HOLOGIC®
The Science of Sure

Powerful images. **Clear answers.**

Manage Patient's concerns about Atypical Femur Fracture*

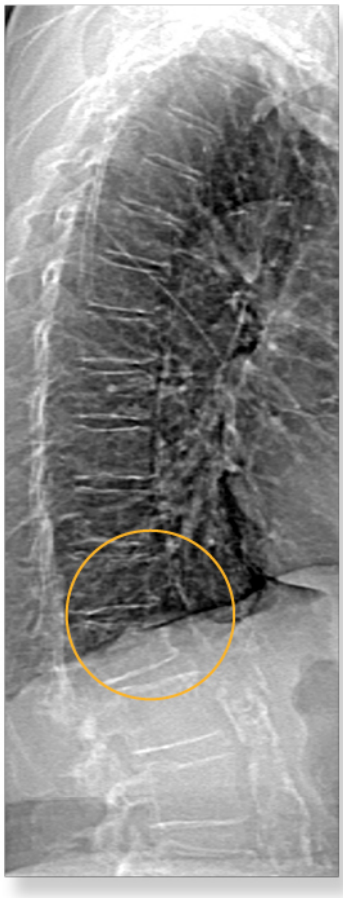

Vertebral Fracture Assessment – a critical part of a complete fracture risk assessment

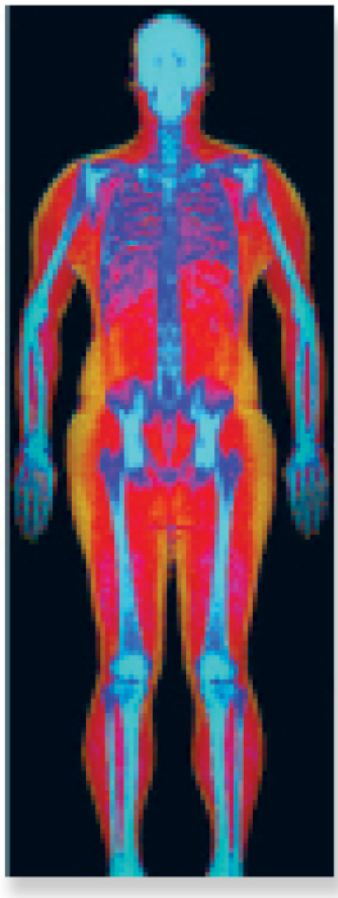

Advanced Body Composition® Assessment – the power to see what's inside

Contact your Hologic rep today at BSHSalesSupportUS@hologic.com

*Incomplete Atypical Femur Fractures imaged with a Hologic densitometer, courtesy of Prof. Cheung, University of Toronto

www.hologic.com | dxaperformance.com | 1.800.442.9892

Volume 35
Number S1
November 2020
pp. 1–337

Journal of Bone and Mineral Research

2020 Annual Meeting of the American Society for Bone and Mineral Research

Virtual Event
September 11–15, 2020

Published monthly by
The American Society for Bone and Mineral Research

2020 Annual Meeting of the American Society for Bone and Mineral Research

Virtual Event
September 11-15, 2020

The *Journal of Bone and Mineral Research* (ISSN: 0884-0431 [print]; 1523-4681 [online]) provides a forum for papers of the highest quality pertaining to bone, muscle, and mineral metabolism. Manuscripts are published on the biology and physiology of bone and muscle, relevant systems biology topics (e.g., osteoimmunology), and the pathophysiology and treatment of sarcopenia, and disorders of bone and mineral metabolism. All authored papers and editorial news and comments, opinions, findings, conclusions or recommendations in the *Journal* are those of the author(s) and do not necessarily reflect the views of the *Journal* and its publisher, nor does their publication imply any endorsement.

The JOURNAL OF BONE AND MINERAL RESEARCH (ISSN: 0884-0431), is published monthly on behalf of the American Society for Bone and Mineral Research by Wiley Subscription Services, Inc., a Wiley Company, 111 River St., Hoboken, NJ 07030-5774. Periodical Postage Paid at Hoboken, NJ and additional offices.

Postmaster: Send all address changes to JOURNAL OF BONE AND MINERAL RESEARCH, John Wiley & Sons Inc., C/O The Sheridan Press, PO Box 465, Hanover, PA 17331. **Information for subscribers:** The *Journal of Bone and Mineral Research* is published in 12 issues per year. Institutional subscription prices for 2020 are: Print & Online: US$1601 (US), US$1701 (Rest of World), €1222 (Europe), £1042 (UK).. Prices are exclusive of tax. Asia-Pacific GST, Canadian GST and European VAT will be applied at the appropriate rates. For more information on current tax rates, please go to www.wileyonlinelibrary.com/tax-vat. The price includes online access to the current and all online back files to January 1st 2012, where available. For other pricing options, including access information and terms and conditions, please visit www.wileyonlinelibrary.com/access. **Commercial Reprints:** Beth Ann Rocheleau, Reprints and Eprints Manager, Rockwater, Inc., PO Box 2211, Lexington, SC 29072, USA; Tel: +00 (1)803 359-4578; Fax: +00 (1)803-753-9430; E-mail: asbmr@rockwaterinc.com. For submission instructions, subscription and all other information, visit: www.jbmr.org

The *Journal of Bone and Mineral Research* is the official journal of the American Society for Bone and Mineral Research, 2001 K Street, NW, 3rd Floor North, Washington, D.C. 20006, USA. **Advertising:** Address advertising inquiries to Joseph Tomaszewski, Advertising Sales Executive, Wiley, 111 River St., Hoboken, NJ 07030, (201) 748-8895 (Tel); jtomaszews@wiley.com (email). Advertisements are subject to editorial approval and must adhere to ASBMR's advertising policy as specified here: https://onlinelibrary.wiley.com/page/journal/15234681/homepage/Advertise.html. Publication of the advertisements in JBMR® is not an endorsement of the advertiser's product or service or the claims made for the product in such advertising. **Disclaimer:** No responsibility is assumed, and responsibility is hereby disclaimed, by the American Society for Bone and Mineral Research, the *Journal of Bone and Mineral Research,* and the Publisher for any injury and/or damage to persons or property as a matter of products liability, negligence or otherwise, or from any use or operation of methods, products, instructions or ideas presented in the *Journal*. Independent verification of diagnosis and drug dosages should be made. Discussions, views and recommendations as to medical procedures, choice of drugs and drug dosages are the responsibility of the authors. Advertisers are responsible for compliance with requirements concerning statements of efficacy, approval, licensure, and availability. The *Journal of Bone and Mineral Research* is a **Journal Club™** selection. The Journal is indexed by *Index Medicus, Current Contents/Life Science, CABS (Current Awareness in Biological Sciences), Excerpta Medica, Cambridge Scientific Abstracts, Chemical Abstracts, Reference Update, Science Citation Index,* and Nuclear Medicine Literature Updating and Indexing Service.

GUIDELINES FOR ABSTRACT READERS

The JBMR® Supplement 1 Abstracts serves as a compiled version of the Abstracts. Authors submit their own abstracts and are charged a fee to do so. Each abstract must be sponsored by a current ASBMR member. Authors are responsible for the accuracy of the content that they post. Authors are responsible for ensuring compliance with applicable human subject and animal subject procedures. When an abstract is submitted, one person is identified as the Presenting Author, the person who is expected to present the abstract at the ASBMR Annual Meeting.

The ASBMR depends upon the honesty of the authors and presenters and relies on their assertions that they have had sufficient full access to the data to be and are convinced of its reliability. The ASBMR expects that authors and presenters:

- Will disclose any conflicts of interest, real or perceived.
- Should disclose any relationship that may bias one's presentation or which, if known, could give the perception of bias.
- Will affirm, for any study funded by an organization with a proprietary or financial interest, that they had full access to all the data in the study.
- Are responsible for the content of abstracts, presentations, slides, and reference materials.
- Keep the planning, content and execution of abstracts, speaker presentations, slides, abstracts and reference materials free from corporate influence, bias or control.
- Should give a balanced view of therapeutic options by providing several treatment options, whenever possible, and by always citing the best available evidence.
- Should disclose when any commercial product is not labeled for the use under discussion or that the product is still investigational.

The ASBMR:

- Will note those speakers who have disclosed relationships, including the nature of the relationship and the associated commercial entity.
- Will peer-review the abstracts according to categories, but only to determine which will be selected for oral presentation, for poster presentations or for any awards. Abstracts are not otherwise subject to any quality or content review by ASBMR or JBMR®.
- Expects the audience for the Abstracts to be researchers, physicians and other health and allied health professionals.
- Protects the Abstracts by copyright, and prohibits the reproduction, distribution or transmission of the abstracts without the express written permission of ASBMR.
- Embargoes the Abstracts for public release in written, oral or electronic communications – until the start time of the session in which the presentation is being made at the ASBMR Annual Meeting

Disclaimer. All authored abstracts, findings, conclusions, recommendations or oral presentations are those of the author(s) and/or speaker(s) and do not reflect the views of the American Society for Bone and Mineral Research or imply any endorsement. No responsibility is assumed, and responsibility is hereby disclaimed, by the American Society for Bone and Mineral Research for any injury and/or damage to persons or property as a matter of products' liability, negligence or otherwise, or from any use or operation of methods, products, instructions or ideas presented in the abstracts or at the ASBMR Annual Meeting. Independent verification of diagnosis and drug dosages should be made. Discussions, views and recommendations regarding medical procedures, choice of drugs and drug dosages are the responsibility of the authors and presenters.

TABLE OF CONTENTS

JBMR® Editorial Board

ASBMR BUSINESS OFFICE

20001 K Street, NW
Third Floor North
Washington, DC 20006
USA
Tel: +1 (202) 367-1161
Fax: +1 (202) 367-2161
E-mail: asbmr@asbmr.org
Website: http://www.asbmr.org

2020 PROGRAM COMMITTEE

President: Teresita Bellido, Ph.D.
Program Chair: Lorenz Hofbauer, M.D.
Program Co-Chair: Tamara Alliston, Ph.D.
Program Co-Chair: Stavroula Kousteni, Ph.D.
Program Co-Chair: Nicola Napoli, M.D., Ph.D.

2020 PROGRAM ADVISORY COMMITTEE

Bjorn Busse, Ph.D.
Peter Croucher, Ph.D.
Roberta Faccio, Ph.D.
Theresa Guise, M.D.
Ed Guo, Ph.D.
Ivo Kalajzic, M.D.
Brendan Lee, M.D., Ph.D.
Fanxin Long, Ph.D.
Laurie McCauley, DDS, Ph.D.
Martina Rauner, Ph.D.
David Roodman, M.D., Ph.D.
Ernestina Schipani, M.D., Ph.D.
Dolores Shoback, M.D.
Natalie Sims, Ph.D.
Hanna Taipaleenmaki, Ph.D.
Marjolein van der Meulen, Ph.D.
Jennifer Westendorf, Ph.D.

2020 ABSTRACT REVIEWERS

Natasha Appelman-Dijkstra, M.D.
Cristiana Cipriani, M.D., Ph.D.
Bart Clarke, M.D.
Peter Ebeling, FRACP, M.D., MBBS
Mary Bouxsein, Ph.D.
Elise Morgan, Ph.D.
Michael Ominsky, Ph.D.
Joseph Wallace, Ph.D.
Maria Luisa Bianchi, M.D.
Craig Langman, M.D.
Michael Levine, M.D.
Andrea Trombetti, M.D.
Deborah Wenkert, M.D.
Natalie Sims, Ph.D.
Florent Elefteriou, Ph.D.
Dana Gaddy, Ph.D.
Lilian Plotkin, Ph.D.
Hiroaki Saito, Ph.D.
Roberto Pacifici, M.D.
Elena Ambrogini, M.D., Ph.D.
Giacomina Brunetti, Ph.D.
Marta Galan-Diez, Ph.D.
Serk In Park, DDS, Ph.D.
Sakamuri Reddy, Ph.D.
Benjamin Frisch, Ph.D.
Beata Lecka-Czernik, Ph.D.
Christa Maes, Ph.D.
Rhonda Prisby, Ph.D.
Michelle McDonald, Ph.D.
Claire Edwards, Ph.D.
Bin Wang, Ph.D.
Hiroshi Kawaguchi, M.D.
Yianglin Bae, Ph.D.
Frederic Cailotto, Ph.D.
Fatma Mohamed, DDS, Ph.D., MS
Salvatore Minisola, M.D.
Zhanna Belaya, M.D., Ph.D.
AMBRISH MITHAL, M.D.
Roman Natoli, M.D., Ph.D.
LUISA PLANTALECH, M.D.
Robert Wermers, M.D.
Janet Rubin, M.D.
Neha Dole, Ph.D.
David Karasik, Ph.D.
Ryan Riddle, Ph.D.
CHUANJU LIU, Ph.D.
Yi-Hsiang Hsu, M.D., Ph.D.
Jitesh Pratap, Ph.D.
Reinhold Erben, M.D., DVM
Stephen Harris, Ph.D.
Holger Henneicke, M.D., Ph.D.
Eva Liu, M.D.
Hinori Yamamoto, Ph.D.
Edward Guo, Ph.D.
Daisuke Inoue, M.D., Ph.D.
Chao Liu, Ph.D.
Xiaowei Sherry Liu, Ph.D.
Meghan McGee-Lawrence, Ph.D.
Bettina Willie, Ph.D.
Alberto Falchetti , M.D.
Lucas Brun , M.D., Ph.D.
Peter Friedman, Ph.D.
Aline Martin, Ph.D.
Dobrawa Napierala, Ph.D.
Lauren Surface, Ph.D.
Maria Schuller Almeida, Ph.D.
KRISTINA AKESSON, M.D., Ph.D.
Debra Bembem, Ph.D.
Ghada El-Hajji Fuleihan, M.D., MPH
Joshua Farr, Ph.D.
RENNY FRANCESCHI, Ph.D.
Jonathan Lowery, Ph.D.
Koichi Matsuo, M.D., Ph.D.
Ling Qin, Ph.D.
Josephine Tauer, Ph.D.
MIchael Hadjiargyrou, Ph.D.
Elizabeth Bradley, Ph.D.
MOTOMI ENOMOTO-IWAMOTO, DDS, Ph.D.
MOTOMI ENOMOTO-IWAMOTO, DDS, Ph.D.
Brya Matthews, Ph.D.
Toru Ogasawara, Ph.D.
Roman Thaler, Ph.D.
Natalie Glass, Ph.D.
Rolando Espinosa-Morales, M.D.
Mary Goldring, Ph.D.
Nancy Lane, M.D.
Martina Rauner, Ph.D.
Francesca Gori, Ph.D.
Anyonya Guntur, Ph.D.
Srividhya Iyer, Ph.D.
Charles O'Brien, Ph.D.
Tadayoshi Hayata, Ph.D.
Melissa Kacena, Ph.D.
Merry Jo Oursler, Ph.D.
Sarah Dallas , Ph.D.
Murat Bastepe, M.D., Ph.D.
Mary Farach-Carson, Ph.D.
David Findlay, Ph.D.
Valerie GEOFFROY, Ph.D.
Yuji Yoshiko, Ph.D.
Claus Glueer, Ph.D.
Lorie Fitzpatrick, M.D.
Benjamin Khoo, Ph.D.
Lynn Kohlmeier, M.D.
John Schousboe, M.D., Ph.D.
Bo Abrahamsen, M.D., Ph.D.
Cyrus Cooper, M.D., Ph.D.
Kristine Ensrud, M.D., MPH
Carola zillikens, Ph.D.
Jane Cauley, Ph.D.
Michael Bolognese, M.D.
Stefan Goemaere, Ph.D.

Eugene McCloskey , M.D.
roger Bouillon, M.D., Ph.D.
Thomas Levin Andersen, Ph.D.
Suzanne Morin, M.D., MS
Jeri Nieves, Ph.D.
dolores Shoback, M.D.
Karl Jepsen, Ph.D.
Christopher Kovacs, M.D.
Laura McCabe, Ph.D.
Jan Bruder, M.D.
charlles castro, M.D., Ph.D.
Robert Marcus, M.D.
Thierry Thomas, M.D., Ph.D.
Elena Tsourdi, M.D.
Robert Adler, M.D.
serge ferrari, M.D.
Bente Langdahl, M.D., Ph.D.
maria belen zanchetta, M.D.
Edith Gardiner, Ph.D.
T.J. (Jack) Martin, FRACP, DSc., M.D.
Takuma Matsubara , DDS, Ph.D.
Shigeki Nishimori, M.D., Ph.D.
Yongmei Wang, M.D., Ph.D.
Cheryl Ackert-Bicknell , Ph.D.
Jinwoo Kim, DDS, Ph.D.
Wei Yao, M.D.
Abhishek Chandra, Ph.D.
Stephen Deacon, Ph.D.
Jiliang Li, M.D., Ph.D.
Maya Styner, M.D.
Michael Whyte, M.D.
Michael Econs, M.D.
Diala El Maouche, M.D., MS
Seiji Fukumoto, Ph.D.
Luigi Gennari, M.D., Ph.D.
Daniela Merlotti, M.D., Ph.D.
Eileen Shore, Ph.D.
Marja Hurley, M.D.
Roy Morello, Ph.D.
Yves Sabbagh, Ph.D.
Bram van der Eerden, Ph.D.
Dennis Villareal, M.D.
Dana Bliuc, M.D., Ph.D.,MPH
Vincent T. Carpentier, MS
Peggy Cawthon, Ph.D., MPH
Andrea Giusti, M.D.
Elsa Strotmeyer, Ph.D., MPH

ASBMR COMMITTEE MEMBERS AND REPRESENTATIVES

ADVOCACY/SCIENCE POLICY COMMITTEE

Patricia Ducy, Ph.D., *Chairperson*
Julia Charles, M.D., Ph.D.
Maureen Devlin, Ph.D.
Amel Dudakovic, Ph.D.
Michael Hadjiargyrou, Ph.D.
Lisa Langsetmo, Ph.D., M.S.
Yi-Xian Qin, Ph.D.
Elsa Strotmeyer, Ph.D., M.P.H.
Marc Wein, M.D., Ph.D.
Deneen Wellik, Ph.D.
Deborah Wenkert, M.D.
Roberta Faccio, Ph.D., *Council Liaison*
Katie Duffy, *Staff Liaison*
Hannah Miller, *Staff Liaison*

DEVELOPMENT COMMITTEE

Melissa Kacena, Ph.D., *Co-Chairperson*
Larry Suva, Ph.D., *Co-Chairperson*
Andrea Alford, Ph.D.
Charles Farber, Ph.D.
Marian Hannan, DSc.
Julia Hum, Ph.D.
Nancy Lane, M.D.
Gabriel Mbalaviele, Ph.D.
Fayez Safadi, Ph.D.
Marcella Walker, M.D.
Marja Hurley, M.D., *Council Liaison*
Deborah Kroll, *Staff Liaison*
Hannah Miller, *Staff Liaison*

DIVERSITY, EQUITY, AND INCLUSION COMMITTEE

Nicole Wright, Ph.D., MPH, *Co-Chairperson*
Rhonda Prisby, Ph.D., *Co-Chairperson*
Ejigayehu Abate, M.D.
Lucas Brun, Ph.D.
Jesse Goliath, Ph.D.
Nilsson Holguin, Ph.D.
Karl Lewis, Ph.D.
Orhan Oz, M.D., Ph.D.
Ling Qin, Ph.D.
Tiahana Spencer
Sylvia Christakos, Ph.D., *Ex-Officio*
Kristy Nicks, Ph.D., *Ex-Officio*
Lauren Taggart, *Staff Liaison*
Lauren Strup, *Staff Liaison*
Kim Durante, *Staff Liaison*

EDUCATION ADVISORY COMMITTEE

Jesus Delgado-Calle, Ph.D., *Co-Chairperson*
Anne Schafer, M.D., *Co-Chairperson*
Joshua Farr, Ph.D.
Deborah Mitchell, M.D.
Luisa Plantalech, M.D.

ETHICS ADVISORY COMMITTEE

Robert Adler, M.D., *Chairperson*
Eva S. Liu, M.D.
Richard Bockman, M.D., Ph.D.
Catherine Gordon, M.D., M.S.
Núria Guañabens, M.D., Ph.D.
Karl Jepsen, Ph.D.
Richard Lee, M.D.
Laurie McCauley, D.D.S., Ph.D.
Eileen Shore, Ph.D.
Kristine Ensrud, M.D., MPH, *Council Liaison*
Bart L. Clarke, M.D., *Ex-Officio*
Doug Fesler, *Staff Liaison*
Katie Duffy, *Staff Liaison*
Hannah Miller, *Staff Liaison*

FINANCE COMMITTEE

Juliet Compston, M.D., FRCP, *Chairperson*
Johannes van Leeuween, Ph.D., *Co-Chairperson*
Mary Bouxsein, Ph.D.
Peggy Cawthon, Ph.D.
Clarissa Craft, Ph.D.
Robert Jilka, Ph.D.
Richard Kremer, M.D., Ph.D.
Teresita Bellido, Ph.D., *Ex Officio*
Kurt Hankenson, M.D., *Council Liaison*
Doug Fesler, *Staff Liaison*
Brian Teague, *Staff Liaison*
Sunny Patel, *Staff Liaison*

INNOVATION COMMITTEE

Michael Mannstadt, M.D., *Chairperson*
Rachelle Johnson, Ph.D.
Hanna Taipaleenmaki , Ph.D.
Natalie Sims, Ph.D.
Suzanne Jan de Beur, M.D., *ASBMR President Elect*

MEMBERSHIP ENGAGEMENT COMMITTEE

Anne Gingery, Ph.D., *Co-Chairperson*
Jonathan Lowery, Ph.D., *Co-Chairperson*
Maria Belen Zanchetta, M.D.
Jesus Delgado-Calle, Ph.D.
Morten Frost Nielsen, M.D., Ph.D.
Patricia Juarez-Camacho, Ph.D.
Amna Khan, MBBS, M.D.
Melissa Premaor, Ph.D.
Martina Rauner, Ph.D.
Erica Scheller, D.D.S., Ph.D.
Jad Sfeir, M.D.
Pawel Szulc, M.D., Ph.D.
Cristiana Cipriani, Ph.D., *Ex-Officio*
Katherine Motyl, Ph.D., *Ex-Officio*
Roman Thaler, Ph.D., *Ex-Officio*
Paola Divieti Pajevic, M.D., Ph.D., *Council Liaison*
Megan Weivoda, Ph.D., *Early Stage Investigator SubCommittee Chair*
Rachelle Johnson, Ph.D., *Early Stage Investigator SubCommittee Chair*
Lauren Taggart, *Staff Liaison*
Lauren Strup, *Staff Liaison*
Hannah Miller, *Staff Liaison*

EARLY STAGE INVESTIGATOR SUBCOMMITTEE

Megan Weivoda, Ph.D., *Co-Chairperson*
Rachelle Johnson, Ph.D., *Co-Chairperson*
Beth Bragdon, Ph.D.
Adriana Carvalho, Ph.D.
Shilpa Choudhary, Ph.D.
Kathleen Hill-Gallant, Ph.D.
Debra Irsik, Ph.D.
Aaron Hudnall, D.O.
Maureen Lynch, Ph.D.
Patrick Mulcrone, Ph.D.
Sun Peck, Ph.D.
Neha Shashank Dole, Ph.D.
Sabashini Ramchand, FRACP, MBBS
Elena Tsourdi, M.D.
Liesbeth Winter, M.D., Ph.D.
Anne Gingery, Ph.D., *MEEC Liaison*
Jonathan Lowery, Ph.D., *MEEC Liaison*
Lauren Taggart, *Staff Liaison*
Lauren Strup, *Staff Liaison*
Kim Durante, *Staff Liaison*

PROFESSIONAL PRACTICE COMMITTEE

Matthew Drake, M.D., Ph.D., *Chairperson*
Pauline Camacho, M.D.
Carolyn Crandall, M.D., MS
Beatrice Edwards, M.D.
Sabrina Gill, M.D., M.P.H.
Nicholas Harvey, MBBC
Aliya Khan, M.D.
Valerie Peck, M.D.
Micol Rothman, M.D.
Thomas Weber, M.D.
Vishnu Garla, M.D., *Ex-Officio*
Mahshid Mohseni, M.D., *Ex-Officio*
Anna Spagnoli, M.D., *Council Liaison*
Katie Duffy, *Staff Liaison*
Hannah Miller, *Staff Liaison*

PUBLICATIONS COMMITTEE

Sarah Dallas, Ph.D., *Chairperson*
Manju Chandran, M.D.
Ruban Dhaliwal, M.D., MPH
Roman Eliseev, M.D., Ph.D.
James Fleet, Ph.D.
Struan Grant, Ph.D.
Meryl S. LeBoff, M.D.
David Monroe, Ph.D.
Roberto Civitelli, M.D., *Ex-Officio*
Peter Ebeling, AO, M.D., FRACP, *Ex-Officio*
John P. Bilezikian, M.D., *Ex-Officio*
S. Serra Ucer Ozgurel, Ph.D., *Ex-Officio*
Daniel Youngstrom, Ph.D., *Ex-Officio*
Kate Ward, Ph.D., *Council Liaison*
Christopher Kovacs, M.D., *Council Liaison*
Katie Duffy, *Staff Liaison*
Hannah Miller, *Staff Liaison*

WOMEN IN BONE AND MINERAL RESEARCH COMMITTEE

Michaela Reagan, Ph.D., *Chairperson*
Alesha Castillo, Ph.D.
Lamya Karim, Ph.D.
Laura McCabe, Ph.D.
Michelle McDonald, Ph.D.
Meghan McGee-Lawrence, Ph.D.
Allison Pettit, Ph.D.
Lilian Plotkin, Ph.D.
Christine Swanson, M.D., MCR
Catherine Van Poznak, M.D.
Naga Yalla, M.D., *Ex-Officio*
Emma Duncan, FRACP, MBBS, M.D., Ph.D., *Council Liaison*
Lauren Taggart, *Staff Liaison*
Lauren Strup, *Staff Liaison*
Kim Durante, *Staff Liaison*

ASBMR REPRESENTATIVES TO FASEB

Brendan Boyce, M.D.
Member, Board of Directors

Thomas L. Clemens, Ph.D.
FASEB Finance Committee

Patricia Ducy, Ph.D.
Science Policy Committee
Research Conferences Advisory Committee

Roberta Faccio, Ph.D.
Excellence in Science Award Committee

David Karasik, Ph.D.
FASEB Publications and Communications Committee

Thomas Lang, Ph.D.
FASEB Editorial Board

Yousef Abu-Amer, Ph.D.
FASEB BioAdvances Editorial Board

Katie Duffy
Staff Liaison

ASBMR REPRESENTATIVES TO OTHER GROUPS

Meryl Leboff, M.D.
U.S. Bone and Joint Initiative

Stuart L. Silverman, M.D.
National Osteoporosis Foundation
Interspecialty Medical Council

Roland Baron, D.D.S, Ph.D
International Federation of Musculoskeletal Research Societies Board Co-Chair

Nicola Napoli, M.D.
International Federation of Musculoskeletal Research Societies Board
ASBMR Representative

Meghan McGee-Lawrence, Ph.D.
IFMRS Future Global Leaders Committee

Lynda Bonewald, Ph.D.
IFMRS Big Data Working Group, Co-Chair

AWARDS

WILLIAM F. NEUMAN AWARD
John P. Bilezikian, M.D.

FULLER ALBRIGHT AWARD
Martina Rauner, Ph.D.

FREDERIC C. BARTTER AWARD
Felicia Cosman, M.D.

LOUIS V. AVIOLI FOUNDERS AWARD
Moustapha Kassem, M.D., Ph.D.

LAWRENCE G. RAISZ AWARD
Claes Ohlsson, M.D., Ph.D.

PAULA STERN ACHIEVEMENT AWARD
Natalie Sims, Ph.D.

SHIRLEY HOHL SERVICE AWARD
Douglas P. Kiel, M.D., M.P.H.

STEPHEN M. KRANE AWARD
Theresa Guise, M.D.

GIDEON A. RODAN AWARD
G. David Roodman, M.D., Ph.D.

ADELE L. BOSKEY AWARD
Tamara Alliston, Ph.D.

2020 ASBMR MOST OUTSTANDING BASIC ABSTRACT AWARD
Fatma Mohamed, B.D.S, M.S., Ph.D.

2020 ASBMR MOST OUTSTANDING CLINICAL ABSTRACT AWARD
Sandra Iuliano, Ph.D.

2020 ASBMR MOST OUTSTANDING TRANSLATIONAL ABSTRACT AWARD
Jingwen Yang, Ph.D

2020 ASBMR PRESIDENT'S AWARD
Shawon Debnath, Ph.D.

2020 ASBMR YOUNG INVESTIGATOR AWARD
Tala Azar
Named in memory of Robert Heaney and given to the most outstanding abstract in nutrition research.

2020 ASBMR FELIX BRONNER YOUNG INVESTIGATOR AWARD
Frederica Scotto di Carlo, Ph.D.

2020 ASBMR FUND FOR RESEARCH AND EDUCATION YOUNG INVESTIGAOR AWARDS

Samantha Weaver, Ph.D.
Kosei Nagata, M.D.

2020 ASBMR FUND FOR RESEARCH AND EDUCATION YOUNG INVESTIGAOR DIVERSITY AWARD
Claudia Cristina Biguetti, D.D.S., M.Sc., Ph.D.

2020 ASBMR FUND FOR RESEARCH AND EDUCATION YOUNG INVESTIGATOR EMERGING COUNTRY AWARD
Priyanka Singh

2020 ASBMR YOUNG INVESTIGATOR AWARDS

Tala Azar
Lena Batoon
Cora Best, Ph.D., M.H.S., R.D.N.
Scott Birks
James Boorman-Padgett
Lianzhi Chen, Ph.D.
Ruiying Chen
Guillaume Courbon, Ph.D., M.S.
Bhaba Krishan Das, Ph.D.
Elizabeth Duchow
Katelyn Guerriere, M.S.
Gali Guterman Ram, Ph.D.
Shawn Hallett
Zixue Jin, Ph.D.
Cynthia Kahari
Ho Jun Kang
Ismael Karkache
Jenna Leser
Huili Lyu
Hirotsugu Maekawa
Mohit M Mahatma
Adel Mandl
David Molstad
Shuangfei Ni, Ph.D.
Chase Pagani
Peter Sang Uk Park
Shuqun Qi, Ph.D.
Noemi Roza, Ph.D.
Bhavya Senwar
Betty Shum, M.D.
Cassandra Smith
Anne Sophie Sølling, M.D.
Amy Strong, M.D., Ph.D.
Tuuli Suominen, M.Sc.
Dana Trompet
Christie Turin, M.D.
Bowen Wang
Jialiang Wang, Ph.D.
Wenzheng Wang
Zheng Wang, D.D.S., M.S.
Komal Waqas
Yulong Wei
Karin C. Wu, M.D.
Jiajia Xu, Ph.D.
Huiliang Yang, M.D.
Lutian Yao, M.D., Ph.D.
Tetsuya Yoshimoto, D.D.S., Ph.D.
JungeunYu, Ph.D.
Wei Yu, M.D.
Zhenjian Zhuo, Ph.D.

2020 CLASS OF ASBMR FELLOWS

Dennis Black, Ph.D.
Jacques Brown, M.D.
Dong Won Byun, M.D., Ph.D.
Peggy Cawthon, Ph.D.
Robin Daly, Ph.D.
Michael Econs, M.D.
Ghada El-Hajj Fuleihan, M.D., M.P.H.
Rachel Gafni, M.D.
Struan Grant, Ph.D.
Gail Greendale, M.D.
Theresa Guise, M.D.
Harry Hogan, Ph.D.
Carlos Isales, M.D.
Deborah Kado, M.D.
David Karpf, M.D.
Hua Zhu (David) Ke, Ph.D.
Aliya Khan, M.D.
Jung-Eun Kim, Ph.D.
Henry Kronenberg, M.D.
Meryl LeBoff, M.D.
Michael Levine, M.D.
Joshua Lewis, Ph.D.
Xiaodong Li, Ph.D.
Subburaman Mohan, Ph.D.
Susan Ott, M.D.
Nathan Pavlos, Ph.D.
Rhonda Prisby, Ph.D.
Stuart Ralston, M.B., ChB, FRCP, M.D., FFPM, FMedSci, FRSE
Yumie Rhee, M.D., Ph.D.
Deborah Sellmeyer, M.D.
Joseph Stains, Ph.D.
Thomas Thacher, M.D.
Katherine Tucker, Ph.D.
Marjolein van der Meulen, Ph.D.
Deepak Vashishth, Ph.D.
Connie Weaver, Ph.D.
Jiake Xu, Ph.D., MB

2020 SUPPORTERS

The ASBMR gratefully acknowledges the following companies for their support (as of August 26, 2020)**:**

SILVER LEVEL
Ascendis Pharma A/S

BRONZE LEVEL SUPPORTERS
Alexion Pharmaceuticals
Inozyme Pharmaceuticals
Ipsen Biopharmaceuticals, Inc.
Takeda
Ultragenyx Pharmaceutical, Inc.

FRIEND LEVEL SUPPORTERS
Amgen, Inc.
Kyowa Kirin
Radius Health
Regeneron Pharmaceuticals, Inc.
Scanco Medical
UCB

DISCLOSURE POLICY

The ASBMR is committed to ensuring the balance, independence, objectivity and scientific rigor of all its individually sponsored or industry-supported educational activities. Accordingly, the ASBMR adheres to the requirement set by ACCME that audiences at jointly-sponsored educational programs be informed of a presenter's (speaker, faculty, author, or planner) academic and professional affiliations, and the disclosure of the existence of any significant financial interest or other relationship a presenter or their spouse has with any proprietary entity over the past 12 months producing, marketing, re-selling or distributing health care goods or services, consumed by, or used on patients, with the exemption of non-profit or government organizations and non-health care related companies. When an unlabeled use of a commercial product, or an investigational use not yet approved for any purpose, is discussed during the presentation, it is required that presenters disclose that the product is not labeled for the use under discussion or that the product is still investigational. This policy allows the listener/attendee to be fully knowledgeable in evaluating the information being presented. The On-Site Program book will note those speakers who have disclosed relationships, including the nature of the relationship and the associated commercial entity.

Disclosure should include any affiliation that may bias one's presentation or which, if known, could give the perception of bias. This includes relevant financial affiliations of a spouse or partner. If an affiliation exists that could represent or be perceived to represent a conflict of interest, this must be reported in the abstract submission program by listing the name of the commercial entity and selecting the potential conflict(s) by clicking in the box next to the relationship type. Disclosures will be printed in the program materials. These situations may include, but are not limited to:

- Grant/Research Support
- Consultant
- Speakers' Bureau
- Major Stock Shareholder
- Other Financial or Material Support

1001 - 1024	Friday Oral Presentations
1025 - 1048	Saturday Oral Presentations
1049 - 1072	Sunday Oral Presentation
1073 - 1096	Monday Oral Presentations
1097 - 1120	Tuesday Oral Presentations
P-001 - P-868	Poster Sessions
*	Denotes Abstract Presenting Author

1001

Skeletal stem cells are maintained in a Wnt-inhibitory environment within the resting zone of the growth plate *Shawn Hallett[1], Noriaki Ono[1]. [1]University of Michigan School of Dentistry, United States

Chondrocytes in the resting zone of the postnatal growth plate are characterized by their slow-cycling nature, which include a population of skeletal stem cells that form columnar chondrocytes, osteoblasts and bone marrow stromal cells over time. Slow-cycling chondrocytes express parathyroid hormone-related protein (PTHrP), constituting the PTHrP-indian hedgehog feedback loop essential for growth plate maintenance. However, the molecular mechanisms regulating resting chondrocyte differentiation into proliferating, columnar chondrocytes are unknown. Here, we utilized a genetic pulse-chase approach to isolate slow cycling chondrocytes (LRCs) from the postnatal growth plate resting zone using a chondrocyte-specific doxycycline-controllable Tet-Off system regulating expression of histone-linked GFP (H2B-GFP). FACS sorting of dissected growth plates was conducted to isolate H2B-GFPhigh; Col2a1-creERtdTom LRCs versus H2B-GFPlow; Col2a1-creERtdTom non-LRCs. An RNA-seq transcriptomic analysis of LRCs identified significant enrichment of Wnt inhibitors and resting zone chondrocyte markers while non-LRCs were enriched for pre-hypertrophic and hypertrophic chondrocyte markers. To define the functional role of Wnt signaling on LRCs, we activated Wnt/ß-catenin signaling in PTHrP+ resting chondrocytes by conditionally inducing haploinsufficiency of Adenomatous polyposis coli (Apc), a component of the ß-catenin degradation complex, using a PTHrP-creER line and Apc-floxed allele combined with a tdTomato reporter allowing cell-lineage analyses. Animals were injected with tamoxifen at postnatal day 6 (P6) and chased until P12, 21, 36 and 96. PTHrP+ resting chondrocytes and short (10 cells) columnar chondrocytes were quantified to assess PTHrP+ skeletal stem cell formation and short/long-term self-renewal capability. By P12 and P21, Apc-haploinsufficient PTHrP+ resting chondrocytes and the number of short columns were significantly reduced compared to controls. After 3 months of chase at P96, Apc-haploinsufficient PTHrP+ resting chondrocytes established long columns less effectively than their controls. These data indicate that Wnt/ß-catenin activation impairs formation and short and long-term self-renewal of PTHrP+ chondrocytes. These findings reveal that slow-cycling chondrocytes are maintained in a canonical Wnt-inhibitory environment, unraveling a novel mechanism regulating self-renewal and differentiation of PTHrP+ skeletal stem cells of the postnatal growth plate.

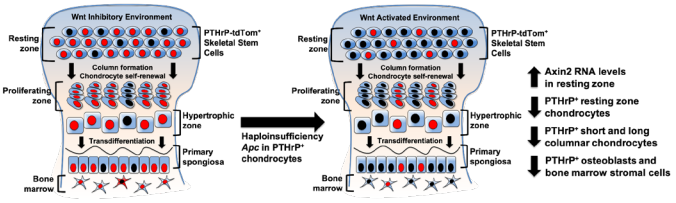

***Disclosures: Shawn Hallett**, None*

1002

Phlpp1 inhibition improves post-traumatic osteoarthritis through independent effects on chondrocytes and neurons *Samantha Weaver[1], Ian Lorang[1], Xiaodong Li[1], Elizabeth Bradley[2], Jennifer Westendorf[1]. [1]Mayo Clinic, United States, [2]University of Minnesota, United States

Osteoarthritis (OA) in the knee is a debilitating condition that causes significant pain and morbidity. Phlpp1 and Phlpp2 are highly expressed in human OA tissue but not normal articular cartilage and genomic variants are associated with human OA in GWAS studies. Inhibition of Phlpp1 protein phosphatase has previously been shown to preserve cartilage, reduce allodynia, and improve function in a murine model of post-traumatic OA (PTOA). Phlpp1-/- mice and WT mice given an intra-articular injection of a small-molecule Phlpp inhibitor into the knee joint space are protected from PTOA. To investigate the specific cell type responsible for cartilage preservation in Phlpp1-depleted mice, Phlpp1 was deleted in Aggrecan-expressing (Agc+) cells at 12 weeks of age (Phlpp1-CKOAgc). At 17 weeks old, male mice were subjected to destabilization of the medial meniscus (DMM) surgery in the right knee. PTOA progression was monitored over the subsequent 12 weeks through activity assays, at which point mice were euthanized and limbs collected for histology. Phlpp1-CKO-Agc mice were not protected from functional impairments as previously demonstrated in Phlpp1-/- mice. However, Phlpp1-CKOAgc knee articular cartilage was preserved compared to WT-AgcCre+ mice, with an overall lower summed OARSI score. These data suggest that Phlpp1 expression in chondrocytes contributes to cartilage degradation following PTOA. To test the effects of Phlpp1 inactivation on sensory neurons responsible for pain signaling, primary rat dorsal root ganglia (DRG) were treated in culture with increasing doses of Phlpp inhibitor NSC117079 for 28 days. NSC117079 reduced neurite outgrowth and expression of small/medium sensory neurons (NTrk1) and neurotransmitters (Cgrp), but not a common neuronal gene (Uchl1) in a dose dependent manner. To translate these findings in vivo, Phlpp1-CKOAgc mice were given an intra-articular injection of NSC117079 into the DMM-operated knee 7 weeks post-surgery. Both Phlpp1-CKOAgc and WT-AgcCre+ administered NSC117079 spent less time resting during subsequent weekly activity assays, indicating improved pain. Bone sections from mice injected with NSC117079 indicated reduced staining of pain neurotransmitters Substance P in the subchondral bone and NF200 in the periosteum. Taken together, these data suggest that Phlpp1 inhibition preserves cartilage and improves pain during OA progression by simultaneously working in different cell types, including chondrocytes and neurons.

***Disclosures: Samantha Weaver**, None*

1003

Feedback-regulatory loop between MYC and NRF2 controls osteoclastogenesis and pathological bone erosion *Peter Sang Uk Park[1], Sehwan Mun[1], Steven Zeng[1], Seyeon Bae[1], Kyung-Hyun Park-Min[2]. [1]Arthritis and Tissue Degeneration Program, David Z. Rosensweig Genomics Research Center, Hospital for Special Surgery, United States, [2]Arthritis and Tissue Degeneration Program, David Z. Rosensweig Genomics Research Center, Hospital for Special Surgery, New York, NY, USA, United States

Osteoclasts are bone-resorbing cells that play an essential role in homeostatic bone remodeling, and defects in osteoclasts result in unbalanced bone resorption and pathological bone loss such as inflammatory arthritis and osteoporosis. Receptor activator of NF-kappa B ligand (RANKL) is an essential regulator of osteoclast formation and activity. Therefore, developing targeted therapies of the molecular pathways downstream of RANKL has been a promising approach to alleviating bone disease. However, the RANKL-RANK network is involved in various biological processes, and a deeper understanding of the molecular pathways specific to osteoclasts is needed. Recently, the crucial role of MYC and its downstream effectors in driving osteoclast differentiation and pathological bone loss has been demonstrated, suggesting that MYC-driven transcriptional cascade in osteoclasts is a potential treatment target downstream of RANKL. Despite these advances, upstream regulators of the MYC network in osteoclasts are not well defined. In this study, we identify Nuclear factor erythroid-derived 2 (NRF2), a transcription factor known to regulate the expression of phase II antioxidant enzymes, as a novel upstream regulator of MYC and promising target for bone diseases. We find that RANKL-induced transcription and stability of MYC are negatively regulated by NRF2. Pharmacological activation of NRF2 completely suppresses MYC expression while NRF2-deficiency increases MYC expression. Mechanistically, NRF2 negatively regulates MYC through suppressing RANKL-induced ERK activation, and blocking ERK completely inhibits NRF2 deficiency-induced osteoclast formation. To further understand the pathophysiological role of MYC in NRF2-mediated suppression of osteoclastogenesis, we generated osteoclast-specific MYC/NRF2-deficient mice. The ablation of MYC in osteoclasts reverses enhanced osteoclast differentiation and activity by NRF2 deficiency both in vivo and in vitro. Furthermore, we also find that MYC is responsible for the accelerated arthritic bone destruction in NRF2 deficient mice in a murine model of inflammatory arthritis.Collectively, our results identify the functional feedback loop between MYC and NRF2 during osteoclastogenesis. Our findings also indicate that this novel NRF2-ERK-MYC axis could be instrumental for the fine-tuning of osteoclast formation and provide additional ways in which osteoclasts could be therapeutically targeted to prevent pathological bone erosion.

***Disclosures: Peter Sang Uk Park**, None*

1004

Live Cell and Intravital Imaging of Osteoclast Resorption Dynamics and Osteocyte Fate During Resorption *Sarah Dallas[1], Valerie Kirtley[1], LeAnn Tiede-Lewis[1], Eleanor Ray[1], Yixia Xie[1], Lora Shiflett[1]. [1]University of Missouri Kansas City, United States

Transgenic gain and loss of function models, osteoclast culture models and naturally occurring mutations have advanced understanding of the mechanisms regulating osteoclast differentiation and function. However, only a few studies have used live cell imaging to determine the dynamic behaviors of osteoclasts in situ within bone. Using transgenic mice with fluorescently tagged osteoclasts, osteocytes and collagen, live cell and intravital imaging was used to understand the dynamic and resorptive behavior of osteoclasts in bone and determine the fate of osteocytes undergoing resorption.Transgenic lines crossed in various combinations for 2-color imaging included mice with osteoclast expression of tdTomato (LysM-Cre/tdTom), osteocyte expression of GFP (Dmp1-AcGFPmem) or tdTomato (Dmp1-cre/tdTom) and mice with GFPtpz-tagged type I collagen (Col-GFP). Widefield or confocal live cell imaging was done in calvarial explants with & without PAM3CSK4, a proinflammatory stimulator of resorption, and intravital multiphoton imaging was done in 4-6wk mice. Live imaging in LysM-Cre/tdTom calvaria revealed that osteoclasts were highly motile, with maximum velocities up to 52.6+/-5.7µm/h and a mean of 13.5+/-1.4µm/h and had a highly branched, multi-lobed morphology, with many cell projections. Over 48h of imaging the osteoclast morphology continually changed, with extension & retraction of cell processes, amoeboid-like streaming of the cell and formation of multiple transient actin rings(sealed zones) that correlated with advancing resorption fronts. Some osteoclasts underwent fusion with adjacent osteoclasts or fission into 2 or more osteoclasts that continued to resorb. PAM3CSK4 significantly reduced the maximum & mean osteoclast velocity to 38.3+/-2.1 & 8.8+/-0.4µm/h, promoted resorption and osteoclast survival, increased the directionality of motion, increased the mean # of actin rings per osteoclast from 0.27+/-0.11 to 1.4+/-0.25 and decreased fusion with a trend towards increased fission. Dual imaging of osteoclasts/osteocytes and collagen/osteocytes showed that ~93% of osteocytes in resorbed bone underwent cell death, 6% were internalized into osteoclasts and in rare cases (~1%), they

survived resorption by migrating out of their lacunae (n=91 osteocytes). These data provide new insight into the dynamic behavior of osteoclasts in the natural bone environment, how these dynamics are altered in inflammatory bone resorption, and reveal the fate of osteocytes undergoing resorption.

***Disclosures: Sarah Dallas**, None*

1005

Endoplasmic reticulum stress induced inhibition of mitochondrial transfer and cathepsin K secretion in osteocyte network - a novel mechanism of glucocorticoid induced bone loss *Junjie Gao[1], Jun Yuan[2], Delin Liu[2], Changqing Zhang[3], Minghao Zheng[4]. [1]Perron Institute for Neurological and Translational Science, Nedlands, Western Australia, 6009, Australia, Australia, [2]Centre for Orthopaedic Translational Research, Medical School, University of Western Australia, Nedlands, Western Australia, 6009, Australia., Australia, [3]Department of Orthopaedics, Shanghai Sixth People's Hospital, Shanghai Jiaotong University, Shanghai, 200233, China., China, [4]Centre for Orthopaedic Translational Research, Medical School, University of Western Australia, Nedlands, Western Australia, 6009, Australia., Australia

Glucocorticoid (GC) associated osteoporosis is common but GC-triggered bone loss remains largely unclear. Accounting for 90% of cell population, osteocytes and their network may play critical role in response to GC administration. Previously we showed that endoplasmic reticulum (ER) regulated activity and transfer of mitochondria within osteocyte dendritic processes is critical for bone hemostasis. Here we showed for the first time that GC inhibits osteocyte homeostasis by suppressing mitochondrial transfer between osteocytes and induced secretion of cathepsin K through the induction of mitophagy of osteocytes. We first showed that dexamethasone (Dex) modified the configuration of ER in osteocytes from a tubular-like form to a stressed condensed sheet-like pattern. The change of configuration lead to the arrest of MitoTracker® Green labelled mitochondrial movement along the dendritic network and compromise mitochondrial transfer within the osteocyte dendritic network. Degradation of Mfn2 by GC induced PINK1 activation is responsible for the inhibition of mitochondrial transfer evidenced by siRNA study in MLO-Y4 cells. We further showed that PINK1-mediated mitophagy has resulted in the induction of cathepsin K in mouse calvaria culture. Knocking down PINK1 gene but not Atg5 abolished the GC-triggered cathepsin K production suggesting that production of cathepsin K in osteocytes following GC treatment is mediated by a non-canonical autophagy pathway. In summary, our results indicate that GC-induced PINK1 modulates both of the mitochondrial transfer, and the production of cathepsin K in osteocytes, thereby contributing to the GC-induced bone loss.

***Disclosures: Junjie Gao**, None*

1006

Mmp9 and Mmp14 Cooperatively Orchestrate Osteoclast Activation via Surface Galectin-3 Lattice Proteolysis *Lingxin Zhu[1], Yi Tang[2], Xiao-Yan Li[2], Samuel Kerk[3], Evan Keller[4], Jung-Sun Cho[2], Tamar Feinberg[2], Costas Lyssiotis[3], Stephen Weiss[2]. [1]School and Hospital of Stomatology, Wuhan University, China, [2]Life Sciences Institute, University of Michigan, United States, [3]Department of Molecular and Integrative Physiology, University of Michigan, United States, [4]Department of Pathology, University of Michigan, United States

During bone resorption, osteoclasts (OCs) undergo extensive transcriptional and metabolic reprogramming while reorganizing cytoskeletal structure, and secreting protons along with proteases into resorption lacunae. We recently identified a cathepsin K-independent collagenolytic system in OCs that includes a functionally redundant network of the matrix metalloproteinases, Mmp9 and Mmp14 (Sci Transl Med 12:529, 2020). However, whether Mmp9/Mmp14 might also impact the cellular transcriptional and metabolic landscape of OCs remains unknown. To address this issue, we generated a myeloid-specific Mmp14 conditional knockout mice (Csf1r-Cre/Mmp14f/f) in either Mmp9 wild-type or null backgrounds. Primary bone marrow-derived macrophages were isolated and differentiated into OCs, then subjected to integrated transcriptional-metabolic profiling. Unexpectedly, over 700 transcript changes were detected with remarkable transcriptional alterations noted in cytoskeleton- and carbohydrate metabolism-associated gene products in Mmp9/Mmp14 double-knockout (DKO) OCs. Nevertheless, OC differentiation, mitochondrial abundance, tricarboxylic acid cycle- and glycolysis-related metabolic products were unaffected in the DKO OCs. Interestingly, however, the compromised sealing zone formation and hypo-resorptive phenotype - observed both in vitro and in vivo - in tandem with alterations in carbohydrate metabolism, drew our attention to galectin-3, a putative regulator of OC function and a known substrate for both Mmp9 and Mmp14. Indeed, osteoclastic Mmp9 and Mmp14 cooperatively regulated the proteolytic turnover of galectin-3, wherein the DKO OCs displayed significant increases in membrane-associated levels of the lectin. Consistent with recent studies demonstrating that Lgals3-/- mice display decreased bone mass with increased OC activity in vivo, we find that exogenous galectin-3 significantly inhibited sealing zone formation and bone resorption in wild-type OCs without affecting OC differentiation. Importantly, the galectin-3 inhibitor, GCS-100, which blocks surface galectin-3 binding, significantly reversed the defective sealing zone formation and bone resorption by DKO OCs. Together, these studies characterize a previously unsuspected Mmp9/Mmp14 axis that not only participates in mediating bone type I collagenolytic activity, but also serves to control transcriptional programs underlying the galectin-3-dependent regulation of sealing zone formation and bone resorptive activity.

***Disclosures: Lingxin Zhu**, None*

1007

Loss of Function of PFN1 Drives the Development of Pagetic and Primary Osteosarcoma *Federica Scotto di Carlo[1], Sharon Russo[2], Francesc Muyas[3], Laura Pazzaglia[4], Teresa Esposito[1], Carmine Settembre[5], Isidro Cortés-Ciriano[3], Fernando Gianfrancesco[1]. [1]Institute of Genetics and Biophysics, National Research Council of Italy, Italy, [2]Institute of Genetics and Biophysics National Research Council of Italy, Italy, [3]European Molecular Biology Laboratory, European Bioinformatics Institute, Wellcome Genome Campus, United Kingdom, [4]IRCCS Istituto Ortopedico Rizzoli, Laboratory of Experimental Oncology, Italy, [5]Telethon Institute of Genetics and Medicine (TIGEM), Italy

Osteosarcoma (OS) is an aggressive tumor of mesenchymal origin, characterized by a great genetic heterogeneity due to highly rearranged genomes. Rarely, it arises as degeneration of Paget's disease of bone (OS/PDB), a late-onset bone remodeling disorder, and shows a 5-year survival rate almost nil. We recently identified a loss-of-function mutation in the PFN1 gene, encoding the Profilin 1, as responsible for early-onset Paget's disease complicated by OS (Scotto di Carlo et al., J Bone Miner Res. 2020. doi: 10.1002/jbmr.3964). Interestingly, the analysis performed on our cohort of human tumor samples detected genomic loss of PFN1 in 15 out of 28 (54%) OS/PDB and 15 out of 50 (30%) primary OS, resulting in downregulation Profilin 1. More importantly, we observed reduced PFN1 protein levels also in tumors without the genomic loss of PFN1. We explained this last result through luciferase assay that demonstrated PFN1 as transcriptional target of p53, a well-known tumor suppressor in OS.To obtain additional clues on the PFN1 pathogenic role, we generated a Pfn1 knock-in mouse model. Micro-CT analysis revealed that heterozygous mice (n=9) as young as 4 months show a reduction of bone volume in their femurs by 25% (P=0,003), compared with wild type (n=9), further confirming the early development of bone remodeling alterations. Mutant spleen-derived osteoclasts confirmed the accelerated osteoclast differentiation in vitro. Intriguingly, mesenchymal cells isolated from Pfn1-KI calvariae (n=7) showed a 30% higher proliferation rate compared to WT cells (n=4), suggesting a predisposition to sarcomatous transformation. We performed whole genome sequencing (WGS) on 4 OS/PDB and their normal counterparts, highlighting high burden of genomic rearrangements in tumor samples. Accordingly, MC3T3 pre-osteoblasts, engineered through CRISPR-Cas9 to knock-out the Pfn1 gene, acquired features of malignant transformation, namely enhanced proliferation and migration. These cells also exhibited nuclear abnormalities (binucleation, micronuclei, chromatin bridges), indicative of chromosome segregation defects and genomic instability. In fact, WGS on eight independent Pfn1-KO clones confirmed extensive numerical and structural chromosomal alterations, similar to what observed in OS/PDB (see figure). In conclusion, we describe the loss of function of PFN1 as a novel mutational event underlying imbalanced bone remodeling and genomic rearrangements in OS.

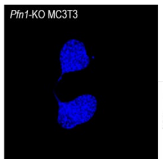

Profilin 1 knock-out forms chromatin bridges connecting two daughter cells due to cell division defects, resulting in chromosome mis-segregagtion and copy number alterations (below).

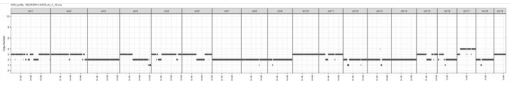

***Disclosures: Federica Scotto di Carlo**, None*

1008

Integrin alpha-5 in human breast cancer is a mediator of bone metastasis and a therapeutic target for the treatment of osteolytic lesions *Francesco Pantano[1], Martine Croset[2], Keltouma Driouch[3], Natalia Bednarz-Knoll[4], Michele Iulialni[5], Giulia Ribelli[5], Edith Bonnelye[2], Harriet Wikman[4], Sandra Geraci[2], Florian Bonin[3], Sonia Simonetti[5], Bruno Vincenzi[5], Saw See Hong[6], Sofia Sousa[2], Klaus Pantel[4], Giuseppe Tonini[5], Daniele Santini[5], Philippe Clezardin[2]. [1]University of Rome, Italy, [2]INSERM, UMR_S1033, University of Lyon, France, [3]Institut Curie, France, [4]University Medical Centre Hamburg-Eppendorf, Germany, [5]Campus Bio-Medico University of Rome, Italy, [6]INRA, UMR-754, Lyon, France

Bone metastasis remains a major cause of mortality and morbidity in breast cancer. Therefore, there is an urgent need to better select high-risk patients in order to adapt patient's treatment and prevent bone recurrence. Here, we found that integrin alpha 5 (ITGA5) was highly expressed in bone metastases, compared to lung, liver or brain metastases. High ITGA5 expression in primary tumors correlated with the presence of disseminated tumor cells in bone marrow aspirates from early-stage breast cancer patients (n = 268; P = 0.039). ITGA5 was also predictive of poor bone metastasis-free survival in two separate clinical data sets (n = 855, HR = 1.36, P = 0.018 and n = 427, HR = 1.62, P = 0.024). This prognostic value remained significant in multivariate analysis (P = 0.028). Experimentally, ITGA5 silencing

impaired tumor cell adhesion to fibronectin, migration, and survival. ITGA5 silencing also reduced tumor cell colonization of the bone marrow and formation of osteolytic lesions in vivo. Conversely, ITGA5 overexpression promoted experimental bone metastasis. Pharmacological inhibition of ITGA5 with humanized monoclonal antibody M200 (volociximab) recapitulated inhibitory effects of ITGA5 silencing on tumor cell functions in vitro, and tumor cell colonization of the bone marrow in vivo. M200 also markedly reduced tumor outgrowth in experimental models of bone metastasis or tumorigenesis, and blunted cancer-associated bone destruction. ITGA5 was not only expressed by tumor cells but also osteoclasts. Being selective to human ITGA5, this antibody did not interfere with murine osteoclast differentiation and activity in vitro. However, a clinically relevant concentration of M200 antibody was nearly as effective as the anti-RANKL antibody denosumab to inhibit human osteoclast differentiation and activity in vitro. Thus, in addition to its anti-tumor effect, M200 may also be effective at inhibiting bone resorption in vivo. Overall, this study identifies ITGA5 as a mediator of breast-to-bone metastasis and raises the possibility that volociximab/M200 could be combined with the best standard of care for the treatment of ITGA5-positive breast cancer patients with bone metastases.

***Disclosures: Francesco Pantano**, None*

1009

Activation of the Sympathetic Nerve System Weakens Anti-Tumoral Immunity in Bone via Beta 2 Adrenergic Receptors in Osteoblast and Myeloid-Derived Suppressor Cells, Contributing to Bone Metastasis Progression *Eun Jung Lee[1], Kyung Jin Lee[1], Serk In Park[1]. [1]Korea University College of Medicine, Republic of Korea

The sympathetic nerve system (SNS) regulates bone homeostasis via β2 adrenergic receptor (Adrb2) on osteoblasts, and chronic psychological stress-induced SNS activation was shown to promote bone metastasis tumor growth, osteolysis, angiogenesis via osteoblastic cytokine expression in immunocompromised mouse models. We further investigated the effects of SNS activation on immune cells in the bone microenvironment using immune-competent mouse models of breast cancer bone metastasis. Chronic immobilization stress (CIS, 2 hours daily) increased 4T1 syngeneic breast tumor growth in bone that was reversed by administration of ICI-118551 (1mg/kg/day), a pharmacologic inhibitor of Adrb2. Moreover, CIS-treated tumors had increased CD11b+Gr1+ myeloid-derived suppressor cells (MDSC), a group of immature bone marrow cells with T cell suppression activity, compared with control-treated mice. Two-week CIS pre-treatment before intra-tibial tumor implantation increased EdU+ proliferating MDSC, supporting that CIS primes the pre-metastatic niche in bone by tipping anti-tumoral immunity balance in favor of tumor growth. Based on previous publications showing that SNS activation and/or CIS effects are dependent on Adrb2 expressed on osteoblasts, we determined the effects of osteoblastic Adrb2 on MDSC function using in vitro co-culture system. Arginase 1 (Arg1), a functional marker of activated MDSC, expression in bone marrow cells increased when co-cultured with isoproterenol (an Adrb2 agonist)-stimulated MC3T3E1 osteoblasts. In addition, isoproterenol increased C-C chemokine ligand (CCL)-2, one of the known inducers of MDSC expansion, in MC3T3E1 osteoblasts. Our data collectively demonstrate that activation of the SNS contributes to breast cancer bone metastasis partly by expanding MDSC and subsequent T cell suppression. The SNS activation-dependent MDSC expansion is mediated by osteoblastic Adrb2 and CCL2 expression. Further studies using osteoblast-specific Adrb2 knockout mice and CCR2-dependent MDSC depletion/reconstitution experiments will provide more clear molecular mechanism underlying the SNS-dependent bone marrow immunity regulation.

***Disclosures: Eun Jung Lee**, None*

1010

Stromal cell-guided transformation of MDS to AML *Álvaro Cuesta-Domínguez[1], Ioanna Mosialou[2], Abdullah Ali[3], Junfei Zhao[4], Marta Galán-Díez[5], Julie Teruya-Feldstein[6], Ellin Berman[7], Raúl Rabadán[4], Azra Raza[3], Stavroula Kousteni[2]. [1]Department of Physiology and Cellular Biophysics, Vagelos College of Physicians & Surgeons, Columbia University Irving Medical Center, United States, [2]Department of Physiology and Cellular Biophysics, Vagelos College of Physicians & Surgeons, Columbia University Irving Medical Center, United States, [3]Department of Medicine, Vagelos College of Physicians & Surgeons, Columbia University Irving Medical Center, United States, [4]Department of Systems Biology, Vagelos College of Physicians & Surgeons, Columbia University Irving Medical Center, United States, [5]Department of Physiology and Cellular Biophysics, Vagelos College of Physicians and Surgeons, Columbia University Irving Medical Center, United States, [6]Department of Pathology, Icahn School of Medicine at Mount Sinai, United States, [7]Department of Pathology, Memorial Sloan-Kettering Cancer Center, United States

A pathogenic role of stromal cells in the bone marrow in the development of myeloproliferative neoplasia, myelodysplasia (MDS) and acute myeloid leukemia (AML) has been evidenced by a growing body of evidence. Activation of β-catenin signaling in osteoblast precursors induces AML in mice (βcat(ex3)2.3Col1a1 mice), is seen in approximately 38% of MDS/AML patients and correlates with disease severity and progression to AML. To examine whether it is involved in MDS to AML transformation, we constitutively activated β-catenin in mature osteoblasts (βcat(ex3)OCN mice). Similar to the leukemic βcat(ex3)Col1a1 mice, βcat(ex3)OCN mice, presented with anemia, neutrophilia, thrombocytopenia, lymphocytopenia and dysplasia in the erythroid lineage. As opposed to 40% blasts detected in the bone marrow of βcat(ex3)Col1a1 mice, less than 15% blast blasts were detected in the bone marrow of βcat(ex3)OCN mice. In contrast to βcat(ex3)Col1a1 mice, βcat(ex3)OCN mice showed extensive apoptosis in approximately 90% of myeloid cells in the bone marrow, spliceosome deregulation and increased methyltransferase expression, all hallmark characteristics of MDS. To gain mechanistic insight into the transformation of MDS to AML we compared the transcriptional profile of hematopoietic stem cell progenitors (LSK, Lin-/cKit+/Sca+ cells)) from βcat(ex3)OCN (MDS) and βcat(ex3)Col1a1 (AML) mice as well as of bone marrow mononuclear cells (BM-MNCs) from 25 MDS patients and the same patients after they transformed to AML. We found that in both the mouse models and patients, expression of the Nucleoporin (NUP) family members was decreased with transformation to AML. Similarly, a comparison between the AML TCGA database and the human GEO MDS database indicated decreased expression of NUPs, in AML as compared to MDS samples. NUPs expression is also decreased in MDS cells of 58% of patients compared to healthy subjects; and, in LSK cells of two MDS mouse models, NUP98-HOXD13 and PU.1URE-hetMsh2-/- mice, as compared to LSK cells from their wild type littermates. Notably, low NUPs expression associates with poor prognosis in TCGA AML and with enhanced β-catenin activity in stromal cells of MDS patients transformed to AML. These results indicate that downregulation of NUPs expression may be an important transformative effect of MDS to AML cells. This event is preferentially associated with and can be initiated by constitutive activation of β-catenin in mature, OCN-expressing osteoblasts

***Disclosures: Álvaro Cuesta-Domínguez**, None*

1011

Prostate Cancer-derived Extracellular Vesicles Negatively Affect Osteoblast Function *Giulia Furesi[1], Martina Rauner[1], Lorenz C. Hofbauer[1]. [1]Department of Medicine III and Center for Healthy Aging, Dresden, Germany, Technische Universität Dresden, Germany, Germany

Patients with advanced prostate cancer (PCa) often develop bone metastasis. Extracellular vesicles (EVs) have emerged as key players in the formation of the pre-metastatic niche and mediators of the crosstalk between tumor cells and the host microenvironment. However, the role of PCa-derived EVs in the establishment of a favorable tumor microenvironment in bone remains unclear. Here, we evaluated the effects of PCa-derived EVs on osteoblasts (OB) in vitro and in vivo. EVs were isolated from the murine osteotropic PCa cell line RM1-BM by ultracentrifugation and characterized by transmission electron microscopy, nanoparticle tracking analyzer, and Western blot analyses of surface markers. Internalization of PKH26-labeled EVs by murine primary OB was detected using fluorescence microscopy and flow cytometry. Additionally, OB were cultured with different concentrations (20, 50,100 µg/ml) of PCa-derived EVs to assess dose-dependent effects on OB metabolic activity (Cell Titer Blue assay), vitality (crystal violet), and mineralization capacity (alizarin red staining). Also, RNA sequencing was performed to identify alterations in the gene expression profile of OB after EV treatment. Finally, the effect of PCa-derived EVs on osteogenesis in vivo was evaluated using BMP-2-induced bone formation in a calvarial defect mouse model. PCa-derived EVs displayed both the expected size of 50-100 nm as well as the expression of the common EV markers, CD63 and CD9. Fluorescence microscopy revealed the uptake of PCa-EVs into OB as early as after 1 h. After 24 h, nearly all OB contained tumor-derived EVs. OB treated with PCa-derived EVs showed a dose-dependent increase of cell metabolic activity [+24%; +40%; +58% P<0.001] and viability [+32%; +52%; +65%; P<0.001] compared to untreated cells. In contrast, mineral deposition was significantly reduced [-4% to -37%; P<0.001]. Gene set enrichment analysis of OB treated with PCa-derived EVs versus normal OB showed a significant downregulation of osteoblastic markers [P<0.02] and upregulation of inflammatory factors [P<0.001]. In line with the in vitro studies, PCa-EVs potently inhibited BMP-2-induced bone formation in a calvaria defect model as assessed by µCT (P< 0.01). In summary, our results show that PCa-derived EVs impair OB activity, suggesting a potential role of EVs in the pre-metastatic dysregulation of bone remodeling.

***Disclosures: Giulia Furesi**, None*

1012

Myeloma-modified adipocytes exhibit metabolic dysfunction and a senescence-associated secretory phenotype (SASP) *Michaela Reagan[1], Amel Dudakovic[2], Casper Khatib[3], Mariah Farrell[1], Samantha Costa[1], Carolyne Falank[1], Maja Hinge[4], Connor Murphy[1], Victoria Demambro[1], Jessica Pettitt[5], Christine Lary[1], Heather Driscoll[6], Michelle McDonald[0], Moustapha Kassem[7], Clifford Rosen[1], Thomas Andersen[8], Andre van Wijnen[2], Abbas Jafari[3], Heather Fairfield[1]. [1]Maine Medical Center Research Institute, United States, [2]Mayo Clininc, United States, [3]University of Copenhagen, Denmark, [4]Department of Internal Medicine, Division of Haematology, Vejle Hospital, Denmark, Denmark, [5]Garvan Institute, Australia, [6]Norwich University, United States, [0]Garvan Institute, Australia, [7]Odense University Hospital & University of Southern Denmark, Denmark, [8]Vejle/Lillebaelt Hospital, University of Southern Denmark, Denmark

Bone marrow adipocytes (BMAds) have been implicated in accelerating bone metastatic cancers and multiple myeloma (MM). Importantly, bone marrow (BM) adipose tissue

expands with aging and obesity- two key risk factors for MM- suggesting that BMAds may influence and be influenced by MM cells. BM biopsies showed significant loss of BM adipose volume per marrow volume (AV/MV) in newly-diagnosed MM patients (n=19) versus healthy subjects (n=18), and significant reduction in BMAd size in MM versus MGUS or healthy subjects (Fig. 1). Proximal femurs from MM.1S tumor-bearing SCID-Beige mice (Fig. 1) had significantly fewer BMAds than naïve mice, and similar results were observed in the C57BL/KaLwRiJHsd-5TGM1 model ($p<0.001$). In vitro, murine adipocytes derived from 3T3-L1 cells or BM or ear mesenchymal stem cells (MSCs) had significant reductions in lipid content ($p<0.0001$) and adipogenic gene expression (Adipoq, Fabp4, $p<0.001$) when co-cultured with MM cells via transwell. Microarray and pathway analysis of 3T3-L1s co-cultured with MM cells indicated dysfunctional metabolic pathways, and the SeaHorse assay confirmed their defects in bioenergetic function. In human MSC-derived BMAs, co-culture with MM cells decreased expression of adipogenic genes and elevated expression of genes encoding senescence associated secretory proteins (SASPs), including: SERPINB2 (204x), IL6 (175x), ICAM1 (33x), CXCL1 (58x), CXCL2 (39x) and VEGFA (5x), as assessed by RNA sequencing. The "senescent-like" phenotype was confirmed via cytokine arrays and β-galactosidase staining in adipocytes exposed to MM.1S cells via transwell (p2 FC) in MM cells co-cultured with BMAds, 3 of which are implicated in glucocorticoid receptor signaling. Our findings may help explain the dexamethasone resistance we observed in MM.1S cells co-cultured with BMAds, measured via flow cytometry and bioluminescence quantification. MM patients with higher BM AV/TV prior to dexamethasone and high dose melphalan followed by autologous transplant also exhibited a worse treatment response (-54%, $p<0.05$). These findings suggest that higher BMAd levels prior to treatment provides protection to MM cells. In summary, our findings reveal that bi-directional interactions between BMAds and MM cells have significant implications for the pathogenesis and treatment of MM.

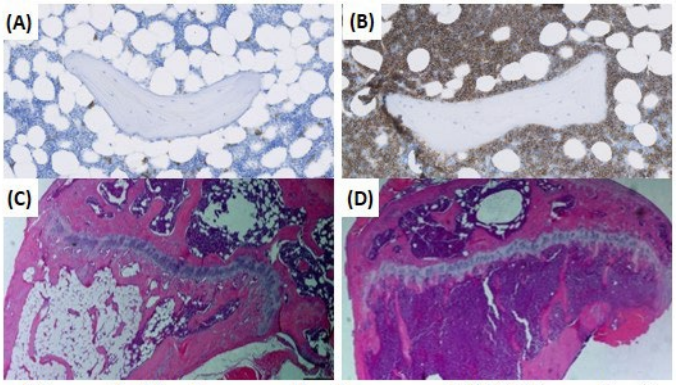

Figure 1. Myeloma cells decrease BMAT in patient biopsies and mice. (A) CD138 IHC (brown) staining of MGUS and (B) MM human biopsies shows MM cells and BMAds co-localizing. (C) Femur H&E staining of 12 female SCID-Beige mice injected i.v. with (C) vehicle or (D) MM.1S cells at endpoints.

***Disclosures: Michaela Reagan**, None*

1013

Control of Osteocytogenesis by a Neuronally−expressed Sp7−dependent Genetic Network *Jialiang Wang[1], Tushar Kamath[2], Evan Macosko[2], Henry Kronenberg[3], Marc Wein[1]. [1]Massachusetts General Hospital, United States, [2]Broad Institute of MIT and Harvard, United States, [3]Massachusetts Generial Hospital, United States

The transcription factor Sp7 coordinates cell type-specific gene expression programs at multiple stages in skeletal cell differentiation. Our previous data demonstrated that severe defects in osteocyte dendrite morphology are noted in mice lacking Sp7 during osteocyte differentiation. The combination of transcriptome and cistrome analyses identified 79 osteocyte-specific Sp7 targets. Osteocytes and neurons bear an elaborate network of cellular dendritic projections used for extensive inter-cellular communication. To explore links between osteocytes and neurons, we examined the enrichment of osteocyte-specific Sp7 targets in mouse brain at the single-cell transcriptomic level. This analysis revealed a significant enrichment of osteocytic Sp7 targets in neurons compared to other cell types in the mouse brain. These results suggest that Sp7 regulates a neuronally-enriched gene expression network in order to coordinate osteocytogenesis.To capture cells undergoing osteoblast-to-osteocyte differentiation at single-cell resolution, we crossed Dmp1-Cre transgenic mice to Ai14 tdTomato reporter mice. Viable tdTomato+ cells were obtained from serial digestions of femora, tibiae and calvariae for single-cell RNA-seq. We successfully identified several osteo-lineage cell populations, including osteoblasts (marked by Bglap3), mineralized osteocytes (Enpp1) and mature osteocytes (Pdpn). To understand the role of Sp7 during osteocyte differentiation, we compared single-cell datasets between Sp7 conditional knockout (cKO) mice to littermate controls. We detected striking changes in the proportions of key subpopulations in Sp7 cKO mice (decrease: mineralized osteocyte; increase: mature osteocyte). Differential gene expression analysis revealed that terminal osteocyte markers are down-regulated in mutants across the entire population, including Pdpn, Atf3 and Ptprz1. Pseudotime analysis demonstrated dysregulated osteocyte differentiation in the absence of Sp7, with a specific block in a group of Lmo2-expressing mineralizing cells prior to becoming mature osteocytes. This suggests that Sp7-deficiency leads to an accumulation of mature osteocyte precursors and a relative paucity of mature osteocytes.Sp7 orchestrates osteocytogenesis via a suite of targets that promote the optimal formation of osteocyte dendrites. Findings from scRNA-seq analyses highlight shared transcriptome between osteocytes and neurons, and suggest novel steps in the treatment of osteoporosis.

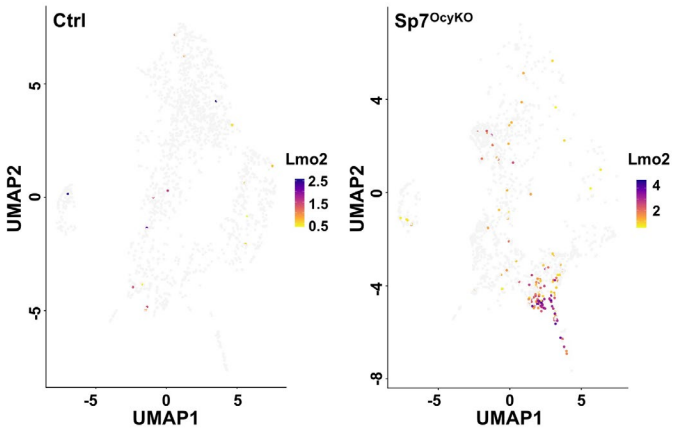

***Disclosures: Jialiang Wang**, None*

1014

Attenuation of Bone Loss by Activation of Connexin Hemichannels during Mechanical Unloading *Chao Tu[1], Manuel A Riquelme[1], Dezhi Zhao[1], Sumin Gu[1], Jean X Jiang[1]. [1]Department of Biochemistry and Structural Biology, The University of Texas Health Science Center, San Antonio, TX 78229, USA, United States

Background: Emerging evidences have demonstrated that connexin 43 (Cx43)-forming gap junctions and hemichannels play a pivotal role in mediating mechanotransduction. However, the specific role of gap junctions and hemichannels in mechanotransduction remains elusive. Our previous study identified that inhibition of Cx43 hemichannels could enhance osteocytes apoptosis and impair periosteal bone remodeling, thereby aggregating the bone loss during unloading. We recently developed a monoclonal antibody, MHC2 that activates Cx43 hemichannels. By using this specific hemichannel-targeting MHC2, we aimed to investigate whether enhanced opening of hemichannel could attenuate the hindlimb unloading (HLU)-induced bone loss. Methods: 15-week-old male C57BL6 mice were tail-suspended or kept under ambulatory conditions for 4 weeks. Age-matched mice were randomly separated into different groups, and intraperitoneally injected with MHC2 or vehicle once per week at a dose of 25mg/kg. At the endpoint, the gastrocnemius and soleus muscle were weighted. The femurs and tibias were examined by micro-computed tomography (uCT) and histomorphometry, and bone turnover markers were measured by immunohistochemistry. Results: Mice exposed to HLU caused a significant muscle atrophy compared with non-unloaded counterparts. Moreover, HLU resulted in impaired cortical bone microstructure, increased empty osteocyte lacunae, restrained bone formation, and enhanced osteoclast activity, as evidenced by uCT, H&E and TRAP staining, respectively. By contrast, mice injected with MHC2 showed less severe muscle atrophy compared with those following vehicle treatments. Notably, MHC2 contributed to elevated cortical thickness, bone volume fraction and BMD, and decreased empty lacunae and osteoclastogenesis in mice following HLU. Furthermore, the sclerostin positive (SOST+) and apoptotic osteocytes in cortical bone caused by HLU were significantly decreased by MHC2 treatment. Conclusions: In this study, we showed that opening of hemichannel by MHC2 attenuated the catabolic function and subsequent bone loss during HLU, at least in part though suppression of osteocyte apoptosis and osteoclast activity. This study indicates an important role of hemichannels in protecting bone loss in response to mechanical unloading, and thus targeting Cx43 hemichannels may offer a new therapeutic strategy for treating bone loss and osteoporosis.

***Disclosures: Chao Tu**, None*

1015

Disrupted Lacunar-Canalicular Networks and Osteocyte Mechanosensation in Bone with Aging and Disrupted TGFb Signaling *Charles Schurman[1], Stefaan Verbruggen[2], Tamara Alliston[1]. [1]UCSF, United States, [2] Columbia University, United States

Aged bone presents several osteocyte-specific defects including a lack of mechanoresponsiveness, uncoupling of bone deposition and resorption, and increased bone fragility. Others have described an age-related degeneration of the Lacunar-Canalicular Network (LCN) marked by loss of osteocyte dendrites and cell bodies in mouse bone. However, the extent to which LCN defects impact osteocyte mechanotransduction, intercellular communication, and mass transport remains unclear. Given technical constraints in experimentally dissecting these processes, we applied two in silico approaches to investigate the functional impact of LCN disruption resulting from aging or from osteocyte-intrinsic defects in TGFb signaling (TbRIIocy-/-). Using 3D reconstructed confocal images of fluorescently-labeled osteocyte networks, we applied Connectomic Network Analysis to model mass transport and Finite Element Analysis (FEA) to model fluid dynamics and osteocyte mechanosensation. Relative to 2 month old wild-type mice, osteocytes from 36 month old C57BL/6 (WT, N=5) and 2 month old TbRIIocy-/- mice (N=5) display 43 and 34%fewer, more tortuous, canaliculi respectively resulting in osteocyte networks with as much as 51 and 44% less surface area (all P<0.01). Network analysis revealed preservation of linear LCN order in aged and TbRIIocy-/- bone, but also localized disruptions caused by canalicular shortening and loss. These blunted networks reduce predicted pericellular diffusion in aging and TbRIIocy-/- bone by as much as 43% (P<0.05). FEA predicts a 53% drop in fluid velocity and a 30-42% reduction in shear stress around aged and TbRIIocy-/- osteocytes, respectively (P<0.01). Modeling of flow through individual canaliculi across a range of tortuosity values did not show any differences to flow parameters, suggesting flow deficits are driven by LCN surface area. To determine if LCN expansion, e.g. by perilacunar/canalicular remodeling (PLR), is sufficient to rescue flow, space around osteocytes was expanded and flow values became indistinguishable from young WT controls (Fig.1) Therefore, PLR regulatory pathways, such as TGFb, have potential to protect or restore function. Accordingly, gene expression analysis of aged bone shows repression of genes implicated in TGFb signaling and PLR. Therefore, in silico modeling shows how LCN degeneration can compromise mass transport and mechanotransduction, and suggests PLR as a possible target to overcome these age-related bone deficits.

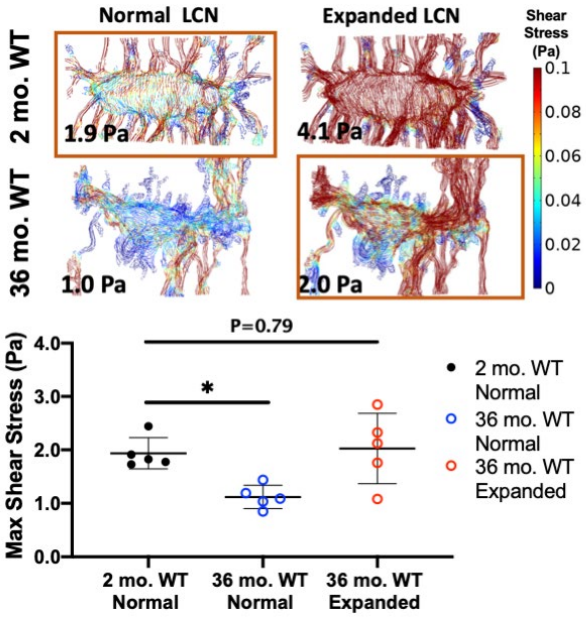

***Disclosures: Charles Schurman**, None*

1016

NADPH Oxidase 2-Mediated Reactive Oxygen Species is Necessary for Osteocyte Mechano-Transduction In Vitro and In Vivo *Nicole Gould[1], Katrina Williams[1], Humberto Joca[2], James Lyons[1], Marcus Hughes[1], Ramzi Khairallah[3], Christopher Ward[1], Joseph Stains[1]. [1]Department of Orthopaedics, University of Maryland School of Medicine, Baltimore, MD, 21201, USA., United States, [2]Center for Biomedical Engineering and Technology, University of Maryland School of Medicine, Baltimore, MD, 21201, USA., United States, [3]Myologica, LLC, New Market, MD 21212, USA., United States

Bone senses mechanical signals and transduces them into biological changes that direct bone remodeling, the concerted action of bone resorbing osteoclasts and bone forming osteoblasts. Osteocytes, mechano-sensitive cells encased in bone, control bone remodeling in part through the expression of the Wnt/β-catenin antagonist, sclerostin. We recently described a novel osteocyte mechano-transduction pathway in vitro that controls sclerostin abundance. Briefly, osteocytes sense mechanical signals through microtubules, which activate NADPH Oxidase 2 (NOX2). NOX2-mediated reactive oxygen species (ROS) trigger calcium influx, activation of calcium/calmodulin-dependent kinase II (CaMKII), and rapid sclerostin protein degradation. Here, we extend these in vitro findings to show that NOX2-dependent ROS are both necessary and sufficient to regulate sclerostin abundance in vitro and in vivo. In vitro, we showed that inhibition of NOX2 function with gp91-dsTAT prevented fluid shear stress-induced calcium influx, CaMKII activation, and rapid sclerostin protein loss in Ocy454 osteocyte-like cells. Conversely, controlled production of ROS using a photo-activated reagent, KillerRed, was sufficient to drive activation of CaMKII and sclerostin degradation. Using a mouse ulnar load model to stimulate mechano-activated bone formation, we showed that a single bout of mechanical load was sufficient to decrease sclerostin protein abundance in bone. Further, acute treatment of mice with apocynin, a NOX2 inhibitor, prior to ulnar loading showed a statistically significant decrease in bone formation rate as determined by dynamic histomorphometry. Together, these data validate the fidelity of the novel osteocyte mechano-sensing pathway in vivo, provide key insights into osteocyte mechano-transduction and the control of sclerostin, and reveal new therapeutic targets to improve bone mass.

***Disclosures: Nicole Gould**, None*

1017

Disruption of LINC complex in skeletal stem cells results in decreased osteogenesis and trabecular architecture *Scott Birks[1], Stacie Loisate[1], Destiny Francis[2], Sarah Manske[2], Gunes Uzer[1]. [1]Boise State University, United States, [2]University of Calgary, Canada

Linker of Nucleoskeleton and Cytoskeleton complexes (LINC), comprised of Nesprin and Sun proteins coupled within the perinuclear space via the Nesprin KASH domain, play an integral role in mesenchymal stem cell (MSC) response to mechanical challenge. Here, we hypothesize disabling LINC function in vitro and in vivo will negatively impact osteogenesis and mechanosensitivity of MSCs.In vitro, a dominant negative form of the Nesprin KASH domain (DNK) was overexpressed in MSCs to disrupt LINC integrity by decoupling Nesprin-Sun binding. Osteogenic differentiation was then assessed at day 7 by measuring alkaline phosphatase (ALP) mRNA levels via qPCR. A 61% (p=0.09) decrease in mRNA ALP levels was found compared to empty plasmid controls suggesting a decrease in osteogenesis (Figure 1).In vivo, a similar DNK mechanism was achieved using a cre/lox model under the Prrx1 promoter. Briefly, Prx1CreER-GFP mice (+CreER) were crossed with Tg(CAG-LacZ/EGFP-KASH2) mice (+LacZ) to produce offspring with tamoxifen inducible, cre-mediated EGFP overexpression localized at the KASH domain. This inhibits endogenous Nesprin-Sun binding, thus disabling LINC function. Tamoxifen was administered to male +CreER/+LacZ and control +CreER/-LacZ mice beginning at 7wks. Tibiae were collected at 7, 9, and 12wks (n=3/group). Compared to controls: BV/TV and TbN decreased 24% (p<.01) and 26% (p<.05), respectively, while TbSp was increased by 35% (p<.05) in 9 wk, +CreER/+LacZ mice (Figure 2).Tamoxifen has an estrogenic effect on bone and comparing tamoxifen treated +CreER/-LacZ mice to a tamoxifen independent Prrx1-Cre line (+Cre) revealed a 9% increase in BV/TV at baseline with tamoxifen administration. We then crossed the +LacZ line with the tamoxifen independent +Cre line. While bone parameters were not different at an 8wk baseline (n=8/grp), +Cre/+LacZ mice allowed voluntary access to a running wheel for 4wks had reduced BV/TV (-39%) and TbN (-45%), and increased TbSp (+15%) compared to +Cre/-LacZ controls (n=1/grp). Four more samples/group were collected and are currently being processed. This recent data implicates LINC functionality for cellular mechanical signal propagation in exercise challenged animals, but not in sedentary counterparts. Completion of this data will lead to a greater understanding of LINC-mediated mechanosignaling in bone progenitor cells.All procedures approved by Boise State University Institutional Animal Care and Use Committee.

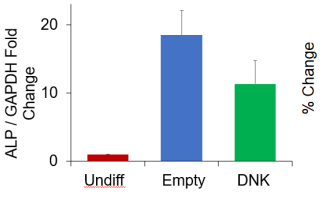

Figure 1 qPCR results probing for alkaline phosphatase expression in undifferentiated MSCs (Undiff), differentiated MSCs transfected with an empty plasmid (Empty), and differentiated MSCs transfected with a DNK plasmid (DNK).

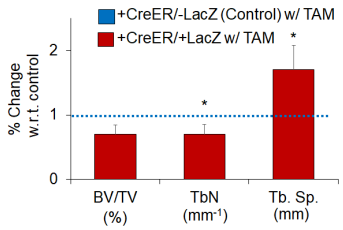

Figure 2 Trabecular bone fraction (BV/TV) and trabecular number (TbN) decreased by -24% and -26%, respectively, and trabecular spacing (TbSp) increased by +35% (n=3/group) in 9 wk, +CreER/+LacZ animals when compared to +CreER/-LacZ controls. Data reported was normalized to TAM treated +CreER/-LacZ control and represented as percent change.

***Disclosures: Scott Birks**, None*

1018

Mechanical stimulation promotes mitochondria function via Piezo1 *Xuehua Li[1], Jacob Kordsmeier[1], Ha-neui Kim[1], Intawat Nookaew[1], Jinhu Xiong[1]. [1]University of Arkansas for Medical Sciences, United States

Mechanical signal plays an essential role in bone growth and homeostasis. Deletion of Piezo1, a mechanosensitive ion channel, from Dmp1-Cre-targeted cells decreases cancellous and cortical bone mass and blunts the response of the skeleton to mechanical stimulus, demonstrating the important role of Piezo1 in skeletal mechanotransduction. However, the molecular mechanisms by which Piezo1 promotes bone formation is not clear. To identify downstream targets and pathways that respond to Piezo1, we performed RNA-seq analysis of MLO-Y4 cells after suppression of Piezo1 using shRNA. GO enrichment analysis indicated that several mitochondria-related categories were down-regulated in Piezo1 knock-down cells. The list included mitochondrial transcription, mitochondrial translation, and protein import to mitochondrial matrix. Consistent with RNAseq analysis, the oxygen consumption rate and ATP production were decreased in Piezo1 knock-down cells. Mitochondria are critical components of cells and their function has been associated with osteoblastogenesis and bone homeostasis in mice. In humans, mitochondrial point mutation m.3243A>G leads to mitochondrial dysfunction and is associated with decreased bone mass and strength. In addition, fluid shear stress increased mitochondrial function in osteoblastic cells in vitro. Consistently, we found that one bout of tibia compressive loading increased expression of genes encoding subunits of the mitochondrial respiratory complex, including Cox-1, Cox-2, Cox-3, and CytB in cortical bone of adult mice. Therefore, we investigated whether Piezo1 is required for increased mitochondria function induced by mechanical stimulation. Yoda1, a small molecule activator of Piezo1, was used in this study because it mimics the effects of fluid shear stress on osteocytes. We found that Yoda1 increased mitochondrial DNA content and mitochondrial mass in calvaria cells indicating increased mitochondrial biogenesis. Yoda1 also increased mitochondrial function as evidenced by increased oxygen consumption rate and ATP production in calvaria cells. However, these changes were significantly blunted in calvaria cells lacking Piezo1. These results suggest that mechanical stimulation promotes mitochondria function via Piezo1.

***Disclosures: Xuehua Li**, None*

1019

High-dose Vitamin D Supplementation Affects Bone Density Differently in Females than Males *Lauren Burt[1], Emma Billington[1], Marianne Rose[2], Richard Kremer [3], David Hanley[1], Steven Boyd[1]. [1]University of Calgary, Canada, [2]Alberta Health Services, Canada, [3]McGill University, Canada

In a 3-year RCT of high-dose vitamin D supplementation (400 vs 4000 or 10,000 IU daily) in vitamin D-sufficient males and females, bone density and strength decreased as a function of the dose. The purpose of this study was to examine whether this response differed between males and females.Participants were healthy males and females 55-70 years with DXA T-scores above -2.5 and serum 25(OH)D between 30 - 125 nmol/L. Participants consuming <1200 mg/day of dietary calcium received calcium supplementation. Participants' radius and tibia were scanned on high-resolution peripheral quantitative computed tomography (HR-pQCT) to measure total volumetric BMD (TtBMD) at baseline, 6, 12, 24 and 36 months. Finite element analysis estimated failure load. Fasting C-telopeptide of type 1 collagen (CTx) and amino-terminal propeptide of type I collagen (P1NP) were assessed. Following an intent-to-treat analysis, we used constrained linear mixed effects models to determine treatment group x time x sex interactions.A total of 311 participants were randomized and enrolled in the study (400 IU: M=61, F=48; 4000 IU: M=51, F=49; 10,000 IU: M=53, F=49). Baseline, three-month, and three-year levels of 25(OH)D were 76.3, 76.7, and 77.4 nmol/L (400); 81.3, 115.3, and 132.2 (4000); and 78.4, 188.0, and 144.4 (10,000). There were significant group x time x sex interactions for TtBMD at the radius (p=0.002) and tibia (p=0.005). Treatment with 4000 or 10,000 compared to 400 IU resulted in greater TtBMD losses in females, but this was not observed with males. At study end females lost 1.8% (400), 3.8% (4000) and 5.5% (10,000), whereas males lost 0.9% (400), 1.3% (4000) and 1.9% (10,000) at the radius. At the tibia, females lost 1.0% (400), 2.0% (4000) and 3.2% (10,000), and males lost 0.1% (400), 0.0% (4000) and 0.6% (10,000) over 3 years. There was no significant group x time x sex effects on bone strength. There was a trend for CTx and P1NP to be higher in females than males, and the females in the 10,000 IU group had higher CTx values than the 400 IU group.Among healthy vitamin D-sufficient females, treatment with 4000 or 10,000 IU of vitamin D, compared with 400 IU per day, resulted in greater losses of TtBMD over three years. The decline in TtBMD was not observed in males. As originally reported, high dose vitamin D supplementation offers no benefit for bone health, and this secondary analysis raises the possibility of increased bone loss for females.

***Disclosures: Lauren Burt**, None*

1020

The Relationship of Total, Bioavailable, and Free 25(OH)D with Indices of Bone Health and Metabolism in Older Adults: A Randomized Controlled Trial *Malak El Sabeh[1], Paola Ghanem[1], Laila Al-Shaar[1], Maya Rahme[1], Rafic Baddoura[2], Georges Halaby[2], Ravinder J. Singh[3], Roger Bouillon[4], Ghada El-Hajj Fuleihan[1]. [1]American University of Beirut, Lebanon, [2]Hotel Dieu de France, Lebanon, [3]Mayo Clinic, United States, [4]Katholieke Universiteit Leuven, Belgium

Questions regarding the superiority of free and bioavailable 25 hydroxy-vitamin D [25(OH)D] in predicting various health outcomes remain unresolved. This study investigates the relative impact of vitamin D metabolites, free, bioavailable or total 25(OH)D, on indices of bone and mineral metabolism, at baseline, and in response to two vitamin D doses. 221 elderly subjects were randomized to receive calcium and oral vitamin D3 (600IU/day or 3,750 IU/day) supplementation. Analyses were performed on serum levels at zero, 6 and 12 months, for > 650 data points for each variable of interest, and on bone mineral density (BMD) at zero and 12 months. We used generalized linear models to account for the lack of independence for variables within each subject, and Bonferroni correction for multiplicity of testing [1]. Vitamin D binding protein was measured by radial immunodiffusion in the Leuven laboratory, and free and bioavailable 25(OH)D were computed using Bikle's equation [2]. Calculated values for the metabolites using the Vermeulen equation were almost identical [2]. Subjects who received the higher vitamin D dose had levels that were 1.3-1.4 folds higher than the lower dose, for all metabolites (p-value < 0.001). Serum bioavailable and free 25(OH)D levels were significantly associated with total 25(OH)D, with r value of 0.942 and 0.943, respectively (p-value <0.001). PTH was negatively associated with all vitamin D metabolites, with correlation coefficients ranging between -0.22 and -0.25; while calcium, and bone turnover markers (carboxy-terminal collagen crosslinks and osteocalcin) were not. Only total 25(OH)D was correlated with % change BMD at the femoral neck at 12 months, while free and bioavailable metabolites did not show any significant relationship with % change BMD at any of the skeletal sites. In conclusion, to-date, calculated free and bioavailable 25(OH)D do not appear to be superior to total 25(OH)D in predicting indices of bone health in an elderly population.References1. Stuart R, et al Journal of the Royal Statistical Society., 2001. 50(No. 1): p. 87-95.2. Bouillon, R., et al. Front Endocrinol (Lausanne), 2019. 10: p. 910.Figure legend: Relationship Between serum PTH and 25(OH)D expressed as Panel A: bioavailable 25(OH)D and Panel B: free 25(OH)D, each divided into their respective quartiles. Star (*) indicates significantly lower PTH levels in fourth quartile of calculated bioavailable and free 25(OH)D compared to the first quartile.

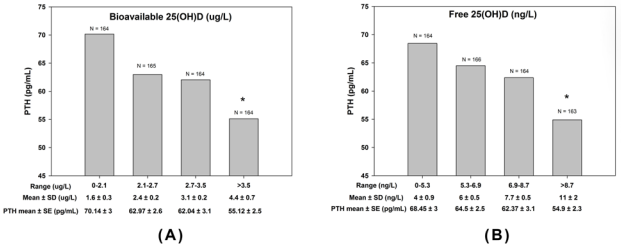

***Disclosures: Malak El Sabeh**, None*

1021

Assessment of Serum and Adipose Tissue Cholecalciferol Concentrations to Investigate Vitamin D Metabolism *Cora Best[1], Leila Zelnick[1], Kenneth Thummel[1], Simon Hsu[1], Gail Cromer[1], Ilona Larson[2], Derek Hagman[2], Howard Sesso[3], JoAnn Manson[4], Mario Kratz[2], Ian de Boer[1], Andrew Hoofnagle[1]. [1]University of Washington, United States, [2]Fred Hutchinson Cancer Research Center, United States, [3]Brigham and Women's Hospital, United States, [4]Brigham and Women's Hospital, United States

The serum 25-hydroxyvitamin D (25OHD) response to vitamin D supplementation is greater when baseline 25OHD concentration is low. Although direct evidence is lacking, this is thought to result from reduced efficiency of 25-hydroxylation as vitamin D input increases. The disposition of the vitamin D not immediately metabolized is unclear. Adipose tissue contains vitamin D, but its contribution to vitamin D homeostasis is unknown.We

used liquid chromatography-tandem mass spectrometry to measure cholecalciferol (D3) in biospecimens from 3 supplementation trials. Study 1 (VITAL-DKD) was a 2x2 factorial randomized placebo-controlled trial (RCT) ancillary to the VITamin D and OmegA-3 TriaL (VITAL) that tested 2000 IU of D3 and/or 1 g of ω-3 fatty acids per day for prevention of diabetic kidney disease. Serum D3 and 25OHD concentrations at baseline and year 2 were obtained for the first 200 participants. Study 2 was a pilot RCT of D3 for reduction of inflammation in obesity. 15 participants with 25OHD concentration < 50 nmol/L received 2000 or 4000 IU of D3/d. Concentrations of D3 and 25OHD3 were measured in serum and subcutaneous adipose tissue at baseline and 3 mo. Study 3 was a pilot RCT of D3 for prevention of diabetic kidney disease. 22 participants with 25OHD concentration < 75 nmol/L received 2000 IU of D3/d or placebo. Serum D3 and 25OHD3 were measured at baseline and 1, 3, 6, and 12 mo.Across studies, there was a hyperbolic relationship between serum D3 and 25OHD3 concentrations with a threshold evident at a 25OHD concentration ≈ 50 nmol/L (Figure 1). In study 1, 16% of participants had baseline 25OHD < 50 nmol/L. Baseline 25OHD < 50 nmol/L (vs. >= 50) was associated with a 16 (95% CI, 1 to 32) nmol/L greater serum 25OHD response but a 15 (95% CI, 2 to 28) nmol/L lesser serum D3 response to supplementation. In study 2, mean serum and adipose tissue D3 concentrations responded proportionally to the dose of D3 administered, whereas 25OHD3 concentrations responded less than proportionally to dose. Adipose tissue D3 was significantly correlated with serum 25OHD3 at baseline (when vitamin D status was low) (r = 0.6) but not after supplementation.Our results support the hypotheses that 25OHD production efficiency declines as vitamin D input increases and that unmetabolized vitamin D is temporarily deposited in fat. These data are proof-of-concept that assessment of parent vitamin D in tissues can fill gaps in understanding of vitamin D homeostasis.

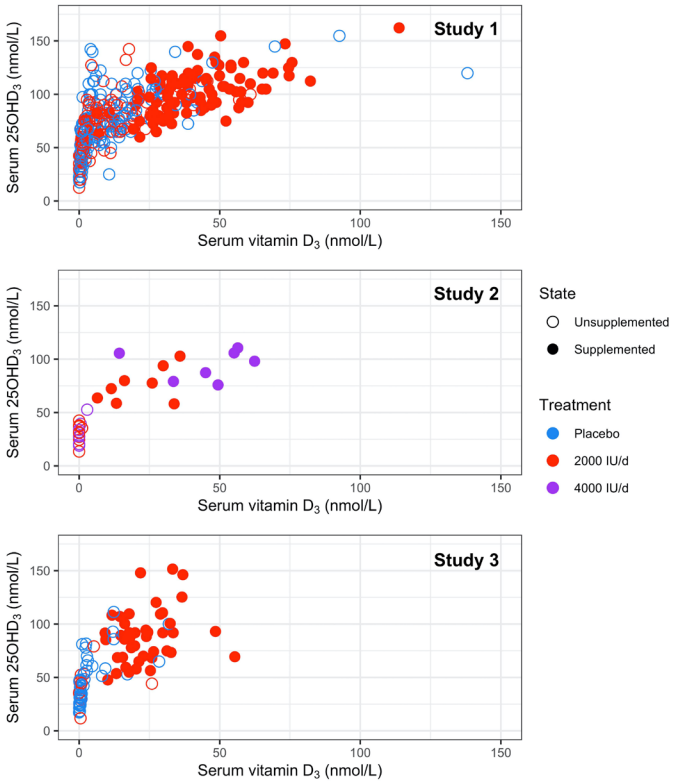

Figure 1. Serum $25OHD_3$ concentration vs. serum vitamin D_3 concentration at baseline and in the placebo group, i.e., in the unsupplemented state (open circles), and during supplementation (closed circles) in three clinical trials of vitamin D_3 supplementation.

***Disclosures: Cora Best**, None*

1022

Dairy Supplementation Reduces Fractures and Falls in Institutionalized Older Adults: a Cluster-Randomized Placebo-Controlled Trial *Sandra Iuliano[1], Shirley Poon[1], Judy Robbins[1], Minh Bui[2], Xiaofang Wang[1], Lisette de Groot[3], Marta Van Loan[4], Tuan Nguyen [5], Ego Seeman[6]. [1]Departments of Medicine and Endocrinology, University of Melbourne / Austin Health, Australia, [2]School of Population and Global Health, University of Melbourne, Australia, [3]Division of Human Nutrition, Wageningen University, Netherlands, [4]US Department of Agriculture-ARS, University of California, United States, [5]Garvan Institute of Medical Research and University of Technology Sydney, Australia, [6] Departments of Medicine and Endocrinology, Austin Health, University of Melbourne and Mary MacKillop Institute for Health Research, Australian Catholic University, Australia

Background: Older adults in aged-care are at the highest risk for fractures and are the source of 30% of hip fractures in the community. These individuals often have inadequate intakes of calcium and protein and have reduced musculoskeletal mass and function. As dairy foods (i.e. milk, yoghurt cheese) are good source of calcium and protein we hypothesized that dairy supplementation would reduce the risk of fractures. Methods: We undertook a 2-year cluster-randomized placebo-controlled trial in 60 aged-care facilities; 30 randomized to provide residents with additional dairy foods to achieve 4 servings daily while the remaining 30 facilities continued with their usual menu. Amongst the 7133 older adults involved (72% females, mean; age 86.0+/-8.2 years, calcium 650 mg/day, protein < 1g per kg body weight, 25(OH)D 73+/-27 nmol/L) falls and fractures were recorded and verified using incident reports and hospital x-ray reports, respectively. Dietary provision was determined from menu analyses and intake determined every 3 months in 10% of residents using validated plate waste analysis. Time to event was determined using multilevel Cox's model to account for the intra-cluster covariance.Results: Dairy supplementation provided an additional 562+/-166 mg/day calcium and 13+/-6 g/day protein with residents achieving intakes of 1153+/-444 mg/day and 69+/-20 g/day respectively, while residents in control facilities continued intakes of 636+/-267 mg/day of calcium and 57+/-16 g/day protein. Dairy supplementation was associated with a 54% reduction in all fractures (HR 0.46; 95CI: 0.27 to 0.80; p=0.002),a 48% reduction in hip fractures (HR 0.60; 95%CI, 0.37 to 0.75; p<0.001), 9% fewer falls (HR0.91, 95%CI, 0.86 to 0.97, p<0.001) and unchanged mortality (HR 1.00, 95% CI, 0.41 to 2.42). Conclusion: Correction of low calcium and protein intakes in aged-care residents using dairy foods is a safe and widely accessible intervention that reduces fractures and falls.

***Disclosures: Sandra Iuliano**, None*

1023

Vitamin D Deficiency Is Independently Associated with COVID-19 Severity and Mortality *Luigi Gennari[1], Irene Campi[2], Daniela Merlotti[1], Christian Mingiano[1], Alessandro Frosali[1], Luca Giovanelli[2], Camilla Torlasco[3], Martino Pengo[3], Francesca Heilbron[2], Davide Soranna[3], Marta Di Stefano[0], Carmen Aresta[0], Marco Bonomi[2], Biagio Cangiano[2], Vittoria Favero[0], Letizia Fatti[2], Giovanni Battista Perego[3], Iacopo Chiodini[0], Gianfranco Parati[3], Luca Persani[2]. [1]Department of Medicine, Surgery and Neurosciences, University of Siena, Italy, Italy, [2]Department of Endocrine and Metabolic Diseases, IRCCS, Istituto Auxologico Italiano, Milan, Italy, Italy, [3]Department of Cardiovascular, Neural and Metabolic Sciences, IRCCS, Istituto Auxologico Italiano, Milan, Italy, Italy, [0]Department of Endocrine and Metabolic Diseases, IRCCS, Istituto Auxologico Italiano, Milan, Italy, Italy

Purpose. Vitamin D exerts well known immunomodulatory functions and there is an ongoing debate on the possibility that vitamin D deficiency might favor a poorer outcome of Coronavirus disease-19 (COVID-19). This is also sustained by epidemiology data suggesting a likely relationship between COVID-19 severity and prevalence areas of vitamin D deficiency. We thus investigated the association between 25-hydroxyvitamin-D (25OHD) levels and COVID-19 severity and mortality. Methods. We prospectively studied 103 patients (age 66.1+/-14.1 yrs) admitted to the hospital for symptomatic COVID-19 and 52 subjects with mildly-symptomatic SARS-CoV-2, without respiratory dysfunction. Vitamin D levels in SARSCoV-2 affected cases were compared to 206 age and sex matched controls obtained from a reference sample of 3174 consecutive subjects that underwent 25OHD measurement between January 01 and March 31, 2020 in the frame of a routine health check.Results: At hospital admission, 25OHD levels were lower in symptomatic COVID-19 patients (18.2+/-11.4 ng/mL) than in mildly-symptomatic SARS-CoV-2 or controls (30.3+/-8.5 ng/mL and 25.4+/-9.4 ng/mL, respectively, p<0.0001 for both comparisons) and were inversely associated with IL-6 levels (β -0.284, p=0.004). After hospital admission, 54 symptomatic COVID-19 patients were admitted to intensive care Unit (ICU), because of severe acute respiratory distress syndrome (ARDS). These patients had lower 25OHD and higher IL-6 levels (14.4+/-8.6 ng/mL and 49.6+/-41.4 pg/mL, respectively), than symptomatic COVID-19 patients not requiring ICU admission (22.4+/-12.7 ng/mL, p=0.0001 and 28.8+/-44.3 pg/mL, p=0.016, respectively). After a mean of 19+/-9 days of hospital stay, 19 symptomatic COVID-19 patients (18.4%) died due to ARDS. As compared to COVID-19 cases who survived, deceased COVID-19 patients had lower 25OHD (13.2+/-6.4 vs 19.3+/-12.0 ng/mL, p=0.03) and higher IL-6 levels (61.0+/-45.6 vs 34.9+/-42.3 pg/mL, p=0.02). Interestingly,

25OHD levels were inversely associated with either ARDS requiring ICU admission [odds ratio, OR1.06, 95% confidence interval (95%CI) 1.01–1.12, p=0.038] or mortality (OR1.18, 95%CI, 1.02–1.37, p=0.029), regardless of IL-6 levels and the presence of major comorbidities.Conclusions. Our data, give a strong observational support to previous suggestions that reduced vitamin D levels may favour the appearance of severe respiratory dysfunction and increase the mortality risk in patients affected with COVID-19.

***Disclosures: Luigi Gennari**, None*

1024

Mediterranean Diet Adherence and its Associations with Circulating Cytokines, Musculoskeletal Health and Incident Falls in Community-Dwelling Older Men *Mavil May Cervo[1], David Scott[1], Markus Seibel[2], Robert Cumming[2], Vasi Naganathan [2], Fiona Blyth[2], David Le Couteur [2], David Handelsman [2], Louise Waite [2], Vasant Hirani[2]. [1]Monash University, Australia, [2]University of Sydney, Australia

Background and Aims: Mediterranean dietary patterns may exert favourable effects on various health conditions. This study aimed to determine associations of adherence to Mediterranean diet with circulating cytokine levels, musculoskeletal health and incident falls in community-dwelling older men.Methods: Seven hundred ninety-four (794) community-dwelling men with mean age 81.1+4.5 years, who participated in the five-year follow-up of the Concord Health and Ageing in Men Project (CHAMP) were included in the cross-sectional analysis, and 616 attended follow-up three years later. Adherence to Mediterranean diet was assessed using MEDI-LITE (literature-derived Mediterranean diet) score which was obtained using a validated diet history questionnaire. Twenty-four evaluable circulating cytokines were analyzed using Bio-Plex Pro Human Cytokine 27-plex Assay kit. Appendicular lean mass (ALM) and bone mineral density (BMD) were measured using dual-energy x-ray absorptiometry (DXA). Three-year changes in gait speed and hand grip strength were assessed by walking a 6-meter course and using a dynamometer respectively. Incident falls over three years were determined through telephone interviews every four months.Results: A higher MEDI-LITE score, indicating greater adherence to Mediterranean diet, was associated with higher appendicular lean mass adjusted for body mass index (ALMBMI) (β: 0.004 kg/kg/m2; 95% CI: 0.000, 0.008), and lower serum interleukin-7 (IL-7) (β: -0.017 pg/mL; 95% CI: -0.031, -0.003), and incident falls rates (IRR: 0.94; 95% CI: 0.89, 0.99). Higher consumption of monounsaturated fatty acids (IRR: 0.76; 95% CI: 0.59, 0.98) and monounsaturated fatty acids to saturated fatty acids ratio (IRR: 0.72; 95% CI: 0.57, 0.90) were associated with 24%, and 28% lower falls risk in older men respectively. MEDI-LITE scores were not associated with BMD or physical function parameters.Conclusion: Adherence to a Mediterranean diet is associated with higher ALMBMI, lower levels of serum IL-7, and fewer falls in community-dwelling older men. Monounsaturated and saturated fatty acids were the most important contributors to the association between Mediterranean diet and falls risk.

***Disclosures: Mavil May Cervo**, None*

1025

Sclerostin Depletion May Induce Inflammation in the Bone Marrow *Cristine Donham[1], Jennifer Manilay[1], Betsabel Chicana[1], Gabriela Loots[2], Deepa Murugesh[2]. [1]University of California, Merced, United States, [2]Lawrence Livermore National Laboratories, United States

Romosozumab, a humanized monoclonal antibody specific for sclerostin, has been approved in the United States for post-menopausal women with osteoporosis at high risk for fracture. In several Phase III clinical trials, romosozumab decreased the risk of vertebral fractures up to 73% and increased total hip area bone mineral density by 3.2%. Our previous work in 12 to 15-week-old sclerostin-knockout mice (SostKO) indicated that changes in immune cell development occur in the bone marrow (BM), which could be a possible side effect to follow in human patients. Our overall goal is to define the mechanisms that guide the behavior of long-term hematopoietic stem cells (LT-HSCs) after exposure to an irregular BM microenvironment. SOST plays an important role in maintaining bone homeostasis, as demonstrated by the increased ratio of bone volume to total volume observed in SostKOs. SOST is secreted mainly by osteocytes and could antagonize Wnt signaling by binding to the low-density lipoprotein related proteins 5 and 6 on other cells in the bone and BM. In this study, we examined the effects of Sost-deficient microenvironments on hematopoiesis using transplantation of wild-type LT-HSCs into an older (at least 6 months of age) cohort of Sost-KO mice (WT→KO chimeras) and in younger mice that that received sclerostin-antibody (Scl-Ab) treatment for 6 weeks. As Wnt signaling is important for LT-HSC maintenance and self-renewal, we hypothesized that that loss of Sost in the microenvironment would result in an expansion and exhaustion of LT-HSCs. Our analyses revealed an increased frequency of hematopoietic progenitors in the BM in WT→KO and Scl-Ab treated mice, including myeloid-biased multipotent progenitors (MPP2 and MPP3), leading to an increased output of monocytes and granulocytes. The lack of Sost in the BM causes permanent changes in hematopoiesis, as this myeloid bias extended to extramedullary hematopoiesis in the spleen, where Sost is not expressed. The bias in myelopoiesis correlates with an increase in inflammatory cytokines TNFα, IL-1α and MCP-1 in the serum of the SostKO BM. In addition, we observed alterations in erythrocyte differentiation in the BM and spleen of SostKOs. Taken together, our current study indicates novel roles for Sost in the regulation of myelopoiesis and control of inflammation in the BM in older subjects. Our animal studies strongly recommend tracking of hematopoietic function in patients treated with romosozumab.

***Disclosures: Cristine Donham**, None*

1026

Non-activated T cells Increase Osteoclastogenesis and Breast Cancer Bone Metastases *Danna L. Arellano[1], Juan A. Corral-Avila[1], Andrea Verdugo-Meza[1], Florian Drescher[1], Samanta Jiménez[2], Felipe Olvera-Rodriguez[3], Patricia Juárez[2], Pierrick GJ. Fournier[2]. [1]Biomedical Innovation Department, CICESE, Posgrado de Ciencias de la Vida, CICESE, Mexico, [2]Biomedical Innovation Department, CICESE, Mexico, [3]Instituto de Biotecnología, UNAM, Mexico

Breast cancer bone metastases cannot be cured, and treatments such as T cell-based immunotherapy need to be tested. However, T cells can be pro-osteoclastic, which would support bone metastases. Thus, we aim to characterize the effect of T cells in breast cancer bone metastases.As a syngeneic model, we used 4T1 breast cancer cells to cause bone metastases in mice. In normal Balb/C mice, osteolytic metastasis was increased when compared to SCID, and T-cell depleted mice (x3.6 and x1.6, respectively, $p<0.05$). Histomorphometry confirmed that the number of osteoclasts was increased at the tumor/bone interface in mice with T cells. Ex vivo, T cells isolated from 4T1 bone metastases increased osteoclastogenesis, consistent with the expression of Rankl and Tnfa mRNA. However, this pro-osteoclastic effect was specific of the non-activated T cells, as activated T cells inhibited the formation of osteoclasts ex vivo, which is consistent with the expression of Ifng and Il4 mRNA. Using flow cytometry, we confirmed that T cells in bone metastases are not activated, as >85% of T cells lacked the activation marker CD69. Thus, immunotherapy activating T cells could benefit patients with bone metastases.While ConA or anti-CD3/CD28 antibodies activated T cells from the spleen ex vivo, they failed to activate T cells from bone metastases. This suggests microenvironment-induced immunosuppression that could be due to an increase of myeloid-derived suppressor cells (MDSC), monocytic (CD11b+Ly6C+), and polymorphonuclear (CD11b+Ly6G+), in 4T1 bone metastases. CellROX and DAF2-DA assays confirmed that these MDSCs produced ROS and NO that suppress T cells.The PDE5 inhibitor, Sildenafil, was reported to inhibit MDSCs. However, treatment with Sildenafil did not decrease 4T1 bone metastases nor improved the effect of zoledronate. Thus, we looked for other therapeutic targets, such as immune checkpoints. Although only 27% of T cells in 4T1 bone metastases were CTLA-4+, >70% of T cells were PD-1+, and 80% of monocytic-MDSCs were PD-L1+, which could trigger T cell suppression in bone.In conclusion, we found that T cells inactivated in the bone metastasis microenvironment increase osteoclast formation and bone metastases, while activated T cells inhibit osteoclastogenesis. Although targeting MDSCs with Sildenafil was not efficient, treatment with immune checkpoint inhibitors (antibodies against PD-1 or PD-L1) could be used for patients with bone metastases.

***Disclosures: Danna L. Arellano**, None*

1027

HDAC inhibitors rescue LIFR repression driven by the bone microenvironment *Courtney Edwards [1], Miranda Clements[2], Lawrence Vecchi[3], Jasmine Johnson[3], Rachelle Johnson[3]. [1]Vanderbilt University Medical Scientist Training Program, United States, [2]Vanderbilt University Graduate Program in Cancer Biology, United States, [3]Division of Clinical Pharmacology Vanderbilt University Medical Center, United States

Breast cancer cells frequently disseminate to the bone marrow, where they either induce osteolysis or enter a dormant state. We have previously demonstrated that down-regulation of leukemia inhibitory factor receptor (LIFR) enables breast cancer cells to exit dormancy in the bone. Hypoxia, or low oxygen tensions, down-regulates LIFR in breast cancer cells independent of hypoxia-inducible factor (HIF) signaling, but the mechanism of hypoxic repression is unknown. Furthermore, we have shown that histone deacetylase (HDAC) inhibitors (entinostat, panobinostat, vorinostat, valproic acid, and romidepsin) stimulate LIFR and, in combination with bisphosphonates, promote dormancy and prevent tumor-induced osteolysis in mouse models of bone colonization. To confirm whether disseminated breast cancer cells encounter hypoxia in the bone, we performed immunostaining for pimonidazole (a hypoxia marker) and cytokeratin (to detect tumor cells) on serial sections and confirmed that approximately 50% of MCF7 breast cancer cells encountered hypoxia in the tibia following intracardiac inoculation. To determine if histone modifications contribute to the mechanism by which LIFR is repressed in hypoxia, we performed chromatin immunoprecipitation (ChIP) for H3K9 methylation and acetylation. ChIP analysis confirmed that H3K9me3, which represses gene transcription, was significantly increased (2.8-fold, $p<0.05$) in the distal LIFR promoter, and H3K9ac, which promotes transcription, was significantly reduced (3.9-fold, $p<0.01$) in hypoxia (0.5% pO2 for 24 hours). Furthermore, entinostat and panobinostat rescued hypoxic repression and dramatically increased LIFR expression (up to 3.7-fold, $p<0.05$-0.001), and increased the known dormancy markers p38β (up to 2.3-fold, $p<0.05$-0.01) and p21 (up to 3.5-fold, $p<0.05$-0.01) by qPCR and Western blot. We previously demonstrated that parathyroid hormone-related protein (PTHrP), which is elevated in bone-disseminated breast cancer cells to promote osteolysis and bone colonization, significantly represses LIFR in vitro. Using ChIP, we confirmed that PTHrP binds to the LIFR distal promoter (up to 25-fold, $p<0.0001$). Furthermore, entinostat rescued LIFR repression by Western blot, and significantly stimulated H3K9ac in the distal LIFR promoter by ChIP (3.2-fold, $p<0.01$) when PTHrP was overexpressed. Together, these data suggest that HDAC inhibitors stimulate LIFR in multiple models of LIFR repression to promote dormancy in the bone microenvironment.

***Disclosures: Courtney Edwards,** None*

1028

Single-cell RNA sequencing of CXCL12+ osteoprogenitors in mechanically loaded mouse tibiae reveals osteogenic mechanosensitive pathways *Pamela Cabahug-Zuckerman[1], Tareq Anani[2], Pablo Atria[3], Anastasia Tikhonova[4], Alireza Khodadadi-Jamayran[5], Nitzan Segal[6], Ioannis Aifantis[4], Alesha Castillo[1]. [1]Dept of Orthopaedic Surgery, New York University Grossman School of Medicine, Veterans Affairs New York Harbor Healthcare System, Manhattan, United States, [2]Dept of Orthopaedic Surgery, Dept of Orthopaedic Surgery, New York University Grossman School of Medicine, United States, [3]Dept of Orthopaedic Surgery, New York University Grossman School of Medicine, United States, [4]Dept of Pathology, New York University Langone Health, United States, [5]Applied Bioinformatics, New York University Langone Health, United States, [6]Dept of Biomedical Engineering, Tandon School of Engineering, New York University, United States

Mechanical loading (ML) is a potent anabolic stimulus in healthy adult bone [1]. A better understanding of cell and molecular processes in load-induced osteogenesis, including underlying mechanosensitive pathways, could yield effective treatment strategies for aged and diseased bone. Cortical bone (CB) osteocytes (OCYs) originate from LepR+ cells, of which 98.8% co-express CXCL12 [2]. Given that skeletal stem cells (SSCs) express an array of overlapping markers, including LepR and CXCL12 [2-6], we sought to determine how these distinct SSC populations respond to ML with regard to their number and gene expression profiles at the single cell level. We hypothesized that ML leads to an expansion of CXCL12+ and LepR+ cell populations and regulates their fate. Following NYU IACUC approval, adult Cxcl12tm2.1Sjm/J dsRed reporter mice (N=19) and C57BL/6 (C57, N=6) mice (Jackson Labs) were subjected to 4 daily bouts of tibial axial compressive loading (L) (6N,2Hz,120cycles) with appropriate non-loaded (NL) controls. Bone marrow (BM) and CB cell suspensions from L and NL tibiae were prepared for FACS and single-cell RNAseq (10XGenomics) as previously described [5]. FACS data are presented as %change and significance determined by a Student's T-test at $\alpha=0.05$; expression data are presented as normalized fold-change. The enriched CXCL12+ cell population was shown to highly express LepR. ML led to a significant increase in the number of LepR+ cells (+114%, $p=0.022$) in the BM. Differentially expressed genes in the L versus NL CXCL12-dsRed+ cells included upregulated osteogenic genes Wnt4 (1.32X, $p<0.0001$) and BMP4 (1.72X, $p<0.0001$), and downregulated adipo-associated genes PPARgamma (0.79X, $p=0.037$) and Apoe (0.92X, $p<0.001$). Unbiased principle component analysis (PCA) yielded 11 cell clusters, including reticular cells [2,5,6] and pre-osteoblasts [5,6]. Loading resulted in a significant increase in BMP4 (2.7X, $p=0.002$) and a significant decrease in sFRP expression (0.55X, $p<0.0001$),

a negative regulator of Wnt signaling [7], in reticular cells. A significant increase in Wnt4 (1.9X, p<0.0001) was also observed in pre-osteoblasts. Our data demonstrate that loading promotes osteogenic differentiation via promotion of Wnt signaling, consistent with previous reports [8-10] while attenuating pro-adipogenic genes in cells expressing both LepR and CXCL12, which are known osteoprogenitors [2]; that is, loading effectively pushes progenitors towards an osteogenic fate.

REFERENCES: [1] Turner+ Sci Sig 2009; [2]Zhou+ Cell Stem Cell 2014; [3] Greenbaum+ Nature 2013; [4] Hanoun+ Cell Stem Cell 2013; [5]Tikhonova+ Nature 2019; [6] Matsushita+ NatComm2020; [7] Haraguchi+ Sci Rep 2016; [8] Holguin+ JBMR 2016; [9] Kelly+ Bone 2016; [10] Chermside-Scabbo+ JBMR2020.

***Disclosures: Pamela Cabahug-Zuckerman**, None*

1029

Interaction between osteocyte SOCS3-dependent signaling and the bone marrow microenvironment maintains cortical bone integrity *Tsuyoshi Isojima[1], Emma C Walker[1], Blessing Crimeen-Irwin[1], Ingrid J Poulton[1], Narelle E McGregor[1], Jonathan H Gooi[1], T. John Martin[1], Natalie A Sims[1]. [1]St. Vincent's Institute of Medical Research, Australia

Cortical structure is a crucial determinant of bone strength, yet the underlying mechanisms that control its organization remain poorly understood. We recently reported that cortical bone develops through pore closure and accumulation of high density bone by SOCS3-mediated suppression of gp130-STAT3 signaling in osteocytes. Since SOCS3 also suppresses G-CSFR signaling, we studied whether global G-CSFR (Csf3r) ablation could improve the structure of Dmp1Cre.Socs3f/f cortical bone.Dmp1Cre.Socs3f/f.Csf3r-/- mice were generated by crossing Dmp1Cre.Socs3f/f mice with Csf3r null mice on a C57BL/6 background. Csf3r null mice exhibited no change in bone structure compared to wild type mice. Surprisingly, bone structure was not improved by Csf3r deletion in Dmp1Cre.Socs3f/f mice at 12 or 26 weeks of age. In fact, the phenotype was worsened. Dmp1Cre.Socs3f/f.Csf3r-/- mice showed a further increase in cortical porosity (by 30%) compared to Dmp1Cre.Socs3f/f. Dmp1Cre.Socs3f/f.Csf3r-/- bone had a higher proportion of low density bone than Dmp1Cre.Socs3f/f (increased by 23%), and very little high density bone (<5%, compared to 15% in Dmp1Cre.Socs3f/f and wild type). Despite this extreme defect in structure, bone shape was normal and femoral strength in three-point bending tests was not different from Dmp1Cre.Socs3f/f. Histology revealed that Dmp1Cre.Socs3f/f.Csf3r-/- cortical bone contained a "double-shell" of lamellar bone separated by a channel of highly porous woven bone, containing 5x more osteoclasts and a 3-fold increase in blood vessel area compared to Dmp1Cre.Socs3f/f control. qPCR of flushed femora in Dmp1Cre.Socs3f/f.Csf3r-/- showed extremely high mRNA levels of osteoclast markers (Dc-stamp, Acp5), RANKL (Tnfsf11) and angiogenesis markers (Endomucin, Tie-1). A significant increase in the number of phospho-STAT1 (~15%) and phospho-STAT3 (~20%) positive osteocytes, and elevations in STAT1 and STAT3 target gene mRNAs (Socs1 and Bcl3), indicated that G-CSFR deletion further increases STAT signaling in Dmp1Cre.Socs3f/f bone.Since G-CSFR is not expressed in osteocytes, we suggest that G-CSFR deficiency promotes STAT signaling in osteocytes through its influence on the bone marrow microenvironment. In the absence of SOCS3 negative feedback, this increases cortical porosity by promoting local vascularization and bone resorption. This suggests that cortical bone integrity requires communication between osteocytes and G-CSFR-mediated signals in the bone marrow microenvironment.

***Disclosures: Tsuyoshi Isojima**, None*

1030

Requirement of Macrophage to Stromal Cell NGF-p75 Signaling in Bone Repair *Jiajia Xu[1], Zhao Li[1], Stefano Negri[1], Seungyong Lee[1], Yiyun Wang[1], Ching-Yun Hsu[1], Ye Tian[1], Qizhi Qin[1], Masnsen Cherief[1], Robert Tower[1], Thomas Clemens[1], Aaron James[1]. [1]Johns Hopkins University, United States

One of the hallmarks of bone injury is pain, yet the role of skeletal sensory nerves in bone repair is only recently becoming understood. In an acute bone injury, we recently reported that nerve growth factor (NGF) – tropomyosin receptor kinase A (TrkA) signaling is necessary for normal skeletal re-innervation and re-ossification. NGF has two known receptors, including the high affinity receptor TrkA and the low affinity receptor p75, the latter of which is expressed in bone-lining cells. Here, we assessed the role of NGF-p75 signaling in macrophage to stromal cell cross-talk during calvarial bone repair. A collection of NGF reporter animals (NGF-eGFP), pan-neuronal reporter animals (Thy1-YFP), NgfLysM conditional knockout mice (Ngffl/fl; LysM-Cre), and p75Pdgfrα conditional knockout mice (Ngfrfl/fl; Pdgfrα-CreERT2) were subjected to calvarial bone defects (1.8 mm diameter, full thickness frontal bone defects). Their bone repair phenotypes were monitored by radiographic, histologic and immunohistochemical means over a four week period. First, NGF and p75 expression patterns were documented after calvarial injury. NGF reporter activity was present both in F4/80-expressing macrophages as well as Pdgfrα-expressing stromal cells upon bone injury (Fig. 1A). P75 immunoreactivity was present principally in Pdgfrα-expressing stromal cells and to a lesser extent in perivascular cells (Fig. 1B). Next, bone repair was assessed upon conditional deletion of p75 in Pdgfrα-expressing stromal cells. Results showed a significant reduction in calvarial bone repair among p75Pdgfrα mice in comparison to p75fl/fl control animals (Fig. 1C-H), including a 68.3% reduction in bone volume, a 40.9% increase in distance between bony fronts, and a 54.8% reduction in bone fractional area at the study endpoint. Histochemical and immunohistochemical staining confirmed a reduction in bone matrix deposition and Osteocalcin+ osteoblast numbers within injured p75Pdgfrα bones. Cell specific deletion of Ngf in LysM-expressing monocyte/macrophages phenocopied these findings. In summary, it appears that NGF signaling via both its high affinity and low affinity receptors are critical for normal bone repair. Future studies will determine how NGF-p75 signaling mediates mesenchymal progenitor cell migration after bone injury, and the extent to which conditional p75 deletion impacts skeletal re-innervation as well as repair.

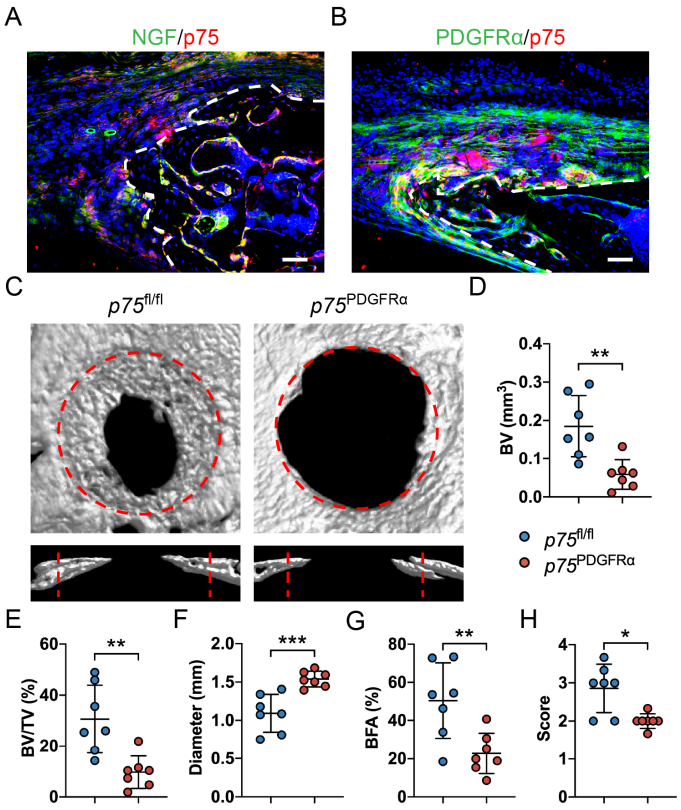

***Disclosures: Jiajia Xu**, None*

1031

The HIF-PHI BAY85-3934 (Molidustat) improves anemia and controls circulating FGF23 in a CKD mouse model *Megan Noonan[1], Pu Ni[1], Rafiou Agoro[1], Elizabeth Swallow[1], Matthew Allen[1], Kenneth White[1]. [1]Indiana University School of Medicine, United States

The phosphaturic hormone FGF23 is a critical factor in chronic kidney disease-mineral and bone disorder (CKD-MBD), with elevated levels in blood associated with increased odds for patient mortality (>6-fold). Anemia is a potent driver of FGF23 expression, and patients with CKD ultimately develop anemia as the kidneys lose the ability to produce erythropoietin (EPO), in concert with FGF23-mediated alterations in mineral metabolism. Our goal was to investigate a HIF-PHI (hypoxia-inducible factor prolyl hydroxylase inhibitor), currently in clinical trials to elevate endogenous EPO, for effects on anemia-dependent FGF23 levels and key outcomes in a mouse model of CKD. Female C57Bl6 mice were fed a casein control or adenine-containing diet to induce CKD, which resulted in markedly elevated iFGF23 and blood urea nitrogen (BUN), hyperphosphatemia, and anemia. After 12 weeks of CKD induction, mice were treated with the HIF-PHI BAY85-3934 ('BAY'; Molidustat) at a human equivalent dose (20 mg/kg) every other day for 3 weeks. Compared to saline controls, BAY elevated serum EPO and restored CBCs to normal levels in CKD mice. iFGF23 was significantly elevated in saline-treated CKD mice (120-fold, p60%; p<0.05) in BAY-treated mice with CKD, coinciding with downregulated renal Egr-1 expression (p<0.01). Renal 1,25D anabolic Cyp27b1 and catabolic Cyp24a1 mRNAs were up and downregulated, respectively, in BAY-treated CKD mice. This extended treatment resulted in decreased BUN (p<0.01) and reduced expression of renal fibrosis markers (p<0.01). The bone marrow Erfe, Transferrin receptor, and EpoR mRNAs were all upregulated (p<0.05-p<0.01), and liver hepcidin expression was downregulated in both control and CKD groups treated with BAY (p<0.05-p<0.01). HIF activation in osteoblasts/osteocytes is associated with increased bone mass, therefore we investigated femur trabecular parameters and cortical porosity, however saw no effect with BAY over this time course. Serum alkaline phosphatase was significantly elevated in CKD-BAY mice compared to CKD controls (p<0.01), suggesting increased osteoblast activity. Collectively, these results support that resolving anemia using a HIF-PHI

improved kidney function and lowered FGF23 during CKD, potentially providing modifiable outcomes beyond improving iron utilization for this patient population.

***Disclosures: Megan Noonan**, None*

1032

Aromatase Deficiency in Hematopoietic Cells Improves Trabecular Bone Quantity, Quality, and Mineralization in Bone Marrow Transplant Recipients *Katie Rubitschung[1], Amber Sherwood[1], Katya Rubinow[2], Rasesh Kapadia[3], Orhan K. Öz[1]. [1]UT Southwestern Medical Center Department of Radiology, United States, [2]University of Washington Diabetes Institute, Department of Medicine, United States, [3]Scanco USA, Inc., United States

Estrogens play important roles in building and maintaining skeletal mass. While gonadally produced estrogens are known to be critical for maintaining bone mass, the role of locally produced estrogens is incompletely understood. Immune cells are hematopoietic descendants that reside in the bone marrow and are known to express aromatase [1]. The aim of this study was to determine whether hematopoietic cell derived estrogens have a role in bone mass regulation.Bone marrow from 9-wk old (WT) and aromatase null (ArKO) male mice littermates was harvested from the femurs and tibias. Nine-week-old male WT C57BL6/J recipient mice (n=24) (Jackson Laboratory, Bar Harbor, ME; strain #000664) underwent sublethal irradiation and bone marrow transplant, receiving either WT or ArKO donor cells. The recipient mice were designated as WT(WT) or WT(ArKO), respectively, and sacrificed 28 weeks after transplant. The lumbar spine was harvested for uCT analysis.MicroCT imaging of the lumbar spine was conducted on a Scanco Medical µCT 40 (Bruettisellen, Switzerland). Morphometric analysis focused on L4. The trabecular regions, encompassing about 350 slices, were contoured using a combination of manual and interpolation process. T-test was applied to normally distributed data while non-normal data were analyzed using the Mann-Whitney U-test.Compared to WT(ArKO), WT(WT) mice had lower bone volume fraction (p=0.0025), trabecular number (p=0.0073), connectivity density (p=0.0107), and average hydroxyapatite equivalent content (p=0.0051). In contrast, there was increased trabecular spacing (p=0.0087) in these mice (Fig. 1). In addition, the structure model index values between the two groups were significantly different (p=0.0003), with WT(WT) mice displaying trabeculae more closely resembling cylindrical rods and WT(ArKO) mice expressing trabeculae with a more parallel plate-like appearance.Aromatase-deficient hematopoietic cells transplanted into WT mice confer greater trabecular bone quantity, quality and mineralization compared to WT cell transplants. This study reveals the importance of estrogen derived from hematopoietic lineage cells and their interaction with marrow stromal cells. Bone marrow from aromatase deficient individuals may have clinical utility in treating bone disorders.Berstein, Lev M., et al. "Ability of lymphocytes infiltrating breast-cancer tissue to convert androstenedione." International journal of cancer 77.4 (1998): 485-487.

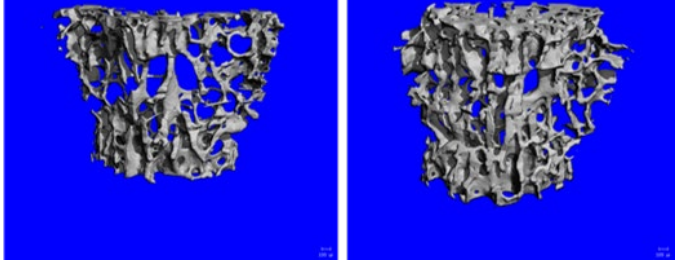

***Disclosures: Katie Rubitschung**, None*

1033

Phlpp1 Is Induced By Estrogen In Osteoclasts And Its Loss In Ctsk-Expressing Cells Does Not Protect Against Ovx-Induced Bone Loss *Marcilline Hanson[1], Ismael Karkache[2], David Molstad[2], Andrew Norton[2], Kim Mansky[2], Elizabeth Bradley[2]. [1]University of Minnesota, United States, [2]University of Minnesota, United States

Prior studies demonstrated that deletion of the protein phosphatase Phlpp1 in Ctsk-Cre expressing cells enhances bone mass, characterized by diminished osteoclast activity and increased coupling to bone formation. Due to non-specific expression of Ctsk-Cre within committed osteoclast and mesenchymal lineage cells, the definitive mechanism for this observation is unclear. To further define the role of bone resorbing osteoclasts within this model, we performed ovariectomy (Ovx) and Sham surgeries on Phlpp1 cKOCtsk and WT littermate mice. We hypothesized that if mesenchymal lineage cells were driving enhanced bone mass, mice would retain enhanced coupling and reduced osteoclast activity despite Ovx. Conversely, if osteoclast activity was dominant, elevated bone mass would be lost following Ovx. Micro-CT analyses confirmed enhanced BV/TV (33.3%), Tb.N (18.2%), Tb.Th (11.1%) and diminished Tb.Sp (12.5%) within the distal femur of Phlpp1 cKOCtsk Sham females (n=4). In contrast, Ovx induced bone loss (40%, 45.8%, 83.3% and 77.8% respectively) with no significant difference between Phlpp1 cKOCtsk and WT mice (n=4). Histomorphometry of the proximal tibia confirmed that Ovx mice lacked significant differences in BV/TV or osteoclasts per bone surface, suggesting that E2 is required for Phlpp1 deficiency to have an effect. We performed high throughput unbiased transcriptional profiling of ex vivo generated Phlpp1 cKOCtsk osteoclasts and identified 290 differentially expressed genes. By cross-referencing these differentially expressed genes with all estrogen-response-element containing genes, we identified Igfbp4 as a potential estrogen-dependent target of Phlpp1. Estradiol (2nM) treatment of osteoclast progenitors induced Phlpp1 expression and reduced Igfbp4. Moreover, genetic deletion or chemical inhibition of Phlpp1 was correlated with enhanced Akt phosphorylation and levels of Igfbp4. We then assessed Igfbp4 expression by osteoclasts in vivo within intact 12-week old females (n=3). Modest Igfbp4 immunohistochemical staining of TRAP+ osteoclasts within WT females was observed. In contrast, TRAP+ bone lining cells within intact Phlpp1 cKOCtsk females robustly expressed Igfbp4, but levels were diminished within TRAP+ bone lining cells following Ovx. These results demonstrate that the effects of Phlpp1 conditional deficiency are due to altered osteoclast activity, potentially due to estrogen-dependent regulation of Igfbp4.

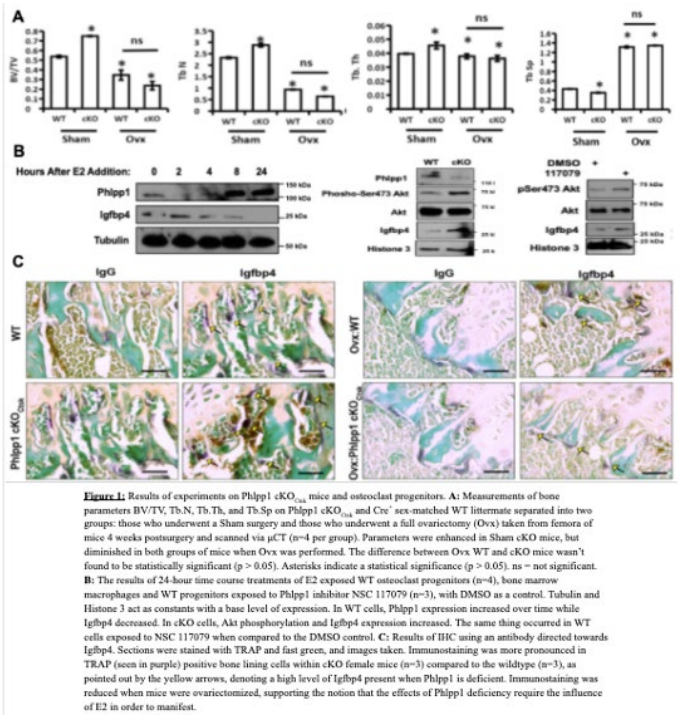

Figure 1: Results of experiments on Phlpp1 cKO_{Ctsk} mice and osteoclast progenitors. **A:** Measurements of bone parameters BV/TV, Tb.N, Tb.Th, and Tb.Sp on Phlpp1 cKO_{Ctsk} and Cre^{+} sex-matched WT littermate separated into two groups: those who underwent a Sham surgery and those who underwent a full ovariectomy (Ovx) taken from femora of mice 4 weeks postsurgery and scanned via µCT (n=4 per group). Parameters were enhanced in Sham cKO mice, but diminished in both groups of mice when Ovx was performed. The difference between Ovx WT and cKO mice wasn't found to be statistically significant ($p > 0.05$). Asterisks indicate a statistical significance ($p > 0.05$). ns = not significant. **B:** The results of 24-hour time course treatments of E2 exposed WT osteoclast progenitors (n=4), bone marrow macrophages and WT progenitors exposed to Phlpp1 inhibitor NSC 117079 (n=3), with DMSO as a control. Tubulin and Histone 3 act as constants with a base level of expression. In WT cells, Phlpp1 expression increased over time while Igfbp4 decreased. In cKO cells, Akt phosphorylation and Igfbp4 expression increased. The same thing occurred in WT cells exposed to NSC 117079 when compared to the DMSO control. **C:** Results of IHC using an antibody directed towards Igfbp4. Sections were stained with TRAP and fast green, and images taken. Immunostaining was more pronounced in TRAP (seen in purple) positive bone lining cells within cKO female mice (n=3) compared to the wildtype (n=3), as pointed out by the yellow arrows, denoting a high level of Igfbp4 present when Phlpp1 is deficient. Immunostaining was reduced when mice were ovariectomized, supporting the notion that the effects of Phlpp1 deficiency require the influence of E2 in order to manifest.

***Disclosures: Marcilline Hanson**, None*

1034

Secreted Frizzled Receptor Protein 4 (Sfrp4) is Required to Maintain Proper Ctsk+ Periosteal Stem/Progenitor Cell Niche Function. *Ruiying Chen[1], Han Dong[2], Dhairya Raval[1], Roland Baron[1], Matthew B. Greenblatt[3], Francesca Gori[1]. [1]1. Division of Bone and Mineral Research, Harvard Medical School and Harvard School of Dental Medicine. 2. Department of Oral Medicine, Harvard Medical School and Harvard School of Dental Medicine., United States, [2]Department of Cancer Immunology and Virology, Dana-Farber Cancer Institute and Harvard University Medical School, United States, [3]Department of Pathology and Laboratory Medicine, Weill Cornell Medicine, United States

The periosteum contains a niche of stem cells and progenitors, which contribute to cortical expansion during growth, and homeostasis and repair in adults. However, in spite of its clinical significance our basic understanding of the local factors which regulate the periosteum remain elusive. We have shown that the cortical bone thinning phenotype seen with deletion or null mutation of the Wnt inhibitor Sfrp4 is due to deregulation of endosteal remodeling and low periosteal bone formation. To gain insight into the function of Sfrp4 in the regulation of the periosteal niche, we generated CtskCre;mTmG;wt and CtskCre;mTmG;Sfrp4-/- mice and investigated Cathepsin K (Ctsk+) labeled and Ctsk+;Sfrp4-/- periosteal cells, which include bona fide stem cells (PSCs) and non-stem progenitors (PP1 and PP2). Importantly, Ctsk+ periosteal cells are enriched for Wnt signaling components, and Sfrp4 is expressed predominantly by PP1 and PP2 progenitors. Long bone periosteum was microdissected from 4 wk-old CtskCre;mTmG;wt and CtskCre;mTmG;Sfrp4-/- mice, digested and FACS performed to isolate and analyze the distribution of Ctsk+ PSCs, PP1 and PP2 cells. This analysis showed that Sfrp4 deletion leads to a significant decrease in the % of PSCs (13.6+0.9 vs 10+0.5, $p<0.01$), while markedly increasing the % of PP2 cells (13.1+2.4 vs

20+1.6, p<0.05), suggesting that Sfrp4 deletion decreases the pool of bona fide stem cells while favoring their transition to progenitors. To test this hypothesis, FACS isolated PSCs were cultured for 10 days and then reanalyzed by FACS. These studies showed that Sfrp4 deletion significantly impaired their ability to give rise to PSCs (1.02%+0.3 vs 0.17%+0.1, p<0.05) and PP1 (93%+1.6 vs 69.2%+9, p<0.05) while favoring their progression into the PP2 non-stem progenitors (0.60%+0.13 vs 10.2%+4.7, p<0.05). Importantly, Sfrp4 deletion markedly decreased both the CFU-OB and CFU-Chondro potential of PSCs, PP1 and PP2 cells as well as their ability to form bone in kidney transplantation assay. Altogether, these studies demonstrate a crucial role for the Wnt inhibitor Sfrp4 in the regulation of periosteal stem cell stemness, favoring the accumulation of periosteal progenitors with impaired capability to differentiate into mature osteoblasts. Elucidating the role of pathways regulated by Sfrp4, may open novel and specific therapeutic options to enhance periosteal cell activity in fracture repair and human diseases associated with cortical bone fragility.

***Disclosures: Ruiying Chen**, None*

1035

The finger 2 tip loop of Activin A is required for the formation of its non-signaling complex with ACVR1 and type II Bone Morphogenetic Protein receptors *Senem Aykul[1], Richard A. Corpina[1], Erich J. Goebel[2], Camille J. Cunanan[1], Alexandra Dimitriou[1], Hyonjong Kim[1], Qian Zhang[1], Ashique Rafique[3], Raymond Leidich[4], Xin Wang[1], Joyce McClain[1], Johanna Jimenez[1], Kalyan C. Nannuru[1], Nyanza J. Rothman[1], John B. Lees-Shepard[1], Erik Martinez-Hackert[5], Andrew J. Murphy[1], Thomas B. Thompson[2], Aris N. Economides[6], Vincent Idone[1]. [1]Regeneron Pharmaceuticals Inc., United States, [2]University of Cincinnati, United States, [3]Regneron Pharmaceuticals Inc., United States, [4]Regeneron Pharmacuticals Inc., United States, [5]Michigan State University, United States, [6]Regeneron Pharmaceuticals Inc., United States

Activin A functions in Bone Morphogenetic Protein (BMP) pathway signaling in two ways: it either engages ACVR1B to activate Smad2/3 signaling or binds ACVR1 to form a non-signaling complex (NSC). Although the former property has been studied extensively, the physiological roles of the NSC remain unexplored. The autosomal-dominant genetic disorder fibrodysplasia ossificans progressiva (FOP) provides a unique window into ACVR1/Activin A signaling because in that disease FOP-mutant ACVR1 recognizes Activin A as an agonistic ligand, initiating signaling akin to that driven by BMPs by activating Smad1/5/8. We have previously shown that signaling induced by Activin A through FOP-mutant ACVR1 is a required driver for the main pathology observed in FOP, the heterotopic ossification (HO) of connective tissue: inhibition of Activin A using neutralizing antibodies ameliorates HO in mouse models of FOP. However, given that FOP is an autosomal-dominant disorder, one wild type copy of ACVR1 remains, and hence can still form NSCs with Activin A (along with the corresponding type II receptors). Deletion of this wild type copy of Acvr1 in mouse FOP results in 6-fold more HO, consistent with an inhibitory role of the NSCs that can still form between wild type ACVR1 and Activin A in that setting. However, no direct evidence for physiological roles of the NSC exists to date. To set the stage to probe this question, we generated 'agonist-only' Activin A muteins that activate ACVR1B but cannot form the NSC with ACVR1. These muteins fail to inhibit BMP7-induced signaling via ACVR1 except to the level expected through competition for binding of these ligands to their type II receptors, a property required for any BMP family ligand to initiate signaling. We also show that these muteins activate ACVR1B just like wild type Activin A, but although they fail to form the NSC with wild type ACVR1 they still activate FOP-mutant ACVR1. Based on this evidence, we hypothesized that these muteins will generate more HO than wild type Activin A in an FOP setting, as they should activate FOP-mutant ACVR1 while simultaneously escaping the tempering effects of the NSC that wild type Activin can still form with the wild type copy of ACVR1. We show that this indeed the case (Figure 1). These results provide the first evidence for a biological role for the NSC in vivo and pave the way for further exploration of the NSC's physiological role in corresponding knock-in mice.

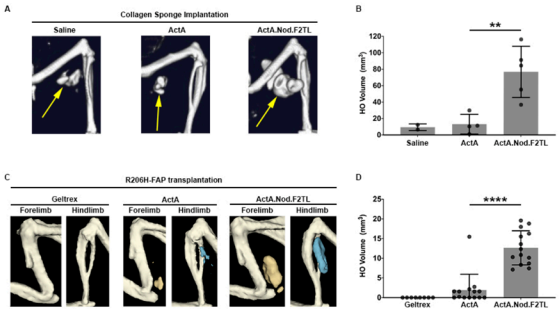

Figure 1: Activin A.Nod.F2TL mutein is a more potent inducer of HO than wild type Activin A

(A) Representative µCT images of HO (yellow arrows) from tamoxifen-treated *Acvr1[R206H]FlEx/+*; *Gt(ROSA26)Sor^CreERT2/+* **mice taken two weeks after implantation of collagen sponges adsorbed with saline, 20 µg wild type Activin A (ActA), or 20 µg Activin A.Nod.F2TL (ActA.Nod.F2TL). (B) HO volume was quantified 2 weeks post-implantation. (C) 11 days post-transplantation, representative µCT images of fore- and hindlimbs from SCID hosts of FOP FAPs (R206H-FAPs) in Geltrex alone, Geltrex contain 5 µg ActA, or Geltrex containing 5 µg ActA.Nod.F2TL. HO is pseudocolored beige for forelimbs and blue for hindlimbs. (D) Quantification of HO volume 11 days post-transplantation of R206H-FAPs. (**=p ≤ 0.01; ****=p ≤ 0.0001)**

***Disclosures: Senem Aykul**, Regeneron Pharmaceuticals Inc, Major Stock Shareholder*

1036

HES1 is a Primary Effector of NOTCH2 Signaling in Osteoclasts *Jungeun Yu[1], Lauren Schilling[1], Ernesto Canalis[1]. [1]UConn Health, United States

Hajdu Cheney Syndrome (HCS) is a rare genetic disorder characterized by craniofacial abnormalities, acroosteolysis and osteoporosis. We created a mouse model termed Notch2tm1.1Ecan replicating a mutation found in HCS. Notch2tm1.1Ecan mice exhibit marked osteopenia secondary to enhanced osteoclastogenesis and bone resorption. Hairy and Enhancer of Split 1 (HES1) is a transcriptional modulator and target of Notch signaling. Hes1 expression is significantly increased in Notch2tm1.1Ecan bone marrow-derived macrophages (BMM) as they mature into osteoclasts. However, the role of HES1 in the HCS phenotype and osteoclastogenesis is not known. To determine whether HES1 is responsible for the phenotype of Notch2tm1.1Ecan mice and the manifestations of HCS, Hes1 was inactivated in osteoclasts from Notch2tm1.1Ecan mice. CtskCre/WT;Hes1loxP/loxP mice were crossed with Notch2tm1.1Ecan;Hes1loxP/loxP mice to inactivate Hes1 in the context of the Notch2 mutation. Notch2tm1.1Ecan mice displayed decreased bone volume/total volume (BV/TV), which was significantly increased in the context of the Hes1 inactivation so that the osteopenia of Notch2tm1.1Ecan mice was nearly resolved. Moreover, the inactivation of Hes1 in Notch2tm1.1Ecan osteoclast precursors decreased the enhanced osteoclastogenesis observed in Notch2tm1.1Ecan mutant cells. To confirm a role of Hes1 in osteoclastogenesis and bone homeostasis, CtskCre/WT;Hes1loxP/loxP mice were crossed with Hes1loxP/loxP mice to generate CtskCre;Hes1Δ/Δ and littermate Hes1loxP/loxP controls. Hes1 mRNA was decreased 50-80% in osteoclasts and tibiae from CtskCre;Hes1Δ/Δ mice. Inactivation of Hes1 in Ctsk-expressing cells markedly increased BV/TV in male and to a greater extent in female mice which exhibited a 52% increase in femoral BV/TV compared to controls. Cultures of BMMs from CtskCre;Hes1Δ/Δ mice displayed a decrease in osteoclast number and size, and decreased bone-resorbing capacity. In contrast, HES1 activation in Ctsk-expressing cells enhanced osteoclast number, size and bone resorption, resulting in osteopenia. RNAseq from these osteoclasts revealed that genes associated with osteoclastogenesis, particularly for cell movement and assembly were significantly increased, whereas inhibitors of osteoclastogenesis were suppressed. In conclusion, HES1 is a determinant of osteoclastogenesis and is a primary effector of NOTCH2 signaling and mechanistically relevant to the skeletal manifestation of HCS.

***Disclosures: Jungeun Yu**, None*

1037

Zoledronic Acid Maintains Areal Bone Density after Denosumab Administration (DATA-HD Extension) *Sabashini K. Ramchand[1], Natalie L. David[1], Hang Lee[2], Joy N. Tsai[1], Benjamin Z. Leder[1]. [1]Department of Medicine, Endocrine Unit, Massachusetts General Hospital, Harvard University, United States, [2]Biostatistics Center, Massachusetts General Hospital, Harvard University, United States

Background: When denosumab (DMAB) is stopped, high-turnover bone loss ensues. The optimal way to prevent this bone loss has not been defined. In DATA-HD, we reported that teriparatide (TPTD) combined with denosumab dramatically increased BMD at all anatomic sites. In DATA-HD Extension, we now test the hypothesis that a single dose of zoledronate (ZOL), given after DMAB, can preserve these large BMD gains for an additional 27 months.Methods: In DATA-HD, postmenopausal osteoporotic women were randomized

to receive 9 months of either 20-µg or 40-µg of TPTD daily in combination with DMAB (60-mg administered at months 3 and 9). At the completion of this 15-month study, women enrolled in the DATA-HD Extension where they received a single dose of ZOL (5-mg i.v.) 24-35 weeks after the last DMAB dose. BMD and bone turnover markers were assessed 12 and 27 months after ZOL.Results: 53 women (mean age 66) completed DATA-HD and enrolled in DATA-HD Extension. At the femoral neck (FN) and total hip (TH), the mean 5.6% and 5.1% gains in BMD achieved from month 0-15 were maintained both 12 and 27 months after ZOL administration (Figure). At the spine, the mean 13.5% gain in BMD achieved from month 0-15 was maintained for the first 12 months but modestly decreased thereafter resulting in a 3.0% reduction (95% CI -2.0 to -4.0%, P<0.0001) 27 months after ZOL. Spine BMD remained 10.1% higher than the original DATA-HD baseline. The pattern of BMD changes between months 15-42 were qualitatively similar in the 20-µg and 40-µg groups. BMD changes were also compared among those who received ZOL early (30 weeks, n=15) by ANOVA. Between months 15-27, FN (but not TH or spine) BMD decreased more in those patients who received ZOL early versus those who received it late (P=0.04) but this difference did not persist to month 42. Analysis of bone turnover markers are pending due to lab closures during the COVID-19 pandemic.Conclusions: A single dose of ZOL effectively maintains the large and rapid TH and FN BMD increases achieved with combination TPTD/DMAB therapy for at least 27 months following the transition. Spine BMD was also largely, though not fully, maintained during this period. These data suggest that the DATA-HD Extension regimen (short-term combination DMAB/TPTD therapy follow by a single dose of ZOL) may be a particularly effective strategy in the long-term management of patients at high risk of fragility fracture.

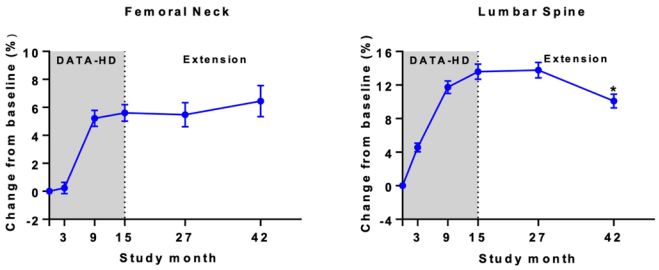

Bone density changes from baseline of pooled data from 53 women (TPTD 20-µg + DMAB and TPTD 40-µg + DMAB groups) who completed DATA-HD and enrolled in the Extension study. Women were given a single dose of zoledronate at month 15 and then completed 27 months of follow-up without further intervention. Data are presented as mean (SEM). *P<0.0001 for percent change from month 15 to 42 at the lumbar spine. Percent changes from month 15 to 27 at the lumbar spine and femoral neck, and from month 15 to 42 at the femoral neck were not significant.

***Disclosures: Sabashini K. Ramchand**, None*

1038

Effect of Zoledronic Acid on Volumetric Bone Density and Microarchitecture after Denosumab Administration (DATA-HD Extension HR-pQCT Study) *Sabashini K. Ramchand[1], Natalie L. David[1], Hang Lee[2], Michael Bruce[1], Mary L. Bouxsein[3], Joy N. Tsai[1], Benjamin Z. Leder[1]. [1]Department of Medicine, Endocrine Unit, Massachusetts General Hospital, Harvard University, United States, [2]Biostatistics Center, Massachusetts General Hospital, Harvard University, United States, [3]Department of Orthopedic Surgery, Harvard Medical School, Beth Israel Deaconess Medical Center, United States

Background: In the original DATA-HD study, we reported that 15-months of combined teriparatide and denosumab resulted in large BMD gains at the hip and spine, and improvements in volumetric BMD (vBMD) and microarchitecture at peripheral anatomic sites. Based on limited evidence from bone turnover marker and areal BMD studies, consolidation treatment with zoledronate (ZOL) has been proposed as a potential strategy to mitigate post-denosumab bone loss. ZOL's capacity to maintain improvements in peripheral volumetric and compartmental BMD and microarchitecture, however, have not been studied previously.Methods: In DATA-HD, postmenopausal osteoporotic women were randomized to receive 9 months of either 20-µg or 40-µg of TPTD daily in combination with DMAB (60-mg administered at months 3 and 9). At the completion of this 15-month study, women enrolled in the DATA-HD Extension where they received a single dose of ZOL (5-mg i.v.) 24-35 weeks after the last DMAB dose. HR-pQCT of the distal radius and distal tibia were assessed 12 and 27 months after ZOL.Results: 53 women (mean age 66) completed DATA-HD and enrolled in DATA-HD Extension. At the distal tibia, total vBMD decreased by 1.0% (95% CI -0.6 to -1.3, P<0.0001) and 2.7% (-2.0 to -3.3, P<0.0001) 12 and 27 months after ZOL (Figure). Cortical vBMD was not significantly decreased at 12 months but decreased by 1.5% (-0.8 to -2.1, P<0.0001) 27 months after ZOL. Cortical thickness decreased by 3.0% (-0.5 to -5.6, P=0.02) and 3.3% (-1.7 to -5.0, P<0.001) 12 and 27 months after ZOL, respectively, with no significant changes in cortical porosity. Results for total vBMD, cortical vBMD and cortical microstructure at the distal radius were similar (not shown). At both anatomic sites, trabecular vBMD, number, thickness, and separation were maintained 12 and 27 months after ZOL administration (P=NS for all comparisons). The pattern of BMD changes were qualitatively similar in the 20-µg and 40-µg groups.Conclusions: A single dose of ZOL effectively maintains trabecular, but not cortical, vBMD and microarchitecture at peripheral anatomic sites after treatment with combination TPTD/DMAB. These results are in contrast to the largely maintained hip and spine areal BMD over this period (as reported separately). Alternative treatment strategies that can fully maintain improvements in peripheral bone parameters require further study.

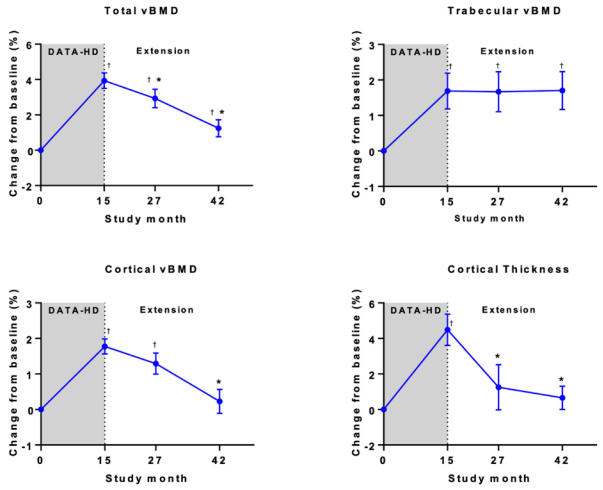

Distal tibia volumetric bone density and cortical thickness changes from baseline of pooled data from 53 women (TPTD 20-µg + DMAB and TPTD 40-µg + DMAB groups) who completed DATA-HD and enrolled in the Extension study. Women were given a single dose of zoledronate at month 15 and then completed 27 months of follow-up without further intervention. Data are presented as mean (SEM). †P<0.05 for percent change from baseline, *P<0.05 for percent change from month 15.

***Disclosures: Sabashini K. Ramchand**, None*

1039

Effects of Teriparatide on Modeling-based and Remodeling-based Bone Formation in the Human Femoral Neck *David Dempster[1], Jeri Nieves[1], Hua Zhou[2], Mathias Bostrom[3], Felicia Cosman[1]. [1]Columbia University, United States, [2]Helen Hayes Hospital, United States, [3]Hospital for Special Surgery, United States

Purpose: We have previously shown that a brief course of teriparatide (TPTD) stimulates bone formation in the cancellous and endocortical envelope of the human femoral neck (1). The purpose of the present study was to determine how much of the new bone was formed by modeling-based formation (MBF) or remodeling-based formation (RBF). Methods: We performed a double-blind trial of TPTD vs Placebo (PBO) in patients about to undergo a total hip replacement (THR) for osteoarthritis. Participants were randomized to receive daily TPTD 20ug or PBO for an average of 6.1 weeks (range 4.1-11.8 weeks) prior to THR. After an average of 3 weeks of study drug, double tetracycline labels were administered per standard protocol. During the THR, an intact sample of the mid-femoral neck (FN) was procured; this was fixed, embedded, and sectioned transversely. Histomorphometric analysis was performed in the cancellous, endocortical, intracortical, and periosteal envelopes, while blinded to treatment group. Sites of new bone formation were identified by the presence of tetracycline labels. Mineralizing surface (MS) was designated as MS.MBF if the underlying cement line was smooth and as MS.RBF if it was scalloped. MS over smooth cement lines adjacent to scalloped reversal lines was designated as overflow (MS.oRBF). The referent for all indices was bone surface (BS).Results: The results are shown in the tables below. In the cancellous and endocortical envelopes, MS.RBF/BS and MS.oRBF/BS were significantly higher in the TPTD-treated than the PBO-treated subjects. Differences were about 2 fold for MS.RBF/BS and about 6 fold for MS.oRBF/BS. There was a trend towards higher MS.MBF/BS in TPTD vs PBO in both envelopes. Eroded surface was not different between groups in either envelope. No significant differences were observed in any parameter in the intracortical and periosteal envelopes.Conclusion: We conclude that the predominant early effect of TPTD in the human femoral neck is to stimulate RBF and oRBF with a trend towards an increase in MBF. Despite the differences in loading between the FN and iliac crest, our findings in the femoral neck are very similar to those seen with early TPTD in the iliac crest. Given the short duration of treatment, and the lack of difference in eroded surface, the TPTD mediated increase in bone formation likely occurred in pre-existing remodeling units1. JCEM 2016;101:1498-1505Values in the table are Mean+/-SD; *Student's t-test.

Cancellous envelope

	MS.MBF/BS (%)	MS.RBF/BS (%)	MS.oRBF/BS (%r)
TPTD (n=18)	**1.14**±1.31	**5.99**±4.26	**1.29**±1.74
PBO (n=17)	**0.49**±0.62	**3.43**±2.93	**0.24**±0.28
P-value*	<0.07	**<0.05**	**<0.02**

Endocortical envelope

	MS.MBF/BS (%)	MS.RBF/BS (%)	MS.oRBF/BS (%r)
TPTD (n=18)	**4.07**±5.85	**11.99**±5.10	**1.78**±1.38
PBO (n=17)	**2.99**±3.63	**6.36**±4.40	**0.33**±0.50
P-value*	NS	**<0.001**	**<0.0005**

***Disclosures: David Dempster**, Eli Lilly, Grant/Research Support*

1040

Effects of Abaloparatide on Modeling and Remodeling Based Bone Formation *David W. Dempster[1], Hua Zhou[1], Sudhaker D. Rao[2], Chris Recknor[3], Paul D. Miller[4], Benjamin Z. Leder[5], Miriam Annett[6], Michael S. Ominsky[6], Bruce H. Mitlak[6]. [1]Regional Bone Center, Helen Hayes Hospital, United States, [2]Bone & Mineral Research Laboratory, Henry Ford Health System, United States, [3]United Osteoporosis Centers, United States, [4]Colorado Center for Bone Research, United States, [5]Mass General Hospital, Harvard Medical School, United States, [6]Radius Health, Inc., United States

Objective: To evaluate abaloparatide-induced changes in the bone formation indices of mineralizing surface (MS), bone formation rate (BFR) and mineral apposition rate (MAR); and to assess the effect of abaloparatide on 3 types of bone formation: modeling-based formation (MBF), remodeling-based formation (RBF), and overflow MBF (oMBF) in transiliac bone biopsies.Methods: Twenty-three postmenopausal women with osteoporosis were enrolled at 4 centers in the US; all received open label abaloparatide (80 µg/day SC) for 3 months. Subjects were administered double fluorochrome labeling at baseline and prior to biopsy at 3 months. Bone formation indices were evaluated by histomorphometry. Changes at 3 months from baseline were assessed for the indices on cancellous, endocortical, intracortical and periosteal bone envelopes. Sites of bone formation were designated as MBF if the underlying cement line was smooth, RBF if scalloped, and oMBF if formed over smooth cement lines adjacent to scalloped reversal lines. Paired t-tests were used to compare the differences of the indices between baseline and 3 months in the 4 bone envelopes. Results: Bone biopsies were obtained from 19 of the 23 subjects were enrolled in the study; all biopsies were evaluable. After 3 months of abaloparatide treatment, MS/ BS increased significantly from baseline in all of the 4 bone envelopes ($p < 0.001$), BFR/BS increased significantly in cancellous, endocortical and intracortical envelopes ($p < 0.001$); no significant change was observed in MAR in the 4 bone envelopes. Consistent with MS/BS, RBF/BS, MBF/BS and oMBF/BS increased significantly from baseline in the cancellous and endocortical envelopes ($p < 0.001$), as did MBF/BS in the periosteum ($p < 0.001$).Conclusions: This study provides histomorphometric evidence that abaloparatide has a robust effect on bone formation in postmenopausal women with osteoporosis after 3 months of treatment. Both modeling- and remodeling-based bone formation were stimulated. This study also shows that abaloparatide has a favorable effect on cortical bone by increasing bone formation in endocortical and periosteal envelopes.

MS/BS Distributed Between Modeling and Remodeling Bone Formation After 3 Months of Abaloparatide Treatment

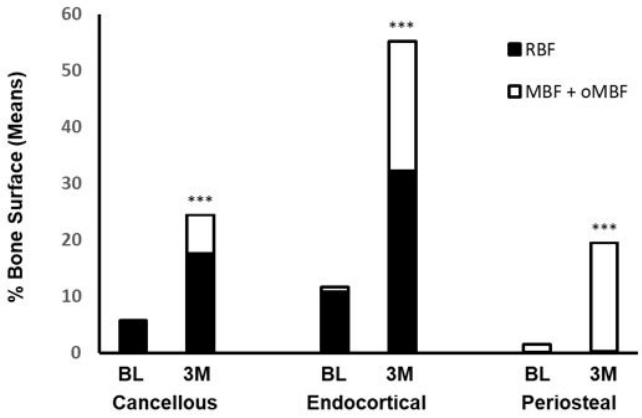

*** P<0.001 for MS/BS comparing 3 months to baseline
BL = Baseline, 3M = 3 Months

***Disclosures: David W. Dempster**, Radius Health, Inc., Speakers' Bureau, Radius Health, Inc., Consultant, Radius Health, Inc., Grant/Research Support*

1041

Kinetic Reconstruction of the Cancellous and Endocortical Remodeling Unit Reveals a Net Positive Bone Balance After 12 Months of Treatment with Romosozumab *Erik F Eriksen[1], Rogely Waite Boyce[2], Yifei Shi[2], Jacques P Brown[3], Stephane Horlait[2], Cesar Libanati[4], Roland Chapurlat[6], Pascale Chavassieux[6]. [1]Oslo University Hospital, Norway, [2]Amgen Inc., United States, [3]CHU de Quebec Research Centre, Canada, [4]UCB BioPharma, Belgium, [6]Université de Lyon, United States, [6]Université de Lyon, France

Purpose: EVENITY® (romosozumab-aqqg (Romo)) is a monoclonal antibody that inhibits sclerostin, leading to a rapid transient increase in modeling-based bone formation and a sustained decrease in resorption (Chavassieux JBMR 2019; Eriksen ASBMR 2019). To assess the effect of Romo on bone formation and resorption at the level of the basic multicellular unit (BMU) and determine integral effects on BMU bone balance (BB) at 12 months, after the bone formation response has attenuated, 3D reconstruction of the cancellous (Cn) and endocortical (Ec) BMU (Eriksen Bone 1986) was performed on biopsies from the FRAME trial (NCT01575834).Methods: In FRAME, transiliac biopsy sections were obtained after 12 months (M12) of Romo or placebo (Pbo) treatment; histomorphometric parameters were measured on Cn and Ec envelopes. Erosion depth (E.De; classified by the predominate resorptive cell type), osteoid thickness (O.Th), and completed and incomplete wall thickness (W.Th) were based on counting of lamellae in polarized light. To assess effects on the formative site at M12, O.Th/mineralized (Md) W.Th at osteoid surfaces was classified using a 4-sector system; the sector containing the nearly completed formative sites provided the reconstructed W.Th. Kinetics of remodeling phases were reconstructed according to Steiniche (Bone 1992). The comparison of Romo vs Pbo on remodeling parameters was done using the Wilcoxon rank-sum test, without multiplicity adjustment.Results: On Cn envelope, Romo resulted in a net positive BB compared with Pbo primarily due to sustained reduction in resorptive cell activity throughout 12 months, resulting in a significant reduction in final (Pre-Ob) E.De. On Ec envelope, Romo also resulted in a net positive BB, not due to effects on resorption but due to positive effects on the formative site. Consequently, Romo significantly increased W.Th in bone packets that had completed by M12. This effect was not sustained in actively forming packets at the end of treatment, suggesting these positive effects on bone formation at the BMU occurred earlier in treatment.Conclusion: After 12 months of Romo, a positive BB at the level of individual BMUs was evident on Cn and Ec envelopes, predominantly due to a net decrease in resorptive cell activity in Cn bone and a net increase in osteoblastic function in Ec bone. These effects likely contribute to the progressive increase in bone mass and microarchitectural improvements with Romo across 12 months of treatment.

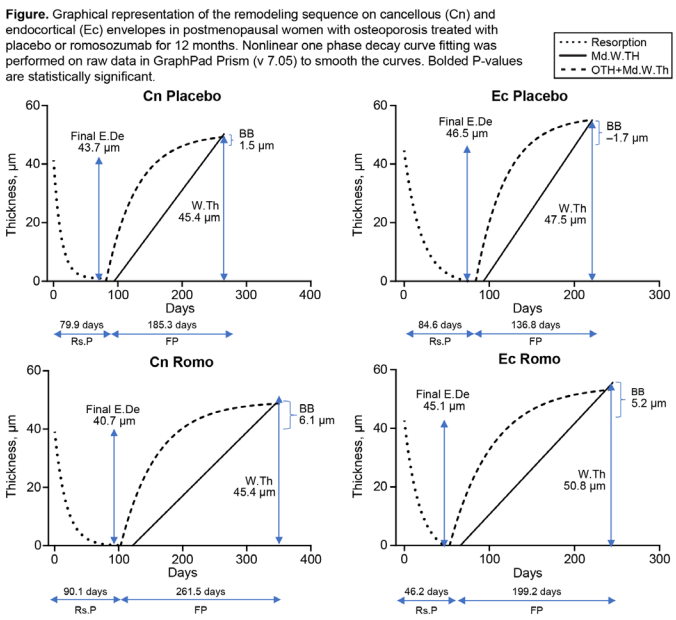

Figure. Graphical representation of the remodeling sequence on cancellous (Cn) and endocortical (Ec) envelopes in postmenopausal women with osteoporosis treated with placebo or romosozumab for 12 months. Nonlinear one phase decay curve fitting was performed on raw data in GraphPad Prism (v 7.05) to smooth the curves. Bolded P-values are statistically significant.

BB = bone balance; FP = formative phase; Md.W.Th = mineralized wall thickness; OTh = osteoid thickness; Final E.De = pre-osteoblast (final) erosion depth; Rs.P = resorptive phase; W.Th = wall thickness

	Placebo N = 31	Romosozumab N = 39	P-value
Remodeling Parameter, µm, median (Q1, Q3)			
Cancellous envelope			
Osteoclast erosion depth	18.1 (14.5, 22.4)	15.4 (11.1, 18.4)	**0.027**
Mononuclear cell erosion depth	33.6 (27.7, 36.9)	29.3 (22.4, 34.1)	0.067
Final erosion depth	43.7 (40.0, 49.0)	40.7 (36.7, 46.2)	**0.05**
Wall thickness	45.4 (41.5, 48.8)	45.4 (41.6, 50.6)	0.57
Reconstructed wall thickness	51.2 (46.2, 55.5)	51.2 (46.7, 57.2)	0.64
Bone balance	1.5 (–6.1, 6.1)	6.1 (1.5, 9.0)	**0.012**
Endocortical envelope			
Osteoclast erosion depth	19.2 (14.9, 23.0)	12.8 (9.6, 17.1)	**<0.001**
Mononuclear cell erosion depth	33.1 (28.6, 40.9)	26.7 (21.5, 30.7)	**<0.001**
Final erosion depth	46.5 (43.3, 55.8)	45.1 (39.2, 52.9)	0.33
Wall thickness	47.5 (41.9, 52.1)	50.8 (45.4, 53.3)	**0.037**
Reconstructed wall thickness	56.0 (48.9, 63.1)	56.5 (49.9, 62.1)	0.84
Bone balance	–1.7 (–6.6, 3.4)	5.2 (–2.0, 11.9)	**0.02**

***Disclosures: Erik F Eriksen**, Takeda, Amgen, Eli Lilly, EffRx, Ascendis, Consultant, Takeda, Amgen, Other Financial or Material Support, Takeda, Amgen, Grant/Research Support*

1042

Treatment Sequences With Romosozumab Before or After Antiresorptive Medication *Felicia Cosman[1], David Kendler[2], Bente Langdahl[3], Benjamin Z Leder[4], E. Michael Lewiecki[5], Akimitsu Miyauchi[6], Maria Rojeski[7], Michele McDermott[7], Mary Oates[7], Cassandra E Milmont[7], Cesar Libanati[8], Serge Ferrari[9]. [1]Columbia University, United States, [2]University of British Columbia, Canada, [3]Aarhus University Hospital, Denmark, [4]Harvard Medical School, United States, [5]New Mexico Clinical Research & Osteoporosis Center, United States, [6]Miyauchi Medical Center, Japan, [7]Amgen Inc., United States, [8]UCB Pharma, Belgium, [9]Geneva University Hospital, Switzerland

Prior studies of anabolic/antiresorptive (AR) treatment sequences indicate that using teriparatide (TPTD) first followed by an AR results in greater BMD gains, particularly at the total hip (TH), vs using an AR first followed by TPTD (Cosman JBMR 2017). Romosozumab (Romo) increases bone formation while decreasing bone resorption, significantly increasing BMD and reducing fracture risk within 1 year. Here we summarize BMD data with Romo prior to or following an AR (alendronate [Aln] or denosumab [DMAb]).We evaluated percentage change from baseline in BMD at the TH and lumbar spine (LS) from four trials where patients received Romo prior to an AR (Phase 3 ARCH [Saag NEJM, 2017] and Phase 3 FRAME [Cosman, NEJM 2016]) or Romo following an AR (Phase 3 STRUCTURE [Langdahl, Lancet 2017] and Phase 2 [Kendler, OI 2019]). Percentage change from baseline BMD was assessed by either an ANCOVA (FRAME) or repeated measures (ARCH, STRUCTURE) model adjusting for baseline covariates, or as summary statistics (Phase 2).TH BMD (Fig 1): In ARCH, BMD increased 6.2% with 1 year of Romo, and a total of 7.1% with the 2-year Romo/Aln sequence; and in FRAME, patients gained 6.8% with 1 year of Romo and a total of 8.8% with the 2-year Romo/DMAb sequence. Patients in STRUCTURE, who were previously treated for >=1 year with Aln, gained 2.9% with 1 year of Romo. In a Phase 2 study, following 1 year of DMAb, 1 year of Romo increased BMD by 0.9%, for a total gain of 3.8% with the 2-year DMAb/Romo sequence.LS BMD (Fig 2): In ARCH, BMD increased 13.7% with 1 year of Romo, and a total of 15.2% with the 2-year Romo/Aln sequence; and in FRAME, patients gained 13.3% with 1 year of Romo and a total of 17.6% with the 2-year Romo/DMAb sequence. Patients in STRUCTURE (previously on Aln for >=1 year) gained 9.8% with 1 year of Romo. In the Phase 2 study (after 1 year of DMAb), 1 year of Romo increased BMD by 5.3%, for a total gain of 11.5% with the 2-year DMAb/Romo sequence.These data demonstrate that treatment with Romo first produces substantial BMD gains at the TH and LS within 1 year, and that subsequent transition to a potent AR can augment those gains. In patients treated with Aln or DMAb, transition to Romo can improve BMD, though gains are not as large as those seen when Romo is used first. Since BMD on treatment is a strong surrogate for bone strength, our findings support the concept that high-risk patients should be offered treatment with Romo first, followed by transition to a potent AR.

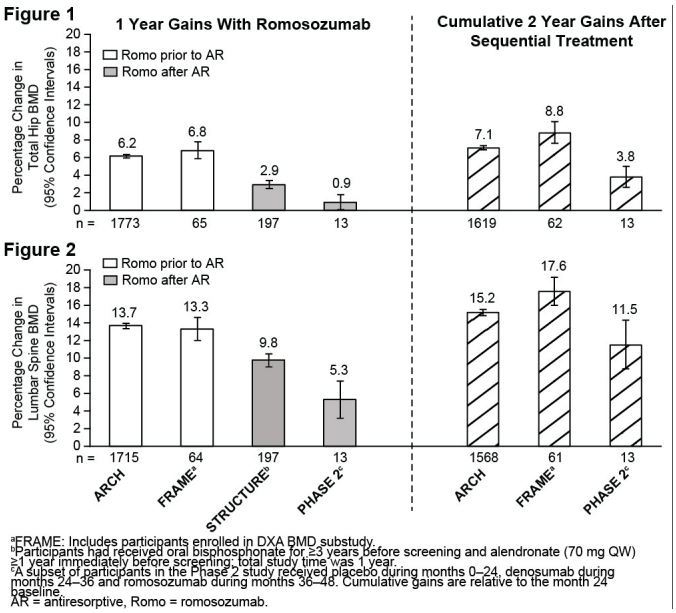

[a]FRAME: Includes participants enrolled in DXA BMD substudy.
[b]Participants had received oral bisphosphonate for ≥3 years before screening and alendronate (70 mg QW) ≥1 year immediately before screening; total study time was 1 year.
[c]A subset of participants in the Phase 2 study received placebo during months 0–24, denosumab during months 24–36 and romosozumab during months 36–48. Cumulative gains are relative to the month 24 baseline.
AR = antiresorptive, Romo = romosozumab.

***Disclosures: Felicia Cosman**, Amgen Inc., Grant/Research Support, Amgen Inc., Consultant, Radius Health, Speakers' Bureau, Amgen Inc., Speakers' Bureau, Radius Health, Consultant*

1043

Burosumab Led to Durable Improvements in Biochemical, Skeletal, and Clinical Features of Tumor-induced Osteomalacia Syndrome (TIO) *Suzanne Jan de Beur[1], Thomas J. Weber[2], Munro Peacock[3], Karl Insogna[4], Rajiv Kumar[5], Paul Miller[6], Diana Luca[7], Tricia Cimms[7], Mary Scott Roberts[7], Thomas Carpenter[4]. [1]Johns Hopkins University School of Medicine, United States, [2]Duke University, United States, [3]Indiana University School of Medicine, United States, [4]Yale University School of Medicine, United States, [5]Mayo Clinic College of Medicine, United States, [6]Colorado Center for Bone Research, United States, [7]Ultragenyx Pharmaceutical Inc, United States

TIO is a rare disease in which tumors produce FGF23, leading to renal phosphate wasting, impaired 1,25(OH)2D synthesis, osteomalacia, fractures, weakness, fatigue, and impaired mobility. In an ongoing, open-label phase 2 trial (NCT02304367), 17 adults with TIO or cutaneous skeletal hypophosphatemia syndrome (CSHS) were enrolled and received burosumab, a fully human monoclonal antibody against FGF23. Here we report safety and efficacy through week 144 (W144). Key endpoints: changes in serum phosphorus and osteomalacia assessed by bone biopsy. Two patients with X-linked hypophosphatemia diagnosed post-enrollment and 1 with CSHS are excluded.Serum phosphorus increased from baseline (BL) and was maintained through W144 (figure). Serum TmP/GFR and 1,25(OH)2D also increased with burosumab.Eleven patients had paired bone biopsies at BL and W48. Mean+/-SE osteoid volume/bone volume decreased (BL: 17.6+/-5.9%; W48: 12.1+/-4.7%; p=0.086). Osteoid thickness decreased (BL: 16.5+/-3.6 µm; W48: 11.3+/-2.8 µm; p<0.05). Using imputation (Dempster 2012), mineralization lag time decreased (BL: 1598+/-420 days; W48: 1032+/-712 days; p=0.41). Osteoid surface/bone surface showed no change (BL: 57+/-9%; W48: 57+/-8%). At BL, 249 fractures/pseudofractures were identified by increased uptake on bone scan; 81 (33%) were fully healed and 32 (13%) were partially healed at W144.Mean (SD) Global Fatigue Score decreased (BL: 5.6 [2.5]; W144: 3.8 [2.2]; p<0.01), indicating reduced fatigue. All domains of the Brief Pain Inventory decreased (W144 Pain Severity and Pain Interference p<0.05), indicating reduced pain. The SF-36v2 mean (SD) physical component summary score increased (BL: 33 [10]; W144: 41 [12]; p<0.01), indicating improved physical functioning. Mean (SD) number of sit-to-stand repetitions increased (BL: 6.7 [4.2]; W48: 8.5 [4.2]; n=10; p<0.01), indicating improved proximal muscle strength and function. All patients had >=1 adverse event (AE). Two discontinued: 1 for chemotherapy to treat neoplasm progression; 1 failed to meet serum phosphorus dosing criteria and received minimal burosumab. There were 16 serious AEs in 7 patients, including 1 death. All were considered unrelated to burosumab. Six patients had a serious AE of tumor progression/compression, 5 of whom had a history of tumor progression.In adults with TIO, burosumab was associated with durable improvements in phosphate metabolism, osteomalacia, fracture healing, and physical functioning and reduced fatigue and pain.

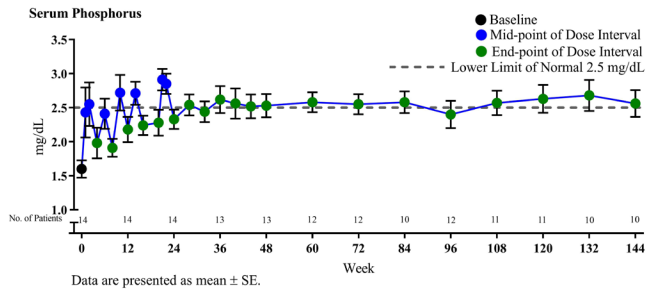

***Disclosures: Suzanne Jan de Beur**, Ultragenyx, Mereo BioPharma Group, Grant/ Research Support, Ultragenyx Pharmaceutical Inc, Consultant, Ultragenyx Pharmaceutical Inc, Other Financial or Material Support*

1044

Efficacy of burosumab in adults with X-linked hypophosphataemia (XLH): A subgroup analysis of a randomized, double-blind, placebo-controlled, phase 3 study *Maria Luisa Brandi[1], Wei Sun[2], Angela Williams[3], Annabel Nixon[4], Karl Insogna[5]. [1]Azienda Ospedaliero Universitaria Careggi, Italy, [2]Kyowa Kirin Pharmaceutical Development, United States, [3]Kyowa Kirin International, United Kingdom, [4]Chilli Consultancy, United Kingdom, [5]Yale University School of Medicine, United States

OBJECTIVE: XLH is a rare, lifelong, progressive phosphate wasting disorder causing substantial musculoskeletal and functional morbidities. Data demonstrate that treatment with burosumab in adults leads to sustained correction of serum phosphate levels, healing of fractures and pseudofractures, and sustained improvement in key musculoskeletal symptoms and impairments. The aim of the exploratory subgroup analyses is to assess whether treatment effects differed for distinct patient clusters by utilizing the data from CL303 (NCT02526160).METHODS: CL303 is a phase 3 multicenter, randomized, double-blind, placebo-controlled study that evaluated the efficacy and safety of burosumab in adults with XLH. Subjects were randomly allocated (1:1) to burosumab or placebo, stratified by pain intensity and region. This comprehensive subgroup analysis was performed to assess the treatment effects of burosumab during a 24-week double blind placebo-controlled period across 14 pre-defined, clinically relevant subgroups defined before the post hoc analysis, including 5 pre-specified subgroups in study design (BPI worst pain at baseline, BPI average pain at baseline, region, gender and race group). Week 24 Primary Analysis Set was used for the 12 efficacy endpoints evaluated in the analysis.RESULTS: This phase 3 study had 134 randomized subjects (68 in burosumab and 66 in placebo; 65% female; median age 41 years [18–65 years]). There were no statistically significant interactions between the pre-defined subgroups and treatment arm on serum phosphate, BPI worst pain, WOMAC stiffness or WOMAC physical function (p for interaction terms >0.05). Results of 12 of the pre-defined subgroup analyses were consistent with the results from the study population with regard to showing a favourable direction of effect of burosumab relative to placebo. However, for two subgroups variation in treatment response was observed (BFI and BPI Pain Interference). CONCLUSIONS: Subgroup analyses with the double-blind treatment period data showed that burosumab was superior to placebo in the primary, key secondary and many other efficacy endpoints across the pre-defined subgroups.

***Disclosures: Maria Luisa Brandi**, Kyowa Kirin International, Consultant*

1045

Three-Year Safety and Efficacy Results of Burosumab for Children Aged 1 to 4 years with X-linked Hypophosphatemia (XLH) *Erik Imel[1], Thomas Carpenter[2], Gary Gottesman[3], Angel Chen [4], Alison Skrinar[4], Mary Scott Roberts[4], Michael P Whyte[5]. [1]Indiana University School of Medicine, United States, [2]Yale University School of Medicine, United States, [3]Shriners Hospitals for Children, St Louis, United States, [4]Ultragenyx Pharmaceuticals Inc., United States, [5]Washington University School of Medicine and Indiana University School of Medicine, United States

XLH is a rare disease involving excess FGF23 that, in children, leads to hypophosphatemia and rickets. Burosumab, a fully human monoclonal antibody against FGF23 approved for XLH treatment, improved rickets in both clinical trials in children aged 5-12 yrs and 1-12 yrs. Here, we report final, 3-year safety and efficacy data from an open label, phase 2 study of burosumab in children aged 1-4 yrs with XLH (NCT02750618).Eligibility criteria included hypophosphatemia and radiographic evidence of rickets. The primary endpoint was fasting serum phosphorus level. Key secondary endpoints were Thacher Rickets Severity Score (RSS) and Radiographic Global Impression of Change (RGI-C). Patients (pts) received SC burosumab every 2 weeks starting at 0.8 mg/kg for 160 weeks (64-week treatment + 96-week extension periods).All 13 enrolled pts completed the 64-week treatment period; 12 completed 160 weeks; 1 withdrew at week 112 (W112) to transition to commercially available burosumab. 8 pts (62%) maintained a dose of 0.8 mg/kg; 5 (38%) had dose increases to 1.2 mg/kg. At baseline (BL), mean (SD) age was 2.9 (1.1) yrs; 69% were male. All had received prior treatment with oral phosphate and active vitamin D starting at a mean (SD) age of 19.6 (18.0) months and a duration of 16.4 (13.8) months.Burosumab rapidly normalized fasting serum phosphorus with mean (SD) levels of 2.5 (0.3) mg/dL at BL and 3.7 (0.5) mg/dL at W1. Levels were maintained through W160 (Table). Serum 1,25(OH)2D increased initially then returned to BL, as reported in other studies. Rickets significantly improved: total RSS decreased, and global RGI-C and lower limb deformity RGI-C scores were positive. Serum alkaline phosphatase (ALP) also improved (Table). Improvements were maintained through W160. Mean (SD) length/height Z-scores were maintained from BL (-1.4 [1.2]) through W160 (-1.5 [1.1]).The safety profile over 160 weeks was similar to previous pediatric studies; no new safety concerns emerged. All pts experienced >=1 treatment-emergent adverse event (TEAE). All but 2 TEAEs were mild (Grade 1) or moderate (Grade 2). One pt had a grade 3 TEAE of food allergy, one had a grade 3 TEAE of increased serum amylase. One pt had a serious TEAE of dental abscess. All were considered unrelated to study drug. Burosumab rapidly restored phosphorus homeostasis in children aged 1-4 yrs. Significant improvements in serum phosphorus and rickets were sustained through W160 with no new safety findings.

Efficacy Parameter, mean (SD)	Baseline	Week 40	Week 64	Week 160
Phosphorus, mg/dL	2.5 (0.3)	3.5 (0.5)	3.4 (0.5)	3.4 (0.5)
1,25(OH)$_2$D, pg/mL	44.8 (17.6)	56.8 (10.3)	55.9 (9.2)	47.2 (8.8)
ALP, U/L	548.5 (193.8)	335.4 (87.6)	333.6 (80.5)	301.8 (70.7)
RSS Total Score	2.9 (1.4)	1.2 (0.5)	0.9 (0.5)	1.0 (0.6)
RGI-C: Global	–	+2.2 (0.3)	+2.2 (0.4)	+2.2 (0.4)
RGI-C: Lower Limb Deformity	–	+1.2 (0.6)	+1.5 (0.5)	+2.0 (0.3)

The normal range for serum phosphorus was 3.2–6.1 mg/dL. The normal range for 1,25(OH)$_2$D was 20.8–105.4 pg/mL.

***Disclosures: Erik Imel**, Ultragenyx Pharmaceutical Inc, Other Financial or Material Support, Ultragenyx Pharmaceutical Inc, Grant/Research Support*

1046

Palovarotene (PVO) for Fibrodysplasia Ossificans Progressiva (FOP): Data from the Phase III MOVE Trial *Robert J Pignolo[1], Mona Al Mukaddam[2], Geneviève Baujat[3], Staffan K Berglund[4], Angela M Cheung[5], Carmen De Cunto[6], Patricia Delai[7], Maja Di Rocco[8], Nobuhiko Haga[9], Edward C Hsiao[10], Peter Kannu[11], Richard Keen[12], Edna E Mancilla[13], Donna R Grogan[14], Rose Marino[14], Andrew Strahs[14], Frederick S Kaplan[2]. [1]Department of Medicine, Mayo Clinic, United States, [2]Departments of Orthopaedic Surgery & Medicine, The Center for Research in FOP and Related Disorders, Perelman School of Medicine, University of Pennsylvania, United States, [3]Département de Génétique, Institut IMAGINE and Hôpital Universitaire Necker-Enfants Malades, France, [4]Department of Clinical Sciences, Pediatrics, Umeå University, Sweden, [5]Department of Medicine and Joint Department of Medical Imaging, University Health Network, University of Toronto, Canada, [6]Pediatric Rheumatology Section, Department of Pediatrics, Hospital Italiano de Buenos Aires, Argentina, [7]Centro de Pesquisa Clinica, Hospital Israelita Albert Einstein, Brazil, [8]Unit of Rare Diseases, Department of Pediatrics, Giannina Gaslini Institute, Italy, [9]Department of Rehabilitation Medicine, The University of Tokyo Hospital, Japan, [10]Division of Endocrinology and Metabolism, UCSF Metabolic Bone Clinic, Institute of Human Genetics, and UCSF Program in Craniofacial Biology, Department of Medicine, University of California-San Francisco, United States, [11]Hospital for Sick children, Canada, [12]Centre for Metabolic Bone Disease, Royal National Orthopaedic Hospital, United Kingdom, [13]Children's Hospital of Philadelphia, Perelman School of Medicine, University of Pennsylvania, United States, [14]Ipsen, United States

Background: FOP is an ultra-rare, severely disabling, life-shortening genetic disorder characterized by progressive and cumulative heterotopic ossification (HO). PVO, an orally available, selective retinoic acid receptor-γ agonist, reduced HO in animal models and phase II trials.Objective: Assess efficacy and safety of chronic and episodic PVO in patients (pts) with FOP.Methods: Pts with FOP aged >=4 years were enrolled in the ongoing, 48-month, single-arm, open-label, phase III MOVE study (NCT03312634). PVO regimen (weight-ad-

justed in skeletally immature pts): chronic (5 mg daily) and episodic (20 mg daily for 4 weeks then 10 mg for >=8 weeks during flare-ups). Primary endpoint: annualized change in new HO volume, assessed by low-dose whole-body computed tomography (excluding head) vs untreated pts from a longitudinal natural history study (NHS; NCT02322255) using a Bayesian compound Poisson model with square-root (sqrt) transformation of new HO volumes. Interim efficacy analyses were planned for when all pts completed Month 12 (IA2) and 18 (IA3) assessments. Futility was prespecified as a <5% posterior probability of a >=30% reduction in sqrt-transformed annualized new HO volume. Post hoc analyses included Bayesian analysis without sqrt transformation and weighted linear mixed effects models (with/without sqrt transformation). Safety is assessed throughout.Results: Futility criteria were met at IA2; however, Bayesian analyses of non-transformed data would have exceeded the prespecified boundary for early efficacy (Table). IA3 analysis set was 97 pts (mean age 15.1 years; 52.6% male) from MOVE; 98 from the NHS (mean age 17.8 years; 55.1% male). At IA3, post hoc Bayesian analyses of non-transformed data continued to be statistically significant (p<0.025 1-sided) with a 62% reduction in mean annualized rate of new HO volume in PVO-treated vs untreated pts (Table). At data cut off, 100% of pts in MOVE had reported >=1 adverse event (AE); 97.0% reported >=1 retinoid-associated (eg mucocutaneous) AE. Maximum AE severity was mild in 32.3% of pts, moderate in 45.5%, and severe in 22.2%. Overall, 29.3% reported >=1 serious AE, including premature physeal closure (PPC) or epiphyseal disorder in 19 of 70 pts skeletally immature at Baseline.Conclusions: Although prespecified futility criteria were met, subsequent post hoc analyses showed substantial efficacy suggesting that, despite the risk of PPC in a subset of pts, PVO may be an important therapeutic option in FOP.

IA2: Bayesian compound Poisson analysis		
	Futility, Pr(γ<0.7) [a]	**Efficacy, Pr(γ<1)** [b]
Prespecified threshold	**<0.0500**	**>0.9932**
Sqrt-transformed (prespecified)	0.0488	0.8019
Non-transformed (ad hoc)	0.7898	0.9952
IA3: Bayesian compound Poisson analysis		
Effect size [95% credible interval]	**Median posterior γ**	**Efficacy, Pr(γ<1)** [c]
Sqrt-transformed	0.93 [0.72, 1.21]	0.6966
Non-transformed	0.62 [0.44, 0.88]	0.9961
IA3: Weighted linear mixed effects model		
Effect size [95% CI]	**Estimate**	**Efficacy P value**
Sqrt-transformed, $mm^{3/2}$	–12.6 [–36.4, 11.1]	0.288
Non-transformed, mm^3	–11,611 [–21,976, –1,246]	0.0292
IA3: Annualized HO volume		
	NHS	**MOVE**
	N=98	**N=97**
Mean [SEM] annualized HO volume, mm^3	23,318 [4,938]	8,821 [2,972]

[a] Futility was predefined as a <5% posterior probability of a ≥30% reduction in sqrt-transformed annualized new HO volume; [b] total type I error of 0.025 (one-sided) using O'Brien-Fleming spending function; [c] Nominal significance: Pr(γ<1)>0.9750; CI: confidence interval; HO: heterotopic ossification; IA2/3: interim analysis 2/3; NHS: natural history study; Pr: probability; SEM: standard error of the mean; sqrt: square root.

***Disclosures: Robert J Pignolo**, Research investigator: Clementia/Ipsen, Regeneron; Advisory board: President of the International Clinical Council on FOP; Chair of the Publications Committee for the IFOPA Registry Medical Advisory Board, Other Financial or Material Support*

1047

Garetosmab, an Inhibitor of Activin-A, Reduces Formation of Heterotopic Bone and Soft Tissue Flare-Ups in Patients with Fibrodysplasia Ossificans Progressiva *Maja Di Rocco[1], Eduardo Forleo-Neto[2], Robert Pignolo[3], Richard Keen[4], Philippe Orcel[5], Thomas Funck-Brentano[5], Christian Roux[6], Sami Kolta[5], Annalisa Madeo[1], Judith S Bubbear[4], Jacek Tabarkiewicz[7], Małgorzata Szczepanek[7], Javier Bachiller-Corral[8], Angela M Cheung[9], Kathryn M Dahir[10], Esmée Botman[11], Pieter G Raijmakers[12], Mona Al Mukaddam[13], Lianne Tile[9], Cynthia Portal-Celhay[2], Melissa Simek-Lemos[2], Bret Musser[2], Neena Sarkar[2], Peijie Hou[2], Anita Boyapati[2], Su Liang[2], Marcella Ruddy[2], Scott Mellis[2], Andrew Rankin[2], Aris N. Economides[2], Dinko Gonzalez Trotter[2], Gary Herman[2], David M. Weinreich[2], George D. Yancopolous[2], E. Marelise W. Eekhoff[14], Frederick S. Kaplan[13]. [1]Department of Pediatrics, Unit of Rare Diseases, IRCCS Istituto Giannina Gaslini, Italy, [2]Regeneron Pharmaceuticals, United States, [3]3Department of Medicine, Mayo Clinic, United States, [4]Centre for Metabolic Bone Disease Royal National Orthopaedic Hospital NHS Trust, United Kingdom, [5]Service de Rhumatologie - DMU Locomotion, AP-HP.Nord - Université de Paris, France, [6]Department of Rheumatology, Cochin Hospital, Assistance Publique - Hôpitaux de Paris, France, [7]Rzeszów University, Rzeszów, Poland, [8]Hospital Universitario Ramón y Cajal, Spain, [9]University Health Network, University of Toronto, Canada, [10]Vanderbilt University Medical Center, United States, [11]Department Internal Medicine section Endocrinology,Amsterdam UMC, Vrije Universiteit, Amsterdam Bone Center, Netherlands, [12]Department Radiology and Nuclear Medicine, Amsterdam UMC, Vrije Universiteit, Netherlands, [13]Departments of Orthopaedics, Medicine and the Center for Research in FOP & Related Disorders, University of Pennsylvania Perelman School of Medicine, United States, [14]Department Internal Medicine section Endocrinology, Amsterdam UMC, Vrije Universiteit, Netherlands*

Background:Fibrodysplasia ossificans progressiva (FOP) is an ultra-rare genetic disorder, characterized by painful flare-ups and episodic yet cumulative bone formation in soft tissues (Heterotopic Ossification, HO), which results in progressive immobility and early mortality. It has been proposed that the FOP mutation converts Activin A into an initiator of HO; a human monoclonal antibody against Activin A (Garetosmab, GAR) is effective in a humanized mouse model of FOP.Methods:LUMINA-1 (NCT03188666) evaluated the safety and efficacy of GAR in adult FOP patients randomized to GAR 10 mg/kg every 4 weeks (Q4w) IV (n=20) or placebo (PBO; n=24). The activity, size and number of HO lesions was assessed by 18F-sodium fluoride positron emission tomography (PET) and whole-body low-dose computerized tomography (CT), over 28 weeks. Flare-ups were evaluated by diary and investigator report.Results:Baseline demographics were similar in both groups, mean age (SD) was 27.6 (8.5) years and 43% male overall. Relative to placebo, GAR treatment decreased the total lesion activity (24.6% by PET, P =0.07) and total volume (24.9% by CT, P=0.37) of HO lesions (new and existing). HO burden was ameliorated by a nearly 90% relative reduction in the total volume of new HO lesions by CT (P =0.017) and a decrease in the number and rate of new HO lesions (number of new bone lesions/patient over 28 weeks in GAR/placebo or rate ratio=0.13 by PET, P=0.006; rate ratio=0.13 by CT, P=0.009; Figure). Fewer patients receiving GAR developed new HO (3/20, 15%) than placebo (11/24, 45.8%) (P=0.05). Patients receiving GAR experienced fewer flare-ups, as assessed by diary (relative risk [RR]=0.49, P=0.03) and investigator reports (RR=0.24, P=0.04). GAR treatment was associated with an increased incidence of epistaxis, headache, acne, madarosis and skin infections.Conclusions:GAR substantially reduces the formation of new HO lesions and flare-ups and demonstrates a favorable benefit/risk profile for adults with FOP. These results support that activin A is a key driver of HO in FOP.IMAGE ATTACHED

Figure: Total Number of Heterotopic Bone Lesions as Assessed by ^{18}F-NaF PET and CT at Week 28[a,b]

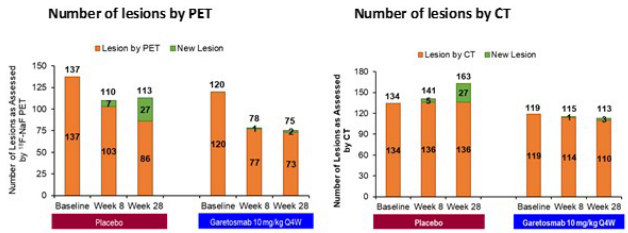

^{18}F-NaF PET, fluorine-18-labelled sodium fluoride positron emission tomography; CT, computed tomography; SUV, standardized uptake value.
[a]Figure shows data at specific timepoints (eg, week 28); the corresponding text in the abstract refers to time course (eg, over 28 weeks).
[b]New lesion criteria by ^{18}F-NaF PET: SUV_{max} that is ≥3 times the SUV_{mean} for the supra-acetabular ROI. New lesion criteria by CT: Density >200 HU with a volume of at least 1 cm^3. Maximum 7 lesions per patient were identified at baseline

***Disclosures: Maja Di Rocco**, None*

Saturday Orals

1048

A Randomized Controlled Trial of Vosoritide in Children with Achondroplasia *Ravi Savarirayan[1], Louise Tofts[2], Melita Irving[3], William Wilcox[4], Carlos Bacino[5], Julie Hoover-Fong[6], Rosendo Ullot Font[7], Paul Harmatz[8], Frank Rutsch[9], Michael Bober[10], Lynda Polgreen[11], Ignacio Ginebreda[12], Klaus Mohnike[13], Joel Charrow[14], Daniel Hoernschmeyer[15], Keiichi Ozono[16], Yasemin Alanay[17], Paul Arundel[18], Shoji Kagami[19], Natsuo Yasui[19], Klane White[20], Howard Saal[21], Antonio Leiva-Gea[22], Felipe Luna-González[23], Hiroshi Mochizuki[24], Donald Basel[25], Dania Porco[26], Kala Jayaram[26], Elena Fisheleva[26], Alice Huntsman-Labed[26], Jonathan Day[26]. [1]Murdoch Children's Research Institute, Royal Children's Hospital, and University of Melbourne, Australia, [2]The Children's Hospital at Westmead, Australia, [3]Guy's and St. Thomas' NHS Foundation Trust, Evelina Children's Hospital, United Kingdom, [4]Emory University, United States, [5]Baylor College of Medicine, United States, [6]Johns Hopkins University, United States, [7]Hospital Sant Joan de Déu, Spain, [8]UCSF Benioff Children's Hospital, United States, [9]Muenster University Children's Hospital, Germany, [10]AI Dupont Hospital for Children, United States, [11]Lundquist Institute Biomedical Innovation, United States, [12]Hospital Universitario Quirón Dexeus, Spain, [13]Universitätskinderklinik Madgdeburg, Germany, [14]Ann and Robert H. Lurie Children's Hospital of Chicago, United States, [15]University of Missouri-Columbia, United States, [16]Osaka University, Japan, [17]Acibadem Mehmet Ali Aydiniar University, Turkey, [18]Sheffield Children's NHS Foundation Trust, Sheffield Children's Hospital, United Kingdom, [19]Tokushima University Hospital, Japan, [20]Seattle Children's Hospital, United States, [21]University of Cincinnati College of Medicine, United States, [22]Hospital Universitario Virgen, Spain, [23]Hospitalario de Málaga, Spain, [24]Saitama Children's Hospital, Japan, [25]Medical College of Wisconsin, United States, [26]BioMarin, United States

Background: Achondroplasia is a disorder caused by specific mutations in the gene encoding the fibroblast growth factor receptor 3 (FGFR3) protein. Open-label, phase 2 trials in children with achondroplasia showed that administration of vosoritide, an analogue of C-natriuretic peptide, resulted in sustained increases in annualized growth velocity.Methods: This international, randomized, double-blind, phase 3 trial compared once-daily subcutaneous administration of vosoritide, at a dose of 15 mg per kg of body weight, with placebo in children with achondroplasia aged 5 to <18 years. Eligible patients had participated, for at least 6 months, in an observational growth study in order to calculate their baseline annualized growth velocity. The primary efficacy endpoint was the change from baseline in annualized growth velocity at week 52 of treatment. The primary analysis of the change from baseline in annualized growth velocity was performed using an ANCOVA model.Results: A total of 121 patients were randomized, with 60 assigned to receive vosoritide and 61 to receive placebo. A total of 119 patients completed the 52-week trial. The adjusted mean difference in annualized growth velocity between patients administered vosoritide and those administered placebo was 1.57 cm per year in favor of vosoritide (95% CI: [1.22, 1.93], two-sided p-value <0.001). A total of 119 patients experienced at least one adverse event (vosoritide group, 59 [98.3%], placebo group, 60 [98.4%]).Conclusions: Daily, subcutaneous administration of vosoritide to children with achondroplasia resulted in a significant increase in mean annualized growth velocity and similar incidence of adverse events compared to placebo.

***Disclosures: Ravi Savarirayan**, BioMarin, Consultant, BioMarin, Grant/Research Support*

1049

Augmentation of BMP signaling causes midfacial defects in mice via suppressing glucose metabolism *Jingwen Yang[1], Masako Toda[2], Shawn A. Hallett[1], Yuji Mishina[1]. [1]1. Department of Biologic and Materials Sciences, School of Dentistry, University of Michigan, Ann Arbor, MI 48109, USA., United States, [2]Department of Biologic and Materials Sciences, School of Dentistry, University of Michigan, Ann Arbor, MI 48109, USA., United States

Midfacial malformation is the most common birth defects among craniofacial abnormalities in humans. The majority of craniofacial tissues are derived from cranial neural crest cells (CNCCs). Energy metabolism, especially aerobic glycolysis, has been recently identified to promote neural crest migration and control posterior embryonic axis elongation. However, the involvement of glycolysis in midfacial development remains unknown. Here we generated a mouse model exhibiting unexpected midfacial defects via conditional expression of a constitutively activated (ca) Acvr1, which encodes a receptor for BMPs, in neural crest cells (ca-Acvr1fx/+;P0-Cre, hereafter referred to as mutant). ca-ACVR1 caused a 1.8-fold increase of pSmad1/5/9 level in nasal processes (NPs), resulting in severe midfacial defects in mutant embryos, including premaxilla bone hypoplasia, duplication of the nasal septum, and absence of philtrum and primary palate. Interestingly, RNA-seq analysis revealed significant downregulation of a series of glycolytic enzymes in mutant NPs, such as H6pd, Gpadh, and Ldhb. Glucose consumption and lactate production were decreased in post-migratory CNCCs from mutant NPs compared with controls. Nevertheless, the mitochondria amount, protein levels of oxidative phosphorylation complexes, and mitochondria membrane potential were unaltered in mutant NPs. Then, we sought to determine whether suppressed glycolysis is involved in ca-ACVR1-induced midfacial defects. Activation of glycolysis via administration of HIF-1α activator Dimethyloxalyl glycine (DMOG) into pregnant females rescued the midfacial defects in mutants. Of note, suppression of glycolysis using 2-Deoxy-D-glucose (2-DG), a competitive inhibitor of glucose metabolism, disturbed the proliferation, survival, and migration of post-migratory CNCCs from control NPs. We have previously found that pSmad interacts with p53 thus inhibiting MDM2-mediated p53 degradation (Development 142:1357, 2015). Here, p53 protein level was upregulated in mutant NPs. We further identified that enhanced BMP signaling suppresses glycolysis via augmentation of p53 signaling. Blockade of p53 activity using pifithrin-α significantly enhanced glycolysis activity and rescued the midfacial defects in mutants. Our results demonstrate that glycolysis regulated by BMP-p53 signaling axis is important for midfacial development and identify a novel therapeutic target for the prevention of midfacial defects.

***Disclosures: Jingwen Yang**, None*

1050

αE-catenin Deletion in Skeletal Stem and Progenitor Cells (SSPCs) Increases their Adipogenic Potential and Protects Against Diet- or Age-induced Obesity and Hyperglycemia *Karen De Samblancx[1], Marion Mesnieres[1], Dana Trompet[1], Naomi Dirckx[1], Katrien Corbeels[2], Elena Nefyodova[1], Ruben Cardoen[1], Jolanda van Hengel[3], Frans van Roy[3], Greetje Vande Velde[4], Bart Van der Schueren[2], Chantal Mathieu[2], Christa Maes[1]. [1]Laboratory of Skeletal Cell Biology and Physiology (SCEBP), Skeletal Biology and Engineering Research Center (SBE), Department of Development and Regeneration, KU Leuven, Belgium, [2]Department of Chronic Diseases, Metabolism and Ageing, KU Leuven, Belgium, [3]Department of Biomedical Molecular Biology, Ghent University; Inflammation Research Center, Flanders Institute for Biotechnology (VIB), Belgium, [4]Molecular Small Animal Imaging Center (MoSAIC), Department of Imaging & Pathology, KU Leuven, Belgium

Links exist between bone, bone marrow adipose tissue (BMAT) and energy metabolism, and understanding this interplay may impact widespread metabolic diseases such as osteoporosis, obesity and diabetes. Here, we generated conditional knock-out (cKO) mice with deletion of the intracellular cell-cell adhesion complex component αE-catenin in Prx1-Cre+ skeletal stem/progenitor cells (SSPCs). MicroCT and histomorphometry showed that, compared with control littermates, αE-catenin cKO mice had reduced trabecular bone mass (BV/TV: 10.6+/-1.1% (control) vs 6.1+/-0.9% (cKO); p=0.006; n=8; 18-week-old) and excessive BMAT (0.15+/-0.05% vs 1.71+/-0.61%; p=0.02; n=11; 12 weeks). Increased adipogenesis in bone was exacerbated by high-fat diet (HFD), ageing or irradiation, and appeared a cell-autonomous consequence of αE-catenin loss, as mutant BMSCs in vitro showed increased adipogenic differentiation.Changes in bone mass and BMAT may influence systemic metabolism. Hence, we investigated whether loss of skeletal αE-catenin affected energy metabolism. Interestingly, when challenged by HFD for 16 weeks, αE-catenin cKO mice were protected against the increased glycemia and glucose intolerance seen in normal mice. While the BW of control mice on HFD doubled compared with those fed a normal diet (p<0.001; n=9-10), αE-catenin cKO mice on HFD did not develop obesity. Indirect calorimetry revealed increased oxygen consumption and energy expenditure in the mutant mice (p<0.0001; n=9-10), despite similar food intake and ambulatory activity as controls, suggesting increased burning and reduced peripheral accumulation of the dietary fat. In accordance, peripheral fat mass was lower in HFD-fed mutants than controls, the average adipocyte size was 3.6-fold reduced (p=0.0012; n=4), and UCP1 mRNA levels were increased 2- to 4-fold in osteoblasts, BM adipocytes, white and brown fat, and muscle of αE-catenin cKO mice. Notably, 1-year-old αE-catenin cKO mice showed a similar beneficial metabolic phenotype, being leaner and more glucose-tolerant than controls. Surprisingly, while increased BMAT was again pertinent, the ageing mutant mice had more trabecular bone than controls. Thus, excessive BMAT rather than bone mass correlated consistently with improved systemic metabolism in αE-catenin cKO mice.In conclusion, αE-catenin deletion in Prx1-Cre+ SSPCs caused increased BMAT and protected against glucose intolerance and obesity, implying novel links between SSPC fate control, BMAT and energy metabolism.

***Disclosures: Karen De Samblancx**, None*

1051

Anabolic effects of nitric oxide on osteoblast metabolism revealed by deficiency of argininosuccinate lyase *Zixue Jin[1], Jordan Kho[1], Brian Dawson[1], Ming-Ming Jiang[1], Chen Yuqing[1], Saima Ali[1], Lindsay Burrage[1], Monica Grover[2], Donna Palmer[1], Dustin Turner[1], Philip Ng[1], Sandesh Nagamani[1], Brendan Lee[1]. [1]Baylor College of Medicine, United States, [2]Stanford School of Medicine, United States

Previous studies have shown that nitric oxide (NO) donors may prevent bone loss and fractures in preclinical models of estrogen deficiency. However, the mechanisms by which NO modulates bone anabolism remain largely unclear. Argininosuccinate lyase (ASL) is the only mammalian enzyme capable of synthesizing arginine, the sole precursor for nitric oxide synthase (NOS)-dependent NO synthesis. Moreover, ASL is also required for channeling extracellular arginine to NOS for NO production. ASL deficiency (ASLD) is thus a model to study cell-autonomous, NOS-dependent NO deficiency. Here, we report that loss of ASL leads to decreased NO production and impairment of osteoblast differentiation in osteoblastic lineage cells and primary osteoblasts derived from a hypomorphic mouse model of ASLD (AslNeo/Neo). Osteoblast-lineage specific Asl knockout mice (Osteocalcin Cre;Asl-flox/flox) have decreased bone mass and reduced bone formation. Mechanistically, we show that the bone phenotype is at least in part driven by the loss of NO-mediated activation of the glycolysis pathway in osteoblasts that leads to decreased osteoblast differentiation and function. Heterozygous deletion of Caveolin-1, a negative regulator of NO synthesis, restores NO production, osteoblast differentiation, glycolysis, and bone mass in AslNeo/Neo mice. The central role of ASL in bone anabolism and the translational significance of these preclinical studies were further reiterated by studies conducted in induced pluripotent stem cells (iPSCs) from an individual with ASLD. The glycolytic gene expression and the ability to differentiate into osteoblasts which was impaired in iPSCs generated from an individual with ASLD was restored in corrected, isogenic cells. Finally, in a convenient sample of ASLD subjects, the proportion with areal bone mineral density Z-score lower than -2.0 at the lumbar spine was higher as compared to the expected proportions from age- and sex-matched data from the general population. Taken together, our findings suggest that ASLD is a unique genetic model for studying NO-dependent osteoblast function and that the NO-glycolysis pathway may be a new target to modulate bone anabolism.

***Disclosures: Zixue Jin**, None*

1052

Load-induced Irisin Signaling in Healthy and Diabetic mice *Marcia Urban-Maldonado[1], Sylvia Suadicani[1], Mia Thi[1]. [1]Albert Einstein College of Medicine, United States

PURPOSE: Bone loss is a complication in diabetes that is often overlooked. The mechanisms underlying osteopenia associated with type I diabetes (T1D) are still not completely understood. Recently, irisin - a hormone released by muscles during exercise - has been shown to not only have anabolic action on bone1 but also directly regulate osteocytes2. Given that irisin levels in serum are positively correlated with bone mineral status in healthy children3, we hypothesized that altered irisin signaling is one of the factors contributing to diabetic bone loss. METHODS: To test this hypothesis, we used the Akita (C57BL/6J) mouse model of T1D and age-matched wildtype (WT) mice (8 wk old, male, n=6/group) that were submitted to mechanical loading by treadmill running (2 wk and 4 wk; 5 days/wk, 300 m/day) or to normal cage control activity. All animals were euthanized immediately after the last running bout. Blood serum and femurs were collected and respectively assayed for levels of irisin using ELISA and qPCR analyses. All experiments were performed under IACUC approval.RESULTS: We found that serum irisin levels in young adult T1D mice markedly decreased during diabetes progression compared to age-matched WTs (Fig. 1A). From our previous studies we showed that in WT mice, load-induced skeletal responses occurred after 2 wks of loading, and by the end of 4 wk running bout, load-induced adaptation was completed4. While no apparent changes in serum irisin levels were observed in WT mice after 2 and 4 wks of loading, load-induced irisin levels were significantly reduced in T1D mice compared to loaded age-matched WT mice at both time points (Fig. 1B). This observation is accompanied by disruption of the Wnt/β-catenin signaling pathway, in which characteristic load-induced changes in mRNA levels of β-catenin (upregulation), Dkk1 and Sost (downregulation) that coincide with anabolic responses normally observed in WT mice, were dysregulated in T1D mice.CONCLUSION: These findings are in line with recent reports of β-catenin regulation by irisin in osteoblasts5 and suggest that a steady level of irisin signaling is critical for load-induced skeletal adaptation. Observed changes in irisin levels in T1D bone are thus likely to alter bone mineral density and quality, and thereby lead to bone loss.1) Colaianni+ PNAS 2015; 2) Kim+ Cell 2018; 3) Colaianni+ Cells 2019; 4) Seref-Ferlengez+ Ann NY Acad Sci 2019; 5) Chen+ Int J Mol Sci 2020.

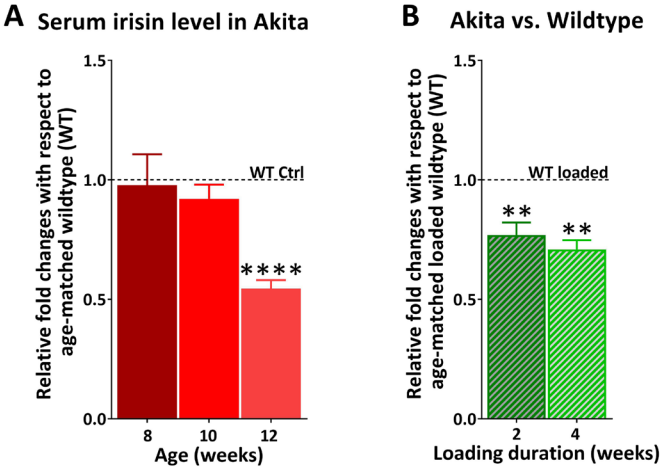

Figure 1. Relative Irisin levels in (A) T1D Akita mice with respect to age-matched wildtypes and (B) Akita mice after 2 and 4 weeks of loading with respect to levels in age-matched loaded wildtype. **P<0.001, ****P<0.00001, t-test followed by Mann-Whitney test. Data presented as means ± SEM. n = 6 / group.

***Disclosures: Marcia Urban-Maldonado**, None*

1053

Targeting Ferroptosis Alleviates Type 2 Diabetic Osteoporosis via Suppressing Osteocyte Lipotoxicity *Yiqi Yang[1], Hanjun Li[1], Tingting Tang[1]. [1]Shanghai Key Laboratory of Orthopaedic Implants, Department of Orthopaedic Surgery, Shanghai Ninth People's Hospital, Shanghai Jiao Tong University School of Medicine, China

Type 2 diabetes is believed to be associated with secondary osteoporosis and trabecular deterioration. However, the underlying pathophysiological mechanisms and effective treatments of diabetic osteoporosis (DOP) remain to be investigated. Ferroptosis is a new form of programmed cell death induced by uncontrolled iron-dependent lipid peroxidation. Since type 2 diabetes is companied by hyperlipidemia, this experiment is designed to investigate the role of ferroptosis in DOP progression. Herein, DOP mice model was established by high fat diet (HFD) with low doses of streptozotocin (STZ) injection. Micro-CT and histology analysis showed significant decreased bone volume, which was companied by increased iron accumulation, morphological change of mitochondria and increased osteocyte death. To mimic metabolic stress in vitro, osteocyte cell line, IDG-SW3, was treated with palmitic acid and high glucose (PA/HG). The data demonstrated that PA/HG treatment significantly decreased cell viability and mineralization ability. In addition, ferroptosis was identified by C11-BODIPY staining and the enhanced transcription of major enzymes involved in lipid oxidation (Ptgs2, Acsl4 and Nox1). Scavenging of lipid peroxides rescued osteocyte viability and promoted osteocyte function in vitro. Finally, ferroptosis inhibitors, Fer-1, further alleviated HFD/STZ-induced bone loss and osteocyte death via inhibiting ferroptosis in vivo. Hence, it is proposed that ferroptosis may play an important role in the progression of DOP and targeting ferroptosis could provide a new horizon for DOP treatment.

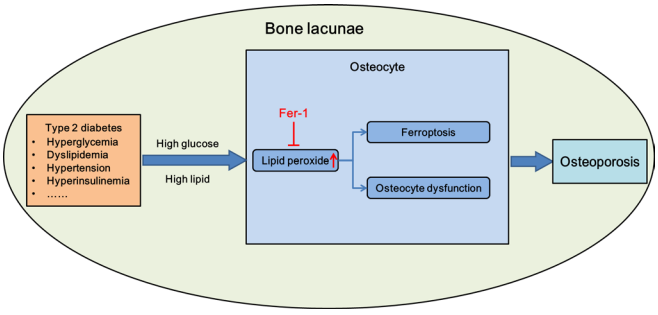

***Disclosures: Yiqi Yang**, None*

1054

Elevated mature osteoblastic 11β-HSD1 contributes to high-fat-diet induced obesity *Chuanxin Zhong[1], Shengzheng Wang[2], Jin Liu[1], Lei Dang[1], Dijie Li[1], Nanxi Li[1], Rongchen Dai[1], Huarui Zhang[1], Chao Liang[1], Shuaijian Ni[1], Aiping Lyu[1], Fuzeng Ren[3], Hong Zhou[4], Ge Zhang[1]. [1]Law Sau Fai Institute for Advancing Translational Medicine in Bone and Joint Diseases, School of Chinese Medicine, Hong Kong Baptist University, Hong Kong SAR, People's Republic of China., Hong Kong, [2]Department of Medicinal Chemistry, School of Pharmacy, Fourth Military Medical University, Xi'an, Shaanxi, People's Republic of China., China, [3]Department of Materials Science and Engineering, Southern University of Science and Technology, Shenzhen, Guangdong, People's Republic of China., China, [4]Bone Research Program, ANZAC Research Institute, University of Sydney, Sydney, Australia., Australia

11β-hydroxysteroid dehydrogenase type 1 (11β-HSD1), a key enzyme converting inactive glucocorticoid (GC) to the physiologically active form, has become an attractive target for anti-obesity drug development. However, the outcomes of the systemic administration of the 11β-HSD1 inhibitors were not clinically satisfactory due to low anti-obesity potency and critical safety concerns.The published data have suggested that the role of 11β-HSD1 in contributing to HFD-induced obesity could not be indispensable in two key metabolic organs (liver and adipose tissue). In addition, the most recent evidence demonstrated that bone behaved as an endocrine organ to influence energy metabolism. Therefore, we examined the 11β-HSD1 expression in the metabolic tissues from HFD-induced obese mice and their chow-fed littermates. The data demonstrated that only intraosseous 11β-HSD1 expression was significantly higher in the HFD group (Fig. 1a). Further, we found the expression level of 11β-HSD1 was significantly higher in the mature osteoblasts in the HFD group (Fig. 1b&c). It implied that the 11β-HSD1 in mature osteoblasts could be involved in HFD induced obesity. To further explore the role of mature osteoblastic 11β-HSD1, we established mature osteoblasts-specific 11β-HSD1 overexpressing mice (11β-HSD1+/+) and induction with HFD. Interestingly, aggravating obese phenotypes were showed in the 11β-HSD1+/+ mice after 20 weeks of induction (Fig. 2). Moreover, after intraosseous injection of 11β-HSD1 inhibitor (AZD 8329) once a week for the last four weeks during HFD induction, the transgenic mice showed lower body weight, gonadal fat weight and intraosseous GILZ mRNA level (a mediator of GC activation by 11β-HSD1) at the end of 20th week. Whereas the intravenous-AZD 8329 group with the same dose showed no significant effect on the above-mentioned phenotype (Fig. 3).Taken together, the present study indicated that elevated mature osteoblastic 11β-HSD1 contributed to HFD-induced obesity. Besides, the clinical failure of anti-obesity 11β-HSD1 inhibitor could be explained by failure in specific inhibition of mature osteoblastic 11β-HSD1. It also suggested that developing the next-generation of 11β-HSD1 inhibitors specifically targeting osteoblastic 11β-HSD1 could provide a potential therapeutic strategy for HFD-induced obesity, which could address the safety concern of abnormal activation of the HPA axis as well.

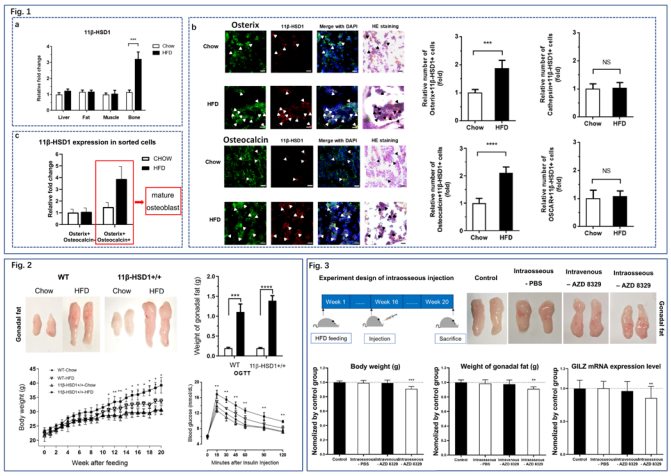

***Disclosures: Chuanxin Zhong**, None*

1055

Single Cell Expression Analysis of Pediatric Bone Reveals Novel Cellular Heterogeneity *Emily Farrow[1], Tammy Brown[1], Jeff Johnston[1], Adam Walter[1], Margaret Gibson[1], Tomi Pastinen[1], Donna Pacicca[1]. [1]Children's Mercy Hospital, United States

There are significant limitations with the use of cell lines and primary cells from rodents in the study of developing human bone. Current published studies are limited to bulk samples, which are unable to detect underlying cellular heterogeneity. We have devised a reliable method for isolation of primary human bone cells and have subsequently harvested

these cells for single cell transcriptome analysis. Deidentified discarded bone samples from healthy pediatric patients (under age 18) were obtained from elective orthopaedic surgeries. A total of 14 individual samples (7 male, 7 female) were used for analysis and included trabecular, cortical, and cartilage samples. Cells were initially processed and clustered by Seurat v3 as described in their SCTransform-based integration workflow, resulting in 40 independent clusters (n=41,0060 cells). Within the large cluster set, known markers of cellular subtypes localized to multiple clusters. Alkaline phosphatase was detected strongly in clusters 18 and 26, but also in clusters 4, 11, 13, 17, 19, 21, 22, 24, 25, 32, 34, and 38. Trap (ACP5) expression was highest in cluster 39, but was also detected in 11, 14, 16, 26, 27, and 38. Hemoglobin cells not fully removed during isolation were detected in cluster 9. Interestingly, SOST was detected at very low levels in clusters 1, 7, 13, 16, 17, 19, 24, 26, and 27 but was not statistically significant between clusters. In order to further refine our analyses and evaluate for novel markers of bone subtypes, we used a classic marker gene set to positively select for known cells types (n=11,862 cells; osteoclasts-OSCAR, osteoblasts-ALPL, osteocytes-PHEX, and chondrocytes-COL2A1). The positive selection resulted in further subclustering between cell types: Osteoclasts = 13 clusters (1359 cells); osteoblasts = 13 (2088 cells), osteocytes = 6 (622 cells), and chondrocytes = 23 (9943 cells). As expected, cellular markers such as DMP1 were detected primarily in osteocytes, but also in osteoblasts. Unexpectedly, PDPN was detected across all 4 cellular subtypes.This is the first human single cell genomics study across multiple primary bone cell / chondrocyte lineages. Classic markers such as SOST may not be as relevant in primary bone. We were able to elucidate novel cellular markers that can be utilized in future studies to identify specific cell populations and will be important to study complex disease mechanisms, such as the impact of diabetes on bone development.

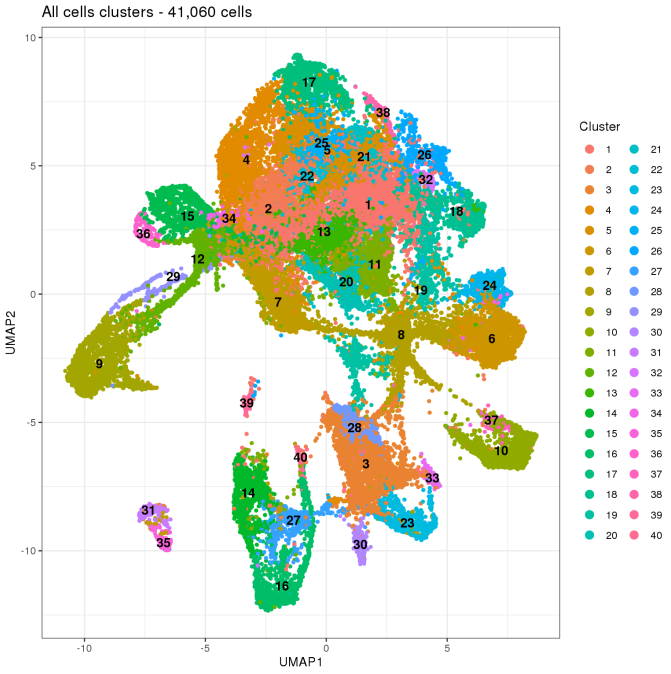

***Disclosures: Emily Farrow**, Illumina, Other Financial or Material Support*

1056

Novel Site-Specific Single-Cell RNA and Single-Nucleus ATAC sequencing of Ectopic Bone Progenitor Cells *Chase Pagani[1], Amanda Huber[1], Charles Hwang[1], Simone Marini[1], Pauline Yu[1], Noelle Visser[1], Nicole Patel[1], Karen Kessel[1], Kaetlin Vasquez[1], Amy Strong[1], Husain Rasheed[1], Reagan Nelson[1], Joseph Greenstein[1], Jane Song[1], Deneen Wellik[2], Benjamin Levi[1]. [1]University of Michigan Medical School, United States, [2]University of Wisconsin - Madison, United States

Traumatic heterotopic ossification (HO) is the formation of ectopic bone in soft tissue following burn/blast wounds, orthopedic surgeries, and sports injuries. It is reported that mesenchymal stem cells (MSCs) undergo altered cell fate following the injury, but it is unclear how these cells progress through aberrant differentiation. Previous methods fail to mark cells effectively in a specific region, leading to confounding results. We hypothesized that performing an HO-forming 30% total body surface area burn with concurrent Achilles' tenotomy on a Hoxa11-CreERT2;ROSA-TdTomato lineage tracing mouse that marks cells important in bone development and healing in the zeugopod (radius/ulna and tibia/fibula region) will allow for a site-specific in-vivo tracing of HO progenitors. We utilized single-cell RNA sequencing (scRNA), single nucleus ATAC sequencing (snATAC), and immunofluorescent histology (IFH) across three time points to characterize and visualize the progression towards HO (A). Canonical analysis of uninjured, 1-week post-injury, and 6-weeks post-injury time points found TdTomato transcript expression in 5 scRNA clusters, 4 of which expressed MSC lineage markers (Pdgfrα and Prrx1). Analyzing individual time points showed TdTomato expression shifts from a TdTomato+ Scx+ Tnmd+ cluster and TdTomato+ Pdgfrα+ Prrx1+ cluster found priory to injury towards a cluster with both osteogenic and chondrogenic gene expression (Sox9, Acan, Runx2, and Spp1) 1 week following injury (B). IFH confirmed Hoxa11 lineage cells were within the injury site following injury and expressed SOX9 and RUNX2. By nine weeks following injury, IFH found Hoxa11 lineage cells within fully formed HO. Monocle pseudo-time analysis of the TdTomato expression clusters shows a stem-like branch prior to injury with an osteo/chondro differentiation branch, mainly occupied by cluster 0, following injury. ScRNA clusters were mapped onto snATAC sequencing clusters and showed increased open chromatin regions of osteogenic, tenogenic, and chondrogenic differentiation genes following injury in cluster 0 (Sox9, Acan, Spp1, Sp7, Comp, Bglap, Ibsp, Dlx5, and Dlx6) (C). These findings suggest that Hoxa11+ bone progenitor cells at the site of injury undergo altered differentiation towards a combined chondrogenic/osteogenic cell type that eventually forms fully formed HO. This is the first study to successfully trace site-specific bone progenitor cells in-vivo towards ectopic bone formation.

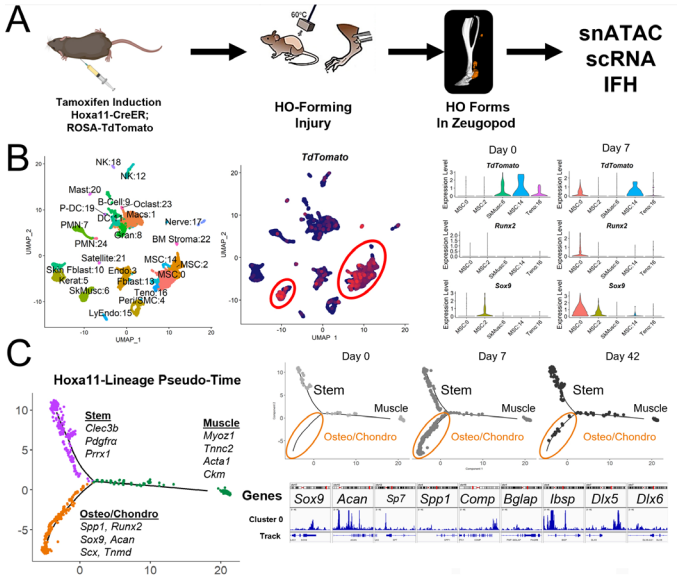

***Disclosures: Chase Pagani**, None*

1057

Single cell analysis reveals transient expansion of marrow adipogenic lineage precursors as the mechanism for bone marrow recovery after radiation *Lutian Yao[1], Leilei Zhong[1], Zhen Miao[1], Mingyao Li[1], Jaimo Ahn[1], Ling Qin[1]. [1]University of Pennsylvania, United States

Radiotherapy treats malignant tumors effectively but also damages surrounding tissues, such as bone marrow. High-dose radiation often leads to fractures and lymphocytopenia. Bone marrow cells, including mesenchymal, hematopoietic, and endothelial cells, attempt to regenerate after radiation injury but the repair mechanism is still largely unknown. To investigate the acute radiation effects on bone marrow, we performed single cell RNA-sequencing (scRNA-seq) on Td+cells (bone marrow mesenchymal lineage cells) sorted from 1-month-old Col2-Cre Tomato (Col2/Td) mouse femurs before and after 5 Gy focal SARRP radiation (day 3). Analyzing these two datasets generated the same clustering pattern consisting of early mesenchymal progenitors (EMPs), late mesenchymal progenitors (LMPs), lineage committed progenitors (LCPs), osteoblasts, osteocytes and marrow adipose lineage precursors (MALPs). Adipoq-Cre Tomato (Adipoq/Td) mice were constructed to visualize MALPs in bone marrow. Interestingly, these cells highly expressed adipogenic markers but had no lipid accumulation. Morphologically, they existed abundantly as pericytes and marrow stromal cells. Computational analysis and EdU incorporation revealed that they normally do not proliferate but acquire highly proliferative ability after radiation, leading to a 7.4-fold increase of MALPs based on flow analysis. Gene enrichment analyses revealed that radiation upregulates pathways related to wound healing and tissue remodeling and particularly myofibroblast-related genes (Acta2, Tagln, Myl9 etc) and collagen genes in MALPs. MALPs have a central cell body with extended cell processes (5.68+0.75/cell) that form 3D network in bone marrow. Shortly after radiation, MALPs lost 67% of cell processes, became more elongated (a 41% decrease in circularity), detached from vessels, indicating a transformation into myofibroblasts. This was coincided with vessel dilation and diminished bone marrow cellularity. At day 14 when bone marrow vessels and cellularity recover, MALPs returned to the baseline number and a normal reticular shape. Cell ablation of MALPs in Adipoq/Td/DTR mice with DT injections starting right after radiation completely blocked the recovery of bone marrow vasculature and cellularity at day 14. In conclusion, we demonstrated that

radiation transiently expands a newly identified bone marrow mesenchymal subpopulation, MALPs, and that this expansion is crucial for bone marrow recovery after radiation injury.

***Disclosures: Lutian Yao**, None*

1058

Compromised mitochondrial dynamics in osteoblasts in MDS to AML transformation *Rossella Labella[1], Abdullah Mahmood Ali[2], Ioanna Mosialou[1], Junfei Zhao[3], Paraskevi Vgenopoulou[1], Andrew W Vandenberg[1], Raul Rabadan[4], Frank Oury[5], Azra Raza[2], Stavroula Kousteni[1]. [1]Department of Physiology and Cellular Biophysics, Columbia University Irving Medical Center, New York, NY, United States, United States, [2]Myelodysplastic Syndromes Center, Columbia University, New York, NY, United States, United States, [3]Department of Biomedical Informatics and Center for Computational Biology and Bioinformatics, Columbia University, New York, NY, United States, United States, [4]Department of Biomedical Informatics and Center for Computational Biology and Bioinformatics, New York, NY, United States, United States, [5]Institut National de la Santé et de la Recherche Médicale (INSERM) U1151, Institut Necker Enfants-Malades (INEM), University of Paris-Sorbonne 75015 Paris, France, France

Cells of the endosteal niche can acquire mutational alterations that promote development of hematological malignancies. In turn, osteoblasts and their precursors can be remodeled by dysplastic cells to favor their propagation. However, it is unknown whether stromal cell remodeling occurs and affects transformation of low to high risk disease. To study the role of osteoblasts in the transformation of myelodysplasia (MDS) to acute myelod leukemia (AML), we compared the osteoblastic transcriptome of 11 MDS patients before and after transformation to AML, and an additional 20 MDS and AML-transformed patients. RNA-seq analysis revealed upregulation of genes encoding mitochondrial proteins in AML compared to MDS patients. Those included components of the mitochondrial respiratory chain, proteins involved in mitochondrial fission, fusion, and trafficking, as well as mitochondrial ribosomal proteins. Consistent with this, whole exome sequencing indicated an increase in mtDNA and Mitotracker fluorescence was increased in bone biopsies of AML transformed patients. In parallel, expression of proteins representing various stages of the autophagy process was decreased. Among them there was a robust downregulation of mitophagy machinery proteins, such as OPTN, MFN2, PINK1, ATG13, and ATG3, involved in selective degradation of dysfunctional mitochondria. In line with decreased autophagy, GSEA and western blot analysis in human osteoblasts indicated a significant downregulation of the FoxO1 signaling pathway in AML transformation, an important trigger of autophagy and mitophagy regulation. Assessment of the functional status of the increased mitochondria of osteoblasts of AML transformed patients has shown compromised mitochondrial activity. To examine whether this metabolic dysregulation in osteoblasts affects MDS to AML progression, we investigated avenues of communication between osteoblasts and dysplastic cells. We found that a dense network of Tunnelling Nanotubes of actin is formed between osteoblasts and leukemic OCI-AML3 cells that allows transfer of mitochondria from osteoblasts to OCI-AML3 cells. These observations demonstrate that compromised mitophagy leads to dysfunctional mitochondria accumulation in osteoblasts during AML transformation. This event may involve exchange of damaged mitochondria with functional ones to overcome metabolic stress in dysplastic cells and favor their hyperproliferation as AML blasts.

***Disclosures: Rossella Labella**, None*

1059

Identifying Drug Targets via Whole Exome Sequencing and CRISPR-Cas9 *Sirui Zhou[1], Laetitia Laurent[1], John Kemp[2], Albena Pramatarova[3], Vincenzo Forgetta[1], John Morris[4], Peter Croucher[5], Graham Williams[6], Duncan Bassett[6], David Goltzman[7], Luca Lotta[8], David Evans[2], Brent Richards[1]. [1]Lady Davis Institute, Jewish General Hospital, Canada, [2]University of Queensland Diamantina Institute, Translational Research Institute, Australia, [3]McGill University and Genome Quebec Innovation Centre, Canada, [4]New York Genome Center, United States, [5]Garvan Institute of Medical Research, Australia, [6]Molecular Endocrinology Laboratory, Department of Medicine, Imperial College London, United Kingdom, [7]Research Institute of the McGill University Health Centre, Canada, [8]Cardiovascular, Metabolic and Musculoskeletal Therapeutic Genetics, Regeneron Genetics Center, United States

Osteoporosis leads to increased susceptibility of bone fracture for which new drugs are needed. A primary risk factor is low bone density; a genetically heritable and polygenic trait. It remains unknown whether whole-exome sequencing (WES) or target gene mapping using GWAS can better identify causal genes to inform drug development. To compare these approaches, we first identified a set of positive control genes for osteoporosis whose perturbation causes a Mendelian form of osteoporosis, or which act as drug targets for approved osteoporosis therapies. We undertook sequence kernel association tests (SKATO) to investigate the association between 18,350 autosomal protein-coding genes and estimated bone mineral density (eBMD), using WES data of 42,404 white British participants from UK Biobank. We also performed a GWAS using imputed data in the same sample followed by an established target gene mapping strategy. We found that genes identified by WES were strongly enriched for positive control genes (odds ratio [OR] = 119, 95% CI (20.1, 502), P=5.2 x 10-6), and that this enrichment was 5-fold higher compared to enrichment of GWAS plus target gene mapping-identified genes (OR=22.5, P=5 x 10-5) (Figure). From WES data, we identified 38 genes with exonic variants impacting protein function, including CADM1, which harbored exonic variants strongly associated with eBMD (SKATO, P=1.8 x 10-9). We used CRISPR-Cas9 to edit CADM1 in SaOS-2 osteoblast like cell lines, suppressing protein abundance at the cell surface, which resulted in increased expression of early bone markers: RUNX2, COL1A1/2 and ALPL. These findings demonstrate that WES is a powerful approach to identify genes influencing bone density, such as CADM1, which could serve as targets for osteoporosis therapies.

Figure: Enrichment for positive control genes using different Target Gene Identification strategies from WES, Imputed and GWAS data. Strategies identify positive control genes are displayed in OR (x-axis). WES (SKATO) represents target genes identified by SKATO using different variant groups from WES. Imputed (SKATO) represents target genes identified by SKATO using different variant groups from imputed data.

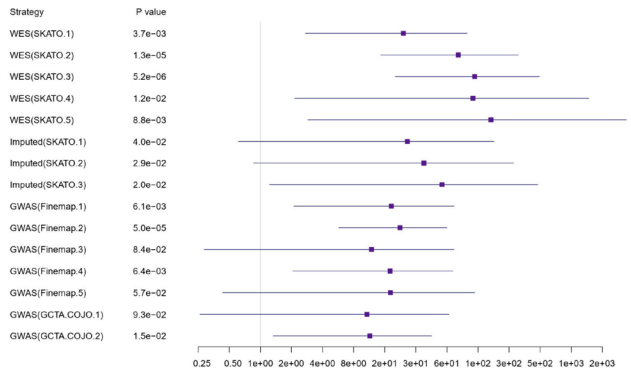

***Disclosures: Sirui Zhou**, None*

1060

Using single cell transcriptomics to characterize the potential role of RNA binding proteins to regulate the early stages of adult human bone marrow-derived mesenchymal stem cell differentiation *Mason Henrich[1], Robert Tower[2], Yuanyuan Wang[3], Yi Xang[3], John S. Adams[1], Rene Chun[4]. [1]Department of Orthopedic Surgery, Orthopedic Hospital Research Center, University of California at Los Angeles, United States, [2]Department of Orthopedic Surgery, Johns Hopkins School of Medicine, United States, [3]Department of Pathology and Laboratory Medicine, Perelman School of Medicine, University of Pennsylvania, United States, [4]Department of Orthopedic Surgery, Orthopedic Hospital Research Center, University of California at Los Angeles, United States

Adult human bone marrow-derived mesenchymal stem cells (hMSC; CD73+/CD90+/CD105+/CD14-/CD34-/CD45-/CD19-/HLA-/DR-) are a heterogeneous cell population that can undergo adipogenesis, chondrogenesis, and osteogenesis when cultured in corresponding media. Understanding the regulatory mechanisms of generating bone forming cells from hMSC is important to the understanding of bone homeostasis and finding of targets for intervention in bone diseases such as osteoporosis. The mechanism of lineage-specific differentiation of hMSC into bone forming osteoblasts and fat accumulating adipocytes is an area of active investigation. While transcription factors (TF) have been proposed as the central regulators of lineage-specific differentiation, RNA binding protein (RBP)-directed alternative splicing of TF has not been examined. Most human genes undergo alternative splicing (AS) through the action of RNA binding proteins (RBPs). With just ~ 20,000 genes, the mechanism of AS expands the repertoire of proteins that is needed for the full diversity of cell types, tissues, and organs found in humans. To explore the role of AS in osteogenesis, we generated single cell RNA-sequencing (scRNA-seq) 3' libraries on the 10x Genomics platform at day 0, 1 and 2 following provoked osteogenesis of hMSC. We examined the expression patterns of 129 RBPs with defined RNA binding motifs and detected four distinct populations of developing progenitors: 1) early non-committed, bipotential progenitors; 2) osteochrondral progenitors marked by high expression of RUNX2; 3) adipogenic progenitors marked by high expression of PPARG; and 4) a purported trans osteogenic-adipogenic population, marked by intermediate expression of both RUNX2 and PPARG. We discovered four RBPs, HNRNPA2B1, FUS, SF3B4, and SRSF1, that were significantly differentially expressed in both scRNA-seq and a concurrently analyzed bulk RNA-seq day 0-12 hMSC osteogenesis time-course dataset. Additionally, using a newly developed analytical pipeline, these four RBPs were motif mapped to exon skipping splice sites of TF identified from the day 0-12 bulk-RNA-seq data. These results provide evidence of a role for differential expression of key RBPs and coupled exon skipping events in TF during the early stages of hMSC maturation down the osteogenic pathway.

***Disclosures: Mason Henrich**, None*

1061

Bisphosphonate Use and Risk of Atypical Femoral Fractures: A Nationwide Danish Analysis with Blinded Radiographic Review *Douglas Bauer[1], Dennis Black[1], Eric Vittinghoff[1], Harry Genant[1], Richard Dell[2], Bo Fan[1], Christopher Smith[3], Martin Thomsen Ernst[3], Bo Abrahamsen[3]. [1]University of California, San Francisco, United States, [2]Southern California Kaiser Permanente Medical Group, United States, [3]University of Southern Denmark, Denmark

BackgroundAtypical femoral fractures (AFF) are a rare but serious complication of anti-resorptive treatments. Previous studies suggest that prolonged bisphosphonate (BP) use is associated with higher AFF risk, but there are few population-based analyses with rigorous long-term documentation of medication use and radiographic validation of AFF. The Danish National Healthcare system maintains longitudinal records of medication use, fracture events, and comorbidities, which allowed us to examine the prospective relationship between BP use and AFFs in the Danish population.MethodsUsing ICD-10 codes we identified and collected digitized pre and post-operative radiographic images from Danish adults >50 with subtrochanteric and femoral shaft fractures between 2010-2015 (n=4973, representing 96% of all fractures at those locations in the country). Images were blindly reviewed by specially trained study radiologists to identify 2014 ASBMR major and minor criteria. BP and other medication use between 1995-2015 was collected from electronic pharmacy records, and comorbidities were assessed from inpatient and outpatient administrative records. We identified a random sample of 35,000 Danish adults >50 and used a case-cohort design to evaluate the relationship between patterns of BP use and AFF outcomes, accounting for demographics, other medication use, comorbidities and previous fractures. ResultsAmong the 1.9 million Danes >50, we confirmed 189 AFFs between 2010-15. 65 individuals with AFF (34%) had no exposure to BPs. After adjustment for potential confounders, the absolute risk of AFF was 0.075/10,000 person-yr in non-users, 1.77 in those with 3-5 yr of BP use, and 4.01 in those with >7 yr of BP use (Table). The Danish nationwide rate of classic hip fracture was 43.8/10,000. One year after BP discontinuation, the risk of AFF fell dramatically (RH=0.29, CI: 0.09, 0.90). AFF risk was increased among those with rheumatoid arthritis or hypertension, but was unrelated to age, gender, diabetes or other medication use. ConclusionsThis study of Danish National Healthcare data found that compared to classic hip fracture rates, the incidence of AFF was extremely low but BP use, particularly >5 years, was clearly associated with an increased risk. One third of AFFs occurred in individuals who had no BP exposure. The risk of AFF falls substantially after BP discontinuation.

Table. Patterns of BP Use and Risk of AFF in Denmark

Duration of BP use (yr)	AFF (N)	Rate/10,000 PY	Adjusted RR (95% CI)
No use	65	0.075	(ref)
>0-1	8	0.45	6.26 (2.89, 13.58)
>1-3	18	0.97	10.67 (6.00, 18.98)
>3-5	21	1.77	17.74 (10.23, 30.77)
>5-7	31	3.71	35.02 (21.28, 57.63)
>7	46	4.01	37.50 (23.25, 60.47)
Time since last use (yr)			
Current use	157	0.17	(ref)
>0-1	27	2.16	1.05 (0.68, 163)
>1-3	<5	0.48	0.27 (0.09, 0.85)
>3	<5	0.28	0.20 (0.05, 0.83)

***Disclosures: Douglas Bauer**, None*

1062

Teriparatide for the healing of incomplete Atypical Femur Fractures: The TAFF Trial *Lianne Tile[1], Robert Bleakney[2], George Tomlinson[3], Aliya Khan[4], Adrian N.C.Lau[5], Rowena Ridout[3], Jessica Chang[6], Jasmine Lakhesar[6], Judy Scher[6], Hanxian Hu[6], Jonathan D.Adachi[7], Angela M. Cheung[3]. [1]Division of General Internal Medicine, Department of Medicine, University of Toronto, Canada, [2]Musculoskeletal Division, Joint Department of Medical Imaging, University of Toronto; Sinai Health Systems, Canada, [3]University Health Network, University of Toronto, Canada, [4]McMaster University, Canada, [5]Division of Endocrinology, Department of Medicine, University of Toronto, Canada, [6]University Health Network, Canada, [7]St Joseph's Healthcare; McMaster University, Canada

Rationale: Atypical femur fractures (AFFs) are bisphosphonate-related stress fractures that are difficult to heal. An incomplete AFF (iAFF) is often present prior to the complete fracture, and can cause pain, ache or weakness in the thigh, especially with or after weight-bearing. Preliminary data suggest that teriparatide may improve healing of these fractures.Methods: We conducted a 2-year double-blind placebo-controlled randomized trial of subcutaneous teriparatide 20 mcg daily versus placebo to assess the effectiveness of teriparatide for the healing of incomplete AFFs (www.clinicaltrials.gov NCT01896011). Women and men over age 30 with incomplete AFFs as defined by the 2014 ASBMR AFF criteria were included in the study. Exclusion criteria included peri-prosthetic, high trauma or pathological fractures from metastases or metabolic bone diseases other than osteoporosis, and contraindications to the use of teriparatide. Our primary outcome was a patient-reported outcome: the change in modified Western Ontario and McMaster Universities Osteoarthritis Index (WOMAC) score from baseline to two years. The modified WOMAC is a self-administered 24-item questionnaire that assesses pain or ache (0-20), weakness (0-8) and physical function (0-68). Our secondary outcomes include radiographic healing, health-related quality of life short form 36 (SF-36), reintegration to normal living index (RNLI), and change in BMD. Continuous outcomes were compared between groups using analysis of covariance, with the corresponding baseline value of the outcome as the covariate at the various time points. Time to radiographic healing was compared using a log-rank test. For the primary outcome, modified WOMAC score, multiple imputation was used to handle missing data. Results: Thirty-four women (mean age 69.2 years; range 33.5 to 82.8yrs) participated in the study. Twenty-seven (27) participants had bilateral AFFs (22 with a complete AFF and a contralateral iAFF, and 5 with bilateral iAFFs). Seven participants had unilateral iAFFs. All study participants had bisphosphonate exposure, with an average duration of bisphosphonate use of 9.96 years (range 2.5 to 28.2 years) years. Average baseline BMD T-score at the lumbar spine and total hip were -1.26 and -0.83, respectively. Over two years, there were no differences between the two groups in modified WOMAC scores, reintegration to normal living, physical or mental component score of SF-36, change in BMD or radiographic healing. Of note, none of the 34 participants progressed from incomplete to complete fractures. Conclusions: This first randomized placebo-controlled trial for the healing of incomplete AFFs failed to show a benefit with teriparatide.

***Disclosures: Lianne Tile**, None*

1063

Risk factors for atypical forearm fractures associated with bisphosphonate usage *Soo Min Cha[1], Hyun Dae Shin[1]. [1]Chungnam National University, School of medicine, Republic of Korea

Background: We performed a complete enumeration survey for patients under the treatment of bisphosphonate (BP), aiming to find the diagnostic factors for atypical forearm fractures additional to atypical femur fractures, via a retrospective case-control study.Methods: We identified 53 patients that met the following inclusion criteria between March 2009 and February 2019: a BP therapy history or ongoing administration of at least 1 year, presence of simple radiographs of bilateral femurs and forearms, and availability of complete medical records and radiological data. The patients were divided into two groups: those with any lesion of atypical fractures of ulna or radius, regardless of the displacement of at least one side extremity in simple radiographs (group 1, 20 patients); and those without any lesions of pathognomonic finding or fractures in either forearm in simple radiographs (group 2, 33 patients).Results: Univariate analyses of basic demographic characteristic such as age, smoking, comorbidity of diabetes mellitus or any connective tissue disease needing steroid treatment, and BMD showed no significant differences between the groups ($P > 0.05$). The co-morbidity of malignant cancer inevitably needing BP usage was not different between the two groups. Multivariate analyses of the several variables that differed significantly between the two groups in univariate analyses demonstrated that total period and single prescribing physician/surgeon were significantly associated with forearm fractures. A cut-off value of 65 months for the total period predicted the presence atypical forearm fractures. Conclusions: Atypical forearm fractures are probably more common than reported in the literature to date, and all forearm lesions were accompanied by preceding atypical femur fractures. The period of BP administration had the main effect on the occurrence of atypical forearm fractures, particularly if more than 65 months. Also, the prescription by multiple physician was predicting factor for forearms lesion additionally to AFFs, however, more evidence-based study is needed to understand the effects of cancer-related BP usage on the forearm.

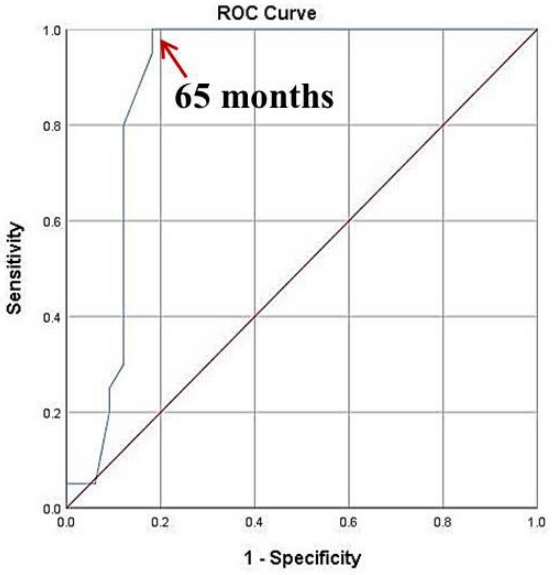

***Disclosures: Soo Min Cha**, None*

1064

BONE MATRIX QUALITY IN TRANSILIAC BIOPSIES FROM POST-MENOPAUSAL WOMEN TREATED WITH DENOSUMAB FOR UP TO 10 YEARS (FREEDOM and FREEDOM Extension TRIALS). *Delphine FARLAY[1], Sébastien RIZZO[1], David D. DEMPSTER[2], Shuang HUANG[3], Li CHEN[3], Arkadi CHINES[4], Jacques P. BROWN[5], Georges BOIVIN[1]. [1]INSERM, UMR 1033, Univ Lyon, University Claude Bernard Lyon 1, France, [2]Department of Pathology and Cell Biology, Columbia University, United States, [3]Clinical Development, Amgen Inc., United States, [4]Clinical Development, Amgen Inc, United States, [5]CHU de Quebec Research Centre, Laval University, Canada

In postmenopausal osteoporotic (PMOP) women, denosumab (DMAb) therapy through 10 years (y) is associated with continued BMD gains and low fracture incidence1. Until 5y, DMAb treatment resulted in significant increases in degree of mineralization of bone (DMB) compared with placebo (Pbo), then plateaued through 10y in both cortical (Ct) and cancellous (Cc) bone2. Our purpose is to assess the microhardness (Hv) of bone reflecting elastic and plastic deformations provided by DMB and the quality of mineral and organic matrix in bone biopsies from PMOP women treated with DMAb for up to 10y (FREEDOM and FREEDOM Extension Trials). Assessments were performed blindly 1) on 72 iliac bone samples from patients treated for 2/3 y either with Pbo or DMAb, and 2) on 49 iliac bone samples from patients treated for 5 (N=28) or 10y (N=21) with DMAb. Intrinsic quality of the mineral and organic matrix were assessed using Fourier transform infrared microspectroscopy. Hv was measured with a Vickers microindenter. Data were obtained separately in Ct and Cc. P-values were calculated using Wilcoxon rank sum test for pairwise comparison. After 2/3y, Ct Hv was significantly higher in DMAb than Pbo (Table) with increased mineral/matrix ratio but without significant variation of other variables of quality of mineral and organic matrix. At 5y and 10y, mineral/matrix ratio, mineral maturity (transformation of precursors into apatite crystals), crystallinity (size/perfection of crystals), were higher compared to 2/3y of DMAb, supporting transition to more mature crystals (within physiological range). Together with the increase in DMB2 and mineral maturation, improvement in Hv was expected. However, Hv was significantly lower at 5y and 10y than to 2/3y while Cc collagen maturity was increased. In conclusion, DMAb improves bone Hv after 2/3y, mainly by changes in bone matrix mineralization characteristics that are consistent with DMAb's mechanism of action as a potent remodeling inhibitor. However, persistently low state of bone remodeling at 5y and 10y is associated with reduced bone Hv, suggesting aging of the poorly remodeled organic matrix (non-collagenous proteins or other factors could be involved). At the organ level, DMAb preserves modeling-based bone formation at weight-bearing sites3 and leads to continued BMD gains and low fracture rate up to 10y. 1-Bone HG Lancet Diabetes Endocrinol 2017,5(7):513 2-Dempster DW JCEM 2018,103:2498 3-Dempster DW JBMR 2020 Mar 12 online

Table

Variables \ Treatment	Placebo 2-3 years	Denosumab 2-3 years	Denosumab 5 years	Denosumab 10 years
Cortical bone				
Microhardness	53.56 ± 3.07	**56.28 ± 3.11** [a]	**50.18 ± 3.86** [b]	**50.38 ± 3.41** [c]
Mineral/matrix	4.43 ± 0.29	**4.65 ± 0.26** [a]	**4.85 ± 0.28** [b]	**4.91 ± 0.37** [c]
Mineral maturity	1.88 ± 0.26	1.88 ± 0.26	**2.13 ± 0.45** [b]	**2.46 ± 0.64** [c]
Mineral Crystallinity	0.0373 ± 0.0016	0.0381 ± 0.0015	**0.0394 ± 0.0014** [b]	**0.0399 ± 0.0009** [c]
Mineral Carbonation	0.0073 ± 0.0004	0.0073 ± 0.0005	**0.0068 ± 0.0004** [b]	**0.0068 ± 0.0004** [c]
Collagen maturity	4.48 ± 0.47	4.42 ± 0.45	4.60 ± 0.33	4.45 ± 0.68
Cancellous bone				
Microhardness	56.53 ± 4.54	56.26 ± 3.72	**53.14 ± 2.60** [b]	**52.82 ± 3.15** [c]
Mineral/matrix	4.39 ± 0.35	**4.62 ± 0.35** [a]	**4.95 ± 0.23** [b]	**4.98 ± 0.17** [c]
Mineral maturity	1.54 ± 0.25	1.53 ± 0.24	**1.80 ± 0.29** [b]	**2.05 ± 0.37** [cd]
Mineral Crystallinity	0.0373 ± 0.0021	0.0379 ± 0.0021	**0.0397 ± 0.0015** [b]	**0.0404 ± 0.0012** [c]
Mineral Carbonation	0.0075 ± 0.0005	0.0073 ± 0.0006	**0.0067 ± 0.0014** [b]	**0.0068 ± 0.0005** [c]
Collagen maturity	3.98 ± 0.68	3.86 ± 0.72	**4.31 ± 0.52** [b]	**4.46 ± 0.34** [c]

Bone matrix quality variables are summarized with mean ± SD.
a : p<0.02 Denosumab Year 2/3 vs Placebo Year 2/3
b : p≤0.008 Denosumab Year 5 vs Denosumab Year 2/3
c : p≤0.006 Denosumab Year 10 vs Denosumab Year 2/3
d : p<0.02 Denosumab Year 10 vs Denosumab Year 5

***Disclosures: Delphine FARLAY**, AMGEN, Grant/Research Support*

1065

Treatment with zoledronate subsequent to denosumab in osteoporosis: a randomized trial *Anne Sophie Sølling[1], Torben Harsløf[1], Bente Langdahl[1]. [1]Department of Endocrinology and Internal Medicine, Aarhus University Hospital, Denmark

Purpose: After discontinuation of denosumab (DMAB) bone resorption increases, bone mass is lost and vertebral fractures have been reported. We have previously shown, that in 60 postmenopausal women and men treated with DMAB for an average of 4.6+/-1.6 years (mean+/-SEM) treatment with zoledronate (ZOL) irrespective of the timing did not fully prevent bone loss 12 months after ZOL treatment. We now report BMD results after 2 years. Methods: In a 2-year randomized, open label, interventional study with 60 patients with osteopenia, we administrated ZOL at 3 different timepoints: 6 months (6M group, n=20) or 9 months (9M group, n=20) after the last DMAB injection or when bone turnover was increased (OBS group, n=20). In the OBS group, ZOL was administered if a patient suffered a low energy hip or vertebral fracture, p-carboxy-terminal collagen crosslinks (p-CTX) increased >= 1.26 ug/l (50% above the range for postmenopausal women and elderly men) or BMD decreased >= 5% 3 months after baseline. Similarly, if p-CTX increased >= 1.26 ug/l or patient suffered a low energy hip or vertebral fracture before month 3, ZOL was administered at that timepoint in the 9M group. All 3 groups were monitored with DXA 6, 12 and 24 months after treatment. If BMD decreased >= 5% or s-CTX increased >= 1.26 ug/l, ZOL was re-administered. The last patient will attend the final visit in August 2020.Results: A total of 54 participants have completed the trial and are included in the results. From baseline to month 24 spine BMD decreased by 4.0+/-0.8%, 4.3+/-0.9%, and 4.4+/-1.7% in the 6M, 9M and OBS groups, respectively (p<=0.001 for all without group differences) and total hip BMD by 3.5+/-0.5%, 3.6+/-0.8%, and 4.4+/-1.2% in the 6M, 9M and OBS groups, respectively (p<0.001 for all without group differences). A total of 26 participants fulfilled the BMD or CTX criteria for re-treatment with ZOL; 14, 6, and 6 patients from the 6M, 9M and OBS groups, respectively. See table 1. In all groups, mean p-CTX was within the premenopausal reference range during the 2nd year of the study. Seven patients suffered a fracture: 2 vertebral fractures and 5 non-vertebral fractures.Conclusion: Treatment with ZOL subsequent to DMAB in osteopenic patients did not prevent loss of bone 2 years after the initial ZOL treatment.

Table 1. Patients that fulfilled the BMD or CTX criteria for retreatment 6, 12 or 24 months after the initial treatment with zoledronate

	6 months after ZOL			12 months after ZOL			24 months after ZOL		
	Total	CTX criteria	BMD criteria	Total	CTX criteria	BMD criteria	Total	CTX criteria	BMD criteria
6-month group	5	1[1]	5[1]	5	1[1]	5[1]	4	0	4
9-month group	3[2]	0	3	1[2]	0	1	3	0	3
Observation group	1	0	1	4	0	4	1	0	1

Number of patients.
C-terminal collagen crosslinks (CTX) criteria: p-CTX increased above 1.26 µg/l.
Bone mineral density (BMD) criteria: BMD decreased more than 5% at the lumbar spine or total hip.
[1] One patient fulfilled both the CTX and BMD criteria for treatment.
[2] One patient from the 9-month groups was retreated twice.

***Disclosures: Anne Sophie Sølling**, None*

1066

Risk of Incident Atrial Fibrillation with Zoledronic Acid Versus Denosumab: A Propensity-Score Matched Cohort Study *Sara J. Cromer[1], Kristin M. D'Silva[2], Elaine W. Yu[1], Michael Fischer[3], Seoyoung C. Kim[3]. [1]Division of Endocrinology, Diabetes, and Metabolism, Massachusetts General Hospital, United States, [2]Division of Rheumatology, Allergy, and Immunology, Massachusetts General Hospital, United States, [3]Division of Pharmacoepidemiology and Pharmacoeconomics, Brigham and Women's Hospital, United States

Zoledronic acid is a highly effective treatment for osteoporosis and malignancy-related bone disease, but questions remain about a possible increased risk of atrial fibrillation (AF). We examined the risk of incident AF among patients receiving zoledronic acid, as compared to denosumab, in the first year of treatment for osteoporosis or malignancy-related bone disease.We performed a new user, active comparator cohort study using claims data from the Clinformatics Data Mart (Optum, Inc.), including privately insured Americans between January 1, 2010, and June 30, 2019. We examined separate propensity score (PS)-matched cohorts of patients with either osteoporosis or active malignancy. Inclusion criteria were age >50 years, incident use of either zoledronic acid or denosumab, and no prior history of arrhythmia or advanced kidney disease. The primary outcome was incident AF (>=1 inpatient or >=2 outpatient diagnostic codes) over one year. Secondary outcomes included: 1) hospitalization for AF, 2) inpatient or outpatient AF diagnosis with initiation of AF medication, 3) stroke/transient ischemic attack (TIA), and 4) non-vertebral osteoporotic fracture. Within each cohort, we used Cox regression to compare outcomes between patients receiving zoledronic acid versus denosumab.In the PS-matched osteoporosis cohort (n=16,235 pairs), the average age was 71 +/- 9 years, and 93% were female. There was an increased risk of AF with zoledronic acid compared to denosumab over one year (incidence rate [IR] 18.6 v 14.9 per 1000 person-years; hazard ratio [HR] 1.25, 95% confidence interval [CI] 1.04 to 1.50). In the PS-matched malignancy cohort (n=7,732 pairs), the average age was 70 +/- 9 years, and 66% were female. There was a trend towards increased AF risk with zoledronic acid compared to denosumab over one year (IR 46.9 v 39.0 per 1000 person-years; HR 1.19, 95% CI 1.00 to 1.43, p=0.06). No increased risk of stroke/TIA occurred in either cohort. In the malignancy cohort, zoledronic acid was less effective than denosumab at preventing non-vertebral fractures (HR for fracture 1.32, 95% CI 1.01 to 1.74).Zoledronic acid, as compared to denosumab, is associated with modestly increased risk of incident AF in the first year after treatment; however absolute risk remained low. Clinicians should consider AF risk in pre-therapy counseling and subsequent monitoring of patients initiating zoledronic acid therapy.

Figure 1: Propensity score-matched Forest plots showing hazard ratios for the primary and secondary outcomes with zoledronic acid vs. denosumab in the osteoporosis cohort (A) and malignancy cohort (B)

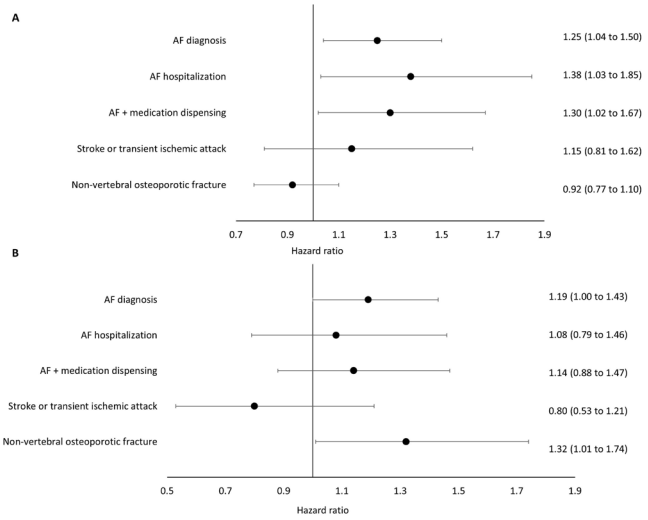

***Disclosures: Sara J. Cromer**, Johnson and Johnson, Other Financial or Material Support*

1067

Effects of the recency of sentinel fractures on conventional estimates of fracture probability using FRAX *John Kanis[1]. [1]Australian Catholic University, Australia

The recency of a prior fracture affects subsequent fracture risk. The aim of this study was to quantify the effect of a recent sentinel fracture, by site, on the 10-year probability of fracture determined with FRAX. The study used data from the Reykjavik Study fracture register that documented prospectively all validated fractures at all skeletal sites in a large sample of the population of Iceland. Fracture probabilities were determined after a sentinel fracture (humeral, clinical vertebral, forearm and hip fracture) from the hazards of death and fracture, firstly in the context of a sentinel fracture occurring within the previous two years, and secondly assuming the presence of a prior osteoporotic fracture irrespective of recency. The probability ratios provided adjustments to conventional FRAX estimates of fracture probability for recent sentinel fractures.Probability ratios to adjust 10-year FRAX probabilities of a major osteoporotic fracture for recent sentinel fractures were age dependent, decreasing with age in both men and women. Probability ratios varied according to the site of sentinel fracture with higher ratios for hip and vertebral fracture than for humerus or forearm fracture. For example, at the age of 50 years, a prior fracture in women from the UK using FRAX is associated with a 10-year fracture probability of a major osteoporotic fracture of 7.2%. Where a fracture occurred within the past two years, fracture probability was uplifted to 19, 17, 14 and 11% where the recent fracture was at the spine, hip, humerus or forearm, respectively. Probability ratios to adjust 10-year FRAX probabilities of a hip fracture for recent sentinel fractures were also age dependent, decreasing with age in both men and women (with the exception of humerus fractures). These probability ratios provide adjustments to conventional FRAX estimates of fracture probability for recent sentinel fractures.

***Disclosures: John Kanis**, None*

1068

Surrogate threshold effect: identifying BMD change linked to different levels of fracture risk reduction. Study-level analysis from the FNIH Bone Quality Project. *Richard Eastell[1], Eric Vittinghoff[2], Li-Yung Lui[3], Charles McCulloch[2], Fernando Marin[4], Anne de Papp[5], Rachel Wagman[6], Sundeep Khosla[7], Jane Cauley[8], Doug Bauer[2], Mary Bouxsein[9], Dennis Black[2]. [1]University of Sheffield, United Kingdom, [2]University of California, San Francisco, United States, [3]California Pacific Medical Center, United States, [4]Eli Lilly and Co., Spain, [5]Merck and Co. Inc., Kenilworth, NJ, United States, [6]Amgen Inc., United States, [7]Mayo Clinic, United States, [8]University of Pittsburgh, United States, [9]Harvard Medical School, United States

Recent work from the FNIH Bone Quality Study suggests that the change in dual-energy X-ray absorptiometry (DXA) bone mineral density (BMD) may be a useful surrogate for fracture endpoints, allowing for smaller and faster clinical trials for new drug approvals in osteoporosis. A key challenge is to identify the surrogate threshold effect (STE), defined as the treatment effect on the surrogate that predicts a beneficial effect on the clinical endpoint with high confidence. We have previously reported the change in total hip BMD at 24 months that predicts any fracture benefit with 95% confidence (ASBMR 2019). In this extension, we use updated methods to estimate STEs predicting clinically meaningful reductions

in fracture risk. We used individual patient data (IPD) including DXA BMD and fracture outcomes collected as part of the FNIH Bone Quality project, a public-private partnership, which compiled IPD from over 150,000 participants in all major clinical trials of osteoporosis therapies. The current analyses include data from 61,415 participants in 18 trials (11 bisphosphonate, 4 SERM, 1 parathyroid hormone analogs (PTH-like), 1 denosumab and 1 odanacatib) that measured total hip (TH) BMD. We used random effects meta-regression to estimate the association of the treatment effect on percent change in TH BMD from baseline to 24 months with the log odds- or hazard-ratio for the effect of treatment on the risk of fracture, accounting for the precision of the two treatment effects for each study. Upper 95% prediction intervals for the treatment effect on fracture risk were calculated for a fine grid of candidate treatment effects on BMD. STEs were estimated for TH BMD difference between active and placebo for different levels of minimum fracture risk reduction (Table).Thus, the STEs are greater the higher the minimum treatment effect and differ by fracture type. A regulatory agency or a sponsor might find the table useful in the interpretation of future clinical trials with total hip as the primary end point.

Table. STEs for different minimum treatment effects.

Minimum Fracture Risk Reduction	Surrogate Threshold Effect, % difference in TH BMD between active and placebo		
	Vertebral fracture	Hip fracture	Non-vertebral fracture
Any	1.4	3.2	2.1
>10%	1.9	3.7	3.5
>20%	2.4	4.5	6.2
>30%	3.0	5.8	-
>40%	3.7	-	-
>50%	4.6	-	-

***Disclosures: Richard Eastell**, Sandoz, Consultant, CL Bio, Consultant, Haoma Medica, Consultant, Samsung, Consultant, IDS, Consultant, Nittobo, Consultant, Lyramid, Consultant, Alexion Pharmaceuticals, Grant/Research Support, Nittobo, Grant/Research Support, Biocon, Consultant, Viking, Consultant, Roche Diagnostics, Grant/Research Support*

1069

Do Women with Lower BMD Benefit More from Anti-fracture Treatment? An Analysis Pooling Individual Patient Data from 134,000 Women in the FNIH-SABRE RCT Database. *Dennis Black[1], Li-Yung Lui[2], Gayle Lester[3], Douglas Bauer[1], Eric Vittinghoff[1], Mary Bouxsein[4], Richard Eastell[5]. [1]University of California, San Francisco, United States, [2]California Pacific Medical Center, United States, [3]NIH-NIAMS, United States, [4]Harvard Medical School, United States, [5]University of Sheffield, United Kingdom

Randomized trials of alendronate, ibandronate and denosumab have shown larger reductions in non-spine fracture in women with low hip BMD T-score (99% women) were at high fracture risk. These data were compiled as part of the FNIH/SABRE Project which is using these data to apply for FDA qualification for BMD change as a surrogate endpoint for fracture in future RCTs.We stratified data into subgroups by baseline femoral neck BMD -2.5. We then calculated the fracture risk reduction in vertebral, non-spine and hip fractures within each BMD subgroups. We then compared and tested the differences between subgroups by calculating the p-value for interaction of BMD group with treatment. We also calculated the number needed to treat (NNT) to prevent 1 fracture within each BMD subgroup. As a sensitivity analysis, we performed subset analyses restricting to trials of bisphosphonates.The figure shows the results for the 3 fracture types. For all 3 fracture types, reductions were statistically significant within both BMD subgroups and numerically larger among those with FN BMD T <-2.5. The difference in fracture reduction between the two groups was significant for vertebral fracture (p for interaction = 0.006), not for hip fractures (p=0.79), with a trend for non-spine fractures (p=0.08). NNTs were smaller in women with BMD T <-2.5. Results in bisphosphonate trials were similar. In summary, fracture risk was reduced in both BMD subgroups with significantly larger vertebral fracture reductions in women with BMD T <-2.5. NNT's for all 3 fracture types were consistently lower in women with BMD T <-2.5 due to higher risks. We conclude that anti-osteoporosis medications are effective in women below and above baseline femoral neck BMD T-score of -2.5 supporting the value of treating both groups of high risk women. The lower NNT in women with BMD T<-2.5 suggests that special consideration be given to treatment for these women.

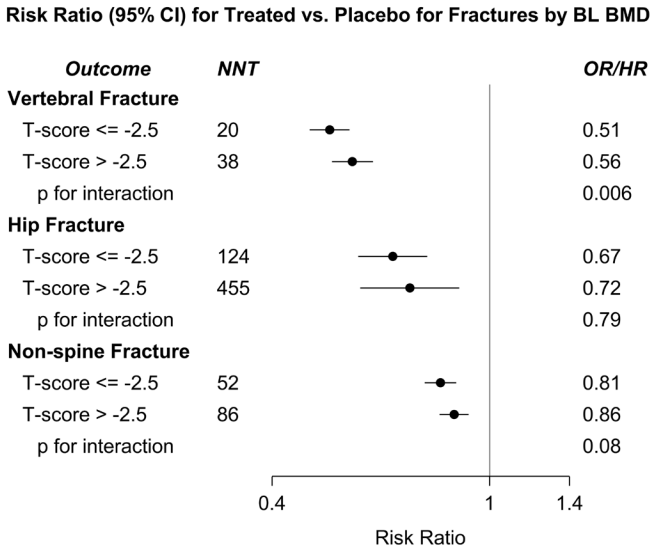

***Disclosures: Dennis Black**, None*

1070

The associations of peak bone mineral density and rate of bone mineral density loss during the menopause transition and early postmenopause with subsequent fracture: results from the Study of Women's Health Across the Nation (SWAN) *Albert Shieh[1], Arun Karlamangla[1], Mei-Hua Huang[1], Weijuan Han[1], Gail Greendale[1]. [1]UCLA, United States

Background. The Study of Women's Health Across the Nation (SWAN) has demonstrated that each standard deviation (SD) decrement of in peak lumbar (LS) or femoral (FN) BMD is linked to 50 and 60% greater risk of incident fracture, respectively. Whether the rate of BMD decline during the menopause transition (MT) contributes independently to fracture risk is unknown. This study examined the independent associations of peak BMD and rate of BMD decline during the MT and early postmenopause with incident fracture.Methods. This analysis included 451 participants from SWAN, a longitudinal study of the MT. The combined MT and early postmenopause period was defined as the interval spanning 1 year before to 5 years after the final menstrual period (FMP). We operationalized peak BMD as the last BMD measurement before 1 year prior to the FMP (BMD did not decrease before that time in SWAN). Rate of BMD decline (% per year) during the MT and early postmenopause was calculated from the peak BMD measurement and the first BMD measurement 5 years after the FMP. We used Cox proportional hazards regression to examine the following as predictors of time to first fracture after early postmenopause: 1) peak BMD; 2) rate of BMD decline during the MT and early postmenopause; and 3) peak BMD and rate of BMD decline. Models were adjusted for age, body mass index, race/ethnicity, study site, and percent of time before or after the observation period that a participant took a bone-detrimental or beneficial medication.Results. Mean (SD) age of participants 1 year before the FMP was 49.6 (2.4) years. 32 women sustained fractures after early postmenopause. Adjusted for covariates, each SD greater peak LS BMD was associated with a 44% lower hazard for fracture (p=0.007). Each 1% per year faster decline in LS BMD was associated with a 56% greater hazard for fracture (p=0.04). Peak LS BMD and rate of LS BMD decline were associated with fracture, independent of the other (Table). Women with a peak LS BMD below the sample median, and a LS BMD decline rate faster than the sample median had a 2.7-fold greater hazard for fracture (p=0.03). Neither peak BMD nor rate of BMD decline at the femoral neck was associated with fracture.Conclusion. Peak LS BMD and rate of decline in LS BMD during the MT and early postmenopause are independent risk factors for subsequent fracture. Women with both below-median peak LS BMD and faster-than-median LS BMD decline have the greatest risk for future fracture.

TABLE
Associations[1] of peak BMD and rate of BMD decline during the menopause transition and early postmenopause with subsequent fracture

	HR per SD increment in BMD or 1% per year faster decline in BMD (95% CI)	p-value
Lumbar spine		
Peak BMD[2]	0.56 (0.34, 0.85)	0.007
Rate of BMD decline[2]	1.56 (1.02, 2.41)	0.04
Peak BMD + Rate of BMD decline	0.54 (0.35, 0.84) 1.49 (1.01, 2.20)	0.005 0.04
Femoral neck		
Peak BMD[2]	0.80 (0.51, 1.26)	0.3
Rate of BMD decline[2]	1.31 (0.87, 1.99)	0.1
Peak BMD + Rate of BMD decline	0.72 (0.45, 1.14) 1.46 (0.94, 2.26)	0.1 0.09

1 Assessed by Cox proportional hazards regression with peak BMD, rate of BMD decline during the menopause transition and early postmenopause), or peak BMD and rate of BMD decline as predictors. Analyses adjusted for age, body mass index (BMI, kg/m^2), race/ethnicity, study site, and percent of time before or after the observation period that participant was exposed to a bone- beneficial or bone-detrimental medication. Mean (SD) observation period was 6.9 (2.8) years.
2 Mean (SD) peak BMD was 1.076 (0.142) g/cm^2 at the lumbar spine, and 0.844 (0.128) g/cm^2 at the femoral neck. Mean rate of BMD decline during the MT and early postmenopause was 1.46 (0.95)% per year at the lumbar spine, and 1.29 (0.86)% per year at the femoral neck.

***Disclosures: Albert Shieh**, None*

1071

Osteocalcin, Muscle Function and 15-year Falls Hospitalizations in Older Women: The Perth Longitudinal Study of Ageing Women Study *Cassandra Smith[1], Joshua R Lewis[2], Marc Sim[2], Wai H Lim[3], Ee Mun Lim[4], Lauren Blekkenhorst[2], Tara C Brennan-Speranza[5], Leon Adams[3], Elizabeth Byrnes[4], Gustavo Duque[6], Itamar Levinger[1], Richard L Prince[3]. [1]Institute for Health and Sport (IHES), Victoria University, Australia, [2]School of Medical and Health Sciences, Edith Cowan University, Australia, [3]Medical School, University Western Australia, Australia, [4]Department of Clinical Biochemistry, PathWest Laboratory Medicine, Queen Elizabeth II Medical Centre, Australia, [5]Bosch Institute for Medical Research, University of Sydney, Australia, [6]Australian Institute for Musculoskeletal Science (AIMSS), University of Melbourne and Western Health, Australia

Purpose: Undercarboxylated osteocalcin (ucOC) has recently been suggested to be involved in muscle mass maintenance and strength, at least in animal models. In humans, the ucOC to total (t)OC ratio, may be related to muscle function, a combined term that includes muscle strength and physical function. As such, the ucOC/tOC ratio may also be related to falls risk, but data are limited. We tested the hypothesis that ucOC and ucOC/tOC ratio are associated with muscle function and 15-year falls-related hospitalizations in a cohort study of older women.Methods: Serum OC and ucOC was assessed in 1261 older women (mean age 75.2 +/- 2.7 years) at year-1 of the Calcium Intake Fracture Outcome Study trial, forming the Perth Longitudinal Study of Ageing Women (PLSAW, 1998 to 2013). Timed-up-and-go and grip strength was assessed at baseline (1998) and at 5 years. Falls-related hospitalizations over a 14.5-year follow-up was captured by the Hospital Morbidity Data Collection, via the Western Australian Data Linkage System. Results: Women with the highest ucOC/tOC ratio (quartile 4) had slower timed-up-and-go test performance compared to quartile 1 by 0.68 secs (p=0.03), grip strength was not significantly different (p>0.05). Those with the highest ucOC/tOC had greater falls-related hospitalizations that remained significant after adjusting for falls risk factors (HR 1.31, 95% CI 1.09-1.57, p=0.004).Conclusions: We identified many older women with high baseline ucOC/tOC ratio also have poorer muscle function. Higher ratio was also related to an increased risk of falls hospitalization. This data supports the concept that a lower ucOC/tOC ratio may be an important indicator towards muscle function and falls-related hospitalizations in older women. Considering links between ucOC/tOC and vitamin K sufficiency, whether this association is due to the vitamin K signal transduction pathway remains to be identified.

***Disclosures: Cassandra Smith**, None*

1072

Uncovering The Total Costs Of Osteoporosis-related Fractures In US Postmenopausal Women *Oth Tran[1], Stuart Silverman[2], Xiaoqing Xu[3], Machaon Bonafede[1], Kathleen Fox[4], Michele McDermott[3], Shravanthi R Gandra[3]. [1]IBM Watson Health, United States, [2]Cedars-Sinai Medical Center and David Geffen School of Medicine, United States, [3]Amgen Inc., United States, [4]Strategic Healthcare Solutions, LLC, United States

Osteoporotic fractures are associated with substantial economic burden in the first year following a fracture regardless of fracture type. Current literature focuses on the short-term costs of osteoporotic fractures; however, fractures can have prolonged effects on patient health and both recent short-term as well as long-term data examining the cost of fracture are lacking. In this study, we compared direct and indirect healthcare costs between postmenopausal osteoporotic women and demographically matched controls in the 5 years after incident fracture, and by fracture type in commercially insured and Medicare populations. Using MarketScan claims data, 226,190 women (91,925 aged 50–64 years; 134,265 aged >=65 years) with incident osteoporotic fracture by type (hip, vertebral, and non-hip non-vertebral [NHNV]) from 2008–2017 were identified. Each fracture case, by type of fracture, was matched to a non-fracture control (1:1) based on age, geographic region, years of follow-up, and insurance type. Direct costs were assessed based on general linear models after adjusting for baseline costs, comorbidities, osteoporosis diagnosis, and treatment. Indirect costs including work loss due to absenteeism and short-term disability (STD) were assessed among commercially-insured patients. Costs were standardized to 2019 US dollars.Baseline osteoporosis diagnosis and treatment rates were low among commercially-insured and Medicare patients. For all fracture types, commercially insured and Medicare patients incurred higher direct costs across all 5 years post-index compared with non-fracture controls. The unadjusted costs among hip fracture patients were 9.5 times higher at Year 1 and 3 times higher at Year 5 than matched controls (Figure). The adjusted mean incremental costs at Year 1 for hip, vertebral, and NHNV fractures were $59,327, $29,987, and $14,390 among commercially-insured patients, and $45,755, $21,169, and $19,209 among Medicare patients, respectively. Further, indirect costs among patients with each fracture type evaluated were higher than controls due to absenteeism and STD at Year 1. Patients with fracture had higher adjusted indirect costs due to STD (incremental cost $5,848, $2,748, and $2,596 for hip, vertebral, and NHNV fracture, respectively) compared with controls during Year 1 post-index. The significant economic burden after an osteoporosis-related fracture underscores the need for early patient identification and timely treatment.

***Disclosures: Oth Tran**, IBM Watson, Consultant*

1073

The Stat3/mitophagy axis coordinates macrophage NLRP3 inflammasome activation and inflammatory bone loss *Zijun Wang [1], Lingxin Zhu[1], Minquan Du[1], Bin Peng[1]. [1]School and Hospital of Stomatology, Wuhan University, China

Accumulating evidence indicates that the inflammasomes are implicated in a wide range of bone destructive diseases driven by both sterile and non-sterile inflammation. Signal transducer and activator of transcription 3 (Stat3) is a cytokine-responsive transcription factor involved in important immune functions including both pro- and anti-inflammatory responses. However, the role of Stat3 in macrophage NLRP3 inflammasome activation and inflammatory osteolysis remains unknown. Here, we found that Stat3 was activated in macrophages during NLRP3 inflammasome activation in vitro and inflammatory osteolysis in vivo. We employed a Stat3 inhibitor Stattic, which inhibits the phosphorylation and DNA binding activity of Stat3, to target Stat3 in macrophages in vitro and inflammatory bone loss in vivo. The Stat3 inhibitor significantly blocked NLRP3 inflammasome activation in primary mouse bone marrow-derived macrophages in vitro, as evidenced by remarkable decrease of cleaved caspase-1 p20 and IL-1β p17 released into the supernatants. The cellular expression level of NLRP3, IL-1β and caspase-1 was unaffected upon Stat3 inhibition. We then sought to determine the molecular mechanisms underlying Stat3-regulated NLRP3 inflammasome activation. Unexpectedly, the Stat3 inhibition caused the notable upregulation of PINK1/Parkin expression and mitophagy occurrence in bone marrow-derived macrophages, leading to a reversed mitochondrial membrane potential collapse, which probably in turn inactivates the NLRP3 inflammasome. Indeed, the mitophagy inhibitor Mdivi-1 significantly reversed the effects of Stat3 inhibition on caspase-1 activation and IL-1β secretion in macrophages, indicating the crucial dependence of Stat3 on mitophagy during inflammasome activation. Importantly, administration of Stat3 inhibitor significantly protected mice from inflammatory osteolysis models of both infection-induced periapical bone destruction and aseptic titanium particle-induced calvarial bone erosion, accompanied with the potent induction of mitophagy, decreased macrophage infiltration and osteoclast number. Together, these studies characterize a previously unsuspected Stat3/mitophagy axis in regulating macrophage inflammasome activation and inflammatory bone loss, and propose a potential therapeutic intervention by targeting this pathway to prevent inflammatory osteolytic bone diseases.

Disclosures: Zijun Wang, *None*

1074

Macrophage Lineage Hdac3 Deletion Enhances Bone Healing and Promotes Lcn2-Dependent Macrophage Metabolic Reprogramming *David Molstad[1], Elizabeth Bradley[1], Jennifer Westendorf[2]. [1]University of Minnesota, United States, [2]Mayo Clinic, United States

Macrophages play a central role in tissue regeneration, participating in both the initial inflammatory response and tissue healing. Although a spectrum exists, inflammatory macrophages (M1) are primarily involved during the initial response to injury; whereas alternative macrophages (e.g., M2) are the primary tissue healing effectors. Altered cellular metabolism, via breaks in oxidative phosphorylation, facilitates M1-associated inflammation. In contrast, M2 exhibits enhanced glucose metabolism that is mediated by PI3K/Akt/mTOR signaling. Genetic and epigenetic studies demonstrate that histone deacetylase (Hdac) 3 plays a critical role in controlling inflammation. Likewise, Hdac inhibitors suppress and conditional deletion of Hdac3 (Hdac3 cKOLysM) enhances M2. Hdac3 deficiency enhances collagen deposition within atherosclerotic lesions and stabilizes plaques, but the impact on bone healing is unknown. We therefore examined how Hdac3 deficiency impacts bone healing and alters macrophage metabolism. We induced single cortex defects in Hdac3 cKOLysM 12-week-old mice or their control littermates and assessed bone healing 14 days after defect generation (n=7). Female Hdac3 cKOLysM mice showed an average 140% increase in BV/TV within the defect site. Unbiased RNA sequencing revealed altered expression of genes related to inflammation and metabolism, including decreased Lipocalin2 (Lcn2), by Hdac3 deficient bone marrow macrophages (BMMs). We confirmed these data and showed diminished Lcn2 levels by ex vivo cultured Hdac3 cKOLysM BMMs, and in vivo within the bone marrow of 12-week-old Hdac3 cKOLysM mice (n=6) via IHC. Moreover, BMMs treated with the PAN Hdac inhibitor SAHA or the Hdac3-specific inhibitor Rgfp966 exhibited increased Akt/mTOR/S6K pathway activation and expression of glycolytic genes, but Lcn2 levels were suppressed. Rgfp966 promoted glycolysis of BMMs, as measured by lactate production, but SAHA did not. As expected, lactate levels were increased by a two hour insulin or IL4 treatment, but Hdac inhibition did not potentiate this effect. Finally, we assessed LCN2 levels as a function of age via IHC using a human bone marrow tissue array. LCN2 levels were lowest in bone marrow biopsies from males and females under the age of 30, but were high in males and females over the age of 65. These data support that myeloid-lineage Hdac3 deficiency, by promoting M2 polarization, enhances bone healing and promotes Lcn2-dependent metabolic reprogramming.

Disclosures: David Molstad, *None*

1075

Preosteoblasts modulate myelopoiesis in the bone marrow by producing the chemokines CCL3 and CCL4 *Alexander Lubosch[1], Franziska Wirth[1], Katrin Huck[1], Caren Zoeller[1], Hiba Ghura[1], Stefan Hamelmann[1], Stefan Porubsky[2], Inaam Nakchbandi[1]. [1]University of Heidelberg, Germany, [2]University Of Mainz, Germany

Osteoblasts affect hematopoiesis and modulate the immune response against cancer (Rossnagl et al. PLoS Biology 2016), in addition to their classical role in bone formation. Integrin signaling modulates the ability of osteoblasts both to differentiate (Sens et al. JBMR 2017, J Biol Chem 2017) and to modify the immune response by exposed myeloid cells. A Rho GTPase called CDC42 located downstream of integrin signaling is additionally able to integrate these signals with those originating from the wnt pathway and various growth factors. We therefore aimed to characterize the influence of CDC42 in osteoblasts on hematopoiesis.Deletion of Cdc42 in vivo in preosteoblasts using the osterix (Osx) promoter to drive cre expression in CDC42 floxed homozygous (conditional knockout: cKO) diminished osteoblast function in vitro (von Kossa staining, $p<0.001$) and in vivo leading to diminished BMD (CT: 290 vs. Osx cKO: 246 mg/cm3, $p<0.0001$). In addition, hematopoietic common myeloid progenitors (CMPs) increased in the bone marrow. These give rise to erythrocytes, thrombocytes, granulocytes and macrophages (CMPs increased by 17%, $p<0.05$). In peripheral blood, a rise in cells derived from these progenitors, namely erythrocytes and platelets was detected (Platelets increased by 18%, $p<0.05$). Interestingly, deletion of CDC42 in differentiating osteoblasts using the collagen α1(I) promoter to drive cre expression in CDC42 floxed mice also diminished BMD (Control: 262 vs. collagen cKO: 242 mg/cm3, $p<0.05$), albeit to a lesser degree than in Osx cKO. This was due to a decrease in osteoblast numbers and function (ObN/BS decreased by 34%, $p<0.001$). Hematopoiesis in the bone marrow and peripheral blood cells were unaffected. Thus, CDC42 expression in preosteoblasts, but not in differentiating osteoblasts modulates hematopoiesis in the bone marrow.To establish causality between CDC42 loss in preosteoblasts and changes in hematopoiesis, we isolated bone marrow stromal cells and treated these with a chemical CDC42 inhibitor. After removal of the inhibitor, pretreated stromal cells were able to advance the differentiation of sorted hematopoietic stem cells and increase myelopoiesis compared to untreated stromal cells (60% increase, $p<0.005$). Bone marrow stromal cells that were treated with CDC42 inhibitor as well as cells isolated from Osx cKO were compared to their respective controls. In the conditioned media of treated and cKO cells two chemokines were increased: CCL3 (4-fold increase, $p<0.05$) and CCL4 (2-fold increase, $p<0.05$). Inhibiting either one of the chemokines in pretreated stromal cells cocultured with stem cells counteracted the increase in myelopoiesis ($p<0.05$).In summary, preosteoblasts, but not differentiating osteoblastic cells modulate myelopoiesis. This effect involves the Rho GTPase Cdc42 and is mediated by the chemokines CCL3 and CCL4.

Disclosures: Alexander Lubosch, *None*

1076

Blocking of osteocyte Toll-like receptor signaling uncouples bone resorption from inflammation *Tetsuya Yoshimoto[1], Mizuho Kittaka[1], Matt Prideaux[2], Lynda F Bonewald[2], Yasuyoshi Ueki[1]. [1]Indiana University School of Dentistry, Indiana Center for Musculoskeletal Health, Indiana University School of Medicine, United States, [2]Indiana Center for Musculoskeletal Health, Indiana University School of Medicine, United States

It is well known that bacterial pathogens are potent inducers of bone resorption. As osteocytes express RANKL to activate osteoclasts, we proposed that osteocytes are the cellular mediators between bacterial infection and osteoclastogenesis. As we found that, like immune cells, osteocytes express Toll-like receptor 2 (TLR2) and its signal transducer MYD88, Dmp1-Cre Myd88fl/fl mice were generated with targeted deletion of Myd88 in osteocytes. Injection of the TLR1/2 agonist Pam3CSK4 onto calvaria of these mice resulted in a reduction in bone erosion (67.2% males; 69.3% females) compared to control Myd88fl/fl mice. The Pam3CSK4-injected Dmp1-Cre Myd88fl/fl mice showed decreased osteoclast numbers and Rankl expression. However, there were no differences in inflammation. As interleukin-1 receptor (IL-1R) also signals via MYD88, we next injected Pam3CSK4 to Dmp1-Cre Il1r1fl/fl mice, but found no reduction in bone loss, suggesting that activation of TLR in osteocytes plays an exclusive role in osteoclast activation. To determine if this signaling mechanism is specific for osteocytes, both osteoblast (Ob)- and osteocyte (Ocy)-enriched cell populations were isolated from calvaria of 10-week-old C57BL/6J mice by sequential enzymatic digestion. Strikingly, stimulation with Pam3CSK4 induced much higher Rankl expression in Ocy-enriched cells compared to Ob-enriched cells (4.3 vs. 1.2-fold at 4 hours, n = 3) and this signaling for Rankl was blocked in the Ocy cells by inhibiting MAPKs. The co-culture of Ocy-enriched cells with osteoclast precursors in the presence of Pam3CSK4 showed a 5.2-fold increase in osteoclast formation compared to co-culture with Ob-enriched cells. Inducing periodontitis by oral infection with P.gingivalis resulted in significantly less alveolar bone loss in Dmp1-Cre Myd88fl/fl mice along with a decrease in Rankl expression in the jawbones, but no decrease in inflammation in the gingiva. Intraperitoneal administration of T6167923, an MYD88 inhibitor, protected against alveolar bone loss in the wild-type mice with P.gingivalis periodontitis. We also found the bacteria within the Ocy lacunar-canalicular system in this model. In summary, our data show that blocking of osteocytic RANKL uncouples bone resorption from inflammation in periodontitis and potentially other bacterial

infections. The osteocytic TLR-MYD88 pathway may be an emerging target to prevent and treat bone loss in pathogen-driven inflammatory bone diseases.

***Disclosures: Tetsuya Yoshimoto**, None*

1077

Ovariectomy Induces Bone Loss Via Microbial Dependent Trafficking of Intestinal TNF Producing T Cells and Th17 Cells to the Bone Marrow

*Roberto Pacifici[1], Mingcan Yu[2], Subhashis Pal[2], Cameron Paterson[3], Jau-Yi Li[2], Abdul Malik Tyagi[2], Jonathan Adams[2], Craig M Coopersmith[4], M. Neale Weitzmann[5]. [1]1 Division of Endocrinology, Metabolism and Lipids, Department of Medicine, Emory University, Atlanta, GA; 2 Emory Microbiome Research Center, Emory University, Atlanta, GA; 6 Immunology and Molecular Pathogenesis Program, Emory University, Atlanta, GA., United States, [2]1 Division of Endocrinology, Metabolism and Lipids, Department of Medicine, Emory University, Atlanta, GA; 2 Emory Microbiome Research Center, Emory University, Atlanta, GA., United States, [3]3 Department of Surgery and Emory Critical Care Center, Emory University School of Medicine; 4 Lieutenant, Medical Corps, United States Navy, NROTC Atlanta., United States, [4]2 Emory Microbiome Research Center, Emory University, Atlanta, GA; 3 Department of Surgery and Emory Critical Care Center, Emory University School of Medicine., United States, [5]1 Division of Endocrinology, Metabolism and Lipids, Department of Medicine, Emory University, Atlanta, GA; 2 Emory Microbiome Research Center, Emory University, Atlanta, GA; 5 Atlanta VA Medical Center, Decatur, GA., United States

Estrogen deficiency causes a gut microbiome dependent expansion of bone marrow (BM) Th17 cells and TNFa (TNF) producing (TNF+) T cells. The resulting increased BM levels of IL-17 and TNF stimulate RANKL expression and activity causing bone loss. However, the origin of BM Th17 cells and TNF+ T cells is unknown. We found that ovariectomy (ovx) expanded the pool of TNF+ T cells and Th17 cells, as well as the transcript levels of TNF and IL-17 in the gut and the BM suggesting that ovx may increase the trafficking of intestinal T cells to the BM. To directly measure T cell trafficking, Kaede mice (which ubiquitously express a photoconvertible protein that changes its fluorescence emission from green to red upon photoactivation with UV light) were sham operated or ovx. Two weeks later intestinal Peyer's patches were surgically exposed and photo-converted by UV light exposure for 1 minute. BM red T cells were counted by flow cytometry 24 hours later. These experiments revealed that ovx increased by ~ 3-6 fold the homing of intestinal TNF+ T cells and Th17 cells into the BM. Studies using eGFP labeled Th17 cells confirmed that ovx increases the tropism of Th17 cells toward the BM. We found the egress of TNF+ T cells and Th17 cells from the intestine to the systemic circulation to be mediated by the S1P-receptor 1 (S1PR1) expressed in T cells and circulating S1P. The influx of TNF+ T cells from the circulation to the BM was mediated by the chemokine receptor CXCR3. The resulting increase in BM TNF levels upregulated the expression of the CXCR6 ligand CCL20 by BM cells. CCL20 then recruited CXCR6+ Th17 cells to the BM, causing and expansion of the pool of Th17 cells and the levels of IL-17 in the BM. Attesting to the functional relevance of T cell trafficking, the loss of trabecular bone and the increase in bone turnover induced by ovx were completed prevented by either: a) treatment with the S1PR1 functional antagonist FTY720, an agent that blocks T cell egress from the intestine, b) blockade of TNF+ T cells trafficking to the BM by silencing of CXCR3, or c) arrest of Th17 cells influx to the BM via treatment with anti CCL20 Ab. In summary, the Th17 cells and TNF+ T cells that accumulate in the BM of ovx mice originate in the gut. Intestinal T cells are a proximal target of sex steroid deficiency relevant for bone loss. Blockade of intestinal T cell migration may represent a therapeutic strategy for the treatment of postmenopausal bone loss.

***Disclosures: Roberto Pacifici**, None*

1078

TNFR2 signaling pathway mediated by 14-3-3ε instructs macrophage plasticity in inflammatory arthritis

*Wenyu Fu[1], Young-su Yi[1], Aubryanna Hettinghouse[1], Wenjun He[1], Guodong Sun[1], Yufei Bi[1], Chuan-Ju Liu[1]. [1]New York University Medical Center, United States

Inflammatory arthritis is a polyarticular chronic inflammatory disease characterized by deregulated immune response and bone erosion. Increasing evidences document that macrophages contribute significantly to the inflammation in inflammatory arthritis, thus therapeutic strategy targeting the unbalanced M1/M2 ratio represents an attractive target in treating inflammatory arthritis. Although it is well recognized that TNFR2 plays a beneficial anti-inflammation function in inflammatory diseases, its role in macrophage polarization, particularly under inflammatory arthritis, remains unknown.Here we found that activation of TNFR2 with its novel ligand progranulin (PGRN) markedly skewed the macrophage toward anti-inflammatory M2 macrophage. Using biochemical co-purification and mass spectrometry approaches, we isolated the signaling molecule 14-3-3ε as a novel component of TNFR2 complexes in response to PGRN stimulation in macrophages. PGRN's effects on macrophage polarization were largely abolished in 14-3-3ε knockout Raw264.7 and primary BMDMs, and re-expression of 14-3-3ε restored 14-3-3ε knockout cells' response to PGRN, suggesting that 14-3-3ε serves as a mediator of PGRN/TNFR2 signaling. Global or macrophage specific 14-3-3ε deficiency resulted in an overt pro-inflammatory response through skewing macrophage toward M1 and unbalanced M1/M2 ratio relative to control littermates; in addition, PGRN's anti-inflammation action was largely abolished in 14-3-3ε deficient mice, suggesting that unbalanced M1/M2 ratio played a pathologic role in inflammatory arthritis, and targeting macrophage plasticity through 14-3-3ε by PGRN/TNFR2 may hold a therapeutic promise for inflammatory arthritis.Combining transcriptome profiling and GSEA analysis, examination of activation status of key signaling molecules, along with DNA binding activity analysis revealed that TNFR2/14-3-3ε signaled through PI3K Akt mTOR to restrict NF-κB activation while simultaneously to stimulate C/EBPβ activation, thereby instructing macrophage functional plasticity (Fig. 1).In summary, our study identified 14-3-3ε as a novel regulator which is necessary and sufficient to mediate TNFR2's regulation on macrophage polarization. This study not only provides new insights into TNFR2 signaling, but may also lead to the development of new interventions for various inflammatory diseases, particularly inflammatory diseases.

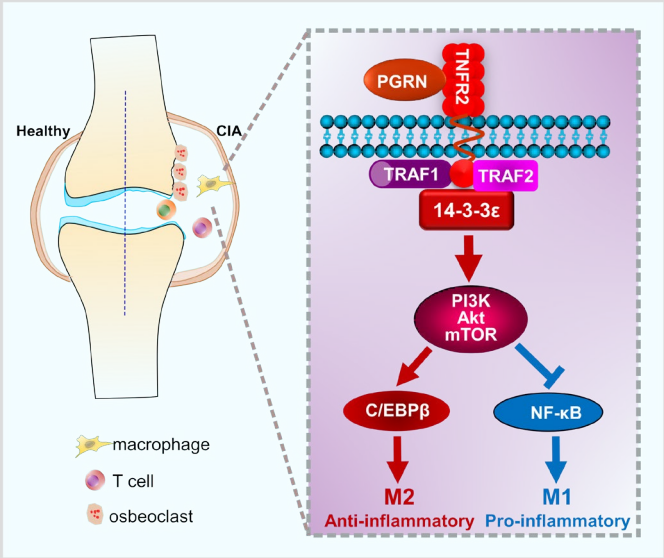

***Disclosures: Wenyu Fu**, None*

1079

Fracture Risk in Type 2 Diabetes: Longitudinal Glycemic Control Based Prediction and the Efficacy of Medications

*Bowen Wang[1], Zehai Wang[1], Atharva Poundarik[1], Mohammed Zaki[2], Richard Bockman[3], Deepak Vashishth[1]. [1]Center for Biotechnology and Interdisciplinary Studies, Department of Biomedical Engineering, Rensselaer Polytechnic Institute, United States, [2]Department of Computer Science, Rensselaer Polytechnic Institute, United States, [3]Division of Endocrinology and Metabolic Bone Disease, Hospital for Special Surgery, United States

The increased fracture risk in people with type 2 diabetes (T2D) is underestimated in clinical BMD-based fracture risk assessments, such as such as the FRAX tool. The loss of glycemic control in patients with T2D has been associated with multiple tissue modifications, including bone quality alteration. In this study, we proposed to use longitudinal HbA1c, a serum based glycemic marker routinely measured in people with T2D over a period of time, to independently predict T2D fractures. The efficacy of longitudinal anti-diabetic and anti-osteoporotic medication use was also examined.The OptumLabs® Data Warehouse (OLDW) is a longitudinal, real-world data asset with de-identified administrative claims and electronic health record (EHR) data. Over the period of 01/01/2007 to 09/31/2015, a cohort of 154,345 patients with T2D (age >= 55 years) with available HbA1c measurements was identified from OLDW. Correlations were assessed based on different durations of HbA1c aggregate and following fracture incidences. Kaplan-Meier survival analysis and Cox proportional hazard model were used to evaluate the relationship between longitudinal HbA1c, medications, and fracture risk. The covariates selected in the multivariate model include sex, age, use of three types of medication (metformin, insulin, bisphosphonates), and comorbidities.A strong positive correlation was shown between one-year follow-up fracture rate and two-year average HbA1c (Fig. 1A, $R2 = 0.97$; $p < 0.005$). Figure 1B illustrates the survival curves of two-year cumulative fracture rate stratified by HbA1c bins (two-year average). The fracture rate between groups were significantly different ($p < 0.005$). With 13 covariates adjusted, a 1% increase in two-year average HbA1c is responsible for 2% increase in risk of fracture for the following two years ($p=0.03$). Two-year use of metformin correlated with decreased fracture risk, while insulin and bisphosphonates were associated with higher risk of fracture (all $p < 0.005$). We also discovered that fracture risk has a more linear response to longitudinal HbA1c with a lower threshold, compared to other comorbidities.Our finding suggests longitudinal two-year HbA1c average independently predicts the subsequent two

years' fracture risk. Maintenance of glycemic control, and the use of metformin is beneficial in managing fracture risk in people with T2D.

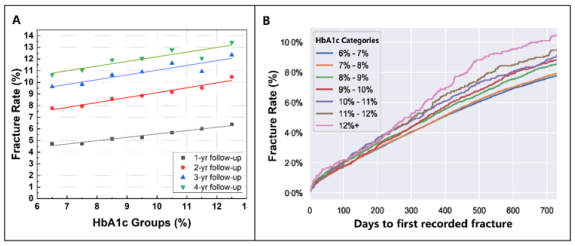

Figure 1. (A) Correlations between fixed two-year longitudinal HbA1c average and one to four-year of following fracture rate. **(B)** . Kaplan-Meier estimation of fracture rate for two years of follow-up period, stratified by two-year HbA1c average.

***Disclosures: Bowen Wang**, None*

1080

Use of Sodium-glucose Co-transporter-2 Inhibitors, Changes in Body Mass Index and Risk of Fracture in the United Kingdom (UK) *Nikki Werkman[1], Judith van Dalem[1], Johanna Driessen[1], Bernardette Rossi[2], Peter Vestergaard[3], Joop van den Bergh[4], Richard Eastell[5], Andrea Burden[6], Nicklas Rasmussen[7], Olaf Klungel[8], Martijn Brouwers[9], Frank de Vries[1]. [1]Department of Clinical Pharmacy and Toxicology, Maastricht University Medical Centre+, Netherlands, [2]Directorate Pharmaceutical Affairs, Department for Policy in Health, Ministry for Health, Malta, [3]Aalborg University Hospital and Aalborg University, Denmark, [4]Department of Internal Medicine, Division of Rheumatology, Maastricht University Medical Center+, Netherlands, [5]Department of Oncology and Metabolism, University of Sheffield, United Kingdom, [6]Department of Chemistry and Applied Biosciences, Institute of Pharmaceutical Sciences, Switzerland, [7]Steno Diabetes Center North Denmark, Aalborg University Hospital, Denmark, [8]Division of Pharmacoepidemiology and Clinical Pharmacology, Utrecht Institute of Pharmaceutical Sciences, Netherlands, [9]Department of Internal Medicine, division of Endocrinology and Metabolic Disease, Maastricht University Medical Centre+, Netherlands

Background: Type 2 diabetes (T2D) is a metabolic disorder associated with decreased bone quality. Clinical trials showed that sodium-glucose co-transporter 2 inhibitors (SGLT2-Is) were associated with considerable weight loss in T2D. There is conflicting evidence regarding a potential reduction of bone mineral density associated with these drugs. Former studies presented contradicting results regarding the association of SGLT2-Is and major osteoporotic fracture risk. However, the potential role of weight loss due to SGLT2-I use was not considered.Objectives: The aim of the current study was to investigate the association between SGLT2-I use, changes in body mass index (BMI) and the risk of major osteoporotic fractures.Methods: A retrospective population-based cohort study was conducted using data from the UK Clinical Practice Research Datalink (CPRD) GOLD (2013-2018). The study population (N=34,960) consisted of T2D patients aged 18+ who received a first ever prescription of a sulphonylurea (SU) or SGLT2-I. The date of the first prescription defined the start of follow-up. Time-varying Cox proportional hazards models were used to estimate the hazard ratios (HRs) of major osteoporotic fracture with current SGLT2-I use versus current SU use, stratified by change in BMI. Analyses were adjusted for age, sex, lifestyle variables, comorbidities and concomitant drug use.Results: Current use of SGLT2-Is was not associated with increased risk of major osteoporotic fracture (adjusted HR 1.19; 95% confidence interval 0.80-1.79) compared to SU users. This finding remained consistent after stratification by change in BMI (see table).Conclusions: Current use of SGLT2-Is was not associated with osteoporotic fracture risk compared to current use of SUs. Among current SGLT2-I users, loss of BMI was not associated with risk of major osteoporotic fracture. These results suggest that SGLT2-I use is not associated with an increased risk of osteoporotic fractures, irrespective of change in BMI.

Table The risk of major osteoporotic fractures with current use of SGLT2-Is versus current use of SUs, by change in BMI since index date.

	Number of MOFs (N=415)	IR (/1000 PY)	Age/sex adjusted HR (95% CI)	Adjusted HR[a] (95% CI)
Current SU use	124	5.28	Reference	Reference
Current SGLT2-I use	33	4.53	1.22 (0.82 - 1.82)	1.19 (0.80 - 1.79)
By change in BMI[b]				
Loss or gain of ≤0.5kg/m^2	14	4.85	1.32 (0.76 - 2.32)	1.26 (0.72 - 2.23)
Loss of ≥ 0.51 kg/m^2	15	4.09	1.09 (0.63 - 1.89)	1.11 (0.64 - 1.93)
Gain of ≥ 0.51 kg/m^2	<5	5.54	1.50 (0.55 - 4.09)	1.30 (0.47 - 3.58)

Abbreviations: MOF: major osteoporotic fracture; IR: incidence rate; PY: person years; HR: hazard ratio; CI: confidence interval; SU: sulphonylurea; SGLT2-I: sodium-glucose cotransporter-2 inhibitor; BMI: body mass index. Current use: most recent prescription within 90 days before the start of an interval.
[a] Adjusted for sex, age, alcohol use, diabetes duration, falls in the previous 7-12 months, a history of fracture, chronic obstructive pulmonary disease, congestive heart failure, cancer and use of the following drugs in the previous 6 months: insulin, antidepressants, anxiolytics/hypnotics, bisphosphonates, calcium and glucocorticoids.
[b] Change since start of follow-up.

***Disclosures: Nikki Werkman**, None*

1081

Greater Serum Carboxy-Methyl-Lysine (CML) is Associated with Increased Fracture Risk in Type 2 Diabetes: The Health, Aging and Body Composition Study *Ruban Dhaliwal[1], Susan Ewing[2], Deepak Vashishth[3], Richard Semba[4], Ann Schwartz[2]. [1]State University of New York, Upstate Medical University, United States, [2]University of California San Francisco, United States, [3]Department of Biomedical Engineering, Rensselaer Polytechnic Institute, United States, [4]The Johns Hopkins University School of Medicine, United States

Purpose: Accumulation of advanced glycation end-products (AGE) occurs with aging and diabetes in tissues with low turnover, including bone collagen. This accumulation alters collagen structure and function. Data on the relationship of fluorescent AGEs and fractures are not consistent. We examined the association of a non-fluorescent AGE, Carboxy-methyl-lysine (CML) with incident clinical and prevalent vertebral fractures by type 2 diabetes (T2DM) status, in men and women ages 70-79 years from the Health, Aging, and Body Composition study.Methods: Determinants of T2DM were self-report, use of hypoglycemic medication, elevated fasting glucose (>=126 mg/dl), or impaired glucose tolerance (2-hour plasma glucose during oral glucose tolerance test >=200 mg/dl). Incident clinical fractures and baseline vertebral fractures were assessed. Cox proportional hazards models were used to analyze the associations between log-transformed baseline serum CML and risk of clinical fractures, and logistic regression models for prevalent vertebral fractures.Results: At baseline, mean +/- SD age was 73.7 +/- 2.8 and 73.6 +/- 2.9 years in T2DM (n = 712) and non-DM (n = 2,332), respectively. Baseline CML levels were significantly higher in T2DM than non-DM (893 +/- 332 vs. 771 +/- 270 ng/ml, p <0.0001). Incident clinical fractures occurred in 136 T2DM participants over mean follow-up of 9.6 years and in 509 non-DM participants over mean 10.9 years. Among the subset with lateral scout data (n = 1,038), 11 T2DM and 18 non-DM participants had prevalent vertebral fracture. In models adjusted for age, race, gender, and clinic, greater CML was significantly associated with higher risk of clinical fracture in T2DM (Hazard Ratio (HR) 1.45; 95% CI: 1.22, 1.73 per 1 SD increase in log CML) but not in non-DM (HR 1.07; 95% CI: 0.98, 1.16; p for interaction = 0.004). Further adjustment for weight, weight loss, smoking, A1c, BMD, cystatin-C, and medications had little effect (Table 1). Greater CML was also associated with increased prevalence of vertebral fracture in T2DM but not in non-DM (Table 1).Conclusion: Higher CML levels are associated with increased risk of incident clinical fractures and higher likelihood of prevalent vertebral fractures in T2DM, independent of BMD. These results implicate CML in the pathogenesis of bone fragility in diabetes.

Table 1. Relative risk[a] and 95% CI for clinical fractures and prevalent vertebral deformities associated with 1 SD increase in CML[b]

		Minimally adjusted[c]			Multivariable model[d]		
	n[e]	RR[a]	95% CI	*P*	RR[a]	95% CI	*P*
Clinical fracture[f]							
Diabetes	136	1.45	1.22, 1.73	<0.001	1.46	1.22, 1.75	<0.001
Non-diabetes	509	1.07	0.98, 1.16	0.16	1.03	0.94, 1.13	0.50
Moderate or severe vertebral deformity[g]							
Diabetes	11	1.51	0.82, 2.79	0.19	2.28	0.92, 5.63	0.07
Non-diabetes	18	0.79	0.52, 1.19	0.27	0.75	0.48, 1.19	0.22

[a] Relative hazard ratio for clinical fracture models; odds ratio for vertebral deformity models
[b] Log-transformed CML
[c] Adjusted for age, race, gender and clinic
[d] Adjusted for age, race, gender, clinic, current smoker, baseline total hip BMD, baseline weight, weight loss of 5+ pounds in year before baseline, cystatin-C, A1C, and use of vitamin D supplements, calcium supplements, oral steroids, osteoporosis drugs (bisphosphonates, calcitonin, raloxifene), thiazide diuretics, statins, oral estrogen and, in models with diabetes participants, use of insulin and thiazolidinediones
[e] Number of participants with at least one fracture
[f] *P* value for interaction between log CML and diabetes status = 0.004 in minimally adjusted model and = 0.001 in multivariate model
[g] *P* value for interaction between log CML and diabetes status = 0.09 in minimally adjusted model and = 0.06 in multivariate model

***Disclosures: Ruban Dhaliwal**, None*

1082

Dietary Advanced glycation end-products (dAGEs) and bone health: a cross-sectional analysis in Rotterdam study *Komal Waqas[1], Jinluan Chen[2], Trudy Voortman[2], Fernando Rivadeneira[2], Andre G Uitterlinden[2], M. Carola Zillikens[3]. [1]Department of internal Medicine, Erasmus Medical Centre, Netherlands, [2]Department of Epidemiology, Erasmus Medical Centre, Netherlands, [3]Department of Internal Medicine, Erasmus Medical Centre, Netherlands

We recently showed that subjects with high skin advanced glycation end products (AGEs) have more prevalent vertebral (VFs) and major osteoporotic fractures (MOFs). No studies have yet investigated the association of dietary intake of AGEs namely, Carboxymethyllysine (CML), in human subjects with bone mineral density and fractures. A cross-sectional analysis was performed in 3939 participants from Rotterdam study by using CML estimated from food frequency questionnaires and a dAGE database. Bone mineral density (BMD) was estimated using insight dual X-ray absorptiometry. We defined MOFs as hip, wrist, humerus and clinical VFs; and VFs as Genant's radiological grade 2 and 3 + clinically reported VFs. Multivariate linear and logistic regression models were performed adjusting for sex, age, RS-cohorts, physical activity, diet quality, energy intake, eGFR, diabetes status, smoking and BMI and subsequently BMD. Mean age of our cohort was 66.7+/-10.5 years with 43% males and 12% subjects with diabetes. In fully adjusted models, we observed no association of CML with TBS (β=-0.015; p=0.48) and BMD at both femoral neck (β=-0.006; p=0.70) and lumbar spine (β=-0.013; p=0.38). Higher intake of CML was found to be associated with vertebral fractures (Odds ratio, OR=1.16, 95% confidence interval, (1.02-1.32), p=0.02) and a similar but non-significant trend with MOFs (OR=1.12 (0.98-1.27), p=0.10). Adjustment for BMD did not change associations with fractures. Stratification showed a significant association for VFs in females and subjects without diabetes. Top 6 food categories contributing to more than 70% of daily dietary CML intake, namely: Sweets, Whole grains, Unprocessed Meat, Refined grains and Processed Meat in descending order. Together, CML intake of top 6 food categories were significantly associated with VFs (OR=1.15 (1.03-1.29), p=0.02) with almost a similar effect size as all 21 categories but not with MOFs (OR=1.09 (0.97-1.22), p=0.17). In conclusion, dietary intake of CML was associated with VFs independent of BMD. CML from milk, grains and meat might impact bone health negatively but future studies are needed to elucidate whether associations found are causal and related to intake of CML alone or other constituents of these foods.

***Disclosures: Komal Waqas**, None*

1083

Saturated and Unsaturated Bone Marrow Lipids Have Distinct Effects on Bone Density and Fracture Risk in Older Adults *Gina Woods[1], Susan Ewing[2], Sigurdur Sigurdsson[3], Eric Vittinghoff[2], Deborah Kado[1], Trisha Hue[2], Thomas Lang[2], Tamara Harris[4], Clifford Rosen[5], Vilmunder Gudnason[6], Anne Schafer[2], Xiaojuan Li[7], Ann Schwartz[2]. [1]University of California, San Diego, United States, [2]University of California, San Francisco, United States, [3]Icelandic Heart Association, Iceland, [4]National Institutes of Health, United States, [5]Maine Medical Center Research Institute, United States, [6]University of Iceland, Iceland, [7]Cleveland Clinic, United States

Greater bone marrow adiposity (MAT) is associated with low bone density (BMD) and vertebral fractures, yet less is known about MAT composition and bone outcomes. We studied the associations between 1H-MRS measures of vertebral MAT saturation and unsaturation and bone outcomes in 465 older adults from the Age Gene/Environment Susceptibility (AGES)-Reykjavik study. MAT saturation was defined as the ratio of saturated lipid (1.3 ppm peak) to total marrow contents, and MAT unsaturation as the ratio of unsaturated lipid (5.3 ppm peak) to total marrow contents. Associations between MAT composition and QCT and DXA bone parameters were evaluated with linear regression models. Logistic regression models were used to evaluate associations with prevalent and incident radiographic vertebral fractures, and Cox proportional hazards models for incident clinical fractures. All models included both saturated and unsaturated lipids. At baseline, mean age was 81.7 (SD 4.3) years, mean MAT unsaturation was 3.5% (SD 1.0) and mean saturation was 46.3% (SD 7.2). Prevalent vertebral fractures were present in 21.0% of participants, and incident clinical fractures occurred in 21.3% of participants over 5.1 (SD 2.4) years. Incident vertebral fractures occurred in 14.8% of 298 participants attending follow up visits over 3.0 (SD 1.5) years. In cross-sectional analyses, each SD increase in MAT saturation was associated with lower BMD (Table). Conversely, higher MAT unsaturation was associated with higher BMD. Each SD increase in MAT saturation was associated with 46% greater odds (95% confidence interval [CI] = 1.11-1.92) of prevalent vertebral fracture and 55% greater odds (95% CI = 1.03-2.34) of incident vertebral fracture, while each SD increase in MAT unsaturation was associated with 42% lower odds (95% CI = 0.38-0.89) of incident vertebral fracture. In men, there was a 45% increased risk (95% CI = 0.97-2.19) for incident clinical fracture per SD increase in MAT saturation versus a 45% decreased risk (95% CI = 0.37-0.83) per SD increase in MAT unsaturation. There was no association between MAT composition and incident clinical fractures in women. MAT composition was not associated with change in bone parameters. In conclusion, saturated and unsaturated marrow lipids have distinct relationships to bone density and fracture risk. Therefore, combining these peaks into total MAT content may not be an effective approach when evaluating the relationship between MAT and bone outcomes.

Mean Percent Difference in Bone Parameter per SD Increase in MAT Saturation and MAT Unsaturation, Cross-Sectional Analysis, Full Cohort (n=465)		
	Percent Difference (95% CI) Per SD Increase in MAT Saturation	Percent Difference (95% CI) Per SD Increase in MAT Unsaturation
Spine trabecular BMD	**-23.64 (-27.14, -20.13)**	**17.53 (14.03, 21.04)**
Spine integral BMD	**-8.46 (-10.19, -6.74)**	**7.02 (5.30, 8.74)**
Spine compressive strength index	**-26.83 (-30.61, -22.86)**	**26.24 (19.73, 33.11)**
Total hip trabecular BMD	**-13.03 (-18.39, -7.66)**	**11.51 (6.14, 16.88)**
Total hip integral BMD	**-4.52 (-6.25, -2.79)**	**3.66 (1.93, 5.39)**
Total hip cortical BMD	**-1.20 (-1.90, -0.50)**	0.60 (-0.10, 1.30)
Femoral neck trabecular BMD	**-23.47 (-34.76, -12.18)**	**21.96 (10.66, 33.26)**
Femoral neck integral BMD	**-4.18 (-5.96, -2.39)**	**2.54 (0.75, 4.33)**
Femoral neck cortical BMD	**-1.01 (-1.83, -0.19)**	0.43 (-0.39, 1.25)
Lumbar spine areal BMD	**-4.87 (-6.38, -3.37)**	**5.52 (4.01, 7.03)**
Total hip areal BMD	**-3.51 (-4.87, -2.15)**	**2.86 (1.50, 4.22)**
Femoral neck areal BMD	**-3.24 (-4.66, -1.83)**	**2.33 (0.92, 3.75)**
No significant gender interactions All models include both lipid measures, saturated and unsaturated, as well as age, gender, visit window, BMI, diabetes, serum estradiol and testosterone.		

***Disclosures: Gina Woods**, None*

1084

Role of the Gut Microbiome in Bone Metabolism in Severe Obesity and After Sleeve Gastrectomy *Karin Wu[1], Kathryn McCauley[1], Susan Lynch[1], Anne Schafer[1]. [1]University of California, San Francisco, United States

Sleeve gastrectomy, the most common bariatric procedure, leads to durable weight loss and improves obesity-related comorbidities. However, it induces abnormalities in bone metabolism. One unexplored potential contributor to the negative skeletal effects is the gut microbiome, which influences bone metabolism and is altered after bariatric surgery. We characterized the relationship between the gut microbiome and skeletal outcomes in severe obesity and after sleeve gastrectomy.A cohort of 22 obese adults underwent skeletal health assessment and stool collection preoperatively, and 15 submitted stool 6 months after sleeve gastrectomy. Using 16S rRNA gene sequencing, stool microbial alpha diversity (richness, evenness), beta diversity (compositional dissimilarity), and taxon relative abundances were characterized. Linear mixed effect models and PERMANOVA analyses were applied to as-

sess relationships between fecal microbiota and serum bone turnover markers (BTM) or areal bone mineral density (aBMD). Differential in silico prediction of bacteria functional pathways enrichment (Piphilin) was performed with a paired negative binomial test.Variance in gut microbiota beta diversity (composition) was related to serum C-telopeptide (CTX; p=0.04) and to procollagen-1 N-propeptide (P1NP; p=0.02) levels. Microbial diversity positively correlated with BTM levels. Six months after surgery, microbial beta diversity, relative abundance of specific bacterial taxa, and predicted microbiota function were significantly altered. Most notably, microbiota were predicted to encode a lower capacity for butyrate metabolism. Concurrently, CTX and P1NP increased (by median 229% and 68%, both p<0.01), and femoral neck aBMD decreased (by mean 4.4 +/-4.7%, p<0.01). Those with greater within-subject change in microbial composition had greater increases in P1NP (p=0.02) and insulin-like growth factor 1 (IGF-1; p=0.045). Change in alpha diversity was positively associated with percent change in femoral neck aBMD (p=0.03).Gut microbial composition co-varied with BTM levels in severe obesity. Six months after sleeve gastrectomy, microbial compositional changes were correlated with change in P1NP, and those with greater increases in microbial diversity had smaller declines in femoral neck BMD. These findings suggest that sleeve gastrectomy-induced alterations in the gut microbiome may influence skeletal outcomes. Microbial influences on IGF-1 and butyrate production are possible mechanisms.

***Disclosures: Karin Wu**, None*

1085

The Stem Cell Basis of Bifurcation between Adipogenic versus Osteogenic Lineages *Shawon Debnath[1], Alisha R. Yallowitz[1], Jason Mc. Cormick[2], Michelle Cung[1], Matthew B. Greenblatt[1]. [1]Department of Pathology and Laboratory Medicine, Weill Cornell Medicine, United States, [2]Flow Cytometry Core Facility, Weill Cornell Medicine, United States

Concurrent decrease in osteoblast differentiation and increase in adipocyte differentiation are a signature of nearly every disorder of low bone mass, implying that alterations in a bipotent progenitor able to produce both osteoblasts and adipocytes represent a convergent pathogenic mechanism for a wide range of skeletal disorders. However, the cell type where the osteoblast and adipocyte differentiation pathways diverge and where the decision to form osteoblasts versus adipocytes is made are unknown under either physiologic or pathologic conditions. Here, we have applied a combination of 16+ color FACS for deep cellular phenotyping with fate mapping and in vivo transplantation studies to identify a specific subset of skeletal stem cells (SSCs, Lin-Thy-6C3-CD200+CD105- cells) accounting for less than 20% of total SSCs as the only bipotent fraction of SSCs. Specifically, only this bipotent fraction of SSCs are able to both generate bone organoids after transplantation to the kidney capsule and reconstitute adipogenesis when implanted into "fatless" A-Zip/F1 mice. In keeping with these findings, only this bipotent fraction of SSCs are able to both self-renew and generate all other SSC fractions in a transplantation-based differentiation hierarchy assay, indicating that this SSC fraction represents true stem cells. This bipotent SSC fraction in turn gives rise to 2 non-overlapping SSC fractions that function as committed adipocyte and committed osteoblast progenitors in organoid-based tissue formation assays. Further, this bipotent SSC fraction is a key cellular effector in the ovariectomy model of postmenopausal osteoporosis, as after ovariectomy only this fraction of SSC is capable of switching from osteogenesis to adipogenesis as shown in transplantation based organoid formation assays. Thus, here we identify the specific cellular point where the decision to form osteoblasts versus adipocytes is made, and thereby the bone versus fat balance of mesenchymal tissue is determined. Additionally, only this bipotent cell displays full stemness features, restricting skeletal stem cells to only a small fraction of the cells meeting the current definitions.

***Disclosures: Shawon Debnath**, None*

1086

CD10: A novel marker of bone marrow adipocyte progenitors *Abbas Jafari[1], Asma Alshammary[2], Adiba Isa[2], Linda Harkness[2], Alexander Rauch[2], Michaela Tencerova[3], Maria Nielsen[4], Jens Andersen[4], Thomas Levin Andersen[5], Abdullah Aldahmash[6], Moustapha Kassem[2]. [1]Department of Cellular and Molecular Medicine, University of Copenhagen, Denmark, [2]Laboratory of Molecular Endocrinology (KMEB), Odense University Hospital, Denmark, [3]Molecular Physiology of Bone, Institute of Physiology of the Czech Academy of Sciences, Czech Republic, [4]Department of Biochemistry and Molecular Biology, University of Southern Denmark, Denmark, [5]Clinical Cell Biology, Department of Pathology, Odense University Hospital, Denmark, [6]Stem Cell Unit, Department of Anatomy, King Saud University, Saudi Arabia

The biological functions of human bone marrow adipocytes (BMAds) are under intensive investigation. It is now accepted that BMAds are derived from skeletal (stromal or mesenchymal) stem cells (hBMSCs) that reside in a perivascular niche within the bone marrow stroma. However, lineage ontogeny of BMAds is not known due to the absence of prospective identification markers. Here, we employed global quantitative proteomic analysis to identify surface proteins for prospective isolation of BMAd progenitors. CD10 - also known as neprilysin (NEP) - was found to be significantly upregulated during differentiation of hBMSCs to adipocyte lineage (4.7-fold on day 7, p<0.001). Single-cell RNA sequencing of adipogenic hBMSC cultures indicated that induction of adipocyte differentiation induces CD10 expression in non-differentiated progenitor population, and CD10 expression was increased upon further development of the cells into mature adipocytes (650-fold, day 7, p<0.001). Changes of CD10 expression in adipogenic cultures were shown to be due to de novo chromatin remodelling and enhancer activation of cis regulatory elements in the vicinity of CD10 locus, leading to upregulation of CD10 mRNA and protein levels during adipogenesis. Fluorescence-activated cell sorting (FACS) experiments demonstrated that CD10- and CD10+ hBMSC populations did not differ in terms of cell morphology or expression of classical hBMSC markers, whereas adipocyte differentiation potential was higher in CD10- cells, due to higher proliferation rate (2,3-fold, p<0.005) and accumulation of non-committed stem cell population. Immunohistochemical analysis of human bone specimens from healthy individuals indicated CD10 immunoreactivity in PPARG+ Runx2- adipocytic lineage cells within the bone marrow. Finally, we found increased CD10 expression (+10%, p<0.05) in primary hBMSC cultures established from bone marrow aspirates of obese subjects (BMI 40.1 +/- 0.9, age 36 +/- 4) as compared to lean individuals (BMI 22.1 +/- 0.8, age: 33 +/- 5). Our findings demonstrate that CD10 is a marker of BMAd progenitors and thus is relevant for further investigations of BMAd development within the bone marrow.

***Disclosures: Abbas Jafari**, None*

1087

Novel Roles of Tendon Cells in Joint Fibrocartilage Formation that is Regulated by Ihh Signaling *Zheng Wang[1], Chi Ma[2], Diane Chen[1], Yan Jing[1], Jerry Feng[1]. [1]Texas A&M College of Dentistry, United States, [2]Texas Scottish Rite Hospital for Children, United States

In large joints, there are two different cartilage tissues: articular cartilage (lack of type I collagen) and fibrocartilage (rich of type I collagen). The former receives the most research attention, whereas the fibrocartilage is largely unknown except that it is the common tendon rupture site. Additionally, osteochondrogenitors were considered as the sole source for both cartilages, and tendons only move joints. The aim of this study was to test a hypothesis: tendons directly form fibrocartilage, which is under-regulated by Ihh. To test this hypothesis, we 1st used immunostains to show similar ECM protein profiles such as aggrecan and Col X in both cartilages of humerus heads with no expressions of DMP1 and SOST (mature bone markers). Interestingly, fibrocartilage does not express Sox9 but express Runx2 and Col I (two early bone cell markers), while the articular cartilage express Sox 9 but no Runx2 and Col I. 2nd, we traced the cell source of fibrocartilage using the tendon specific Cre Scx-creERT2; R26R-tdTomato line with tamoxifen induction at P3 and harvested at P7 or P9 or P33 or P60. The tracing data revealed only a few tendon-derived Scx+ chondrocytes at P7, with a gradual increase of Scx-cre+ cells in fibrocartilage at P9, P33 and the highest level at P60. The quantitative data showed a significant increase among these groups (n = 4; $p < 0.05$) regarding the ratio of Scx+/DAPI+ cells and fibrocartilage mass (Fig a). We also induced Scx-CreERT2 at P30 and harvested at P60, in which there were more newly added Scx+ cells in the fibrocartilage, suggesting a continuous contribution to fibrocartilage growth. 3rd, we induced diphtheria toxin fragment A (DTA) expression in Scx-cre+ cells using Scx-creERT2 and showed a great reduction in the fibrocartilage ECM (Fig b). 4th, we conditionally deleted the Ihh gene using the Scx-CreERT2 at P3 and harvested at P14. These null-pups displayed few invaded Scx+ fibrocartilage cells and the original chondrocytes remained as they are (Fig c). Finally, we showed that 4-week treadmill exercises greatly increase aggrecan expression in fibrocartilage. Together, our studies support a novel theory (fig d): the fibrocartilage originates from tendon, which grows in and eventually replaces the existing cartilage. This novel finding explains why fibrocartilage is distinct from the articular cartilage and makes the tendon connection to joint extremely strong instead of simply connected to joints.

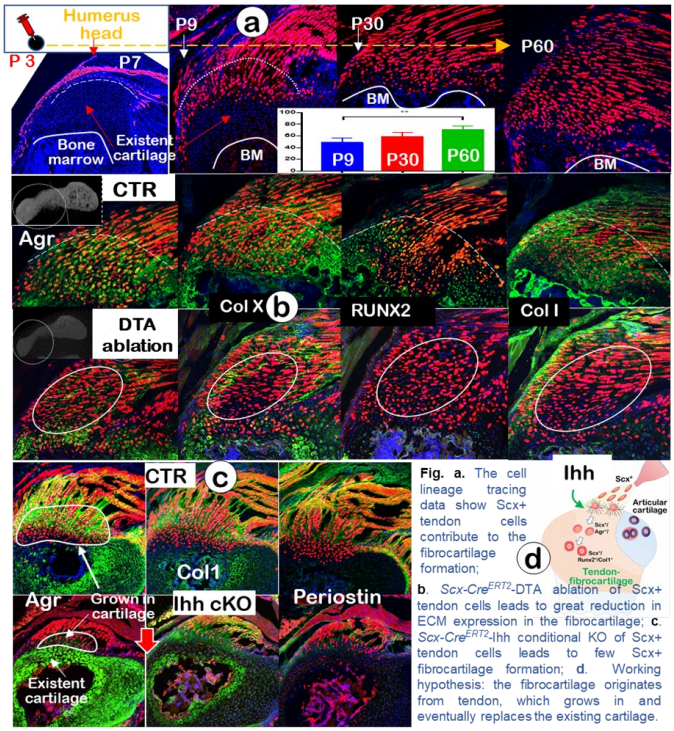

Fig. a. The cell lineage tracing data show Scx+ tendon cells contribute to the fibrocartilage formation; **b.** *Scx-Cre*^{ERT2}-DTA ablation of Scx+ tendon cells leads to great reduction in ECM expression in the fibrocartilage; **c.** *Scx-Cre*^{ERT2}-Ihh conditional KO of Scx+ tendon cells leads to few Scx+ fibrocartilage formation; **d.** Working hypothesis: the fibrocartilage originates from tendon, which grows in and eventually replaces the existing cartilage.

***Disclosures: Zheng Wang**, None*

1088

RhoA Regulates the Quiescence and Cell Fate of Skeletal Stem and Progenitor Cells (SSPCs) *Dana Trompet[1], Marian Dejaeger[1], Marion Mesnieres[1], Elena Nefyodova[1], Ruben Cardoen[1], Cord Brakebusch[2], Jos Tournoy[3], Frank Luyten[4], Christa Maes[1]. [1]Laboratory of Skeletal Cell Biology and Physiology (SCEBP), Skeletal Biology and Engineering Research Center (SBE), KU Leuven, Leuven, Belgium, Belgium, [2]Biomedical Institute, BRIC, Faculty of Health, University of Copenhagen, Copenhagen, Denmark, Denmark, [3]Gerontology and Geriatrics, University Hospitals Leuven, and Department of Chronic Diseases, Metabolism and Ageing, KU Leuven, Leuven, Belgium, Belgium, [4]Skeletal Biology and Engineering Research Center (SBE), Department of Development and Regeneration, KU Leuven, Leuven, Belgium, Belgium

A better understanding of skeletal stem/progenitor cell (SSPC) biology, including the significance and regulation of intrinsic cytoskeleton-centered processes, could provide novel osteo-anabolic therapies. Therefore, we generated conditional knock-out (cKO) mice lacking the key cytoskeletal regulator RhoA in SSPCs and osteolineage cells using Prx1-Cre and Osx-Cre mice.MicroCT and histomorphometry revealed that loss of RhoA led to reduced trabecular bone mass in both mouse models (e.g. BV/TV 12-week-old Prx1-Cre;RhoA cKO mice: 10.91+/-0.97% vs. 15.57+/-0.40% in controls; n=8-9; p<0.001). Interestingly, whereas the reduced BV/TV in Osx-Cre;RhoA mutants could be attributed to decreased osteoblast number and activity, Prx1-Cre;RhoA cKO mice rather showed dominant effects in the earlier stem and progenitor cell populations. Firstly, we found that SSC quiescence was reduced in Prx1-Cre;RhoA cKO mice. Mutant BMSCs showed 2-fold increased proliferation in vitro (n=3; p<0.05) and young Prx1-Cre;RhoA cKO bones contained 40% more CFUs than controls (n=9; p<0.05). Moreover, Prx1-Cre;RhoA cKO mice grew wider bones, and generated larger calluses after fracture (n=16; p<0.01), indicating an increased SSC/SSPC expansion capacity. Compromised stem cell quiescence upon RhoA-inactivation was further supported by reduced long-term EdU-label-retention in vivo, and associated with increased BMSC senescence (p16 qRT-PCR). Moreover, the SSC/SSPC pool displayed premature exhaustion upon loss of RhoA as evidenced by the reduced number of CFUs and of CD45-Ter119-CD31-CD51+Thy-6C3-CD105-CD200+ SSCs in 1-year-old Prx1-Cre;RhoA cKO mice. Secondly, loss of RhoA affected the cell fate and differentiation profile of SSPCs, favoring adipogenesis and chondrogenesis. Cultured mutant BMSCs displayed increased adipogenic differentiation (n=4-5; p<0.05) and Prx1-Cre;RhoA cKO mice showed increased BM adiposity in vivo, which aggravated upon injury (e.g. post-fracture osmium-staining: 0.42+/-0.35% BMAT (control) versus 5.34+/-6.43% (cKO); n=8; p<0.05). Increased chondrogenesis was seen upon fracture (7.1+/-3.6% cartilage (control) versus 12.3+/-1.5% (cKO); post-fracture day 7; n=4-5; p<0.01) and in occasional enchondroma formation. Notably, RhoA-deficient cells showed changes in Wnt/β-catenin and YAP/TAZ-signaling consistent with these alterations.Altogether, we conclude that loss of RhoA in SSPCs increases cellular expansion and alters differentiation, leading to premature SSPC exhaustion and osteopenia.

***Disclosures: Dana Trompet**, None*

1089

Skeletal Abnormalities in Csf1r Knockout Rats Are Rescued by Transplant of Total Bone Marrow *Lena Batoon[1], Melanie Caruso[1], Katharine Irvine[1], Allison Pettit[1], David Hume[1]. [1]Mater Research Institute-The University of Queensland, Australia

Macrophages and osteoclasts (OC) depend on colony-stimulating factor 1 receptor (CSF1R) signaling for proliferation, differentiation and survival. Homozygous CSF1R mutations in humans are associated with flattened and diffusely dense vertebral bodies, metaphyseal and epiphyseal osteosclerosis, thin cortical bone in the long bones (dysosteosclerosis) and hypercalcification of the skull base. Studies of the phenotypic consequences of Csf1r knockout (Csf1rko) in mice have been limited by early postnatal lethality. We recently generated Csf1rko rats which are viable as adults on an outbred background. Here, we explored the impact of Csf1rko in rats on postnatal bone growth on a defined Dark Agouti genetic background. These Csf1rko rats are indistinguishable at birth from littermates but exhibit postnatal growth retardation. However, Alcian blue-Alizarin red staining of newborn skeletons already showed delayed mineralization of the small paw bones and digits. At 1 week, osteopetrosis was evident. The muscle fibers formed around the bones were also reduced in diameter. By 3 weeks, mutant rats had intriguing site-specific skeletal defects: a profound delay in rib cage ventral segment mineralization, vertebral body development, secondary ossification center formation in long bones and digits, and subarticular ossification of small paw bones and carpal-tarsal bones. At 7 weeks, the cranial case of mutant rats lacks calcification and suture closure was impaired. All these skeletal features were shared with the human CSF1R mutation. We examined macrophage and OC distribution by immunohistochemical localization of IBA1 and TRAP. Abundant IBA1+ macrophages in the paw, vertebral body and hind limbs including in both endosteal and periosteal surfaces were detected in 1- and 3-week old wild-type (WT) rats and were almost completely absent in the Csf1rko. TRAP+ OC were also undetectable. IBA1+ macrophages were partly restored in 7-9-week old Csf1rko rats, but OC remained absent. Transplant (Tx) of WT bone marrow (BM) cells into unconditioned 3-week old Csf1rko rats reconstituted tissue macrophages and OC, reversed skeletal abnormalities as early as 7 weeks post-Tx, promoted skeletal and somatic growth, and long-term survival. Our findings have important implications for understanding the consequences of CSF1R mutation for the human skeleton and reveal the therapeutic potential of targeting the CSF1-CSF1R axis in related bone diseases.

***Disclosures: Lena Batoon**, None*

1090

Discoidin Domain Receptor 2 (DDR2) Regulates In Vivo Skeletal Progenitor Cell Differentiation, Collagen Matrix Organization and Hedgehog Signaling *Fatma Mohamed[1], Chunxi Ge[1], Randy L. Cowling[2], Abdul-aziz Binrayes[1], Barry Greenberg[3], Rennu Franceschi[1]. [1]University of Michigan School of Dentistry, United States, [2]UCSD, United States, [3]UCSD School of Medicine, United States

DDR2 is a collagen-activated receptor tyrosine kinase that, together with β1-integrins, mediates extracellular matrix (ECM) signaling. Inactivating mutations in DDR2 cause an autosomal inherited human disorder characterized by dwarfism and bone growth defects that are largely phenocopied in globally Ddr2-deficient mice. In this study, the distribution, lineage and cellular function of Ddr2 was examined in transgenic mice. β-gal staining of Ddr2LacZ/+ mice showed strong Ddr2 expression in metaphysis, periosteum, and growth plate resting zones. This pattern partially overlapped with Gli1, a mediator of Hedgehog signaling previously identified in skeletal stem/progenitor cells. Lineage analysis using Ddr2mer-iCre-mer; R26RtdTomato reporter mice revealed initial tdTomato labeling of skeletal precursors that subsequently contributed to chondrogenic and osteogenic lineages including osteocytes, but not to osteoclasts. Ddr2 conditional knockout (cKO) in skeletal progenitors using Gli1-CreERT or Col2a1-Cre recapitulated skeletal phenotypes of global knockout mice including low bone mass, stunted skull growth and shortened growth plates. In addition, defects were observed in chondrocyte organization, proliferation, and ECM distribution. In wild type mice, type II collagen was uniformly detected around chondrocytes while in cKO animals it displayed an abnormal distribution with little staining in the cartilage interterritorial matrix. Conditional knockout of Ddr2 in mature osteoblasts using osteocalcin-Cre did not result in an observable skeletal phenotype, thereby providing further evidence for lineage-restricted functions of Ddr2 in skeletal progenitors. Gene expression analysis showed enrichment of Ddr2 together with stem cell markers (Gli1, LepR and Nestin) in non-hematopoietic, non-endothelial PDGFRα+CD51+ skeletal progenitor cells. Ddr2 knockdown in these cells did not affect clonogenic activity; rather it reduced osteogenic (CFU-Ob) while enhancing adipogenic (CFU-Ad) differentiation potential. Similarly, Ddr2 knockout in embryonic limb bud micromass cultures reduced cartilage nodules and down-regulated chondrocyte differentiation markers. Ddr2 loss also markedly downregulated Ihh, Gli1 and Ptch Hedgehog signaling intermediates. These studies establish cell autonomous functions of Ddr2 in Gli1+ skeletal progenitor cells and chondrocytes that are

related to changes in ECM organization and Hedgehog signaling critical for chondrogenesis and osteogenesis.

***Disclosures: Fatma Mohamed**, None*

1091

Loss of Transferrin Receptor 1 in Osteoclast Lineage Cells Attenuates Osteoclast Energy Metabolism and Cytoskeleton Organization Resulting in a Dramatic Increase of Trabecular Bone Mass in Long Bones of Female Mice *Bhaba K Das[1], Lei Wang[2], Toshifumi Fujiwara[3], Renny Lan[4], Jian Zhou[2], Jian Q Feng[5], Michael L Jennings[6], Nukhet Aykin-Burns[7], Weirong Xing[8], Subburaman Mohan[8], Haibo Zhao[1]. [1]Southern California Institute for Research and Education, Office of Research, Tibor Rubin VA Medical Center, VA Long Beach Healthcare System, United States, [2]Department of Orthopedics, First Affiliated Hospital, Anhui Medical University, China, [3]Department of Orthopedic Surgery, Kyushu University Hospital, Japan, [4]Department of Biochemistry and Molecular Biology, University of Arkansas for Medical Sciences, United States, [5]Department of Biomedical Sciences, Texas A&M college of Dentistry, United States, [6]Department of Physiology and Biophysics, University of Arkansas for Medical Sciences, United States, [7]Division of Radiation Health, Department of Pharmaceutical Sciences, University of Arkansas for Medical Sciences, United States, [8]Musculoskeletal Disease Center, Jerry L Pettis Memorial VA Medical Center, United States

Both osteoclast (OC) differentiation and bone-resorbing activities demand high energy. Fe is a nutritional element essential for mitochondrial metabolism and the biosynthesis of heme and Fe-S clusters, which are critical components of the mitochondrial respiratory complexes. Mammalian cells acquire Fe predominantly through the transferrin (Tf)/Tf receptor (TfR1)-dependent pathway. However, how the cellular iron homeostasis impacts OC metabolism has not been well elucidated. To address this question, we generated myeloid and mature OC-specific TfR1 deficient mice by crossing TfR1-floxed mice with LysM-Cre (TfR1ko/LysM) and Cathepsin K-Cre (TfR1ko/CTSK) mice, respectively. By μ-CT and histomorphometric analysis of distal femurs of 10-week old mice, we found a near three-fold increase in trabecular BV/TV, number, and thickness in female but not male TfR1ko/LysM mice compared to gender-matched control littermates. Although increased trabecular bone volume was seen in both TfR1ko/CTSK male and female mice, the phenotype was more pronounced in female mice. The OC number and serum level of TRAP in both TfR1ko/LysM and TfR1ko/CTSK mice were similar to controls. Surprisingly, loss of TfR1 in OCs led to marked increases in the osteoblast (OB) number and serum level of P1NP, suggesting that enhanced bone formation might also contribute to increased bone mass. In vitro mechanistic studies revealed that loss of TfR1 abolished Tf-dependent Fe uptake in OC precursor and mature cells as measured by the Tf-Fe59 uptake assay and caused a 75% decrease in mitochondrial respiration as assayed by the Seahorse Extracellular Flux analyzer. In consistence, quantitative proteomics identified a profound downregulation of proteins associated with mitochondrial oxidative phosphorylation in TfR1KO OCs. OC differentiation of TfR1KO bone marrow monocytes was normal. However, TfR1KO OCs exhibited a significant delay in the formation of podosome-belt and actin-ring on glass coverslips and on bone slices, respectively. While loss of TfR1 impaired OC bone resorption, bone marrow stromal cells derived from TfR1KO mice were able to differentiate into OB and form bone nodule. In conclusions, TfR1-dependent iron uptake plays an important role in OC energy metabolism and cytoskeleton organization but not OC differentiation. Deletion of TfR1 in OC lineage cells inhibits bone resorption and indirectly promotes bone formation leading to increased trabecular bone mass in a gender-dependent manner.

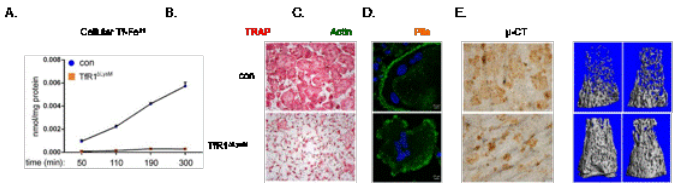

***Disclosures: Bhaba K Das**, None*

1092

Osteoblastic Deletion of PKA Regulatory Subunit1A Causes Severe Bone Pathology in Mice *Carole Le Henaff[1], Brandon Finnie[1], Joshua Johnson[1], Yasaman Nahaei[1], Zhiming He[1], Krishnakali Dasgupta[1], Juhee Jeong[1], Johanna Warshaw[1], Henry M Kronenberg[2], Lawrence S Kirschner[3], Nicola C Partridge[1]. [1]Department of Molecular Pathobiology - College of Dentistry - New York University, United States, [2]Endocrine Unit, Massachussetts General Hospital, Harvard Medical School, United States, [3]Department of Cancer Biology and Genetics and the Division of Endocrinology, Diabetes and Metabolism - Department of Internal Medicine - The Ohio State University Wexner Medical Center, United States

Parathyroid hormone (PTH) was the first osteoanabolic hormone for treating osteoporosis. We have previously shown that PTH acts through PTHR1 and protein kinase A (PKA) activation to regulate osteoblastic gene expression. Our study aimed to elucidate the effects of increased PKA activity in vivo and better understand the actions of PTH (1-34) in bone. Tamoxifen (1mg/10g) was injected weekly to 1 or 5 month-old C57Bl/6J male col-1CREERT/Prkar1afl/fl mice or Prkar1afl/fl mice as controls for 3-4 weeks to delete the PKA regulatory subunit 1A in osteoblasts and increase PKA activity. At both ages, col1CREERT/Prkar1afl/fl mice demonstrated bone pathologies in their skulls, femurs and vertebrae and tumors in their tails. Deletion of Prkar1a increased bone turnover with a considerable increase in osteoblast activity shown by serum-P1NP levels (6.5-13 fold), only single instead of double fluorescent labeling of bone and a substantial increase in osteoclast activity shown by CTX levels (4.4-12 fold) and TRAP staining. MicroCT showed cortical bone breakdown with apparent trabecular bone in the cortical area in femurs and vertebrae (Figure 1). In both age groups, cortical and trabecular bone RNAs showed a large increase in bone sialoprotein mRNA levels (3 to 6 fold) with a sharp decrease in osteocalcin (0.2-0.4 fold) showing a change in osteoblast differentiation. Furthermore, PTH responsive genes were significantly changed: SOST expression was decreased to 0.1-0.2 fold, RANKL was upregulated by 2-3 fold and MMP13 was increased by at least 3 fold. Surprisingly, the col1CREERT/Prkar1afl/fl skulls showed thicker but more porous and disorganized calvariae, shown by alizarin red staining and μCT images. At 7 weeks-old, uCT analyses showed a decrease in calvarial thickness (-15.7%) resulting from apparent increased trabecular bone in the calvariae and a 16% increase in porosity. No change was observed in mandibles or teeth. At both ages, Col-1CREERT/Prkar1afl/fl mice had tumors in their tails evident by an invasion of stromal and osteoclastic cells with disappearance of bone marrow and decreased growth plate but intact cartilage and intervertebral discs. In conclusion, elevated PKA activity in osteoblasts appears to be involved with high bone turnover and pathological events mimicking hyperparathyroidism, Jansen's metaphyseal chondrodysplasia or McCune-Albright syndrome.

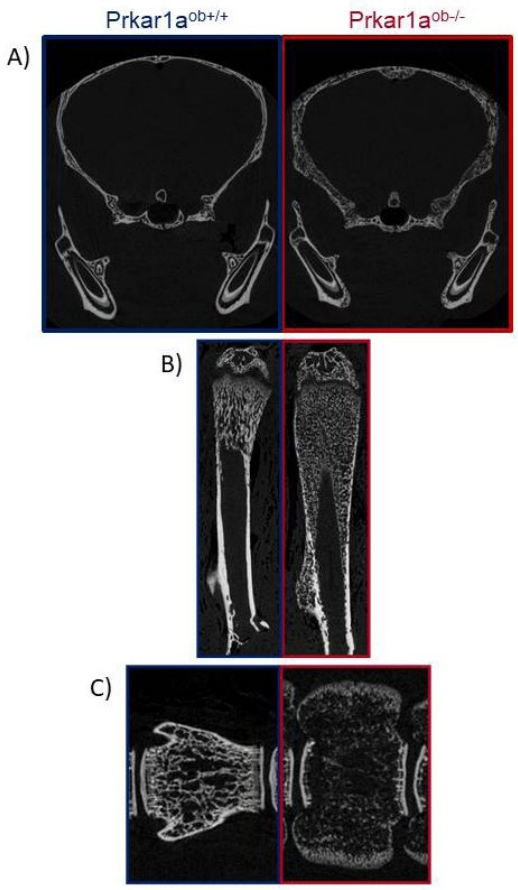

***Disclosures: Carole Le Henaff**, None*

1093

Dynamics of Modeling- and Remodeling-Based Bone Formation in Response to Intermittent Parathyroid Hormone (PTH) Treatment and Discontinuation *Wenzheng Wang[1], Wei-ju Tseng[1], Hongbo Zhao[1], Tala Azar[1], Nathaniel Dyment[1], Xiaowei Sherry Liu[1]. [1]McKay Orthopaedic Research Laboratory, Department of Orthopaedic Surgery, Perelman School of Medicine, University of Pennsylvania, United States

Both modeling-based bone formation (MBF), de novo bone formation (BF) on quiescent surfaces without prior resorption (Fig A), and remodeling-based BF (RBF), BF coupled with resorption by osteoclasts (Fig B), are important mechanisms by which anabolic agents such as PTH rapidly improve bone mass. Despite the potent effect of PTH on promoting new BF, treatment benefit rapidly diminishes upon treatment discontinuation. To study the dynamics of activation and retention of MBF and RBF, we injected calcein (green, G), alizarin complexone (red, R), and tetracycline (yellow, Y) mineral labels to ovariectomized rats in a G-R-Y-G sequence at days -2, 5, 12, and 19 (initiation of PTH on day 0, 20 μg/kg/day), followed by euthanasia at day 21 (end of PTH), 28, and 42 (1- and 3- wks after PTH discontinuation, n=6/group). Mineral labels and cement lines on cryo-sections of tibial trabecular bone were used to identify BF sites as MBF (smooth cement line, Fig A) or RBF (scalloped cement line, Fig B) that were further stratified by activation time (within wk 1, 2, or 3, Fig D). We hypothesized that MBF and RBF respond differently to anabolic treatment and discontinuation.Mineralizing surface (MS/BS) or mineral apposition rate (MAR) did not differ between MBF and RBF in VEH-treated rats. Three-week PTH treatment led to greater MBF- and RBF- induced MS/BS (4.3- and 3.4- fold) and MAR (67% and 39%) compared to VEH, respectively (Fig C). PTH activated 87% of MBF surfaces during wk 1 and 13% by wk 2, while PTH activated 32, 66, and 2% of all RBF surfaces during wks 1, 2, and 3, respectively (Fig E).No BV/TV reduction was found after 1-wk discontinuation from PTH. However, discontinuation for 3 weeks led to a 43% reduction in total BV/TV. The BV/TV of MBF was unchanged while that of RBF and pre-existing bone was 81% and 34% lower in wk 3 vs. wk 0, respectively (Fig F). Consistently, 41% of RBF and 40% of pre-existing bone surfaces were TRAP+ while only 2% of MBF was TRAP+. Furthermore, 82% of MBF surfaces were ALP+ and 16% had mixed TRAP and ALP signal. However, only 34% of RBF surfaces were ALP+ and 25% had mixed signals (Fig G-K). Moreover, 60% of pre-existing bone surfaces remained quiescent (Fig K).In summary, PTH induces BF through rapid activation of new MBF, followed by continuous activation of RBF. During discontinuation, bone loss occurs mostly at pre-existing bone and RBF sites, whereas MBF is highly resistant to PTH withdrawal.

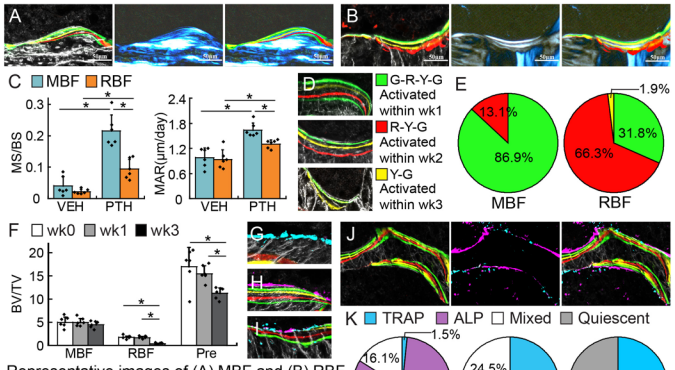

Representative images of (A) MBF and (B) RBF sites. (C) MS/BS and MAR of MBF and RBF in response to VEH and PTH, *: p<0.05 by two-way ANOVA with Bonferroni corrections. (D) Bone formation sites stratified by activation time based on mineral labels. (E) Percentage of MBF and RBF surfaces stratified by activation time in ovariectomized female rats treated with PTH. (F) BV/TV of MBF, RBF and pre-existing bone tissue after 0-, 1-, and 3- week PTH discontinuation. *: p<0.05 by one-way ANOVA. Representative images of (G) TRAP+ surface, (H) ALP+ surface, and (I) Mixed surface. (J) Representative images of TRAP and ALP staining after 1-wk PTH discontinuation. (K) Percentage of different types of surfaces on MBF, RBF, and pre-existing bone.

***Disclosures: Wenzheng Wang**, None*

1094

A Sex Dimorphic Mechanism Links Protection from Bone Loss and Promotion of Gut Microbiome Diversity Induced by a Nutritional Intervention *Amy Y Sato[1], Cindy H Nakatsu[2], Meloney Cregor[1], Kevin McAndrews[3], Gretel G Pellegrini[3], Mario G Ferruzzi[4], Mary A Lila[4], Connie M Weaver[5], Teresita M Bellido[6]. [1]Department of Anatomy, Cell Biology, and Physiology, Indiana University School of Medicine, Indianapolis, IN, United States, [2]Department of Agronomy, Purdue University, West Lafayette, IN, United States, [3]Department of Anatomy, Cell Biology, and Physiology, Indiana University School of Medicine, Indianapolis, IN, United States, [4]Department of Food Bioprocessing and Nutrition Sciences, North Carolina State University, Kannapolis, NC, United States, [5]Department of Nutrition, Purdue University, West Lafayette, IN, United States, [6]Department of Anatomy, Cell Biology, and Physiology, Indiana University School of Medicine, Indianapolis, IN; Richard L. Roudebush Veterans Affairs Medical Center, Indianapolis, IN, United States

We previously showed that a blueberry-enriched diet counteracts the effects of estrogen deficiency in female mice on bone, skeletal muscle, and peripheral fat, and alters the gut microbiome. Here, we compare between female and male mice the impact of the diet on the skeleton and the microbiome. Four-month old B6.129X1/J mice were gonadectomized or sham operated, each group separated in two groups, which then were fed either control AIN-93M diet (C) or AIN-93M diet containing 10% lyophilized/freeze dried Montgomery blueberry (MONT); N=9-20 females and N=10-26 males. In contrast to full protection from OVX-induced bone loss, MONT failed to prevent the loss in BMD induced by ORX. Further, while MONT completely prevented OVX-induced architectural deterioration of cancellous and cortical bone, the diet did not prevent the decrease in BV/TV, Tb.Th, Tb.N, Ct.Ar/Tt.Ar, and Ct.Th, quantified by micro-CT, induced by ORX. Likewise, MONT prevented OVX-induced increases in circulating resorption marker CTX, but it had no effect on CTX levels in ORX mice. We next quantified gut microbiome diversity, by analyzing fecal bacterial DNA using 16S rRNA gene sequences from high throughput paired end MiSeq technology. OVX or ORX did not alter the variety of bacterial communities (α-diversity) within either C or MONT-fed mice. However, MONT increased α diversity overall, and to a greater extent in females than in males, measured by the Shannon Index. MONT also shifted the relatedness of bacterial communities (β diversity) farther in females than in males, detected by two different metrics Jaccard distance (absence/presence of taxa), and weighted Unifrac (phylogenetic relatedness and relative taxa abundance). Moreover, MONT increased the prevalence of the taxon Ruminococcus1 exclusively in females and not in males, detected by Analysis of Composition of Microbiomes. In summary, the MONT diet protects from estrogen, but not androgen deficiency-induced bone loss and architectural deterioration; and promotes a healthier microbiome signature to a greater extent in females than males. These findings demonstrate that skeletal and microbiome responses to nutritional interventions are sex dimorphic and suggest a link between bone protection and gut microbiome diversity.

***Disclosures: Amy Y Sato**, None*

1095

Overexpression of antibody against oxidized phospholipids attenuates the age-associated, but not the ovariectomy- or unloading- induced, bone loss in mice *Michela Palmieri[1], Teenamol E Joseph[1], Aaron D Warren[1], Horacio Gomex-acevedo[2], Jinhu Xiong[3], Joseph L Witztum[4], Stavros C Manolagas[1], Elena Ambrogini[1]. [1]Center for Osteoporosis and Metabolic Bone Diseases and Center for Center for Musculoskeletal Disease Research, University of Arkansas for Medical Sciences and the Central Arkansas Veterans Healthcare System, United States, [2]Department of Biomedical Informatics, University of Arkansas for Medical Sciences, United States, [3]Department of Orthopaedics Surgery, University of Arkansas for Medical Sciences, United States, [4]Department of Medicine, University of California San Diego, United States

Overexpression of a single chain (scFv) form of the antigen-binding domain of E06 IgM – a natural antibody that recognizes the phosphocholine (PC) moiety of oxidized phospholipids (OxPLs) – protects against atherosclerosis and hepatic steatosis. Moreover, the E06-scFv transgene increases cancellous and cortical bone mass in both male and female adult mice, by increasing bone formation. Age-related bone loss is characterized by a decline in osteoblast number and bone formation and is associated with increased oxidative stress and lipid peroxidation. We have searched for and found that the age-associated bone loss seen in 22 and 24 month-old female and male wild type C57BL/6 mice was greatly attenuated in homozygous E06-scFv transgenic littermates, as determined by serial DXA BMD every 3 months. Micro-CT analysis upon euthanasia revealed that the effect of the E06-scFv was due to the attenuation of the age-associated decline in cancellous, but not cortical, bone mass. Both male and female E06-scFv transgenic mice also accumulated less fat mass than WT littermates during aging. As shown in histological analysis of the vertebrae, the aged E06-scFv transgenic mice had increased osteoblasts and decreased osteoclasts compared to the wild type mice. Oxidative stress (OS) is involved in the bone loss caused by sex-steroid deficiency and elevated OS markers are found in unloading-induced bone loss, raising the possibility that an increase of OxPLs induced by OS might be contributing to the pathogenesis of these conditions as well. We, therefore, investigated whether the beneficial effect of the E06-scFv extends to these two other conditions. To this end, 4.5 month old females E06-scFv homozygous mice and WT controls were ovariectomized (OVX). Unlike aging, the E06-scFv transgene did not protect against OVX-induced bone loss in either the cancellous or the cortical compartment, as measured by DXA and micro-CT 6 weeks post-surgery. Lastly, we tail- suspended 5.5 month old male mice and sacrificed them 21 days later. E06-scFv transgenic mice had similar cortical bone loss compared to WT mice. These results indicate that the increase of oxidative stress with aging and the resulting increase in the generation of lipid peroxidation products, such PC-OxPLs, is an important pathogenetic mechanism for the age-associated bone loss in the cancellous bone compartment. These mechanisms, however, may not contribute to the OVX- or unloading –induced bone loss.

***Disclosures: Michela Palmieri**, None*

1096

Osteocytes regulate bone resorption via Sclerostin and Lrp4 signaling through Rankl dependent and independent mechanisms *Jesus Delgado-Calle[1], Ashley Daniel[1], Hayley Sabol[1], Serra Ucer[1], Kevin McAndrews[1], Jessica Nelson[1], Megan Sweet[1], Alexander Robling[1], Teresita Bellido[1]. [1]Indiana University School of Medicine, United States

Earlier studies demonstrated that activation of canonical Wnt signaling in pre- and differentiated osteoblasts versus in osteocytes (Ots) inhibits or stimulates bone resorption, respectively. In both cases, osteoprotegerin (Opg) is upregulated. However, when the pathway is activated in Ots, receptor activator of NfKB ligand (Rankl) is also upregulated, explaining the increased resorption; and also Sost/sclerostin (scl) expression is increased. We hypothesized that the mechanism by which canonical Wnt signaling in Ots increases resorption requires Sost/scl, a gene/protein expressed only in these cells. Here, we tested this hypothesis in vivo by crossing mice with canonical Wnt signaling activation in Ots (daβcatOt mice) with SOST KO mice to generate control (C), daβcatOt, SOSTKO, and daβcatOt;SOSTKO littermate mice. daβcatOt mice had the expected elevated Sost and Rankl mRNA expression and cancellous bone mass, and more osteoclasts (Ocls) compared to C. SOSTKO mice also had increased cancellous bone mass but no changes in Rankl or Ocls. Sost deletion in daβcatOt mice increased by 25% femoral cancellous bone mass, restored to C levels the elevated Ocl number and decreased by 30% Rankl expression and the number of Rankl positive Ots, without affecting Opg. These results demonstrate that Sost/Scl regulates Rankl expression in Ots to stimulate bone resorption. We examined next whether Scl upregulates Rankl expression in Ots via Lrp4, known to retain and facilitate Scl's actions. We crossed daβcatOt mice with mice with conditional deletion of Lrp4 in Ots (Lrp4Ot) and generated C, daβcatOt, Lrp4Ot, and daβcatOt;Lrp4Ot littermate mice. Lrp4Ot mice exhibited increased cancellous bone mass due to increases in osteoblasts (Obs) and the bone formation marker P1NP, but no changes in Rankl or Ocls. Deletion of osteocytic Lrp4 in daβcatOt mice increased by 25% femoral cancellous bone mass, restored Ocl number to control levels, and reduced by 20% the levels of the resorption marker CTX, but it did not alter their elevated Obs number. Surprisingly, deletion of Lrp4 in Ots did not affect Rankl (or Opg) mRNA or Rankl protein expression in Ots, which remained increased and similar to those found in daβcatOt mice. In conclusion, our findings demonstrate that Scl exerts catabolic actions in bone by increasing Rankl expression in Ots, and suggest that osteocytic Lrp4 signaling also stimulates bone resorption through autocrine mechanisms in Ots independent of Rankl regulation.

***Disclosures: Jesus Delgado-Calle**, None*

1097

Bone microarchitecture and composition contribute to bone fracture risk in the genetically diverse diversity outbred (DO) founder mouse strains

*Bhavya Senwar[1], Michael A. Friedman[2], Charles R. Farber[3], Henry J. Donahue[2], Virginia L. Ferguson[1]. [1]University of Colorado, Boulder, CO, United States, [2]Virginia Commonwealth University, Richmond, VA, United States, [3]University of Virginia, Charlottesville, VA, United States

Bone strength is a function of the bone mass, morphology, and material quality which contribute to the structural rigidity of bone. While it is understood that bone strength varies with genetics, how these factors contribute to bone strength and fragility remains poorly understood. Within low (C57BL/6J) and high (A/J) bone mass mouse strains, bone strength depends on both micro-architecture and bone quality, specifically cortical tissue mineral density (Ct.TMD; Jepsen et al., 2008, Courtland et al., 2008). We sought to evaluate if this relationship persists across a wider range of genetic backgrounds from the eight DO founder mouse strains (n=6/group; males; 19 weeks). Femurs were evaluated using micro-CT, Raman spectroscopy, and three-point bending. Slenderness ratio (total area/bone length, Tt.Ar/Le) was calculated where A/J had the most slender bones (mean Tt.Ar/Le = 0.086), followed by CAST (0.089), NOD (0.093), 129S1 (0.1), NZO (0.13), WSB (0.15), PWK (0.18), and C57BL/6 (0.35). Pearson correlations were calculated across these strains to evaluate relationships between bone morphology, tissue chemistry (mineral:matrix ratio and crystallinity) and strength. Tt.Ar/Le negatively correlated with cortical thickness, Ct.Th (r=-0.61, p<0.0001), indicating that more slender bones have thicker cortices. Tt.Ar and relative cortical area (RCA) were negatively correlated (r=-0.68, p<0.0001) indicating that smaller bones (lower Tt.Ar) had thicker cortices. Small bones with thicker cortex (Ct.Th) also had higher Ct.TMD (r= 0.7, p<0.0001), mineral:matrix (r=0.33, p<0.05) and crystallinity (r=0.29, p=0.06). These smaller bones (Tt.Ar) also had higher modulus (r=-0.73, p<0.0001) and lower work to fracture (r=0.61, p<0.0001). Across these strains, smaller bones had higher mineralization and highly organized mineral crystals, which could contribute towards ability of bone to bear normal, physiological loads. However, this increased mineralization could result in a more brittle and fracture-prone bone. These findings were earlier investigated in the A/J, C57BL/6J mouse strains and their recombinant inbred strains. The current study demonstrates these findings for a genetically diverse population of eight DO founder strains which motivates evaluating how specific genes associated with bone traits vary among these individual strains. Following this work, we aim to incorporate bone material composition into prediction of fracture risk for a genetically diverse population.

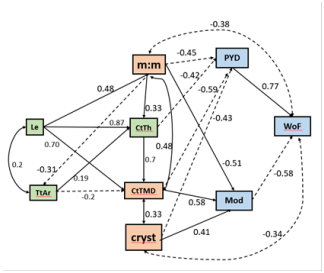

Figure 1: Correlation map showing bone morphology, microarchitecture and material quality contributes to bone fracture risk in a genetically diverse population of 8 DO founder strains. Solid line represents positive and dashed represent negative correlations. Green, orange, and blue boxes represent bone morphology, bone quality and bone mechanical properties, respectively. Abbreviations are defined in the text. PYD- post yield deformation, Wof- work of fracture and Mod- modulus.

***Disclosures: Bhavya Senwar**, None*

1098

Alterations to the Gut Microbiome Impair Bone Tissue Strength in Aged Mice

*Macy Castaneda[1], Kelsey Smith[2], Jacob Nixon[1], Sheldon Rowan[2], Christopher Hernandez[1]. [1]Cornell University, United States, [2]Tufts University, United States

Recent studies have shown that the gut microbiome can regulate bone remodeling, bone quantity, bone quality and whole bone strength. Preclinical work, however, has been limited to young adult mice (less than 6 months of age), and it is unclear if modifications to the gut microbiome can also improve bone tissue strength in aged animals. Here we ask if alterations to the constituents of the gut microbiome influence bone strength in older mice (1-2 years of age).In this IACUC approved opportunistic study, male C57Bl/6 retired breeder mice were raised on a standard diet, divided into three groups (n=7-11/group, 28 total) and starting at 12-13 months of age had the starch content of their diet altered as follows: high glycemic index (100% amylopectin), low glycemic index (30% amylopectin/70% amylose) or low glycemic index diet supplemented with antibiotics to modify the constituents of the gut microbiome (320 mg ampicillin + 640mg neomycin /kg chow). The special diets continued until 22-24 months of age when femurs were collected to analyze diaphyseal geometry and strength (Fig. 1A).The low glycemic index group with altered gut microbiome showed reductions strength that could not be explained by geometry (section modulus) indicating reduced bone tissue strength (p = 0.006, Fig. 1B). No differences in tissue strength were observed between low- and high glycemic index groups, although the high glycemic index diet group had larger body mass, larger bone cross-sectional area (Fig. 1C) and moment of inertia, and an associated increase in whole bone stiffness (p < 0.05 each).Guss et al. (JBMR 2017) showed that modification to the gut microbiome caused by oral ampicillin and neomycin during rapid bone acquisition (1-4 months of age) led to reduced bone tissue strength at skeletal maturity. Here we show that the same stimulus to the gut microbiome applied in late adulthood (12-24 months of age), causes a similar reduction in bone tissue strength. Although the current study was opportunistic and is therefore limited (no baseline assessment, no high glycemic index Amp+Neo group), it shows that microbiome-induced modifications to bone tissue strength are not limited to young, rapidly growing animals. Current osteoporosis interventions focus on enhancing bone quantity and do not directly address impaired bone tissue properties. Our findings raise the possibility that microbiome-based interventions could improve bone tissue material properties in the elderly.

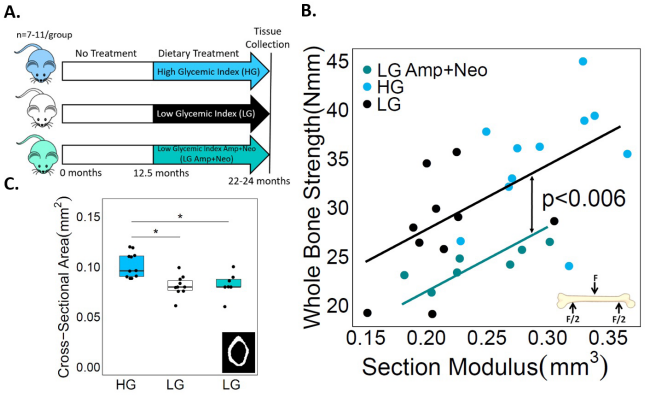

Figure 1. A) The experimental design includes mice on diets including high glycemic index (HG), low glycemic index (LG) and low-glycemic index supplemented with ampicillin and neomycin to alter the gut microbiome (LG Amp+Neo). B) Alterations to the gut microbiota (Amp+Neo) caused reductions in bone strength that could not be explained by geometry (difference expected value between regression lines). C) The high glycemic index diet group had larger bone cross-sectional area. *p<0.05 using Tukey-Kramer HSD comparisons for all pairs.

***Disclosures: Macy Castaneda**, None*

1099

Small changes in structure and mineral density after exercise can have profound effects on mechanical strength

*Mariana Kersh[1], Hyunggwi Song[1], John Polk[2]. [1]University of Illinois at Urbana-Champaign, United States, [2]University of Illinois, United States

Bone modeling occurs during development, an optimal time for adaptation due to exercise, that may have lifelong benefits. Axial loading has demonstrated a link between mechanical stimulation and adaptation, but their translation to exercise is challenging.Healthy juvenile sheep were exercised on a flat (n=11) or inclined (n=11) treadmill, and compared to non-exercised controls (n=8) (Fig 1A). Micro-CT analyses of subchondral (Sbch) and trabecular (Tb)structure and density were analyzed throughout the joint followed by mechanical testing. Sheep used more flexed knee angles during inclined exercise but less range of motion resulting in a preferential loading of a smaller region of the posterior condyle. Larger areas of increased Sbch and trabecular Tb and density occurred due to flat exercise compared to inclined exercise (Fig 1B,C). Increases in Tb thickness became larger moving towards the joint center (2.0+/-1.2\% to 3.4+/-1.1), while density decreased (4.9+/-2.4% to 3.5+/-1.4%). Elastic modulus and yield stress was significantly greater than the control group (flat: 90% and 76%, incline: 59% and 41%, p<0.01, Fig1E). Yield strain did not change. The ultimate stress significantly increased by 45% (p0.1)). The ultimate strain in the inclined group significantly decreased to 60% of that in controls (p<0.05). Relatively small percent increases in subchondral and trabecular density (9 to 14%) due to exercise induced much larger increases in mechanical strength (41 to 90%) compared to controls. Yield and ultimate strength are among the most clinically important because it implies when plastic deformation and failure occurs. The decrease in ultimate strain due to exercise implies that the exercised bone is more brittle as seen in the increase in elastic moduli. However, this result does not imply that the exercised bone became weaker because the energy needed to fracture was larger in the exercise groups (see area under curves in Fig 1E). The differential response in mechanical properties of the two exercise groups (compared to control) suggests that changes in the nature of mechanical loading - here induced via inclined exercise - results in differing adaptive response. Small changes in joint loading can result in spatially correlated changes to bone properties providing a mechanism for targeted exercise strategies aimed to improve bone health.

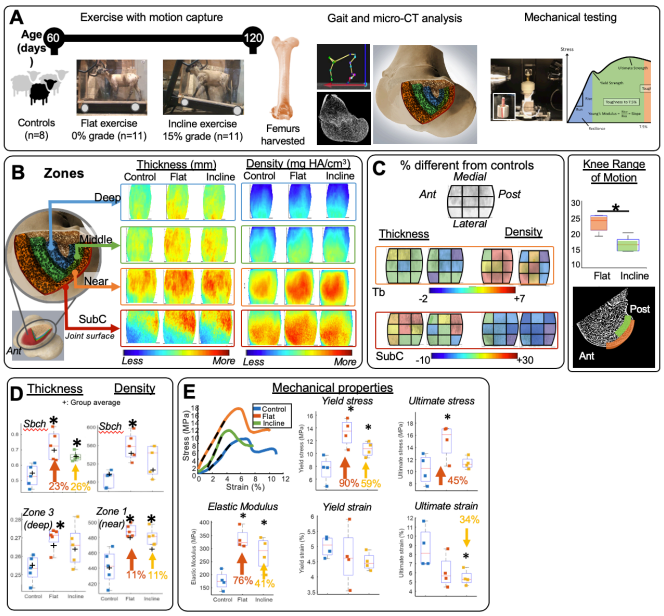

***Disclosures: Mariana Kersh**, None*

1100

Military Trainees Who are More Physically Fit Have More Favorable Tibial Bone Microarchitecture at Military Entry *Katelyn Guerriere[1], Kristin Popp[1], Soothesuk Kusumpa[1], Leila Walker[1], Melissa Richardson[1], Kathryn Taylor[2], Susan Proctor[1], Stephen Foulis[1], Mary Bouxsein[3], Julie Hughes[1]. [1]U.S. Army Research Institute of Environmental Medicine, United States, [2]U.S. Army Research Institute of Envrionmental Medicine, United States, [3]Beth Israel Deaconess Medical Center, United States

Physical activity (PA) history has a positive impact on bone density, structure, and fracture risk. Stress fractures are a particular concern for individuals undergoing U.S. Army Basic Combat Training (BCT). Measures of historical PA are not taken before beginning BCT, however, all incoming trainees complete one or more multi-event physical fitness (PF) tests to determine military readiness. Purpose: The purpose of this study was to assess the relationship between multi-event PF test performance and bone microstructure and density in young men and women entering BCT. Methods: This analysis uses a subset of data from an on-going prospective study collecting HR-pQCT images of the distal tibia before and after BCT in 4,000 trainees. Using the U.S. Army Research Institute of Environmental Medicine's Soldier Performance Health and Readiness database, we obtained Occupational Physical Assessment Test (OPAT) and/or the first recorded Army Physical Fitness Test (APFT) scores from 1141 men and 630 women with pre-BCT HR-pQCT scans. The OPAT consists of a deadlift, standing long jump, power throw, and shuttle run with overall scores ranging from 1 (best) to 3 (worst). The APFT consists of a 2-mile run, 2-minute sit ups, and 2-minute pushups with overall scores between 0 (worst) and 300 (best). We used generalized linear models to determine the association between PF test scores and bone parameters. Results, presented as effect estimates, were adjusted for age, race/ethnicity, and BMI. Results: Men and women enrolled in this study were similar in age and BMI. OPAT scores were significantly inversely associated with cortical area (Ct.Ar) and thickness (Ct.Th) in men (-2.21, p=0.007; -0.02, p=0.042) and women (-2.54, p=0.001; -0.02, p=0.026). Ct.Ar (0.067) and Ct.Th (0.001) were also positively associated with APFT scores in men (p<0.001), but not women. Total vBMD, trabecular (Tb.) vBMD, and most Tb. parameters were also significantly inversely associated with OPAT scores and significantly positively associated with APFT scores in men (p<0.04 for all), but not women. Conclusion: These results indicate that trainees who are more physically fit have more favorable bone microarchitecture at entry into BCT, although relationships may be modified by sex. Objective measures of PF at military entry may identify trainees at increased risk for musculoskeletal injury, although this remains to be demonstrated.

***Disclosures: Katelyn Guerriere**, None*

1101

Low Magnitude Mechanical Signals Enhance the Effects of Zoledronic Acid to Reduce Osteolytic Lesion Area and Improve Cardiac Function in a Murine Model of Breast Cancer Bone Metastases *Gabriel M. Pagnotti[1], Monte S. Willis[1], Trupti Trivedi[1], Sreemala Murthy[1], Sukanya Suresh[1], Yun She[1], Clinton T. Rubin[2], William R. Thompson[0], Khalid S. Mohammad[1], Theresa A. Guise[1]. [1]Indiana University, United States, [2]Stony Brook University, United States, [0]Indiana University, United States

Breast cancer bone metastases are characterized by osteolytic lesions and associated with systemic skeletal muscle dysfunction. Treatment for estrogen receptor(+) disease includes complete estrogen(E2)-deprivation and osteoclast bone resorption inhibitors, such as bisphosphonate zoledronic acid(ZA) to suppress bone destruction. Patients can experience disease recurrence and muscle weakness, which may include cardiac muscle dysfunction. Low intensity vibrations(LIV), a low-magnitude mechanical signal, improved bone mass and muscle strength in the setting of complete E2-deprivation (ovariectomy(OVX)+aromatase inhibitor(AI) letrozole) mouse models. We hypothesized that combining LIV with ZA could mitigate musculoskeletal decline in the setting of complete E2-deprivation(OVX+AI) and bone metastases. 5w-old athymic nude mice divided into 4 tumor-bearing and 2 non-tumor-bearing groups(n=20). Non-tumor groups were either sham or E2-deprived while all tumor-bearing groups were E2-deprived, receiving either no treatment, ZA alone, LIV alone or combined(Table1). LIV treatment(90Hz, 0.5g acceleration) began at 5w of age, complete E2-deprivation and ZA treatment at 9wk and intracardiac inoculation of 1x105 MDA-MB-231 cells at 12wk. Four weeks post-tumor inoculation, radiographs showed a significant reduction in osteolytic lesion areas in the ZA treated group(p<0.05) versus untreated tumor-bearing mice. Combined treatment(LIV+ZA) reduced osteolytic lesion area more than either treatment alone(p<0.01). Both untreated and ZA treated tumor-bearing E2-deprived mice had significantly reduced grip strength, which marginally improved with LIV either alone or in combination with ZA. Since we observed significant effects on skeletal muscle function, we hypothesized that cardiac muscle function might also be affected. We assessed mouse cardiac function by echocardiography calculation of fractional shortening(FS); non-tumor(p<0.05) and tumor-bearing(p<0.01) E2-deprived mice showed a reduction versus sham-mice(14d post-inoculation). This was partially prevented with LIV, ZA or in combination, exhibiting no effects on systolic cardiac function(FS%). Together, these data show that osteolytic breast cancer bone metastases are associated with skeletal muscle weakness and cardiac muscle dysfunction, both of which are improved by LIV, ZA or in combination and suggest that systemic effects of the growth factors released from the bone matrix may affect cardiac as well as skeletal muscle.

Table.1	Non-Tumor-Bearing		Tumor-Bearing			
E-Deprivation	Sham	OVX+AI	OVX+AI	OVX+AI	OVX+AI	OVX+AI
Treatment	No	No	No	ZA	LIV	ZA+LIV

***Disclosures: Gabriel M. Pagnotti**, None*

1102

Preclinical supplementation of Human Milk Oligosaccharides (HMOs) during early life positively impacts long-term bone quality. *Nicolas Bonnet[1], Kathrin Mletzko[2], Michael Baruchet[1], José Manuel Ramos-Nieves [1], Laurent Favre[3], Dominique Brassart [4], Felix Schmidt[2], Bjorn Busse[2], Sietse-Jan Koopmans [5], Marie Noelle Horcajada[1]. [1]Nestlé Research, EPFL Innovation Park, 1015 Lausanne, Switzerland, Switzerland, [2]Department of Osteology and Biomechanics, University Medical Center Hamburg, Germany., Germany, [3]Nestlé Research, Vers-chez-les-Blanc, 1000 Lausanne 26, Switzerland, [4]Nutrition Business Unit. Nutrition Research. Avenue Nestlé 55. 1800 Vevey. Switzerland, Switzerland, [5]Wageningen UR Livestock Research, Wageningen, The Netherlands, Netherlands

Bone growth during infancy is a key period for bone strength later in life. Human milk oligosaccharide (HMO) supplementation rescues bone growth in malnourished infants. However, it is not known which specific HMOs are involved and if it is a long lasting effect. Hence, we tested if sialylated and/or neutral HMOs intake during early life can impact determinants of bone strength later in life. Göttingen female Minipigs (n=48) were randomly allocated to be artificially reared with milk substitutes containing blends of either sialylated (2-HMOs: 3'SL and 6'SL; 0.68 g/L), neutral (4-HMOs: LNnT, LNT, 2'FL and di-FL; 4 g/L), both sialylated or neutral (6-HMOs: 4 g/L) or lactose as control group (C:4 g/L) from 10 days to 11 weeks of age (weaning). A naturally-reared reference group (NR; n=8) was kept. At weaning, all groups received a mild-western chow diet up to 48 weeks of age (sacrifice). Tibial BMD, microstructure, bone quality indices (matrix maturity, mineral-to-matrix ratio, degree of mineralization) and strength were evaluated by DXA, microCT, FTIR, quantitative backscattered electron microscopy and axial compression, respectively. Protocol was approved by Dutch Centrale Commissie Dierproeven, NL, N191114. Control group (C) exhibit low BMD, Tb BV/TV, CtBV, failure and post failure energy and high Ct.Po (-7.3%, -5.6%, -8.9%, -8.5%, -22.5% and +129%, p<0.05) vs NR. 2-4 and 6-HMOs blends reduced Ct. Po and increased mineral-to-matrix ratio vs C in regions of interest (respectively -50%, -52%, -53% and +8.4%, +8.3%, +8.7% all p<0.05) without any effect on collagen maturity. 4-HMOs blend significantly increased BMD, Tb BV/TV and Tb.N vs C (+7.7%, +4%, +27%

all p<0.05). This intervention decreased the degree of mineralization specifically at the periosteal vs C (-2.5% p<0.05), signs of higher bone formation. Similar trends were observed with 6-HMO. As a consequence, both 4-HMO and 6-HMO increased elastic energy vs C (+29.4% and +20.2%; all p<0.01) and yield force (+6.3%, p=0.07 and +10.7%, p<0.05), reaching energy to failure levels similar to NR. In conclusion, early life lactose milk substitute is not as efficient as natural-rearing to promote bone strength. Addition of neutral HMO to lactose rescued elastic tibial mechanical properties by improving BMD, trabecular and cortical bone quality. These findings further delineate the important role of HMO on long-term bone strength at milk substitution.

***Disclosures: Nicolas Bonnet**, Nestlé, Speakers' Bureau*

1103

FGF and Klotho Phosphate Regulatory Pathways Linking Placenta and Bone *Claire Stenhouse[1], Katherine M Halloran[1], Makenzie G Newton[1], Dana Gaddy[2], Larry J Suva[3], Fuller W Bazer[1]. [1]Department of Animal Science, Texas A&M University, United States, [2]Department of Veterinary Integrative Biosciences, Texas A&M University, United States, [3]Department of Veterinary Physiology and Pharmacology, Texas A&M University, United States

Phosphate and calcium are essential for fetal bone development and post-natal growth. Calcium transport across the placenta to the developing fetus is mediated by PTHrP but little is known regarding mechanisms of placental transport of phosphate. This study sought to identify whether the phosphate regulatory pathways recently uncovered in the skeleton have roles in the ovine endometrium and placenta throughout gestation. On Days 9, 12, 17, 30, 70, 90, 110 or 125 of pregnancy, ewes were euthanized and hysterectomized. On Days 9-17, the uterine horns were flushed with PBS to recover conceptuses. Sections of conceptus tissue (Day 17), placentae and endometria were frozen in liquid nitrogen or fixed in 4% paraformaldehyde. Inorganic phosphate was detected spectrophotometrically in uterine flushes, allantoic and amniotic fluid, and homogenates of placentae and endometria. Concentrations of phosphate were influenced by gestational day in all samples except for amniotic fluid (P<0.05). Phosphate concentration was greater in placentae than endometria on Days 30, 70 and 90 (P<0.05). On Day 125, phosphate concentrations in the endometria were greater than placentae (P<0.001). Next, expression of mRNA for sodium-dependent phosphate transporters (SLC20A1 and SLC20A2) and klotho signaling pathway mediators (FGF21, FGF23, FGFR1, KL and KLB) were quantified by qPCR. Day 17 conceptuses expressed SLC20A1, SLC20A2, KLB, FGF21, FGF23 and FGFR1 mRNAs. Endometrial expression of FGFR1 (P<0.001) and FGF21 (P<0.05) mRNAs was highest on Day 30, as was KL mRNA (Days 30 and 110; P<0.001). Placental expression of KLB (P=0.06) and FGF21 (P<0.05) mRNAs increased between Days 110 and 125. Placental FGF23 mRNA expression increased with stage of gestation (P<0.01). Placental expression of FGFR1 mRNA was lowest at Day 90 and increased by Day 125 (P=0.05). SLC20A1 mRNA expression peaked at Day 30, before decreasing to Day 110 (P<0.001). Further, KL and FGF23 proteins were detected using immunohistochemistry in conceptus trophectoderm and endoderm, uterine luminal and glandular epithelia, and uterine stratum compactum. KL and FGF23 were also expressed by placental cotyledons and caruncles in early pregnancy and localized to cotyledons in late pregnancy. These data suggest an important role for multiple phosphate regulatory pathways and direct our attention to the need to understand the impact that placental phosphate transport has on both placental pathophysiology and fetal mineralization.

***Disclosures: Claire Stenhouse**, None*

1104

A Neuroskeletal Atlas of the Mouse Limb *Madelyn R. Lorenz[1], Jennifer Brazill[1], Alec Beeve[1], Kristann Magee[1], Erica L. Scheller[1]. [1]Washington University in St. Louis, United States

In addition to the well-established role of the nervous system in bone pain and vasoregulation, the function of nerves in and around bone has been associated with progression of skeletal disorders including osteoporosis, fracture, arthritis and tumor metastasis. Though this has renewed interest in the study of neuroskeletal disorders, isolation of the region-specific mechanisms surrounding these relationships is limited by our lack of comprehensive local maps of skeletal innervation.To overcome this, we used 50 µm, thick-section histology and confocal immuno-microscopy to map the tyrosine hydroxylase positive sympathetic adrenergic nerves and calcitonin gene related peptide expressing sensory peptidergic nerves within the mouse tibia, femur, ulna, and radius in 12-week-old C57BL6 and C3H mice. In the periosteum, these maps were then related to the surrounding musculature, including entheses and myotendinous attachments to bone, in addition to major nerve branches and surrounding adipose tissues.Locally, distinct patterns of innervation were detected within established sites that are important for bone repair and homeostasis, including regions of the metaphysis, mid-diaphysis, and periosteum. Within the periosteum, innervation patterns fall into three categories: aneural (Type I), anchored (Type II), and fascial (Type III). Finally, confocal imaging, tissue clearing, and light sheet microscopy were used to map aspects of secondary neural architecture, defining areas of myelination, Schwann cells and specialized mechanoreceptors, within the context of the musculoskeletal system.Overall, these results demonstrate that nerves are an integrated component of the skeleton with distinct spatial patterns of organization. This provides guidance that can be used during the design and implementation of future neuroskeletal studies and suggests that local differences in the neuroskeletal microenvironment may result in diverse, region-specific responses during skeletal disease and repair. This work was compiled as a resource for the field as part of the NIH SPARC consortium.

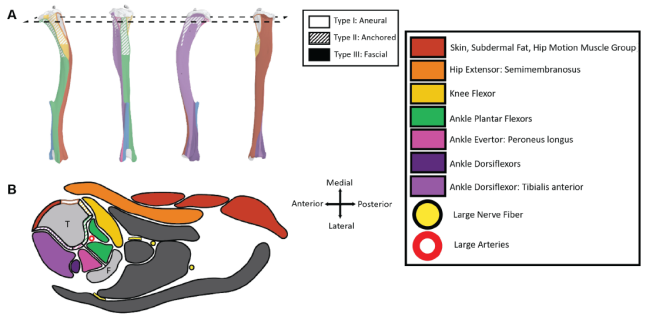

Figure 1. (A) Four views of a 12-week old C3H uCT tibia image with annotation of Types I-III neural attachments. (B) 2D cross section of the distal tibial metaphysis (T), including surrounding muscle and fibula (F), as indicated by the dotted box in Panel A.

***Disclosures: Madelyn R. Lorenz**, None*

1106

Beyond the Brain: Neurodegeneration risk-factor TREM2 R47H mutation causes distinct sex-dependent bone and cardiovascular phenotype in the absence of neuropathology *Alyson Essex[1], Padmini Deosthale[2], Allison Wagner[3], John Damrath[4], Joseph Wallace[5], Monte Willis[6], Andrea Bonetto[7], Lilian Plotkin[2]. [1]Department of Anatomy, Cell Biology& Physiology, Indiana University School of Medicine, United States, [2]Department of Anatomy, Cell Biology&Physiology, Indiana University School of Medicine, United States, [3]Life Health Science Internship, Indiana University- Purdue University, United States, [4]Weldon School of Biomedical Engineering, Purdue University, West Lafayette, Indiana, United States, [5]Department of Biomedical Engineering, Indiana University- Purdue University Indianapolis, United States, [6]Indiana Center for Musculoskeletal Health, Indiana University, United States, [7]Department of Surgery, Indiana University School of Medicine, United States

Age is the most critical risk factor for Alzheimer's disease (AD). Along with its complications, including osteoporosis and cardiovascular disease, AD prevalence is expected to increase over the next few decades due to the aging population. Clinical data shows exacerbated bone loss in AD, but no demonstrated mechanistic or causal links between the two conditions have been reported. Genome-wide analysis suggests that the Triggering Receptor Expressed on Myeloid Cells 2 R47H variant (TREM2R47H) confers high risk of developing AD. TREM2 contributes to neuroinflammation in AD, but, interestingly, TREM2 mutant mice only exhibit cognitive deficits when co-expressing AD neuropathology-conferring mutations. TREM2 is also critical for osteoclast differentiation and activity. Cardiomyocytes also express TREM2, suggesting that altered TREM2 function could also lead to deficient peripheral cell function, contributing to exacerbate bone and cardiovascular disease in AD patients. To test this possibility, TREM2 R47H variant hemizygous (TREM2R47H/+) mice were created by CRISPR-Cas9 on C57B6/J (WT) background. We found decreased systolic function by ultrasound echocardiography in 15-month-old (mo) TREM2R47H/+female (76.9+/-3.6 vs 85.0+/-2.3 ejection fraction, EF%) and male (78.3+/-1.3 vs 84.1+/-1.5 EF%) mice, but not in 1mo mutants, compared to WT littermates. Left ventricular (LV) end diastolic and systolic diameters, indicators of dilation, were higher in female but not male 15mo TREM2R47H/+ mice. Femoral cortical and cancellous bone µCT analysis showed no change in 4mo mice, but lower cortical and cancellous BV/TV in 13mo female TREM2R47H/+ compared to WT mice; with no changes in males up to 20 months of age. Higher cortical cross-sectional area (5%), marrow area (13.5%), and endocortical bone surface (4.6%) with lower cortical thickness (7.4%) indicate that the TREM2 variant may accelerate age-related endocortical resorption and periosteal expansion in female TREM2R47H/+ mice. Lower biomechanical strength [yield force (20%) and work to yield (31%)] and material properties [stress (22%) and resilience (37%)] tested by 3-point bending were seen in female mutant compared to WT mice. Overall, our data indicate that by 13-15 months, female TREM2R47H/+ mice have aggravated loss of femoral bone mass and mechanical strength compared to age and sex-matched controls, with more profound cardiovascular dysfunction than males, suggesting a sex-dependent systemic role of TREM2 with aging.

***Disclosures: Alyson Essex**, None*

1107

Transplantation of the Gut Microbiota from Healthy Mice Ameliorates Bone Loss in Sickle Cell Disease Recipient Mice *Liping Xiao[1], Donyell Williams[1], Marja Hurley[1]. [1]UConn Health, United States

Although 80% of adults with sickle cell disease (SCD) have low bone mineral density, the molecular mechanisms of bone loss in SCD are not yet fully defined. Recent studies

Tuesday Orals

showed gut microbiota dysbiosis in SCD in both humans and mice harboring the humanized sickle hemoglobin gene. Short chain fatty acids (SCFAs) are the major metabolite produced by gut bacteria that can affect bone growth by regulating insulin like growth factor 1 (IGF1) production. Serum IGF1 was low in SCD subjects and we published decreased IGF1 in bone and serum of SCD mice. Currently, there is no report on SCFA levels in SCD subjects or SCD mice. It is unknown if decreased IGF1 associated with low bone mass in SCD is due to reduced SCFA production by gut microbiota. Therefore, we performed fecal microbiota transplantation (FMT) in SCD mice. SCD female mice (3 months old, 10 mice/group) were fasted for 1h, then mice were subjected to bowel cleansing by oral gavage with four doses of 200µl PEG (polyethylene glycol, Macrogol 4000) at 20min intervals to deplete the majority of their gut flora and then used as RECIPIENTS of the FMT. Pooled fecal matter from 8 healthy control (Ctrl) mice (DONOR mice) was given by oral gavage 4h after last PEG treatment to recipient mice. FMT was performed once per week. This is SCD-FMT group. As controls, Ctrl mice received FMT from Ctrl mice (Ctrl group) and SCD mice received FMT from SCD mice (SCD group). Six weeks post FMT, samples were collected. uCT analysis of femur showed significantly decreased bone volume/total volume (Fig1.A&B) and trabecular number, and significantly increased trabecular spacing and structure model index in SCD mice compared to Ctrl mice; these parameters were partially rescued in SCD-FMT group. Bone formation marker genes alkaline phosphatase, type-1 collagen, Dmp1, and Igf1 mRNA (Fig.1C) were significantly decreased in flushed tibiae from SCD mice compared with Ctrl, which was rescued after FMT from healthy Ctrl feces. SCFAs levels in cecal content were quantified by gas chromatograph coupled to a mass spectrometer detector (GC-MS). Propionate and butyrate (2 types of SCFA) levels were significantly lower in SCD mice vs. Ctrl that was rescued after receiving FMT from healthy Ctrl mice (Fig.1D&E). These results suggest that the healthy gut microbiota community from healthy Ctrl mice confers protection from SCD bone loss by changing the production of bone growth factor IGF1 in response to altered bacterial metabolites SCFAs.

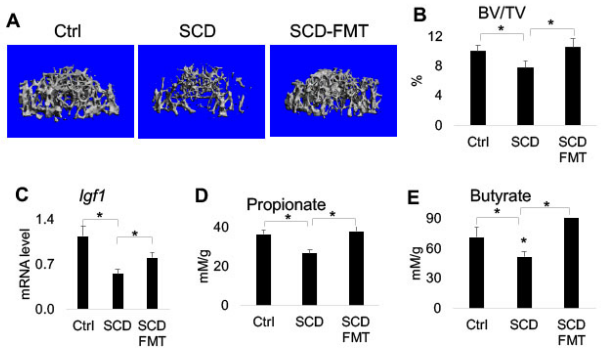

Figure 1. (A&B) uCT analysis of femur, (C) qPCR analysis of Igf1 mRNA in flushed tibia, (D&E) GC-MS analysis of propionate and butyrate (2 types of SCFA) in cecal content of Ctrl, SCD, and SCD-FMT mice. n=10 mice/group. Data are mean±SE. *p<0.05 ; t-test.

***Disclosures: Liping Xiao**, None*

1108

Sensory Innervation in Porous Endplates by Netrin-1 from Osteoclasts Mediates PGE2-induced Spinal Pain *Shuangfei Ni[1], Jianzhong Hu[2], Xu Cao[3]. [1]Zhengzhou University, China, [2]Central South University, China, [3]Johns Hopkins University, United States

INTRODUCTION: Low back pain (LBP) is the leading cause of activity limitation and work absence as a common health problem. 90% of LBP is nonspecific LBP, however, its origins and underlying mechanisms remain unclear.METHODS: The lumbar spine instability (LSI) and aging mouse model were established. Heterozygous male Avil-Cre mice were crossed with EP4flox/flox mice to knockout EP4 in sensory nerves. Heterozygous Dmp1-Cre mice were crossed with Ranklflox/flox to inhibit osteoclast formation. Heterozygous Trap-Cre mice were crossed with Netrin-1flox/flox to delete Netrin-1 secreted by osteoclasts. The pressure hyperalgesia, spontaneous activity, and mechanical hyperalgesia of hindpaw were conducted to evaluated spinal pain-associated behaviors. All mice were maintained at the animal facility of The Johns Hopkins University School of Medicine. Human endplate samples were obtained from patients undergoing spine fusion surgery in the Department of Spine Surgery at Xiangya Hospital (China).RESULTS SECTION: Here we report that osteoclasts initiate the endplate sclerosis accompanied by sensory innervation for the LSI- and aging-induced spinal pain. Sensory innervation into the porous areas of sclerotic endplates was validated by retrograde and anterograde tracing. we also evaluated the pathological changes in the endplates of the lower lumbar spines of patients with or without LBP history. Severe endplate lesions were observed in patients with history of frequent LBP, whereas the cartilaginous structure was preserved in patients without history of frequent LBP. Abundant TRAP+ osteoclasts and CGRP+PGP9.5+ nociceptive nerve fibers were observed in the porous endplates of patients with LBP. We show that lumbar spine instability (LSI) or aging induces spinal pain. Elevated levels of PGE2 activate sensory nerves, ultimately leading to sodium influx through Nav 1.8 channels through PKA/CREB signaling. Particularly, we show that knockout of PGE2 receptor 4 (EP4) in sensory nerves significantly reduces the spinal pain. Inhibition of osteoclast formation by knockout Rankl in the osteocytes significantly inhibits LSI-induced porosity of endplates, sensory innervation, and spinal pain. Knockout of Netrin-1 in osteoclasts abrogates sensory innervation into porous endplates and spinal pain.DISCUSSION: LBP is difficult to diagnose and treat because of limited knowledge about its source. Importantly, endplates undergo sclerosis during aging and become porous, which is clinically associated with LBP. In this study, we demonstrate that osteoclasts initiate porosity of endplates with sensory innervation into porous areas, which is the potential source of spinal pain.

***Disclosures: Shuangfei Ni**, None*

1109

INZ-701 prevents ectopic tissue calcification and restores growth in ENPP1 deficient mice *ZHILIANG CHENG[1], Kevin O'Brien[1], Caitlin Sullivan[1], Jennifer Howe[1], Denis Schrier[2], David Thompson[1], Steve Jungles[1]. [1]Inozyme Pharma, United States, [2]Inozyme Phrma, United States

Ectonucleotide pyrophosphatase/phosphodiesterase 1 (ENPP1) is the major enzyme that generates extracellular pyrophosphate (PPi), an inorganic metabolite with potent anti-calcification activity. Loss-of-function mutations lead to a state of ENPP1 deficiency and hypopyrophosphatemia, which in turn cause extensive calcification of the heart, arteries, and kidney, impaired growth and premature mortality. The acute infantile form of ENPP1 deficiency (referred to as Generalized Arterial Calcification of Infancy (GACI)) presents with pathological mineralization in multiple tissues, arterial stenoses, growth impairment, and a 50% mortality in the first year of life. INZ-701 is a recombinant, soluble, human ENPP1-Fc protein being developed as potential enzyme replacement therapy for the treatment of ENPP1 deficiency. We performed a dose-response study to investigate the pharmacological effects of INZ-701 in Enpp1asj/asj mice, a murine model of acute infantile ENPP1 deficiency. These mice harbor a missense mutation, p.V246D, in the Enpp1 gene, which produces undetectable levels and activity of ENPP1 protein and closely mimics the human condition. Starting from 2 weeks of age, Enpp1asj/asj mice were subcutaneously dosed either with vehicle or with 0.2, 1, or 5 mg/kg of INZ-701 every other day for 8 weeks. Clinically relevant endpoints, including PPi levels, tissue calcium by colorimetric assay and µCT, body weight, and clinical signs and symptoms were measured. While plasma PPi levels in Enpp1asj/asj mice were confirmed to be undetectable, dosing of INZ-701 normalized PPi levels to ~2 µM in all 3 groups. Enpp1asj/asj mice treated with vehicle ceased to gain weight from ~4 weeks of age, and showed signs of hunched back, stilted gait, and impaired growth. Significant increases in tissue calcium levels were recorded in heart, kidney, spleen, lung, liver and vibrissae, and µCT revealed extensive calcification in the areas of aorta, coronary artery and heart in the vehicle-treated group (Figure). Our results showed that INZ-701 treatment at a dose of 1mg/kg or higher prevented pathological calcification in all the tested organs, restored growth parameters, and improved signs and symptoms of ENPP1 deficiency. In summary, INZ-701 restored circulating levels of PPi, a critical calcification inhibitor, and demonstrated a dose dependent prevention of pathological calcification and improvement of growth and symptoms in a murine model of ENPP1 deficiency.

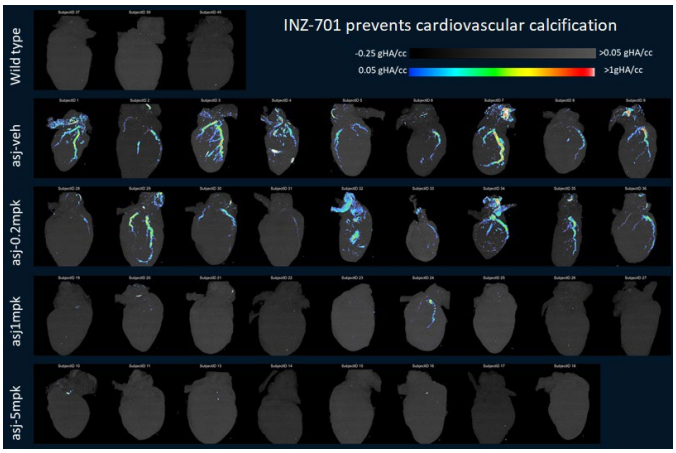

***Disclosures: ZHILIANG CHENG**, INOZYME PHARMA, Grant/Research Support*

1110

A MyD88 Inhibitory Peptide Reduces Endochondral Heterotopic Ossification in the ALK2R206H-FlEx model of FOP *Huili Lyu[1], Cody Elkins[1], Nikash Hari[2], Joshua Johnson[2], Carlos Serezani[3], Daniel Perrien[1]. [1]Division of Endocrinology, Department of Medicine, Emory University, United States, [2]Vanderbilt Center for Bone Biology, Division of Clinical Pharmacology, Department of Medicine, Vanderbilt University Medical Center, United States, [3]Division of Infectious Disease, Department of Medicine, Vanderbilt University Medical Center, United States

Fibrodysplasia ossificans progressiva (FOP) is a genetic disease caused by aberrant BMP signaling through mutated ACVR1/ALK2 and characterized by episodic muscle inflammation and endochondral heterotopic ossification (EHO) of skeletal muscles frequently induced by injury or inflammatory events. Hyperinflammation plays an essential role in FOP flares and endochondral heterotopic ossification, but the mechanisms that trigger the hyperinflammatory responses are not described. DAMPs and members of the IL-1 superfamily are among the first inflammatory signals released from damaged tissues. Their signaling through Toll-Like Receptors (TLRs) and IL-1 receptors, respectively, is critical to initiating the inflammatory cascade and largely dependent on the adapter protein MyD88 and TLR-signaling has been linked to the enhancement of canonical BMP signaling. Hence, we hypothesized that inhibition of MyD88 may reduce inflammation and EHO in FOP and tested the hypothesis in an established mouse model of FOP. ALK2R206H-FlEx;R26creERt2/creERt2 mice received tamoxifen starting at 8 days old by feeding the dam 40mg/kg/d for 8 days followed by bilateral injury of the lower hindlimb muscles by injection of 1.5µg cardiotoxin at 20 days old. All mice received 100µg of a palmitoylated MyD88-inhibitory peptide (Anti-MyD) ip or control peptide (Con) every 3 days starting 1 day before injury until sacrifice. Analysis of weekly radiographs revealed significantly less EHO in Anti-MyD mice vs Con at 14- ($p<0.0001$) and 21-days post-injury ($p<0.001$), which was confirmed by ex vivo µCT ($p=0.0014$). To determine the possibility of a direct role for MyD88 in mesenchymal commitment to osteogenesis, BMSCs from MyD88+/+ or MyD88-/- mice were cultured in non-osteogenic media with Vehicle, 100ng/ml of the TLR agonist LPS, 100ng/ml BMP2, or BMP2+LPS. BMP alone significantly increased the number of alkaline phosphatase positive cells from both MyD88+/+ ($p<0.05$) and MyD88-/- BMSCs. LPS alone had little effect on AP expression but synergistically increased the osteogenic effect of BMP2 in MyD88+/+ cells ($p<0.01$). However, in MyD88-/- cells, LPS blocked the osteogenic effect of BMP2, suggesting that MyD88-independent signaling pathways may antagonize osteogenic BMP signaling. These results suggest that MyD88-dependent pathways may be critical for EHO formation in FOP and that, in addition to controlling inflammation, blockade of MyD88 may inhibit aberrant BMP signaling in chondrogenic progenitors.

***Disclosures: Huili Lyu**, None*

1111

A self-amplifying, self-propagating loop of Yap and Shh drives formation and expansion of heterotopic ossification *Qian Cong[1], Yuchen Liu[1], Taifeng Zhou[2], Peiqiang Su[3], Paul B Yu[4], Yingzi Yang[2]. [1]Department of Developmental Biology, Harvard School of Dental Medicine, Harvard Stem Cell Institute, United States, [2]Department of Developmental Biology, Harvard School of Dental Medicine, United States, [3]First Affiliated Hospital of Sun Yat-sen University, China, [4]Department of Medicine, Brigham and Women's Hospital, United States

Heterotopic ossification (HO) refers to extraskeletal pathological bone formation that occurs as a common complication after injury or as a manifestation of particular genetic disorders. However, limited by poor understanding of underlying cellular and molecular mechanisms, there is currently no effective treatment and surgical eviction ofter results in recurrence. We have found that in both genetic and injury-induced HO, activated ectopic Shh expression drives HO progression by forming a positive feedback loop that results in non-cell- autonomous and self-propagation of osteoblast differentiation of wild type cells. In mouse models of progressive osseous heteroplasia (POH), a human disease caused by null mutations in GNAS that encodes Gαs, we found that progressively expanded ectopic bone was formed by progressively recruited wild type cells. Mechanistically, Gnas-/- mesenchymal cells differentiate into osteoblasts and recruit wild-type cells to form bone by activating Yap, a transcription factor that regulates Shh expression and secretion. Secreted Shh further induces Yap activation, Shh expression and osteoblast differentiation in surrounding wild type cells. This self-propagating positive feedback loop is both necessary and sufficient for ectopic bone formation and expansion and can independently of Gαs. Importantly, Yap and Shh activation was also found in fibrodysplasia ossificans progressive (FOP), Achilles tendon puncture (ATP)-induced HO mouse models and in human HO samples. Genetic removal of Yap and Shh abolished HO not only in POH, but also in FOP and acquired HO mouse models. We therefore indentify a Yap-Shh positive feedback loop as a common cellular and molecular mechanism underlying HO initiation and expansion. Our work highlights the importance of rare genetic disease studies in identifying a shared core pathological mechanism underlying a class of diseases. As Shh is not required for normal bone formation, our results further suggest that Shh is a promising new therapeutic target for HO without affecting the normal bone.

***Disclosures: Qian Cong**, None*

1112

Evaluation of Epigenetic Regulation of Osteogenesis Imperfecta Severity with Circulating microRNAs: the miROI Study *Alexandre Mercier[1], Marjorie Millet[2], Martine Croset[2], Blandine Merle[2], Jean-Paul Roux[2], Elisabeth Sornay-Rendu [2], Olivier Borel[2], Pawel Szulc[2], Deborah Gensburger[3], Emmanuelle Vignot[4], Elisabeth Fontanges[3], Roland Chapurlat[1]. [1]Division of Rheumatology, Edouard Herriot University Hospital; INSERM UMR 1033, Université de Lyon, France, France, [2]INSERM UMR 1033, Université de Lyon, France, France, [3]Division of Rheumatology, Edouard Herriot University Hospital, France, France, [4]Division of Rheumatology, Edouard Herriot University Hospital, France, France

Objectives: In about 85% of individuals, Osteogenesis Imperfecta (OI) is caused by dominant autosomal mutations in COL1A1 and COL1A2. For the same mutated gene (COL1A1 or COL1A2) and for the same variant (in the same family) there is a great heterogeneity of phenotypic severity, without biomarker of disease severity for the physician. As epigenetic regulators of gene expression, circulating microRNAs (miRs) have been described in other bone diseases as potential markers regulating gene expression. The aim of this study was to identify serum miRs potentially associated with the OI severity.Methods: Ten patients were recruited in consultation and hospitalization at the University Hospital Edouard Herriot Hospital in Lyon. Ten age- and sex-matched control patients from the population-based OFELY, MODAM and STRAMBO cohorts were involved. We measured all circulating microRNAs (miRome) in both groups by next generation sequencing (NGS). Total RNA extracted from serum was analysed by miRs sequencing on Illumina platform and the miRs levels were normalized by the M-trimmed mean prior to Tags-per-million expression and comparison between groups by the Log2(Fold Change). Multiple comparisons were accounted for by the false discovery rate (FDR) adjustment method of Benjamini-Hochberg.Results: The mean age of OI patients was 41 (29-61) with a balanced sex-ratio. All patients had type I OI. We found 79 miRNAs differently expressed with FDR corrected p-values<0.05 and 27 miRs with corrected $p<0.0005$. Among these, 5 were down-regulated, 22 were up-regulated in OI. Several miRs transcribed from physically adjacent miR genes clustered : miR-183/96/182 and miR-25/93/106b. After a literature review, we found 22/27 miRs known to be involved in bone homeostasis. We used the MiRWALK database to screen these miRs interactions and we found 23/79 miRs predictably targeting either COL1A1 or COL1A2 with a probability of 100%.Conclusion: We have established the miR signature in OI by highlighting significant dysregulation in circulating miRs involved or potentially involved in the regulation of genes with a major role in the pathophysiology of OI. These miRs will be remeasured in a validation phase in a larger cohort to link the biological dysregulation to the clinical phenotype.

***Disclosures: Alexandre Mercier**, None*

1113

Role of FGF Receptor, FGF23 Signaling in Enthesopathy of Achilles Tendon in High Molecular Weight FGF2 Transgenic Mice *Donyell Williams[1], Liping Xiao[1], Nathaniel Dyment[2], Marja Hurley[1]. [1]UConn Health, United States, [2]University of Pennsylvania, United States

Background: Subjects with X-linked hypophosphatemic rickets (XLH) and the Hyp mouse homolog of XLH develop osteomalacia and enthesopathy. FGF receptor (FGFR) inhibitor BGJ398 partially rescued osteomalacia in Hyp mice, which we have reported overexpress the high molecular weight isoform of fibroblast growth factor 2 (HMWFGF2) in osteoblasts and osteocytes. HMWFGF2Tg mice phenocopy Hyp mice with increased FGFR and FGF23 expression in osteoblasts and osteocytes, and BGJ398 also partially rescued the osteomalacia in HMWFGF2Tg mice. Therefore, in this study, we aimed to determine if HMWFGF2Tg mice develop enthesopathy at the Achilles tendon insertion site. Additionally the effects of FGF inhibition on enthesopathy in Hyp and HMWFGF2Tg mice have not been reported. Thus, we also examined whether in vivo treatment with BGJ398 would modulate development of the enthesopathy phenotype at the Achilles tendon enthesis of HMWFGF2Tg mice.Methods: All Animal care and use protocols were approved by the Animal Care and Use Committee at UConn Health. VectorTg and HMWFGF2Tg mice (21 days of age) were treated with vehicle (HCL 3.5 mM, DMSO 5%) or BGJ398 (2 mg/kg, sq daily) for 13 weeks at which time they were sacrificed. Ankles were dissected, fixed, and frozen undecalcified sagittal sections including the Achilles tendon were prepared for histology and immunohistochemistry.Results: Achilles tendon entheses from HMWFGF2Tg vehicle-treated mice had higher alkaline phosphatase (AP) activity but weaker Safranin O staining (i.e., proteoglycans) compared with VectorTg. HMWFGF2Tg vehicle-treated mice also had increased FGF23, phospho-ERK, and Runx2 protein expression compared with VectorTg. BGJ398 treatment rescued the observed abnormalities in mineralization, proteoglycan, and expression of FGF23, phospho-ERK and Runx2 in HMWTg entheses.Summary and Conclusion: This study demonstrates that overexpression of the HMWFGF2 isoform in Col1a1-expressing cells results in the enthesopathy of the Achilles tendon enthesis that can be partially rescued by FGFR inhibition.

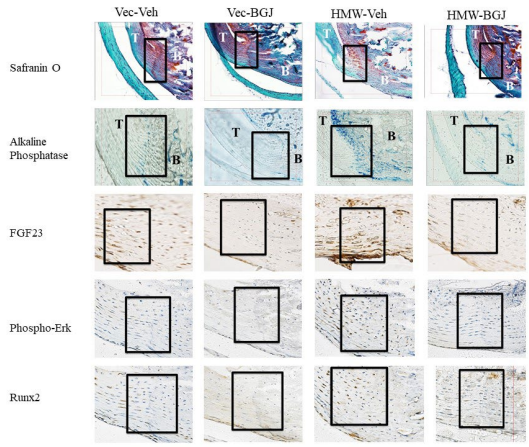

***Disclosures: Donyell Williams**, None*

1114

Activating Fgfr3 Mutation In Immature Osteoblasts Affects Appendicular And Cranio-facial Skeleton *Martin Biosse Duplan[1], Emilie Dambroise[2], Valentin Estibals[2], Joelle Veziers[3], Jerome Guicheux[3], Laurence Legeai-Mallet[2]. [1]Université de Paris, Imagine Institute, Laboratory of Molecular and Physiopathological Bases of Osteochondrodysplasia. INSERM UMR 1163. Service de Medecine Bucco-Dentaire, Hopital Bretonneau, AP-HP, France, [2]Université de Paris, Imagine Institute, Laboratory of Molecular and Physiopathological Bases of Osteochondrodysplasia. INSERM UMR 1163, France, [3]INSERM 1229, Université de Nantes, France

Achondroplasia (ACH), the most common form of dwarfism, is caused by a missense mutation of the gene coding for fibroblast growth factor receptor 3 (FGFR3) that leads to increased FGFR3 signaling. In ACH, the proliferation and differentiation of the growth plate chondrocytes (CCs) are disturbed, thus altering the long bone elongation. Several patients with ACH also show membranous bones defects and reduced bone mineral density, indicating that increased FGFR3 signaling could also impair osteoblasts (OBs) differentiation or activity.In this study, we examined whether or not Fgfr3 overactivation in OBs leads to bone modifications in a mouse model of ACH. We took advantage of a model carrying a Fgfr3 activating mutation (Fgfr3Y367C/+) and targeted the mutation in immature OBs and hypertrophic CCs or in mature OBs using respectively the Osx-cre and collagen 1α1 (2.3kb-Col1α1)-cre mouse lines.We observed that activation of Fgfr3 in immature OBs and hypertrophic CCs perturbed the hypertrophic CCs of the femoral growth plate resulting in a reduced hypertrophic zone (-22.1% compared to Osx-cre mice, p<=0.05; n>=6 for each genotype, 3-week old males). Accordingly, the growth of the long bones was affected, and adult mutant mice had shorter femur (-28.3%, p<=0.001) and tibia (-26.1%, p<=0.001; n>=8 for each genotype, 3-month old males). Increased Fgfr3 signaling in immature OBs and hypertrophic CCs also led to osteopenia as shown by the decreased BV/TV (-46%, p<=0.005) and reduced cortical thickness of femurs (-19%, p<=0.05; n>=6 for each genotype, 3-month old males). Importantly, cranio-facial membranous bones defects were present in mutant mice, with a defective growth of frontal and nasal bones. In contrast, activation of Fgfr3 in mature OBs had very limited effects on skeletal shape, size and micro architecture of long bones as well as cranio-facial membranous bones. Finally, we observed that Fgfr3 activation in immature OBs did not affect the proliferation, viability or differentiation of the cells, but reduced their mineralization activity (-51%, p< 0.01; n>=6 for each genotype). In conclusion, immature OBs are affected by Fgfr3 overactivation and contribute to the bone modifications observed in ACH, independently of CCs. This study emphasizes the role of FGFR3 during the early steps of OB differentiation.

***Disclosures: Martin Biosse Duplan**, None*

1115

The Effect of Low-dose Oral Glucocorticoid Therapy on Osteoporotic Fracture Risk in Patients with Rheumatoid Arthritis: the UK Clinical Practice Research Datalink *Shahab Abtahi[1], Johanna H.M. Driessen[1], Andrea M. Burden[2], Patrick Souverein[3], Joop P. van den Bergh[4], Tjeerd van Staa[3], Annelies Boonen[4], Frank de Vries[1]. [1]Department of Clinical Pharmacy and Toxicology, MUMC+, Netherlands, [2]Institute of Pharmaceutical Sciences, Department of Chemistry and Applied Biosciences, ETH-Zurich, Switzerland, [3]Division of Pharmacoepidemiology and Clinical Pharmacology, Utrecht. Institute for Pharmaceutical Sciences, Netherlands, [4]Department of Internal Medicine, Division of Rheumatology, MUMC+, Netherlands

Background and Purpose: Randomized clinical trials (RCTs) showed that low-dose glucocorticoid (GC) therapy in patients with rheumatoid arthritis (RA) was associated with reduced bone mineral density (BMD) loss in hands or hip. However, the effect on osteoporotic fractures is not yet clear and observational studies mostly reported contrasting results compared to the BMD studies. Thus, we investigated the use of low-dose oral GCs on osteoporotic fracture risk among patients with RA in the UK.Methods: This was a retrospective cohort study including all RA patients aged 50+ from the Clinical Practice Research Datalink (CPRD) between 1997-2017. Exposure to oral GCs was stratified into current (1 year), based on the time since the most recent prescription. Current use was further stratified by average daily and cumulative doses. Time-dependent Cox proportional-hazards models estimated risk of osteoporotic fracture (included hip, vertebrae, humerus, forearm, pelvis, or ribs) in RA patients with current use of low-dose oral GCs (average daily dose <=7.5mg prednisolone equivalent dose [PED]/d) versus past use. The analyses were statistically adjusted for life-style parameters, comorbidities and comedications.Results: Among 15,123 patients with RA (mean age 68.8 years, 68% females), 1640 osteoporotic fractures occurred. Current low-dose oral GC therapy (<=7.5mg PED/d) in RA patients was not associated with an increased risk of osteoporotic fractures compared with past GC use (adjusted hazard ratio 1.14, 95%CI 0.98-1.33, Table 1). Clinical vertebral fracture was the only one among the six studied osteoporotic fractures that observed higher rates with low-dose GC use (adjusted hazard ratio 1.59, 95%CI 1.11-2.29) versus past use. High-dose (>7.5mg PED/d) long-term (>=1g PED) oral GC therapy in RA patients was associated with a 1.5-fold increased risk of osteoporotic fractures compared to past use.Conclusion: Low-dose GC therapy was not associated with an increased risk of osteoporotic fractures in RA patients compared with past GC use, except for clinical vertebral fractures. Our results are in line with findings from RCTs reporting a similar effect of low-dose GC use on BMD in various anatomical sites. Clinicians should be aware that even in RA patients who receive low daily GC doses (<=7.5mg PED/d), clinical vertebral fracture risk is increased.

Table 1. Use of oral glucocorticoids and risk of osteoporotic fracture in patients with rheumatoid arthritis, by average daily dose.

Oral Glucocorticoid Use By recency of use	OP fractures (N=1640)#	IR per 1000 Pys	Age/Sex adjusted Hazard Ratio (95%CI)	Fully adjusted Hazard Ratio* (95%CI)
Current●	428	21.3	**1.36 (1.18-1.56)**	**1.22 (1.06-1.40)**
Mean daily dose ≤7.5mg PED/day	301	20.3	**1.26 (1.08-1.46)**	1.14 (0.98-1.33)
Mean daily dose 7.6-14.9mg PED/day	101	23.3	**1.60 (1.29-2.00)**	**1.38 (1.11-1.73)**
Mean daily dose ≥15mg PED/day	26	27.9	**2.09 (1.40-3.11)**	**1.84 (1.23-2.74)†**
Recent●	36	11.1	0.76 (0.54-1.06)	0.71 (0.51-1.00)
Past●	375	15.7	Reference	Reference
Non-use	801	12.6	0.90 (0.80-1.02)	0.94 (0.83-1.07)

Abbreviations, OP: Osteoporotic, IR: incidence rate, Pys: person years, CI: confidence interval, PED: prednisolone equivalent dose.
Statistically significant hazard ratios are shown in bold.
1640 osteoporotic fracture events among all included patients.
* Adjusted at baseline for sex, body mass index, smoking status and alcohol use, and during follow-up for age, a history of ankylosing spondylitis, chronic obstructive pulmonary disease, dementia, falls (in the past 7-12 months), inflammatory bowel disease, and the use in the past 6-months of antidepressants, antihypertensives, proton pump inhibitors, paracetamol, non-selective non-steroidal anti-inflammatory drugs, cyclooxygenase-2 selective inhibitors, tramadol, opioids stronger than tramadol and conventional synthetic disease modifying antirheumatic drugs.
● The most recently recorded prescription within 6 months, 7-12 months, and >12 months before a period, respectively.
† Statistically different from low GC use group (Avg. daily dose ≤7.5mg/day), Wald test p < 0.05.

***Disclosures: Shahab Abtahi**, None*

1116

Causal Assessment of the Association Between Bone Mineral Density and the Risk of Dementia *Samuel Ghatan[3], Katerina Trajanoska[3], Petroula Proitso[2], Arfan Ikram[3], Ling Oei[4], Angela Hodges[5], Fernando Rivendeneria[3]. [3]Erasmus MC, Netherlands, [2]Kings college London, United Kingdom, [3]Erasmus MC, United Kingdom, [4]Erasmus Mc, Netherlands, [5]King's college london, United Kingdom

Introduction: Evidence for an association between BMD and cognitive decline has been postulated for many years. As both dementia and osteoporosis are prominent age-related diseases the association is expected to be driven by shared comorbid factors, until proven otherwise. The aim of this study was to establish if there is a causal association between bone mineral density (BMD) and dementia. Methods: We included 5,545 participants (58%

females) from a prospective population-based cohort (age:66.3+/-10.3). Participants underwent DXA to measure femoral neck (FN) and lumbar spine (LS) BMD. We assessed dementia at the time of DXA measurement and during a follow-up of maximum 12 years. We used time-to-event analysis to determine the observational relationship between BMD and incident dementia, including Alzheimer's disease (AD) adjusted for age, sex, cohort effect, smoking, education, apoE (genotype) and hormone use. Next, we applied a two-sample bidirectional Mendelian Randomization approach, leveraging genetic data from large-scale genome-wide association studies (GWAS) of AD (n = 74,046 with 25,580 cases) and family history of AD (n=314,278 from UK Biobank; 42,034 paternal/maternal cases; meta analysed against n = 74,046 with 25,580 cases), as well as, FN- and LS-BMD (n=~32,000) seeking to provide robust evidence of causality. Results: Among the 5,545 non-demented participants included in in the study 397 (7.2%) developed AD (n=264 AD cases) during a mean follow-up of 7 years. Lower levels ofFN-BMD were associated with higher risk of AD (HR:1.20) and AD (HR:1.27). In contrast, LS-BMD was not associated with incidence dementia (HR:1.07) or Alzheimer disease (HR:1.10). These observational results were not supported by the MR analysis. A causal association was found between BMD and family history of AD (LS-BMD: OR=1.08, 95%: 1.02 - 1.14) (FN-BMD: OR=1.06, 95%: 1.00 – 1.13), AD and LS-BMD were non-significant but concordant (LS-BMD: OR=1.10, 95% 0.98 – 1.24), however FN-BMD showed no causal association (FN-BMD: OR=1.04, 95% 0.91 – 1.19). Conclusion: The results from the MR analysis provide evidence for a causal association between LS-BMD levels and AD risk, but not FN-BMD. While treating BMD won't be by itself an effective intervention to modify the risk of dementia, investigating the mechanism by which the diseases interact with each other will help us understand the complex aetiology of AD.

***Disclosures: Samuel Ghatan**, None*

1117

Preflight Biomarkers of Bone Remodelling Predict Bone Loss on Long-Duration Spaceflight *Leigh Gabel[1], Paul Hulme[1], Anna-Maria Liphardt[2], Martina Heer[3], Sara Zwart[4], Jean Sibonga[4], Scott Smith[4], Steven Boyd[1]. [1]University of Calgary, Canada, [2]Friedrich-Alexander University Erlangen-Nuremberg, Germany, [3]University of Bonn, Germany, [4]NASA Lyndon B. Johnson Space Center, United States

Bone loss remains a major health concern for astronauts on long-duration spaceflight, despite in-flight countermeasures. This study examined changes in bone microarchitecture, density and strength before and after long-duration spaceflight. Seventeen astronauts (14 men; age 38 to 60 years) had their distal tibiae and radii imaged before and after flight with high-resolution peripheral quantitative computed tomography (HR-pQCT; XtremeCT II; 61µm). Postflight bone images were 3D-registered to baseline images. Finite element analysis was applied to estimate bone strength. Blood and urine biochemical markers of bone remodelling were acquired before, during, and after flight. Spearman correlations evaluated the relationship between changes in bone variables and biomarkers. Mixed effects models examined changes in bone and biochemical variables across time and the relationship between changes in bone variables and mission duration. At the distal tibia, median cumulative postflight losses in total volumetric BMD (Tt.BMD) and bone strength (F.Load) were -2 to -4% (-0.5 to -0.8% per month), while trabecular BMD, bone volume fraction, thickness (Tb.BMD, BV/TV, Tb.Th) and cortical BMD (Ct.BMD) declined 1-3%. Mission duration ranged from 115 to 204 days and was negatively related to change in bone variables after flight. Tibia Tt.BMD, Ct.BMD and F.Load significantly deteriorated on missions longer than 5-months, while Tb.BMD and BV/TV demonstrated a steeper rate of decline on missions longer than 6-months. Less severe postflight changes occurred at the distal radius, where Tt.BMD and F.Load significantly increased on missions shorter than 5.5 months and decreased on missions greater than 6.5-months. Bone resorption markers (carboxy- and amino-terminal cross-linked telopeptides of type 1 collagen; CTx, NTx) were elevated during- and immediately after flight, while bone formation markers (procollagen type 1 amino-terminal propeptide, P1NP; bone specific alkaline phosphatase, BSAP, osteocalcin, OC) were elevated from mid-flight onwards. Preflight CTx and P1NP were negatively associated with changes in tibia Tt.BMD and F.Load (r =-0.56 to -0.92; p<0.05), suggesting that heightened preflight bone remodelling may predict greater in-flight bone loss. Study findings highlight the integral relationship between mission duration and bone deterioration. Pre-flight markers of bone remodeling may help identify individuals most susceptible to bone loss on long-duration spaceflight.

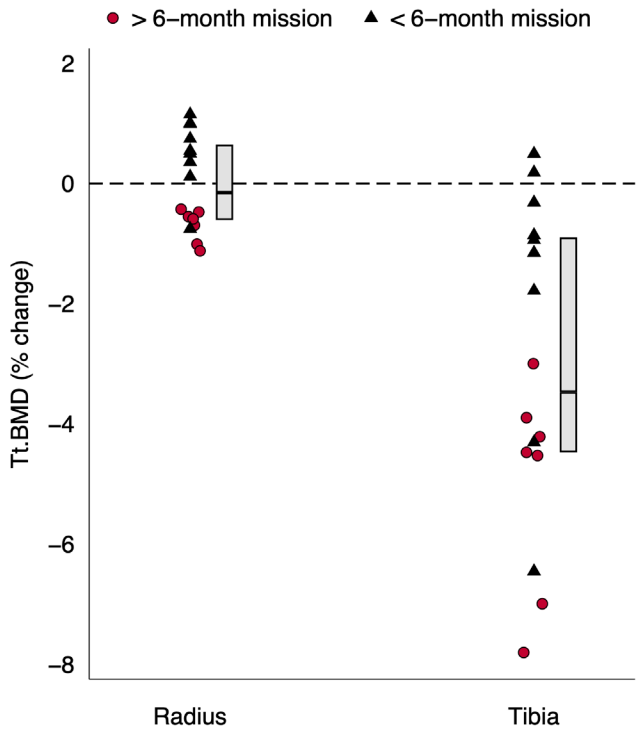

***Disclosures: Leigh Gabel**, None*

1118

Children Living With HIV In Zimbabwe Have Impaired Trabecular Bone Density, Despite Treatment With Anti-Retroviral Therapy: A Cross-Sectional Study *Cynthia Kahari[1], Andrea Rehman[2], Mícheál Ó Breasail[3], Ruramayi Rukuni[1], Tafadzwa Madanhire[4], Tsitsi Bandason[4], Lynda Stranix-Chibanda[5], Lisa K. Micklesfield[6], Rashida A. Ferrand[1], Kate A. Ward[7], Celia L. Gregson[8]. [1]Biomedical Research and Training Institute, Harare, Zimbabwe/ London School of Hygiene and Tropical Medicine, London, United Kingdom, Zimbabwe, [2]London School of Hygiene and Tropical Medicine, London, United Kingdom, United Kingdom, [3]MRC Nutrition and Bone Health Research Group, Cambridge, United Kingdom, United Kingdom, [4]Biomedical Research and Training Institute, Harare, Zimbabwe, Zimbabwe, [5]University of Zimbabwe-College of Health Sciences, Harare, Zimbabwe, Zimbabwe, [6]SAMRC/Wits Developmental Pathways for Health Research Unit (DPHRU), University of the Witwatersrand, Johannesburg, South Africa, South Africa, [7]MRC Lifecourse Epidemiology, University of Southampton, Southampton, United Kingdom, United Kingdom, [8]Musculoskeletal Research Unit, Bristol Medical School, University of Bristol, Bristol, United Kingdom, United Kingdom

The majority of children with HIV live in sub-Saharan Africa. HIV infection has multi-system consequences. Whilst stunting is common, specific effects on the growing skeleton are unclear. We aimed to determine the effect of chronic HIV infection on bone density in children with HIV in Zimbabwe.We conducted a cross-sectional observational study of children with HIV (8-16 years) established on antiretroviral therapy (ART), and children without HIV, from schools serving the same population in Harare, Zimbabwe. Non-dominant tibial pQCT was used to measure 4% trabecular and 38% cortical volumetric bone density (vBMD), cross-sectional area (CSA) and predicted bone strength (38% cross-sectional moments of inertia [CSMI]). Puberty was assessed by Tanner staging. Multivariable linear regression assessed associations between HIV status and bone outcomes, adjusting for age, sex, puberty and height.We recruited 264 children with and 281 without HIV; 50.2% female. Children with HIV were similar in age to those living without HIV ([mean+/-SD] 12.4+/-2.5 and 12.5+/-2.5 years), but more were prepubertal (41.8% vs. 22.1%; p<0.001). Mean age at ART initiation was 4.7+/-3.5 years. Children with HIV had impaired growth compared with those without HIV; stunting (height-for-age Z-score<-2) prevalence was 33% vs. 7.4% (p<0.001), underweight (weight-for-age Z-score<-2) prevalence was 28% vs 8% with a mean weight-for-age Z-score of -1.38+/-1.37 vs. -0.42+/-1.2 (p<0.001). Before adjustment, children with HIV had lower trabecular vBMD (mean difference -12.1 [95%CI -18.5, -5.73]mg/cm^3; p<0.001), smaller 4% and 38% CSA (-82.6 [-116.6, -48.7]mm2 and -46.6 [-58.4, -34.7]mm2 respectively, both p<0.001) and lower CSMI (-1947 [-2487, -1406] mm4; p<0.001) than those without HIV. Adjustment for age, sex and puberty did not attenuate these findings. Additional height adjustment partially explained differences in bone out-

comes. However, deficits in trabecular vBMD (-8.86 [-15.97, -1.75]mg/cm³; p=0.015, 38% CSA (-13.50 [-22.6, -4.9]mm2; p=0.004) and CSMI (-420 [-824.4, -16.32]mm4; p=0.041) persisted.This is the largest pQCT study to date, of children with HIV in Africa. We identified marked bone density and size deficits including impairment in predicted bone strength, despite long-term ART. These findings are concerning, as if generalizable across sub-Saharan Africa they suggest impaired bone development is common, which may lead to increased fracture risk amongst children with HIV in Africa.

***Disclosures: Cynthia Kahari**, None*

1119

Results of the PaTH Forward Phase 2 Trial Demonstrating Potential of TransCon PTH as a Replacement Therapy for Hypoparathyroidism *Aliya Khan[1], Mishaela Rubin[2], Lars Rejnmark[3], Peter Schwarz[4], Tamara Vokes[5], Bart Clarke[6], Intekhab Ahmed[7], Lorenz Hofbauer[8], Andrea Palermo[9], Claudio Marcocci[10], Uberto Pagotto[11], Erik Eriksen[12], Sanchita Mourya[13], Denka Markova[13], Susanne Pihl[14], David B Karpf[13]. [1]Bone Research & Education Center, McMaster University, Canada, [2]Columbia University, United States, [3]Aarhus University Hospital, Denmark, [4]Rigshospitalet, Denmark, [5]University of Chicago, United States, [6]Mayo Clinic, United States, [7]Thomas Jefferson University, United States, [8]Universitätsklinikum Dresden, Germany, [9]Campus Bio-Medico University, Italy, [10]University of Pisa, Italy, [11]Alma Mater Studiorum University of Bologna, Italy, [12]Oslo University Hospial, Institue of Clinical Medicine, Norway, [13]Ascendis Pharma Inc., United States, [14]Ascendis Pharma A/S, Denmark

Background:PTH deficiency in hypoparathyroidism (HP) causes low serum calcium (sCa) and high phosphate (sP). Standard of Care (SoC), consisting of high doses of active vitamin D and calcium, raises sCa and sP and increases burden of illness on HP patients by worsening hypercalciuria and the CaxP product. Recently approved injections of PTH(1-84) (t1/2 ~2-3 hrs) can raise sCa and allow partial withdrawal of SoC, but does not control urinary calcium (uCa) or symptomatic hypo- or hypercalcemia.1,2 TransCon PTH, an investigational prodrug of PTH(1-34) transiently bound to an inert carrier via a linker, is under development for the treatment of HP. At physiological temperature/pH, linker auto-cleavage occurs, releasing active PTH at a controlled rate with a t1/2 ~60 hrs. Methods:PaTH Forward is a phase 2, double-blind, placebo-controlled, multicenter trial investigating safety and tolerability of TransCon PTH in adult HP patients treated with SoC. TransCon PTH was given as daily doses of 15, 18, or 21 µg/day PTH(1-34) vs. placebo for 4 weeks followed by an open-label extension trial during which each subject is optimized to their individual dose of TransCon PTH. The primary endpoint required 1) normal sCa, and 2) normal (or >=50% decrease from baseline) fractional excretion of calcium (FECa), and 3) not taking active D, and 4) taking <=1000 mg/d of Ca. Results:At week 4, significantly more subjects (50%) on TransCon PTH achieved the primary endpoint vs. (15%) subjects on placebo (Table). sP decreased from baseline by 20% in subjects on TransCon PTH vs 1% on placebo. Increase from baseline in subjects meeting FECa endpoint was 42% on TransCon PTH vs. 0% on placebo. Free PTH showed stable levels in the lower half of the normal range at both 2 and 4 weeks. TransCon PTH was well-tolerated; no subjects discontinued the study treatment or from the trial during the 4-week period, and no SAEs or severe AEs were reported. No subjects on TransCon PTH showed symptomatic hypocalcemia vs. 7% of subjects on placebo. Conclusions: These data from the initial 4-week phase of the PaTH Forward Trial demonstrated that TransCon PTH met the primary endpoint for efficacy, potentially representing a true PTH replacement therapy for HP patients. Results from this trial help inform the starting dose and SoC titration schedule for the phase 3 trial. Shire Pharmaceuticals. 2018. NATPARA (package insert)Khurana M et al. Clin Pharm Ther. 2019 105(3):710-8.

Table. Week 4 (Visit 3)

	TransCon PTH	Placebo	P-value
N	44	13	
Off Active vitamin D and ≤ 500 mg calcium	82%	15%	P<0.0001
Off Active vitamin D and calcium	50%	0%	P=0.0008
Primary Endpoint	50%	15%	P=0.0305

***Disclosures: Aliya Khan**, Takeda, Grant/Research Support, Ascendis Pharma A/S, Grant/Research Support, Ultragenyx, Other Financial or Material Support, Amgen, Consultant, Alexion, Other Financial or Material Support, Chugai, Grant/Research Support*

1120

Long bone fractures in fibrous dysplasia/McCune-Albright Syndrome: prevalence, natural history, and risk factors *Raya Geels[1], Maartje Meier[2], Amanda Saikali[3], Natasha Appelman-Dijkstra[1], Alison Boyce[3]. [1]Department of Medicine, Division of Endocrinology, Centre for Bone Quality, Leiden University Medical Centre, Leiden, The Netherlands, Netherlands, [2]Department of Orthopedic Surgery, Centre for Bone Quality, Leiden University Medical Centre, Leiden, The Netherland, Netherlands, [3]Skeletal Disorders and Mineral Homeostasis Section, National Institute of Dental and Craniofacial Research, National Institutes of Health, Bethesda MD, USA, United States

Introduction: Fibrous dysplasia/McCune-Albright Syndrome (FD/MAS) is a rare bone and endocrine disorder caused by somatic GNAS mutations. Proliferation of abnormal skeletal stem cells results in osseous lesions that present along a broad clinical spectrum, ranging from trivial to severe disease. Long bone fractures are a common, painful, and potentially disabling complication. However, fracture prevalence and risk factors have not been well-established, making it difficult to predict which patients are at-risk for a severe course. Methods: Clinical data and imaging were reviewed from 2 large FD/MAS cohorts (NIH and LUMC) to identify long bone fractures at FD sites. Skeletal burden score was quantified using bone scintigraphy. Multiple linear regressions were performed to identify risk factors for fracture rate and age at first fracture.Results: 419 total patients were included (186 NIH, 233 LUMC). 79 (19%) had polyostotic FD and 146 (35%) had monostotic FD. 194 (46%) had MAS endocrinopathies. Median age at last follow-up was 30.2 years (range 3.2-84.6, IQR 25.5), and median skeletal burden score was 16.6 (range 0-75, IQR 33). 48 (59%) patients suffered >=1 lifetime fracture (median 1, range 0-70, IQR 4). Median age at first fracture was 8 years (range 1-76, IQR 10). Fracture rates peaked between 6-10 years of age and decreased thereafter. Lifetime fracture rate was associated with skeletal burden score (β=0.40, p7)(p<0.01).Conclusion: Higher skeletal burden score and MAS hyperthyroidism are primary risk factors for long bone fractures in FD/MAS. First fracture occurrence at age <=7 years is associated with a higher lifetime fracture risk and may predict a more severe clinical course. These results may allow clinicians to identify FD/MAS patients at-risk for severe disease who may be candidates for early therapeutic interventions.

***Disclosures: Raya Geels**, None*

The influence of undercarboxylated osteocalcin on endothelial function in normal and high glucose conditions *Alexander Tacey[1], Tawar Qaradakhi[1], Alan Hayes[1], Anthony Zulli[1], Itamar Levinger[1]. [1]Victoria University, Australia

Purpose: The bone derived protein undercarboxylated osteocalcin (ucOC) improves glucose regulation and is associated with a reduced risk of diabetes. In animals, in vivo treatment with ucOC improves vascular function, but this may be due to improved glucose control rather than a direct influence on blood vessels. Moreover, there are conflicting reports on the role and association of ucOC with cardiovascular outcomes in humans, including reports of adverse effects. The aim of this study was to examine whether ucOC directly influences (positively or negatively) endothelial function in rabbit arteries following incubation in different glucose concentrations.Methods: Male New Zealand white rabbit arteries were fed a normal or atherogenic diet for 4-weeks. Arteries were incubated ex vivo in 11mM or 20mM glucose solutions for 2-hours and the vasoactivity of ucOC was assessed via several different techniques. Isometric tension analysis was use to assess the vasoactivity of abdominal aortic rings to ucOC pre-incubation (10ng/ml or 30ng/ml). To replicate haemodynamic flow, pressure and shear stress that occur physiologically, perfusion myography techniques were used to assess the vasoactivity of carotid artery segments to ucOC dose response curves (0.3 – 45ng/ml). The immunoreactivity of nitrotyrosine (NT), endothelial nitric oxide synthase (eNOS), protein kinase B (p-Akt) and mammalian target of rapamycin (p-mTOR) were assessed in the aorta via immunohistochemistry (IHC) following the assessment of vasoactivity.Results: In the abdominal aorta, both 10ng/ml and 30ng/ml doses of ucOC did not significantly alter endothelium-dependent (acetylcholine) (Attached figure) or endothelium-independent (sodium nitroprusside) blood vessel relaxation in aortic rings following incubation in 11mM or 20mM glucose solutions after either the normal or atherogenic diet ($p > 0.05$). In the carotid artery, ucOC treatment did not cause any alteration in vasoactivity at any dose of ucOC, compared to a control treatment following either the normal or atherogenic diet ($p > 0.05$). Further, ucOC (10ng/ml and 30ng/ml) did not alter the immunoreactivity of NT, eNOS, p-Akt or p-mTOR in any group ($p > 0.05$).Conclusion: ucOC does not have a direct adverse effect on endothelial function in rabbit arteries. The improvement in endothelial function previously reported with ucOC is likely to be as a result of improved glucose regulation, an indirect effect and not a direct regulatory effect on the vasculature.

***Disclosures: Alexander Tacey**, None*

P-001

Validation of the Hypoparathyroidism Patient Experience Scale (HPES): Understanding and Assessing Burden of Disease *Meryl Brod[1], David B Karpf[2], Alden Smith[2], Jill Gianettoni[2], Denka Markova[2], Sanchita Mourya[2], Lori McLeod[3]. [1]The Brod Group, United States, [2]Ascendis Pharma Inc., United States, [3]RTI Health Solutions, United States

BackgroundHypoparathyroidism (HP) is an endocrine disorder characterized by absent or low levels of parathyroid hormone (PTH). Patients with HP, including those on standard-of-care therapy (SoC), report debilitating physical and cognitive symptoms and reduced health-related quality of life. Assessing these HP impacts are critical for the optimal management of HP. The HPES-Symptom and HPES-Impact measures were developed according to FDA guidance on development of patient reported outcome measures (PROs). These measures were assessed to evaluate the HPES structure, reliability, validity, and ability to respond to treatment. MethodsData come from 2 sources: a noninterventional observational study and a phase 2, multicenter, double-blind, placebo-controlled study of TransCon PTH. Key inclusion/exclusion criteria for both studies: age >=18 years; confirmed diagnosis of post-surgical, autoimmune or idiopathic HP and stable on SoC. ResultsThe analysis data set included 359 patients (observational study=300, clinical trial=59). For the observational study, factor analysis confirmed all a priori hypothesized domains (Symptom: Physical and Cognitive; Impact: Physical Functioning, Daily Life, Psychological Well-being, Social Life and Relationships). Internal consistency Cronbach's alphas were high for total score and for all domains (Symptom=0.91-0.93; Impact=0.87-0.96). Test-retest reliability for subjects with no treatment change was acceptable with all values for total and domains with 0.70 included within the 95% confidence intervals, with the exception of one domain. HPES validity was strong, with all a priori construct validity hypotheses supported by moderate to strong correlations with the exception of one domain which had mixed results (Symptom r=0.39-0.72; Impact r=0.46-0.77) and significant discriminant validity values for groups based on global ratings, calcium levels and number of comorbid issues (Symptom p< 0.004; Impact p< 0.003). For the clinical trial, both measures were highly responsive to active treatment at Week 4 (Symptom p=0.0001; Impact p=0.0026).ConclusionThese data show that HP, even when a patient is stable on SoC, has a significant impact on both patients' reported symptoms, overall functioning and well-being. The HPES Symptom and Impact are reliable, valid and responsive PRO measures of these impacts. Assessing HPES symptoms and impacts are key to studying new treatments and improving clinical care for patients with HP.

***Disclosures: Meryl Brod**, Ascendis Pharma A/S, Consultant*

P-002

Real-World Clinical Profiles of Adults With Hypophosphatasia (HPP) From the Global HPP Registry *Kathryn M. Dahir[1], Priya Kishnani[2], Anna Petryk[3], Wolfgang Högler[4], Agnès Linglart[5], Gabriel Ángel Martos-Moreno[6], Keiichi Ozono[7], Shona Fang[3], Cheryl Rockman-Greenberg[8], Lothar Seefried[9]. [1]Vanderbilt University Medical Center, United States, [2]Duke University Medical Center, United States, [3]Alexion Pharmaceuticals, Inc., United States, [4]Universitätsklinik für Kinderheilkunde, Johannes Kepler University, Austria, [5]Paris-Sud University, APHP and INSERM, France, [6]Hospital Infantil Universitario Niño Jesús, Universidad Autónoma de Madrid, CIBERobn, ISCIII, Spain, [7]Osaka University, Suita, Japan, [8]University of Manitoba, Canada, [9]9University of Würzburg, Germany

Introduction: HPP is a rare, inherited, metabolic disease caused by low activity of tissue nonspecific alkaline phosphatase (ALP). Due to multiple musculoskeletal and systemic manifestations, HPP in adults has a heterogeneous clinical presentation that can lead to misdiagnosis and substantial delays in diagnosis. Methods: To better understand the most common clinical profile of adults with HPP, this study analyzed data from 270 adults with HPP (>=18 years of age, low ALP and/or ALPL variant) from the Global HPP Registry. Results: Most adults were women (75.2%). The median age at registry enrollment was 50.0 years, and the median ALP activity was 25.0 U/L (normal range: 40–150 U/L). Review of medical histories showed that pain (74.8%) was the principal symptom, followed by dental manifestations (60.4%) and skeletal manifestations (47.8%). Fatigue (35.2%) and muscle weakness (26.3%) were also reported. For adults with quality-of-life data, the median Short-Form-36v2 (SF-36v2) Physical Component Score was 42.4 (range: 17.9, 63.3; n=203; population norm score=50). The median pain interference score based on the Brief Pain Inventory-Short Form (BPI-SF) was 3.3 (range: 0.0, 10.0; n=196; scale ranges from 0=does not interfere to 10=completely interferes). Of 212 adults with available data, most (66%) reported some disability on the Health Assessment Questionnaire Disability Index (HAQ-DI). Treatment with enzyme-replacement therapy (asfotase alfa) was reported in 77/270 (28.5%) adults, while 193/270 (71.5%) adults had never received treatment. Demographics and baseline ALP activity were similar between treated and untreated adults. Treated adults reported poorer quality of life before treatment initiation and had a higher occurrence of pain, dental issues, recurrent and poorly healing fractures/pseudofractures, fatigue, and muscle weakness compared with untreated adults. Conclusions: These results establish pain, dental manifestations, skeletal manifestations, fatigue, and muscle weakness as the principal symptoms characterizing the real-world clinical profile of adults with HPP. For clinicians taking medical histories, it is important to recognize that the most common symptoms of HPP may not be immediately associated with bone disease.

***Disclosures: Kathryn M. Dahir**, Alexion Pharmaceuticals, Inc., Consultant*

P-003

Risk Factors for the Development of Heterotopic Ossification After Hip Arthroplasty: A Retrospective Review *Sukhmani Singh[1], Joseph Kidane[1], Kelly Wentworth[1], Saam Morshed[1], Edward Hsiao[1]. [1]UCSF, United States

Purpose: Heterotopic ossification (HO) is a process where normal bone forms in soft tissue. It arises as a complication of trauma, surgery and inflammation. Risk factors for development of HO include male gender, spinal cord injury, and bone producing diseases like ankylosing spondylitis [1]. We investigated other risk factors associated in the development of HO after total hip arthroplasty and acetabular repair.Methods: A retrospective review of medical records was performed for individuals who underwent total hip arthroplasty or acetabular repair surgeries (CPT 27130, 27076, 27137, 27220, 27222, 27226, 27227, 27228, 27254, 29915) from September 2010 to October 2019. Demographics, anthropometrics, length of hospital stay, medication use and comorbid conditions were obtained. Logistic regression was used to identify predictors for HO development.Results: A total of 4373 patients who underwent surgery were identified (2038 men and 2335 women, mean age at procedure: 59.2+/-15.6 years). The incidence of HO development was 2.6% (N=115). The average age was 58.8+/-15.7 years in those who did not develop HO compared to 62.7+/-13.2 years in those who did. The average length of stay was 2.92+/-3.0 days in non-HO group vs 3.23+/-1.7 days in the HO group. A larger proportion of individuals in the HO group had spinal cord injury or spine disease (20% vs 7.7%, p<0.001), osteoporosis (44.4% vs 16.7%, p<0.001), unspecified diabetes type (8.7% vs 2.4%, p<0.001), type 2 diabetes (36.5% vs 16.4%, p<0.001), prior motor vehicle accidents (9.6% vs 5.2%, p=0.042), vitamin D deficiency (33.0% vs 10.9%, p<0.001), and were post-menopausal (40% vs 16.7%, p<0.001). Significant predictors for HO development were African American race (OR 4.44, p=0.010, 95% CI 1.42-13.87), osteoporosis (OR 2.11, p=0.006, 95% CI 1.24-3.59), diabetes (OR 2.38, p=0.039, 95% CI 1.04-5.44), vitamin D deficiency (OR 1.85, p-0.020, 95% CI 1.10-3.10) and use of NSAIDs within 14 days of surgery (OR 0.58, p=0.038, 95% 0.35-0.97). A low estrogen state (post-menopausal status and amenorrhea patients combined) was associated with HO development but was non-significant (OR 1.69, p=0.056, 95% CI 0.99-2.88).Conclusions: Risk factors of African American race, diabetes, osteoporosis, vitamin D deficiency and potentially low estrogen states carry an increased risk for development of HO and may benefit from HO prophylaxis.References: [1] Kurz AZ, Leroux E, Riediger M, et al. Curr Rev Musculoskelet Med. 2019;12(2):147-155

***Disclosures: Sukhmani Singh**, None*

P-004

Vitamin D Status and COVID-19 Clinical Outcomes in Hospitalized Patients *Betsy Szeto[1], Jason E. Zucker[2], Elijah D. LaSota[2], Mishaela R. Rubin[2], Marcella D. Walker[2], Michael T. Yin[2], Adi Cohen[2]. [1]Columbia University Vagelos College of Physicians and Surgeons, United States, [2]Columbia University Irving Medical Center, United States

Populations severely affected by COVID-19 are also at risk for vitamin D (VitD) deficiency. Common risk factors include older age, chronic illness, obesity, and non-Caucasian race. Countries most affected by VitD deficiency also have had the highest COVID-related mortality. VitD levels, deficiency and/or receptor polymorphisms may play a role in immune function and have been associated with risk for respiratory infections and failure, susceptibility and response to therapy for enveloped virus infection, and immune-mediated inflammatory reaction. We hypothesized that vitD deficiency may be a risk factor for severity of COVID-19 respiratory and inflammatory complications.Among the first 700 COVID+ nonpregnant adults with COVID-related admissions at Columbia University Medical Center [median (IQR): aged 63(IQR:50–74) yrs, 43% female, BMI 28.3 (IQR:24.6–33.3) kg/m2], 22% were intubated and mortality was 21%.We searched health records for serum 25-hydroxy VitD levels measured within 12 months of admission. VitD deficiency was defined as <20 ng/mL. Outcomes included discharge status, mortality, length of hospital stay, intubation, length of intubation, need for dialysis, and peak levels of inflammatory markers: erythrocyte sedimentation rate, c-reactive protein, ferritin, interleukin 6.VitD levels were available in 93/700 [vitD: 25 (IQR:17–33) ng/mL; measured 136 (IQR:75–248) days preadmission]. Compared to those without vitD levels, those with vitD measurements did not differ in age, BMI or the distribution of sex and race, but were more likely to have ICD-defined hypertension, diabetes, chronic kidney disease and pulmonary disease.Those with VitD deficiency (n=35) did not differ from those with vitD >=20ng/mL in terms of age, sex, race, BMI, or comorbidities. VitD deficiency tended to be associated with younger age and a lower frequency of preexisting pulmonary disease. There were no between-group differences in any outcome including intubation (29 vs 17%, p=0.2). Results were similar in those over 50 yrs (n=75;intubation 30 vs 17%; p=0.2) and in male/female only cohorts. There was no relationship between vitD as a continuous variable and any outcome, even after controlling for age and pulmonary disease. In summary, preliminary data do not clearly support a relationship between vitD status and COVID-19 clinical outcomes. Larger studies with VitD measurements on samples obtained at the time of hospital admission may better address this hypothesis.

	VitD Deficiency (< 20 ng/mL) N=35	Normal VitD (≥ 20 ng/mL) N=58	P value
Cohort Characteristics			
Age (Years)	58 (IQR: 36–74)	64 (IQR: 54–73)	0.1
Sex (% Female)	18 (51%)	31 (53%)	0.9
BMI (kg/m^2)	28.5 (IQR: 23.1–33.8)	27.0 (IQR:22.4–32.2)	0.5
Race (% Black/African American)	32%	28%	0.7
ICD-Defined Comorbidities:			
Hypertension	27 (77%)	49 (84%)	0.4
Diabetes	23 (66%)	37 (64%)	0.9
Chronic Kidney Disease	18 (51%)	28 (48%)	0.8
Any Pulmonary Disease	7 (20%)	22 (38%)	0.07
Predefined Outcomes			
Discharge status:			
Deceased/Discharged to Hospice	8 (23%)	14 (24%)	0.3
Discharged (not death)	25 (71%)	37 (64%)	
Still Admitted – Intubated	2 (6%)	2 (3%)	
Still Admitted – Not Intubated	0	5 (9%)	
Deceased	8 (23%)	14 (24%)	0.9
Ever-Intubated	10 (29%)	10 (17%)	0.2
Length of Intubation (#days)	8 (IQR: 4–34)	15 (IQR: 7–23)	0.7
Renal Replacement (HD or CVVH)	10 (29%)	14 (24%)	0.6
Length of Stay (#days)	8.8 (IQR: 4.9–16.7)	9.4 (IQR: 5.0–16.2)	0.8
Peak Level Inflammatory Markers:			
ESR (mm/hr)	83 (IQR: 54–114)	80 (IQR: 59–110)	0.9
CRP (mg/L)	118 (IQR: 37–274)	131 (IQR: 62–223)	0.9
Ferritin (ng/mL)	1030 (IQR: 555–1802)	933 (IQR: 311–2165)	0.7
IL-6 (pg/mL)	12 (IQR: 5–76)	26 (IQR: 8–63)	0.7

Values represent median (interquartile range) or frequency (percentages); BMI= body mass index, ICD=International Classification of Diseases, HD=hemodialysis, CVVH=Continuous Veno-Venous Hemofiltration, ESR=erythrocyte sedimentation rate, CRP=C reactive protein, IL-6=interleukin 6

***Disclosures: Betsy Szeto**, None*

P-005

Diagnosis of Adult-Onset Hypophosphatasia Presenting with Metatarsal Stress Fracture: Proof-of-Concept for a Case Finding Strategy *Kenna Koehler[1], Said Atway[2], James Pipes[2], Steven Ing[3]. [1]The Ohio State University College of Medicine, United States, [2]The Ohio State University Wexner Medical Center Department of Orthopaedics, Division of Podiatry, United States, [3]The Ohio State University Wexner Medical Center Department of Internal Medicine, Division of Endocrinology, Diabetes & Metabolism, United States

Background: Hypophosphatasia (HPP) is a rare metabolic bone disorder due to loss-of-function mutations in ALPL that encodes tissue nonspecific alkaline phosphatase (ALP), resulting in decreased activity of ALP, an enzyme largely responsible for skeletal mineralization. Adult-onset HPP includes metatarsal stress fractures (MSF). Population prevalence of HPP is estimated at 1/6370 (0.016%). The primary objective was to determine how many cases of metatarsal fractures and low ALP levels presenting to our medical center's podiatry clinic have an ALPL mutation and to phenotype their clinical course and symptoms. Methods: We queried our Electronic Health Record (EHR) for patients (age >= 18 years) presenting with MSF and metatarsal fracture (MF) (by ICD-9 and ICD-10CM codes) from 10/1/2011 to 10/1/2017 and who had a serum ALP concentration measured at some time. Patients with low ALP values (reference range, 38-126 U/L before and 32-126 U/L after 6/24/2013, when a new assay platform was implemented) were eligible to receive genetic testing for ALPL (Prevention Genetics) and complete surveys: Short Form 36 version 2 (SF36v2), Brief Pain Inventory-Short Form (BPI), and Health Assessment Questionnaire Disability Index (HAQ). Cases with and controls without ALPL pathogenic mutation were compared by survey scores and clinical variables relevant to the fracture. We present descriptive data due to small sample size.Results: In 1611 patients with MSF/MF, 937 had ALP measurements and of these, 13 (1.4%) had low ALP. In 8 patients consenting to participate, 2 had heterozygous pathogenic ALPL mutations. Pathogenic ALPL mutations were found in 0.12% (2/1611) with MSF/MF, 0.21% (2/937) in MSF/MF & ALP value, and 15% (2/13) in MSF/MF & low ALP. Mean ALP in cases was 32.5 U/L (range, 30-35) and in controls was 29.2 U/L (range, 23-35). Cases vs. controls rated lower scores on 8/8 scales and both physical component (30.5 vs. 56.5) and mental component (45.1 vs. 56.8) scores on SF36v2 (range, 0-100); higher scores for worst pain (8.0 vs. 0.8) and average pain (6.0 vs. 0.7) on the BPI (range, 0-10); and higher standard disability score (1.4 vs. 0) on the HAQ (range, 0-3).Conclusion: These data provide proof-of-concept for HPP case identification in patients presenting to podiatry clinics with MSF/MF. Review of EHR for low ALP levels may be useful for consideration of HPP diagnosis and supports the need for a prospective study to determine an optimal case finding strategy.

***Disclosures: Kenna Koehler**, None*

P-006

The Voices of Hypopara Survey: Journey of Patients Living with Hypoparathyroidism *Danette Astolfi[1], Deb Murphy[1], Bob Sanders[1], Loretta Gulley[1], Ami Knoefler[2], Minyoung Park[2], Susana Tsao[2], Sanchita Mourya[2], Mishaela Rubin[3]. [1]HypoPARAthyroid Association, Inc., United States, [2]Ascendis Pharma Inc., United States, [3]Columbia University, United States

BackgroundHypoparathyroidism (HP) is a rare disease that is characterized by insufficient levels of parathyroid hormone, resulting in hypocalcemia, hyperphosphatemia and hypercalciuria. Standard of care (SoC) consists of calcium and active vitamin D supplementation. The HypoPARAthyroidism Association (HPA) is a nonprofit organization dedicated to improving the lives of HP patients. The HPA developed the "Voices of Hypopara" survey to characterize the patient journey of HP individuals in the US.MethodsThe online survey was distributed to all HPA members in May 2020. Questions focused on evaluating patients' experiences including diagnosis, treatment, quality of care, and impact on daily living.ResultsThe survey was completed by 146 HPA members (89% female; mean age 51). The majority of participants (80%) were diagnosed with post-surgical HP. Diagnosis of HP was delayed >6 months in 55% of participants despite symptoms of chronic HP; 51% underwent >5 physician visits before obtaining a HP diagnosis. The most frequently cited challenges included the impact of HP on quality of life (87%), long-term complications (87%) and daily symptoms (78%).Most participants reported they are currently taking SoC (calcium in 91%; active vitamin D in 77%). However, over half felt that this did not optimally address their disease and 29% were extremely concerned about hypocalcemia despite supplementation. Many (69%) felt that taking SoC was moderately to extremely burdensome. Almost all participants (97%) had to adjust their regimens over the course of their disease, with 61% adjusting >5 times since diagnosis.More than two-thirds (69%) of participants reported a "calcium crash" (sudden hypocalcemia symptoms requiring medical attention) in the past year; of these, 43% reported calcium crashes monthly or weekly. Almost half (42%) of all participants visited an emergency room/urgent care in the last year as a result of HP symptoms; of these, 56% believed that the staff was inexperienced with management of a calcium crash.ConclusionsThis survey, one of the largest conducted in HP patients, demonstrates key gaps in HP management. These findings underscore the limitations of SoC and the urgent need for greater disease and treatment understanding to best support patients with HP.

***Disclosures: Danette Astolfi**, None*

P-007

Risk Factors for Multifocal Disease in Patients with Glucocorticoid Induced Avascular Necrosis *Alexandra Krez[1], Joseph Lane [2], Kyung Park-Min[2], Kaichi Kaneko[2], Tania Pannellini[2], Derek Hansen[2], Douglas Mintz[2], Donald McMahon[2], Richard Bockman[2], Emily Stein[1]. [1]Hospital for Special Surgery, United States, [2]Hospital for Special Surgery, United States

Osteonecrosis is a debilitating musculoskeletal condition that results in significant pain and compromised quality of life. Blood supply to bone is interrupted leading to death of bone cells which often results in mechanical failure and joint destruction. Patients may have multiple joints affected, compounding their pain and disability. While glucocorticoid (GC) use is a common cause of atraumatic osteonecrosis, the specific features of GC therapy that increase risk of multifocal disease are poorly understood. This study investigated risk factors for multifocal disease (MON) in patients with GC-induced osteonecrosis. We hypothesized that patients with the highest cumulative GC exposure have the greatest risk of MON. Fifty-five adults with GC-induced osteonecrosis were prospectively enrolled. MON was defined as osteonecrosis in >= 3 joints. Total cumulative dose, average dose, peak dose and duration were calculated separately as prednisone equivalents for oral and IV GCs. Mean age of subjects was 44+/-17 years, 58% women. The most common indications for GCs were rheumatologic disease and hematologic malignancy. Half of subjects had an additional risk factor for osteonecrosis: systemic lupus erythematosus (29%), acute lymphoblastic leukemia (11%), HIV (9%) and alcohol use > 320 g/week (4%). Mean daily oral dose of GCs was 29 +/- 34 mg, duration 5.4 +/- 7.7 years. Average cumulative oral dose was 29,847 +/- 35,467 mg. Half of the cohort received both IV and oral GCs. Surgical intervention was performed in 73%: 69% total arthroplasty and 31% core decompression. MON was found in 36%. Among all features of oral and IV GC exposure, the best predictor of MON was cumulative oral GC dose. For each increase of 1,000 mg, risk of MON increased by 3.2% (95% CI = 1.03, 1.67). GC exposure in the first 6 months of therapy, peak dose (oral or IV) and mean daily dose did not independently increase risk of MON. In summary, among patients with GC-induced osteonecrosis cumulative oral GC dose was the best predictor of multifocal disease. Our findings indicate that high initial doses of IV and oral glucocorticoids, often necessary to rapidly reduce inflammation, may not increase risk of MON as much as total cumulative dose. They suggest that strategies for reducing the risk of MON in GC treated patients be aimed at lowering total cumulative exposure. Further research is needed to better define optimal strategies for prevention and treatment of MON.

***Disclosures: Alexandra Krez**, None*

P-008

Quantitative histone acetylation analysis of GATA3 and PAX1 transcription factor genes in primary hyperparathyroidism *PRIYANKA SINGH[1], Ashutosh Arya[2], Divya Dahiya[3], Uma Nahar Saikia[4], Jyotdeep Kaur[4], Naresh Sachdeva[3], Sanjay Bhadada[4]. [1]PhD, India, [2]PhD, India, [3]Associate Professor, India, [4]Professor, India

Introduction: Loss of histone acetylation is associated with tumorigenesis and may act as a potential biomarker for detecting cancer. The aim of the present study was to explore the histone acetylation status (H3K9ac) of the GATA3 and paired box 1 (PAX1) developmental transcription factor genes in a spectrum of parathyroid tumor in an Indian population.Materials and methods: A total of 40 parathyroid adenomas and 10 normal parathyroid tissue were recruited for the study. Gene expression analysis was done by quantitative real time PCR (qRT-PCR) and histone acetylation analysis was performed by chromatin immunoprecipitation (ChIP) -qPCR.Results: The qRT-PCR analysis showed significantly reduced expression of GATA3 and PAX1 in parathyroid adenoma when compared to normal parathyroid samples with fold reduction of 0.25+/-0.22 ($p <=0.0001$) and 0.18+/-0.21 ($p <=0.0001$) respectively. However, expression of PAX1 was inversely related to serum calcium ($r= -0.54$; $p=0.03$) and plasma iPTH ($r= -0.61$; $p = 0.01$) but not with other clinicopathological parameters. We found active histone mark i.e. H3K9ac was decreased by 3 fold ($p= 0.01$) at GATA3 and 6.2 fold ($p= 0.004$) at PAX1 promoter gene in sporadic parathyroid adenoma compared to control parathyroid samples. A strong positive correlation between H3K9ac and mRNA expression of GATA3 ($r= 0.58$; $p= 0.01$) and PAX1 ($r= 0.63$; $p= 0.003$) was observed respectively.Conclusion: Our study reported the altered expression of GATA 3 and PAX1 in parathyroid adenoma. Thus, suggesting the role of histone deacetylation in altered expression of GATA3 and PAX1 might possible epigenetic regulator for parathyroid tumors and is crucial for diagnostic purposes.Sources of research support: DST-SERB 2018 and PGIMER Intramural Research Grant 2016.

***Disclosures: PRIYANKA SINGH**, None*

P-010

Factors associated with volumetric bone mineral density in people with severe obesity *Anne-Frédérique Turcotte[1], Suzanne N Morin[2], Fabrice MacWay[3], Jenna C Gibbs[4], Audrey St-Laurent[5], Sonia Jean[6], Laurent Biertho[7], Stefane Lebel[7], André Tchernof[8], Amin Andalib[9], Vanessa Tardio[2], Claudia Gagnon[10]. [1]Endocrinology and Nephrology Unit, CHU de Quebec Research Centre, Quebec City, Canada; Quebec Heart and Lung Institute Research Centre, Quebec City, Canada, Canada, [2]Department of Medicine, McGill University, Montreal, Canada, Canada, [3]Endocrinology and Nephrology Unit, CHU de Quebec Research Centre, Quebec City, Canada; Department of Medicine, Laval University, Québec City, Canada, Canada, [4]Department of Kinesiology and Physical Education, McGill University, Canada, [5]Endocrinology and Nephrology Unit, CHU de Quebec Research Centre, Quebec City, Canada, Canada, [6]Institut National de Santé Publique du Québec, Canada, Canada, [7]Quebec Heart and Lung Institute Research Centre, Quebec City, Canada; Department of Surgery, Laval University, Quebec City, Canada, Canada, [8]Quebec Heart and Lung Institute Research Centre, Quebec City, Canada; Institute of Nutrition and Functional Foods, Laval University, Quebec City, Canada, Canada, [9]Department of Surgery, McGill University, Montreal, Canada, Canada, [10]Endocrinology and Nephrology Unit, CHU de Quebec Research Centre, Quebec City, Canada; Quebec Heart and Lung Institute Research Centre, Quebec City, Canada; Department of Medicine, Laval University, Quebec City, Canada, Canada

Context: People with severe obesity are at increased risk of fracture. The mechanisms of bone fragility in obesity remain unclear but factors such as higher visceral adipose tissue (VAT), hyperglycemia, advanced glycation end-products (AGEs) and poor muscle strength due to muscle fat infiltration could be implicated.Objective: We explored the association of the above-mentioned factors with volumetric bone mineral density (vBMD) at the lumbar spine and hip in people with severe obesity before bariatric surgery.Methods: We used baseline data from an ongoing prospective observational study investigating the impact of bariatric surgery on bone health. Quantitative computed tomography (QCT) was used to assess lumbar spine (L2-L3), total hip and femoral neck (FN) vBMD using Mindways QCTPro software. Spearman correlations before and after adjustment for age and sex were used to explore the correlations between total vBMD at each site and body weight, BMI, VAT (CT at L2-L3), glycemic control using glycated hemoglobin (HbA1C), AGEs levels by non-invasive skin auto-fluorescence (AGE Reader) and muscle strength (handgrip and Biodex-measured knee extensor strength).Results: 29 participants were included (22F/7M, mean age 47.2+/-8.2 y, mean BMI 42.9+/-6.6 kg/m2, 66% with type 2 diabetes). Significant inverse correlations were found between L2-L3 vBMD and visceral fat ($r=-0.45$, $p=0.02$), HbA1C ($r=-0.51$, $p=0.005$) and AGEs ($r=-0.55$, $p=0.002$), and a positive correlation with knee extensor strength ($r=0.44$, $p=0.02$). We also found a significant inverse correlation between total hip vBMD and HbA1C ($r=-0.51$, $p=0.006$), and a positive correlation with knee extensor strength ($r=0.38$, $p=0.05$). Finally, FN vBMD was inversely correlated with AGEs ($r=-0.44$, $p=0.02$) and visceral fat ($r=-0.40$, $p=0.04$). After adjusting for age and sex, correlations only remained statistically significant between L2-L3 vBMD and knee extensor strength ($r=0.40$, $p=0.05$), and between total hip vBMD and HbA1C ($r=-0.40$, $p=0.05$). No correlations were found with body weight, BMI, and handgrip strength.Conclusion: Our preliminary results suggest that after taking into account age and sex, lower HbA1c and lower limb muscle strength are associated with higher vBMD at the hip and lumbar spine in people with severe obesity.

***Disclosures: Anne-Frédérique Turcotte**, None*

P-011

Analysis of bone status by 3D DXA measures in patients with acromegaly or growth hormone deficiency *Manuel Muñoz-Torres[1], Sheila González-Salvatierra[2], Antonia García-Martín[3], María Dolores Avilés-Pérez[4], Enrique Moratalla-Aranda[5], Diego Becerra-García[5], Beatriz García-Fontana[3], Luis Gracia-Marco[6]. [1]Bone Metabolic Unit, Endocrinology and Nutrition Division. Hospital Universitario San Cecilio. Instituto de Investigación Biosanitaria de Granada (Ibs.GRANADA); CIBERFES, Instituto de Salud Carlos III; Department of Medicine. Universidad de Granada, Spain, [2]Bone Metabolic Unit, Endocrinology and Nutrition Division. Hospital Universitario San Cecilio. Instituto de Investigación Biosanitaria de Granada (Ibs.GRANADA); Department of Medicine. Universidad de Granada, Spain, [3]Bone Metabolic Unit, Endocrinology and Nutrition Division. Hospital Universitario San Cecilio. Instituto de Investigación Biosanitaria de Granada (Ibs.GRANADA); CIBERFES, Instituto de Salud Carlos III., Spain, [4]1. Bone Metabolic Unit, Endocrinology and Nutrition Division. Hospital Universitario San Cecilio. Instituto de Investigación Biosanitaria de Granada (Ibs.GRANADA); CIBERFES, Instituto de Salud Carlos III., Spain, [5]Medicine Nuclear Division. Hospital Universitario San Cecilio., Spain, [6]PROFITH "PROmoting FITness and Health Through Physical Activity" Research Group, Sport and Health University Research Institute (iMUDS), Department of Physical and Sports Education, Faculty of Sport Sciences, University of Granada, Spain

Purpose: Growth hormone (GH) and insulin-like growth factor-I (IGF-I) exert significant actions on the adult skeleton. Acromegaly and adult growth hormone deficiency (GHD) can be associated with an increased risk of bone fragility. However, areal dual-energy x-ray absorptiometry (aDXA) does not capture bone quality or discriminate trabecular and cortical compartment. We aimed to explore the hypothesis that 3D-DXA would be useful in the bone evaluation of patients with GHD and acromegaly.Patients and methods: This cross-sectional study includes 20 patients with acromegaly (mean age 54.8 +/- 11.5.6 years; 75% women), 14 patients with GHD (mean age 57.4 +/- 12.3 years; 78% women) and 40 healthy subjects matched by gender and age (mean age 56.1 +/- 12.8 years). Areal bone mineral density (aBMD) at femoral neck (FN), trochanter, shaft and total hip (TH) was determined by conventional DXA (Hologic QDR 4500). Volumetric bone mineral density (vBMD) at cortical and trabecular compartments as well as cortical surface bone mineral density (sBMD) and cortical thickness at total hip was evaluated using the 3D-Shaper software (v2.6, Galgo Medical).Results: 3D-DXA parameters showed poorer cortical vBMD ($p=0.004$) and integral vBMD ($p=0.048$) in the GHD group compared to the control group and higher cortical sBMD ($p=0.003$) and cortical vBMD ($p=0.0024$) in the ACRO group compared to the GHD group. More specifically, the cortical vBMD, integral vBMD and cortical sBMD was 7.3%, 8.4% and 9.9% lower in the GHD group compared to the control group and; 16.2%, 8.5%, 12.2% and 7.3% higher in the ACRO group compared to the GHD group for the cortical sBMD, cortical vBMD, integral vBMD and cortical thickness, respectively.Conclusions: According to our results, new techniques applied to DXA provide additional information on bone in states of deficiency or excess of GH.

***Disclosures: Manuel Muñoz-Torres**, None*

P-012

Frequency and Causes of Elevated Bone Mass: The French Multicentre Elevated Bone Mass Study *JULIEN PACCOU[1], Rose-Marie Javier[2], Isabelle Henry-Desailly[3], Aurore Nottez[1], Isabelle Legroux-Gérot[1], Camille Ternynck[1], Eric Lespessailles[4], Pascal Guggenbuhl[5], Sami Kolta[6], Bernard Cortet[1]. [1]Lille University Hospital, France, [2]Strasbourg University Hospital, France, [3]Amiens Picardie University Hospital, France, [4]University of Orleans, France, [5]University of Rennes, France, [6]Cochin Hospital, Assistance Publique-Hôpitaux de Paris, France

IntroductionReports of Elevated bone mass (EBM) on routine Dual energy X-Ray Absorptiometry (DXA) scanning are not infrequent. However, epidemiological studies of EBM are few and definition thresholds variable. The purpose of this French multicentric study was to evaluate the prevalence and causes of EBM in adult patients who underwent DXA scanning over a 10-year period.Material and methodsThis multicentric, retrospective study was conducted in six French regional bone centres (Amiens, Lille, Orléans, Paris, Rennes, and Strasbourg). DXA databases were initially searched for individuals with a bone mineral density (BMD) Z-score >=+4 at any site in the lumbar spine or hip from April 1st, 2008 to April 30st, 2018.ResultsThe number of patients who had at least one DXA scan was 72,225, of which 66% were women. Of these 72,225 patients, 909 had a Z-score >=+4 at any site, i.e. a prevalence of 1.26% [1.18%-1.34%]. The DXA scans, imagery and medical records of 322

men and 587 women with EBM were reviewed to assess causes. In a few patients, EBM was attributed to several causes, which explains the difference between the total number of causes (n=936) and the total number of patients (n=909). An artefactual cause was found in 752 patients (80%) with EBM (mostly degenerative disease of the spine in 613 patients (65%)), and an acquired cause of focal EBM was found in 12 patients (1%) including sclerotic bone metastases (n=3), Paget's disease (n=7), and fibrous dysplasia of bone (n=2). An acquired cause of generalized EBM was found in 84 patients (9%), with renal osteodystrophy (n=32), followed by haematological disorders (n=20, e.g. myeloproliferative syndromes and mastocytosis), hypoparathyroidism (n=15) and diffuse bone metastases from solid cancer (n=12). Of the remaining causes, rare hereditary diseases (e.g. X-linked hypophosphatemia and osteopetrosis) and unexplained EBM were found in 19 (2%) and 69 (7%) cases, respectively. ConclusionThe prevalence of EBM (Z-score >=+4 at any site) is 1.26% [1.18%-1.34%]. In nearly all instances (93%) the explanation for EBM came from the medical record and conventional investigation. This study suggests that the main cause of EBM is degenerative disease of the spine. However, EBM can also reveal acquired or hereditary diseases.

***Disclosures: JULIEN PACCOU**, None*

P-013

Potential Interactions between SQSTM1, KEAP1 and PARK2 in Paget's Disease of Bone *Yvette Oppong[1], Britta Petersen[1], Cynthia Alander[1], Marc Hansen[1]. [1]Center for Molecular Oncology, UConn School of Medicine, United States

Paget's Disease of Bone (PDB) is a metabolic disease resembling excessive bone remodeling causing disorganized, structurally weak bone. The genetic etiology of PDB is heterogeneous, but a significant portion is attributed to mutations in the SQSTM1 gene. The SQSTM1 gene product (p62) is a 62kD protein linked to a number of cellular processes including autophagy. KEAP1 and PARK2 are proteins that have been shown to interact with p62 during autophagy. The hypothesis is that mutations in SQSTM1 associated with PDB could alter KEAP1 and/or PARK2 interaction with p62. A wildtype osteoblastic cell line (hFOB1.19) and a marrow stromal cell line developed from a pagetic lesion (PSV10) were treated with a combination of 15nM 1α,25-(OH)2D3 (VitD) and 1μg/ml lipopolysaccharide (LPS) with or without 1μM Simvastatin, a drug that blocks p62 activity in autophagy. The cells were then fixed and analyzed by immunofluorescence using antibodies against RELA, KEAP1 or PARK2. Activation of RELA (a known downstream target of p62 activation), KEAP1 and PARK2 were detected by changes in cellular localization of these proteins to the nucleus. Results, as measured by nuclear accumulation, showed activation of RELA in the PSV10 but not hFOB1.19 cells in response to the low dose VitD and LPS. Simvastatin addition appeared to eliminate this activation. There was also nuclear accumulation of KEAP1 in the PSV10 cells following VitD and LPS stimulation, which was again blocked by Simvastatin addition. However, for PARK2, while there was nuclear accumulation in the PSV10 cells following LPS and VitD stimulation, Simvastatin addition did not eliminate the nuclear accumulation of PARK2. In conclusion, VitD and LPS appeared to activate RELA, KEAP1 and PARK2 in PSV10 cells but not hFOB1.19 cells. Simvastatin appeared to suppress activation of RELA and KEAP1 but not PARK2 in the PSV10 cells. This suggests that mutations in SQSTM1 associated with PDB may play different roles in activating RELA, KEAP1 and PARK2 and that Simvastatin affects only some of those roles.

***Disclosures: Yvette Oppong**, None*

P-014

Vitamin D3 (D3) supplementation in subjects with primary hyperparathyroidism (PHPT): evaluation of safety and biochemical response *STHEFANIE GIOVANNA PALLONE[1], Monique Nakayama Ohe[1], Livia Marcela Santos[1], Isabela Ohki Nacaguma[1], Renata Elen Costa Silva[0], Ilda Sizue Kunii[1], José Gilberto Vieira[1], Marise Lazaretti-Castro[1]. [1]Federal University of São Paulo, Brazil, [0]Federal University of São Paulo, Brazil

Introduction: Vitamin D deficiency is common in PHPT, which frequently is associated with a secondary hyperparathyroidism component. Therefore, it is essential to improve the levels of 25hydroxyvitamin D (25OHD), avoiding a higher elevation of PTH and its deleterious consequences in bone quality. However, the safety of 25OHD replacement in such patients is uncertain, given the risk of worsening of hypercalcemia. Objective: We aim to evaluate the effectivity of 14,000 UI/week D3 supplements on subjects with PHPT and healthy controls to achieve 25OHD levels above 30 ng/mL and the safety regarding hypercalcemia by analyzing (tCa) and ionized calcium (iCa). Materials and methods: We studied 54 patients with PHPT prior surgery and 65 healthy age-and-sex-matched subjects prospectively for 12 weeks with the administration of 14,000 IU of D3 weekly. Exclusion criteria were: taking Vitamin D supplementation in the last 3 months, creatinine clearance < 45 and use of calcimimetics. Fasting blood samples were collected at baseline and the end of the study and used a general linear model with repeated measures approach to investigate the main effect of time and diagnosis, and diagnosis x time interactions. Results: At baseline, 25OHD levels were similar in both groups (42.8% of subjects in the PHPT group and 52% of healthy subjects had levels of 25OHD <20 ng / mL. p-value=0.342). The mean of tCa and iCa were higher in PHPT than in controls. Diagnosis groups also differed in PTH values, as expected in these populations. The mean values of 25OHD increased over time in both groups (achieving the goal of 30 ng/mL), albeit more intensively among controls. The administration of D3 did not significantly change tCa, iCa, or PTH (Table 1). Conclusion: Vitamin D3 14000 UI administered weekly for 12 weeks successfully raised 25OH D levels to a goal of 30 ng/ml without changes in calcemia in PHPT and control subjects, demonstrating the effectivity and the safety of this dosage in these patients. The impact of D3 replacement on 25OHD levels differed between PHPT and controls, with a smaller increase among PHPT patients.

	25OHD (ng/mL)		tCa (mg/dL)		iCa (mmol/L)		PTH (pg/mL)	
	Baseline	After 12 weeks	Baseline	After 12 weeks	Baseline	After 12 weeks	Baseline	After 12 weeks
PHPT (mean±SD)	22.84 ± 6.12	31.60 ± 6.95	11.26 ±0,94	11.16 ± 0.88	1.52±0,14	1.53 ± 0.16	132.40 ± 91.20	132.94 ± 66.22
Controls (mean±SD)	20.47 ± 5.77	32.59 ± 6.47	9.67±0.36	9.64 ± 0.34	1.29±0.03	1.28 ± 0.03	62.30 ± 28.84	56.78 ± 25.31
Main effect of diagnosis (p-value)	0.513		<0.001		<0.001		<0.001	
Main effect of time (p-value)	<0.001		0.160		0.769		0.516	
Diagnosis x time interaction (p-value)	0.003		0.460		0.288		0.431	

***Disclosures: STHEFANIE GIOVANNA PALLONE**, None*

P-015

Vitamin D, Glucose and Lipid Metabolism: Analysis in Healthy Subjects *Vittoria Danese[1], Cristiana Cipriani[1], Federica Ferrone[1], Jessica Pepe[1], Luciano Colangelo[1], Mario Renella[1], Valentina Piazzolla[1], Viviana De Martino[1], Luciano Nieddu[2], Frank Blocki[3], Salvatore Minisola[1]. [1]Department of Clinical, Internal, Anesthesiologic and Cardiovascular Sciences, Sapienza University of Rome, Italy, [2]Faculty of Economics, UNINT University of Rome, Italy, [3]DiaSorin Inc, United States

Purpose. The study aimed to evaluate the mutual relationship between vitamin D, glucose and lipid metabolism in a large cohort of healthy subjects.Methods. We studied 1240 blood donors (age range 18-68 years). We excluded subjects treated with drugs that may affect mineral metabolism. In all subjects, we measured serum 25-hydroxy-vitamin D [25(OH)D], parathyroid hormone (1-84PTH, hereafter PTH) and 1,25(OH)2D by chemiluminescence-immunoassay (LIAISON® and LIAISON XL®); ionized calcium (Ca++) and magnesium (Mg++) by biochemical analyzer NOVA 8; serum total and HDL cholesterol, triglycerides, and plasma glucose by enzymatic test with the Cobas c 311 analyzer (Cobas®); serum LDL was calculated by the Friedewald formula: LDL cholesterol = total cholesterol - HDL - (triglycerides/5).Results. Table 1 shows demographic and anthropometric characteristics and laboratory findings in all subjects. We observed significant negative associations between serum 25(OH)D and BMI (R= -0.11, p<0.0001), PTH (R= -0.16, p<0.0001), total cholesterol (R= -0.06, p<0.05), and triglycerides (R= -0.13, p<0.0001). Conversely, serum 25(OH)D was positively associated with 1,25(OH)2D (R= 0.12) and creatinine (R= 0.17) (p<0.0001 for all). Interestingly, there was a significant direct association between serum PTH and total (R= 0.08, p<0.01) and LDL cholesterol (R= 0.1, p<0.001), triglycerides (R= 0.09, p<0.01) and glucose (R= 0.15, p<0.0001); serum PTH inversely correlated with HDL cholesterol (R= -0.09, p<0.01). In the group of subjects with serum 25(OH)D < 20 ng/mL (n=670), the associations between PTH, glucose and lipid metabolism were substantially maintained: total (R= 0.07, p=0.06) and LDL cholesterol (R= 0.09, p<0.02), glucose (R= 0.19, p<0.0001); HDL cholesterol (R= -0.08, p<0.05). When we divided the cohort in two groups according to PTH levels below (n=1155) and above (n=85) the upper limit of normal (36.6 pg/mL), PTH positively correlated with total (R= 0.08, p<0.01) and LDL cholesterol (R= 0.11, p<0.001), triglycerides (R= 0.08, p<0.01), glucose (R= 0.14, p<0.0001), and negatively with HDL cholesterol (R= -0.09, p<0.01) in subjects whose PTH was < 36.6.Conclusions. Our study demonstrates that within the scope of the vitamin D-PTH axis, glucose and lipid metabolism are mutually related and influenced. Hypovitaminosis D appears to predispose towards worse glucose and lipid profiles, as impacted directly by the action of PTH. Conversely, while higher serum PTH levels per se have no relationship with glucose and lipid metabolism, they do associate with higher levels of bad LDL cholesterol.

Table 1. Demographic and anthropometric characteristics and laboratory findings (mean ± SD) in all subjects

	All subjects (n = 1240)	Normal range
Age, years	41.9 ±11.7	-
Female/male ratio	1/3.3	-
Weight, kg	76.7±13	-
Height, cm	175±8	-
BMI, kg/m^2	24.9±3.3	18.5 - 25
25(OH)D, ng/mL	19.9 ± 8.4	> 30
PTH, pg/mL	23.5 ± 8.3	6.5 - 36.6
1,25(OH)$_2$D, pg/mL	50.5 ± 13.2	19.9 - 79.3
Ca^{++}, mmol/L	1.29 ± 0.03	1.17 - 1.33
Mg^{++}, mmol/L	0.53 ± 0.05	0.45 – 0.6
Creatinine, mg/dL	0.89 ± 0.15	0.7 – 1.2
Total cholesterol, mg/dL	195 ± 34.2	80 - 232
LDL cholesterol, mg/dL	116.4 ± 32	69 - 118
HDL cholesterol, mg/dL	60 ± 15.2	44 - 64
Triglycerides, mg/dL	91 ± 46.5	45 - 163
Glucose, mg/dL	86.2 ± 9.5	68 - 99

***Disclosures: Vittoria Danese**, None*

P-016

Evaluating quality of life and symptoms in primary hyperparathyroidism *Raghad Alyousefi[1], Sunnah Aziz[1], Afroze Abbas[2], Rebecca Sagar[2]. [1]University of Leeds, United Kingdom, [2]Leeds Teaching Hospitals Trust, United Kingdom

Background: Patients with symptomatic primary hyperparathyroidism (PHPT) are usually considered for parathyroidectomy, the gold-standard treatment for this condition. Identifying symptomatic patients is challenging as symptoms are non-specific. Assessing quality of life is not routinely objectively evaluated pre or post-surgery. Our study aims to both assess evaluation of symptoms in PHPT and validate these against quality of life outcomes. Methods: We prospectively collected data on 101 UK patients with confirmed PHPT. 2 questionnaires were completed, 1 a validated symptom scoring tool (Pasieka, Pasieka et al), the other assessed quality of life (PHPQoL, Webb et al). Data analysed included demographics, biochemistry and questionnaire scores. For Pasieka the higher the score, the more symptomatic. A score >200 has been validated as symptomatic. Conversely, the lower the score in PHPQoL questionnaire, the worse the quality of life. Results: 89% of the patients were female. Median age was 84 years (21-91). Time since diagnosis ranged from 0-5.5 years. Mean serum calcium at time of questionnaire was 2.68mmol/L +/- 0.1, mean PTH was 17.6 pmol/L +/- 9.1. 82% of patients had a Pasieka score >200, mean 529 +/- 310. PHPQoL mean score was 49 +/- 23. There was significant negative correlation between Pasieka and PHPQoL score (r2= 0.69, p<0.0001). We compared different symptom groups (neurocognitive, fatigue, bone pain, thirst and other). PHPQoL scores for neurocognitive and fatigue symptoms were significantly higher than scores for bone pain (p=0.001 and p=0.003 respectively). Similar results were seen in Pasieka with neurocognitive and fatigue symptoms the highest scoring, 'other' symptoms scored lowest. Calcium and PTH were not correlated with Pasieka (p=0.30 and p=0.74 respectively) nor PHPQoL (p=0.81 and p=0.59). Conclusion: Our study shows the PHPQoL and Pasieka tools correlate strongly in this UK cohort, demonstrating the significant impact of PHPT symptoms on quality of life. Degree of biochemical derangement was not predictive of symptoms/quality of life. Neurocognitive and fatigue domains were scored more highly than others on both tools. Thus, routine use of PHPQoL may detect subtle neurocognitive impacts of PHPT and facilitate patient selection for surgery. Post-surgery, clinical focus is on normalisation of biochemical indices, but in the future tracking change in quality of life may better assess impact on patient well-being.

***Disclosures: Raghad Alyousefi**, None*

P-017

Bone Health in Type 1 Diabetes with and without Neuropathy; a Cross-Section Study *Tatiane Vilaca[1], Margaret Paggiosi[1], Fatma Gossiel[1], Dinesh Selvarajah[2], Jennifer Walsh[1], Richard Eastell[1]. [1]Academic Unit of Bone Metabolism, The University of Sheffield, United Kingdom, [2]Department of Oncology and Metabolism, The University of Sheffield, United Kingdom

Background Fracture risk is increased in diabetes, especially in type 1 diabetes. The underlying mechanisms are not fully established. Some evidence suggests that abnormalities in microarchitecture might be involved, especially in patients with microvascular disease. Methods We assessed bone microarchitecture (high resolution peripheral quantitative computed tomography) and bone turnover markers (CTX and PINP) in patients with type 1 diabetes with (T1DN+, n=20) and without (T1DN-, n=20) distal symmetric polyneuropathy and healthy controls (n=20). Participants were scanned at the standard site and at 14% bone length at the radius and tibia. Results At the 14% length site, favourable trabecular microarchitecture was found in T1DN- compared to controls at both radius and tibia (key findings in the table). At the standard site, tibial cortical porosity was 56% higher (p=0.009) in T1DN+ compared to T1DN-. PINP and CTX were decreased in participants with diabetes (T1DN+ and T1DN-) compared to controls. PINP was 34% (p=0.006) and 28% (NS) lower in T1DN- and T1DN+ compared to controls, while CTX was 87% (p=0.016) and 90% (p=0.011) lower, respectively. DiscussionDiabetes is associated with low bone turnover, as shown by the decrease in bone turnover markers. This low bone turnover preserved trabecular microarchitecture, resulting in favourable findings at the 14% site. At the standard, more distal site, an increase in cortical porosity was found only at the tibia in patients with neuropathy. This finding suggested that microvascular complications, especially neuropathy, could affect bone vascularization and/or innervation and impact on cortical porosity. Overall, impaired microarchitecture is unlikely to be the main mechanism of bone fragility in type 1 diabetes.

Percentage differences in trabecular features between T1DN- and T1DN+ and control

	Radius				Tibia			
	T1DN- vs control (%)	p	T1DN+ vs control (%)	p	T1DN- vs control (%)	p	T1DN+ vs control (%)	p
Trabecular vBMD (mgHA/cm3)	↑46	0.017*	↑39	0.056	↑25	0.024*	↑20	0.083
Trabecular number	↑30	0.010*	↑17	0.221	↑22	0.014*	↑16	0.087
Trabecular BV/TV (no units)	↑46	0.017*	↑39	0.055	↑25	0.023*	↑20	0.081
Trabecular thickness	↑20	NS	↑13	NS	↑6	NS	↑4	NS

NS non-significant

* statistically significant difference between groups

***Disclosures: Tatiane Vilaca**, None*

P-018

Lower femoral neck bone mineral density and higher body fat are associated with vascular calcification in Chronic Obstructive Pulmnonary Disease patients *Roberta Grauman[1], Vera Lúcia Szejnfeld[1], Marcelo Pinheiro[1], Charlles Castro[1]. [1]Escola Paulista de Medicina - Universidade Federal de São Paulo, Brazil

Introduction: Chronic Obstructive Pulmonary Disease (COPD), a chronic disorder characterized by not fully reversible expiratory airflow limitation, has been associated with comorbidities as cardiovascular disease and osteoporosis. Higher risk for osteoporosis, vertebral fractures and low lean mass and increased cardiovascular mortality have been observed in COPD patients. As cardiovascular mortality due to vascular calcification and bone fragility might share pathophysiological mechanisms, in this study we aimed at evaluating the association between osteoporosis and vertebral fragility fractures with cardiovascular calcification in a series of patients with COPD. Patients and Methods: A total of 97 COPD patients underwent bone mineral density (BMD) and body composition analyses by DXA, spirometric evaluation and laboratorial tests. Conventional X-ray of thoracic and lumbar spine was used to assess vertebral fractures using semiquantitative Genant's criteria and vascular calcification of abdominal aorta using Kauppila's method. The study was approved by our local Ethics Committee. Results: Ninety-six patients had data available for this analysis: 44 (45.8%) were men (mean age 65.8 years-old; min 51 - max 83) and 52 (54.2%) were women (mean age 64.3 years-old; min 44 – max 85) with mean Kauppila's index of 4.8 (0-19). As compared to values below 7, a Kauppila´s index >= 7 was significantly associated with older age (67.9 vs 63.5 years-old; p<0.05), lower femoral neck BMD (0.784 vs 0.877 g/cm2; p<0.05) and higher serum creatinine (1.0 vs 0.8 mg/dL; p<0.05). Patients with Kauppila's index >= 7 tend to have more vertebral fractures (Gentant's grades II and III) than those with a Kauppila's index < 7 (33.3% vs 17,5%; respectively; p=0.07). After adjustments for all confounding variables, multiple logistic regression analyses demonstrated that age and low femoral neck BMD for women and age and high body fat for men were the main determinants for having a Kauppila's index >= 7. Conclusion: Our results demonstrate a high prevalence of vascular calcification in COPD patients and this outcome is associated with low bone mass at the femoral neck and higher rates of morphometric vertebral fractures.

***Disclosures: Roberta Grauman**, None*

P-019

Tumor-induced osteomalacia (TIO): Clinical Experience of a Mexican Reference Institution *Alfredo Adolfo Reza-Albarrán[1], Ramón G De los Santos[1], Anabel Rodríguez-Romo[2], Dania L Quintanilla Flores[3], Nicole M Íñiguez Ariza[1], Arturo Angeles Angeles[1]. [1]Instituto Nacional de Ciencias Médicas y Nutrición Salvador Zubirán, Mexico, [2]Clínica de Especialidades Indianilla, ISSSTE, Cd. de México, Mexico, [3]Clínica de Especialistas; Monterrey, Nuevo León, Mexico

TIO is a rare disease caused by a FGF-23-producing tumor, usually benign; its major features are low serum phosphate and 1,25 (OH)2 vitamin D, along with severe osteomalacia and muscular weakness. Case series: We describe 22 cases of TIO of a mexican institution of tertiary attention. 12 men and 10 women are included; median age was 48.6 years (+/- 11.3); the age at onset of symptoms was 35.9 +/- 11.7. The median follow up period was 34.1

months (10.2-55). Generalized bone pain (100%), severe weakness (95%) and limitation for deambulation (95%) were the most frequent symptoms. Mean tumor size was 39.8 mm (+/-) 18.9 mm and location was from head to feet. Fractures were present in 21 patients (the most frequent sites were femur, ribs and spine). Median serum phosphate at diagnosis was 1.51 mg/dl. Mean serum bone-specific alkaline phosphatase (BSAP) was 127.71+/- 50.04 U/l (normal range: 9-22); mean PTH at diagnosis was 81.6 pg/ml and mean N-telopeptides (N-Tx) value was 91 nM/mmol cr (range of this series from 62.3-671.6; normal values 5-65). FGF-23 values (measured in 7 cases) was 857 RU (range from 324-1017; normal values less than 180). Scan with octreotide (with or without SPECT) was done in 18 patients and it was useful for tumor location in 15; other studies used for tumor location were CT, MRI and PET-CT with galium-DOTANOC. 21 patients have been treated with surgery and 19 of them are cured; the 2 patients without cure have tumors located in bone (5 patients from this series had tumor located only at bone and 4 more in soft tissue with bone infiltration). Two cases with tumors located in brain are cured. Histologic report was phosphaturic mesenchymal tumor. BSAP drecreased to normal values in 50% of cases at 23 months and N-Tx in 42% of cases at 21.6 months. Values of bone mineral density increased at all sites; at total hip, Z score increased from -3.72 to +0.19 SD. All cured patients informed improved quality of life and are able to walk; the 2 with surgical failure (and more than one surgical procedure in both) are now able to walk and also inform improved deambulation and functionality. Discussion: We inform cure in 19 of 21 surgically treated patients. Clinical improvement was noted in all of them. Until 2019, only 19 cases with "intracraneal" location had been informed; we report 2 cured cases with tumor located inside brain and one more with tumor possibly located in sellar area, whose cardiopulmonary function makes surgery very risky.

***Disclosures: Alfredo Adolfo Reza-Albarrán**, None*

P-020

Is hyperparathyroidism associated with blood clots? Evidence from a systematic review and meta-analysis *Kavindra Ratnaweera[1], Alexander Rodríguez[2]. [1]School of Medicine, Griffith University, Australia, [2]Bone and Muscle Health Research Group, Department of Medicine, Monash University, Australia

Calcium is critical in coagulation. Parathyroid hormone (PTH) maintains calcium homeostasis. Patients with elevated PTH are at increased risk of cardiovascular disease, but it is unclear if these patients are predisposed to thrombosis which may be related to PTH action on calcium. We aimed to determine if PTH was associated with increased clots or markers of coagulation in a systematic review. We searched MEDLINE and EMBASE (29 March, 2020) for original studies that were non-randomized; directly measured PTH levels or specifically enrolled patients with hyper/hypo-parathyroidism; measured any clotting factor; or reported thromboembolic or haemorrhagic events. We excluded interventional studies, case reports, studies of patients with surgical correction of hyperparathyroidism or receiving therapies that would interfere with mineral metabolism or haemostasis. The primary outcome was the association between PTH and clotting factors and the association of PTH with the incidence of thromboembolic or haemorrhagic events. Study quality was assessed using the Newcastle-Ottawa Scale. Continuous data were meta-analysed if reported in at least 100 patients in more than one study. Random-effects models were fitted and reported as standardized mean difference (SMD) with 95% confidence intervals (95%CI). Heterogeneity was determined by the I2 statistic. All data were computed using R (4.0.0). 2404 records were screened. Eight were eligible for inclusion. Seven studies were cross-sectional analyses of patients with primary (PHPT) or secondary (SHPT) hyperparathyroidism compared to controls. Study quality was poor. In pooled analyses comparing PHPT to controls, there was no statistical difference in fibrinogen [SMD=0.01 (-0.92–0.94); k=3 trials; n=133 patients; I2=86%]; D-dimer [0.46 (0.03–0.97); 3; 133; 52]; PAI [0.01 (-0.54–0.57); 3; 181; 69]. Other outcomes were reported in less than 100 patients as were outcomes in studies involving SHPT patients. One high-quality prospective study (n=27000 healthy adults) found serum PTH was not associated with venous thromboembolism [adjusted hazard ratio: 1.03 (0.74-1.42)], deep vein thrombosis (1.00; 0.66-1.52) or pulmonary embolism (1.09; 0.65-1.80). Overall, there was little evidence to support an association between PTH and increased coagulation. Prospective data are needed to understand what role if any, PTH plays in coagulation and if patients with elevated or reduced PTH are predisposed to clots or bleeds.

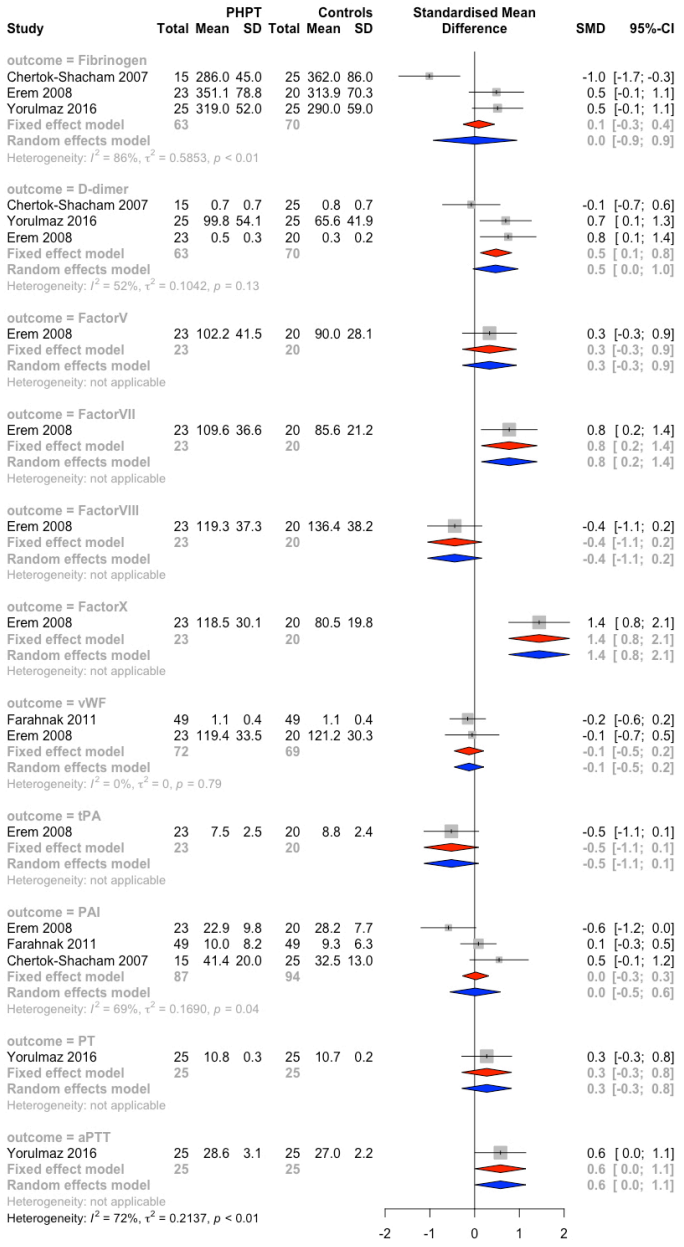

***Disclosures: Kavindra Ratnaweera**, None*

P-021

Risk Factors for Low Bone Mass in Spanish patients treated for HIV infection. *Gonzalo Allo Miguel[1], Joaquín Puerma[2], Gemma Villa[1], José Napky[1], Mercedes Oliet[1], Mercedes Aramendi Ramos[3], Rafael Rubio[4], Guillermo Martínez Díaz-Guerra[1]. [1]Endocrinology Service. 12 de Octubre University Hospital, Spain, [2]Endocrinology Service.12 de Octubre University Hospital, Spain, [3]Laboratory Service. 12 de Octubre University Hospital, Spain, [4]Internal Medicine Service. 12 de Octubre University Hospital, Spain

Background: Patients with human immunodeficiency virus (HIV) infection show lower bone mineral density (BMD) and higher rates of fragility fracture than general population. The pathogenesis of bone disease in HIV patients remains unclear but it seems to be multifactorial. Low BMD has been associated with different risk factors, such as age, sex, smoking and anti-retroviral therapy (ART). As nowadays HIV is a chronic disease, it is mandatory to identify associated risk factors in those patients. Aim: This study describes BMD status in a group of HIV patients and evaluates potential risk factors for low BMD in those patients.Material and methods: 107 HIV patients were evaluated in this retrospective study. BMD was assessed by DXA, (densitometer QDR 4500, Hologic) at lumbar spine (LS), femoral neck (FN) and total hip (TH). Serum 25OHD was measured by enzyme immunoassay (Roche). 25OHD deficiency was defined as a 25(OH)D level of 30 ng/ml

were categorized as 25OHD sufficiency. ART drugs included: Tenofovir disproxil (TED); Tenofovir alafenamide (TAF) and Protease inhibitors (PI). Statistics: Data are expressed as mean+/-s.d. for continuous variables and percentages for categorical ones. Regression techniques were used to evaluate the association between continuous variables. p-value <0.05 was considered as statistically significant.Results:79 male/28 female. Mean age: 55.8+/-7.3 years. 91(85.0%) patients were treated with TED; 15(14.0%) with TAF and 31(29.3%) with PI. Mean serum 25OHD was in the insufficiency range 27.09+/-12.63 ng/ml. 29(27%) patients showed 25OHD deficiency and 43 patients (40.1%) insufficiency. Mean T-score was in the osteopenia range in FN (-1.35+/-0.93) and LS (-1.43+/-1.26). 28(26,2%) patients suffered osteoporosis. Combined treatment with TED+PI was associated with lower TH T-score (p=0.02). Longer duration of the disease showed statistically significant association with FN (p=0.01); TN (p=0.02) and LS (p=0.03) T-score. Lower 25OHD level was associated with lower TN T-score (p=0.02).Conclusion: Low BMD, osteoporosis and 25OHD deficiency are common findings in HIV patients in our group. Our study shows that long-lasting disease and treatment with the combination of TED+PI are associated with lower BMD. This data should contribute to understand the pathogenesis of bone disease in HIV patients and provide practical recommendations for its evaluation and treatment.

***Disclosures: Gonzalo Allo Miguel**, None*

P-022

Lower bone mineral density is associated with primary hyperparathyroidism patients with abnormal vitamin D metabolite ratio (VMR): A case-control study *Jonathan Tang[1], Mushood Malik[1], Jeremy Turner[2], William Fraser[1]. [1]University of East Anglia, United Kingdom, [2]Norfolk and Norwich University Hospital NHS, United Kingdom

Introduction The role of vitamin D and calcium metabolism has long been implicated in the clinical manifestation of primary hyperparathyroidism (PHPT). The skeletal response to the overproduction of parathyroid hormone (PTH) is less predictable, and the effect on bone loss can be greater in some patients. The aim of this study was to establish associations between vitamin D metabolism, including vitamin D metabolite ratio (VMR) with rates of bone loss in PHPT, particularly in patients who did not undergo surgery.Methods An audit was conducted from the electronic health records of patients diagnosed with PHPT who attended the Endocrinology clinic at the Norfolk and Norwich University Hospital (NNUH), UK during the 2017-2019 period. The search identified cases with abnormal vitamin D metabolism 1,25(OH)2D:24,25(OH)2D VMR of >=51, and excluded those who had parathyroid surgery or had received steroid therapy. For each case, the age and gender were matched to controls, i.e. 1,25(OH)2D:24,25(OH)2D VMR of <51, with the same exclusion criteria as described. Cases (n=13) were identified (age mean(range): female 70.6(50-94)yrs, male 73(63-79)yrs). Each case was matched to controls in the ratio of 2:1 for females, and 1:1 for males. Laboratory measurements of serum 25OHD, adjusted calcium (ACa), phosphate, and plasma PTH were retrieved. In addition, we obtained the bone mineral density (BMD) T-score values (lumbar, left hip and left femoral neck) from DEXA scans carried out +/-1 month from the biochemical measurements.Results We observed a significantly lower Lumbar Spine T-score in the cases, mean (95%CI) -1.85 (-0.9 to -2.77) than in the matched controls -0.2(0.30 to -0.79), p<0.001. Whilst the left hip and left femoral neck T-scores in the cases were not significantly lower (Figure). 25OHD and 24,25(OH)2D were significantly lower in the cases than controls; mean (SEM), 42.9(6.6) v 69.4(3.9)nmol/L, p<0.01 and 2.0(0.44) v 5.0(0.38)nmol/L, p<0.001, respectively. In contrast, the 25OHD:24,25(OH)2D VMR in the cases were higher 27(2.0) v 15(0.8), p<0.001. PTH, 1,25(OH)2D and ACa were elevated above the upper limit of the reference interval in both groups but no significant relationships were observed between the groups.Conclusion Our cohort of non-surgically managed PHPT patients presented with grossly elevated 1,25(OH)2D:24,25(OH)2D VMR were strongly associated with lower Lumbar Spine T-score. By using VMR we demonstrated an imbalance between the active and catabolic forms of vitamin D metabolites that might contribute to the accelerated bone loss in PHPT patients.

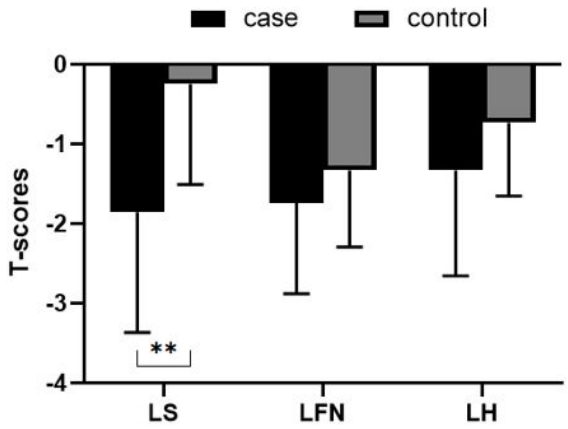

Figure showing the lumbar (LS), left femoral neck (LFN) and left hip (LH) T-score values (mean, SEM) for the cases and controls. Denotes **(p<0.01).

***Disclosures: Jonathan Tang**, None*

P-023

Association of Testosterone, Dehydroepiandrosterone, and 17-Alpha-Progesterone with Bone, Muscle, and Fat in Women with Congenital Adrenal Hyperplasia *Seung-Gyun Im[1], Sung Hye Kong[1], Jung Hee Kim[1], Chan Soo Shin[0]. [1]Seoul National University Hospital, Republic of Korea, [0]Seoul National University Hospital, Republic of Korea

Congenital Adrenal Hyperplasia (CAH) is a disorder with disruption of cortisol synthesis pathway, which leads to adrenal insufficiency and testosterone excess. It is thought that inadequate or excessive replacement of lifelong corticosteroid in patients with CAH exposes them to an increased risk of bone loss and changes in body composition. This study aimed to analyze the relationship of hormonal status with bone mineral density (BMD) and body composition in women with CAH. Women diagnosed with CAH at Seoul National University Hospital from 2000 to 2020 with bone densitometry scan results were included in the final analyses. Patients with low BMD were defined as having less than -2.0 Z-score among the lumbar spine, femur neck, and total hip. Lean body mass and fat mass were measured using bioelectrical impedance analysis, and percent lean and percent fat mass were defined as lean body and fat mass divided by body weight, respectively. Among a total of 138 participants, the mean age was 26.5 years, and the mean body mass index (BMI) was 23.1 kg/m^2. Women with low BMD were older and had lower percent lean mass, while their BMIs were similar. Cumulative and daily doses of corticosteroids, ACTH, renin, 17-alpha-progesterone (17-α-PG), and dehydroepiandrosterone sulfate (DHEA-S) were similar between women with low and normal BMD. In correlation analyses, testosterone levels were positively correlated with the lumbar spine, femur neck, and total hip BMD after adjustments for age and BMI (r=0.69, p<0.001; r=0.60, p<0.001; r=0.51, p=0.001, respectively). Also, DHEA-S was positively correlated with the lumbar spine and total hip BMD (r=0.33, p=0.003; r=0.25, p=0.019, respectively), and 17-α-PG was positively correlated with lumbar spine BMD after adjustments (r=0.45, p=0.001), while doses of steroid replacements were insignificantly correlated with BMDs. The percent fat mass was positively correlated only with renin (r=0.30, p=0.025). Also, percent lean mass did not show significant correlation with hormonal levels and the amount of steroid replacement. To summarize, in women with CAH, women with higher testosterone and DHEA-S levels had better trabecular and cortical BMD, while those with higher 17-α-PG had higher trabecular BMD only. Also, women with increased renin levels were likely to have increased proportions of body fat. However, the degree of steroid replacement was not associated with BMD and body composition.

***Disclosures: Seung-Gyun Im**, None*

P-024

Changing Landscapes, Altered Patterns - Hungry Bone Syndrome following Parathyroidectomy for Primary Hyperparathyroidism *Aye Chan Maung[1], Nurshazwani Mat Salleh[1], Jeremy Chung Fai Ng[2], Manju Chandran[3]. [1]Department of Endocrinology, Singapore General Hospital, Singapore, [2]Department of Surgery, Singapore General Hospital, Singapore, [3]Osteoporosis and Bone Metabolism Unit, Singapore General Hospital, Singapore

Introduction: Hungry Bone Syndrome (HBS) following parathyroidectomy (PTX) for primary hyperparathyroidism (PHPT) has an incidence rate that varies widely from 4-87% depending on the country of origin of the study, with the lower rates reported from some

western developed countries and the highest rates from less developed ones in Asia. No study has explored its incidence rates in a developed country in Asia and therefore this was our aim.Method: 118 patients operated on for PHPT during 2012-2019 at the largest public hospital in the only developed country in SE Asia were retrospectively analysed. All patients had incidentally detected high serum Calcium (Ca) or had been admitted with acute symptoms of hypercalcemia or had elevated Parathyroid hormone (PTH) and high Ca during work-up for osteoporosis. Pre-operative clinical and laboratory parameters assessed were age, gender, race, radiographic bone abnormalities, BMD and use of Bisphosphonate (BSP), Denosumab (DMB) or vitamin D, serum corrected Ca, PTH, PO4, Alkaline Phosphatase (ALP) and 25(OH)D levels. HBS was defined as serum Ca <=2.1 mmol/l with normal/raised serum PTH levels lasting more than 4 days postoperatively, requiring intravenous (IV) Ca.Results: Mean age(SD) of the patients was 60.92(12.01). Chinese constituted 73.7%, Malays 13.6%, Indians 8.5% and other races 4.2%. 70.3% were females. 45% had osteoporosis on DXA scanning. 13.5% had renal calculi. No patient had osteitis fibrosa cystica. 27% of the patients had ever received a BSP and 3.3% had received DMB in the 6 months prior to surgery. 62.7% were on vitamin D supplementation (mean dose:1607.7 IU) in the month prior to surgery. The mean(SD) immediate preoperative levels of PTH (0.9-6.2pmol/l) was 25.66(30.77), corrected Ca (2.10-2.60 mmol/l) was 2.72(0.15), 25(OH)D was 20.75(7.47) ng/ml, PO4 (0.77-1.38mmol/l) was 0.86(0.20) and ALP (32-103U/L) was 117.86(64.48). Only 1/118 (0.8%) developed HBS.Conclusion: The very low incidence of HBS in unselected, consecutive, multi-ethnic patients undergoing PTX for PHPT at a medium volume, multi-surgeon, public hospital, in a developed country in SE Asia likely reflects the changing patterns of PHPT in the developed world. Automated measurements that include serum Ca and screening for PHPT amongst osteoporosis patients results in a pickup of the disease when it is mild or asymptomatic. The absence of severe vitamin D deficiency in our population also likely contributed to this low incidence rate.

***Disclosures: Aye Chan Maung**, None*

P-025

Impact of curative treatment in symptomatic primary hyperparathyroidism on trabecular bone score, bone mineral density, and bone turnover markers - A prospective study from southern India *Jinson Paul[1], Shrinath Shetty[1], Kripa Elizabeth Cherian[1], Nitin Kapoor[1], Deepak Abraham[1], Thomas Vizhalil Paul[1]. [1]Christian Medical College, India

Background: The significance of preoperative PTH in predicting recovery of trabecular bone score (TBS) and other bone mineral parameters following curative parathyroidectomy in symptomatic primary hyperparathyroidism (PHPT) is not well studied. This prospective study was done to objectively assess trabecular bone score, bone mineral density (BMD) and bone mineral profile in Indian subjects with symptomatic PHPT and to study the influence of baseline PTH on recovery of these parameters following curative surgery.Materials & Methods: This was a two year prospective study conducted at a tertiary care centre in southern India. Baseline assessment included demographic details, mode of presentation, bone mineral biochemistry, BMD, TBS and bone turnover markers (BTMs). These parameters were reassessed at the end of the first and second years following curative parathyroid surgery.Results: Fifty one subjects (32 men and 19 women) with PHPT who had undergone curative parathyroidectomy were included in this study. The mean(SD) age was 44.6(13.7) years. On follow-up at two years, BTMs, BMD at femoral neck, lumbar spine and distal forearm as well as TBS showed significant steady improvement when compared to baseline($P<0.05$). The TBS, BTMs and BMD at lumbar spine and forearm were significantly worse at baseline in subjects with higher PTH(>= 250 pg/mL) when compared to the group with lower PTH(<250 pg/mL). However, at the end of two years the difference between high versus low PTH groups (mean+/-SD) persisted only for forearm BMD(0.638+/-0.093 versus 0.698+/-0.041 g/cm2;$P=0.01$).Conclusion: This study found that BMD at forearm remained significantly worse in individuals with high PTH even at two years after surgery, while other parameters including TBS improved significantly from baseline.

***Disclosures: Jinson Paul**, None*

P-026

Assessing The Impact Of Calcitonin In Management Of Hypercalcemia *Malik Faheem[1], Fahim Abbasi[2], Marina Basina[1]. [1]Division of Endocrinology, Stanford University, United States, [2]Division of Cardiovascular Medicine, Stanford University, United States

Purpose:Hypercalcemia accounts for about 0.6% of all the hospital admissions and hypercalcemia of malignancy, seen in up to 20% of all the malignancy cases, is the most common cause in the inpatient setting. Choice of therapeutic options is usually dictated by initial serum calcium level, rapidity of its rise and presence of hypercalcemia symptoms. Due to the high cost of calcitonin (minimum of $3539.20 per 48-hour therapy), we sought to evaluate whether calcitonin therapy with and without bisphosphates was superior to bisphosphonates alone in reducing calcium levels in patients with hypercalcemia. Method: This is a retrospective chart review of 71 consecutive patients admitted to Stanford Hospital between 10/1/2018-09/30/2019 with ICD-10 codes for hypercalcemia. Patients who received bisphosphonate alone (Group B), calcitonin alone (Group C) or bisphosphonates and calcitonin dual therapy (Group BC) were included. All patients received intravenous hydration. Patients receiving Denosumab were excluded due to small sample size, and no patients received medications known to cause hypercalcemia. Percent decline in corrected serum calcium was compared between the groups. One-way ANOVA followed by Bonferroni pairwise comparison tests were used for statistical analysis.Results: The patients had a mean age of 64.3 years, 41 (57.8%) were male, and 61 (85.9%) had hypercalcemia of malignancy. Mean baseline corrected calcium was 12.2 +/- 1.5 mg/dl in bisphosphonate group (B), 13.4 +/- 1.7 mg/dl in calcitonin group (C) and 13.8 +/- 1.6 mg/dl in bisphosphonates + calcitonin group (BC). Between baseline and day 5, group C had a significantly lower mean percentage decrease in corrected calcium (11.8 +/- 11.6) compared to group B (28.6 +/- 4.1) and group BC (26.0 +/- 12.9) ($p=0.02$), and there was no statistically significant difference between group B and group BC. There was no significant difference between initial symptoms, baseline serum creatinine and length of stay between the three groups.Conclusion: Use of calcitonin, whether alone or in combination with bisphosphonates, did not provide a superior reduction in serum calcium levels compared to bisphosphonates alone in patients with hypercalcemia. Due to its high cost, calcitonin use should be limited to patients with severe symptomatic hypercalcemia. Further studies are warranted to determine the calcium level cut off when calcitonin therapy would be beneficial.Disclosure: None

***Disclosures: Malik Faheem**, None*

P-027

Hypercalcemia in Cirrhotic Liver Disease: A Clinical Case Series *Diana Athonvarangkul[1], Anika Anam[1], Renata Belfort de Aguiar[1]. [1]Yale University, United States

Hypercalcemia due to advanced liver disease without neoplasia is a complex process with increasing prevalence, but its evaluation and management remains puzzling. Here, we present 8 patients with hypercalcemia due to cirrhosis of varying causes including viral, alcoholic and genetic. The peak serum corrected calcium level ranged from 12.76-14.56 mg/dL (normal 8.8-10.2 mg/dL). As hypercalcemia due to cirrhosis is a diagnosis of exclusion, all patients had an extensive evaluation for other causes of hypercalcemia. All patients had low intact PTH, low to normal 25-hydroxyvitamin D, and low to normal 1,25-dihydroxyvitamin D. Seven patients had low to normal PTHrP and one patient had elevated PTHrP in the context of renal dysfunction. Phosphorus level was normal to mildly elevated. Four patients had CTX level measured, and all were elevated. Of all patients, three had elevated total alkaline phosphatase (ALP); although all four patients with measured bone specific ALP had normal levels. No patient had evidence of hepatic neoplasm at the time of hypercalcemia. Six patients had negative workup for monoclonal gammopathy and one patient had a discrete abnormal band in the gamma region. Thyroid and cortisol hormones were normal in all patients. No patient had elevated vitamin A. One patient screened negative for sarcoid with ACE. Four patients were considered bedbound. Three patients had exogenous calcium intake with calcium or nutritional supplements. Three patients with DXA scans had T-scores in the normal to osteopenic range. For treatment of hypercalcemia, patients received calcitonin (n=4), bisphosphonates (n=5) and denosumab (n=1), either alone or in combination. One patient achieved normocalcemia after discontinuation of calcium supplements only. Three patients who received zolendronic acid developed hypocalcemia requiring calcium supplementation. Many patients were not able to tolerate intravenous fluid therapy due to cirrhosis related volume overload. Although the mechanism of hypercalcemia due to cirrhosis is unclear, it has been postulated to involve inflammatory cytokines. The presence of elevated bone turnover marker CTX, but normal bsALP, preserved bone mineral density and, in some cases, only transient hypercalcemia, suggests that there is an acute uncoupling of bone remodeling favoring resorption, which may respond to bisphosphonates and denosumab. Additional studies are needed to determine the mechanism and to guide treatment options.

***Disclosures: Diana Athonvarangkul**, None*

P-028

Evaluation of Bone Mineral Density and Trabecular Bone Score (TBS) in X-linked hypophosphatemic patients *Pablo Florenzano[1], Danisa Ivanovic-Zuvic[1], Macarena Jimenez[1]. [1]Pontificia Universidad Catolica de Chile, Chile

X-linked hypophosphatemia, the most common cause of inherited hypophosphatemia, manifests as rickets in children and osteomalacia in adults. To date, Bone Mineral Density (BMD) reports in this population have been discordant, with a tendency towards a higher BMD at the lumbar spine that could be partially explained spinal by paravertebral ligament calcifications. The Trabecular Bone Score (TBS), an index that is determined from DXA scans, assesses the microarchitecture of the spine, with less influence by spinal artifacts. To date, no information has been published regarding TBS in this group of patients.Objective: To describe BMD and TBS in XLH patients, and to determine its association with clinical and biochemical presentation. Design: Cross-sectional.Methods: Adult subjects with PHEX-confirmed XLH were included. All patients underwent DXA scans (Lunar) at the lumbar spine and femoral neck. In addition, TBS values were determined. Z-scores were calculated compared to NHANES. Clinical and biochemical data were obtained to determine its association with BMD and TBS.Results: Eighteen patients were included, 13 (72%) women, median age of 33 (IQR, 25-37 years). Three patients had never received calcitriol and/or phosphate. Median of proportion of lifetime with treatment was 0.53 (IQR, 0.12-0.75). All patients were hypophosphatemic, 56% had elevated ALP and 44% had hyperparathyroidism. Mean BMD at lumbar spine and femoral neck were 1.45 gr/cm2 (Z-score= 2.4) and 1.02 gr/cm2 (Z-score =0.2). BMD at lumbar spine, but not at femoral neck, was increased compared to normative data ($p<0.05$). Mean TBS was 1.511, with a mean Z-score of 1.2+/-1.1, significantly higher than norm-based population. Spine BMD and TBS Z-scores exceed-

ing 2SD were present in 44% and in 17%, respectively ($p<0.05$). TBS had no significant correlation with spine BMD. TBS Z-score, but not spine BMD, had a negative correlation with ALP Z-score ($r=-0.47$, $p<0.05$). Neither the proportion of lifetime with treatment nor other biochemical parameters, including Phosphorous Z-score, ALP Z-score, PTH, FGF23 and CTx were associated with TBS index.Conclusions: Our population presents with high lumbar spine BMD and TBS compared to reference data, not associated to exposure to treatment. These findings suggest that elevated spine BMD is not only explained by extra skeletal calcifications and highlight the need of further studies in order to elucidate the high lumbar bone mass phenotype in XLH.

***Disclosures: Pablo Florenzano**, None*

P-029

Correlations Between Preoperative Intact Parathyroid Hormone Levels and Adenoma Volumes Estimated by Ultrasound or Sestamibi Scintigraphy in Primary Hyperparathyroidism *Sandra Haide Aguilar Maciel[1], Aldo Ivan García Contreras[1], Michelle Ninoska García González[1]. [1]Department of Endocrinology, General Hospital of Mexico, Mexico City, Mexico, Mexico

Background: Primary hyperparathyroidism is a common endocrine disorder that can be associated with skeletal complications and nephrolithiasis. Its primary etiology is the parathyroid adenoma which resolves with minimally invasive surgery and requires imaging localization studies such as ultrasound and sestamibi scintigraphy. Purpose:This study aims to determine the association between intact parathyroid hormone levels with the volume of parathyroid adenomas in patients with primary hyperparathyroidism caused by a single adenoma . Methods: Retrospective, observational study, which included 37 patients with primary hyperparathyroidism diagnosed in the endocrinology outpatient clinic of the General Hospital of Mexico during a period of five years between 2013-2018. Serum parathyroid hormone levels were evaluated in all patients before surgery. The volume of parathyroid adenomas was measured by using the formula of a rotating ellipsoid in localization studies performed (ultrasound or sestamibi scintigraphy) before surgery.Results: Thirty seven cases, including 33 females (89%) and 4 males (10.8%) with an average age of 53.6 years (+/-13.21) in which the average parathyroid hormone level preoperatively was 507 pg/ml. A positive correlation was observed between the volume of parathyroid adenomas using ultrasound and parathyroid hormone levels with a correlation coefficient of 0.47 ($p=0.004$). The correlation between the volume of parathyroid adenomas using sestamibi scintigraphy and parathyroid hormone levels was also found positive with a correlation coefficient of 0.55 ($p=0.001$). Additionally, a positive correlation was also observed between the parathyroid hormone levels and the area of the adenoma with a correlation coefficient of 0.53 ($p=0.002$). No correlation existed between serum calcium levels or phosphorus levels and the volume of the adenoma or its area. Although a significant positive correlation was found between the levels of alkaline phosphatase and the volume of parathyroid adenomas with a correlation coefficient of 0.432 ($p=0.012$).Conclusion: Preoperative parathyroid hormone levels have a positive correlation with the volume of parathyroid adenomas using the formula of a rotating ellipsoid in both ultrasound and sestamibi scintigraphy. No correlation was found between preoperative calcium or phosphorus levels and the volume of parathyroid adenomas.

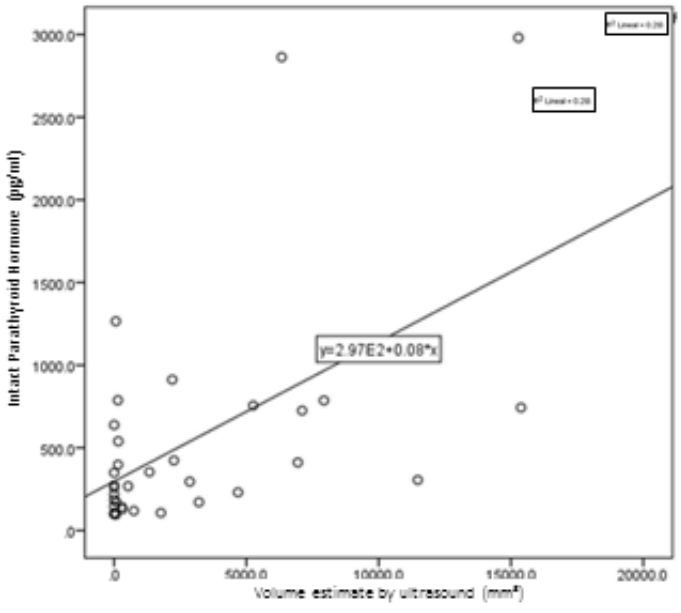

***Disclosures: Sandra Haide Aguilar Maciel**, None*

P-030

Normocalcaemic hyperparathyroidism (NPHPT) and primary hyperparathyroidism (PHPT): Least significant change (LSC) for adjusted serum calcium *MARIAN SCHINI[1], Richard Jacques[2], Eleanor Oakes[3], Nicola Peel[3], Jennifer Walsh[1], Richard Eastell[1]. [1]Department of Oncology and Metabolism, University of Sheffield, UK, United Kingdom, [2]School of Health and Related Research (ScHARR), University of Sheffield, UK, United Kingdom, [3]Sheffield Teaching Hospitals National Health Service Foundation Trust (STH NHS FT), UK, United Kingdom

The least significant change (LSC) is a term used in individuals in order to evaluate whether one measurement has changed significantly from the previous one. It is widely used when assessing bone mineral density (BMD) scans. To the best of our knowledge, there no such estimate available in the literature for patients with disorders of calcium metabolism. Our aim was to provide an estimate of the least significant change in patients with normocalcaemic hyperparathyroidism (NPHPT) and primary hyperparathyroidism (PHPT). Methods: We adjusted total serum calcium for albumin based on an equation derived from our laboratory and used the within-subject standard deviation calculated using the method of Bland and Altman (1996) in a population of NPHPT (n=11) and PHPT (n=17) for our LSC estimation.Results: The LSC for NPHPT and PHPT were found to be 0.25 and 0.24 mmol/L respectively (1.00 and 0.96 mg/dL). Intermittent hypercalcemia was present in 7 of the 11 NPHPT patients and 6 of the 17 PHPT patients. Figure 1 shows the follow-up measurements from a patient with NPHPT (left panel) and PHPT (right panel), both having intermittent hypercalcaemia yet all results falling within the LSC (grey areas).Discussion: The least significant change calculated in this way could be used to interpret the changes in serum adjusted calcium in patients with NPHPT or PHPT.

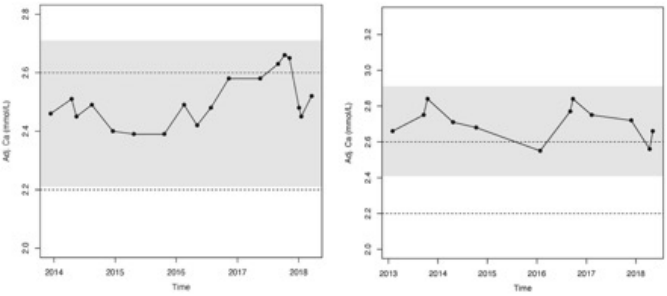

***Disclosures: MARIAN SCHINI**, Roche Diagnostics, Grant/Research Support*

P-031

Changes in Composition of the Gut Microbiota with Correction of Vitamin D Deficiency Using Cholecalciferol or Calcifediol in Young, Healthy Adults *Albert Shieh[1], Sungeun Lee[1], Jonathan Jacobs[1], Carter Gottlieb[1], Venu Lagishetty[1], John Adams[1]. [1]UCLA, United States

Background. Vitamin D may impact gut immune function and gut microbiota composition. We examined whether correcting vitamin D deficiency with cholecalciferol (D3) or calcifediol (25D3) in young, healthy adults changes gut microbiota composition. Methods. 18 adults with 25-hydroxyvitamin D [25D] <20 ng/ml were randomized to 60 mcg / day of D3 or 20 mcg/day of 25D3 for 8 weeks with study visits every 4 weeks. Serum 25D, 1,25(OH)2D (1,25D), and 24,25(OH)2D (24,25D) were assayed using liquid chromatography/tandem mass spectrometry. A vitamin D activation ratio was calculated as the 100*(1,25D/25D. A vitamin D catabolism ratio was calculated as 24,25D/25D. Gut microbiota composition was assessed using 16S rRNA sequencing. α-diversity (within-individual diversity) was examined by species richness (Chao1), phylogenetic diversity (Faith's PD), and species evenness (Shannon Index). β-diversity (between-individual diversity) was assessed using DEICODE. We used a supervised, sparse Partial Least Squares Discrimination Analysis (sPLA-DA) to test for changes in gut microbial composition. Associations of vitamin D metabolites with α-diversity, β-diversity, and individual taxa were assessed using multivariable linear regression or DESeq2. Results. Subjects in D3 and 25D3 groups were similar; mean basal 25D, BMI, and age were 17.2 ng/ml, 26.5 kg/m2 and 29.8 years, respectively. After 8 weeks of D3, mean 25D and 24,25D increased significantly, but mean 1,25D did not (25D: 17.8 to 30.1 ng/ml [$p=0.002$]; 24,25D: 1.1 to 2.7 ng/ml [$p=0.003$]; 1,25D: 49.5 to 53.0 pg/ml [$p=0.9$]). After 8 weeks of 25D3, mean 25D, 24,25D, and 1,25D all increased significantly (25D: 16.7 to 50.6 ng/ml [$p<0.0001$]; 24,25D: 1.3 to 6.2 ng/ml [$p=0.0001$]; 1,25D: 56.5 to 74.2 pg/ml [$p=0.05$]). 25D and 24,25D were greater at weeks 4 and 8 in the 25D3 group. Gut microbial α-diversity did not change with D3 or 25D3 supplementation. There was a trend towards change in gut microbial β-diversity with D3 or 25D3 supplementation (groups pooled) ($p=0.09$), but there were no clustering or taxonomic profile changes specific to supplement type. In sPLA-DA, there was a shift in some taxa after 4 weeks of D3 or 25D3 (groups pooled) that did not persist to week 8 (Figure). Vitamin D metabolites, activation and catabolism ratios were not associated with gut microbiota composition.Conclusion. D3 and 25D3 supplementation in vitamin D deficient, young, health adults did not change gut microbial composition.

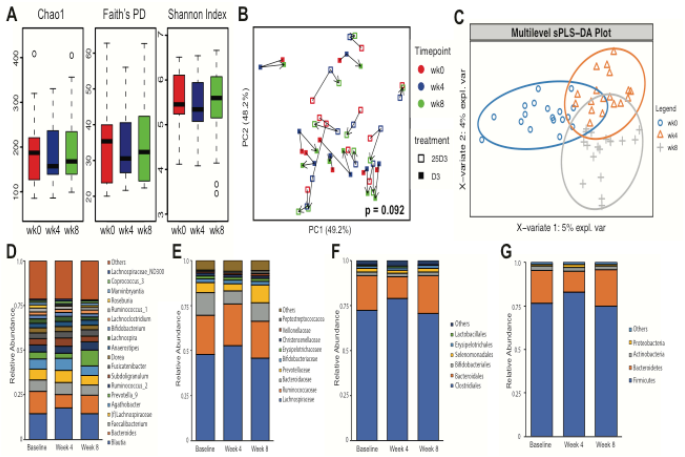

***Disclosures: Albert Shieh**, None*

P-032

Vitamin D Metabolism after PTH Therapy in Hypoparathyroidism *Isabelle Piec[1], Chloe Simper[1], Jeremy Turner[2], William D. Fraser[1]. [1]University of East Anglia, United Kingdom, [2]Norwich and Norfolk University Hospital, United Kingdom

Chronic hypoparathyroidism (hypoPT) is a rare disease characterized by insufficient parathyroid hormone (PTH) production/secretion, usually secondary to damage or removal of the parathyroid glands during head and neck surgery and often associated with hypocalcaemia and other clinical findings.Until recently, standard therapy for this disorder consisted of calcium and vitamin D analog supplementation frequently associated with hypercalciuria, potentially resulting in long-term renal complications such as nephrocalcinosis, nephrolithiasis, and renal insufficiency.Recently, it has been shown that daily subcutaneous doses 20µg of recombinant human PTH(1-34) or 50-100 µg rhPTH(1-84) (NatPar), were effective in maintaining serum calcium concentrations and enabling significant decreases in vitamin D analog and oral calcium doses.We present preliminary data from a follow-up study, comparing vitamin D metabolism in patients on standard treatment (n=7) vs PTH (n=7). Group comparison was performed for adjusted calcium (ACa), phosphate (PO4), 25(OHD), 1,25(OH)2D and 24,25(OH)2D using a Mann Whitney U tests (IBM SPSS version 25.0.0.1) at baseline and after 2, 4, 6, 8, 12 and 16 weeks of either treatment. Within group comparison were performed using ANOVA with Bonferroni post-hoc using SPSS.ACa, PO4 and 25(OH) D did not show any significant differences between the two treatments at any time point. In both cases. ACa increased within the reference range (2.1-2.5 mmol/L) and PO4 decreased to mid reference range (0.8-1.5 mmol/L). 25(OH)D concentrations decreased while those of the active form 1,25(OH)2D increased from baseline when treated with PTH achieving significant difference after 16 weeks of daily injections of PTH. 24,25(OH)2D was significantly decreased in patients treated with PTH, resulting in a significant ($p<0.05$ after 8 weeks of treatment) difference of the ratios 25:24,25 and 1,25:24,25 vitamin D, while standard treatment with calcium and vitamin D showed no significant effect on these ratios.In patients with HypoPT, daily injection of PTH induced a significant (ANOVA, $p<0.05$) increase of 1,25(OH)2D concentrations, by activating 1-alpha hydroxylase (CYP27B1) in the kidney and by decreasing the degradation of 25(OH)D to 24,25(OH)2D by CYP24A1. Lower concentrations of 24,25(OH)2D may also increase the number of available vitamin D receptors for 1,25(OH)2D resulting in beneficial effects such as faster and greater decrease of PO4 and increase of ACa.Chronic hypoparathyroidism (hypoPT) is a rare disease characterized by insufficient parathyroid hormone (PTH) production/secretion, usually secondary to damage or removal of the parathyroid glands during head and neck surgery and often associated with hypocalcaemia and other clinical findings.Until recently, standard therapy for this disorder consisted of calcium and vitamin D analog supplementation frequently associated with hypercalciuria, potentially resulting in long-term renal complications such as nephrocalcinosis, nephrolithiasis, and renal insufficiency.Recently, it has been shown that daily subcutaneous doses 20 µg of recombinant human PTH(1-34) or 50-100 µg rhPTH(1-84), (NatPar) were effective in maintaining serum calcium concentrations and enabling significant decreases in vitamin D analog and oral calcium doses.We present preliminary data from a follow-up study, comparing vitamin D metabolism in patients on standard treatment (n=7) vs NatPar (n=7). Group comparison was performed for adjusted calcium (ACa), phosphate (PO4), 25(OHD), 1,25(OH)2D and 24,25(OH)2D using a Mann Whitney U tests (IBM SPSS version 25.0.0.1) at baseline and after 2, 4, 6, 8, 12 and 16 weeks of either treatment. Within group comparison were performed using ANOVA with Bonferroni post-hoc using SPSS.ACa, PO4 and 25(OH) D did not show any significant differences between the two treatments at any time point. In both cases. ACa increased within the reference range (2.1-2.5 mmol/L) and PO4 decreased to mid reference range (0.8-1.5 mmol/L). 25(OH)D concentrations decreased while those of the active form 1,25(OH)2D increased from baseline when treated with PTH achieving significant difference after 16 weeks of daily injections of PTH. 24,25(OH)2D was significantly lowered in patients treated with PTH, resulting in a significant ($p<0.05$ after 8 weeks of treatment) difference of the ratios 25:24,25 and 1,25:24,25 vitamin D, while standard treatment of calcium and vitamin D showed no significant effect on these ratios.In patients with HypoPT, daily injection of PTH induced significant (ANOVA, $p<0.05$) increased of 1,25(OH)2D concentrations, by activating 1-alpha hydroxylase (CYP27B1) in the kidney thereby decreasing the degradation of 25(OH)D to 24,25(OH)2D by CYP24A1. Lower concentrations of 24,25(OH)2D may also increase the number of available vitamin D receptors for 1,25(OH)2D resulting in beneficial effects such as faster and greater decrease of PO4 and increase of ACaChronic hypoparathyroidism (hypoPT) is a rare disease characterized by insufficient parathyroid hormone (PTH) production/secretion, usually secondary to damage or removal of the parathyroid glands during head and neck surgery and often associated with hypocalcaemia and other clinical findings.Until recently, standard therapy for this disorder consisted of calcium and vitamin D analog supplementation frequently associated with hypercalciuria, potentially resulting in long-term renal complications such as nephrocalcinosis, nephrolithiasis, and renal insufficiency.Recently, it has been shown that daily subcutaneous doses 20µg of recombinant human PTH(1-34) or 50-100 µg rhPTH(1-84) (NatPar), were effective in maintaining serum calcium concentrations and enabling significant decreases in vitamin D analog and oral calcium doses.We present preliminary data from a follow-up study, comparing vitamin D metabolism in patients on standard treatment (n=7) vs PTH (n=7). Group comparison was performed for adjusted calcium (ACa), phosphate (PO4), 25(OHD), 1,25(OH)2D and 24,25(OH)2D using a Mann Whitney U tests (IBM SPSS version 25.0.0.1) at baseline and after 2, 4, 6, 8, 12 and 16 weeks of either treatment. Within group comparison were performed using ANOVA with Bonferroni post-hoc using SPSS.ACa, PO4 and 25(OH) D did not show any significant differences between the two treatments at any time point. In both cases. ACa increased within the reference range (2.1-2.5 mmol/L) and PO4 decreased to mid reference range (0.8-1.5 mmol/L). 25(OH)D concentrations decreased while those of the active form 1,25(OH)2D increased from baseline when treated with PTH achieving significant difference after 16 weeks of daily injections of PTH. 24,25(OH)2D was significantly decreased in patients treated with PTH, resulting in a significant ($p<0.05$ after 8 weeks of treatment) difference of the ratios 25:24,25 and 1,25:24,25 vitamin D, while standard treatment with calcium and vitamin D showed no significant effect on these ratios.In patients with HypoPT, daily injection of PTH induced a significant (ANOVA, $p<0.05$) increase of 1,25(OH)2D concentrations, by activating 1-alpha hydroxylase (CYP27B1) in the kidney and by decreasing the degradation of 25(OH)D to 24,25(OH)2D by CYP24A1. Lower concentrations of 24,25(OH)2D may also increase the number of available vitamin D receptors for 1,25(OH)2D resulting in beneficial effects such as faster and greater decrease of PO4 and increase of ACa.

***Disclosures: Isabelle Piec**, None*

P-033

Analysis of Parathyroid Treatment in Murine Studies *Laura Zweifler[1], Amy Koh[2], Stephanie Daignault-Newton[2], Laurie McCauley[2]. [1]University of Michgian, United States, [2]University of Michigan, United States

Parathyroid hormone (PTH) is produced by the parathyroid glands in response to low serum calcium concentrations where it targets bone, kidneys, and intestines. The N-terminus of PTH has been investigated over decades for its ability to stimulate bone formation when administered intermittently and is used clinically as an effective anabolic agent for the treatment of osteoporosis. Despite great interest in PTH and its clinical use, the mechanisms of action remain complicated and continues to be an interest for researchers. Data was compiled from twenty years of studies that have used PTH in murine models with a focus on anabolic actions in the trabecular compartment. In total, 103 studies were included that reported an anabolic dose of PTH. The data was stratified based on gender (male, female, or both), bone site (tibia, femur, vertebrae), days per week of treatment (5-5.5 days or 7 days), age at the start of treatment (0-2 weeks, 4-8 weeks, 9-10 weeks, 11-12 weeks, or >12 weeks), duration of treatment (<4 weeks, 4 weeks, 5-6 weeks, or 7-12 weeks), and dose of PTH (11 weeks. Additionally, PTH had a greater anabolic effect when administered for a duration of 5-6 weeks compared to all other timepoints. This analysis provides critical insight for improved future study design and interpretation.

***Disclosures: Laura Zweifler**, None*

P-034

Calcium-phosphorus Metabolism In Patients With Cushing's Disease *Alexandra Povaliaeva[1], Ekaterina Pigarova[1], Artem Zhukov[1], Larisa Dzeranova[1], Larisa Nikankina[1], Liudmila Rozhinskaya[1]. [1]Endocrinology Research Centre, Moscow, Russia, Russian Federation

Objective: to study the response of calcium-phosphorus metabolism to the cholecalciferol loading dose in patients with an active Cushing's disease in comparison with healthy individuals.Materials and methods: The study included 12 patients (10 female and 2 male) with an active Cushing's disease, median age 39.7 [37.5;47.3] years, BMI 31.3 [27.6;33.1] kg/m2, 25(OH)D level 13.3 [7.8;18.7] ng/ml (immunochemiluminescent method, DEQAS certified), as well as 13 conditionally healthy individuals. The groups did not differ significantly in age, sex, BMI and level of 25(OH)D. All participants were tested for PTH, total and ionized calcium, albumin, magnesium and creatinine blood levels as well as calcium- and phosphorus-creatinine ratio in single void urine before oral administration of 150 000 IU of an aqueous solution of cholecalciferol and 1, 3, 7 days after administration.Results: In the Cushing's disease group we observed higher levels of ionized calcium at all points ($p<0.05$) and higher levels of magnesium on the 3rd and 7th day ($p<0.05$), lower phosphorus levels on

the 7th day (p<0.05). We also observed non-significant trends for higher levels of baseline albumin-adjusted serum calcium (p=0.07) and on day 1 (p=0.06), lower levels of baseline serum albumin (p=0.06), higher levels of PTH on the 3rd day (p=0.07).In the Cushing's disease group phosphorus levels increased by day 1 after taking a loading dose of cholecalciferol (p=0.04) and later decreased from day 3 to day 7 (p=0.04); levels of albumin-adjusted serum calcium decreased from day 1 to day 7 (p=0.03). In the control group we observed a significant increase in ionized calcium by day 3 (p=0.008), as well as a decrease in serum albumin by day 3 (p=0.03), followed by an increase by day 7 (p=0.01).In the Cushing's disease group magnesium levels showed significant negative correlation with total calcium levels at all points, as well as with ionized calcium levels at baseline and on day 7, with albumin-adjusted serum calcium at baseline, on day 1 and 7 (p<0.05). In the control group there were no such associations.Conclusion: the observed changes in calcium-phosphorus metabolism in patients with Cushing's disease are probably associated with magnesium-mediated prevention of an increase in blood calcium level, followed by an increase in PTH secretion, which led to a decrease in blood phosphorus. More studies are needed to characterize the observed changes accurately, including vitamin D metabolites.

***Disclosures: Alexandra Povaliaeva**, Russian Science Foundation (project No. 19-15-00243), Grant/Research Support*

P-035

Post-surgical permanent hypoparathyroidism: can we anticipate it? A cohort study *Giselle A Mumbach[1], Romina Speroni[1], Elbio Genovesi[1], Mariana González Pernas[1], Ana Paula Lisdero[1], María Jimena Otero[1], Ana Segarra[1], María Laura García[1]. [1]Sanatorio Dr Julio Méndez, Argentina

Introduction: Hypoparathyroidism (HypoPTH) is a disease manifested by hypocalcemia, hyperphosphatemia and inappropriate or low level of Parathyroid hormone (PTH). Common causes are thyroid or parathyroid surgery. HypoPTH could be classified: permanent (P) or transient (T). P-HypoPTH is the feared complication associated with high morbidity in follow-up . Recognize which patient has a higher risk to develop this unwanted complication will help us to achieve an earlier and prompt treatment.Objectives: Predict P-HypoPTH in post-surgical (PS) patients obtaining a cut-off value before 6 months follow-up.Methods: PS patients from Endocrinology Registry of Sanatorio Dr. Julio Méndez were retrospectively follow-up for 12 months. We defined P-HypoPTH as hypocalcemia and inadecuated or low PTH for more than 6 months post surgery. Calcium (Ca), PTH, phosphorous (P), vit D, magnesium and requirement of supplementation were measured a day after, a week and every three months. Two groups were formed and compared by Mann Whitney U Test, logistic regression, univariate and multivariate lineal regressions were performed as well as ROC curves and Logistic ROC curves. Data is expressed by variable distribution, OR with CI95%. p<0,05 is considered significant.Results: Seventy two patients were included. Logistic regressions and ROC curves were performed in order to find a predictable variable Table1.After several ROC curves we've determined a predictive diagnostic triad for P-HypoPTH: week ca level of 8.9mg/dl under >=3grams of calcium supplements + 3rd month P level >4mg/dl; reporting S-E of 86-78% respectively AUC: 0,87 Conclusion: P-HypoPTH is an unwanted PS complication. Identifying a predictive data to determine which patient is at a higher risk to develop it will help us improve and quicken treatment response. We've found multiple risk variables and propose a diagnostic triad constructed by: Week ca level of 8.9mg/dl under >=3grams of calcium supplements and 3rd month P level >4mg/dl, but further studies with a larger number of patients is needed to confirm or improve our findings adding a better sensitivity and specificity.

	OR	CI95%	S%	E%	p
PS Trousseau	7	1,4-35	50	87,5	0,019
Week ca treatment	1,9	1,2-3	53	85	0,007
Week calcitriol treatment	19	2-192	33	96	0,012
3rd month P	6,3	2-21	61,1	81,25	0,002
3rd month ca treatment	4,5	1,8-11	76,5	89,5	0,001
3rd month calcitriol treatment	389	3,5-4366	69	81,25	0,013
6th month P	7,6	1,3-44	64,3	73,3	0,022

***Disclosures: Giselle A Mumbach**, None*

P-036

Aldosterone is positively associated with circulating FGF23 levels in chronic kidney disease across four species, but does not drive FGF23 secretion directly *Judith Radloff[1], Maximilian Pagitz[1], Olena Andrukhova[1], Rainer Oberbauer[2], Iwan Burgener[1], Reinhold Erben[1]. [1]Veterinary University of Vienna, Austria, [2]Medical University of Vienna, Austria

Chronic kidney disease (CKD) is accompanied by increases in circulating fibroblast growth factor 23 (FGF23) and aldosterone levels. The mechanism underlying increased secretion of intact FGF23 from the skeleton in CKD still remains enigmatic. Here, we tested the hypothesis that aldosterone may be one of the driving forces behind increased FGF23 secretion in CKD. Using data from a prospective study in humans (n = 14), a retrospective study in cats and dogs (n = 21 and 17), and an experimental study in 5/6-nephrectomized (5/6-Nx) mice (n = 45), we analyzed the relationship between circulating intact FGF23 and serum aldosterone levels in CKD across four species. To assess the effects of acute inhibition of aldosterone signaling on circulating FGF23, we treated mice with established CKD with the mineralocorticoid receptor blocker canrenone (50 mg/kg iv) and measured intact FGF23 before and 24 h after administration of the drug. As expected, serum intact FGF23 was closely associated with serum creatinine in human, canine, and feline CKD patients as well as in 5/6-Nx mice (humans: Spearman rank correlation coefficient rS = 0.60, p = 0.0195; dogs: rS = 0.74, p < 0.0001; catS: rS = 0.70, p < 0.0001; mice: rS = 0.62, p < 0.0001), underscoring the tight association between elevated serum intact FGF23 and declining renal function across all four species tested. Interestingly, we found a strikingly close association between circulating intact FGF23 and serum aldosterone in human, canine, and feline CKD patients, as well as in experimental murine CKD (humans: rS = 0.58, p = 0.0368; dogs: rS = 0.66, p = 0.0019; cats: rS = 0.72, p = 0.0016; mice: rS = 0.49, p = 0.0004). However, injection of canrenone in 5/6-Nx mice, 14 weeks postsurgery, did not lead to changes in the elevated intact FGF23 blood levels within 24 h post-injection. Hence, despite the tight positive association between circulating intact FGF23 and aldosterone in human, canine, and feline CKD patients as well as in experimental CKD models, the increased levels of circulating aldosterone in CKD are not directly driving FGF23 secretion.

***Disclosures: Judith Radloff**, None*

P-037

Differences in Material Properties of Trabecular Bone Tissue from Modeling- and Remodeling-Based Bone Formation in Rats *Xiaowei Sherry Liu[1], Wei-Ju Tseng[1], Wenzheng Wang[1], Hongbo Zhao[1], Alexander Bennett[2], Lisa Mariani[2], Yihan Li[1], Tala Azar[1], Nathaniel Dyment[1], Do-Gyoon Kim[3], Kevin Turner[2]. [1]McKay Orthopaedic Research Laboratory, Department of Orthopaedic Surgery, Perelman School of Medicine, University of Pennsylvania, United States, [2]Department of Mechanical Engineering and Applied Mechanics, University of Pennsylvania, United States, [3]College of Dentistry, Division of Orthodontics, The Ohio State University, United States

Activation of modeling-based bone formation (MBF), i.e., bone formation (BF) on quiescent surfaces, has been identified as an important mechanism by which anabolic agents, e.g. PTH1-34, rapidly elicit new BF. However, the quality of the bone tissue generated from MBF vs. remodeling-based BF (RBF, BF coupled with osteoclast resorption) is unclear. To identify MBF and RBF, we injected calcein (green, G), alizarin complexone (red, R), and tetracycline (yellow, Y) fluorochrome labels to 7-mo-old female rats (n=5-6/group) in a G-R-Y-G sequence on days -2, 5, 12, and 19 (PTH 20μg/kg on days1-21), followed by euthanasia on day 84. Based on fluorochrome labels, cement lines, and collagen fiber alignment under fluorescence and second harmonic generation (SHG) microscopes, BF sites were identified as MBF (smooth cement line and uniform collagen fibers) or RBF (scalloped cement line with interrupted surrounding collagen fibers) on the 3-mm-thick PMMA sections of the rat tibia (Fig A-C). We hypothesize that the homogeneous collagen structure of MBF may lead to reduced heterogeneity of tissue material properties when compared to RBF.Compared to VEH, PTH treatment led to marked increases in both MBF- and RBF-induced mineralizing surface (MS/BS, Fig H). MS/BS was 136% greater for MBF vs. RBF with no difference in mineral apposition rate (MAR, Fig H). Nano-indentation tests were performed on PTH-treated specimens (10+/-2 MBF and 9+/-2 RBF sites per specimen) where BF sites were labeled with all 4 markers (G-R-Y-G, tissue age 10-12 wks, ~90% of BF sites). At each BF site, individual indents were performed first on the pre-existing bone, then on the MBF or RBF site, and lastly on the PMMA as internal controls (Fig D-G). While no difference in elastic modulus (E) or hardness (H) was found between MBF and RBF, both MBF and RBF had lower E (19% and 21%) and H (25% and 23%) vs. pre-existing bone (Fig I). Surprisingly, the full width at half maximum (FWHM) in E (EFWHM) of MBF was 27% and 28% greater vs. that of RBF and pre-existing bone, respectively, indicating increased heterogeneity in MBF. Similar results were also found for the coefficient of variance (CV) of E (ECV) and H (HCV).Our findings indicate greater heterogeneity in nano-scale E and H in bone tissue from MBF than those from RBF and pre-existing bone, rejecting our original hypothesis. Our results suggest that targeting MBF not only maximizes the net bone mass increase, but also leads to higher tissue heterogeneity.

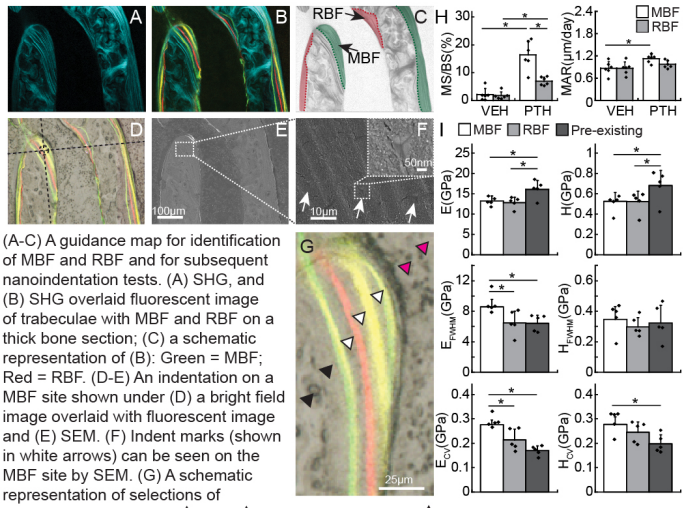

(A-C) A guidance map for identification of MBF and RBF and for subsequent nanoindentation tests. (A) SHG, and (B) SHG overlaid fluorescent image of trabeculae with MBF and RBF on a thick bone section; (C) a schematic representation of (B): Green = MBF; Red = RBF. (D-E) An indentation on a MBF site shown under (D) a bright field image overlaid with fluorescent image and (E) SEM. (F) Indent marks (shown in white arrows) can be seen on the MBF site by SEM. (G) A schematic representation of selections of indentation locations on △MBF, ▲pre-existing bone, and ▲PMMA. (H) MS/BS and MAR of MBF and RBF in response to VEH and PTH, *: p<0.05 by two-way ANOVA with Bonferroni corrections. (I) Comparisons of material properties between MBF, RBF, and pre-existing bone tissue. *: p<0.05 by one-way ANOVA with Bonferroni corrections.

***Disclosures: Xiaowei Sherry Liu**, None*

P-038

Whole bone geometry effects on functional compensation in the radius

*Randee Hunter[1], Karen Briley[2], Amanda Agnew[1]. [1]The Ohio State University; Skeletal Biology Research Laboratory, United States, [2]Wright Center of Innovation in Biomedical Imaging, United States

Fracture prediction requires an understanding of multiple contributors to strength augmented by using a systems approach. Functional compensation has been demonstrated in the tibia suggesting a coupling of the amount of bone and its mineralization. Furthermore, whole bone geometry has been shown to affect age-related changes in the radius. The purpose of this study is two-fold: investigate functional compensation trends as well as quantify effects of whole bone geometry on these trends in the radii of males and females. Quantitative computed tomography (QCT) was performed on bilateral radii (n=286) from post-mortem human subjects (n=92 males; n=51 females) ranging in age from 35-98 years at 50% and 30% of total length (Le). Robustness (Tt.Ar/Le), a measure of whole bone geometry, and vBMD were quantified at each location. No significant side differences (p>0.05) were found. Data were analyzed by sex as well as divided into "slender" and "robust" groups using height-adjusted Tt.Ar/Le values. Tt.Ar/Le and vBMD were significantly different (p<0.01) between 30 and 50% (whether analyzed by sex or group) such that an inverse relationship indicates functional compensation where mineralization is increased in areas with less bone. After controlling for age, significant correlations between Tt.Ar/Le and vBMD were found in males (p=0.01, r=-0.13) and females (p=0.01, r=0.18). Robust radii demonstrated a significant negative correlation (p<0.01, r=-0.19) whereas, there was no relationship in slender radii (p=0.68). Further investigation of sex-specific effects within each size group found only slender males (n=35) exhibited a significant inverse correlation (p=0.02, r=-0.21). Slender females (n=37) had a non-significant correlation within the radius and a positive trend (p=0.2, r=0.11) similar to trends seen in the female only group. Although the inverse relationship between variables in robust radii seem to demonstrate functional compensation, neither robust males (n=57) nor robust females (n=13) had significant correlations when considered separately despite obvious inverse trends (males r=-0.09; females r=-0.18). To maintain function, bone has the ability to synchronously alter features in response to age-related changes through mechanisms influenced by whole bone geometry. These results suggest functional compensation may occur differently depending on whole bone geometry likely mediated by sex-specific differences.

***Disclosures: Randee Hunter**, None*

P-039

Identifying Components of the Gut Microbiome that Regulate Bone Tissue Mechanical Properties

*Marysol Luna[1], Jason Guss[1], Laura Vasquez-Bolanos[1], Macy Castaneda[1], Manuela Vargas Rojas[1], Jasmin Strong[1], Denise Alabi[1], Sophie Dornevil[1], Erik Taylor[1], Rodrigo Bicalho[1], Eve Donnelly[1], Christopher Hernandez[1]. [1]Cornell University, United States

Modifications to constituents of the gut microbiome can influence bone density and tissue strength, but the specific microbes that influence bone are not known. Here we use narrow spectrum oral antibiotics to selectively "knock out" distinct parts of the gut microbiota to help isolate the organisms responsible for modifications in bone tissue quality and strength.Under IACUC approval, male C57Bl/6 mice were divided into groups receiving oral treatment from 4-16 weeks of age to remove some or all of the gut microbial organisms as follows (n=7-10/group, 57 total): 1) ampicillin; 2) neomycin; 3) vancomycin; or 4) metronidazole; 5) a cocktail of all 4 antibiotics with aspartame sweetener to remove 99% of gut microbes; 6) sweetener only control; and 7) an untreated control. Femora were collected, submitted to micro-CT for microarchitecture analysis, and tested in 3-point bending to determine whole bone strength. Tissue composition was obtained with FTIR spectroscopy. Taxonomic composition of the gut microbiota was determined by 16S rRNA sequencing and a subsequent PICRUSt analysis was used to predict the functional capacity of the gut microbiota.After accounting for differences in geometry, bone strength was reduced in the neomycin group (p=0.002, Fig.1A) as was the tissue mineral:matrix ratio (Fig.1B). Taxonomy did not indicate differences between the neomycin and untreated groups (the vancomycin and sweetener groups differed from untreated, Fig.1C). However, the predicted functional capacity of the gut microbiota in the neomycin group showed reduced ability to synthesize vitamin K (43.2 +/- 27.1% less than untreated animals). The sweetener only group showed increase tissue strength and metaphyseal bone volume fraction (Fig.1A,1D). This unexpected finding in the sweetener group suggests that sweeteners commonly used in microbiome studies may influence bone.Changes in the constituents of the gut microbiome caused by neomycin led to alterations in bone tissue strength. Our findings illustrate how taxonomy (which species are present, determined with 16S rRNA sequencing) may not be as good at explaining microbiome-induced phenotypes as microbial functional capacity (which genes are present), which requires more expensive metagenomic sequencing. Furthermore, our findings are consistent with the idea that microbiome-derived vitamin K can influence bone tissue strength, possibly by modulating vitamin K dependent bone matrix proteins such as osteocalcin.

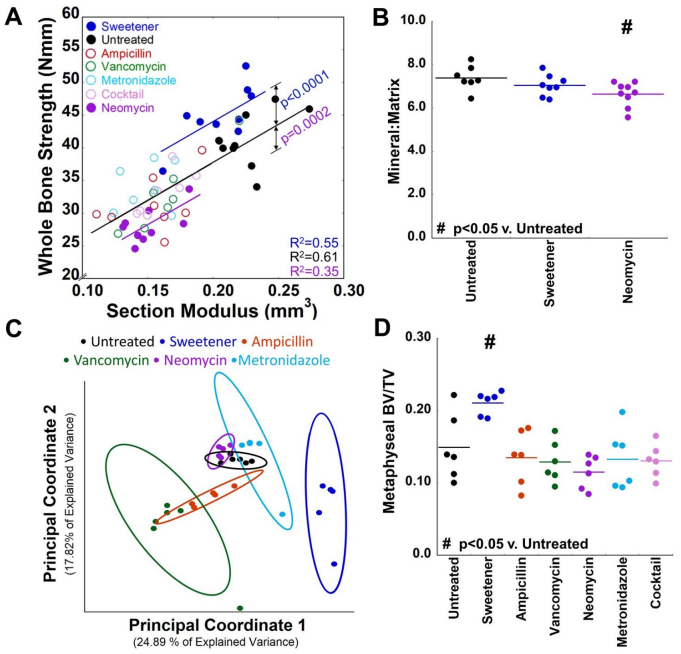

Fig 1. A) Alterations to the gut microbiota caused by neomycin reduced whole bone strength more than expected from changes in geometry (see different regression lines). Tissue strength increased in the sweetener group. B) Mineral to matrix ratio was reduced in the neomycin group. C) Principal coordinate analysis of the gut microbiota using unweighted UniFrac distance shows that vancomycin and sweetener groups are distinct from others (95% confidence ellipses). D) Bone volume fraction in the distal femoral metaphysis was increased in the sweetener group.

***Disclosures: Marysol Luna**, None*

P-040

Investigation of human trabecular bone quality in osteoporosis with and without type 2 diabetes

*Praveer Sihota[1], Ram Naresh Yadav[1], Ruban Dhaliwal[3], Jagadeesh Boss[3], Vandana Dhiman[4], Deepak Neradi[3], Shailesh Karn[3], Sidhartha Sharma[5], Sameer Aggrawal[6], Vijay Goni[6], Vishwajeet Mehandia[7], Deepak Vashishth[8], Sanjay Bhadada[9], Navin kumar[10]. [1]PhD student, India, [3]MD, United States, [3]MD, India, [4]PhD, India, [5]Assistant Professor, Orthopedicas, PGIMER Chandigarh, India, [6]Professor, orthopedics, PGIMER, India, [7]Assistent Professor, IIT Ropar, India, [8]Professor, RPI, United States, [9]Professor,Endocrinology, PGIMER, India, [10]Associate proffesor, IIT Ropr, India

Purpose: Individuals with type 2 diabetes (T2D) have a two to three-fold greater hip fracture risk than those without diabetes despite normal to high areal bone mineral density (aBMD). Mechanisms underlying diabetic skeletal fragility are poorly understood, making the clinical identification of those at risk for fractures difficult. Poor bone quality has been implicated in diabetic skeletal fragility but its role in altering the biomechanical proper-

ties, associated with fracture due to lack of glycemic control over an extended period (>5 yrs.), at the microstructural and bone matrix levels is not established.Method: Bone samples were taken from two groups of patients who were undergoing total hip replacement for low-energy hip fractures. These include patients without diabetes (n=40) and those with diabetes (n=30) of duration >5 years. The mean age of the diabetic and non-diabetic group was 67.8+/-9.2 and 71.2+/-10.8 years respectively. The mean duration of diabetes was 7.5 +/-2.8 years. None of the patients had a history of hip fracture. The study was approved by the Institutional Ethics Committee (PGI/IEC/2015/171) of PGIMER, Chandigarh.Results: Baseline characteristics were similar for both groups. The bone quality parameters were found to be degraded in the diabetic group whereas no significant difference was observed in aBMD. Bone volume fraction was lower for the diabetic group than for non-diabetic group due to fewer and thinner trabeculae. Apparent-level (strength) and tissue-level (nanoindentation determined) modulus and hardness were lower in those with diabetes. Compositional differences between the non-diabetic and diabetic groups included lower mineral to matrix ratio, wider mineral crystals and bone collagen modifications assessed as higher total fluorescent advanced glycation end-products (fAGEs) and non-enzymatic cross-link ratio (NE-xLR), lower enzymatic cross-link ratio (E-xLR) and altered secondary structure (Amide I and II bands). NE-xLR was strongly and negatively correlated with post-yield-strain, and fAGE was strongly and negatively correlated with post-yield-strain energy and toughness. These bone quality changes directly explain enhanced bone fragility in T2D.Conclusions: Our findings provide evidence of the detrimental effects of diabetes on trabecular bone quality at multiple scales due to lack of glycemic control over an extended period (> 5 yrs.) and provide new insight on skeletal fragility in individuals with diabetes.

***Disclosures: Praveer Sihota**, None*

P-041

RAGE Removal in Developing Mice on High-Fat Diet Alters Bone Matrix Quality *Samuel Stephen[1], Stacyann Bailey[1], Divya Krishnamoorthy[2], Danielle D'Erminio[2], James Iatridis[3], Deepak Vashishth[1]. [1]Rensselaer Polytechnic Institute, United States, [2]Ichan School of Medicine at Mount Sinai, United States, [3]Icahn School of Medicine at Mount Sinai, United States

Adolescent obesity, a growing worldwide epidemic, is related to chronic inflammation and elevated fracture risk. Recent work has highlighted that the receptor for advanced glycation end products (RAGE), a key inflammatory mediator, affects bone metabolism. RAGE is believed to control reactive oxygen species synthesis, which is linked to matrix damage. Yet, the effect of RAGE on matrix quality in obese patients remains unknown. This study aimed to delineate how matrix quality is mediated by RAGE in obesity. We hypothesized that RAGE removal challenged with obesity would help retain bone matrix quality.Six-week old C57BL/6J (WT) and RAGE knockout littermates (KO, n=36; 50% Female/50% Male) were fed either a low fat (LF, 10% kcal) or high fat (HF, 60% kcal) diet for 12 weeks starting at 6 weeks of age. Tibiae and humeri (n=9/group) were excised at 18 weeks of age. Humeri were notched at diaphysis and loaded to failure in three-point bending to evaluate fracture toughness. Tibiae were scanned for cortical morphology with µCT and imaged with confocal Raman to assess matrix chemical composition. Two-factor ANCOVA with Tukey post-hoc test was used to identify any significant ($p<0.05$) differences between WT and KO groups with body mass normalized. WT HF and KO HF females displayed reduced tibial cortical area, cortical thickness, and BMD over respective LF littermates (Table 1). No morphological differences were seen in males. Mechanical testing revealed WT HF females had a higher toughening effect over WT LF females, but this diet effect was reversed in the KO female group (Fig. 1A). Raman imaging showed increased mineral-to-matrix ratio in KO groups over WT groups in both sexes (Fig. 1B). Additionally, WT HF females showed high pentosidine (PEN) and carboxymethyl-lysine (CML) over WT LF females that was not observed in KO female groups (Fig. 1C-D).The effects of HF diet on biomechanical properties seen in WT females were reversed in the RAGE KO group, implying that RAGE alters diet affects bone quality in a sex dependent manner. Compared to WT controls, RAGE KO groups displayed enhanced mineral-to-matrix ratio but attenuated glycoxidative and glycation-based damage in the bone matrix, seen by reduced CML and PEN. Thus, ablation of RAGE conserves bone quality despite degraded geometry and BMD. Therapeutic targeting of RAGE may have a promising role in reducing fracture risk in the obese population through management of bone quality.

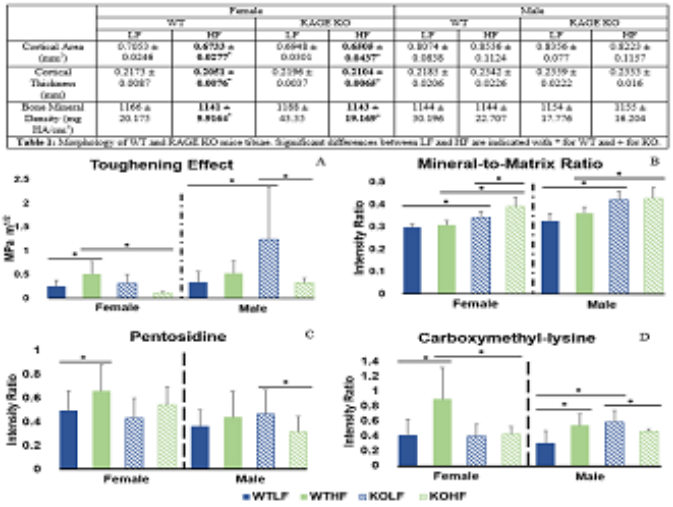

Figure 1: Data illustrated as mean ± standard deviation. WT HF females displayed higher toughening effect (A), pentosidine (PEN, C) and carboxymethyl-lysine (CML, D) over WT LF littermates, but RAGE KO reduced these effects. These parameters were higher in KO LF males and HF diet lowered their magnitudes. KO in both LF and HF groups showed higher mineral-to-matrix ratio (B) over WT controls. Lines with * indicate significant difference ($p < 0.05$) between groups.

***Disclosures: Samuel Stephen**, None*

P-042

Changes in Bone Quality after One Year of Teriparatide Treatment *Florence Lima[1], Madhumathi Rao[1]. [1]University of Kentucky, United States

Background: We studied bone biopsies at baseline and after 1 year of treatment with teriparatide (TPD), in patients with low-energy fractures and low bone turnover, to examine the effect of teriparatide on bone quality using Fourier transform infrared spectroscopy (FTIR). FTIR assesses changes in bone mineral and matrix properties and parameters measured are Mineral-to-Matrix ratio (MM), Carbonate-to-Phosphate ratio (CP), Collagen Crosslinks (Cx) and Crystal size (C). Methods: We studied 10 patients who had paired biopsies a year apart. We also evaluated bone mineral density (BMD) by DXA, bone turnover markers (bone specific alkaline phosphatase, n-telopeptide and osteocalcin) at baseline and 1 year. Undecalcified bone biopsies with tetracycline labeling were obtained from iliac crest and evaluated by qualitative histology and quantitative histomorphometry. FTIR results were compared against normal control samples. Results: As expected, DXA results and BV/TV by histomorphometry showed a significant improvement after 1 year of TPD treatment (Lumbar BMD: 8.0+/-3.6%, $P<0.01$ and BV/TV: 50+/-57%, $P<0.05$). Bone turnover markers were significantly increased after 1 year of TPD treatment ($P<0.01$); bone turnover parameters by histomorphometry were also increased but did not reach significance (BFR/BS: 55+/-113%, $P = 0.40$ and Acf: 64+/-106%, and $P = 0.14$). FTIR studies showed that Mineral-to-Matrix ratio and Crystal size were overall increased compared to baseline (MM: 8.1+/-9.6%, $P = 0.03$ and C: 4.9+/-3.5%, $P<0.01$, Fig. 1). At baseline, the overall Mineral-to-Matrix mean was lower than controls (MMbas = 4.16 vs. MMCont = 4.54, $P = 0.08$), while 1 year after TPD treatment, the overall mean values were close to the control mean value (MM1yr = 4.50 vs. MMCont = 4.54, $P = 0.80$). Crystal size parameter increased after 1 year of treatment; the overall mean at baseline was not different from controls (CBas = 1.14 vs. CCont = 1.15, $P = 0.53$, Fig. 1) while 1 year later, the overall mean was significantly higher than controls (C1yr = 1.19 vs. CCont = 1.15, $P = 0.04$, Fig. 1). CP ratio and Cx parameters were not significantly different between baseline and 1 year of TPD treatment ($P = 0.06$ and $P = 0.54$, resp.). Conclusion: Studies on the effect of TPD on bone quality are limited. We show that TPD improves bone quality and microarchitecture by increasing Mineral-to-Matrix ratio and crystal size. This effect occurs in addition to the improvement demonstrated in Bone Volume.

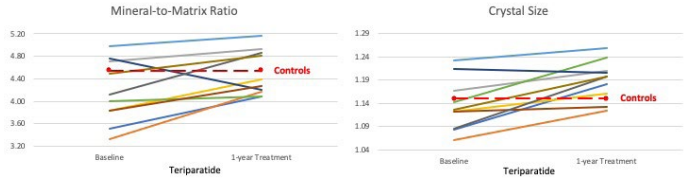

***Disclosures: Florence Lima**, None*

Posters

P-043

One Year of Denosumab after Two Years of Teriparatide in Premenopausal Idiopathic Osteoporosis (IOP): Changes in Skeletal Indices using High Resolution Peripheral Computed Tomography (HR-pQCT) *Sanchita Agarwal[1], Adi Cohen[1], Stephanie Shiau[2], Nayoung Kil[1], Mafo Kamanda-Kosseh[1], Mariana Bucovsky[1], Elizabeth Shane[1]. [1]Division of Endocrinology, Department of Medicine, Columbia University, United States, [2]Department of Biostatistics & Epidemiology, Rutgers School of Public Health, United States

Premenopausal women with IOP (PreMenIOP) have marked deficits in volumetric BMD (vBMD), microstructure and bone strength of the peripheral skeleton by HR-pQCT. We previously reported that 24 months (M) of teriparatide (TPTD) improved trabecular (Tb) microstructure, increased cortical (Ct) area, thickness (Th) and porosity (Po) and estimated bone strength that were more consistent at tibia than radius in 34 women with PreMenIOP. In a subset of 26 TPTD-treated women, we now report sequential treatment with 12M of denosumab (Dmab; 60 mg SC q6M) and overall effect of treatment with 24M TPTD + 12M Dmab. 22 women had complete data at tibia and 14 at radius (7 excluded for motion >3 or corruption). 11 had baseline scans on 1st-(XCT1) and follow-up on 2nd-generation HR-pQCT (XCT2). Common ROI generated by standard 2D matching was analyzed for all 3 visits. XCT2 data were calibrated to XCT1 by regression. Changes after 24M TPTD, 12M Dmab and 24M TPTD + 12M Dmab were analyzed by paired Student's t-tests. Primary outcomes were total, Ct and Tb vBMD, CtPo and stiffness. Tibia: After 24M of TPTD, Tb number (N) increased by 3.1% (Table; p<0.05), CtTh and Po by 2.5% and 18.6%, and stiffness and failure load (FL) by 2.8% and 2.3% respectively (all p<0.01); density measures did not change. After 12M of Dmab, total, Ct and Tb vBMD, Tb BV/TV and CtTh increased by 2.5%, 1.4%, 2.9%, 2.8% and 1.0% (all p<0.01), TbTh and FL increased by 1.5% and 1.1% (both p<0.05); CtPo did not change. Compared to baseline, TPTD+Dmab (24+12M) was associated with higher total vBMD and CtTh (2.4% and 3.6%; p<0.01) and TbN (4.2%; p<0.05). CtPo remained 16.4% above baseline (p<0.01), but stiffness increased by 3.8% (p<0.01). Radius: Despite improvements in Tb microstructure (increased TbN and TbTh, decreased TbSp, p<0.05) during TPTD, total, Ct and Tb vBMD and stiffness did not change. During Dmab, total and Ct vBMD increased by 2.5% and 1.7% (both p<0.01) and CtTh by 1.2% (p<0.05). After TPTD+Dmab, there were increases in total vBMD (1.8%), Tb BV/TV (1.7%), TbN (6.1%) and TbTh (5.1%, all p< 0.05), with no statistically significant increase in stiffness or FL. In summary, we observed that sequential therapy with 24M TPTD + 12M Dmab resulted in improved Tb and Ct microstructure and strength at the tibia and to a lesser extent at the radius, possibly due to lower power in the latter. We hypothesize that Dmab permits bone formed during TPTD to mineralize, thus increasing overall density and strength.

Table: Skeletal indices from HRpQCT presented as Mean (SD) values at Baseline, 24 months of Teriparatide (TPTD) followed by 12 months of Denosumab (Dmab) treatments, * p<0.05 and ** p<0.01.

	Baseline	24M TPTD	12M Dmab	% change Baseline to 24M TPTD	% change 24M TPTD to 12M Dmab	% change Baseline to 36M (24M TPTD + 12M Dmab)
	TIBIA (N=22)					
Tot.vBMD (mgHA/ccm)	243 (51)	243 (53)	249 (52)	0.0 (3.1)	**2.5 (2.0)****	**2.4 (2.9)****
Tb.vBMD (mgHA/ccm)	112 (27)	111 (26)	113 (26)	-1.5 (5.4)	**2.9 (4.2)****	1.2 (5.1)
Tb.BV/TV	0.093 (0.022)	0.092 (0.021)	0.094 (0.022)	-0.7 (5.7)	**2.8 (4.1)****	2 (5.1)
Tb.N (1/mm)	1.59 (0.32)	1.65 (0.35)	1.66 (0.36)	**3.1 (7.9)***	1.2 (4.6)	**4.2 (7.6)***
Tb.Th (mm)	0.064 (0.010)	0.064 (0.008)	0.065 (0.009)	0.2 (5.2)	**1.5 (2.9)***	1.6 (4.9)
Tb.Sp (mm)	0.603 (0.205)	0.601 (0.247)	0.596 (0.232)	-1.2 (6.3)	-0.6 (5.2)	-1.9 (6.4)
Ct.Po (%)	3.4 (1.1)	4.0 (1.1)	3.9 (1.0)	**18.6 (16.0)****	-1.2 (11.5)	**16.4 (15.9)****
Ct.Th (mm)	1.16 (0.23)	1.19 (0.24)	1.20 (0.24)	**2.5 (2.4)****	**1.0 (1.8)****	**3.6 (2.5)****
Ct.vBMD (mgHA/ccm)	873 (60)	865 (58)	877 (52)	-0.9 (2.4)	**1.4 (1.3)****	0.5 (2.2)
Ct.Area (mm2)	98 (16)	100 (17)	101 (16)	**2.6 (2.3)****	**1.3 (2.0)****	**3.9 (2.9)****
Tb.Area (mm2)	526 (130)	522 (130)	521 (129)	**-0.7 (0.5)****	-0.2 (0.4)	**-0.9 (0.5)****
Stiffness (N/mm)	107080 (17312)	110025 (18049)	111134 (18571)	**2.8 (4.8)****	1 (2.8)	**3.8 (4.8)****
Failure Load (N)	4910 (737)	5022 (756)	5078 (767)	**2.3 (3.8)****	**1.1 (2.4)***	**3.5 (4)****
	RADIUS (N=14)					
Tot.vBMD (mgHA/ccm)	259 (71)	258 (71)	264 (69)	-0.6 (2.7)	**2.5 (3.2)****	**1.8 (2.3)***
Tb.vBMD (mgHA/ccm)	107 (33)	107 (33)	108 (33)	-0.3 (3.7)	1.4 (3.9)	1.0 (3.2)
Tb.BV/TV	0.088 (0.026)	0.088 (0.027)	0.090 (0.027)	-0.2 (4)	1.9 (4.1)	**1.7 (3.7)***
Tb.N (1/mm)	1.71 (0.26)	1.79 (0.20)	1.80 (0.22)	**5.8 (9.3)***	0.4 (2.5)	**6.1 (8.6)***
Tb.Th (mm)	0.052 (0.008)	0.054 (0.007)	0.055 (0.007)	**2.6 (4)***	**2.5 (3.8)***	**5.1 (5.8)****
Tb.Sp (mm)	0.547 (0.108)	0.522 (0.078)	0.526 (0.09)	**-3.8 (6.3)***	0.5 (4)	-3.4 (5.9)
Ct.Po (%)	0.9 (0.4)	1.0 (0.4)	1.1 (0.4)	15.0 (39.3)	9.5 (17.9)	24.4 (42.2)
Ct.Th (mm)	0.78 (0.20)	0.78 (0.20)	0.79 (0.19)	0.4 (1.3)	**1.2 (1.6)***	**1.6 (1.5)****
Ct.vBMD (mgHA/ccm)	871 (66)	868 (75)	882 (70)	-0.4 (3.4)	**1.7 (1.3)****	1.2 (3)
Ct.Area (mm2)	44 (9)	44 (10)	45 (9)	**0.7 (1.1)***	**1.3 (1.8)***	**2.0 (1.4)****
Tb.Area (mm2)	187 (40)	186 (39)	186 (39)	**-0.3 (0.4)***	**-0.3 (0.5)***	**-0.6 (0.4)****
Stiffness (N/mm)	40570 (8629)	40869 (8602)	41472 (8137)	0.9 (4.8)	1.7 (3.3)	2.6 (5.2)
Failure Load (N)	1800 (342)	1807 (352)	1835 (325)	0.4 (3.9)	1.9 (3.7)	2.2 (4.3)

***Disclosures: Sanchita Agarwal**, None*

P-044

Age-changes in femoral neck cortical and trabecular traits vary with region and sex *Karl Jepsen[1], Daniella Patton[1], Erin Bigelow[1], Robert Goulet[1], Stephen Schlecht[2], David Kohn[1], Carrie Karvonen-Gutierrez[1], Todd Bredbenner[3]. [1]University of Michigan, United States, [2]Indiana University, United States, [3]University of Colorado Colorado Springs, United States

Hip bone mineral density (BMD) provides a simple measure of femoral neck mass but obscures regional changes in cortical and trabecular structures that contribute to strength decline. Age-related bone loss is thought to occur nonuniformly within the proximal femur with loss in mass of the secondary and tensile arcades preceding that of the compressive arcade. However, these studies were not conducted using high resolution 3D imaging. We mapped cortical and trabecular structure for the femoral neck and tested for regional and sex differences in how structure changed with age.Femoral neck cortical (Ct.BVF) and trabecular bone volume fraction (Tb.BV/TV) were measured for white male (n=50, 18-89 years) and female (n=44, 21-97 years) cadavers using nanoCT (27µm). The femoral neck was divided into 4 cortical and 4 trabecular regions resulting in 8 regions designated as superior-proximal (SP), superior-distal (SD), inferior-proximal (IP), and inferior-distal (ID) for each bone type. There was a significant negative correlation between Tb.BV/TV and age in all regions for females (SP R2=0.30, p<0.001; SD R2=0.27, p<0.001; IP R2=0.11, p=0.026; ID R2=0.17, p=0.005) and males (SP R2=0.16, p=0.004; SD R2=0.18, p=0.003; ID R2=0.17, p=0.003) except for the male IP region (R2=0.04, p=0.173). Regression y-intercepts (p0.4, ANCOVA) differed by sex for all regions, indicating that males had greater Tb.BV/TV than females but that both sexes showed similar rates of Tb.BV/TV loss with age. Males showed nonsignificant age associations with Ct.BVF for all regions (R2=0.002-0.05, p=0.12-0.73). In contrast, females showed significant negative correlations with age in the inferior cortical regions (IP R2=0.24, p<0.001; ID R2=0.13, p=0.016). The slopes of the IP (p<0.001) and ID (p=0.006) regressions differed significantly by sex suggesting that cortical porosity increased in the inferior cortex of females at a faster rate than for males. Regional age-changes in structure were mapped in 3D for the first time revealing similar rates of change in Tb.BV/TV among most regions within the proximal femur and suggesting that bone loss declined more uniformly than expected. Sex differences in cortical bone loss were localized to the inferior cortex where fractures originate. Females had lower Tb.BV/TV across all ages including the compressive arcade; these trabecular losses combined with greater Ct.BVF losses (ie, increased porosity) within the inferior cortex would greatly reduce femoral neck fracture resistance and may contribute to the greater fracture rate of women compared to men.

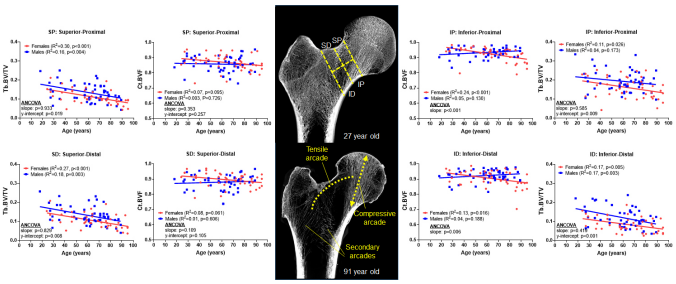

***Disclosures: Karl Jepsen**, None*

P-045

Voluntary Jumping Exercise Pre-Treatment Enhances Cancellous Bone Strength and Density in the Tibia of Hindlimb Unloaded Rats *Scott Lenfest[1], Jon Elizondo[1], Jessica Brezicha[2], Amelia Looper[3], Susan Bloomfield[4], Harry Hogan[1]. [1]Dept. of Mechanical Engineering, Texas A&M University, United States, [2]Dept. of Biomedical Engineering, Texas A&M University, United States, [3]College of Veterinary Medicine, Texas A&M University, United States, [4]Dept. of Health and Kinesiology, Texas A&M University, United States

Resistance exercise is an important component of in-flight countermeasures for mitigating bone loss in astronauts. The hindlimb unloading rat model allows for ground-based study of skeletal effects due to simulated microgravity, but simulating exercise is more challenging in this animal model. The goal of our current study was to assess the efficacy of a voluntary jumping exercise (VJE) protocol that uses positive reinforcement. Adult male rats (5 mo.) were placed in a custom jumping cage and trained over 5 weeks to jump onto a 10" platform. Rats were then assigned to aging control (AC, n=63), hindlimb unloading control (HU, n=27) or exercise (VJE, n=45) groups by body weight and jumping ability. VJE animals performed 30 jumps/d, 5 d/wk, for 4 wks at an average rate of 1 jump each 20-25 sec. After the 28d period, HU and VJE animals did 28d of unloading. In vivo pQCT scans of the proximal tibia metaphysis (PTM) were taken before (d0) and after (d28) VJE pre-treatment, at the end of HU (d56), and at the end of 56d of recovery (d112). Reduced platen compression (RPC) testing was performed on the proximal tibia metaphysis of bones harvested on d28, d56, and d112 to assess cancellous bone. Following exercise (d28), total vBMD was higher (+4.7%) for the VJE group vs. AC. Cancellous vBMD also trended higher for VJE (8.8%) vs. HU. After HU (d56), the VJE group had significantly higher cancellous vBMD (+21.2%) compared to HU. The VJE group maintained significantly higher cancellous vBMD compared to both AC and HU throughout recovery. RPC showed similar results, but the magnitude of difference was much greater. At the end of exercise (d28), the VJE group had higher Ultimate Stress (US, +45%) and Elastic Modulus (EM, 31%) vs. AC, but these differences were not significant. VJE rats had significantly higher US and EM vs. HU at the end of unloading (d56, +239%, +208%, resp.) and at the end of recovery (d112, +107%, +58%, resp.). These data indicate that our new VJE protocol induces an anabolic bone response that conserved bone integrity, particularly in the cancellous compartment, during a subsequent period of disuse. These findings further demonstrate that the magnitude of change in densitometric properties underpredicts the magnitude of change in mechanical properties. The results have important implications for situations when patients

on bed rest or crew members aboard ISS are unable to exercise, as the benefits persist long after cessation of exercise.

***Disclosures: Scott Lenfest**, None*

P-046

Maximizing Precision for Estimated Bone Strength in Longitudinal Analyses by HR-pQCT and the Finite Element Method *Ryan Plett[1], Steven Boyd[2]. [1]Biomedical Engineering Graduate Program, University of Calgary, Canada, [2]McCaig Institute for Bone and Joint Health, Cumming School of Medicine, University of Calgary, Canada

Three-dimensional (3D) imaging with high-resolution peripheral quantitative computed tomography (HR-pQCT) and micro-finite element analysis (μFEA) provides important insight into bone health. Longitudinal analyses of bone morphology maximize precision by using slice-matching or 3D rigid body registration to account for repositioning error between scans. However, the compatibility of these techniques with μFEA for longitudinal bone strength estimates are limited. This study develops and validates a μFEA methodology for HR-pQCT scans using image registration to maximize reproducibility and compares it to current methods.Using a standard imaging protocol, ex vivo HR-pQCT (XtremeCT II, Scanco Medical) distal radius images were acquired for 10 cadaveric specimens in addition to three serial scans of each sample. The intact forearm was repositioned with relative angles (~1o, ~3o, ~6o) simulating a range of typical repositioning errors. Reaction force and failure load were estimated with μFEA (Faim v8.0, Numerics88 Ltd.) for three conditions: non-registered, the current standard slice-matched, and the newly developed 3D registered images. In our proposed method, only the common bone volume across serial scans is used for μFEA. We quantified least significant change (LSC) to estimate the precision of serial measures. Since cadaveric bone was used, the gold-standard was zero change in serial estimates. Comparisons of precision were based on repeated-measures ANOVA ($p<0.05$). Reaction force LSC significantly improved with slice-matching (74.27 N) and 3D registration (51.02 N) compared to non-registered estimates (285.28 N). Similarly, failure load LSC significantly improved with slice-matching (34.63 N) and 3D registration (27.57 N) compared to non-registered estimates (123.96 N). LSCs did not differ significantly between 3D registration and slice-matching; however, at repositioning errors 3o or greater 3D-registered failure load was significantly improved from no registration, but slice-matching was not.We found that μFEA reproducibility improved using both slice-matching and 3D rigid-body image registration, and that 3D registration was advantageous as repositioning error increased. Although 3D registration does not negate motion artifacts and aliasing, it plays an important role in providing the best LSC possible for longitudinal study designs and is ideally suited for estimating in vivo effects of interventions in longitudinal studies of bone strength.

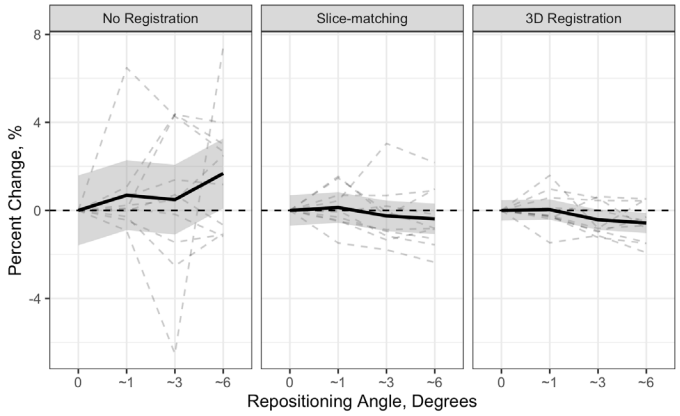

***Disclosures: Ryan Plett**, None*

P-047

Metacarpal strength and porosity predict strength and porosity at other skeletal sites in a sex-specific manner *Erin Bigelow[1], Daniella Patton[1], Bonnie Brooker-Nolan[1], Antonio Ciarelli[1], Stephen Schlecht[2], Todd Bredbenner[3], David Kohn[1], Carrie Karvonen-Gutierrez[1], Karl Jepsen[1]. [1]University of Michigan, United States, [2]Indiana University, United States, [3]University of Colorado Colorado Springs, United States

The metacarpal has been examined as a proxy of bone health at fracture prone sites like the proximal femur as it can be imaged at higher resolution and lower radiation dose. Prior work focused on metacarpal morphology and bone mineral density, but a systematic inter-skeletal comparison of bone strength and porosity has not been conducted. Herein, we tested how direct measures of metacarpal strength and porosity correlate across skeletal sites. We also tested whether these associations are sex-specific.Third metacarpals, radii, and femurs were obtained from white male (M, 18-89 years) and female (F, 21-97 years) cadavers with IRB approval. Mid-shaft porosity and proximal femur trabecular bone volume fraction (BV/TV) were obtained using nanoComputed Tomography. Whole bone strength was determined for diaphyses loaded in four-point bending and proximal femurs loaded in a sideways fall configuration.Metacarpal strength correlated significantly with strength measured at the radius (n=31, R2=0.33, p<0.001), femoral diaphysis (n=28, R2=0.51, p<0.001), and proximal femur (n=24, R2=0.48, p<0.001) for males (Fig 1). Likewise, metacarpal strength correlated with strength at the radius (n=37, R2= 0.55, p<0.001), femoral diaphysis (n=34, R2=0.65, p<0.001), and proximal femur (n=34, R2=0.53, p<0.001) for females. Sex-specific differences in the y-intercept for the radius (p<0.001) and the slope for the proximal femur (p=0.026) indicated that males had stronger radial diaphyses and proximal femora relative to the metacarpal compared to women.Metacarpal porosity for males correlated with porosity at the radius (R2=0.55, p<0.001) and femoral (R2=0.13, p=0.057) diaphyses, and with proximal femur BV/TV (R2= 0.17, p=0.030). For females, metacarpal porosity correlated with porosity at the radius (R2= 0.36, p<0.001) and femoral (R2=0.15, p=0.02) diaphyses, and with trabecular BV/TV of the femoral neck (R2=0.33, p=0.032). Differences in the y-intercept for the radius (p=0.002), and proximal femur BV/TV (p=0.014) indicated that females had greater radius porosity but lower femoral neck BV/TV relative to the metacarpal compared to males.Thus, metacarpal strength and porosity predict strength and porosity at other skeletal sites with known inter-site differences in age-related bone loss patterns. Critically, these associations were sex-specific suggesting further research is needed to understand how peripheral sites can be used to monitor bone health at fracture prone sites.

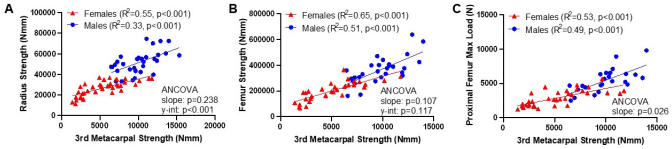

Figure 1. Linear regressions between strength of the 3rd metacarpal and radial diaphysis (A), femoral diaphysis (B), and proximal femur (C) showed significant correlations.

***Disclosures: Erin Bigelow**, None*

P-048

Altered otic capsule morphology of the oim mouse model of osteogenesis imperfecta *Annalisa De Paolis[1], Brendyn Miller[2], Michael Doube[3], Andrew J Bodey[4], Christoph Rau[4], Claus-Peter Richter[5], Luis Cardoso[1], Alessandra Carriero[6]. [1]The City College of New York, United States, [2]Clemson University, United States, [3]City University of Hong Kong, Hong Kong, [4]Diamond Light Source, United Kingdom, [5]Northwestern University Feinberg School of Medicine, United States, [6]The City college of New York, United States

Osteogenesis imperfecta (OI) is a genetic disorder caused by mutations in the encoding of type I collagen. Skeletal fragility, deformities, and functional disabilities, including hearing loss, are typical symptoms of OI. Hearing loss in OI is progressive and in 11-31% of cases occurs in children below 10 years old [1-3]. There is no cure or treatment for OI hearing loss, and very little is known about the properties of the OI inner ear or the mechanisms leading to hearing loss. In this study we investigate the morphology of the otic capsule and the cochlear spiral duct in the oim mouse model of OI, which also suffers hearing loss [4]. High-resolution images of 8 week old oim and WT inner ears (N=6/group) were acquired using synchrotron microtomography at sub-micron resolution. Morphological indexes were evaluated on the coronal and sagittal planes at their intersection with the cochlear modiolus and on two transverse planes crossing the middle and apical turn of the cochlea (Fig. 1a-b). Otic capsule thickness was measured on the aforementioned planes and otic capsule length was measured in the coronal plane. At the tissue level, cortical bone porosity, canals and lacunae were measured [5]. The total volume of the duct and of the helicotrema, and the external spiral length were quantified on 3D renderings of the fluid scalae. Duct and helicotrema surface area and perimeter were measured on the coronal and sagittal planes, turn pitches on the coronal plane, and maximum axes on the transverse planes. The morphology of the oim inner ear is mainly preserved in the 8 week old mouse, but increased coronal cortical thickness and intracortical canal density, volume and connectivity affect the oim otic capsule (Fig. 1c-i). These results portray a state of compromised bone quality in the oim otic capsule which may contribute to hearing loss by making the bone tissue more susceptible to microfractures and/or by varying the hydrodynamics inside the cochlear duct. Further studies are also needed to examine the growth and development of oim ear bones in relation to osteoprotegerin distribution and hearing loss.References1. Pedersen, Scand Audiol, 13:2, 19842. Pillion et al., Genet Res Int, 20113. Ting et al., Clin Otolaryngol, 37:3, 20124. Chen et al., Clin Genet, 71:5, 20075. Miller et al., ORS Annual Meeting, 2017

Posters

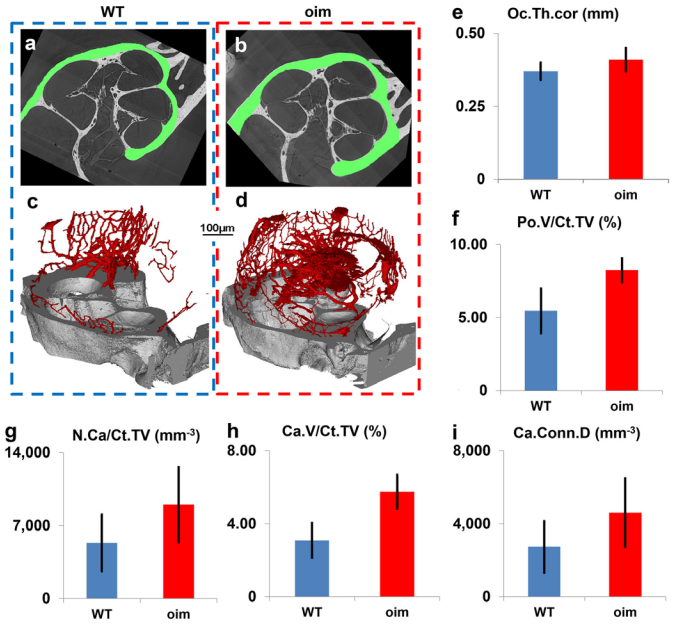

Figure 1. (**a**, **b**) Synchrotron x-ray microtomographic slice of WT and *oim* representative otic capsule showing the difference in coronal cortical thickness. The region of interest considered for the calculation of the mean Oc.Th.cor is reported in green. (**c**, **d**) Surface render of the canal network (red) respectively within the WT and *oim* cochlear otic capsule (gray). (**e-i**) Bar graphs comparing WT and *oim* otic capsule morphological indexes (mean ± SD; $p<0.05$): thickness in the coronal plane (Oc.Th.cor), porosity (Po.V/Ct.TV), canal number density (N.Ca/Ct.TV), canal volume density (Ca.V/Ct.TV), and canal connectivity density (Ca.Conn.D).

***Disclosures: Annalisa De Paolis**, None*

P-049

Two Years of Teriparatide Followed by One Year of Denosumab in Premenopausal Idiopathic Osteoporosis (IOP): Effect on Lumbar Spine Volumetric BMD by Central QCT *Sanchita Agarwal[1], Thomas Lang[2], Stephanie Shiau[3], Mafo Kamanda-Kosseh[1], Mariana Bucovsky[1], Robert Recker[4], Joan Lappe[4], Julie Stubby[4], Jennifer Larsen[4], Elizabeth Shane[1], Adi Cohen[1]. [1]Division of Endocrinology, Department of Medicine, Columbia University, United States, [2]School of Dentistry, University of California San Francisco, United States, [3]Department of Biostatistics & Epidemiology, Rutgers School of Public Health, United States, [4]Department of Medicine, Creighton University Medical Center, United States

Premenopausal women with IOP (PreMenIOP) have large deficits in lumbar spine (LS) total and trabecular (Tb) volumetric BMD (vBMD) measured by central QCT (cQCT). We have reported that 24 months (M) of teriparatide (TPTD; 20mcg SC QD) markedly increased LS BMD by DXA in 41 PreMenIOP (age 36.9+/-7.6 yrs). In 32 of the 41 women, vBMD of L1-L2 was imaged by cQCT at baseline and after 24M of TPTD; a calibration phantom was scanned to convert CT Hounsfield Units to equivalent concentration of calcium hydroxyapatite. QCT parameters included total density (with posterior elements; Tot_vBMD), Tb density (Tb_vBMD) and strength index (SI; =density2*area). SI, computed from the 10mm mid-section of the vertebral body, approximates vertebral compressive strength. After 24M of TPTD, there were significant increases in all parameters (Table; within-group change analyzed by paired Student's t-test). Tot_vBMD and its DXA equivalent LS BMD increased by 9% and 13% respectively; Tb_vBMD increased by 25% and SI by 57% (all p<0.001). Five women had no BMD increase by DXA (12M LS BMD change <0.026 g/cm2). These women had no significant increase in Tot_vBMD (3+/-5%; p=0.3), while Responders did (10+/-9%; p<0.01). Similarly, Tb_vBMD did not increase in Nonresponders (9+/-11; p=0.12), while Responders increased by 26+/-22% (p<0.01). SI increased in Nonresponders (26+/-25; p=0.02) and Responders (62+/-44%; p<0.01), but trended smaller in Nonresponders (p=0.12).After completing TPTD, 30 PreMenIOP took denosumab (Dmab; 60 mg SC q6M) for 12M; 27 had cQCT scans at all 3 timepoints (baseline, 24M TPTD, 12M Dmab). For each time period, changes were analyzed by paired Student's t-test. After 12M of Dmab (Table), LS BMD increased further by 6%, Tot_vBMD by 4% (p<0.05), Tb_vBMD by 10%, and SI by 15% (all p<0.001). Compared to baseline, 24M TPTD + 12M Dmab was associated with large and statistically significant improvements in all parameters: Tot_vBD, LS BMD, Tb vBMD and strength index increased by 15%, 20%, 43% and 85% respectively (all p<0.001).In summary, 24M of TPTD was associated with statistically significant increases in Tot_vBMD, Tb vBMD and SI by cQCT and LS BMD by DXA. Sequential Dmab therapy resulted in further statistically significant increases in all indices. Compared to pretreatment, 24M TPTD + 12M Dmab led to marked overall improvements in vBMD and strength by cQCT and LS BMD by DXA. We conclude that Dmab further enhances bone mass and strength gains made during TPTD therapy in PremenIOP.

Table: Skeletal indices from QCT of Lumbar Spine (L1 and L2) and Lumbar Spine areal BMD by DXA (L1-L4) presented as Mean (SD). Analyzing percent changes on (I) 24 months (M) of Teriparatide (TPTD) from baseline, (II) 12 months of Denosumab (Dmab) after completion of TPTD, (III) 24 months of TPTD + 12 months of Dmab from baseline. * p<0.05 and ** p<0.001

	Analysis I (N=32) TPTD Rx: Baseline to 24M			Analysis II (N=30) Dmab Rx: end of TPTD to 12M			Analysis III (N=27) Sequential Rx: Baseline to 36M		
	Baseline	24M TPTD	% change	24M TPTD	12M Dmab	% change	Baseline	36M (24M TPTD + 12M Dmab)	% change
Tot_vBMD (g/cm^3)	0.22 (0.03)	0.24 (0.03)	9 (9)**	0.23 (0.03)	0.24 (0.03)	4 (8)*	0.21 (0.02)	0.24 (0.03)	15 (11)**
Tb_vBMD (g/cm^3)	0.13 (0.03)	0.16 (0.04)	25 (22)**	0.15 (0.03)	0.17 (0.04)	10 (13)**	0.12 (0.03)	0.17 (0.04)	43 (37)**
Strength Index (g^2/cm^4)	0.16 (0.06)	0.25 (0.09)	57 (43)**	0.23 (0.08)	0.27 (0.10)	15 (17)**	0.15 (0.05)	0.27 (0.10)	85 (61)**
DXA LS BMD (g/cm^2)	0.78 (0.09)	0.88 (0.10)	13 (9)**	0.87 (0.09)	0.92 (0.08)	6 (4)**	0.77 (0.07)	0.92 (0.08)	20 (8)**

Tot_vBMD – Average vertebral volumetric BMD; whole vertebra including posterior elements and excluding transverse elements. Similar to DXA LS BMD
Tb_vBMD – Average Trabecular volumetric BMD from whole vertebra
Strength Index – Average vertebral compressive strength (density^2*area) from a 10mm-section of mid-vertebra excluding transverse and posterior elements
DXA LS BMD – Average areal BMD from DXA; whole vertebra in antero-posterior (AP) direction

***Disclosures: Sanchita Agarwal**, None*

P-050

Trabecular bone structural units (BSU) in the human lumbar spine decrease in size with age and bone volume fraction *Britney Lamarche[1], Christina Møller Andreasen[2], Jesper Skovhus Thomsen[3], Thomas Levin Andersen[2], Brent Lievers[1]. [1]Bharti School of Engineering, Laurentian University, Canada, [2]Clinical Cell Biology, Pathology Research Unit Dept. of Molecular Medicine & Dept. of Clinical Research, University of Southern Denmark, Denmark, [3]Dept. of Biomedicine, Aarhus University, Denmark

Age-related fractures are common at skeletal sites with high proportions of cancellous bone such as the hip and spine. Because of their ageing populations, the incidence of such fractures is expected to increase in industrialized countries. Previous research has shown that measures of bone quantity (e.g., bone mineral density) are imperfect predictors of fracture risk, so recent efforts have focused on combining them with measures of bone quality such as the microarchitecture or composition. Trabeculae are composed of a patchwork of bone structural units (BSU), also known as hemiosteons or trabecular packets, bonded together by cement lines. The BSU-composition of trabeculae has received little attention. Any age-related changes in BSU morphometry due to remodeling can be expected to alter the mechanical properties and failure behaviour of cancellous bone.The present study focuses on whether the most recently formed BSU in vertebral cancellous bone undergo morphometric changes with age. The study was conducted on L2 vertebrae from eight young (18.5–37.6 years) and eight old (69.1–96.4 years) females with no history of osteoporotic fractures. The vertebrae were scanned with µCT and embedded in plastic. Thin frontal sections (7.5 µm) from the centre of each vertebral specimen were prepared and immunostained for osteopontin to highlight the cement lines. The cement lines of the recently formed BSU (i.e., intact with no new resorption or formation) were manually traced using ImageJ on high resolution scans of the sections. Polarized light microscopy was used to clarify any ambiguous staining. The area, thickness, and direct length (Fig. 1) of 4,230 BSU (181–385 per vertebra) were measured. A nested t-test indicated that BSU in the old group had significantly smaller area, thickness, and length compared to the young group (p<0.0140), and there was a negative linear correlation between age and the three measured BSU parameters (p<0.0172). The BSU measurements were also highly correlated to bone volume fraction (BV/TV, p<0.0017) and structure model index (SMI, p<0.0072) obtained by µCT. The results show that vertebral trabecular BSU decrease in area, thickness, and length with both increasing age and decreasing bone volume fraction. The mechanical consequences of the changes in BSU morphometry on fracture risk warrant further investigation.

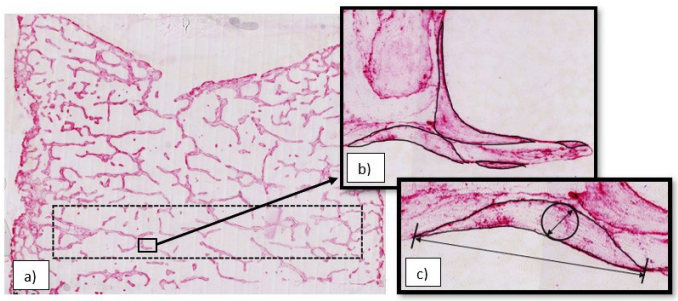

***Disclosures: Britney Lamarche**, None*

P-051

Predicting Patient-Specific Bone Atrophy using Level-Set Methods and HR-pQCT Measurements *Tannis Kemp[1], Bryce Besler[2], Lauren Burt[2], David Hanley[2], Steven Boyd[2]. [1]Department of Mechanical and Manufacturing Engineering, Schulich School of Engineering, University of Calgary, Calgary, Canada, Canada, [2]McCaig Institute for Bone and Joint Health, University of Calgary, Calgary, Canada, Canada

Previous studies attempted to model age-related bone atrophy; however, these studies used bone atrophy rates that were not specific to individual participants and therefore did not capture patient-specific changes. This study aims to 1) extract patient-specific bone atrophy rates from serial in vivo high resolution peripheral quantitative computed tomography (HR-pQCT) measurements, and 2) predict bone microstructure by comparing our new simulated bone atrophy results to ground-truth HR-pQCT data at multiple time points. A subset of participants (N=30) from the Calgary Vitamin D Study, investigating effects of high-dose vitamin D supplementation on bone quality in healthy adults (55-70 years) are used. Distal tibia HR-pQCT scans were taken at baseline, 6, 12, 24 and 36 months. The baseline and 6-month scans are used to determine patient-specific atrophy rates; the remaining timepoints are used to compare simulated and ground-truth microstructure. Individual bone atrophy rates are determined using level-set methods, least squares and gradient descent to optimize the difference between simulated and ground-truth trabecular bone volumes. Dice coefficient evaluated the difference between simulated and ground-truth bone volume data, where values closer to 1 indicate good agreement. Root mean square error (RMSE) measured the error in trabecular bone volume fraction (Tb.BV/TV) between simulation and ground-truth. The results for a representative participant are presented (Fig 1). For this participant at month 6, the dice coefficient is 0.89 and the RMSE in Tb.BV/TV is 0.004. These results indicate the algorithm successfully determined atrophy rates. For this participant over months 12-36, the average dice coefficient is 0.80+/-0.05 (strong prediction) whereas the RMSE in Tb.BV/TV is 0.028 (10.2% of peak Tb.BV/TV). The strong dice coefficient is likely from optimizing simulated and ground-truth bone volumes, and not optimizing for specific morphologic parameters such as Tb.BV/TV. To our knowledge, this is the first attempt to predict future bone health by determining patient-specific bone atrophy rates from serial in vivo HR-pQCT data. Future work will employ strain-adaptive models and all participants will be examined to determine the method's feasibility in a population.

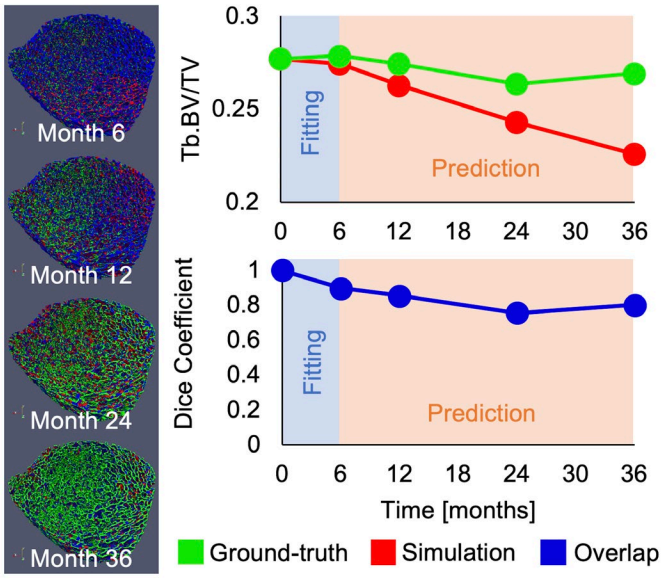

***Disclosures: Tannis Kemp**, None*

P-052

The Role of Matrix Metalloproteinase-13 on Perilacunar/Canalicular Remodeling During Lactation *Michael Sieverts[1], Cristal Yee[2], Minali Nemani[2], Tamara Alliston[2], Claire Acevedo[1]. [1]University of Utah, United States, [2]University of California, San Francisco, United States

PURPOSEPerilacunar/canalicular remodeling (PLR) is a dynamic process in which osteocytes resorb and replace local bone extra cellular matrix (ECM) surrounding their perilacunar and pericanalicular spaces by secreting matrix metalloproteases (MMPs) and resorptive enzymes. We and others have found that PLR is crucial to maintain bone quality, systemic mineral homeostasis, and the osteocyte lacuno-canalicular network (LCN). PLR is increased during lactation to meet the metabolic demand of supplying minerals from the mother's skeleton to their offspring. This change in mineral homeostasis during lactation results in a reduction of bone mass, change in bone morphology and increase skeletal fragility. In addition to changes at the whole bone level, local volumetric changes also occur in the ECM surrounding osteocyte lacunae. Since matrix metalloproteinase-13 (MMP13) is essential for PLR and maintaining bone quality, we used MMP13 osteocyte specific cell knockout mice (MMP13ocy-/-) to study MMP13 osteocyte role during lactation-induced PLR.METHODSFemale mice (n=4-5 mice per group) with osteocyte specific knockout of MMP13 (DMP1Cre+;MMP13fl/fl, referred to as MMP13ocy-/-) and littermate controls (DMP1Cre-;MMP13fl/fl, referred to as WT) were used. For lactation study, MMP13ocy-/- and WT mice at 10 weeks were time-mated, allowed to be pregnant, adjusted litter size to 8-10 pups after delivery, and lactated for 14 days. Lactated mice and 16-week-old aged-matched virgin mice were euthanized and tibias were harvested for imaging on the micro-computed tomography beamline 8.3.2 at the Advanced Light Source at Lawrence Berkley National Laboratory.RESULTSAt the whole bone level, significant reductions in bone volume and cortical thickness were observed due to lactation regardless of genotype. Bone volume of the WT and MMP13ocy-/- were reduced by 22% and 14% respectively. This reduction of bone is consistent with current knowledge of lactations effect on bone. Another common response to lactation is an increase in lacunar volume attributed to PLR. Analysis of lacunar volume showed evidence of PLR in the lactating WT mice. The lacunar volume of the WT mice significantly increased by 31% with lactation. In contrast, no significant difference in volume was observed within the MMP13ocy-/- genotype due to lactation.CONCLUSIONFindings indicate that MMP13 deficiency inhibits PLR during lactation. This shows that MMP13 is a vital gene for PLR to occur during lactation.

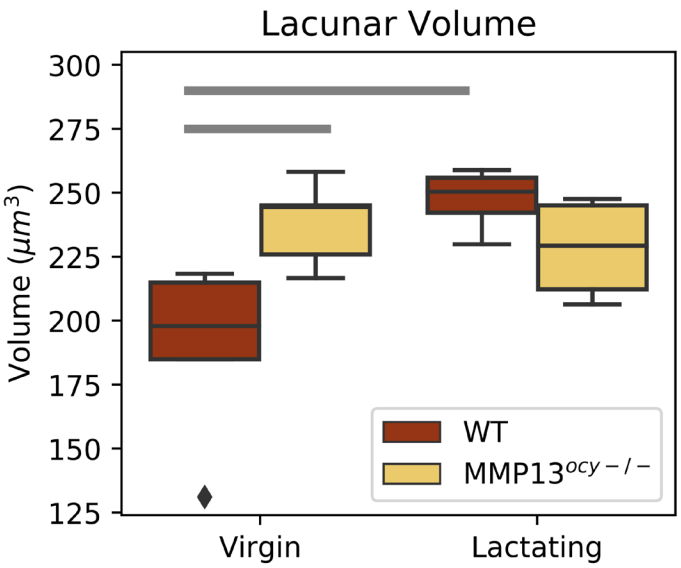

***Disclosures: Michael Sieverts**, None*

P-053

Abaloparatide Improves Bone Mass and Microarchitecture, without Increasing Bone Resorption, in Adult Rats Subjected to Hindlimb Unloading *Dian A. Teguh[1], Amanda E. Craven[1], Jordan L. Nustad[1], Daniel J. Brooks[1], Heike Arlt[2], Beate Lanske[2], Mary L. Bouxsein[1]. [1]Beth Israel Deaconess Medical Center, United States, [2]Radius Health, Inc, United States

Disuse osteoporosis occurs due to a reduction in mechanical loading, commonly caused by prolonged bed rest, paralysis, casts/braces, or microgravity exposure during spaceflight. Abaloparatide (ABL) is a PTHrP analog that has been shown to promote bone formation with limited bone resorption activity (Culler et al., 2001, Doyle et al., 2013), though its ability to prevent bone loss due to disuse has not been studied. Here, we assessed whether ABL prevents bone loss due to hindlimb unloading. Adult male rats (14 wks of age) were assigned to one of four groups (10-12 per group): ambulatory+vehicle (CON-VEH), ambulatory+ABL (CON-ABL), hindlimb unloading+vehicle (HLU-VEH), or HLU+ABL (HLU-

Posters

ABL). Rats received a daily injection of ABL (25µg/kg/day, SC) or VEH for 28 days. We measured trabecular (Tb) and cortical (Ct) bone microarchitecture ex vivo using µCT (15 µm voxel size); dynamic histomorphometry and serum markers of bone metabolism. MicroCT analyses revealed that HLU led to deficits in bone microstructure that were prevented by ABL treatment. In particular, at the distal femur, Tb.BV/TV, Tb.Th and Tb.BMD were -44%, -13% and -27% lower, respectively, in HLU-VEH vs. CON-VEH ($p<0.05$ for all); whereas these same outcomes were 67%, 39%, and 50% higher, respectively, in HLU-ABL vs. HLU-VEH. A similar positive impact of ABL treatment on bone morphology was seen in the normally ambulating rats. Tb. bone formation indices (MS/BS and BFR/BS) and osteoblast number were significantly reduced by HLU. In contrast, bone formation increased with ABL treatment in both HLU and CON rats, accompanied by either a significant decrease or no change in osteoclast number. Serum TRAcP5b did not differ among groups, whereas osteocalcin had a trend of increase in both ABL-treated groups compared to VEH. Gene expression levels for bone formation and resorption markers are currently being tested.In sum, this study demonstrated positive effects of ABL on the trabecular and cortical bone in both normally ambulating and unloaded animals, with increases in bone formation and no increase in resorption. These results are consistent with prior studies showing positive effects of ABL on bone mass, structure and strength in OVX and ORX rats, as well as glucocorticoid-treated rabbits (Chandler et al., 2019a, Chandler et al., 2019b, Varela et al., 2017), and provide a strong rationale for investigating the ability of abaloparatide to prevent disuse-induced bone loss in humans.

***Disclosures: Dian A. Teguh**, None*

P-054

Alignment of the Femur with the Upper Body Protects Against Atypical Femoral Fractures Independent of Antiresorptive Therapy *Hanh Nguyen[1], Catherine Shore-Lorenti[1], Cherie Chiang[2], Frances Milat[3], Roger Zebaze[1], Peter Ebeling[1]. [1]Monash University, Australia, [2]Austin Health, Australia, [3]Hudson Institute of Medical Research, Australia

Bisphosphonate (BP) treatment to prevent fragility fractures is threatened by fear of atypical femur fractures (AFFs). As AFFs are rare, identifying the majority who are at very low risk is a priority. Stress on the lateral femoral shaft from loading patterns during upright stance may be critical in AFF aetiology. We hypothesized that femoral alignment (FA) with the upper body is associated with AFFs, and the greater the FA with the upper body, the better the protection from AFF. In this case-control study,in 23 Caucasian postmenopausal women on BPs who sustained AFFs and 51 AFF-free peers [median(IQR) age: 74(67-80) vs. 69(58-77) years, $p>0.05$], we computed DXA-derived spine and hip BMD, and hip structural parameters. Femoral alignment was quantified by a novel FA Score (FAS), expressed as a percentage.After adjusting for BP use and other co-variates, a higher FAS was associated with a lower likelihood of AFF [OR(95%CI)=0·89(0·84, 0·95), p=0·001]. Median FAS was lower in AFF cases (39·4% vs 51·9%, $p<0·001$). FAS was a better predictor of those who did not sustain AFFs [AUC(95%CI): 0·80(0·69, 0·90)]. The greater the FAS, the greater the positive predictive value (PPV) in identifying AFF-free women (R2=0·92). At a FAS of 49·6%, the PPV was 100%, capturing 57·4% of the population who did not sustain an AFF. Conversely, the lower the FAS, the greater the risk for AFFs, although no threshold with a PPV of 100% was identified. Body mass index, hip BMD, and structural fragility indicators did not predict AFF. FAS has the potential to increase the uptake of osteoporosis treatment by ameliorating fear of AFFs. The majority of women with FAS>49·6% can be reassured that antiresorptives can be initiated or continued; whilst those with a very low FAS score may require further screening for AFFs, or alternative treatment with anabolic drugs.

***Disclosures: Hanh Nguyen**, None*

P-055

Micro-Geometry in Metal Scaffold Regulates Angiogenesis and Osteogenesis *Chengyu Yang[1], Yang Liu[1], Chao Liu[1]. [1]Southern University of Science and Technology, China

INTRODUCTIONThe advent of precision manufacturing of metals, such as 3D printing, will enable the creation of bone-interfacing implants with cell-scale geometries. Micron-sized geometric features could regulate both osteoinduction and angiogenesis. However, it is unclear how precision-manufactured structures with micron-sized features will affect cellular behavior. In this study, pre-osteoblasts and endothelial cells were cultured on stainless steel disks with microgeometries in vitro to observe the effect of micron-scale features on osteogenesis and angiogenesis. We hypothesized that acute angles in the pores of a metallic substrate will enhance angiogenesis and osteogenesis, due to the formation of stress concentrations within cells. METHODSMC3T3-E1 preosteoblasts and C166 endothelial cells were cultured on flat stainless-steel scaffolds with 3 types of pores: isosceles triangle, square, and circle. On day 4, proliferation of C166 cells was measured. Phalloidin and DAPI was used to stain actin and nuclei after 24 h. Actin and nucleus area was quantified. After culturing with different scaffolds for 4 days, osteogenic genes and angiogenic genes were measured by qPCR for MC3T3-E1 C166 cells respectively, and normalized to 18s. RESULTSThe actin area ratio was highest in the triangular group. Proliferation was reduced in both endothelial cells (28.6-37.5%) and preosteoblasts (30.0-37.1%) after 4 days regardless of scaffold geometry. Triangular scaffold induced highest expression of angiogenic genes VEGFR2, VEGF-A and S1PR1 in C166 cells, and highest expression of osteogenic genes OPN and Runx2 in MC3T3-E1 cells. ALP mRNA expression was similar in triangle and square groups; with 24% reduction in the circular feature group. DISCUSSIONAcute angles at the micron-scale induced more actin fibrils, as well as higher expressions of angiogenic genes in endothelial cells and osteogenic genes in preosteoblasts. The findings represent a step closer in controlling bone formation at the implant interface at multiple length scales, up from the nano-surface texture5 to the millimeter structures. We have utilized a standard 2D culture protocol and geometric features on stainless steel disks, which has the drawback of lacking the 3D ultrastructural information from physiological conditions. Future work will include 3D lattice scaffold designs that are validate with in vivo experiments.

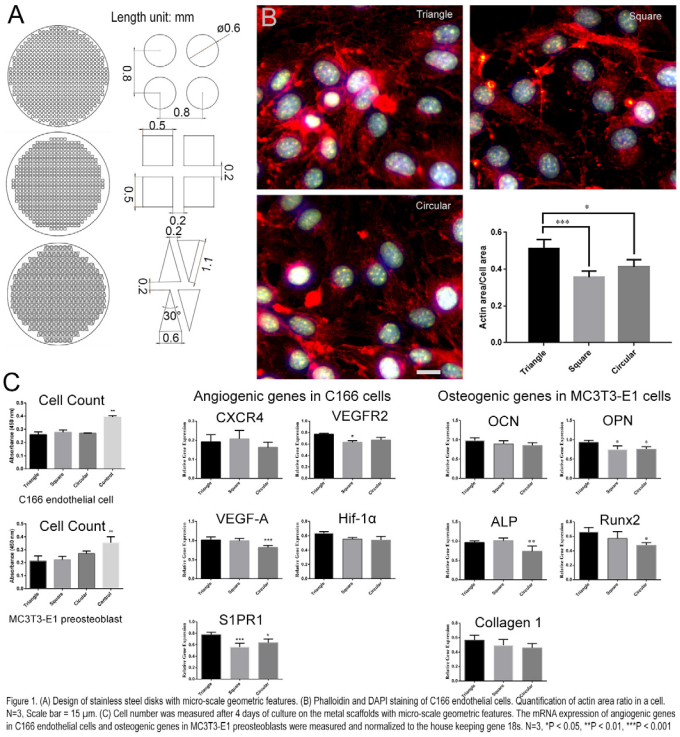

Figure 1. (A) Design of stainless steel disks with micro-scale geometric features. (B) Phalloidin and DAPI staining of C166 endothelial cells. Quantification of actin area ratio in a cell. N=3, Scale bar = 15 µm. (C) Cell number was measured after 4 days of culture on the metal scaffolds with micro-scale geometric features. The mRNA expression of angiogenic genes in C166 endothelial cells and osteogenic genes in MC3T3-E1 preosteoblasts were measured and normalized to the house keeping gene 18s. N=3, *P < 0.05, **P < 0.01, ***P < 0.001

***Disclosures: Chengyu Yang**, None*

P-056

Different relationships between cortical bone design and bone tissue mass and quality (mineralization) in limb bones of 3 anuran species, in relation with the mechanostat control of bone structure. *Miriam Corina Vera[1], Jose Luis Ferretti[2], Gustavo Roberto Cointry[2], Virginia Abdala[3]. [1]Laboratorio de Genética Evolutiva, Instituto de Biología Subtropical, Universidad Nacional de Misiones-CONICET, Misiones, Argentina, Argentina, [2]Center for P-Ca Metabolism Studies (CEMFoC), Natl Univ of Rosario and Arg NRC (CONICET), Argentina, [3]Cátedra de Biología General, Facultad de Ciencias Naturales e IML, Universidad Nacional de Tucumán, Tucumán, Argentina, Argentina

Bone mechanostat is a feedback mechanism that regulates bone structural stiffness by spatially orienting bone modeling accordingly with the strains induced by mechanical usage. The mechanostat efficiency to optimize the diaphyseal design (CSMIs) can be evaluated as a function of either the availability or the vBMD of cortical tissue in negative 'distribution/quality' (d/q) curves, or how well bone mass (BMC) is utilized to optimize diaphyseal design (CSMI) in positive 'distribution/mass' (d/m) curves, respectively. Anurans' long bones offer a suitable model to test the efficiency of the mechanostat that way because of the wide variety of mechanical challenges derived from their different locomotion modes and habitats. We aimed to show that both d/q and d/m relationships would describe differences in the efficiency of the bone mechanostat under different mechanical loads, and the curves would show similar patterns between jumper and swimmer species and different patterns between these and walker frogs. To test it, we scanned by pQCT the femur and tibia-fibula of an arboreal-walker (Ar-W, 5 specimens), an arboreal-jumper (Ar-J, 6 specimens), and an aquatic-swimmer (Aq-S, 5 specimens) frog species at 9 sites placed at every 10% of their length.The d/q relationships showed a highly significant adjustment to common curves for Ar-J and Aq-S ($r=0.85$, $p<0.001$), with Aq-S data shifting to the upper-left zone of the graph, showing higher CSMI and lower cortical vBMD values than Ar-J. In contrast, the walking frogs plotted in a different region of the graph, especially in the case of data from mid diaphysis, both in femur and tibia-fibula. This could be explained by the slow movement of the Ar-W frogs compared to the quick and powerful movement of Ar-J and Aq-S species.The d/m associations confirmed that idea. The Ar-J and Aq-S data were significantly adjusted to common correlation curves ($r=0.82$, $p<0.001$), suggesting that both movements respond to a common pattern, although its location in different zones would indicate some habitat

influence. In contrast, the Ar-W data correlated significantly (r=0.80, p <0.001) at a different height and with a different slope (ANCOVA p<0.001) with respect to those of Ar-J and Aq-S.These findings show that the movements of the jumping and swimming frogs present common patterns, involving higher mechanical demands than those followed by walker frog.

***Disclosures: Miriam Corina Vera**, None*

P-057

Compound Deletion of Thrombospondin-1 and -2 Results in a Skeletal Phenotype not Predicted by Single Gene Knockouts *Andrea Alford[1], Chris Stefan[1], Anita Reddy[1], Kenneth Kozloff[1], Kurt Hankenson[1]. [1]University of Michigan, United States

The trimeric thrombospondin homologs, TSP1 and TSP2, are both components of bone tissue and contribute in distinct ways to skeletal physiology. TSP1-null mice exhibit high trabecular and cortical bone mass with an osteoclast functional deficit. TSP2-null mice exhibit higher endocortical bone mass with increased MSC proliferation and osteoblast differentiation capacity. Both TSPs affect collagen fibrillogenesis. The functional effects of combined TSP1 and TSP2 deficiency remain to be elucidated. Here, we examined the spectrum of detergent soluble proteins in diaphyseal cortical bone of growing (6-week old) male and female mice deficient in both thrombospondins (double knockout (DKO)). Equal amounts of detergent soluble cortical bone protein were subject to Tandem Mass Tags (TMT) quantitative proteomics. 3,429 proteins met the selection criteria (FDR<= 1% and ³2 peptide spectral matches). 181 proteins were differentially abundant in both male and female DKO bones (>=2 fold or <=0.5 fold compared to wild-type). Physiologically relevant annotation terms identified in Ingenuity Pathway Analysis included “ECM degradation” and “Quantity of Monocytes.” Manual inspection revealed a number of proteins with shared expression among osteoclasts and osteocytes were reduced in DKO bones. To associate changes in protein content with phenotype, we examined 12-week old male DKO (N=4) and WT (N=5) mice. Marrow-derived colony forming unit-fibroblastic was reduced in DKO mice (18 vs. 52 CFU per million cells plated). DKO mice were smaller than WT (22.25+/-1.9 vs. 27.60+/- 0.5 grams p<0.001). DKO femora had reduced cross-sectional area (1.65+/-0.3 vs. 2.13+/-0.1 mm2 p<0.01) with a flattened, less circular cross-section (0.76+/-0.1 vs. 0.91+/-0.03 Welch’s corrected p=0.05). DKO bones were less stiff in bending (142.20+/-25.1 vs. 201.90+/-33.2 N/mm2 p<0.05), but a disproportionate reduction in anterior-posterior bending moment on nanoCT (0.103+/-0.02 vs. 0.18+/-0.01 mm4 p<0.001) lead to a modest increase in predicted modulus (stiffness/bending moment, p=0.07). DKO displayed a lower ultimate load (28.55+/-3.7 vs. 36.89+/-2.7 N p<0.01) along with a decreased ratio of ultimate displacement to yield displacement (1.10+/-0.02 vs. 1.39+/-0.2 Welch’s corrected p<0.05), which suggests a brittle bone phenotype. Tissue mineralization was not affected on nanoCT. Together our data suggest that when both TSP1 and TSP2 are absent, a unique bone phenotype not predicted by the single knockouts, is manifested.

***Disclosures: Andrea Alford**, None*

P-058

Vitamin D receptor signaling prevents long-term glucocorticoid induced bone fragility by preserving several components of bone quality *Amy Y Sato[1], Meloney Cregor[1], Charlie A Schurman[2], Jennifer Shutter[1], Punit Vyas[1], David Halladay[1], Kevin McAndrews[1], Tamara Alliston[2], Teresita Bellido[3]. [1]Department of Anatomy, Cell Biology, and Physiology, Indiana University School of Medicine, Indianapolis, IN, United States, [2]Department of Orthopaedic Surgery, University of California San Francisco, San Francisco, CA, United States, [3]Department of Anatomy, Cell Biology, and Physiology, Indiana University School of Medicine, Indianapolis, IN; Richard L. Roudebush Veterans Affairs Medical Center, Indianapolis, IN, United States

Bone fracture incidence with excess of glucocorticoids (GC) surpasses the risk predicted by the loss of bone mineral density (BMD), implicating GC effects on other determinants of bone quality such as microarchitecture, remodeling rate, degree of collagen mineralization, and mechanical properties of collagen fibrils. We showed earlier that ligands of the vitamin D receptor (VDR) prevent GC-induced BMD loss. We investigated here their effect on bone fragility at the tissue, micro, and nanoscale levels. Skeletally mature 4mo C57Bl6 female mice (N=10) received for 8wks placebo or GC (2.1 mg/kg/d prednisolone pellets), and vehicle, 1,25D3 or eldecalcitol-71 (ED) (50ng/kg/d 5x/wk, gavage, starting 3d prior pellet implantation). GC decreased the structural (extrinsic) properties ultimate force, energy to ultimate load, and stiffness by ~20%, and the material (intrinsic) properties ultimate stress and toughness ~17%, tested by femoral 3-point bending. VDR ligands did not affect mechanical properties, but prevented all GC effects; although 1,25D3 increased ultimate force and GC decreased this index even with 1,25D3. We then investigated the mechanisms underlying bone strength preservation by the VDR ligands. GC-induced microarchitectural deterioration in cancellous bone (low BV/TV and Tb.N, and increased Tb.Sp) was fully prevented by the ligands. In contrast, ED fully protected from GC-induced cortical bone deterioration (low Ct.Ar/Tt.Ar, Ct.Th, and Ct.Ar, and increased Ma.Ar), but 1,25D3 did not. Regarding bone remodeling, both VDR ligands prevented GC-induced resorption, quantified by circulating CTX and osteoclast number/surface; and ED by itself markedly decreased resorption. In contrast, the VDR ligands did not prevent GC-induced reduction in bone formation, quantified by circulating P1NP, osteocalcin, and MS/BS and BFR. Consistent with the effects on resorption, GC decreased material density measured by micro-CT and the VDR ligands prevented this effect. Small-Angle X-ray Scattering (SAXS) with in situ tensile testing showed a GC-dependent increase in bone deformation (ultimate and yield strain), which was prevented by the VDR ligands. Further, VDR ligands alone decreased tissue ductility. Moreover, GC transferred strain away from collagen fibrils increasing collagen ductility, which was prevented by VDR ligands. These findings demonstrate that VDR signaling prevents GC-induced bone fragility by preserving bone mass and several key components of bone quality.

***Disclosures: Amy Y Sato**, None*

P-059

Effects of bone strain of rat tibia during electrical stimulation-induced muscle contraction on bone strength in the early stages of disuse musculoskeletal atrophy *Hiroyuki Tamaki[1], Kengo Yotani[1], Futoshi Ogita[1]. [1]National Institute of Fitness and Sports in Kanoya, Japan

Mechanical loading of bone tissue is essential to maintain bone volume and muscle contraction force generates bone strain in vivo. We determined the in vivo bone strain magnitude and strain rate during electrical stimulation-induced muscle contraction (ES) and tested whether daily muscle ES treatment can ameliorate the decrease in tibial bone strength after sciatic denervation (DN) in aged rats.In vivo bone strain was measured during ES using thin-film strain gauges (Kyowa) attached under anesthesia to the medial surface of the tibial bone in adult rats (n=6). ES was applied to the tibialis anterior (TA) muscle using bipolar surface electrodes connected to an electrical stimulator (stimulation intensity: 1-60 V; frequency: 1-100 Hz). Peak strain magnitude (με), as well as maximal and minimal strain rates (με/s) during the increasing and descending phases of ES, were analyzed using a time-strain curve. Twenty-four male rats were assigned to one of the following groups: the age-matched control group; the DN group; or the DN + ES group. Denervated TA muscle in the DN+ES group received ES at 10 Hz for 30 min/day, six days/week, for 1 week.ES-generated twitch and tetanic force induced bone strain for a duration of approximately 30-70 ms. Peak strain magnitude and strain rate increased linearly with ES intensity and frequency up to 30 V and 50 Hz, respectively. A significant correlation was found between bone strain magnitude and strain rates during ES. ES at 10 Hz generated a constant repetitive bone strain at 10 cycles/s. ES-induced muscle contraction force mitigated denervation-induced muscle and trabecular bone loss and deterioration of the mechanical properties of the tibia mid-diaphysis, such as the stiffness, but not the maximal load, in aged rats. The TA muscle in the DN+ES group showed significant improvement in the myofiber cross-sectional area and muscle force relative to the DN group.These results suggest that 1) the in vivo strain magnitudes and strain rates of the rat tibia obtained during ES depend on the level of muscle contractile force, 2) low-frequency ES-induced muscle contraction treatment retards trabecular bone and muscle loss in aged rats in early-stage disuse musculoskeletal atrophy, and has beneficial effects on the functional properties of denervated skeletal muscle.

***Disclosures: Hiroyuki Tamaki**, None*

P-060

Mechanisms of Crack Growth Toughness in Young Osteogenesis Imperfecta Mouse Bone *Anxhela Docaj[1], Alessandra Carriero[1]. [1]The City College of New York, United States

In osteogenesis imperfecta (OI or brittle bone disease), mutations in the collagen genes alter the whole bone hierarchical structure and composition, increasing its vulnerability to spontaneous fractures and fragility [1]. We recently showed that bone fracture toughness is low in the oim mouse model of OI [1], already at a very young age [2], and that increases as the mouse grows [2]. To explain this behaviour, we examined the path of the crack during growth in 4 and 12 week old oim mice to determine the presence of toughness mechanisms, e.g. crack deflections, uncracked ligament bridging, and splitting, and their contribution to the bone fracture resistance.Femora from the oim and WT mice at 4 and 12 week old (N=3-6/group) were notched and loaded in 3-point bending at 1 μm/sec using a micro-testing device within an environmental scanning electron microscope used in backscattering mode at 25kV and 35 Pa [3]. Toughness was calculated for each crack growth. The presence and occurrence of toughening mechanisms was examined for each crack extension and the relative toughness was estimated.Examination of the crack path shows that the most common toughening mechanism is deflection, followed by splitting in WT bone, while in oim bone splitting and bridging are equally detected (Table 1). In 4 w.o. WT bone, bridging is the highest contributing mechanism to crack growth toughness, followed by deflection and splitting. In 4 w.o. oim bone, deflections and splitting contribute more to toughness than bridging, but less than in WT. In 12 w.o. mice, crack deflections, splitting and bridging are observed in WT bones, while they are almost absent in oim bones showing an almost flat crack path (Table 1).This study shows for the first time the presence of toughening mechanisms in brittle oim mouse bone at a young age, but not in older oim mice. Interestingly, these mechanisms could be beneficial to rescue oim bone from their fragility if we could increase their initiation toughness. Our future studies will examine the changes in the structure and composition in oim bone affecting their fracture toughness during mouse growth.

Mechanism of Crack Growth	WT					
	4 w.o. WT			12 w.o. WT		
	Oc.	*ki*	*ki+1*	*Oc.*	*ki*	*ki+1*
Bridging	1	0.29	0.41	0	-	-
Deflection	7	0.28±0.11	0.12±0.07	11	0.29±0.13	0.17±0.21
Splitting	5	0.18±0.08	0.10±0.09	7	0.22±0.17	0.08±0.13
Mechanism of Crack Growth	***oim***					
	4 w.o. *oim*			12 w.o. *oim*		
	Oc.	*ki*	*ki+1*	*Oc.*	*ki*	*ki+1*
Bridging	2	0.03±0.03	0.12±0.17	0	-	-
Deflection	7	0.15±0.09	0.08±0.10	0	-	-
Splitting	2	0.15±0.07	0.06±0.08	1	0.05	0

Table 1*. Fracture toughness in terms of stress intensity factor (MPa*m$^{1/2}$) before (ki) and after (ki+1) crack growth mechanisms. Oc. indicates the occurrence of the mechanism.*

Disclosures: Anxhela Docaj*, None*

P-061

Biomechanical and MicroCT Conclusions Are Different Based on Method of Bodyweight Control: Pair-feeding versus Linear Regression *Mikhail Gurevich[1], Alexander Chirokikh[2], Sardar Uddin[2], David Komatsu[1]. [1]Renaissance School of Medicine at Stony Brook University, United States, [2]Stony Brook University, United States

Understanding the morphometric and biomechanical properties of bone is fundamental to appreciating its overall integrity and function. Animal models are commonly used to study the effects of genetic perturbations or drug treatments on skeletal integrity; however, these interventions often alter body size as well as skeletal structures. Since morphometric and biomechanical properties correlate with body size, it is challenging to discern whether experimental outcomes are a result of direct effects on bone or are secondary to alterations in body mass. In past studies of the effects of methylphenidate (MP) on rat bone, we employed pair-feeding in an effort to control for body mass. Recently, analytical methods of body mass normalization, such as linear regression have been introduced, prompting us to ask if we would arrive at the same conclusions using these two methods. Therefore, the goal of this study was to compare the conclusions regarding the effects of MP treatment on bone reached using the pair-fed method to those acquired using the linear regression method. Four-week-old male and female Sprague-Dawley rats were divided into 5 groups (n=12/group): Water (water for 8 hours), LD MP (4 mg/kg first hour, 10 mg/kg next 7 hours), LD PF (no MP, same food intake as LD MP), HD MP (30 mg/kg first hour, 60 mg/kg next 7 hours), and HD PF (no MP, same food intake as HD MP). After 13 weeks of treatment, femurs were assessed for longitudinal growth, microCT, and biomechanical outcomes. The HD MP group had a significantly lower final bodyweight relative to Water (-15.2%), LD MP (-15.1%), and LD PF (-14.8%) in males and relative to Water (-11.5%), LD MP (-15.8%), LD PF (-11.1%), and HD PF (-13.7%) in females. Without adjusting for body size, HD MP treatment significantly reduced energy to failure (-23.4%), stiffness (-11.5%), and ultimate force (-11.2%) in males, while having no significant effects in females. After normalizing with linear regression, significant differences among male groups were no longer present, while relatively longer (+3.0%) and wider femurs (+3.7%), with a greater maximum moment of inertia (+18.3%) were observed in the female HD MP group as compared to Water. Pair-fed comparisons revealed no significant differences between groups in either sex. We consider the linear regression method to hold significant merit by allowing us to adjust for experimental variables and potentially reduce the number of animals needed to draw meaningful conclusions.

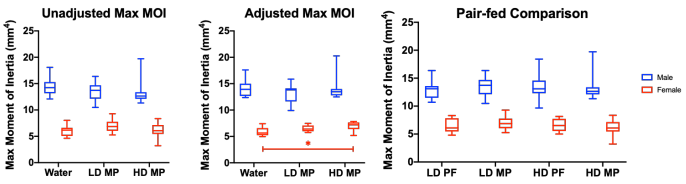

Disclosures: Mikhail Gurevich*, None*

P-062

A Novel Micro-FE Based Model to Investigate the Role of Osteocyte Lacunae in Microcracking of Human Bone *Elliott Goff[1], Francesco Vicentini[1], Ralph Müller[1]. [1]Institute for Biomechanics, ETH Zürich, Switzerland

Microcracks propagate through the mineralized bone matrix in the vicinity of osteocyte lacunae. Lacunae have been shown to guide cracking, so greater understanding of this biomechanical interaction is warranted. Researchers have previously created micro-finite element (micro-FE) models to explore crack progression, yet they are oversimplified and lack clinical relevance. We present a novel model using clinically relevant human data to address crack propagation and lacunar interaction.The cortical region of a complete human iliac crest biopsy embedded in PMMA was imaged using a µCT50 (Scanco Medical, Switzerland) at a nominal voxel resolution of 1.2µm. A cubic subvolume with side length of 180µm was segmented, which included a vascular canal and 79 lacunae. The image volume was meshed using ParOSol and vertical compression was iteratively simulated in steps of 0.1% strain until failure with the bottom fixed. Crack initiation was defined as voxels exceeding a maximum principle strain of 0.8%. A directional vector was calculated accordingly and the immediate voxel bordering the crack tip in the vector path was deleted. The method was applied to several rotated versions of the original image subvolume to evaluate differences in cracking patterns. Lacunar volume (Lc.V), stretch (Lc.St), and oblateness (Lc.Ob) as defined previously were calculated using a custom Python script.As the subvolume's angle changed, so did the crack pattern and the lacunae intersected. Yet, crack propagation remained parallel to the axis of compression while the number of intersected lacunae differed between image rotations. The crack in Figure 1B intersected with ten lacunae while the crack in Figures 1A&1C intersected with three lacunae. Intersected lacunar morphometric parameters in the table adjacent to Figure 1 demonstrate a range of volume, stretch, and oblateness mean values that approximate ellipsoidal geometries.Our model confirms previous experimental work by demonstrating that microcracks propagate parallel to the axis of compression, originate at large canals (such as vascular canals) and are interwoven with lacunae. The mean Lc.St and Lc.Ob values reported suggest that these intersected lacunae approximate ellipsoidal geometries. The lacunar shape could serve a mechanobiological function such as crack tip blunting, crack energy dissipation, or even a future biomarker for bone health.

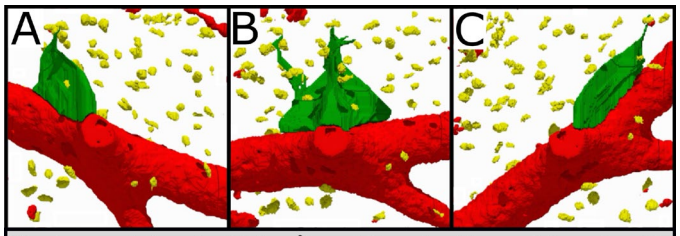

Region	Mean Lc.V (µm^3)	Mean Lc.St	Mean Lc.Ob
A	219+/-84.4	.493+/-.012	-.620+/-.094
B	235+/-90.5	.525+/-.133	-.398+/-.425
C	132+/-81.6	.520+/-.073	-.053+/-.261

Figure 1: Microcrack (green) initiating at the vascular canal (red) and propagating through regions of lacunae (yellow). A) Initial orientation (0° rotation), 2.4% strain, 3 intersected lacunae B) 30° rotation, 3.0% strain, 10 intersected lacunae C) 60° rotation, 2.1% strain, 3 intersected lacunae.

Disclosures: Elliott Goff*, None*

P-063

Experimental Validation of Finite Element Models of the Proximal Tibia Using Digital Volume Correlation *Dylan Zaluski[1], Saija Kontulainen[2], James Johnston[1]. [1]Department of Mechanical Engineering, University of Saskatchewan, Canada, [2]College of Kinesiology, University of Saskatchewan, Canada

Background: Finite element (FE) models of bones incorporating geometry and material properties from quantitative computed tomography (QCT) (generally referred to as QCT-FE) can help researchers understand the effects of altered bone mechanics on joint health [1]. Current QCT-FE models of the tibia have been experimentally validated for surface strains [2] but not internal bone mechanics. The objective of this study was to validate QCT-FE models of the tibia for internal bone displacements using digital volume correlation (DVC). Methods: Five embalmed cadaveric tibiae were subjected to compressive loading inside a high-resolution peripheral QCT (HR-pQCT) scanner using a custom mechanical testing rig. HR-pQCT scans (41µm voxel) were taken before load application and subsequently between steps of 0.5, 1.0 and 1.5mm of applied displacement. Experimental displacements were obtained using DVC software (DaVis 10.01, LaVision). QCT-FE models were generated from HR-pQCT scans by first downsampling to clinical QCT resolution (0.5mm voxel), adding noise, segmenting and converting bone voxels to linear hexahedral elements. Each element was assigned an elastic modulus (E) derived from bone mineral density (BMD) using 3 different E-BMD relationships [3-5]. Boundary conditions were replicated by mapping DVC displacements to nodes on the contact surface and the fixed distal end. FE models were solved using a custom MATLAB program. Agreement between FE-predicted and DVC-measured displacements was assessed using linear regression and root mean square error normalized to maximum measured displacement (RMSE%). Results: Regression intercepts ranged from -0.0008 to 0.0324mm and slopes ranged from 1.00 to 1.10 (Fig. 1); all were significantly different from 0 and 1, respectively. RMSE% ranged from 3.5 to 5.5%, and all R2 were greater than 0.99. For each E-BMD tested, x and y displacement predictions

were nearly identical, while Nazemi et al. more accurately predicted larger magnitude z-displacements (Fig. 1c). Conclusions: Internal bone displacements within the elastic regime in the proximal tibia are accurately predicted by QCT-FE. The E-BMD relationship of Nazemi et al. is recommended due to lower error for large-magnitude z-displacements. Future work is required to validate models for reaction forces and to develop optimized E-BMD relationships. References: [1] McErlain et al. 2011; [2] Gray et al. 2008; [3] Nazemi et al. 2017; [4] Rho et al. 1995; [5] Morgan et al. 2003

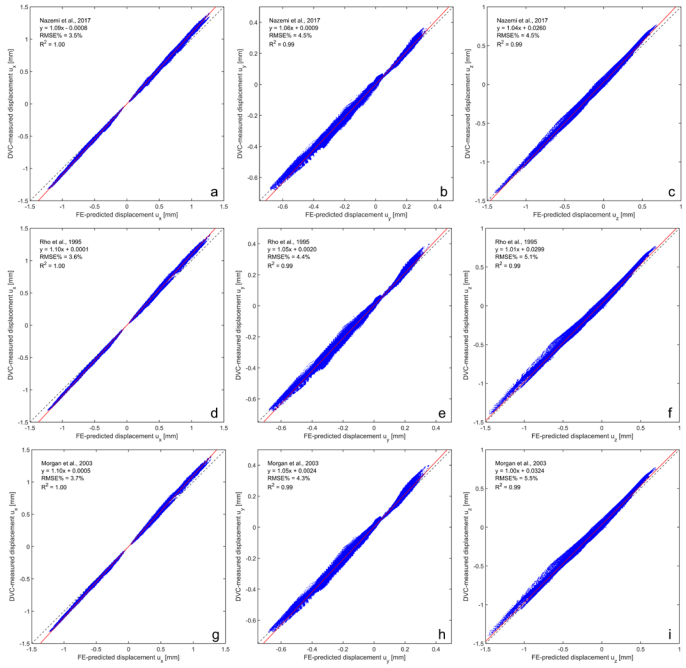

***Disclosures: Dylan Zaluski**, None*

P-064

Skeletal Repercussions of Concomitant Methylphenidate and Fluoxetine Treatment *Alexander Chirokikh[1], Mikhail Gurevich[1], Sardar Uddin[1], Carly Connor[2], Panayotis Thanos[2], Michael Hadjiargyrou[3], David Komatsu[1]. [1]Department of Orthopaedics, Stony Brook University, United States, [2]BNNLA - Research Institute on Addictions, Department of Pharmacology and Toxicology, SUNY University at Buffalo, United States, [3]Department of Biological and Chemical Sciences, New York Institute of Technology, United States

Concomitant administration of methylphenidate (MP) with selective serotonin reuptake inhibitors (SSRI) such as fluoxetine (FLX) is a common strategy used to treat attention-deficit/hyperactivity disorder in pediatric patients with depression or anxiety comorbidities. Previously, our laboratory demonstrated that chronic MP treatment of male adolescent rats resulted in reduced longitudinal growth, mineralization, and biomechanical integrity in appendicular bones. Similarly, clinical data have shown that long-term SSRI treatment is linked to increased fracture risk and reduced bone mineral density, prompting the question of whether the skeletal repercussions associated with MP treatment are exacerbated when administered in combination with SSRI. As such, the objective of this study was to investigate the effects of MP and FLX treatment on bone morphology and biomechanical properties using a rat model. Four-week-old male Sprague-Dawley rats were randomly divided into the following 4 groups (n=10/group) and administered treatments via drinking water for 8 hours per day: Water (water for 8 hours), HD MP (30 mg/kg first hour, 60 mg/kg next 7 hours), FLX (15mg/kg for 8 hours), and MP+FLX (MP and FLX). Following 4 weeks of treatment, significantly lower bodyweights in the HD MP (-17.3%), FLX (-15.8%), and MP+FLX (-50.1%) groups were observed relative to Water. Since bone morphological and biomechanical properties are associated with animal size, data were compared directly and after normalization to bodyweight via linear regression. Without adjusting for bodyweight, MP+FLX animals had significantly shorter (-12.4%) and narrower (-17.2%), but higher density (+2.3%) femora compared to Water animals. The MP+FLX group also had a significantly lowered energy to failure (-24.8%) and ultimate force (-14.4%) relative to the Water group. In contrast, the MP+FLX group showed no significant differences in longitudinal growth, microCT parameters, or biomechanical outcomes relative to any other group after normalization. We conclude that the adverse skeletal effects of MP+FLX treatment seen via direct comparison are predominantly attributable to reductions in bodyweight rather than direct effects on the bone. Future studies will investigate MP+FLX treatment on trabecular microarchitecture and cortical porosity to better understand the effects on the skeleton, as well as to recognize all the possible sequelae for adolescents being treated with this combination therapy.

***Disclosures: Alexander Chirokikh**, None*

P-065

Local Bone Remodeling in Distal Radius Fracture Healing Is Not Isolated to the Fracture Region: A Time-lapse HR-pQCT Imaging Study *Penny Atkins[1], Kerstin Stock[2], Caitlyn Collins[1], Nicholas Ohs[1], Lukas Horling[2], Patrik Christen[3], Michael Blauth[2], Ralph Müller[1]. [1]Institute for Biomechanics, ETH Zurich, Switzerland, [2]Department for Trauma Surgery, Innsbruck University Hospital, Innsbruck, Austria, Austria, [3]Institute for Biomechanics, ETH Zurich; Institute for Information Systems, FHNW, Olten, Switzerland, Switzerland

Clinically, fracture healing is evaluated using 2D radiographic images; however, these images are only used to assess fracture bridging, without consideration for other aspects of bone quality post-fracture. By using a high-resolution peripheral quantitative computed tomography (HR-pQCT) time-lapse imaging protocol, fracture healing can be more accurately monitored through microstructural bone remodeling. Therefore, we investigated local bone formation and resorption rates (BFR and BRR, respectively) in the region of the fracture, as well as proximally and distally, hypothesizing that microstructural bone remodeling would be greatest in, but not isolated to, the region of the fracture.Patients (3 female, 33, 52, and 56 years of age; 1 male, 21 years of age) with conservatively treated radius fractures provided informed consent prior to participation (Ethics Committee, Medical University of Innsbruck). HR-pQCT (XtremeCT II, Scanco Medical AG) images were acquired at 1, 3, 5, 13, 26, and 52 weeks post-fracture. Three image stacks (504 slices, 61 µm voxels) were acquired to ensure full imaging of the fracture. Voxel intensities of the radius were isolated with a mask and registered using a pyramid-based approach (Python v3.7). Registered images were Gaussian filtered (sigma 0.8, support 1.0) and binarized (threshold 320 mg/ccm) prior to calculation of volume-based BRR and BFR, which were quantified relative to images from the previous time point. Proximal, distal, and fracture regions were isolated using manually-defined cutting planes (ParaView v5.4; Figure 1, left).In the region of the fracture, maximum BRR was observed from 1-3 weeks (1.39-3.92%/day), while maximum BFR was observed either from 1-3 or 3-5 weeks (2.31-3.01%/day) (Figure 1, right). Cortical bridging was evident at 13 weeks. In the region distal to the fracture, BRR was highest from 1-3 or 3-5 weeks (1.78-3.05%/day), while BFR was highest from 3-5 weeks (1.21-1.76%/day). For all patients, BFR and BRR remained below 1.25%/day in the region proximal to the fracture site.BRR and BFR were highest in the region of the fracture, however, even in this relatively young cohort, we observed high BRR in the trabecular-rich distal region during early fracture healing. The use of this protocol to quantify fracture related remodeling may help to identify clinically relevant changes in bone quality post-fracture, especially in patients with a pre-existing imbalance of BFR and BRR (i.e. osteoporosis).

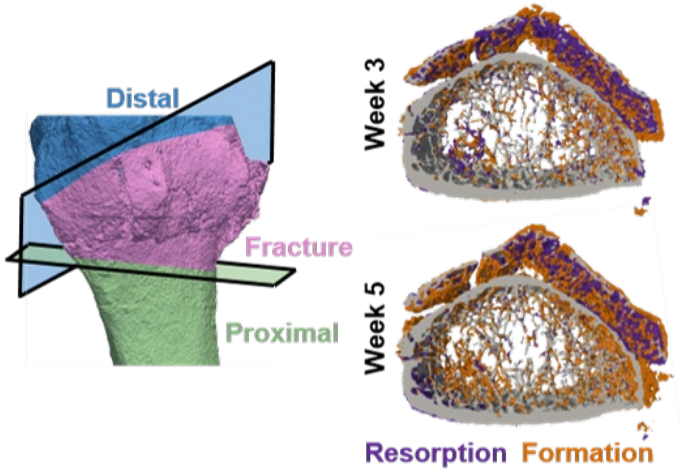

Figure 1: Isolated regions for analysis (left). Representative transverse section within the fracture region showing local resorption and formation (right).

***Disclosures: Penny Atkins**, None*

P-066

Female Volleyball Players: A within-subject controlled model of the lower limb *Claudia Romero Medina[1], Sena Harlley[1], Daniel Den Briones[1], Jorge Gonzalez[1], Vanessa Yingling[1]. [1]Cal State East Bay, United States

Introduction: High impact loading common in some sports affect bone structure that may influence bone strength across a lifetime. A within-subject controlled model for studying lower limb bone adaptation to loading is needed especially in females. Weatherholt and Warden (2016) examined male jump athletes as a potential model reporting small side-to-side bone strength differences in the tibia. The fibula only shares 6.4% of weight distribution with the ankle joint in neutral (Takebe et al, 1984). The relative disuse of the fibula may make it more responsive to increased loading. Volleyball may serve as a with-in subject

Posters

model of the lower limb due to the high-impact jumps that are common in the sport. Purpose: To determine bilateral differences in bone architecture and strength of the tibia and fibula. Methods: 16 Division II female volleyball players (age 19 yrs + 1.2, Ht 1.74 + 0.69 m, BM 69.8 + 8.1 kg, BF% 23.9 + 5.7%) underwent peripheral quantitative computed tomography (pQCT) scans to measure bone strength on both the lead leg (dominant) and gather leg (non-dominant) tibia and fibula. Trabecular bone strength at the 4% epiphyseal site (BSIc mg2/mm4 =ToA x ToD2) and cortical bone strength at the 66% site (strength strain index (pSSI mm2) were measured. Significance was determined using two-tailed paired T-tests. Results: No significant differences between dominant and non-dominant limbs were detected for either the 4% or 66% site in both the tibia and the fibula. BSIc measures resulted in the following for tibia and fibula at the 4% site: -2.3% (95% CI = -5.7%-1.1%) and -3.8% (95% CI = -10.8%-3.2%). pSSI measures for tibia and fibula at the 66% site: -1.6% (95% CI = -4.6%-1.4%) and 7.0% (95% CI = -2.4%-16.4%). Conclusion: No significant side to side differences were detected in either the tibia or the fibula. The 95% CI were much larger compared to Weatherholt and Warden (2016) and much larger in the fibula compared to the tibia, suggesting a subset of the VB players could potentially reveal the effects of loading on the fibula depending on factors such as position played and years playing the sport. Under normal conditions the fibula is underloaded, therefore greater differences are expected as a result of sudden high impact loading; a larger sample size is needed to determine this. The results may also conclude that volleyball may not result in loading significant enough to cause large bilateral differences in the lower limb.

***Disclosures: Claudia Romero Medina**, None*

P-067

Preclinical evaluation of a novel 3D-printed composite scaffold using a rodent posterolateral spinal fusion model *Mark Plantz[1], Joseph Lyons[1], Allison Greene[1], Chawon Yun[1], Silvia Minardi[1], Soyeon Jeong[1], Kenneth Blank[2], Robert Havey[2], Muturi Muriuki[2], Avinash Patwardhan[2], Stuart Stock[1], Wellington Hsu[1], Erin Hsu[1]. [1]Northwestern University Feinberg School of Medicine, United States, [2]Edward Hines Jr. VA Hospital, United States

Despite recent advances in bone graft technology, there are significant shortcomings with current bone graft substitutes for spinal fusion. Options such as iliac crest bone graft and recombinant human bone morphogenetic protein-2 (rhBMP-2), while unquestionably effective for promoting bone healing, are limited by morbidity and complications, respectively. Synthetic materials are promising but remain insufficiently effective. To address this issue, we previously developed a recombinant growth factor-free, 3D-printed composite material comprised of hydroxyapatite (HA) and demineralized bone matrix (DBM) for bone regeneration. Herein, we perform a preclinical comparative evaluation of the scaffold relative to a positive control (rhBMP-2/ACS; Infuse™) using a preclinical small animal model. Fifty female Sprague-Dawley rats underwent L4-L5 posterolateral spine fusion (PLF) and were implanted with either the HA-DBM scaffold or with 10 µg rhBMP-2/ACS (Infuse™) (A). Fusion was evaluated 8 weeks postoperatively. Fusion scoring was assessed by 3 blinded investigators using an established scoring system where 0=no fusion (motion between segments), 1=unilateral fusion (motion unilaterally), and 2=bilateral fusion (no motion between segments). Spines that received an average score >=1.0 were considered successfully fused. Biomechanical testing quantified the segmental flexion-extension range of motion (ROM) and stiffness of the fused segments. The same PLF model was used for a mechanistic assessment of osteogenesis. Explants were removed at increasing time points up to 8 weeks for assessment of pro-osteogenic gene expression via qPCR and Western blotting. Fusion rates were not significantly different between the scaffold (93%) and Infuse™ (100%) (B); however, fusion scores were greater with Infuse™ (p=0.008) (C). Both treatments resulted in significantly reduced segmental range of motion (ROM; p<0.001) (D) and greater stiffness (p=0.009) when compared with non-operated controls; this effect was greater with Infuse™ (L4-5 flexion-extension ROM: non-operated control: 28°; scaffold: 15°; Infuse™: 4°). Patterns of gene expression appeared similar between groups, with both Infuse™ and scaffold treatments resulting in significant elevations of several pro-osteogenic markers including Alp, Osx, and Runx2. The HA-DBM scaffold represents a recombinant growth factor-free biomaterial for promoting bone regeneration, with potential to be used as a bone graft substitute for spinal fusion.

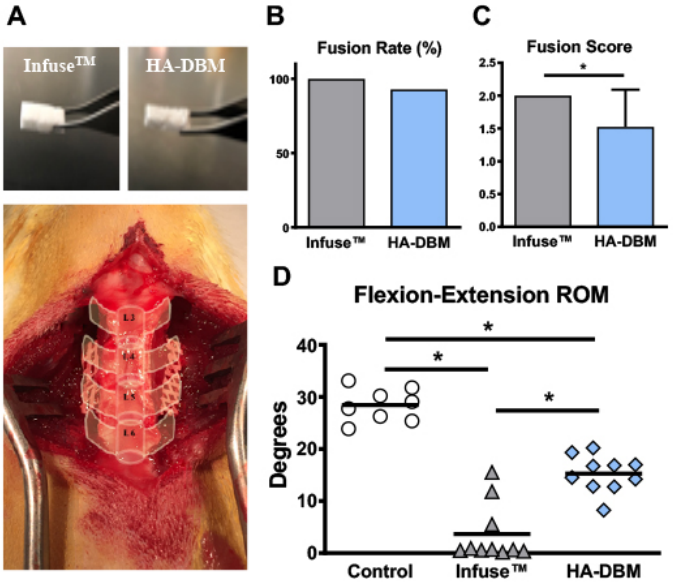

***Disclosures: Mark Plantz**, None*

P-068

Deep learning-based image segmentation performs well when trained and tested on similar, dissimilar, and combined image data *Emilie N. Henning[1], Ryan J. Reger[1], Daniella M. Patton[2], Rob W. Goulet[2], Benjamin Provencher[3], Nicolas Piché[3], Mike Marsh[3], Roberto J. Fajardo[4], Ellen E. Quillen[5], Karl J. Jepsen[2], Todd L. Bredbenner[1]. [1]Department of Mechanical and Aerospace Engineering, University of Colorado Colorado Springs, United States, [2]Department of Orthopedic Surgery, University of Michigan, United States, [3]Object Research Systems, Canada, [4]Clinical and Applied Science Education, University of the Incarnate Word School of Osteopathic Medicine, United States, [5]Section on Molecular Medicine and Center for Precision Medicine, Wake Forest School of Medicine, United States

Separating bone from background is a crucial step in quantifying bone structure in image data. We previously demonstrated that image segmentation via deep learning with fully convolutional neural networks (FCNNs) outperforms methods based on global or local thresholding [1]. The objective of this study was to investigate the performance of FCNN-based segmentation of human vertebral body and femoral neck data when segmented using similar, dissimilar, and combined data.Human L1 vertebral bodies (14 M, 25-88 yrs; 14 F, 28-80 yrs) were imaged using microCT (53µm voxels). Human proximal femurs (15 M, 18-89 yrs; 13 F, 24-95 yrs) were imaged using nanoCT (27µm voxels), and the femoral necks were isolated. Six image slices were extracted from each bone and manually segmented to create ground truth masks (Dragonfly 4.0, ORS). FCNNs (2D U-Net) were separately trained with femoral neck data, vertebral body data, and a combined dataset using a nested four-fold cross-validation approach. Each FCNN was tested by segmenting femoral neck and vertebral body data. Segmentation performance was evaluated using five metrics to quantify similarity between segmented and ground truth masks. Nonparametric multivariate analyses (Wilks' lambda test) were used to simultaneously consider all metrics in evaluating the relative segmentation performance of the FCNN models.Relative model effects were significant ($p < 0.001$), indicating differences in the segmentation performance of the FCNNs (Fig 1). FCNNs trained separately on femoral neck or vertebral body data both outperformed the FCNN trained on the combined dataset in segmenting femoral neck data. Similarly, FCNNs trained on femoral neck or vertebral body data outperformed the FCNN trained on combined femoral neck and vertebral body data in segmenting vertebral body data. All FCNNs reported in the present work performed significantly better than most segmentation methods based on global or local thresholding and not significantly different than the others [1]. Simultaneous consideration of multiple performance metrics indicated that FCNNs trained and tested on dissimilar data performed well compared to FCNNs trained and tested on similar data. Further, a network trained with combined datasets (but not including the test data) performed well on both datasets, suggesting that deep learning-based segmentation may allow broad application of FCNNs trained with varied imaging data on unseen data.1. Patton, et al. Trans. ORS. 2020

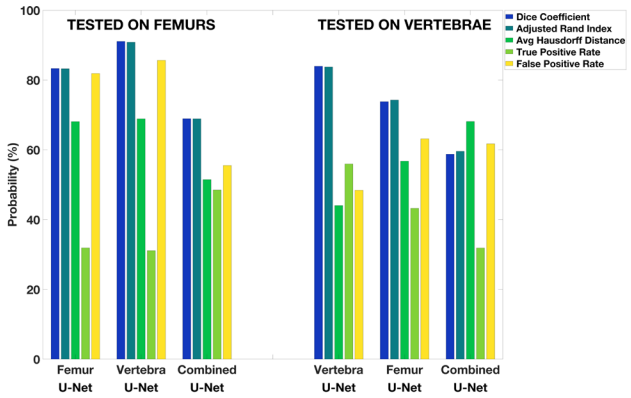

Figure 1. Relative FCNN model effects indicate the probability that segmentation from each model outperforms segmentation from a randomly chosen FCNN model.

***Disclosures: Emilie N. Henning**, None*

P-069

Mechanical Behavior of the Vertebral Endplate *Yuanqiao Wu[1], Elise Morgan[1]. [1]Boston University, United States

Introduction: Vertebral fractures frequently occur in or near the vertebral endplate (VEP) [1], a thin layer of cortical-like bone that helps transfer loads between the intervertebral disc and the interior of the vertebral body. Evidence of changes in the density of the VEP with factors such as age [2] suggests that the mechanical behavior of the VEP may influence the risk of vertebral fracture. In addition, clinical outcomes of vertebral fracture may be worse if the VEP itself becomes cracked or broken [3,4]. Thus, the goal of this study was to quantify the mechanical behavior of the VEP and the dependence of this behavior on VEP density. Methods:80 VEPs were dissected from 39 fresh-frozen human spine segments (L1-L4; M: 24, F:15; age: 77.72+/-11.56 years). A ~30mm×12mm×1.5mm rectangular specimen was cut from the central region of each VEP after stripping off the cartilage endplate. Specimens were imaged using micro-computed tomography (μCT) (μCT40, Scanco Medical; 16μm/voxel, 70kV, 114μA) to quantify bone volume fraction (BV/TV), apparent density (app), and tissue mineral density (TMD). Then each specimen underwent a four-point bend test (Instron 5565) to measure elastic modulus (E), yield stress (σy), and ultimate strain (strain at maximum force, εu), fracture strain (εf)). Linear regression was used to examine the dependence of each mechanical property on each measure of density (JMP Pro 13, SAS Institute). Regressions were performed separately for specimens from the superior vs. inferior VEPs (defined relative to the vertebral body). The mechanical and densitometric measures were also compared between superior and inferior VEPs, using paired analysis where appropriate. Results: Both the elastic modulus and yield stress increased with increasing ρ_app and BV/TV, in both superior and inferior VEPs (r2>0.51, p<0.001). In contrast, ultimate strain and fracture strain decreased with increasing BV/TV in inferior (r2>0.32, p0.08). The yield stress was higher in inferior vs. superior VEPs (p=0.04); no other properties differed with location (p>0.05). Conclusions: With decreasing density, the stiffness (modulus) and strength (yield stress) of the VEP decreased but the ductility (ultimate and fracture strains) decreased. These results suggest a potential compensatory mechanism in the VEP whereby bone loss leads to a more flexible and less strong VEP, yet one that is less prone to breakage. Reference:[1] AO.Ortiz.Am J Neuroradiol,32(1):115-20.[2]Ferguson SJ. Eur Spine J,2003(12): S97-S103. [3] S Dudley. Spine J, 14(7):1256-64. [4]AT Trout.J Bone Miner Re,21(11):1797-802.[5] F.-D Zhao. Bone,44(2):372-9.

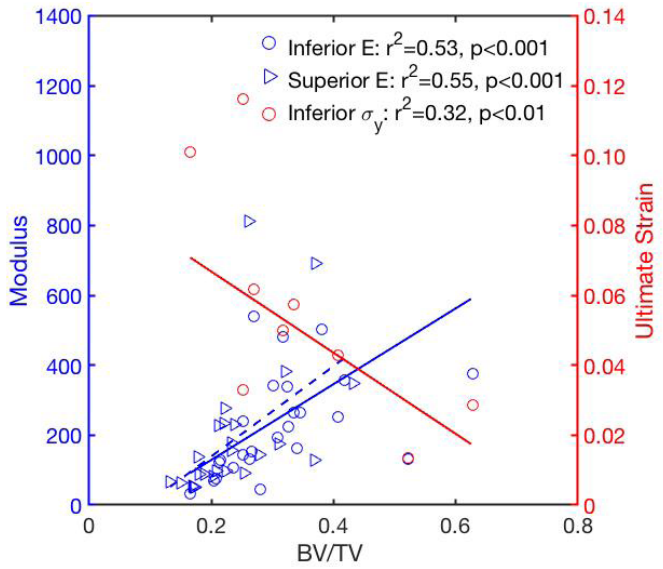

***Disclosures: Yuanqiao Wu**, None*

P-070

Effects of SGLT2 Inhibitor Therapy on the Fracture Resistance of Diabetic Mouse Bone *Jeffry Nyman[1], Clay Bunn[2], Sasidhar Uppuganti[1], Philip Ray[2], Iuliana Popescu[2], Evangelia Kalaitzoglou[2], John Fowlkes[2], Kathryn Thrailkill[2]. [1]Vanderbilt University Medical Center, United States, [2]University of Kentucky Medical Center, United States

As a selective sodium-dependent glucose co-transporter inhibitor (SGLT2I) that causes glucosuria, canagliflozin is an effective therapy to lower blood glucose (BG) levels in patients with T2D. Because hypercalciuria also results from the blocking action of the drug on the renal reabsorption of Na and glucose, there is concern that SGLT2I therapy could exacerbate the T2D-related increase in fracture risk. Using the TallyHO (TH) model (JAX #5314) of juvenile-onset T2D, we tested whether SGLT2I therapy improves or worsens the fracture resistance of diabetic bone. Female TH mice maintain normal glucose levels, while ~75% of male TH mice develop frank T2D. Thus, we assigned male TH mice with established hyperglycemia at 8-10-wk of age to chow (High-BG, n=43) or to chow supplemented with canagliflozin at 100 ppm (Cana, n=52). These mice, along with male TH mice with normal BG (Low-BG, n=16), were euthanized at 20-wk of age after collecting serum. Low-BG mice and Cana-treated mice gained weight between 8-wk and 20-wk, while High-BG mice stopped gaining weight such that their weight was 15% lower than the final weight of the other mice (p0.5). As expected, Cana did not restore urine glucose and calcium excretion to normal levels, which were both similarly elevated in Cana and High-BG compared to Low-BG mice (p<0.0001). As assessed by μCT, the cross-sectional area (Ct.Ar, p=0.001) and cortical thickness (Ct.Th, p<0.0001) of the femur mid-shaft were lower for the hyperglycemic than for the euglycemic mice. Cana normalized Ct.Ar to the level of Low-BG (p=0.252), but only partially rescued Ct.Th still being lower compared to Low-BG mice (p=0.007). The ultimate force endured by the femur mid-shaft during three-point bending was significantly lower in the High-BG than in the Low-BG group (p<0.0001). Cana-treatment increased this structural-dependent measurement of strength by 6.2% (p=0.033 vs. High-BG), with no significant difference between Cana and Low-BG (p=0.505). The ultimate stress was also lower for untreated mice with high BG compared to Low-BG. Cana did not significantly improve this estimate of material strength. Cortical tissue mineral density did not significantly vary among the 3 groups (p=0.070), despite persistent hypercalciuria occurring in Cana and High-BG. There was a significant difference in the distal femur BV/TV between all 3 pair-wise comparisons (pCana>High-BG. Thus, the positive effects of SGLT2I on BG and weight partially corrects the T2D-related deterioration in bone and does not worsen the fracture resistance of diabetic bone.

***Disclosures: Jeffry Nyman**, None*

P-071

Individual Trabecula Segmentation (ITS) Based Analysis of 2nd Generation HR-pQCT Scans of the Human Distal Radius and Tibia Compared to 1st Generation HR-pQCT and μCT Scans *A. Teodora Dinescu[1], Yizhong Jenny Hu[1], Sanchita Agarwal[2], Elizabeth Shane[2], X. Edward Guo[1]. [1]Columbia University, United States, [2]Columbia University Medical Center, United States

High-resolution peripheral quantitative computed tomography (HR-pQCT) has been used for in vivo 3D visualization of trabecular microstructure with low radiation. Sec-

ond-generation HR-pQCT (XCTII) has been shown to have good agreement with first generation HR-pQCT (XCTI) and has an enhanced voxel size from 82 µm to 61 µm. Advanced Individual Trabecula Segmentation (ITS) decomposes the trabecula network into individual plates and rods and has been used to identify subtle bone microstructure features. ITS based on XCTI showed strong correlation to ITS based on micro computed tomography (µCT) and identified important trabecular changes in various diseases. ITS based on XCTII has new potentials in musculoskeletal studies but has yet to be validated. The objective of this study was to assess the agreement between ITS based on XCTII, ITS based on XCTI and ITS based on µCT to assess the capability of ITS on XCTII as a clinical tool.Twenty sets of fresh-frozen tibia and radius bones obtained from the Life Legacy Foundation were scanned in the distal region using XCTI at 82 µm, XCTII at 61 µm and µCT at 37 µm. The µCT image was registered to the corresponding XCTII image to ensure analysis of same regions. XCTII images were registered to XCTI images. A Laplace-Hamming filter was applied to XCTI images and a Gaussian filter applied to the XCTII and µCT images for noise reduction and a global threshold used to binarize the images. ITS analysis was performed on the trabecular region of the registered images. Bone volume fraction (pBV/TV, rBV/TV), number density (pTb.N, rTb.N), thickness (pTb.Th, rTb.Th) and plate-to-rod (PR) ratio (pBV/rBV) of trabecular plates and rods were obtained. Difference between these measurements in XCTII vs µCT and XCTI vs XCTII was calculated. Paired student's t-tests were used to examine the difference. Linear regression was used to determine the correlation coefficient of these parameters.Difference and correlation coefficients of ITS based measurements are shown in Table 1. The XCTII parameters were statistically different from the µCT measurements except BV/TV in the distal tibia and rTb.N in the distal radius and the XCTI parameters were statistically different from the XCTII measurements except pTb.Th. The strong correlation between XCTII and µCT microstructural analysis suggests that XCTII can be used to clinically assess changes in plate and rod microstructure and that values from XCTI can be corrected to XCTII parameters.

Table 1. XCTI vs XCTII and XCTII vs uCT ITS differences and correlations. *(p<0.05)

	Distal radius				Distal tibia			
	Difference (XCTI - XCTII)	R^2 (XCTI vs XCTII)	Difference (XCTII - µCT)	R^2 (XCTII vs µCT)	Difference (XCTI – XCTII)	R^2 (XCTI vs XCTII)	Difference (XCTII - µCT)	R^2 (XCTII vs µCT)
BV/TV	0.032*	0.57	-0.018*	0.80	0.036*	0.86	-0.002	0.91
pBV/TV	-0.043*	0.67	-0.037*	0.77	-0.058*	0.86	-0.021*	0.88
rBV/TV	0.075*	0.50	0.019*	0.74	0.095*	0.48	0.020*	0.43
pTb.N	-0.129*	0.78	-0.299*	0.50	-0.123*	0.78	-0.224*	0.46
rTb.N	0.272*	0.66	0.051	0.54	0.490*	0.37	0.102*	0.33
pTb.Th	0.001	0.35	0.040*	0.71	-0.006	0.40	0.045*	0.79
rTb.Th	0.033*	0.41	0.019*	0.64	0.017*	0.57	0.021*	0.80
PR Ratio	-1.623*	0.80	-1.757*	0.82	-2.382*	0.71	-2.291*	0.74

***Disclosures: A. Teodora Dinescu**, None*

P-072

Effect of vitamin D supplementation on hip structural geometry in the elderly *Aya Bassatne[1], Thomas Beck [2], Ghada El-Hajj Fuleihan[1]. [1]American University of Beirut, Lebanon, [2]Beck Radiological Innovations, United States

Vitamin D in conjunction with calcium reduces the risk of hip fractures in institutionalized elderly subjects but the effect on BMD is less consistent. We hypothesize that the beneficial effects of vitamin D supplementation on fracture risk may result from improved bone strength and geometry rather than BMD. We used data from a trial that randomized 257 overweight elderly individuals to calcium citrate 1000mg daily and cholecalciferol at a daily equivalent dose of 600 or 3,750IU. 221 participants completed the trial. We assessed the effect of vitamin D on Hip Structural Analysis (HSA) parameters including cross-sectional area (CSA), section modulus (Z), subperiosteal width/outer diameter (OD) and buckling ratio (BR). The HSA program measures bone structural geometry of the femoral neck using conventional DXA images. Three regions are analyzed: the narrow neck (NN), the intertrochanter (IT) and the femoral shaft (FS). We ran unadjusted and also adjusted analyses for subtotal lean mass. In the overall group (combining both doses), total hip BMD, NN CSA and Z, IT CSA, FS CSA, subperiosteal width and Z significantly increased between baseline and 12 months, in the direction of increased strength. Within treatment groups, there was a beneficial effect of vitamin D on BMD at the total hip and HSA parameters at the IT and FS in the low dose arm, and on BMD at the total hip, and on HSA parameters including NN, IT and FS in the high dose arm. Subtotal lean mass decreased with vitamin D supplementation in the low dose group but did not change in the high dose group. The favorable effect of vitamin D on HSA parameters at 12 months remained significant at the IT and FS and became significant at the NN in the low dose group after lean mass adjustments. All values at 12 months in the high dose lost significance on adjusted analyses. The only difference in unadjusted HSA parameters between treatment arms was for the delta BR at the intertrochanteric site, with a decrease in the low dose and an increase in the high dose. However, this difference disappeared in the adjusted analyses. Supplementation with 1000mg calcium citrate and vitamin D3 (600 IU/day) for one year had a beneficial effect on total hip BMD and parameters of bone structural geometry and strength that persisted after lean mass adjustments in the low dose, but not high dose arms. More vitamin D is not better, and the reduction in hip fracture with CaD may be mediated by structural as opposed to BMD changes.

Table 1: BMD and HSA parameters at baseline and after 12 months of vitamin D supplementation per treatment group[1]

	Low dose (N=111)		High dose (N=110)	
	Baseline	12 months	Baseline	12 months
BMD				
Total hip BMD (g/cm²)	0.827 ± 0.122[2]	**0.831 ± 0.121***	0.824 ± 0.118	**0.828 ± 0.118***
Femoral Neck BMD (g/cm²)	0.679 ± 0.103	0.682 ± 0.101	0.671 ± 0.101	0.675 ± 0.099
Subtotal lean mass	41015.5 ± 7620.0	**40656.3 ± 7694.9****	40509.9 ± 8166.3	40323.7 ± 7013.5
HSA Narrow Neck				
Cross sectional area (cm²)	2.698 ± 0.469	2.708 ± 0.455	2.667 ± 0.486	**2.702 ± 0.480***
Subperiosteal width[3] (cm)	3.416 ± 0.319	3.416 ± 0.326	3.421 ± 0.357	3.446 ± 0.362
Section modulus (cm³)	1.469 ± 0.366	1.482 ± 0.365	1.432 ± 0.391	**1.464 ± 0.394***
Buckling ratio	12.314 ± 2.628	12.219 ± 2.489	12.565 ± 2.605	12.571 ± 2.503
HSA Intertrochanter				
Cross sectional area (cm²)	4.664 ± 0.938	**4.723 ± 1.009***	4.592 ± 0.896	**4.646 ± 0.931***
Subperiosteal width (cm)	5.659 ± 0.504	5.651 ± 0.526	5.635 ± 0.490	**5.680 ± 0.537***
Section modulus (cm³)	4.233 ± 1.212	4.287 ± 1.249	4.187 ± 1.107	4.209 ± 1.176
Buckling ratio	9.396 ± 1.945	9.297 ± 1.877	9.418 ± 1.795	9.494 ± 1.815
HSA Femoral Shaft				
Cross sectional area (cm²)	4.289 ± 0.811	4.312 ± 0.814	4.283 ± 0.822	**4.314 ± 0.819***
Subperiosteal width (cm)	3.062 ± 0.229	**3.078 ± 0.236***	3.061 ± 0.251	**3.074 ± 0.259***
Section modulus (cm³)	2.502 ± 0.572	**2.530 ± 0.576***	2.473 ± 0.549	**2.508 ± 0.559***
Buckling ratio	2.986 ± 0.697	2.998 ± 0.697	2.975 ± 0.704	2.979 ± 0.695

[1]Independent t-tests were used to compare variables between treatment groups at baseline and 12 months. Paired t-tests were used to compare variabl at baseline and 12 months in the overall group and each treatment group separately.
[2] Mean ± SD (all such values)
[3] Subperiosteal width = outer diameter
* p<0.05 (baseline vs 12 months in each treatment group)
** p<0.01 (baseline vs 12 months in each treatment group)

***Disclosures: Aya Bassatne**, None*

P-073

A Clinically Handy Novel Mechanical Parameter to Quantify the Microarchitecture Effect on Apparent Modulus of Trabecular Bone *Yongqiang Jin[1], Teng Zhang [1], Kam Yim Sze[1], Jason Pui Yin Cheung[1], William Weijia Lu[1]. [1]The University of Hong Kong, Hong Kong

An important aspect of bone quality is the trabecular microarchitecture which can vary the apparent modulus (E) of trabecular bone independent of bone volume fraction (BV/TV). Previous studies have employed morphological/topological indices to quantify E. However, E itself is a mechanical quantity and those non-mechanical indices are not easily interpretable in clinical practice. This study aims to propose a novel mechanical parameter that is clinically handy to quantify the microarchitecture effect on E.Fourteen human female cadaveric vertebrae were scanned with a µCT at 18 µm isotropic resolution. Four trabecular specimens (3.46×3.46×3.46 mm) were obtained from each vertebral body and converted to voxel-based finite element (FE) models. E value of the FE model was computed using linear FE analysis. The normalized apparent modulus (E*) was computed as E divided by BV/TV. Linear regression was performed between E* and BV/TV. Ineffective bone mass (InBM) was defined as the bone mass with a negligible contribution to the load-resistance and represented by elements with von Mises stress less than a certain stress threshold. InBM was quantified as the low von Mises stress ratio (LSVMR), which is the ratio of the number of InBM elements to the total number of elements in the FE model. An incremental search technique with coarse and fine search intervals of 10 and 1 MPa, respectively, was adopted to determine the stress threshold for calculating LSVMR. Correlation between E* and LSVMR was analyzed using linear and power-law models for each stress threshold with the one producing the highest coefficient of determination (R2) taken as the optimal threshold. Linear regression was performed between E and LSVMR. Multiple linear regression of E against both BV/TV and LSVMR was further analyzed. E* has no significant ($p = 0.75$) correlation with BV/TV. Incremental search suggests 59 MPa to be the optimal stress threshold. BV/TV alone can explain 59% of the variation in E ($E = 2254.64BV/TV1.04$, $R2 = 0.59$, $p < 0.001$). LSVMR alone can explain 48% of the variation in E ($E = 1696.4 – 1647.1LSVMR$, $R2 = 0.48$, $p < 0.001$). With both, 95% of the variation in E can be explained ($E = 1364.89 + 2184.37BV/TV – 1605.38LSVMR$, adjusted $R2 = 0.95$, $p < 0.001$). We conclude LSVMR can be adopted as the mechanical parameter to quantify the microarchitecture effect on the apparent modulus of trabecular bone and it is clinically handy with the interpretation of ineffective bone mass.

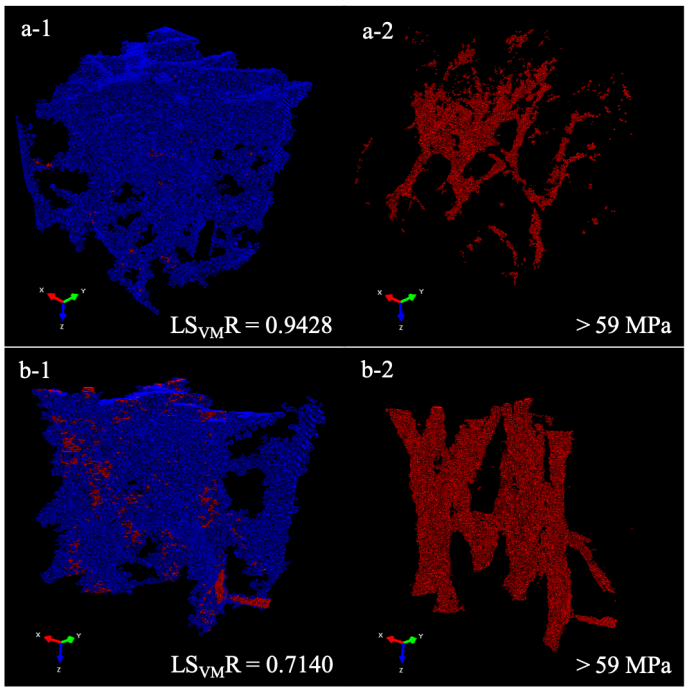

***Disclosures: Yongqiang Jin**, None*

P-074

3D printed tough magnesium phosphate-based implants induce bone regeneration in an equine defect model *Miguel Castilho[1], Nasim Golafshan[1], Elke Vorndran[2], Uwe Gbureck[2], Harold Brommer[3], René van Weeren[3], Jos Malda[1]. [1]University medical Center Utrecht, Netherlands, [2]Universitätsklinik Würzburg, Germany, [3]Utrecht University, Netherlands

Introduction: Magnesium phosphates (MgP) have shown to significantly enhance bone formation when compared with the standard calcium phosphate-based ceramics. However, such materials can hardly be shaped into large and complex geometries and more importantly lack adequate mechanical properties for the treatment of load-bearing and complex shape bone defects. In this study, we have engineered bone implants through extrusion assisted three-dimensional (3D) printing of MgP ceramics modified with Sr2+ ions (MgPSr) and a medical grade polycaprolactone (PCL) polymer phase.Materials and methods: MgPSr based powders were first synthesized and then combined with PCL at different weight ratios (70:30, 60:40, and 50:50 wt.%). Printability of MgPSr-PCL composite pastes was investigated using a pneumatic-driven 3D printer (regenHU, Switzerland). Full characterization of the printed materials in terms of their physico-chemical, structural and mechanical properties was performed. Cytotoxicity, resorbability and osteo-conductive (and inductive) properties of printed materials was first accessed in vitro, in the presence of equine mesenchymal stem cells (MSc), and then in vivo in an equine model (Shetland ponies, n=8). Bone tissue formation was evaluated after 6 months of implantation by micro-CT, histology and energy-dispersive X-ray spectroscopy combined with scanning electron microscope.Results and Discussion: MgPSr with 30wt.% PCL (MgPSr-PCL30) allowed the printability of relevant size structures (>780 mm3) with an interconnected macroporosity (>40%) and elastic mechanical properties (~ 40MPa elastic modulus, ~ 300 kJ/m3 toughness) (Fig 1). Notably, MgPSr-PCL30 implants were able to promote in vitro bone formation without the supplementation with osteo-inducing components. In addition, long-term in vivo performance of MgPSr-PCL30 implants in equine tuber coxae model for 6 months showed these implants induced bone regeneration without eliciting any negative inflammatory reaction, while no bone formation was observed in the empty defects (Fig 1A-C).Conclusion: Overall, the developed MgP-based composite materials and extrusion-based 3D printing process presented here open promising avenues to satisfy the growing need for fully resorbable and mechanically competent bone implants.

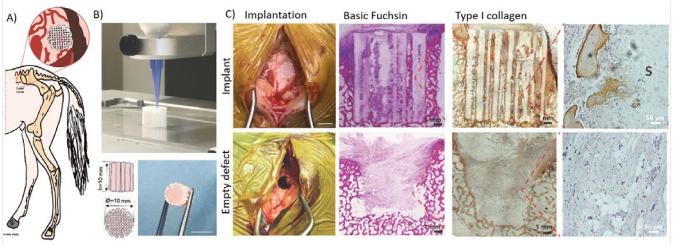

Fig 1: Workflow of the work: from implant fabrication to in vivo evaluation. A) Schematic of equine tuber coxae model. B) Implant extrusion-based 3D printing. C) Histological assessment of new bone formed (*) within the MgPSr based composite after 6 months *in vivo* evaluation

***Disclosures: Miguel Castilho**, None*

P-075

Are wide proximal femurs weaker? *Karl Jepsen[1], Erin Bigelow[1], Daniella Patton[1], Robert Goulet[1], Stephen Schlecht[2], David Kohn[1], Carrie Karvonen-Gutierrez[1], Todd Bredbenner[3]. [1]University of Michigan, United States, [2]Indiana University, United States, [3]University of Colorado Colorado Springs, United States

In simple terms, biomechanical principles dictate that wide bones should be stronger than narrow since strength is proportional to outer width cubed. However, wide femoral necks show increased fracture risk in some studies. The biomechanical mechanism that explains this association in terms of structure-function relationships is not fully understood. We tested the hypothesis that wide proximal femurs will show greater loss of strength and structural traits with age compared to narrow.Proximal femurs were obtained for 50 white male cadavers (18-89 years; IRB approved). Femoral neck trabecular architecture and narrow-neck cortex traits were quantified from nanoCT images (27µm). Whole bone strength (max load) was determined by loading proximal femurs in a sideways fall configuration. Samples were sorted into 5 groups using total cross-sectional area (TtAr), cortical area (CtAr), and trabecular BV/TV (K-means cluster analysis). Two clusters containing 1-2 samples each were not examined. The three remaining clusters overlapped in CtAr and BV/TV but not TtAr. Based on TtAr, groups were designated as narrow (n=13), intermediate (n=20), or wide (n=14).The wide (R2=0.41, p=0.019) and intermediate (R2=0.32, p=0.019) but not narrow (R2=0.12, p=0.301) groups showed significant negative associations between strength and age (Fig 1). TtAr showed nonsignificant associations with age for all groups. The wide group showed significant negative correlations with age for both CtAr (R2=0.45, p=0.009) and BV/TV (R2=0.38, p=0.019). In contrast, the intermediate group showed a significant negative correlation with age only for BV/TV (R2=0.36, p=0.005), whereas the narrow group showed no significant associations with age for either CtAr (R2=0.06, p=0.405) or BV/TV (R2=0.01, p=0.713).This analysis showed that wide, male proximal femurs are stronger than narrow at younger ages (<65 years; p=0.006, 2-way ANOVA) consistent with biomechanical principles. However, age-related changes in the cortical and trabecular tissues lead to a greater decline in strength of wide proximal femurs and a convergence of strength values at the older ages. Age-related losses of cortical and trabecular tissues varied among the three groups suggesting that outer bone size may predict individual trait-age trajectories. Further research is needed to understand why cortical and trabecular mass decline with age in wide but not narrow proximal femurs and how combinations of change affect bone strength.

Fig 1. Linear regression analysis showed different strength-age associations for proximal femurs sorted into wide, intermediate, and narrow subgroups.

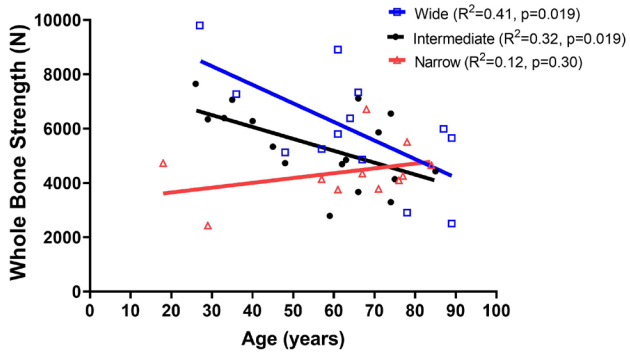

***Disclosures: Karl Jepsen**, None*

Posters

P-076

Pull out strength of the screw and compression force of vertebra gain with a 3-month course of romosozumab treatment: Prospective study using finite element analysis *Koji Ishikawa[1], Soji Tani[1], Koki Tsuchiya[1], Hiro Hasegawa[2], Takako Negishi-Koga[3], Yoshifumi Kudo[1], Toshiyuki Shirahata[4], Takashi Nagai[1], Tomoaki Toyone[2], Katsunori Inagaki[1]. [1]Department of Orthopaedic Surgery, Showa University School of Medicine, Japan, [2]Department of Orthopaedic Surgery, Showa University School of Medicine, Japan, [3]Division of Malaria Immunology, Department of Microbiology and Immunology, The Institute of Medical Science, The University of Tokyo, Japan, [4]Department of Orthopaedic Surgery, Showa University Koto Toyosu Hospital, Japan

Introduction: Romosozumab (Romo) recieved the first in the world approval in Japan for the treatment of osteoporosis. Several studies have investigated the effect of osteoporosis treatment in patients undergoing spinal surgery. However, the lack of evidence to support use of Romo during spinal surgery. The aim of the present study was to investigate the effect of Romo on spinal surgery using FEA (finite element analysis).Methods: Fourteen patients (age: 73.1 +/- 6.0 years: mean +/- SD) with postmenopausal osteoporosis were included for this prospective study. All patients were analyzed using blood samples, DXA, and CT. In performing FEA analysis, each 3D model of L4 vertebra was constructed from the CT data. The 3D-FE models of the pedicle screw were developed separately from high solution micro-CT and inserted in the 3D vertebra model using traditional trajectory. Pull out strength (POS) of the screw and compression force of vertebra were assessed at baseline and 3 months following treatment.Results: Thirteen patients (92.9 %) completed 6 months follow-up with no fracture events. There were a significant change in TRACP-5b and total-P1NP from baseline to 3 months (P<0.01, vs baseline: Wilcoxon). The percent LS BMD changes increased significantly from baseline to 6 months (14.4 %, P<0.01, vs baseline: Wilcoxon). Notably, percent POS changes and compression force of vertebra were significantly increased from baseline in only 3 months treatment (POS: 24.1%, Compression force: 13.5%, P<0.01, vs baseline: Wilcoxon).Discussion: In summary, our prospective biomechanical study using FEA showed 3 months treatment of Romo was effective in both screw fixation and compression force of vertebra. Romo may be useful for patients undergoing spine surgery.

Finite element analysis: Pull out strength

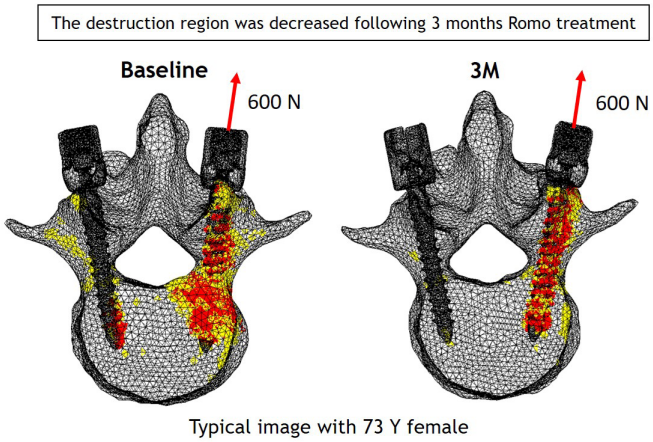

***Disclosures: Koji Ishikawa**, None*

P-077

Fracture Risk in Lower Extremity High Rate Loading - A Probabilistic Statistical Shape and Density Finite Element Analysis *Lance Frazer[1], Daniel Nicolella[1]. [1]Southwest Research Institute, United States

Background: Anti-vehicular landmines and improvised explosive devices (IEDs) can produce catastrophic lower extremity injuries. As such, lower extremity injury prevention is of high concern but requires a better understanding of high-rate impacts and fracture risk. In this study, a probabilistic finite element model of the tibia and talus was developed to produce a fracture risk assessment and was compared to experimental cadaveric testing. Methods: We developed a high-fidelity statistical shape and density model of the tibia to provide a means of generating physiologically plausible anatomies to investigate the effect of anatomical variability on the risk of injury. Probabilistic descriptions of bone material properties for the tibia were taken from literature and internal sources to account for natural variation and uncertainty. A 7.5 kN distal tibia impact simulation was developed following the methodology of a previously described framework. This 7.5 kN load corresponds to nearly a 10% tibial fracture risk, which was experimentally derived using cadaveric specimens. Using the probabilistic descriptions of anatomy and material properties, a Latin Hypercube probabilistic finite element analysis was performed using the 2nd percentile strain as a failure criterion. Results and Discussion: The probabilistic analysis resulted in a computed risk of fracture of 10% given the 7.5 kN impact force on the distal tibia. Uncertainty and variability in the bone failure strain, material properties, and tibia anatomy substantially influenced fracture risk. The described probabilistic model reproduced experimentally derived fracture risk and can be used as a comprehensive surrogate to cadaveric testing for high-rate distal tibia impacts. This model can be used for the design of protective equipment, the identification of high-risk individuals, and the development of novel injury mitigation strategies.

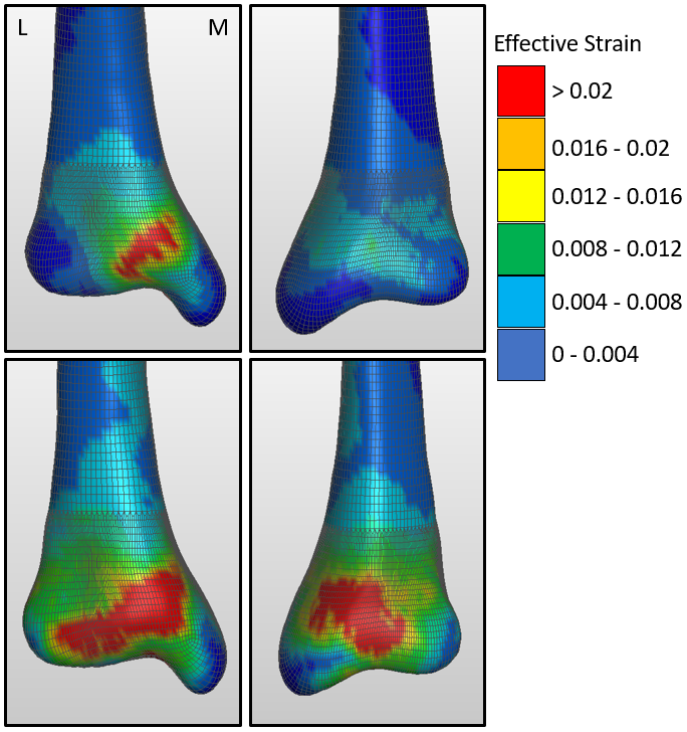

***Disclosures: Lance Frazer**, None*

P-078

Bilateral Asymmetry in the Healing Distal Radius: An in vivo HR-PQCT Micro-Finite Element Analysis Study *Caitlyn Collins[1], Penny Atkins[1], Nicholas Ohs[1], Lukas Horling[2], Kerstin Stock[3], Patrik Christen[0], Michael Blauth[2], Ralph Müller[1]. [1]Institute for Biomechanics, ETH Zurich, Switzerland, [2]Department for Trauma Surgery, Innsbruck University Hospital, Austria, [3]Department for Trauma Surgery, Innsbruck University Hospital, Austria, [0]Institute for Biomechanics, ETH Zurich; institute for Information Systems, FHNW, Switzerland

Despite evidence of inhibited recovery in non-dominant arm fractures, hand dominance in fracture healing remains under investigated. With the advent of high-resolution peripheral quantitative computed tomography (HR-pQCT), changes in microstructural and biomechanical properties can be assessed in vivo. The objective of the current study was to assess the effect of hand dominance on fracture healing using HR-pQCT-based micro-finite element (microFE) analysis.Patients (3 males, 26-70 years; 8 females, 27-81 years) with a conservatively treated, unilateral radius fracture provided informed consent prior to participation (Ethics Committee, Medical University of Innsbruck). Standard clinical HR-pQCT scans (XtremeCT II, Scanco Medical AG, isotropic voxel size: 61 µm) were taken of the fractured (F) and contralateral (C) radii (168 slices) at 1, 3, 5, 13, 26, and 52 wks post-fracture. Additional data, proximal and distal to the standard scan, were captured for the F-radii (504 total slices). MicroFE models, generated from registered HR-pQCT data via direct conversion from voxels to hexahedral elements (Python v3.7), were assigned scaled, linear elastic material properties (Poisson's ratio=0.3). "High friction" compression tests with a prescribed 1% axial displacement were performed on all models. Anterior-posterior (AP) strain ratios were compared after isolation of the two regions using a cutting plane with surface normal from the center of mass to the dorsal tubercle (Figure 1, right).Median Effective (Eff) strain was consistently higher (20-55%) posteriorly for both non-dominant and dominant C-radii. AP Strain ratio was significantly larger (p=0.027) and more consistent for the dominant C-radii (Figure 1, left). This behavior was irrespective of patient age. As a result of the fracture, AP Strain ratios (+/-sd) were inverted until 13 wk (0.84+/-0.14; 1 wk: 1.18+/-0.42) and 26 wk (0.98+/-0.18; 1 wk: 1.27+/-0.36) in the dominant and non-dominant F-radii, respectively. The disparity in AP strain ratio between non-dominant and dominant C-radii suggests that C-radii cannot be used as a patient-specific, "healthy" reference. Full recovery after fracture may take more than one-year, as subjects in the current study have yet to achieve reference C-radii AP Strain ratios at 52 wk. Despite limited size of the current subset, the results

indicate that HR-pQCT-based microFE analysis is sensitive enough to detect and track dominance-related contributions to bone fracture healing.

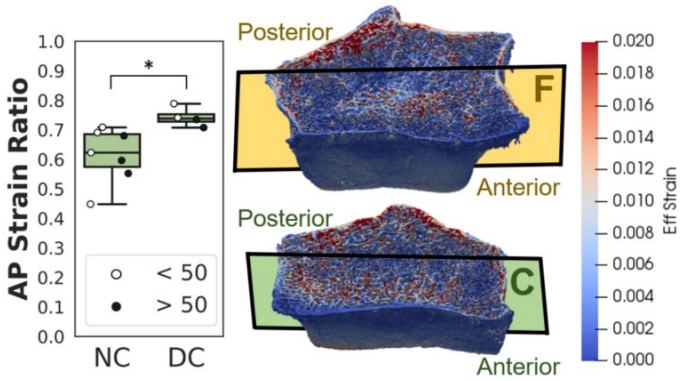

Figure 1: (Left) Anterior-Posterior (AP) Median Effective (Eff) Strain ratios for the non-dominant and dominant contralateral radii (NC and DC, respectively), markers indicate patient age. (Right) Contour plots of Eff Strain for representative fracture (F) and contralateral (C) radii.

***Disclosures: Caitlyn Collins**, None*

P-079

Effects of In Vitro Vitamin B Treatment on Advanced Glycation End-Products and Human Cortical Bone Mechanical Properties *Taraneh Rezaee[1], Rachana Vaidya[2], Jacob Aaronson[2], Lamya Karim[2]. [1]Department of Bioengineering, University of Massachusetts Dartmouth, United States, [2]Department of Bioengineering, University of Massachusetts Dartmouth, United States

T2D patients experience 3x increased fracture risk compared to non-diabetics even with normal to high bone mineral density. It is likely the high risk is due to poor bone quality, which results from many factors including increased advanced glycation end-products (AGEs). It is important to test methods to prevent these harmful AGEs from forming. Vitamin B6 (VitB) is an AGE inhibitor that has been used to treat diabetic complications such as neuropathy and cardiovascular issues1,2. Here, we investigated the effects of in vitroVitB treatment on bone material properties and hypothesized treatment with VitBwill decrease AGEs and improve bone mechanical properties.Twenty cortical beams were acquired from cadaveric human tibias and randomly divided into groups: vehicle, ribose (R), R + 0.5mM VitB, R + 5 mM VitB, and R + 50 mM VitB. Beams were incubated for 10 days at 37°C in solutions with 5 mM benzamidine, 25 mM e-amino-n-caproic acid, 10 mM n-ethylmaleimide, and 30 mM HEPES in Hank's Buffer. Ribose and VitB groups had 0.6 M ribose and respective concentrations of VitB. Beams were imaged by microCT, mechanically tested by cyclic Reference Point Indentation (cRPI) and 4-point bending, and assessed for total fluorescent AGEs.Tissue mineral density and cortical porosity were not different between groups. AGEs were increased in the ribose group compared to vehicle control ($p<=0.05$), but there were no differences in AGEs in Vitamin B treated groups vs ribose group. Mechanical testing variables by bending tests did not differ between groups. Majority of cRPI variables were not different between groups, except unloading slope (US) and average unloading slope were lower ($p<=0.05$) in 5 and 50 mM Vitamin B6 treated groups compared to the ribose group.We observed lower US and average US in VitB treated groups, indicating the treatment made bone less stiff, but this change was not explained by altered AGE levels. In contrast, a previous in vitro study showed VitB had an inhibitory effect on AGEs and improved indentation distance increase (IDI) in the presence of glucose3. This indicates 1) vitamin B6 may not be as effective on ribose-derived crosslinks, or 2) we may need to further assess individual AGEs such as pentosidine and carboxymethyllysine in addition to increasing sample size to get a full understanding.References: 1) Kilhovd, et al., 1999; 2) Jimenez, et al., 2009; 3) Abar, et al., 2018Ack:University of Massachusetts Dartmouth Multidisciplinary Seed Funding

Table 1. Average and standard deviation per group for AGEs, cRPI variables and microCT variables for in vitro ribose and Vitamin B6 incubated bone. Asterisks (*) denote that the average values of the groups are significantly different than the ribose groups ($p<0.05$), and black dot (•) represents that the average value of the group is significantly different than the vehicle group ($p<0.05$).

	Cortical Porosity (%)	TMD (mgHA/cm3)	ID (µm)	US (N/mm)	CID (µm)	TID (µm)	IDI (µm)	Avg ED (µJ)	Avg US (N/µm)	Avg LS (N/µm)	AGEs (ng quinine/mg collagen)
Vehicle	7.47±1.42	1057.88±15.15	64.67±5.71	0.33±0.03	5.33±1.88	65.42±6.12	9.2±2.65	15.57±2.74	0.362±0.02	0.28±0.02	339.76±97.28
Ribose	7.81±1.32	1057.83±5.30	58.83±8.41	0.35±0.03	4.75±2.05	63.58±9.27	8.78±3.52	16.19±4.37	0.38±0.02	0.29±0.02	974.63±221.80*
R+0.5mM VitB	9.65±3.43	1065.89±9.95	60.17±8.10	0.33±0.03	5.17±1.57	64.08±7.80	8.14±1.73	15.59±2.13	0.36±0.01	0.29±0.01	1008.90±198.14
R+5mM VitB	7.86±1.94	1064.41±12.70	61.42±11.03	0.31±0.03*	5.08±2.46	65.41±11.21	8.23±2.92	16.72±3.65	0.34±0.03*	0.27±0.03	770.40±114.18
R+50mM VitB	9.86±3.81	1050.67±12.43	57.92±5.04	0.31±0.05*	4.83±1.14	62±5.38	8.14±1.79	17.36±3.02	0.33±0.05*	0.26±0.04	1634.00±748.69

***Disclosures: Taraneh Rezaee**, None*

P-080

Effects of High-dose Bisphosphonate Therapy on the Fatigue-life of Whole-bone and Bone Tissue *W. Brent Edwards[1], Ifaz Haider[1], Andrew Sawatsky[1], Rebecca Page[1]. [1]University of Calgary, Canada

Long-term bisphosphonate (BP) use has been linked to atypical femoral fractures (AFF) defined as fatigue-like fractures of the femoral shaft. The prevailing hypothesis for AFF is that BP related suppression of bone remodeling impairs tissue-level fatigue resistance; however, BPs are also associated with increases to bone mineral density and cortical thickness at the whole-bone level. It remains unclear how BP-induced changes to bone across these different length scales influence fatigue-life measurements. In this study, we quantified the effects of high-dose BP therapy on the fatigue-life of whole-bone and bone tissue in New Zealand white rabbits treated for 6 months with alendronate (ALN; 0.15 mg/kg; n=3) or vehicle (VEH; n=3) via subcutaneous injection; the dosage was 50-times higher than the clinical dosage in humans. After treatment, whole-tibiae were imaged using computed tomography (CT) then cyclically loaded in zero-compression at 50% ultimate strength until failure or a run-out of 500,000 cycles. Tissue-level tests were performed on 44 cortical beam-samples (1.1 x 1.1 x 16 mm) prepared from femora. Samples were cyclically loaded in four-point bending at either 140, 120 or 100 MPa until failure. After fatigue assessment, sections of bone near the fracture site were imaged using µCT (5 µm isotropic voxel size). Median volumetric bone mineral density and content were 4.1% and 14.2% higher for ALN, respectively, demonstrating a marked osteogenic response to drug. In general, whole-tibiae from ALN rabbits (median=500,000, IQR=214,631 cycles) illustrated a longer fatigue-life than VEH (median=28,300, IQR=76,201 cycles), with the majority of ALN bones reaching 500,000 cycles (Figure 1); the Cohen's d effect size between groups was large (d = 1.62). At the tissue-level, generalized linear modeling verified a relationship between load magnitude and fatigue-life ($p < 0.001$); however, no effect of treatment group ($p=0.243$) or group x load interaction ($p=0.224$) was observed. The overall porosity and size of the Haversian systems were lower in ALN when compared to VEH (d=0.66-1.82, depending on measure). To summarize, 6-months high-dose BP therapy illustrated improvements to whole-bone fatigue-life, no changes to bone-tissue fatigue-life, and structural and microarchitectural changes consistent with long-term BP therapy. These preliminary findings open doors to alternative hypotheses for the increased risk of AFF associated with prolonged BP treatment.

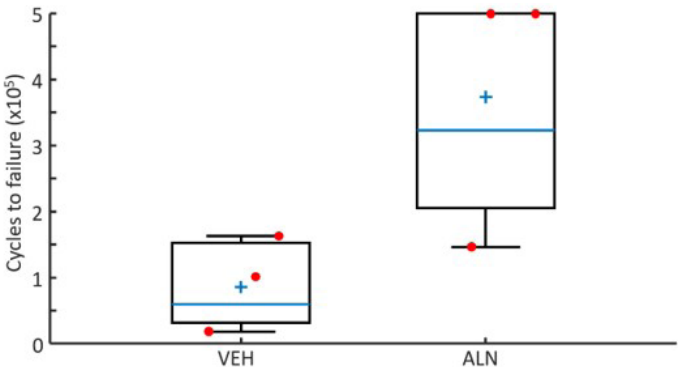

***Disclosures: W. Brent Edwards**, None*

Posters

P-081

Why the cervical spine doesn't break – a biomechanical examination by load testing the vertebrae of 13 body donors *Guido Schröder[1], Sven Spiegel[1], Marko Schulze[2], Rene Trezack[3], Reimer Andresen[4], Hans-Christof Schober[5]. [1]University Medical School Rostock, Germany, [2]Institute of Anatomy, University Medical School Rostock, Germany, [3]Faculty of Mechanical Engineering and Marine Engineering, Department of Construction Technology/ Lightweight Structures, University of Rostock, Germany, [4]Institute of Diagnostic and Interventional Radiology/Neuroradiology, Westkuestenklinikum Heide, Academic Teaching Hospital of the Universities of Kiel, Luebeck and Hamburg, Germany, [5]Department of Internal Medicine IV, Municipal Hospital Suedstadt Rostock, Academic Teaching Hospital of the University of Rostock, Germany

IntroductionOsteoporotic fractures of the cervical spine (CS) are seldom described. This raises the question of whether cervical cancellous bone differs in structure from that of thoracic (TS) and lumbar (LS) vertebrae. Structural and material characteristics of the cervical, thoracic and lumbar spine were compared in terms of the bone structure, structure model index (SMI), degree of anisotropy (DA) and failure load.MethodsCancellous bone was extracted using a Jamshidi Needle® from each of the cervical, thoracic and lumbar vertebrae of 13 body donors (Age: 84.2+/-8.5 y, 5 f, 4m). The investigations were carried out using a µ-CT (SKYSCAN 1172, RJL Micro & Analytic GmbH, Germany). A flat-field correction and a reference comparison with phantoms of density 0.25 g/cm³ and 0.75 g/cm³ were performed. We measured the force required to generate a first-degree fracture (20% height loss) in 104 vertebral bodies using a load test. The load tests of vertebral bodies C5, C6, T7, T8, T9, T12, L1, L3 were performed on a servo-hydraulic testing machine (MTS 858, MTS Systems Cooperation, Eden Prairie, USA). ResultsWith regard to SMI and DA, bone density (BV/TV), trabecular thickness (Tb.Th.) and trabecular separation (Tb.Sp.), statistically significant differences were found between cervical spine and thoracic spine and between cervical spine and lumbar spine.SMI: CS vs. TS p=0,009; CS vs. LS p=0,002; DA: CS vs. TS p=0,026; CS vs. LS p=0,025. The force required to produce a first-degree fracture was approximately twice as high in the cervical spine compared to the thoracic and lumbar spine. Failure strength CS vs. TS p= 0,002; CS v. LS p= 0,002. ConclusionCervical vertebrae have significantly greater load capacity before fracturing compared to thoracic and lumbar vertebrae due to their denser structure, higher SMI and a lesser degree of anisotropy. These morphological differences may explain why osteoporotic fractures in vivo rarely occur in the cervical spine.

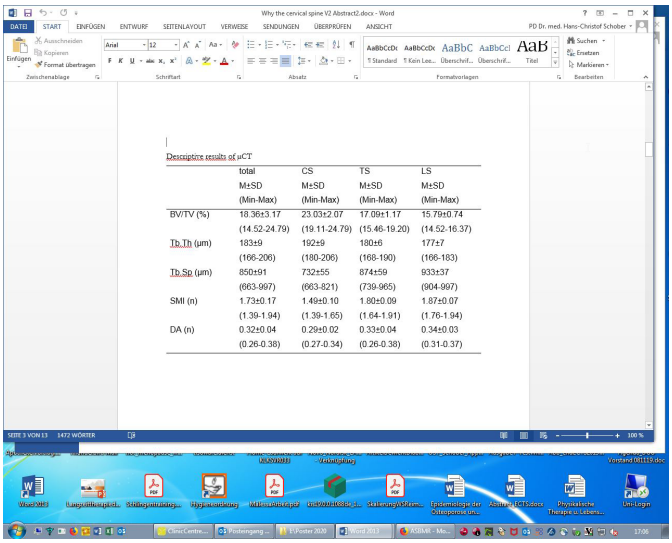

Descriptive results of µCT

	total M±SD (Min-Max)	CS M±SD (Min-Max)	TS M±SD (Min-Max)	LS M±SD (Min-Max)
BV/TV (%)	18.36±3.17 (14.52-24.79)	23.03±2.07 (19.11-24.79)	17.09±1.17 (15.46-19.20)	15.79±0.74 (14.52-16.37)
Tb.Th (µm)	183±9 (166-206)	192±9 (180-206)	180±6 (168-190)	177±7 (166-183)
Tb.Sp (µm)	850±91 (663-997)	732±55 (663-821)	874±59 (739-965)	933±37 (904-997)
SMI (n)	1.73±0.17 (1.39-1.94)	1.49±0.10 (1.39-1.65)	1.80±0.09 (1.64-1.91)	1.87±0.07 (1.76-1.94)
DA (n)	0.32±0.04 (0.26-0.38)	0.29±0.02 (0.27-0.34)	0.33±0.04 (0.26-0.38)	0.34±0.03 (0.31-0.37)

***Disclosures: Guido Schröder**, None*

P-082

Dietary Supplements Do Not Improve Bone Quality in C57BL/6J Female Mice *Amy Creecy[1], Collier Smith[2], Joseph Wallace[2]. [1]Indiana University, United States, [2]IUPUI, United States

There are multiple dietary supplements marketed for their ability to improve health outcomes, including reducing the symptoms of osteoarthritis or improving skin and nail quality. Some of these dietary supplements contain components of the extracellular matrix of bone and could possibly impact bone quality. Beginning at 11 weeks of age, female C57BL/6J mice were given dietary supplements (hydrolyzed collagen, chondroitin sulfate, fish oil, or glucosamine) 5 times per week for 8 weeks (n=10 per group). Supplements were suspended in Milli-Q water and then deposited onto a Bacon Softie® food supplement. Mice had access to eat these supplements ad libitum. Control mice were given the same food supplement soaked with only Milli-Q water. Femurs and vertebrae were collected and stored in PBS-soaked gauze at -20°C. Femurs and vertebra were scanned with µ-computed tomography (9.8 µm voxel size) to determine bone structure. Femurs were tested to failure in 3-pt bending to determine mechanical properties. One-way ANOVA was used for data analysis, followed by Dunnett's multiple comparison tests where dietary supplement groups were compared to the control group if one-way ANOVA values were significant. Body weights were not different among the groups. Trabecular bone parameters were similar between all groups in both the femur and vertebrae. There were no significant changes in bone volume fraction (BV/TV), trabecular number or spacing. Structural model index was lower in the femurs for collagen-treated mice, indicating more parallel plate-like structure of trabeculae. There were few differences in cortical bone structure of the femur. Marrow area and endocortical bone surface of glucosamine-treated mice were larger compared to controls, but there was no effect on cortical area or thickness. For the mechanical tests, there were no differences in extrinsic mechanical properties. For material properties, elastic modulus was lower for glucosamine-treated and fish oil-treated mice. This difference in modulus was not accompanied by differences in ultimate stress or toughness. Overall, dietary supplements had minimal effects on bone quality or quantity.

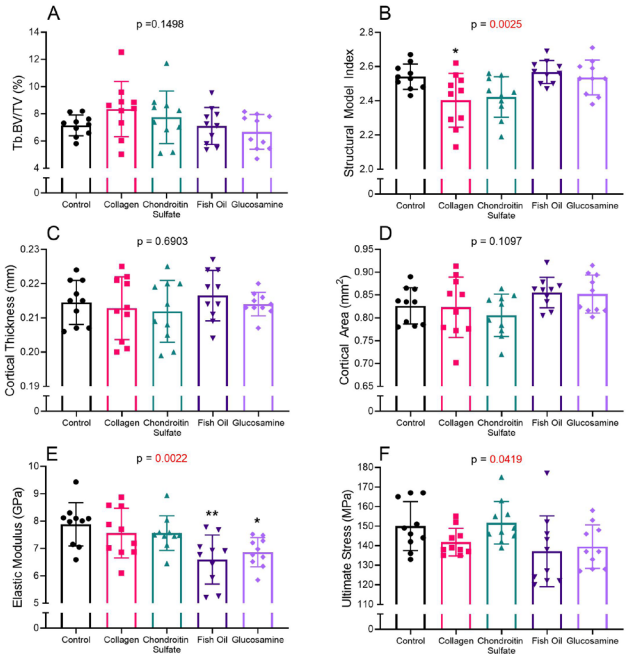

Figure 1: Average and standard deviation of trabecular bone volume (A) and structural model index (B) of the femur metaphysis. Average and standard deviation of cortical thickness (C), cortical area (D), modulus (E) and ultimate stress (F) of the femur mid-shaft. P valuesfrom one-way ANOVAs are shown above the graphs. Asterisks indicate a significant difference when compared to the control group.

***Disclosures: Amy Creecy**, None*

P-083

Enhanced Formation of Carboxymethyllysine in Bone Matrix through Designed Glycation Reaction *Grazyna Sroga[1], Deepak Vashishth[1]. [1]Rensselaer Polytechnic Institute, United States

Formation of advanced glycation end products (AGEs) is of great interest to health and medicine as they are formed at a slow but constant rate in human body and continue to accumulate with time altering key processes and functions. Due to its connection with the in vivo oxidative stress, carboxymethyllysine (CML) is of considerable importance to various oxidative stress-related diseases. Recently, it has been shown that CML accumulates in human aging bone [1] and correlates with fracture incidences [2]. Still, the mechanistic implications of CML accumulation in bone remain to be elucidated. Such studies have been hindered by the lack of suitable experimental strategies generating CML in bone. Thus, the goal of our study was to develop an in vitro strategy for enhanced formation of CML in bone matrix. In vivo, CML can be formed through a number of different glycation and glycoxidation pathways. Of importance to this study is the in vivo oxidative route known as the Namiki pathway [3]. It inspired the development of our new strategy enhancing formation of CML in extracellular bone matrix based on using glyoxal and glyoxylic acid as the substrates. Tibiae (posterior area) from human donors (3 age groups: young (25 y/o), middle-age (48 y/o) and elderly (84 y/o)), served as the source of cortical bone. We determined that on average, glyoxal led to the formation of higher levels of CML. Generally, the developed strategy produced approx. 3.1-fold higher levels of CML over the controls for glyoxal (Fig. 1A) and approx. 2.4-fold for glyoxylic acid (Fig. 1B). We also observed a moderate increase of the AGE levels either with glyoxal or glyoxylic acid, which was expected due to the presence of other amino acids with free functional groups (e.g., arginine, tyrosine or cys-

teine) in matrix proteins, known to react with glyoxal and/or glyoxylic acid. We propose that under the developed reaction conditions, the in vitro generation of CML using glyoxal may be a dominant pathway towards CML formation. In summary, we developed new strategy enhancing formation of CML in bone matrix. Our study presents a new experimental tool to investigate the role and mechanistic aspects of specific AGEs, here CML. We believe that the developed procedure may have general applications beyond skeletal research. References: [1] Thomas et al, Bone 2018, 110: 128-133; [2] Barzilay et al, JBMR 2014, 29(5):1061-1066; [3] Namiki N, Adv Food Res, 1988, 32: 115–184

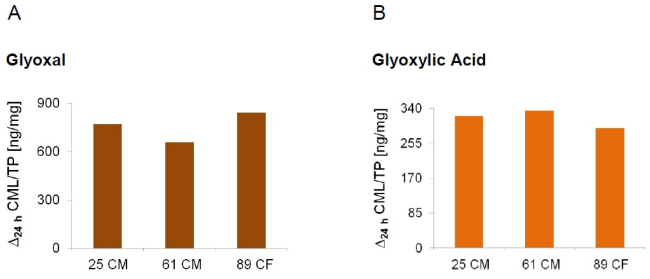

Figure 1. **Increase of total CML levels in bone matrix when using either glyoxal or glyoxylic acid**. The values are expressed as ng of CML per mg of total protein (TP). On average, the developed strategy produced approx. 3.1-fold higher levels of CML (after 24 h; Δ24h) over the controls for glyoxal (**A**) and approx. 2.4-fold for glyoxylic acid (**C**).

***Disclosures: Grazyna Sroga**, None*

P-084

Hypercaloric diet, polyphenols and microarchitecture of Wistar rats femoral neck *Beatriz Almeida Rodrigues[1], Fabiana Cirinos dos Santos[1], Felipe Peressini[1], Matheus Nobile[1], Mark Hurtig[2], Lizandra Amoroso[1]. [1]Universida Estadual Paulista "Julio de Mesquita Filho" - Faculdade de Ciências Agrarias, Brazil, [2]Ontario Veterinary College, University of Guelph, Canada

The objective of this work was to evaluate the influence of the red orange Moro Citrus sinensis (L.) Osbeck and the swimming practice, on the ultrastructural aspects of the femoral neck of male and adult Wistar rats, treated with a high calorie diet. The experimental groups with twelve animals each were organized as follows: normocaloric diet (Dn), hypercaloric diet (Dh), normocaloric diet and phytotherapic (DnF), hypercaloric diet and phytotherapic (DhF), normocaloric diet and swimming (DnS), hypercaloric diet and swimming (DhS), hypercaloric diet, swimming and phytotherapic (DhSF). The dry extract of the red orange was diluted in distilled water and administered at a dose of 7mg/kg, once a day, via gavage. After a week of adaptation, swimming was performed for 30 min a day in a heated pool. After 84 days of treatment, the animals were euthanized, the femurs were dissected and frozen. For microCT analysis on the GE Brightspeed Elite equipment, the samples were thawed gradually at room temperature and kept at the same temperature during scanning. An 80 kv power radiograph and a 4000x2624 charge-coupled device (CCD) camera were used. The voxel size was 5.9 µm. Then, they were placed in acrylic containers and positioned longitudinally, in the craniocaudal direction. After acquiring the 3D images, the reconstruction of the longitudinal sections in the program began. The material was analyzed using Parallax Innovations' Microview software, with selection of the femoral neck as the area of interest (ROI). In the evaluation by computed microtomography (micro-CT) of the femoral neck, there was a greater total volume (VT) and greater bone volume (BV) in the group treated with a high calorie diet and swimming (DhS). Bone mineral content (BMC), bone mineral density (BMD), bone tissue mineral content (TMC) stood out in the DhSF group, while the tissue mineral density was higher in the Dh group. Higher bone volume of the femoral neck was observed after the group that practiced swimming and had access to the high calorie diet. Although there is no change in bone microarchitecture, the morphological changes and BMC, BMD and TMC values may reflect on beneficial effects of the phytotherapic on the femur, minimizing the influence of the high calorie diet on the femoral neck.

***Disclosures: Beatriz Almeida Rodrigues**, None*

P-085

Optimization of a High-Resolution Peripheral Quantitative Computed Tomography(HR-pQCT) Protocol in the Distal Tibia and Radius in Children and Adolescents *Kyla Kent[1], Jin Long[1], Mary Leonard[1], Ariana Strickland[1], Jessica Whalen[1], Babette Zemel[2], Keenan Brown[3], Andrew Burghardt[4]. [1]Department of Pediatrics, Stanford University, United States, [2]Department of Pediatrics, Children's Hospital of Philadelphia, United States, [3]Mindways Software, Inc., United States, [4]Department of Radiology & Biomedical Imaging, University of California San Francisco, United States

HR-pQCT provides novel measures of bone quality that are increasingly used to study bone accrual in healthy children and those with chronic disease. To date, pediatric studies are hampered by lack of consistent methods for reference line placement (endplate vs. growth plate) or scan site (fixed or percent distance). The goal of this study was to establish a protocol for the XCT II scanner that best captures variability in metaphyseal bone outcomes related to sex and maturation. First, we measured the distance from the endplate (tibia plafond or radius medial endplate) to the proximal margin of the distal growth plate in 84 participants (ages 5-29 yr), demonstrating the distance did not scale with total bone length in the tibia or radius (both $R < 0.05$). The distance scaled inversely as a percentage of bone length (tibia R = - 0.59; radius R = - 0.49; both $p < 0.001$), so use of the endplate reference will introduce significant bias with a relatively more proximal scan site in those with shorter bones. Accordingly, we recommend reference line placement at the proximal margin of the distal growth plate. Second, we acquired two consecutive stacks (336 slices over 20 mm) beginning 2 mm proximal to the proposed reference line in 322 participants (ages 5-29 yr). The Figure illustrates the systematic changes in HR-pQCT outcomes within individuals along the length of the tibia metaphysis: e.g. trabecular thickness and cortical thickness increased a mean (SD) of 17% (9.2) and 173% (33) over the scan region, respectively. We used multivariable regression to compare results in a single stack obtained a fixed 2 mm distance from the reference line vs. a single stack centered at 4%. Tests for interaction demonstrated that the 4% site revealed significantly greater sex and maturation effects on trabecular and cortical outcomes, compared with the fixed stack in the tibia: e.g. $p < 0.001$ for greater sex and Tanner maturation effects on trabecular thickness and cortical thickness at the 4% site. Exploratory analyses comparing stacks centered at 3, 3.5, 4, or 4.5% did not demonstrate consistent advantages across HR-pQCT outcomes. Similar results were observed in the radius. Test-retest precision for trabecular and cortical outcomes were comparable at each scan site. In summary, we recommend that the HR-pQCT community adopt a standard pediatric protocol with reference line placement at the proximal margin of the growth plate and a single stack centered at 4% of bone length.

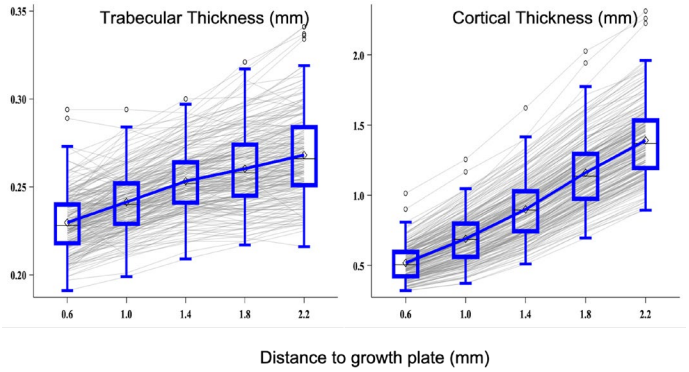

***Disclosures: Kyla Kent**, None*

P-086

Urinary Calcium Excretion is Negatively Associated with Bone Mineral Accrual in Youth with Type 1 Diabetes *David Weber[1], Kimberly O'Brien[2], Noya Rackovsky[1], George Schwartz[1]. [1]University of Rochester Medical Center, United States, [2]Cornell University - College of Human Ecology, United States

Background: The skeletal complications of type 1 diabetes (T1D) include an increased risk of fracture and mild to modest deficits in bone density. The mechanism underlying T1D-related bone disease is unknown. Hypercalciuria has been described in conjunction with T1D, however its relationship with bone accrual has not been evaluated. The objective of this study was to determine if urinary calcium excretion was associated with bone accrual in T1D youth. Methods: Youth with T1D of >=1 yr duration were evaluated with DXA, blood, and urine tests at baseline and 12-months. Whole body less head (WBLH) bone mineral content (BMC) was converted into age and sex specific Z-scores, adjusted for height Z-score. Bone accrual was assessed by WBLH BMC velocity (gm/yr), expressed as Z-scores adjusted for baseline BMC, age, height, weight, growth, and puberty. Urinary calcium excretion was assessed by spot urine calcium to creatinine ratio (Uca/Ucr). Means were expressed (+/- SD) and compared using t-tests; medians as (interquartile range) and compared using Wilcoxon rank sum. Associations between variables were tested by Spearman's rho and multivariable linear regression.Results: 53 subjects (62% male, 83% white) aged 8-20 yr (mean 14.9+/-3.5) completed the study. Mean hemoglobin A1c (A1c) was 8.6+/-1.5%; median duration of T1D was 6.4 (3.5-8.9) yr. WBLH BMC-Z declined from −0.16+/-0.83 to −0.21+/-0.90, p=0.15. Mean WBLH BMC velocity-Z was −0.31+/-0.98, which was significantly lower than the reference population, p=0.03. Spot Uca/Ucr was significantly negatively associated with WBLH BMC velocity-Z, ρ=−0.49, p=0.003 (Fig. 1). This relationship persisted after adjusting for sex, puberty, growth velocity, and biochemical markers of bone mineral metabolism. WBLH BMC velocity-Z was significantly lower in the 6 subjects (11%) with hypercalciuria (Uca/Ucr >0.2) compared to those without hypercalciuria, −0.85 (−2.04-−0.83) vs −0.07 (−0.74-0.55), p=0.02. Positive correlations were seen between Uca/Ucr and both urine glucose to creatinine (ρ=0.31, p=0.03) and urine sodium to creatinine (ρ=0.46, p=0.001) ratios. A1c, a marker of long-term glycemic control, was not associated with bone accrual or Uca/Ucr.Conclusions: Greater urinary calcium excretion was associated with lower rate of bone accrual in T1D youth. Further studies are needed to

Posters

determine if Uca/Ucr is simply a marker of impaired bone mineral accrual or if it may be a potentially modifiable factor to improve bone health in T1D.

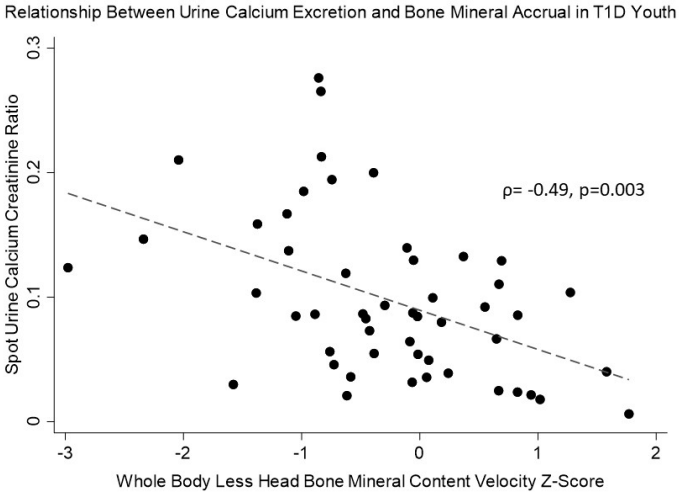

***Disclosures: David Weber**, None*

P-087

Associations of Sex, Sexual maturation, IGF1 and Muscle Mass with Bone Failure Load in the Tibia and Radius Metaphysis and Diaphysis during Development *Tandy Aye[1], Jin Long[1], Kyla Kent[1], Jessica Whalen[1], Ariana Strickland[1], Andrew Burghardt[2], Mary Leonard[1]. [1]Dept of Pediatrics, Stanford University, United States, [2]Dept of Radiology and Biomedical Imaging, University of California San Francisco, United States

Puberty is a time of rapid growth and bone accrual and these gains influence fracture risk across the life course. The independent roles of sex, sexual maturation, insulin-like growth factor -1 (IGF1) and muscle mass on the development of the long bone metaphysis and diaphysis have not been established. Micro-finite element analysis (μFEA) generated failure load (FL) has been associated with fractures in multiple studies but has not been assessed using 2nd generation HR-pQCT (XCT-II, Scanco, Inc) in children and young adults. The objective of this cross-sectional study in 284 healthy participants (151 females), ages 5-30 years, was 1) to identify effects of sex and maturation on metaphysis and diaphysis μFEA FL in the tibia and radius; and 2) to determine the impact of adjustment for IGF1 or muscle mass. Tibia and radius scans were obtained with 10.2 mm volumes centered at distances 4% (metaphysis) and 30% (diaphysis) proximal to the distal growth plate. Failure load was estimated for a 1% axial compression, assuming a homogenous tissue modulus of 10 GPa and failure to occur when 7.5% of elements exceed 7000 μ. Leg and arm muscle mass were obtained from whole body DXA scans. All log-linear regression models for FL were additionally adjusted for age, age2 and bone length as covariates. At all four sites, FL did not differ according to sex within Tanner 1,2 independent of age and bone length. The figure illustrates the study findings in the tibia diaphysis as a representative example. Beyond Tanner 1,2, FL was progressively and significantly greater with successive Tanner stages and was significantly greater in males than females. Sex differences were amplified in Tanner 5 (sex-tanner interaction, p=0.001). IGF1 was positively associated with FL at both sites in the tibia (metaphysis: p<0.001; diaphysis: p<0.01), independent of sex and maturation, but was not significantly associated with FL in the radius. Adjustment for IGF1 did not attenuate the sex and sexual maturation associations with FL in the tibia (Figure). Muscle mass was significantly and positively associated with FL at all 4 sites (all p < 0.001), independent of sex and maturation. Adjustment for muscle largely attenuated the sex and maturation effects on FL at all 4 sites. These novel data will provide the foundation for studies of the impact of chronic childhood disease on bone health and studies of interventions to improve bone strength during growth and development.

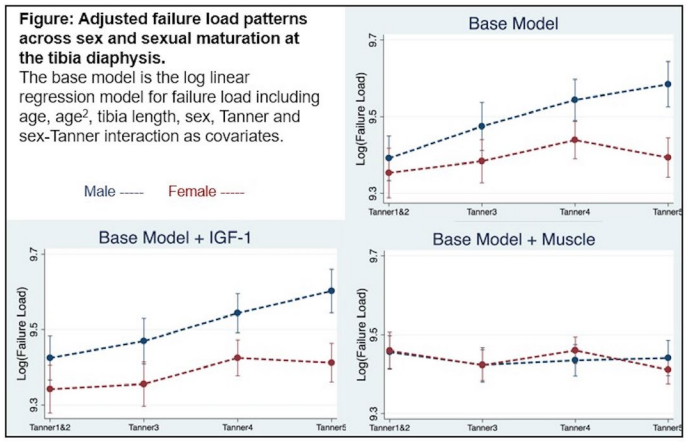

***Disclosures: Tandy Aye**, None*

P-088

Type 1 Diabetes is Associated with Bone and Muscle Deficiencies in Children and Adolescents *Jin Long[1], Hilary Seeley[1], Jessica Whalen[1], Ariana Strickland[1], Kyla Kent[1], Tandy Aye[1], Laura Bachrach[1], Mary Leonard[1]. [1]Department of Pediatrics, Stanford University, Stanford, CA, United States

The bone disease in Type 1 Diabetes (T1D) is characterized by impaired bone formation, resulting in increased fracture risk across the lifespan. Biomechanical forces exerted by muscle are a strong anabolic stimulus to bone formation during childhood and adolescence, and recent data suggest that T1D compromises muscle mitochondrial oxidative capacity. The objective of this study was to assess bone failure load, muscle mass and muscle strength in 50 children and adolescents (ages 10-18 years) with T1D of at least 3 years duration, compared with 182 controls. Tibia and radius HR-pQCT scans (XCT-II, Scanco, Inc) were obtained in the metaphysis and diaphysis at a distance 4% and 30% proximal to the distal growth plate, respectively. Failure load (FL) was estimated using micro-finite element analysis. Leg lean mass was obtained from whole body DXA scans and isokinetic leg strength in knee extension from dynamometry. All bone and muscle measures were converted to sex-specific Z-scores relative to age based on the data in the healthy controls. Participant characteristics were notable for higher BMI Z-scores in the T1D females compared with controls (0.76 +/- 0.57 vs. 0.31 +/- 0.91, p=0.03); BMI Z-scores did not differ in T1D males and controls (0.24 +/- 0.94 vs. 0.26 +/- 0.98). Among males, FL in the tibia metaphysis and diaphysis and leg muscle strength were significantly lower in T1D, compared with controls (Table, all p <= 0.01). The significant bone deficits persisted in the males after adjustment for lower muscle mass or strength. Among females, T1D was not associated with muscle or bone deficits at any site. However, bone deficits were evident in the tibia diaphysis when adjusted for the greater BMI in the female T1D participants. IGF-1 levels were positively associated with tibia FL in the metaphysis and diaphysis within the controls, and were significantly lower in T1D compared with controls (Z-score: -1.01 +/- 1.18 vs. -0.003 +/- 1.00, p < 0.001). However, adjustment for IGF-1 levels had negligible and inconsistent effects on the FL estimates summarized below. Future studies are needed to determine the impact of glycemic control and exercise interventions on musculoskeletal health in children and adolescents with T1D.

Table 1. Bone and Muscle Z-scores in T1D, Compared with Controls

	Male	Female	Male	Female
			Adjusted for BMI Z-Score	
Tibia Metaphysis Failure Load	**-0.57 (p < 0.05)**	-0.11 (p = 0.66)	**-0.56 (p < 0.05)**	-0.37 (p = 0.09)
Tibia Diaphysis Failure Load	**-0.71 (p < 0.01)**	-0.13 (p = 0.60)	**-0.69 (p < 0.01)**	**-0.45 (p < 0.05)**
Radius Metaphysis Failure Load	-0.27 (p = 0.22)	-0.09 (p = 0.69)	-0.27 (p = 0.22)	-0.27 (p = 0.23)
Radius Diaphysis Failure Load	-0.24 (p = 0.29)	0.18 (p = 0.46)	-0.24 (p = 0.28)	0.04 (p = 0.87)
Leg Muscle Mass	-0.34 (p = 0.14)	0.19 (p= 0.43)	-0.33 (p = 0.88)	-0.20 (p = 0.26)
Leg Strength in Knee Extension	**-0.67 (p < 0.01)**	0.01 (p = 0.95)	**-0.66 (p < 0.01)**	-0.27 (p = 0.23)

***Disclosures: Jin Long**, None*

P-089

Preferential maternal transmission of STX16-GNAS mutations responsible for autosomal dominant pseudohypoparathyroidism type Ib (PHP1B): another example of Transmission Ratio Distortion *Zentaro Kiuchi[1], Monica Reyes[1], Harald Jüppner[2]. [1]Endocrine Unit, Massachusetts General Hospital and Harvard Medical School, United States, [2]Endocrine Unit and Pediatric Nephrology Unit, Massachusetts General Hospital and Harvard Medical School, United States

The preferential transmission of a genetic mutation to the next generation, referred to as Transmission Ratio Distortion (TRD), has been described for several autosomal dominant disorders, but the underlying mechanisms remain undefined. Recently, TRD was reported for the offspring of patients affected by either pseudohypoparathyroidism type Ia (PHP1A) or pseudo-pseudohypoparathyroidism (PPHP). These individuals, who carry mutations involving the maternal or the paternal GNAS exons 1-13, respectively, transmit the mutant allele to approximately two thirds of their children (odds ratio: ≈2:1). To determine whether TRD is observed also for the offspring of patients affected by autosomal dominant pseudohypoparathyroidism type Ib (AD-PHP1B), we analyzed numerous cohorts in which STX16 deletions or an inversion involving the GNAS locus leads to loss-of-methylation at GNAS exon A/B, if inherited from a female, thus leading to PTH-resistant hypocalcemia and hyperphosphatemia, and frequently resistance to other hormones that mediate their actions through Gsα-coupled receptors. In our studies, 72 females who are either unaffected carriers of the STX16/GNAS mutation (n=50) or are affected by PHP1B (n=22), had given birth to a total of 181 children (52.5% boys, 47.5% girls). 113 of these offspring (54.0% boys, 46.0% girls) had inherited the genetic defect, while 68 (50.0% boys, 50.0% girls) had inherited the wild-type allele; the mutation was thus transmitted to almost two thirds of the children (p=0.00082). Mothers with a STX16/GNAS mutation on their paternal (unaffected carriers) or their maternal allele (affected by PHP1B) revealed an indistinguishable TRD. No evidence for TRD was observed for paternally inherited STX16/GNAS mutations. Furthermore, unaffected carriers and females affected by PHP1B showed no difference in fertility (2.7 and 2.0 offspring/female, respectively; p=0.14). The underlying mechanisms resulting in TRD for maternally transmitted mutations are unclear. It is, however, conceivable that maturing oocytes carrying a STX16/GNAS mutant have lower intracellular cAMP levels and may therefore have shortened meiotic arrest than oocytes comprising the wild-type allele, thus potentially prolonging for each secondary oocyte the window for fertilization. Our findings provide insights into a previously not recognized aspect of AD-PHP1B, which is likely to have implications for genetic counseling and possibly oocyte biology.

***Disclosures: Zentaro Kiuchi**, None*

P-090

Sex-specific Differences in Radius Bone Size, Density and Micro-Architecture between Children with Type 1 Diabetes and Typically Developing Children *Yuwen Zheng[1], Anthony Kehrig[1], James Johnston[2], Munier Nour[3], Saija Kontulainen[1]. [1]College of Kinesiology, University of Saskatchewan, Canada, [2]College of Engineering, University of Saskatchewan, Canada, [3]College of Medicine, University of Saskatchewan, Canada

Introduction: Weak bone structure at the fracture prone radius, particularly in boys, may underpin the greater pediatric fracture risk related to type 1 diabetes (DM1). Sex-specific comparisons of bone structure, micro-architecture, density and estimated strength between children with DM1 and typically developing children (TDC) are lacking. Our objectives were: 1) to assess the role of DM1 and sex in radius bone properties, micro-architecture and strength; 2) to characterize bone differences between children and youth with DM1 and TDC. Methods: We categorized 169 children and youth (6-15yrs) based on DM1 diagnosis into DM1 (N=35, 22F) and TDC groups (N=134, 74F). We imaged distal radius structural (e.g., area), micro-architectural (e.g., porosity) properties and quantified trabecular and cortical bone density using high resolution peripheral quantitative computed tomography (HR-pQCT). We estimated bone strength (failure load and stiffness) from HR-pQCT images using finite element modeling. We imaged radius shaft bone structure, density and estimated strength (density-weight polar section modulus) as well as the surrounding muscle area at the forearm using pQCT. We assessed the role of group (DM1 vs. TDC) and group*sex interaction using MANCOVA, adjusted for maturity, forearm muscle area and body mass, followed by (sex-specific) between group comparison of bone outcomes. Significance was set at p<.05. Results: Adjusted bone outcomes at the distal radius and shaft sites differed between the DM1 and TDC groups (Pillai's trace=0.740, p<.01) with a group*sex interaction in bone outcomes (Pillai's trace=0.236, p<.01). At the distal radius, both sexes in DM1 group had 10-49% lower trabecular bone area and cortical porosity and 5-22% higher cortical density and thickness (p<.05, Table 1). Girls also had 8-10% lower trabecular bone density, volume fraction and thickness, while boys had 18% higher trabecular separation, 14% lower total bone area and trabecular number in DM1 group (p<.05, Table 1). At the radius shaft, both sexes in DM1 group had 5-11% higher cortical bone density, while girls had 9-11% lower total and cortical bone area and boys had 8% higher cortical bone content in DM1 group (p<.05, Table 1). Conclusion: Bone difference in children and youth with DM1 are likely influenced by sex. Children with DM1 had deficits in distal radius bone size, trabecular bone properties and micro-architecture, but a denser and thicker cortical bone compared to TDC.

Table 1: Mean radius outcomes (adjusted for maturity, muscle area and body mass) for girls and boys in DM1 and TDC groups and between group %-differences with 95% confidence intervals (CI). Bolded values illustrate between group differences.

	Girls				Boys			
	DM1	TDC			DM1	TDC		
	Mean (SD)	Mean (SD)	*p*-value	%-Difference (95% CI)	Mean (SD)	Mean (SD)	*p*-value	%-Difference (95% CI)
Distal Radius – HR-pQCT								
Total Bone Area (mm²)	184.3 (28.8)	198.1 (27.9)	0.055	-6.9 (-14.0, 0.2)	**190.8 (29.7)**	**222.6 (29.2)**	**0.001**	**-14.3 (-22.5, -6.1)**
Total Bone Mineral Density (mg HA/cm³)	253.2 (40.1)	249.7 (38.9)	0.727	1.4 (-6.5, 9.2)	278.2 (37.9)	255.1 (37.2)	0.052	9.1 (-0.1, 18.2)
Trabecular Bone Area (mm²)	**151.1 (29.8)**	**166.9 (28.9)**	**0.034**	**-9.5 (-18.2, -0.8)**	**153.6 (30.1)**	**189.5 (29.6)**	**<0.001**	**-18.9 (-28.7, -9.2)**
Trabecular Bone Mineral Density (mg HA/cm³)	**159.0 (28.5)**	**175.6 (27.6)**	**0.019**	**-9.5 (-17.4, -1.6)**	172.4 (29.9)	186.5 (29.3)	0.130	-7.6 (-17.4, 2.3)
Trabecular Bone Volume Fraction (%)	**13.2 (2.4)**	**14.6 (2.6)**	**0.018**	**-9.6 (-17.8, -1.4)**	14.4 (2.5)	15.5 (2.3)	0.127	-7.7 (-17.4, 1.9)
Trabecular Number (1/mm)	2.1 (0.2)	2.2 (0.2)	0.215	-2.9 (-7.6, 1.7)	**2.0 (0.2)**	**2.3 (0.2)**	**<0.001**	**-13.6 (-18.8, -8.5)**
Trabecular Thickness (µm)	**62.0 (9.4)**	**66.0 (8.6)**	**0.036**	**-7.6 (-13.6, 0.0)**	72.0 (10.8)	67.0 (7.7)	0.143	6.0 (-1.5, 14.9)
Trabecular Separation (µm)	412.0 (46.9)	391.0 (43.0)	0.080	5.1 (-0.5, 11.0)	**434.0 (39.7)**	**368.0 (38.7)**	**<0.001**	**17.9 (11.4, 24.5)**
Cortical Bone Area (mm²)	35.9 (6.5)	38.4 (6.3)	0.115	-6.6 (-14.8, 1.6)	40.7 (6.6)	43.2 (6.5)	0.225	-5.7 (-15.1, 3.6)
Cortical Bone Mineral Density (mg HA/cm³)	**752.9 (49.3)**	**704.3 (47.8)**	**<0.001**	**6.9 (3.5, 10.3)**	**754.4 (43.6)**	**688.5 (42.8)**	**<0.001**	**9.6 (5.7, 13.5)**
Cortical Tissue Mineral Density (mg HA/cm³)	790.4 (35.3)	773.8 (34.2)	0.060	2.1 (-0.1, 4.4)	**802.0 (31.1)**	**763.7 (30.5)**	**<0.001**	**5.0 (2.5, 7.5)**
Apparent Cortical Thickness (µm)	650.0 (126.6)	606.0 (120.4)	0.161	7.3 (-3.0, 17.5)	**753.0 (115.3)**	**615.0 (116.1)**	**<0.001**	**22.4 (10.9, 34.1)**
Fine-Structured Cortical Thickness (µm)	**471.0 (75.0)**	**405.0 (68.8)**	**0.001**	**16.3 (7.2, 25.2)**	**462.0 (50.4)**	**387.0 (46.5)**	**<0.001**	**19.6 (11.4, 27.6)**
Cortical Porosity (%)	**3.5 (2.3)**	**6.8 (2.6)**	**<0.001**	**-48.5 (-64.7, -32.4)**	**5.3 (2.5)**	**7.9 (2.3)**	**0.001**	**-32.9 (-51.9, -15.2)**
Failure Load (kN)	1.7 (0.3)	1.8 (0.3)	0.344	-3.5 (-10.7, 3.8)	2.0 (0.3)	2.0 (0.3)	0.500	3.3 (-6.4, 13.0)
Stiffness (kN/mm)	35.2 (2.3)	34.6 (2.6)	0.634	1.9 (-6.0, 9.8)	41.9 (6.9)	38.0 (6.7)	0.068	10.3 (-0.8, 21.4)
Radius Shaft- pQCT								
Total Bone Area (mm²)	**112.7 (19.3)**	**123.5 (18.7)**	**0.025**	**-8.8 (-16.4, -1.1)**	125.8 (22.6)	134.8 (22.1)	0.197	-6.7 (-17.0, 3.6)
Cortical Bone Area (mm²)	**70.7 (9.3)**	**79.2 (9.0)**	**<0.001**	**-10.8 (-16.5, -5.1)**	80.4 (9.7)	82.8 (9.5)	0.427	-2.9 (-10.1, 4.3)
Cortical Bone Content (mg/mm)	64.3 (9.2)	67.8 (8.9)	0.126	-5.1 (-11.8, 1.5)	**74.4 (8.9)**	**68.9 (8.7)**	**0.049**	**8.0 (0.0, 15.9)**
Cortical Bone Density (mg/mm³)	**895.3 (69.5)**	**853.2 (67.4)**	**0.016**	**4.9 (1.0, 8.9)**	**917.2 (60.0)**	**830.3 (58.8)**	**<0.001**	**10.5 (6.0, 14.9)**
Density-Weighted Polar Section Modulus (mm³)	189.4 (36.9)	196.7 (35.7)	0.425	-3.7 (-12.9, 5.5)	231.1 (38.4)	215.1 (37.6)	0.180	7.4 (-3.5, 18.4)

***Disclosures: Yuwen Zheng**, None*

P-091

Neonatal severe hyperparathyroidism. New analysis causes new guideline. *Stephen Marx[2], Ninet Sinaii[0]. [2]Office of the Scientific Director, NICHD, United States, [0]Clinical Center, NIH, United States

Context: Neonatal severe hyperparathyroidism (NSHPT) is a rare and life-threatening emergency. It includes generalized hyperparathyroid bone disease and respiratory distress from combinations among a narrowed thorax, rib fractures, hypotonia, and biochemical disturbances. Neuromotor retardation may persist after otherwise successful therapy. Early intervention seems critical. NSHPT is usually caused by homozygous or heterozygous pathogenic variant(s) of the CASR. Homozygotes and heterozygotes are often not distinguished. In theory, their management should differ. Optimum treatment in homozygotes is early total parathyroidectomy. Optimal management of heterozygotes varies from careful observation without surgery, to bisphosphonates and/or calcimimetics, and/or to subtotal parathyroidectomy. Evidence Acquisition: Each case met strict criteria for "severe" disease. To compare different immunoassays, PTH was analyzed as a ratio (thus without units) of the raw data divided by the upper limit of its normal range. This is a major extension on a recent report (JCEM April 2020). We now include many variables about presentation and therapy. Evidence Synthesis: There were 98 cases with homozygous pathogenic CASR variants and 35 cases with heterozygous pathogenic or likely pathogenic variants. Maximal serum calcium was far higher in homozygotes 5.8 +/- 1.5 versus 3.2 +/- 0.2 (P<.001) (normal 2.2-2.6 mM). Maximal serum PTH as a ratio was also far higher in homozygotes 17 +/- 12 versus 8 +/- 9 (P=.003) (normal ratio 0.3-1.0). We defined extreme hypercalcemia empirically as any calcium value above 4.5 mM. No heterozygote had a maximal calcium above 3.7 mM; however, 30 of 36 (83%) of the homozygotes had maximal calcium above the conservative cutoff of 4.5 mM. A more aggressive cutoff of 4.0 mM would capture 95% of homozygotes and no heterozygotes. The linear regression of the highest levels of extreme hypercalcemia versus day number confirmed frequent clustering of recognition in the first 10 days. Conclusions: Extreme hypercalcemia greater than 4.5 mM was newly identified as a conservative cutoff that was 100% predictive of homozygosity for pathogenic CASR variants. Extreme hypercalcemia in NSHPT is an early, facile, rapid, and inexpensive determinant of homozygosity. It should be sought and used as a guideline to promote early and definitive total parathyroidectomy in homozygotes.

***Disclosures: Stephen Marx**, None*

P-092

Bisphosphonates for Sickle Cell Bone Morbidity: A Multicenter Canadian Pediatric Experience *Chelsey Grimbly[1], Aisha Bruce[2], Jacob L Jaremko[3], Rose Girgis[1], Marie-Eve Robinson[4], Ewurabena Simpson[5], R. Todd Alexander[6], Leanne M Ward[7]. [1]Division of Pediatric Endocrinology, Department of Pediatrics, University of Alberta, Canada, [2]Division of Pediatric Hematology, Department of Pediatrics, University of Alberta, Canada, [3]Department of Radiology and Diagnostic Imaging, University of Alberta, Canada, [4]Department of Pediatrics, Division of Endocrinology, University of Ottawa. Children's Hospital of Eastern Ontario Research Institute, Canada, [5]Division of Pediatric Hematology, Department of Pediatrics, University of Ottawa, Canada, [6]Division of Pediatric Nephrology, Department of Pediatrics, University of Alberta, Canada, [7]Research Chair in Pediatric Bone Health, University of Ottawa, Canada

Purpose: Sickle Cell Disease (SCD) has severe bone morbidity, including avascular necrosis and bone infarcts that are often under-recognized in childhood. To date, there are no proven medical treatments, although bisphosphonates may be of benefit. We set out to describe the type and skeletal locations of symptomatic bone morbidity and the use of bisphosphonates in children with SCD being followed at two Canadian, tertiary care pediatric hospitals. Methods: This was a bi-institutional, retrospective study that included children and adolescents with SCD and a history of symptomatic bone morbidity. Clinical data collected included sex, age of initial presentation, sickle cell genotype, serum 25-hydroxyvitamin D

(25OHD), hydroxyurea intake, the indication for bisphosphonate therapy, and the response to treatment. Results: We identified 32 children with Sickle Cell bone morbidity, 14 in Edmonton who were identified from 2014-2019, and 18 in Ottawa from 2003-2020. The mean +/- SD age at presentation with bone disease was 12.1 +/- 4.2 years (range 2.6-17.3). Bone morbidity included avascular necrosis (AVN) of the femur and humerus, vertebral end-plate infarcts, and bone infarcts in the femur, tibia, fibula, pelvis, jaw, and skull (See Table 1). The average 25OHD level was 46.8 +/- 25.8 nmol/L with 56% of 25OHD levels < 50 nmol/L and 10% < 25 nmol/L. Ten patients were treated with intravenous (IV) bisphosphonate therapy (pamidronate n=2, and zoledronic acid n=8) because of bone pain. The acute phase reaction with the first infusion occurred in 4/10 children. There were no reports of bisphosphonate-induced sickle cell crisis, or hypocalcemia requiring intervention. In all cases, children reported significant or complete resolution of pain. Three children with limited mobility resumed full ambulation after bisphosphonate therapy. Two children underwent trans-iliac biopsies that demonstrated significantly elevated bone formation prior to bisphosphonates (348% and 578% of the healthy average), with drastic reduction two years later (45% and 90%, respectively). Conclusions: Long bone AVN and infarcts, as well as vertebral body, jaw and skull infarcts, can be symptomatic enough to warrant IV bisphosphonate therapy for children with SCD. Bisphosphonate therapy was well tolerated and effective in this retrospective study. This merits further study in prospective, controlled studies to confirm and further assess this promising therapy in SCD.

Table 1: Clinical characteristics of children with SCD bone morbidity

	N = (%)
Male	21 (68%)
Genotype	
HbSS	24 (77%)
HbSS/G6PD	3 (9.7%)
HbSS/Beta 0	2 (6.5%)
HbS/O-Arab	1 (3.2%)
HbSC	1 (3.2%)
Vertebral AVN	21 (70%)
Femoral head AVN	11 (37%)
Humeral head AVN	2 (7%)
Bone Infarcts	11 (37%)

***Disclosures: Chelsey Grimbly**, None*

P-093

Hip geomtery in adolescents and young adults with type 1 diabetes *sowmya krishnan[1], Jennifer Chadwick[1], Madhusmita Misra[2]. [1]University of Oklahoma Health Sciences Center, United States, [2]MassGeneral Children's hospital, Boston, United States

Type 1 Diabetes (T1D) in adults is associated with low bone mineral density (BMD) and higher risk for osteoporotic fracture. The effect of T1D on the skeleton when peak bone mass is being laid is still uncertain. Bone mineral density obtained by dual energy x-ray absorptiometry (DXA) has traditionally been used as the surrogate measure for bone health but it is not a true measure of volumetric density and is influenced by bone size. Recently hip geometry measures obtained by routine DXA scans have been shown to be predictive of osteoporotic fractures in adults. It is uncertain if hip geometry is altered in adolescents and young adults with T1D. We conducted a cross-sectional pilot study to look at differences in BMD and hip geometry scores among adolescents and young adults with and without T1D. We hypothesized that subjects with T1D would have lower BMD and unfavorable hip geometry scores. Due to the influence of race on BMD, only subjects who identified themselves as white were included in the study. Subjects with any other illness (eg: celiac disease, history of cancer) or medications (eg: glucocorticoids, oral contraceptive pills) that can influence bone health were excluded from the study. All scans were performed on GE lunar iDXA. We present data on the initial 6 subjects with type 1 diabetes and 8 control subjects who have completed the study. Mean age of subjects with and without T1D was 18.3 +/-1.4 and 17.9 +/-1.6 years respectively. Total body BMC, spine BMC, spine BMD did not differ between subjects with and without T1D (2578.4 +/- 335.4 g vs 2881.7 +/-599.4 g; p: 0.19; 63.0 +/- 10.2g vs 73.9 +/- 13.1 g p: 0.72; 1.05 +/- 0.14 g/cm2 vs 1.20+/- 0.11 g/cm2; p: 0.62 respectively). Similarly bone mineral apparent density at the spine did not differ between subjects with and without diabetes (0.32 +/- 0.05 g.cm3 vs 0.35 +/- 0.03 g/cm3 respectively. However there was a significant difference in cross sectional area (CSA: index of resistance to axial forces) and cross-sectional moment of inertia (CSMI: estimate of resistance to bending forces in a cross-section) on hip structural analysis. CSMI was 11376.0 +/-3057.7 mm4 vs 13917.3 +/-5720.3 mm4 (p: 0.02) while CSA was 165. 2+/-19.8 mm2 vs 184.6 +/- 36.8 mm2 (p: 0.018) for subjects with and without diabetes respectively. We conclude based on this pilot study that subjects with type1 diabetes may have altered hip geometry that contributes to the skeletal fragility later in life.

***Disclosures: sowmya krishnan**, None*

P-094

Bone Health in Treatment-Naïve, Ambulatory Boys with Duchenne Muscular Dystrophy *Stefan Jackowski[1], Jinhui Ma[2], Maya Scharke[1], Victor Konji[1], Jacob Jaremko[3], Khaldoun Koujok[4], MaryAnn Matzinger[4], Nazih Shenouda[4], Scott Walker[1], Colleen Hartigan[1], Hugh McMillan[4], Kerry Siminoski[3], Pradeep Bista[5], Joanne Donovan[5], Maria Mancini[5], Leanne Ward[4]. [1]Children's Hospital of Eastern Ontario Research Institute, Canada, [2]McMaster University, Canada, [3]University of Alberta, Canada, [4]University of Ottawa, Canada, [5]Catabasis Pharmaceuticals, Inc., United States

Introduction and Aims: Boys with Duchenne muscular dystrophy (DMD) are predisposed to low-trauma vertebral and long bone fractures due to osteoporosis. The purpose of this study was to determine whether clinically significant skeletal abnormalities are present early in the disease course, including vertebral fractures and low whole-body BMD (WB-BMD) Z-scores. We also sought to examine the factors associated with low WB-BMD. Methods: Baseline data were analyzed from treatment-naïve ambulatory boys 4 to 7 years (up to 8th birthday) with genetically-confirmed DMD not on glucocorticoids who were participating in a global phase III trial of the NF-kB inhibitor edasalonexent (NCT03703882). Boys underwent functional assessments including the North Star Ambulatory Assessment and dual-energy x-ray absorptiometry (DXA) for Lean and Fat Mass Indices (expressed lean or fat mass/height2, kg/m2), and WB-BMD (less head, g/cm2). Lateral spine radiographs were analyzed for vertebral fractures according to the Genant semi-quantitative method. Results: At baseline, 108 boys underwent lateral spine radiographs (mean +/- standard deviation [SD] age 5.8+/-1.1 years); 72 boys also had DXA machine cross-calibrated WB-BMD scans (age 5.9+/-1.1 years). Three boys (2.8%) had a total of four low-trauma vertebral fractures (all Genant 1, mid-thoracic). WB-BMD and anthropometry measures (mean +/- SD) were as follows: WB-BMD Z-score -2.7+/-1.2 (p <0.001 compared with the healthy average; 74% with a WB-BMD Z-score ? -2.0), height Z-score -0.8+/-1.1 (p <0.001), weight Z-score -0.1 +/-1.0 (p =0.27), and body mass index Z-score 0.8+/-0.9 (p <0.001). A multiple linear regression model controlling for age and height Z-score showed higher Fat Mass Index (β -0.25, 95% CI -0.46, -0.04; p=0.02), and lower Lean Mass Index (β 0.45, 95% CI 0.20, 0.704; p=0.001) were associated with lower WB-BMD Z-scores. Logistic regression adjusted for age and height Z-score showed every 1 kg/m2 decrease in Lean Mass Index was associated with a 46% increase in the odds of a WB-BMD Z-score < -2.0 (95% CI 24%, 90%; p=0.02).Conclusions: Mean WB-BMD Z-scores are low in young, ambulatory boys with DMD not on glucocorticoids. A small percentage have mild vertebral fractures, further supporting the negative impact of early DMD on bone health even prior to glucocorticoid use. In addition to lower lean mass, higher fat mass may also play a role in the abnormal bone strength development of pediatric DMD.

***Disclosures: Stefan Jackowski**, None*

P-095

A Six Years Longitudinal Cohort Study on the Changes in Bone Density and Bone Quality up to Peak Bone Mass in Adolescent Idiopathic Scoliosis with and without 2 Years of Calcium and Vitamin D Supplementation *Guangpu YANG[1], Tsz-ping LAM[1], Henry PANG[1], Benjamin Hon-kei YIP[2], Wayne Yuk-wai LEE[1], Alec Lik-hang HUNG[1], Nelson Leung-sang TANG[3], Kenneth Kin-wah To[4], Yong QIU[5], Jack Chun-yiu CHENG[1]. [1]SH Ho Scoliosis Research Lab, Joint Scoliosis Research Center of the Chinese University of Hong Kong and Nanjing University, Department of Orthopaedics & Traumatology, The Chinese University of Hong Kong, Hong Kong, [2]The Jockey Club School of Public Health and Primary Care, The Chinese University of Hong Kong, Hong Kong SAR, China, Hong Kong, [3]Department of Chemical Pathology, Faculty of Medicine, The Chinese University of Hong Kong, Hong Kong, [4]School of Pharmacy, Faculty of Medicine, The Chinese University of Hong Kong, Hong Kong, [5]Spine Surgery, The Affiliated Drum Tower Hospital of Nanjing University Medical School, Nanjing, China, China

Introduction:Adolescent idiopathic scoliosis(AIS) is associated with low bone mass which could persists into adulthood. Given that AIS girls have low dietary calcium intake and high prevalence of Vitamin D(Vit-D) insufficiency, our group has previously reported the first 2-year randomized double-blinded placebo-controlled trial with calcium(Ca) and Vit-D supplementation to AIS girls with low bone mass (the Cal study) showing strong evidences of positive bone accretion effects with Ca+Vit-D supplementation.This study is an extension of the Cal study investigating the changes in bone density and bone quality at 4-year after discontinuation of Ca+Vit-D supplementation.Objective:This 6-year longitudinal cohort study aimed to investigate whether improvement in BMD and bone quality induced by Ca and Vit-D supplementation (600mg Ca and 400/800IU Vit-D3 per day) persisted after supplement discontinuation for low bone mass in AIS girls.Methods:This was a randomized double-blinded placebo-controlled trial on AIS girls (11-14 years old, mean age = 12.9 years, Tanner stage<IV) with femoral neck aBMD Z-score<0 and Cobb angle>=15°. 330 subjects were randomized to Group1(placebo), Group2(600 mg Ca and 400 IU Vit-D3 per day) or Group3(600mg Cal and 800 IU Vit-D3 per day) for 2-year treatment. Investigations were done at baseline, 2-year and 6-year including High-resolution Peripheral Quantitative Computed Tomography(HR-pQCT) at distal radius and Dual Energy X-ray Absorptiometry(DXA) at proximal hips. ANCOVA was used for analysis.Results and

Discussion:270(81.8%) subjects completed treatment. At 2-year time-point, the increases in serum 25(OH)Vit-D, left femoral neck aBMD in Group3, average volumetric BMD(vBMD), trabecular vBMD, Trabecular BV/TV, Trabecular Number in both Group2 and 3 were significantly greater than in Group1($p<0.05$). At 6-year follow up after 4-year discontinuation of supplementation with a mean age of 19.15 years old, no difference was noted except increase in Cortical Area and Cortical Thickness were greater only in Group3 than in Group1. Conclusion and Significance:This study provided strong evidences that 2-year supplementation with Ca+Vit-D can improve bone health for low bone mass in AIS. At 6-year follow up with 4-year discontinuation of treatment, the treatment effect mostly regressed towards the null hypothesis indicating the need of continued supplementation to sustain the therapeutic effect on bone health up to the stage of peak bone mass.

***Disclosures: Guangpu YANG**, None*

P-096

Influence of Puberty on Bone Deficits in Ambulatory Youth with Spina Bifida

*Tishya Wren[1], Nicole Mueske[1], Susan Rethlefsen[1], Robert Kay[1], Alexander Van Speybroeck[1], Wendy Mack[2]. [1]Children's Hospital Los Angeles, United States, [2]University of Southern California, United States

Pathologic fractures of the femur and tibia are common in youth with spina bifida (SB). These fractures may be associated with deficient bone accrual due to decreased ambulation and skeletal loading. This prospective cohort study used quantitative computed tomography (QCT) to assess three-dimensional bone properties in children and adolescents with SB. Eighty-three ambulatory youth with SB underwent QCT imaging of the tibia at up to 4 annual visits between ages 6-16 years (294 total visits averaging 3.5 visits/patient). 177 controls without disability and 10 non-ambulatory youth with SB underwent imaging once. Bone geometric properties (cortical bone area, cross-sectional area, cortical thickness, cortical density, and moments of inertia) were measured at the mid-diaphysis (50% of bone length); cross-sectional area, cancellous density, and density-weighted area were measured in the proximal (13% of bone length) and distal (90% of bone length) metaphyses. Bone properties were compared between the ambulatory SB and control participants, among SB neurosegmental subgroups (sacral, low lumbar, mid lumbar and above) as a function of pubertal stage (pre-pubertal, pubertal, post-pubertal), and considering SB type (myelomeningocele or lipomyelomeningocele) using linear mixed effects models adjusted for sex, age, height percentile, and body mass index percentile. Only cancellous density of both metaphyses and weighted area of the proximal metaphysis differed between ambulatory children with SB and controls before puberty. However, significant deficits in all bone properties manifested during and after puberty as moderate bone growth in the SB group failed to keep pace with the large increases normally observed during puberty (Figure, top). The bone deficits primarily affected patients with myelomeningocele, and similar deficits were observed at all neurosegmental levels except that cancellous density was closer to normal in the sacral group (Figure, middle and bottom). Descriptive analysis of the 10 non-ambulatory youth with SB showed greater bone deficits than ambulatory children, particularly for cancellous density in the distal metaphysis. Therefore, both ambulatory and non-ambulatory youth with spina bifda have deficits in bone, particularly during and after puberty.

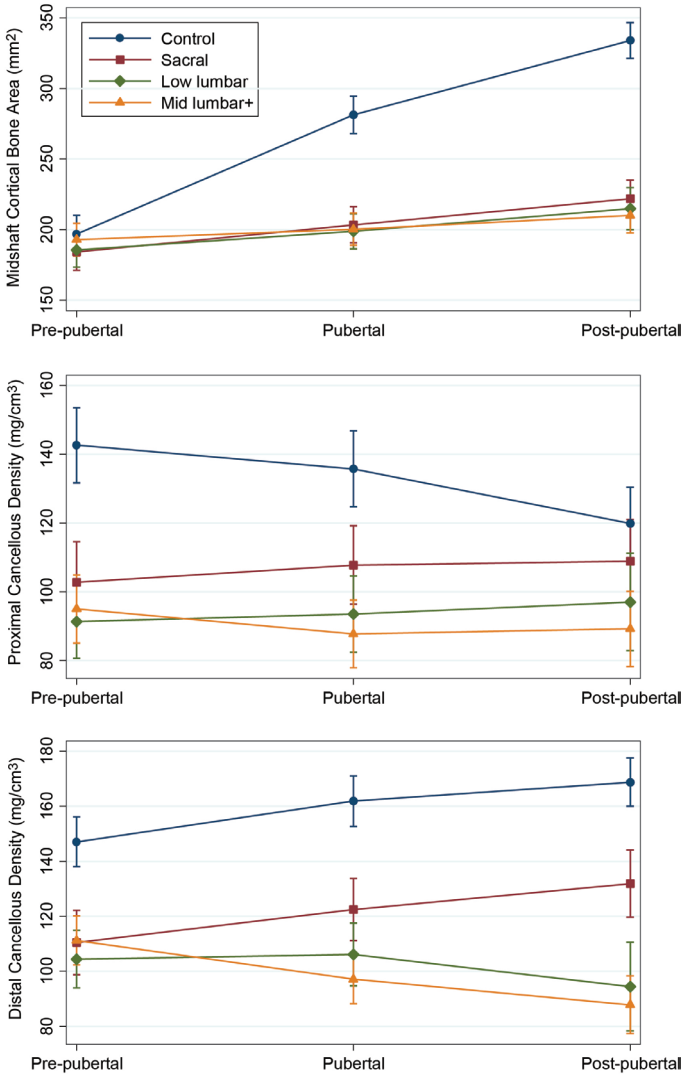

***Disclosures: Tishya Wren**, None*

P-097

The Impact of Oral Bisphosphonate Therapy on Vertebral Morphometry and Fractures in Patients with Duchenne Muscular Dystrophy and Glucocorticoid-Induced Osteoporosis

*Nat Nasomyont[1], Cuixia Tian[1], Lindsey Hornung[1], Jane Khoury[1], Paul Hochwalt[2], Joshua Cole Tilden[3], Irina Rybalsky[1], Brenda Wong[4], Meilan Rutter[1]. [1]Cincinnati Children's Hospital Medical Center, United States, [2]University of Cincinnati, United States, [3]Yale University, United States, [4]University of Massachusetts Children's Medical Center, United States

Objective: Osteoporosis and vertebral fractures are common in patients with Duchenne Muscular Dystrophy (DMD) treated with glucocorticoids. We aimed to evaluate the effects of oral bisphosphonate (BP) therapy on vertebral morphometry and fractures in patients with DMD and glucocorticoid-induced osteoporosis.Methods: We retrospectively studied children and adolescents with DMD who had been treated with oral BP for glucocorticoid-induced osteoporosis at a tertiary-care pediatric center from 2010-2017. Demographic data, and glucocorticoid and oral BP treatment histories were obtained from electronic medical records. Treatment outcomes were changes in lumbar (L1-L4) vertebral morphometry and fractures, as assessed by the Genant semi-quantitative method. Patients were included if they had both baseline and at least one follow-up spine radiograph available for review. Chi-square was used to examine change in fracture prevalence at each vertebra.Results: Fifty-eight patients with DMD (median age 12.2y, range 5.5-19.6y) were treated with glucocorticoids for a median duration of 4.7y (range 1.3-12.6y) and 33% were non-ambulatory at BP start. Vertebral fractures, defined by Genant grading >=1, were present in 6%-19% of L1-L4 vertebrae at baseline. Among patients who had radiographs at both baseline and 1 or 2y-post BP start, the prevalence of vertebral fractures remained stable at 1y (n=43; 5-18% at baseline vs 8-18% at 1y, p=0.31-1.00) and 2y of treatment (n=42; 5-23% at baseline vs 11-33% at 2y, p=0.11-1.00). Among patients who had serial radiographs for comparison, longitudinal examination showed no change in Genant grading the majority of vertebrae

up to 5y of treatment (Figure).Conclusions: In our experience of oral BP therapy in patients with DMD, we observed stable prevalence of lumbar vertebral fractures after 1 and 2y of treatment. Longitudinal Genant grading remained overall unchanged for up to 5y of treatment. Our findings suggest oral BP may be beneficial for secondary prevention of glucocorticoid-induced osteoporosis in patient with DMD and may mitigate development or progression of vertebral fractures in the majority of patients. Longer-term data and in-depth quantitative analysis of vertebral fracture severity are needed to determine the efficacy of oral BP in children and adolescents with DMD.

Table: Changes in Genant grading in L1-L4 vertebrae from baseline up to 5 years of treatment

	Baseline vs 1 year (N = 39, n = 156)	Baseline vs 2 year (N = 41, n = 164)	Baseline vs 3 year (N = 30, n = 120)	Baseline vs 4 year (N = 26, n = 104)	Baseline vs 5 year (N = 26, n = 104)
Unchanged	102 (80%)	92 (68%)	73 (70%)	55 (64%)	64 (71%)
Improved	12 (10%)	12 (9%)	8 (8%)	8 (9%)	10 (10%)
Worsen	13 (10%)	31 (23%)	23 (22%)	23 (27%)	16 (18%)
NA	29	29	16	18	14

Data presented in number of vertebrae (%).

Abbreviations: N, number of patients; n, number of vertebrae; NA, number of vertebrae not readable.

***Disclosures: Nat Nasomyont**, None*

P-098

The Timing and Tempo of the Skeletal Maturational Spurt is Independent of Racial or Ethnic Background *Melanie Boeyer[1], Emily Leary[2], Richard Sherwood[3], Bone Mineral Density in Childhood Study bmdcs.nichd.nih.gov[4], Dana Duren[1]. [1]Department of Orthopaedic Surgery, University of Missouri, Columbia, MO, United States, [2]Department of Orthopaedic Surgery and the Thompson Laboratory for Regenerative Orthopaedics, University of Missouri, Columbia, MO, United States, [3]Department of Pathology and Anatomical Sciences, University of Missouri, Columbia, MO, United States, [4]NICHD, United States

An accurate assessment of a child's future growth and/or development is contingent, in part, on their skeletal maturational trajectory. Because the tempo of skeletal maturation often does not track linearly with chronological age, knowledge of an impending bout of rapid skeletal maturation (i.e., a maturational spurt) would be helpful, particularly in the treatment of pediatric skeletal disorders. Yet, the characterization of a maturational spurt has only been established for Non-Hispanic White children, and it is unknown whether the maturational spurt is influenced by racial and/or ethnic background. We, therefore, aimed to assess the maturational spurt in 420 children from four different racial and/or ethnic backgrounds from the Bone Mineral Density in Childhood Study (Asian or Pacific Islander, 23; Hispanic, 53; Black Non-Hispanic, 78; White Non-Hispanic, 266), each of whom had seven consecutive left hand-wrist radiographs between the chronological ages of 6 and 19 years. The relationship between chronological age and skeletal age, assessed via the Fels Method, was evaluated separately in each child using a fixed effect fifth order polynomial. Milestones related to the maturational spurt, including the chronological age and maturational rate of onset, peak, and cessation, were compared between children from each racial and/or ethnic background using a one-way analysis of variance in both boys and girls. In boys, the chronological age of attainment for each maturational milestone was similar across all racial and/or ethnic groups. In girls, the chronological age at which onset and peak were attained in Asian or Pacific Islanders was significantly earlier (onset, 9.1 yr; peak, 10.9 yr) than other racial and/or ethnic backgrounds, particularly those from Non-Hispanic White backgrounds (onset, 11.2 yr; peak, 12.9 yr). No differences were observed in the rate of skeletal maturation at any milestone in either boys or girls. Although some groups had a low number of children, these analyses indicate that the chronological age and rate of skeletal maturation at each milestone may be similar in children of different racial and/or ethnic backgrounds, despite documented variation in milestones for other growth-related skeletal phenotypes, such as height or bone mineral accrual.

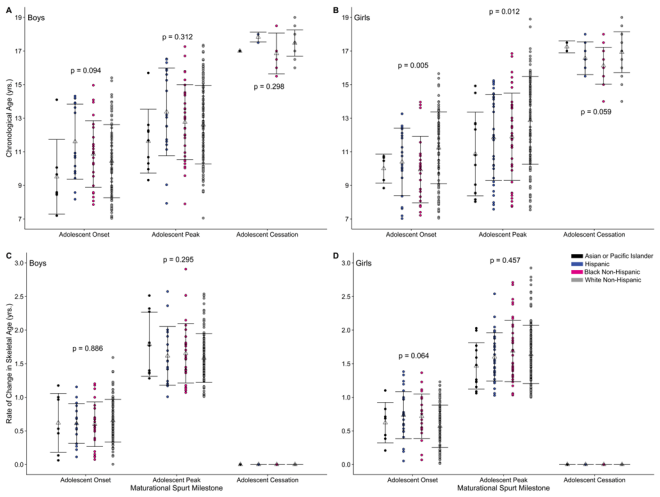

***Disclosures: Melanie Boeyer**, None*

P-099

Trends in emergency department visits for fall-related fractures among U.S. children 2001-2015. *Jack Orces[1], Carlos Orces[2]. [1]Nicklaus Children Hospital, United States, [2]Laredo Medical Center, United States

Background: Although fractures in children are a major publich health problem, it is unknown whether fall-related fractures have decreased among children in the U.S. Objective: To examine nationwide trends in emergency department (EDs) visits for fall-related fractures among children beween 2001 and 2015.Methods: The National Electronic Injury Surveillance System-All Injury Program was used to generate national estimates of unintentional fall-related fractures among children aged 0 to 19 years treated in EDs. Population estimates were used as the denominator to calculate age-specific fracture rates per 100,000 persons. Fracture rates were then directly standardized to the 2000 U.S. population. The Joinpoint regression program software version 4.7.0.0 was used to identify points where a statistically significant change occurred in the linear slope of fracture rates. The results are presented as the average annual percent change (AAPC) with their corresponding 95% confidence interval (95% CI).Results: An estimated 7.9 million U.S. children were treated in EDs for unintentional fall-related fractures between 2001 and 2015. Overall, upper extremity fractures accounted for 70% of the cases. Trend analysis demonstrated that fracture rates significantly decreased among those aged 10 to 15 years on average by -2.5% (95% CI, -3.4% to -1.6%) per year. After adjusting for age, fracture rates in boys decreased annually by -1.9% (95% CI, -3.1% to -0.6%), whereas the decrease in rates in girls was less accentuated by - 1.4% (95% CI, -1.8% to -1.0%) per year. As shown in Figure 1, forearm and/or wrist fracture rates significantly decreased by -1.6% (95% CI, -2.4% to -0.8%) during the study period. Notably, a marked annual decrease in rates by -2.4% (95% CI, -2.9% to -1.9%) was seen from 2004 onwards. Likewise, hand/finger fracture rates linearly decreased on average by -3.5 (95% CI, -4.3% to -2.8%) per year. In contrast, shoulder, arm, and/or elbow fracture rates remained unchanged during the study period. Conclusions: EDs visits for fall-related fractures significantly decreased in U.S. children between 2001 and 2015. This finding was predominantly attributed to a marked downward trend in fracture rates seen among children aged 10 to 14 years, boys, and forearm/wrist fractures.

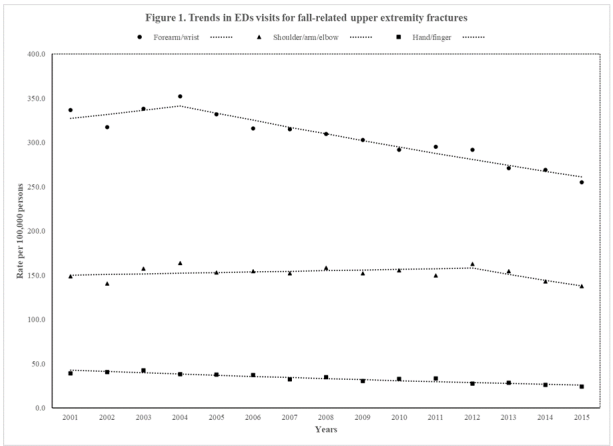

***Disclosures: Jack Orces**, None*

P-100

Alternative splicing of CYP11B1 is involved in adrenal steroidogenesis and skeletal maturation of children *Olja Grgic[5], Matthew R. Gazzara[2], Alessandra Chesi[3], Carolina Medina-Gomez[5], Diana L. Cousminer[2], Jonathan A. Mitchell[4], Vid Prijatelj[5], Enisa Shevroja[5], Shana E. McCormack[4], Heidi J. Kalkwarf[6], Joan M. Lappe[7], Vicente Gilsanz[8], Sharon E. Oberfield[9], John A. Shepherd[10], Kelly Andrea[4], Soroosh Mahboubi[11], Fabio R. Faucz[12], Richard A. Feelders[5], Frank H. de Jong H. de Jong[5], Andre G. Uitterlinden[5], Jenny A. Visser[5], Louis R. Ghanem[4], Eppo B. Wolvius[13], Leo J. Hofland[5], Constantine A. Stratakis[12], Babette S. Zemel[4], Yoseph Barash[2], Struan F. A. Grant [4], Fernando Rivadeneira[5]. [5]Erasmus MC, University Medical Center Rotterdam, Dr Molewaterplein 40, 3015 GD, The Netherlands, Department of Internal Medicine;, Netherlands, [2]Perelman School of Medicine, University of Pennsylvania, 2615 Civic Center Boulevard, Philadelphia, PA 19104, USA, Department of Genetics;, United States, [3]Children's Hospital of Philadelphia, 3401 Civic Center Boulevard, Philadelphia, PA 19104, USA, Center for Spatial and Functional Genomics;, United States, [4]Perelman School of Medicine, University of Pennsylvania, 3400 Civic Center Boulevard, Philadelphia, PA 19104, USA, Department of Pediatrics;, United States, [5]Erasmus MC, University Medical Center Rotterdam, Dr Molewaterplein 40, 3015 GD, The Netherlands, Department of Internal Medicine;, Switzerland, [6]Cincinnati Children's Hospital Medical Center, University of Cincinnati College of Medicine, 3333 Burnet Ave, Cincinnati, OH 45229, USA, Department of Pediatrics;, United States, [7]Creighton University, 2500 California Plaza, Omaha, NE 68178, USA, Division of Endocrinology;, United States, [8]Children's Hospital Los Angeles, Keck School of Medicine, University of Southern California, 1975 Zonal Ave, Los Angeles, CA 90033, USA, Division of Orthopedic Surgery;, United States, [9]Morgan Stanley Children's Hospital, Columbia University Irving Medical Center, 622 West 168th Street, PH17 W 307, New York, NY 10032, USA, Division of Pediatric Endocrinology;, United States, [10]University of Hawai'i Cancer Center, 701 Ilalo St, Honolulu, HI 96813, USA, Cancer Epidemiology;, United States, [11]Children's Hospital of Philadelphia, 3401 Civic Center Boulevard, Philadelphia, PA 19104, USA, Department of Radiology;, United States, [12]Eunice Kennedy Shriver National Institute of Child Health and Human Development (NICHD), National Institutes of Health, 6710 Rockledge Dr. Bethesda, MD 20817, USA, Section on Endocrinology and Genetics;, United States, [13]Erasmus MC, University Medical Center Rotterdam, Dr Molewaterplein 40, 3015 GD, The Netherlands, Department of Oral and Maxillofacial Surgery;, Netherlands

Objectives: While aberrant splicing has been established as a cause of Mendelian diseases, the effect of alternative splicing on phenotypic variability remains unclear. CYP11B1 locus was in recent GWAS meta-analysis robustly associated with skeletal age (SA). Several GWS variants are located in proximity to the intron-exon boundary of the CYP11B1, and therefore, we hypothesized that splicing of CYP11B1 may be the mechanism underlying reported GWAS association. Methods: Data was obtained from 208 adrenal gland RNA-seq samples from GTEx (where gene showed major expression) and used to screen CYP11B1 for splicing quantitative trait loci (sQTL). We focused on rs6410, the second most significant SNP in SA meta-analysis, and the one closest to the intron-exon boundary. Inclusion levels of alternative splice junctions were evaluated by the Modeling Alternative Junction Inclusion Quantification algorithm which quantifies local splicing variations denoted as Percent Selected Index (PSI) - percent of transcripts that made certain splicing choice. The sQTL pipeline was used to test the association between rs6410 genotypes and PSI values. Reverse transcription polymerase chain reaction (RT-PCR) was performed using adrenal gland RNA samples isolated from 6 donors from the Erasmus Medical Center (EMC) and 9 donors from the NIH repository. Spearman correlation between rs6410 genotypes and splicing event of interest was then calculated. Results: The C allele of rs6410 was associated with intron 2 retention (ΔPSI=21.1%; P=4.38x10-41), exon 2a inclusion (ΔPSI=5.3%; P=6.14x10-31), decreased exon 2 and 3 splicing (ΔPSI=-26.4%, P=5.29x10-43) and decreased use of the intron-proximal 3'ss which creates a longer exon 7 (ΔPSI=-20.3%; P=8.78x10-28). RT-PCR recapitulated the same conclusions with intron 2 retention levels being significantly associated with the rs6410 C allele in samples from both EMC and NIH (r2=0.93, P=0.008 and r2=0.95, P=7.3x10-5 respectively). Conclusion: Our study demonstrates that alternative splicing of CYP11B1 was the mechanism of rs6410 underlying reported association. In light of the already demonstrated pleiotropic effect of rs6410 on SA, height, cross-sectional area and hypertension, our study underpins the role of naturally occurring variation in splicing for both physiological traits and complex diseases. Evaluation of the impact of genomic variants on alternative splicing should be considered an integral part of clinical variant prioritization.

***Disclosures: Olja Grgic**, None*

P-101

Bone mineral density in children with cerebral palsy and spina bifida treated with ibandronate *Vladimir Kenis[1], Andrey Sapogovskiy[1], Tatiana Prokopenko[1]. [1]H.Turner National Medical Research Center for Children's Orthopedics and Trauma Surgery, Russian Federation

Bisphosphonates has become a common method for the prevention and treatment of osteoporosis in children with neuromuscular diseases. Purpose. To assess mid-term changes of bone mineral density in patients with cerebral palsy and spina bifida treated with ibandronic acid. Materials and methods. 34 patients were examined and treated: 19 children with cerebral palsy (GMFCS levels III-IV) and 15 children with spina bifida (thoracic and upper lumbar neurosegmental levels), mean age 9.8 +/- 2.9 years. Ibandronic acid was administered to all patients (3 consecutive intravenous infusions, 0.1 mg per 1 kg every 3-4 months). Assessment of bone mineral density was carried out using dual-energy X-ray absorptiometry. Results. Z-score increased from -2.55 to -2.1 (total body less head) and from -2.7 to -1.65 (lumbar spine). Improvement of the Z-score for the lumbar spine was noted after the first, and for the whole body after the first two infusions. Conclusion. Ibandronic acid infusions improved bone mineral density in children with cerebral palsy and spina bifida for both the whole body and the lumbar spine. Given the data obtained, expanded weight-bearing excersises can be recommended 3 months after the first infusion, and dynamic exercises preferably expanded after 6 months.

***Disclosures: Vladimir Kenis**, None*

P-102

Primary Hyperparathyroidism in children and adolescents: A far cry from Adult Hyperparathyroidism- A series from South India *Smitha Rao[1], Dhalapathy Sadacharan[2], Shriraam Mahadevan[3], Anjali Sathya[4], Jayashree Gopal[4], Shanmugasundar S[4], S Murthy[4]. [1]Senior resident in Endocrine Surgery, Madras Medical College, India, [2]Associate Professor, Endocrine Surgery, Madras Medical College, India, [3]Endocrinology, Diabetes & Metabolism, Sri Ramachandra Institute of Medical Sciences, India, [4]Endocrinology & Metabolism, India

Background: Primary hyperparathyroidism (PHPT) is a common endocrine condition but rare in the paediatric and adolescent population. The presentations can be unique, under cover of various differentials accounting for significant morbidity in case of untimely detection.Aim: To study surgically treated paediatric PHPT retrospectively and review literatureMethods: We retrospectively analysed 37 surgically treated cases of PHPT with presenting age of up to 20 years between 2010 to 2019. All of them were operated by a high volume, single endocrine surgeon and team.Results: A total of 37 cases were included with 22 males (59.5%). Mean age of the study population was 16.54 years (1-20), including 4 cases of neonatal severe HPT (NSPHPT). Multiple Endocrine Neoplasia type 1 (MEN1) was diagnosed and genetically confirmed in 10 cases. Presenting manifestations were: Various presentations included bone pain (35.13%), renal stones (27.02%), incidental asymptomatic detection (18.9%), failure to thrive (10.8%) and pancreatitis (8.1%). Mean serum calcium was 12.9mg/dl (highest-14.1, N-8.8-10.8mg/dl), mean parathormone levels were 386.91pg/ml (N-10-65) and vitamin D levels ranged from 2.9-22.8ng/ml. Localization was done with ultrasound and 99mTc- SESTAMIBI scans. All patients underwent a bilateral neck exploration and parathyroidectomy, with 14 cases having an additional thymectomy, 2 cases with thyroidectomy and a single case of hemithyroidectomy. The cure rate was 97.3%, with one case of NSPHPT of persistent disease (postop PTH-110pg/ml). Uniglandular disease was seen in 54.05% and the rest had multiglandular disease. All cases had a postoperative histopathological confirmation with an average follow up of 2 years.Conclusion: Childhood PHPT was more common among females with nearly one third of them having MEN1. In contrast to adults with more asymptomatic manifestation, bone disease followed by renal stones were the most common mode of presentation. Uniglandular involvement was more common than multi glandular disease in our series as compared to rest of the world data. Regular long-term follow up for MEN1 is mandatory.

***Disclosures: Smitha Rao**, None*

P-103

Oral Risedronate Treatment In Children With Osteogenesis Imperfecta *Antoine Nguyen[1], Pisit Pitukcheewanont[2], Anna Ryabets-Lienhard[3]. [1]Children's Hospital Los Angeles (CHLA) Division of Endocrinology, Diabetes, and Metabolism, Los Angeles, CA, USA, United States, [2]Ascendis Pharma Inc., Palo Alto, CA, USA, United States, [3]Children's Hospital Los Angeles (CHLA) Division of Endocrinology, Diabetes, and Metabolism; Keck School of Medicine, USC; Saban Research Institute, CHLA., Los Angeles, CA, USA, United States

To date, there are no approved pharmaceutical therapies for children with OI. Intravenous bisphosphonates have been used for years to treat children with OI with variable efficacy and tolerability. However, a few studies have evaluated the effects and tolerability of oral risedronate in children with OI (1)(2). In this study, we aimed to present our experience with oral risedronate treatment in children with OI. A retrospective chart review of patients with OI and history of multiple fragility fractures, who were treated with oral risedronate

and followed in our bone clinic between the years of 2013 and 2019. Primary outcomes included changes in fracture rate, urinary N-terminal telopeptide (uNTX), height z-scores, and lumbar and femur BMD z-scores. Safety and tolerability of risedronate were reviewed. Wilcoxon matched-pairs sign-ranks test was used to assess the medians (IQR) between pre- and post-treatment with p value of < 0.05 set as statistically significant. A total of 17 patients ages 5—19 ys were reviewed (11 males, 65% type I OI, 12% type III, 18% type XI, and 5% unknown). At the time of the review, 69% were on weekly, 19% on daily, and 12% on monthly risedronate treatment. Mean duration of therapy was 2.7 y ? 2.3 y, ranging 0.5 to 8 ys.The bone resorption marker, uNTX, decreased > 30% from baseline in 93% of subjects within the first year of treatment, and was statistically lower by the end of treatment period [245 (159, 393) to 170 (39, 261), p=0.02]. Height z-score did not change with treatment, -0.80 (-1.20, 0.10) pre- and -0.85 (-1.60, -0.40) post-treatment, p = 0.2 in patients with Type I OI. There was a clinically significant reduction in the rate of fractures from baseline 0.6 per y (0.4, 0.8) to 0.24 (0, 0.5) by the end of the treatment period. Within a year of treatment, 80% of children were fracture free with improvement in bone pain and mobility. BMD pre- and on treatment for lumbar and femur were -2.5 (-3.43, -1.94) and -2.36 (-3.25, -1.35), and -2.05 (-2.95, 0.3) and -1.18 (-1.73, 2.13), respectively. However, there was no statistical significance. There was one case of reflux without erosive esophagitis, which resolved with reflux treatment. Overall, risedronate was well tolerated with no cases of clinically significant acute phase reaction, hypocalcemia, erosive esophagitis, or osteonecrosis of the jaw.Based on our experience, oral risedronate effectively decreased bone resorption, showed a trend towards decrease in fracture rate with improvement in symptoms, and was well tolerated in children with OI. More data are needed to systematically evaluate its long-term effects on growth, bone mineral density, fracture frequency, and quality of life in children with different types of OI.(1)Rauch et al., J Bone Miner Res. 2009; 24: 1282-1289 (2) Bishop et al., Lancet. 2013;382(9902):1424-32.

***Disclosures: Antoine Nguyen**, None*

P-104

Parathyroid Hormone Response to Different Vitamin D Levels in Young People Living in the Arctic Region *Galina Kostrova[1], Svetlana Malyavskaya[1], Aleksandra Strelkova[1], Andrey Lebedev[1]. [1]Northern State Medical University, Russian Federation

Background: Low vitamin D (VD) is not always followed by a development of secondary hyperparathyroidism (SHPT). The climate-geographical specificity of the Arctic region provides conditions for vitamin D deficiency (geographical latitude, peculiarities of photoperiodicity, high geomagnetic activity, severity of weather conditions) due not only to the limited possibilities for natural production of vitamin D in skin but also to adaptive metabolic shifts. This study assesses prevalence of functional hypoparathyroidism (FHPT) in relation to VD deficiency/insufficiency in young people living in the city of Arkhangelsk. Methods: The participants of the cross-sectional (one-stage) study were 174 young people aged 18 to 20 years, including 48 (27.6%) men and 126 (72.4%) women. The level of 25(OH)D in blood serum was measured by enzyme immunoassay (DRG Instruments kits, Germany). The levels of provision of vitamin D depending on the level of 25(OH)D were as follows: normal level at 30–80 ng/mL, insufficiency at 20–30 ng/mL, deficiency at 10–19 ng/mL, and severe deficiency at less than 10 ng/mL. The level of parathormone was measured by enzyme immunoassay, pg/mL (normally, 16–65.0 pg/mL). Results: Levels of vitamin D in young people were normal in 40 subjects (23%); 25-OH vitamin D concentration was 20–30 ng/mL in 59 subjects (34%); 10–19 ng/mL in 56 subjects (32%), and <10 ng/mL in 19 subjects (11%). The correlation analysis has shown a weak negative relationship between the levels of vitamin D and total calcium (R = –0.164, p = 0.033). Increased level of PTH was detected in 37 subjects (21.3%). Level of PTH was higher in the group with 25(OH)D below 30 ng/mL. There was no correlation between the levels of PTH and vitamin D. More than 75% of the subjects showed normal level of PTH at the 25(OH)D levels below 30 ng/mL and below 20 ng/mL (FHPT). There was a positive correlation between the levels of parathormone and total calcium (R = 0.21, p =0.018) in the group with 25(O?)D below 30 ng/mL; the same group demonstrated a weak correlation between the levels of vitamin D and total calcium (R =0.18, p = 0.037). Conclusions: Lack of parathyroid hormone response to vitamin D deficiency in 75% of young people may be due to desensitization and reduced expression of the calcium-sensitive receptor of the parathyroid glands determined by living in an area with low insolation and high probability of vitamin D deficiency.

***Disclosures: Galina Kostrova**, None*

P-105

A Case Control Study of Food Selectivity and Bone Health in Children with Autism Spectrum Disorder (ASD) *Karen Loechner[1], Rashelle Berry[2], Lindsey Burrell[1], Scott Gillespie[1], Scahill Larry[1], William Sharp[1]. [1]Emory University School of Medicine, United States, [2]Children's Healthcare of Atlanta, United States

Introduction: Provisional evidence suggest that children with ASD are at risk for decreased bone mineral density (BMD). High prevalence of severe food selectivity (SFS) in ASD may contribute to reduced BMD; however, the consequences of restricted patterns of intake in ASD are not well understood. In this case control pilot study, we applied a tiered framework to evaluate the relationship between food selectivity and BMD status. Study Design: Recruitment of 30 boys (6-10 years of age) divided into 3 groups: (1) ASD and severe food selectivity (SFS) (n=10); (2) ASD with mild/no FS (NFS) (n=10); and (3) without ASD and NFS (n=10, controls). Clinical assessment/diagnostic testing confirmed ASD status. Presence/absence of FS involved a FS screening tool supported by a nutrition evaluation of regular (3-day) dietary intake. Exclusion criteria included (1) medical issues known to affect BMD (e.g., glucocorticoids); (2) enteral feeding (suggesting feeding disturbance beyond SFS), and/or 3) eating disorder (e.g., anorexia nervosa), which involves a different etiology. Measurement Approach: Feasibility outcomes included recruitment, attrition, and successful collection of clinical, BMD, and serologic/urine laboratory assessments. Study measures included radiological assessment involving DXA (TBLH, spine). Serologic/urine laboratory assessments included bone metabolism markers (25 OH vitamin D, PTH, Calcium, Magnesium, Phosphorus, and alkaline phosphatase (formation marker) and urine NTX (resorption marker), and markers of malabsorption included CRP and celiac screen. Endocrine tests included thyroid, growth hormone indices and testosterone. PreliminaryResults See Table 1: Enrollment thus far involves 23/30 boys (study held due to covid restrictions). Feasibility outcomes indicated high retention and completion of study measures (>90%). A trend to lower TBLH Z-score in SFS than NFS or controls is seen and indicates larger group sizes are needed. Of note, no difference in vitamin D noted. Conclusion: FS is a common problem for children with ASD. These preliminary findings suggest that children with ASD and severe FS may be at risk for adverse health outcomes including decreased BMD. Increased group numbers will provide greater power to see if these findings are significant. Further study, in turn, directed to intervention models (feeding therapy; vitamin supplementation) would be indicated.Abbreviations: DXA: dual energy absorptiometry, TBLH: total body less head; NTX: N-telopeptide; PTH: parathyroid hormone

Table 1: Demographics, Bone Mineral Density and Vitamin D analysis

Outcome	N	Controls (1) N=9	N	ASD, Non-Selective Eating (Mild) (2) N=10	N	ASD, Selective Eating (Severe) (3) N=10	Omnibus P-Value[1]	Pairwise P-Values[1]		
								P-Value 1 vs. 2	P-Value 1 vs. 3	P-Value 2 vs. 3
Age (yrs)	6	7.06 ± 0.49	9	8.31 ± 1.41	8	8.41 ± 1.59	0.019	0.023	0.035	0.892
Male Gender	6	6 (100%)	8	8 (100%)	8	8 (100%)	NA	NA	NA	NA
Spine Z-score, Mean ± SD	5	-0.28 ± 0.88	9	-0.03 ± 0.93	7	-0.91 ± 1.35	0.359	0.628	0.338	0.158
TBLH Z-score, Mean ± SD	5	-1.28 ± 1.13	7	-0.37 ± 1.34	6	-1.60 ± 0.74	0.149	0.224	0.594	0.055
Vitamin D, Mean ± SD	5	24.1 ± 8.20	8	24.3 ± 5.30	7	22.8 ± 11.1	0.944	0.959	0.812	0.738

[1]Omnibus p-value is the overall ANOVA p-value; Pairwise p-values are based on post-hoc ANOVA tests

***Disclosures: Karen Loechner**, None*

P-106

PROPEL2: a phase 2, open-label, dose-escalation and dose-expansion study of infigratinib in children with achondroplasia (ACH) *Ravi Savarirayan[1], Peter Kannu[2], Carl Dambkowski[3], Daniela Rogoff[3], Melita Irving[4]. [1]Murdoch Children's Research Institute, Australia, [2]The Hospital for Sick Children, Toronto, Canada, [3]QED Therapeutics Inc., United States, [4]Guy's and St Thomas' NHS Trust, United Kingdom

Background: ACH, the most common non-lethal form of skeletal dysplasia, is characterized by defective endochondral ossification resulting from gain-of-function mutations in the fibroblast growth factor receptor 3 (FGFR3) gene, a negative regulator of endochondral bone formation. Current treatment options are non-targeted, ineffective, or painful interventions aimed at preventing or treating complications. Infigratinib is an orally bioavailable and selective FGFR1–3 tyrosine kinase inhibitor in development for FGFR-related conditions. In vitro data with infigratinib showed inhibition of FGFR1–3 activity with reversal of established growth arrest in chondrocytes. In vivo studies revealed dose-dependent improvements in foramen magnum and long bone length in Fgfr3Y367C/+ mice following treatment with infigratinib.Methods: PROPEL2 is a prospective, phase 2, open-label study of infigratinib in children with ACH. It consists of dose escalation with an extended treatment phase (ESC-ET), designed as dose finding, followed by a dose-expansion phase (EXP) to confirm the selected dose and to provide evidence of efficacy. The primary endpoints of ESC-ET are treatment-emergent adverse events and change from baseline in annualized growth velocity. Subjects (n=40) will be enrolled in ascending dose cohorts of approximately 10 subjects/cohort (4 cohorts planned) and treated for 6 months at their assigned dose, continuing for an additional 12 months with dose modifications as required. The primary endpoint of EXP is change from baseline in annualized growth velocity at the dose identified from ESC. Up to 20 new subjects will be enrolled in this phase and receive infigratinib (mini-tablets, administered orally once daily) for 12 months. Secondary objectives include: safety/tolerability of infigratinib; changes from baseline in anthropometric parameters, including body proportions; pharmacokinetic/pharmacodynamic profile of infigratinib. An exploratory objective is evaluation of changes in ACH disease burden. Eligible children with ACH 3–11 years of age who completed at least 6 months of observation in PROPEL will participate in PROPEL2. Current status: PROPEL2 is currently enrolling; the planned total enrollment is 60 children with ACH (40 ESC-ET, 20 EXP). Following completion of PROPEL2, subjects have the opportunity to enroll in an open-label long-term extension study to assess the safety and efficacy of long-term administration of infigratinib in children with ACH.

***Disclosures: Ravi Savarirayan**, QED Therapeutics Inc., Grant/Research Support, QED Therapeutics Inc., Other Financial or Material Support, BioMarin, Consultant, BioMarin, Grant/Research Support, Ascendis, Other Financial or Material Support, BioMarin, Other Financial or Material Support, Ascendis, Grant/Research Support, Theracon, Grant/Research Support*

P-107

A Randomized Double Blind Placebo Controlled Trial in Healthy School Children to Evaluate the Adequacy and Efficacy of Daily Supplementation of Milk Fortified with 1200 IU Vitamin A and D2 in one litre of Milk *Raman Marwaha[1], Aashima Dabas[2], Seema Puri[3], Mani Kalaivani[4], Arjun Dang[5], Vineet Dabas[2], Sangeeta Yadav[2], R Pullakhandam[6], Susheel Gupta[7], Archana Narang[8]. [1]SEHEAC, India, [2]Maulana Azad Medical College, India, [3]Department of Food and Nutrition, Institute of Home Economics, University of Delhi, India, [4]Department of Biostatistics, All India Institute of Medical Sciences, New Delhi, India, [5]Dr Dangs Lab, India, [6]Biochemistry Division, Indian Council of Medical Research- National Institute of Nutrition, India, [7]Department of Endocrinology, Sanjay Gandhi Post Graduate Institute, India, [8]Department of Homeopathy, BR Sur Homeopathic College, India

In view of high prevalence of vitamin A & D deficiencies in Indian children, we undertook a double-blind placebo-controlled randomized trial in prepubertal children, to evaluate the adequacy of daily supplementation of milk fortified with 1200 IU of vitamin A & D2 in one litre of milk. A total of 235 out of 266 children with vitamin D insufficiency were randomized into an intervention (n=119) and control (n=116) group. Intervention group was supplemented with 200 mL milk fortified with approximately 240 IU of A & D2 and control group with200 mL of plain milk every day for 12 weeks from Oct to December 2019. A total of 210 children completed the study. Baseline and post supplementation fasting blood samples were evaluated for calcium, phosphate, alkaline phosphatase, 25 hydroxy vitamin D, parathyroid hormone, bone markers (CTx and PINP), retinol and urinary calcium/creatinine ratio. Mean? SD of baseline serum 25(OH)D level was 11.7?3.7 ng/mL with levels<12ng/mL in 100 (42.5%) children. The decline in control group was significantly greater(11.97?3.79 to 6.73?3.5ng/mL; P<0.001) than the intervention group (11.42?3.63 to 10.81?3.45ng/mL; P=0.1) following supplementation. Secondary hyperparathyroidism significantly increased from 18.1% to 39%in the control group and decreased from 22.7% to 13.3%in intervention group post supplementation; P<0.001. Subclinical vitamin A deficiency was recorded in 2.2% subjects. Supplementation of milk fortified with 240 IU Vitamin D2 is not adequate to achieve vitamin D sufficiency, though it does reduce the decline in serum 25(OH)D levels during winter in prepubertal Indian children with vitamin D deficiency.Trial registration: CTRI/2019/09/021073

Comparison serum vitamin D and parathyroid hormone levels between the groups

Outcomes	Control		Intervention		Mean Difference (95% CI)		P value
ITT Analysis	n=116		n=119				
[1]S.25(OH)D	11.9	3.8	11.4	3.6	0.55	(-0.40,	0.257
Baseline	6.7	3.5	10.8	3.5	4.1	1.50)	<0.001
Endline	***5.2	(4.5, 6.0)	0.60	(-0.12, 1.32)	-4.6	(3.2, 4.9)	<0.001
Difference (95%	45.8	(17.9,173.4)	49.5	(14.2,129.1)		(-5.7, -3.6)	0.392
CI)	52.6	(14.9,549.3)	46.5	(9.7,121.5)			0.007
[1,2]S. PTH	***-13.5	(-217.7, 55.9)	†††3.9	(-218.8, 72.1)			<0.001
Baseline							
Endline							
% Change							
PP Analysis	n=104		n=106				
[1]S. 25(OH)D	12.3	3.8	11.4	3.6	0.89	(-0.11,	0.082
Baseline	6.4	3.5	10.7	3.4	4.3	1.91)	<0.001
Endline	***5.8	(5.1, 6.6)	†††0.68	(-0.13, 1.49)	-5.2	(3.3, 5.2)	<0.001
Difference (95%	47.5	(17.9,172.9)	47.4	(14.2,129.1)		(-6.3, -4.0)	0.754
CI)	55.9	(15.0,549.3)	44.4	(9.7,121.5)			<0.001
[1,2]S. PTH	***-18.7	(-217.7,55.9)	†††11.4	(-218.8,72.1)			<0.001
Baseline							
Endline							
% Change							

N= 235 in ITT and 210 in PP analysis; ITT, intention to treat, PP, per protocol, 25(OH)D- 25 hydroxy vitamin D, PTH, parathyroid hormone; Values S. 25(OH)D expressed as mean and SD and S/ PTH as median and IQR;[1]statistical analysis between baseline and endline values, [2]statistical analysis between baseline and endline values in intervention group; *P values between baseline and endline values in control group, **P*<0•05, ***P*<0•01, ****P*<0•001, †P values between baseline and endline values in intervention group, †*P*<0•05, ††*P*<0•01, †††*P*<0•001

***Disclosures: Raman Marwaha**, None*

P-108

PROPEL: a prospective clinical assessment study in children with achondroplasia (ACH) *Ravi Savarirayan[1], Peter Kannu[2], Carl Dambkowski[3], Daniela Rogoff[3], Melita Irving[4]. [1]Murdoch Children's Research Institute, Australia, [2]The Hospital for Sick Children, Toronto, Canada, [3]QED Therapeutics Inc., United States, [4]Guy's and St Thomas' NHS Trust, United Kingdom

Background: ACH is the most common non-lethal form of skeletal dysplasia, affecting between 1 in 15,000 to 1 in 30,000 live births [Horton et al. 2007; Waller et al. 2008]. Children and adults with ACH have disproportionate short stature, with a final height of approx. 131 cm for males and 124 cm for females. Growth velocity for individuals with average stature is 1.7- to 2.2-fold higher than individuals with ACH during infancy and puberty and 1- to 1.8-fold higher during childhood [Hoover-Fong et al. 2008]. People with ACH are prone to significant co-morbidities, including obstructive sleep apnea, chronic otitis media with conductive hearing loss, spinal stenosis, and a propensity towards obesity. In some infants, narrowing of the foramen magnum may result in compression of the spinal cord with neurologic sequelae, requiring timely neurosurgical intervention. There are currently no approved therapies for the treatment of ACH in either the US or the EU, and management is supportive in nature. There is no widely accepted consensus about treatment, and current treatment options are non-targeted, ineffective, or painful interventions aimed at preventing or treating complications of ACH [Unger et al. 2017; FDA 2018].Methods: Children with ACH between the ages of 2.5 and 10 years are eligible for enrollment in PROPEL, a prospective, non-interventional study examining baseline growth parameters and health status in children being assessed for potential enrollment into interventional studies with infigratinib, an oral FGFR1–3 inhibitor in development for ACH. Participants will be assessed at baseline, month 3, month 6, and every 6 months thereafter. The primary endpoint is annualized height growth velocity. Secondary endpoints include change from baseline in other growth parameters (including body proportionality); analysis of bone biomarkers (e.g. bone alkaline phosphatase, collagen X fragment); and the occurrence of medical events and surgical procedures. Participants will be enrolled in the study for a minimum of 6 months up to a maximum of 2 years.Current status: The PROPEL study is underway; the first participant was enrolled in August 2019. Planned total enrollment is 200 children with ACH. The sample size of approx. 200 participants is considered enough to characterize the natural history of children with ACH and lead to sufficient enrollment in a QED-sponsored Phase 2 and/or 3 interventional trial of infigratinib in children with ACH (PROPEL2).

***Disclosures: Ravi Savarirayan**, QED Therapeutics Inc., Grant/Research Support, Ascendis, Grant/Research Support, QED Therapeutics Inc., Other Financial or Material Support, BioMarin, Other Financial or Material Support, BioMarin, Consultant, BioMarin, Grant/Research Support, Theracon, Grant/Research Support, Ascendis, Other Financial or Material Support*

P-109

Protocol for a Comprehensive Understanding of Bone and Muscle in Children with Systemic Lupus Erythematosus: a Pilot Study of Bone-muscle Interactions *Sarah L West[1], Linda Hiraki [2], Andrea Knight[2], Deborah Levy[2], Reza Vali[2], Amer Shammas[2], Andy Kin On Wong[3], Greg Wells[2], Etienne Sochett[2]. [1]Trent University, The Hospital for Sick Children, Canada, [2]The Hospital for Sick Children, Canada, [3]University Health Network, Canada

Childhood-onset Systemic Lupus Erythematosus (cSLE) is a rare chronic autoimmune disease that can negatively impact the musculoskeletal system. Bone health is recognized to be compromised in cSLE, especially deficits in bone quantity and quality which place children at risk for current and future fracture. Muscle function may also be impaired in cSLE; chronic inflammation may result in impaired oxidative metabolism via free radical damage to mitochondria, and reduced endothelial function may disrupt blood flow and/or oxygen delivery to muscles. The muscle-bone interaction is an important factor contributing to bone health; however, no studies have examined the link between impaired bone & skeletal muscle metabolism/perfusion in cSLE. This study will address the knowledge gap by non-invasively measuring bone quantity, quality, and muscle metabolism/perfusion in cSLE. Our hypothesis is that bone health and muscle function (metabolism and perfusion) will be impaired in children with cSLE compared to healthy matched controls. We also hypothesize that there will be a relationship between the impairment in bone health and muscle function in cSLE. This study will be performed at the Hospital for Sick Children in Toronto, Canada. We will recruit 16 children with cSLE and 16 healthy controls (9-18 years old). After informed consent, non-invasive imaging techniques will be used to measure bone and muscle function. More specifically, clinical bone densitometry reports (total body less head and spine) will be obtained. Bone quality will be measured at the non-dominant radius and tibia by high resolution peripheral quantitative computed tomography (HRpQCT). 31P-magnetic resonance spectroscopy (via magnetic resonance imaging; MRI) will be used in conjunction with exercise protocols (that target aerobic and anaerobic energy systems using a MRI safe ergometer) to assess skeletal muscle metabolism of the quadriceps muscle. Blood-oxygen level-dependent functional (BOLD) MRI imaging will provide a measure of blood flow/volume and oxygen saturation (skeletal muscle perfusion). We will use T-tests, general linear model and regression analyses to assess outcomes, controlling for factors such as corticosteroid use. If we find that poor bone and muscle health are correlated in cSLE, the results will support a larger exercise intervention study that will aim to evaluate the impact of exercise on bone health and muscle function improve bone, muscle, and quality of life in cSLE.

***Disclosures: Sarah L West**, None*

P-110

Lactobacillus reuteri prevents Early Stages of Glucocorticoid-induced Avascular Necrosis of Femoral Head. *Ho Jun Kang[1], Jonathan D Schepper[2], Soumya Chennupati[1], Morgan Roegner[1], Narayanan Parameswaran[1], Laura R McCabe[1]. [1]Michigan State University, United States, [2]BioTek Instruments, United States

Glucocorticoids (GC) are effective anti-inflammatory drugs commonly used to treat patients with autoimmune diseases. Over time, chronic GC treatment can negatively affect both gut and bone health. In the gut this leads to intestinal dysbiosis and increased gut permeability. In bone, this leads to glucocorticoid-induced osteoporosis and can cause osteonecrosis (GCON, i.e., avascular necrosis of the femur head). Patients with late stages of GCON in the hip suffer from pain and stiffness, resulting in long-term disability and hip replace-

ment. Identifying non-invasive ways to prevent or treat GCON would be of great benefit to patients. Our lab and others have shown that the gut microbiota and barrier function are involved in regulating bone homeostasis and density. We also identified that the probiotic Lactobacillus reuteri 6475 (LR) prevented GC-induced femoral and vertebral trabecular bone loss in male and female mice. Based on these findings, we examined if LR treatment could prevent GCON of the femur head (avascularization, cell apoptosis, adiposity, abnormal bone surface and architecture). Male C57BL/6J (16-weeks-old) mice were treated for 8-weeks with subcutaneous pellets containing GC (2.5 mg/kg/day) or vehicle. Simultaneously, mice were orally supplemented with vehicle, the probiotic LR or a mixture of 8 strains of probiotics (VSL#3) at a dose of ~109 CFU bacteria/day. Femur immunohistochemistry examining von Willebrand factor (vWF) positive blood vessels and the gene expression of vWF revealed that the GC induced avascularization of the femur head was completely prevented by LR supplementation. Specifically, compared to controls, GC treatment caused more than 50% reduction in the number of the blood vessels in the marrow area of the femur head, whereas LR treated mice did not exhibit any change in vascularization compared to controls. VSL#3 treated mice had a response that was in-between controls and GC-treated mice (~25% reduction in vascularization). Similarly, TUNEL analyses and mRNA markers of apoptosis (Bax/Bcl-2, pro/anti-apoptotic) determined that LR treatment prevented GC-induced apoptosis of trabecular osteoblasts and osteocytes. Also, only LR treatment prevented GC-induced marrow adiposity and bone architecture changes. Together, these data indicate that probiotic LR supplementation prevents the pathological bone effects of GCs and may be an effective way to prevent early stages of avascular necrosis of femoral head.

***Disclosures: Ho Jun Kang**, None*

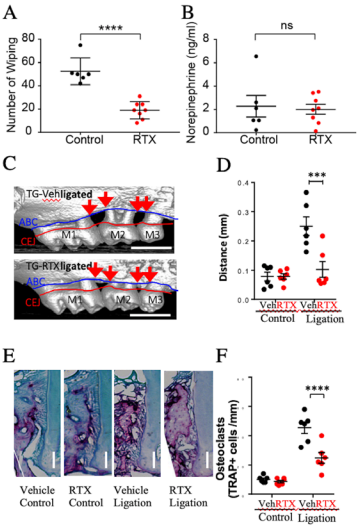

A. Number of eye wiping motions measured for 5 minutes following the application of capsaicin (0.03% in 20 µl) to the left eye a week after intra-TG injection of RTX or Veh. ***p < 0.001 in t-test; n=6/group; mean ± s.e.m. **B**. ELISA assay for evaluating circulating level of norepinephirine in blood collected 3 weeks after TG injection of RTX or vehicle. **C.** Three dimensional reconstruction of µCT scanned Images (Siemens Inveon small animal CT; 9.9 µm resolution). ABC, alveolar bone crest; CEJ, cementoenamel junction; M2, maxillary second molar; The red arrows indicate four points where distances between ABC and CEJ were evaluated in each image, Scale bar, 1 mm. Four measurements were averaged in each sample. **D.** Averaged distances from ABC to CEJ assessed in µCT. ***p< 0.001 in Bonferroni post-test following two-way ANOVA. N=6/group. **E.** Histological evaluation of osteoclasts. Osteoclasts were stained red by TRAP staining. Scale bar=100 µm. Scale bar=50 µm. **F.** The number of osteoclasts (TRAP+ cells/mm of the alveolar bone surface) Multinucleated dark red cells with three or more nuclei lying along the alveolar bone surface around 2nd molar were counted. ****p< 0.0001 in Bonferroni post-test following two-way ANOVA. N=6/group.

***Disclosures: Sheng Wang**, None*

P-112

Ablation of TRPV1+ Afferents Decreases Periodontal Bone Destruction in Mice *Sheng Wang[1], Man Kyo Chung[1], Xiaobei Wang[2], Vivek Thumbigere-Math[2]. [1]University of Maryland School of Dentistry, Neural and Pain Science Department, United States, [2]University of Maryland School of Dentistry Advanced Oral Sciences & Therapeutics Department, United States

Objectives: Periodontal tissues are innervated by multiple subsets of sensory afferents including peptidergic nociceptive afferents, majority of which expresses transient receptor potential vanilloid 1 (TRPV1). It is well established that neuropeptides derived from sensory neurons affect vascular responses (e.g., neurogenic inflammation) indicating the contribution made by afferents to local inflammatory responses. Significant questions remain regarding the functions of peptidergic sensory nerves in periodontal host responses and alveolar bone remodeling. The objective of this study was to determine the roles of TRPV1+ peptidergic subsets of sensory afferents in alveolar bone homeostasis.Methods: In adult C57bl/6 mice, TRPV1+ trigeminal afferents were selectively ablated by intraganglionic injection of resiniferatoxin (RTX) into trigeminal ganglia (TG). One week later, periodontitis was induced by tying a silk suture around the maxillary 2nd molar. Unligated contralateral tooth served as a control. Two weeks after ligature placement, the mice were euthanized for microCT followed by histology study. In a separate cohort of periodontitis-induced mice, maxillary alveolar bone including three molars were dissected and used for multiplex assay. Results: In vehicle (PBS) injected group, ligature produced alveolar bone resorption around the second molar. In contrast, the alveolar bone resorption was significantly lower in RTX injected group. Tartrate-resistant acid phosphatase (TRAP) staining demonstrated significantly increased number of osteoclasts in the ligated side, which was comparably lower in RTX group than vehicle group. Ligature significantly increased periodontal expression of RANKL, IL1β and TNFα, which was significantly lower in RTX group compared to vehicle group.Conclusion: Ablation of TRPV1+ trigeminal afferents decreases proinflammatory cytokines and the numbers of osteoclasts in periodontium, which leads to decreased bone destruction in the mouse model of periodontitis. These results suggest that specific targeting of neuroimmune and neuroskeletal regulation can offer promising therapeutic targets for periodontitis.

P-113

Minocycline-Induced Gut Dysbiosis Disrupts Metabolism and Post-Pubertal Skeletal Development *Matthew Carson[1], Amy Warner[1], Jessica Hathaway-Schrader[1], Brooks Swanson[1], Joy Kirkpatrick[1], Alexander Alekseyenko[1], Jose Aguirre[2], Caroline Westwater[1], Chad Novince[1]. [1]Medical University of South Carolina, United States, [2]University of Florida, United States

Our group has shown the commensal gut microbiota critically regulates skeletal maturation through liver derived mechanisms. We have also shown that broad spectrum antibiotic perturbation of gut microbiota dysregulates post-pubertal skeletal development. Study purpose was to investigate immediate and sustained effects of minocycline (MINO) therapy, the most common systemic antibiotic treatment (Tx) for adolescent acne, on post-pubertal skeletal development. Sex-matched specific-pathogen-free (SPF) C57BL/6T mice were administered a clinically relevant dose of MINO or vehicle-control (VEH) from age 6-12wks; groups were euthanized at ages 12 and 18wks to assess immediate and sustained MINO Tx effects. In a separate experiment, germ-free (GF) C57BL/6T mice were administered MINO or VEH Tx from age 6-12wks. 16S rDNA analysis was performed on colon contents. Ex vivo µCT was performed in femurs. Tibia and vertebrae were embedded for histomorphometry. Livers were isolated for histopathology. Flow cytometry was carried out in gut draining mesenteric lymph nodes (MLNs) and liver draining lymph nodes (LLNs). In vivo µCT was performed to assess changes in peripheral adipose tissue volume fraction. Bone marrow stromal cells (BMSCs) were isolated from naïve mice to assess direct MINO Tx effects on osteoblastogenesis. MINO Tx induced phylum level dysbiotic shifts in the gut microbiome. Bone mineral density and bone volume fraction were blunted in MINO vs. VEH treated SPF mice at age 12wks, and these effects persisted at age 18wks. The osteopenic phenotype in MINO treated SPF mice was attributed to suppressed bone formation and mineral apposition rates, which was validated by decreased serum OCN and P1NP. Liver weight and hepatic glycogen content were reduced in MINO vs. VEH treated SPF mice at age 12wks, and these effects persisted at age 18wks. Proinflammatory TH1 and TH17 cells were elevated in LLNs of MINO vs. VEH treated SPF mice. There was a 3-4X greater fold increase in peripheral adipose tissue from age 12 to 18wks, in MINO vs. VEH treated SPF mice. Skeletal and metabolic outcomes were similar in MINO vs. VEH treated GF mice, and exogenous MINO stimulation did not alter osteoblast outcomes in vitro, which implies that MINO Tx effects are dependent on the microbiota. MINO-induced gut dysbiosis has detrimental effects on murine metabolism and skeletal maturation, which highlights potential clinical implications for adolescents subjected to systemic MINO Tx for acne.

***Disclosures: Matthew Carson**, None*

P-114

Role of Estrogen Receptor β in Bone and Muscle Crosstalk *Nuria Lara[1], Julian Vallejo[1], Mark Dallas[1], Yixia Xie[1], Mohammad Niroobakhsh[1], Mark Gray[1], Eleanor Ray[1], Derek Nelson[1], Kashif Javid[1], Sarah L. Dallas[1], Ganesh Thiagarajan[1], Michael Wacker[1], Mark Johnson[1]. [1]UMKC, United States

Estrogen signaling through its two main receptors, ERα and ERβ, plays essential roles in bone and muscle health and we hypothesize in bone-muscle crosstalk. We investigated the role of ERβ mediated signaling in bone-muscle crosstalk by deleting ERβ in late osteoblast/osteocytes (ERβ-/-oy; ERβf/f crossed with the 10-kb Dmp-1 Cre mice) or in skeletal muscle (ERβ-/-sm; ERβf/f crossed with the tamoxifen inducible MCM-HSA-Cre mice). Mice (m/f; n=3-7) were analyzed at 6 months of age. Cre negative littermates were used as controls.

Body weight (BW) was identical over their lifespan between knockout and control mice. Femurs were used for μCT and biomechanical analysis and EDL and Soleus muscles were used for contractility analysis. Trabecular BV/TV (3.4+/-0.8% vs 7.7+/-1.2%, p<.05) was lower in male ERβ-/-oy due to decreased trabecular number (0.7+/-0.1 1/mm vs 1.7+/-0.2 1/mm, p<.05) and increased trabecular separation (0.4+/-0.02mm vs 0.3+/-0.02mm, p<.05). Male ERβ-/-oy had increased elastic stiffness (200.6+/-6.4N/mm vs 174.2+/-6.8N/mm, p<.05) and modulus of elasticity (4.2+/-0.3GPa vs 3.2+/-0.2GPa, p<.05). Soleus muscles were smaller (9.5+/-0.2mg vs 10.7+/-0.4mg, p<.05) and recovered from fatigue to a lesser degree (56.7+/-3.4%vs 72.9+/-3.6%, p<.05) in male ERβ-/-oy compared to controls. In contrast, no differences were seen in the EDL. EKG showed decrease in QT interval corrected for heart rate (QTc). While femurs of ERβ-/-oy females had lower modulus of elasticity (3.2+/-0.4GPa vs 4.5+/-0.4GPa, p<.05), no other differences were detected in bone or muscle properties. Soleus muscles of ERβ-/-sm males and females showed enhanced recovery from fatigue. Interestingly, Heart weight/BW was lower in ERβ-/-sm males, but higher in ERβ-/-sm females, which also showed a decrease in QTc. We did not observe any major difference in architectural or biomechanical properties in the bones of ERβ-/-sm in male or female mice. These data identify a previously unrecognized role for ERβ in bone and show that Dmp1-Cre targeted deletion of ERβ in bone affects trabecular bone in males but not in females. Moreover, deleting ERβ in bone impairs Soleus muscle recovery from fatigue, suggesting a role for bone crosstalk with muscle adaptation to applied stress. Muscle ERβ deletion beginning at adulthood had effects on the soleus and heart, but not on bone properties. Together, these data support the hypothesis that ERβ mediated signaling plays an important role in bone to muscle crosstalk at the biochemical level.

***Disclosures: Nuria Lara**, None*

P-115

Depletion of Replicating Osteolineage Cells Leads to Fracture Nonunion in Col1-tk Mice *Katherine Hixon[1], David Sykes[1], Susumu Yoneda[1], Austin Hensley[1], Jennifer McKenzie[1], Anna Miller[1], Matthew Silva[1]. [1]Washington University in St. Louis, United States

Nonunion is defined as the permanent failure of a bone to heal and occurs clinically in 5% of fractures. Atrophic nonunion, characterized by failure of osteochondral callus formation, is poorly understood and difficult to treat. To date, most animal models of atrophic nonunion involve osteotomy, periosteal stripping, etc., yet such destructive surgical methods are not representative of many clinical cases. Thus, there is an unmet need for a clinically relevant "failure of biology" atrophic nonunion model. Jilka et al. created the 3.6Col1A1-tk (Col1-tk) mouse where treatment with the nucleoside analog ganciclovir (GCV) depletes replicating osteoprogenitor cells. Heterozygous Col1-tk+ mice and WT littermates, 12-weeks old, male and female, were subjected to femur full fracture. All animals were dosed with GCV (8 mg/kg i.p.) twice daily starting at fracture for 2 or 4 weeks. Mice were sacrificed at 3 weeks for micro-CT and histology to examine an early healing timepoint. Additional animals were monitored weekly by X-ray and micro-CT for 12 weeks post fracture to assess longer term outcomes; following sacrifice, micro-CT was performed and samples were processed for either histology or biomechanics. Weekly radiographs (n=12-18/group) were scored for the degree of healing using a modified Goldberg score and revealed that WT vs. Col1-tk mice were significantly different (Figure 1A; $\chi 2$, $p < 0.05$). After 3 weeks, WT mice had a large callus with the normal appearance of woven bone (red) and cartilage (blue). In contrast, Col1-tk mouse had negligible callus formation with reduced or absent bridging (Figure 1B). For in vivo micro-CT, the Col1-tk callus did not significantly change in size, whereas the WT mice saw a large increase in volume when the callus formed and a decrease as it remodeled (n=7-9/group; $p < 0.05$, ANOVA). Histologically, by 12 weeks all WT mice had bridged and remodeled. While the Col1-tk mice did display some bridging, the cortical bone remodeling/resorption was reduced and fibrotic tissue and cartilage persisted (n=7/group). Finally, when the femurs were biomechanically tested, Col1-tk mice were significantly weaker and less stiff than WT mice ($p < 0.05$), indicating inferior function. In summary, depletion of replicating osteolineage cells in the first 2 weeks after fracture in Col1-tk mice leads to greatly diminished callus formation resulting in functionally impaired healing. This represents a new model of atrophic (or oligotrophic) nonunion.

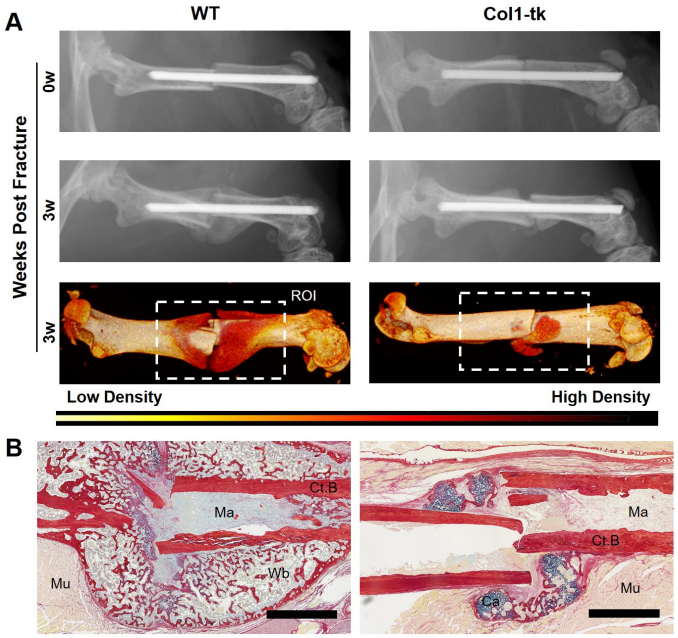

Figure 1. (A) Radiographs scored for bridging and micro-CT 3D reconstruction demonstrated significantly different healing in WT vs. Col1-tk mice ($\chi 2$, $p < 0.05$). **(B)** Histologically, WT mice had complete bridging with the callus almost entirely composed of woven bone, while Col1-tk mice had a smaller callus composed of mostly cartilage and fibrotic tissue. Abbreviations: Cortical Bone = Ct.B.; Cartilage = Ca; Marrow = Ma; Muscle = Mu; Woven Bone = Wb. Black scale bars denote 1 mm.

***Disclosures: Katherine Hixon**, None*

P-116

Cardiovascular disease miRNAs are associated with BMD in a non-human primate model of osteoporosis. *Ellen Quillen[1], Roberto Fajardo[2], Todd Bredbenner[3]. [1]Wake Forest School of Medicine, United States, [2]University of the Incarnate Word School of Osteopathic Medicine, United States, [3]University of Colorado Colorado Springs, United States

The overlap between cardiovascular health and bone health has been a topic of clinical interest for decades, with evidence suggesting a link between vascular disease, bone mineral density, and fracture risk. Accumulating evidence implicates circulating miRNAs as gene regulators across tissues and potential biomarkers of disease states. The baboon animal model is used in studies of cardiovascular disease, osteoporosis, and other conditions because disease processes are naturally occurring and often replicate human pathophysiology. To better understand the potential role of miRNAs in cardiovascular and bone health, we evaluated the association of miRNAs previously associated with cardiovascular disease with vertebral bone mineral density in the aging baboon. No work was done on living animals and no animals were euthanized specifically for this study. We evaluated 192 baboons (126 female) ranging in age from 10-29 years (30-90 human-equivalent years) with a mean of 19.4 years.RNA was extracted from whole blood samples collected at necropsy and miRNA libraries sequenced on the Illumina HiSeq2500. miRNAs were identified based on miRbase alignments. miRNA counts were analyzed using the R statistical package DESeq2 to identify miRNAs associated with aBMD, measured using DXA in both the anterior-posterior (AP) and medio-lateral (ML) orientation for the intact L2-L4 vertebrae. Six of eleven cardiovascular-related miRNAs investigated are associated with differences in AP aBMD in the baboon ($p < 0.05$). Four miRNAs are upregulated in animals with lower aBMD (miR-320a, miR-197-3p, miR-191-5p, miR-27b-3p), while two are downregulated (miR-126-3p, miR-21-5p).Most notably, miR-320a and miR-126 are known regulators of VEGF signaling which regulates both angiogenesis and endochondral ossification, while miR-27b targets PPARγ, a transcriptional factor regulating cardiac fibrosis, glucose metabolism, and bone homeostasis. Additionally, miR-191 and miR-197 regulate NF-kB signaling which regulates both platelet activation contributing to heart disease and RANK ligand-induced osteoclastogenesis. Future analyses will evaluate miRNA associations with material and structural properties, and thus, fracture risk. We expect this work to identify miRNAs that modulate signaling between tissues or represent shared biomarkers of dysregulation in cardiovascular and skeletal diseases (e.g. arising from common dysregulation of calcium metabolism).

***Disclosures: Ellen Quillen**, None*

Posters

P-117

FGF23 Neutralizing Antibody Rescues Reduced Bone Nodule Formation in Bone Marrow Stromal Cell Cultures from Sickle Cell Disease Mice *Marja Hurley[1], Liping Xiao[1], Donyell Williams[1]. [1]UConn Health, United States

Osteoporosis and osteopenia are common bone complications in sickle cell disease (SCD), the most common genetic blood disorder in humans. The molecular mechanisms of bone loss in SCD are not yet fully defined. Fibroblast growth factor 23 (FGF23) is a phosphaturic hormone that is mainly produced by osteocytes and osteoblasts. Production of FGF23 is up regulated by iron deficiency, hypoxia, and high erythropoietin, which are often seen in SCD. In this study we examined the involvement of FGF23 in impairing bone mineralization in SCD mice. Since in addition to being a regulator of serum phosphate, FGF23 has been shown to have direct inhibitory effects on bone formation, we also assessed whether bone formation was decreased in SCD mice in vitro and whether FGF23 blocking antibody could modulate bone nodule formation in vitro. Analysis of biochemical markers in 6 months old male control (Ctrl) and SCD littermate mice showed serum calcium was similar in Ctrl and SCD mice (Fig.1A). Serum phosphate was significantly decreased in SCD mice compared to Ctrl (Fig.1B). Serum 1,25(OH)2D was inappropriately normal in the setting of decreased serum Pi (Fig.1C). Serum FGF23 (intact) was significantly increased in SCD mice (Fig.1D). Serum ?Klotho (an essential cofactor for FGF23 signaling) was increased in SCD mice (Fig.1E). Bone marrow stromall cells (BMSCs) harvested from 3 months old Ctrl and SCD female mice were plated at 2 million cells/well in 6-well dishes and cultured for 3 days in proliferation media (αMEM supplemented with 10% heat-inactivated fetal bovine serum, 100-U/mL penicillin-streptomycin), then switched to osteogenic media (proliferation media plus 50 ug/ml ascorbic acid and 4mM β-glycerophosphate). BMSCs from Ctrl and SCD were treated with control IgG (IgG, rat-anti- NGFPb-3F8-raIgG2a) or a rat anti-rat FGF23 neutralizing antibody (FGF23Ab, clone 58.5, 100 nM) (a gift from Amgen Inc., Thousand Oaks, CA) throughout the 14 days of culture. After staining for alkaline phosphatase, dishes were re-stained for von Kossa to assess mineralized bone nodules. As shown in Fig.1F&G, von Kossa staining and Image J quantitative analysis showed area of mineralized bone nodules was reduced in SCD cultures and was rescued by FGF23Ab. We conclude that FGF23 contributes to the pathogenesis of abnormal phosphate homeostasis and bone loss in SCD mice, and there is an intrinsic mineralization defect in BMSCs from SCD mice that could be rescued by blocking FGF23 signaling.

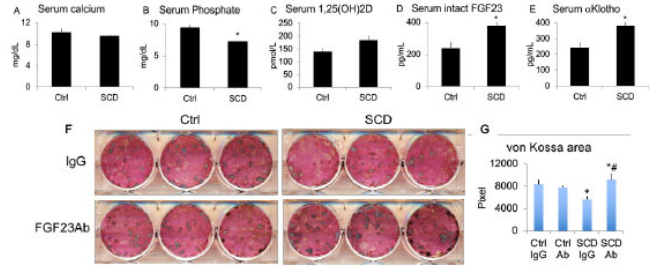

Figure 1. Serum biochemical markers in Ctrl and SCD mice and effect of FGF23 neutralizing antibody on bone formation in BMSC culture from Ctrl and SCD mice. (A) Serum calcium, (B) Pi, (C) 1,25(OH)2D, intact FGF23, and (E) aKlotho in 6 months old male mice, n=4 mice/group. *p<0.05 compared with Ctrl by T-Test. (F) representative images of von Kossa staining at 14 days of culture. (G) Quantitative analysis of von Kossa-positive colony area utilizing ImageJ software. *: compared with Ctrl-IgG P < .05; #: compared with SCD-IgG P<0.05.

***Disclosures: Marja Hurley**, None*

P-118

Modulation of Bone Marrow Mesenchymal Stem Cell Differentiation by Osteocytic Connexin Hemichannels *Jingruo Zhang[1], Rui Hua[1], Manuel Riquelme[1], Sumin Gu[1], Jean Jiang[1]. [1]Department of Biochemistry and structural biology, UT Health San Antonio, United States

Differentiation of bone marrow mesenchymal stem cells (MSCs) in marrow cavity is modulated by multiple factors. Osteocytes, the most abundant bone cell type in mineral matrix, form an extensive cellular network and provide an extracellular tunnel connecting bone matrix to bone marrow cavity. The factors released from osteocytes could function in a paracrine manner to influence bone marrow microenvironments and MSCs. Connexin 43 (Cx43) hemichannels richly present in osteocytes allow small molecules, such as prostaglandins, to release from inside cell to extracellular space. In this study, by using two transgenic mice models with a predominantly overexpression of Cx43 mutants in osteocytes: R76W mice (dominant-negative Cx43 mutant inhibiting gap junctions) and Δ130–136 mice (dominant-negative Cx43 mutant inhibiting both hemichannels and gap junctions), we found increased numbers of bone marrow adipocytes in Δ130–136 mice as compared to wild type (WT), while there was no change in R76W mice. In vitro MSC differentiation induction study showed that MSCs isolated from Δ130-136 mice bone marrow preferred adipogenic pathway as compared with WT and R76W mice. mRNA levels of adipogenic markers were also increased during adipogenic induction in Δ130-136 mice, including peroxisome proliferator-activated receptor gamma (PPARγ) and adipocyte protein 2 (aP2). Contrary to Δ130-136 mice, MSCs from R76W mice preserved a relatively normal differentiation process with a slightly enhanced osteogenic differentiation as compared to WT. Osteocytic Cx43 hemichannels serve as a major portal for prostaglandin E2 (PGE2) release. The PGE2 level in bone marrow of Δ130-136 mice was mitigated compared to WT and R76W mice. To access the involvement of PGE2 released from Cx43 hemichannels in this paracrine effect, we treated isolated MSCs with PGE2. The adipogenic differentiation was attenuated with PGE2 in MSCs isolated from Δ130-136. Additionally, we observed an increase of apoptotic bone marrow cells in Δ130-136 mice. PGE2 protects cells from apoptosis in many cell types so that the decreased PGE2 level may result in an increased apoptosis in Δ130-136 mice bone marrow. Overall, our data suggest that Cx43 hemichannels play an important role in MCS differentiation in bone marrow and factor(s), possibility PGE2, released by Cx43 hemichannels in osteocytes may act in a paracrine manner to modulate adipogenic and osteogenic pathways.

***Disclosures: Jingruo Zhang**, None*

P-119

Chronic Treatment with Sildenafil Stimulates Bone Regeneration in a Calvarial Bone Defect in Rats *Esteban Matias Brenna[1], Sandra Judith Renou[2], Victoria Interlandi[1], Viviana Andrea Centeno[1], Pablo Alejandro Fontanetti[1]. [1]Universidad Nacional de Cordoba. Facultad de Odontología. Departamento de Biologia Oral. Cordoba, Argentina, Argentina, [2]Universidad de Buenos Aires. Facultad de Odontología. Cátedra de Anatomía Patológica. Buenos Aires, Argentina, Argentina

Guided bone regeneration (GBR) is a process by which new bone is formed in an area where it was lost. This technique is performed by creating a space between the surface of the bone and surrounding soft tissues, using membranes that allow the formation of new bone in the created space. A factor involved in the GBR process is the vascularization of the area. Sildenafil citrate (SC) is a phosphodiesterase-5 inhibitor and due to its vasodilator action, it showed healing benefits in different experimental models.Objective: To evaluate the effect of SC in the GBR process in a calvarial bone defect in rats.Methods: Ten male Wistar rats aged 30-day-old underwent surgery to perform a bone defect in calvaria. The day after surgery, the animals were randomly divided into two groups which were administered, by orogastric tube, physiological solution (Control Group (CG); n=5) or SC solution at a dose of 10mg / kg body weight (Sildenafil Group(SG), n=5). After 28 days of treatment animals were euthanized by cervical dislocation. Prior to euthanasia, blood samples were taken to measure liver transaminases (GOT and GPT) and plasma Ca and P levels. Subsequently tissue samples were extracted from the regenerated area for histological processing. Frontal sections of 6 µm thickness were obtained at the level of the middle defect area, which were then colored with H&E. On digital microphotographs of these sections, the following histomorphometric parameters were measured using Image ProPlus program: bone volume [BV/TV(%)] and soft tissue volume [SV/TV(%)]. The results were statistically analyzed by Student t test, setting a p-value <0.05 for significant differences.Results: No significant differences in plasma levels of GOT and GPT were observed between the groups studied (p>0.05). The animals treated with SC showed an increase in P levels (p<0.05). Qualitatively, a more compact and continuous cortical was observed at the base of the bone defect in sections from the SC group. BV/TV(%) was significantly higher in bone defects of SG compared to CG (41.03 +/- 11.76 vs. 18.26 +/- 3.54; p<0.01) while SV/TV(%) was significantly lower in SG compared to CG (28.94 +/- 11.26 vs. 42.47 +/- 5.08; p<0.05). Conclusion: The SC did not generate liver toxicity assessed by the absence of changes in transaminase levels. In addition, the results suggest that SC stimulates the bone regeneration in a calvarial bone defect in rats.

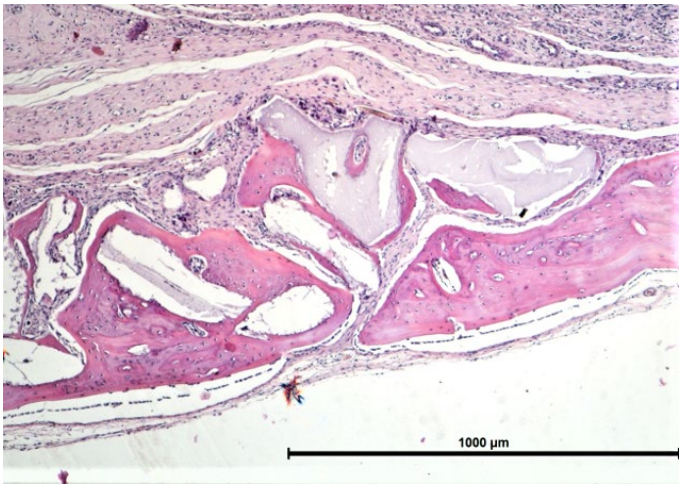

***Disclosures: Esteban Matias Brenna**, None*

P-120

Role of the phytoestrogen Genistein on cellular events involved in bone remodeling: bone-vascular cells crosstalk *Marisa J. Sandoval[1], Adrián E. Campelo[2], Sabrina B. Cepeda[3], Virginia L. Massheimer[4]. [1]Dto Biología, Bioqca y Farmacia, Universidad Nacional del Sur (UNS). Instituto de Ciencias Biológicas y Biomédicas del Sur- Consejo Nacional de Investigaciones Científicas y Técnicas (INBIOSUR-CONICET). Bahía Blanca, Buenos Aires, Argentina, Argentina, [2]Instituto de Ciencias Biológicas y Biomédicas del Sur (INBIOSUR), Dto de Matemática-Universidad Nacional del Sur (UNS). Consejo Nacional de Investigaciones Científicas y Técnicas (CONICET), Bahía Blanca, Buenos Aires, Argentina, Argentina, [3]Dto. Biología, Bioquímica y Farmacia, Universidad Nacional del Sur (UNS). Bahía Blanca, Buenos Aires, Argentina, Argentina, [4]Instituto de Ciencias Biológicas y Biomédicas del Sur (INBIOSUR), Dto Biología, Bioqca y Farmacia-Universidad Nacional del Sur (UNS). Consejo Nacional de Investigaciones Científicas y Técnicas (CONICET), Bahía Blanca, Buenos Aires, Argentina, Argentina

Phytoestrogens (PE) as Genistein (Gen) are proposed as natural therapy for bone loss prevention. We studied the mechanism of action of Gen on osteoblast (OB) differentiation; and on bone-vascular cells interactions with focus on angiogenesis. Aortic rings (AR, ex vivo assays) or murine primary cell cultures (in vitro assays) of aortic endothelial cells (EC) or calvarial OB exposed to 10 nM Gen were employed as experimental models. Using RT-PCR technique, we found that Gen increased estrogen receptor alpha (ERα) and Runx2 mRNA levels at 3-5 days of culture (2; 20 fold a/c, respectively, $p<0.05$). When OB differentiation markers were evaluated, the evidence shows that Gen enhanced osteocalcin expression (immunofluorescence analysis), alkaline phosphatase activity (ALP, spectrophotometry) and extracellular collagen deposition (Sirius Red staining) after 11 days of culture (34, 40 and 60% a/c, respectively, $p<0.001$). In presence of the high affinity ER antagonist ICI182780 (10 µM) or the NO synthase (NOS) inhibitor L-NAME (10 µM) the enhancements on ALP activity and collagen deposition elicited by Gen were suppressed ($p<0.001$). Cell preincubation with the ERK inhibitor PD98059 (10 µM) or the PI3K signaling pathway antagonist LY294002 (10 µM), completely blunted the enhancement of collagen deposition produced by Gen treatment ($p<0.001$), meanwhile the antagonists partially reduced the stimulation triggered by the PE on ALP activity (70 vs 36%; absence vs presence of the blockers). Since vascularization and microcirculation are events required for bone remodeling, we tested whether Gen could exert an angiogenic action via an interaction between OB and EC. New capillaries formation depends on EC proliferation and migration. Experiments using conditioned medium (CM) obtained from OB exposed 24 h to Gen (CMGen) were performed. The presence of CMGen increased EC proliferation and migration (1.4 and 2.5 fold, respectively, $p<0.05$). Then, new tubes formation around AR seeded on a collagen matrix (15 days) were evaluated using optical microscopy and ImageJ software quantification. The stimulation of capillaries formation exerted by Gen was significantly potentiated in presence of CMGen (95%, $p<0.05$). In conclusion, Gen promoted osteoblastogenesis through the participation of ER and NOS pathways, and the contribution of ERK or PI3K signal transduction pathways. Indeed, Gen stimulated angiogenesis through a crosstalk between bone and vascular cells.

***Disclosures: Marisa J. Sandoval**, None*

P-121

The Changing Partners of FOXO1 Under High Serotonin Levels in Winnie Mouse Model of Spontaneous Chronic Colitis *Shilpa Sharma[1], Ahmed Al Saedi[1], Kulmira Nurgali[2], Gustavo Duque[1]. [1]Australian Institute for Musculoskeletal Science, The University of Melbourne and Western Health, Melbourne, Australia. Department of Medicine-Western Health, The University of Melbourne, Melbourne, Australia, Australia, [2]Institute for Health and Sport, Victoria University, Melbourne, Australia, Australia

The most common extraintestinal manifestations of inflammatory bowel disease (IBD) are skeletal dysfunctions. It is likely that risk factors are multifactorial, such as systemic inflammation, malnutrition and use of glucocorticoids. Notwithstanding, large gaps remain in our knowledge of mechanisms underlying bone loss in IBD. The consistent feature of colitis is increased gut-derived serotonin (GDS) availability in the intestinal mucosa, which could have a negative impact on osteoblastogenesis in this model. We tested the hypothesis that GDS plays an important role in the pathogenesis of bone loss in IBD. Using Winnie mouse model of spontaneous chronic colitis, closely representing human IBD, we showed for the first time that elevated GDS cross talks with molecular pathways involved in bone formation. Winnie male mice prior to onset of colitis (6 weeks old (6wk)) and progression of colitis (14wk) were compared to age- and sex- matched control C57BL/6 mice. High levels of peripheral GDS at 14wk in Winnie male mice bind to serotonin receptors (5-HTR1B) on bone marrow-derived mesenchymal stem cells (BM-MSCs) to regulate transcriptional activity of FOXO1. This was evidenced by increased mRNA expression of 5-HTR1B and FOXO1 from BM-MSCs of 14wk Winnie male mice compared to 14wk male controls as determined by qPCR. To elucidate downstream molecular mediators of GDS in bone, immunohistochemical analysis unveiled dissociation of FOXO1 and CREB1 complex at 14wk in Winnie male mice. This relieves the suppressive effect of CREB on FOXO1, resulting in decreased osteoblast proliferation as compared to strong association of CREB and FOXO1 in control group. Additionally, FOXO1 (CREB-free) association with ATF4 was observed in 14wk Winnie male mice, in which ATF4 promotes the transcriptional activity of FOXO1, contributing to suppression of osteoblast proliferation (Figure 1). In contrast, 6wk Winnie male mice showed no significant change in association/ dissociation of complexes with FOXO1 compared to 6wk male controls. This is agreeable to similar 5-HTR1B expression levels in 6wk Winnie male mice and age-matched male controls. These findings identify FOXO1 as the molecular node of an intricate transcriptional machinery that confers the signaling of high GDS levels to inhibit bone formation. Further exploration of the mechanisms explaining this skeletal phenotype is warranted.

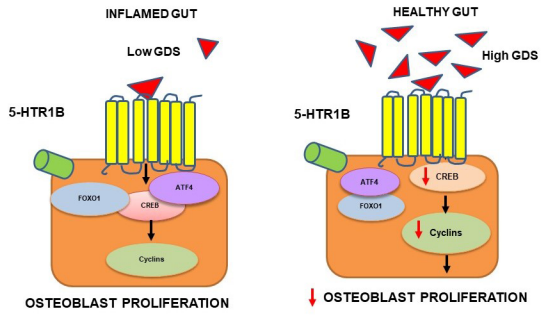

Figure 1. Mechanism of GDS mediated bone loss in *Winnie* mice model of colitis

***Disclosures: Shilpa Sharma**, None*

P-122

Pathogenic role of fibroblast like synoviocyte in the particle induced periprosthetic osteolysis *Supriya Jagga[1], Yeon-Hee Lee[1], Ju-Suk Nam[1], Sang-Soo Lee[1], Ashish Ranjan Sharma[1]. [1]Hallym University, Republic of Korea

Pathogenic role of fibroblast like synoviocyte in the particle induced periprosthetic osteolysis Ashish Ranjan Sharma, Supriya Jagga, Yeon-Hee Lee, Ju-Suk Nam, Sang-Soo LeeInstitute for Skeletal Aging/Orthopedic Surgery, Hallym University-Chuncheon Sacred Heart Hospital, Chuncheon, South KoreaINTRODUCTION Wear debris from prosthetics often leads to failure of implants by causing periprosthetic osteolysis. Under inflammatory conditions, fibroblast-like synoviocytes (FLS) displays pathogenic behavior by releasing a number of pro-inflammatory cytokines and are crucial for the pathogenesis. Henceforth, the purpose of this study was to investigate the effect of Ti particles on FLS and the mechanism by which it might participate in the process of periprosthetic osteolysis. METHODS1) Sterilized Ti particles (1~3 µm). 2) For viability assessment, MTT and LDH assays were performed. 3) mRNA expression levels were analyzed by real-time RT-PCR. 4) TRAP staining was performed for osteoclastogenesis. 5) Alkaline phosphatase activity (ALP), mineralization, and collagen synthesis were analyzed to study changes in osteogenic activity. 6) For WNT and BMP signaling, Axin-2 and BRE reporter construct was utilized. 7) Western blot was performed to detect the activation of signaling molecules. RESULTS1. 1:400 (cells to Ti particles) to human FLS increased the expression of COX-2 and pro-inflammatory cytokines.2. Conditioned medium (CM) collected from Ti stimulated FLS induced osteoclastogenesis in RAW 264.7 cells.3. Ti CM suppressed osteogenic parameters as well as WNT and BMP signaling activity in osteoblasts.4. Ti particles induced the mRNA expression of various antagonists to the WNT and BMP signaling pathways in FLS.5. Inhibition of Sclerostin (SOST) partially recovered the Ti CM suppressed osteogenic activity in osteoblasts. CONCLUSIONFLS might contribute toward the bone loss as observed during periprosthetic osteolysis by not only stimulating osteoclastogenesis but also by suppressing bone-forming ability of osteoblasts. Secretion of antagonists for WNT and BMP signaling pathways like SOST might be helpful in understanding the participatory role of FLS in wear debris induced osteolysis. In the clinical setting, targeting FLS for the secretion of antagonists like SOST might be a novel therapeutic approach for preventing bone loss during periprosthetic osteolysis.Keywords: Periprosthetic osteolysis, Wear debris, Biomaterials, Fibroblast-like synoviocytes, osteoblasts, Osteoclasts Acknowledgments This research was supported by Hallym university research Fund and by a grant from the National Research Foundation of Korea (NRF-2017R1A2B4012944 & NRF-2020R1C1C1008694) funded by the Ministry of Education, Science and Technology.

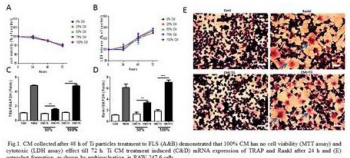

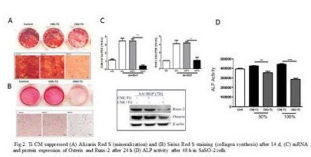

Posters

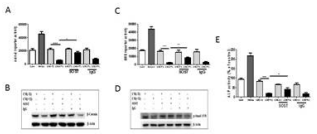

Fig 3. Neutralization of SOST in Ti CM partially restores the suppressed (A&B) WNT and (B&C) BMP signaling and (E) ALP activity.

***Disclosures: Supriya Jagga**, None*

P-123

LECT2 mediates the interaction between liver and bone by inhibiting osteoclastogenesis *Seong Hee Ahn[1], JinMi Park[1], Cho-Rong Kim[1], Seongha Seo[1], Da Hea Seo[1], Yongin Cho[1], So Hun Kim[1], Seongbin Hong[1]. [1]Department of Endocrinology and Metabolism, Inha University Hospital, Inha University School of Medicine, Republic of Korea

Objective: Although several clinical data suggested the deterioration of bone metabolism in patients with chronic liver diseases, the direct interaction between liver and bone has been rarely demonstrated in vitro. We investigated the effects of hepatocyte-conditioned medium (HepG2-CM), which probably contains secreted proteins from hepatocyte, and leukocyte cell-derived chemotaxin 2 (LECT2), a known hepatokine, on osteoclasts.Methods: The conditioned medium from HepG2 cell line was collected after 48 hours of culture without fetal bovine serum. Osteoclasts were differentiated from mouse bone marrow macrophages (BMMs). HepG2-CM and LECT2 were treated on BMMs with M-CSF and RANKL. Tartrate resistant acid phosphatase-positive multinucleated cells were considered as osteoclasts, and the resorption area was determined by incubating the cells on dentine discs. Signaling pathways were investigated using qRT-PCR and western blot.Results: HepG2-CM inhibited both osteoclastogenesis and in vitro bone resorption without any significant effect on the viability of preosteoclasts. LECT2 also inhibited both osteoclastogenesis and in vitro bone resorption without any significant effect on the viability of preosteoclasts. Consistently, the expressions of osteoclast differentiation markers were significantly decreased by LECT2. Western blot analyses suggested that LECT2 inhibits p38 signaling pathways in osteoclasts. Conclusion: LECT2 is a candidate hepatokine that connects liver and bone by inhibiting osteoclastogenesis.

***Disclosures: Seong Hee Ahn**, None*

P-124

Identify the role of osteopontin in Shn3/SLIT3 pathway of osteoblasts-type H endothelial cells coupling *Jia-Fwu Shyu[1], Cheng-Yuan Hsiao[1], Tzu-Hui Chu[1], Ting-Han Taso[1], Yu-Chih Lo[1]. [1]Department of Biology and Anatomy, National Defense Medical Center, Taiwan, Province of China

Recent studies have highlighted roles for blood vessels during bone remodeling and fracture healing. Type H endothelial cells (ECs) express high level of junctional protein CD31 and endomucin. ECs are emerging as a crucial source of signals that control bone remodeling, thereby allowing the coupling of angiogenesis and osteogenesis during both development and regeneration. Schnurri-3 (SHN3) knocked out mice have unexpectedly identified increased bone mass due to augmented osteoblast function. Transcriptomic analysis of osteoblast-lineage specific Shn3 deletion mice have identified the axon-guidance cue SLIT3 as a proangiogenic factor whose expression in bone is restricted to osteoblasts and is negatively regulated by SHN3. Osteopontin (OPN), produced by osteoblasts, is one of the most abundant non-collagenous proteins in extracellular matrix. OPN is an acidic phosphorylated glycoprotein, which belongs to the protein family of "Small Integrin-Binding Ligand N-linked Glycoproteins" (SIBLINGs) and plays a decisive role in the biology of bone mineralization and angiogenesis. Taken together, SHN3/SLIT3 and OPN are emerging novel bone anabolic molecules targeting type H ECs. In this study, we set up osteoblast/HUVEC transwell co-culture system to examine the angiogenic effects induced by SHN3/SLIT3 and OPN. The angiogenesis was measured by tube formation by HUVEC in Matrigel (bottom well). The osteoblasts (upper well) were pre-cultured in osteogenesis medium (containing b-glycerophosphate and ascorbate) with or without PTH for one week. Increase tube formation was observed in HUVECs co-cultured with osteoblasts in osteogenesis medium without PTH. Elisa analysis showed increase expression of osteopontin but decrease expression of SLIT3 in PTH-stimulated osteoblast culture medium. In addition, immunofluorescent labeling and Western blot analysis showed increase expression of CD31 and endomucin in SLIT3- and OPN-stimulated HUVECs. In conclusion, these results may provide in-depth understanding of the osteo-angio coupling and safe and more effective treatment for osteoporosis and fracture healing.

***Disclosures: Jia-Fwu Shyu**, None*

P-125

Inhibition of PAD4 Mediated Neutrophil Extracellular Traps Prevents Fibrotic Osseointegration Failure in a Murine Model of Tibial Implantation *Emile-Victor Kuyl[1], Fei Shu[1], Branden Sosa[1], Matthew B Greenblatt[2], Mathias PG Bostrom[1], Xu Yang[1]. [1]Hospital for Special Surgery, United States, [2]Weill Cornell Medicine, United States

Purpose: The formation of peptidyl arginine deiminase (PAD4) mediated neutrophil extracellular traps (NETs) are a recently discovered defense mechanism that responds to sterile triggers with detrimental effects in tissue healing. Patients with aseptic loosening, a cause of failure in uncemented total joint arthroplasty (TJA), often present with fibrotic tissue at the bone-implant interface. In this study, we explore the role of NETs in peri-implant fibrosis and osseointegration failure through a murine model of tibial implant with instability. Methods: A 3D printed Ti-6Al-4V implant was inserted in an oversized drill-hole in the right proximal tibia of 8-week-old male C57BL/6J and PAD4-/- mice (n=3 per group). Fourteen days post-implantation, all mice were euthanized, and tibias were dissected and analyzed for the presentation of fibrosis at the bone-implant interface. Trabeculae were assessed by micro-computed tomography (microCT), hematoxylin and eosin staining and immunofluorescence for extracellular DNA, citrullinated histones (CitH3) and myeloperoxidase (MPO). Peri-implant membrane was retrieved from patients undergoing total hip revision surgery for aseptic loosening and analyzed for the presence of NETs. Results: NETs (MPO+CitH3+ with extracellular DNA) were present in the peri-implant area only and not in other neutrophil populations (MPO+citH3-) of the bone marrow (Figure 1a). NETs were identified in peri-implant fibrotic tissue collected from aseptic loosening patients (Figure 1b). Unstable implants in wild type mice failed to properly osseointegrate, as indicated by the presence of fibroblast-like cells and immature bone matrix in the peri-implant area (Figure 1c)and low bone volume fraction (BV/TV) and bone surface area (BS) around the implant (Figure 1e). In PAD4-/- mice, we observed well-formed trabeculae, few fibroblast cells (Figure 1d), higher peri-implant BV/TV and BS (Figure 1f). These indicate better osseointegration in these mice.Discussion: NETs have been characterized in human peri-implant fibrotic tissue and have been identified at early time points in a murine model of unstable tibial implantation, indicating a possible damage induced activation. The lack of peri-implant fibrosis through inhibition of NETs via PAD4 deficiency in mice indicates that NETs play a role in osseointegration failure, leading the way for potential therapeutic targets in treating fibrotic osseointegration failure and aseptic loosening.

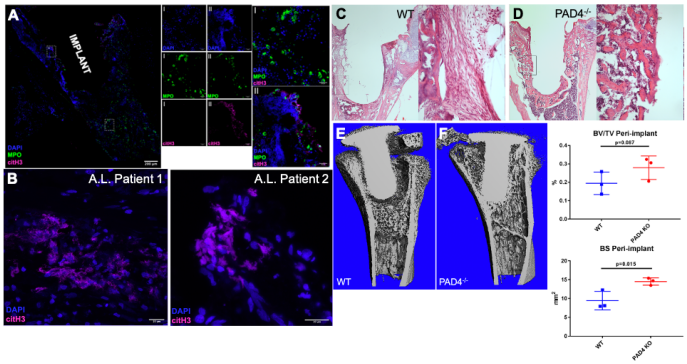

Figure 1. Immunofluorescence indicates NETs are isolated to the peri-implant area at day only, indicating a damage-associated response (*A*). NETs are also present in the intramedullary fibrotic membrane of two aseptic loosening (A.L.) revision surgery patients (*B*). In unstable implant conditions, wildtype mice exhibit extensive fibroblast-like cells around the implant area (*C*), while inhibition of PAD4 mediated NETs promotes enhanced osseointegration as indicated by well-formed and mature peri-implant trabeculae and lack of fibroblast-like cells (*D*). Inhibition of PAD4 mediated NETs enhances peri-implant bone volume (BV/TV, $p<0.10$) and trabeculae bone surface area (BS, $p<0.05$) in conditions of unstable tibial implantation (*E,F*).

***Disclosures: Emile-Victor Kuyl**, None*

P-126

Deletion of Transferrin Receptor 2 (Tfr2) Aggravates Inflammation and Bone Loss in Serum Transfer Arthritis in Mice *Maria G. Ledesma-Colunga[1], Ulrike Baschant[1], Lorenz C. Hofbauer[1], Martina Rauner[1]. [1]Department of Medicine III & Center for Healthy Aging, Technische Universität Dresden, Dresden, Germany, Germany

Rheumatoid arthritis is an autoimmune disease characterized by chronic inflammation and progressive joint destruction with frequent synovial iron deposition. Transferrin receptor 2 (Tfr2) is a focal point in the regulation of systemic iron levels and bone mass. Loss of Tfr2 functions results in low hepcidin expression and iron overload. As neither the role of iron nor Tfr2 has been explored in arthritis, here, we aimed to investigate whether Tfr2 deletion and/or iron overload impacts on the pathogenesis of inflammatory arthritis.We compared iron overloaded Tfr2-deficient mice (Tfr2-/-), and their wild-type (Tfr2+/+) littermate controls for their capacity to develop K/BxN serum transfer arthritis (STA). Arthritis severity was assessed by clinical scores and hind paws were collected for micro-CT, histomorphometry, quantitative PCR, and flow cytometry.Tfr2-/- mice developed more pronounced joint

swelling with enhanced mRNA expression of inflammatory markers (Il1b, Inos), synovial hypertrophy, and bone erosion as compared to Tfr2+/+ mice. Furthermore, the infiltration of myeloid cells including GR1pos neutrophils and F4/80pos macrophages/monocytes at day 7 was increased in the joints of Tfr2-/- mice, suggesting a role of Tfr2 and/or iron overload in arthritis progression. To elucidate whether Tfr2 has a direct role in the pathogenesis of arthritis or whether the effects are merely mediated via the systemic iron overload, we induced STA in mice with a conditional deletion of Tfr2 in the myeloid lineage, that have been previously described with normal iron loading. Tfr2fl/fl-LysMCre+ showed increased disease development with enhanced synovial hypertrophy and bone erosion in the arthritic joints compared to Cre- control littermates.Taken together, these findings suggest a protective role of endogenous Tfr2 on the progression of arthritis.

***Disclosures: Maria G. Ledesma-Colunga**, None*

P-127

Erythropoietin receptor in B cells plays a role in bone remodeling in mice *Naamit Deshet-Unger[1], Albert Kolomansky[1], Nathalie Ben-Califa[1], Sahar Hiram-Bab[2], Dafna Gilboa[1], Tamar Liron[2], Maria Ibrahim[1], Zamzam Awida[1], Anton Gorodov[1], Howard S. Oster[3], Moshe Mittelman[3], Martina Rauner[4], Ben Wielockx[5], Drorit Neumann[1], Yankel Gabet[2]. [1]Department of Cell and Developmental Biology, Sackler Faculty of Medicine, Israel, [2]Department of Anatomy and Anthropology, Sackler Faculty of Medicine, Tel Aviv University, Israel, [3]Department of Medicine A, Tel Aviv Sourasky Medical Center, Sackler Faculty of Medicine, Tel Aviv University, Israel, [4]Department of Medicine III, Dresden University Medical Center, Germany, [5]Institute for Clinical Chemistry and Laboratory Medicine, Technische Universität Dresden, Germany

Erythropoietin (EPO) is a key regulator of erythropoiesis. However, EPO receptors (EPO-Rs) are also expressed on non-erythroid cell types, including myeloid and bone cells. Immune cells also participate in bone homeostasis. B cells produce receptor activator of nuclear factor kappa-B ligand (RANKL) and osteoprotegerin (OPG), two pivotal regulators of bone metabolism. Here we explored the ability of B cells to transdifferentiate into functional osteoclasts and examined the role of EPO in this process in a murine model. Methods: We have combined specifically-designed experimental mouse models and in vitro based osteoclastogenesis assays, as well as PCR analysis of gene expression.Results: (i) EPO treatment in vivo increases RANKL expression in bone marrow (BM) B cells, suggesting a paracrine effect on osteoclastogenesis; (ii) B cell-derived osteoclastogenesis occurs in vivo and in vitro, as demonstrated histologically by B cell lineage tracing in murine models, respectively; (iii) B-cell-derived osteoclastogenesis in vitro is restricted to Pro-B cells expressing CD115/CSF1-R and is enhanced by EPO; (iv) EPO treatment increased the number of B-cell-derived preosteoclasts (β3+CD115+), suggesting a physiological rationale for B cell derived osteoclastogenesis; (v) finally, mice with conditional EPO-R knockdown in the B cell lineage (cKD) displayed a higher cortical and trabecular bone mass. Moreover, cKD attenuated EPO-driven trabecular bone loss, an effect that was observed despite the fact that cKD mice attained higher hemoglobin levels following EPO treatment.Conclusions: Our work highlights B cells as an important extra-erythropoietic target of EPO-EPO-R signaling and suggests their involvement in the regulation of bone homeostasis and possibly in EPO-stimulated erythropoietic response. Importantly, we present here the first histological evidence for B cell-derived osteoclastogenesis in vivo.

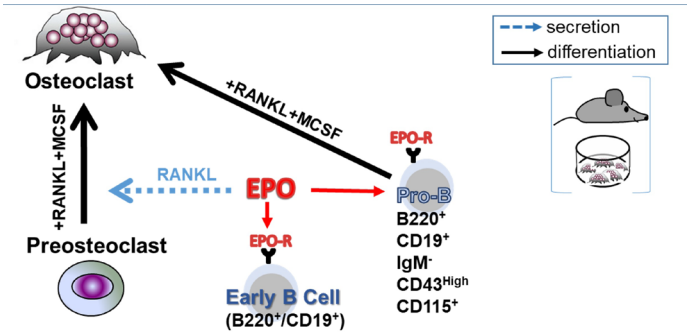

***Disclosures: Naamit Deshet-Unger**, None*

P-128

Assessing the host inflammatory response to a novel 3D-printed hydroxyapatite (HA) and demineralized bone matrix (DBM) composite using a rodent posterolateral spinal fusion model *Mark Plantz[1], Joseph Lyons[1], Allison Wintring[1], Elianna Fred[1], Eileen Phan[1], James Foley[1], Chawon Yun[1], Silvia Minardi[1], Soyeon Jeong[1], Stuart Stock[1], Wellington Hsu[2], Erin Hsu[1]. [1]Northwestern University Feinberg School of Medicine, United States, [2]Wellington.Hsu@nm.org, United States

A wide range of biologic bone graft materials have been assessed for spinal fusion applications. However, the two options that remain the most effective – iliac crest bone graft and recombinant human bone morphogenetic protein-2 (rhBMP-2) – are limited by morbidity and complications, respectively. We recently described a recombinant growth factor-free, 3D-printed composite material comprised of hydroxyapatite (HA) and demineralized bone matrix (DBM) as a potential bone graft substitute. Herein, we compare the host inflammatory response of our previously described 3D-printed hydroxyapatite (HA)-demineralized bone matrix (DBM) composite scaffold to a positive control (rhBMP-2/ACS; Infuse™) using a preclinical rodent posterolateral lumbar fusion (PLF) model. Sixty female Sprague-Dawley rats, aged 12-16 weeks, underwent bilateral posterolateral intertransverse lumbar spinal fusion using 1 of 3 adjuncts: (1) type I absorbable collagen sponge (ACS) alone (n=20), (2) 10 μg rhBMP-2/ACS (n=20), or (3) HA-DBM composite scaffold (HA-DBM) (n=20). The host inflammatory response was assessed at 2, 5, and 10 days post-operatively using magnetic resonance imaging (MRI) to quantify local edema and cytokine analysis (ELISA) of various pro-inflammatory markers – IL-1β, IL-18, TNF-α, MCP-1, MIP-1 – to quantify and compare the inflammatory response between the different treatment groups. At days 2 and 5 post-operatively, the HA-DBM scaffold yielded significantly less soft tissue edema relative to rhBMP-2 ($p<0.05$). Additionally, the HA-DBM scaffold yielded comparable volumes of soft tissue edema to the ACS control at all the time points in the post-operative period. The concentrations of various cytokines – IL-18, TNF-α, MCP-1 – were significantly elevated in the rhBMP-2 group relative to the ACS control in the peri-operative period ($p<0.05$). This elevation in cytokine markers was not observed for the HA-DBM group relative to the ACS control. In summary, the 3D-printed HA-DBM composite has a favorable host response that is comparable to that of an absorbable collagen sponge, when assessed preclinically. The minimal inflammatory response elicited by this material provides a notable advantage relative to recombinant growth-factor containing materials (e.g. rhBMP-2).

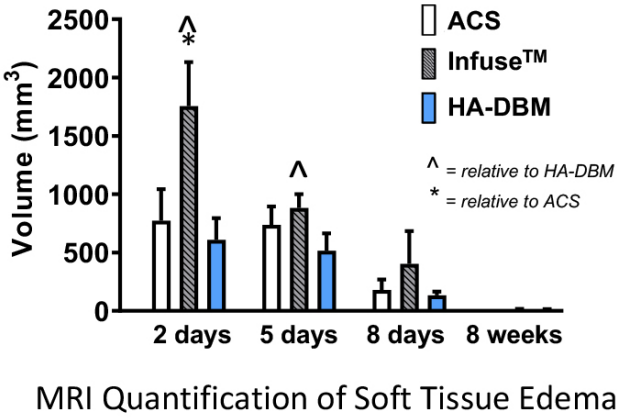

***Disclosures: Mark Plantz**, None*

P-129

Osteal Macrophage Contributions to Post-Menopausal Osteoporosis Bone Pathology *Lena Batoon[1], Susan Millard[1], Andy Wu[1], Wenhao Sun[1], Simranpreet Kaur[2], Martin Wullschleger[3], Liza Raggatt[1], Nathan Pavlos[4], Allison Pettit[1]. [1]Mater Research Institute-The University of Queensland, Australia, [2]The University of Queensland Diamantina Institute, Australia, [3]Gold Coast University Hospital, Australia, [4]University of Western Australia, Australia

Osteal macrophages (osteomacs) support osteoblast function and promote bone anabolism, but their contributions to osteoporosis have not been explored. While mouse ovariectomy (OVX) models have been repeatedly used, spontaneous osteoporosis in female C57Bl/6 mice limits utility of this strain and there are no comprehensive studies confirming OVX recapitulated all pathological features of osteoporosis in other mouse strains. We characterized OVX model of post-menopausal osteoporosis in C3H/HeJ mice. OVX caused reduced trabecular bone volume (-46%), thickness (-21%) and number (-23%) as well as reduced cortical thickness (-8%) with increased cortical porosity (17.5%) at 4-weeks post-surgery. High resolution micro-CT revealed enlargement of cortical vascular canals post-OVX. Bone loss was associated with increased osteoclasts on trabecular ($p<0.0001$) and endocortical bone ($p<0.0016$), and decreased osteoblasts on trabecular bone ($p<0.0001$). While there was no impact on overall osteocyte number, the TRAP-expressing osteocyte frequency was increased in cortical bone ($p=0.0005$) which is suggestive of osteocytic osteolysis, especially

when considered in the context of the increased cortical porosity. Unexpectedly, osteomac frequency was increased on both trabecular (p<0.0001) and endocortical bone (p<0.0001) post-OVX. Dual F4/80 (pan-macrophage marker) and TRAP staining revealed osteomacs frequently located in close proximity to TRAP+ osteoclasts and containing TRAP+ intracellular vesicles, suggesting osteomac-mediated phagocytosis of extracellular TRAP at resorption sites. Using an in vivo inducible macrophage depletion model (CD169-DTR mouse), that does not simultaneously deplete osteoclasts, we observed that osteomac loss was associated with elevated serum TRAP (p=0.0017). Using in vitro high-resolution confocal imaging of mixed osteoclast-macrophage cultures on bone substrate, we observed macrophages juxtaposed to osteoclast basolateral functional secretory domains scavenging degraded osteoclast by-products. These data demonstrate a role for osteomacs in supporting bone resorption through sequestering resorption byproducts. Overall, our data expose a novel role for osteomacs in supporting osteoclast function and provide the first evidence of their involvement in osteoporosis bone pathology.

***Disclosures: Lena Batoon**, None*

P-130

Commensal Oral Microbiota Induces Osteoimmune Response Effects that are Separate from the Systemic Microbiota *Jessica Hathaway-Schrader[1], Johannes Aartun[1], Nicole Poulides[1], Megan Kuhn[1], Blakely Graham[1], Michael Chew[1], Emily Huang[1], Richard Darveau[2], Caroline Westwater[1], Chad Novince[1]. [1]Medical University of South Carolina, United States, [2]University of Washington, United States

The commensal microbiota is a critical regulator of osteoimmune mechanisms in the healthy skeleton. Yet, the influence of specific commensal microbiota communities (i.e. oral, gut, lung, skin, urogenital) on osteoimmune response effects is unknown. Study purpose was to discern osteoimmunoregulatory effects imparted by the commensal oral microbiota that are separate from the systemic microbiota. Study outcomes were assessed at both oral and non-oral skeletal sites in 12wko male C57BL/6T mice bred under specific-pathogen-free (SPF) or germfree (GF) conditions. Trabecular/cortical bone parameters were evaluated by µCT, and histomorphometric analyses were performed in maxillae and tibiae. Flow cytometry and nCounter gene expression were carried out in mandibular bone marrow and long bone marrow. SPF vs. GF mice had reduced cortical and trabecular parameters in alveolar bone, while only trabecular bone outcomes were decreased at non-oral skeletal sites. Osteoclast numbers and size were enhanced lining alveolar bone, whereas only osteoclast size was increased lining non-oral skeletal sites, of SPF vs. GF mice. Consistent with the enhanced pro-osteoclastic phenotype, SPF mice had upregulated Nfatc1 and Rank in alveolar bone marrow, but not long bone marrow. Toll-like receptor(TLR) and MHC class-II antigen presentation pathways were upregulated in alveolar bone marrow, but not long bone marrow, of SPF vs. GF mice. These results were supported by elevated antigen-presenting cells, activated CD4+ helper T-cells, and proinflammatory TH1 and TH17 cells in alveolar bone marrow, but not long bone marrow, of SPF vs. GF mice. To validate the commensal oral microbiota has osteoimmunomodulatory effects distinct from the systemic microbiota, SPF mice were subjected to twice daily 0.12% chlorhexidine (CHX) oral antiseptic rinses from age 8-12wks. 16S rDNA analysis showed a 50% reduction in oral bacterial load, with no alterations in gut bacterial load, in CHX vs. saline treated mice. µCT revealed inferior alveolar bone parameters in saline vs. CHX treated mice. Paralleling outcomes in SPF vs. GF mice, TLR and MHC class-II pathways were increased in alveolar bone marrow of saline vs. CHX treated mice. This research delineates that the commensal oral microbiota has osteoimmunomodulatory actions separate from the systemic microbiota. Findings from this study reveal that oral antiseptic rinses may be employed to protect against commensal oral microbiota driven alveolar bone loss.

***Disclosures: Jessica Hathaway-Schrader**, None*

P-131

Shedding "LIGHT" on the link between bone and fat in obesity in obese children and adolescents *Giacomina Brunetti[1], Maria Felicia Faienza[2], Laura Piacente[2], Giuseppina Storlino[3], Gabriele D'Amato[4], Gianpaolo De Filippo[5], Silvia Colucci[1], Maria Grano[3]. [1]Department of Basic and Medical Sciences, Neurosciences and Sense Organs, Section of Human Anatomy and Histology, University of Bari, Italy, [2]Department of Biomedical Science and Human Oncology, Paediatric Unit, University of Bari, Italy, [3]Department of Emergency and Organ Transplantation, Section of Human Anatomy and Histology, University of Bari, Italy, [4]Neonatal Intensive Care Unit, Di Venere Hospital, Italy, [5]Assistance Publique-Hôpitaux de Paris, Hôpital Robert Debré, Service d Endocrinologie Diabétologie Pédiatrique, France

Obesity may affect bone health, but literature reports are contradictory about the correlation of body mass index (BMI) and bone markers. LIGHT, one of the immunostimulatory cytokines regulating the homeostasis of bone and adipose tissue, could be involved in obesity. Our objective was the evaluation of LIGHT/TNFSF14 levels in obese children and adolescents and the influence of different grades of obesity on bone status. The human study involved 111 obese subjects (12.21 +/- 3.71 years), and 45 age and sex-matched controls. Patients were subjected to the evaluation of bone status by QUS, showing that the averages of Ad-SoS-Z-score and BTT Z-score were within the normal range but significantly reduced respect to the controls (p<0.05). 25(OH) Vitamin D levels were reduced compared to the controls, but the difference did not reach the statistical significance. Obese patients showed significant high BMI-SDS, weight-SDS, and HOMA-IR that negatively correlated with the reduced AD-SoS-Z-score and BTT-Z-score. They also displayed significantly higher serum levels of LIGHT compared with healthy controls (497.30 +/- 363.45 pg/ml vs 186.06 +/- 101.41 pg/ml, p<0.001). LIGHT levels positively correlated with age (r= 0.29, p<0.03), Tanner stage (r= 0.207, p<0.05), weight-SDS (r= 0.448, p<0.0001), BMI-SDS (r= 0.416, p<0.0002), conversely a negative correlation with 25 (OH) Vitamin D (r= -0.173, p<0.0001), and osteocalcin (r= -0.232, p<0.0001), Ad-Sos-Z-score (r= -0.445, p<0.02) and BTT-Z-score (r= -0.341, p<0.05) was found. The expression of LIGHT on monocytes, CD3+-T-cells, and neutrophils, was also higher in obese patients than in the controls. Furthermore, in vitro experiments carried out on peripheral blood mononuclear cell (PBMCs) cultures, demonstrated that the addition of anti-LIGHT antibodies induced a significant inhibition of osteoclastogenesis. With adjustment for age multiple linear regression analysis for LIGHT as dependent variable showed that Tanner stage, weight-SDS, BMI-SDS, cholesterol, 25 (OH) Vitamin D, Osteocalcin, AD-SoS-Z-score, and BTT-Z-score are the most important predictors (r = 0.768, p<0.0001).In conclusion, our study highlighted the elevated serum levels of LIGHT in obese children and adolescents, and its relationship with both the grade of obesity and bone impairment. Our results also emphasized the key role of the immune system in the cross-talk between bone and fat in obesity.

***Disclosures: Giacomina Brunetti**, None*

P-132

The Role of Toll-like Receptors 2 and 9 in Host Responses to Staphylococcus aureus Osteomyelitis *Jenna Petronglo[1], Nicole Putnam [1], Caleb Ford[2], Jacob Curry[3], Jim Cassat[4]. [1]Vanderbilt University, United States, [2]Vanderbilt University Department of Biomedical Engineering, United States, [3]Vanderbilt University Medical Center, United States, [4]Vanderbilt University Medical Center Department of Pediatric Infectious Diseases, United States

Staphylococcus aureus is the most common etiologic agent of bone inflammation, or, osteomyelitis (OM). During S. aureus OM, treatment difficulty is compounded by inflammatory processes that dysregulate skeletal homeostasis, altering the differentiation and function of bone-building osteoblasts and bone-resorbing osteoclasts (OCs) to favor bone loss. Toll-like receptor 2 (TLR2), which detects bacterial lipoproteins, and TLR9, which detects bacterial CpG-DNA, have emerged as major pattern recognition receptors responsible for immune cell sensing of S. aureus. Thus, in this study, we sought to determine the role of TLR2 and TLR9 in host immune responses and dysregulation of skeletal homeostasis during S. aureus OM. Using in vitro assays, we discovered that S. aureus-induced osteoclastogenesis proceeds in a TLR2-and TLR9-dependent manner. To evaluate how TLR2 and TLR9 contribute to increased osteoclastogenesis and to dysregulation of bone homeostasis during an in vivo infection, we surgically induced S. aureus OM in Tlr2-/- and Tlr9-/- mice. Despite our previous findings showing that mice deficient in the common TLR adapter protein MyD88 incur increased bacterial dissemination and mortality, we found that TLR2 and TLR9 were individually dispensable for host survival and bacterial control. Moreover, in contrast to our in vitro findings, there were no differences in trabecular OC abundance or bone loss compared to wildtype (WT). We posited that compensation between TLR2 and TLR9 masked the role of TLR2/9 in OM in these studies. To test this, we induced OM in Tlr2/Tlr9-/- mice. We did not observe defects in local bacterial burden control or dissemination in Tlr2/Tlr9-/- mice over an infection time course. However, we did find a significant decrease in reactive, cortical bone formation in Tlr2/Tlr9-/- mice compared to WT, suggesting TLR2/9 may be involved may be involved in changes to osteoclast or osteoblast function in response to S. aureus. We have begun in vitro experiments to further understand how TLR2/9 functions in skeletal cells responding to S. aureus. Overall, our data suggest that redundancy in innate immune responses to S. aureus in bone renders TLR2 and 9 individually expendable for the regulation of skeletal homeostasis and the control of bacterial burdens during OM, but also establish that TLR signaling in the skeletal niche contributes to regulation of bone homeostasis in infection.

***Disclosures: Jenna Petronglo**, None*

P-133

Deletion of von-Hippel Lindau in Dmp1-expressing cells impairs B cell development *Betsabel Chicana[1], Joel Spencer[1], Jennifer Manilay[1]. [1]University of California, Merced, United States

The von-Hippel Lindau protein (VHL) regulates hypoxia-inducible factor degradation in response to low oxygen environments. Osteoblasts (OBs) support B cell development and mature into osteocytes (OCYs). We utilized Dmp1-Cre;Vhl conditional knockout mice (cKO), in which Vhl is deleted in OBs and OCYs. The cKO display dysregulated bone growth, high bone density, smaller bone marrow (BM) cavity volume and cellularity compared to wild-type (WT) mice, and impaired B cell development. B cells produce antibodies, which are crucial for a robust adaptive immune response. Our current objective is to further characterize how the altered cKO bone microenvironment influences B cell development. Using multiparameter flow cytometry, we found that long-term hematopoietic stem cells (HSCs), short-term HSCs, common lymphoid progenitors, multipotent progenitors-2, 3 and 4 and B cell progenitors were increased in % and absolute numbers in the cKO BM. In contrast, later stages of B cell development were decreased. As no splenic Dmp1+ cells

have been described, we were surprised that the % of mature peripheral B cells were also reduced, implying that the altered BM microenvironment in the cKO permanently affected B cells outside of the bone. Our observation of altered B cell development in the BM and in the periphery of lethally irradiated WT→cKO BM chimeras supports the idea that Vhl deletion in Dmp1+ cells results in cell-extrinsic changes that cannot support normal B cell development. We are utilizing Ai9 reporter mice to sort Vhl deficient Dmp1+ cells to test the hypothesis that B cell development is impaired due to reduction of key niche cells and decreased production of IL7, SCF, CXCL12, and Flt3. Furthermore, our preliminary intravital and ex vivo imaging studies of the cKO BM revealed abnormal structure of the marrow cavity, with noticeably increased vascular permeability and the appearance of an increased vessel density. The functional consequences of the cKO microenvironment on B cell proliferation, death and output from the BM are being addressed. In future studies, we will apply our intravital imaging approach to perform longitudinal analyses of B cell development in individual cKO mice to determine how the distinct physical properties in the bone change and affect the progression of B cell defects in cKO bones as a function of time. This information could be applied to future studies of the effects of bone-building drugs on BM niches and immune cell development.

***Disclosures: Betsabel Chicana**, None*

P-134

The central role of TRPM7 kinase in magnesium ion-induced immunomodulation in macrophage during bone healing *Wei Qiao[1], Karen H.M. Wong[1], Yun Wah Lam[2], Kelvin W.K. Yeung[1]. [1]The University of Hong Kong, Hong Kong, [2]City University of Hong Kong, Hong Kong

The use of magnesium ion (Mg2+)-modified biomaterials in bone regeneration is a promising and cost-effective therapeutic. Despite the widespread observation on the osteogenic effects of Mg2+, the diverse roles played by Mg2+ in the complex biological process of bone healing have not been systematically dissected. Here, we reveal a previously unknown biphasic mode of action of Mg2+ in bone repair. In the early inflammation phase, Mg2+ primarily targets the monocyte-macrophage lineage to promote their recruitment, activation, and polarization. We showed that an increase in extracellular Mg2+ contributes to an upregulated expression of transient receptor potential cation channel member 7 (TRPM7) and a TRPM7-dependent influx of Mg2+ in the monocyte-macrophage lineage, resulting in the cleavage and nuclear accumulation of TRPM7-cleaved kinase fragments (M7CKs). This then triggers the phosphorylation of Histone H3 at serine 10, in a TRPM7-dependent manner at the promoters of inflammatory cytokines like IL-8, leading to the formation of a pro-osteogenic immune microenvironment. In the later active repair/remodeling phase of bone healing, however, continued exposure of Mg2+ and IL-8 leads to over activation of NF-κB signaling in macrophages, turning the immune microenvironment into pro-osteoclastogenesis. Moreover, the presence of Mg2+ at this stage also decelerates bone maturation through the suppression of hydroxyapatite precipitation. The negative effects of Mg2+ on osteogenesis can override the initial pro-osteogenic benefits of Mg2+, as we found prolonged delivery of Mg2+ compromises overall bone formation. Taken together, this study establishes a paradigm shift in understanding the diverse and multifaceted roles of Mg2+ in bone healing.

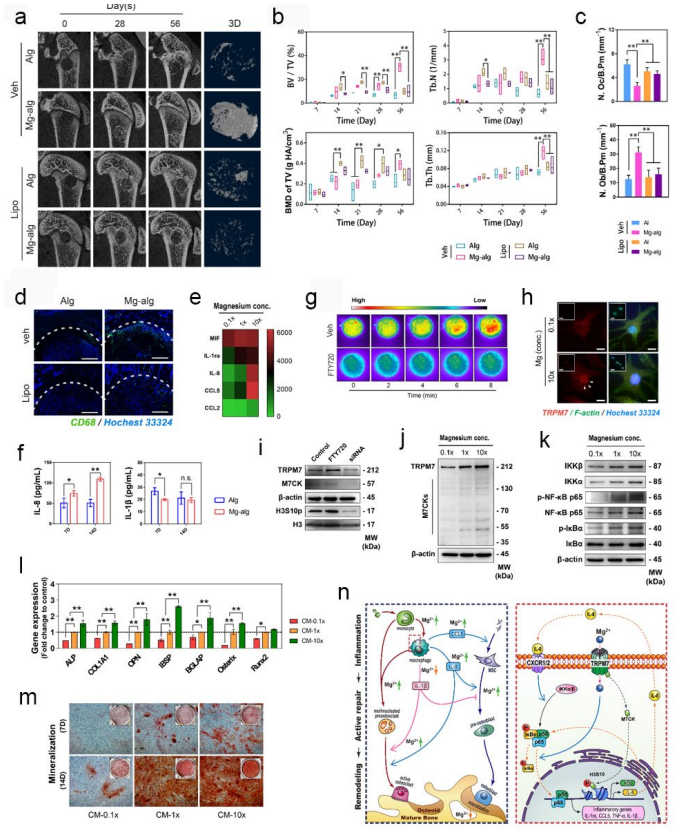

***Disclosures: Wei Qiao**, None*

P-135

Sodium Benzoate (NaB) attenuates osteoporosis and enhances bone health via modulating host osteoimmune system *Rupesh K. Srivastava[1], Leena Sapra[1], Asha Bhardwaj[1], Ayaan Ahmad[1], Zaffar Azam[1]. [1]All India Institute of Medical Sciences (AIIMS), India

Purpose: NaB is predominantly used as a food additive with medicinal properties. NaB is an FDA approved drug for treating urea cycle disorder and kidney disorders. Recent studies reported that administration of NaB enhances Treg cell population by up regulating expression of TGF-β via activating STAT6 transcription factor. But no study till date had delineated the immunomodulatory role of NaB in regulating bone-health in osteoporosis.The present study aims to elucidate the immunomodulatory role of NaB in regulating bone health in osteoporotic mice model.Methods Used: To investigate the same, firstly we performed in vitro cultures of bone marrow derived osteoclasts in the presence of NaB in a dose dependent manner along with examining the underlying molecular mechanism involved in osteoclastogenesis via Western blotting. For in vivo study female BALB/c mice were divided into three group's (n=8 mice/gp) viz. Sham, Ovx and Ovx+NaB. NaB was administered orally (100 mg NaB/kg bw) and after 45 days mice were sacrificed and tissues analyzed for various parameters via various cutting-edge technologies such as SEM, AFM, μCT, FTIR, FACS and CBA/ELISA.Results: Our in vitro results clearly indicated that NaB inhibits osteoclastogenesis in a dose dependent manner by reducing the development of multi-nucleated TRAP positive osteoclasts. NaB ameliorated osteoclastogenesis via suppressing PI3K-Akt-mTOR mediated signaling pathway involved in differentiation of osteoclasts. From in vivo results, we observed that administration of NaB attenuated bone loss in Ovx mice. Both the cortical and trabecular bone content (BMD) and bone heterogeneity of NaB treated group was significantly higher than Ovx group. Remarkably, the percentages of osteoclastogenic progenitors i.e macrophages (F4/80+CD11b+) and osteoclastogenic Th17 (CD4+Rorγt+) cells at distinct immunological sites such as BM, spleen, MLN and PP were significantly reduced ($p < 0.01$). On the contrary the percentages of anti-osteoclastogenic Tregs (CD4+Foxp3+ and CD8+-Foxp3+) and Bregs (CD19+CD5+CD1d+IL-10+) were significantly enhanced ($p < 0.01$) in NaB treated group, thereby attenuating bone loss. The immunomodulatory role of NaB was further supported by serum cytokine data with a significant reduction in osteoclastogenic cytokines (IL-6, IL-17 and TNF-α) along with enhancement in anti-osteoclastogenic cytokines (IL-10, IFN-γ) in NaB treated group.Conclusion: Altogether our present findings for the first time demonstrate that NaB has the potential to inhibit osteoclastogenesis and thereby inhibit bone loss in osteoporotic mice via the modulation of host immune system. The present study thus highlights the novel osteoprotective role NaB (an FDA approved food additive) in the treatment and management of osteoporosis.

***Disclosures: Rupesh K. Srivastava**, None*

Posters

P-136

Dose-dependent Effect of Zolendronic Acido n the Development of Medication-associated Jaw Osteonecrosis (MRONJ) Like-lesion in C57Bl/6 Mice – A Histological Preliminary Study *Nataira Momesso[1], Vinicius Rosa[1], Raquel Parra[1], Ramez Mahmoud[1], Edilson Ervolino[1], Claudia Biguetti[2], Mariza Matsumoto[1]. [1]Department of Basic Sciences, School of Dentistry, São Paulo State University (UNESP), Araçatuba, SP, Brazil, [2]Bone-Muscle Research Center, College of Nursing and Health Innovation, University of Texas at Arlington, Arlington, TX 76019, USA., United States

Medication-related osteonecrosis of the jaw (MRONJ) is a potentially painful condition that affects patients with previous or continuous treatment with antiresorptive or antiangiogenic agents. In this context, the cumulative use of zoledronic acid (ZL) is important duration medication-related risk factors for patients needing tooth extraction. In this preliminary study, we investigated the development of MRONJ-type lesions in C57Bl/6 male mice (ethical committee approval n°00262-2019) at the late time point of socket healing, after continuous and cumulative administration of zoledronic acid (ZL) in two different dosages. Mice at age of 4 to 6 months were divided, receiving intraperitoneal injection of saline solution (SS, control, n=3) or ZL at a concentration of 250ug / Kg (n=3) and 500ug/Kg (n=4), once a week, starting 4 weeks before extraction of the upper right incisor and continuing until day 30 after the surgery. At the end of 30 days, bone samples were collected for histological (H&E and Goldner Trichrome [GT] staining), histomorphometric and immunohistochemical analyzes for bone (RANKL) and inflammatory (COX-2) markers. While control group exhibited the dental socket filled with mature bone, ZL-250 and ZL-500 groups presented a significant and gradual increase in the area density of inflammatory infiltrate dependent of each dosage. Bone matrix area density was significantly lower in ZL-250 and ZL-500 groups, and GT staining revealed a gradual impairment in bone matrix in ZL-250 and ZL-500 groups compared to control (Figure 1). Area density of COX2+ cells, an inflammatory parameter positively related to bone neoformation, was also decreased in both treated groups compared to the control. On the other hand, area densities of fibroblasts, RANKL+ cells, and empty osteocyte lacunae were increased in ZL-250 and ZL-500 groups. Interestingly, the area density of detached osteoclasts, a typical characteristic of ZL effect, was higher in the ZL250 group compared to the SS, while ZL500 group presented a lower density of attached osteoclasts compared to the others. The final outcome of alveolar bone healing was significantly affected in C57BL/6 mice using both dosages used in this study, but with increasing effects on histological MRONJ parameters at the higher dosage.

***Disclosures: Nataira Momesso**, None*

P-137

High-throughput cathelicidin bioassay utilizing HiTCA, a novel CRISPR Cas9-edited human monocytic cell line *Carter Gottlieb[1], Rene Chun[2], Jeffrey Wang[2], Vahe Yacoubian[2], John S Adams[2]. [1]Department of Orthopaedic Surgery, Orthopaedic Hosital Research Center, UCLA, United States, [2]Department of Orthopaedic Surgery, Orthopaedic Hosital Research Center, UCLA, United States

The purpose of this project is to create a novel serum 25-hydroxyvitamin D (25D)-driven bioassay for cathelicidin gene (CAMP) expression in human innate immune cells. Cathelicidins are anti-microbial peptides with potent broad-spectrum activity against bacteria, fungi, and viral pathogens. The human CAMP gene encodes a single anti-microbial peptide, LL-37. CAMP is expressed by innate immune cells such as monocytes and macrophages (mono-macs). Owing to the insertion of a retrotransposon bearing a consensus vitamin D response element in the proximal CAMP promoter, only in humans and higher apes is CAMP expression responsive to vitamin D and limited by the 25D-deficient state of the host.Our lab has previously developed a CAMP expression bioassay whereby plastic-adherent, primary cultures of single donor monocyte-macrophages (mono-macs) are conditioned with heterologous donor serum before measuring CAMP expression by qPCR. Based on the concentration of 25D in the conditioning serum, this assay has proved valuable for measuring the ability of donor serum to alter ex vivo CAMP expression in mono-macs. However, the assay suffers from (1) donor variability, requiring a different mono-mac donor in each experiment, (2) low throughput, and (3) contamination with a small number of neutrophils or other CAMP-expressing plastic-adherent cells. We circumvented these problems by creating a CRISPR-Cas9-directed knock-in of a cDNA containing the mCherry fluorescent reporter at the C-terminal end of the endogenous CAMP gene in the human VDR and CYP27B1-hydroxylase expressing SC monocytic cell line (ATCC CRL-9855), creating the High Throughput Cathelidicin Assay (HiTCA) cell line. After confirming that mCherry inserted in the correct location and orientation, we validated the responsivity of HiTCA cells exposed to physiologically-relevant levels of 25D3 (1nM, 10nM, and 100nM) in serum-free media by observing a 25D3 dose-dependent CAMP-mCherry response (Figure 4). The robust response to 25D3 in HiTCA cells suggests intracellular activation to I,25-dihydroxyvitamin D3 by endogenous CYP27B1. We then tested the HiTCA cell line using 16 donor human serum samples (total 25D3 ranging from 6.7 to 36.2 ng/mL) and noted a statistically significant CAMP-mCherry expression difference ($p < 0.0001$) among donors. In conclusion, the HiTCA cell line enables a high-throughput and reproducible bioassay for 25D-containing human sera.

Figure 4. **25D induces CAMP-mCherry expression in HiTCA cells**

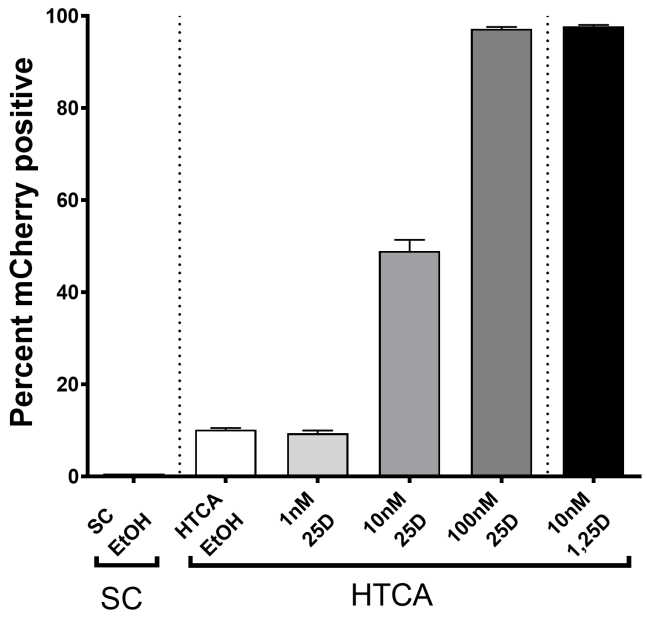

***Disclosures: Carter Gottlieb**, None*

P-138

Regulation of macrophage polarization by IL-3 *Shubhanath Behera[1], Juilee Karhade[1], Garima Pandey[1], Mohan R. Wani[1]. [1]National Centre for Cell Science, India

Regulation of macrophage polarization by IL-3 Shubhanath Behera, Juilee Karhade, Garima Pandey, Mohan R. Wani National Centre for Cell ScienceS. P. Pune University Complex, Pune 411004, IndiaMacrophages play a major role in the immune system. These cells can be polarized into classically activated pro-inflammatory M1 phenotype or alternatively activated anti-inflammatory M2 phenotype. It is recently shown that M1/M2 macrophage ratio is increased in bone marrow of ovariectomized osteoporotic mice and treatment with estrogen restore the M1/M2 ratio by preventing M2 macrophages from being differentiated into osteoclasts. Thus, alteration in M1/M2 macrophage ratio may participate in the pathogenesis of postmenopausal osteoporosis. Macrophages and bone resorbing osteoclasts share the same myeloid cell lineage. We have recently shown that IL-3, a cytokine secreted by activated T lymphocytes inhibits osteoclast differentiation by diverting the cells to macrophage lineage. IL-3 also prevents the development of inflammatory arthritis in mice and protects cartilage and bone destruction in the joint. In the present study we investigated the role of IL-3 in polarization of macrophages. When bone marrow-derived CD11b+ F4/80+ macrophages were incubated for 24 hours with IL-3 alone, we found that there was increase in the expression of M2 macrophage markers CD206 and Arginase 1, however, the expression of M1 macrophage marker iNOS was unchanged by IL-3. We then induced macrophages into M1 phenotype by Th1 cytokines interferon gamma and/or lipopolysaccharide; and M2 phenotype by Th2 cytokine IL-4 in presence of IL-3. We found that IL-3 significantly increased the expression of CD206 and Arginase 1 induced by IL-4. IL-3 showed no effect on expression of M1 phenotype. These results indicate that IL-3 regulate macrophage polarization by diverting the cells towards anti-inflammatory M2 macrophages. Thus, IL-3 may play an important role in regulation of M1/M2 ratio in osteoporosis.

***Disclosures: Shubhanath Behera**, None*

P-139

Modulation of osteoclast behaviors by the immune microenvironment *Margaret Durdan[1], Sonya Royzenblot[1], Megan Weivoda[1]. [1]University of Michigan, United States

Osteoclasts (OCs) are bone resorbing cells and are increasingly recognized to exhibit functional heterogeneity. Understanding how OC behaviors are regulated could lead to novel therapeutic targets to promote/inhibit specific activities without affecting OC numbers. Because OCs are closely related to macrophages (MΦ) that are phenotypically polarized by the immune microenvironment, we tested the effects of a subset of immune cytokines (LPS, IL4, and TGFβ) on mature OC gene expression. OCs were differentiated from mouse BM

(M-CSF and RANKL, 20 and 25ng/mL, respectively). Mature OCs were treated (tx) with immune cytokines for an additional 24 hrs. Following treatment, there were no differences in OC numbers. RNA was isolated for RT-qPCR of OC and MΦ functional gene sets. LPS potently induced inflammatory MΦ genes (Adgre1, Casp1, Cd38, Fpr2, Il1b, Il6, Nlrp3, Nos2, Tnf), and to a lesser extent, OC genes (Acp5, Ctsk, Dcstamp, Ocstamp, Oscar). IL4 inhibited expression of inflammatory MΦ and OC genes and stimulated repair/resolution MΦ genes (Arg1, Egr2, Mrc1, Myc). TGFβ uniquely stimulated coupling-factor genes that have been shown to promote osteoblast proliferation, migration or differentiation (Lif, Pdgfa, Pdgfb, Sphk1, Vegfa, Wnt1). In addition, TGFβ reduced inflammatory MΦ genes (Adgre1, Casp1, Cd38, Fpr2, Il18, Nos2) and potently increased OC genes (Acp5, Ctsk, Dcstamp, Itgav, Itgb3, Ocstamp, Oscar). Because bone-derived TGFβ is released and activated during resorption, our data suggest that TGFβ may act as negative feedback during inflammatory resorption and transition OC activity toward coupling. To further understand mature OC response to TGFβ we performed single cell RNA-seq of vehicle or TGFβ tx OCs (FludigmC1). Using the Seurat toolkit, we identified two mature OC clusters (Acp5, Ctsk, Csf1r, Itgb3, Oscar, Tnfrsf11a), one being vehicle and the other TGFβ tx. Differential analysis of these clusters confirmed TGFβ qPCR data. Interestingly, whereas vehicle tx OCs exhibited increased lysosomal pathways and elevated Clcn7, Car2, Mmp9 expression, TGFβ tx OCs skewed towards phagosome and focal adhesion pathways, and increased Atp6v1g1, Atp6v1b2, and Atp6v0e expression, suggesting potentially altered resorption mechanics. This is in line with previous reports of pit- vs trench-forming OCs. Thus, our current working hypothesis is that the immune microenvironment, including bone-derived TGFβ, regulates OC resorptive, inflammatory, and coupling behaviors.

***Disclosures: Margaret Durdan**, None*

P-140

Comparative Evaluation of 99mTc-WBC SPECT/CT and MR Imaging for Diagnosis of Osteomyelitis in Subjects with Diabetes and Foot Infection *Orhan K. Öz[1], Amber Sherwood[1], Katie Rubitschung[1], Javier La Fontaine[2], Uma Thakur[1], Nathan Dettori[1], Avneesh Chhabra[1], Larry Lavery[2]. [1]UT Southwestern Medical Center Department of Radiology, United States, [2]UT Southwestern Medical Center Department of Plastic Surgery, United States

Osteomyelitis is a common complication in diabetic foot ulcers. Accurate diagnosis of diabetic foot osteomyelitis (DFO) is key to proper treatment and avoiding amputations. The best imaging approach in DFO diagnosis is an area of active investigation. Using bone biopsy as the diagnostic gold standard, we compare the sensitivity and specificity of radiolabeled white blood cell imaging combined with CT (99mTc-WBC SPECT/CT) to MRI for the evaluation of DFO.Subjects with diabetes and foot ulcerations presenting to the Emergency Room of a large tertiary care facility were examined by the podiatry service. Those with suspected osteomyelitis were offered participation in an IRB approved protocol comparing 99mTc-WBC SPECT/CT and MR imaging with and without contrast in the diagnosis of DFO. Bone biopsy was used as a reference standard. Forty-eight subjects consented to participate in the study. A total of 41 subjects completed all imaging and underwent biopsy. Nineteen subjects who were positive for DFO on biopsy also returned for follow up imaging and biopsy six weeks after initial treatment. In all cases WBC scans and MRI were performed within 24h of each other and prior to bone biopsy. MR scans were independently interpreted by two readers, a fellow and a fellowship trained musculoskeletal (MSK) radiologist. In the two instances of disagreement, a third reader fellowship trained in MSK radiology adjudicated. The WBC SPECT/CT scans were read by a radiologist with more than 20 years experience in Nuclear Medicine. All readers were blinded to biopsy results. Pathology was performed in the hospital laboratory and interpreted by pathologist with experience in MSK infections. MRI, SPECT/CT, and pathology interpretations were coded as either positive or negative for osteomyelitis. Sensitivity, specificity, and predictive values were calculated in GraphPad Prism Version 8.0.Imaging in the diagnosis of DFO revealed the sensitivity and specificity of MRI was 87.9% and 31.8%, respectively (n=45), with a 57.14% positive predictive value (PPV). The negative predictive value (NPV) of MRI was higher at 70.0%. 99mTc-WBC SPECT/CT performance was better overall with 90.9% sensitivity, 73.7% specificity, 80.0% PPV, and 87.5% NPV (n=41).Using bone biopsy results as the reference standard, radiolabeled 99mTc-WBC SPECT/CT demonstrates both greater sensitivity and specificity for DFO when compared to MRI.

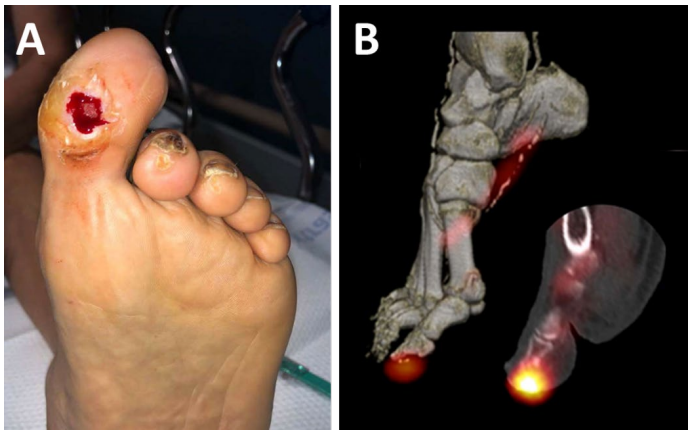

***Disclosures: Orhan K. Öz**, None*

P-141

Investigation of the Molecular Mechanism of TNF-α-Induced RANK on Osteoclast Precursors in Orthodontic Tooth Movement *Takahiro Noguchi[1], Hideki Kitaura[1], Saika Ogawa[1], Fumitoshi Ohori[1], Aseel Marahleh[1], Yasuhiko Nara[1], Adya Pramusita[1], Ria Kinjo[1], Itaru Mizoguchi[1]. [1]Division of Orthodontics and Dentofacial Orthopedics, Tohoku University Graduate School of Dentistry, Japan

Osteoclasts are required for bone resorption and remodeling. Two cytokines, M-CSF and RANKL, are important for osteoclast formation. TNF-α has also been recognized as an important factor for osteoclastogenesis. It has also been reported that TNF-α plays an important role in osteoclastogenesis and bone resorption during orthodontic tooth movement (OTM). RANK is known as the receptor for RANKL. RANK is expressed in osteoclast precursors and osteoclasts. It has been reported that TNF-α enhances expression of RANK on osteoclast precursors in vitro. However, the effect of TNF-α on RANK expression in vivo and the role of TNF-α on RANK expression during OTM are still unclear. In this study, we investigated the effect of TNF-α on RANK expression in vitro, in vivo and in OTM. Furthermore, we investigated molecular mechanism of TNF-α-induced RANK in osteoclast precursors. For in vitro experiments, RANK expression was enhanced on TNF-α treated osteoclast precursors. NF-κB and MAPKs inhibitors significantly decreased RANK expression by TNF-α. Furthermore, TNF-α priming stimulates RANKL-induced osteoclast formation in vitro. For in vivo experiments, TNF-α was injected into mice calvariae by daily subcutaneous injection for 5 days. After sacrifice, RANK expression was evaluated by real-time PCR and immunohistochemistry. The results showed that RANK mRNA expression and the number of RANK-positive cells in TNF-α-injected mice are higher than PBS-injected mice. For OTM, a Ni-Ti closed-coil spring was fixed between the upper incisors and upper-left first molar to move the first molar to the mesial direction in wild-type (WT) mice and TNFR1/TNFR2-deficient (TNFRsKO) mice to analyze the effect of TNF-α on RANK expression. After OTM, the number of RANK-positive cells at the compression side was evaluated by immunohistochemistry. RANK-positive cells increased at the compression side of the alveolar bone in WT mice as a function of time by mechanical loading. In addition, the number of RANK-positive cells at the compression side in WT mice was significantly higher than that in TNFRsKO mice after OTM. These results suggest that TNF-α induced RANK expression in osteoclast precursors by the activation of NF-κB and MAPKs, and the enhanced expression of RANK by TNF-α might increase RANKL-induced osteoclastogenesis. Furthermore, TNF-α induced RANK expression at the compression side of OTM. It might enhance osteoclast formation at the compression side during OTM.

***Disclosures: Takahiro Noguchi**, None*

P-142

Possible Involvement of Elastase in Enhanced Osteoclast Differentiation by Neutrophils Through Degradation of Osteoprotegerin *Risa Sugisaki[1], Yoichi Miyamoto[2], Daichi Chikazu[1], Ryutaro Kamijo[2]. [1]Department of Oral and Maxillofacial Surgery, Tokyo Medical University, Japan, [2]Department of Biochemistry, Showa University School of Dentistry, Japan

[Purpose] Periodontitis and rheumatoid arthritis are chronic inflammatory diseases accompanied by bone resorption by osteoclasts (OC). Neutrophils are one of the most abundant leukocytes in the sites of lesion of inflammatory diseases such as periodontitis and rheumatoid arthritis. Besides the roles of reactive oxygens and proteases including elastase in antimicrobial activity of neutrophils, the role of these agents derived from neutrophils in inflammatory bone resorption has not been fully investigated. On the other hand, we previously reported that Kgp, a cysteine protease produced by Porphyromonas gingivalis, enhanced OC differentiation through degradation of osteoprotegerin (OPG), a decoy receptor for nuclear factor κB (RANK) ligand (RANKL), expressed by osteoblasts. The purpose

of this study is to clarify the role of neutrophil elastase in OC differentiation. [Methods] We examined the effects of neutrophils and recombinant neutrophil elastase on osteoclast differentiation in co-cultures of mouse calvarial osteoblasts and bone marrow cells in the presence and absence of the inhibitors of elastase. We also evaluated the degradation of human recombinant OPG by neutrophils isolated from human peripheral blood and recombinant human elastase by western blotting using an anti-OPG antibody. The primary cleavage site of OPG cleaved by neutrophil elastase was determined by N-terminal amino acid sequence analysis of the fragment. [Results] We found that human neutrophils enhanced osteoclast differentiation, which was significantly suppressed by elastatinal, an inhibitor of neutrophil elastase. Also, we found that human neutrophils degraded human recombinant osteoprotegerin (OPG), which was suppressed by human α1-protease inhibitor, the major endogenous inhibitor of neutrophil elastase. Recombinant human neutrophil elastase degraded human OPG in its death domain-like region. [Conclusions] These results indicated that the degradation of OPG by elastase contributed at least in part to the enhanced osteoclast differentiation by neutrophils. There is a possibility that neutrophils play an important role in inflammatory bone loss found in rheumatoid arthritis and periodontitis.

***Disclosures: Risa Sugisaki**, None*

P-143

Investigation of Effect of IL-33 on TNF-α-Induced Osteoclast Formation and Orthodontic Tooth Movement *Fumitoshi Ohori[1], Hideki Kitaura[1], Saika Ogawa[1], Takahiro Noguchi[1], Aseel Marahleh[1], Yasuhiko Nara[1], Adya Pramusita[1], Ria Kinjo[1], Itaru Mizoguchi[1]. [1]Division of Orthodontics and Dentofacial Orthopedics, Tohoku University Graduate School of Dentistry, Japan

Interleukin (IL)-33 is a member of the IL-1 family, which acts as an alarmin. IL-33 is likely to inhibit osteoclast formation and bone resorption. Tumor necrosis factor-α (TNF-α) can promote osteoclast formation by directly stimulating the osteoclast precursors. It has been reported that TNF-α plays an important role in orthodontic tooth movement (OTM). However, there has been no detailed report regarding the effect of IL-33 on TNF-α-induced osteoclast formation and OTM. There are two objectives in this study. The first is to investigate the role of IL-33 on TNF-α-induced osteoclast formation and bone resorption. The second is to examine the effect of IL-33 during OTM. For in vitro analyses, osteoclast precursors, which were derived from bone marrow cells of eight-week-old male C57BL/6J mice, were treated with or without IL-33 in the presence of TNF-α. Tartrate-resistant acid phosphatase (TRAP) staining was performed to assess osteoclast formation. To investigate the molecular mechanism of osteoclast formation, we performed immunoblotting and immunofluorescence on osteoclast precursors. For in vivo analyses of mouse calvariae, TNF-α with or without IL-33 was subcutaneously administrated into the supracalvarial region of eight-week-old male C57BL/6J mice daily for 5 days (n = 4). Histological sections were stained for TRAP, and osteoclast numbers were determined. Using micro-CT reconstruction images, the ratio of bone destruction area on the calvariae was evaluated. As an OTM model, a Ni-Ti closed-coil spring connecting the anterior alveolar bone and upper-left first molar was fixed to move the first molar to the mesial direction for 12 days in eight-week-old male C57BL/6J mice (n = 4). IL-33 or PBS were injected on the buccal side of upper-left first molar at 2-day intervals. The number of osteoclasts induced by TNF-α was significantly decreased with IL-33. Bone resorption was also reduced. IL-33 inhibited IκB phosphorylation and NF-κB nuclear translocation. OTM distance was smaller in the IL-33 group than in the PBS group. These results suggest that IL-33 inhibited TNF-α-induced osteoclast formation and bone resorption. In addition, the result of OTM indicates that IL-33 inhibited tooth movement.

***Disclosures: Fumitoshi Ohori**, None*

P-144

Reprogramming Metabolism in Osteolineage and Osteoblasts by Inflammatory and Pro-resolution Cytokines *Rajeev Aurora[1], Di Wu[1], Anna Cline-Smith[1], Elena Shashkova [1]. [1]Saint Louis University School of Medicine, United States

Studies by Albright and Reifenstein (1946) showed that estrogen (E2) loss initiates a rapid phase of bone loss leading to osteoporosis in half of postmenopausal women, but the mechanism is not fully understood. Recently we described a new pathway by which ovariectomy (OVX) produced E2 loss leads to chronic low-grade production of the proinflammatory cytokines: TNFα and IL-17 by memory T-cells in a IL-7 and IL-15 dependent mechanism (Cline-Smith, 2020). Our results provided a piece of the puzzle that has remained unsolved for 75 years: how does E2 loss lead to osteoporosis? Bone homeostasis is maintained by coupled bone resorption by osteoclasts followed by formation of new bone by osteoblasts. We showed previously that TNFα and IL-17 are needed to elicit uncoupled bone resorption observed in postmenopausal women and in OVX mice. The effect of TNFα and IL-17A on osteoclastogenesis is well studied. While the bone formation and mineralization rates increase during the acute phase, postmenopause and post-OVX, how the osteoblasts are restrained from matching bone resorption is not well understood. We will present results that show that TNFα and IL-17A restrain osteolineage differentiation pathway but increase osteoblast activity. Interestingly, in both instances the proinflammatory cytokines reprogram the cellular metabolism through differential regulation of the two mTOR complexes. These data provide new insights into how E2 loss restrains bone formation allowing for uncoupling between osteoblasts and osteoclast activity. Our laboratory has also shown that induction of regulatory CD8 T-cells (TcREG) by pulsed low-dose RANKL (pRANKL) is bone anabolic. Interestingly, TcREG suppress osteoclasts and therefore lead to uncoupled bone formation. We will present data that shows that pRANKL treatment of OVX IL-10-/- mice did not increase bone formation and mineral apposition rates. We will also show that IL-10 reprograms metabolism of MSC and mature OB through regulation of mTOR complexes. Together these data provide a fascinating view of how inflammation and resolution of inflammation regulates osteogenesis.

***Disclosures: Rajeev Aurora**, None*

P-145

Associations between household income and proinflammatory cytokines related to bone early in the life-course: A Systematic Review *Stefanie Bird[1], Jason Talevski[1], Jack Feehan[2], Ghazala Naureen[1], Joanne May Ling Tay[3], Priya Goyal[3], Morgan Scott Berman[3], Gustavo Duque[1], Rachel L Duckham[4], Sharon L Brennan-Olsen[5]. [1]Australian Institute of Musculoskeletal Science & University of Melbourne, Australia, [2]Australian Institute of Musculoskeletal Science & Victoria University, Australia, [3]University of Melbourne, Australia, [4]Australian Institute of Musculoskeletal Science & Deakin University, Australia, [5]Australian Institute of Musculoskeletal Science & University of Melbourne & Deakin University, Australia

The life-course association between socioeconomic inequalities and bone health is becoming well-documented. Yet, little is known about the impact of socioeconomic factors on bone-related proinflammatory cytokines in the years before the achievement of peak bone mass. We aimed to systematically identify and synthesise existing data to investigate the relationship between household income, an important parameter of socioeconomic status (SES) known to influence child health, and bone-related pro-inflammatory cytokines during the years prior to peak bone mass attainment (ages 6 to 30 years).We applied a defined e-search strategy to PubMed, Ovid (Medline), EMBASE, PsycINFO and CINAHL databases, with no set limits of publication date. All full-text peer-reviewed articles written in English that encompassed household income data and levels of proinflammatory cytokines associated with bone accrual (C-reactive protein [CRP], interleukin-6 [IL-6], and tumour necrosis factor-alpha [TFN-α]) were screened for eligibility; epidemiological cross-sectional, case-control, and/or cohort studies in children and young adults aged 6-30 years, and baseline data from randomised control trials, where relevant, were included. The Lievense et al.1 scoring system was used to determine the level of evidence.In total, 14 studies met the inclusion criteria; 4 cohort studies (from USA and Australia) and 10 cross-sectional studies (from USA, Puerto Rico and Canada). These studies included a total of 52,586 participants (~54% female). We found limited evidence for an association between low household income and higher levels of IL-6. However, moderate-strong evidence was observed regarding a lack of association between TFN- and CRP, respectively.This review suggests that an association may exist between low household income with increased levels of IL-6, although based on a paucity of data. Future analyses should investigate associations between other parameters of SES and proinflammatory cytokines, given the importance of early life influences on later life bone health.[1] Lievense A, Bierma-Zeinstra SMA, Vergahen AP, van Baar ME, Verhaar JAN, Koes BW (2002) Influence of obesity on the development of osteoarthritis of the hip: a systematic review. Rheumatol 41:1155–1162

***Disclosures: Stefanie Bird**, None*

P-146

The Phosphate Hypothesis: ACE2 Stabilizes Anti-polar Phenotypes of COVID 19 *Robert S Fredericks[1]. [1]Endocrine-Associates, United States

COVID 19 exposes discordance between conventional expectations and the reality of nature, necessitating strategies to discover transformative principles that coherently organize the data. Engaging tactics to kill the SARS-CoV-2 virus while ignoring metabolic complexity of the host leaves us vulnerable to unanticipated health and economic consequences. ACE2, the viral conduit to intracellular replication, is also disrupted as a metabolic signal deserving of attention. Models demonstrating a capacity to differentially activate innate and acquired immunity have been developed during investigation of the role of phosphate in manifestations of Chronic Fatigue Syndrome (CFS) that can incorporate ACE2 disruption as a generator of divergent phenotypes. It is proposed that COVID 19 pandemic severity requires both victims of cytokine storm manifesting ARDS and recurrent asymptomatic spreaders, plausibly mediated by enhanced innate viral killing, both stemming from compromised ACE2, Previous work demonstrated that mutations in the HFE gene, when homozygous responsible for hemochromatosis, are associated with divergent metabolic phenotypes similar to those proposed for COVID 19. Additional validation of the models includes demonstrations that Grave's disease remits with paricalcitol, Bechet's improves with doxercalciferol and that severe metabolic syndrome can respond to etidronate. Recognition of heat as a fundamental metabolic signal integrating phosphate, sodium and calcium with FGF23/aKlotho/PTH/PTHrP signaling clarifies CFS findings relating to innate and acquired immunity. Central to the phosphate hypothesis is the principle of anti-polarity where an initial signal produces divergent outcomes due to each individual's complex signaling structure. Mitigation of the COVID 19 pandemic appears to require appropriate choice of differing interventions for the victims versus asymptomatic spreaders with ACE2 disruption contributing to both phenotypes. ACE2 disruption appears to negate

fatigue responses that could otherwise ameliorate pandemic manifestations of SARS-CoV-2 infection. Interventions, including SGLT2 inhibitors, vitamin D analogues, RAAS modifiers and renal protective agents are proposed as favorable to metabolic integrity and vaccine efficacy. Recognizing the kidney as a reporter organ and the skeleton as an expression of systemic metabolic organization facilitates needed exploration for modeling personalized predispositions.

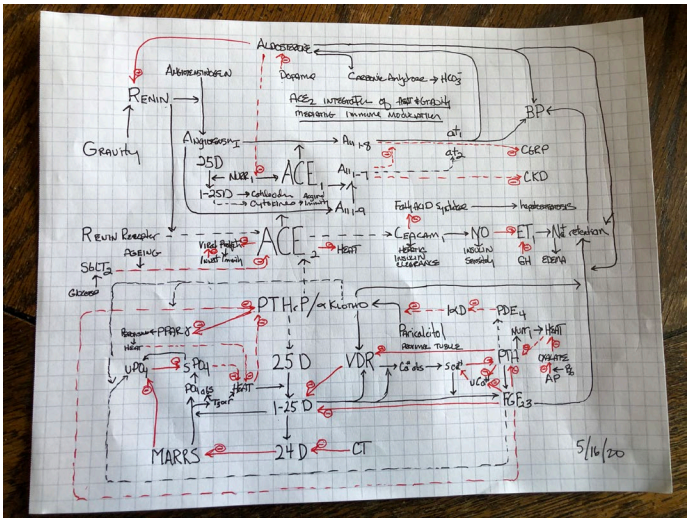

***Disclosures: Robert S Fredericks**, None*

P-147

Bone marrow adipogenic lineage precursors (MALPs) promote osteoclastogenesis in bone remodeling and pathologic bone loss *Wei Yu[1], Leilei Zhong[1], Lutian Yao[1], Yulong Wei[1], Tao Gui[1], Ziqing Li[2], Hyunsoo Kim[3], Nathaniel Dyment[1], Xiaowei Liu[1], Shuying Yang[4], Yongwon Choi[3], Jaimo Ahn[1], Ling Qin[1]. [1]Department of Orthopaedic Surgery, Perelman School of Medicine, University of Pennsylvania, United States, [2]University of Pennsylvania, United States, [3]Department of Pathology and Laboratory Medicine, Perelman School of Medicine, University of Pennsylvania, United States, [4]Department of Basic & Translational Sciences, School of Dental Medicine, University of Pennsylvania, Philadelphia, United States

Bone resorption by osteoclasts is a critical step in bone remodeling. It is well known that osteogenic cells support osteoclastogenesis via synthesizing RANKL. Recently, we identified a novel mesenchymal subpopulation, marrow adipogenic lineage precursors (MALPs), which highly expresses adipogenic markers but has no lipid accumulation, and demonstrated their functions in regulating marrow vessels and bone formation. In this study, using a single cell RNA-sequencing (scRNA-seq) dataset containing 17,494 mouse bone marrow mesenchymal and hematopoietic cells, we computational delineated the in vivo differentiation route of osteoclasts from MΦα cells, an intermediate macrophage cell type that also gives rise to terminally differentiated MΦβ cells. Surprisingly, ligand-receptor pair analysis suggested that MALPs, but not osteoblasts nor osteocytes, have the most signal interactions with macrophage lineage cells due to their high expression of osteoclast regulatory factors, including RANKL. Lineage tracing revealed that Adipoq-Cre only labels MALPs and their descendant lipid-laden adipocytes (LiLAs, which are hundred times less than MALPs in bone marrow) but not mesenchymal progenitors, osteoblasts, and osteocytes. Interestingly, nearly all osteoclasts in bone were touched by MALP cell processes. Thus, we constructed Adipoq-Cre Tnfsf11 flox/flox (RANKL CKOAdipoq) mice to study the role of RANKL from MALPs. These mice in both genders displayed a drastic increase of trabecular bone mass (BV/TV) in long bones (61%) and vertebrae (33%) starting from 1 mo of age but their growth plate and cortical bone were normal (n=6/group). At 3 mo of age, they displayed a more striking increase of BV/TV (1.7-fold, n=6/group). In comparison, osteoblasts/osteocytes-specific RANKL knockdown using Dmp1-Cre merely increased tibial BV/TV by 18% (n=6/group, 1 mo of age). RANKL CKOAdipoq mice showed reduced osteoclast number (65%), osteoblast number (52%), and bone formation rate (58%) at trabecular bone surface (n=6/mice). MALPs also exist in calvarial bone marrow. Osteolytic lesion in calvaria induced by LPS injection was completely abolished in RANKL CKOAdipoq mice due to diminished osteoclast activation (n=6/group). In ovariectomized mice, elevated bone resorption in vertebrates was also partially attenuated in these mice (n=6/group). In summary, our studies identified MALPs as a critical player in controlling bone remodeling during normal bone metabolism and pathological bone loss.

***Disclosures: Wei Yu**, None*

P-148

MarrowQuant across Aging and Aplasia: A Digital Pathology Tool for Quantification of Bone Marrow Compartments in Histological Sections *Josefine Tratwal[1], Ibrahim Bekri[1], Chiheb Boussema[1], Nicolas Kunz[2], Rita Sarkis[1], Tereza Koliqi[1], Shanti Rojas-Sutterlin[1], Frédérica Schyrr[1], Daniel Naveed Tavakol[1], Vasco Campos[1], Erica L. Scheller[3], Rossella Sarro[4], Carmen Barcena[5], Bettina Bisig[6], Valentina Nardi[7], Laurence de Leval[4], Olivier Burri[8], Olaia Naveiras[9]. [1]Laboratory of Regenerative Hematopoiesis, Institute of Bioengineering and Institute for Experimental Cancer Research, Ecole polytechnique fédérale de Lausanne (EPFL), Switzerland, [2]Animal Imaging and Technology Core, Center for Biomedical Imaging, Ecole polytechnique fédérale de Lausanne (EPFL), Switzerland, [3]Division of Bone and Mineral Diseases, Department of Internal Medicine, Washington, United States, [4]Institute of Pathology, Lausanne University Hospital (CHUV) and Lausanne University (UNIL), Switzerland, [5]Department of Pathology, University Hospital 12 de Octubre, Spain, [6]Institute of Pathology, Lausanne University Hospital (CHUV) and Lausanne University (UNIL), Switzerland, [7]Department of Pathology, Massachusetts General Hospital, Harvard Medical School, United States, [8]Bioimaging and Optics Core Facility, Ecole polytechnique fédérale de Lausanne (EPFL), Switzerland, [9]Laboratory of Regenerative Hematopoiesis, Institute of Bioengineering and Institute for Experimental Cancer Research, Ecole polytechnique fédérale de Lausanne (EPFL) and Department of Oncology, Hematology Service, Lausanne University Hospital (CHUV), Switzerland

The bone marrow (BM) exists heterogeneously as hematopoietic/red or adipocytic/yellow varying with skeletal location, age, and physiological condition. Mouse models and patients undergoing radio/chemotherapy or suffering acute BM failure, endure a rapid adipocytic conversion of the BM (red-to-yellow transition). Following hematopoietic recovery, such as upon BM transplantation, functional hematopoiesis is restored (yellow-to-red transition). These changes as evaluated on histological sections of trephine biopsies are a diagnostic feature of hematopoietic failure.Here we report the development of a semi-automated image analysis plug-in, MarrowQuant operating through an open-source software (QuPath), to systematically quantify multiple bone components in hematoxylin and eosin stained sections in an unbiased manner. MarrowQuant reproducibly analyses the areas occupied by bone, hematopoietic cells, the interstitial/microvascular compartment, as well as adipocyte ghosts and their size distribution. BM hematopoietic cellularity analysis with MarrowQuant lies within the range of scoring by independent pathologists as the gold standard. Quantification of total BM adipocyte area in murine whole bone sections compares with volumetric measurements of osmium-tetroxide stained lipids by micro-computerized tomography. Due to user-dependent variables, reproducibility in longitudinal studies is a challenge, and MarrowQuant thus offers a complementary standardized approach.With our tool, we were able to develop a consistent map of BM hematopoietic cellularity and adiposity in mid-sections of murine bones in homeostatic conditions, including quantification of the highly predictable red-to-yellow transitions in the proximal caudal vertebrae and in the tibia. We present a comparative skeletal map induced by lethal irradiation, with longitudinal quantification of the red-to-yellow-to-red transition over two months in femurs and tibiae. Following BM transplantation, BM adiposity inversely correlates with kinetics of hematopoietic recovery conserving a proximal-to-distal gradient. Analysis of recovery in vivo with magnetic resonance imaging reveals comparable kinetics. Applying MarrowQuant to acute myeloid leukemic biopsies at different timepoints of treatment, confirms the plasticity of the human BM and a reciprocal relationship between the hematopoietic and adipocytic BM compartments. This opens avenues for its application in contexts requiring standardized BM evaluation.

***Disclosures: Josefine Tratwal**, None*

P-149

Senolytics improve the in vivo bone remodeling potential of bone marrow mesenchymal stem cells obtained from aged mice *Yueying Zhou[1], Xiaonan Xin[1], Li Chen[2], Lichao Wang[1], Ming Xu[2], David Rowe[2]. [1]UConn Health, United States, [2]UCONN Health, United States

The in vitro osteogenic potential of bone marrow mesenchymal stem cells (BMSCs) declines with aging. To explore this observation, BMSCs from 27-month-old C57BL/6 male mice were isolated and cultured in a 6 well plate for 7 days reaching 80% confluency. Four wells received a senolytic cocktail (0.2μM dasatinib+20μM quercetin; D+Q) and 2 wells vehicle (V) for 24 hours. One day later, the cell confluency of the D+Q treated wells fell to 50%, but recovered to 80% after 2 additional days of culture. The treated and control wells, as well as BMSCs from young donors (Y), were harvested and 5 x 105cells/defect absorbed into a Healos scaffold and implanted into a calvarial defect of NSG mice that also carried a Col3.6GFPtpz reporter. Calvarial were harvested at 6 weeks after a single i.p. injection of alizarine complexone (AC) 1 day prior to sacrifice. Calvarial defects were fixed in formalin, x-rayed and processed for cryohistology. The planar area of new bone formation relative to the defect size was assessed by ImageJ (Fig. A: Y = 0.88+/-0.05, V = 0.51+/-0.06 while D+Q = 0.82+/-0.05, p<0.001). The transverse histological sections revealed the mineralized cortical shell surrounding a bone marrow space and the adjacent membraneous bone of the host. Relative to the Y and D+Q treated aged cells, the V cells had wide cortices and a small marrow space (Fig B: marrow area/total area: Y = 0.48+/-0.05; V=0.22+/-0.03; DQ=

Posters

0.46+/-0.03, p<0.0001). Although AP and AC positive surfaces were similar on all samples, the V-treated cells had fewer TRAP positive cells on the endocortical surface and outer cortical shell, and more unresorbed Healos-derived hydroxyapaptite within the cortical bone. In addition, the osteoblasts expressing the Col3.6GFPtpz reporter were abundant on the endocortical surfaces of the V-treated cells but rarely found in the D+Q or young donor samples. This histological study suggests that the D+Q treatment improves overall osteogenesis by enhanced bone remodeling of the woven bone that is initially deposited within the calvarial defect model to form a cortical shell and the environment necessary for intramarrow hematopoiesis. It accomplishes this outcome with little contribution from the host osteoblasts. The study reveals properties of osteogenesis that are not evident in primary in vitro BMSC cultures and provides a model for simultaneously evaluating the cellular basis for the in vitro and in vivo effects of senolytic agents on the aged osteogenic lineage.

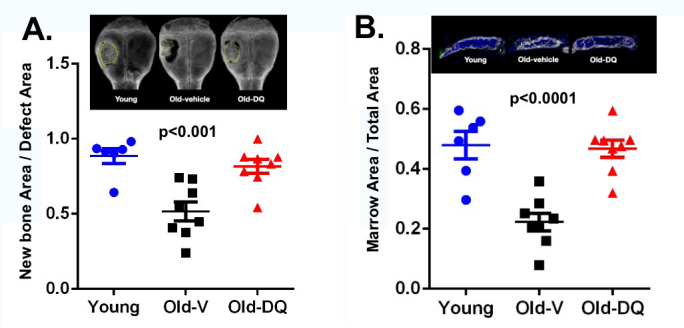

***Disclosures: Yueying Zhou**, None*

P-150

Oxylipins Mediate Radiation-induced Marrow Adipose Tissue Expansion *Jason A Horton[1], Aaron Maymin[2], James Boyer[2]. [1]Upstate Medical University, United States, [2]Upstate Medical University, Dept. Orthopedic Surgery, United States

INTRODUCTION: Marrow adipose tissue (MAT) expansion following radiation exposure may be implicated in radiation-induced bone disease. We hypothesized that radiation-induced lipid oxidation could be a key factor driving marrow adipose expansion by activating P-PARγ which is endogenously activated by oxidized lipids. METHODS: With IACUC consent, bilateral hind limbs of 12-week old female c57BL/6J mice received four daily 5Gy fractions of 225kVp x-radiation; sham-irradiated mice served as controls. Tissues were harvested at 1, 3, 7 and 14 days after the final radiation exposure(n=10/group). Femurs were fixed and prepared for µCT-based morphometry and OsO4 enhanced imaging of MAT. The left tibia was homogenized in saline with 0.05% BHT, and lipids purified in C18 columns for measurement of neutral lipids, PUFAs, total lipid peroxidation (Cell Biolabs), or quantitative oxylipin analysis by LC-MS/MS. RNA was extracted from the right tibia to assess adipogenesis related gene expression (Adipogenesis PCR arrays, Qiagen). Differences between sham and irradiated mice were accepted as statistically significant when p<=0.05 by ANOVA.RESULTS: Bone morphometry (table 1) showed increased trabecular bone at 1 and 3 days post-irradiation (p<=0.0215) and gradual increase of diaphyseal cortical bone density (p<0.0001). MAT expansion (Ad.V/TV) was rapid, achieving significance by day 3 (p<=0.0004); Neutral lipid content was significantly increased by days 7 and 14 (p<0.01). While total lipid peroxides and PUFA were reduced at 1, 3 and 7 days (p<=0.0101), several oxidized lipid species including P-PARγ agonist 9-HODE were increased (p<0.05) vs. controls at all time points. Reactome pathway analysis revealed two dominant themes of upregulated gene expression 1,3, and 7 days post irradiation, centering P-PARγ-mediated regulation of white adipocyte differentiation, and DNA damage signaling mediated by p53, p21 and FOXO1. In contrast pro-adipogenic Wnt signaling pathways, were downregulated by day 14. DISCUSSION: This experiment identified 9-HODE as mediator of radiation-induced MAT expansion, likely acting via P-PARγ. Our gene expression studies suggest that MAT expansion may also involve p53-dependent and/or FOXO1-dependent transcription of the p21, known to be necessary for adipogenesis and prohibitive of osteoblastic differentiation. ACKNOWLEDGEMENTS: This research was funded by NIAMS/NIH 4R00AR066737-02 (JAH)

Table 1. Morphometric data by µCT

Group	BV/TV	Tb.N (1/mm)	Tb.Th mm	Tb.Sp mm	Diaphy. BMD mg/CCM HA	Ad.V/TV
Sham	0.056 ± 0.009	3.55 ± 0.21	0.044 ± 0.003	0.281 ± 0.017	1206.7 ± 9.6	0.031 ± 0.048
1d	0.083 ± 0.015*	4.02 ± 0.23*	0.047 ± 0.003	0.245 ± 0.016*	1210.2 ± 11.0	0.121 ± 0.095
3d	0.080 ± 0.015*	3.88 ± 0.19*	0.047 ± 0.002	0.253 ± 0.015*	1213.0 ± 10.5	0.277 ± 0.1051*
7d	0.075 ± 0.025	3.83 ± 0.40	0.048 ± 0.004*	0.259 ± 0.025	1214.0 ± 9.6	0.488 ± 0.1172*
14d	0.0496 ± 0.013	3.50 ± 0.24	0.045 ± 0.003	0.286 ± 0.022	1230.7 ± 12.3*	0.501 ± 0.1037*

* indicates p<0.05 by ANOVA

***Disclosures: Jason A Horton**, None*

P-151

Differential bone effects with lipoxinA4: steady state vs. wound healing *Koh Amy[1], Ann Decker[1], Justin Do[1], Hernan Roca[1], Laurie McCauley[1]. [1]University of Michigan, United States

LipoxinA4 (LXA4), an eicosanoid lipid mediator derivative metabolized from arachidonic acid, is one of the most abundant lipoxin specialized pro-resolving mediators. LXA4 binding to its G protein coupled receptor promotes inflammation resolution and wound healing in concert with macrophages. Bone marrow F4/80+ macrophages are known to facilitate anabolic actions of parathyroid hormone (PTH) and PTH increases bone marrow lipoxins. Studies of LXA4 in bone report direct inhibitory actions on osteoclasts and enhanced macrophage efferocytosis in vitro. This study investigated LXA4 effects on bone in steady state (growth and adult) and wound healing (tooth extraction) scenarios. C57Bl/6 male mice (12wk) were anesthetized and the first maxillary molar extracted. LXA4 (10ng/g) or vehicle (V) was administered daily for 14d. Using a growth model, pups (4d) were given daily LXA4 for 17d. Using an adult model, 16wk mice were given 5d of daily LXA4, then 3x/wk for 6wks. Bone turnover markers TRAcP5b and P1NP were determined in serum and µCT analyses performed of tibiae and socket bone fill. Vertebral TRAP+ osteoclast (OC) numbers were determined. In vitro, LXA4 effects on mCSF+RANKL induced osteoclastogenesis in primary bone marrow cultures was determined. After 14d of LXA4, µCT analyses revealed significantly increased bone volume/total volume (BV/TV: 0.25+/-0.03 V vs 0.38+/-0.04 LXA4) within the distal socket. There was a significant decrease in trabecular (Tb) number (20.6+/-0.5 V vs 18.9+/-0.2 LXA4) and increases in Tb thickness (0.044+/-0.001 V vs 0.050+/-0.022 LXA4) and BMD (183+/-25 V vs 268+/-24 LXA4) with no change in Tb spacing. Tibial µCT revealed no differences in BV/TV and no differences in serum TRAcP5b, an indicator of OC numbers, and serum P1NP, an indicator of bone formation. There were no LXA4 BV/TV differences found in adult mice. In contrast, the growth model µCT revealed significantly increased BV/TV (0.21+/-0.02 V vs 0.28+/-0.02 LXA4), Tb number (5.96+/-0.22 V vs 7.15+/-0.34 LXA4) and BMD (124.3+/-6.6 V vs 155.18+/-9.99 LXA4) and a trend of increased Tb thickness and decreased Tb spacing. Serum TRAcP5b was decreased (13.12+/-1.49 V vs 9.71+/-0.88 LXA4; p=0.07) while P1NP was unchanged. TRAP staining in vertebrae revealed no differences, yet OC numbers in vitro decreased with LXA4. These data reveal the pro-resolving mediator, LXA4, increased bone growth favorably in rapid growth and wound healing scenarios which may be partly attributed to an inhibition of bone resorption.

***Disclosures: Koh Amy**, None*

P-152

The Influence of Interleukin-1 Receptor Antagonism and Bone Marrow Ablation on Vasodilator Capacity, Bone Marrow Blood Vessel Ossification, and Bone Microarchitecture in Old Fischer-344 Rats *Sunggi Noh[1], Ryan Pohlig[2], Rhonda Prisby[1]. [1]The University of Texas at Arlington, United States, [2]The University of Delaware, United States

BACKGROUND: A pro-inflammatory marrow microenvironment reduces vasodilator capacity of bone blood vessels and increases bone marrow blood vessel (BMBV) ossification. We theorized that bone marrow ablation and administration of an interleukin-1 receptor antagonist would eliminate the pro-inflammatory marrow microenvironment and reduce BMBV ossification.Thus, we assessed vasodilator capacity of the femoral principal nutrient artery (PNA), ossified BMBV, and bone microarchitecture in old rats. METHODS: Male Fischer-344 rats (24-mon) were assigned accordingly: Control (CON, n=15), interleukin-1 receptor antagonism (IL-1RA, n=13), bone marrow ablation (BMA, n=13) and combined treatment (IL-1RA+BMA, n=11). Rats underwent surgery to create a defect in the right femoral shaft. The bone marrow of the BMA and IL-1RA+BMA groups was flushed with PBS. During 3 weeks of recovery, CON and BMA received injections of PBS (100 µl, 3 d/wk, i.p.), while IL-1RA and IL-1RA+BMA received the antagonist (3 µg/kg, 3 d/wk, i.p.). At sacrifice, endothelium-dependent (ACh; 10-9-10-4 M) and independent (DEA NONOate; 10-10-10-4 M) vasodilation in the absence and presence of marrow was assessed. MicroCT (µCT) was used to determine ossified vessel volume (OsVV, %) and thickness (OsV.Th, mm). Bone microarchitecture (i.e. BV/TV, %; Tb.N, /mm; Tb.Th, mm Tb.Sp, mm and Ct.Th, mm) and bone density (mg HA/ccm) were assessed via µCT. Mixed Models and ANOVAs were used. RESULTS: In the presence of marrow, endothelium-dependent vasodilation was reduced (p<0.05) in IL-1RA and BMA vs. the other groups. For endothelium-independent vasodilation, it was diminished (p<0.05) in the presence vs. the absence of marrow. OsVV and OsV.Th did not differ. Trabecular BV/TV, Tb.N and Tb.Sp did not differ among groups; however, Tb.Th was higher (p<0.05) in BMA (90+/-3 mm) vs. CON (79+/-2 mm). Trabecular density was highest (p<0.05) in IL-1RA+BMA (1136+/-7 mg HA/ccm) vs. the other groups and IL-1RA (1073+/-26 mg HA/ccm) was higher (p<0.05) vs. CON (994+/-4 mg HA/ccm) and BMA (1022+/-7 mg HA/ccm). Ct.Th did not differ, and cortical density was higher (p<0.05) in IL-1RA+BMA (1325+/-3 mg HA/ccm) vs. BMA (1304+/-4 mg HA/ccm). CONCLUSION: The marrow microenvironment reduced endothelium-independent vasodilation. Although BMBV ossification was not altered, combined treatment (i.e., IL-1RA+BMA) augmented bone density.

***Disclosures: Sunggi Noh**, None*

P-154

GNAS product XLαs, but not Gsα, exhibits variable allele-specific expression in bone marrow stromal samples: "next-generation" sequencing (NGS) to determine parental contribution. *Qiuxia Cui[1], Claire Elizabeth Remillard[2], Antonius Plagge[3], Mina Gardezi[4], Margret Dunlap[4], Louis C Gerstenfeld[4], Qing He[5], Murat Bastepe[2]. [1]Endocrine Unit, Department of Medicine, Massachusetts General Hospital and Harvard Medical School; Zhongnan Hospital, Wuhan University, United States, [2]Endocrine Unit, Department of Medicine, Massachusetts General Hospital and Harvard Medical School, United States, [3]Institute of Systems, Molecular & Integrative Biology, University of Liverpool, United Kingdom, [4]Department of Orthopaedic Surgery, Boston University School of Medicine, United States, [5]Endocrine Unit, Department of Medicine, Massachusetts General Hospital and Harvard Medical School; School of Stomatology, Wuhan University, United States

The GNAS locus gives rise to multiple transcripts including the stimulatory G protein alpha-subunit (Gsα). GNAS mutations cause multiple inherited diseases and are found in various endocrine and non-endocrine tumors. Another GNAS product is the extra-large G-alpha protein (XLαs), which differs from Gsα in its promoter and first coding exon. XLαs expression has been shown to be paternal, and therefore, with the exception of those located in Gsα exon 1, all disease-causing GNAS mutations affect XLαs when they are on the paternal allele. However, a previous study observed biallelic XLαs expression in bone marrow stromal cells (BMSCs) from normal individuals and patients from fibrous dysplasia of bone. We therefore investigated allelic XLαs expression in different tissues. We initially compared the XLαs transcript levels in paternal, maternal, or homozygous XLαs knockout (XLKO) mice to the levels in wild-type littermates; however, conclusive results could not be obtained owing presumably to the variable levels of remnant XLαs mRNA from the disrupted allele. We then employed "next-generation" sequencing of RT-PCR amplicons and a polymorphism common to both XLαs and Gsα, as well as A/B, another paternally expressed GNAS transcript. In mouse BMSCs, bone tissue, and cerebellum, Gsα transcripts were biallelically derived (48.4+/-0.3%; n=6, 53.0+/-0.7%; n=6, and 51.9+/-0.3%; n=6, respectively), while A/B was nearly exclusively paternal (99.8+/-0.2%; n=4, 99.6+/-0.1%; n=4, and 99.9+/-0.1%; n=3, respectively). In contrast, XLαs expression varied substantially among individual samples in each of the three tissues. Strikingly, the paternal XLαs contribution in six independent BMSC samples ranged from 43.0% to 99.9% (p=0.02 vs. the data distribution in A/B; Wilcoxon rank-sum test). In two unrelated human BMSC samples, XLαs expression also appeared to be variable, albeit predominantly monoallelic (91.3% or 99.6%). In contrast, murine calvarial osteoblasts did not show evidence of such variable allelic XLαs expression, even after 2 weeks of differentiation in culture (99.4+/-0.2%; n=4), arguing against a role of cell culture in the observed variation of allelic XLαs expression. Considering that BMSCs consist of multiple cell populations whose relative abundance may differ from sample to sample, it is possible that XLαs expression is biallelic in a certain subset of BMSCs. These findings have important implications in understanding the role of altered XLαs actions in GNAS-related diseases.

***Disclosures: Qiuxia Cui**, None*

P-155

Osteocyte Vegf-a Contributes to Myeloma-associated Angiogenesis and Is Regulated by Fgf23 *Patrick Mulcrone[1], Daniela Petrusca[1], Jesus Delgado-Calle[2], G. David Roodman[1]. [1]Indiana University School of Medicine, United States, [2]Indiana University School of Medicien, United States

Osteocytes regulate normal bone homeostasis and the development of multiple myeloma bone disease (MMBD). Previous studies demonstrated when osteocytes interact with multiple myeloma cells (MM), these interactions stimulate tumor growth and production of osteocytic factors that increase osteoclast resorption and suppress osteoblast activity. In addition, the MMBD tumor microenvironment is very hypoxic, and increased bone marrow angiogenesis is a characteristic of patients with active MM. Further, the level of increased marrow angiogenesis correlates negatively with patient survival. Although osteocytes can produce pro-angiogenic factors during mechanical load stress and in the presence of pro-inflammatory cytokines, it is unclear if osteocyte-MM interactions also contribute to enhanced bone marrow vascularization seen with MMBD. We report that hypoxia and direct interactions with MM cells increase pro-angiogenic signaling in osteocytes. Vascular endothelial growth factor-a (Vegf-a) increases in MLOA5 cells cultured in hypoxia compared to those grown under normoxic conditions. Co-culture of MM cells with MLOA5 under hypoxia induces greater than two-fold increases in production of Vegf-a in osteocytes when compared to normoxic mono-culture, and a 42-55% increase compared to normoxic co-culture conditions. Conditioned media (CM) from both hypoxic mono and co-cultures increases HUVEC tube length at 8hrs when compared to CM from normoxic cultures. These increases induced by hypoxic CM are prevented by addition of a neutralizing antibody targeting murine Vegf-a or using CM derived from MLOA5s lacking Vegf-a via siRNA. Angiogenic changes are also prevented with Ad-Cre treatment of calvarial biopsies from or primary osteocytes derived from calvariae of Vegf-a flox/flox mice. In vivo, we detected an increased number of Vegf-positive osteocytes in 5TGM1 MM-bearing tibiae that correlated positively with MM vascular area. Finally, we demonstrate a novel angiogenic role of Fgf23, an osteocyte-specific hormone. Fgf23 promotes Vegf-a expression and secretion in osteocytes via upregulation of the Egr1 transcription factor, and knockout of Fgf23 in osteocytes blocks MM-induced upregulation of Vegf-a. Together, these results demonstrate that hypoxia and MM cells trigger a pro-angiogenic phenotype in osteocytes via Fgf23 and Vegf-a signaling. Our results support that angiogenic signals from osteocytes contribute to MM vascularization.

***Disclosures: Patrick Mulcrone**, None*

P-156

Differential Pathway Activation by GP130 Cytokines in Breast Cancer *Tolu Omokehinde[1], Alec Jotte[1], Rachelle Johnson[2]. [1]Vanderbilt University, United States, [2]Vanderbilt University Medical Center, United States

Bone-disseminated breast cancer cells oftentimes home to the osteogenic niche, where they are exposed to glycoprotein130 (GP130) cytokines secreted by osteoblast-lineage cells. Leukemia inhibitory factor (LIF), oncostatin M (OSM) and ciliary neurotropic factor (CNTF) are GP130 cytokines that can all signal through LIF receptor (LIFR) and are known to induce JAK/STAT, AKT, and ERK signaling. Our lab previously showed that breast cancer cell expression of LIFR and JAK/STAT signaling promotes tumor dormancy in bone, but it is unclear which pathways in breast cancer cells are stimulated by the LIFR-binding ligands. We hypothesized that LIF, OSM, and CNTF induce pro-dormancy signaling pathways and promote tumor suppression. Treatment with recombinant LIF, OSM or CNTF (50ng/ml) robustly stimulated pSTAT3 (up to 34-fold, p<0.01-0.0001), LIF and OSM induced pERK (up to 4-fold, p<0.01-0.001), and only OSM induced pAKT (up to 9-fold, p<0.0001) in MCF7 breast cancer cells by Western blot. LIF and CNTF induced no signaling in MDA-MB-231 breast cancer cells, which have a non-functional LIFR, but OSM robustly stimulated pSTAT3 and pAKT (up to 26-fold, p<0.05-0.0001) in MDA-MB-231b cells, suggesting OSM may signal through OSM receptor (OSMR) on breast cancer cells. Reverse phase protein array (RPPA) analysis of MCF7 cells treated with recombinant LIF, OSM, and CNTF revealed several previously unknown signaling pathways and effectors to be activated, including ATM, CREB, HSP27, and N-RAS. Overexpression of OSM in MCF7 cells reduced the expression of 4/18 the pro-dormancy genes BMP7, FOXA1, IGFBP5, and TGFB2 (by 41-97.5% p<0.05-0.0001) in vitro, while treatment with recombinant cytokines or CNTF overexpression resulted in no significant changes. When orthotopically inoculated into mice (n=10/group), neither OSM nor CNTF overexpressing MCF7 cells altered the progression of tumor formation, tumor volume or weight in vivo. Since we were unable to generate LIF over-expressing MCF7 cells, possibly due to induction of dormancy, we have created a Tet-on inducible overexpression system for LIF, OSM, and CNTF and these experiments are in progress. Together, these data suggest that the GP130 cytokines robustly stimulate multiple signaling pathways with tumor-suppressive and tumor-promoting activity, but further studies are needed to determine their effect on tumor progression and dissemination to the bone.

***Disclosures: Tolu Omokehinde**, None*

P-157

Osx marks distinct subsets of CD45Neg and CD45Pos stromal populations in extra-skeletal tumors that enhance tumor growth *Biancamaria Ricci[1], Eric Tycksen[2], Hamza Celik[3], Francesca Fontana[4], Roberto Civitelli[4], Roberta Faccio[1]. [1]Washington University in St Louis-Department of Orthopedics, United States, [2]Washington University in St Louis-Department of Genetics, United States, [3]Washington University in St Louis-Department of Medicine, United States, [4]Washington University in St Louis-Department of Internal Medicine, United States

The contribution of stromal populations to support tumor progression and metastasis is increasingly recognized. Cancer-associated fibroblasts (CAFs) are a heterogeneous population of mesenchymal cells providing pro-tumorigenic signals, extra-cellular matrix (ECM) support and protection from anti-tumor therapies. While their function is well established, their origin and cellular phenotype remain to be fully elucidated. Osterix (Osx) is a master regulator of osteogenic differentiation expressed in perinatal skeletal mesenchymal stem cells (MSC) and post-proliferative osteoblasts. We detect Osx expression in CAFs from primary breast tumors and melanomas. By using Osx-cre/TdTomato reporter mice we confirm presence of 10-15% TdTOSX+ cells in extra-skeletal tumors, but also 12-20% TdTOSX+ cells in bone marrow (BM) and 13-18% TdTOSX+ cells in circulation. Co-injection of tumor-derived TdTOSX+ cells with B16 melanomas significantly increases tumor growth compared to tumor cells alone. Unexpectedly, the majority of TdTOSX+ cells are also positive for the hematopoietic marker CD45. RNAseq analysis and flow cytometry reveal that the genetic and phenotypic profiles of tumor-derived TdTOSX+CD45+ cells resemble that of tumor infiltrating immune cells, indicating that Osx does not mark a specific immune subset. Indeed, such heterogeneity is explained by Osx expression early during hematopoiesis, where Osx transcripts are detected in long and short-term HSC and multipotent progenitors but not in the mature immune populations such as T cells, dendritic cells or macrophages. In contrast, RNAseq data from the TdTOSX+CD45- population show expression of genes involved in ECM deposition and remodeling, closely resembling the CAFs. Our results indicate that Osx marks distinct subsets of tumor promoting CD45- and CD45+ stromal populations in extra-skeletal tumors and challenge the dogma that expression of osteogenic and hematopoietic markers are mutually exclusive.

***Disclosures: Biancamaria Ricci**, None*

P-158

Autocrine and paracrine Notch receptor 3 signaling in the myeloma niche stimulates tumor growth and bone destruction. *Hayley Sabol[1], Tania Amorim[1], David Halladay[1], Noriyoshi Kurihara[1], Judith Anderson[1], Meloney Cregor[1], G David Roodman[1], Teresita Bellido[1], Jesus Delgado-Calle[1]. [1]Indiana University School of Medicine, United States

In multiple myeloma (MM), Notch is activated in the tumor niche to stimulate MM proliferation and survival and bone destruction. We showed before that osteocytes (Ots) activate Notch, increase Notch receptor (NR) 3 expression, and stimulate proliferation in MM cells. To investigate the role of NR3 in MM cells and their communication with Ots, we used lentiviral-mediated shRNA stable gene inhibition. NR3 mRNA was undetectable in 5TGM1 MM cells transduced with shRNA-NR3 and NR3 activation (NICD3) was reduced by 80% compared to control shRNA-scramble cells, whereas NR1, 2 or 4 NICD protein levels remained unchanged compared to controls. NR3 knockdown decreased Notch target gene expression and cyclin D1, reduced proliferation by 35%, and modestly increased apoptosis of MM cells. Further, knockdown of NR3 decreased Rankl and increased Opg expression and abrogated the ability of MM cells to promote osteoclastogenesis in vitro. Together, these results demonstrate that autocrine NR3 signaling stimulates proliferation, favors survival, and increases the osteoclastogenic potential of MM cells. Next, we examined NR3's role in MM-Ots communication. Direct co-culture with Ots increased MM cell proliferation by 2.7 fold in control cells compared to only 1.6 fold in shRNA-NR3 MM cells. NR3 knockdown in MM cells partially prevented the upregulation of Notch target genes and cyclinD1 induced by contact with Ots. Inhibition of signaling downstream all NRs with GSI was required to fully prevent the increases in MM proliferation and gene expression induced by Ots. These results show that paracrine NR3 signaling mediates MM-Ots communication, but other NRs also contribute to Ot's effects. Lastly, we studied the effects of NR3 knockdown in MM cells in ex vivo and in vivo models. Ex vivo, we found less tumor growth and lower levels of the resorption marker CTX in conditioned media from bones bearing shRNA-NR3 MM cells compared to bones bearing control cells. For the in vivo study, we injected 105 shRNA-NR3 or shRNA-scramble 5TGM1 MM cells in the tibias of 6-wk-old C57BL/KaLwRijHsd mice. After 5 wks, mice bearing shRNA-NR3 cells had a 50% decrease in tumor burden, 50% reduction in osteolytic lesions, and exhibited 30% more cancellous bone compared to mice bearing control MM cells. These findings identify NR3 as a key mediator of autocrine and paracrine communication in the MM tumor niche and warrant future studies to target NR3 as a therapeutic approach for the treatment of MM.

***Disclosures: Hayley Sabol**, None*

P-159

Non-bone metastatic cancers promote osteocytic bone destruction *Fabrizio Pin[1], Joshua R. Huot [2], Matthew Prideaux[1], Lynda F. Bonewald[1], Andrea Bonetto[2]. [1]Department of Anatomy, Cell Biology Physiology, Indiana University School of Medicine, Indianapolis, United States, [2]Department of Surgery, Indiana University School of Medicine, Indianapolis, United States

The effects of bone metastatic cancer are well described, whereas considerably less is known regarding the effects of non-metastatic pro-cachexiogenic cancer on bone. In this study we investigated the effects of three well-characterized models of cancer cachexia in mice; Colon-26 adenocarcinoma (C26), ES-2 ovarian cancer and Lewis lung carcinoma (LLC). Even though C26, ES-2 and LLC tumor growth resulted in comparable body and muscle wasting, the ES-2 and LLC hosts exhibited severe bone loss by microCT analysis, whereas only a modest bone loss was observed in the C26-bearing mice. In line with the loss of bone mass, histomorphometrical analysis showed increased osteoclast numbers on the femoral bone surface from ES-2 and LLC hosts (+149% and +178%, respectively, $p<0.01$), while no significant effects were observed in the mice bearing C26 tumors. TRAP+ osteocytes were increased in the femurs of C26 (+635%) and ES-2 bearers (+698%), along with increased lacunar area (+24% and +37% respectively, $p<0.01$) showing osteocytic osteolysis. In addition, C26 and ES-2 hosts displayed dramatically increased osteocyte death (+1569% and +4890% respectively, $p<0.001$), as well as empty lacunae (+108% and +93% respectively, $p<0.001$). To test the hypothesis that tumor-secreted factors were responsible for osteocyte cell death, IDG-SW3 cells differentiated for 21 days to acquire a mature osteocyte phenotype were co-cultured for 24 and 72 hours with cancer cells or 3T3 fibroblast as a control. Cell death was assessed by an LDH assay. An increase in LDH was observed in the culture medium at 24h of day 21 IDG-SW3 cells exposed to all three cancer cell lines (C26: +160%; ES-2: +257%; LLC: +512%; $p<0.001$) suggesting that all tumors were cytotoxic for osteocytes. Further, elevated osteoclast markers, including Acp5, CtsK, Atp-6v0d2 and Mmp13, support the in vivo observation of osteocytic osteolysis. A reduction in mRNA levels for both the early osteocyte marker Dmp1 and the late marker Sost was also observed. Osteocytic bone destruction and extensive osteocyte cell death (osteonecrosis) along with muscle wasting may generate a musculoskeletal system that is incapable of full recovery upon eradication of tumor. Consideration of co-treatments that maintain musculoskeletal health while simultaneously using chemotherapy should be taken.

***Disclosures: Fabrizio Pin**, None*

P-160

HIF Signaling Prevents Outgrowth of Breast Cancer Cells in Lung but not Bone *Vera Todd[1], Lawrence Vecchi[2], Rachelle Johnson[2]. [1]Vanderbilt University, United States, [2]Vanderbilt University Medical Center, United States

As tumors enlarge and outgrow their blood supply, they frequently become hypoxic, activating hypoxia-inducible factor (HIF) signaling. Previous studies suggest that HIF signaling in breast cancer cells promotes lung dissemination in genetic models and bone colonization following intracardiac inoculation, but the impact of HIF1α in the primary tumor on spontaneous dissemination to bone has never been evaluated. Based on these studies, we hypothesized that HIF1α deletion in the primary tumor would reduce spontaneous dissemination to bone. To test this, we generated MMTV-Cre.Hif1αf/f.PyMT mice, which spontaneously develop mouse mammary carcinomas with conditional deletion of HIF1α in the mammary fat pad / tumors. As we reported last year, CreT/w/Hif1αf/f/PyMTT/w (Hif1α-/-) and Crew/w/Hif1αf/f/PyMTT/w (Hif1αf/f) littermate and cousin controls were used and mice sacrificed when the largest tumor reached 1cm3, which was delayed in Hif1α-/- mice ($p<0.001$). Our recent data now indicate that despite experiencing similar levels of intratumoral hypoxia (as assessed by pimonidazole staining), Hif1α-/- mice (n=21 mice) had an 85% reduction in Hif1α expression in whole mammary tumors compared to Hif1αf/f mice (n=19 mice) ($p<0.0001$). Histological inspection of lung sections previously revealed that Hif1α-/- mice had greater incidence of macroscopic tumor nodules (n=15/21 Hif1α-/-, n=6/19 Hif1αf/f, $p<0.05$), and greater average lesion number (1.9-fold increase, $p<0.05$) and area (2.2-fold fold increase, $p<0.05$), and we now confirm that only one Hif1α-/- mouse had discernible tumor burden in the bone upon histological inspection of tibiae. Since PyMT mice have low baseline levels of tumor cell dissemination to bone, we used qPCR detection of Pymt mRNA, which is specifically expressed in mammary carcinoma cells, as an additional tool to measure tumor burden. Last year we reported a small but significant decrease in Pymt mRNA in the spine of Hif1α-/- mice, but with the addition of more samples and new statistical analyses, we now report there was no significant difference in tumor burden by Pymt expression in the lung, femora, spine, or brain. These data suggest that blocking HIF1α signaling in primary breast tumors and metastatic tumor cells may promote tumor cell dissemination or outgrowth in the lung, where tumor cells only encounter hypoxia as they grow and expand, but not in the physiologically hypoxic environment encountered in the bone.

***Disclosures: Vera Todd**, None*

P-161

FOXP1 Drives Osteosarcoma Development by Repressing P53 Signaling *Hanjun Li[1], Tingting Tang[1]. [1]Shanghai Key Laboratory of Orthopaedic Implants, Department of Orthopaedic Surgery, Shanghai Ninth People's Hospital, Shanghai Jiao Tong University School of Medicine, China

Osteosarcoma has poor prognosis, and poor understanding of the genetic drivers of osteosarcoma hinder further improvement in therapeutic approaches. Here, we determined the role and regulatory mechanisms of the transcription factor forkhead box P1 (FOXP1) in osteosarcoma. We examined FOXP1 expression in osteosarcoma cells by qRT-PCR and Western blot and the pathological characteristics associated with FOXP1 expression through tissue microarray. FOXP1 overexpression and knockdown osteosarcoma cell lines were established by lentiviral transfection. Functional analyses of FOXP1 in osteosarcoma were performed in vitro and in vivo using cell-derived xenograft and patient-derived xenograft models. RNA-sequencing, chromatin immunoprecipitation, coimmunoprecipitation, proximal ligation assay, and luciferase reporter assay were applied to determine the downstream genes, protein interactions, and upstream regulators of FOXP1. We found that higher FOXP1 expression correlated with malignancy in both osteosarcoma cell lines and clinical biopsies. FOXP1 promoted proliferation, tumor sphere formation, migration and invasion, and inhibited anoikis in osteosarcoma cells. FOXP1 acted as a repressor of P21 and RB (retinoblastoma protein) transcription, and directly interacted with the tumor suppressor p53, thereby inhibiting p53 activity. Extracellular signal-regulated kinase/c-Jun N-terminal kinase (ERK/JNK) signaling and c-JUN/c-FOS transcription factors were found to be upstream activators of FOXP1. Silencing of FOXP1 suppressed the development and progression of osteosarcoma in cell-derived and patient-derived xenograft animal models. In conclusion, we demonstrate that the FOXP1 drives osteosarcoma development by regulating the p53 signaling cascade, suggesting that FOXP1 is a potential target for osteosarcoma therapy.

***Disclosures: Hanjun Li**, None*

P-162

Macrophage Efferocytosis of Apoptotic Prostate Cancer Cells Activates TIM-3/CEACAM1/SHP-2 Signaling to Support Bone Metastatic Progression

*Veronica Mendoza-Reinoso[1], Dah Youn Baek[1], Adrianne Kurutz[1], John Rubin[1], Morgan Kuczler[2], Danielle M. Zambito[3], Kenneth Pienta[3], Laurie K. McCauley[1], Hernan Roca[1]. [1]Department of Periodontics and Oral Medicine, University of Michigan School of Dentistry, United States, [2]Department of Urology Johns Hopkins University School of Medicine, United States, [3]Department of Urology Johns Hopkins University School of Medicine, United States

Apoptotic cell clearance by macrophages, aka efferocytosis, is crucial for maintaining tissue homeostasis. During tumor growth, millions of cancer cells undergo apoptosis and are cleared by macrophages. Various studies have found that efferocytosis of cancer cells by macrophages promotes chronic inflammation and immunosuppression supporting tumor growth and metastases. Little is known of the unique role that bone marrow macrophages play in skeletal metastasis. T-cell immunoglobulin and mucin-domain containing-3 (TIM-3) is implicated in T-cell responses and cancer progression; however, TIM-3 signaling in efferocytic macrophages remains to be defined. Activation of the TIM-3 signaling pathway relies on interaction of TIM-3 with carcinoembryonic antigen-related cell adhesion molecule 1 (CEACAM1). TIM-3 was found to be upregulated in macrophages efferocytosing apoptotic prostate cancer cells. A CEACAM1 fragment was synthesized to interact with TIM-3 and then used to treat efferocytic bone marrow-derived macrophages. TIM-3 protein expression was reduced in macrophages efferocytosing cancer cells when treated with the CEACAM1 peptide. CEACAM1 is a critical binding partner of Src-homology 2 domain-containing phosphatase (SHP-2) in the cytosol and SHP-2 regulates macrophage polarization and activates pro-inflammatory and immunosuppressive mechanisms. When a specific SHP2 inhibitor (SHP099) was used in efferocytic macrophages it significantly reduced TIM-3 expression. In addition, SHP2 inhibition led to STAT3 hyperphosphorylation suggesting STAT3 as a SHP-2 target in this mechanism. To investigate the potential role of TIM-3 expression in monocytes/macrophages in relation to prostate cancer progression, we isolated mononuclear CD14+ cells from blood and bone marrow samples of prostate cancer patients with varying grades of disease and analyzed TIM-3 expression. Flow cytometric analysis revealed a population of TIM-3+/FSChigh monocytes/macrophages that was significantly increased in the bone marrow but not in the matched blood samples from Grade 5 (high risk metastatic) vs. lower grade prostate cancer patients. These results suggest that CD14+/TIM-3+/FSChigh cell population may play a critical role in bone metastasis. Together these findings reveal a signaling pathway triggered in efferocytic macrophages that connects the TIM-3/CEACAM1/SHP-2 axis, and suggests a mechanism that promotes an immunosuppressive microenvironment and bone metastatic cancer progression.

***Disclosures: Veronica Mendoza-Reinoso**, None*

P-163

Bone marrow adipocytes induce multiple myeloma cell adipomimicry and dexamethasone resistance

*Mariah Farrell[1], Anastasia D'Amico[1], Heather Fairfield[1], Connor Murphy[1], Carolyne Falank[1], Michaela Reagan[1]. [1]Maine Medical Center Research Institute, United States

Purpose: Multiple myeloma (MM) is a cancer of plasma cells that is characterized by MM cell colonization of the bone marrow (BM) and painful osteolytic lesions. The relationship between bone marrow adipocytes (BMAds) and MM cells holds great promise as a novel therapeutic avenue. Our group and others have published that BMAds support MM cell survival and drug resistance, however, the mechanisms governing this are still relatively unknown.Approach: BMAds were differentiated from BM-MSCs for 21 days and then conditioned media (CM) was collected for 48hr. Flow cytometric or bioluminescence assays assessed OPM2 and MM.1S cell apoptosis, cell cycle, and proliferation after 72hr with BMAd CM, 80 μM dex or both. RT-PCR, adipokine arrays, and RNAseq (GSE132604) were used to look at adipogenic phenotype of MM cells. Finally, SCID beige mice were treated for 5 weeks with an anti-sclerostin antibody (Scl Ab) to decrease BMAds and then inoculated with MM.1S cells. Scl Ab continued during MM progression and 9 mg/kg dex was given to mice 4x/week for 2 weeks after tumor burden was established. Controls received vehicles, dex alone, or Scl Ab alone.Results: MM1S cells and OPM2 cells had a 50% reduction in cell number and a 3-fold increase in apoptosis with dex treatment. BMAd-CM reduced dex-induced apoptosis to 1.3-fold in these cells and rescued cell numbers. Dex reduced KI67%+ cells to 75%, but BMAd-CM recovered this level to 95%. Both an adipokine array and gene expression revealed an increase in adipogenic genes in MM cells exposed to BMAd CM (eg. FABP4, Pref-1, Leptin, IL-6, and adiponectin). RNAseq analysis revealed that many adipogenic genes were increased in obese MM patients relative to lean such as PPARγ, CEBPA, and FOXO1. Mice co-treated with Scl Ab and dex had the least amount of tumor burden and had significantly increased survival compared to all other treatment groups (Fig. 1).Conclusion: BMAd-CM supported MM cells and inhibited dex-induced apoptosis. MM cells increased their expression of adipokines after BMAd-CM treatment, and obese patients' MM cells expressed higher levels of adipocyte genes. Our data suggest that MM cells may evade dex-induced apoptosis by undergoing adipomimicry. Additionally, targeting BMAds with Scl Ab in vivo increased efficacy of dex, resulting in decreased tumor burden and increased survival. Together our data demonstrate BMAds support MM cell survival and drug resistance, and provide translational insight for MM treatment.

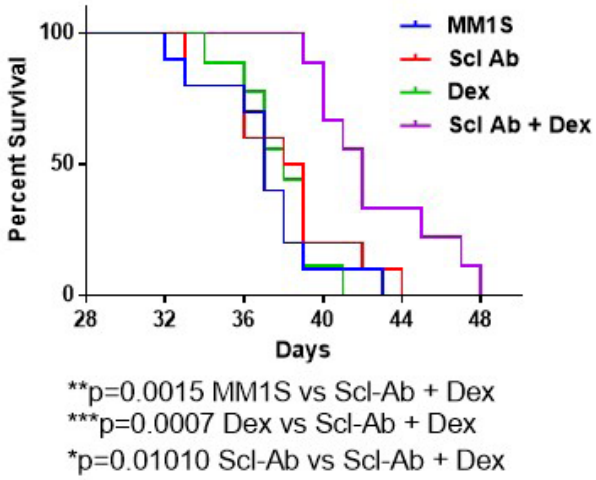

Figure 1. In the MM1S/SCID Beige Mouse xenograft model, sclerostin-neutralizing antibody (Scl Ab) in combination with dexamethasone (Dex) increased mouse survival significantly, compared to Dex alone, Scl-Ab alone, or vehicle controls (MM1S).

***Disclosures: Mariah Farrell**, None*

P-164

Aberrant DNA methylation and gene expression profiles in the bone marrow stroma of AML patients carrying IDH1 or IDH2 mutations

*Paraskevi Vgenopoulou[1], Junfei Zhao[2], Raul Rabadan[2], Martin Carroll[3], Stavroula Kousteni[4]. [1]Department of Physiology and Cellular Biophysics, Columbia University Irving Medical Center, United States, [2]Department of Biomedical Informatics and Center for Computational Biology and Bioinformatics, Columbia University Irving Medical Center, United States, [3]Division of Hematology and Oncology, Perelman School of Medicine, University of Pennsylvania, United States, [4]Department of Physiology and Cellular Biophysics, Columbia University Irving Medical Center, United States

Gain-of-function mutations in isocitrate dehydrogenase genes (IDH1 and IDH2) are found in 3% of myelodysplasia (MDS) and 20% of acute myeloid leukemia (AML) patients. They drive the synthesis of the oncometabolite 2-hydroxyglutarate (2HG) which inhibits α-KG-dependent dioxygenases and alters histone and DNA methylation in MDS/AML cells. However, IDH1/2 mutations are not disease-causing by themselves and require additional cooperative signals to become fully transforming. We examined whether such signals could emanate from potential epigenetic alterations in the bone marrow (BM) stomal niche. We found that 2HG is present and elevated in the BM plasma of MDS or MDS/AML patients carrying IDH mutations as compared to patients without such mutations. It can be uptaken by stromal cells as treatment of BM stromal cells with 2HG leads to its detection in cell lysates. Methylome analysis by Enhanced Reduced Representation Bisulfite Sequencing of BM stromal cells showed that BM stroma of IDH-mutant AML exhibited a characteristic methylation pattern that was significantly different from that of IDH-wild type AML stroma. Gene Set Enrichment Analysis demonstrated alterations in transcription factor targets associated with chromatin remodeling in malignancies such as acute lymphoblastic leukemia (LYF1), cell proliferation (SRF, HNF3, CREB), integrin beta chain associated with leukocyte adhesion deficiency (LFA1), as well as pathways indicating metabolic deregulation. In parallel, RNAseq analysis of the same stromal cell samples revealed a robust gene expression signature associated with IDH1/2-mutant patients. Genes contained within the aberrant IDH-mutant gene expression and DNA methylation signatures were integrated and common targets were used to identify biological pathways and functions that are perturbed in the stroma of IDH-mutant leukemias. Pathway analysis revealed a significant overrepresentation of genes involved in vascular endothelial growth factor activity, signaling by receptor tyrosine kinases and extracellular matrix organization and interactions, all pathways implicated in the interaction between stromal cells and hematopoietic stem cells (HSCs) in health and disease. This study unveils the epigenetic landscape of the BM stroma in IDH-mutant MDS/AML and sets the stage for the identification of cooperating signals that drive IDH-mutant HSC transformation; targeting such signals, in combination with IDH1/2 inhibitors, could improve treatment outcome.

***Disclosures: Paraskevi Vgenopoulou**, None*

Posters

P-165

Treatment of established bone metastases can be achieved by combinatorial osteoclast blockade and depletion of Gr1+ cell subsets *Seunghyun Lee[1], Aude-Hélène Capietto[1], Roberta Faccio[0]. [1]Washington University in St.Louis, United States, [0]Washington University in St.Louis, United States

The bone is the third most common site of metastasis for a variety of solid tumors including breast, prostate, and melanoma, among others. While osteoclast (OC) blockade has been successful in reducing tumor growth in bone in pre-clinical settings, anti-resorptives failed to improve the overall survival rate of cancer patients with bone metastasis despite ameliorating skeletal complications. To address this unmet clinical need, we established a murine model of bone metastasis insensitive to the anti-tumor effects of OC blockade (Zoledronic acid; ZA), consisting of delayed ZA administration starting 7 days after intratibial (i.t) or intracardiac (i.c.) tumor cell inoculation. By using this tumor model, we interrogated what other cells modulate tumor growth in bone in addition to the OCs. CD11b+Gr1+ myeloid cells, also known as myeloid-derived suppressor cells, originate in the bone marrow and promote tumor progression by suppressing anti-tumor immunity. Thus, we hypothesized that accumulation of CD11b+Gr1+ populations might hinder ZA anti-tumor effects in the context of established bone metastases. To address this hypothesis, we administered anti-Gr1 3x/week to mice with established B16 melanoma, PyMT carcinoma and 4T1 breast cancer metastases to bone or bearing subcutaneous and mammary tumors as control. While anti-Gr1 significantly reduced primary tumor progression, this treatment had no effects on bone metastases either following i.t or i.c. tumor delivery, and both in the preventive and curative settings. By profiling immune populations from the bone marrow and the primary tumor of anti-Gr1 treated mice, we found efficient depletion of CD11b+Gr1+ populations only at extraskeletal sites, while increased numbers in bone marrow. Subset specific analysis revealed that anti-Gr1 expanded a specific subset CD11b+Ly6CintLy6Gint, while depleting the Cd11b+/Ly6Ghigh and Ly6Chigh populations. Intriguingly, CD11b+Gr1+ cells from bone marrow of tumor bearing anti-Gr1 treated mice gave rise to more OCs in vitro than CD11b+Gr1+ cells from tumor bearing IgG controls. Based on this observation, we treated established metastases to bone with a combination of anti-Gr1 + ZA and found that the combinatorial treatment significantly reduced metastases to bone compared to each agent alone. In summary, we provide evidence that amelioration of established skeletal metastases can be achieved by a combination therapy consisting of depletion of Gr1+ subsets and osteoclast blockade.

***Disclosures: Seunghyun Lee**, None*

P-166

The Wnt-Inhibitor DKK-1 as a Prognostic Marker and Molecular Target in Human Triple-Negative Breast Cancer *Teresa Stefania Dell'Endice[1], Andrew Browne[1], Lorenz Hofbauer[2], Andy Göbel[1], Tilman Rachner[2]. [1]Division of Endocrinology, Diabetes and Bone Diseases, Department of Medicine III, TU Dresden Medical Center, Fetscherstraße 74, D-01307 Dresden, Germany, Germany, [2]Division of Endocrinology, Diabetes and Bone Diseases, Department of Medicine III and Center for Healthy Aging, TU Dresden Medical Center, Fetscherstraße 74, D-01307 Dresden, Germany, Germany

The Wnt-signalling antagonist Dickkopf-1(DKK-1) promotes the formation of osteolytic bone metastases by affecting the osteoblastic function in advanced breast cancer. Several studies underline the importance of DKK-1 as a tumor promotor with pleiotropic supportive effects on cancer cell growth and disease progression. In this study, we aimed at clarifying the biological role and the potential as a therapeutic target of DKK-1 in human triple-negative breast cancer (TNBC).DKK-1 protein expression was evaluated by immunohistochemistry in a tissue microarray of 396 patients with primary breast cancer. Immunoreactivity was assessed by grading the stain intensity from 0 to 3 and multiplied by a value in order to calculate the percentage of the stained cancerous tissue. Patients were divided into DKK-1 low/negative and DKK-1 positive groups. The survival curves were plotted for the total number of patients, as well as subdivisions of estrogen receptor negative (ER-) and estrogen receptor positive (ER+) patients. Cell metabolism in MDA-MB-231 control and DKK-1 knock-out (KO) cells was assessed in vitro by Cell Titer Blue® viability assay. In vivo, normal and DKK-1 KO cells were subcutaneously inoculated into NMRI-nu female mice and tumour growth was assessed after 5 weeks.DKK-1 expression was significantly increased by up to 3-fold between stages T1 and T2 compared to carcinoma in situ ($p<0.05$). When patients were stratified according to the ER- status, DKK-1 was a decisive predictor of survival with a significant association between positive DKK-1 expression and decreased survival ($p<0.05$) in ER- patients only. Assessment of cell viability demonstrated a significant reduction in the DKK-1 KO compared to the control cells ($p<0.001$) under serum-deprived culture conditions after 72 h. Subcutaneous tumor growth was significantly suppressed by using DKK-1 KO cells (61%, $p<0.05$) compared to control cells.Our findings show that DKK-1 expression in breast cancer is a negative prognostic factor in ER-, but not in ER+ patients indicating DKK-1 as a potential therapeutic target in TNBC. Furthermore, the growth of human MDA-MB-231 breast cancer cells is significantly reduced in NMRI-nu mice supporting a pro-tumourigenic role of DKK1 in ER- breast cancer. These results warrant further research to define the role of DKK-1 in primary and metastatic breast cancer.

***Disclosures: Teresa Stefania Dell'Endice**, None*

P-167

Denosumab is Non-inferior to Zoledronic Acid as Bone Protection in Post-menopausal Breast Cancer: A 2-year Prospective Follow-up Study *Kristian Buch-Larsen[1], Michael Andersson[2], Peter Schwarz[1]. [1]Department of Endocrinology, Rigshospitalet, Denmark, [2]Department of Oncology, Rigshospitalet, Denmark

BackgroundStandard treatment for post-menopausal women with oestrogen receptor positive (HR+) breast cancer (BC) is aromatase inhibitors (AI), known to cause loss of BMD. Guidelines recommend the use of intravenous (i.v.) bisphosphonates i.e. zoledronic acid, which increase overall survival. Bisphosphonates reduce BMD loss and risk of fractures. In this study we investigate whether denosumab is a valid second option for patients unable to receive standard i.v. zoledronic acid for various reasons.MethodsIn total 212 patients have been evaluated after they did not receive i.v. zoledronic acid at baseline at the department of Oncology and of those 199 were in AI treatment. After endocrine evaluation all patients were offered zoledronic acid as first choice (N=30) or secondly denosumab (N=169). The patients were followed prospectively with blood tests at baseline, 1, 3, 6, 12 and 24 months and DXA scans at baseline and 24 months.Results We saw no difference between the two treatment groups at baseline, with regard to anthropometry and standard biochemistry. Plasma ionized calcium (p-Ca2+) was significantly decreased (non-symptomatic) after 1 month of treatment in both the denosumab (mean change -0.05 mmol/L, $p<0.001$) and zoledronic acid (-0.05 mmol/L, $p<0.001$) group with a corresponding p-PTH elevation. We observed no significant difference between the groups and p-Ca2+ was normalized after 1 year. Markers of bone turnover (p-P1CP, p-CTX, p-bone specific alkaline phosphatase and p-osteocalcin) all showed significant suppression from month 1 compared to baseline and remained supressed for both groups throughout the 2 years. BMD showed small and significant increases at the spine (0.023 g/cm2, $p<0.01$) and total hip (0.020 g/cm2, $p<0.001$) in the denosumab group but no change at the femoral neck (-0.012 g/cm2, $p=0.14$). In the zoledronic acid group we observed no significant change at spine (0.014 g/cm2, $p=0.63$) and total hip (-0.001 g/cm2, $p=0.90$) and a small and significant drop at the femoral neck (-0.037 g/cm2, $p=0.03$). However, when we compared BMD change between the treatment groups, we found no significant difference.ConclusionOur data indicate that for post-menopausal HR+ BC patients in AI treatment who for various reasons cannot be treated with zoledronic acid, denosumab might be recommended as a safe second choice. Regarding bone protection denosumab is non-inferior to zoledronic acid.

***Disclosures: Kristian Buch-Larsen**, None*

P-168

Identification of senescent plasma cells in a mouse model of monoclonal gammopathy of undetermined significance *Gabriel Borges[1], Sonya Royzenblat[1], Iyabode Ajayi[1], Claire Edwards[2], Ming Xu[3], Tamara Tchkonia[4], James Kirkland[4], Matthew Drake[4], Megan Weivoda[1]. [1]Department of Periodontics and Oral Medicine, School of Dentistry, University of Michigan, United States, [2]Nuffield Department of Orthopaedics, Rheumatology & Musculoskeletal Sciences, Botnar Research Centre, University of Oxford, United Kingdom, [3]University of Connecticut Center on Aging, University of Connecticut Health, United States, [4]Robert and Arlene Kogod Center on Aging, Mayo Clinic, United States

Monoclonal gammopathy of undetermined significance (MGUS) is a precursor condition for multiple myeloma (MM) characterized by clonal plasma cell (PC) derived monoclonal antibody. Despite similar oncogenes to MM, MGUS PCs are non-proliferative and the mechanisms that trigger disease progression remain unclear. Because oncogene activation is a stressor known to cause senescence-induced growth arrest, we hypothesized that MGUS clonal PCs are senescent. Thus, we have employed the KaLwRij mouse model of MGUS to assess senescence markers in KaLwRij PCs and the response of these cells to senolytic therapy (dasatinib+quercetin, D+Q).Age and sex-matched KaLwRij mice (10-12 mo) were treated (tx) with D+Q (5, 50mg/kg) or placebo for 3 days, biweekly for 2.5 months. The related C57BL/6 mice served as controls. Blood samples were collected biweekly to measure serum antibody (Ab) content. Following euthanasia, bone marrow PCs were enriched via magnetic sorting, followed by staining for senescence-associated βGal activity (SA-βGal) and further isolation/analysis of PCs by fluorescence-activated cell sorting.Male and female KaLwRij mice exhibited significantly reduced total PC numbers compared to C57BL/6, with increased percentage (%) SA-βGal+ PCs. The % SA-βgal+ PCs was significantly decreased in female D+Q tx KaLwRij mice, and these mice exhibited a rescue in total PC number. Male D+Q tx KaLwRij mice showed no differences in these parameters compared to placebo. RT-qPCR revealed increased senescence gene expression (Bcl2, Bmi, Fas, Irf4, Nfkb1, Prdm1, and Relb) with reduced proliferation marker, Mki67, in SA-βGal+ PCs. D+Q tx significantly improved the expression of PC markers Cd40, Slamf7, and Xbp1, with trends for improved Sdc1 and Cd40Ig in SA-βGalNeg PCs. Serum Ab content served as a functional readout of MGUS. While individual Ab isotype levels were variable, total Ab content significantly increased with time in placebo mice. This increase was not observed in D+Q tx female KaLwRij mice. The increased Ab content was driven by increased IgG1, and D+Q tx female KaLwRij mice exhibited a significant decrease in IgG1 percent change compared to placebo.Overall, these results are consistent with senescence in clonal PCs. Recent findings suggest senescent cells can exhibit increased genomic instability. Thus, further evaluation of

PC senescence phenotypes in MGUS may lead to the identification of biomarkers to predict risk of progression to MM.

***Disclosures: Gabriel Borges**, None*

P-169

Bone Loss Evaluation after One Year of Combined GnRH Agonist and Aromatase Inhibitors Therapy for Premenopausal Early Breast Cancers *XAVIER NOGUES[1], Irene Petit[2], Sonia Servitja[3], Isabel Campodarve[2], Isabel Aymar[2], Marta Pineda-Moncusi[4], Diana Ovejero[4], Natalia Garcia-Giralt[4]. [1]IMIM (Hospital del Mar Research Institute), Centro de Investigación Biomédica en Red de Fragilidad y Envejecimiento Saludable (CIBERFES);Internal Medicine Department, Hospital del Mar, Universitat Autònoma de Barcelona, Spain, [2]Internal Medicine Department, Hospital del Mar, Universitat Autònoma de Barcelona, Spain, [3]Cancer Research Program, IMIM (Hospital del Mar Research Institute), Spain, [4]IMIM (Hospital del Mar Research Institute), Centro de Investigación Biomédica en Red de Fragilidad y Envejecimiento Saludable (CIBERFES), Spain

Aromatase Inhibitors (AI) have been constituted as a first line adjuvant therapy for estrogen receptor-positive breast cancer patients. Recent therapeutic strategies in premenopausal patients involve ovarian function suppression (OFS) for menopause induction plus AI treatment. Even though these combined therapies increased benefits in terms of disease-free survival, several endocrine-deprivation symptoms like osteoporosis and fractures are raised as frequent complications. Up to day, little evidences about bone health have been described in these patients. The present study aimed to describe the bone mineral density (BMD) changes one year after AI-therapy initiation.Data of Caucasian women candidates for OFS plus AI (OFS+AI) were collected prospectively since January 2018. Participants were supplemented with 25(OH)vitD3 and those with bone antiresorptive treatments were excluded. The main outcomes of the study were the relative change in lumbar spine (LS), femoral neck (FN) and total hip (TH) BMD from baseline to one year of AI therapy. Patient characteristics and clinical variables were also registered at baseline and each year during treatment. Bone mass changes were compared between these patients and postmenopausal breast cancer women treated only with AI (B-ABLE cohort). T Student was used for group comparisons in SPSS vs23.26 patients initiated combined OFS plus AI (OFS+AI) and 758 patients were included in the B-ABLE cohort at the beginning of AI therapy at postmenopause (AI-post). Of those patients, 13 OFS+AI and 640 AI-post had BMD values at one year after AI starting. As it is expected, OFS+AI patients were significantly younger and thinner than AI-post (age mean+/-SD:46+/-6 vs 61+/-7.6; BMI mean+/-SD:24.5+/-4 vs 29+/-5.4, respectively; p<0.0001). No differences were found in basal BMD at three body locations, or in Vitamin D levels at baseline and after 1 year of treatment. OPF+AI patients suffered a striking bone loss (mean+/-SD) of -6.7%+/-3 at LS, -7.8%+/-4 at FN, and -5.2%+/-2.8 at TH. AI-post patients also underwent bone loss although it was significantly slighter (LS: -1.4%+/-4.1, FN: -1.3%+/-6, TH: -0.3%+/-3.7; p<0001 compared to OPF+AI patients).In summary, an important bone loss was detected in OFS+AI patients during the first year of AI therapy, even higher than AI-postmenopausal women, which need to be considered and monitored for clinical interventions.

***Disclosures: XAVIER NOGUES**, None*

P-170

Low doses of the bone-targeted Notch inhibitor BT-GSI exhibit higher anti-myeloma activity and preserve bone compared to unconjugated GSI or zolendronic acid. *Tania Amorim[1], Adam Ferrari[1], Hayley Sabol[1], Judith Anderson[1], Meloney Cregor[1], Megan Sweet[1], Venkatesan Srinivasan[2], Frank Ebetino[2], Robert Boeckman[2], G David Roodman[1], Teresita Bellido[1], Jesus Delgado-Calle[1]. [1]Indiana University School of Medicine, United States, [2]University of Rochester, United States

Multiple myeloma (MM) cells communicate with cells in the MM niche via Notch signaling, leading to tumor growth and bone destruction. γ-secretase inhibitors (GSIs) block Notch and decrease MM growth, but their clinical use is limited by severe gut toxicity. To overcome GSI side-effects, we generated a bone-targeted Notch inhibitor (BT-GSI). We previously showed that BT-GSI inhibits Notch in bone, decreases MM growth, and preserves bone without inducing gut toxicity. Here we compared BT-GSI's anti-MM efficacy to an equimolar dose of systemic GSI or to zolendronic acid (ZA); and examined the effects of lower doses of BT-GSI on mouse models of established MM. KaLwRijHsd mice were injected with 105 5TGM1 MM cells or saline (control). 3 wks after MM cell inoculation, mice bearing MM were randomized by tumor burden and osteolysis, and received either vehicle (DMSO), BT-GSI (10mg/Kg, 3x/wk), unconjugated GSI (5mg/kg, 3x/wk), bone-targeting moiety (BT) (5mg/kg, 3x/wk), or ZA (0.1 mg/kg, 2x/wk) for 3 more wks. Vehicle-treated mice exhibited a 6-fold increase in tumor burden. Similar tumor progression was seen in mice receiving ZA or GSI. In contrast, BT-GSI and BT decreased MM growth by 50% compared to vehicle-treated mice. Futher, vehicle-treated mice had a 5-fold increase in osteolytic lesions. ZA, GSI, and BT reduced osteolytic number by 45%, whereas BT-GSI reduced osteolysis by 70% compared to vehicle-treated mice. Morevoer, BT-GSI, BT, and ZA decreased the levels of the systemic bone resorption biomarker CTX, by 30-50% while no CTX changes were seen with GSI. To test the efficacy of lower doses of BT-GSI, KaLwRijHsd mice were injected with 105 5TGM1 cells and randomized after 3 wks as indicated above. Mice bearing MM received either vehicle and equimolar doses of BT-GSI (5 and 2mg/Kg) and BT (2.5 and 1 mg/kg) 3/wk. Mice receiving vehicle injections exhibit a 5-fold increase in tumor burden and 2-fold increase in osteolysis. Both doses of BT-GSI decreased tumor growth by 50-60% and osteolytic lesions by 40-50% compared to vehicle-treated mice. In contrast, none of the lower BT doses affected tumor or bone disease progression. All BT-GSI and BT doses reduced systemic CTX levels. Collectively, these results demonstrate that BT-GSI inhibits MM growth and bone destruction at doses in which GSI and BT are ineffective; and support that bone-targeted Notch inhibition with BT-GSI is a promising therapeutic approach to treat MM disease.

***Disclosures: Tania Amorim**, None*

P-171

Zoledronic Acid Improves Bone Quality and Muscle Function in High Bone-Turnover State *Trupti Trivedi[1], Mohamed Manaa[1], Sutha John[1], Steven Reiken[2], Gabriel Pagnotti[1], SreeMala Murthy[1], Neha Dole[3], Yun She[1], Sukanya Suresh[1], Brian Hain[4], Jenna Regan[1], Rachel Ofer[2], Laura Wright[5], Alex Robling[6], Xu Cao[7], Tamara Alliston[3], Andrew Marks[2], David Waning[4], Khalid Mohammad[5], Theresa Guise[5]. [1]Indiana University School of Medicine, United States, [2]Columbia University, United States, [3]University of California San Francisco, United States, [4]The Pennsylvania State University College of Medicine, United States, [5]Indiana University School of Medicine, United States, [6]Indiana University, United States, [7]Johns Hopkins University School of Medicine, United States

Previous evidence showed that zoledronic acid (ZA), a bisphosphonate inhibitor of osteoclastic bone resorption, prevented the development of muscle weakness induced by bone-derived TGFβ in mice with osteolytic bone metastases. To determine the effects of ZA on bone and muscle function in a nonmalignant setting, we used mouse model Camurati-Engelmann disease (CED), a bone dysplasia with TGFβ-induced accelerated bone remodeling. Wild-type (WT) and CED mice were treated with vehicle (V) or ZA (5μg/kg;3x/wk) for 4 and 10wks; bone and muscle parameters were assessed. CED-V mice showed increased bone remodeling as indicated by increased osteoclasts number (p<0.01), osteoid volume (p<0.05), and BFR (p<0.05) versus WT-V. ZA treatment reduced bone remodeling in CED mice. MicroCT showed CED-V mice had reduced BV/TV in the tibia (p<0.05) and L5 vertebrae (p<0.001) with increased tibial cortical porosity (Ct.Po) (p<0.001) versus WT-V. 3pt-bending of the femur and uniaxial compression of L5 showed decreased resistance to fracture in CED-V compared to WT-V mice. In CED, ZA increased BV/TV, reduced Ct.Po, and improved fracture resistance in the femur and L5. Collectively, ZA had significant effects to improve bone volume and strength in CED mice. Increased pSmad2/3 (p<0.05) in CED skeletal muscle indicated systemic effects of bone-derived TGFβ activity. Excess TGFβ in CED was associated with significant muscle weakness shown by reduced muscle fiber diameter (p<0.001), muscle cross-sectional area (CSA) (p<0.001), forelimb grip strength (p<0.01) and muscle force (p<0.01) relative to WT-V. In CED mice, 4wks and 10wks of ZA treatment reduced muscle pSmad2/3 (p<0.05), increased CSA (p<0.05) and fiber diameter (p<0.05). There was a marginal increase in muscle force after 4wks of ZA in CED mice. However,10wks of preventative ZA significantly increased forelimb grip strength (p<0.05) and muscle force (p<0.001) in CED mice. Reduced muscle force in CED mice was due to Nox4 mediated oxidation of Ca+2 release channel Ryanodine Receptor1(RyR1) and loss of Calstabin in skeletal muscle. ZA improved muscle function by preventing oxidation of RyR1 in CED mice. Our data highlight the profound impact of ZA in maintaining bone health and preserving function in an extreme state of high bone turnover, not associated with malignancy. These effects on muscle are likely indirect, by blocking osteoclastic bone destruction. Potential direct effects cannot be ruled out and are under investigation.

***Disclosures: Trupti Trivedi**, None*

P-172

Syngeneic Murine Bladder Cancer Growing in Bone Responds to Anti-PD-1 Treatment *Mari I. Suominen[1], Katja Fagerlund[1], Jukka P. Rissanen[1], Arne Scholz[2]. [1]Pharmatest Services, Finland, [2]Bayer AG, Germany

The first immunotherapy treatment approved by FDA was for bladder cancer in 1990 when intravesical introduction of weakened, live bacillus Calmette-Guérin (BCG) was found to reduce the cancer recurrence by stimulating an immune response. The overall 5-year survival rate of bladder cancer is 77%, so there are still patients recurring and having distant metastases, approximately half presenting with bone metastases. Today, also bladder cancer patients with metastases can be treated with immunotherapy, since 5 drugs targeting the PD-1/PD-L1 pathway are approved for treatment. However, the effects of immunotherapies in bone metastases are severely understudied. The aim of the study was to establish a novel syngeneic model for bladder cancer bone metastasis that could be utilized in such research. The optimal number of murine MBT-2 bladder cancer cells inoculated into the tibia of 5-6 week-old female C3H/HeN mice was established based on weekly observation of tumor-induced bone changes by X-ray imaging and confirmed by histology. For the anti-PD-1 treatment study, the mice were stratified into two groups based on similar bone lesion areas 10 days post-inoculation and treated with anti-PD-1 therapy or isotype control. Bone changes

were followed by X-ray imaging one week after start of treatment and at sacrifice after three weeks on treatment.In the model establishment study, tumor take rate of 50% was observed. The tumor-induced bone reaction was osteolytic resulting in substantial local bone loss in the mice. The osteolytic bone lesions became visible 7-14 days post-inoculation, and the mice had to be euthanized 4 weeks from the cancer cell inoculations. In histology, large tumors and reduced bone volume of the inoculated tibia were observed. The anti-PD-1 treatment inhibited the increase of osteolytic area. A trend of inhibition was found already after one week of treatment, and significantly lower bone lesion area was observed at sacrifice.The established novel syngeneic bladder cancer bone metastasis model presented good response to anti-PD-1 therapy. These results are in concordance with the clinical efficacy of PD-1/PD-L1 pathway inhibitors, suggesting that the intratibial MBT-2 model could be utilized to increase the knowledge of the effects of these pathway inhibitors in tumor - bone microenvironment. In addition, the efficacy of new immunotherapies and combination therapies could be tested in this model.

***Disclosures: Mari I. Suominen**, None*

P-173

Vitamin D regulates extracellulair vesicle communication of bone metastatic prostate cancer cells *Joelle A Z Klazen[1], Iris J Robbesom[1], Martin E van Royen[1], Andre J van Wijnen[2], Jeroen A Demmers[1], M Carola Zillikens[1], Johannes P T M van Leeuwen[1], Marjolein van Driel[1]. [1]Erasmus MC, Netherlands, [2]Mayo Clinic, United States

The skeleton is a preferential site for metastatic invasion by cancer cells. The metastatic process is determined by complex interactions between cancer cells and the bone microenvironment.In order to unravel a potential mechanism underlying the complexity of bone metastases, we studied the role of extracellular vesicles (EVs). EVs are nano-sized particles that transfer information from cell to cell and thereby support pre-metastatic niche formation in the bone.Since therapeutic intervention is not beneficial in bone metastases yet, we aimed to study the effects of a candidate therapeutic compound on the behavior of bone metastatic prostate cancer cell derived EVs. We selected 1α,25(OH2)D3 vitamin D because of its beneficial effects on bone and negative effects on cancer cell growth.EVs from vitamin D (10-7 M 1α,25-OH2D3) treated and untreated GFP-expressing human bone metastatic prostate cancer cells (PC-3) were isolated by ultracentrifugation (20.000 g and 100.000 g fractions) after one week of culture. EVs were counted by high-resolution flow cytometry (BD influx) and microscopy-image-guided counting (EVQuant). PC-3 EV mRNA content was analyzed by high-throughput next generation sequencing and confirmed by qPCR. PC-3 EV uptake by human osteoblasts (SV-HFO) was measured by flow cytometry (BD Accuri C6). Proteomic profile of PC-3 EVs was analyzed by liquid chromatography-mass spectrometry.Vitamin D treatment decreased the number of PC-3 cells by almost 70%. The surviving cancer cells produced a significantly higher number of EVs per cell in the 100,000 g fraction (increase of 82%, p=0.0008). This 100,000 g EV fraction of the vitamin D treated PC-3 cells contained a different set of preferentially packaged mRNAs compared to the EVs from untreated cells. Interestingly, vitamin D treatment of PC-3 cells resulted in less uptake of EVs by human osteoblasts (15% reduction (p=0,013) for the 100.000 g and 43% (p=0.0260) for the 20.000 g fraction). This was accompanied by a lower adhesion protein profile on the EV membrane. Remarkably, despite this decreased EV uptake by osteoblasts, gene expression levels of the preferentially packaged EV mRNAs of the vitamin D treated PC-3 cells were highly upregulated (towards 200 fold) in the recipient osteoblasts.Our data identify new ways in which vitamin D affects the communication route of bone metastatic prostate cancer cells, but cannot prevent surviving cancer cells to set their landmarks for metastatic outgrowth.

***Disclosures: Joelle A Z Klazen**, None*

P-174

Runx2 Regulates Cytoskeletal Dynamics in Bone Metastatic Breast Cancer Cells *Ahmad Othman[1], Marcus Winogradzki[1], Jitesh Pratap[1]. [1]Rush University Medical Center, United States

Bone metastasis is a significant contributor to breast cancer mortality, with no current treatment available. Aberrant expression of the transcriptional regulator Runx2 facilitates bone metastasis. Recently, Runx2 has been shown to enhance autophagy, a process of degradation of damaged organelles and proteins into subunits for biosynthesis. Autophagosomes traffic along microtubules (MTs). Acetylation of a-Tubulin (Ac-a-Tub) stabilizes MTs and prevents it from buckling under the forces of traffic. High levels of Ac-a-Tub and autophagy are independently linked with breast cancer metastasis. We found that Runx2 promotes Ac-a-Tub and MTs stability. However, questions regarding the mechanism of Runx2 mediated-Ac-a-Tub and MTs stability remain. Using patient biopsies, bone-derived breast cancer cells, gene and tumor arrays, we examined autophagy, Ac-a-Tub, and dynamics of MTs polymerization. The tumor array showed a significant association between high levels of Runx2 and autophagy, while patient biopsies showed increased Ac-a-Tub staining in bone metastatic samples compared to primary tumors. Profiling of 168 autophagy and cytoskeletal-related genes revealed that the majority of the genes were unchanged with Runx2 silencing. We found a 2.5 fold decrease in mRNA and protein levels of Transglutaminase-2 (TGM2) in control cells, however, its inhibition did not change autophagy or Ac-a-Tub. Furthermore, no significant changes were observed in regulators of Ac-a-Tub (HDAC6, SIRT2, and ATAT1) with Runx2 silencing. Additionally, expression of WT and transcriptionally inactive mutant of Runx2 increased Ac-a-Tub and MT polymer mass, while a C-terminal deletion mutant failed to recapitulate these findings. These results indicate a novel transcriptional independent regulation of Ac-a-Tub via Runx2. We tested whether Runx2 alters activity or subcellular localization of regulators of Ac-a-Tub via protein-protein interaction. Inhibition of HDAC6 activity increased Ac-a-Tub and autophagy, while SIRT2 silencing resulted in minimal changes. We used Leptomycin-B to suppress protein shuttling between the nucleus and cytoplasm and found enhanced Ac-a-Tub in both control and Runx2 silenced cells. Taken together, these results show that Runx2 may alter localization and activity of the regulators of Ac-a-Tub. Our studies suggest that autophagy, Runx2, and Ac-a-Tub levels may help stratify bone metastatic patients for effective treatments with FDA approved MTs targeting agents.

***Disclosures: Ahmad Othman**, None*

P-175

Modeling Spontaneous Bone Metastasis of Human Prostate Cancer in Mice *Vera Labitzky[1], Ann-Kristin Ahlers[1], Anke Baranowsky[1], Udo Schumacher[1], Tobias Lange[1]. [1]University Medical-Center Hamburg-Eppendorf, Germany

Purpose: The prognosis of prostate cancer (PCa) patients largely depends on whether or not distant metastases occur with the bone marrow (BM) being a frequent metastatic site. One efficient and common approach for studying BM metastasis in vivo is to inject human tumor cells intracardially into immunodeficient mice. However, such procedure circumvents early steps of the metastatic cascade due to the lack of a primary tumor. The purpose of this study was therefore to develop a xenograft model of human PCa in which BM metastases are spontaneously formed.Methods: Establishment of subcutaneous (s. c.) xenografts of human PCa cells (PC-3 expressing firefly luciferase (Luc2)) in SCID and NSG mice; at ~1cm³ primary tumor volume: necrospy (control group) or tumor resection (OP group); post-surgical monitoring of BM metastasis outgrowth by in vivo-bioluminescence imaging (BLI); detection of skeletal and pulmonary metastases by ex vivo-BLI at necropsy, corresponding histology; quantification of spontaneous dissemination to the blood, lung and BM by Alu-PCR at necropsy; establishment of PC-3-Luc2 sublines by re-cultivation of xenograft primary tumor and BM metastasis cells.Results: The baseline level of spontaneous lung and BM metastasis formation (control group) was low for PC-3-Luc2 cells. For instance, we could only detect single disseminated tumor cells in the lung by histology while metastatic cells in the BM were only detectable by Alu-PCR. Primary tumor resection prolonged the life span, thereby enabling outgrowth of lung, but not BM metastases (OP group). Skeletal lesions could be identified by ex vivo-BLI, but were not visible by histology, when every 10th section (4 µm each) of the area of interest was examined (OP group). The overall level of circulating tumor cells and metastatic cells at both sites (Alu-PCR) was higher in the more immunodeficient NSG as compared to SCID mice. Despite the lack of detectable outgrowth of BM metastases, human PC-3-Luc2 cells could regularly be recovered from the BM of long bones after surgery for in vitro expansion.Conclusion: In spontaneous metastasis xenograft models of PC-3, higher metastasis yields can be obtained in NSG as compared to SCID mice. Primary tumor resection enables the outgrowth of lung, but not BM metastases. This model might be particularly useful for future studies on how metastatic outgrowth is regulated in a dormancy-inducing (BM) vs. metastasis-permissive (lung) environment.

***Disclosures: Vera Labitzky**, None*

P-176

Anti-resorptive Off-medications May Yield Differential Remodeling vs. Exposure on Alveolus in Cancer-survivors: Analysis of the Outcome-variables *Yen Chun Grace Liu[1], Andy Yen-Tung Teng[2]. [1]Center for Osteoimmunology & Biotechnology Research (COBR) & Dept. of Oral Hygiene, School of Dentistry & College of Dental Medicine, Kaohsiung Medical University (KMU) & KMU-Hospital, Kaohsiung, Taiwan, Taiwan, Province of China, [2]Center for Osteoimmunology & Biotechnology Research (COBR), College of Dental Medicine, Kaohsiung Medical University & Hospital, Kaohsiung, Taiwan, Taiwan, Province of China

Objectives: It is clear that specific anti-resorptive drugs (ARDs), including bisphosphonates, anti-RANKL MAbs (Prolia/Xgeva), anti-angiogenics on VEGF signaling and selective estrogen receptor modulators (SERM) are clinically associated with patients who suffer from adverse reactions in the maxillofacial regions, via quiescent or progressive bone or mucosal destruction, termed MRONJ. Thus, we proposed to correlate the clinical manifests, based on the therapeutic timing on off-medications(holidays) for their latency to follow-ups over the clinical courses where the resulting healing or improvements of bony or mucosal lesions with/without exposures were end-marked over time for analyses. Methods: Among 96 MRONJ-diagnosed patients from the clinics (e.g., 40% cancer survivors, 30% osteoporosis & 30% arthritis; M:64+/-5.8yrs & F:66+/-7.2yrs), clinical data were retrieved from established records of MRONJ, whose ARDs were dichotomized for on- or off-holidays (i.e., 4-to-48 months), drugs' intervals and the effects assigned as (co)-variables for the statistical correlations with other measures, where the off-holidayed was primarily due to related medical concerns. Student t-test was to compare variables among on- vs. off-holidayed MRONJ-stages (i.e.,-1,-2,-3) & timing employed, and the one-way ANOVA was to compare the clinical (co)-variables among all different ARDs employed. Level of significance was set at $p<0.05$; all data analyzed using SAS8.2. Results: The analyses showed that: i) the on-holidayed with Prolia/Xgeva in the cancer survivors was significantly effective in alleviating the episodic attacks and progressive frequencies of MRONJ's bone manifests ($p<0.01$) on

comparisons; ii) conversely, such on- or off-holidays (i.e., Prolia) was detected non-equally effective in MRONJ subjects with severe osteoporosis vs. osteoarthritis, in contrast to those amongst the cancer-survivors; iii) such differential outcomes on bone manifests in cancer survivors appeared significantly associated with the drugs' dosing & timing applied ($p<0.05$, ANOVA), compared to other (co)-variables analyzed. Concludion: The present findings suggest that specific ARDs (i.e., Prolia/Xgeva) were associated with specific causes on alveolus on distinctive bone vs. mucosal remodeling measures in cancer survivors over time (i.e., 48-month), whose underlying mechanisms, once revealed, will facilitate the development & designs of the new treatment modalities/protocols with urgent needs.

***Disclosures: Yen Chun Grace Liu**, None*

P-177

Osteoblasts Derived from Mouse Mandible Enhance Tumor Growth of Prostate Cancer More Than Osteoblasts Derived from Long Bone *Yusuke Shiozawa[1], Matthew Eber[1], Sun Park[1], Fang-Chi Hsu[1]. [1]Wake Forest University Health Sciences, United States

Prostate cancer (PCa) metastasizes to bone, where the bone marrow microenvironment controls disease progression. However, the cellular interactions that result in active bone marrow metastases are poorly understood. A better understanding of these interactions is critical to success in the pursuit of effective treatments for this life ending disease. Anecdotally, we observe that after intracardiac injection of PCa cells, one of the greatest tools to investigate the mechanisms of bone-metastatic disease, animals frequently present with mandible metastasis before hind limb metastasis. Therefore, in this study, we investigated whether the bone cells derived from the mouse mandible influence PCa progression differently than those from the hind limb.We first validated that in the intracardiac model of metastatic PCa, mandible bone lesions often occur before hind limb bone lesions, which is anecdotally well-recognized. We then showed that cells derived from both the mandible and hind limb bones of mice have osteoblastic properties, and that mandible osteoblasts (MaOBs) have a higher potential for osteoblastic differentiation than hind limb osteoblasts (HLOBs) both in vitro and in vivo. Interestingly, when PCa cells were co-cultured with these osteoblasts, PCa cells grew significantly faster in co-culture with MaOBs compared to HLOBs. Consistently, PCa cells co-implanted with MaOBs into the animals grew faster and larger tumors than those co-implanted with HLOBs. This may be due to the observation that MaOBs grow faster than HLOBs, but not that MaOBs are more differentiated than HLOBs, as differentiation of osteoblasts through L-Ascorbic acid and β-Glycerophosphate supplementation failed to increase PCa growth in vitro.Together, our study demonstrated that faster growing osteoblasts can lead to the proliferation of PCa cells. Although further studies are clearly needed, these findings suggest that the proliferation status of osteoblasts plays a crucial role in the regulation of the growth of bone metastatic cancer cells. Therefore, by developing drugs that are able to alter osteoblastic proliferation, perhaps we can mitigate the problem of recurrence in PCa patients either by perpetuating dormancy of bone metastatic cells indefinitely, or by releasing bone metastatic cells from dormancy and making them more susceptible to anti-cancer therapies that rely on proliferation pathways in order to eradicate the disease entirely.

***Disclosures: Yusuke Shiozawa**, None*

P-178

The Value of SSTR2A Immunohistochemistry in Tumor- Induced Osteomalacia *Seunghyun Lee[1], Namki Hong[2], Sang-kyum Kim[3], Yumie Rhee[2]. [1] Department of Internal Medicine, Severance Hospital, Endocrine Research Institute, Yonsei University College of Medicine, Republic of Korea, [2]Department of Internal Medicine, Severance Hospital, Endocrine Research Institute, Yonsei University College of Medicine, Republic of Korea, [3]Department of Pathology, Yonsei University College of Medicine, Republic of Korea

Tumor-induced osteomalacia(TIO) is a paraneoplastic disease with hypophosphatemia in which phosphaturic mesenchymal tumor-mixed connective tissue variant(PMT-MCT) secrete excessive fibroblast growth factor 23(FGF23). The localization of the tumor is important because curative surgery is possible. However, it is difficult to make a confirmative diagnosis from a histologic perspective because PMT-MCT is similar in appearance to other tumors such as hemangiopericytoma, osteosarcoma. Therefore, a more sensitive histologic biomarker is needed to support the diagnosis of TIO. To date, FGF23 immunohistochemistry(IHC) or RT-PCR has been proposed as a useful adjunctive tool to confirm the diagnosis of TIO. However, the staining pattern of FGF23 IHC is often focal, limiting diagnostic utility, particularly in small biopsies. Recently, a 68Ga-DOTATOC scan, which sensitively detects expression of somatostatin receptor 2A (SSTR2A) in the tumor, demonstrated diagnostic value in localizing TIO. Based on this finding, we compared the diagnostic performance of FGF23 and SSTR2A IHC in patients with TIO, along with results of the 68Ga-DOTATOC scan. Medical records of patients with surgically confirmed TIO in Severance hospital from November 2010 to July 2019 were reviewed. Unstained slides of 13 patients (7 males, 6 females) were obtained from the pathology repository of Severance hospital to perform additional IHC for FGF23 and SSTR2A. Among 13 patients, 12 patients underwent a 68Ga-DOTATOC scan, which successfully detected suspicious lesion except for one case. Histological evaluation was performed by a single pathologist based on the H-score system using three components: the degree of dysplasia of the spindle cell, the presence of osteoclast type giant cell reaction, and the presence of rich vasculature. H-score was calculated by multiplying expression percentage and intensity with score 0 to 2 for each component(total score 0 to 6 points). SSTR2A showed higher H-score(median 6[IQR 6-6] vs. 4[2-6], p=0.009) compared to FGF23 IHC. When the nuclear pattern was counted as nonspecific, even greater difference of H-score was observed (SSTR2A 6 [6-6] vs. FGF23 0 [0-2], p=0.001). Our findings suggest that SSTR2A IHC with H-score quantitation might be a sensitive, adjunctive diagnostic tool to ascertain the histologic diagnosis of TIO compared to FGF23 IHC. Further validation with negative controls is needed to evaluate the diagnostic accuracy of SSTR2A IHC.

***Disclosures: Seunghyun Lee**, None*

P-179

Serum total periostin is an independent marker of overall survival in non-small cell lung cancer *Jean-Charles Rousseau[1], Emmanuel Massy[2], Madiagne Gueye[3], Edith Bonnelye[4], Marie Brevet[5], Laurianne Chambard[3], Michael Duruisseaux[6], Olivier Borel[1], Christelle Roger[1], Raphaelle Guelminger[6], Jean-Baptiste Pialat[7], Evelyne Gineyts[8], Lamia Bouazza[1], Marjorie Millet[1], Jean-Michel Maury[9], Philippe Clezardin[1], Nicolas Girard[10], Cyrille Confavreux[11]. [1]Inserm UMR 1033, France, [2]Inserm UMR1033 - Hospices Civils de Lyon - Université de Lyon, France, [3]Service de Rhumatologie - Hospices Civils de Lyon, France, [4]Inserm UMR1033 - CNRS ERL 6001/inserm U1232 - Institut de Cancérologie de l'Ouest - St Herblain, France, [5]Anatomie Pathologie-Hospices Civils de Lyon, France, [6]Service de Pneumologie - Hospices Civils de Lyon, France, [7]Service de Radiologie - Hospices Civils de Lyon, France, [8]inserm UMR 1033, France, [9]Service de Chirurgie Thoracique, Hospices Civils de Lyon, France, [10]Institut du Thorax Curie-Montsouris, France, [11]Inserm UMR1033 - Hospices Civils de Lyon - Université de Lyon, France

Introduction. Lung cancer is a worldwide leading cause of mortality. At diagnosis, 30 to 50% of non-small cell lung cancers (NSCLC) have bone metastases. The set-up of a metastatic niche between cancer cells and bone microenvironment is a key step of bone metastasis physiopathology. Periostin, an extracellular matrix protein, is expressed in bone in response to mechanical stress. In cancer setting, in vivo experiments have shown that periostin in microenvironment was an early event of the niche process favoring cancer cell proliferation through Wnt signaling. Moreover, some cancer cells overexpressed periostin. Thus, we wanted to test the prognosis value of serum total periostin level in NSCLC patients.Methods. Blood samplings were performed in NSCLC patients either with localized tumor or with a first bone metastasis (metastatic group). Patients were prospectively followed. NSCLC patients were paired on age and gender to healthy controls from OFELY and STRAMBO cohorts. Serum periostin was assessed using Biomedica® ELISA kit. Survival analysis and multivariate Cox model have been conducted in the overall cancer population and in the bone metastatic sub-group. Results. 133 patients, aged 64+/-11 years, have been enrolled into non-metastatic (n=67) and metastatic (n=65) group. Median follow-up was 2.8 years. Median serum periostin level was 1092 pmol/L in the whole cancer population. Periostin level was similar between localized tumor patients and controls but significantly higher (+40%) in bone metastases patients (medians : 887 vs 1009 vs 1703 pmol/L respectively; $p<0.0001$).Metastatic status and a high serum periostin level (>= 1092 pmol/mL) was associated with a higher risk of death (HR [95% CI]=2.80 [1.59-4.95]; p=0.0003 and HR=2.09 [1.06-4.13]; p = 0.03 respectively) in multivariate Cox model. In bone metastatic group, the Cox multivariate model including age, CRP, CTX, Ca, albumin lymphocytes index, showed that an elevated periostin (above the highest value of localized group) remained associated with a higher risk of death (HR=3.62 [1.74-7.52]; p=0.0005). Moreover, using the same antibody than the ELISA, we performed immunohistochemistry on bone metastasis biopsies. Beyond bone matrix expression, we observed intranuclear expression in tumoral cells.Conclusion. Our results in NSCLC, showed that serum periostin was associated with overall survival and that periostin might be overexpressed by lung cancer cells in bone metastatic niche.

***Disclosures: Jean-Charles Rousseau**, None*

P-180

Investigating the Effect of Yoda1 on Osteocytes Mechanoregulation of Breast Cancer Bone Metastasis *Chun-Yu Lin[1], Liyun Wang[2], Lidan You[1]. [1]University of Toronto, Canada, [2]University of Delaware, United States

Introduction: Bone metastasis is a severe complication causing the major mortality of breast cancer patients. Since metastasized breast cancer disrupts the balanced bone remodeling through the crosstalk with bone cells, exercise which mediates bone remodeling through mechanical loading and attenuates metastatic tumor growth could act as a preventive strategy. However, commonly prescribed exercise can be physically challenging for cancer patients who are frail and can increase their risk of accidental injury, keeping them from benefiting from exercise. Yoda1, an activator of the mechanosensitive Piezo1 channel, provides a unique target to simulate bone condition under exercise without actual significant movement of patients by enhancing mechanosensitivity of osteocytes, the major mechanosensory bone cells with high expression of Piezo1 [1]. Building from our previous results showing stimulated osteocytes with oscillatory fluid flow (OFF) inhibit cancer invasion using a microflu-

idic platform [2], this project aims to study if similar inhibition could be achieved under low shear stress OFF stimulation combining with Yoda1.Methods: Cell viability of MLO-Y4 osteocytes-like cells and 4T1.2 breast cancer cells under Yoda1 treatment are tested by Calcein AM. Then, rescuing mechanosensitivity of MLO-Y4 under 0.5 Pa low shear stress OFF by various concentration of Yoda1 is evaluated by intracellular calcium imaging (flow-on for 3 mins). Finally, using microfluidic platform, we study the inhibition of 4T1.2 extravasation by Yoda1 treated MLO-Y4 under low shear stress OFF. MLO-Y4 seeded in the platform is treated with optimized concentration of Yoda1 and stimulated by 0.5Pa OFF 2 hrs/day for 4 days, while adjacent non-stimulated lumen channel is coated with C166 endothelial cells and seeded with 4T1.2. The invasion distance and percentage that 4T1.2 migrate across lumen into side channels are monitored by fluorescence microscope.Results: MLO-Y4 and 4T1.2 both demonstrate high cell viability under Yoda1 treatment (Figure A). Align with our hypothesis, preliminary data shows pretreating MLO-Y4 with 5 μM Yoda1 increases osteocytes response rate under 0.5Pa OFF by 21.5 % compared with untreated group (Figure B). 4T1.2 extravasation distance decreases in stimulated MLO-Y4 group (Figure C). To conclude, this project provides a novel treatment concept to prevent bone metastases for the fragile population.References: [1] Li. eLife. 2019. [2] Mei. Integr Biol. 2019.

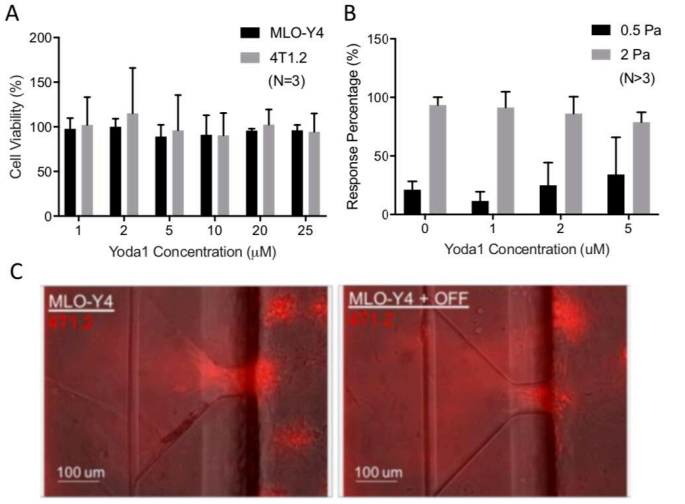

A) Cell viability of MLO-Y4 and 4T1.2 under different concentration of Yoda1. B) Intracellular calcium response percentage of MLO-Y4 under 0.5 or 2 Pa OFF with or without Yoda1 pre-treatment. C) Fluorescence images of 4T1.2 migration with or without MLO-Y4 exposed to 1 Pa OFF (anticipated results with Yoda1 treatment under 0.5 Pa OFF)

***Disclosures: Chun-Yu Lin**, None*

P-181

Targeting Cartilage Epidermal Growth Factor Receptor (EGFR) Pathway for Osteoarthritis Treatment *Yulong Wei[1], Ling Qin[1], Tao Gui[1]. [1]University of Pennsylvania, United States

Osteoarthritis (OA) is the most common chronic condition of the joints. Despite the fact that OA patients have a great level of pain and disability, neither a cure nor disease-modifying treatment exists. Our previous studies revealed that mice lacking EGFR activity specifically in cartilage (Col2-Cre) have accelerated knee OA during aging or after DMM surgery. To test whether this pathway can be targeted as a novel OA therapy, we overexpressed HBEGF, an EGFR ligand, using constitutive Col2-Cre and inducible Aggrecan-Cre (Tamoxifen x 5d at 3 mo of age). These mice had elevated p-EGFR and p-ERK levels specifically in cartilage. Compared to WT, Col2-Cre HBEGFOver mice had persistently enlarged articular cartilage (23% and 34% increases at 1 and 5 mo of age, respectively, n=8/group), due to an expanded pool of chondroprogenitors (79%) with elevated proliferation ability (49%), survival rate (68%), and lubricant production (52%). Strikingly, after receiving DMM surgery at 3 mo of age, both HBEGFOver models were resistant to cartilage degeneration (Mankin Score: sham: 0.9; DMM WT 10.0, DMM Col-Cre 2.1, DMM Aggrecan-CreER 2.5, n=8/group) and OA-induced joint pain 4 mo later. Treating mice with Gefitinib, an EGFR inhibitor, abolished the protective action against OA in HBEGFOver mice (Mankin Score: 9.0, n=8/group). To pharmacologically target EGFR, we conjugated TGFα, a potent EGFR ligand, to polymeric micellar nanoparticles (NPs) via copper-free click chemistry. Cationic diblock copolymer PLL-PCL was introduced into the PEG-PCL NP to reduce the surface charge for improved cartilage binding. The resultant TGFα-NPs were stable and non-toxic with superior cartilage uptake, penetration, and joint retention abilities. They bound to primary chondrocytes and potently activated EGFR downstream targets in a TGFα/EGFR-specific manner. Intra-articular delivery of TGFα-NPs once every 3 wk for 3 mo effectively attenuated DMM surgery-induced OA cartilage degeneration (Markin Score: veh 8.9, TGFα 8.1, NP 8.4, TGFa-NP 3.3, n=8/group), subchondral bone plate sclerosis, and joint pain. Genetic or pharmacologic activation of EGFR revealed no obvious side effects in knee joints and major vital organs in mice. Taken together, our studies demonstrate the feasibility of targeting EGFR signaling for OA treatment as a novel therapeutic approach using nanotechnology.

***Disclosures: Yulong Wei**, None*

P-182

Runx3 protects articular cartilage by direct induction of Prg4 *Kosei Nagata[1], Taku Saito[1], Fumiko Yano[1], Hironori Hojo[2], Yasuhide Iwanaga[1], Sakae Tanaka[1]. [1]Department of Orthopaedic Surgery Faculty of Medicine The University of Tokyo, Japan, [2]Department of Bioengineering, The University of Tokyo, Japan

Runx transcription factor family, including Runx1, Runx2, and Runx3, modulates skeletal development and osteoarthritis pathogenesis. Here, we examined expression and roles of Runx3 in these processes.Runx3 was expressed in the hypertrophic zone of mouse epiphyseal cartilage, and Col2a1-Cre;Runx3fl/fl mice displayed no obvious abnormality in skeletal formation.In adult mouse articular cartilage, Runx3 was dominantly detected in superficial zone. Runx3 proteins decreased with cartilage degeneration in both mouse and human cartilage.We next prepared Col2a1-CreERT2;Runx3fl/fl and Prg4-CreERT2;Runx3fl/fl mice for Runx3 deletion in total and superficial articular cartilage after skeletal growth, respectively, and compared with Runx3fl/fl littermates. Notably, osteoarthritis development was significantly accelerated in surgically-induced model by resection of medial meniscus and medial collateral ligament (medial model, n = 12, each) and aging model (n = 10, each) of Col2a1-CreERT2;Runx3fl/fl mice. Immunohistochemistry of sham joints showed that rate of Runx3 positive cells and Prg4 and Aggrecan positive area were decreased in Runx3-knockout articular cartilage. Prg4-CreERT2;Runx3fl/fl mice also displayed enhanced osteoarthritis progression both in the medial model (n = 10, each) and destabilization of medial meniscus model (n = 8, each).To identify target genes of Runx3, we isolated superficial chondrocytes from Col2a1-Cre;Runx3fl/fl and Runx3fl/fl mice and performed RNA- and ChIP sequencing. Extracellular matrix formation and collagen fibril organization were indicated as the Runx3 roles in superficial chondrocytes. Prg4 was identified as a target gene of Runx3 in the superficial chondrocytes, and other extracellular matrix genes were decreased by Runx3 knockout in deep zone chondrocytes.In primary chondrocytes, Runx3 knockout leaded to downregulation of anabolic genes such as Acan/Aggrecan, and Prg4/Lubricin, while Runx3 overexpression induced these factors.Finally, we performed intra-articular administration of Runx3 or GFP adenoviral vectors into knee joints of wild-type mice after the medial model surgery (n = 10, each). Runx3 overexpression was confirmed by immunohistochemistry, and osteoarthritis development was significantly suppressed by Runx3 maintenance. We conclude that Runx3 protects articular cartilage through its anabolic roles, and may be a potential therapeutic target for osteoarthritis.

***Disclosures: Kosei Nagata**, None*

P-183

Notch signaling contributes to articular cartilage homeostasis by suppressing differentiation of superficial zone cells *Yasuhide Iwanaga[1], Kosei Nagata[1], Fumiko Yano[2], Sakae Tanaka[3], Taku Saito[4]. [1]graduate student, Japan, [2]Specially Appointed Associate Professor, Japan, [3]Professor, Japan, [4]Associate Professor, Japan

Notch is a single-pass transmembrane cell-surface receptor that plays a crucial role in cell-fate determination and differentiation during development. We previously reported that Notch-Hes1 pathway promotes osteoarthritis (OA) development; however, there are a few paradoxical reports and the mechanism underlying regulation of joint homeostasis by Notch signaling has not been fully elucidated. Recent studies have shown that superficial zone (SFZ) of articular cartilage not only contributes to joint surface lubrication by producing lubricin/Prg4, but contains progenitors of articular chondrocytes. Here, we examined expression and functions of Notch signaling in the SFZ. mRNA levels of Notch-related molecules, including Notch1, 2, and Hey1, were highly expressed in SFZ cells, compared to deep zone cells. For in vivo experiments, we generated Prg4-CreERT2;Rbpjfl/fl (KO) mice to delete Rbpj, an intranuclear cofactor of Notch intercellular domain (NICD), and to suppress Notch signaling activity specifically in the SFZ. After tamoxifen (TM) injection for 5 days at 11 weeks of age, surgical destabilization of medial meniscus (DMM) was conducted in the right knee. TM-treated KO mice displayed marked OA development, i.e., cartilage destruction and osteophyte formation, 3 months after the surgery. Similarly, OA development was markedly enhanced in 12-month-old KO mice which received TM injection at 9 months. We further mated KO mice with Ai14 reporter mice, and examined fate of Rbpj-knockout SFZ cells, indicated as red fluorescent protein (RFP)-positive cells. Notably, RFP-positive cells were broadly distributed in the deep zone, while they disappeared in the SFZ within 8 weeks. RFP-positive cells were also detected widely in ectopic endochondral ossification in peri-articular regions. In explant culture of femoral heads, chondrocyte maturation, determined by mRNA levels of Col2a1 and Acan, were enhanced by Rbpj knockout. In contrast, these markers were significantly suppressed in SFZ cells by NICD overexpression. In conclusion, Notch signaling is essential for SFZ cells to maintain the undifferentiated nature, and contributes to homeostasis of articular joints.

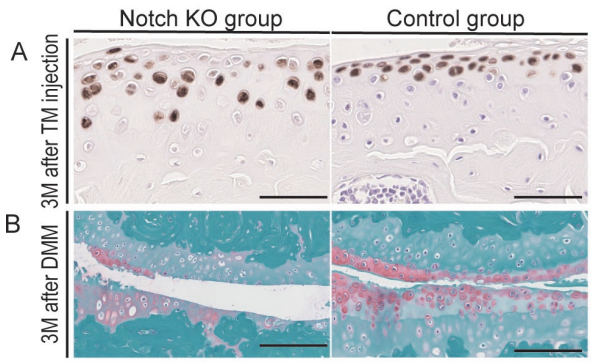

(A) Cell tracking of SFZ cells in using Prg4-Cre^{ERT2};Rbpj$^{fl/fl}$;*Ai14* (KO), and Prg4-Cre^{ERT2};*Ai14* (control), 3 months after TM injection. RFP-positive cells were distributed in deep zone in KO mice, while they were localized in SFZ in control mice. (B) Medial knee joints of KO and control mice 3 months after the DMM surgery. Scale bars, 100 μm.

***Disclosures: Yasuhide Iwanaga**, None*

P-184

A Transgenic Rat for Noninvasive Assessment of Chondrogenesis In Vivo *Elisabeth Ferreira[1], Hong Wu[2], Landon Gatrell[2], Ryan Porter[1]. [1]1University of Arkansas for Medical Sciences, Department of Internal Medicine. 2Department of Orthopaedic Surgery. 3Center for Musculoskeletal Disease Research., United States, [2]University of Arkansas for Medical Sciences, Department of Internal Medicine, United States

Chondroprogenitor cell (CPC) differentiation, or chondrogenesis, represents an important bottleneck in the repair of not only articular cartilage, but also appendicular bone. Rat models of skeletal injury and repair are frequently employed in the preclinical development of novel treatments for stimulating new chondrogenesis. To support these efforts, we generated a transgenic rat strain that can be used to either noninvasively report endogenous chondrogenesis, for correlation with endpoint measures of tissue repair, or provide a source of exogenous reporter CPCs for use in transplantation studies. A transgene was constructed in which bioluminescent (firefly luciferase) and fluorescent (mCherry) reporters were placed under control of regulatory sequences from rat Col2a1. This transgene was injected into Lewis rat embryos, transgene-positive pups were bred with wild type Lewis rats, and the candidate lines were imaged by serial bioluminescence imaging. For two lines, substantial bioluminescence signal was detected from cartilaginous regions, including the appendicular synovial joints, spine, sternum, nose, and ears. Bioluminescent radiance was intense at 1 month of age and rapidly declined with continued development, though signal was still readily detected above background in 17 month old animals. For the most promising line, reporter activity was evaluated at 5, 8, 12, and 23 weeks of age ex vivo. Explant imaging and immunohistochemistry confirmed that both firefly luciferase and mCherry expression are localized to cartilage, while non-cartilaginous tissues (e.g., fat, muscle, kidney) exhibited negligible reporter levels. Longitudinal trends in reporter mRNA levels and luciferase activity agreed with in vivo imaging. To determine whether this model can report de novo chondrogenesis, we overexpressed bone morphogenetic protein 2 within the gastrocnemius muscle, which leads to ectopic bone formation through an endochondral pathway. Two to three weeks after initiating BMP2 overexpression, bioluminescence signal was detected from the muscle; this signal preceded heterotopic ossification, as determined by concurrent X-Ray imaging. Histology of explants taken during peak bioluminescence confirmed that this signal was associated with ectopic cartilage in the muscle. This animal model can help develop new strategies for stimulating cartilage and endochondral bone formation or for inhibiting chondrogenesis associated with heterotopic ossification.

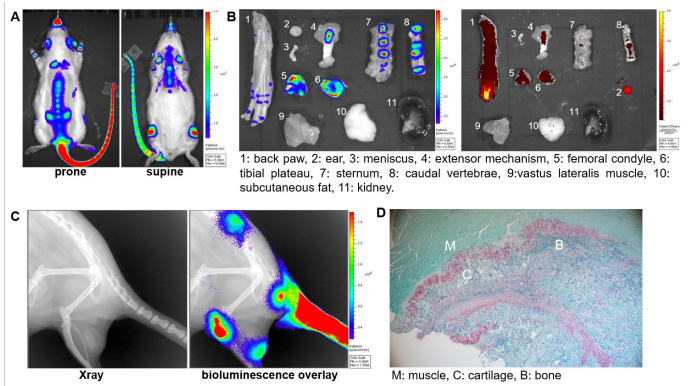

(**A**) Representative images of an adult 30-week old rat imaged after intra-peritoneal injection of D-Luciferin (150 mg/kg). (**B**) Bioluminescent (left) and fluorescence (right) imaging of explants from a 5-week old rat; luminescence was acquired 10 min after tissue incubation in D-Luciferin (0.5 mg/mL). (**C**) X-ray (left) and X-ray/bioluminescence overlay (right) from a 34-week old rat, 21 days after induction of BMP2 overexpression in the gastrocnemius msucle. (**D**) Safranin O / Fast Green stain of explant harvested from rat in (C).

***Disclosures: Elisabeth Ferreira**, None*

P-185

The role of Sox9 SUMOylation during mouse skeletal development *Masafumi Inui[1]. [1]Meiji University School of Agriculture, Japan

Sox9 is a transcription factor essential for the chondrocyte differentiation in vertebrate. As the skeletal morphology alters sensitively to the change of Sox9 dosage, Sox9 activity is tightly regulated in multiple layers including post-translational modifications (PTMs). In vitro studies have reported the possible inhibitory role of ubiquitination or SUMOylation on Sox9 transcriptional activity, but the in vivo relevance of these PTMs during the skeletal development remains unknown. To elucidate the role of Sox9 PTMs in skeletal development, we introduced a point mutation to the genomic sequence of mouse Sox9 so that 396th lysine, an evolutionary conserved PTM target residue, is substituted to arginine. The mouse carrying Sox9K396R mutation showed reduced body size, delayed endochondral ossification, and up-regulation of Sox9 target genes, indicating that Sox9 activity is negatively regulated by the PTMs on K396 during skeletal development. The long bones of Sox9K396R mouse became shorter and thicker, probably due to the disturbed columnar alignment of proliferation zone chondrocytes. Sox9 protein level was not altered in Sox9K396R chondrocyte, implying that K396 was targeted by regulative modification. Consistently, K396R mutation on Sox9 abolished its SUMOylation, but not the ubiquitination, indicated that SUMOylation is the major PTM on K396. We found that SUMO-fused Sox9 localized in nucleus, bound DNA, but could not activate the target gene expression. Furthermore, SUMO-fused Sox9 repressed the transcriptional activity of co-expressed non-SUMOylated Sox9 in a promoter dependent manner. As the SUMOylation level was reduced in mutant Sox9 that could not bind DNA, SUMOylation could act as a negative feedback regulation on Sox9 transcriptional activity. In sum, our study revealed the in vivo relevance of PTMs on Sox9 in mammalian skeletal development.

***Disclosures: Masafumi Inui**, None*

P-186

The Epigenetic Reader Brd4 Regulates Long Bone Formation *M. Lizeth Galvan[1], Christopher Paradise[1], Sofia Jerez[1], Eva Kubrova[1], S. Sharare Dehghani[1], Oksana Pichurin[1], Roman Thaler[1], Andre van Wijnen[1], Amel Dudakovic[1]. [1]Mayo Clinic, United States

Formation of long bones by endochondral ossification, a process in which a cartilaginous matrix is replaced by mineralized tissue, is controlled by signaling pathways that regulate key transcription factors, including Sox9 and Runx2. The accessibility of these factors to chondrogenic genes is modulated by chromatin structure which is linked to post-translational modifications on histone proteins. We recently showed that the epigenetic regulator Brd4, a bromodomain protein that binds and interprets acetylated lysines on histones, supports osteogenic differentiation in vitro. Our current studies assess the functional contribution of Brd4 on long bone formation and chondrogenesis. Conditional (cKO) ablation of Brd4 in the mesenchyme (Prrx1-Cre) yields viable mice that are smaller and exhibit impairments in endochondral ossification. Specifically, mesenchymal Brd4 loss delays long bone formation (46% decline in femoral length at 3 weeks) and causes abnormal growth plate morphology. In support, a significant reduction in proliferative zone (25% decline at 1 week) and hypertrophic zone (40% decline at 1 week) within the physis and impaired formation of the secondary ossification center (60% decline at 3 weeks) is observed in Brd4 cKOPrrx1 mice. We also generated mice in which Brd4 function is ablated in chondrocytes (Col2a1-Cre). With the exception of a few survivors, the majority of Brd4 cKOCol2a1 perish immediately after birth. Preliminary assessment of surviving mice and embryos reveals shortened long bones, suggesting that chondrocyte-specific Brd4 loss impairs endochondral ossification. In vitro assessment of ATDC5 cells and ex vivo analysis of immature mouse articular chondrocytes

reveals that Brd4 supports chondrogenic differentiation and maturation, reflected by reduced expression of endochondral genes, Alcian Blue staining and Alizarin Red staining. Loss of Brd4 function significantly suppresses expression of genes that are regulated by Sox9 (e.g., Col2a1 and Acan) and Runx2 (e.g., Sp7/Osx and Mmp13) in differentiating chondrocytes. Hence, our results suggest that Brd4 is required for long bone formation and facilitates the transcriptional activities of Sox9 and Runx2 to support endochondral bone formation.

***Disclosures: M. Lizeth Galvan**, None*

P-187

Glutamine Metabolism in Cartilage Tumors *Hongyuan Zhang[1], Vijitha Puviindran[1], Puviindran Nadesan[1], Hidetoshi Tsushima[2], Yuning Tang[3], Leyao Shen[1], Guofang Zhang[4], Courtney Karner[1], Benjamin Alman[1]. [1]Department of Orthopaedic Surgery, Duke University, United States, [2]Department of Orthopaedic Surgery, Kyushu University, Japan, [3]Department of Genetics, Stanford University, United States, [4]Duke Molecular Physiology Institute, Duke University, United States

INTRODUCTION: Enchondromas (ECA) are cartilage tumors that arise from growth plate chondrocytes that fail to undergo terminal differentiation. They affect approximately 3% of the population causing pain, deformity, and can progress into malignant chondrosarcomas (CSA). There are currently no effective drugs for this condition. The majority of ECAs and around 50% of CSAs harbor somatic mutations in isocitrate dehydrogenases (IDH). Our lab reported that a chondrocyte specific Idh1 mutation was sufficient to initiate ECA formation and cause defects in chondrocyte differentiation during endochondral bone development. Mutant IDH produced the unique “oncometabolite” D-2-hydroxyglutarate (D-2HG), however, inhibition of the ability of mutant IDH to produce 2-HG has minimal effects on the tumorigenic properties of cartilage tumors. Previous studies demonstrated D-2HG was primarily derived from glutamine in glioma cell lines with IDH1 mutations, and inhibiting glutamine metabolism slows down tumor growth of glioma. In this study, we investigated the role of glutamine metabolism in cartilage tumors and test whether glutaminase (GLS), the enzyme catalyzes the first step of glutamine metabolism, could be a therapeutic target for enchondroma and chondrosarcoma. RESULTS: We found glutaminase activity in Idh1 mutant chondrocytes were significantly higher while the GLS protein level remained unchanged. Carbon tracing experiment showed glutamine is the primary source for the generation of D-2HG. Deleting Gls in Idh1 mutant chondrocytes exacerbated enchondroma-like phenotype in adult mice. During embryonic development, deleting Gls in Idh1 mutant chondrocytes inhibited hypertrophic differentiation of chondrocytes and caused an increase in proliferation. However, in the study of chondrosarcoma, inhibiting glutaminase reduced cell viability of multiple patient samples in vitro and in vivo. SIGNIFICANCE: This study identifies the role of glutamine metabolism in cartilage tumors may differ at different stages of tumor development. It will help identify novel therapeutic targets for enchondroma and chondrosarcoma.

***Disclosures: Hongyuan Zhang**, None*

P-188

Generation of a Quantitative Luciferase Reporter for Sox9 SUMOylation *Masafumi Inui[1], Hideka Saotome[1], Atsushi Kubo[2]. [1]School of Agriculture, Meiji University, Japan, [2]Institute of Development, Aging and Cancer, Tohoku University, Japan

Sox9 is a master transcription factor for chondrogenesis, which is essential for chondrocyte proliferation, differentiation, and maintenance. Sox9 acts in a dose-dependent manner in mammalian skeletal development, and its haploinsufficiency causes bone malformation and perinatal death in both mice and humans, while the overexpression of Sox9 also causes abnormalities in skeletal elements. To maintain its activity within appropriate levels, Sox9 is regulated by multiple layers, including post-translational modifications, such as SUMOylation. Although Sumoylation represses the Sox9 activity in the neural crest cells of Xenopus laevis, its role in the chondrogenic process remains unclear. As SUMOylation could be involved in Sox9 dose regulation, its quantitative detection during chondrogenesis is important. However, quantitative and dynamic detection of SUMOylation of specific proteins is technically difficult. Therefore, a detection method for visualizing the SUMOylation in live cells is required to fully understand the role of Sox9 SUMOylation. To solve this probrem, we generated a quantitative reporter for Sox9 SUMOylation that is based on the NanoBiT system. The simultaneous expression of Sox9 and SUMO1 constructs that are conjugated with NanoBiT fragments induced luciferase activity in SUMOylation target residue of Sox9-dependent manner. In HEK293T cell, the reporter signal could be detected from both cell lysates and live cells. The signal from live cells could be visualized by the microscope. Furthermore, the signal level of our reporter responded to the co-expression of SUMOylation or deSUMOylation enzymes by several fold, showing dynamic potency of the reporter. The reporter was active also in ATDC5 cells, which have chondrogenic potential. Finally, using this reporter, we revealed an extracellular signal conditions that can increase the amount of SUMOylated Sox9. In summary, we generated a novel reporter that was capable of quantitatively visualizing the Sox9-SUMOylation level in live cells. It will be interesting to apply this reporter for detecting SUMOylation level of Sox9 during chondrocyte differentiation to understand the role of Sox9 regulation by SUMOylation in cartilage formation. This reporter will be useful for understanding the dynamism of Sox9 regulation during chondrogenesis.

***Disclosures: Masafumi Inui**, None*

P-189

Targeted Deletion of the Glucocorticoid Receptor in Chondrocytes Attenuates Cartilage Degradation in Murine Osteoarthritis *Eugenie Macfarlane[1], Jan Tuckermann[2], Markus Seibel[1], Hong Zhou[1]. [1]ANZAC Research Institute, University of Sydney, Australia, [2]University of Ulm, Germany

Although glucocorticoids (GCs) are often used in the treatment of osteoarthritis (OA) for pain relief, the function of endogenous GCs in the pathogenesis of OA remains unknown. We have previously shown that disruption of endogenous GC signaling in osteoblasts and osteocytes mitigates OA in mice by reducing the severity of cartilage damage, subchondral bone sclerosis and osteophyte formation. This finding led us to investigate whether disruption of endogenous GC signaling in chondrocytes also affects the development of OA.Osteoarthritis of the knee joint was induced by surgical destabilization of the medial meniscus (DMM) in tamoxifen-inducible glucocorticoid receptor-knockout (chGRKO) mice and their wild-type (WT) littermates at 22-weeks of age (n=10-11 per group). Sham surgery was used as a control (n=4-5 per group). Both WT-DMM and chGRKO-DMM mice developed apparent OA 16-weeks after surgery, characterized by cartilage degradation, subchondral bone sclerosis and osteophyte formation. No obvious signs of inflammation were observed histologically at this time point. Histological semiquantitative scoring revealed that compared to WT-DMM mice, cartilage damage was significantly less pronounced in chGRKO-DMM mice, particularly at the medial tibial plateau and femur condyle (Fig. 1A, B). Medial tibial cartilage area assessed by histomorphometry was 5912µm2 and 4632µm2 in chGRKO-DMM and WT-DMM mice respectively (p=0.0149; Fig. 1B). Similarly, intact medial femoral cartilage area was 6728µm2 and 5384µm2 in chGRKO-DMM and WT-DMM mice respectively (p=0.0116; Fig. 1B). Deletion of the glucocorticoid receptor in chondrocytes appeared to have no impact on subchondral bone sclerosis, osteophyte formation or synovial inflammation as no differences were observed between chGRKO-DMM and WT-DMM mice by either micro-CT or histomorphometry analyses (Fig. 1C).We conclude that endogenous GC signaling in chondrocytes promotes cartilage degradation but not abnormal bone formation (subchondral bone sclerosis and osteophytes) in a mouse model of surgically induced OA.

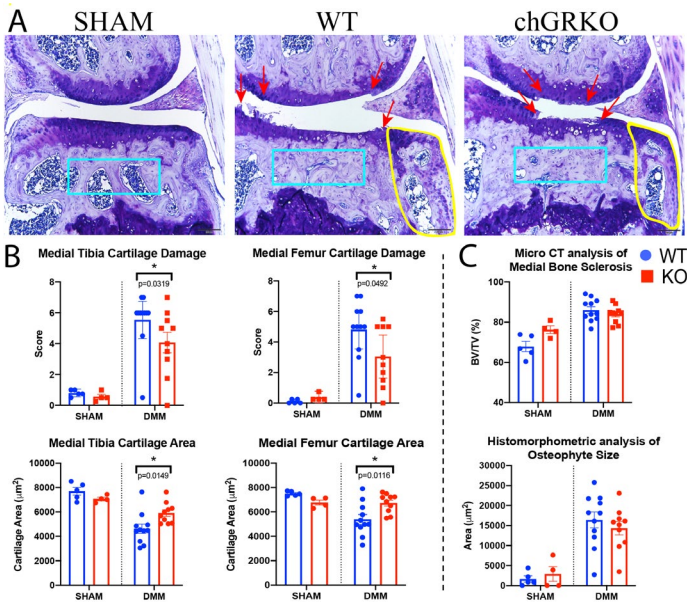

***Disclosures: Eugenie Macfarlane**, None*

P-190

Role of PHOSPHO1 in the Biogenesis and Function of Matrix Vesicles *Flavia Amadeu de Oliveira[1], Colin Farquharson[2], José Luis Millán[1], Massimo Bottini[1]. [1]Sanford Burnham Prebys Medical Discovery Institute, United States, [2]University of Edinburgh, United Kingdom

Matrix vesicles (MVs) are a class of extracellular vesicles released by mineral-competent cells that play a key role in the deposition of hydroxyapatite during physiologic mineralization and ectopic calcification1. MV-mediated mineralization is driven by a constellation of proteins present both on the outer surface of the MV membrane and in the MVs’ lumen and acting in concert to regulate the extracellular concentration of calcification inhibitors as well as the intraluminal concentration of Ca2+ and Pi ions. Orphan phosphatase 1 (PHOS-

PHO1) is present in the cytosol as well as the MVs' lumen where it produces Pi from phosphocholine and phosphoethanolamine generated by distinct enzymatic cascades acting upon the vesicle's phospholipid membrane2. Recently, we have shown that Phospho1-/-chondrocytes have impaired MV biogenesis and function3 - the latter phenomenon correlated to the absence of a mineralization precursor, the nucleation core (NC), in the MVs' lumen by AFM-based analyses4. Herein, to further assess the role of PHOSPHO1 on MV biogenesis and function, we used chondrocytes isolated from the growth plate of C57BL/6J mice cultured in osteogenic medium in the presence or absence of a PHOSPHO1 inhibitor (MLS-0263839). Calcium deposition, assessed by Alizarin-Red staining, showed that MLS-0263839 significantly hampered mineralization. We then assessed the mRNA expression of chondrocyte markers (Runx2, Col10a1), molecules involved in nucleotide signaling (Entpd1, Nt5e, P2rx7), enzymes responsible for Pi turnover on the MV surface (Alpl, Enpp1, S pp1, Slc20a1, Slc20a2) and inside MVs (Phospho1, Enpp6, Pla2g4a, Smpd3, Chka, Etnk1), enzymes responsible for Ca2+ turnover (Anxa5, Anxa6), markers of mitochondrial biogenesis (Tfam, Ppargc1a, Nrf1), and proteins participating in autophagy (Becn1, Atg5, Map1lc3a, Map1lc3b) and mitophagy (Pink1, Park2, Sqstm1). Our data show that the expression of all these mRNAs increased in mineralizing chondrocytes with time, except for Anxa5, Anxa6, Nrf1 and Becn1 whose expression did not significantly change. Our data also show that the presence of MLS-0263839 in the culture medium blunted the expression of all these mRNAs, except for Anxa6, Nrf1 and Map1lc3b, without affecting cell viability. Taken together, our results suggest that PHOSPHO1 enzymatic activity is involved in upstream processes driving MV biogenesis and function.1.Bottini M et al. 20182.Dillon S et al. 20193.Yadav M et al. 20164.Plaut JS et al. 2019

***Disclosures: Flavia Amadeu de Oliveira**, None*

P-191

SLC26A11 implicated in a new sulfate transport disease *Smrithi Salian[1], Thi Tuyet Mai Nguyen[1], Justine Rousseau[3], Julie Gauthier[0], Jacques L Michaud[0], Benjamin Ellezam[1], Peter Glavas[0], Marie Laberge-Malo[0], Antonio Rossi[0], Johan Thevelein[0], Philippe M Campeau[1]. [1]CHU Sainte-Justine Research Center, University of Montreal, Montreal, QC H3T 1C5, Canada, Canada, [3]CHU Sainte-Justine Research Center, University of Montreal, Montreal, QC H3T 1C5, Canada, Canada, [0]CHU Sainte-Justine Research Center, University of Montreal, Montreal, QC H3T 1C5, Canada, Canada, [0]Department of Molecular Medicine, Unit of Biochemistry, University of Pavia, 27100 Pavia, Italy, Italy, [0]Laboratory of Molecular Cell Biology, Institute of Botany and Microbiology, KU Leuven, Flanders, Belgium, Belgium

Solute carrier 26 (SLC26) gene family encodes a conserved membranous protein that functions as anion exchangers capable of transporting a wide variety of monovalent and divalent anions across the plasma membrane. So far three SLC26 genes have been known to be implicated in Mendelian diseases: SLC26A4 in deafness with enlargement of the vestibular aqueduct, SLC26A3 chloride diarrhea and SLC26A2 is implicated in several skeletal dysplasias, including achondrogenesis, atelosteogenesis II, multiple epiphyseal dysplasia and diastrophic dysplasia. SLC26A11 was reported to be localized to cytoplasm and lysosome, where it was proposed to serve as a sulfate exporter. It is expressed broadly including in the brain.In this study, we have identified a mutation in SLC26A11 in a patient and we hypothesize that lack of functional SLC26A11 results sulfate accumulation in lysosomes and a relative lack of cytoplasmic availability of sulfate essential for GAG synthesis.The patient was born to consanguineous Iranian parents with significant joint hypermobility at birth and club feet, and eventually presented microcephaly, intellectual disability, proptosis, hip dysplasia, coxa vara, lordosis, scoliosis and feet contractures. She was given a clinical diagnosis of Larsen syndrome at birth, and the current phenotype resembles musculocontractural Ehlers-Danlos. Exome sequencing revealed a homozygous missense variant c.206A>G (p.Tyr69Cys) in SLC26A11 (NM_173626.3). We have obtained fibroblasts from this patient and stably corrected them with a lentivirus encoding wildtype SLC26A11.We will analyze the lysosomal sulfate export as well as GAG synthesis in patient fibroblast and iPSC-derived chondrocytes. We generated codon-optimized constructs to express SLC26A11 in yeast to assess the variant's effect on sulfate import.In conclusion, we identified a new disorder of sulfate transport and are actively looking for additional patients to corroborate our findings and define the extent of the disease.

***Disclosures: Smrithi Salian**, None*

P-192

Chondrogenic Differentiation of Mesenchymal Stem Cell-Like KS483 Cells *Katja Fagerlund[1], Natalia Habilainen-Kirillov[2], Clemens Löwik[3], Alan Chan[4], Jukka Rissanen[1], Jenni Mäki-Jouppila[1]. [1]Pharmatest Services, Finland, [2]Pharmatest Services, Finland, [3]Department of Radiology, Leiden University Medical Center, Netherlands, [4]Percuros, Netherlands

KS483 cells, a murine mesenchymal progenitor cell line, can differentiate into chondrocytes, adipocytes and osteoblasts and are a well-characterized model for the study of osteoblast differentiation and bone formation. For chondrogenic differentiation, KS483 cells were cultured in three-dimensional (3D) pellet culture system in 96-well plates in serum-free differentiation medium. The pellets were cultured in the presence and absence of BMP-6 for 17-28 days and the medium was refreshed in 2-3 day intervals. The pellets were embedded in paraffin, sectioned, and stained for Safranin O and Alcain blue for assessment of sulfated glycosaminoglycan (sGAG) content, and processed for immunohistochemistry to visualize type II collagen. For biochemical analysis, the pellets were digested with proteinase K and assayed for sGAG at days 17, 24 and 28. Type II collagen carboxyterminal propeptide (CP-II) was determined in the culture medium collected at day 17. BMP-6 showed concentration-dependent stimulatory effects on chondrogenic differentiation visualized by histological stainings, increased sGAG content of the pellets, and increased CP-II released into the culture medium. These results suggest that the KS483 cells can be used for in vitro chondrogenic differentiation model and for identifying novel chondrogenic compounds or compounds with inhibitory effects on chondrogenesis. The cells can be easily expanded and utilised for studies including large number of study groups and replicates.

***Disclosures: Katja Fagerlund**, None*

P-193

A Novel Regulatory Role of TRAPPC9 in Osteoarthritis *Nazar Hussein[1], Fayez Safadi[2]. [1]Kent State University, United States, [2]Northeast Ohio Medical University, United States

Osteoarthritis (OA) is the most prevalent joint disease worldwide, causing chronic disability in older people. Various factors are associated with its pathogenesis, including aging, obesity, joint instability, and joint inflammation. The articular cartilage cells, chondrocytes, are responsible for maintaining homeostasis of the ECM by producing its major components. Several activators (pro-inflammatory mediators) such as Interleukin 1 beta (IL-1β) is able to activate NF-kB signaling pathways. There are two distinct pathways, which can activate the NF-kB signaling cascades. The first one termed canonical or classical pathway, activation of IKKα/IKKβ/IKK?-NEMO complex will activate this pathway. On the other hand, the non-canonical or alternative pathway activation relies on NF-kB-inducing kinase (NIK). Trafficking Protein Particle Complex 9 (TRAPPC9) is a major subunit of TRAPPII Complex. Our data showed that TRAPPC9 binds IKKβ and NIK in chondrocytes. We believe such interaction could lead to a potential regulatory role of TRAPPC9 during NF-kB signaling cascades given that the role of TRAPPC9 in OA has not been studied yet. To explore the role of TRAPPC9 in OA, first, we assessed the gene expression/protein levels in primary human chondrocytes and found that TRAPPC9 expression is increased in IL-1β-treated chondrocytes compared to controls. Next, we determined the effect of TRAPPC9 downregulation using a viral system. TRAPPC9 downregulation might lead to positive or negative regulation of NF-kB signaling cascades. Studies are underway to determine the effects of modulating TRAPPC9 using in vivo studies, which include injection of viral particles of TRAPPC9 downregulation into the knee articular cartilage of C57BL6 mice after OA is surgically induced (DMM model). For OA histopathology assessment, The OARSI cartilage grading system will be used. Collectively, these studies are the first to report a novel role of TRAPPC9 in OA development.

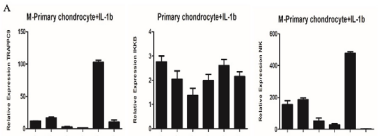

Figure 1: Gene expression and protein assessment of TRAPPC9, NIK , and IKKb post IL-1b treatment. (A) mRNA level of TRAPPC9 was measured following different time points following IL-1b treatment (B) IKKB mRNA and (C) NIK mRNA. *P<0.05, **P <0.01, ***P<0.001

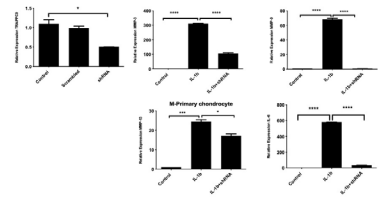

Figure 2: TRAPPC9, MMPs 3,9,13, and IL-6 expression levels TRAPPC9 knockdown mediated inflammation. After transfection, TRAPPC9 was successfully knockdown in primary mouse chondrocytes (A). Inflammatory markers MMP-3 (B), MMP-9 (C), MMP-13 (D), and IL-6 (E) gene expression was measured by qPCR. *P<0.05, **P <0.01, ***P<0.001.

***Disclosures: Nazar Hussein**, None*

P-194

Excessive mechanical strain accelerates intervertebral disc degeneration by disrupting the intrinsic circadian rhythm of nucleus pulposus cells *Li-Bo Jiang[1]. [1]Zhongshan Hospital, Fudan University, China

Objective. Night shift workers with disordered rhythmic mechanical loading are more prone to have low back pain and intervertebral disc degeneration (IDD). We aim to investigate the effect of mechanical loading on the intrinsic circadian rhythm (CR) of nucleus pulposus (NP) cells and IDD progression.Methods. Human tissues, aged rat IVDs and a punctured rat intervertebral discs (IVDs) were established, collected and analyzed by RNA sequencing and histology. NP cells were treated with excessive cyclic tensile strain (CTS) to detect the intrinsic CR and the involved mechanism. An upright rat models with longtime light-dark (LD) shift for 12 months mimicking Night shift workers were established to detect the effect of mechanical loading on IDD.Results. The CR was dampened in the degenerated and aged NP cells. Longtime environmental CR disruption promoted IDD in rats. Moreover,

excessive mechanical strain disrupted the CR and inhibited the expression of core clock proteins. The inhibitory effect of mechanical loading on the expression of extracellular matrix genes could be reversed by BMAL1 overexpression in NP cells. The Rho/ROCK pathway was demonstrated to mediate the effect of mechanical stimulation on CR. Prolonged mechanical loading, for 12 months, disrupted the intrinsic CR and induced IDD in a model of upright posture in a normal environment. Unexpectedly, the mechanical loading further accelerated the IDD in a LD cycle-disrupted environment.Conclusion. These results indicate that intrinsic CR disruption might be a mechanism involved in loading-induced IDD and a potential drug target for night shift worker.

***Disclosures: Li-Bo Jiang**, None*

P-195

Dietary Supplementation with Hydrolyzed Hyaline Cartilage Mitigates Posttraumatic Osteoarthritis: Potential Role of Shifts in Gut Microbiome *Yuan-Haw Wu [1], Samantha H. Landgrave[2], Honey Hendesi[1], Lacey J. Favazzo[1], David A. Villani[3], William Schroeder[1], Stacey M. Thomas[1], Karin A. Payne[3], Janne Prawitt[4], Michael J. Zuscik[3]. [1]Department of Orthopedics, Anschutz Medical Campus, Aurora, Colorado, United States, [2]Department of Orthopedics, Anschutz Medical Campus, Aurora, Colorado; Cell Biology, Stems Cells and Development Program, Anschutz Medical Campus, University of Colorado, Aurora, Colorado, United States, [3]Department of Orthopedics, Anschutz Medical Campus, Aurora, Colorado; Cell Biology, Stems Cells and Development Program, Anschutz Medical Campus, University of Colorado, Aurora, Colorado, United States, [4]Rousselot BVBA, Gent, Belgium, Belgium

Objective: Osteoarthritis (OA) is a leading cause of disability globally. Symptom palliation is the only option for treatment as there is no available disease-modifying therapy. It has recently been suggested that changes in the gut microbiome can influence OA progression; in fact, the chondroprotective effects of various nutraceuticals, including dietary supplements comprised of cartilage components, may be due to their ability to shift the gut microbiome composition. One supplement in particular, known as hydrolyzed hyaline cartilage (hHC), has anecdotally been identified as joint protective. However, the exact mechanism of this protection and the potential involvement of the gut microbiome is yet to be explored. This study aimed to investigate the basis for joint protection conferred by hHC in OA. Method: Posttraumatic OA (PTOA) was surgically induced via destabilization of the medial meniscus in male C57BL/6J mice consuming a defined diet from OpenSource (D1245H). Injured mice were provided a daily oral supplement of hHC (0.62mg/gm body weight) or vehicle, beginning 2 weeks prior to injury. Three- and 12-weeks post-injury, knee joints were harvested, fixed, embedded in paraffin and cut sections were stained with Safranin O. Histomorphometry analyses were performed to measure the area of femur and tibial cartilages. TNF immunohistochemistry was performed to study joint inflammation and TUNEL staining was performed to assess chondrocyte apoptosis. Fecal material was also collected to support analysis of the gut microbiome via 16S rDNA sequencing. Result: Histomorphometry revealed that hHC-supplemented mice had more tibial and femoral uncalcified cartilage at both 3- and 12-week post-injury. These results may be related to suppression of inflammation in the hHC cohort, which displayed a trend toward reduced synovial TNF. This paralleled a reduction in chondrocyte apoptosis in hHC-supplemented mice. Suggesting a potential mechanistic association, hHC supplemented mice displayed significant shifts in the gut microbiome that included loss of proinflammatory Peptococcaceae family members, particularly the species rc4-4. Conclusion: Findings suggest that oral dietary supplementation with hHC confers joint protective effects in PTOA as well as parallel alterations in the gut microbiome. This sets the stage for follow-on study of the potential mechanistic link between the microbial shifts induced by hHC and its ability to support chondroprotection.

***Disclosures: Yuan-Haw Wu,** None*

P-196

Acquired Autoimmune Parathyroid Hormone (PTH) Resistance due to PTH1 Receptor Autoantibodies *Adel Mandl[1], Peter D. Burbelo[1], Giovanni DiPasquale[1], James Welch[1], Michail S. Lionakis[1], Meryl A. Waldman[1], Michael T. Collins[1], William F. Simonds[1], Sunita K. Agarwal[1], Jenny E. Blau[1], Lee S. Weinstein[1]. [1]NIH, United States

Background: Parathyroid hormone (PTH) resistance is a hallmark of pseudohypoparathyroidism, an inherited genetic disorder of PTH/PTH-related Peptide (PTHrP) signaling. However, PTH1 receptor-related autoimmune etiology has not yet been identified as the underlying mechanism for this disease.Here we describe the first case of acquired autoimmune PTH resistance that is secondary to PTH1R autoantibodies.Clinical Case: A 60-year-old African-American woman, who previously had normal calcium homeostasis, presented with acute, symptomatic hypocalcemia, hyperphosphatemia and markedly elevated serum PTH, consistent with parathyroid hormone resistance. She did not have a clinical or biochemical phenotype suggestive of pseudohypoparathyroidism. Whole-exome sequencing and GNAS methylation analysis revealed no genetic or epigenetic defects of the PTH/PTHrP signaling pathway. Treatment with Calcitriol and Calcium supplements was initiated with good clinical response. Within 10 years of follow-up, the patient developed autoimmune hypothyroidism, alopecia and an unusual form of membranous glomerulonephritis, raising the suspicion for an autoimmune etiology for PTH resistance. Luciferase immunoprecipitation system assay identified antibodies against PTH1R. Using an in vitro biological assay in GP-2.3 cells, we found that the antibodies derived from the patient's serum blocked PTH downstream signaling via Gsalpha/cAMP/protein kinase A pathway in a concentration-dependent manner. The patient's autoantibody profile led to the diagnosis of additional autoimmune diseases, including atrophic gastritis and Sjogren syndrome. Lymphocyte immunophenotyping using flow cytometry revealed an overall normal B and T cell profile, but with increased frequency of autoreactive CD21 low CD38-negative B cell subset, which is known to be enriched in patients with certain immune disorders. Genes associated with autoimmune inflammatory disorders were sequenced but no pathologic changes were detected.Conclusions: Identification of the first case of autoimmune PTH resistance secondary to PTH1R autoantibodies extends the etiologic spectrum of hypoparathyroidism and should be considered when a patient presents with findings consistent with pseudohypoparathyroidism, especially in the presence of additional autoimmune diseases.

***Disclosures: Adel Mandl**, None*

P-197

A Rare De Novo Mutation In Lrp5 Gene In An Adolescent Female With Juvenile Onset Primary Osteoporosis *Betty Shum[1], Anna Ryabets-Lienhard[1], Clement Cheung[1]. [1]Children's Hospital Los Angeles, United States

Background: Juvenile onset of primary osteoporosis is a rare skeletal disorder with a highly heterogenous clinical presentation and complex poorly understood genetic etiology. Low-density lipoprotein receptor-related protein 5 (LRP5), a Wnt-β-catenin pathway receptor involved in bone mineral density (BMD) regulation, has been reported in children with primary osteoporosis mainly due to missense and frame-shift mutations. To our knowledge, there is only one report of in-frame deletions in exon 21 possibly being implicated in pregnancy related osteoporosis (1). We report the first case of a rare heterozygous de novo in-frame deletion in exon 21 of LRP5 gene in a girl with juvenile onset primary osteoporosis.Clinical Case: A 7.5 yo previously healthy European-African-American female born to non-consanguineous family, was noted to have left ankle and bilateral wrists fractures during sport activities occurring over the span of 1 y. On exam, she was of normal stature, had normal sclerae and vision, but was found to have hypermobile joints. Initial blood work revealed an elevated iPTH 72 pg/mL (9-59), normal Ca 9.6 mg/dL (8.9-10.4), and low 25OH-Vitamin D 17 ng/mL (30-100), which normalized with supplementation to 30.4 ng/mL. By 10.5 yo, she had sustained multiple sports related and pathologic fractures of long bones with progressive bone pain and functional ambulatory impairment. Radiographic evaluation showed osteopenia, multiple healed long bone fractures with presumed non-ossifying fibroma in the distal right femoral metaphysis, and subtle height loss of T4-5 vertebrae. CT bone densitometry at 12 yo showed low mean cancellous lumbar vertebral BMD of 190 mg/cm3 (ref. 285 +/- 45) and normal cortical BMD of the femoral midshaft of 1977 mg/cm3 (ref. 2000 +/- 60). Genetic testing for Osteogenesis Imperfecta returned negative for COL1A1 and COL1A2 mutations. Whole exome sequencing (WES) revealed a rare, de novo heterozygous mutation in exon 21 that involved deletion of nucleotides 4454 to 4465 resulting in an in-frame deletion of amino acid 1485 to 1488. This mutation is predicted to be deleterious by in silico analysis.Conclusion: We present the first case of a young female with progressive pathologic fractures, functional ambulatory impairment, and low BMD in childhood, consistent with juvenile onset primary osteoporosis. WES revealed a rare de novo heterozygous in-frame deletion mutation in LRP5, providing a plausible biological mechanism for her clinical presentation, and further contributing to the increasing genetic heterogeneity of juvenile onset primary osteoporosis and LRP5-related bone disorders. Reference: (1) Cook, F., Mumm, S., Whyte, M., Wenkert, D. Pregnancy-associated osteoporosis with a heterozygous deactivating LDL receptor-related protein 5 (LRP5) mutation and a homozygous methylenetetrahydrofolate reductase (MTHRF) polymorphism. JBMR. 2014;29 (4): 922-8.

***Disclosures: Betty Shum**, None*

P-198

Hypophosphatemia Associated with Intravenous Ferric Carboxymaltose Complicated by Multiple Insufficiency Fractures *Christie Turin[1], Christopher Hvisdas[1], Amna Khan[2]. [1]University of Pennsylvania, United States, [2]University of Pennsylvani, United States

Background: Hypophosphatemia is a well-documented side effect of intravenous iron, mostly reported with ferrous carboxymaltose (FCM). However, associated severe osteomalacia resulting in bone fractures is largely under-recognized. Herein, we report a case of FCM-induced hypophosphatemia complicated by multiple insufficiency fractures. Case:A 73-year-old woman with history of Crohn's disease, breast cancer and renal cell carcinoma was referred for evaluation of low bone mineral density (BMD). On evaluation, she was found to have hypophosphatemia. Workup revealed normal calcium (9.0 mg/dL), low phosphorus (1.8 mg/dL), low 1,25-dihydroxyvitamin D (19.2 pg/mL, NR: 19.9-79.3), and high alkaline phosphatase (200 U/L, NR: 38-126). 25 OH vitamin D (32 ng/mL) and iPTH (5 pmol/L, NR: 1.6-6.9) were normal. 24-hour urine phosphate was 0.533 g/d (NR: 0.6-1.2 g/d) considered inappropriately high given low serum phosphorus. Lowest BMD was at the left hip with a T score of -2.9. She was started on calcitriol and phosphate supplements. However, she experienced non-traumatic multiple nondisplaced fractures in tarsal bones. Given history of malignancies and concern for tumor-induced osteomalacia, FGF23 levels were checked which were inappropriately normal (110 RU/mL, NR<180). Also noted to

have elevated C-telopeptide levels (1004 pg/mL, NR: 30 – 826). She revealed she was receiving IV iron infusions for iron-deficiency anemia, prescribed by local Hematologist, and had recently been switched from iron sucrose to IV FCM 700 mg/dose for total of 7 doses. Biochemical evaluation prior to FCM was unremarkable. FCM was discontinued and she was able to wean off Calcitriol and phosphate after 4 months. Phosphate levels remained stable, did not experience recurrent fractures and her BMD increased significantly one year after. Conclusion: Hypophosphatemia is a well-documented side effect of IV iron, mostly with FCM that causes rapid increase in active FGF23 leading to phosphate wasting. Severe hypophosphatemia could last up to 12 weeks and can result in osteomalacia and bone fractures which are largely under-recognized. Only few studies describe long term effects on bone health as evident by our case. Clinicians should be aware of this complication and should consider using alternatives especially in patients at high risk for osteoporosis and fragility fractures.

***Disclosures: Christie Turin**, None*

P-199

Pathogenic Variants of GNAS Gene Generating Abnormal Amino Acid Sequences in the β6 Strand / α5 Helix of Gsα in 2 Unrelated Japanese Patients with Pseudohypoparathyroidism 1A / Pseudopseudohypoparathyroidism

*Yasuhisa Ohata[1], Haruna Kakimoto[2], Yasuki Ishihara[3], Makoto Fujiwara[3], Shinji Takeyari[1], Taichi Kitaoka[1], Hirofumi Nakayama[4], Yukako Nakano[1], Kenichi Yamamoto[5], Chieko Yamada[1], Takeshi Ishimi[1], Takuo Kubota[1], Keiichi Ozono[1]. [1]Department of Pediatrics, Osaka University Graduate School of Medicine, Japan, [2]Department of Pediatrics, Kagoshima University Graduate School of Medical and Dental Sciences, Japan, [3]Department of Pediatrics, Osaka University Graduate School of Medicine; The first Department of Oral and Maxillofacial Surgery, Osaka University Graduate School of Dentistry, Japan, [4]Department of Pediatrics, Osaka University Graduate School of Medicine; The Japan Environment and Children's Study, Osaka unit center, Japan, [5]Department of Pediatrics, Osaka University Graduate School of Medicine; Department of Statistical Genetics, Osaka University Graduate School of Medicine, Japan

Pseudohypoparathyroidism type 1A (PHP1A) is a rare disease characterized by Albright's hereditary osteodystrophy (AHO) and hormonal resistance including parathyroid hormone (PTH) and thyroid-stimulating hormone (TSH). PHP1A is caused by loss-of-function mutations in the imprinted GNAS gene, encoding Gsα, in the maternal allele. On the other hand, mutations in the paternal allele result in pseudopseudohypoparathyroidism (PPHP) characterized by AHO and no hormonal resistance. [Case 1] A 5-year-old boy with subcutaneous heterotopic ossification diagnosed by biopsy was referred to us since he had hypocalcemia and hyperphosphatemia. His height and body weight were 110.8 cm (+0.81SD) and 24.2 kg (+28.1%), respectively. He had AHO symptoms including round and flat face, brachydactyly, and knuckle sign and mild mental retardation. We started the treatment with active vitamin D and thyroid hormone since laboratory test showed hypocalcemia, hyperphosphatemia, and hypothyroidism: serum Ca 6.9 mg/dl, Pi 7.8 mg/dl, Alb 4.1 g/dl, ALP 681 U/l, PTH 524.9 pg/ml, 25(OH)D 17 ng/ml, TSH 14.27 μIU/ml, FT4 1.2ng/dl. Genetic test revealed heterozygous c.1141delG (p.Asp381Thrfs23*) of his and his mother's GNAS gene. [Case 2] A 1-year-old boy with subcutaneous heterotopic ossification diagnosed by biopsy was referred to us. He did not have any symptoms of AHO except ossification. His height and body weight were 69.2 cm (-0.53 SD) and 9.3 kg (+0.70 SD), respectively. The laboratory data were as follows: serum Ca 9.9 mg/dl, Pi 6.6 mg/dl, Alb 4.0 g/dl, ALP 449 U/l, PTH 44 pg/ml, 25(OH)D 25.8 ng/ml, TSH 7.32 μIU/ml, FT4 0.87 ng/dl. Since hypothyroidism was diagnosed, we started thyroid hormone treatment. Genetic analysis revealed heterozygous c.1117delC (p.Arg373Alafs*30) of his GNAS gene, although his mother did not harbor this mutation.These mutations we found have not been reported in the databases (LOVD and HGMD). The frameshift mutations introduce the addition of 23 or 30 amino acids in β6 strand / α5 helix of Gsa, which interact with G protein coupling receptor (GPCR) (Figure 1). When we predict the affinity between the Gsa with and without mutations and GDP by I-TASSER, there was no significant difference among these group: the confidence score of the prediction was 0.87, 0.83, and 0.94 in WT, c.1141delG (p.Asp381Thrfs23*), and c.1117delC (p.Arg373Alafs*30), respectively. Therefore, we concluded that these mutations do not affect the affinity with GDP but alter the association with GPCR and cause PHP1A or PPHP.

Figure 1

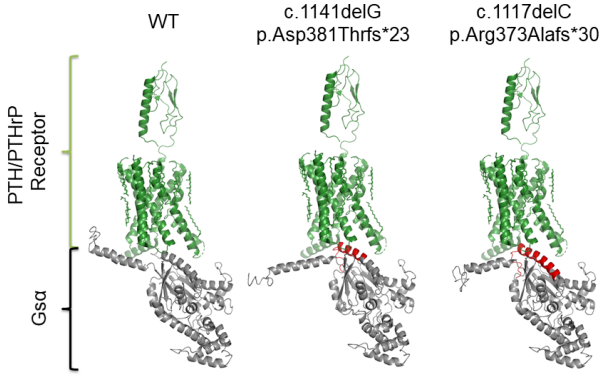

Ribbon diagrams of Gsα and PTH/PTHrP receptor complex. Gsα is shown in grey, receptor in green. The abnormal amino acid sequences caused by the mutations are shown in red.

***Disclosures: Yasuhisa Ohata**, None*

P-200

Alopecia due to Sub-Cutaneous Scalp Calcifications in a Patient with Pseudo Hypoparathyroidism

*Jaspreet Hehar[1], Arti Bhan[1], Sudhaker Rao[1]. [1]Henry Ford Hospital, United States

Pseudo-hypoparathyroidism (PHP) is a genetic disorder characterized by end organ resistance to parathyroid hormone (PTH) action, resulting in hypocalcemia, hyperphosphatemia and elevated PTH levels. PHP is sub classified into types 1A, 1B and 2. Patients with PHP-1A have the classical phenotypic features with short stature, round facies, and bilateral short 4th and 5th metacarpals. Types 1B and 2 lack this phenotypic features, but share similar biochemical abnormalities. We present a patient with PHP-1A, with prolonged asymptomatic hypocalcemia and hyperphosphatemia that resulted in alopecia due to entire scalp calcification.A 40y African American woman with past medical history of hypothyroidism, seizure disorder, scalp alopecia, and low IQ, presented to the clinic for management of hypocalcemia and hyperphosphatemia. On initial evaluation, she reported worsening alopecia for the past several years, for which she was evaluated by dermatology and diagnosed with central centrifugal cicatricial alopecia after biopsy of the scalp. She had been hypocalcemic for several years and reported no symptoms or seizure episodes. Her vital signs were normal: BP 106/72 mmHg, PR 83/m, Ht 150cm, Wt 72.8 kg, and BMI 33.8kg/m2. On examination she had multiple diffusely scattered palpable small nodules on the entire scalp. Serum and ionized calcium levels were 6.6mg/dL (reference range[RR]: 8.6-10.4) and 0.89mmol/L (RR 1.00-1.35), respectively, serum phosphorous was 5.7mg/dL (RR 2.5-4.5), and total and bone specific alkaline phosphatase 111 IU/L (RR 40-120), and 73 U/L (RR 11.6-29.6), respectively. Serum intact PTH was 650pg/mL (RR 15-65), 25-hydroxyvitamin D 50ng/mL (RR >20), 1,25-dihydroxyvitamin D 36 pg/mL (RR 20-79). BMD left femoral neck: -1.0SD, lumbar spine +0.2SD and forearm +0.5SD. A CT of the head showed dense calcifications of the basal ganglia and dentate nuclei, and unusual subcutaneous calcifications of the entire scalp. The diagnosis of PHP 1A was confirmed with phenotypic, biochemical, and radiological features, and was started on calcitriol and calcium carbonate, with eventual improvement in her lab abnormalities.Although intracranial calcifications are a well-known of idiopathic hypoparathyroidism, it is less commonly seen in post-surgical and PHP. We believe the extensive subcutaneous scalp calcifications due to underlying PHP most likely contributed to the progressive scarring resulting in alopecia totalis, which has not been previously reported in any form of hypoparathyroid states.

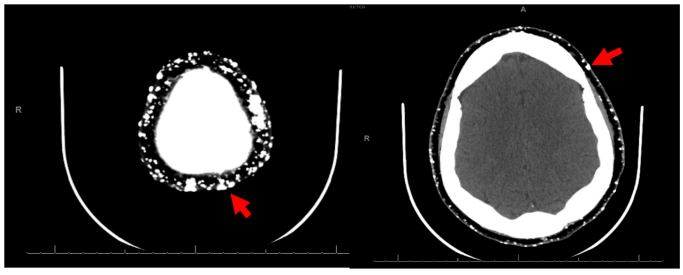

Figure 1. Non-contrast head CT. Arrows denote areas of intracranial scalp calcification

***Disclosures: Jaspreet Hehar**, None*

Posters

P-201

Hyperphosphatemic Familial Tumoral Calcinosis Secondary to fibroblast Growth Factor 23 (FGF23) Mutation: Response to Teriparatide. *Carlos Gomez-Alonso[1], Eduardo Eduardo J Banegas-Deras[2], Carmen García Gil-Albert[3], Noelia Avelló-Llano[4], Minerva Rodríguez Garcia[5], Jorge B Cannata-Andía[6], Manuel Naves Díaz[6]. [1]UGC Bone and Mineral. ISPA. Hospital Universitario Central de Asturias. Universidad de Oviedo. Oviedo (Spain), Spain, [2]AGC of Nephology HUCA. Oviedo (Spain), Spain,[3] AGC Medicine Laboratory, HUCA, Oviedo (Spain), Spain, [4]AGC Medicine Laboratory, HUCA. Oviedo (Spain, Spain, [5]AGC of Nephology, HUCA. Universidad de Oviedo. Oviedo (Spain), Spain, [6]UGC Bone and Mineral. ISPA . Hospital Universitario Central de Asturias. Universidad de Oviedo. Oviedo (Spain), Spain

Hyperphosphatemic familial tumoral calcinosis (HFTC) is a rare genetic disorder with shared clinical features, characterized by hyperphosphatemia and recurrent ectopic calcifications, in addition to other visceral and vascular manifestations, in absence of any inflammatory or neoplastic disorder.We present 3 cases of a family with two brothers and their uncle, with a mutation ((homozygous c.985G>A, p.G329R) in exon 4 GALNT3G leading to a missense mutation), with various degrees of involvement and response to treatment.Case 1: female, 44 years old, an episode of vertebral osteitis D11-D12Case 2: Male, 42 years old, moderate calcinosis in subcutaneous cellular tissue and incipient masses in hips and shoulders.Case 3: Male 67 years old, type II diabetes the last 3 years, with severe calcifications in all large joints and severe diffuse calcification of subcutaneous cellular tissue in lower limbs as well as severe vascular calcifications with grade IV ischemia and left foot amputation.All three had normal serum creatinine 0.7-1.1 mg/dL (Ref 0.7-1.2) high phosphate (P) 2-2.3 mmol/L (Ref 0.9-1.4), normal calcium, inappropriately low intact PTH 15-25 pg/mL (Ref 15-65) and very high FGF23 (C-Terminal FGF23 (Biomedica)) > 417 RU/mL (Ref 25-130). Low urinary P removal 12-18 mmol/24h (Ref 13-42) and high tubular P reabsorption 95-97%The initial treatment with restriction of dietary P and administration of phosphate binders with meals (Algamate 1.5 g/8h) had a very limited effect on phosphatemia. The use of acetazolamide (250 mg/12h) decreased and normalized serum P in case 1, but remained high in cases 2 and 3. In case 3, due to the severity of the clinical picture, once obtained the Ethical Committee authorization, started treatment with teriparatide 20 mg SC/24h to promote phosphaturia and increase P uptake by the bone. The evolution of this patient (figure) was an important reduction in ectopic calcifications after 6 months of treatment. CTX and P1NP bone turnover markers increased from 0.11 to 0.46 ng/mL and from 22.1 to 70.2 ng/L respectively. TRP decreased from 97 to 90%.In view of the PTH values in this family and the response observed in case 3, we consider whether the loss of function of FGF23 is limited to the renal tubule or if it could start inhibiting the secretion of PTH. In some cases of HFTC, the treatment with teriparatide could be an alternative or a complement to the dietary P restriction on, use of P binders, acetazolamide and thiosulfate.

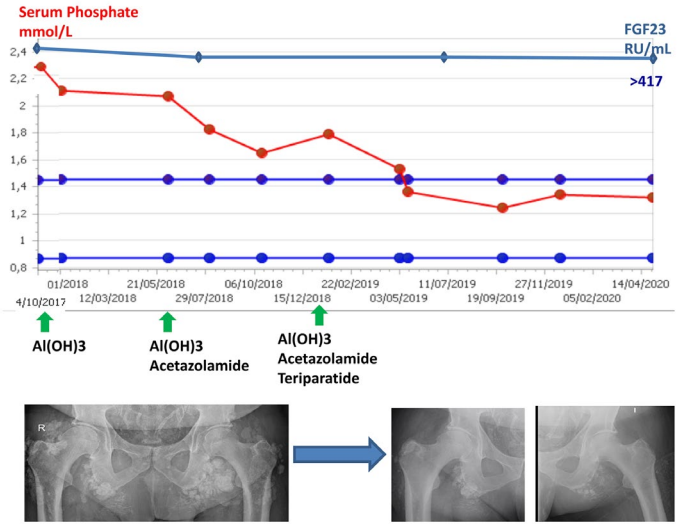

***Disclosures: Carlos Gomez-Alonso**, None*

P-202

Eye Inflammation Associated With Bisphosphonate Treatment *Vicente Ricardo González[1], María Diehl[1], Mirena Buttazzoni[1], Ariela Kitaigrodsky[1], María Marcela García[1], Ana María Galich[1]. [1]Hospital Italiano de Buenos Aires, Argentina

Bisphosphonates (BP) are first-line drugs in the treatment of osteoporosis and other bone diseases. Uveitis is a rare complication associated with their use.We describe 6 patients with ocular inflammation associated with BP use. The age range was between 50 and 86 years. Four received BP for osteoporosis and two for oncologic disease. Five patients developed the inflammatory reaction after the first infusion of zoledronate and one patient after pamidronate. The time of presentation of this adverse effect varied between 12 hours and 7 days after infusion. In five cases anterior uveitis was diagnosed and one patient had posterior scleritis associated with optic perineuritis. In all patients the engagement was monocular. Three of them had received previous oral BP, without any adverse ocular reaction. One patient who was treated with a second zoledronate infusion repeated a new episode of uveitis.Patients who had anterior uveitis (n= 5) resolved with topical corticosteroids. The patient with posterior scleritis and perineuritis required systemic corticotherapy and hospitalization for pain management. All presented favorable evolution and ocular inflammation resolved within four weeks.Discussion:Drug induced uveitis is infrequent (<0.5%). Other more frequent causes include infections and systemic immune-mediated disease. BP act by inhibiting farnesyl pyrophosphate synthase. This leads to the accumulation of isopentenyl pyrophosphate which has a molecular similarity to a microbial compound and may therefore trigger the activation of gamma delta T cells. This activation leads to the release of cytokines and inflammatory mediators that lead to the acute phase reaction. Eye inflammation associated with BP treatment is an uncommon complication, but it should be suspected in patients who have pain, photophobia or red eye after BP application. It may recur in case of a new BP infusion. In our series all the patients had received intravenous BP. The evolution was favorable with the establishment of local or systemic corticotherapy. Early intervention is essential to improve pain and reduce the risk of complications. Multidisciplinary work is necessary for a proper diagnosis and treatment.

Case	Age	Sex	Indication of BP	Type of BP	Ocular disease	Time of onset after BP use	Corticosteroid therapy
1	73	M	Prostate cancer	Zoledronate	Distal perineuritis, episcleritis	3 days	Systemic
2	58	F	Osteoporosis	Zoledronate	Uveitis	5 days	Topic
3	86	F	Osteoporosis	Pamidronate	Uveitis	2 days	Topic
4	62	F	Osteoporosis	Zoledronate	Uveitis	7 days	Topic
5	55	F	Osteoporosis	Zoledronate	Uveitis	12 hours	Topic
6	66	F	Plasmocytoma	Zoledronate	Uveitis	7 days	Topic

***Disclosures: Vicente Ricardo González**, None*

P-203

Hungry Bone Syndrome in Tumor-Induced Osteomalacia *Layne N. Raborn, BS[1], Iris R. Hartley, MD[1], Kristen S. Pan, MD[1], Gina Woods, MD[2], Karen A. Pozo, RN[1], Jamie Streit, RN[1], Michael T. Collins, MD[1], Rachel I. Gafni, MD[1]. [1]Skeletal Diseases and Mineral Homeostasis Section, National Institute of Dental and Craniofacial Research, National Institutes of Health, United States, [2]University of California San Diego, United States

Background: Tumor-induced osteomalacia (TIO) is a rare paraneoplastic syndrome caused by phosphaturic mesenchymal tumor (PMT) overproduction of fibroblast growth factor 23 (FGF23), resulting in hypophosphatemia and osteomalacia. Complete tumor resection is curative, with normalization of blood FGF23 and renal phosphate reabsorption, increase in 1,25-(OH)2-vitamin D and bone healing. Rapid postoperative changes in mineral homeostasis in the setting of chronic osteomalacia have the potential to induce accelerated bone mineralization associated with hypocalcemia and secondary hyperparathyroidism, reminiscent of the hungry bone syndrome following surgical cure of hyperparathyroidism. We present 2 patients with TIO who experienced postoperative hypocalcemia and secondary hyperparathyroidism, requiring significant calcium supplementation following curative PMT resection.Cases: Patient 1 was a 56 yo man who underwent complete resection of a chest wall PMT, with FGF23 falling from 482 RU/mL (nl < 180) to <50 RU/mL 12 hours after surgery. On postoperative day (POD) 2, blood calcium decreased to 8.4 mg/dL (8.6-10.2) and PTH increased to 69.9 pg/mL (15-65) (Fig). Oral calcium was initiated to prevent further decline, requiring up to 5 g/d of elemental calcium. In addition to a calcium-rich diet, gradually decreasing doses of supplemental calcium were needed for about 2y to prevent elevated iPTH. His preoperative alkaline phosphatase of 222 U/L (40-129) slowly fell to 95 U/L as his skeleton healed. Patient 2 was a 57 yo man with a rib PMT. Prior to surgery, due to inadequate dietary calcium, he was managed with 0.5-2g/d calcium supplementation, in additional to calcitriol and phosphate. After PMT removal, FGF23 levels decreased from 352 RU/mL to <50 RU/mL by POD2. Within 12 hours of surgery, calcium fell from 8.80 mg/dL to 7.32mg/dL and iPTH rose to 125.6 pg/mL (Fig). Calcium and PTH levels normalized on 5 g/d of elemental calcium. Three months after surgery, he continues to require 4 g/d calcium to maintain a normal iPTH. In both patients, oral phosphate and calcitriol were discontinued at time of surgery; phosphate was given briefly for severe hypophosphatemia on POD1&2. Conclusion: These cases of osteomalacia-induced hungry bone syndrome demonstrate the

expected physiological perturbation of mineral homeostasis following tumor resection in TIO, underscoring the importance of attentive post-surgical monitoring and calcium supplementation following PMT resection.

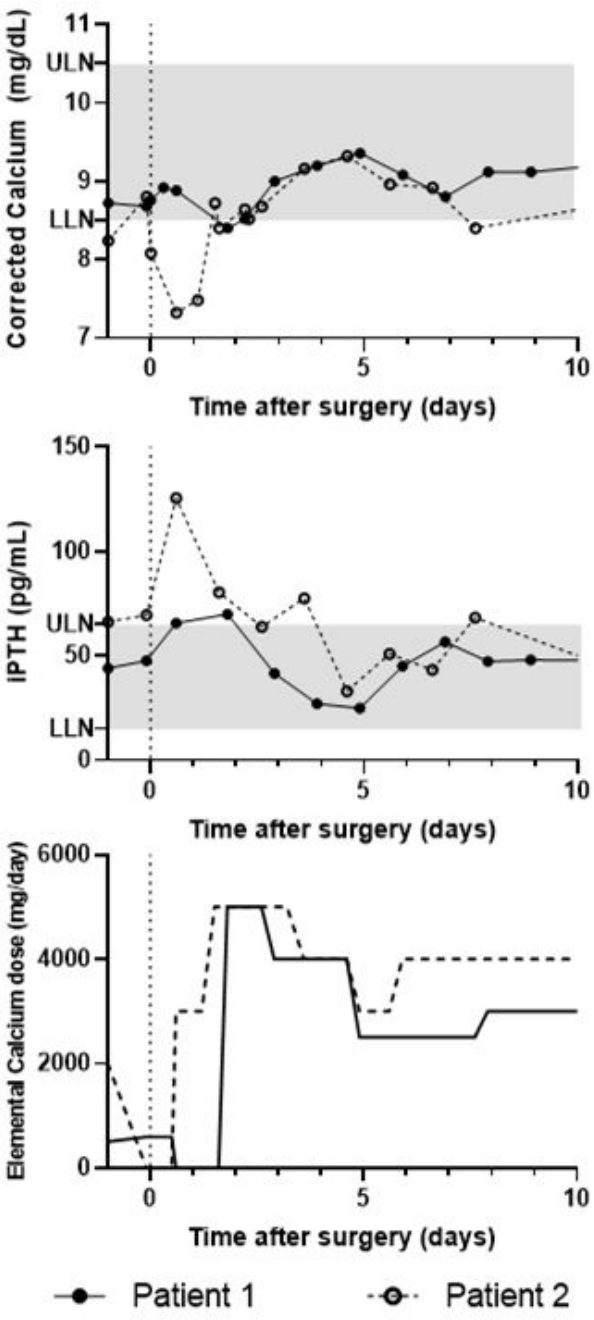

***Disclosures: Layne N. Raborn, BS**, None*

P-204

A rare and challenging disease: successful treatment with pamidronate in Sternocostoclavicular Hyperostosis *A.T. Leerling[1], A. Navas Cañete[1], N.M. Appelman-Dijkstra[1], E.M. Winter[1]. [1]Leiden University Medical Center, Netherlands

Background: Sternocostoclavicular hyperostosis (SCCH) is a rare disease, constituting a sterile osteomyelitis with elevated bone turnover, mainly affecting the sternocostoclavicular region. It causes pain and shoulder dysfunction, and severely interferes with daily activities, work, and quality of life. SCCH has a relapse-remitting disease course, but local sclerotic transformation, is slowly progressive and ultimately predisposes tissue degeneration. Low awareness amongst physicians and consequent diagnostic and therapeutic delay therefore construct a major problem, as unrecognized patients risk irreversible damage and associated morbidity. There is no established treatment for SCCH, but in our center we often observe a favorable effect of intravenous bisphosphonates. The rationale for bisphosphonates rests on them decreasing painfully increased bone turnover, and their anti-inflammatory effect in general.Clinical cases: Two adult female SCCH-patients presented with longstanding pain and swelling of the anterior chest wall, and compromised shoulder function. Complaints had existed without diagnosis for respectively 3 and 1.5 years. SPECT/CT illustrated elevated bone activity and sclerosis, with osteitis and hyperostosis, thereby confirming the diagnosis of SCCH (see attachment). Intravenous pamidronate in 3-month cycles was started for both, resulting in clinical remission as established by lower pain levels, improved shoulder function and decreased bone turnover on scintigraphy. Sclerosis persisted in one patient and completely resolved in the other. Conclusions and discussion: SCCH remains a rare but impactful bone disorder and lacks recognition. Here we described two SCCH cases treated with intravenous pamidronate, leading to clinical remission in both, and even complete resolution of sclerosis in one of them, which in our experience is a novel finding. The rationale for pamidronate treatment is reinforced by the clinical response together with the sclerotic regression, as this reversal lowers the chances of eventual permanent degeneration, associated with further disease burden and impaired quality of life.

SCCH disease course on CT-scan and skeletal scintigraphy

Case 1

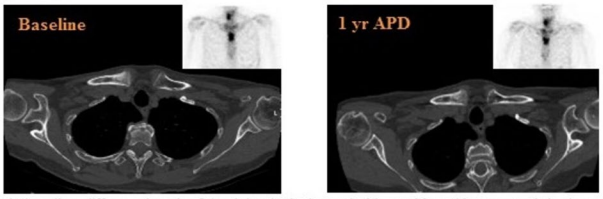

At baseline, diffuse sclerosis of the right clavicular end with osteitis and hyperostosis is observed on CT, with elevated local bone activity on scintigraphy. After one year of pamidronate (APD) treatment, coinciding with clinical remission, this rate of bone turnover is reduced, but sclerosis remains unchanged.

Case 2

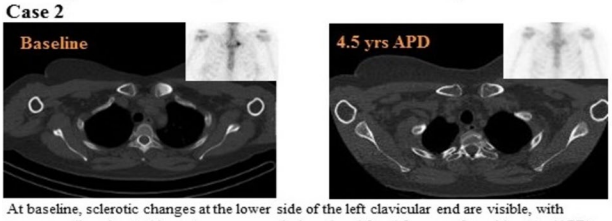

At baseline, sclerotic changes at the lower side of the left clavicular end are visible, with corresponding elevated bone turnover on scintigraphy. After 4.5 years of pamidronate (APD) treatment and at the point of clinical remission, bone activity has normalized and sclerosis has almost completely resolved.

***Disclosures: A.T. Leerling**, None*

P-205

Novel use of Burosumab (Crysvita) in a girl with Fanconi syndrome. *Nandini Vijayakanthi[1], Joshua B Kaltman[2], Roshan P George [3], Karen J Loechner [4]. [1]Division of Pediatric Endocrinology, Department of Pediatrics, Emory University School of Medicine, Children's Healthcare of Atlanta, United States, [2]Emory University School of Medicine, United States, [3]Division of Pediatric Nephrology, Department of Pediatrics, Emory University School of Medicine, Children's Healthcare of Atlanta, United States, [4]Division of Pediatric Endocrinology, Department of Pediatrics, Emory University School of Medicine, Children's Healthcare of Atlanta, United States

Introduction: Phosphate (phos) is critical for mineralization and skeletal development. Hypophosphatemia can result in metabolic bone disease. We describe a 9-year-old girl with Fanconi syndrome, hypophosphatemic rickets and nephrocalcinosis. After an allergic response to calcitriol, Burosumab (Crysvita) was initiated. Case Discussion: She presented at 18 months of age with renal tubular acidosis (proteinuria, glucosuria, hypercalciuria, metabolic acidosis); evaluation for cystinosis, tyrosinemia, secondary causes of hypercalciuria, Lowe syndrome and Dent disease were negative. Hypophosphatemia (1.7-3 mg/dL) with phosphaturia (FeP04 50%) noted at 4 years old led to diagnosis of Fanconi syndrome. Potassium citrate, phos and cholecalciferol started, yet she still progressed to nephrocalcinosis, weight loss and poor linear growth. At 8 years, bone pain and genu valgum, along with laboratory (Table 1) and radiographic evidence of metaphyseal widening/fraying (Figure 1), were consistent with hypophosphatemic rickets. Standard therapy with phos and calcitriol was started but stopped abruptly due to hives. Given bone pain and rickets, we initiated Burosumab (FDA approved for XLH; dosing per "prescriber packet"). Although Fanconi syndrome is not a known condition of FGF23 excess, we postulated that Burosumab might offset her phosphaturia by blocking any FGF23 contribution (pretreatment FGF23 181 RU/mL; Mayo Clinic, reference< 230). Within 5 doses, (10mg q2 weeks) serum phosphorus increased (1.7 to 3.0 mg/dL) and urine phosphorus decreased (81 to 34.5 mg/dL). However, 3 months later, serum phosphorus was again 1.7 mg/dL. We increased Burosumab (20mg q2 weeks) but repeat phos remained 1.7 mg/dL. Clinically, bone pain improved along with early radiological changes in rickets (Figure1). Conclusion: FGF23 diminishes Na-dependent phosphate reabsorption,1,25 (OH)2 vitamin D and PTH action. Burosumab, a recombinant

human IgG1 monoclonal antibody targeting FGF23, binds to/inhibits FGF23 and decreases phosphaturia and improves rickets in XLH. Our patient's response to Burosumab suggests FGF23 inhibition may be clinically useful in other phosphaturic states for symptomatic relief and possibly bone mineralization, but it does not appear to normalize serum phos levels in Fanconi syndrome at recommended dosing. Abbreviations : FePO4: Fractional excretion of phosphate, XLH: X linked hypophosphatemic rickets, FGF 23: Fibroblast growth factor 23, PTH-Parathyroid hormone.

Table 1 : Lab values at rickets presentation

	At presentation	Reference range
Calcium (mg/dL)	8.4	8.9-10.4
Phosphate (mg/dL)	2.4	4.1-5.9
Magnesium (mg/dL)	2.5	1.6-2.3
25 hydroxy vitamin D (ng/mL)	60	30-80
1,25 di hydroxy vitamin D (pg/mL)	175	24-86
PTH (pg/mL)	24.6	8.5-77.1
Alkaline phosphatase (IU/mL)	741	156-369
Random urine phosphate/ creatinine ratio (mg/mg)	2.7	<0.97
FePo4 (%)	50	10-20

Figure 1 : Xray of left wrist showing rachitic changes before & after Burosumab

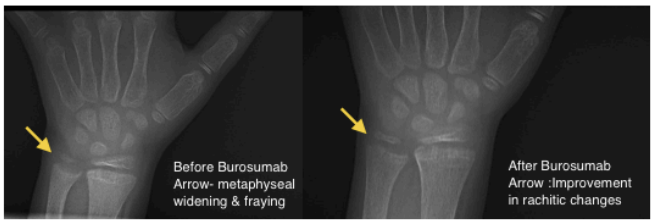

***Disclosures: Nandini Vijayakanthi**, None*

P-206

Multiple fractures in a young woman with normal bone mineral density: insights from bone microarchitectural assessment *Madhuni Herath[1], Catherine Shore-Lorenti[2], Peter Ebeling[1], Frances Milat[3]. [1]Department of Endocrinology, Monash Health; Department of Medicine, School of Clinical Sciences, Monash University, Australia, [2]Department of Medicine, School of Clinical Sciences, Monash University, Australia, [3]Department of Endocrinology, Monash Health; Centre for Endocrinology & Metabolism, Hudson Institute of Research; Department of Medicine, School of Clinical Sciences, Monash University, Australia

Introduction: Fracture prevention in young adults with chronic disease and glucocorticoid (GC) exposure is complex and limited by insufficient data. Current guidelines(1) recommend monitoring of bone mineral density (BMD) with dual x-ray absorptiometry (DXA); oral bisphosphonates are recommended over anabolic therapy for those at moderate-high fracture risk.Clinical Case: A 47-year-old woman with a 30-year history of severe rheumatoid arthritis presented for review of osteoporosis management. She had a 20-year fracture history including vertebral, metatarsal and periprosthetic fractures of the left ulna and a more recent non-healing left patella and tibia-fibula fracture. Risk factors for fracture included over 20 years of GC exposure, premature ovarian insufficiency (POI) secondary to cyclophosphamide and pancreatitis secondary to sulfasalazine. She had received oral bisphosphonates for over five years followed by four doses of zoledronic acid. Two years after her final dose of zoledronic acid, she developed osteonecrosis of the jaw (ONJ) after a dental extraction.The patient had normal vitamin D (25-OH vitamin D 102nmol/L; 50-250), creatinine 63umol/L (45 – 85) and corrected calcium 2.44mmol/L (2.15-2.55) levels. Bone turnover markers were unremarkable: CTx 220ng/L (150-800), P1NP 50ug/L (15-70) and ALP 59U/L (20-105). BMD was normal on DXA: L1-L4 (LS) 1.254g/cm2, Z-score -0.3, left neck of femur (NOF) 0.921g/cm2, Z score -1.1 in 2010, increasing to 1.353g/cm2 LS and 1.142g/cm2 NOF by 2018. However, high resolution peripheral quantitative computed tomography (HR-pQCT) identified reduced trabecular and cortical bone volume and a 7.8x6.5x6.7mm area of focal bone loss (Figure 1). While her ONJ improved, trabecular volumetric BMD (Tb.vBMD: 157mgHA/cm3 at radius and 144.3 mgHA/cm3 at tibia) and cortical volumetric BMD (Ct.vBMD; 845.3 mgHA/cm3 radius and 889.5 mgHA/cm3 tibia) did not, (Tbv.BMD 119.0 mgHA/cm3 radius and 114.3 mgHA/cm3 tibia, Ct.vBMD 848.4 mgHA/cm3 radius and 889.1 mgHA/cm3 tibia) after eight months of teriparatide.Conclusions: HR-pQCT provides additional insights into bone quality, enabling detailed assessment of cortical and trabecular bone structure and quality. This case highlights the complexity of bone disease encountered in young adults with chronic disease. The importance of navigating pitfalls of routine imaging modalities and utilising alternatives to obtain information and guide management are important learning points.

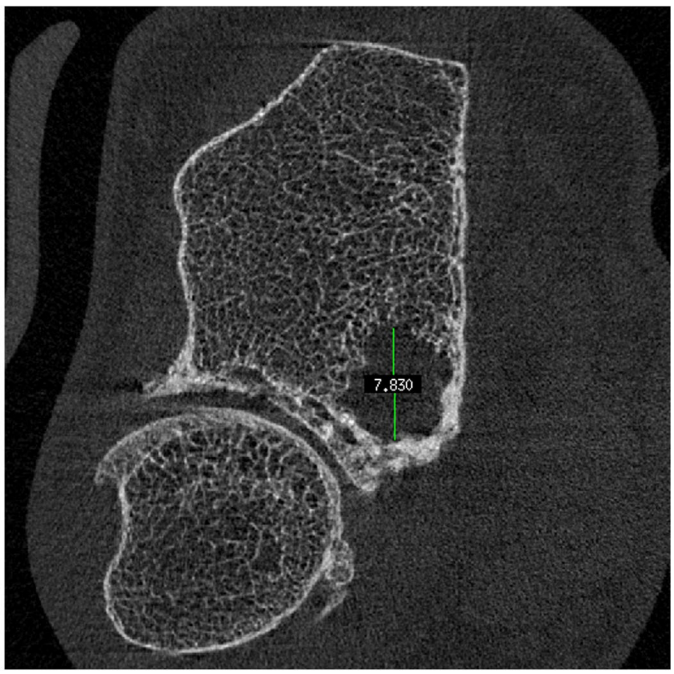

***Disclosures: Madhuni Herath**, None*

P-207

Symptoms of Multicentric Carpotarsal Osteolysis Respond to Anti-inflammatory Treatment *Nina Ma[1]. [1]Section of Endocrinology, Children's Hospital Colorado and Department of Pediatrics, University of Colorado School of Medicine, United States

Multicentric carpotarsal osteolysis (MCTO) is a rare diagnosis associated with MAFB mutations and characterized by osteolysis, nephropathy and craniofacial anomalies. Affected individuals are frequently diagnosed with juvenile idiopathic arthritis (JIA) due to joint pain and swelling. Treatment for JIA does not prevent the progressive destruction of carpal and tarsal bones; consequently, "misdiagnosis" of JIA is suggested. However, we present a case of MCTO that responded clinically to treatment for JIA, suggesting that inflammatory arthropathy may co-exist with or be a feature of MCTO.A 21 mo-old child was not standing or walking and cried when she put weight on her feet. She learned to "walk" on her knees. She was healthy and her development typical otherwise. Exam was notable for bilateral wrist/ankle swelling, limited range of motion, metatarsal medial curvature and subtle craniofacial changes (shortened palpebral fissures, periorbital fullness, narrowed nasal bridge, small nasal alae and long underdeveloped slit philtrum). Radiographs showed small wrist/ankle compartments and atypical carpal/tarsal bones. Ankle MRI showed asymmetric talus bones, joint effusions and synovitis. She was diagnosed with JIA and trialed various treatments (NSAIDs, MTX +/- adalimumab, oral/intraarticular corticosteroids). The most effective treatment was MTX + tocilizumab. Treatment relieved pain and improved function. She began to put weight on her legs and walk independently (with orthotics). Her right foot remained more inverted than the left and she was unable to jump, go up or down stairs. On exam, she had significant improvement in range of motion and minimal active disease. Musculoskeletal ultrasound showed no active inflammatory arthritis or tenosynovitis. Whole exome sequencing later revealed a novel variant in MAFB (c.212 C>G, p.P71R). Despite a genetic diagnosis of MCTO, her treatment for JIA continued due to significant clinical improvement of symptoms and inflammation. She had no medication side effects and had normal renal function.Clinical Lessons: 1. Inflammatory arthropathy may co-exist with or is a characteristic of MCTO. Anti-inflammatory/rheumatic treatment may be adjunctive therapy in some patients with MCTO1. 2. Small joint compartments and atypical carpal/tarsal bones may be an early clue that individuals presenting with inflammatory arthropathy have MCTO. 3. Small wrist/ankle compartments may support the notion that MAFB gene expression is important for chondrocyte function and the preparation for ossification in wrists/ankles2. Thus, MCTO may not be purely an osteolytic disorder which has implications for treatment.References: 1. Upadia J, et al. J Pediatr Genet 2018;7(4):174-9. 2. Lazarus S, et al. Am J Pathol 2017;187(9):1923-34.

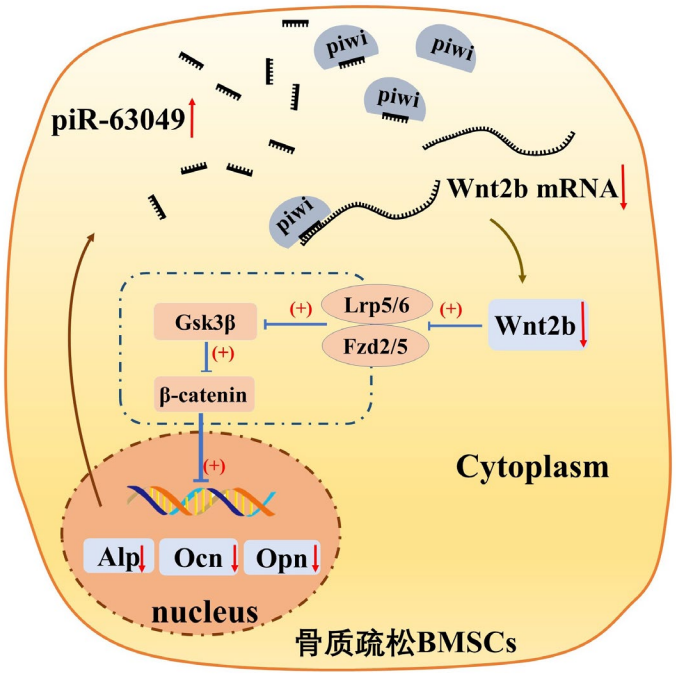

***Disclosures: Nina Ma**, None*

P-208

Humoral Hypercalcemia of Malignancy in Recurrent Pulmonary Papillomatosis *Ansha Goel[1], Julianna Barsony[1]. [1]Medstar Georgetown University Hospital, United States

Background: Hypercalcemia is defined as serum calcium greater than 10.5 mg/dL and/or ionized calcium greater than 1.3 mmol/L. Primary hyperparathyroidism and malignancy account for over 90% of all hypercalcemia cases. Humoral hypercalcemia of malignancy involves the secretion of parathyroid hormone-related peptide (PTHrP). Given its homology with PTH, PTHrP binds to the same receptors and causes hypercalcemia by increasing bone resorption, renal distal tubular calcium resorption, and intestinal calcium absorption. We present a case of humoral hypercalcemia of malignancy in a patient with recurrent respiratory papillomatosis (RRP), a rare disease caused by human papillomavirus (HPV) where papillomas grow throughout the upper and lower respiratory tracts.Clinical case: Our patient is a 32-year-old male with a history of RRP with multiple pulmonary papillomas who has previously had over 350 papilloma excisions. Prior biopsies were positive for HPV 6 and 11, without evidence of high-grade squamous intraepithelial lesion or malignancy. He initially presented with shortness of breath and was found to be hypercalcemic with a serum calcium of 14.6 mg/dL (corrected for albumin of 2.2 gm/dL) and ionized calcium of 1.92 mmol/L. Additional workup revealed acute kidney injury (creatinine 1.86 mg/dL), suppressed PTH (6.3 pg/ml), elevated PTHrP (43 pmol/L), normal 25-hydroxyvitamin D (57.2 ng/ml), and normal 1,25-dihydroxyvitamin D (47.1 pg/mL). Electrocardiogram did not reveal a shortened Q-T interval. His clinical picture was consistent with humoral hypercalcemia of malignancy, presumably due to squamous cell transformation of previous pulmonary papillomas. He initially received intravenous fluids, calcitonin, and Denosumab. As his renal function improved, he also received one dose of intravenous Zoledronic acid with subsequent improvement in his hypercalcemia to 12.6 mg/dL.Conclusion: Squamous cell carcinoma, via PTHrP secretion, is the most common cause of hypercalcemia of malignancy. Malignant transformation of previously benign respiratory papillomas into squamous cell carcinoma can occur in up to 4% of RRP cases. This illustrates the need for careful monitoring for malignant transformation in patients with RRP as they may possibly develop life-threatening hypercalcemia. A comprehensive diagnostic evaluation and urgent treatment with intravenous fluids and bisphosphonate therapy may be indicated in order to prevent morbidity and mortality in these patients.

***Disclosures: Ansha Goel**, None*

P-209

Osteomalacia Secondary to Fanconi Syndrome Induced by Antiretroviral Drugs in a Patient with HIV/AIDS *Sara Gariela Bayas[1], Francisco Umaña [1], Luisa Plantalech[1], Betiana Mabel Perez[1], Mirena Buttazzoni[1], Ariela Veronica Kitaigrodsky[1], Maria Diehl[1]. [1]Hospital Italiano de Buenos Aires, Argentina

HIV may cause an imbalance in mineral and bone metabolism. This effect is multifactorial and induced by pro-inflammatory molecules with an increase in osteoclast activity and suppression of osteoblast function. Tenofovir has been associated with Fanconi syndrome, accelerated bone mass loss and osteomalacia.We report a case of severe hypophosphatemia and osteomalacia induced by tenofovir.A 49-year-old woman consulted with invalidating bone and muscle pain, asthenia and multiple spontaneous fractures (vertebral, hips, tibia, patella, humerus, distal femur) in the last 3 years that lead her to prostation. She reported a history of non-Hodgkin's lymphoma, Hepatitis C and HIV diagnosed at 31 years of age. She received lopinavir/ritonavir, lamivudine and tenofovir as antiretroviral therapy. Physical examination showed scoliosis, severe kyphosis and marked limitation in mobility of upper and lower limbs. Biochemical studies revealed: serum phosphate 1.4 mg/dl (NR 2.5-4.5), calcium 8.1mg/dl (NR 8.5-10.5), magnesium (Mg) 2 mg/dl (NR 1.9-2.5), creatinine 0.48 mg/dl, PTH 38 pg/ml (NR 16-77.1), beta crosslaps 2.48 ng/ml (NR 0.1-0.55), bone alkaline phosphatase 300 ug/l NR (3.8-22.6), 25 OH vitamin D 25 ng/ml (>30), calciuria 556 mg/day (NR 250), calcium/creatinine urinary index 0.9 (NR 0.1-0.25), Mg fractional excretion 2.15 (3-5%), tubular phosphorus reabsorption: 74% (NR >85). BMD showed a T- score of -3.6 in lumbar spine. X-rays showed severe demineralization. She received intravenous and oral phosphate, calcium, calcitriol, magnesium, hydrochlorothiazide and cholecalciferol. Tenofovir was withdrawn. Once hypocalcemia and hypophosphatemia were corrected, zoledronate 4 mg was indicated. She continued with oral ibandronate for two years. Lumbar spine BMD improved (+27.5%) as well as X-ray images and bone markers. She evolved with progressive clinical improvement and is now able to walk unaided. She has not suffered new fractures after five years of treatment.Conclusion: In this patient with AIDS / HIV two metabolic bone disturbances were found, osteomalacia due to Fanconi syndrome induced by antiretroviral drugs with severe hypophosphatemia and devastating clinical consequences, treated with mineral substitution, and high bone turnover which was controlled by bisphosphonates. The importance of suspecting the possibility of hypophosphatemic osteomalacia in patients with AIDS / HIV treated with tenofovir is highlighted.

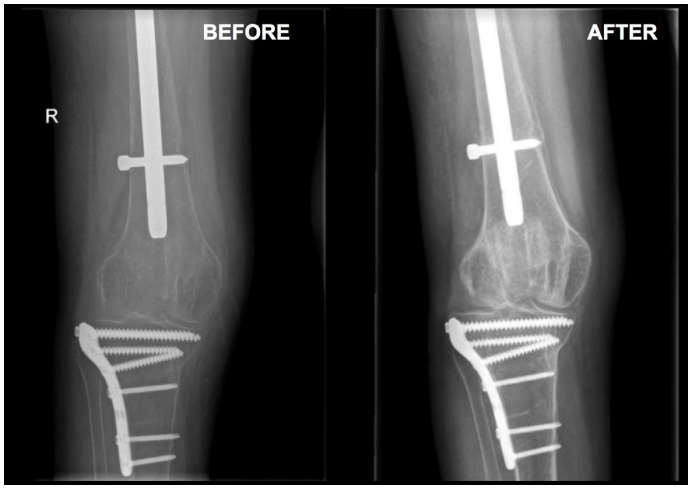

***Disclosures: Sara Gariela Bayas**, None*

P-210

Aneurysmal Bone Cysts: A Case Series *Milena Komornicki[1], Mirena Butazzoni[2], Maria Diehl [1], Ana María Galich[1], Luisa Plantalech[1]. [1]MD Hospital Italiano de Buenos Aires, Argentina, [2]Hospital Italiano de Buenos Aires, Argentina

Introduction: Aneurysmal bone cysts (ABC) are rare benign skeletal lesions. They most frequently involve metaphysis of long bones, pelvis or spine. They may occur as a primary bone tumor or secondary to preexisting bone lesions (e.g., simple bone cyst, fibrous dysplasia, giant cell tumor, etc.). They are usually diagnosed in the first two decades of life. Clinically they present with pain, swelling and palpable mass. Spinal lesions may present with back pain or stiffness, neurologic deficits and radicular pain. Treatment goals are to eradicate the lesion, minimize recurrence, relieve pain and avoid functional impairment. Treatment options are surgery, sclerotherapy, selective embolism, cryotherapy, etc. Recently bisphosphonates have been successfully used as definitive treatment.The aim of this presentation is to describe three different cases of this entity.Case 1: a 28-year-old woman presented with rib tumor and local pain. The initial histology showed a fibrohistiocytic lesion with multinucleated giant cells. Given the probability of being a giant cell tumor surgical excision was performed and fibrous dysplasia with ABC was diagnosed. Local pain resolved after surgery,Case 2: a 38-year-old woman with ABC in C7 and axial pain. Selective embolization of the lesion was performed with partial response. Due to its location with potential risk of spinal cord injury, she underwent intravenous ibandronate therapy, three doses during six month, with symptoms improvement. RMI showed reduction in the size of the lesion and less bone edema. No other adjunctive therapy or surgical intervention was required. Case 3: a 34-year-old woman, diagnosis of fibrous dysplasia with secondary ABC in sixth rib in posterior localization and back pain. She refused surgery and medical treatment with bisphosphonates was indicated. Three doses of intravenous ibandronate were administered within one year. She reported significant pain improvement without evidence of recurrence

during the follow up.Conclusions: ABC are a diagnostic and therapeutic challenge. It is important to consider this entity in patients with fibrous dysplasia. Considering its symptoms, location, extent, recurrence rate and benign nature, different treatment alternatives may be considered including surgery and antiresorptive therapy. The use of bisphosphonates could be a viable treatment option.

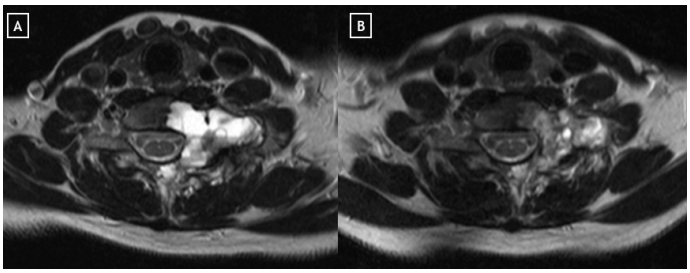

***Disclosures: Milena Komornicki**, None*

P-211

Chronic Treatment of Hypercalcemia caused by Methacrylate-induced Granulomas *Luisa Plantalech[1], Maria Diehl[1], Maria Eugenia Vera[1], Diana gonzalez[2], Carlos Federico Varela[1]. [1]Hospital Italiano de Buenos Aires, Argentina, [2]Mautalen, Argentina

Introduction: Granulomatous diseases can produce hypercalcemia mediated by 1.25 OH2 Vitamin D due to increased activity of 1α-hydroxylase. In recent years, granulomatosis has been reported as a reaction to foreign bodies after the use of methacrylate for aesthetic purposes.Corticosteroids are a first-line therapy in granulomatosis and antiresorptive drugs are part of the usual treatment of hypercalcemia. Other options are hydroxychloroquine, ketoconazole and anti TNF alpha antibodies.The purpose of this presentation is to communicate the long-term treatment of a patient with granulomas induced by methacrylate and hypercalcemia of difficult management.Case report: A 34-year-old woman consulted in 2014 with hypercalcemia, lithiasis and renal failure. She had a previous injection of methacrylate in her lower limbs for aesthetic purposes. Laboratory tests: hypercalcemia 13 mg/dl (8.5-10.5), phosphatemia: 4.1 mg/dl (2,5-4,5), PTH <3 pg/ml (8.7-77.1), 1.25 OH2 Vitamin D 180 pg/ml (18-60), creatinine 2.1 mg% (0.3-1.2), alkaline phosphatase 61 (31-100u/l), PET-CT: hypermetabolic nodular images in both buttocks and thighs. In a renal biopsy nephrocalcinosis and acute tubular necrosis were found. The biopsy of the gluteal area showed a foreign body-type granulomatous reaction. She received treatment with hydration, corticotherapy, bisphosphonates and hydroxychloroquine which was suspended due to intolerance. Ketoconazole (400-200 mg/day) was initiated combined with meprednisone 6 mg/day and alendronate 70 mg/week with normalization of serum calcium (9.6 mg /dl) and improvement of kidney function (creatinine: 1.40 mg/dl). After 5 years of treatment, she presented asthenia, hypotension and oligomenorrhea that was related to adrenal insufficiency due to a decrease in meprednisone to <4 mg (carried out by the patient) associated with ketoconazole. The patient recovered by lowering the dose of ketoconazole to 200 mg/d and increasing meprednisone to 6 mg/d. In the last year she had stable kidney function and normal calcium and PTH values.Conclusions: Treatment of granuloma-induced hypercalcemia associated with methacrylate application is a challenge. The combination of low doses of corticosteroids, ketoconazole and alendronate was effective at long-term. The dose of ketoconazole and meprednisone must be titrated in each patient, to be effective to inhibit the synthesis of calcitriol and avoid adverses events like suppression of corticoids and sexual steroid synthesis

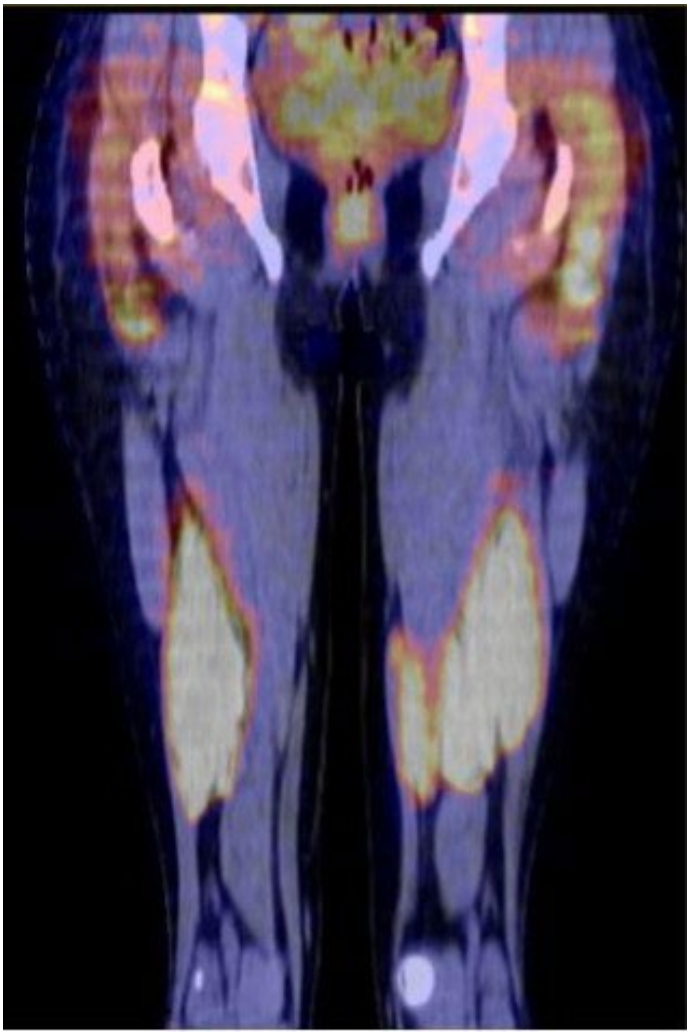

***Disclosures: Luisa Plantalech**, None*

P-212

A Case Of Rebound Hypercalcemia After Cessation Of Denosumab In Adult Patient With McCune-Albright Syndrome *Radhika Jaiswal[1], Stuart Weinerman[1]. [1]Long Island Jewish Medical Center, United States

Introduction: Denosumab, a fully human monoclonal antibody, is an inhibitor of RANKL (a cell surface protein involved in many cellular processes, including osteoclastogenesis, and is reported to be overexpressed in FD-like bone cells) and is mainly used for the treatment of postmenopausal osteoporosis and for the prevention of skeletal-related events from bone metastases 1,2. It is used off label in patients with McCune-Albright syndrome (MAS) because of its potent anti-resorptive properties 3,4. Rebound hypercalcemia following cessation of high dose Denosumab have been reported previously in adult patients with osteoporosis and juvenile patients with giant cell tumor and Paget's disease 5-7. There has been only one case report so far from Denosumab discontinuation causing life-threatening hypercalcemia requiring hospitalization in a juvenile patient with MAS 8. However, to the best of our knowledge, it has not been reported in an adult patient with MAS.Case description:A 25-year-old male with a history of MAS with polyostotic FD (who previously did not respond to aminobisphosphonates, being managed as outpatient with 120 mg subcutaneous injection of Denosumab every 1.5 months) and no prior history of hypercalcemia presented with worsening migraine, nausea, and vomiting for a week. His last dose of Denosumab was 4 months ago as he had a planned tooth extraction. Initial corrected serum calcium was 15.7 mg/dl [8.4-10.5 mg/dl]. PTH was appropriately low 9.85 pg/ml [15-65 pg/ml], vitamin D 25-OH low 25.5 ng/ml [30-80 ng/ml] and vitamin D 1,25-dihydroxy low <5.0 pg/ml [199-79.3 pg/ml]. PTHrP within normal range, <2.0. Serum calcium trended down to 14.4 mg/dl after fluids but again worsened to 15.1 mg/dl. The patient received a dose of Calcitonin 330 IU intramuscularly with improvement in serum calcium to 14.5 mg/dl. Further doses of Calcitonin were held due to an adverse reaction in form of abdominal pain, nausea and shakiness. Aggressive hydration was continued and a dose of Denosumab 120 mg subcutaneously was administered, following which the serum calcium continued to trend down and was 11.6 mg/dl on discharge from hospital. When checked as an outpatient within a week, repeat calcium was 9.0 mg/dl. Patient resumed his Denosumab every 1.5 months. Multiple repeat calcium

have been normal since the hospital admission.Conclusion:Rebound hypercalcemia can occur in a patient with MAS upon cessation of Denosumab and thus warrants close monitoring for electrolyte derangements following discontinuation.

***Disclosures: Radhika Jaiswal**, None*

P-213

Fractures in the Intensive Care Unit (ICU): Continuous Renal Replacement Therapy Masking Immobility Hypercalcemia *Preethika Ekanayake[1], Tudor Hughes[2], Gina Woods[3]. [1]University of California, San Diego Division of Endocrinology, Diabetes and Metabolism, United States, [2]University of California, San Diego, Department of Radiology, United States, [3]University of California, San Diego Division of Endocrinology, Diabetes and Metabolism; VA San Diego Healthcare System, United States

IntroductionContinuous renal replacement therapy (CRRT) is utilized for the treatment of renal failure in critically ill patients with hemodynamic instability. The citrate used in CRRT prevents activation of the coagulation cascade by chelating with calcium. This complex is then removed by the filter, leading to calcium loss. Thus, serum calcium levels must be maintained via a post filter calcium infusion. Here we present a case of hypercalcemia and bone resorption masked by CRRT.Clinical CaseA 46-year-old woman with gastric ulcers and bilateral oophorectomy presented with unintentional weight loss, jaundice, cirrhosis, and necrotizing pancreatitis. Following a month and a half of a protracted critical illness requiring intubation and vasopressors, exacerbated by fluid shifts, the patient developed acute renal failure. CRRT with citrate anticoagulation was initiated. Prior to CRRT, her albumin-adjusted calcium was 9.0-9.6mg/dL and ionized calcium 1.16 (ref 1.13-1.32mmol/L). When CRRT was initiated, the patient received the customary calcium infusion to maintain her ionized calcium within the target range of 1.05-1.1mmol/L. However, within five days of CRRT initiation, her ionized calcium started rising above goal (1.12-1.3mmol/L) and thus the post filter calcium infusion was stopped. Despite ongoing citrate use with CRRT, her ionized calcium remained within the desired range without supplementation. After 23 days of CRRT, a CT scan of the chest showed incidental findings of acute sternal and bilateral rib fractures with severe bone demineralization. Her intact parathyroid hormone (PTHi) was elevated at 248 (ref 15-65pg/mL), calcitriol 16.7 (ref 19.9-79.3pg/mL), and vitamin D-OH 21 (30-80ng/mL). Subsequent CT scans showed additional acute fractures of the thoracic and lumbar spine, sacrum, pubic rami, and bilateral femoral necks. Unfortunately, two months after CRRT was initiated, the patient expired.ConclusionIn the above case, citrate used with CRRT masked hypercalcemia and bone resorption until the patient suffered multiple fractures. The etiology of her hypercalcemia was attributed to immobilization. Normalization of post filter serum calcium without supplemental calcium infusion, in a patient on CRRT using citrate as an anticoagulant, should raise suspicion for endogenous calcium loss via accelerated bone resorption.

***Disclosures: Preethika Ekanayake**, None*

P-214

Voriconazole Induced Periostitis *Ariela Veronica Kitaigrodsky[1], Maria Diehl[1], Aldana Maria Degrave[1], Marina Scolnik[1], Diana Carolina Fernandez Avila[1], Adela Aguirre[1], Mirena Buttazzoni[1], Tatiana Pereira[1], Ana Basquiera[2]. [1]Hospital Italiano de Buenos Aires, Argentina, [2]Hospital Privado Universitario de Córdoba, Argentina

INTRODUCTIONDrug-induced periostitis is a recognized entity. Voriconazole is a triazole agent used in prophylaxis and treatment of fungal infections. There is recent evidence that prolonged therapy with voriconazole may cause diffuse periostitis.CLINICAL CASEA 42-year-old woman diagnosed with high risk acute myeloid leukemia in June 2017, underwent bone marrow transplant with a mismatched unrelated donor in December 2017. Two months after transplant, gastrointestinal grade 4 graft-versus-host disease developed and she received treatment with high dose steroid and infliximab. As a result of severe immunosuppression she suffered a mycosis by Scedosporium apiospermum with lung and brain compromise. She was treated with voriconazole with close monitoring of plasma levels. She began with arthralgias in hands and generalized bone pain after 9 months of treatment with voriconazole. Physical examination showed swelling and nodular lesions in both hands and relative functional impotence. Bone scan revealed morphological changes at phalanges and metacarpal and severe periosteal reaction along with increased soft tissue. Laboratory showed increased levels of bone remodeling markers (bone ALP 191.8 ug/l (NR< 22.6), osteocalcin 152 ng/ml (NR 11-46), beta-crosslaps 4.86 ng/ml (NR < 0.573) and high levels of 24-hour urine fluoride (17.22 mg/l, NR <3 mg/l). Calcemia, phosphatemia, and creatininemia were normal. Positron emission tomography determined hypermetabolic periosteal lesions of exophytic growth towards soft tissues in multiple axial and appendicular bone structures. Findings were compatible with extensive periostitis. On suspicion of voriconazole-induced periostitis, its use was discontinued and liposomal amphotericin was started. Days after discontinuing therapy, symptoms improved and radiographic abnormalities decreasedDISCUSSIONVoriconazole-induced periostitis has been recently described. Fluoride included in voriconazole molecule may cause elevated fluoride levels and increased osteoblastic activity with periosteal lesions. The history of multifocal and asymmetric bone pain and imaging evidence of diffuse periosteal reaction in the context of chronic treatment with voriconazole suggested the diagnosis. Increased fluoride levels has diagnostic utility in this entity. Although the suspension of therapy usually achieves rapid symptomatic improvement in 2 to 21 days, as in the case of our patient, radiological alterations may persist for years.

***Disclosures: Ariela Veronica Kitaigrodsky**, None*

P-215

Presentation of a Late Diagnosis of Larsen Syndrome with a Novel Mutation of the Gene Encoding Filamin B (FLNB) *Deepshree Gupta[1], Deborah Wenkert[2]. [1]UCLA, United States, [2]Wenkert&Young, LLC, United States

Background: FLNB mutations cause autosomal dominant osteochondrodysplasias including Spondylocarpotarsal Synostosis Syndrome, Larsen syndrome and 3 typically lethal disorders. Clinical case: A 65-year-old Caucasian female, referred for diagnosis and fracture risk assessment, had congenital anomalies (bilateral clubfeet and bilateral dislocated hips and knees) and patellar dislocation. Surgeries included 12 at age 50, and left femoral rodding of a fracture. Endocrine history: Age 45-left oophorectomy (endometriosis); Age 50-menopause (no HRT). Fracture history: 2 femur fx-ages 14 and 58 yrs; wrist fx-age 51 yrs. In her 50s, 5 yrs of bisphosphonates, preceded 4 doses of Prolia over 4 yrs through age 63. Additional history: supraventricular tachycardia s/p ablation, androgenic alopecia, actinic keratosis, kidney stones, vertigo. Family & Social History: Ashkenazi Jewish descent, unmarried, no children. 63 yo sister has 2 children, age 32 and 43. No FH of a skeletal dysplasia. Physical exam: weight 81.6 kg, height 155cm, BMI 34. Alopecia, normal lips and palate, no thyromegaly, mild heart murmur, and wide based gait and features of Larsen syndrome (Table). DXA (age 59): T&Z scores: L1-L4 Spine -1.7 & -0.3, Femoral neck -0.8 & 0.5, Total hip -0.8 & 0.1. A clinical diagnosis of Larsen Syndrome was confirmed by FLNB gene analysis (heterozygous c533G>C (Cys178Ser) mutation in exon 2 of FLNB, not present in dbSNP, ESP, ExAC). Discussion: Our patient's novel mutation occurs in a highly conserved region in exon 2 of FLNB near the coding region of an actin binding domain (ABD) of filamin B. Other mutations in this region are presumed to affect actin binding, but her presentation is mild for an FLNB associated disorder. This spontaneous, likely pathogenic, variant explains her atypical facies, bilateral clubfeet and chronic joint dislocations, but not fracture history which may be related to her postmenopausal status. Indeed, neither osteoporosis nor fractures are known features of Larsen Syndrome. She has not had respiratory, cardiac, ophthalmologic, nor neurologic manifestations of Larsen Syndrome and has only mild scoliosis; she has extremity disproportionality, but her height is normal. Significant variability occurs even within families with Larsen syndrome making it difficult to ascribe her milder FNLB associated phenotype to her novel mutation.

Defects seen in Larsen syndrome (per OMIM)	Reported prevalence within Larsen Syndrome	Phenotype of case being presented
Facial dysmorphology: mid-face hypoplasia, prominent forehead, hypertelorism, depressed nasal bridge		Mid-face hypoplasia, mild frontal bossing, depressed flat nasal bridge, appearance of proptosis, button nose
Conductive hearing loss; Ossicle malformation	Malformations of the middle ear ossicles (21%)	Patient wearing right hearing aid since age 61, possibly had symptoms of hearing loss several years earlier
Anterior corneal lens opacities		Only after age 62
Cleft palate, uvula, lip	Cleft palate or bifid uvula (15%)	No
Hypodontia		No missing baby or adult teeth
Cardiovascular defects: Aortic dilatation, atrial or ventricular septal defect		No (per echocardiogram)
Respiratory: tracheal stenosis, tracheomalacia, bronchomalacia		No
Chest appearance: pectus excavatum and carinatum		Short trunk, Mild pectus excavatum with depressed sternum
Skull: Flattened frontal bone, small skull base, shallow orbits		No
Cervical vertebrae: hypoplasia, subluxation, fusion, or kyphosis and spinal cord compression	Cervical kyphosis (50%), secondary cervical cord damage and secondary paralysis (at least 15%)	No
Thoracic and lumbar: Scoliosis, wedged vertebrae, spondylolysis, spinabifida occulta	Spine abnormalities (scoliosis and kyphosis) including cervical (84%)	Age 64: mild levoscoliosis of L2 L3, moderate to severe degenerative discogenic disease from the L2-L4 levels, mild lateral and posterior subluxation of L2 on L3 and no compression fracture
Joint laxity; wrist, elbow, hip, knee dislocations; dysplastic epiphyseal centers	Present at birth: dislocation of large joints (80% hip, 80% knee, and 65% elbow)	Joint laxity, knee/patellar and hip dislocations. Has hypomobility of wrist and fingers with swan neck deformity with extension
Hands: Cylindric fingers, spatulate thumbs, short metacarpals, supernumerary carpal bones, multiple carpal ossification centers		Spatulate thumbs
Feet: Talipes equinovalgus or equinovarus; Short metatarsals; Supernumerary tarsal bones; Delayed coalescence of calcaneal ossification centers; Short nails	Clubfoot (75%)	Equinovalgus with a medially deviated, broad hallux and overlapping 4th and 5th toe
Mental retardation		No. Studied business after high school for a few years
Growth abnormality: Short stature (final adult height less than 152cm); and prenatla growth deficiency	Height is below the tenth percentile (70%)	155 cm (10th percentile); short trunk, upper and lower extremity rhizomelia and lower extremity mesomelia. Birth weight- over 6 lbs

***Disclosures: Deepshree Gupta**, None*

P-216

The efficacy of denosumab treatment for hypercalcemia in a patient with primary hyperoxaluria type 1. *Liudmila Rozhinskaya[1], Sofia Gronskaia[1], Tatiana Grebennikova[1], Zhanna Belaya[1]. [1]The National Medical Research Centre for Endocrinology, Russian Federation

Primary hyperoxaluria type 1 (PH1) is a rare, metabolic, autosomal recessive disease, characterized by a deficiency of liver glyoxylate aminotransferase enzyme (AGT) and consequent oxalate overproduction due to enzyme defects. These oxalate deposits lead to various abnormalities including kidney failure and oxalate osteopathy.We report a 19-year-old male referred to our clinic due to complaints about severe pain in the pelvic bones, weight loss, low appetite, muscle and general weakness. PH1 was confirmed based on a heterozygous c508 G>Amutation in exon 4 of AGXT gene. He suffered from nephrolithiasis and nephrocalcinosis since childhood which led to kidney failure and peritoneal dialysis at the age of 11; hemodialysis at the age of 17. At the age of 18 the patient underwent liver and kidney transplantation. At the age 19, PTH non-dependent hypercalcemia (the corrected serum calcium 3.62 (2,15-2,55) mmol/L) with low PTH level 3(12-88) pg/mL) was found for the first time which coexisted with symptoms of severe pain in the pelvic bones. Computed tomography (CT) revealed severe abnormalities: diffuse sclerosis and cortical thickening of the vertebrae and pelvic bones, periosteal proliferation, abnormal bone texture in the sacroiliac joints with patchy sclerosis and several lytic lesions in the subchondral areaOn basal evaluation the patient had severe kyphosis, reduced mobility in the hip joints, low body weight (BMI 16.4kg/m2; height 1.62m; weight 43kg). According to laboratory tests the following changes were revealed: leukopenia 2.9 (3.9-10) 109/L with severe neutropenia 0.6 (1.5-6.8)109/L, thrombocytopenia 107 (148-339) 109/L, anemia Hb-108 (132-172) g/L with serum iron at a normal level, hypercalcemia (calcium corrected for albumin- 3.62 (2.15-2.55) mmol/L, serum phosphate 1.69 (0.74-1.52) mmol/L, uric acid 518 (202-416) µmol/L, PTH 8.12 (15-65) ng/ml, creatinine 266 (63-110) µmol/L, eGFR 30 ml/min 1.73 m2, carboxylterminal cross-linked telopeptide of type I collagen (CTx) – 3.94 (0.01-0.6) ng/ml, osteocalcin - 235 (11-43) ng/ml; TSH 2.65 (0.35-4) mclU/ml, testosterone – 11.4 (11-28.2) nmol/l.Due to kidney failure and high bone turnover, denosumab 60mg was administered subcutaneously in order to control hypercalcemia. Three days after denosumab administration, the patient reported a reduction in bone pain which coincided with a decline in serum calcium levels and the bone resorption marker (serum calcium – 2.82 (2.15-2.55) mmol/L, CTx -0.64 (0.01-0.6) ng/ml, serum phosphate 0.99 (0.74-1.52) mmol/L). A month later biochemical parameters were within the reference range: serum calcium 2.32 mmol/L, serum phosphate 1.03 mmol/L with a slight improvement in creatinine levels- 184 (63-110) µmol/L, eGFR 45 ml/min 1.73 m2 and bone pain was alleviated.Conclusion: treatment with denosumab 60mg was effective at alleviating bone pain and non-PTH-dependent hypercalcemia in a PH1 patient.

***Disclosures: Liudmila Rozhinskaya**, None*

P-217

Atypical Parathyroid Adenoma Causing Parathyroid Crisis *Tammy Tavdy[1], Justin Mathew[1], Vafa Tabatabaie[1]. [1]Montefiore Medical Center/Albert Einstein College of Medicine, United States

Background: Primary hyperparathyroidism (PHPT) is a common endocrine disorder that often presents as asymptomatic hypercalcemia in the setting of excess parathyroid hormone (PTH) secretion. Patients with PHPT rarely present with parathyroid crisis - a sequelae of severe hypercalcemia with signs of multiple organ dysfunction. Parathyroid carcinoma and atypical parathyroid adenomas are rare diagnoses that account for approximately 2% of all patients with PHPT. While a definitive diagnosis for these conditions relies on pathology, severe hypercalcemia and PTH elevations strongly correlate with a parathyroid carcinoma. We describe a rare case of a patient with profound PTH-dependent hypercalcemia and parathyroid crisis who was found to have atypical parathyroid adenoma.Case: A 43-year-old woman presented with worsening abdominal pain associated with constipation and vomiting for one month. Laboratory results revealed hypercalcemia to 21 mg/dL (reference range 8.5-10.5), intact PTH of 920.2 pg/mL (15.0-65.0), and creatinine 4.54 mg/dL from a baseline of 0.7 (30.0) and vitamin D 1,25-dihydroxy was suppressed to 8 pg/mL (18.0-72.0). PTHrP was normal. She had no family history of endocrinopathies and imaging did not reveal any jaw tumors.Neck imaging revealed a 3x2.5 cm nodule along the right posteroinferior aspect of the thyroid, concerning for a parathyroid carcinoma or adenoma. She was initially treated with aggressive intravenous fluid hydration, calcitonin, and bisphosphonates, and then started on cinacalcet. However, her hypercalcemia was refractory to medical management, and she underwent emergent right inferior parathyroidectomy. Pathology revealed peripheral fibrosis, increased mitoses, and cytologic atypia without necrosis or invasion, meeting criteria for atypical parathyroid adenoma.Conclusions: This case describes an aggressive biochemical presentation of an atypical parathyroid adenoma. Severe PTH-dependent hypercalcemia often raises concern for parathyroid carcinomas. However, standard consideration should also be given to atypical adenomas, an intermediate form of parathyroid neoplasms with uncertain malignant potential and atypical histologic features. Germline mutations of CDC73 are a common genetic anomaly and suggest that these cases could be variants of the hyperparathyroidism-jaw tumor syndrome. Identification of genetic markers in atypical adenomas is necessary to guide appropriate postoperative monitoring.

***Disclosures: Tammy Tavdy**, None*

P-218

Bilateral Atypical Femur Fractures as a Presenting Manifestation of Unrecognized Hypophosphatasia. *Madhav Chittimalla[1], Tamara Roumayah Ivers[1], Leika Raychouni[1], Sudhaker Rao[1]. [1]Henry Ford Health System, United States

Introduction: Hypophosphatasia (HPP) is a rare inherited disorder of the ALPL gene which leads to low serum alkaline phosphatase (ALP) levels and abnormal bone matrix mineralization due to accumulation of pyrophosphate, a known inhibitor of mineralization. Although severe symptoms are seen in infancy and childhood, adult onset HPP is milder and often asymptomatic except for low BMD, thus escapes diagnosis. Manifestations of adult HPP include: low serum ALP, atraumatic or pseudo-fractures of femur, and premature tooth loss. We present an unusual case of previously unrecognized HPP in an otherwise healthy adult. Case: A 56y old man presented for evaluation of sequential bilateral atypical femur fractures (AFF). He had a low impact slip-and-fall in September 2019 sustaining left mid-shaft AFF while working in China. Twelve weeks later he returned to the USA, and he stepped oddly while walking and felt pain in right thigh resulting in fall; x-ray showed mid-shaft non-displaced transverse right AFF. He had no history of tooth loss, fractures or osteoporosis, nor use of bisphosphonate (BP), steroids, rheumatoid arthritis, or diabetes, well known predisposing factors for AFF. Review of lab results in electronic medical record showed low levels of ALP for at least 9y, but he was unaware. Despite the 2 AFFs, serum ALP was still inappropriately low-normal.Discussion: Review of the literature suggests that initial presenting symptoms of adult HPP are usually bone pain related to pseudo-fractures or premature loss of teeth. AFFs have been reported in the setting of undiagnosed HPP and concurrent bisphosphonate therapy, which is an independent risk factor for AFF. However, our case is unusual in whom bilateral AFFs were the only presenting manifestation of an underlying undiagnosed adult onset HPP in an otherwise healthy individual not taking bisphosphonates.

***Disclosures: Madhav Chittimalla**, None*

P-219

Coracoid Stress Fracture in a Tennis Player – A Rare Sports Injury *Clay Larkin[1], Elijah Kakani[1], Scott Mair[1], Florence Lima[1], Madhumathi Rao[1]. [1]University of Kentucky, United States

BackgroundA coracoid stress fracture is a rare injury, especially unusual in non-traumatic settings. In a recent systematic review, acute trauma, usually direct impact or avulsion, was responsible for 71% (n=15/21) of coracoid fractures, sometimes also associated with acromioclavicular joint injury. The remaining were fractures caused by recurrent stresses placed directly over the coracoid bone, such as recoil from a firearm, often referred to as “trap shooter’s shoulder”. This report describes a non-traumatic right coracoid stress fracture in a 62-year-old female, who is a life-long, predominately right-handed tennis player.Clinical CaseThe patient presented to the bone clinic with acute pain located anterior to the right shoulder that occurred during a game of tennis. She was diagnosed with a coracoid stress fracture on standard shoulder 3-view X-rays. Due to the non-displaced nature of the coracoid fracture, the patient was treated conservatively with a sling and cessation of sporting activities.Her past medical history was significant for post-menopausal osteoporosis complicated by stress fractures in the left radius and ulna, and bilateral breast cancer treated with chemotherapy and radiation; past surgical history was significant for surgical repair for right rotator cuff injury.She underwent complete workup for metabolic bone disease and was treated with denosumab. An anterior iliac crest bone biopsy was also performed showing normal bone turnover in the cortical and subcortical areas, but decreased turnover in the deeper areas. A follow up x-ray at one month showed mild displacement of the base of coracoid fracture with minimal interval healing and persistent significant rotator cuff arthropathy. The patient then underwent reverse shoulder replacement. After ten months the patient was able to return to playing tennis at a level similar to baseline.ConclusionThis report serves as an in-depth account of a singular patient with a stress fracture at the base of the right coracoid process, a highly unusual injury. Post-menopausal osteoporosis, prior radiation to the region, chemo-

therapy and tamoxifen, coupled with intensified mechanical stress from previously injured rotator cuff and continued use during tennis, culminated in this rare skeletal injury. As prior radiation therapy precluded the use of anabolic agents, the patient was successfully treated with denosumab.

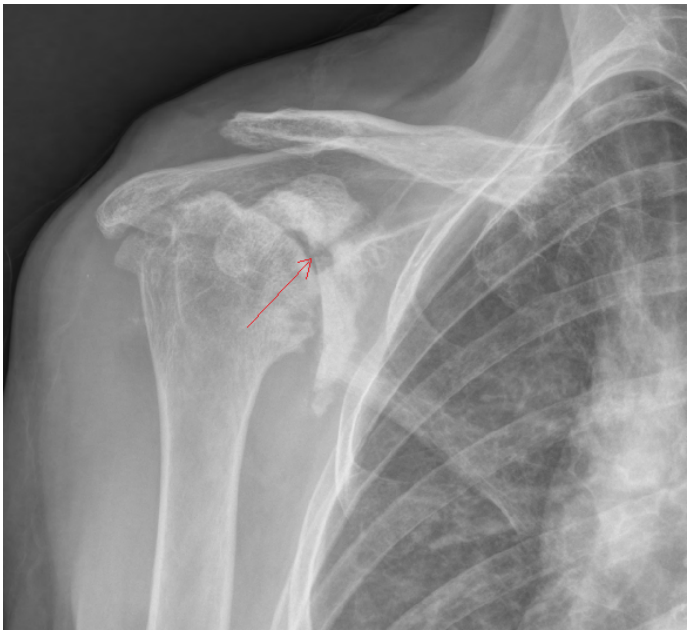

***Disclosures: Clay Larkin**, None*

P-220

Sacral Fractures in the Setting of Newly Diagnosed Rectal Cancer in Pregnancy: A Gravid Issue. *Parvathy Madhavan[1], Samaneh Rabieihashemi[1], Pamela Taxel[1]. [1]University of Connecticut Health Center, United States

Introduction:Fragility fractures are rare during pregnancy and commonly occur in the thoracic and lumbar vertebrae during late pregnancy or early postpartum period. We discuss a case of a pregnant patient with bilateral sacral and SI joint insufficiency fractures and rectal cancer.Case:A 36-year-old female patient presented to our clinic at 31 weeks gestation after right sacral fracture several weeks prior. She was diagnosed with stage IIIb, locally advanced rectal carcinoma at 18 weeks gestation and underwent neoadjuvant chemotherapy followed by radiation treatment. Follow-up MRI revealed non-displaced incomplete fracture of right sacrum without definitive underlying pathologic lesion, retrospectively associated with moderate pain while walking on treadmill. A 2nd fracture of left sacral ala occurred 4-weeks later, and a 3rd fracture at right SI joint occurred 5-months post-partum, both atraumatic. MRI findings were most consistent with insufficiency fractures.Her history was significant for menarche at 15 years, with irregular cycles consistent with PCOS. A prior child was conceived via IVF without fracture occurrence. After delivery, menstrual cycles were regular, and the current pregnancy spontaneous. The patient had several childhood fractures related to sports injuries. Family history was significant for osteopenia in her mother, without other metabolic bone disorders.We noted intake of prenatal vitamin and Vitamin D 2000 IU/day but limited calcium intake. Physical exam revealed a healthy-appearing gravid female without significant lumbosacral pain and otherwise normal exam. She was counseled regarding the increased demand of calcium in the 3rd trimester for fetal skeletal health, with a goal of 1500 mg/d. Labs: See table.Due to fractures, she underwent C-section and a health boy was delivered. After delivery she underwent successful bowel surgery, around which she took enoxaparin. She is now 15 months postpartum, pain-free and without further fractures. Conclusion:Sacral insufficiency fractures are rare in pregnancy, and in this case prompted suspicion for bone metastases, often seen in the pelvis or vertebrae in rectal cancer. However, bone metastases on MRI could not be documented. This patient had several risk factors for insufficiency fracture, including very low calcium intake. After pregnancy, BMD generally improves within 6-12 months; thus, we will monitor her progress closely and consider anti-resorptive therapy if indicated.

Labs	Reference	value
Serum Calcium	8.9-10.4 mg/dL	8.9
25- OH vitamin D	30-80 ng/ml	48
Albumin	3.8-5.3 g/dL	3.6
PTH rP	0-3.4 pmol/L	<2
Bone- specific alkaline phosphatase	11.6-29.6 U/L	20.2
PTH	15-88 pg/ml	32
Spot urine calcium: creatinine ratio	mg/g creatinine	633
collagen cross -linked N-telopeptide	17-94 nM BCE/mM creatinine	57

***Disclosures: Parvathy Madhavan**, None*

P-221

The Impact of Drug Therapy on Osteogenesis Imperfecta *Sarah Souza[1], Rayanne Peinado[1], Nathalia Cordeiro[1], Monise Carvalho[1]. [1]Universidade São Francisco, Brazil

Introduction: Osteogenesis imperfecta (OI) is a genetic disorder with heterogeneous manifestations, characterized mainly by fragility in the bones due to defects in the structure or quantity of type 1 collagen. The main clinical manifestations of this disorder are: skeletal deformities, blueish scleras, imperfect dentinogenesis and deafness. The diagnosis can be done in utero by the ultrasounds. After birth, the diagnosis becomes prominently clinical, with supplementary lab work and imaging scans. Treatment should be precocious and multidisciplinary, using drug therapy with Pamidronate Disodium in patients under 18 years old, with the intention of diminishing the risk of fractures. Clinical Case: M.V.S.C., 1 year and 3 months old, female, born at 40 weeks of gestation, no family history of OI. The hypothesis of OI came up with the 30 week ultrasound, that showed long bones dysplasia (femur=4,4cm consistent with a 24 week fetus; ulna=4,47cm consistent with a 28 week fetus), and the suspicion of a fracture in the right femur. At birth, radiological exams highlighted fracture in the right femur, genu varus (Picture 1) and bone thinning, including in the skull. The case was forwarded to a reference service where the patient was diagnosed with OI Type III in the Sillence Classification. Due to the lack of availability of the medication through the public health system, the start of treatment with Pamidronate Disodium was delayed. In the mean time the patient had various fractures throughout her first year of life. At 1 year of age, the patient received her first dose of Pamidronate Disodium, wich is an inhibitor of bone reabsorption mediated by osteoclasts (1st day: 0,25mg/kg, 2nd and 3rd days: 0,5mg/kg). And also takes Cholecalciferol, 4 drops/day, and calcium carbonate, 500mg/day. In addition to the drug treatment, the patient also is also being monitored by a multidisciplinary team. After beginning medication, the patient hasn't had any more fractures until now, which supports the importance of the drug therapy at the prognosis. Conclusion: This report is a classic example of how drug therapy benefits the prognosis, with the caveat of an early intervention being needed. However, the late start to the therapy due to the lack of availability of the medication through the public health system at first, leads to the worsening of the clinical presentation during the waiting time for the medication, resulting in various fractures during this period.

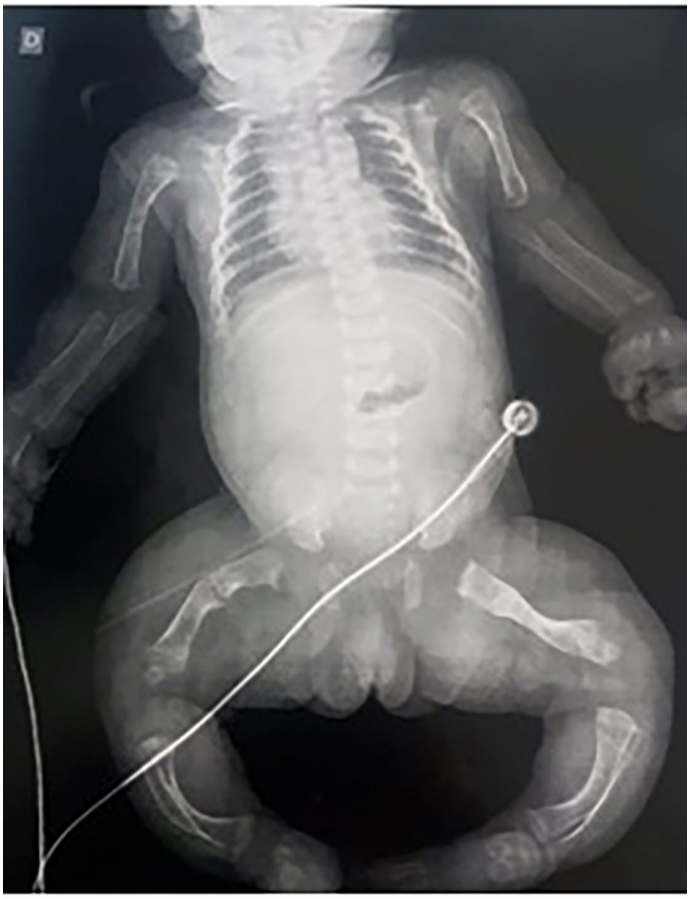

***Disclosures: Sarah Souza**, None*

P-222

Pregnancy associated Osteoporosis - Transient Osteoporosis of Hip *Krishna Mori[1], Sathish Kumar[1], Amulya Yalamanchi[1], Karthik Balachandran[1], Adlyne Reena Asirwatham[1], Shriraam Mahadevan[1]. [1]Sri Ramchandra Medical College, India

Introduction: Transient osteoporosis of hip (TOH) is a rare condition, often associated with pregnancy. The risk factors include pregnancy, smoking, alcohol, steroid intake, inflammation, vascular injury and osteogenesis imperfecta. The most important challenges include differentiating from avascular necrosis of hip (AVN), regional migratory osteoporosis (RMO) and deciding on treatment.Presentation: 25 year old lady, G2P1L1, at term pregnancy presented with waddling gait and lower limb pain. She delivered a healthy neonate. Two weeks postpartum, her pain in left hip worsened for which she was re-evaluate and was found to have fracture of left neck of femur. She was operated and plate and screw fixation was done. On further evaluation she was found to have Vit D deficiency. Since Vit D deficiency as a cause of non-traumatic hip fracture is unlikely, alternative diagnosis was sought. DEXA scan (right hip-Z Score – 4.1 and LS spine-Z Score – 3.9) showed osteoporosis. She was diagnosed to have TOH, associated with pregnancy. In view of active lactation and the fact that the patient had already been operated, bisphosphonate therapy was avoided. She was given Vitamin D 60000 IU/week for 8 weeks and calcium supplementation of 1000 mg/day. The patient showed remarkable improvement on follow up.Discussion: The pathophysiology of TOH is debated and is currently thought to be due to microfractures and edema in the marrow, with contribution from the hormonal changes occurring during and after pregnancy. The closest differential is AVN which is progressive and irreversible, while TOH is not. The other differential is index episode of RMO but it typically affects men in the fifth-sixth decade of life. Treatment modalities for TOH include conservative management with rest, core decompression in the marrow edema stage and screw fixation in the presence of fractures.Medical treatment can potentially hasten recovery in TOH. The treatment options include Bisphosphonates (not preferred during lactation), Calcitonin and Teriparatide along with Calcium and Vit D supplementation.Conclusion: TOH is a rare cause of acute onset hip pain, usually associated with pregnancy. The pathophysiology and prevalence are largely unknown. The condition recovers with rest and conservative management with or without surgery, over six months to one year. Timely detection and early initiation of anti-osteoporotic therapy can avert surgery or hasten recovery. Keywords: Osteoporosis, Pregnancy

***Disclosures: Krishna Mori**, None*

P-223

Hypercalcemia in A Young Patient: What is the Deal? *Dr. Carmen Cartwright, MD[1], Dr. Janna Prater, MD[1], Dr. Catherine Anastasopoulou, MD, PhD, FACE[1]. [1]Albert Einstein HealthCare Network, United States

Introduction: Hypercalcemia can have detrimental effects leading to nephrolithiasis, renal dysfunction or failure, osteoporosis, cardiac arrhythmias, and a malady of symptoms captured in the classic medical student mnemonic of "stones, bones, groans, and psychic moans". We present a case of a young patient with hypercalcemia of unclear etiology to emphasize the importance of understanding the underlying causes of the problem that ultimately could help in the final diagnosis and decision of appropriate treatment.Clinical Case: The patient is a 30-year-old male with attention deficit hyperactivity disorder, Asperger's syndrome, gastroesophageal reflux disease, mixed hyperlipidemia, seizure disorder, and Bell's palsy, who was found to have asymptomatic hypercalcemia since age 24. Calcium levels have ranged between 10.1 – 12.2 mg/dl (Normal: 8.7 -10.2), with low-normal parathyroid hormone (PTH) levels 18-35 pg/ml (Normal: 15-65). The patient denied any excess calcium, vitamin D3, or vitamin A intake. He has had mildly elevated 1,25 dihydroxy vitamin D levels and low-normal 25 hydroxy vitamin D levels. different laboratory tests (see Table 1) have ruled out familial hypocalciuric hypercalcemic syndrome, thyroid dysfunction, multiple myeloma, lymphoma, sarcoidosis, tuberculosis, or other pulmonary infections that can lead to hypercalcemia. Imaging studies were negative for Primary Hyperparathyroidism. An elevated ratio of 24, 25 dihydroxy-vitamin D to 25 hydroxy-vitamin D was found. This was suspected to be due to relative 25 hydroxy-vitamin D deficiency and genetic testing was pursued but did not show evidence of mutations to CYP24A1 or SLC34A1. A trial of Ketoconazole was instituted due to high suspicion of an unknown mutation, but this did not prove to be successful. Discussion/Conclusion: The etiology of the hypercalcemia in our patient was presumed to be non-PTH mediated and an even more extensive workup is ongoing to cover the most unusual differential diagnoses. Endocrinologists sometimes come across cases where the etiology of the hypercalcemia is not attributable to well-known causes. These rare cases demonstrate that our knowledge of the mechanisms of hypercalcemia is far from complete and as we get a better understanding of the underlying processes in the pathogenesis of hypercalcemia, it is likely that we will recognize better ways of its management.

LABORATORY RESULTS

DATE	Calcium N:(8.7-10.2 mg/dl)	Albumin N: (4.1-5.2 g/dl)	Parathyroid Hormone N: (15-64 pg/ml)	25-hydroxy Vitamin D N: (30-100 ng/ml)	1,25 dihydroxy Vitamin D N: (19.9-79.3 pg/ml)	24-hour Urinary Calcium N: (100-300 mg/24hour)	24,25 dihydroxy Vitamin D level (ng/ml, no reference range)	24,25 Vit D: 25 Vit D Ratio (level 25-80 considered high)
6/2016	10.1	4.3	23	25.4				
8/2017	10.6	4.2	18	37.9	80.3	226.5		
7/2018	11.5	4.2	35	25.2				
1/2019	10.5	4.3	29	14.1	65.6			
2/2019				18			0.56	32.14
4/2020	12.2	4.4	23	18	21.3			
No evidence of CYP24A1 or SLC34A1 mutations								
SPEP, UPEP negative on two separate occasions								

***Disclosures: Dr. Carmen Cartwright, MD**, None*

P-224

An Atypical Case of Steroid Induced Bone Infarctions *Jessica Lucier[1], Jawairia Shakil[2]. [1]Houston Methodist Hospital, United States, [2]Houston Methodist Hospital, United States

Introduction: Glucocorticoid use is a well known cause of bone osteonecrosis. Glucocorticoids have a direct toxic effect to osteoblasts and lead to increased osteoclast activity. Patients who have received a transplant are at an increased risk of osteonecrosis when com-

pared to the general population. Bone infarcts in this patient population are most commonly seen in weight bearing long bones, specifically the femoral head. Case: A 47 year old female with a past medical history of double lung transplant secondary to interstitial lung disease and chronic anemia presented to our institution with left knee and right ankle pain. Endocrinology was consulted for evaluation of bone infarcts found on imaging. The patient's bone pain started developing shortly after her transplant, which was three years prior to presentation. She had no know history of joint swelling, trauma, radiation therapy, heavy alcohol use, or hematological disorders. She had been on chronic steroids for her anti-rejection medications. Initially after her surgery she was on high dose steroids, but had now been on 5mg prednisone daily for two years. Her other medications included vitamin D3, calcium, and fosamax, which she started 3 months prior to presentation. During her hospitalization, she had an MRI of the spine and upper/lower extremities. She was found to have acute and chronic bone infracts in the distal diaphysis of the femur, proximal diaphysis of the tibia/fibula, anterior calcaneus, navicular, first metatarsal, and proximal diaphysis of the left humerus. Hematology was consulted and performed an extensive work up for possible hematological causes. There work up was negative for multiple myeloma, sickle cell disease, thalassemia, Gaucher disease and hypercoagulability. It was concluded that though atypical in location for steroid induced osteonecrosis, her chronic steroids were the likely underlying cause of her bone infarcts. Discussion: Steroids are commonly used for anti-rejection purposes in the transplant population. It is important to remember that even low doses of chronic steroids can induce osteonecrosis. Though the femoral head is the most commonly affected area by steroid induced osteonecrosis, bone infarcts can occur anywhere. Patients who have received a transplant often also have multifocal osteonecrosis. Prompt recognition of bone infarctions and early treatment with bisphosphonates can greatly decrease pain and increase ambulation in this patient population.

***Disclosures: Jessica Lucier**, None*

P-225

Interactions between CXCL12+ bone marrow stromal cells and hematopoietic cells regulate murine bone marrow adipogenesis *Yuki Matsushita[1], Noriaki Ono[1]. [1]University of Michigan, United States

Bone marrow stromal cells (BMSCs) expressing C-X-C motif chemokine ligand 12 (CXCL12), generally termed as CXCL12-abundant reticular (CAR) cells, are a multifunctional mesenchymal cell population that regulates hematopoiesis, osteogenesis, and adipogenesis. Recent studies have revealed that these CXCL12+ BMSCs are comprised of two distinct subsets of pre-osteoblast-like and pre-adipocyte-like cells, termed as Osteo-CAR and Adipo-CAR cells, respectively. The latter pre-adipocyte-like cells are dormant in physiological conditions and localized to sinusoidal surfaces, with particular enrichment for hematopoiesis-regulating cytokines. However, the nature of interactions between CXCL12+ BMSCs and hematopoietic cells, and how these interactions play a role in marrow adipogenesis are unknown. Here we show that many CXCL12+ BMSCs marked by Cxcl12-GFP are physically coupled with hematopoietic cells in single cell preparation, and loss of CXCL12 in these cells using Col2a1-cre and Cxcl12-floxed alleles leads to extensive marrow adipogenesis. We found in imaging cytometry that a substantial fraction of Cxcl12-GFP+ cells intertwined with CD45+ cells in a way indistinguishable from purely single cells, which rendered these cells falsely appearing in a CD45+ fraction in flow cytometry. Deletion of CXCL12 in CXCL12+ BMSC using Cxcl12 GFP/flox; Col2a1-cre; R26R-tdTomato triple transgenic mice led to a significant reduction of hematopoietic cells and CD45+Cxcl12-GFP+ cells, suggesting functional CXCL12 is important in maintaining interactions between CXCL12+ BMSCs and CD45+ hematopoietic cells. In addition, CXCL12 deletion in BMSCs caused extensive marrow adipogenesis in adult mice, despite the fact that CXCL12-deficient mesenchymal progenitor cells exhibited normal capabilities for colony formation, self-renewal and adipocyte differentiation in cultured conditions. Our findings support the notion that CXCL12 inhibits an adipogenic fate of CAR cells in a non-cell-autonomous manner, suggesting a link between CXCL12-dependent stromal-hematopoietic interactions and marrow adipogenesis. Interactions with surrounding hematopoietic cells might be important for bone marrow stromal cells to maintain their proper cell fates under normal conditions.

***Disclosures: Yuki Matsushita**, None*

P-226

Hepatocyte Nuclear Factor 4 alpha (HNF4α) is a key mediator of bone metabolism *Marta Martinez Calle[1], Guillaume Courbon[1], Connor Francis[1], Xueyan Wang[1], Bridget Hunt-Tobey[1], Jadeah Spindler[1], Emily Lynch[1], Aline Martin[1], Valentin David[1]. [1]Division of Nephrology and Hypertension, Department of Medicine, and Center for Translational Metabolism and Health, Institute for Public Health and Medicine, Northwestern University Feinberg School of Medicine, Chicago, IL, USA, United States

Hepatocyte nuclear factor 4 alpha (HNF4α) is a transcription factor controlling the expression of genes involved in gluconeogenesis and lipid metabolism in liver. Several studies have shown that mutations in HNF4α are associated with osteoporosis and other bone and mineral metabolism outcomes, but the role of HNF4α in bone has not been studied. We tested the hypothesis that HNF4α is expressed in bone and regulates osteoblastogenesis and bone turnover.We verified expression of HNF4α in bone and generated mice harboring a conditional deletion of HNF4α in osteoblasts and osteocytes by crossing HNF4αflox/flox mice with Oc-Cre mice (HNF4αOc-cKO). We studied the bone phenotype of wild-type (WT) and HNF4αOc-cKO mice at 6, 12 and 35 weeks of age. We also performed RNA sequencing (RNA-seq) analyses in bones and RT-PCR in primary osteoblast cultures isolated from WT and HNF4αOc-cKO mice and in MC3T3 cells overexpressing HNF4α (Hnf4αTg). Finally, we performed Chromatin Immunoprecitation Sequencing (ChIP-seq) analyzes and metabolomics in control and Hnf4αTg and Hnf4αKO MC3T3 osteoblasts to define the impact of HNF4α on osteoblastic genes and signaling pathways.We show that HNF4α is expressed in bone cells of mesenchymal origin (osteoblasts and osteocytes), and that HNF4α expression in bone declines with aging, from 6 to 35 weeks. HNF4αOc-cKO mice, showed an age dependent reduction in trabecular bone volume, reaching a ~40% reduction in 12-weeks-old mice. They also showed decreased bone formation, bone resorption and mineralization, suggesting that HNF4α regulates bone metabolism. Consistent with the in vivo phenotype, HNF4α deletion reduced the number of alkaline phosphatase positive colonies and mineral deposits by ~50 %. ChIP-seq analyses showed that HNF4α is a transcriptional regulator of genes of osteoblastic differentiation, such as Runx2, osteocalcin and osterix, and Hnf4αTg cells showed a 3-5 fold increased expression of these genes. Finally, by RNA-seq, RT-PCR and metabolomics, we demonstrate that HNF4α is a master regulator of mitochondrial function and energy homeostasis in bone cells.Our results demonstrate a crucial role for HNFα in osteogenesis and suggest that osseous HNF4α plays a central role in bone dynamics by modulating the expression of osteoblastic genes and cellular energetic program.

***Disclosures: Marta Martinez Calle**, None*

P-227

Longitudinal Changes in Visceral Adiposity are Associated with Bone Density, Microarchitecture and Strength: The Framingham Osteoporosis Study *Douglas Kiel[1], Marian Hannan[1], Ching-Ti Liu[2], Thomas Travison[1], Timothy Tsai[1], Mary Bouxsein[3]. [1]Hebrew SeniorLife, United States, [2]Boston University School of Public Health, United States, [3]Beth Israel Deaconess Medical Center, United States

The belief that higher body weight protects the skeleton is so widely embraced in clinical medicine, the FRAX® risk predictor uses BMI in place of BMD when that measure is not available. Despite this view, the protective effects of increased fat mass on skeletal health have recently been challenged, implicating visceral obesity as having a negative impact on skeletal health, possibly mediated through systemic factors such as adipokines, cytokines, or sex steroids. To better determine the role of visceral adipose tissue (VAT) on bone density, microarchitecture and strength, we tested the hypothesis that longitudinal increases in VAT are associated with lower volumetric density, worse microarchitecture and lower bone strength.We determined the association between 8-yr changes in VAT and distal tibia and radius measures of volumetric density, microarchitecture and strength (measured by micro-finite element analysis) in 1,443 men and 1,691 women from the Framingham Study Generation 3 cohort. Participants had both baseline and follow-up whole body DXA scans 8 yrs apart that were used to measure longitudinal changes in VAT, and HRpQCT scans (Scanco XCTII) at the follow-up visit. Information on age, BMI, menopause status, self-reported physical activity, and use of estrogen was obtained from the follow-up visit. Multiple linear regression was used to quantify the association between changes in VAT (follow-up minus baseline) and distal tibial/radius measures of trabecular and cortical bone density, microarchitecture and strength, adjusting for baseline age, BMI, menopausal status and physical activity.At follow-up, the mean age was 54 yrs, mean height was 175 cm for men and 163 cm for women, and mean BMI was 29 kg/m2 in men and 27 kg/m2 in women. The mean (SD) change in VAT was 345 cm3 (800) for men, and 243 cm3 (541) for women. After adjustment for covariates, in men larger increases in VAT over 8 yrs were associated with significantly higher cortical density (CtBMD), lower cortical porosity (CtPo), lower cortical thickness (CtTh) and area (CtAr), trabecular density (TbBMD) and total area (TtAr), and most strikingly, lower failure load (FL). For every SD gain in VAT over the 8 yrs, the FL declined by 234 Newtons. In women, greater increases in VAT were associated with significantly lower CtTh, CtAr, TbBMD, TbN, Tb.BV/TV, TtBMD, TtAr and FL (a decline of 170 Newtons). Findings were similar for the distal radius but some measures did not reach statistical significance.In conclusion, after accounting for BMI and physical activity, gains in visceral adiposity over time are associated with unfavorable bone density, microarchitecture and strength, especially in women. In both men and women lower bone strength among those with the greatest visceral adiposity indicates that visceral fat may be deleterious to bone health.

***Disclosures: Douglas Kiel**, None*

P-228

The role of mechanical loading in preventing obesity-induced bone loss *Xinle Li[1], Jie Li[1], Daquan Liu[1], Hiroki Yokota[2], Ping Zhang[3]. [1]Department of Anatomy and Histology, School of Basic Medical Sciences, Tianjin Medical University, Tianjin 300070, China., China, [2]Department of Biomedical Engineering, Indiana University-Purdue University Indianapolis, IN 46202, USA, United States, [3]Department of Anatomy and Histology, School of Basic Medical Sciences, Tianjin Medical University, Tianjin 300070, China. Department of Biomedical Engineering, Indiana University-Purdue University Indianapolis, IN 46202, USA, China

Obesity and its associated metabolic sequela are increasing globally and they are closely related to bone homeostasis. The balance of adipocytes and osteoblasts from bone marrow mesenchymal stem cells (BM-MSCs) is linked to bone mass and fat mass in the bone marrow milieu. While it is reported that mechanical loading not only stimulated bone formation but also inhibited obesity-associated hepatic steatosis, little is known about the loading effects on obesity-associated bone loss. Using obese mice induced by high-fat diet and ovariectomy (OVX), we examined whether knee loading prevents bone loss associated with obesity through regulating the Wnt pathway. C57BL/6 female mice (~14 weeks) were sorted into five groups (n=22 each group): standard diet group (SC), high-fat diet group (HF), loading-treated HF group, HF with OVX group (HO), and loading-treated HO group. Knee loading was applied with 1 N force at 5 Hz for 6 min/day for 4 weeks, and femurs were harvested for histomorphometry analysis. Bone marrow-derived cells were isolated to examine the differentiation of adipocytes and osteoblasts. Western blotting was performed to evaluate the expression of markers for adipocytes, osteoblasts, and Wnt signaling. The results showed that a high-fat diet (HF and HO groups) presented higher body weight, body fat, and body mass index (BMI) as well as bone loss than a standard diet (SC and HF groups), in which the changes in OVX mice was even higher. However, knee loading significantly decreased body weight, fat, and BMI. It also reduced the numbers and perimeter of adipocytes and the differentiation of adipocytes from BM-MSCs. The expression of C/EBPα and PPARγ were suppressed by knee loading. The loaded group also presented a significant increase in bone mineral density and contents, and the circumference of trabecular bone. Regarding osteoblasts, knee loading enhanced the number of osteoblasts on bone surface, differentiation of osteoblasts, and the level of Runx2 and ALP. Furthermore, knee loading attenuated obesity-induced bone loss through regulating the Wnt pathway. Collectively, high-fat diet induced obesity aggravates bone loss in OVX mice. This study indicates that knee loading prevents obesity-related bone loss by regulating cellular fates in the differentiation of adipocytes and osteoblasts from BM-MSCs via the Wnt pathway. Further understanding of mechanical loading may contribute to developing potential therapies for obesity-associated disease.

***Disclosures: Xinle Li**, None*

P-229

Gli1 labels a subpopulation of FAP cells that preferentially promote muscle regeneration with less fat accumulation *Lutian Yao[1], Elisia Tichy[1], Leilei Zhong[1], Sarthak Mohanty[1], Luqiang Wang[1], Foteini Mourkioti[1], Ling Qin[1]. [1]University of Pennsylvania, United States

Skeletal muscle has a remarkable regeneration capacity after injury. Fibro-adipogenic progenitors (FAPs) are critical for supporting injured muscle regeneration but their heterogeneity remains largely unknown. Here, using Gli1-CreER Tomato (Gli1/Td) mice, we found that Gli1-labeled Td+ cells are located in the interstitial area of myofibers expressing FAP markers PDGFRα and Sca1. Flow cytometry identified 71.3% of Td+ cells as FAPs, 17.3% of FAPs as Td+ cells, and none of Td+ cells as satellite cells. Aging markedly decreased muscle Td+ cells (2 mo: 7.6%; 12 mo: 4.9%, n=4/group, p<0.01). Sorted Td+ FAPs formed 6.2-fold more CFU-Fs and generated much fewer adipocytes when subjected to adipogenic differentiation than Td- FAPs. Next, we created acute muscle injury by Notexin injection and chronic muscle injury by crossing dystrophic mdx mice with Gli1/Td mice. In both models, Td+ FAPs were preferentially expanded. Specifically, Notexin injury increased the percentage of Td+ cells in FAPs from 17% to 37% at d3 and Gli1/Td/mdx mice contained 1.8-fold more Td+ cells than Gli1/Td mice (n=4/group). Cell ablation in Gli1/Td/DTA mice with Tam injections reduced Td+ cells by 80% and eliminated Td+ CFU-F colonies from muscle (n=3/group). After Notexin injury, myofibers regenerated at d7 and d28 in Gli1/Td/DTA mice were 34.1% and 22.7%, respectively, smaller than those in Gli1/Td mice (n=5/group), suggesting an impairment of myogenesis. Gli1 is an effector of Hedgehog (Hh) signaling. Intramuscular injection of purmorphamine (pur), an Hh agonist, resulted in 1.6-fold larger sizes of myofibers at d30 after Notexin injury (n=4/group). Local glycerol injection causes muscle degeneration with fat infiltration. Interestingly, Td+ FAPs were less likely to become adipocytes compared to Td- FAPs and ablation of Td+ cells led to 39.9% more adipocytes in muscle (n=4/group). Hh signaling inhibitor, GANT61, induced 78.3% more adipocytes, while pur almost completely depleted adipocyte infiltration (n=5/group).Single cell RNA-sequencing of mouse muscle mononucleated cells showed that FAPs can be subclustered into Gli1+ and Gli1- cells. Pathway analysis suggested that Gli1+ cells are more metabolic active and more related to tissue regeneration. In conclusion, our study revealed a subpopulation of FAPs that preferentially promotes muscle regeneration with less fat accumulation and implied a potential therapeutic effect of Hh signaling in muscle diseases.

***Disclosures: Lutian Yao**, None*

P-230

PTHrP Overexpression in Mammary Tumors Causes Anorexia: A Possible Role of Lipocalin-2 *Diego Grinman[1], Pamela Dann[1], Marya Shanabrough[1], Tamas Horvath[1], John Wysolmerski[1]. [1]Yale University, United States

Cancer Anorexia Cachexia Syndrome (CACS) is a life threatening complication caused by the release of soluble factors by tumor cells that lead to pronounced loss of weight, appetite, skeletal muscle and fat mass. It occurs in up to in 26% of breast cancer patients and is directly responsible for 20% of all cancer deaths. CACS not only reduces quality of life, but also blunts responses to chemotherapy, having a dramatic impact on patient survival. One of the secreted factors implicated in CACS is parathyroid hormone-related protein (PTHrP), however, whether PTHrP contributes to CACS in breast cancer patients has not yet been fully explored. To study the metabolic effects of PTHrP in a breast cancer setting, we created a tetracycline-regulated model of PTHrP overexpression in mammary tumors. Administering doxycycline (Dox) to Tet-PTHrP;PyMT mice (10-12 weeks old) activated human PTHLH cDNA expression in mammary tumors, leading to elevated circulating PTHrP levels and severe hypercalcemia. Tet-PTHrP;PyMT mice on Dox experienced profound anorexia, rapid fat wasting and weight loss. To determine whether PTHrP overexpression in mammary tumors caused alterations in the central nervous system (CNS) appetite center/s, we performed c-Fos immunohistochemistry, a marker of neuronal activation, in coronal sections of the mouse brain. Tet-PTHrP;PyMT mice on Dox had a significant activation of neurons from the lateral parabrachial nucleus (LPBN), an area previously linked to appetite regulation. Also, treatment of Tet-PTHrP;PyMT mice with Dox caused more than a ten-fold increase in circulating levels of Lipocalin-2 (LCN2), an osteoblast secreted protein that has been shown to cause anorexia and is associated with reduced breast cancer patient survival. Upregulation of the LCN2 mRNA levels was observed in whole bones and also in mammary tumors, suggesting that both tissues may contribute to the LCN2 circulating pool in response to PTHrP. Overall, our data suggest that mammary tumor derived PTHrP induces anorexia possibly through activation of neurons in the LPBN. Although more experiments are needed to determine whether LCN2 is mediating the PTHrP-induced anorexia, these studies highlight a potential mammary tumor to bone to brain axis that could broaden our understanding of the suppression of appetite in CACS.

***Disclosures: Diego Grinman**, None*

P-231

Connexin43 Controls Body Adiposity and Glucose Tolerance in Mice via Gap Junction Dependent and Independent Functions *Seung-Yon Lee[1], Manuela Fortunato [1], Marcus Watkins[1], Francesca Fontana[1], Roberto Civitelli[1]. [1]Divisions of Bone and Mineral Diseases, Department of Medicine; Musculoskeletal Research Center, Washington University School of Medicine, United States

The gap junction protein, connexin43 (Cx43) is expressed in mesenchymal lineages including adipocytes and osteogenic cells. Others have shown that Cx43 mediates white adipose tissue (WAT) “beiging” in response to cold exposure, and is involved in ensuring mitochondrial integrity and metabolic activity of brown adipose tissue (BAT). Using Twist2(Dermo1)-Cre to induce mesenchymal lineage specific ablation of Cx43 (cKOTw2), we asked whether lack of Cx43 affects body adiposity and energy metabolism, in addition to its action on bone modeling and homeostasis. In standard diet and temperature conditions, body weight and fat mass are only modestly reduced in cKOTw2. Likewise inguinal WAT is significantly reduced in cKOTw2 mice, but not other WAT depots. Notably, cKOTw2 mice are metabolically more active compared with control mice, based on indirect calorimetry, despite equal food consumption; and have better glucose tolerance on a standard chow diet. Importantly, significantly lower gains in body weight, fat mass, and WAT weight occur in cKOTw2 mice on a high fat diet (HFD) relative to control mice, and cKOTw2 mice are partially protected from HFD-induced glucose intolerance. Such protective effect is not seen with Gja1 deletion in mature adipocyte (cKOAdipoq); and Cx43 ablation in osteogenic lineage cells (cKOOsx and cKODMP1) does not affect body weight and fat mass, suggesting that Cx43 acts at early steps of adipocyte development. Intriguingly, Tw2-Cre-driven induction of mutations that interfere with either Cx43 channel function, as in oculodentodigital dysplasia (cODDD), or Cx43 signaling function, as with C-terminus 5-aminoacid truncation (cDel5Tw2), also results in lesser body fat gains on HFD, relative to controls. Hence, Cx43 favors WAT accumulation via both its gap junction channel and signaling functions. Intriguingly, glucose metabolism is normal in cODDD mice, whereas cDel5Tw2 mice are modestly glucose intolerant on standard or HFD, as are cKOAdipoq mice, suggesting that this Cx43 effect is linked to its signaling/scaffolding function, consistent with an action in mitochondria. Thus, Cx43 has multiple actions in energy metabolism, ultimately serving to decrease energy expenditures while maximizing glucose utilization and fat tissue metabolism. Interference with specific functions of Cx43 may help improve metabolic balance in obesity and during weight reduction programs, while preserving bone health.

***Disclosures: Seung-Yon Lee**, None*

P-232

Impaired zinc signaling is involved in muscle atrophy in type 1 diabetic mice *Fuka Takeuchi[1], Marina Morimoto[1], Yoshinori Mizuno[1], Yoko Horikawa[1], Yukinori Tamura[1]. [1]Department of Physiology & Biochemistry, Graduate school of Nutrition, Kobe Gakuin University, Japan

Type 1 diabetes induces serious skeletal muscle atrophy and impaired muscle repair, which are important risk factors for falls and subsequent fractures. However, the detailed mechanisms of skeletal muscle dysfunction in diabetic state remain unclear. Zinc is an essential micronutrient for regulating metabolism, and intercellular zinc distribution is regulated by 24 zinc transporters (Zip1~14, ZnT1~10) located in plasma/organelle membranes. Recent studies suggest that changes in the expressions of zinc transporters are associated with the regulation of muscle cell function. In this study, we therefore investigated the role of zinc transporters in the pathogenesis of diabetic muscle atrophy in vivo and in vitro. Quantitative CT analysis showed that tibial muscle mass was decreased in streptozotocin-induced diabetic female mice compared with control mice. Analysis of the gastrocnemius muscle revealed that protein degradation was enhanced, and protein synthesis and myogenic differentiation were suppressed in muscle of diabetic mice. The mRNA levels of zinc transporters, such as Zip1, 3, 9, 11, 13 and ZnT6, 9 were decreased in muscle of diabetic mice, suggesting that zinc signaling in muscle is altered in diabetic state. Moreover, oral zinc supplementation for 4 weeks significantly ameliorated muscle loss in diabetic mice along with the increase in the expression of Zip9 and Zip13 in muscle. We next examined the role of Zip9 and Zip13, which transport zinc from the Golgi apparatus to the cytoplasm, in muscle function using mouse myoblastic C2C12 cells. Knockdown of Zip9 or Zip13 by specific siRNA markedly increased the levels of marker genes of ubiquitin proteasome system (MuRF-1, Atrogin1) in C2C12 cells. In addition, knockdown of Zip9 or Zip13 also markedly decreased the levels of myogenic genes (MyoD, Myogenin, MyHC) along with suppressed Akt phosphorylation in C2C12 myotubes. Moreover, knockdown of Zip13 but not Zip9 enhanced autophagy as well as increased protein levels of FoxO1 in C2C12 myotubes. In conclusion, our study demonstrated that zinc signaling is altered in muscle of diabetic mice, and the down-regulation of Zip9 and Zip13 is associated with enhanced protein degradation and suppressed myogenesis through Akt/FoxO1 signaling pathway in muscle cells. These data suggest that impaired zinc signaling is involved in the pathogenesis of diabetic muscle atrophy, and it may be a novel therapeutic target in musculoskeletal disorders induced by diabetes.

***Disclosures: Fuka Takeuchi**, None*

P-233

Accelerated Osteocyte Senescence and Skeletal Fragility in Mice with Type 2 Diabetes *Japneet Kaur[1], Brittany Eckhardt[1], Jennifer Rowsey[1], Daniel Fraser[1], Sundeep Khosla[1], David Monroe[1], Joshua Farr[1]. [1]Mayo Clinic, United States

The prevalence of type 2 diabetes (T2D) is increasing worldwide and collective evidence indicates a three-fold higher fracture risk in this population despite normal to higher bone density. In addition to the more rapid accumulation of advanced glycation end products (AGEs) in T2D, recent studies have demonstrated that insulin resistance is associated with increased expression of p16Ink4a, a marker of cell senescence - i.e., stress-induced irreversible cell growth arrest, in pancreatic β-cells of mice. We previously showed that increased senescence mediates age-related bone loss; therefore, we hypothesized that premature cell senescence and SASP factors contribute to skeletal dysfunction in adult-onset T2D. To investigate this, we established T2D in adult C57BL/6N male mice using high-fat diet (HFD) and a single dose of streptozotocin (STZ). HFD/STZ mice demonstrated key features of T2D such as increased body weight, fat mass, consistently higher glucose (>=250 mg/dL) and HbA1C levels, and reduced insulin levels and pancreatic β-cell area. Longitudinal assessments of the skeletal phenotype of T2D mice showed deteriorated cortical bone microarchitecture relative to control mice. Additionally, these mice displayed altered bone turnover markers, diminished bone strength, and impaired material properties such as failure load, ultimate stress, and stiffness at multiple skeletal sites as compared to controls. Histomorphometric assessment showed higher bone resorption and lower bone formation rates in T2D vs control mice. The skeletal dysfunction in T2D mice was accompanied by increased levels of Nε-(1-carboxymethyl)-L-Lysine (CML), an activator of the receptor for AGE (RAGE) pathway in serum and bone. In addition, analysis of osteocyte-enriched bone samples of mice with T2D showed significantly elevated mRNA expression of cell senescence markers, namely p16Ink4a and p21Cip1, as well as multiple senescence-associated secretory phenotype (SASP) factors, particularly metalloproteinases (Mmp3, Mmp9, Mmp12, and Mmp13) and NFkb1. Finally, advanced histological techniques showed a significantly increased percentage of senescent osteocytes in T2D as compared to control mice. Based on our findings, the HFD/STZ model represents a promising model for future mechanistic studies in mice with T2D as it mimics the typical characteristics of the human disease and suggests that increased cell senescence in conjunction with elevated AGEs mediate T2D-related skeletal fragility.

***Disclosures: Japneet Kaur**, None*

P-234

Findings to unravel the underlying mechanisms of in vivo interactions involving Wnt10a in bone, fat and muscle *Manabu Tsukamoto[1], Ke-Yong Wang[2], Takashi Tasaki[3], Yoshiaki Yamanaka[1], Eiichiro Nakamura[1], Sohsuke Yamada[4], Hiroto Izumi[5], Qian Zhou[6], Kagaku Azuma[6], Yasuyuki Sasaguri[3], Kimitoshi Kohno[7], Akinori Sakai[1]. [1]Department of Orthopaedic Surgery, University of Occupational and Environmental Health, Japan, [2]Shared-Use Research Center, University of Occupational and Environmental Health, Japan, [3]Department of Pathology and Cell Biology, University of Occupational and Environmental Health, Japan, [4]Department of Pathology and Laboratory Medicine, Kanazawa Medical University, Japan, [5]Department of Occupational Pneumology, University of Occupational and Environmental Health, Japan, [6]Department of Anatomy, University of Occupational and Environmental Health, Japan, [7]Kurate Hospital, Japan

Purpose: Wnt10a is a member of the WNT family. Although deficiency of this gene causes symptoms related to teeth, hair, nails, and skin, we recently demonstrated a new phenotype of Wnt10a knockout (KO) mice involving bone and fat. The in vivo effect of the Wnt10a gene on bone and fat is unclear, and the relationship between bone/fat and muscle in Wnt10a signaling is also interesting. We aimed to evaluate the tissue changes in Wnt10a KO mice compared to wild-type mice and show the findings as a starting point to unravel the underlying mechanisms of in vivo interactions involving Wnt10a in bone, fat and muscle. Methods: Experiments were performed on Wnt10a KO male mice and WT littermates. In vivo images of visceral and subcutaneous fat were acquired by micro CT. Mice were euthanized at 16 weeks of age, and blood samples, bones, fat tissues, and muscles were obtained for analysis (bone histomorphometry, cell cultures, RT-PCR, Immunohistochemical staining, western blot and DNA microarray, etc).Results: Trabecular bone loss in the lower limbs of Wnt10a mice and decreased bone mineralization were observed. The adipose tissue in bone marrow was also decreased, and adipocyte differentiation was reduced. The body fat mass in Wnt10a KO mice was decreased, and white adipocytes in subcutaneous fat were converted to beige adipocytes. The muscle weight of the lower limbs was not decreased despite trabecular bone loss, but Gdf8/myostatin expression was reduced in the subcutaneous fat and gastrocnemius muscles of Wnt10a KO mice. Thus, in vivo deletion of Wnt10a inhibited osteogenic activity, promoted beige adipogenesis of white adipocytes and maintained muscle mass. These results suggest that regulation of Gdf8 by Wnt10a may help maintain the muscle mass of Wnt10a KO mice. Conclusions: This study was the first to histologically evaluate the bone, fat and muscle phenotypes of Wnt10a KO mice. The results of this study, which were obtained by investigating the three tissues together, could influence the understanding of in vivo interactions involving the Wnt10a gene.

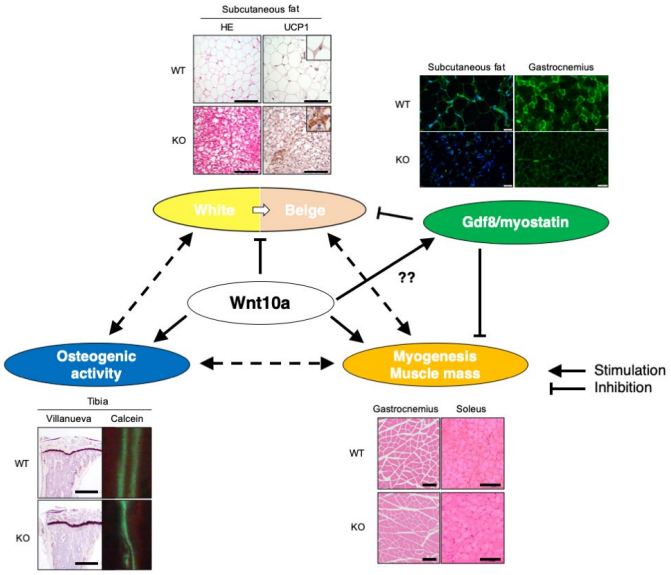

The schema of in vivo interactions between organizations via Wnt10a gene

***Disclosures: Manabu Tsukamoto**, None*

Posters

P-235

Endothelial cell function is mediated by BMP-2 treatment during Type 2 Diabetes *Hanisha Battina[1], Ushashi Dadwal [1], Fazal Ur Rehman Bhatti[1], Olatundun Awosanya[1], Seungyup Sun[1], Caio Staut[1], Stephen Mendenhall[1], Anthony Perugini[1], Conner Valuch[2], Nikhil Tewari[1], Rohit Nagaraj[1], Murad Nazzal[1], Rachel Blosser[1], Jiliang Li[2], Melissa Kacena [1]. [1]Department of Orthopaedic Surgery, Indiana University School of Medicine, IN, USA, United States, [2]Department of Biology, Indiana University Purdue University Indianapolis, IN, USA, United States

Type 2 diabetes (T2D), in the presence of coexisting osteoporosis, results in increased fracture risk and impaired fracture healing. The latter is associated with impaired angiogenesis, a vital process during regeneration of bone tissue. The aim of this study was to investigate the angiogenic and proliferation potential of endothelial cells (ECs) isolated from the lungs (LECs) and bone marrow (BMECs) from obesity-induced mice that were treated with bone morphogenetic protein-2 (BMP-2, 4μg, local administration at the time of surgery) to heal a femoral segmental bone defect (SBD). Male C57BL/6 mice were fed a high fat diet (HFD, n = 27) beginning at 8 weeks of age to induce a type 2 diabetic-like phenotype. This phenotype was confirmed by Glucose and Insulin Tolerance testing 12 weeks later. Low fat diet (LFD, n = 26) fed animals served as controls. The HFD and LFD groups were treated with either saline or BMP-2 at the time of SBD surgery. LECs and BMECs were isolated 3 weeks post-surgery, and their angiogenic potential was evaluated by proliferation, tube formation, cell migration, and gene expression. Proliferation was examined by DAPI or crystal violet staining. The proliferation of LECs and BMECs was not altered by diet or BMP-2 treatment. HFD enhanced vessel-like properties of both LECs and BMECs as demonstrated by tube formation assay. Three-way ANOVA results for humeri BMECs had significant effects (p£0.05) in all three migration parameters (Wound width (μm), Relative wound density (%), and wound confluence (%)) by time, diet, and treatment, as well as a diet by treatment effect. The HFD-fed mice treated with BMP-2 showed the highest migration potential. Additionally, irrespective of diet, ECs isolated from BMP-2 treated mice exhibited increased migration compared to those isolated from saline treated mice. Analysis of angiogenic genes CD31, FLT-1, ANGPT1, and ANGPT2 showed similar changes in expression levels between humeri BMECs and LECs. Interestingly, BMP-2 treatment enhanced angiogenic gene expression in LFD fed mice but attenuated expression in HFD fed mice. This data demonstrates that LECs and BMECs undergoing HFD feeding have enhanced angiogenic potential. Taken together, this study shows that diet, fracture surgery, and local BMP-2 treatment all result in important systemic changes in angiogenesis.

***Disclosures: Hanisha Battina**, None*

P-236

Insulin-Like Growth Factor Binding Protein 2 Knockout Mice (Igfbp2-/-) Are Protected Against Vertical Sleeve Gastrectomy-Induced Bone Loss *Alison Pletch[1], Benjamin Harris[2], Phuong Le[3], Clifford Rosen[3]. [1]Maine Medical Center, United States, [2]University of New England, United States, [3]Maine Medical Center Research Institute, United States

Vertical Sleeve Gastrectomy (VSG) is the most common weight loss surgery in America. It is a successful treatment for obesity, however it leads to bone loss via undefined mechanisms. Previously, we have shown that Insulin-like Growth Factor Binding Protein 2 (IGFBP2) is necessary for osteoclast proliferation and differentiation in mice, and its deletion results in resistance to bone loss. Shah et al (2019) has shown that serum IGFBP2 level is markedly increased after VSG in humans. Based on these observations, we hypothesized that genetic loss of Igfbp2 would protect Igfbp2 knockout (-/-) mice from VSG-induced bone loss. To test this hypothesis, 36 male Igfbp2-/- mice and their littermate controls (+/+) were fed a 60% Kcal (high fat diet) starting at 8 weeks old. At 16 weeks, 9 Igfbp2-/- mice underwent VSG while 9 underwent a sham surgery. Similarly, 9 Igfbp2+/+ mice underwent VSG while 9 underwent a sham surgery. Mice were eye-bled and DEXA scanned at 15 and 18 weeks. At 20 weeks, mice were DEXA scanned again and euthanized; serum was collected to measure levels of carboxy-terminal collagen crosslinks (CTx), total procollagen type 1 N-terminal propeptide (P1NP), and IGFBP2. At 20 weeks of age, both +/+ and -/- mice that underwent VSG lost significant weight compared to their sham controls (+/+ VSG mean = 29.87g, +/+ sham mean = 37.65g, p=0.0003. -/- VSG mean = 31.65g, -/- sham mean = 36.89g, p=0.0251). This weight loss was associated with lower fat mass (+/+ VSG mean = 6.578g, +/+ sham mean = 13.25g, p=0.0004. -/- VSG mean = 8.363g, -/- sham mean = 13.57g, p=0.0082) with no change in fat free mass (data not shown). Total areal bone mineral density (aBMD) was significantly lower in +/+ VSG mice compared to +/+ sham (+/+ VSG mean = 0.04622g/cm2, +/+ sham mean = 0.04925g/cm2, p=0.0150). Femoral BMD was significantly lower as well (+/+ VSG mean = 0.05717g/cm2, +/+ sham mean = 0.06530g/cm2, p=0.0313), as was femoral bone mineral content (+/+ VSG mean = 0.007667g, +/+ sham mean = 0.009000g, p=0.0190). Serum markers of CTx were significantly higher in the +/+ VSG group compared to the +/+ sham group (+/+ VSG mean = 40.35ng/mL, +/+ sham mean=27.54ng/mL, p=0.0127). This was also seen with serum markers of P1NP (+/+ VSG mean = 38.96ng/mL, +/+ sham mean=20.06ng/mL, p=0.0008). No differences were observed among -/- mice. Taken together, our data suggest that Igfbp2-/- mice are protected from significant bone loss after VSG.

***Disclosures: Alison Pletch**, None*

P-237

Low bone mass in female mice fed high-fat diet is associated with elevated bioenergetics and ER stress in cells of the osteoblast lineage. *Veronica Butler[1], Lakshmi Divya Kolora[1], Natalie Hohos[2], Yuan-Haw Wu[1], Malgorzata Skaznik-Wikiel[2], Vanessa Sherk[1], Srividhya Iyer[1]. [1]Department of Orthopedics, University of Colorado, School of Medicine, Anschutz Medical Campus, United States, [2]Department of Obstetrics and Gynecology, Division of Reproductive Sciences, University of Colorado School of Medicine, Anschutz Medical Campus, United States

Obesity is detrimental to bone health, especially in children. However, the cellular mediators and mechanisms of this negative effect remain unclear. Differentiation of pluripotent stem cells is influenced by changes in energy metabolism and nutrient availability. Bioenergetics and protein folding in the endoplasmic reticulum (ER) are closely linked. Damage due to accumulation of misfolded proteins results in ER stress and activates the unfolded protein response (UPR) by three sensor proteins: PERK, IRE1, and ATF6. ER stress mediates progression of multiple obesity-related comorbidities including glucose metabolism, liver and heart diseases. Previous studies have shown that elevated UPR in the osteoblast lineage increases apoptosis and expression of RANKL. The purpose of this study was to determine the effects of high-fat diet (HFD) on osteoblast differentiation. To this end, 5-week-old C57BL/6 female mice were fed either low-fat diet (LFD) or HFD for 10 weeks and were divided based on body weight into high-fat obese (HF-Ob: >25 g) and high-fat lean (HF-Ln: <22 g). Exposure to HFD increased body fat and blood glucose. Importantly, this metabolic imbalance was accompanied by low cancellous bone mass of the femur that was primarily due to decreased trabecular number and increased separation. Although the cortical thickness was unaffected, mice fed HFD exhibited a reduction in the mineral density at femoral midshaft. Furthermore, cultures of osteoblastic cells obtained from bone marrow of HF-Ln and HF-Ob mice had elevated glycolytic and oxygen consumption rates suggesting that excess caloric intake regulates their bioenergetics. We also found that elevated protein levels of PERK target p-eIF2a and ATF6 in bone shafts of HF-Ob mice compared to LFD controls, suggesting UPR dysregulation in osteoblast lineage cells may contribute to obesity-related bone deficits. Our findings suggest that HFD adversely affects skeleton by acting directly on cells of osteoblast lineage. This is in part by regulating their bioenergetics and UPR signaling.

***Disclosures: Veronica Butler**, None*

P-238

Inhibition of Hypoxia Inducible Factor (HIF) Signaling Ameliorates Radiation Induced Marrow Adiposity *Wendi Guo[1], Kassandra Spiller[1], Colleen Wu[1]. [1]Duke University School of Medicine, United States

While radiation therapy effectively eliminates malignant cells, damage to healthy tissue surrounding tumors remains a persistent clinical issue. For bone, normal tissue toxicity is marked by impaired hematopoietic function, diminished bone volume, and accumulation of marrow adipose tissue (MAT). Importantly, cancer patients who receive radiation treatment have an increased risk for fracture. Because marrow adiposity is associated with an increased risk for fracture and diminished hematopoietic stem cell frequency; we sought to identify strategies to prevent radiation induced expansion of MAT. Of note, the bone microenvironment (BME) is characterized by low oxygen tension or hypoxia and active hypoxia inducible factor (HIF) signaling regulates many cellular interactions in the BME to maintain healthy bone. In our initial studies, histological analysis and μCT quantification of bones isolated from mice exposed to total body irradiation showed, unlike bone volume, that there was a rapid and persistent accumulation of MAT. Moreover, endomucin and CD31 staining of long bones revealed a disruption of the bone marrow vasculature, suggesting a perturbation of the hypoxic bone niche. Bone marrow adipocytes arise from multipotent mesenchymal progenitors (MMPs) which have the capacity to differentiate into lineage specific adipocyte progenitors. We next sought to determine if HIF signaling was required for radiation induced MAT formation. For this purpose, mice were generated in which HIFαtranscription factors were conditionally ablated in either MMPs or lineage specific adipocytes by crossing LepRCre and aP2Cremice to mice homozygote for the conditional alleles Hif-1fl/fland Hif-2fl/fl.Intriguingly, histological analysis and μCT quantification of osmium tetraoxide staining revealed radiation induced MAT was ameliorated in aP2Cre;Hif-1fl/fl;Hif-2fl/flmutant animals when compared to littermate controls. In contrast, genetic ablation of HIFain LepR-Creexpressing MMPs did not affect the expansion of marrow adiposity in irradiated bones. Intriguingly, after exposure to ionizing radiation examination of bones isolated from aP-2Cre;Rosa26tdTomato/+conditional reporter mice showed tdTomato+cells localized to the bone marrow stroma; however, they did not co-stain for the adipocyte marker perilipin. In addition, co-localization of enodmucin+and tdTomato+cells in bone sections was not observed. This data suggests that within the BME, aP2Cre expressing cells do not contribute to lipid laden adipocytes nor do they comprise cells of the vasculature. Collectively, this data suggests aP2Cre expressing cells in the BME constitute a population of bone marrow stromal cells that require HIF signaling to support radiation induced adipogenesis via a non-cell automatous mechanism. These studies reveal the potential to exploit the HIF signaling pathway to protect bone against normal tissue toxicity associated with radiation exposure.

***Disclosures: Wendi Guo**, None*

P-239

The L enantiomer of β-aminoisobutyric acid (BAIBA), a contracting muscle metabolite, has positive effects on muscle in vitro and in vivo *Fabrizio Pin[1], Yukiko Kitase[1], Anika Shimonty[1], Joshua R. Huot[2], Alberto Smargiassi[2], Andrea Bonetto[2], Lynda F. Bonewald[1]. [1]Department of Anatomy, Cell Biology Physiology, Indiana University School of Medicine, Indianapolis, United States, [2]Department of Surgery, Indiana University School of Medicine, Indianapolis, United States

β-aminoisobutyric acid (BAIBA) is a non-protein amino acid produced by skeletal muscle during physical activity via a PGC-1α-dependent mechanism. We have shown previously that L-, but not D-BAIBA is secreted by contracted mouse soleus and EDL muscle and that L-BAIBA is 100-1000 times more potent than D-BAIBA in protecting osteocytes from cell death. Others have shown that the racemic mixture of L- and D-BAIBA enhances adipose tissue browning, increases insulin sensitivity, and protects against diet-induced obesity, but effects of the pure enantiomers have not been examined. The potential autocrine effects of L-BAIBA on muscle were compared to the D- enantiomer by in vitro experiments using C2C12 myotubes and in vivo by administering it in drinking water of mice (100mg/day/kg) for 5 (acute) or 30 days (chronic). In vitro studies showed that 20 mM L-BAIBA increased C2C12 mitochondrial respiration, whereas 20 mM D-BAIBA resulted in reduced myotube diameter (-10%, $p<0.05$). In vivo, no significant effects were observed with either enantiomer in the acute experiments. However, chronic administration of L-BAIBA increased gastrocnemius and quadriceps muscle size compared to control mice (+18%, +15%, $p<0.05$) and increased grip strength (+16%, $p<0.01$). We also observed a glycolytic-to-oxidative fiber shift (+42%, $p<0.05$) in the tibialis anterior muscle. An increase in protein expression of markers of mitochondrial biogenesis, such as PGC-1α and Cytochrome C, and markers of fusion, such as OPA1 (+300%, + 63% and +285% respectively, $p<0.05$) was also observed. Notably, similar to L-BAIBA, D-BAIBA increased grip strength (+15%, $p<0.01$). However, D-BAIBA had no significant effects on muscle mass, but did significantly reduce spleen size (19%, $p<0.01$). Together these in vitro and in vivo data show the positive potential autocrine effects of L-BAIBA to improve oxidative metabolism resulting in increased muscle function. In mice, L-, but not D-BAIBA, acts as an exercise mimetic.

***Disclosures: Fabrizio Pin**, None*

P-240

Linagliptin Does Not Alter Bone Mass but Reduces Body Weight and White Adipose Tissue *Giulia Leanza[1], Francesca Fontana[2], Rocky Strollo[1], Paolo Pozzilli[1], Nicola Napoli[1], Roberto Civitelli[3]. [1]Unit of Endocrinology and Diabetes, Campus Bio-Medico University, Italy, [2]WASHINGTON UNIVERSITY IN ST. LOUIS, United States, [3]Division of Bone and Mineral Diseases, Washington University in St Louis, United States

Dipeptidyl peptidase-4 (DPP-4) inhibitors are used to lower blood glucose in type 2 diabetes (T2D). Their mechanism of action is based on inhibiting DPP-4-mediated degradation of glucagon-like peptide-1 (GLP-1), a hormone that favors glucose utilization. Clinical studies suggest that DPP-4 inhibitors also reduce fracture risk among T2D patients; and circulating DPP4 positively correlates with body weight. In preclinical studies, GLP-1 stimulates proliferation of mesenchymal stem cells and inhibits differentiation to adipocytes; while DPP4 expression increases with adipocyte differentiation, suggesting a role of GLP-1 in regulating body adiposity. We tested whether linagliptin, a commonly used DPP-4 inhibitor, may improve bone mass and body adiposity in non-diabetic conditions. To this end, we randomized 6-week-old female C57BL/6J mice to receive either linagliptin (0.15 mg/ml in drinking water; n=15) or placebo (drinking water; n=10) for 8 weeks. To minimize variation in baseline body weight, we used mice with body weight between 15.5 and 16.5 g. We observed no differences in bone mineral density (BMD) and bone mineral content (BMC) by DXA between treatment groups at 4 and 8 weeks after starting linagliptin. Likewise, we found no differences between groups in lean and fat mass by DXA. By contrast, the linagliptin-treated group experienced a reduced gain in body weight with time relative to the placebo-treated group with a significant difference at the end of the observation period (18.1+/-1.4 vs. 19.2+/-1.1 g, respectively; $p<0.05$ t-test). Random blood glucose was lower in treated vs. control mice (144+/-10.8 vs. 172+/-20.4 mg/dl, respectively; $p<0.05$, t-test); however, no hypoglycemic episodes were observed on linagliptin. Notably at 8 weeks, mice treated with linagliptin showed a significant reduction in both gonadal (0.10+/-0.02 vs. 0.19+/-0.04 g; $p<0.001$, t-test) and retroperitoneal white adipose tissue depots (0.017+/-0,007 vs. 0.04+/-0.01 g; $p<0.001$, t-test) relative to untreated mice, even after normalization to body weight. In summary, linaglitptin reduces body adiposity and body weight without altering bone mass, suggesting a potential use of DPP-4 inhibitors in obesity and weight reduction programs in non-diabetic individuals, without effects on bone mass.

***Disclosures: Giulia Leanza**, None*

P-241

Ankle flexor torque and muscle composition are differential determinants of distal tibia bone strength and trabecular plate-rod morphometry *Andy Kin On Wong[1], Eva Szabo[1], Hugo Jern Wai Fung[2], Adrian Chan[2], Sunita Mathur[2], Lora Giangregorio[3], Angela M Cheung[1]. [1]University Health Network, Canada, [2]University of Toronto, Canada, [3]University of Waterloo, Canada

For a fixed bone volume fraction, trabecular plates contribute more to mechanical properties of trabecular bone than rods. Muscle properties are known to affect bone strength, but it is unclear how it affects different components of trabecular structure. Hypothesis: Peak torque or size of muscles around the ankle, as well as muscle and myotendinous density are associated with a more plate-like architecture at the distal tibia. Methods: A convenience sample of women and men >= 50 years old with no metal, reconstructive surgery, muscular dystrophies, or tendinopathies in any leg were recruited. Isometric ankle dorsi-plantarflexion and inversion-eversion peak torques were measured using Biodex dynamometry. HR-pQCT distal tibia scans were completed. Dynamometry and HR-pQCT assessments were completed on the same day on the non-dominant leg. Standard periosteal contouring was performed followed by an automated script to define the endosteal surface. Integral and trabecular vBMD were derived from typical analyses, failure load (FL) was obtained from finite element analysis, plate-specific parameters were computed from Individual Trabecula Segmentation (ITS) analysis, myotendinous density (MyD) and volume fraction (MyV/TV) were computed from soft tissue analysis. pQCT scans of the 66% mid-leg were performed (500 µm at a CT speed of 15 mm/s) to obtain muscle density (MD). Statistical Analysis: General linear models estimated how ankle flexor and extensor torque and muscle composition differentially relate, both separately and together, to whole-bone properties (integral vBMD, FL) and trabecular morphometry (ITS plate parameters). Models were adjusted for age, sex, BMI, use of glucocorticoids, current osteoarthritis, and participation in moderate to vigorous physical activity. Results: Among 81 women and 24 men (mean age: 63(10)y, BMI: 25.8(5.4) kg/m2, 25% with OA, 17% fracture history, 42% falls history), all torque measures, particularly ankle dorsiflexion, were determinants of plate-plate/rod junction density and failure load. However, muscle composition measures but not peak torque were associated with vBMD. The effect of greater ankle flexor-extensor torque on more intact bone parameters was stronger when MyD was higher (interaction $p<0.001$). Conclusion: Strength of muscles around the ankle are correlates of trabecular morphometry at the distal tibia, while muscle and myotendinous density surrounding it are associated with whole-bone density and strength.

Table 1. General Linear Model examining the relationship between HR-pQCT bone density and trabecular morphometry and each of dorsiflexion torque and myotendinous tissue volume fraction (MyV/TV) or density (MyD). Bold = significant at 95% confidence level. Underline = effect size representing larger than 10% of mean of the dependent variable.

DEP	IND1	IND2	R^2	B1	LCL	UCL	P-val	Effect Size	B2	LCL	UCL	P-val	Effect Size
ppJuncD	DTORQ	MyV/TV	0.298	**0.227**	**0.088**	**0.370**	**0.002**	0.106	0.099	-0.026	0.224	0.118	0.046
rpJuncD	DTORQ	MyV/TV	0.296	**0.405**	**0.172**	**0.640**	**0.001**	0.111	0.070	-0.139	0.279	0.506	0.019
FL	DTORQ	MyV/TV	0.442	**813**	**494**	**1132**	**<0.001**	0.159	**335**	**49**	**622**	**0.022**	0.065
vBMDtr	DTORQ	MyV/TV	0.296	**15.43**	**4.54**	**26.32**	**0.006**	0.099	**11.65**	**1.87**	**21.43**	**0.020**	0.075
vBMDi	DTORQ	MyV/TV	0.320	11.32	-3.59	26.24	0.135	0.041	**21.63**	**8.23**	**35.03**	**0.002**	0.078
vBMDc	DTORQ	MyV/TV	0.406	-0.55	-14.90	13.80	0.940	0.001	12.35	-0.55	25.24	0.060	0.015
ppJuncD	DTORQ	MyD	0.293	**0.231**	**0.089**	**0.370**	**0.002**	0.108	0.092	-0.042	0.226	0.174	0.043
rpJuncD	DTORQ	MyD	0.299	**0.392**	**0.158**	**0.630**	**0.001**	0.108	0.099	-0.122	0.321	0.375	0.027
FL	DTORQ	MyD	0.454	**782**	**463**	**1100**	**<0.001**	0.153	**409**	**107**	**710**	**0.009**	0.080
vBMDtr	DTORQ	MyD	0.276	**16.41**	**5.27**	**27.55**	**0.004**	0.106	9.52	-1.02	20.07	0.076	0.061
vBMDi	DTORQ	MyD	0.341	9.59	-5.23	24.42	0.202	0.035	**25.68**	**11.66**	**39.71**	**<0.001**	0.093
vBMDc	DTORQ	MyD	0.469	-5.75	-19.46	7.94	0.406	0.007	**24.18**	**11.21**	**37.13**	**<0.001**	0.030

***Disclosures: Andy Kin On Wong**, None*

P-242

Sympathetic Inhibition Is Associated with Lower BMD and Higher Body Fat in Young Female UCP1 Knockout and Wildtype Mice *Maisey Schuler[1], Rebecca Tutino[1], Miranda Cosman[1], Rachel Hurwitz[1], Taylor Spencer[1], Alexis Stokel[1], Isabel Hermsmeyer[1], Cleo Moursi[1], Maureen Devlin[1]. [1]University of Michigan, United States

Brown adipose tissue (BAT) helps maintain body temperature through nonshivering thermogenesis, in which uncoupling protein-1 (UCP1) releases energy as heat. BAT is correlated with higher bone mass in humans, and experimental studies in adult rodents show BAT may protect the skeleton from cold-induced bone loss due to elevated sympathetic tone. To investigate interactions of cold stress, sympathetic tone, and BAT on body composition and skeletal acquisition in subadults, we studied the effects of housing temperature and sympathetic inhibition in young C57BL/6J (B6) mice and UCP1 knockout (UCP1KO) mice. We hypothesize that 1) cold-housed UCP1KO mice will have lower BMD vs. B6 mice and 2) sympathetic inhibition via the beta-blocker propranolol (PRO) will reduce cold-induced bone loss, particularly in UCP1KO mice. To test these hypotheses, male and female B6 and UCP1KO mice were pair housed at 26C (thermoneutrality) or 22C (mild cold stress) from 3-12 wks of age with food and water ad lib. Half of each group were given PRO in drinking water (0.5 mg/mL) and half were controls (CON) (N=4-11/group). Outcomes at 12 wks of age included body mass, food intake, whole body bone mineral density (BMD, g/cm2), bone mineral content (BMC, g), and percent body fat (%) via PIXImus, and cortical and trabecular bone architecture at the midshaft and distal femur via µCT (results pending due to research hiatus). In females, BMC was lower at 12 wks and body fat was higher at 9 and 12 wks in UCP1KO at 22 vs. 26C, and in UCP1KO vs. B6 at 22C. In males, there were no significant differences in UCP1KO vs. B6 at either temperature. In B6 PRO females at 22C, BMD was

lower at 12 wks, BMC was lower at 9 and 12 wks, and body fat was higher at 9 wks. In UCP-1KO PRO females at 22C, BMD was lower at 6 and 9 wks of age and BMC was lower at 6 wks of age, and body fat was higher at 9 and 12 wks of age vs. CON. In male PRO vs. CON mice, there were no significant differences in bone density or body fat for either genotype or temperature. These data show UCP1KO mice have lower BMC, consistent with a protective effect of BAT on the skeleton. Contrary to our hypotheses, sympathetic inhibition was associated with lower BMD and BMC and higher body fat in both B6 and UCP1KO females, but not in males, suggesting a sex-specific trade-off between bone and body fat. Future work will investigate whether skeletal effects of sympathetic tone differ in subadult skeletal acquisition vs. adult bone maintenance.

***Disclosures: Maisey Schuler**, None*

P-243

Effects of Chronic Hypoxia on Osteocyte Energy Metabolism, Differentiation and Function *Yukiko Kitase[1], Matthew Prideaux[1], Lynda F. Bonewald[1]. [1]Indiana University, United States

Chronic hypoxia, one of the contributing factors to aging- and disuse-induced osteoporosis, modulates cellular energy metabolism. Osteocytes under unloaded conditions undergo hypoxia, however few studies have investigated the effects of chronic hypoxia on osteocyte energy metabolism, differentiation and function. To determine how chronic hypoxia affects osteocyte energy metabolism, IDG-SW3 cells that model late osteoblast to mature osteocyte differentiation were treated with Roxadustat, an inhibitor of HIF prolyl-hydroxylase, known to cause the stabilization of HIF-α. Short-term treatments for 24 and 72h, at d15 revealed dysregulation of energy metabolism genes. To determine the effects on osteocyte differentiation, cells at d0-15 were treated with the inhibitor and harvested on d15. Lipid droplet accumulation was confirmed by Oil red O staining while Alizarin Red staining showed a dose-dependent inhibition of mineralization. Roxadustat-induced chronic hypoxia[DS3] resulted in sustained induction of Glut1 mRNA (2.8-fold, Glucose uptake), Gpd1 & Pck1 (3.3 & 13.6, Glyceroneogenesis), Lpl, Cd36 & Fabp4 (4.5, 7.1 & 5.7, FA uptake/transport), Dgat2, Cidec & Plin4 (3.4, 5.2 & 4.9, Triglyceride synthesis/ lipid droplet) and PPARg (3.3, Lipogenic transcription factor), but not Acaca & Fasn (De novo lipogenesis). Gene expression of HIF-2a was increased (3.9), but not HIF-1a suggesting that HIF-2a is responsible for the observed changes. Osteocyte differentiation, as determined by gene expression of Dmp1, Phex, and Mepe was inhibited but podoplanin (E11) (2.7) and Rankl (6.1) were significantly increased. To examine the effects of chronic hypoxia on mature osteocytes, cells were treated between d15-28. Roxadustat disrupted FA/lipid droplet metabolism by elevating the expression of Lpl (2.7), Fabp4 (2.3), Dgat2 (3.9), and Plin4 (2.0). Osteocyte genes that regulate bone turnover, Rankl (2.0) & Rankl/Opg ratio (1.7) showed a significant increase, while Sost/Sclerostin (0.2/0.1) was almost completely blocked. Surprisingly, Fgf23 (10.2) was highly increased suggesting that phosphate metabolism is altered under chronic hypoxia. These data suggest that in osteocytes chronic hypoxia may modulate FA/lipid droplet metabolism via HIF-2α, and alters osteocyte differentiation and function. Understanding the effects of chronic hypoxia on osteocyte lipid metabolism may identify novel targets for developing new therapeutic interventions against aging- and disuse-induced osteoporosis.

***Disclosures: Yukiko Kitase**, None*

P-244

Impaired bone healing in type 2 diabetes is caused by defective bone microenvironment functions of skeletal progenitor cells. *FLORENCE FIGEAC[1], MICHAELA TENCEROVA[2], DALIA ALI[1], THOMAS L. ANDERSEN[3], DAN REMI APPADOO[1], GREET KERCHKOFS[4], JUSTYNA MAGDALENA KOWAL[1], NICHOLAS DITZEL[1], MOUSTAPHA KASSEM[1]. [1]KMEB, University of Southern Denmark and Odense University Hospital, Denmark, [2]Molecular Physiology of Bone, Institute of Physiology, the Czech Academy of Sciences, Prague, Czech Republic, Czech Republic, [3]KCB, Odense University Hospital, University of Southern Denmark, Denmark, [4]Biomechanics lab, Institute of Mechanics, Materials, and Civil Engineering, UCLouvain and institute for experimental and clinical research and department of material science and engineering, Belgium

Purpose: The cellular mechanisms of obesity and type 2 diabetes (T2D)-associated impaired fracture healing are poorly studied. In a murine model of T2D reflecting both hyperinsulinemia due to high fat diet (HFD) (60% fat) and insulinopenia induced by streptozotocin (STZ:40mg/kg), we examined the cellular dynamics of bone healing in a tibia monocortical bone defect model.Methods: A cortical bone defect recapitulating phases of a stabilized fracture was performed, and the dynamics of bone healing were studied using µCT-scanning and quantitative histology. BM-MSCs number, functions and bone marrow microenvironment composition were analysed employing molecular biology assays, quantitative in situ hybridization and immunostaining.Results: During hyperinsulinemia, a delayed bone healing was observed. Newly formed bone was reduced by 28.4+/-7.7% and associated with accumulation of marrow adipocytes at the defect site +124.1+/-38.7%, and increased density of SCA1+ (+75.0+/- 29.2%) but not Runx2+osteoprogenitor cells. We also observed increased in reactive oxygen species (ROS) production (+101.8+/- 33.0%), senescence gene signature (≈106.66+/- 34.03%) and LAMIN B1- as marker for senescent cell density (+225.2+/- 43.1 %), suggesting accelerated senescence phenotype. During insulinopenia, a more pronounced delayed bone healing was observed with decreased newly formed bone to -34.9+/- 6.2% which was inversely correlated with glucose levels (R2=0.48, p<0.004) and callus adipose tissue area (R2=0.3711, p<0.01). Senescent phenotype present in hyperinsulinemic condition was absent during insulinopena. To test for the human relevance, we observed that sera from obese and T2D patients exerted inhibitory effects on osteoblastic differentiation of human marrow stromal MSC.Conclusions: Our data suggest that T2D exerts negative effects on bone healing through inhibitory effects of differentiation of osteoblastic stem cells and that the degree of hyperglycaemia and not insulin levels per se, are detrimental to bone healing.

***Disclosures: FLORENCE FIGEAC**, None*

P-245

Acute Relapse in Mice Increases Dietary Fat Retention in Cortical Bone *Beatriz Bermudez[1], David Presby[2], Ginger Johnson[3], Matthew Jackman[3], Yuan-Haw Wu[3], Vanessa Sherk[3]. [1]University of Colorado Denver, United States, [2]Harvard Medical School, United States, [3]University of Colorado Anschutz Medical Campus, United States

Bone remodeling is known to expend energy, thereby contributing to energy balance. Bone marrow is an adipose depot and has a potential role as a local energy reservoir. Weight loss induces metabolic adaptations in non-skeletal tissues and increases the propensity for weight regain. It is unclear whether this also occurs in bone. Testing how energy balance alters nutrient trafficking in bone is crucial to understanding how undernutrition or overnutrition influences bone health. We aim to determine how fat trafficking and retention are altered by weight loss and relapse in exercise trained mice. The study design utilized mice over expressing human lipoprotein lipase (mckLPL) due to previously observed decreases in dietary and de novo derived fat retention in mckLPL mice. Wild type mice (WT) and mckLPL mice (6 wks old; n=14-18/grp) were fed a high-fat, high-sucrose diet for 8 weeks. All mice were then switched to a calorically-restricted medium fat diet and subjected to high intensity interval treadmill running for 3 weeks to induce and maintain 20% weight loss. For the final day of study, mice were randomized to either receive a food allotment to stay in energy balance (WtL, n=7,8/grp) or were allowed ad libitum feeding (Relapse, n=7-10/grp). To determine trafficking of lipids, we provided food with 14C labelled oleate and palmitate to trace retention of dietary fat and we injected mice with 3H2O just prior to the final 24-hour period of study to trace de novo derived lipids. Tissues were harvested after the 24-hour experiment and lipids were extracted from hindlimb cortical bone and plasma. Data are mean +/- SEM. Lean and fat mass were similar among groups. Fat intake was highest in Relapse groups (p<0.05, mckLPL Relapse: 449+/-42; WT Relapse: 437+/-45 vs mckLPL WtL: 325+/-48; WT WtL: 244+/-11 mg). Additionally, total energy expenditure and respiratory quotient (RQ) were highest in Relapse groups. Total lipid amount and de novo derived lipid product in hindlimb cortical bone were not different between groups, however dietary fat retention in cortical bone lipid was highest in Relapse groups (p<0.05, mckLPL Relapse: 0.11+/-0.01; WT Relapse: 0.14+/-0.03 vs mckLPL WtL: 0.07+/-0.01; WT WtL: 0.06+/-0.01 mg). Dietary fat retention in cortical bone was positively correlated with fat intake and RQ (p<0.05, r=0.61-0.66). Our results indicate that an acute relapse increases fat retention and exercise did not alter energy expenditure or nutrient trafficking between groups.

***Disclosures: Beatriz Bermudez**, None*

P-246

The Effects of High Fat Diet, Fracture Healing, and BMP-2 Treatment on Endothelial Cell Function in Ipsilateral and Contralateral Limbs *Olatundun Awosanya[1], Ushashi Dadwal[1], Caio Staut[1], Nikhil Tewari[1], Conner Valuch [2], Stephen Mendenhall[1], Rohit Nagaraj[1], Rachel Blosser[1], Jiliang Li[2], Melissa Kacena [1]. [1]Department of Orthopaedic Surgery, Indiana University School of Medicine, IN, USA, United States, [2]Department of Biology, Indiana University Purdue University Indianapolis, IN, USA, United States

Type 2 diabetes (T2D) results in physiological and structural changes in bone which contribute to poor fracture healing outcomes. Most prominently, T2D compromises microvascular performance which negatively impacts bone regeneration as angiogenesis is required for new bone formation. Here we sought to examine the effects of locally administered BMP-2 on femoral segmental bone defect (SBD) surgery and its angiogenic impacts on endothelial cells (ECs) isolated from the ipsilateral tibia or the contralateral tibia during T2D. Male C57BL/6 mice were fed a low fat diet (LFD, 10 kcal % fat, n=26) or high fat diet (HFD, 45 kcal % fat, n=27) starting at 8 weeks of age to induce a T2D-like phenotype. After 12 weeks, the T2D phenotype was confirmed via glucose and insulin tolerance testing and mice underwent a femoral SBD surgery. Mice were treated with BMP-2 (4µg) or saline at the time of surgery. The ipsilateral and contralateral tibia were removed 3 weeks post-surgery and bone marrow ECs were isolated and their proliferation, angiogenic potential, and gene expression were analyzed. Crystal violet staining showed a significant 2-fold increase in BMP-2 treated LFD contralateral tibia ECs (p<0.05, n=3). However, no differences in proliferation were detected in surgical tibia ECs. Enhanced tube formation was observed in saline treated compared to BMP-2 treated, LFD ECs isolated from both the ipsilateral and contralateral tibia. Interestingly, for HFD fed mice, in both ipsilateral and contralateral tibia ECs, BMP-2 enhanced tube formation parameters. In LFD ipsilateral tibia ECs, BMP-2 treatment increased expression of all angiogenic genes examined (CD31, FLT-1, ANGPT1,

and ANGPT2), whereas with HFD BMP-2 treatment did not alter the expression of CD31 or FLT1 and decreased the expression of ANGPT1 and ANGPT2. For the contralateral tibia, although BMP-2 treatment resulted in no differences in CD31 or ANGPT2 expression between LFD and HFD ECs, significant increases were observed in HFD compared to LFD ECs in FLT-1 and ANGPT1 expression. As expected with impaired angiogenesis in T2D, LFD ECs had enhanced tube formation compared to HFD ECs. Thus, for the ipsilateral tibia ECs it appears that tube formation is inversely related to expression of CD31, FLT-1, ANGPT1, and ANGPT2 expression. However, this same trend is not observed in contralateral tibia ECs, perhaps suggesting that microenvironment at local versus distal sites of injury impact angiogenic properties.

***Disclosures: Olatundun Awosanya**, None*

P-247

Bone-derived PDGF-AA Promotes Pancreatic β cell Proliferation and Function in Aging *Xiaonan Liu[1], Yu Chai[1], Lei Wang[1], Bin Yu[1]. [1]Southern Medical University, China

The platelet-derived growth factors (PDGFs), key factors regulating pancreatic β cells proliferation and function, are secreted by bone tissue. However, the contribution of PDGF signaling from bone cells in β cells senescence and age-related type 2 diabetes remains unexplored. In this study, we report that the reduced number of osteoprogenitors in metaphysis of the long bone in aging results in a declined level of serum PDGF-AA, which contributes to decreased pancreatic β cell proliferation and function. 22-month-old mice had reduced level of both serum and pancreas PDGF-AA protein compared with 6-month-old control mice, which correlates with decreased serum insulin level and increased fasting glucose level, suggesting a declined pancreas function. RT-PCR analysis of different tissues and different cell types in bone marrow showed the decline in serum PDGF-AA level in aging was due to decreased expression of bone marrow osteoblast lineage cells. In situ immunofluorescence staining of bone tissue sections confirmed osterix+ osteoprogenitors are the primary source of PDGF-AA in bone. However, the number of osteoprogenitors, as well as their PDGF-AA secretion, decreased as shown by immunofluorescence staining in 22-month-old mice. To determine whether bone-derived PDGF-AA modulates β cell proliferation and function, we evaluated the senescence phenotype and insulin secretion of rat insulinoma INS1 cells using standard medium(CON) or osterix+ osteoblast conditioned medium without(CM) or with (CM+AN) addition of PDGF-AA neutralizing antibody. Percentage of insulinoma INS1 cells that expressed p16INK4a was 8.7% in CM group and increased to 23.9% in CM+AN group. Importantly, the expression of insulin markedly increased in CM group compared with CON group but was significantly lowered in CM+AN group, suggesting PDGF-AA secreted by osteoprogenitors promotes β cell proliferation and function. Finally, we found transplantation of osteoblast lineage cells directly to bone marrow increased serum PDGF-AA level and β cell proliferation as well as function in aging mice, as shown by a reduced number of senescence-associated beta-galactosidase (SA-βGal)+ cells in pancreas tissue and improved glucose tolerance. These findings show the importance of bone-derived PDGF-AA in mediating pancreatic β cell proliferation and function in aging and raised the possibility of targeting bone secretion as a strategy to overcome age-related type 2 diabetes.

***Disclosures: Xiaonan Liu**, None*

P-248

Low energy availability reduces skeletal benefits in female long-distance triathletes as detected by HR-pQCT *Eduardo Medeiros Ferreira da Gama[1], Leandro Kasuki[2], Franscisco de Paula Paranhos Neto[3], Miguel Madeira[4], Laura Maria Carvalho Mendonça[5], Annie Schtscherbyna[4], Maria Lucia Fleiuss Farias[4]. [1]Division of Endocrinology of Clementino Fraga Filho University Hospital, Federal University of Rio de Janeiro (HUCFF-UFRJ), Brazil, [2]Division of Neuroendocrinology Research Center of Clementino Fraga Filho University Hospital, Federal University of Rio de Janeiro (HUCFF-UFRJ), Brazil, [3]Division of Endocrinology of Clementino Fraga Filho University Hospital, Federal University of Rio de Janeiro (HUCFF-UFRJ)., Brazil, [4]Division of Endocrinology of Clementino Fraga Filho University Hospital, Federal University of Rio de Janeiro (HUCFF-UFRJ)., Brazil, [5]Division of Rheumatology of Clementino Fraga Filho University Hospital, Federal University of Rio de Janeiro (HUCFF-UFRJ)., Brazil

ABSTRACTIntroduction: The female athlete triad, initially described as the association of disordered eating, amenorrhea and osteoporosis, was further rede?ned to focus on low energy availability (EA), which has a central role in the development of hypoestrogenism and low bone mineral density (BMD), as measured by DXA. Objectives: To evaluate bone status in long-distance triathletes with and without low EA compared to non-athletes using DXA and HR-pQCT. Methods: Forty pre-menopausal women 20 years and older, 23 triathletes and 17 non-athletes were included. The athletes denied previous menstrual alterations and had spontaneous regular menses or were on hormonal contraceptives at entry in the study. Results: Although no significant difference was detected by DXA, triathletes showed better bone density and microstructure than non-athletes at HR-pQCT, and median (range) values at distal tibia were, respectively: Total Ar=646.6 (487-869) vs 615.6 (499-816) p=0.014; Tb.Ar=527.5 (374-764) vs 473 (384-686) p=0.018; Ct.Pm=101 (87-114) vs 96 (87-111) p=0.011; Dtrab=167.4 (124-215) vs 131.3 (109-206) p=0.018; BV/TV=0.14 (0.10-0.18) vs 0.11 (0.09- 0.17) p= 0.017; Tb.Sp=0.45 (0.33-0.61) vs 0.49 (0.34-0.69) p=0.034; Tb.Sp/N SD=0.19 (0.12-0.29) vs 0.22 (0.14-0.35) p=0.040. At distal radius significant differences were found for Total Ar, Tb.N, Tb.Sp and Tb.Sp/N SD. The positive association of exercise was maintained in the subgroup of athletes with low EA as compared to controls. However, athletes with low EA, as compared to those with adequate EA, showed increased fat mass index=6.5 (3-11) vs 3.0 (2-11) p=0.016, and lower D100=293 (244-341) vs 344 (275-405) p=0.025, Ct.Ar=46.4 (32.2-59.2) vs 54.4 (40.5-62.4) p=0.038 and Ct.Th=0.66 (0.48-0.85) vs 0.86 (0.62-1.01) p=0.025 at the radius and lower Dcomp=923 (873-962) vs 950 (919-994) p=0.048 at the tibia. Stress fractures were reported by 33% of athletes with low EA and by 18% of those with adequate EA. No impact on bone health was found between users compared to non-users of hormonal contraceptives. Conclusions: HR-pQCT detects better bone density and microstructure in female long-distance triathletes, unrevealed by DXA. Low EA partially compromises the beneficial effects of exercise on bone. These innovative findings reinforce the importance of an adequate EA in female athletes, irrespective of an apparently adequate BMD at DXA, to guarantee skeletal health.

***Disclosures: Eduardo Medeiros Ferreira da Gama**, None*

P-249

Incidence and predictors of fractures in older adults with and without obesity defined by body mass index versus body fat percentage *Anoohya Gandham[1], Ayse Zengin[1], Maxine P Bonham[2], Tania Winzenberg[3], Saliu Balogun[3], Feitong Wu[3], Dawn Aitken[3], Flavia Cicuttini[4], Peter R Ebeling[1], Graeme Jones[3], David Scott[1]. [1]Department of Medicine, School of Clinical Sciences at Monash Health, Monash University, Clayton, Victoria, Australia, Australia, [2]Department of Nutrition, Dietetics and Food, Monash University, Notting Hill, Victoria, Australia, Australia, [3]Menzies Institute for Medical Research, University of Tasmania, Hobart, Tasmania, Australia, Australia, [4]Department of Epidemiology and Preventive Medicine, School of Public Health and Preventive Medicine, Monash University, Melbourne, Victoria, Australia, Australia

Purpose: To determine and compare risk factors associated with incident fractures in older adults with and without obesity, defined by both body mass index (BMI) and body fat percentage. Methods: 1,099 older adults (mean +/- standard deviation age = 63.0 +/- 7.5) years, participated in this prospective cohort study. Obesity status at baseline was defined by BMI (>=30 kg/m2) obtained by anthropometry and body fat percentage (>=30% for men and >=40% for women) assessed by dual-energy X-ray absorptiometry (DXA). Total hip and lumbar spine areal bone mineral density (aBMD) were assessed by DXA up to five years. Incident fractures were self-reported up to 10 years. Results: Prevalence of obesity was 28% according to BMI and 43% according to body fat percentage. Obese older adults by BMI, but not body fat percentage, had significantly higher aBMD at the total hip and spine compared with non-obese (both p0.05). Mediation analysis confirmed that aBMD meditated the effects of BMI, but not body fat percentage, on all incident fractures. Higher baseline falls risk score was the only consistent predictor of increased likelihood of incident fractures in obese individuals only, according to both BMI and body fat percentage (both p-value<0.05).Conclusions: Obesity defined by body fat percentage is associated with increased likelihood of incident fractures in community-dwelling older adults, whereas those who are obese according to BMI have reduced likelihood of incident fractures due to higher aBMD. Falls risk assessment may improve identification of obese older adults at increased risk of incident fractures.

***Disclosures: Anoohya Gandham**, None*

P-250

GPR109A gene deletion ameliorates gonadectomy-induced bone loss in mice *Jin-Ran Chen[1], Oxana P. Lazarenko [1]. [1]Arkansas Children's Nutrition Center, and the Department of Pediatrics, University of Arkansas for Medical Sciences, United States

Sex steroid deficiency plays critical roles in the pathophysiology of bone as the result of increased bone resorption. The G protein-coupled receptor 109A (GPR109A), also known as hydroxycarboxylic acid receptor 2 (HCAR2), HM74A or PUMA-G, is expressed in a variety of cells and tissue types, and robustly in osteoclastic precursor macrophages. We have previously provided evidence that suggested that GPR109A controls osteoclastogenesis and bone resorption, and systemic GPR109A gene deletion resulted in decreased osteoclast bone resorption but increased bone mass. Here, we used ovariectomized (OVX), orchidectomized (ORX) and GPR109A gene deletion mouse models, and investigated the role of GPR109A in gonadectomy-induced bone loss in female and male mice. 6 month old GPR109A-/- mice and their littermate wild type C57Bl6 mice were allocated to Sham control groups or gonadectomized groups for six weeks. Using densitometric micro-CT confirmed by peripheral quantitative CT (pQCT) scan on tibia and spine ex vivo, we determined that bone mass including bone volume, trabecular number, and bone mineral density and content in both trabecular and cortical site were significantly decreased in wild type OVX and ORX mice compared with their respective Sham control mice. While bone mass in GPR109A-/- Sham groups were higher compared with respective wild type Sham groups, gonadectomy-induced bone loss was ameliorated in GPR109A-/- mice compared with their respective Sham mice. In females especially, most parameters measured by micro-CT and pQCT had no differences between Sham and OVX groups. Bone remodeling marker mea-

surements indicated that both bone resorption (Cathepsin K) and bone formation (bone specific ALP) markers were increased in gonadectomized mice compared with their respective Sham mice. However, expression of bone resorption markers (NFATc1, MMP9) were significantly lower in GPR109A-/- mice compared with their wild type littermates. These data indicate that GPR109A systemic gene deletion ameliorates sex steroid deficiency-induced bone loss through suppressed bone resorption. Supported by USDA-ARS Project #6026-51000-012-06S.

***Disclosures: Jin-Ran Chen**, None*

P-251

C3H substrain variation results in decreased bone density and fat mass in C3H/HeJ mice *Talia Lizotte[1], Oraya Zinder[2], Victoria DeMambro[3], Daniel Brooks[4], Melissa Mariano[1], Eryn Harrington[1], Mary Bouxsein[4], Laura Reinholdt[2], Clifford Rosen[3], Kathleen Becker[1]. [1]University of New England, United States, [2]The Jackson Laboratory, United States, [3]Maine Medical Center Research Institute, United States, [4]Beth Israel Deaconess Medical Center, United States

C3H/HeJ (HeJ) mice, a model of both high bone density and increased marrow fat, are commonly compared to C57BL/6J mice. HeJ mice harbor a mutation in TLR4 and an inversion on Chr 6 which are absent in C3H/HeOuJ (OuJ) mice. In order gain a greater understanding how genetic differences in C3H substrains impact bone and adipose tissue, body composition was analyzed by DXA in OuJ and HeJ mice (n=15) at 8, 14, and 18 wks of age. Female and male HeJ mice displayed decreased body mass (26% and 18% respectively), decreased fat mass, and increased percent fat-free mass when compared to OuJ mice. Inguinal and gonadal depot weights and adipocyte size were also reduced in HeJ mice. While no difference in food consumption was observed, HeJ mice had decreased energy expenditure likely resulting from changes in body composition. DXA analysis also indicated that total and femoral aBMD and aBMC were reduced in HeJ mice vs OuJ. When DXA results were normalized to body weight using a multiple linear regression model, substrain differences in bone were eliminated or reversed. These data suggest that body weight is a major factor in regulating bone mass in C3H substrains. Bone microarchitecture was analyzed by μCT in femurs from OuJ and HeJ mice at 18 weeks of age (n=5). No overt differences in trabecular bone were present. However, Ct.Ar was decreased in HeJ mice. Decreases in periosteal circumference were observed only in female HeJ mice likely resulting in decreased pMOI, Imax, and Imin. Following adjustment for body weight, HeJ mice still showed decreased Ct.Ar while female mice still had decreased pMOI and Imax compared to normalized OuJ data. Taken together, these results indicate that the HeJ mice have smaller bones than OuJ mice likely due to body weight differences. To further investigate differences in cell differentiation, bone marrow stromal cells (BMSCs) were differentiated into adipocytes and osteoblasts in vitro. No strain differences in adipogenesis were detected, but increased mineralization was observed by Von Kossa staining in BMSCs isolated from female HeJ mice. It is likely that genetic changes in HeJ mice result in increased osteogenesis, but body composition factors may play a major role in dictating bone density in vivo. Further analysis of marrow fat and gene expression may provide additional evidence to support a more informed choice of C3H substrains as an experimental model to study the genetic determinants of bone mass.

***Disclosures: Talia Lizotte**, None*

P-252

The Dynamics of Mice and Human Bone Marrow Adipose Tissue in Response to Feeding and Fasting *Gisela Pachon-Pena[1], Pouneh K Fazeli[2], Miriam A Bredella[2], Elizabeth K O'Donell[2], Anne Klibanski[2], Clifford Rosen[1]. [1]MMCRI, United States, [2]MGH, United States

The administration of a high fat diet (HFD) is an accelerating factor for metabolic syndrome, impaired glucose tolerance, and early type 2 diabetes mellitus (T2DM). The present study aims to assess the impact of a high fat diet or acute weight gain on human marrow adipose tissue. Adipose tissue secrete numerous active substances termed adipokines, including adiponectin, leptin, resistin, interleukin-6, etc. Adipokines physiologically regulate development, metabolism, fat storage, insulin sensitivity, homeostasis, blood pressure, immunity, and inflammation. To determine the effect of HFD on adipokines marrow adipose tissue, marrow/peripheral blood serum and marrow adipocytes from healthy adult human who underwent either 10 days of HFD or 10 days of fasting, were collected according to published protocols. To analyze the expression of resistin, IL-6, TNF-α and adiponectin in human serum from marrow and peripheral blood, we used DuoSet ELISA kit respectively. To analyze the expression of resistin, TNF-α, RCAN2 and SEMA3E/PLXND1 on marrow adipocyte, qRT-PCR were performed. Our results show that in paired aspirates, resistin increased markedly with a HFD, but not with fasting, and not in the circulation, without significant changes on adiponectin neither IL-6 levels. Resistin is a cytokine produced in WAT (adipocytes in rodents, macrophages in human) and is thought to mediate T2DM and cardiovascular disease and to mark macrophage activation and TLR4 signaling. In our previous studies with mouse models, PLXIND1 is highly expressed on marrow stromal cells and has been linked to adiposity and type 2 diabetes. PLXIND1 also was one of the most highly expressed genes in MSCs from a mouse with high marrow adiposity and consistent with our finding noted in human volunteers. Our data show that expression of SEMA3E/PLXIND1, RCAN2 and TNF-α were increased on marrow adipocytes from the HFD volunteers. Also we identified up-regulation of the macrophage gene marker, EMR-1 (Homologous to F4/80 in mice), suggestive of an inflammatory response in the marrow of normal volunteers on a HFD but not fasting. The bone microenviroment can be modulated by various factors including aging, obesity, and inflammation. Stress signal could be modulated by SEMA3E/PLXND1 axis as a chemoattractant for macrophages, provoking adipose tissue inflammation. Further analysis is needed to understanding the immune response in the context of marrow adiposity in humans and mouse models.

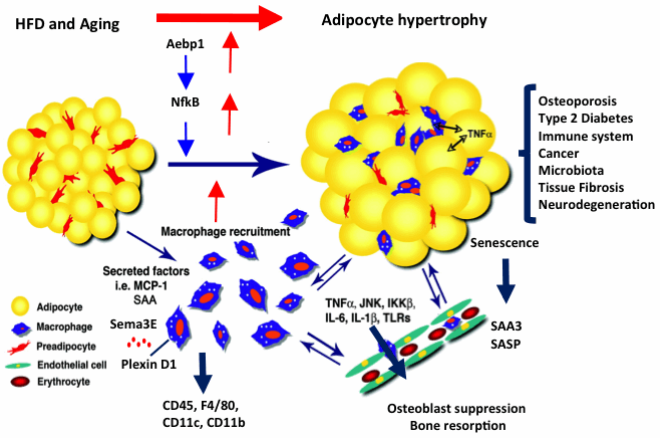

***Disclosures: Gisela Pachon-Pena**, None*

P-253

Higher diet quality score increases weight loss during moderate caloric restriction with no greater loss of bone mineral density. *Anna Ogilvie[1], Yvette Schlussel[1], Stephen Schneider[2], Sue Shapses[3]. [1]Rutgers University, United States, [2]Robert Wood Johnson Medical School, United States, [3]Rutgers University and Robert Wood Johnson Medical School, United States

Purpose: Weight loss (WL) has been shown to reduce bone mineral density (BMD). Observational data indicate that a high-quality diet is beneficial to bone and may reduce fracture risk. However, whether the quality of the diet affects BMD during WL is not known. Methods: In this prospective study design, we examined body composition, BMD, and diet quality in overweight/obese subjects during 6 months of WL (Osteoporosis, Weight loss and Endocrine; OWLE dataset). Subjects were provided nutrition counseling whether they were randomly assigned to weight loss (72%) or maintenance (28%); both groups were analyzed together due to similar diet quality scores over 6 months. The Healthy Eating Index 2015 (HEI) was calculated from monthly food records (11+ daily intakes/person). The HEI, based on the Dietary Guidelines for Americans, is a compilation of 13 food components that assesses nutrient density of the diet. Subjects were retrospectively separated into two groups by median HEI score (Higher HEI, H-HEI and Lower HEI; L-HEI; n=116/group) and analyzed by repeated measures ANOVA.Results: Subjects (n=232) were aged 54.5 y (53.1, 55.8), with body mass index of 28.9 kg/m2 (28.4, 29.4), and were predominantly female (87%). During WL, subjects in H-HEI and L-HEI groups scored 68 (67, 69) and 54 (53, 55), respectively ($p<0.001$). Those in the H-HEI group lost more weight [-4.1 kg (-4.9, -3.4)] than those in the L-HEI group [-3.0 kg (-3.8, -2.1); $p<0.05$]. WL was associated with higher intake of whole grains and protein (fish/plant sources), and reduced intake of saturated fat and refined grains ($p<0.05$). Loss of total and visceral fat was greater in H-HEI versus L-HEI ($p<0.05$). As expected, there was WL-induced BMD-loss (total hip, 33% radius; $p<0.001$; and trend for lumbar spine, LS; p0.05) or a trend to attenuate BMD loss (total hip and total body; $p=0.073$, $p=0.095$, respectively) in the H-HEI compared to L-HEI.Conclusions: Individuals with higher diet quality scores lost more weight, and total and visceral fat. However, for a given amount of WL, BMD loss was similar in H-HEI and L-HEI groups. These data suggest the quality of the diet during caloric restriction, in addition to the amount of WL, is potentially another factor contributing to BMD loss.

***Disclosures: Anna Ogilvie**, None*

P-254

Bioactive Glass-Ceramic Granules Induce New Bone Formation in a Rat Preclinical Model of Type-1 Diabetes Mellitus *Fátima Gomez Gramajo[1], Gabriela Vargas[2], Rosa Alicia Araoz[3], Rosa Vera Mesones[2], Teresita Bellido[4], Aldo Roberto Boccaccini[5], Alejandro Gorustovich[6]. [1]CONICET, Salta, Argentina, Argentina, [2]Salta National University, Argentina, [3]University of Buenos Aires, Argentina, [4]Indiana University School of Medicine; University of Arkansas for Medical Sciences, United States, [5]Institute of Biomaterials, Department of Materials Science and Engineering, University of Erlangen-Nuremberg, Germany, [6]Interdisciplinary Materials Group-IESIING-UCASAL, INTECIN UBA-CONICET, Argentina

Therapeutic strategies to increase bone formation which is defective in type-1 diabetes mellitus (T1DM) are sorely needed. Incorporation of therapeutic ions into the structure of bioactive glasses for direct stimulation of cells is a very attractive approach for bone tissue regeneration. Lithium (Li) has recently been identified as a biologically active ion which can stimulate osteoblast cell activity. Here, we evaluated the osteogenic effects of glass-ceramic (G-C) granules developed from bioactive glass of the 45S5 system and 5 wt% Li-doped 45S5 glass (45S5.5Li), in a Streptozotocin-induced T1DM model. Male Wistar rats (5 weeks old) were assigned to two groups: control (n=10) and DM (n=10). After a week, DM was confirmed by quantifying fasting blood glucose levels and G-C granules (250 µm) were intraosseously implanted under anesthesia. Each animal was implanted with 15 mg of 45S5 G-C granules inside the medullary compartment of one tibia and 15 mg of 45S5.5Li G-C granules in the contralateral tibia. At 30 days post-treatment, glycemia levels and body weight were recorded and the rats then euthanized. All procedures were approved by the IACUC. Tibias were fixed, decalcified and embedded in paraffin. Histological sections transverse to the tibial longitudinal axis were subsequently obtained, stained with hematoxylin-eosin, and examined under optical microscope. Bone volume/tissue volume (BV/TV) of neoformed bone around GC granules was quantified by histomorphometry. As compared to controls (C), DM rats showed a significant increase ($p< 0.01$) in blood glucose (C 110+/-11 mg/dL, DM 531+/-102 mg/dL) and a significant decrease ($p< 0.01$) in body weight (C 263+/-23 g, DM 103+/-34 g). Microscopically, both groups showed lamellar bone around the G-C granules at 30 days post-implantation. The histomorphometric analysis showed similar % BV/TV of bone around the G-C granules induced by 45S5 or 45S5.5Li granules in both C and DM groups (C/45S5 21+/-4, C/45S5.5Li 18+/-4; DM/45S5 14+/-1, DM/45S5.5Li 15+/-4). The present results demonstrate that 45S5 and 45S5.5Li G-C granules equally stimulate the neoformation of bone under physiological or diabetic conditions. These findings provide the basis for the use of bioactive glass-ceramics to promote bone regeneration in DM.

***Disclosures: Fátima Gomez Gramajo**, None*

P-255

Musculoskeletal and metabolic responses to low fat and high fat diet in athymic nude mice *Sukanya Suresh[1], Laura Wright[1], Sutha John[1], Sreemala Murthy[1], Yun She[1], Trupti Trivedi[1], Gabriel Pagnotti[1], Khalid Mohammad[1], Theresa Guise[1]. [1]Indiana University, United States

Advanced breast cancers are frequently associated with bone metastases. Bone marrow microenvironment provides metastatic niche for tumor cells to survive and grow. Bone marrow adipose tissue (BMAT); abundant in the marrow increases with age, excess body fat accumulation and during adjuvant endocrine therapy, conditions which are experienced by breast cancer patients. Since the role of BMAT in breast cancer metastatic niche is unknown, it is essential to develop xenograft models of excess body fat and BMAT accumulation mirroring the development of obesity in humans. Athymic nude mice are T cell deficient outbred mice widely used in xenograft studies. Here, we characterized the effect of feeding high fat diet (HFD, 60 kcal % fat) or nutrient matched low-fat diet (LFD, 10 kcal % fat) on body fat, bone, BMAT, muscle and glucose metabolism in 9-week-old female athymic nude mice for 4 weeks and 18 weeks. We observed no body weight differences in the initial 4 weeks, but from 12 weeks of age the LFD-fed mice showed more body weight gain compared to the HFD fed mice ($p<0.05$). However, between the two diet groups there was no difference in body fat, lean mass, glucose tolerance, insulin sensitivity, forelimb grip strength or muscle specific force measured by ex vivo contractility measurement of extensor digitorum longus muscle. Despite the lack of excess body fat accumulation, micro-CT analysis showed that 4 weeks of HFD feeding resulted in 32% reduction in trabecular bone volume (BV/TV, $p<0.05$) and significant induction in marrow adiposity ($p<0.05$) compared to the LFD-fed mice. In contrast, 18 weeks of HFD feeding increased the trabecular BV/TV by 50% in the HFD fed mice relative to LFD-fed mice ($p<0.05$), with no induction of excess BMAT. Histomorphometric analysis of tibiae showed that HFD reduced bone formation rate, mineral apposition rate and osteoid volume at both 4 weeks ($p<0.05$) and 18 weeks ($p<0.05$) but reduction in osteoclasts only at 18 weeks ($p<0.05$). Cortical bone parameters and mechanical properties of the bone were unaffected by either diets.Thus, for bone metastases studies where impact of excess body fat, BMAT accrual and metabolic dysfunction are essential to study disease progression and metastases, the athymic nude mouse model is not ideal. Whether modifications to the model, including sex steroid deficiency, or others will improve responsiveness to HFD induced metabolic disruption in athymic nude mice should be assessed in future studies.

***Disclosures: Sukanya Suresh**, None*

P-256

Relationship between Serum PTH and Metabolic Biomarkers *Syu Mi Sam [1], Sabashini Ramchand[2], Rachel Davey[2], Samantha Richardson[3], Jeffrey Zajac[2], Janine Danks[2]. [1]RMIT University, School of Health and Biomedical Sciences, Australia, [2]University fo Melbourne DOM, Austin Health, Australia, [3]RMIT University, School of Science, Australia

Parathyroid hormone (PTH) is known for its classical role in calcium homeostasis and bone metabolism. However, evidence shows that bone, as an endocrine organ, can exert feedback regulation on aspects of glucose homeostasis by secreting bone-derived factors. For example, osteocalcin has been implicated in glucose homeostasis via the regulation of insulin secretion. This cross-talk between glucose and bone demonstrates the significance of hormones/factors which act on bone cells and could in turn contribute to the physiological pathways involved in glucose metabolism or vice versa. Our aim was to investigate the relationship between serum PTH levels and metabolic biomarkers in diabetic patients. These biomarkers were selected for their involvement in glucose homeostasis or calcium regulation. Biochemistry blood results from 12,068 diabetic patients attending an outpatient clinic from 2008-2015 were examined. Only 2,032 patients from this group had their PTH level determined. Pearson's correlational analyses were performed to determine the association of PTH with these biomarkers which included: fasting plasma glucose, C-peptide, uncorrected calcium (not adjusted to albumin), 25-hydroxy vitamin D, glycated haemoglobin, total cholesterol, high-density lipoprotein and low-density lipoprotein. Serum PTH levels were positively correlated with C-peptide, a marker of endogenous insulin production. This correlation was strongest in the group of patients who had PTH levels above the normal reference interval (1.6- 6.0 pmol/L ($r=0.30$, $p<0.01$)). These findings suggest that the interaction of PTH with biomarkers may be affected by impaired beta-cell function.

***Disclosures: Syu Mi Sam,** None*

P-257

Visceral Adipose Tissue and Major Adverse Cardio-vascular Events:A Systematic Review and Meta-analysis Protocol of Observational and Randomized Controlled Trials *Randa Saad[1], Malak Ghezzawi[1], John Batsis[2], Katherine Saunders[3], Marlene Chakhtoura[1]. [1]American University of Beirut Medical Center, Lebanon, [2]Dartmouth-Hitchcock Medical Center, United States, [3]Weill Cornell Medicine, United States

Introduction:The diagnosis of obesity has been traditionally based on using body mass index (BMI) which has known limitations. Visceral Adipose Tissue (VAT) assessment by imaging (MR, CT or Dual-energy X-ray absorptiometry (DXA)) represents a specific and sensitive method for measuring ectopic fat at specific sites, including central obesity.Objectives:The aim is to evaluate the association of increased VAT with major adverse cardiac events (MACE) (non-fatal stroke, non-fatal myocardial infarction, and cardiovascular death), and to identify a VAT cutoff that implies a significantly increased risk of MACE. Methods:We will search MEDLINE (1946 to present), EMBASE, COCHRANE, and CINAHL without time or language limitation. We will include observational studies and trials conducted in adults (>=18 years), evaluating the association of VAT area (cm2) with 3-point MACE outcomes, combined (primary outcome), separately (secondary outcome). Two reviewers (RS and MG) will review citations and abstracts, in duplicate and independently after training, and will screen full texts using a priori prepared screening forms. We will use the Newcastle-Ottawa Quality Assessment Scale and the Cochrane Collaboration tool for risk of bias assessment of observational and randomized studies, respectively. We will calculate the relative risk (RR) of the 3-point MACE, comparing a specific cutoff or range of VAT area, or comparing different tertiles or quartiles, depending on data available in individual studies. Adjusted results in individual studies will be used. The primary analysis will be done using a random effects model, using RevMan version 5.3Results: This project is currently ongoing and full results will be available by September 2020. Discussion:Since BMI may be sometimes an insufficient parameter in the assessment of individuals with obesity, additional measurements, such as VAT, may be needed to help providers risk stratify patients. The diagnostic threshold of abnormal visceral fat is unknown and our meta-analysis will provide evidence of its relationship with long-term adverse cardiovascular outcomes.

***Disclosures: Randa Saad**, None*

P-258

Sirt3 Deficiency Causes Hyper-acetylation of Mitochondrial Proteins and Mitochondrial Dysfunction in Osteoclasts of Old Mice *Wen Ling[1], Kimberly Krager[1], Aaron Warren[1], Nukhet Aykin-Burns[1], Stephanie Byrum[1], Maria Almeida[1], Ha-Neui Kim[1]. [1]University of Arkansas for Medical Sciences, United States

Mitochondrial protein acetylation plays a key role in aging and Sirt3 is the primary mitochondrial protein deacetylase. Sirt3 is indispensable for the increased bone resorption and the accompanying enhanced mitochondrial function in osteoclasts from old mice but the molecular details remain elusive. We have analyzed the global proteome of bone marrow-derived macrophages (BMMs) and pre-osteoclasts (pOCs) from 16-month-old Sirt3 deficient (KO) B6/Sv129 female mice and WT controls by mass spectrometry. Of a total

4400 identified proteins 387 were mitochondrial proteins. Gene Ontology enrichment analysis confirmed that several Sirt3 target pathways, including oxidative phosphorylation, mitochondrial translation, transmembrane electron transfer carrier, and respiratory chain were down regulated in Sirt3 null cells. However, the overall protein-fold changes were minimal between genotypes, suggesting that changes in acetylation, rather than protein levels may be responsible for the mitochondrial dysfunction in osteoclasts of the Sirt3 null mice. Following data acquisition in MS/MS mode we used the Uniprot Mus musculus database to identify acetylated peptides and proteins. A total of 567 acetylated peptides were identified with a fold change of >2.5 and a p value of <0.05. RANKL enhanced 69 acetyl-lysine peptides in WT cells whereas Sirt3 deletion resulted in the hyperacetylation of 305 peptides. In RANKL-treated Sirt3 null osteoclasts 18 mitochondrial proteins were identified with significant hyperacetylation at multiple sites. Importantly, five lysine residues (K49, K52, K62, K83, and K103) quantified in ATPIF1 – an essential protein for mitophagy – displayed a 3.9- to 213-fold acetylation increase in the absence of Sirt3, indicating that ATPIF1 is a major target of Sirt3 in osteoclasts. Consistent with this, osteoclasts lacking Sirt3 exhibited a striking decrease in the protein levels of mitophagy markers such as Bnip3 and Nix compared to osteoclasts from WT mice. Deletion of Sirt3 also reduced the conversion of LC3-I to LC3-II, indicating suppression of autophagic flux. These results demonstrate that Sirt3 deficiency causes significant changes in the acetylome of osteoclasts and Sirt3 target proteins are culprits of excessive bone resorption associated with old age.

***Disclosures: Wen Ling**, None*

P-259

Novel BMD Loci Identified by Whole Genome Sequencing and CRISPR editing in Zebrafish: The NHLBI Trans-Omics for Precision Medicine (TOPMED) Study *Yi-Hsiang Hsu[1], Joyce W Tang[2], Hanfei Xu[3], Cecily Choy[2], May Montasser[4], Carolyn Crandall[5], Ming-Ju Tsai[1], Mao Fu[4], Jeffrey R. O'Connell[4], James Perry[4], Shabnam Salimi[4], Elizabeth Streeten[4], Chris Delaney[6], Anne Justice[7], Charles R. Farber[8], David Karasik[9], David M. Evans[10], Jonathan Tobias[11], Brent Richards[12], Ching-Ti Liu[3], Robert Wallace[13], John Blangero[14], Kerri Wiggins[15], Rebecca Jackson[16], Douglas Kiel[9], Braxton D. Mitchell[4], Ronald Kwon[17]. [1]HSL Marcus Institute for Aging Research and Harvard Medical School, United States, [2]Institute for Stem Cell and Regenerative Medicine, Sch of Med, University of Washington, United States, [3]Boston University, School of Public Health, United States, [4]School of Medicine, University of Maryland, United States, [5]School of Medicine University of California, Los Angeles, United States, [6]University of Washington, United States, United States, [7]University of North Carolina, United States, [8]Center for Public Health Genomics University of Virginia, United States, [9]HSL Marcus Institute for Aging and Harvard Medical School, United States, [10]University of Queensland Diamantina Institute, Australia, [11]Department of Clinical Science at North Bristol, University of Bristol, United Kingdom, [12]Lady Davis Institute, Jewish General Hospital, McGill University, Canada, [13]University of Iowa, United States, [14]University of Texas Rio Grande Valley School of Medicine, United States, [15]University of Washington, United States, [16]Ohio State University Wexner Medical Center, United States, [17] Institute for Stem Cell and Regenerative Medicine, Sch of Med, University of Washington, United States*

The discovery of causal genetic variants creates opportunities for new disease diagnostics and therapies. Whole-genome sequencing (WGS) is rapidly being incorporated into mainstream biomedical research to provide comprehensive enumeration of sequence variation. To identify novel coding variants that are associated with BMD, we utilized the deep-coverage WGS (average 30X coverage) in 10K Caucasian participants obtained from Amish, CHS, FHS, SAFOS and WHI studies (the NHLBI TOPMED Program) as well as ALSPAC and TWINSUK studies (10X coverage). We performed gene-based collapsing association tests (allele-count and SKAT tests) to identify rare functional coding variants (MAF <= 0.5%) associated with BMD adjusting for age, age2, sex, weight, height, ancestral genetic background, cohort, and menopausal status (women). Only loss-of-function (LoF), protein-altering short insertion/deletion, and missense variants with deleterious effects were included. The most significant gene-based association was found in the IGHE gene ($p=7.18x10-8$) with lower lumbar spine (LS) BMD (genome-wide significance $p < 4.27x10-6$ after Bonferroni correction). The other novel findings included SLC26A11, ERGIC3 and STMN1 genes with LSBMD and TFAP2E, CYP2B6, GDF10 and IL6 genes with FNBMD. Among these genes, Gdf10 and Il6 has been reported to be the most highly expressed in skeletal structures during early mouse development. GDF10 (growth differentiation factor 10) also known as BMP3B is a member of the transforming growth factor ß superfamily. In the GDF10 gene, four less-common potential functional variants were associated with FNBMD. Among them, SNP P468S is located in the mature region downstream of the RXXR cleavage site and predicted to be a LoF mutation that suppresses GDF10 function. To address the involvement of GDF10 in bone metabolism, we generated zebrafish mutants for gdf10a and gdf10b and analyzed them using microCT-based spinal phenomics (160 measures/animal). We administered CRISPR-Cas9:gRNA complexes targeting three sites on gdf10a or gdf10b. Sequencing analysis revealed that this produced bi-allelic out-of-frame mutations with an efficiency of ~90% for each gene. During early development (12 days), somatic mutants for both gdf10a and gdf10b exhibited increased vertebral ossification. As adults (3mo), somatic mutants for gdf10a exhibited reduced vertebral bone mass and mineralization. Our studies support a function for GDF10 in the development and growth of the skeleton.

***Disclosures: Yi-Hsiang Hsu**, None*

P-260

Single-cell analyses in a comparative primate skeletal cell culture model reveal evolutionarily divergent patterns of gene expression *Genevieve Housman[1], Yoav Gilad[1]. [1]University of Chicago, United States*

Skeletal anatomy is important for comparative primate research, but the molecular mechanisms that drive the development and evolution of complex skeletal traits are not well characterized. Studying gene regulation in primate skeletal tissues is particularly challenging because samples are difficult to obtain, often have preservation issues, and contain heterogenous populations of cells. Further, human skeletal transcriptomic data have not been collected in consortia like GTEx. Thus, we have established a comparative primate skeletal cell culture model as a more accessible way of evaluating gene expression in the skeleton. We optimized protocols for differentiating six human and six chimpanzee induced pluripotent stem cell lines (iPSCs) into mesenchymal stem cells (MSCs) and subsequently into osteoblasts; we then validated cell differentiation using standard methods. Using the 10X Genomics platform, we collected single-cell RNA-seq data from over 100,000 cells that represent samples and replicates at each stage of differentiation (n=21).Technical replicates were collected for each species and cell type, and the strong correlations of their average gene expression patterns ($r=0.99$ for each cell type) validate the reproducibility of collected data. Across all samples, humans and chimpanzees share patterns of marker gene expression that denote pluripotency in iPSCs, commitment to the mesodermal lineage in MSCs, and osteogenic potential in osteoblasts. Simultaneously, hundreds of genes are differentially expressed (DE) between humans and chimpanzees in each cell type, with some DE genes shared across cell types and others unique to specific cell types. DE genes present in later stages of skeletal cell differentiation are enriched in functions associated with extracellular matrix organization – processes essential for skeletal tissue development. Further, these single-cell data allow for species-specific DE gene assessment in more detailed classifications of osteogenic cells, such as preosteoblast, osteoblast, and embedding osteoblast stages. Altogether, these gene expression patterns during primate skeletal cell development hint at possible evolutionarily divergent gene regulation mechanisms that may contribute to skeletal trait differences between species. Continued evaluation of this cell culture system using controlled developmental and environmental manipulations will further enhance our understanding of these genotype-phenotype relationships in the skeleton.

***Disclosures: Genevieve Housman**, None*

P-261

Whole Genome Association Study Identifies and Replicates Novel Loci Associated with Bone Microarchitecture and Fracture Risks Independent of aBMD: The Bone Microarchitecture International Consortium (BoMIC) *Yi-Hsiang Hsu[17], Fredrick Kinyua[2], Ching-Ti Liu[3], Ming-Ju Tsai[1], Maria Nethander[0], Elizabeth J. Atkinson[0], Elisabeth Sornay-Rendu[0], Claire Watson Watson[7], Andy Kin On Wong[8], Danielle Whittier[9], Andrew Burghardt[10], Shreyasee Amin[5], Eric Lespessailles[11], Jonathan D. Adachi[12], David Karasik[13], Blandine Merle[14], Brent Richards[15], David Goltzman[16], David A. Hanley[0], Steven K. Boyd[17], Mary L. Bouxsein[18], Ronald Y. Kwon[7], Mattias Lorentzon[19], Eric Orwoll[20], Claes Ohlsson [21], Pawel Szulc[6], Serge Livio Ferrari [22], Roland D. Chapurlat [23], Sundeep Khosla[24], Douglas Kiel[1]. [17]HSL Marcus Institute for Aging and Harvard Medical School, United States, [2]Marcus Institute for Aging Research, Hebrew SeniorLife, United States, [3]Biostatistics, Boston University School of Public Health, United States, [1]HSL Marcus Institute for Aging and Harvard Medical School, United States, [0]University of Gothenberg, Emmaneul Biver, University of Geneva, Swaziland, [0]Mayo Clinic, United States, [0]INSERM and University of Lyon, France, [7]Musculoskeletal Systems Biology Lab, Orthopaedics and Sports Medicine, University of Washington, United States, [8]Toronto General Research Institute, University Health Network and McMaster University, Canada, [9]University of Calgary, Canada, [10]Department of Radiology and Biomedical Imaging at University of California, San Francisco, United States, [5]Mayo Clinic, United States, [11]University of Orleans, France, [12]Charlton Medical Centre, McMaster University, Canada, [13]Marcus Institute for Aging Research, Hebrew SeniorLife, United States, [14]INSERM, University of Lyon, Dan Mellström, Univ of Gothenburg, France, [15]Lady Davis Institute and Department of Human Genetics, McGill University, Canada, [16]Departments of Medicine and Physiology, McGill University, Canada, [0]Cumming School of Medicine, University of Calgary, Canada, [17]Cumming School of Medicine, University of Calgary, Canada, [18]Beth Isreal Deaconess Medical Center, Harvard Medical School, United States, [19]Sahlgrenska University Hospital, UNIV. OF GOTHENBURG, Sweden, [20]Division of Endocrinology, Diabetes and Clinical Nutrition, School of Medicine, Oregon Health & Science University, United States, [21]Center for Bone and Arthritis Research at the Sahlgrenski Academy, Sweden, [6]INSERM and University of Lyon, France, [22]Geneva University Hospital and Faculty of Medicine, Switzerland, [23]INSERM and University of Lyon, Hospital E. Herriot, France, [24]Mayo Clinic College of Medicine, United States

Peripheral bone density, microarchitecture and strength assessed by HR-pQCT is genetically heritable and associated with fracture risk even after adjusting for DXA-based areal BMD (aBMD). Genetic studies of these phenotypes may reveal unique, novel genes that contribute to skeletal integrity not identifiable in previous genome-wide association studies (GWAS) of aBMD and CT-derived vBMD. We performed genome-wide association meta-analyses to discover novel GWAS loci and replicated these novel findings in additional studies. The discovery GWAS meta-analysis was done in 5,692 adult Caucasians from 7 cohort studies (FHS, Mayo Clinic, GeRiCo, OFELY, STRAMBO, MrOS Sweden and GOOD). Replication was done in 2,636 adult Caucasians (MrOS US, CaMOS and Lyon QUALYOR). HR-pQCT (XtremeCT, Scanco Medical AG) distal radius and tibia phenotypes were assessed. Except for CaMOS and Qualyor (de novo genotyping for replication), SNPs in all other studies were genotyped by SNP chips and whole genome imputed to ~40 million SNPs. Multiple linear regression or mixed-effects model (family-based) were used for SNP-phenotype associations. Additive genetic effect models were applied, adjusted for age, sex, weight, height and genetic ancestry. We identified and replicated 17 GWAS loci with $p < 5x10\text{-}8$ and 7 suggestive GWAS loci with $5x10\text{-}8 < p < 5x10\text{-}7$. Among 17 GWAS loci, 11 were not reported by previous aBMD GWAS, including EFEMP1_PNPT1, FMN2, Chr3q25.2, CPED1, Chr9q22.2, Chr13q21.32, VAPA, DIS3L2, FGFRL1, PELO and PCDH15 genes. Most of these novel loci were primarily associated with bone structure phenotypes (TbTh, TbN, TtAr, CtPo and CtTh) and bone strength estimated via µFEA-FL. Six out of 7 suggestive GWAS loci were also primarily associated with bone structure phenotypes. In contrast, the six previously reported aBMD GWAS loci (ZBTB40, MEF2C-AS1, WNT16-FAM3C and AKAP11-TNFSF11, PTHLH-CCDC91 and EN1) were associated with both density (e.g., TtBMD, CtBMD, TbBMD) and structure phenotypes. The most significantly associated SNP, rs10254825, was positively associated with µFEA-FL ($p=5x10\text{-}26$) and previously associated with fracture. Our findings suggest that the genetic control of bone microarchitecture may provide additional insights into the pathogenesis of skeletal integrity not available from aBMD. Genome editing in zebrafish using the CRISPR/Cas9 on selected genes from the novel loci is underway to dissect their potential functional involvement in bone biology.

***Disclosures: Yi-Hsiang Hsu**, None*

P-262

Zinc Finger Protein 384 (ZNF384) identified in early-onset familial osteoporosis *Melissa M Formosa[1], Dalila Palazzo[1], Robert Formosa[2], Nikita Camilleri[1], Josanne Vassallo[3], M Carola Zillikens[4], André G Uitterlinden[5], Fernando Rivadeneira[5], Annemieke JMH Verkerk[4], Angela Xuereb-Anastasi[1]. [1]Department of Applied Biomedical Science, Faculty of Health Sciences, University of Malta, Malta, [2]Department of Medicine, Faculty of Medicine and Surgery, University of Malta, Malta, [3]Department of Medicine, Faculty of Medicine and Surgery, University of Malta, Msida, Malta, [4]Department of Internal Medicine, Erasmus University Medical Center, Netherlands, [5]Department of Internal Medicine, Erasmus University Medical Center; Department of Epidemiology, Erasmus University Medical Center, Netherlands

Objectives: Osteoporosis is a metabolic skeletal disease with a strong underlying genetic component. The study aimed to identify the genetic determinants of a penetrant form of early-onset osteoporosis in an extended Maltese family. Methods: A 3-generation pedigree of 29 relatives with ages ranging from 21 to 81 years was recruited. Osteoporosis was defined using T-score or Z-score measures of the lumbar spine and hip derived from DXA scans. The proband had a hip T-score of -2.9. A genome-wide linkage scan followed by whole exome sequencing was performed, whereas shortlisted variants were tested using Competitive Allele Specific PCR in a case-control collection of Maltese postmenopausal women. Pre-mRNA splicing aberrance was tested using an exon-trapping vector transfected in SaOS2 and hFOB cells. Results: Multipoint parametric linkage with dominant inheritance identified two suggestive peaks with a LOD score of 2.1 mapping to chromosomes 12p13.33-12p13.1 and 19p13.2-q13.12. Comprehensive exome variant filtering revealed the presence of a conserved variant rs146089604 (c.686+32G>A) in intron 7 of ZNF384 in all 7 affected relatives, having a MAF of <=1% in gnomAD. In silico modeling predicted the G>A substitution to abolish an exon splicing enhancer motif and branch site. Indeed, in vitro functional assessment demonstrated that the A allele leads to exon 8 and part of intron 8 to be retained, both of which were spliced out in transcripts with the G allele. Targeted expression profiling confirmed that ZNF384 transcripts harboring exon 8 are weakly expressed in healthy bone tissue, indicating that levels would be altered in the presence of the variant. Replication of ZNF384 rs146089604 in 1018 Maltese postmenopausal women strengthened the association with BMD and fracture susceptibility; women with the GA genotype (n=67) had a two-fold increased risk of low hip BMD (adjusted odds ratio: 2.0 [95% CI 1.1-3.8]) and fractures (all-type: 2.0 [1.1-3.8], hip: 2.6 [1.0-6.4]), which was not attenuated after adjusting for BMD. Only 2 women with the AA genotype were detected, both having a low hip BMD. Conclusion: Observations suggest that ZNF384 rs146089604 could be a causal variant. ZNF384 transactivates COL1A1 and matrix metalloproteinases, and suppresses BMP and canonical Wnt signaling. ZNF384-deficient mice had increased bone formation and bone volume. Thus, impaired splicing mechanisms could alter ZNF384's function culminating in reduced bone quality.

***Disclosures: Melissa M Formosa**, None*

P-263

Potential role of RNA binding proteins and skipped exon alternative splicing events in the regulation of osteogenesis *Yuanyuan Wang[1], Rene F Chun[2], Lan Lin[3], Samir Adhikari[3], Christopher M Lopez[4], Mason Henrich[2], Vahe Yacoubian[2], John S Adams[2], Yi Xing[3]. [1]Bioinformatics Interdepartmental Graduate Program, UCLA, United States, [2]Department of Orthopaedic Surgery, Orthopaedic Hospital Research Center, UCLA, United States, [3]Department of Pathology and Laboratory Medicine, Perelman School of Medicine, University of Pennsylvania, United States, [4]Biology Scholars Advanced Research Program, University of California, Davis, United States

Age-related bone loss resulting in osteoporosis with increased fracture risk represent a major health problem with increased morbidity and decreased quality of life. A more complete understanding of how stem cells produce bone forming cells during osteogenesis could be vital to discovering new therapeutic interventions. Nearly all genes of the human genome undergo alternative splicing (AS) through the action of RNA binding proteins (RBPs). From a mere ~ 20,000 genes, the mechanism of AS expands the repertoire of proteins that is needed for the full diversity of cell types, tissues, and organs found in humans. There has been no unbiased, transcriptome-wide analysis of AS of human bone marrow mesenchymal stem cells (hMSC; CD73+/CD90+/CD105+/CD14-/CD34-/CD45-/CD19-/HLA-DR-) undergoing osteogenic differentiation. In this study, we conducted osteogenic day 0-12 time-course differentiation of hMSC, RNA-sequencing, and bioinformatic analysis with a focus on RBPs and exon-skipping (SE) the most common mode of AS. As anticipated, a number of genes had expression that were up- and down-regulated over the time course including a number of RBPs. Additionally, a number of genes showed no change in expression level but exhibited AS. We then explored our dataset to identify RBPs whose significant differential expression over the time course was robustly correlated ($R2 > 0.5$) with SE events that had significant percent-spliced-in (PSI) changes with time. RBP binding motif scanning was then conducted on the 300-base upstream intron, exon-body, and 300-base downstream intron window of sequences of these SE events. Motifs with position weight matrix scores > 0.8 were deemed as hits. Motif hit/not-hits on foreground and background SE events were statistically analyzed for region specific enrichment yielding nine candidate RBPs (CPEB2, FUS, HNRNPA2B1, KHDRBS3, PCBP3, PTBP1, RBM38, SF3B4, SRSF1) that could be

potential regulators of osteogenesis. One candidate, KHDRBS3, was knocked down by siRNA and found to significantly reduce osteogenesis as assayed by quantitative real-time PCR of osteogenic markers RUNX2 and BGLAP and functional alkaline phosphatase staining in comparison to non-targeting siRNA negative control. The analytical pipeline also identifed genes with SE that maybe the targets of regulation by the candidate RBPs inferred from the RBP binding motif mapping. These results suggest the potential and power of AS to regulate the osteogenesis differentiation process.

***Disclosures: Yuanyuan Wang**, None*

P-264

Transcriptomic analysis of aged mouse bone identifies novel genes enriched for genetic associations with bone fracture and bone mineral density in human *Serra Kaya[1], Neha S. Dole[1], Charlie Schurman[2], Daniel S. Evans[3], Tamara Alliston[1]. [1]University of California San Francisco, United States, [2]UC Berkeley-UCSF Graduate Program, United States, [3]California Pacific Medical Center Research Institute, United States

Ongoing efforts to identify new genetic determinants of bone fragility in mice or humans promise to yield therapies for bone fragility in aging. However, RNA sequencing (RNAseq) in mouse models of fragility can yield thousands of differentially expressed genes (DEGs) and prioritizing new candidates for functional analyses is difficult. Human genome-wide association studies (GWAS) report many single variants associated with BMD and fracture, but GWAS alone is unable to identify causal variants. We sought to integrate data generated in mouse RNAseq and human GWAS to improve the identification of novel genes that are clinically relevant and functionally involved in regulating human BMD and fracture in aging.Unbiased RNAseq of cortical bone (marrow and periosteum removed) from 2mo, 1, 2, and 2.5yr mice (n=4/group) was used to identify DEGs for three aging sets: 2m-1y, 2m-2y, and 2m-2.5y (1499, 1685, and 5525 DEGs, respectively, FDR<0.1). To determine if human homologs of mouse DEGs were associated with human BMD or fracture, MAGMA was used to calculate gene-based scores from published GWAS results from 426,824 UK Biobank participants. Scores were based on the most significant variant within 50kb of the gene region, after adjusting for several potential confounders. MAGMA was also used for enrichment analysis of mouse DEG sets for human BMD and fracture associations.While all aging mouse DEGs sets were enriched for BMD, only the 2m-2.5y set was significantly enriched for fracture (Fig. 1). Of this group, 1046 genes were associated with BMD and 19 genes were associated with fracture (Bonferroni, P<0.05). Of the 19 fracture-associated genes, this in-silico approach identified WNT16 and LRP5, which have known functions in bone and clinical relevance to fracture. Several others have yet to be investigated in the skeleton. These include FAM3C and CPED1, which are among 11 genes significantly associated with fracture at the whole genome level; and MPP3 and ERP27, which are not.Therefore, this approach of integrating mouse RNAseq and human GWAS prioritizes an unbiased selection of <0.5% of 5525 DEG in aging mouse bone for further mechanistic study to elucidate their functional relevance in bone fragility. Accordingly, we generated a publicly available tool (mouse2human.org) so that others can leverage new and published RNAseq and GWAS datasets to accelerate identification of new genetic determinants of bone fragility and, ultimately, corresponding therapies.

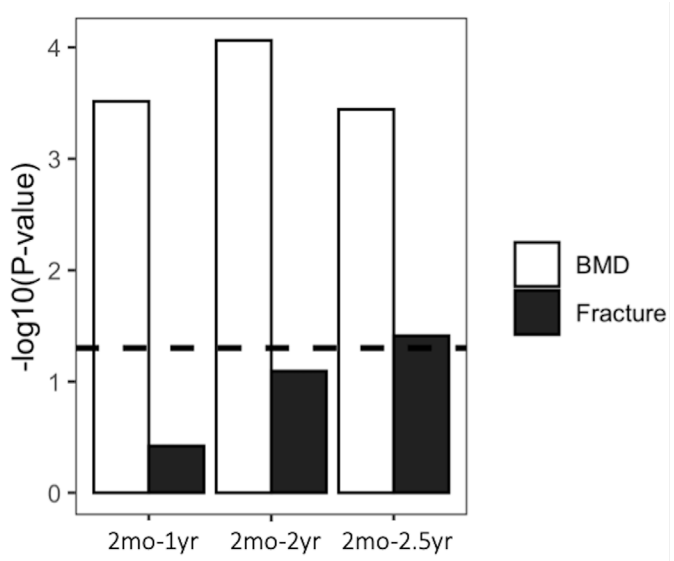

Figure 1: Gene set enrichment analysis using differentially expressed genes in mouse RNAseq of 2mo-1yr, 2mo-2yr, and 2mo-2.5yr male mice, and GWAS of human BMD and bone fractures in the UK Biobank. Dashed line shows the significance threshold (P<0.05)

***Disclosures: Serra Kaya**, None*

P-265

A whole genome sequencing to identify genetic variants associated with lean mass: The NHLBI Trans-Omics for Precision Medicine (TOPMED) Program *Xiaoyu Zhang[1], Ching-Ti Liu[1], Hanfei Xu[1], Mao Fu [2], Kerry Wiggins [3], Yi-Hsiang Hsu[4], Michelle Yau[4], Carolyn Crandall [5], Braxton Mitchell [6], Rebecca Jackson[7], May Montasser [2], Douglas P Kiel[4], David Karasik[8]. [1]Biostatistics, Boston University School of Public Health, United States, [2]University of Maryland, Baltimore, United States, [3]U Washington, United States, [4]Marcus Institute for Aging Research, Hebrew SeniorLife, United States, [5]UCLA HEALTH SCIENCES, United States, [6]U Maryland, United States, [7]Ohio State University, United States, [8]Azrieli Faculty of Medicine, Bar-Ilan University, United States

Lean mass (LM), a proxy of muscle mass, predicts a range of morbidities, including frailty and fractures. Although genome-wide association studies (GWAS) have identified loci associated with whole-body (WB-) and appendicular LM, they only detect a fraction of genetic heritability and are unlikely to identify rare genetic variants that have larger effect sizes.To comprehensively discover new signals, we utilized the whole-genome sequencing (WGS) with average 30x in ethnically diverse (85% European-Ancestry, 7% African-Ancestry, 8% Hispanic) participants (5744 for WB LM and 5690 for appendicular LM) from the Amish, CHS, FHS, SAFOS and WHI studies, members of the Trans-Omics for Precision Medicine (TOPMed) program. Participants had amean age of 60.7 years (SD: 14.8) and >65% of them were women.Lean mass residuals were generated adjusting for age, age2, sex, height, weight, total fat and study-specific variables. Genetic associations with inverse normal transformed residuals were evaluated using linear mixed-effects models adjusting for principal components, with random effects for relatedness. We identified four less frequent variants (all MAF<0.013) associated with LM at p<5x10-8 in the single-SNP analysis (Table 1). rs76791411 (intronic of LOC101928882) was associated with WB-LM. For appendicular LM, intergenic rs76740061 (chr.1), as well as rs1356970370 (intronic of DLGAP2) and rs75017738 (intronic of AUH) were significantly associated. There were no known GWAS SNPs in their vicinity (+/-500K bp); these new SNPs were not analyzed in prior published GWAS for LM. In the gene-based association (SKAT) tests, no gene reached a stringent Bonferroni corrected threshold p < 1.53x10-6.We used GTEx and FUSION quantitative trait loci of expression (eQTLs) and DNA methylation (meQTLs of CpG sites) in human skeletal muscle tissue, to assess muscle function. Variants on chr.1 and in AUH gene corresponded to histone marks (H3K4me1_Enh and H3K27ac_Enh), suggesting these loci may function as enhancers in the H1 Derived Mesenchymal Stem Cells, as well as HSMM Skeletal Muscle Myoblasts and Cultured Satellite Cells.Additional tests are underway, including sex- and ancestry-specific analyses with a larger sample size, as well as replicating these results in other WGS cohorts. The discovery of previously not-observed genetic variants creates new opportunities to reveal unique pathways influencing muscle metabolism for disease diagnostics and therapies.

TABLE 1

phenot	chr	pos	n	MAC	MAF	Est	Est.SE	Wald.p	Ref all	Alt all	rsid	Function	gene
aLM	1	178714575	5690	58	0.005	-0.79603	0.137233	6.61E-09	G	T	rs76740061	None	
aLM	1	178716541	5687	58	0.005	-0.79568	0.137233	6.71E-09	G	A	rs77930692	None	
aLM	1	178716731	5684	59	0.005	-0.77264	0.13615	1.39E-08	G	A	rs77442648	None	
WB LM	3	180712844	5744	78	0.007	-0.63565	0.11566	3.89E-08	A	G	rs76791411	Intron variant	LOC101928882
aLM	9	91209881	5690	75	0.007	0.688193	0.122709	2.04E-08	C	T	rs146650246	None	3.9kb 3' of AUH
aLM	9	91218781	5690	72	0.006	0.692129	0.12454	2.74E-08	C	T	rs75017738	Intron variant	AUH
aLM	8	1642255	5538	143	0.013	0.515583	0.093927	4.04E-08	G	A	rs1356970370	Intron/downstream transcript variant	DLGAP2

***Disclosures: Xiaoyu Zhang**, None*

P-266

Activated Apoptosis and Inhibited Cell Migration: Molecular Etiology Behind Spaceflight-Induced Impairment of Male Mouse Fracture Repair *Nabarun Chakraborty[1], Ariane Zamarioli[2], Aarti Gautam[3], Stephen Mendenhall[4], Paul Childress[4], George Dimitrov[5], Bintu Sowe[6], Aamir Tucker[4], Liming Zhao[4], Rasha Hammamieh[7], Melissa Kacena[4]. [1]Geneva Foundation, US Army for Environmental Health Research, United States, [2]Ribeirão Preto Medical School, Brazil, [3]Integrative Systems Biology US Army Center for Environmental Health Research, United States, [4]Indiana University School of Medicine, United States, [5]Advanced Biomedical Computing Center, United States, [6]ORISE, US Army Center for Environmental Health Research, United States, [7]US Army Center for Environmental Health Research, United States

Spaceflight adversely impacts musculoskeletal health and increases the risk of bone fracture and impaired healing, yet the molecular underpinnings remain elusive. Here we examined the effect of spaceflight on bone healing using a 2 mm femoral segmental bone defect (SBD) model. Forty, 9-week old, C57BL/6J male mice were randomized by cage into spaceflight or ground groups. In both groups 10 mice underwent SBD surgery and 10 mice served as unoperated sham controls. Surgery/sham procedures for spaceflight mice occurred 4 days prior to launch. Ground control surgery/sham procedures and all subsequent procedures were asynchronous by 5 days to match spaceflight conditions. Mice were euthanized 24-28 days post-launch. The surgical femur from 5 mice/group were preserved for micro-computed tomography (μCT) analysis, and the callus region (corresponding area in sham mice) was probed by whole genome transcriptomics and metabolomics assay in the remaining 5 mice/group. μCT confirmed bone loss in sham spaceflight compared to ground femurs as well as impaired fracture healing. Concomitantly a trending sign of habituation to spaceflight became apparent, as gene-metabolite networks linked to cellular homeostasis and morbidity became activated and inhibited, respectively. The regulation of the morbidity signal was switched in the spaceflight surgery mice and μCT analyses revealed increased trabeculae spacing and decreased trabecular connectivity. Inhibited signals of cell migration synchronized with suppressed signals of growth factors, cytokines, and angiogenic agents were observed in spaceflight SBD femurs. Thus, in spaceflight there was a failure to recruit necessary agents for successful bone regeneration. Furthermore, the activated apoptosis signal escalated cell death. With pro-apoptotic and anti-migration characteristics, the RANK-NFκB axis emerged as the central node in spaceflight. Concluding, the consequence of SBD in spaceflight was unique and customized solutions are needed to facilitate facture healing in spaceflight.

***Disclosures: Nabarun Chakraborty**, None*

P-267

Genome-wide association (GWAS) meta-analysis of skull bone mineral density identifies determinants of osteoporosis and craniosynostsis *Carolina Medina Gomez[1], Benjamin Mullin[2], Alessandra Chesi[3], Vid Prijatelj[1], Hana Mlcochova[4], Tavia Evans[1], Maria Knol[1], Mikolaj Pawlak[5], Bram van der Erden[1], Sjur Reppe[6], Andrew Wilkie[7], GEFOS Consortium[8], Jeroen van der Peppel[1], Hieab Adams[1], Kaare Gautvik[6], Stephen Twigg[7], Andre G Uitterlinden[1], Cheryl Ackert-Bicknell[9], Erika Kague[10], Fernando Rivadeneira[1]. [1]ErasmusMC, Netherlands, [2]University of Western Australia, Australia, [3] Children's Hospital of Philadelphia, United States, [4]Oxford University, United Kingdom, [5]Poznan University of Medical Sciences, Poland, [6]Oslo University Hospital, Norway, [7]University of Oxford, United Kingdom, [8]GEFOS Consortium, Netherlands, [9]University of Colorado Denver, United Kingdom, [10]University of Bristol, United Kingdom

Background: Skull bone mineral density (SK-BMD) has been shown to have high heritability (low environmental influence) and moderately strong genetic correlation (shared heritability) with BMD measured at other skeletal sites. We aimed at assessing the genetic determinants of SK-BMD with functional follow-up of associated signals Methods: GWAS meta-analysis comprising 43,800 individuals from 21 different studies. SK-BMD associated variants were tested for pathway and tissue enrichment using DEPICT, GARFIELD and in-house pipelines; and examined for association on a skull shape GWAS of the UK-BioBank (N~38,000). A phenotype scan was performed on a mouse KO model of a gene underlying one of the novel associated signals specific to the skull. Results: We identified 59 genome-wide significant loci (P<=5x10-8) of which 4 were novel, explaining up to 12.5% of SK-BMD variance. Pathway and tissue enrichment analysis of the association signals resulted in clustering within gene-sets involved in the regulation of the skeleton development; overexpressed in the musculoskeletal system; and enrichment in enhancer and transcribed regions in osteoblasts. Variants mapping to CPED1, previously associated with BMD at different skeletal sites and fracture, are associated not only with SK-BMD (P=1.0x10-37) but also presented the strongest evidence among interrogated markers for association with parameters of skull shape (P<1x10-16). Whereas, in-depth analysis of one of the novel associated genes, ZIC1 (P=1.2x10-10) showed that mice mutants for this gene exhibited an irregular pattern of skull mineralization. Conclusion: SK-BMD provides a suitable trait for the discovery of genes important to global bone biology and osteoporosis. The study of SK-BMD also offers the advantage of identifying components unique to intramembranous ossification, which cannot be captured at other skeletal sites. The genetic connection between SK-BMD and other cranial abnormalities, could open new avenues to the understanding of the pathophysiology of craniofacial defects. For instance, ZIC1, a transcription factor implicated in craniosynostosis was shown to have a role in the regulation of skull bone mineralization.

***Disclosures: Carolina Medina Gomez**, None*

P-268

Serum profile of microRNAs linked to bone metabolism during sequential treatment for postmenopausal osteoporosis *Elena Tsourdi[1], Athanasios Anastasilakis[2], Polyzois Makras[3], Athanasios Papatheodorou[3], Martina Rauner[1], Lorenz Hofbauer[4], Maria Yavropoulou[5]. [1]1Department of Medicine III, 2Center for Healthy Aging, Technische Universität Dresden Medical Centre, Dresden, Germany;, Germany, [2]3Department of Endocrinology, 424 General Military Hospital, Thessaloniki, Greece; 4Department of Medicine III;, Greece, [3]4Department of Medical Research, 251 Hellenic Air Force & VA General Hospital, Athens, Greece;, Greece, [4]1Department of Medicine III, 2Center for Healthy Aging, Technische Universität Dresden Medical Centre, Dresden, Germany; 5Center for Regenerative Therapies Dresden, Technische Universität Dresden, Dresden, Germany;, Germany, [5]6Endocrinology Unit, 1st Department of Propaedeutic Internal Medicine, School of Medicine, National and Kapodistrian University of Athens, Greece, Greece

Objective: The expression of serum microRNAs (miRs) related to bone metabolism is potentially affected by anti-osteoporotic treatment. Here, we investigated the effect of sequential treatments on serum miR expression profile.Patients and Methods: This was an observational, open label, non-randomized clinical trial. Denosumab (Dmab) was administered for 12 months in 37 women who were treatment-naïve (naïve-group) (n=11) or previously treated with teriparatide (TPTD-group) (n=20) or zoledronate (ZOL-group) (n=6). Main outcome measures were the relative serum expression of miRs linked to bone metabolism and secondary outcome measures were serum concentrations of the bone turnover markers (BTMs) pro-collagen type 1 N-terminal propeptide (PINP), C-terminal-crosslinking telopeptide of type 1 collagen (CTX), and tartrate-resistant acid phosphatase 5b (TRAP-5b). Time points were baseline, 3 and 6 months after the first Dmab injection.Results: Baseline relative expression of miR-21a-5p, miR-23a-3p, miR-29a-3p, and miR-338-3p was higher in the TPTD-group, while the relative expression of miR-21a-5p was lower in the -ZOL group compared to the naive-group. Dmab decreased the relative expression of miR-21a-5p at 3 months [fold change (FC) 0.43, p<0.001] and 6 months (FC 0.34, p<0.001), and miR-338-3p and miR-2861 at 6 months (FC 0.31, p=0.041; FC 0.52, p=0.016, respectively) in the whole cohort. In subgroup analyses, Dmab decreased the relative expression of miR-21a-5p, miR-29a-3p, miR-338-3p and miR-2861 at 3 months (FC 0.13, p<0.001; FC 0.68, p=0.044; FC 0.46, p=0.012; FC 0.16, p<0.001, respectively), and 6 months (FC 0.1, p<0.001; FC 0.52, p<0.001; FC 0.04, p=0.006; FC 0.2, p<0.001, respectively) only within the TPTD group. Serum concentrations of CTX and TRAP-5b were positively correlated with the relative expression of several circulating miRs at both 3 and 6 months of Dmab treatment. No correlation was observed between serum PINP levels and the relative expression of the tested miRs at 3 and 6 months after Dmab treatment in the entire cohort.Conclusions: TPTD treatment potentially affects the expression of the pro-osteoclastogenic miR-21a-5p and miRs related to the expression of osteoblastic genes RUNX2 (miR23a-3p), COL1 (miR-29a-3p) and HDAC5 (miR-2861), while sequential treatment with Dmab acts in the opposite direction.

***Disclosures: Elena Tsourdi**, None*

P-269

In Silico Analysis of Limb Bud Formation in the Prrx1-Cre Anti-microRNA-23a-27a-24-2 Cluster Mouse *Delores Stacks[1], Benjamin Wildman[1], Yuechuan Chen[1], Theodore Busby[1], Ashlee Williams[1], Quamarul Hassan[1]. [1]University of Alabama at Birmingham, United States

Objective: The microRNA cluster 23a-27a-24-2 (miR-23a cluster) inhibits osteogenesis by repressing the Runx2 – Ezh2 axis of osteoblast differentiation. We established a murine phenotype of increased trabecular and cortical bone when the miR-23a cluster was repressed in a Col1a1-Cre anti-miR-23a cluster mutant model. Col1a1 is expressed in committed osteoblasts as the collagen matrix is created prior to mineralization, which occurs in the mouse at days E18.5 and PN18. In this study, by changing the conditions of anti-miR-23a cluster expression to an earlier time course using a Prrx1-Cre, which is expressed at day E9.5, the

resulting offspring exhibit a unilateral rostral limb malformation phenotype that expresses with incomplete penetrance. Before beginning in vivo experiments to determine the cause of this abnormality, we surveyed mRNA seed sequences in the 3' UTR that match the miR-23a cluster and its components to find possible targets for transcriptional interruption. Method: Here we utilized three different in silico methods of miRNA target prediction (DianaTools, PicTar, and TargetScan) to determine if limb bud proteins are targets of members of the entire miR-23a cluster. Gene ontology analysis (Panther) was used to classify genes into their respective functions and pathways. Results: 2988 possible miR-23a cluster gene targets were identified. 8 molecular functions, 21 biological processes, 14 cellular components, 21 protein classes, and 122 pathways were recognized based on gene ontology terms. Notably, bone morphogenetic protein (BMP) signaling, Fibroblast growth factor signaling, Wnt signaling, Hedgehog signaling, Notch signaling, and TGF-β signaling pathways are possible targets and are interesting due to their notoriety for being vital to osteogenesis and limb bud development. Conclusions: Computational prediction verifies that pathways involved in limb bud development are likely affected when the miR-23a cluster is repressed at an early embryonic stage. Future experiments include immunohistological assessment of the embryonic limb bud and RNA sequencing of isolated limb bud tissues. Funding statement: Research reported in this publication was supported by the National Institute of Dental & Craniofacial Research of the National Institutes of Health under Award Number T90DE022736. The content is solely the responsibility of the authors and does not necessarily represent the official views of the National Institutes of Health.

***Disclosures: Delores Stacks**, None*

P-270

Independent effects of estrogen and follicle stimulating hormone on marrow cell populations identified by single cell RNA-Seq analysis *Vanessa Sherk[1], Paul MacLean[1], T. Rajendra Kumar[1], Douglas Adams[1], Yuan-Haw Wu[1], Rebecca Foright[1], Matthew Jackman[1], Ginger Johnson[1], Cheryl Ackert-Bicknell[1]. [1]University of Colorado Anschutz Medical Campus, United States

Estrogen (E2) and follicle stimulating hormone (FSH) are purported to have independent effects on bone loss during the menopausal transition. While FSH receptors are found on osteoclasts and not on osteoblasts, changes in FSH positively correlate with both formation and resorption markers in peri- and postmenopausal women, suggesting that FSH impacts the mesenchyme in an as-of-yet undefined manner. Further, it is known that changes in both E2 and FSH are correlated with changes in energetics, both at the whole organism level and at the cellular level. The purpose of this study was to determine if treatment of rats with E2 and or FSH altered composite populations found within bone marrow stromal cells (BMSC), if cellular energy metabolism was different among these cells, and if this was correlated with osteoblast mineralizing potential. In a 2-factor design, adult female Wistar rats were ovariectomized and treated with a GnRH antagonist (Degarelix; 2mg/kg, 5% mannitol) +/- E2 (drinking water; 1.0μM to target ~40 pM) and +/- FSH (implanted peristaltic pump; 6ug/kg/day) for 3 weeks. Degarelix effectively blocked FSH (<2 ng/mL). FSH treatment resulted in concentrations of 60+/-13 and 67+/-11 ng/mL for FSH and FSH+E2. Marrow was centrifuged from hindlimb bones and adherent cells were passaged 3 times and collected for Single cell RNA-Seq at 50,000 reads per cell and 4 replicates. Clustering and differential expression profiles were performed using the Seurat 3.0 R package. Oxygen consumption rate (OCR) and extracellular acidification rate (ECAR) were measured with Seahorse XFe96. Cell heterogeneity differed between all 4 conditions with the greatest differences observed for cells obtained from the E2 treated animals. Relative to the other three conditions, E2 BMSCs presented with an alteration in osteoblast maturation profile and a greater ability to mineralize as determined by Alizarin Red staining of cells. FSH treatment was also associated with decreased expression of genes related to IGF-1 signaling relative to all other treatments. Genes associated with glycogen, aerobic glycolysis, and the pentose phosphate pathway were most highly expressed with E2 treatment, which was in concordance with having the highest ECAR and state 3 OCR. Our scRNAseq analyses demonstrate that in vivo treatment of E2 and FSH changes the heterogeneity, identity, and gene expression of marrow-derived cells in a manner that may influence their metabolic phenotype and bone forming capacity.

***Disclosures: Vanessa Sherk**, None*

P-271

Functional Characterization of Primary Bone Transcriptome Reveals SOX7, CPED1, AC145124.1, FAM167A, TSLP and FCN3 as Bone Mineral Density Effector Genes *Vid Prijatelj[1], Sjur Reppe[2], Matthew Dietz[3], Joost A. M. Verlouw[1], Carolina M. Medina-Gomez[1], Andre J. van Wijnen[0], Kaare M. Gautvik[2], Eppo B. Wolvius[1], Fernando Rivadeneira[1]. [1]Erasmus MC, University Medical Center Rotterdam, the Netherlands, Netherlands, [2]Institute of Basic Medical Sciences, University of Oslo, Norway, Norway, [3]Mayo Clinic, Rochester, MN, USA, Department of Orthopedic Surgery, United States, [0]Mayo Clinic, Rochester, MN, USA, Department of Orthopedic Surgery, United States

BACKGROUND: Expression quantitative trait loci (eQTLs) are characterized by variants influencing messenger RNA (mRNA) expression that are often tissue-specific. We performed cis-eQTL analysis on primary bone tissue, with a functional follow-up analyses, including a summary data-based Mendelian randomization (SMR) to combine multi-omics data for the prioritization of gene targets.METHODS: Donor iliac-crest biopsy samples (n=76) underwent microarray genotyping (Affymetrix Axiom 432) and transcriptome sequencing (Illumina Hiseq2000). A custom computational profiling method was utilized in the cis-eQTL analysis to quantify and correct blood contamination. This computational method offers substantial decrease in analysis time as compared to similar tools, and is provided as a shareable R programming language package. Analysis was performed in regions encompassing 1,000,000 base pairs upstream of transcription start sites (TSS) and downstream of transcription end sites (TES). Significant eQTLs were tested for enrichment of genomic features across several cell lines (including human osteoblasts), and amidst variants associated at genome-wide significant level with estimated bone mineral density (eBMD) from heel bone ultrasound in UK-Biobank (N=435K). Colocalization tests and multi-variant SMR integrative analysis (for eQTLs with Chi2 statistic >10) were performed. Bonferroni corrected P-value < 0.05 was considered significant.RESULTS: In total, 1277 e-genes had significant eQTLs. The majority of eQTLs were located around the TSS. In human osteoblasts, they were significantly enriched for CCCTC-binding factor (CTCF) and transcribed chromatin states, as well as significantly depleted for repressed chromatin states. From the 13,126 analyzed transcripts, FAM167A (P < 0.05) and CPED1, SOX7, AC145124.1 (P 50% only for colocalization of TSLP and FCN3, most likely due to conditional nature of eQTLs. CONCLUSION: We were able to integrate transcriptomic and genotyping information of primary bulk bone tissue to predict "unconfounded" associations between tissue specific gene expression and clinical phenotypes. CPED1 and SOX7 have established roles in skeletal biology, while the other prioritized eBMD genes are all related to immunological response, coagulation and complement activation, and autoimmune diseases. Such triangulation of evidence aids the identification of implicated biologic pathways.

***Disclosures: Vid Prijatelj**, None*

P-272

Leveraging data from bivariate genome-wide association meta-analysis to unravel novel pleiotropic pathways of bone-muscle crosstalk *Katerina Trajanoska[4], Niki Dimou[2], David Karasik[3], Fernando Rivadeneira[1], on behalf of GEFOS Consortium[0]. [4]Department of Internal Medicine, Erasmus MC University, Netherlands, Netherlands, [2]Section of Nutrition and Metabolism, International Agency for Research on Cancer, France, [3]Azrieli Faculty of Medicine, Bar-Ilan University, Israel, [1]Department of Internal Medicine, Erasmus MC University, Netherlands, Netherlands, [0]Bivariate analysis group, Netherlands

Background: The intimate relationship between bone and muscle is governed by various mechanical and biochemical interactions; regulated by a complex network of pleiotropic genes with common biological pathways. We aimed to assess pleiotropy between bone and muscle by performing a bivariate genome-wide association study (GWAS). Methods: We included 20 cohorts from populations of European ancestry (Ntotal= 38,457). Total body bone mineral density (TB-BMD; g/cm2) and lean mass (TB-LM; kg) were measured in all cohorts using Dual-energy X-ray absorptiometry (DXA. Genetic variants were imputed to the Haplotype Reference Consortium (HRC) reference panel. In each cohort we performed univariate and bivariate GWAS adjusting for age, gender, height, fat percentage, and principal components using 8,027,751 variants and results were combined in a meta-analysis. We defined lead significant SNPs with $P < 5 \times 10\text{-}8$ that were independent of each other at r2 300 kilobases (kb) apart from each other represented independent loci. Results: In the univariate TB-BMD GWAS we identified 42 signals mapping to 27 loci; all known BMD loci. Five loci were associated with TB-LM, three of which were novel mapping to SPEG (rs1810144-T, beta=0.04SD), TMEM18 (rs73139123-T, beta=0.05SD) and MYPN genes (rs7081213-G, beta=0.04SD). Evidence from animal models links SPEG and MYPN genes with muscle biology. Notably, the bivariate meta-analysis yielded 16 pleiotropic signals mapping in or near MEF2C, XYLB/ACvr2B, PPP6R3, RSPO3 genes among others, linked with both bone and muscle biology. Conclusion: Our findings provide basis for future functional assessments aiming to unravel biological mechanisms underlying complex bone-muscle interactions; with the potential of pinpointing strategies for the joint prevention and intervention of osteoporosis and sarcopenia.

***Disclosures: Katerina Trajanoska**, None*

P-273

Identifying circulating biomarkers for osteoporosis *Sirui Zhou[1], Erin Oerton[2], John Morris[3], Eleanor Wheeler[2], Vincenzo Forgetta[1], Claudia Langenberg[2], Brent Richards[1]. [1]Lady Davis Institute, Jewish General Hospital, Canada, [2]MRC Epidemiology Unit, University of Cambridge, United Kingdom, [3]New York Genome Center, United States

Circulating causal protein biomarkers for osteoporosis may help risk prediction, diagnosis, and can be putative drug targets. In this study we used Mendelian randomization (MR) to identify clinically relevant circulating biomarkers for heel bone mineral density (eBMD). We then confirmed these findings using direct measurements of prioritized biomarkers in another cohort with BMD measurement. Cis-acting SNPs associated with 863 circulating proteins were identified from two studies of 6,501 individuals. These were used as instrumental variables in a hypothesis free, two-sample MR scan for their causal effect on eBMD from a GWAS of 426,824 individuals from UK Biobank. Candidate biomarkers were validated in the Fenland cohort (N=?11,183?) by ?their protein-level association with total body BMD (tBMD).?We identified 62 candidate protein biomarkers for eBMD using MR (P < 6.45 x 10-

5), from which 17 biomarkers showed high probability of colocalization (COLOC posterior probability>0.7). Measuring these candidate proteins in the Fenland cohort we found that 21 had significant associations with tBMD, where direction of effect was concordant with the MR finding; further analysis highlighting three prioritized biomarkers with high probability of colocalization in eCAVIAR with CLPP > 0.01 (MRC2, COLEC11, SEMA3C). These results suggest that MR can prioritize circulating protein levels as biomarkers for BMD outcomes. The identified biomarkers have been tested through MR and direct measurement and may serve as causal biomarkers and inform drug development.? ?

***Disclosures: Sirui Zhou**, None*

P-274

Role of Senescence in Age- and Radiation- Associated Bone Marrow Adiposity *Abhishek Chandra[1], Anthony Lagnado[1], Joshua Farr[1], David Monroe[1], Christine Hachfeld[1], Sundeep Khosla[1], Joao Passos[1], Robert Pignolo[1]. [1]Mayo Clinic, United States

Clearance of senescent cells has been shown to suppress bone marrow adiposity, and ameliorate age- and radiation-associated bone loss, but molecular events that precede the occurrence of marrow adiposity are unknown. Using radiation as a model to understand age-associated changes in bone, we have shown that p21 peak expression on day 1 post-radiation precedes major detrimental changes in radiated bones. RNA sequencing in radiated(R) and non-radiated(NR) femurs from mice revealed that p21, and several of the genes linked to adiposity, were the most significantly up-regulated in the R-bones as compared to the NR-bones. For a longitudinal assessment of adiposity related genes, NR-and R- bones were collected post sham and actual exposure, respectively, at days 1, 7, 21 and 42 for mRNA analysis and at day 1 and 7 for histology. Significantly high levels of telomere dysfunction-induced foci(TIF)+ senescent osteoblasts were detected in the R-bones at day-1 and -7. The qRT-PCR of 20 adiposity-related genes only connected by a highly stringent String-Network was performed. Only Pparg was upregulated on day 1 post-radiation. Significant up-regulation in adipose-related genes was observed in R-bones at day 7(Adipoq, Fabp4, Fabp5, Ghr, Igf-1 and -2, Lpl, Pparg, Plin-1 and -2, Rarres2 and Rxra), day 21(Cfd, Ctsc, Igf1, Mlxipl, Plin-1, -2 and -4, Rarres2 and Rxra) and at day 42(Adipoq, Cfd, Cidec, Ctsc, Ghr, Igf-1 and -2, Lpl, Lipe, Plin-1,-2 and-4, Pparg, Rarres2, Rbp4, Rxra and Scd1). In aging studies, 24 month bone samples showed high p21 (~6-fold increase, p=0.0002), high p16Ink4a(~3.5 fold increase, p=0.005) and 19 out of the 20 adiposity-related genes were significantly up-regulated, as compared to young (5m old) mouse bones. Significant down-regulation of microRNA(mir)-106b-5p(targeting p21 mRNA) was observed in aged bones(p=0.02) and across all time points in the radiated bones(day 1[p=0.09], day 7[p=0.013], day 21[p=0.006] and day 42[p=0.09], while mir-20a-5p(targeting p21 mRNA) was down-regulated only at day 21 post-radiation (p=0.006). Intriguingly, mir-27a-3p, reported to be elevated during obesity and in adipose tissue, was found to be elevated in aged- (p=0.04), and in R- bones(-day 1[p=0.005], day 21 [p=0.18] and day 42[p=0.04]. In summary, our data indicate the interplay between pathways of senescence and bone marrow adiposity which follow a similar pattern in aging and radiation.

***Disclosures: Abhishek Chandra**, None*

P-275

Detection of musculoskeletal GWAS-associated lncRNAs in human, rodent and fish models *Bodhisattwa Banerjee[1], Ines Föβl[2], David Karasik[3], Barbara Obermayer-Pietsch[2]. [1]Bar-Ilan University, Israel, [2]Medical University Graz, Austria, [3]Bar-Ilan University; Hebrew SeniorLife, Israel

Background: The musculoskeletal (MSK) system possesses fundamental functions in the human body. Long non-coding RNAs (lncRNAs) are now emerging as critical regulators of major biological processes affecting development, differentiation, and disease. The importance of lncRNAs just began to be recognized in bone (patho)physiology. Therefore, our study aims to prioritize candidate lncRNAs involved in MSK GWAS and determine the functionality of these lncRNAs in humans, mice, and zebrafish.Methods: We have mined the existing MSK GWAS databases and prioritized candidate lncRNAs based on their sequence conservancy in humans, zebrafish, and mouse. The expression of the lncRNAs in the bony tissues (cranium and operculum) in fish of various ages (3 and 6 months, 1 and 1.5 years) was tested using qPCR. Furthermore, the expression of these candidate lncRNAs in human plasma, serum, and bones was examined by qPCR. The qPCR data were statistically analyzed by Student's t-test. The expression of these three lncRNAs was analyzed in RNA-seq data of human posterior iliac crest biopsies (GEO: GSE72815) and differentiating mouse osteoblasts (GEO: GSE54461).Results & Discussion: The lncRNAs MALAT1, GAS5, and OIP5-AS1 were selected for their potential regulatory functions in skeletal phenotypes. In zebrafish bones, malat1 and gas5 lncRNA expressions were significantly elevated ($p < 0.05$) in young adults (3 and 6 mo) compared to the older fish (1 and 1.5 y old). Expression data from the human bone RNA-seq demonstrated slight upregulation of MALAT1 and GAS5 lncRNA in younger women compared to the older. During murine osteoblast differentiation, Gas5 showed higher expression in the early time points (2, 4, 6 days) compared to the later time points (10, 14, 18 days). Therefore, it could be seen that at least one of these three lncRNAs, GAS5, shows a similar pattern of expression across species suggesting functional conservation and age-specific functions in the MSK system. Furthermore, in human serum and plasma, lncRNA GAS5 shows the highest expression, followed by MALAT1. The current data do not clarify the tissue of origin of the lncRNAs or their release mechanism into the bloodstream. However, the presence of these two lncRNAs in serum/plasma suggested that they might serve as potential biomarkers. In the future, expression of GAS5 lncRNA during murine osteoblast differentiation will be validated by qPCR.

***Disclosures: Bodhisattwa Banerjee**, None*

P-276

Genetic and miRNA associations underlying beta-blocker effects on bone mineral density *Kathleen Nevola[1], Douglas Kiel[2], Katherine Motyl[3], Christine Lary[3]. [1]Tufts University, United States, [2]Hebrew SeniorLife, United States, [3]Maine Medical Center Research Institute, United States

Many studies have shown a positive association between beta blocker (BB) use and bone outcomes such as fracture and bone mineral density (BMD). Response to BBs can be variable which may be due to genetics, with previous studies implicating beta-adrenergic receptor genes (ADRB1 and ADRB2). We hypothesized that variants in these and other genes in the beta adrenergic signaling mechanism on bone cells (see Figure) may influence BB response on BMD, and this may be due to microRNA expression (miRNA). We selected 13 genes from this pathway that have single nucleotide polymorphisms (SNPs) with prior association with BMD. We measured associations between SNPs, BB use, and their interaction, on femoral neck BMD (FN BMD) measured via DXA in a sample of N = 1,527 members of the Framingham Study Offspring cohort. Genetic data were imputed to the HRC (Haplotype Reference Consortium), and SNPs within 2 kB upstream to 0.5 kB downstream of each gene were analyzed with the alternative allele dosage using a sex-stratified linear mixed effects model, with kinship as a random effect and covariates (age, sex, height, weight, and estrogen use in women). We then used conditional joint analysis with Genome-wide Complex Trait Analysis (GCTA) to select independent signals within each gene, identifying 11 SNPs that had significant interactions with BB use ($p < 0.05$) in ADRB1, HDAC4, PRKACB, PRKAR2B, RANK, and RANKL. We plan to bring 4 SNPs forward for validation: 2 in females (ADRB1 rs12414657 p=0.046; HDAC4 rs11124190 p=0.0093) and 2 in males (RANK rs34170507 p=4.4e-5; RANK rs6567268 p=0.0051). These SNPs are intron variants except rs12414657 which is an upstream transcript variant. To determine potential miRNA-related mechanisms, we analyzed the association between miRNA from whole blood with each of the 11 SNPs ($p < 0.05$), focusing on miRNAs with prior bone associations or miRNA that target the gene containing the SNP. For example, the SNP in ADRB1 (rs12414657) is associated with increased expression of miR-19a-3p, a miRNA associated with BB use and BMD, which has been shown to target ADRB1. We hypothesize that the increased expression of this miRNA with the alternative allele decreases ADRB1 expression, down-regulating adrenergic signaling in bone, leading to a decrease in bone remodeling. We plan to validate this and other findings in future clinical and in vivo studies. This work has implications for biomarkers and personalized therapy regimes for beta blocker use in bone.

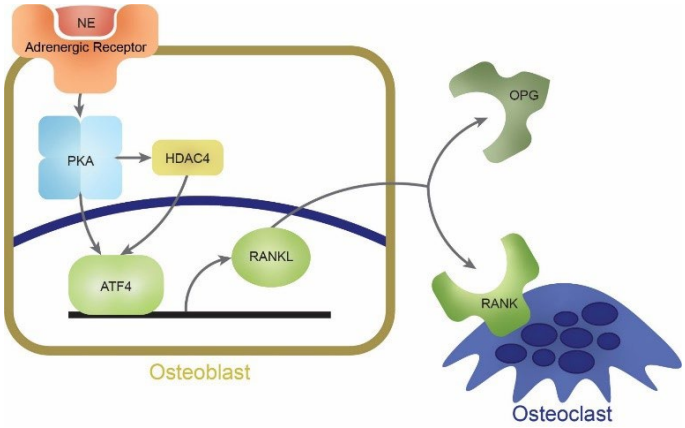

***Disclosures: Kathleen Nevola**, None*

Posters

P-277

Improved prediction of fracture risk leveraging a genome-wide polygenic risk score *Tianyuan Lu[1], Vincenzo Forgetta[2], Julyan Keller-Baruch[2], Maria Nethander[3], Derrick Bennett[4], Marie Forest[2], Sahir Bhatnagar[1], Robin Walters[4], Kuang Lin[4], Zhengming Chen[4], Liming Li[5], Magnus Karlsson[6], Dan Mellström[3], Eric Orwoll[7], Eugene McCloskey[8], John Kanis[8], William Leslie[9], Robert Clarke[4], Claes Ohlsson[3], Celia Greenwood[1], Brent Richards[1]. [1]McGill University, Canada, [2]Lady Davis Institute for Medical Research, Canada, [3]University of Gothenburg, Sweden, [4]University of Oxford, United Kingdom, [5]Peking University, China, [6]Lund University, Sweden, [7]Oregon Health & Science University, United States, [8]University of Sheffield, United Kingdom, [9]University of Manitoba, Canada

Accurately quantifying risk of osteoporotic fracture is important for directing appropriate clinical interventions. While skeletal measures such as heel quantitative speed of sound (SOS) and DXA bone mineral density have been shown to be able to predict risk of osteoporotic fracture, the utility of such measurements is subject to availability of equipment and human resources. Using data from 341,449 individuals of white British ancestry, we previously developed a genome-wide polygenic risk score (PRS), called gSOS, that captured 25.0% of the total variance in SOS. We aim to test whether gSOS can improve fracture risk prediction.We examined the predictive power of gSOS in five large genome-wide genotyped cohorts, including 90,172 individuals of a European ancestry and 25,034 individuals of an Asian ancestry. We calculated gSOS for each individual and tested for association between gSOS and incident major osteoporotic fracture and incident hip fracture. We tested whether adding gSOS to risk prediction models had added value over models using other clinical risk factors.A standard deviation decrease in gSOS was strongly associated with an increased odds of incident major osteoporotic fracture in European populations, with odds ratios ranging from 1.35-1.46 in four cohorts. It was also associated with a 1.26-fold (95% CI: 1.13-1.41) increased odds of incident major osteoporotic fracture in the Asian population. We demonstrated that gSOS was more predictive of both incident major osteoporotic fracture (AUROC = 0.734; Interquartile Range (IQR): 0.727-0.740) and incident hip fracture (AUROC = 0.798; IQR: 0.791-0.805) than most traditional clinical risk factors, including prior fracture, smoking, use of corticosteroids, rheumatoid arthritis. We also showed that adding gSOS to FRAX, the commonly used fracture risk prediction tool, could significantly refine risk prediction with a likelihood ratio test p-value < 0.05 and a positive net reclassification index ranging from 0.024 to 0.072.In conclusion, we generated and validated a PRS for SOS which is strongly associated with risk of fracture. This score provides modestly better fracture risk discrimination than most clinical risk factors. We propose that gSOS should be explored as a tool to provide better risk stratification to identify individuals at high risk of fracture, particularly considering that PRSs can be generated for multiple diseases from one single investment in genome-wide genotyping.

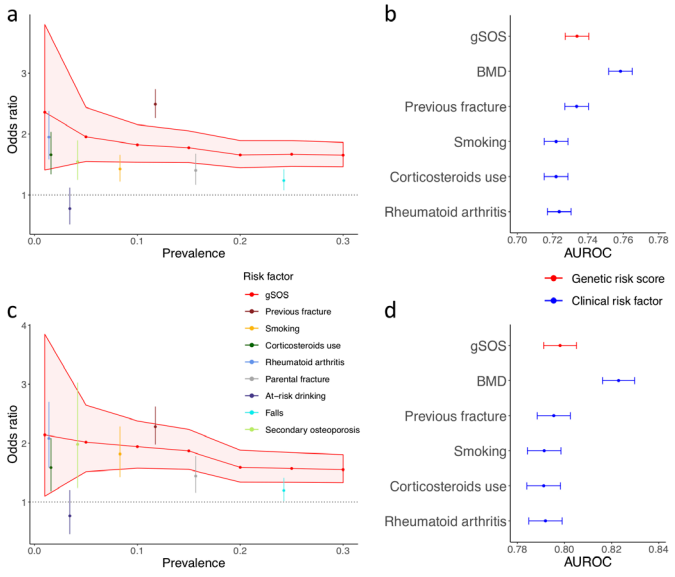

***Disclosures: Tianyuan Lu**, None*

P-278

Proteomic Approach in Aorta of Rheumatoid Arthritis-Induced 5-LO KO Mouse Model *Cintia Kazuko Tokuhara[1], Flavia Amadeu de Oliveira[2], Talita Mendes Oliveira Ventura[1], Jose Burgos Ponce[3], Joao Paulo Domezi[1], Adriano de Souza Pessoa[1], Gabriela Silva Neubern de Oliveira[1], Mariana Liessa Rovis Sanches[1], Vimal Veeriah[2], Mariana Rodrigues Santesso[4], Marilia Afonso Rabelo Buzalaf[1], Rodrigo Cardoso de Oliveira[1]. [1]University of São Paulo, Brazil, [2]Sanford Burnham Prebys Medical Discovery Institute, United States, [3]University Center of Adamantina, Brazil, [4]Sao Paulo State University, Brazil

It has been established that rheumatoid arthritis (RA) mainly affects the joints, however, extra-articular involvement is common. Thus, it is reported that patients with RA have higher risk of mortality in comparison with health people, due mainly to increased cardiovascular disease related to both traditional risk factors and disease-induced chronic inflammation. Leukotrienes (LTs) are lipid mediators derived from arachidonic acid by 5-lipoxygenase (5-LO) pathway and play an important role in the inflammatory response. Thus, we sought to study in detail the role of leukotrienes on protein profile from aorta in rheumatoid arthritis condition. We conducted a quantitative proteomics analysis by using mass spectrometry comparing 5-LO Knockout (KO) and wild type (WT) mice under arthritis-induced condition. 60-days old KO and WT mice were intravenously immunized with 1.5 mg of arthrogen cocktail at day 0 and 10 µg of LPS was intraperitoneally administered at day 3. After 14 days of immunization, mice were euthanized and protein samples from aorta were isolated, purified and processed for proteomics analysis using LC-ESI-MS/MS. Results showed several changes of aorta protein profile between 5-LO KO RA and WT RA. In total, over 1075 proteins were identified by proteomic approach. Among them, 341 proteins were exclusive from 5-LO KO RA and 385 from WT RA and 349 proteins were identified in both groups. Regarding quantitative analysis, 60 and 15 proteins were up and downregulated, respectively in the comparison 5-LO KO RA vs. WT RA. The following proteins histone H4 and nuclear mitotic apparatus protein 1 were increased more than 2-fold in 5-LO KO RA and 15 proteins were decreased more than 2-fold in the same group. Results clearly demonstrated that absence of leukotriene causes significant changes in proteome profile of RA aorta and it may have important functions on metabolism and clinical implications in rheumatoid arthritis.

***Disclosures: Cintia Kazuko Tokuhara**, None*

P-279

Comparison of Week-by-Week Changes in Serum Levels of Bone-related Circulating MicroRNAs and Bone Turnover Markers *Patryk Zarecki[1], Fatma Gossiel[1], Johannes Grillari[2], Miguel Debono[3], Matthias Hackl[4], Richard Eastell[1]. [1]University of Sheffield, Department of Oncology & Metabolism, United Kingdom, [2]Ludwig Boltzmann Institute for Experimental and Clinical Traumatology, Austrian Cluster for Tissue Regeneration, Austria, [3]Sheffield Teaching Hospitals NHS Foundation Trust, United Kingdom, [4]TAmiRNA GmbH, Austria

MicroRNAs are involved in post-transcriptional regulation of gene expression. Due to the regulatory role, microRNAs are differently expressed during certain conditions in healthy and diseased individuals and could be used as diagnostic and prognostic biomarkers for various diseases and conditions. We want to investigate the variability of microRNAs and bone turnover markers in weekly time intervals.In a single site longitudinal study, a panel of 19 bone-related miRNAs was measured using the osteomiR™ RT-qPCR assay in serum samples of 35 postmenopausal women divided into 3 groups: healthy controls (n = 9), low BMD (n= 14) and vertebral fractures (n= 12). Blood samples were collected once per week for 8 weeks at 9:00 am after overnight fasting. Bone turnover markers were measured on the IDS-iSYS Multi-Discipline Automated Analyser.We have analysed the data using a mixed model analysis of variance approach and we found no significant changes between week-by-week time-points in any of groups. To estimate intra-individual variability between weekly time-points we have calculated the median coefficient of variation (CV).In healthy control group microRNAs median intra-individual CV was between 28.4% (hsa-miR-19b-3p) and 80.2% (hsa-miR-214-3p); in low BMD group 33.8% (hsa-miR-188-5p) and 77.9% (hsa-miR-127-3p); in vertebral fractures group 29.5% (hsa-miR-19b-3p) and 61.4% (hsa-miR-214-3p). Combined assay CV including RNA isolation, reverse transcription and real-time qPCR was 21.3%. CTX median CV was 13.4% in healthy control group, 16.8% in low BMD group and 17.9% in vertebral fractures group, with assay CV of 6.5%. PINP median CV was 13.6% in healthy control group, 13.2% in low BMD group and 15.6% in vertebral fractures group, with assay CV of 7.2%. Osteocalcin median CV was 12.7% in healthy control group, 8.5% in low BMD group and 11.8% in vertebral fractures group, with assay CV of 6.3%. Bone alkaline phosphatase median CV was 9.2% in healthy control group, 9.8% in low BMD group and 11.1% in vertebral fractures group, with assay CV of 3.5%.Circulating microRNAs measured in serum seem to have higher weekly intra-individual variability compared to bone turnover markers. MicroRNAs with high serum levels are on average less variable than microRNAs with low serum levels.

***Disclosures: Patryk Zarecki**, None*

P-280

Comparative messenger RNA expression analysis of vitamin D receptor, calcium-sensing receptor, cyclin D1, and PTH in symptomatic and asymptomatic primary hyperparathyroidism in Asian Indians *Dwijaraj Hegde[1], Parjeet Kaur[1], Sunil Mishra[1], Deepak Sarin[1], Dheeraj Gautam[1], Priyanka Singh[2], Sanjay Bhadada[2], Ambrish Mithal[3]. [1]Medanta The Medicity, India, [2]Postgraduate Institute of Medical Education and Research, India, [3]Max superspeciality Hospital Saket, India

Background: Although classic symptoms of primary hyperparathyroidism (PHPT) have been reported to be common in the India, data on increasing number of asymptomatic PHPT cases have been emerging from this part of the world as well. The exact underlying mechanistic reasons for this differential clinical profile remain unknown and efforts to define the molecular mechanisms underlying PHPT phenotypic heterogeneity have been limited. Aim: To explore underlying molecular mechanisms in the pathogenesis of symptomatic and asymptomatic sporadic PHPT. Methods: A prospective single centre study from India. Patients diagnosed with PHPT undergoing parathyroidectomy, were included. Patients lacking specific symptoms or signs traditionally associated with hypercalcemia or PTH excess were diagnosed as having asymptomatic PHPT. The mRNA expression of vitamin D receptor (VDR), calcium sensing receptor (CASR), cyclin D 1 (CD1), and parathyroid hormone (PTH) in parathyroid adenoma cells and controls (eight parathyroid tissues obtained from euthyroid patients without PHPT during thyroid surgery) was determined using quantitative real-time PCR (qRT-PCR) by SYBR Green I dye method (Fermentas, Life Sciences). Results: Total of 42 PHPT patients (18 men, 24 women) were studied. Mean (SD) age was 49.7 (12.8) years. 21 patients were asymptomatic. Mean plasma PTH levels were significantly higher in symptomatic group compared with asymptomatic group (538.26 vs 347.47 pg/ml). CaSR and VDR mRNAs were significantly reduced in both symptomatic and asymptomatic cases compared with controls. CD1 and PTH mRNAs were significantly increased in symptomatic patients whereas they were not significantly different in asymptomatic PHPT patients compared with controls. Symptomatic PHPT patients had significantly higher expression of CD1 mRNA and significantly lower expression of CaSR mRNA compared with asymptomatic patients. There were no correlations between VDR, CASR, PTH and CD1 mRNA levels and serum Ca, plasma intact PTH, 25-hydroxyvitamin D levels or adenoma weight. Conclusion: This study addressed the molecular mechanisms underlying PHPT phenotypic heterogeneity. Asymptomatic PHPT had significantly lower expression of CD1 mRNA and significantly higher expression of CaSR mRNA compared with symptomatic PHPT in Asian Indians.

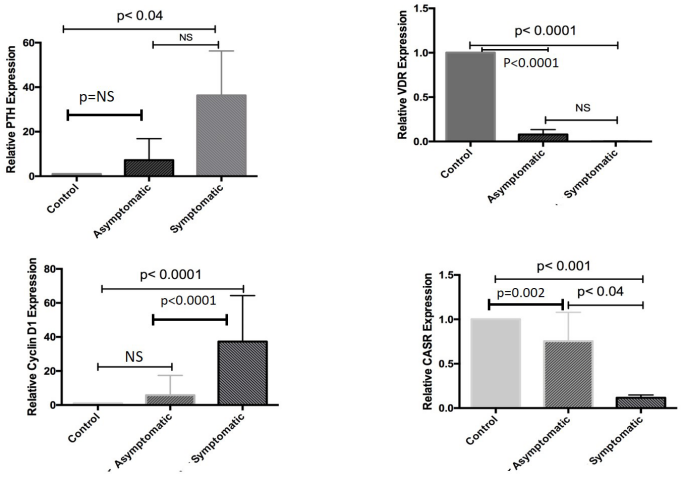

***Disclosures: Dwijaraj Hegde**, None*

P-281

DBP Is Required for the Utilization of Skin-Generated Vitamin D *Elizabeth Duchow[1], Lori Plum[1], Hector DeLuca[1]. [1]University of Wisconsin-Madison, Department of Biochemistry, United States

The primary source of vitamin D is skin exposure to ultraviolet B light (UVB). Despite the importance of this source, the mechanisms surrounding the transport of cutaneously produced vitamin D into the circulation remain undefined. We tested the hypothesis that vitamin D binding protein (DBP) is required for the utilization of skin-generated vitamin D. Mutant mice lacking DBP (DBP-/-) and wild-type control mice (DBP+/+) were made vitamin D deficient. All mice lacked detectable serum 25-hydroxyvitamin D (25-OHD) levels and were equally hypocalcemic. All mice were irradiated with 8kJ of UVB daily for up to 4 days. Serum calcium and 25-OHD were measured using atomic absorption spectrometry and the DiaSorin Liason 25 OH Vitamin D Total Assay, respectively. Skin vitamin D content was analyzed using a biological assay and/or high-performance liquid chromatography. All data are expressed as mean+/-SEM and statistical significance is defined as p<0.05. Treatment with UVB normalized serum 25-OHD and serum calcium in DBP+/+ mice, but had no effect on either in DBP-/- mice (Table 1). Vitamin D-deficient, hypocalcemic test rats responded with a comparable increase in serum calcium following administration of lipid extracts of skin from DBP+/+ and DBP-/- mice immediately following UVB treatment, indicating vitamin D production was normal in DBP-/- mice. Skin vitamin D levels decreased over a 2-day period in DBP+/+ mice but remained high in DBP-/- mice, suggesting impaired mobilization in the absence of DBP (40+/-2ng/g vs. 140+/-15ng/g, p<0.05 vs. DBP+/+). Repletion of DBP-/- mice by intravenous injection of increasing amounts of recombinant DBP (2μg, 7.5μg, or 23μg) prior to UVB restored responsiveness to UV-generated vitamin D. After two rounds of treatment, a significant increase in serum calcium was observed in the middle and high-dose group compared to controls that received saline prior to UVB and controls that were injected with highest amount of protein but did not receive UVB. A significant decrease in the total amount of vitamin D retained in the skin at 48 hours following the final treatment was observed at all dose levels with respect to the saline control. These results demonstrate that DBP is required for the utilization of vitamin D produced in skin by UVB.

Group	Serum measurement	Pre-UVB (±SEM)	Post-UVB (±SEM)
DBP$^{+/+}$	25-OHD (ng/mL)	*below detection limit* [A]	22.4 ± 3.7 [B]
	Calcium (mg/dL)	5.0 ± 0.1	8.2 ± 0.1 [C]
DBP$^{-/-}$	25-OHD (ng/mL)	*below detection limit* [A]	*below detection limit* [A]
	Calcium (mg/dL)	5.0 ± 0.1	5.1 ± 0.2

[A] Less than 4 ng/mL [B] Serum 25-OHD levels in vitamin D-sufficient DBP$^{+/+}$ mice: ~23.7ng/mL
[C] Serum calcium level in vitamin D-sufficient DBP$^{+/+}$ mice: ~8.0mg/dL

***Disclosures: Elizabeth Duchow**, None*

P-282

Secreted Frizzled Receptor Protein 4 (Sfrp4) is required for proper response of the periosteal stem/progenitor cells to PTH *Ruiying Chen[1], Han Dong[2], Dhairya Raval[1], Shawn Berry[1], Matthew B. Greenblatte[3], Roland Baron[1], Francesca Gori[1]. [1]1. Division of Bone and Mineral Research, Harvard Medical School and Harvard School of Dental Medicine. 2. Department of Oral Medicine, Harvard Medical School and Harvard School of Dental Medicine., United States, [2]Department of Cancer Immunology and Virology, Dana-Farber Cancer Institute and Harvard University Medical School, United States, [3]Department of Pathology and Laboratory Medicine, Weill Cornell Medicine, United States

The periosteum is essential in the cortical response to anabolic drugs. The identification of periosteal stem cells offers an opportunity to explore the mechanisms by which anabolic drugs such as PTH(1-34) influence the periosteum and might help identify drug targets for the treatment of skeletal diseases associated with cortical thinning and fragility. We have shown that lack of the Wnt inhibitor Sfrp4 leads to Pyle's disease, characterized by low periosteal bone formation, cortical thinning and bone fragility. We found that PTH induces Sfrp4 in periosteal cells, suggesting that Sfrp4 might be a downstream effector of PTH in the periosteum. Whether PTH regulates specific pools of periosteal cells and whether Sfrp4 is involved is not known. To test this hypothesis, we generated CtskCre;mTmG;wt and Ctsk-Cre;mTmG;Sfrp4-/- mice and studied the response of periosteal cells labeled by Cathepsin K (Ctsk+ and Ctsk+:Sfrp4-/-) to iPTH (25 nmol/kg, daily for 4-wk starting at 4-wk of age). Ctsk+ cells include bona fide stem cells (PSCs), with high PTH receptor expression, and non-stem progenitors (PP1 and PP2), the predominant source of Sfrp4. We have shown that Sfrp4 is required for proper maintenance and function of Ctsk+ cells. The periosteum of CtskCre;mTmG;wt and CtskCre;mTmG;Sfrp4-/- mice was microdissected and digested and Ctsk+ PSCs, PP1 and PP2 cells FACS-sorted. We found that in Ctsk-Cre;mTmG mice, iPTH increased the % of Ctsk+ cells (0.39+0.06 vehicle vs 0.55+0.08 iPTH, p<0.05) and this was due to the increase in the % of PSCs (15.5+0.3 vehicle vs 18.8+0.2, p<0.005). In contrast, in the absence of Sfrp4, iPTH was unable to significantly increase the pool of Ctsk+ cells, (0.35+0.04 vehicle vs 0.40+0.06 iPTH, NS) and the % of PSC (11+0.6 vehicle vs 12.1+0.3 iPTH, NS). Importantly, mCT analysis showed that iPTH treatment, while significantly increasing cortical thickness in Ctsk-Cre;mTmG tibiae (0.145+0.004 mm vehicle vs 0.165+0.005 mm iPTH, p<0.005), failed to do so in the absence of Sfrp4 (0.095+0.002 mm vehicle vs 0.096+0.004 mm iPTH, NS). Our data raise the possibility that Ctsk+ bona fide stem cells are associated with the anabolic effect of PTH in the periosteum and that Sfrp4 contributes to the cortical bone response to PTH. Further analysis of signaling molecules regulating periosteal stem cells may have clinical implications for fracture repair and the treatment of diseases associated with bone fragility

***Disclosures: Ruiying Chen**, None*

Posters

P-283

Conditional Loss of Nmp4 In Mesenchymal Stem Progenitor Cells Enhances PTH-Induced Bone Formation *Emily Atkinson[1], Michele Adaway[1], Crystal Korff[2], Daniel Horan[1], Angela Klunk[1], Joseph Wallace[3], Alexander Robling[1], Joseph Bidwell[1]. [1]Anatomy, Cell Biology & Physiology Indiana University School of Medicine, United States, [2]Medical & Molecular Genetics, Indiana University School of Medicine, United States, [3]Department of Biomedical Engineering IUPUI, United States

Activation of bone anabolic pathways is a fruitful approach for treating severe osteoporosis. Yet, FDA-approved osteoanabolics, e.g. parathyroid hormone (PTH) have limited efficacy. Improving their potency is a promising strategy for maximizing their benefits. Mice harboring a global loss-of-function mutation in nuclear matrix protein 4 (Nmp4) are healthy and exhibit an extended and enhanced bone formation response to PTH compared to wild type (WT) mice. This transcription factor is expressed in all tissues. To identify the cell type responsible for heightened PTH-induced osteoanabolism, we conditionally deleted Nmp4 at different stages of osteoblast-lineage differentiation. Nmp4-floxed mice (Nmp4fl/fl) were crossed to one of three different bone-lineage Cre drivers: Prx1-Cre, which targets mesenchymal stem progenitor cells (MSPCs) in developing limb bud, Bglap-Cre, which targets mature osteoblasts, and Dmp1-Cre, which targets transitional osteocytes. PCR and Western analyses demonstrated genetic recombination and loss of Nmp4 protein expression in the appropriate Cre+ bone cells whereas Cre- control mice showed robust Nmp4 protein expression and an absence of recombination. Virgin female Cre+ and Cre- mice (10 wks of age) were randomly sorted into treatment groups by weight and genotype. Mice received a daily injection of human PTH 1–34 at 30 µg/kg, or vehicle (VEH) for 4 wks. At the end of treatment areal bone mineral density (aBMD; g/cm2) was measured for the post-cranial skeleton by dual-energy X-ray absorptiometry. Femoral bone volume/total volume (BV/TV, %) was assessed with microcomputed tomography. Protocols were approved by IACUC. RESULTS: Nmp4fl/fl;Prx1Cre+ mice showed a significantly enhanced whole body aBMD vs. Nmp4fl/fl;Prx1Cre- mice (VEH Cre- 0.051 +/- 0.002; PTH Cre- 0.054 +/- 0.002; VEH Cre+ 0.052 +/- 0.002; PTH Cre+ 0.055 +/- 0.002, avg +/- SD treatment p<0.0001, genotype p=0.04, 2W ANOVA, n=12-16/cohort). Nmp4fl/fl;BglapCre+ and Nmp4fl/fl;Dmp1Cre+ did not show this effect. The Nmp4fl/fl;Prx1Cre+ mice exhibited an enhanced PTH-induced increase in femoral BV/TV compared to the Nmp4fl/fl;Prx1Cre- animals (Cre- VEH 2.3+/-0.7; Cre- PTH 5.6+/-1.7; Cre+ VEH 3.1+/-1.3; Cre+ PTH 8.4+/-3.6; avg +/- SD, treatment p<0.0001; genotype p= 0.0001; genotype x treatment p=0.03, 2W ANOVA, n=25-34/cohort). CONCLUSION: conditional loss of Nmp4 from MSPCs amplifies bone response to anabolic PTH. This cell-type specific pathway is a novel target for improving osteoanabolics.

***Disclosures: Emily Atkinson**, None*

P-284

Mechanisms Controlling The High Level Of Vitamin D Receptor Gene Expression In Mouse Intestine. *James Fleet[1], Sylvia Christakos[2], Michael Verzi[3]. [1]Purdue University, United States, [2]Rutgers New Jersey Medical School, United States, [3]Rutgers University, United States

The hormone 1,25 dihydroxyvitamin D (1,25(OH)2D) is a critical regulator of calcium, phosphorus, and bone metabolism whose actions are mediated through the Vitamin D Receptor (VDR), a ligand-activated transcription factor. While VDR is expressed in many tissues, the highest levels of VDR are found in the intestine. We examined the DNA regions and sequences that control intestine-specific expression of the mouse Vdr gene. Samples were obtained from the three different intestinal locations: the duodenal villi, the duodenal crypt, and the colon. In addition, we examined three different ages: developmental (12-15 d post natal), adult (90 d), and aged (20 months). Samples were analyzed by ATAC-seq with a MACS2 peak calling protocol. Comparisons between these groups were conducted using DiffBind. A topologically associated domain of 240 kb containing the Vdr gene and 6 other genes was identified using CH12 cell Hi-C data from the 3Dgenome.org (5 kb resolution). 15 ATAC peaks were identified in adult duodenal villi and crypt and all were within a 125 kb region from intron 3 of the Vdr gene to -55.8 kb from exon 1. Two novel ATAC peaks were also found in this region for the adult colon. Peaks were similar in adult and old mouse intestine but peaks were missing or reduced in the developing duodenum (7 peaks) and colon (4 peaks). All adult duodenal villi/crypt and colon peaks overlapped with ChIP-seq peaks for the intestine-specific transcription factor, Cdx2 (GSM2610627). Some ATAC peaks also overlapped with HNF4α/γ (9 peaks, GSE112946) or SMAD4 (9 peaks, GSM1688778) ChIP-seq peaks while 5 ATAC peaks overlapped with ChIP-seq peaks for all three transcription factors. Consistent with the importance of these transcription factors, Vdr mRNA levels fell by >70% in the intestine of Cdx2 or HNF4α/γ KO mice. Our ATAC peaks were similar to DNAse-Seq peaks from ENCODE for large intestine and kidney (which also had 2 novel peaks). However, the majority of intestine ATAC peaks were distinct from regulatory regions identified for other VDR expressing tissues including NIH 3T3 cells, lung alveolar macrophages, and MC3T3 osteoblasts. Our analysis demonstrates that the regulation of intestinal Vdr gene expression requires the complex interaction of multiple distal regulatory regions and is controlled by a combination of intestine-specific (Cdx2) and other (HNF4, SMAD4) transcription factors.

***Disclosures: James Fleet**, None*

P-285

Regulation of CRTC1/2/3 by Protein Phosphatases and Salt-inducible Kinases in Osteoblastic RankL Transcription *Michael Mosca[1], Zhiming He[1], Carole Le Henaff[1], Nicola Partridge[1]. [1]Department of Molecular Pathobiology, New York University College of Dentistry, United States

Parathyroid hormone (PTH) is a key regulator of bone homeostasis and has been used to treat osteoporosis. Unfortunately, prolonged treatment with PTH leads to excessive bone resorption through the stimulation of RankL. Denosumab has been used in trials to ameliorate the catabolic effects of RankL stimulated by PTH-derived treatments, but to date has not been proven to eliminate long term adverse effects. Current models suggest that CREB regulated transcription coactivators 1, 2, and/or 3 (CRTC1/2/3) are potential co-activators responsible for RankL transcription upon PTH-induction in osteoblasts. Our laboratory has previously shown that dephosphorylation of CRTC2/3 in the cytoplasm leads to their subsequent nuclear translocation and RankL transcription, but it is not known exactly how this occurs. To elucidate regulatory mechanisms involved in CRTC regulation, primary calvarial osteoblasts were harvested from C57BL/6J mice aged 2-3 days postnatal; calvariae were digested and cells were plated. siRNA knockdowns for salt-inducible kinases (SIK) and individual catalytic subunits of protein phosphatases (PP) of interest were performed (SIK1, 2 & 3; PP1, 2A, 3, 4, 5, 6 & 7) to determine their individual and combined roles on RankL transcription using qPCR and Western blotting. Data suggest SIK inhibition mimics PTH-induction but alone is insufficient to explain CRTC1/2/3 translocation after cAMP signaling. PPs likely assist in removal or regulation of the phosphate group on CRTC1/2/3 upon PTH stimulation. Initial data show specific catalytic subunits of PP1, PP2A, and PP3 may play critical roles in this cascade as siRNA knockdowns produce significant changes in RankL mRNA compared to controls ($p < 0.001$). Additionally, we have investigated the direct interactions of each factor of interest with the CRTCs via co-IP using anti-CRTC2/CRTC3 antibodies followed by Western blots. Results indicate that CRTC2/3 interact with PP1/PP2A upon PTH-stimulation while SIKs do not, and this interaction likely facilitates dephosphorylation and subsequent translocation of the CRTCs. These data lead us to believe that several PPs act together to regulate CRTCs after PTH-stimulated cAMP signaling and that understanding the exact mechanisms will illuminate novel drug targets in the treatment of osteoporosis.

***Disclosures: Michael Mosca**, None*

P-286

Beta-catenin regulates PTH receptor signaling through its armadillo residue to association with PTH receptor *Bin Wang[1], Hong Lei[1], Roger Armen[1], Yanmei Yang[1]. [1]Center for Translational Medicine, Department of Medicine, Sidney Kimmel Medical College, Thomas Jefferson University, United States

The optimal use of parathyroid hormone (PTH) therapy in osteoporosis depends in part on our understanding of the regulation of PTH signaling to maintain the anabolic actions of PTH while mitigating its catabolic effects. Although PTH receptor (PTHR) signaling pathways are being studied in increasing detail, the regulation of PTHR functions has not been fully elucidated. The anabolic PTH effects on bone are mostly mediated by the Gs/cAMP signaling pathway, whereas Gq/PLC activation may antagonize this osteoanabolic action. Our data and those from other groups show that beta-catenin interacts with the PTHR and switches the PTHR signaling from Gs/cAMP to Gq/PLC activation in chondrocytes, osteoblast-like (Saos2) cells, and HEK293 cells transfected with PTHR. Beta-catenin interacts with the PTHR carboxyl-terminal region, but which position of beta-catenin is bound by PTHR remains unknown. The primary structure of beta-catenin includes an N-terminal region of 130 residues, an C-terminal 100-residue segment, and a central region of 12 armadillo repeats spanning (130 – 668) residues. To explore which position of beta-catenin is associated with the PTHR, we generated beta-catenin knockout Saos2 cells and their control wild-type cells using CRISPR/Cas9 technology. Knockout of beta-catenin significantly increased PTH(1-34) stimulation of cAMP formation but inhibited PTH-induced intracellular calcium mobilization, an index of PLC activity. Knockout of beta-catenin also significantly facilitated PTH(1-34) stimulation of phosphorylation of the cAMP-dependent protein kinase PKA substrate (VASP) signal by using anti-VASP antibody. We transfected Flag-tagged full-length beta-catenin into beta-catenin knockout Saos2 cells, and found that exogenous beta-catenin could also mediate PTHR signaling switch compared with beta-catenin knockout cells transfected with vector plasmid. We than transfected plasmids with Flag-tagged N-terminal region, central region of armadillo repeats, or C-terminal region. Our data showed that only central region of armadillo repeats but not N- or C- terminal region was able to mediate PTHR signaling switch. Molecular modeling data also suggest that the central region of armadillo repeats have positively charged amino acid residues that bind to multiple negative charged residues of C-terminal region of the PTHR. Collectively, beta-catenin through its armadillo residue to association with PTHR regulates PTHR signaling and targeting these biding sites by designing new small molecules may enhance anabolic effect of PTH for the treatment of osteoporosis.

***Disclosures: Bin Wang**, None*

P-287

Cardiac Fgf23 Production Promotes Myocardial Fibrosis In A Pressure Overload Model In Mice *Nejla Latic[1], Ana Marek[1], Ute Zeitz[1], Wenhan Chang[2], Reinhold Erben[1]. [1]University of Veterinary Medicine, Austria, [2]University of California San Francisco, United States

Increased cardiac expression of fibroblast growth factor (FGF23) has been observed in left ventricular (LV) hypertrophy in mice and men. However, the pathophysiological role of cardiac FGF23 secretion in the development of LV hypertrophy and dysfunction is unknown. To specifically ablate FGF23 in cardiomyocytes, we crossed Fgf23fl/fl mice with MLCv2-Cre transgenic mice, expressing Cre in cardiomyocytes. The specificity of Cre expression was confirmed by crossing the MLCv2-Cre mice with ROSAmT/mG reporter mice. Cardiac mRNA expression of FGF23 was reduced 86% in cardiomyocyte-specific FGF23 knock-out (Fgf23CM-KO) mice, relative to wild-type controls. Body weight and mineral metabolism were unchanged in Fgf23CM-KO mice.Cardiac hypertrophy was induced by transverse aortic constriction (TAC), a chronic pressure overload model. TAC or sham surgery were performed in 5-month-old Fgf23CM-KO animals, using wild-type, Fgf23fl/fl, and MLCv2-Cre mice as controls. Serum levels of FGF23 were equally increased in all genotypes after TAC, suggesting that cardiac-derived FGF23 does not contribute to the rise in circulating FGF23 after TAC. Parameters of heart hypertrophy such as heart-to-body weight ratio and cardiomyocyte size were similarly increased in all groups of TAC animals, 4 weeks post-surgery, showing that LV hypertrophy developed independently of cardiac FGF23. However, intra-arterial catheterisation revealed that mean arterial pressure was significantly reduced in Fgf23CM-KO TAC mice, compared to Fgf23fl/fl TAC controls. LV internal diameter in systole and diastole measured by echocardiography as well as LV diameter measured histologically were increased in Fgf23CM-KO in comparison to Fgf23fl/fl controls, indicating more pronounced eccentric hypertrophy in Fgf23CM-KO mice after TAC. Interestingly, histological evaluation revealed a distinct reduction in TAC-induced cardiac fibrosis in Fgf23CM-KO compared to Fgf23fl/fl controls. Mechanistically, treatment of isolated cardiac fibroblasts with recombinant FGF23 increased collagen I expression ~4-fold. Collectively, our data suggest that local production of FGF23 promotes cardiac fibrosis in afterload-induced LV hypertrophy via a paracrine crosstalk between cardiomyocytes and fibroblasts.

***Disclosures: Nejla Latic**, None*

P-288

1,25-Dihydroxyvitamin D and Anti-FGF23 Blocking Antibody Treatments Improve Dentoalveolar Tissues in the Hyp Mouse Model of X-linked Hypophosphatemia *Eva Liu[1], Elis Lira dos Santos[2], Michael Chavez[2], Tamara Kolli[2], Brian Foster[2]. [1]Brigham and Womens Hospital, United States, [2]Ohio State University College of Dentistry, United States

Purpose: X-linked hypophosphatemia (XLH) is caused by PHEX mutations, leading to elevated serum levels of fibroblast growth factor 23 (FGF23). The high FGF23 levels result in decreased production of 1,25-dihydroxyvitamin D (1,25D), hypophosphatemia, and rickets. Patients with XLH develop dental complications, including caries and abscesses. Hyp mice replicate the XLH phenotype as they develop significant dentoalveolar mineralization defects. We aimed to compare the effects of 1,25D monotherapy or an anti-FGF23 blocking antibody (FGF23Ab) treatment on dentoalveolar development and mineralization in Hyp mice.Methods: Male Hyp mice injected subcutaneously with daily 1,25D (175 pg/g) or thrice weekly with FGF23 blocking antibody (35 mcg/g) from postnatal days 2 to 35 were compared to wild-type (WT) controls and untreated Hyp mice. Mandibular first molar teeth were analyzed by high resolution micro-computed tomography (micro-CT). Decalcified first molar tissue morphology was assessed by hematoxylin and eosin (H&E) and picrosirius red (PR) stains. Results: First molar enamel volume and density both trended lower in Hyp vs. WT mice, and both appeared improved with either treatment. Dentin/cementum volume and density were both dramatically decreased in Hyp vs. WT mice. Dentin/cementum volumes increased about 20% with either 1,25D or FGF23Ab, while dentin/cementum mineral density was not improved by either therapy. Alveolar bone fraction (bone volume/tissue volume; BV/TV) and mineral density (BMD) around the first molar were both reduced in Hyp vs. WT mice. BV/TV increased about 10% in Hyp mice treated with either 1,25D or FGF23Ab, while BMD did not respond to therapy. H&E stain of the first molar demonstrates that treatment of Hyp mice with either therapy improves acellular cementum morphology and reduces the widened predentin, though there is still substantial osteoid present in treated molars. Examination of PR stained Hyp molar tissue under polarized light microscopy revealed disorganization of the periodontal ligament (PDL) attachment. Both therapies improved PDL organization, indicating improved attachment. Conclusions: Taken together, these findings demonstrate similarly limited improvements in dentoalveolar tissues with 1,25D or FGF23Ab therapy, suggesting 1,25D and/or phosphate partially contribute to dentoalveolar mineralization in XLH. They show that the defects in Hyp dentoalveolar tissue are not due to FGF23 specific actions.

***Disclosures: Eva Liu**, None*

P-289

Sex differences in skeletal development and maintenance mediated by the osteoblastic glucocorticoid receptor *Anuj Sharma[1], Reginald Benson[1], Candee Barris[1], Jessica Pierce[1], Jennifer Dorn[1], Rachel Roberts[1], Kanglun Yu[1], Sadanand Fulzele[1], William Hill[2], Mark Hamrick[3], Carlos Isales[3], Xingming Shi[3], Meghan McGee-Lawrence[3]. [1]Augusta University, United States, [2]Medical University of South Carolina, United States, [3]Medical College of Georgia, Augusta University, United States

While the harmful effects of exogenous glucocorticoids (GC) on the skeleton are well understood, the role of endogenous GC and their glucocorticoid receptor (GR)-mediated signaling in bone are not clear, particularly during musculoskeletal aging. We originally predicted that blocking GR signaling would protect against aging-induced osteoblast dysfunction, but previously found that conditional knockout (CKO) of the GR in osteoprogenitors using Osx Cre promoted low bone mass and increased marrow adiposity in young (3-6 month old) female mice that was further exacerbated with age (21-24 month old). This suggests a critical function for the GR in skeletal maintenance with aging. In the current study, we extended these observations into young (3-6 month old) male GR-CKO mice. Surprisingly, the in vivo effects of loss of the skeletal GR were sex-specific, demonstrating more harmful effects in GR-CKO females than in males. For example, marrow adiposity (Ad.Ar/M.Ar) and marrow adipocyte density (N.Ad/M.Ar) were increased by 747% and 400%, respectively, in female GR-CKO as compared to female WT mice, but only by 176% and 59% in male GR-CKO as compared to male WT mice (genotype x sex interaction p-values: p=0.027 and 0.017, respectively). To further explore this finding, we developed an inducible (Tet-off) Osx-Cre GR-CKO mouse model, where mice were maintained on doxycycline chow until 12 weeks of age and studied at 24 weeks of age to negate any developmental defects related to the Osx Cre or GR deficiency during rapid growth; the sex differences of GR-CKO mice persisted in this model. Despite the differences seen in vivo, bone marrow stromal cells (BMSCs) from young male and female GR-CKO mice cultured for 21 days under osteogenic conditions behaved similarly in vitro, showing increased lipid droplets and decreased mineralized matrix production as compared to cells from wildtype (WT) sex-matched mice. Similarly, mesenchymal stem cells (MSCs; cell surface marker sorted) from WT male mice treated with the GR antagonist RU486 developed intracellular lipid droplets and decreased matrix mineralization similar to BMSC isolated from GR-CKO mice. The similar in vitro results between sexes despite disparate findings in vivo suggest the involvement of hormonal mechanisms that interact with GC signaling in musculoskeletal aging biology. In ongoing studies, male GR-CKO mice and WT littermates are being aged to determine whether sex differences persist during aging.

***Disclosures: Anuj Sharma**, None*

P-290

Role of Endogenous Parathyroid Hormone - related Protein (PTHrP) in Skeletal Anabolic Actions *Takeshi Shimoide[1], Loan Nguyen-Yamamoto[1], Aimee-Lee Luco[1], Lucie Canaff[1], Laetitia Laurent[2], Andrew C Karaplis[2], David Goltzman[1]. [1]Research Institute of the McGill University Health Centre, Canada, [2]Lady Davis Institute for Medical Research, Canada

Purpose: Parathyroid Hormone (PTH) acts via the type 1 PTH receptor (PTHR1). PTH-related protein (PTHrP), which plays a critical role in skeletal development, can act in a paracrine or autocrine mode either by also interacting with the PTHR1 receptor through its N-terminal domain, or independently of the receptor, in an intracrine fashion, through its nuclear localization sequence (NLS) and C-terminal region. In the present study, we aimed to compare the role of the N-terminal PTHR1-interacting domain relative to the NLS and C-terminus of PTHrP in modulating bone formation. Methods: To elucidate the role of PTHrP via PTHR1 in bone formation, we conditionally deleted Pthr1 and/or PthrP from cells of the osteoblast lineage in mice. We used mice with either a floxed Pthrp allele or Pthr1 allele and crossed them with either osteocalcin (OC)-Cre- positive or osterix(OSX)-Cre-positive mice to create conditional knockouts specific to mature osteoblasts (PthrpOB-/- and Pthr1OB-/-)or immature osteoblasts (Pthrpob-/- and Pthrpob-/-) respectively. Mice were then crossed to create double conditional knockouts of both Pthrp and Pthr1 in mature osteoblasts (PthrpOB-/-;Pthr1OB-/-) or immature osteoblasts (Pthrpob-/-;Pthr1ob-/-). Cre negative littermates or Cre+ mice without the floxed allele were used as controls for the conditional knockouts. Mice with global Pth deletion (Pth-/- mice) were derived as previously described. The skeletal phenotype of each strain was then analyzed in mice at 8 weeks of age. Growth curves, femoral bone mineral density (BMD), and femoral bone micro-architecture using micro-computed tomography (μCT) and serum biochemistry were evaluated. Results: Preliminary results show that Pthr1OB-/- mice were significantly smaller than their Cre- littermates and had significantly shorter femur lengths, and double knock-out PthrpOB-/-;Pthr1OB-/- mice were also smaller. In contrast, PthrpOB-/- mice displayed no significant difference in body weight, femur length, serum calcium or phosphorus, femoral BMD or μCT parameters and global Pth deletion did not alter the size and femur lengths of the Pth-/- mice. Pthrpob-/- mice, however, were smaller than controls. Conclusions: This work is currently ongoing to fully phenotype and elucidate the mechanism responsible for these phenotypes, however preliminary results suggest that the Pthrp ligand for Pthr1 in mature osteoblasts, may derive from less mature osteoblasts and act in a paracrine manner.

***Disclosures: Takeshi Shimoide**, None*

Posters

P-291

High susceptibility to collagen-induced arthritis in mice with progesterone receptors selectively inhibited in osteoprogenitor cells *Lixian Liu[1], Junjing Jia[1], Min Jiang[1], Xueping Liu[1], Chenlin Dai[1], Barton Wise[1], Nancy Lane[1], Wei Yao[1]. [1]University of California, Davis Medical Center, United States

Background. Progesterone receptor (PR) affects immunomodulation, and lack of PR in osteoprogenitor cells primarily affects pathways associated with immunomodulation, especially in the males. In this study, we selectively deleted PR from osteoprogenitor cells using Prx1-Cre to evaluate the tissue-specific effects of PR on inflammatory arthritis (IA). Methods. Collagen-induced arthritis (CIA) was used as an IA animal model, which we induced in PRΔPrx1 mice and their wild type (WT) littermates were immunized with collagen II (CII) emulsified incomplete Freund's adjuvant (CFA) in both sexes. Joint erosion, inflammation, and cartilage damages were assessed using a semiquantitative histologic scoring system. Bone volume and erosions in knee and ankle joints were quantitated using microCT. We found that knee and paw joint erosions developed in 37.5% and 41.7% of the WT and PRΔPrx1 female mice, respectively, and in 45.4 and 100%, respectively, of the male mice. Also, both knee and ankle joint inflammation scores, joint damage scores, and subchondral bone erosions were significantly more severe in male PRcKO mice than in male WT mice (figure). Although of lower severity than in male mice, female PRΔPrx1 mice also developed higher inflammation scores and bone erosions than the KO-normal or WT-CIA females. Immunohistochemistry staining of the NLRP3 inflammasome revealed the male PRΔPrx1 mice had significantly higher expression of NLRP3 inflammasome in the knee joints. Conclusion. Our observations indicate that the presence of PR in osteoprogenitor cells counteracts the development of collagen-induced arthritis and might help to explain the sex differences observed in human inflammatory arthritis.

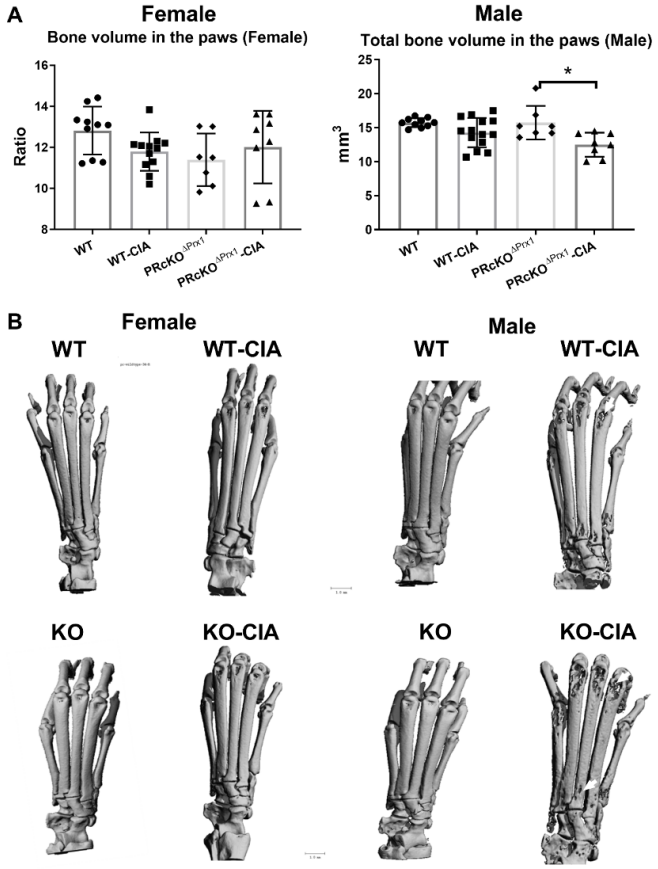

***Disclosures: Lixian Liu**, None*

P-292

Vitamin D and bone mineral density in Argentinian patients with multiple sclerosis: preliminar results of a pilot study *Maria Rosa Ulla[1], Carlos Vrech[2], Elena Peralta Lopez[3], Maria Jose Castro[1], Florencia Martos[1], Maria Angelica Rivoira[3]. [1]Fundacion ILAIM, Cordoba, Argentina, Argentina, [2]Sanatorio Allende, Argentina, [3]Facultad de Ciencias Medicas, UNC, Argentina

Multiple sclerosis (MS) is a chronic, inflammatory, autoimmune, demyelinating disease of the nervous system. Currently, relapsing-remitting multiple sclerosis (RRMS) is the most common type of the disease. These patients are frequently exposed to high doses of corticosteroids, thus having risk for secondary osteoporosis, frequently aggravated by restriction of mobility due to physical deficit, which can predispose to fractures and cause further deterioration in the quality of life. Recent statistics from Argentina have shown an increasing prevalence of 32 patients in every 100,000 inhabitants. Since there is no similar study in local literature so far, we aimed at assessing bone health and vitamin D levels in these patients. Materials and methods: Observational, prospective, open case-control study evaluating serum levels of 25(OH)vitamin D as well as bone mineral density (BMD) in femoral neck, total hip and lumbar spine, in self-reliant patients with RRMS, compared to healthy controls. Thirty-six patients with RRMS (8 men and 28 women) between 20 and 59 years of age and 36 healthy patients of similar age and sex were included. All the women were pre-menopausal. The patients had an Expanded Disability Status Scale less than 5.0 and all had received a corticosteroid pulse the year prior to bone densitometry. A survey of physical activity and dairy consumption was carried out. Results: RRMS patients had inferior serum 25(OH)vitamin D levels than controls (21.1+/-7,8 ng/mL vs 40,2+/-18.8 ng/mL, respectively; p<0.001). However, BMD (g/cm2) was almost the same in RRMS patients and controls in all the skeletal areas (Femoral neck: RRMS 0.802 vs 0.792 in controls; Total hip: RRMS 0.916 vs 0.921 in controls; Lumbar spine: RRMS 0.988 vs 0.970 in controls). Z-score BMD (expressed in media +/- standard deviation) was similar in both groups, as well (Femoral neck: RRMS -0.15 +/- 1.18 vs 0.14 +/- 0.93 in controls; Total hip: RRMS -0.11 +/- 1 vs -0.04 +/- 0.97 in controls; Lumbar spine: RRMS -0.28 +/- 1.16 vs 0.36 +/- 1.12 in controls). Consumption of dairy products was low but similar in both groups (500 mg Ca/day), whereas patients with RRMS practised physical activity more regularly. Conclusions: the inferior levels of vitamin D detected in patients with RRMS did not have a significant correlate on BMD, when compared with controls. This might be partially due to a more committed physical activity among RRMS patients. Bone parameters other than BMD remain to be studied.

***Disclosures: Maria Rosa Ulla**, None*

P-293

Gestational Bisphenol-A Exposure Negatively Impacts Trabecular Microarchitecture and Cortical Geometry in Male, but not Female, Adult Offspring *Rebecca Dirkes[1], Rebecca Welly[1], Jiude Mao[1], Jessica Kinkade[1], Victoria Vieira-Potter[1], Cheryl Rosenfeld[1], Pamela Bruzina[1]. [1]University of Missouri, Columbia, United States

Bisphenol-A (BPA) and bisphenol-S (BPS) are estrogen disruptors found in the environment and common household items. Estrogen is a primary hormonal regulator of bone growth and development; however, the impact of gestational BPA or BPS exposure on skeletal health of offspring remains unknown. In this longitudinal study, adult female mice were randomized into three groups: BPA exposure (BPA), BPS exposure (BPS) or control (CON). BPA/BPS/CON treatment continued through mating, gestation, and lactation. One male and one female offspring from each dam (n=6/group/sex) were selected and given ad lib access to a high-fat diet until 16 weeks of age, when body weight was measured and femora collected. Cortical geometry of the mid-diaphysis and trabecular microarchitecture of the distal femur were assessed via micro-computed tomography with a voxel size of 12 mm. Biomechanical strength of the femoral diaphysis was assessed via three-point bending. Two-factor ANOVA or ANCOVA with final body weight as a covariate were used to determine the effects of maternal BPA or BPS on trabecular and cortical bone outcomes, respectively. There were no group differences in body weight or femoral length in male or female offspring. There were no group differences in cortical geometry or trabecular microarchitecture in female offspring. Male offspring exposed to BPA had significantly lower trabecular bone volume, trabecular number, connectivity density and greater trabecular spacing compared to BPS or CON animals. Cortical thickness was also reduced in male offspring of BPA-treated dams. There were no group differences in biomechanical strength in male or female offspring. In conclusion, gestational BPA exposure significantly impairs trabecular microarchitecture and cortical geometry in male, but not female, adult offspring.

***Disclosures: Rebecca Dirkes**, None*

P-294

Genistein improves bone healing via estrogen receptor alpha-mediated activation and maturation of osteoblasts *Jui-Tai Chen[1], Yi-Ling Lin[1], Ruei-Ming Chen[1]. [1]Taipei Medical University, Taiwan, Province of China

Osteoporosis-associated fractures may cause higher risks or morbidity and mortality. Our previous study showed that genistein, a nonsterol phytoestrogen, could induce estrogen receptor alpha (ERα) expression and stimulate osteoblast mineralization. This study used rat calvarial osteoblasts and an animal bone defect as our experimental models to evaluate the effects of genistein on bone healing and its possible mechanisms. Exposure of rat calvarial osteoblasts to genistein caused a time-dependent increase in activity of alkaline phosphatase (ALP), a biomarker of osteoblasts, without affecting cell survival. Levels of cytosolic and nuclear ERα significantly increased following genistein treatment. Subsequently, treatment with genistein induced ALP mRNA and protein expressions in primary osteoblasts. Knocking-down ERα using RNA interference concurrently inhibited genistein-induced ALP mRNA expression. Moreover, genistein induced other osteogenesis-associated runt-related transcription factor 2 and osteocalcin mRNA and protein expressions. Attractively, administration of ICR mice suffering bone defects with genistein caused significant increases in the callus width, chondrocyte proliferation, and ALP synthesis. Results of micro-computed

tomography revealed that administration of genistein increased trabecular bone numbers and improved the bone thickness and volume. This study showed that genistein can improve bone healing via triggering ERα-mediated osteogenesis-associated gene expressions and subsequent osteoblast maturation.

***Disclosures: Jui-Tai Chen**, None*

P-295

Progesterone (Pg) and Medroxyprogesterone acetate (MPA) regulate same events with opposite actions in bone and vascular cells *Pablo Hernan Cutini[1], Adrián Esteban Campelo[2], Virginia Massheimer[1]. [1]Instituto de Ciencias Biológicas y Biomédicas del Sur (INBIOSUR), Universidad Nacional del Sur (UNS), Consejo Nacional de Investigaciones Científicas y Técnicas (CONICET), Bahía Blanca, Buenos Aires, Argentina., Argentina, [2]Instituto de Ciencias Biológicas y Biomédicas del Sur (INBIOSUR), Dpto. de Matemática, Universidad Nacional del Sur (UNS), Consejo Nacional de Investigaciones Científicas y Técnicas (CONICET), Bahía Blanca, Buenos Aires, Argentina., Argentina

Bone and cardiovascular diseases are multifactorial clinical entities that often coexist in postmenopausal women. Clinical and epidemiological studies have shown an interesting relationship between high bone turnover and cardiovascular disease mortality. Disorders in bone metabolism reversely correlate with vascular calcification (VCa). Hormone replacement therapy including natural Pg or synthetic progestins such as MPA emerged as a therapeutic option, although the risk/benefit of its use is controversial. VCa developed within atherosclerotic plaque is partly due to the osteogenic transdifferentiation of vascular smooth muscle cells (VSMC). The aim of this work was to investigate the effect of Pg and MPA on cellular/molecular events involved in VCa and in osteoblastogenesis. Primary cultures of calvarial osteoblasts (OB) and aortic VSMC, were in vitro exposed to 10 nM Pg or 10 nM MPA. Measurements of matrix extracellular calcium content and alkaline phosphatase (ALP) activity were employed as osteoblastic differentiation markers.In order to promote osteoblastic differentiation, VSMC were cultured for 21 days in osteogenic medium (10 mM β-glycerophosphate and 4 mM CaCl2). When VSMC were cultured in osteogenic medium (VSMC-OB), treatment with Pg for 21 days significantly reduced ALP activity (15% below control, $p<0.02$) and calcium content (32% below control, $p<0.02$). Similar treatment with the synthetic progestin also showed a significant reduction in ALP activity (239.9 +/- 21.0 vs. 159.6 +/- 19.1 x103 IU/mg protein, control vs MPA, $p<0.02$), as well as in the extracellular calcium deposition (365.1 +/- 38.2 vs 253.6 +/- 21.9 µg/mg protein, control vs MPA, $p<0.02$). Conversely, exposure of OB cells to Pg or MPA significantly increased ALP activity (59%; 290% above control, Pg; MPA, $p<0.02$) and matrix calcium levels (12%; 55% above control, Pg; MPA, $p<0.02$). The mechanism of action of Pg and MPA on both cells involves the participation of Pg receptor (PgR), since pre-treatment of cells with RU486, a PgR antagonist, completely reversed the hormonal action. However, we ruled out the involvement of the androgen receptor (AR), since in the presence of the AR antagonist flutamide, the effect of the progestogens was sustained. In conclusion, although Pg and MPA exert opposite effects on OB and VSMC-OB, both steroids would exhibit a potential beneficial effect by promoting osteoblastic differentiation and inhibiting VCa.

***Disclosures: Pablo Hernan Cutini**, None*

P-296

Mass spectrometry profiling of estrogens in bones derived from a rat model to identify potential targets for the prevention of postmenopausal osteoporosis *Tine Albrecht[1], Daniela Pemp[1], Sebastian Müller[2], Lukas Häfner[1], Günter Vollmer[2], Leane Lehmann[1]. [1]University of Würzburg, Germany, [2]University of Dresden, Germany

The impact of exogenous factors, as xenobiotics, on bone density and the risk of postmenopausal osteoporosis, is often tested using an animal model based on ovariectomy with or without additional oral exposure to the estrogen 17beta-estradiol (E2) to simulate the postmenopausal situation. Although it is well established that estrogens significantly contribute to the maintainance of the bone homeostasis, the estrogen profile in bone has not been determined in this model before.Thus, female mature Wistar-Hannover rats were either sham operated (sham group, n=18) or subjected to ovariectomy and were either fed a diet containing E2 benzoate (0.825 ppm to mimick menopausal estradiol levels; ovx+E2B group, n=15) or unsupplemented diet (ovx-E2B group, n=15) for 8 weeks. Then, the estrogen profile was analyzed in femur specimens by GC (estrone (E1), E2, 2- and 4-methoxy (MeO)-E1 and -E2) and UHPLC (E1-sulfate, E1-glucouronide), coupled with mass spectrometry and using deuterated internal reference standards for identification and quantification.Only E2, E1 and 2-MeO-E1 were detected and also quantified (E2 <16-124 fmol/g; E1 <16-104 fmol/g; 2-MeO-E1 <19-118 fmol/g). As expected, frequencies of detection of both E2 and E1 were significantly higher in bones derived from the sham group than from the ovx-E2B group ($p<0.05$, Fischer´s exact test). Frequency of detection of E2 did not differ between bones derived from ovariectomized animals with or without oral exposure to E2B. In contrast, frequencies of detection of E1 did not differ between bones derived from the sham and the ovx+E2B groups. Despite comparable levels of E1 were observed after in sham group and ovx+E2B group, 2-MeO-E1 was detected exclusively in specimens derived from the ovx+E2B group (27%). Since direct ingestion of 2-MeO-E1 was excluded (<0.05% of E2 benzoate), differences in biotransformation between endogenous and exogenously administered E2 seem to be reflected in the bone.In conclusion, the oxidative metabolite 2-MeO-E1 seems only be present above limit of detection in the bone under the conditions of the animal model. Ovariectomy decreases levels of E2 within the bone which cannot be recovered by oral exposure to 0.825 ppm E2 benzoate which instead seems to restore E1 levels. The characterization of the estrogen profile in the ovariectomized rat model, allows to understand and target the estrogen profile as a potential key factor related to changes in bone density.

***Disclosures: Tine Albrecht**, None*

P-297

In vivo effects of 1α25(OH)2D3-glycosides from Solanum glaucophyllum leaves in mice and skeletal muscle cells *Paula Irazoqui[1], Veronica Gonzalez Pardo[1], Claudia Buitrago[1], Kathrin Bühler[2], Ana Russo de Boland[1]. [1]Universidad Nacional del Sur-INBIOSUR, Argentina, [2]Herbonis Animal Health GmbH, Switzerland

We have previously shown that Solanum glaucophyllum leaves extract (SGE) enriched with 1a,25(OH)2D3-glucosides exhibits at least equal or greater effects on early myoblast differentiation as synthetic 1a,25(OH)2D3 thus being an effective substitute to promote muscle growth. Recently, we reported the effects of SGE compared to synthetic 1a,25(OH)2D3 in the regulation of mitogen activated protein kinases (MAPKs), genes involved on the differentiation of murine skeletal muscle cells C2C12, and their role on myotube formation. Since MAP kinase phosphatases (MKPs) deficiency impairs skeletal muscle regeneration and exacerbates muscular dystrophy, we further studied the effects of SGE on MKP1 and MKP5 which function to specifically dephosphorylate and inactivate MAPKs. SGE did not statistically modified MKP-1 and MKP-5 protein levels although basal changes were observed. MKP-1 protein levels remained unchanged at 1, 24 and 48 hours and decreased at 6 and 72 hours. MKP-5 protein levels increased at differentiation onset (24-72 h). We found that SGE significantly induced biphasic changes in phosphatase activity, decreased at 1 and 24 hours (which correlates with the pro-differentiation cell arrest previously reported), and increased at 6 hours. We also investigated the effects of SGE on Akt-mTOR signaling during the differentiation phase. SGE, decreased Akt phosphorylation after 5-day and increased its phosphorylation after 7-day of treatment. However, SGE did not induced changes in mTOR phosphorylation during time (3-7-day). Following with this approach, we investigated in vivo effects of SGE on skeletal muscle function in mice. Results from the first in vivo pilot test, have evidenced that 2 mg SGE/kg BW for 30 days did not show statically significant differences in phosphorus, calcium and glucose parameters from SGE groups compared to control. However, SGE leads to an increase in soleus muscle VDR protein expression in line with a significant decrease in 25(OH)D3 in blood serum while lower SGE doses did not change biochemical parameters measured in serum or protein content in mice muscle. These results contribute to elucidate the mechanism of action of the herbal active form of vitamin D when used as substitute to promote muscle growth

***Disclosures: Paula Irazoqui**, None*

P-298

Osteocyte Ca2+ Responses to in vivo Mechanical Loading in Mice Expressing Genetically Encoded Calcium Indicators with Different Sensitivities *James Boorman-Padgett[1], David Spray[2], Mia Thi[2], Jelena Basta-Pljakic[1], Karl Lewis[3], Robert Majeska[1], Mitchell Schaffler[1]. [1]City College of New York, United States, [2]Albert Einstein College of Medicine, United States, [3]Cornell University, United States

PURPOSE: Lewis+ in our laboratory recently reported the first ever studies using a genetically encoded calcium indicator (GECI) targeted to osteocytes (Ot) to measure Ca2+ responses to mechanical loading in vivo1. We discovered that increasing strain levels recruited more Ca2+ responding Ot following a well-defined response curve. These studies used an early GECI, GCaMP31. New GECIs, like GCaMP6f, have increased dynamic range and sensitivity compared to GCaMP32-4 but we do not know if Ot Ca2+responses in vivo are modified by the GECI used. Here, we examined how Ot Ca2+ responses to loading in vivo differ with GCaMP3 vs GCaMP6f. METHODS: Ot-targeted GCaMP3 or GCaMP6f mice were obtained from crossing DMP1-Cre with Ai38 or Ai95 mice, yielding OtGP3 and OtGP6 mice respectively [16-18 week old females, IACUC approved]. Under anesthesia, 3rd metatarsals (MT3) were cyclically loaded to strains between 250 and 3000 µstrain1. Multiphoton microscopy was used to visualize Ot fluorescence in the mid-diaphyseal cortex during loading. For each Ot, fluorescence intensity was measured (ImageJ) at baseline and during loading; cells >25% intensity increases were counted. Linear regression was used to model strain vs Ot responses.RESULTS: Within the physiological strain range (250-2000 µstrain), Ca2+ signaling Ot in both OtGP6 and OtGP3 mice rose monotonically ($r^2>0.9$ for both) (Fig). Signal intensity in OtGP6 was higher than OtGP3 cells, with ~twice as many responding Ot/strain level. Critically, loading-response curve slopes were equivalent (ANCOVA, $p>0.4$).DISCUSSION: OtGP6 mice show more Ot responding to a given mechanical strain level than OtGP3 mice consistent with higher fluorescence intensity reported in GCaMP6f. However, the Ot-loading-Ca2+ response curve slopes were equivalent, revealing that the recruitment relationship between Ca2+ responding Ot number vs strain magnitude is the same in both reporter systems, and thus represents a fundamental characteristic of the system. Finally, we note that linear extrapolation of the OtGP6 response curve

to the y-axis implies that ~40% of cells are responding at zero load, which was not what we observed. We speculate a different Ot response curve might exist for very low strain loading (dashed line, Fig) that can now be elucidated using the higher sensitivity of the GCaMP6f reporter.REFERENCES: 1) Lewis+ PNAS, 2017; 2) Chen+ Nature 2013; 3) Tian+ Nat Methods 2009; 4) Ohkura+ PLoS One 2012

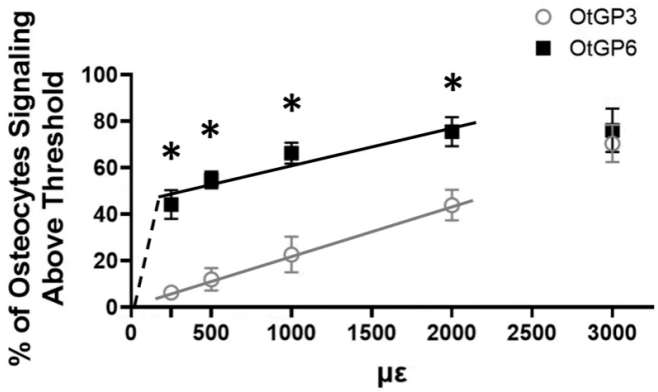

Figure: Ca^{2+} responding osteocytes in mechanically loaded MT3 *in vivo*. Data presented as mean ± sem. Asterisks indicates p<0.05 between OtGP3 and OtGP6 at a given strain level. Data shown as mean±SEM.

***Disclosures: James Boorman-Padgett**, None*

P-299

Unloading Induces Site-Specific Bone Loss in Cannabinoid Receptor 1 (CB1) Deficient Mice *Rachel DeNapoli[1], Aron Lichtman[1], Henry J. Donahue[1]. [1]Virginia Commonwealth University, United States

The endocannabinoid system (eCBS) plays an important role in postnatal bone metabolism. Preliminary results from our laboratory suggest that male C57BL/6J CB1 receptor (CB1KO) mice show increased sensitivity to age-related epiphyseal bone loss compared to wild type (WT).Age-related bone loss shares many traits with unloading-induced bone loss; however, the role of CB1 receptor expression in unloading-induced bone loss has not been examined. Therefore, we tested the hypothesis that CB1KO mice are more sensitive to unloading-induced bone loss than WT littermates.All animal procedures were conducted with approval of Virginia Commonwealth University IACUC. Adult 20-week-old male C57BL/6J WT mice (n=11) and constitutive global CB1KO mice (n=8) were placed in casts to immobilize the left hindlimb. The right hindlimb was used as a contralateral control. After 21 days of immobilization, mice were sacrificed, and femurs harvested. The skeletal phenotype was assessed using ex vivomicro-CT scans (Bruker Skyscan 1172; 8.9 um). Cortical bone at the diaphysis and cancellous bone at epiphyseal and metaphyseal regions were analyzed by standard micro-CT methodology. Data were compared using repeated measures 2-way ANOVA ($p<0.05$).At femoral diaphyseal bone sites, there were no differences in micro-architecture endpoints between male WT and CB1KO limbs after three weeks of immobilization. Unloading induced femoral epiphyseal bone loss in both WT and CB1KO mice. However, at femoral metaphyseal bone sites,unloading significantly decreased femoral metaphyseal BV/TV, Tb.N, and Tb.Th and increased Tb.Sp in CB1KO males, but not in WT males (Figure 1). These data indicate that male CB1KO mice are more sensitive, relative to WT mice, to unloading induced trabecular bone loss at metaphyseal bone sites.This study demonstrates that CB1 receptor expression protects against bone loss from unloading. Therefore, activating the CB1 receptor may represent a potential therapeutic target for disuse and age-related bone loss.

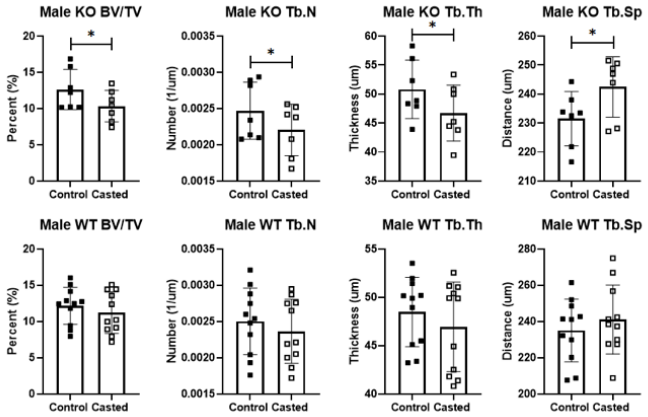

***Disclosures: Rachel DeNapoli**, None*

P-300

NaQuinate: A drug that Selectively Synergizes with Mechanical Loading Stimuli In Vivo to Generate Greater Cortical Bone Mass and Architectural Modifications *Behzad Javaheri[1], Amy Lock[1], Robin Soper[2], Alan Boyde[3], Ruby Chang[1], Stephen Hodges[1], Andrew Pitsillides[1]. [1]Royal Veterinary College, United Kingdom, [2]Haoma Medica Ltd, United Kingdom, [3]Queen Mary's College, United Kingdom

Background: Response to applied mechanical loading is pivotal in the generation of bone mass and architecture sufficient to withstand habitual use and resist fracture. We have previously found that NaQuinate, a naphthoquinone carboxylic acid, contributes to maintaining bone quality and quantity in rat and mouse ovariectomy models of rapid bone loss. Herein, NaQuinate's ability to alter mechanoadaptive response in cortical and trabecular tibial bone following mechanical loading has been investigated.Methods: Female 12wk-old C57/Bl6 mice (n=8/group) were randomly allocated to two groups, receiving either NaQuinate (750 µg/Kg/day) or vehicle 5d/wk over 3 wks. On three alternate days in the last 2wks, the right tibia of all mice was subjected to non-invasive, dynamic axial loading (12N, 40cycles/day, 2Hz, with 10s rest periods between cycles), with the left serving as non-loaded contralateral control. Three days after the last load episode, tibiae were removed and scanned by high-resolution micro-CT (5um) for measurement of traditional indices of bone mass and architecture in defined trabecular regions and along the whole of the cortex. A linear mixed effects model followed by Fisher's least significant difference post-test was used for statistical analysisResults: Comparison of non-loaded tibiae in the two groups showed small, significant NaQuinate-related increases in cross-sectional area (CSA) at restricted midshaft and tibio-fibular junction locations (Fig 1A/C). NaQuinate markedly enhanced mechanoadaptive cortical responses, generating significantly greater load-related increases in CSA, thickness and J score across extensive proximal tibia regions (Fig. 1B/D); revealing clear synergy, with increases in CSA and J significantly greater than their distinct additive effects (Fig 1E). NaQuinate treatment also amplifies load-related increases in trabecular thickness and generates more vertically-orientated trabeculae when compared to load alone; which was not evident in contralateral tibiaeConclusions: These data reveal that NaQuinate significantly interacts with mechanical loading in the trabecular compartment and targeted cortical bone regions. This constructive interaction between NaQuinate and mechanical loading indicates functional utilisation of bones' mechanostat in the regulation of bone mass and architecture and supports the notion that NaQuinate treatment can provide a novel therapeutic approach to skeletal disorders such as osteoporosis.

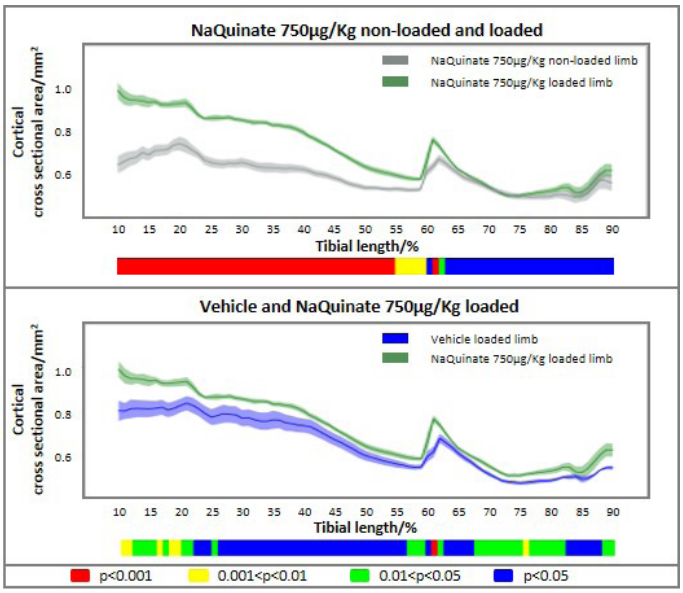

***Disclosures: Behzad Javaheri**, None*

P-301

β-catenin and Cx43 Interact to Mediate the Effect of Mechanical Signals on Osteocytes *Yue Zhang[1], Caleb Ryan[1], Henry Donahue[1]. [1]Virginia Commonwealth University, United States

Introduction: Gap junctions (GJ) play a key role in mechanotransduction in bone. Osteoblast- and osteocyte-selective Cx43 deficient mice have effects in response to mechanical load and unloading in vivo [1, 2]. However, the mechanism is unknown. Osteocytes are the cells sense and communicate to bone effector cells, osteoblasts and osteoclasts. The WNT/β-catenin pathway has been shown to be integral to bone response to mechanical signals [3]. There is also evidence that suggests β-catenin interacts with Cx43 [4]. In this study, we examined the hypothesis that Cx43 regulates osteocytic cell response to fluid flow through a β-catenin dependent mechanism.Materials and Methods: OCY454 cells were cultured at 33°C for 3 days, then differentiated at 37°C for 12 more days. Differentiated wild type (WT) OCY454 cells were lysed, incubated with Phospho- or Non-phospho- β-catenin antibodies, precipitated, and subjected to western blot analyses with Cx43 antibody. Mouse osteocytic OCY454 cells had the Cx43 gene deleted using Crispr/Cas9. Western blotting and a parachute assay were used to verify deletion and gap junctional communication (GJC). A Topflash, was used to quantify β-catenin mediated transcription. A Fobflash, a mutated Topflash, was used as a control. WT and Cx43 deficient cells were both co-transfected with Topflash or Fobflash, and TK-Renilla for 48 hours. Cells were then exposed to oscillating fluid flow (10dyns/cm2 at 1Hz) for 2 hours. After 2 hours later, cells were collected for dual luciferase assay. Relative luciferase activity for both WT and Cx43 KO cells was calculated as (TopFlow-FobFlow)/(TopCtrl-FobCtrl).Results and Discussion: Cx43 KO cells displayed reduced Cx43 protein expression and GJC relative to WT cells. Co-IP results showed that non-phosporylated β-catenin (active form) co-precipitated with Cx43 but not the phosphorylated form (Fig 1). These data suggest that in osteocytes, Cx43 directly binds with the active form of β-catenin, reducing its availability for nuclear translocation. Exposure to fluid flow significantly increased luciferase activity to a greater degree in osteocytic Cx43 KO cells compared to WT cells (Fig 2). This suggests that fluid flow activates β-catenin mediated nuclear translocation and gene transcription to a greater degree in Cx43 KO relative to WT cells. Taken together, these results suggest that Cx43 binds activated β-catenin and that in Cx43 KO cells there is more β-catenin available in response to mechanical signals. This at least partly explains the increased anabolic response to mechanical load in Cx43 deficient mice.Conclusions: Our results decreasing Cx43 expression has a strong potential to enhance the anabolic response of bone to mechanical load.Acknowledgements: This research was funded by the NIH 9R01AR068132-120.References: 1. Zhang Y PLOS 2011. 2. Lloyd SA JBMR 2012. 3. Kang KS. Front Endocrinol 2006. 4. Wu JC. JBC 2013.

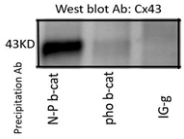

Figure 1. Cx43 Co-IP with non-phospho β-catenin.

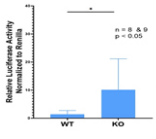

Figure 2. Relative luciferase activity of WT and Cx43 KO OCY454 cells after exposure to fluid flow.

***Disclosures: Yue Zhang**, None*

P-302

Skeletal disuse from unilateral hindlimb immobilization decreases the formation of osteocyte plasma membrane disruptions (PMD) and causes cortical bone loss *Anik Tuladhar[1], Mackenzie Hagan[1], Kanglun Yu[1], Mohamed Awad[1], Emily Parker[1], Mark Hamrick[1], Meghan McGee-Lawrence[2]. [1]Augusta University, United States, [2]Medical College of Georgia, Augusta University, United States

Disuse (such as from spaceflight) leads to bone loss, and better strategies to maintain bone health in astronauts during weightlessness and upon return to gravitational forces are needed. Therapeutic approaches to enhance musculoskeletal mechanosensitivity would address this need, but a critical barrier to designing such an intervention is that the mechanosensing osteocytes in bone cannot be properly targeted because the physical mechanism of load sensation by osteocytes is not fully understood; most osteocyte mechanosensation mechanisms observed in vitro have failed to fully explain bone's ability to detect and adapt to loading in vivo. We and others have recently reported that osteocytes utilize plasma membrane disruptions (PMD) as a mechanism to sense mechanical loads and initiate mechanotransduction cascades which direct subsequent bone adaptation, and that this mechanism functions in osteocytes both in vitro and in vivo. Importantly, we consistently observe that ~20% of long bone osteocytes develop PMD with routine cage activity in mice, suggesting that formation of osteocyte PMD may be essential to bone's sensation of and response to normal gravitational loads. Accordingly, the goal of this study was to test the effects of disuse on osteocyte PMD formation. Twenty female CD-1 mice (11 weeks old) were subjected to unilateral hind-limb immobilization for two weeks. Left limbs were casted using gauze and tape and right limbs were left untreated as loaded controls. Ten mice were sacrificed two weeks after cast application, five were remobilized for 24 hours prior to sacrifice, and another five were remobilized for 72 hours prior to sacrifice. MicroCT analyses showed significant decreases in cortical bone thickness and area of the femur following two weeks of immobilization. Histological detection of intracellular albumin staining in tibial osteocytes, indicative of PMD formation, showed significantly fewer PMD-labeled osteocytes in the immobilized left limb as compared to the control right limb (-74%, p=0.017). Mice remobilized for 24 hours also showed significantly fewer PMD in the immobilized limb, whereas following 72 hours of remobilization there were no differences between the immobilized and control limbs. These data suggest skeletal disuse results in decreased osteocyte PMD formation, contributing to blunted mechanotransduction and bone loss; these results further support the importance of osteocyte PMD formation in skeletal mechanobiology.

***Disclosures: Anik Tuladhar**, None*

P-303

NF-κB activation is required for mechanoresponsive nerve growth factor expression in osteoblasts *Ibtesam Rajpar[1], Ryan Tomlinson[1]. [1]Thomas Jefferson University, United States

In response to physiological loads, osteoblasts actively synthesize new bone tissue at the sites of highest mechanical strain. Recent studies have shown that mechanical loading induces nerve growth factor (NGF) expression in mature osteoblasts, which subsequently signals through TrkA receptors on resident sensory nerves to support load-induced bone formation. In this study, we sought to determine whether the NF-κB signaling pathway modulates NGF expression and the resultant bone formation in response to loading. First, we assessed the time course of NGF expression following load in vitro. Monolayer cultures of the pre-osteoblastic MC3T3 cell line were subjected to fluid shear stress using a previously developed microfluidics fluid flow device. Triplicate wells were loaded at 1 mL/min for 10, 15, 30, or 60 minutes. Significant increases in NGF gene expression were observed at 30 (+1.5 fold) and 60 minutes (+2.2 fold) of load as compared to non-loaded controls. To assess the requirement for NF-κB in NGF expression by osteoblasts in vitro, culture media was supplemented with the NF-κB inhibitors BAY-11-7082 or pyrrolidine dithiocarbamate (PDTC), or DMSO (vehicle control), starting 60 minutes before loading. NGF gene expression and protein level was analyzed using qRT-PCR and ELISA, and an NF-κB reporter assay was used to determine the extent of NF-κB inhibition. As compared to vehicle controls, a significant reduction of NGF expression and NF-κB subunits was observed in response to both inhibitors. These results suggested that NF-κB may be required for NGF expression and the ensuing anabolic load-response in adult bones. To test this hypothesis, adult mice expressing a dominant negative IkB kinase under the control of a Col1a1 promoter (Col1a1.IKK-DN) were subjected to three bouts of axial forelimb compression (3 N, 100 cycles, 2 Hz rest-inserted) over three consecutive days. Surprisingly, our preliminary results indicate no significant differences between Col1a1.IKK-DN mice and wildtype littermate controls in load-induced bone formation (Figure), suggesting a complex role of mechanoresponsive pathways under the control of NF-κB signaling as well as potential compensation for the constitutive loss of IkB kinase activity. In conclusion, our study reveals new understanding of the regulation of NGF-TrkA signaling in bone, which may enable new therapeutic options for diseases of low bone mass and inform the development of anti-NGF antibodies for pain relief.

Posters

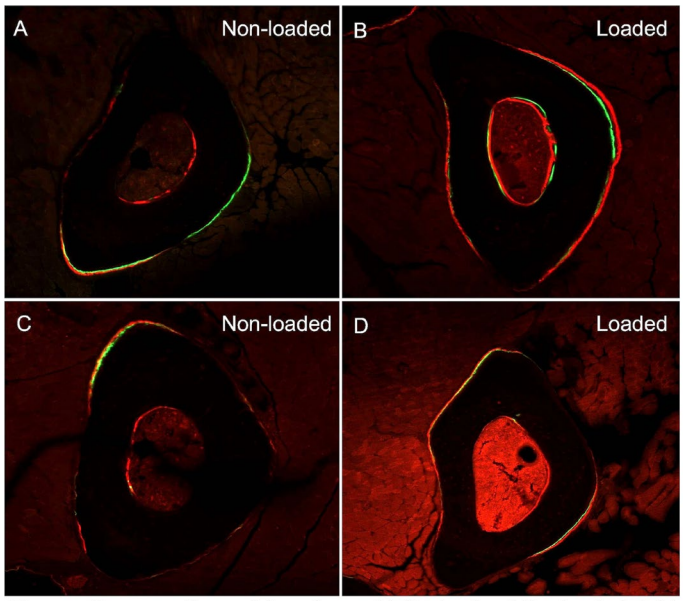

Figure: Cross-sections of the ulnar mid-diaphysis of the loaded right and contralateral (non-loaded) forelimbs in Col1a1.IKK-DN (A,B) and WT (C,D) mice. Increased mineralized surface and mineral apposition is depicted on the medial surface in loaded limbs by Alizarin Red S labeling.

***Disclosures: Ibtesam Rajpar**, None*

P-304

Evidence for site-specific mechanoregulation of osteocyte perilacunar/canalicular remodeling *Courtney Mazur[1], Tamara Alliston[1]. [1]University of California, San Francisco, United States

Together, bone mass and bone quality determine bone strength. Bone quality metrics such as modulus, ultimate stress, and mineralization are improved by treadmill running or axial loading protocols in mice, but the cellular mechanisms linking applied loads to changes in quality parameters have not been identified. Osteocyte perilacunar/canalicular remodeling (PLR), which involves changes in gene expression, lacunar and canalicular geometry, and matrix mineralization, regulates bone quality. While others have investigated the effect of unloading on lacunar area, the effect of applied load on PLR is not understood. Therefore we sought to study the effect of load on the canalicular network and the genes involved in shaping it.We applied axial compressive load to the tibia of 8-week-old male mice (600 cycles/day, 1 Hz, 700-1200 με peak) and compared loaded and contralateral non-loaded limbs. PLR outcomes were assessed in the proximal and distal tibia by blinded histologic analysis of canalicular length (10 days after three loading sessions) and by mRNA analysis of 8 acidification and proteolysis genes implicated in PLR using a custom Nanostring array (24 hrs post-load). Loading caused the expected repression of SOST (immunofluorescence, n=9, $p<0.05$) and the expected induction of Akt phosphorylation (Western, n=6, $p<0.01$) and bone formation (dynamic histomorphometry, MS/BS, MAR, BFR, n=6-7, $p<0.02$). In the proximal tibia, this loading regimen increased canalicular length in 5 of 6 analyzed mice by an average of 20%, a difference approaching significance (n=6, p=0.058, 3 mice await analysis). Likewise, loading significantly induced Atp6v0d2 mRNA levels in the proximal tibia (n=6, $p<0.05$), with induction trends for 5 other PLR genes and the Nanostring gene signature score. Parallel analysis of the distal tibia reveals site-specificity, such that no changes in PLR gene expression were observed in this region. Site-specific regulation of TGFβ signaling provides one potential explanation, as we observed load-induced upregulation of TβRI and TβRII only in the proximal bone and repression of the TGFβ-responsive gene Serpine1 only in the distal tibia (n=6, $p<0.05$).Load-induced PLR gene expression in the proximal tibia and accompanying trends in canalicular length suggest that osteocyte PLR may be mechanosensitive and spatially regulated. This result would indicate a role for osteocytes in mechanoregulation of bone quality in addition to bone mass.

***Disclosures: Courtney Mazur**, None*

P-305

Regulation of Piezo1 in Osteoblasts using Ultrasonic Acoustic Radiation Force *Guangdao Zhang[1], Sophie Li[1], Lin Wu[2], Yi-Xian Qin[1]. [1]Stony Brook University, United States, [2]Chinese Medical University, China

Mechanical stimulation has shown promising in bone adaptation, promoting bone formation, and enhancing healing. Piezo1 is proposed as a mechanotransducer in the regulation of cellular response to external loading. As an effective noninvasive method, acoustic radiation force (ARF) elevated by the low-intensity pulsed ultrasound (LIPUS), has been used to promote bone regeneration and fracture healing. We hypothesize that Piezo1, a mechanosensitive ion channel, could transduce ultrasound associated mechanical signals and activate downstream signaling processes. The goal of this study was to evaluate the role of Piezo1 in mouse MC3T3-E1 osteoblastic cells during ARF stimulation. We investigated the Piezo1 expression and localization, cell migration, intracellular calcium oscillations, perinuclear F-actin, and the kinases 1/2 (ERK1/2) signaling in MC3T3-E1 cells and shRNA-Piezo1 knockdown cells, respectively. The results indicated Piezo1 protein was highly expressed in the MC3T3-E1 osteoblastic cells, and mainly localized on the plasma membrane and nucleus. Piezo1 could be knocked down by shRNA transfection. The relative expression of Piezo1 after knocked down was only 0.123 +/- 0.025, which was significantly lower than 0.679 +/- 0.066 in the control cells ($p<0.01$) (Fig. 1A). The cell migration and proliferation results showed that cell-covered area of MC3T3-E1 cells was 45.91 +/- 2.29%, which was significantly higher than the shRNA-Piezo1 cells (32.82 +/- 1.79%, $p<0.01$) at 4 hours after LIPUS stimulation. he fluorescence intensities of the intracellular calcium of MC3T3-E1 cells significantly increased and several calcium spikes have been observed during ARF stimulation, and the F-actin was also found to immediately accumulate at the perinuclear region after LIPUS stimulation (Fig. 1B), which persistently existed until 5-min and returned to its initial level at 30-min. Corresponding to these findings, the protein expression of ERK1/2 after the ARF stimulation found significantly increased from 0.483 +/- 0.069 to 0.975 +/- 0.026 (p0.05) in sh-RNA Piezo1 cells. In conclusion, Piezo1 in MC3T3-E1 osteoblastic cells could transduce ARF associated mechanical signals into intracellular calcium, and the influx of calcium acts as the second messenger in activating ERK1/2 phosphorylation and polymerization of perinuclear F-actin. ARF has the potential to regulate Piezo1 channel and promote osteogenesis.

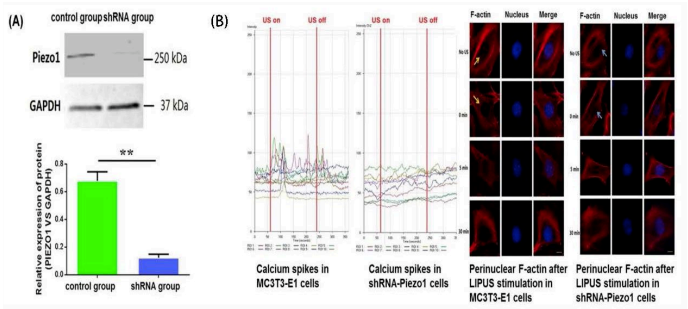

Fig. 1 A. Expression of Piezo1 protein on MC3T3-E1 cells and shRNA-Piezo1 cells. Knock off Piezo1 using shRNA significantly reduces the expression. B. The changes of intracellular calcium intensity and perinuclear F-actin after ARF stimulation.

***Disclosures: Guangdao Zhang**, None*

P-306

Fluid Shear Stress Rapidly Activates TGFβ Family Signaling in Osteocytes *David Monteiro[1], Neha Dole[1], Serra Kaya[1], Luke Campos[1], Cassandra Belair[1], Tamara Alliston[1]. [1]University of California, San Francisco, United States

Bone is a dynamic tissue that constantly adapts to changing mechanical demands. The transforming growth factor beta (TGFβ) pathway plays several important roles in maintaining skeletal homeostasis by coupling the bone-forming and bone-resorbing activities of osteoblasts and osteoclasts and participating in the anabolic response of bone to applied loads. However, the extent to which osteocytic TGFβ signaling is directly regulated by fluid shear stress (FSS) is unknown, despite work suggesting that fluid flow along canaliculi is a major physical cue sensed by osteocytes following bone compression. To investigate the effects of FSS on TGFβ signaling in osteocytes, we stimulated OCY454 cells grown within a microfluidic platform with FSS.Using this system, we found that OCY454 cells rapidly respond to 0.1 Pa FSS with increases in cytosolic Ca2+, Akt phosphorylation, and Ptgs2 expression. Furthermore, this FSS regimen induces Smad2/3 phosphorylation and nuclear translocation within 30 minutes, even in the absence of added TGFβ. In fact, the dynamics of TGFβ signaling by FSS were comparable to treatment with 5 ng/mL TGFβ ligand. However, relative to TGFβ, FSS induced a larger increase in levels of pSmad2/3 and TGFβ target gene Serpine1, which was upregulated 60-fold by FSS compared to 6-fold by TGFβ after 2 hours. The striking effect of FSS stimulation on TGFβ signaling was further augmented when cells were concurrently treated with TGFβ ligand, suggesting that FSS-mediated activation of latent TGFβ is insufficient to explain this enhancement.A closer investigation into the pSmad bands seen by Western blotting revealed subtle differences in the effects of FSS stimulation and treatment with TGFβ that we found to be consistent with concurrent activation of TGFβ and BMP pathways by FSS. While pretreatment with the TGFβ receptor type I inhibitor SB-431542 blocked Smad phosphorylation by TGFβ, it only partly attenuated its induction by FSS. RNA sequencing analysis revealed many biological pathways targeted by FSS, including TGFβ, that remained significantly upregulated even in the presence of SB-431542, suggesting that the effects of FSS on TGFβ signaling occur through TβRI-dependent and -independent mechanisms.Overall, these results show that FSS rapidly enhances Smad signaling through multiple arms of the TGFβ signaling pathway by activating several

distinct subsets of TGFβ type I receptors, implicating both TGFβ and BMP pathways in the osteocytic response to FSS.

***Disclosures: David Monteiro**, None*

P-307

Substrate surface characteristics are transduced through a β-catenin mediated mechanism initiated by focal adhesion turnover and maturation

*Otto Juhl[1], Anna-Blessing Merife [1], Yue Zhang[1], Christopher Lemmon[1], Henry Donahue[2]. [1]Virginia Commonwealth University, United States, [2]Virginia Commonwealth University, United States

The mechanism by which osteoblast precursors and osteoblasts transduce the various substrate surface characteristics associated with bone implants is largely unknown. This lack of understanding makes the design and implementation of implants difficult, especially in diseases such as osteopenia, where bone formation is decreased thus limiting implant osteointegration.In this study, hFOB 1.19 cells, a preosteoblastic cell line, cultured on either tissue culture polystyrene (TCPS) or a pro-osteogenic substrate (POS) were examined for both enzymatic alkaline phosphatase (AP) activity and expression of key osteoblastic genes. In addition, changes in focal adhesion formation and maturation as well as localization and transcriptional activity of b-catenin on either TCPS or POS were assessed. b-catenin binding to TCF/LEF was then inhibited using PNU-74564 in cells on either TCPS or pro-osteogenic substrate. The effect of b-catenin inhibition on osteoblastic differentiation was then evaluated. Significance was considered as values of $p < 0.05$ for all studies.Cells cultured on the POS displayed a significant 2.5 fold increase in AP activity compared to cells cultured on TCPS. Moreover, there was a significant increase in all genes associated with increased osteoblastic differentiation after 7 days in cells cultured on the POS. Focal adhesion turnover and maturation increased from 24-48 hours after seeding to a greater degree in cells on POS relative to cells on TCPS. Interestingly, b-catenin translocation from the membrane to the nucleus and transcriptional activity in cells cultured on POS was greater and more rapid (approximately 24 hours prior) than in cells cultured on TCPS. These variations also coincided with the observed changes in focal adhesion turnover and maturation. Inhibition of b-catenin binding to TCF/LEF also inhibited the increased osteoblastic differentiation in cells cultured on POS such that there was no significant difference in AP activity between cells cultured on TCPS and the POS.These data suggest that substrate surface characteristics may be transduced by a focal adhesion mediated mechanism by which b-catenin translocation acts as a messenger molecule to regulate osteoblastic differentiation. Moreover, inhibition of b-catenin binding to TCF/LEF prevents the upregulation of osteoblastic differentiation associated with POS.

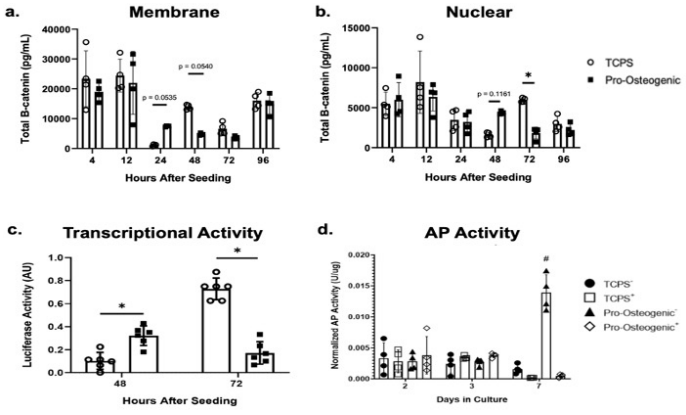

***Disclosures: Otto Juhl**, None*

P-308

A Novel Method for Associating Local Strain and Mineral Formation in Applications of Bone Tissue Engineering

*Julia K. Griesbach[1], Gian N. Schädli[1], Graeme R. Paul[1], Ralph Müller[1], Marina Rubert[1]. [1]Institute for Biomechanics, ETH Zurich, Switzerland

Dynamic mechanical loading increases bone formation both in vitro and in vivo. While micro-CT and micro-FE have shown a relationship linking bone formation, resorption and mechanical environment in vivo, current methods have several limitations. In the Schulte method, the association of multiple strain values to single formation voxels on concave surfaces leads to inaccurate remodeling probability predictions. We have therefore developed and validated a novel surface strain dilation (SSD) method for accurate association of local mechanical stimuli to mineral formation in tissue engineered bone.A remodeling image, obtained through registering and superimposing time-lapsed images, and local strains serve as input. Strain and formation are associated by dilating the surface strain onto the formation. The iterative layer-by-layer extrapolating of the surface data prevents original data distortion (Fig. 1b). Artificial validation images were created representing bone formation on uneven surfaces or multiple layers of formation (Fig. 1c, d) to compare the accuracy of the Schulte and SSD method (Fig. 1a). For real life comparison, cell-seeded scaffolds (n=6) were cultured in compression bioreactors. Cyclic loading was executed 3x/week using 3% strain at 5Hz for 5min. Time-lapsed micro-CT was performed weekly. Images were registered, superimposed and converted to Young's moduli for subsequent micro-FE to compare the two methods using area under the curve of the Receiver Operating Curve (AUC-ROC) scores and probability of formation.SSD showed the same amount of formation voxels for both validation images as the ground truth (c: 32, d: 56) while the Schulte method deviated vastly (c: 72, d: 36). Results from the in vitro study showed SSD to be accurate while the Schulte method showed an average absolute deviation of 108.9% (Fig. 1e). The AUC-ROC score of SSD was substantially better (0.65) than that of the Schulte method (0.54). The resulting probability plots for formation showed different behavior (Fig. 1f).We have developed and validated a novel algorithm that allows more accurate association of local strain and formation for uneven surfaces and large amounts of formation, facilitating the investigation of mechano-regulation for bone tissue engineering applications. This can lead to new insights in mechanical and geometrical design parameters of engineered bone scaffolds.

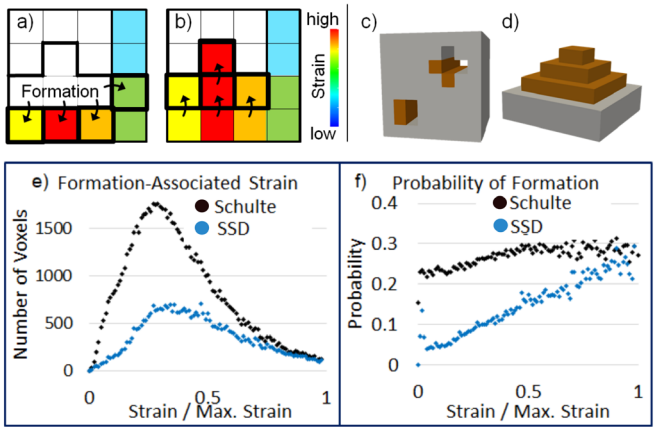

Fig. 1: Association formation and strain values for a) Schulte method, b) SSD method; validation images (quiescent: grey, formation: orange): c) concave surface, d) multiple formation layers; e) Histogram for formation-strain-association for both methods; f) probability of formation for a surface voxel dependent on its strain.

***Disclosures: Julia K. Griesbach**, None*

P-309

3D physiological load estimation based on time-lapsed HR-pQCT images

*Matthias Walle[1], Francisco C. Marques[1], Nicholas Ohs[1], Ralph Müller[1], Caitlyn J. Collins[1]. [1]Institute for Biomechanics, ETH Zurich, Switzerland

Pathological bone morphology observed in patients with type II diabetes mellitus T2DM may indicate changes in cell mechanosensation. Computational models for the characterization of tissue- and cell-level biomechanical properties of bone may be used to investigate such changes, if physiological-mechanical loads can be estimated correctly. However, existing estimation approaches only perform moderately with HR-pQCT data as input. Here, we present a novel approach to improve estimation based on mechanoregulation principles and provide validation using bone geometries from micro-CT images adapted via a micro-structural in silico bone adaptation simulation with a highly controlled mechanical environment. Adaptation to six different target loading conditions (Figure B; Funit=1N, and Munit=1N/mm; α=150) were simulated for patients (n=3) using a model of homeostatic, load adaptive remodeling. Tissue was remodeled using a strain energy density (SED) dependent velocity of +/-8000 µm/year/MPa and a maximum velocity of +/-12 µm/month in regions where SED exceeded average tissue load (0.02 MPa) by +/-2%. From each simulation, six consecutive remodeling steps were selected to include several phases of the adaptation process. The implemented load estimation algorithms were based on independently scaling six unit loads (Figure C) with scaling factors α, until a target tissue load was found. The implemented mechanoregulation-based algorithm (MR), maximized SED in regions of bone formation, while minimizing SED in regions where bone was resorbed. The results were compared to a previously published morphology-based load estimation algorithm (MO), where a homogeneous target load of 0.02 MPa was assumed.MR recovered all load compositions uniquely without bias from initial conditions (Figure A). In comparison, MO was unable to recover simulated loads, resulting in a mixed-load prediction. MR-derived load magnitudes showed acceptable mean differences (+1.07+/-20.30%) to αtarget=150, and were underestimated by MO (-77.05+/-7.30%). Furthermore, mechanoregulation analysis showed that MR derived loading patterns explained 62.67+/-3.40% of remodeling events, while MO explained only 50.61+/-0.70%. These preliminary results indicate that using an MR-based criterion increases accuracy of the estimated loads. In the future, this algorithm may be used to better explore load patterns in patient cohorts furthering our understanding of mechanoregulation in osteo-degenerative diseases such as T2DM.

Posters

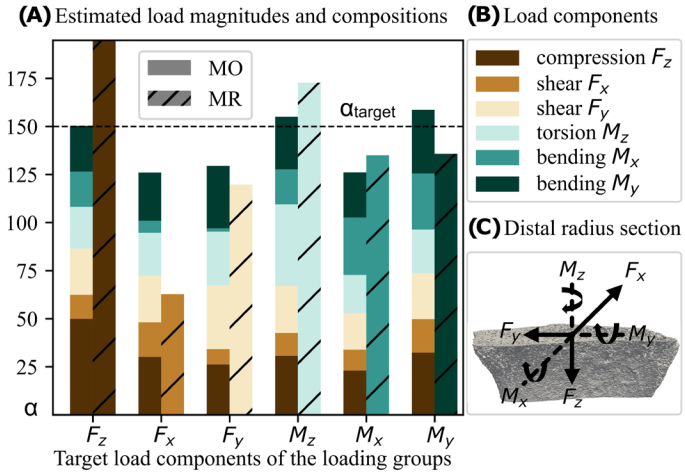

***Disclosures: Matthias Walle**, None*

P-310

Improved Initialisation of a Multiscale in Silico Model of Trabecular Bone Remodelling Using in Vivo Murine Data *Daniele Boaretti[1], Lara Zamboni[1], Duncan Tourolle[1], Ralph Müller[1]. [1]Institute for Biomechanics, ETH Zurich, Zurich, Switzerland, Switzerland

An improved understanding of bone as a mechanobiological system will accelerate the development of treatments for bone related diseases. Current in silico models of bone lack either the spatial fidelity to represent the bone microarchitecture or disregard the complex physiological pathways within the bone. While in vivo micro-CT images allow the use of real bone structures as a basis for such models, it is not possible to determine the spatial distribution of biomolecules and cells from these scans. The largest issue in applying in silico models of bone remodeling is the initialization of the simulations employing experimental data. This makes it very difficult to initialize such models with good estimates of these distributions. Here, we present a novel initialization approach using strain-specific cell seeding and a 1-dimensional (1D) model to determine cell population sizes and molecular concentrations a priori. These results are used to initialize a larger 3D coupled in silico model for trabecular bone remodeling.The governing equations of the in silico model were discretized into a 1D model composed of a set of ordinary differential equations (ODEs). Models were generated using micro-CT scans of mouse caudal vertebrae. The 1D model was used to compute the initial concentration and receptor occupation of a cell. In the 3D model, cells were seeded according to the local mechanical environment, with osteoblasts (OBLs) in areas of higher strain and osteoclasts in areas of lower strain. We were particularly interested in the low-density lipoprotein receptor-related protein 6 (LRP6) receptor occupancy of OBLs and lining cells (LCs).The simulations with the 1D and 3D models show a very similar trend for LRP6 receptor occupancy for both OBLs and LCs (Fig.1, left). OBLs display a smaller range of free LRP6 receptors when compared to LCs for the 3D simulation. Where OBLs can be found on surfaces with high effective strain and have higher free LRP6 receptors, LCs can be found mostly on surfaces with low effective strain and have lower free LRP6 receptors at the end of the simulation in the 3D model (Fig.1, right).The presented method demonstrates how bone remodeling simulations can be initialized with appropriate biochemical concentrations and cell distributions. Such an approach can the current models of health and disease. This will facilitate investigation of population dynamics and the initialization of model agents involved in other signaling pathways.

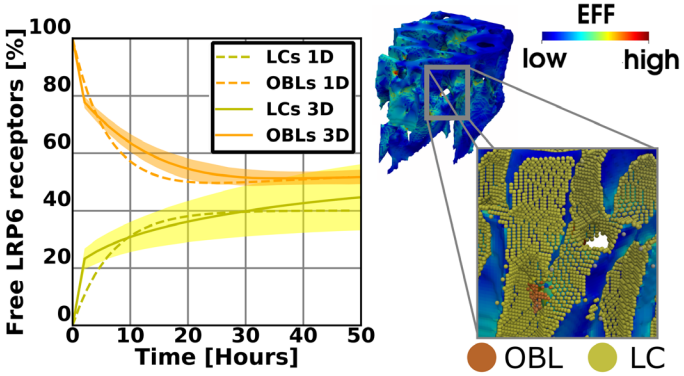

Figure 1 (Left): The predicted mean±3SD of free LRP6 receptors for OBLs and LCs for the 3D multiscale and the 1D ODE model, respectively. (Right) Upper part of the trabecular bone at the end of the 3D simulation. OBLs and LCs are shown with dark orange and dark yellow, respectively.

***Disclosures: Daniele Boaretti**, None*

P-311

Pulsating Fluid Flow Modulates Bone Cell Shape and Mitochondrial Structure – Implications for Bone Cell Function? *Jianfeng Jin[1], Joannes A.M. Korfage[2], Astrid D. Bakker[3], Richard T. Jaspers[4], Jenneke Klein-Nulend[3]. [1]Department of Oral Cell Biology, Academic Centre for Dentistry Amsterdam (ACTA), University of Amsterdam and Vrije Universiteit Amsterdam, Amsterdam Movement Sciences, Amsterdam, The Netherlands, Netherlands, [2]Department of Functional Anatomy, Academic Centre for Dentistry Amsterdam (ACTA), University of Amsterdam and Vrije Universiteit Amsterdam, Amsterdam Movement Sciences, Netherlands, [3]Department of Oral Cell Biology, Academic Centre for Dentistry Amsterdam (ACTA), University of Amsterdam and Vrije Universiteit Amsterdam, Amsterdam Movement Sciences, Netherlands, [4]Laboratory for Myology, Faculty of Behavioral and Movement Sciences, Vrije Universiteit Amsterdam, Amsterdam Movement Sciences, Netherlands

Introduction: Bone cells respond to mechanical cues from the environment by changes in cellular morphology, which requires drastic rearrangements of cytoskeletal structures. Mitochondria form an extensive highly dynamic network undergoing fission and fusion, with clusters moving along the cytoskeleton. Importantly, mitochondrial form and function are intimately linked. However, whether mechanical factors affecting cytoskeletal organization also affect mitochondrial network structure and function in bone cells is unknown. Purpose: To investigate whether bone cell deformation induced by mechanical loading is associated with changes in intracellular mitochondrial network structure.Method: Prior to 1 h pulsating fluid flow (PFF; peak shear stress rate: 6.5 Pa/s; amplitude: 1.0 Pa; frequency: 1 Hz), live MC3T3-E1 pre-osteoblasts were fluorescently stained for F-actin (Sir actin), nuclei (Sir DNA), and mitochondria (MitoTracker). Online live cell imaging was employed (22 cells, n=3 experiments) using LSCM before and during PFF. Cell morphology (area), cell movement (X,Y,Z-direction), cytoskeletal changes (F-actin fluorescence intensity), and mitochondrial network structure and organization (footprint/area, number of branches, junctions, triple/quadruple points, junction/slad/end point voxels, and branch length in live cell top view images; every 1 sec) were determined.Results: PFF reduced cell surface area gradually over time (0.85-fold, 10 min; 0.50-fold, 60 min; Fig. 1). F-actin fluorescence intensity remained unchanged. PFF caused cellular up-and-down movement. PFF modulated mitochondrial network structure and organization, except footprint or area (Fig. 1). The highest peak (value) of the network structure and organization parameters appeared at 5 sec. Mitochondrial movement was along the flow direction.Conclusions: PFF induced temporal and spatial changes in bone cell morphology, which coincided with changes in intracellular mitochondrial network structure. This might suggest that mechanical load-induced bone cell deformation may drive mitochondrial function, and likely bone cell function.Attachment: Figure 1: PFF affected F-actin and mitochondria in pre-osteoblasts. (A) Time course of PFF modulation of F-actin (yellow/red). (B) PFF reduced bone cell area. (C) PFF modulated mitochondrial network structure (green). Black/red wireframe of lines: skeletonized mitochondria. (D) PFF did not change mitochondrial footprint (or area) values. Bar: 20 µm.

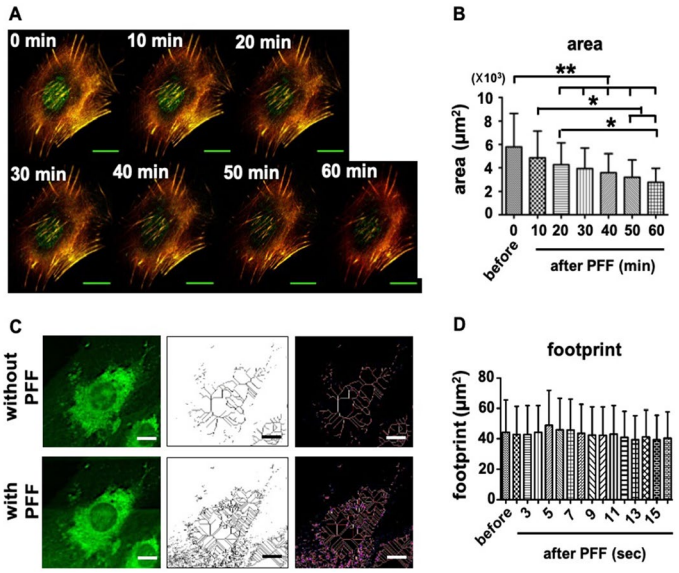

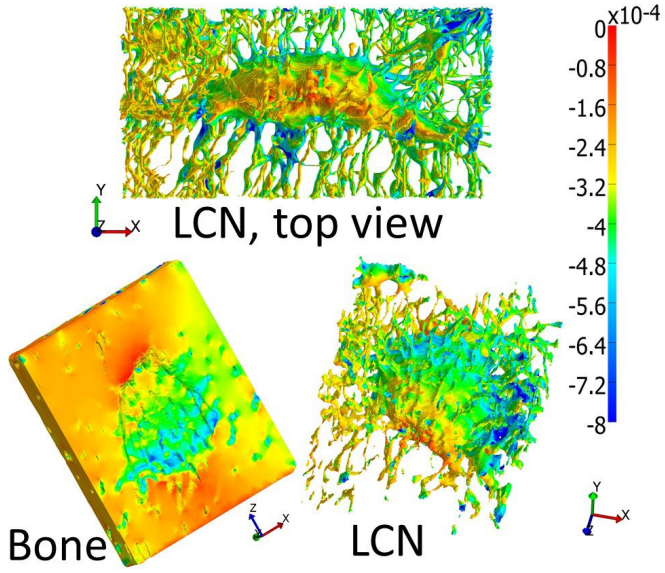

***Disclosures: Jianfeng Jin**, None*

***Disclosures: Loretta Laughrey**, None*

P-312

Mechanotransduction at the Lacuna: Finite Element Modeling in 3D Using Confocal Fluorescence Imaging *Loretta Laughrey[1], Thiagarajan Ganesh[1], Sarah Dallas[2], Mark Johnson[2]. [1]University of Missouri-Kansas City, School of Computing and Engineering, United States, [2]University of Missouri-Kansas City, School of Dentistry, United States

Bone responds to its load environment through mechanisms that are not fully understood. Loading stimulates osteocytes which are key players in bone homeostasis. The effects of global load need to be transduced to the osteocyte in its lacuna. To date, most models have assumed that osteocytes respond to global bone strains homogeneously. Few models demonstrate the complex lacunocanalicular morphology that contributes to a heterogeneous osteocyte response and amplification of the mechanical signals that stimulate bone formation. To interrogate loading dynamics in bone we have developed computer models that simulate the complexity of lacunar and canalicular morphologies using empirical data rather than idealized geometries. Our models represent realistic, 3D models of a single lacuna. Confocal images of a 20x20x11 μm volume of FITC labeled bone, from a 4mo-old mouse femur, were converted into a finite element (FE) model with Materialise Innovation Suite®.Strain analysis was performed to examine the model response to load using FEBio Software Suite. The interior regions of the lacuna and canaliculi were assigned isometric elastic properties similar to water. Bone was assigned an elastic modulus of 5 GPa, Poisson's ratio of 0.17, and density of 2 g/cm3.The results indicate that more strain at the cellular level is concentrated in the canaliculi rather than the lacuna (see figure). Heterogeneity of strain also occurs in the lacunar walls, where strain is higher near canalicular attachments. This, combined with prior observations that osteocyte dendrites are more sensitive to mechanical stimulation than the cell body, suggests that transduction of mechanical load into a biological signal could occur primarily in or near dendrites.The model is composed of about 2 million Tet4 elements. Despite its complexity strain analysis using FEBio Software Suite required less than 20 minutes on a desktop. Linking such models with lower resolution models from the same specimen could simulate the entire path of mechanotransduction from a whole bone to a single osteocyte.Our procedure creates sophisticated FE models of the bone lacuna and its canaliculi for strain analyses based on real geometries. In the future, such models will be combined with multi-scale models, multiplexed images of the osteocyte, and indicators of bone formation to understand the heterogeneity of osteocyte responses to mechanical loading in regions of bone that experience similar global strains.

P-313

Role of Canalicular Loss in Osteocyte Mechanobiology Due to Aging *Mohammadmedhi Niroobakhsh[1], Sarah Dallas[1], Mark Johnson[1], Thiagarajan Ganesh[1]. [1]University of Missouri Kansas City, United States

Prior studies from our group have demonstrated a loss of osteocyte dendrites and connectivity in aged mice, which we hypothesize could explain reduced responsiveness to mechanical loading in the older animals. Two finite element models of idealized single osteocytes in their lacunae, identical except for the number of canaliculi, were created in ANSYS multi-physics software using the fluid-structure interaction (FSI) approach. We examined the effect of the change in number of canaliculi on fluid velocity in the pericellular space (PCS), fluid shear stress, and bone strain. Previous studies by other groups have not examined the effect of canalicular density using computer simulations. Also, they have predicted that load-induced fluid flow plays an essential role in mechanotransduction through fluid flow shear stresses and bone strains.The osteocyte and bone tissue are solid domains, and fluid flows between them through the PCS. To model physiological loading, we applied a compressive strain of 3000 μ? as displacement to one side of the solid and the opposite side was fixed. A fluid inlet pressure of 300 Pa and outlet pressure of 0 Pa were assigned as fluid boundary conditions. The 10 canaliculi model consists of one flow inlet and nine outlets, while the 18 canaliculi model has 5 inlets and 13 outlets.The fluid velocity in canaliculi was higher than in the lacuna. The model with 18 canaliculi showed an average velocity of 11.7 μm/s, average fluid shear stress of 0.39 Pa, and a maximum strain of 29,820 μ? for the osteocyte and bone matrix. An average velocity of 16.1 μm/s, average shear stress of 0.34 Pa, and maximum strain of 26,590 μ? were observed in the model with 10 canaliculi. Although increasing the number of canaliculi results in lower fluid velocity, it yields higher shear stresses and strains. This increase in shear stress and strain may have been due to the incorporation of additional inlets to the model, since inlets experience higher shear stresses. Overall, these data suggest that increased canalicular number results in higher strains. In addition, these simulations support the hypothesis that higher shear stresses occur on the dendrite processes, rather than the cell body.Our findings indicate that it is possible to model aging associated changes in osteocyte morphology and that bone mechanical stimuli may be altered by the consequences of the reduction in PCS fluid flow when osteocyte connectivity changes due to aging.

***Disclosures: Mohammadmedhi Niroobakhsh**, None*

P-314

Prediction of Cyclic Load from Strain Measurement in a Long Bone using an Artificial Neural Network Algorithm *Saeed Mouloodi[1], Hadi Rahmanpanah[2], Colin Burvill[2], Helen MS Davies[3]. [1]Depts Veterinary BioSciences and Mechanical Engineering, The University of Melbourne, Australia, [2]Dept Mechanical Engineering, The University of Melbourne, Australia, [3]Dept Veterinary BioSciences, The University of Melbourne, Australia

Equine third metacarpal (MC3) bones experience a range of surface strains which are a measure of displacement induced by mechanical loading. Bone is a highly nonlinear, inhomogeneous and anisotropic material, thus determining its responses is a daunting task. Inverse finite element analysis has to be solved to predict cyclic loading from strains measurement, which most FEA packages are incapable of doing. Artificial neural network (ANN) is a

gold standard to be employed for prediction of load [1] in preference to relatively inaccurate, expensive and time-consuming tools such as FEA. In addition, examples of areas where such predictive capability is of great value are the design and post-operative analysis of orthopaedic implants [2].Nine hydrated third metacarpal bones (B1-B9) from thoroughbred horses were tested in ex vivo experiments. A set of strain gauges was attached to the lateral, dorsal, and palmar cortices of the bones. Compressive cyclic loads were applied to the bones using an MTS machine. Displacement of the machine ends, the values of six kinds strains, the applied load, and the rate of loading were recorded. The input sector had 10 variables, including time (t), side (left or right limb), age (y), and strains (ε). The output of the simulation was the cyclic load being applied to the bone samples.The ANN model was successfully trained using ex-vivo measurements from B1, B3, B4, and B5. Afterwards, the ANN model was employed to predict the responses of B7. Figure 1a presents the comparison of the ex-vivo experiments and the load prediction of the ANN. The trend of experimental results was consistent with the prediction of the ANN. A force-displacement curve recorded experimentally and that obtained via the ANN model are demonstrated in Figure 1b. A histogram of errors between the ex-vivo load and the prediction of the ANN is presented in Figure 1c. The outcome of regression analysis between experimental results and the prediction of the ANN model is illustrated in Figure 1d.Artificial neural networks (nonlinear mapping approach) were used to solve the forward problem for the estimation of applied load. The ability of ANN to predict load from measurements of displacement, rate of loading, age, side (left or right limb), and strains was discussed. ANN is an invaluable tool for quantifying responses of long bones under mechanical loading.[1] A. A. Zadpoor. (2013). J Mech Behav Biomed Mater. 27: 249-61.[2] S. Mouloodi et al. (2020). J Mech Behav Biomed Mater. 102: 103527.

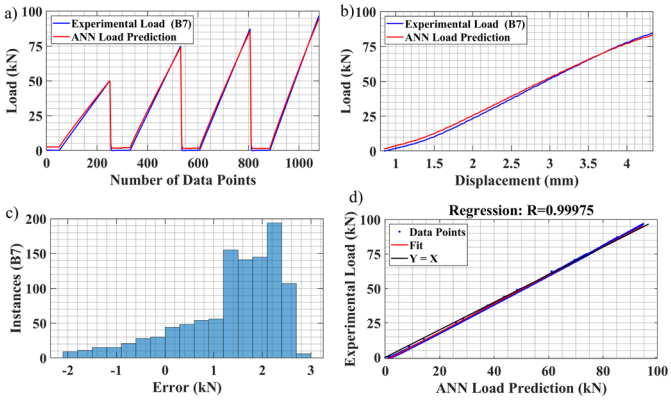

The ANN model was trained using data points from B1, B3, B4 and B5 and then employed to predict the loading of B7. a) Comparison of experimental forces with the prediction of the ANN model. b) Comparison of the second cycle of the force-displacement curve. c) Histogram of errors. d) The regression model.

***Disclosures: Saeed Mouloodi**, None*

P-315

Random Walk in 3D Model of Water Diffusion in the Human Mineralized Collagen Fibril *Fabiano Bini[1], Andrada Pica[1], Andrea Marinozzi[2], Franco Marinozzi[1]. [1]Department of Mechanical and Aerospace Engineering, "Sapienza" University of Rome, Italy, [2]Orthopedy and Traumatology Area, "Campus Bio-Medico" University, Italy

At the nanoscale bone tissue is characterized by the mineralized collagen fibril (MCF), a recurring structure mainly composed of apatite mineral, tropocollagen molecules (TC) and water. The latter has a crucial role in bone biomineralization. In this study, we aim to analyse the mass transport at the collagen-apatite level of porosity by means of a 3D random walk model.We considered a representative building block of the MCF according to [1-2]. We assumed a mineral volume fraction that represents an intermediate mineralized condition (32%vol). The geometrical dimensions of the nanocrystals and TC molecules are obtained with random extractions from Gaussian probability distribution functions within the range indicated in literature. We generated a model of the building block using the Metropolis algorithm in which platelets start in a regular configuration and then are subjected to random displacements and inclinations. The analysed arrangement of the building block is obtained after roughly 6·106 moves and rotations.The water diffusion within the building block is simulated by using a 3D random walk method. We computed the trajectory of the water molecule for 30k time steps Δt = 5·10-10 s and take the average over 300 water particles. We assume that mineral platelets and TC molecules are impermeable obstacles to water diffusion. Periodic boundary conditions are used to prevent error from the finite size of the building block.The diffusion coefficient is calculated from the mean square displacement of water molecules (MSD) according to the equation D=MSD/2nt, where D is the diffusion coefficient, n is the spatial dimension, i.e. n=3, t is the time, i.e. t = nT·Δt, with nT –number of time steps [3].The model provides a good prediction of the apparent diffusion coefficient, i.e. D = 3.25·10-10 m2/s in agreement with previous results achieved from experimental [4] and computational investigations [2]. The 3D random walk model is a valuable tool for investigating the influence of the structural hindrance on the diffusivity since the structure of the building block is included in the diffusion model.Insights into MCF structure and properties enhance the understanding of bone mineralization and may improve the design of smart structural nanomaterials.References:1. Jäger et al. (2000). Biophys. J. 79: 1737-17462. Bini et al. (2019). Sci. Rep. 9:26583. Stylianopoulos et al. (2010). Biophys. J. 99:3119-31284. Marinozzi et al. (2014). Biomatter 4:1 e28237

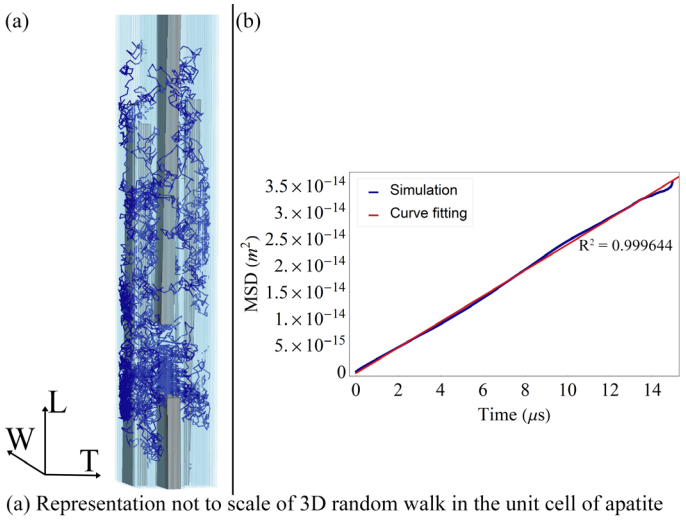

(a) Representation not to scale of 3D random walk in the unit cell of apatite (gray) and collagen (light blue)
(b) MSD plot from simulated trajectories. Diffusion coefficient obtained from linear regression of MSD data is D = $3.25 \cdot 10^{-10}$ $m^2 s^{-1}$

***Disclosures: Fabiano Bini**, None*

P-316

The Interactive Effects of Dynamization Time and Degree on Bone Healing *Ruisen Fu[1], Bettina Willie[2], Haisheng Yang[1]. [1]Department of Biomedical Engineering, Beijing University of Technology, China, [2]McGill University, Shriners Hospitals for Children, Canada

Introduction: Dynamization, reducing the fixation stiffness from a rigid to a more flexible condition, is widely used clinically to promote fracture healing. However, the most effective time to apply dynamization on healing outcomes remains controversial. Preclinical studies have demonstrated that dynamization with a degree of ~0.1 (the ratio of the flexible to rigid stiffness) at an early stage of healing (e.g. one week post-osteotomy) in rat femurs led to delayed healing (1-2). In contrast, a clinical study observed enhanced bone healing with early dynamization (3). It should be noted that the baseline fixation stiffness as well as the dynamization degree are different between those studies. Given the critical role of the fixation stiffness in determining the interfragmentary movement and thus regulating the healing process, it is important to understand how the degree and timing of dynamization interactively affects the healing process. Thus, the aim of the current study was to use finite element modeling to quantify the combined effect of degree and timing of dynamization on healing outcomes in an ovine model.Methods: Based on an ovine tibial fracture healing model which involves a fuzzy logic-based mechano-regulated tissue differentiation algorithm (4-5), we applied varied dynamization degrees (DC=0.1 to 1; 1 represents a rigid fixation) at 1, 2, 3, and 4 weeks (R1wF, R2wF, R3wF, R4wF) and computationally evaluated bone formation and biomechanical integrity during the healing process.Results: Our results demonstrated that early dynamization (at 1 and 2 weeks) significantly affected the healing process and outcomes (Fig. 1). However, the beneficial effect of early dynamization was dependent of the dynamization degree. Specifically, a higher dynamization degree (e.g. 0.1) led to a marked delay in bone formation and unrecovered stiffness whereas moderate dynamization degrees (e.g. 0.3 or 0.5) significantly enhanced bone formation and biomechanical properties of the fractured bone (Fig. 1).Conclusions: Our results suggest that dynamization degree and timing interactively affects the healing process and therefore clinical application of dynamization should consider their interaction carefully to achieve a beneficial healing outcome.References: [1]. Claes et al, JOR, 2009. [2]. Willie et al, CORR, 2011. [3]. Huang et al, Injury, 2012. [4]. Shefelbine et al, JB, 2005. [5]. Simon et al, CMBBE, 2011. Acknowledgement: NSFC (11702008), BJNSF (7202003).

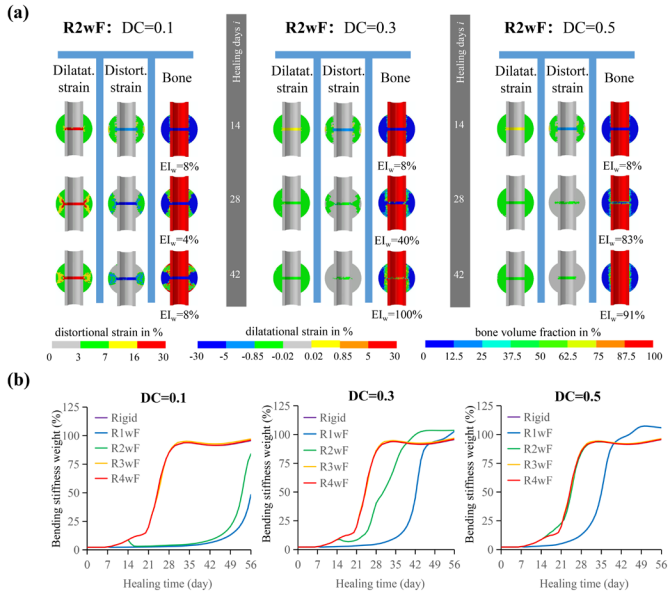

Fig. 1.(a) The strain fields and bone tissue distributions in the callus when dynamization is applied at 2 weeks with varied dynamization degrees (DC=0.1, 0.3, 0.5); (b) Changes in bending stiffness weight of the fractured bone over the healing process when dynamization is applied at 1, 2, 3, and 4 weeks (R1wF, R2wF, R3wF, R4wF) with varied dynamization degrees (DC=0.1, 0.3, 0.5).

***Disclosures: Ruisen Fu**, None*

P-317

Effect of the accordion technique on bone regeneration during distraction osteogenesis *Ruisen Fu[1], David Bertrand[2], Bettina Willie[2], Haisheng Yang[1]. [1]Department of Biomedical Engineering, Beijing University of Technology, China, [2]McGill University, Shriners Hospitals for Children, Canada

Introduction: Distraction osteogenesis (DO) is a surgical technique used to lengthen bone or bridge large segmental bone defects. It is currently employed worldwide to treat congenital and acquired limb length discrepancies and large bone defects resulting from infection, trauma or malignancies. However, a major disadvantage of DO is the prolonged consolidation phase (10-36 months) during which patients must wear a cumbersome external fixator. Thus, strategies are needed to accelerate the healing process in DO. The “accordion” technique (AT), which uses alternating controlled distraction and compression during the consolidation phase of DO, has shown improved healing outcomes in a limited number of patients [1]. However, questions remain as to when is the most effective time to apply the AT following DO.Methods: We performed computational simulations to examine the effect of the AT applied during early, middle and late stages of the consolidation phase of DO on healing outcomes. A 2D axisymmetric finite element model was created based on the cortical and callus geometry of the ovine tibia from experimental data [2]. The initial osteotomy gap was set to 5 mm. Distraction (1mm/day; 0.5mm/12h) was applied to the top of the cortical bone and the bottom cortical end was fixed. Distraction was conducted for 10 days, followed by 40 days of consolidation. An adaptive tissue differentiation algorithm was used to predict mechanically regulated bone regeneration during DO [3]. Four groups of simulations were conducted: (1) Control: no AT; (2) Early AT: day 10-20; (3) Middle AT: day 20-30; (4) Late AT: day 30-40.Results: Results showed enhanced bone formation for the Late AT compared to control. Specifically, by the end of 40 days, the amount of newly formed bone in the callus was 37% greater for the Late AT group than the control group (Fig. 1). In contrast, the Early AT group showed compromised bone regeneration compared to controls. The Middle AT group showed comparable bone healing outcomes with the controls.Conclusion: These results suggest that while application of the AT during the consolidation phase of DO can promote bone regeneration, it is most effective at a later stage in this animal model.References: [1] Makhdom et al, Nanomedicine Nanotechnology, Biol. Med. 11(1): 1-18, 2015. [2] Claes et al, J. Bone Jt. Surg. 82(1): 142-148, 2000. [3] Niemeyer et al, PLoS One. 13(3): 1-31, 2018. Acknowledgement: NSFC (11702008), BJNSF (7202003).

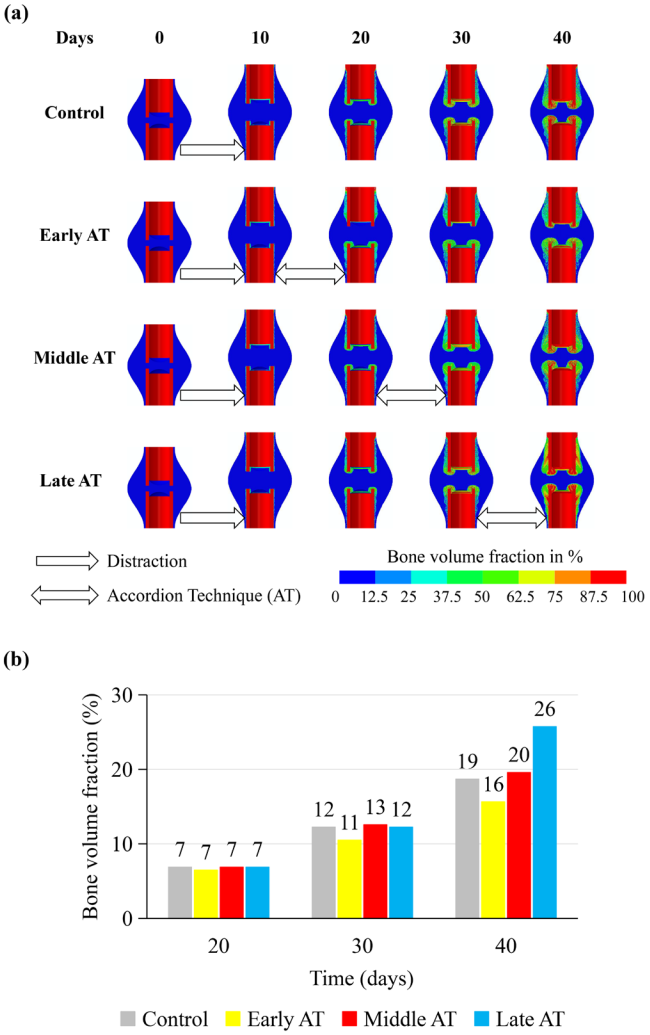

Fig. 1. (**a**) Changes in bone volume fraction over 40 days. Distraction was conducted for 10 days followed by no accordion technique (AT), or AT applied at early (10-20 days), middle (20-30 days) and late stages (30-40 days) in the consolidation phase. (**b**) Bone volume fraction of the callus for Control, Early AT, Middle AT and Late AT at day 20, 30 and 40.

***Disclosures: Ruisen Fu**, None*

P-318

Notum’s role in the response of bone to mechanical loading and aging *Vincent Marshall[1], Bryan Wacker[1], Julia Hum[1]. [1]Marian University, United States

Osteoporosis is a silent, dangerous, pathology frequently undiagnosed until patients experience a major fracture. Fractures from osteoporosis lead to a 20% increase of mortality, revealing a need for novel anabolic therapies. Recently, mice lacking Notum protein expression were reported to have increased endocortical bone formation and strength. Notum is an inhibitory protein of the Wnt pathway, a major growth pathway in mammalian skeletons. The hypothesis for this work is Notum expression is affected by mechanical loading and aging. The goal of these studies is to investigate factors that could affect Notum expression, with the future direction of identifying factors that when pharmacologically modulated could promote anabolic bone growth. After establishing Notum expression in the osteocyte cell line, MLO-Y4, Notum protein expression in response to mechanical loading was assessed, mimicked via fluid shear stress for 15 min, 1hr, and 2hr. Fluid shear stress induced a decrease in Notum protein expression after long bouts of fluid shear stress. Notum gene expression was analyzed from embryonic, >8 weeks old, and <15 weeks old wild-type mice femurs. The aging process increases gene expression of Notum after 15 weeks of age. With these results, our hypothesis is supported and future studies examining the mechanism(s) of mechanical regulation and the aging process on Notum’s expression are underway.

***Disclosures: Vincent Marshall**, None*

Posters

P-319

Loading history changes the morphology and compressive force-induced expression of receptor activator of nuclear factor kappa B ligand/ osteoprotegerin in MLO-Y4 osteocytes *Ziyi Wang[1], Yao Weng[2], Yoshihito Ishihara[3], Naoya Odagaki[3], Ei Ei Hsu Hlaing[1], Takashi Izawa[1], Hiroshiko Okamura[4], Hiroshi Kamioka[1]. [1]Department of Orthodontics, Okayama University Graduate School of Medicine, Dentistry and Pharmaceutical Sciences, Japan, [2]Department of Oral Morphology, Okayama University Graduate School of Medicine, Dentistry and Pharmaceutical Sciences, Okayama, Japan, Japan, [3]Department of Orthodontics, Okayama University Hospital, Japan, [4]Department of Oral Morphology, Okayama University Graduate School of Medicine, Dentistry and Pharmaceutical Sciences, Japan

Background: In this study, we investigated the effect of the mechanical loading history on the expression of receptor activator of nuclear factor kappa B ligand (RANKL) and osteoprotegerin (OPG) in MLO-Y4 osteocytes.Methods: Three h after MLO-Y4 osteocytes were seeded, a continuous compressive force (CCF) of 31 dynes/cm2 with or without additional CCF (32 dynes/cm2) was loaded onto the osteocytes. After 36 h, the additional CCF (loading history) was removed for a recovery period of 10 h. The RANKL/OPG expression, cell numbers, viability, and morphology were time-dependently examined at 0, 3, 6, and 10 h. Then, the same additional CCF was applied again for 1 h to all osteocytes with or without the gap junction inhibitor to examine the RANKL/OPG expression.Results: The expression of RANKL and OPG by MLO-Y4 osteocytes without a loading history was dramatically decreased and increased, respectively, in response to the 1-h loading of additional weight. However, the expression of RANKL, OPG, and the RANKL/OPG ratio were maintained at the same level as in the control group in the MLO-Y4 osteocytes with a loading history but without gap junction inhibitor treatment. No significant difference was observed in the cell number or viability between the MLO-Y4 osteocytes with and without a loading history or among different time checkpoints during the recovery period. The cell morphology showed significant changes and was correlated with the expression of RANKL/OPG during the recovery period.Conclusion: Our findings indicated that the compressive force-induced changes in the RANKL/OPG expression could be habituated within at least 11 h by 36-h CCF exposure. Gap junctional intercellular communication and cell morphology may play roles in the storage of loading history in MLO-Y4 osteocytes.

***Disclosures: Ziyi Wang**, None*

P-320

Local deformation of marrow cells caused by the sinusoidal fluid pressure *Taekyeong Lee[1], THI KHOA MY NGUYEN[1], SooHyeon Hwang[1], Junghwa Hong[1]. [1]Korea university, Republic of Korea

The red marrow of intertrabecular pores PIT, which is a special soft tissue, contains various bone cells, adipocytes, extracellular fluid, and extracellular matrix composed of mostly collagen and proteoglycan. In the intracancellous marrow space, the marrow arteriole divides into capillaries. The capillaries have porous sinusoids, which are drained by venules. The sinusoids are average of 25um wide having thin-walled vessels, which are highly porous. The sinusoidal walls lined by endothelial cells are flown by fluid and traversed by hematopoietic cells in both directions. Importantly, the porous sinusoids role as the primarily local sources and drains of fluid in the PIT. The sinusoids uniformly distribute in the PIT of rats as a density of 90~100 sinusoids per 3×106 micro3. The pressure of sinusoids is unknown. However, it is reported that the intramedullary FP in metaphysis of canine and murine long bone ranges from 1.78 to 2.73 kPa. Since the inner part of metaphysis is composed of the cancellous bone, the intramedullary FP of metaphysis could represent the sinusoidal FP in PIT (PITFPS). As a result, an osmotic pressure equilibrium would be formed in the PIT. Therefore, the sinusoidal FP would generate intramarrow fluid flow for metabolism of marrow cells through the extracellular gaps and matrix pores.Since the cells and adipocytes in the marrow are deformable, applications of the pulsatile PITFPS through the very porous and permeable sinusoidal wall on the boundary between the marrow and a sinusoid would cause local deformation of the bone cells and adipocytes. This could result in changes in configuration of the extracellular gaps (ECG). To understand the changes, murine marrow was loaded in a biochip (Fig. 1a) which has a microchannel. Then, PBS buffer injected to the chamber to make FP that observe the changes in configuration of the extracellular gaps (Fig. 1b).Even though the environment was different that inter trabecular conditions of bone marrow by placing in microchannel after bone marrow aspiration, but the significant local deformations of the marrow cells were occurred at the application line of pressure. In addition, the reductions of the ECG were observed at the line. These reduction of ECG would hinder the intramarrow fluid flow. In vivo, this would cause insufficient mass transport from the sinusoid to the marrow for the metabolisms, and various geneses in the PIT. Therefore, a substantial and assistive mechanism is required to help the intramarrow fluid flow for augmenting mass transport for the metabolisms and geneses of the PIT cells.

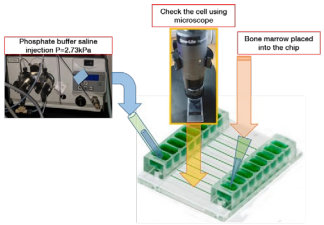

Fig. 1(a) The experimental setup for local deformation of marrow cells

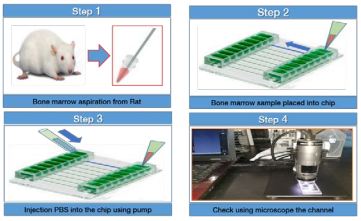

Fig. 1(b) The experiment protocol to understand the marrow cells changes

***Disclosures: Taekyeong Lee**, None*

P-321

Advanced Glycation End-Products Are Related With Cortical Quality And Increased Risk For Bone Fractures In Chronic Kidney Disease Patients *Noemi Roza[1], Kelcia Quadros[1], André Esteves[1], Renata França[1], Wagner Domingues[2], Luzia Furukawa[2], Rodrigo de Oliveira[1]. [1]University of Campinas, Brazil, [2]University of São Paulo, Brazil

INTRODUCTION: The risk of bone fractures is higher in chronic kidney disease (CKD) patients than general population. We aim to investigate the relationships between advanced glycation end-products (AGEs) and cortical bone in a cohort of CKD patients. MATERIALS AND METHODS: 86 CKD patients (stages 3-4, N=26; hemodialysis, N=32; peritoneal dialysis, N=28) were included. AGEs levels were measured in serum (pentosidine and glycated hemoglobin), in skin (by AGE-Reader device) and in cortical bone by immunohistochemistry; receptor activator of nuclear factor kappa-B (RANK) and its ligand (RANKL) and SOST mRNA expression were evaluated by quantitative real-time PCR. Bone histomorphometry was performed to measure cortical porosity, thickness and volume. Fracture risk was predicted using FRAX tool. RESULTS: Age was 51+/-13 years and body mass index (BMI) 26+/-5 kg/m2; 48 (56%) were male, 41 (48%) Caucasian and 16 (19%) diabetics; dialysis vintage was 21 (10-44) months and glomerular filtration rate 6 (5-17) mL/min. AGEs levels in skin were 3.0+/-0.7 AU (reference: <2.0 AU), serum pentosidine 71 (44–121) pmol/mL and glycated hemoglobin 5.4 (5-6)%; cortical bone volume, thickness and porosity were 22.3+/-9.8 µm2, 619+/-213 µm and 1.55 (0.9-2.7)%, respectively. AGEs levels in skin were correlated with age (R=0.538; P=0.0001), risk for major osteoporotic fracture (R=0.562; P=0.0001) and hip fractures (R=0.49; P=0.0001). The mean area of AGEs deposits in the cortical bone was 5.4 (3-12.1)% and a trend of correlation was positively correlated with risk for major osteoporotic fracture (R=0.25; P=0.06); cortical thickness were negatively correlated with serum pentosidine levels (R=-0.27; P=0.02) and age (R=-0.235; P=0.04); cortical porosity were positively correlated with glycated hemoglobin (R=0.278; p=0.02), SOST mRNA expression (R=0.321; p=0.03), RANKL mRNA expression (R=0.414; p=0.004). Finally, RANK mRNA expression was correlated with serum pentosidine levels (R=0.304; p=0.045). CONCLUSION: AGEs were detected in cortical bone and skin of CKD patients and correlates with their risk for osteoporotic fractures. Serum pentosidine levels were associated with low thickness of cortical bone. Cortical porosity was associated with serum glycated hemoglobin levels, SOST and RANKL mRNA expression. RANK was positively influenced by serum pentosidine levels. Together these data point to a direct relationship between AGEs and fractures in patients with CKD.

***Disclosures: Noemi Roza**, None*

P-322

Hypoxia-Inducible Factor 1 Alpha Regulates FGF23 Production and Bone Metabolism in Chronic Kidney Disease *Guillaume Courbon[1], Jadeah Spindler[1], Bridget Hunt-Tobey[1], Emily Lynch[1], Xueyan Wang[1], Marta Martinez Calle[1], Aline Martin[1], Valentin David[1]. [1]Division of Nephrology and Hypertension, Department of Medicine, and Center for Translational Metabolism and Health, Institute for Public Health and Medicine, Northwestern University Feinberg School of Medicine, Chicago, IL, USA, United States

Renal osteodystrophy (ROD) is a complex bone disorder associated with chronic kidney disease (CKD) which affects over one in ten Americans. CKD also leads to increased bone production of the phosphate regulating hormone, fibroblast growth factor 23 (FGF23). ROD and FGF23 are associated with adverse clinical outcomes, including cardiovascular events and death. Hypoxia-inducible factor 1 alpha (HIF1α) regulates FGF23 expression in osteoblasts and osteocytes, and we hypothesized that osseous HIF1α plays an important role in ROD and FGF23 excess in CKD.We generated mice harboring a conditional deletion of Hif1α in osteocytes (Hif1αDmp1-cKO) and crossed them to Col4a3KO mice, a mouse model of progressive CKD. We studied bone and mineral metabolism alterations of wild-type (WT), Hif1αDmp1-cKO, Col4a3KO and compound Col4a3KO Hif1αDmp1-cKO (CPD) mice. In parallel, we also treated WT and Col4a3KO mice with moderate CKD, with a HIF inhibitor (BAY 87-2243) for 4 weeks. Finally, we compared the differentiation and mineralization potential of newly generated MC3T3-E1 osteoblast cell lines overexpressing Hif1α (Hif1αTg) or Hif1α shRNA (Hif1αKO) to MC3T3-E1 transfected with an empty vector (Ctr).As previously reported, Col4a3KO mice show a progressive decline in kidney

function, associated with FGF23 excess, bone loss, mineralization and turnover abnormalities. Deletion of Hif1α delayed progression of CKD, as CPD mice showed reduced levels of BUN compared to age-matched Col4a3KO mice (-25%). In addition, CPD mice showed lower FGF23 levels (-80% vs. Col4a3KO) and we obtained similar results in Col4a3KO mice administered with a HIF inhibitor (-80% FGF23, -30% BUN, vs. Ctr-Col4a3KO). CPD mice also showed improved trabecular and cortical bone parameters (+50% trabecular bone volume, -20% cortical porosity vs. Col4a3KO). Finally, deletion of Hif1α led to increased alkaline phosphatase (ALP) positive colonies and mineral deposits in Hif1αKO cultures compared to Ctr cells, and was accompanied by a 30% reduction in Fgf23 expression. In contrast, Hif1αTg cells showed reduced osteogenic potential, with fewer ALP positive colonies and mineral deposits, together with a 2-fold increase in Fgf23 expression.Our data suggest that osseous HIF1α stimulates FGF23 production in CKD and is a negative regulator of osteoblast differentiation and function. Thus, inhibition of HIF1α in bone might represent a novel therapeutic strategy to improve outcomes in CKD.

***Disclosures: Guillaume Courbon**, None*

P-323

Reduced DMP1 expression precedes bone loss and FGF23 elevation in CKD *Emily Lynch[1], Xueyan Wang[1], Jian Q Feng[2], Thomas Nickolas[3], Valentin David[1], Aline Martin[1]. [1]Division of Nephrology and Hypertension, Northwestern University, United States, [2]College of Dentistry, Texas A&M University, United States, [3]Columbia University Medical Center, United States

Chronic kidney disease (CKD) is associated with major disorders of bone and mineral metabolism, including impaired bone turnover and mineralization, altered osteocyte morphology and differentiation, and increased production of the bone secreted phosphaturic hormone FGF23, which is independently associated with cardiovascular mortality. Dentin matrix protein 1 (DMP1) is an extracellular matrix protein produced by osteocytes that stimulates osteoblast differentiation and inhibits FGF23 production. We previously showed that DMP1 supplementation prevents bone loss, FGF23 elevation and cardiovascular outcomes in mice with advanced CKD.To determine if altered DMP1 expression contributes to the pathogenesis of renal osteodystrophy and FGF23 elevations during CKD progression, we measured DMP1 expression in bone of wild-type (WT) and Col4a3KO mice with spontaneous and progressive CKD every 4 weeks from 4 weeks of age until their death (24 weeks). In parallel, we assessed kidney function, circulating levels of FGF23 and bone microarchitecture. We also assessed osteocyte morphology in mice and in patients with early CKD. Compared to age-matched WT, Col4a3KO mice showed increased albumin to creatinine ratio (ACR) starting at 8 weeks and blood urea nitrogen (BUN) levels starting at 16 weeks indicating onset of proteinuria and impaired kidney function ($p<0.05$). Consistent with BUN levels, serum FGF23 levels showed sustained increases starting at 16 weeks ($p<0.05$). This coincided with alterations in trabecular bone, including reduced trabecular volume (BV/TV), number (Tb.N), thickness (Tb.Th), connectivity-density, and bone mineral density (BMD) measured by 3D-microtomography of femurs from 16 to 24 week-old Col4a3KO mice ($p<0.05$). However, analysis of cortical (Ct) bone showed reductions in BMD, Ct.Th and area (Ct.Ar) as early as 12 weeks of age ($p<0.05$), and alterations in osteocyte morphology as early as 10 weeks in Col4a3KO mice with early CKD and in patient with CKD stage 1-2. Bone DMP1 mRNA was reduced by 50% prior to the onset of proteinuria at 4 weeks of age and remained low at all time points throughout CKD progression ($p<0.05$).These data show that reduction in DMP1 expression occurs prior to major changes in kidney function and precedes altered osteocyte morphology, cortical bone loss and FGF23 elevation in CKD. Although further studies are needed to identify the factors that suppress DMP1 expression in CKD, DMP1 administration might represent an effective therapeutic strategy to prevent alterations in bone and mineral metabolism in early CKD.

***Disclosures: Emily Lynch**, None*

P-324

Ubiquitin-specific Protease USP34 Regulates Dental Root Morphogenesis *Shuang Jiang[1], Yuchen Guo[1], Rui Sheng[1], Xingying Qi[1], Quan Yuan[1]. [1]Sichuan University, China

Dental root morphogenesis is a dynamic process in which dental mesenchymal cells (DMCs) migrate and differentiate into odontoblasts and dental pulp cells, shaping the future root of tooth. There are complex signaling pathways involving in root formation, among which ubiquitin-dependent proteolysis system plays an increasingly important role. However, the precise molecular network controlling deubiquitylation in the process of root formation, is yet to be determined. Here we identify deubiquitinase USP34 as a regulator of dental root morphogenesis.First, we delineated the pattern of USP34 expression in dental pulp tissues from human and mouse. USP34-expressing cells were predominantly observed among odontoblasts and dental pulp cells using immunohistochemical method. Then we found increasing mRNA and protein level of USP34 in human dental pulp stem cells (DPSCs) during odontoblastic induction in vitro. Furthermore, we knocked down the expression of USP34 by siRNA and found the odontoblastic differentiation of DPSCs was inhibited, with reduction of formation of mineralized nodules and intensity of ALP staining.To further validate the role of Usp34 in vivo, we bred Usp34f/+ mice with Sp7-Cre mice to specifically delete Usp34 from DMCs. Via histomorphometry, we observed that Usp34 deletion significantly inhibited root formation in mice, resulting in short root and thin dentin layer 14 days postnatal. This data was also confirmed by micro-CT analysis. Together, we found that Usp34 deletion in DMCs inhibited root morphogenesis.Mechanically, we performed proteome analysis and noticed that knock down of USP34 downregulated the protein level of nuclear factor 1 C (NFIC). Therefore, we assumed that USP34 might control root formation via NFIC, a key regulator in odontoblastic differentiation. Then we examined ectopically expressed NFIC levels in the presence of CHX and observed much faster degradation of this protein after USP34 depletion, indicating that USP34 could regulate the stability of NFIC.Last, we generated DPSCs with NFIC overexpressed using lentiviruses expressing shRNA. Overexpression of NFIC could rescue odontoblastic differentiation, confirming by ALP and ARS staining. Moreover, NFIC overexpression also upregulated the mRNA levels of related markers.In summary, our data demonstrates that USP34 controls odontoblastic differentiation of DMCs during dental root morphogenesis through deubiquitinating and stabilizing NFIC.

***Disclosures: Shuang Jiang**, None*

P-325

Intestinal Vitamin D Receptor in Adult Mice is Essential to Maintain Bone Mass When Calcium Intake is Low but Dispensable When Calcium Intake is Adequate *Heng Jiang[1], Sylvia Christakos[2], James Fleet[1]. [1]Dept. of Nutrition Science, Purdue University, United States, [2]Dept. of Microbiology, Biochemistry and Molecular Genetics, Rutgers New Jersey Medical School, United States

During rapid bone accrual, 1,25(OH)2D/vitamin D receptor (VDR) mediated intestinal Ca absorption (Ca Abs) is necessary to supply adequate Ca. However, the importance of vitamin D-mediated intestinal Ca Abs for adult bone maintenance is unknown. We tested the hypothesis that 1,25(OH)2D-mediated intestinal Ca Abs has a significant role in adult bone health. Transgenic mice were developed to allow inducible VDR gene knockout from the whole intestine (Villin promoter-CreERT2+/- x VDRf/f mice, WIK) or from the large intestine (CDX2 promoter-CreERT2+/- x VDRf/f mice, LIK). Littermates with no CreERT2 transgene were used as controls. At weaning, mice were fed AIN93G diet (0.5% Ca, 0.4% P, 200 IU VD3). At 4 mo of age, mice received tamoxifen (TAM, 1 mg/20 g body weight, i.p. for 5 d) to induce recombination of the floxed VDR alleles. TAM caused complete VDR deletion along the whole intestine in WIK mice whereas LIK mice had limited recombination in ileum, complete recombination in cecum, and partial recombination in the proximal colon (PCo). After TAM, mice were randomized to AIN93M diet with either 0.5% (adequate) or 0.2% (low) Ca for either 2 or 16 wks (n=12/group). On adequate Ca intake, WIK and LIK mice had similar levels of serum 1,25(OH)2D, Ca Abs, BMC and BMD as the controls. In control mice, low Ca intake increased serum 1,25(OH)2D level (+1.9-fold), which upregulated S100g gene expression and Ca Abs in the duodenum (Dd) and PCo (all $p<0.05$). Neither BMD nor BMC were altered by feeding the low Ca diet to control mice, indicating physiologic adaptation was sufficient to prevent bone loss. In WIK mice, the low Ca diet caused a more dramatic increase in serum 1,25(OH)2D (4.4-fold) but the adaptive increases in Dd and PCo Ca Abs and S100g mRNA were eliminated and BMC and BMD levels were significantly reduced (-28.2 and -23.6%, $p<0.0001$). LIK mice adapted to the low Ca diet by increasing serum 1,25(OH)2D (+2.5-fold). While Dd S100g expression and Dd Ca Abs were appropriately increased in the low Ca fed LIK mice, neither PCo S100g levels nor PCo Ca Abs were increased and there was a 12% decline in BMD and BMC. Our data suggest that in adult mice, vitamin D signaling plays a minimal role in regulating Ca Abs and protecting bone mass when dietary Ca intake is adequate. In contrast, vitamin D signaling in the whole intestine, and to a lesser extent the PCo, are critical to upregulate Ca Abs and protect bone when dietary Ca intake is low.

***Disclosures: Heng Jiang**, None*

P-326

In Pediatric X-linked Hypophosphatemia (XLH), Burosumab Improved Clinical Outcomes Versus Higher and Lower Doses of Oral Phosphate and/or Active Vitamin D *Erik A. Imel[1], Francis H. Glorieux[2], Michael P. Whyte[3], Anthony A. Portale[4], Craig F. Munns[5], Ola Nilsson[6], Jill H. Simmons[7], Raja Padidela[8], Noriyuki Namba[9], Hae Il Cheong[10], Pisit Pitukcheewanont[11], Etienne Sochett[12], Wolfgang Högler[13], Koji Muroya[14], Hiroyuki Tanaka[15], Gary S. Gottesman[16], Andrew Biggin[5], Farzana Perwad[4], Angel Chen[17], Mary Scott Roberts[17], Leanne Ward[18]. [1]Indiana University School of Medicine, United States, [2]Shriners Hospitals for Children, Canada, McGill University, Canada, [3]Shriners Hospitals for Children-St Louis, United States, [4]Department of Pediatrics, University of California, San Francisco, United States, [5]The University of Sydney Children's Hospital Westmead Clinical School, The Children's Hospital at Westmead, Australia, [6]Center for Molecular Medicine, Karolinska Institutet, Sweden, [7]Department of Pediatrics, Division of Endocrinology and Diabetes, Vanderbilt University School of Medicine, Vanderbilt University, United States, [8]Department of Paediatric Endocrinology, Royal Manchester Children's Hospital, United Kingdom, [9]Osaka Hospital, Japan Community Healthcare Organization and Osaka University Graduate School of Medicine, Osaka, Japan currently at Tottori University Faculty of Medicine, Japan, [10]Seoul National University Children's Hospital, Republic of Korea, [11]Center of Endocrinology, Diabetes and Metabolism, Children's Hospital of Los Angeles, United States, [12]Department of Pediatrics, Hospital for Sick Children, Canada, [13]Department of Paediatrics and Adolescent Medicine, Johannes Kepler University Linz, Austria, [14]Kanagawa Children's Medical Center, Japan, [15]Okayama Saiseikai General Hospital Outpatient Center, Japan, [16]Shriners Hospitals for Children-St. Louis, United States, [17]Ultragenyx Pharmaceutical Inc., United States, [18]University of Ottawa, Canada

In a phase 3 trial in children with XLH (CL301; NCT02915705), burosumab resulted in greater improvements in hypophosphatemia and related morbidities than continuation with oral phosphate and active vitamin D (Pi/D). Here, we present a post-hoc analysis assessing the response to burosumab vs higher or lower average daily doses of Pi/D over 64 weeks. Children (1-12 years-old) with XLH receiving Pi/D with Rickets Severity Score >=2.0 were randomized 1:1 to 64 weeks of burosumab starting at 0.8 mg/kg subcutaneously Q2W or to resume Pi/D. Pi/D dose categories were assessed as: phosphate >40 mg/kg (HPi), phosphate <=40 mg/kg (LPi), alfacalcidol >60 ng/kg or calcitriol >30 ng/kg (HD), and alfacalcidol <=60 ng/kg or calcitriol <=30 ng/kg (LD). We used the Radiographic Global Impression of Change (RGI-C) to assess rickets healing at 64 weeks based on Pi/D dose categories before (pre-baseline) and during study. The distribution of children in the Pi/D dose categories pre-baseline were: 8 HPi, 21 LPi, 7 HD, and 22 LD in the burosumab group (n=29), and 3 HPi, 29 LPi, 7 HD, and 25 LD in the Pi/D group (n=32). On-study, the distribution was 12 HPi, 20 LPi, 14 HD, and 18 LD in the Pi/D group. Regardless of Pi/D doses administered pre-baseline, children receiving burosumab had an approximately two-fold greater improvement in least square (LS) mean RGI-C score for rickets healing vs those continuing Pi/D (Table). Further, at Week 64, the LS mean RGI-C score with burosumab (2.1 +/-0.1) was greater vs on-study treatment with HPi (1.0 +/-0.2), LPi (1.0 +/-0.2), HD (1.5 +/-0.2), or LD (0.7 +/-0.2). The LS mean improvement in lower limb deformity RGI-C with burosumab (+1.3 +/-0.2) was greater vs HPi (+0.3 +/-0.2), LPi (+0.3 +/-0.1), HD (+0.4 +/-0.2), or LD (+0.2 +/-0.1). The LS mean alkaline phosphatase (U/L) decrease from baseline with burosumab was -174 +/-14 vs HPi (-43 +/-29), LPi (-19 +/-28), HD (-59 +/-30), or LD (-4 +/-24). The mean parathyroid hormone (PTH) percent change from baseline with burosumab was +10.5 +/-13.3 vs HPi (+45.2 +/-41.0), LPi (-9.5 +/-13.1), HD (-29.3 +/-15.5), or LD (+42.5 +/-27.2). Adverse events on burosumab included mild to moderate hypersensitivity and injection site reactions. No discontinuations occurred. In children with XLH, improvements in rickets, lower limb deformity, and decreases in ALP were greater during burosumab than with either higher or lower on-study doses of phosphate or active vitamin D. The increase in PTH was greatest in the HPi and LD groups.

Table: Radiographic Global Impression of Change (RGI-C) for Rickets Healing by Treatment Categories

	Burosumab (N = 29)		Pi/D (N = 32)	
Pre-baseline Dose Categories				
	HPi (n = 8)	**LPi (n = 21)**	**HPi (n = 3)**	**LPi (n = 29)**
Week 64 RGI-C, LS mean ± SE	1.8 ± 0.2	2.1 ± 0.1	0.7 ± 0.2	1.1 ± 0.1
	HD (n = 7)	**LD (n = 22)**	**HD (n = 7)**	**LD (n = 25)**
Week 64 RGI-C, LS mean ± SE	1.9 ± 0.2	2.1 ± 0.1	1.1 ± 0.2	1.0 ± 0.2
On-study Dose Categories				
	Burosumab (n = 29)		**HPi (n = 12)**	**LPi (n = 20)**
Week 64 RGI-C, LS mean ± SE	2.1 ± 0.1		1.0 ± 0.2	1.0 ± 0.2
			HD (n = 14)	**LD (n = 18)**
Week 64 RGI-C, LS mean ± SE			1.5 ± 0.2	0.7 ± 0.2

HPi = phosphate > 40 mg/kg; LPi = phosphate ≤ 40 mg/kg; HD = alfacalcidol > 60 ng/kg or calcitriol > 30 ng/kg; LD = alfacalcidol ≤ 60 ng/kg or calcitriol ≤ 30 ng/kg; LS = least square.

***Disclosures: Erik A. Imel**, Ultragenyx Pharmaceutical Inc., Consultant, Ultragenyx Pharmaceutical Inc., Grant/Research Support*

P-327

Differential iron requirements of osteoblast and adipocyte differentiation *Erica Clinkenbeard[1], Daniel Edwards III[1], Christian Wright[2], William Thompson[2]. [1]Indiana University School of Medicine, United States, [2]Indiana University, United States

Iron is a key mineral component for several cellular and biological processes including oxygen transport. Iron deficiency is highly prolific across the world and often synonymous with chronic kidney disease (CKD). Recent human studies demonstrated that iron deficiency anemia correlated with increased fracture risk independent of other known risk factors. In the adenine diet model of induced kidney failure, iron deficiency anemia correlates with development of severe cortical porosity and marrow adipocyte accumulation. Therefore, we hypothesized iron deficiency impairs normal osteoblast maturation and may enhance adipocyte differentiation. To undertake these studies we used a mouse immortalized mesenchymal progenitor cell (MPC-2), which proliferates continuously and maintains differentiation capacity for chondrocytes, adipocytes and osteoblasts. MPC-2 cells were incubated in osteogenic media (OM) with increasing concentrations of deferoxamine (DFO), to mimic iron deficiency. After 14 days, OM control cells showed a significant induction of osteoblast genes including Bglap, Col1a1 and Dmp1 ($p<0.05$ compared to undifferentiated cells). The highest concentration of DFO significantly blunted the osteoblast gene expression ($p<0.01$ vs OM control) and suppressed mineralized nodule formation. Hypoxia inducible factor 1α (HIF1α), used to adapt to iron deficient/hypoxic conditions, accumulated in the cells treated with DFO. Transferrin receptor (Tfrc), a known HIF1α target, increased in a DFO dose dependent manner. Activation of HIF1α in bone typically enhances osteoblast differentiation suggesting low-iron affects osteoblast function independent of HIF1α. TUNEL staining in these conditions confirmed no increased cell death with prolonged exposure to DFO. MPC2 cells were then differentiated in adipogenic media (AM) with similar DFO concentrations for 14 days. In contrast to the osteoblast experiments, chronic treatment with DFO had no effect on adipocyte differentiation. Gene expression of key factors including Pparγ, Lpl and AdipoQ were similar between DFO treated and AM control cells. Oil red o staining demonstrated no deficits in the ability of the cells to accumulate lipid with or without DFO. In summary, osteoblast differentiation maintains a higher iron requirement for proper differentiation and function compared to adipocytes. Iron deficiency could therefore be a significant contributing factor to bone loss, and elevated fracture risk in CKD.

***Disclosures: Erica Clinkenbeard**, None*

P-328

Osteocyte-specific deletion of FGF23 partially corrects bone growth and mineralization in DMP1KO ARHR mice *Lauriane Hivert[1], Emily Lynch[1], Jadeah Spindler[1], Wenhan Chang[2], Jian Q Feng[3], Valentin David[1], Aline Martin[1]. [1]Division of Nephrology and Hypertension, Northwestern University, United States, [2]Department of Medicine, University of California San Francisco, United States, [3]College of Dentistry, Texas A&M University, United States

Autosomal recessive hypophosphatemic rickets (ARHR) is caused by inactivating mutations of dentin matrix protein 1 (DMP1) that lead to primary increases in fibroblast growth factor 23 (FGF23) expression in osteocytes and circulating intact FGF23 (iFGF23)

levels, which result in hypophosphatemia, rickets and osteomalacia. To determine the role of osteocyte-produced FGF23 and hypophosphatemia on rickets/ostomalacia, we compared the bone and mineral phenotype of wild type (WT), FGF23DMP1-cKO (harboring an osteocyte-specific deletion of FGF23 using DMP1-cre), DMP1KO and compound mutant DMP-1KO/FGF23DMP1-cKO male mice at 12 weeks of age. We measured levels of markers of mineral metabolism in the circulation, measured bone length to evaluate bone growth and assessed trabecular and cortical bone microarchitecture and density by 3D-microtomography. Compared to WT mice, FGF23DMP1-cKO mice showed a 40% reduction in serum iFGF23 levels and a 35% increase in serum phosphate ($p<0.05$). This was associated with reduced cortical bone porosity, increased cortical area (Ct.Ar) and bone mineral density (Ct. BMD) ($p<0.05$), but similar trabecular bone phenotype and bone growth to WT mice. As previously reported, DMP1KO mice showed a 20-fold increase in serum iFGF23, low serum phosphate and increased PTH levels (+5-fold) ($p<0.05$). DMP1KO mice also showed impaired growth demonstrated by reduced body weight and shorter femur and tibia lengths ($p<0.05$), and all the characteristic of rickets and osteomalacia, including larger epiphyses, bone cross-sectional area (CSA) and marrow area (Ma.Ar), and reduced BMD, trabecular BV/TV, and Ct.Ar (each $p<0.05$). Osteocyte-specific deletion of FGF23 in DMP1KO mice corrected iFGF23 levels by 80%, normalized serum phosphate, and lowered PTH levels by 50% ($p<0.05$ vs. DMP1KO). Despite the complete correction of hypophosphatemia, DMP-1KO/FGF23DMP1-cKO mice showed only partial corrections of body weight and bone growth (+70% and +50%, $p<0.05$ vs. DMP1KO) and residual features of rickets. BMD also was only partially improved (+50%, $p<0.05$ vs. DMP1KO) while BV/TV and Ct.Ar showed a near complete rescue (NS vs. WT). These data show that complete correction of hypophosphatemia by the osteocyte specific deletion of FGF23 in DMP1KO mice only partially corrected bone growth and mineralization. Whether the residual phenotype is due directly to DMP1 deficiency or additional effects of FGF23 on bone remains to be determined.

***Disclosures: Lauriane Hivert**, None*

P-329

UK Biobank GWAS Identifies 197 Novel Loci for Serum Alkaline Phosphatase Concentrations *Fadil Hannan[1], Mark McCarthy[2], Diane Smelser[3], Xin Meng[1], Juho Asteljoki[1], Taha Elajnaf[4], William Rayner[1], Gerda Breitwieser[4], David Carey[3], Richard Eastell[5], Anubha Mahajan[2], Rajesh Thakker[1]. [1]University of Oxford, United Kingdom, [2]Genentech, United States, [3]Weis Center for Research, Geisinger, United States, [4]Florida Atlantic University, United States, [5]University of Sheffield, United Kingdom

Alkaline phosphatase (ALP) is a zinc-containing membrane glycoprotein, which plays a key role in skeletal mineralisation, and is widely used in the investigation of bone and liver disease. Serum ALP comprises a mixture of isoforms mainly from liver and bone, and partially from the intestine, especially in individuals with blood groups O and B, or who are secretors of blood group antigens. Serum ALP has >50% heritability, yet the genetic determinants of this biomarker remain to be fully elucidated. We performed a GWAS of serum ALP concentrations involving 274,547 adult individuals of European ancestry from the population-based UK Biobank cohort. Individuals with vitamin D deficiency (25-hydroxyvitamin D <30nmol/L), impaired kidney function (eGFR <60 ml/min/1.73m2), or alterations in bilirubin or gamma glutamyl transferase were excluded. Variant associations were assessed using a linear mixed model adjusted for age, sex, array, and relatedness in samples and population structure. Genome-wide significance was defined at p140,000 individuals. We identified 239 genome-wide significant loci, and the most significant associations were with the reported asialoglycoprotein receptor 1 (ASGR1)(rs55714927, p=3.3e-226), ABO blood group (ABO) (rs550057, p=1.7e-211) and the tissue non-specific ALP (ALPL) (rs72659192, p=2.7e-188) genes. 197 loci were novel and included genes with likely roles in ALP glycosylation (ST3GAL3), zinc incorporation (SLC30A5) and membrane attachment (PIGV, PGAP3). In silico analysis was undertaken to identify gene enrichment in cellular pathways and expression in bone and liver. This identified novel associations between serum ALP and genes involved in osteoclast activation (CFOS, NFATC1) and bone resorption (MMP9), and in bile acid synthesis (BAAT, PROX1, AKR1C4, HSD3B7) and secretion (UGT2B7, SULT2A1, ITPR2). Moreover, genes were enriched in the macro-autophagy pathway, which mediates the clearance of cytosolic components. Thus, serum ALP was associated with genes involved in autophagosome formation (ATG4B, ATG7, ATG10), lysosome activation (TFEB), and autophagosome-lysosome fusion (RILP, UVRAG, FYCO1). In summary, these findings demonstrate a role for genes involved in glycoprotein processing, osteoclast activation and bile acid secretion in regulating serum ALP. In addition, this study highlights a novel association between serum ALP and the macro-autophagy pathway.

***Disclosures: Fadil Hannan**, None*

P-330

Alterations in dental hard tissues in Nogo-A mutant mice *Pierfrancesco Pagella[1], Martin Schwab[2], Thimios Mitsiadis[1]. [1]Institute of Oral Biology, Center of Dental Medicine, Faculty of Medicine, University of Zurich, Zurich, Switzerland, Switzerland, [2]Institute for Regenerative Medicine, University of Zurich, 8952 Schlieren, Switzerland, Switzerland

Initially discovered as a potent inhibitor of neurite outgrowth, in the last decades Nogo-A emerged as a fundamental actor of nervous system development, physiology, pathology and regeneration. In this context, Nogo-A became a promising target for central nervous system (CNS) regeneration- However, despite the already known widespread expression of Nogo-A in non-neuronal tissues, its role outside the CNS has been poorly investigated. We here show a completely novel function for Nogo-A during tooth development. Tooth formation results from a complex set of sequential and reciprocal interactions between the oral epithelium and the cephalic neural crest derived-mesenchyme. The epithelium folds around the mesenchyme that forms the dental follicle and dental pulp. Pulp cells adjacent to the dental epithelium differentiate into odontoblasts and secrete dentin, while epithelial cells adjacent to the pulp differentiate into ameloblasts and secrete enamel. We observed that Nogo-A was expressed in both ameloblasts and odontoblasts from early developmental stages. Transmission and scanning electron microscopy analysis revealed that its deletion in a Nogo-A KO transgenic mouse model led to a general disorganization of ameloblasts and the generation of defective enamel. Conditional deletion of Nogo-A in the dental epithelium (K14:Cre;Nogo-A) was sufficient to cause defects in enamel organization and structure, indicating a completely novel, epithelium-specific role for Nogo-A. RNA sequencing analysis showed that, in this context, the loss of Nogo-A induced the upregulation of genes involved in ameloblastic differentiation. Taken together, these results indicate a completely novel set of functions for Nogo-A outside the neural tissues, revealing it as an important regulator of enamel formation.

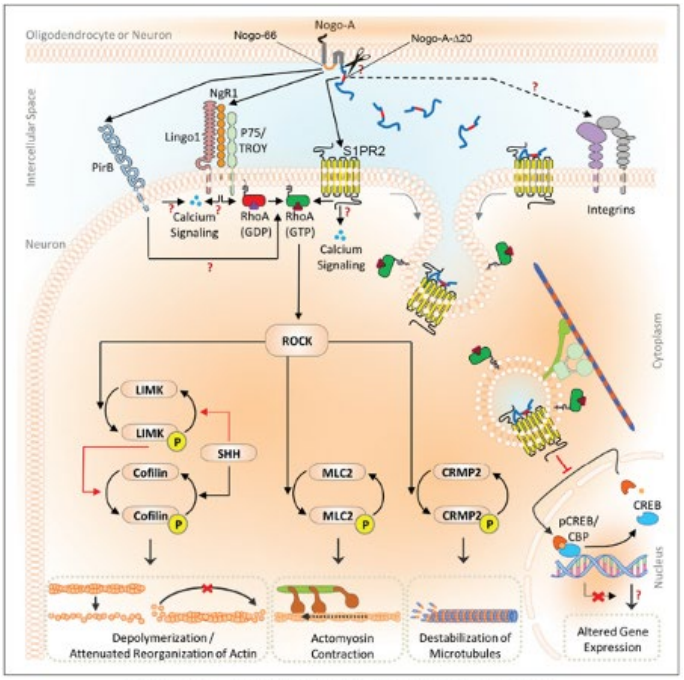

Nogo-A signaling pathway

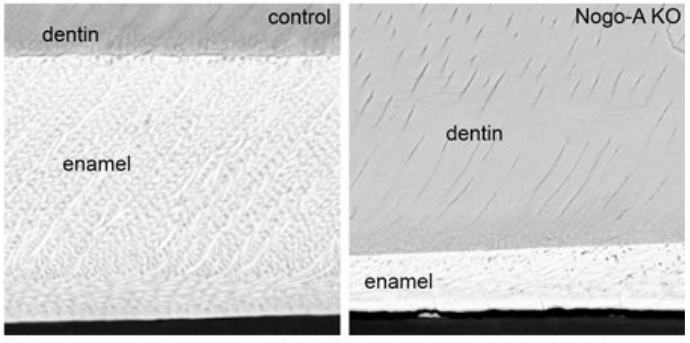

Enamel defects in Nogo-A KO teeth

***Disclosures: Pierfrancesco Pagella**, None*

P-331

Chondrocyte-specific Efnb1 expression promotes angiogenic and bone formation gene expression during fracture repair *Charles Rundle[1], Subburaman Mohan[2]. [1]VA Loma Linda Healthcare System, United States, [2]VA Loma Linda Heathcare System, United States

The ephrin families of ligands and receptors mediate tissue development and homeostasis. We have previously observed the ephrinB1 gene (Efnb1) to exhibit significant changes in

Posters

gene expression during endochondral bone repair. Because EFNB1 is expressed in pre-hypertrophic chondrocytes during fracture repair, we examined fracture healing when Efnb1 expression was disrupted in chondrocytes. We previously reported that Efnb1 deficiency in chondrocytes produced no significant differences in fracture cartilage but resulted in a 25% reduction of the partial bone volume of the fracture callus at 3 weeks post-fracture, a time when the fracture cartilage is replaced by woven bone. To identify molecular pathways by which Efnb1 might regulate this effect, we examined fracture callus gene expression in Col2 chondrocyte-specific Efnb1 knockout mice at 3 weeks healing.Closed femur fractures were performed in chondrocyte conditional knockout (cKO), Cre+Efnb1floxed and control Cre+Efnb1WT mice. Total RNA was isolated from whole fracture calluses at 3 weeks after fracture (n=4/group) and gene expression analyzed by real-time RT-PCR for markers of bone formation, remodeling and angiogenesis, as well as ephrin ligands and receptors that might compensate for Efnb1 deficiency. Statistical analysis was performed by ANOVA with Tukey post-hoc confirmation.Alkaline phosphatase (Alp) expression was significantly reduced in the cKO mouse fractures at 3 weeks post-fracture to 0.70 of control fractures ($P<0.015$) but osteocalcin (Bglap) expression was not different from that of control fractures. None of the remodeling-related genes examined (Tnfsf11, Ctsk and Mmp9) displayed any significant differences in fracture expression between cKO and control mice. Of the angiogenesis-related genes, von Willebrand's Factor (Vwf) expression was down-regulated to 0.37 of the control fractures ($P<0.015$) but Hif1a expression was not different between the two genotypes. The cKO fracture expression of the ephrin ligand Efnb2 was down-regulated to 0.64 of control fractures ($P<0.045$), but the expression of Efnb3 and the ephrin receptor Ephb4 was not different between cKO and control fractures.Based on our results, we propose that: 1) Efnb1 expressed in chondrocytes regulates fracture callus angiogenesis through Vwf, as well as the early stages of mineralization during bone formation through Alp. 2) Efnb1 may recruit other Efn family members to mediate its anabolic effects on fracture healing.

***Disclosures: Charles Rundle**, None*

P-332

Localization of Annexin A6 and its translocation across membrane in matrix vesicles during apatite formation *Ekeveliny Amabile Veschi[1], Maytê Bolean[1], Yubo Wang[2], Agnieszka Strzelecka-Kiliszek[3], Joanna Bandorowicz-Pikula[4], Slawomir Piluka[5], Ofelia Maniti[6], Thierry Granjon[7], Saida Mebarek[8], David Magne[8], Ana-Paula Ramos[1], Nicolas Rosato[9], José Luis Millán[10], He Tian [11], Xiao-Peng He[12], Massimo Bottini[9], Pietro Ciancaglini[13], Rene Buchet[8]. [1]Departamento de Química, FFCLRP-USP, Brazil, [2]East China University of Science and Technology, China, [3]Laboratory of Biochemistry of Lipids, Nencki Institute of Experimental Biology, Poland, [4]Laboratory of Cellular Metabolism, Nencki Institute of Experimental Biology, Poland, [5]Laboratory of Biochemistry of Lipids, Nencki Institute of Experimental Biology, Poland, [6]Universite de Lyon, ICBMS, UMR 5246, CNRS, France, [7]Universite de lyon, ICBMS, UMR 5246, CNRS, France, [8]Universite de Lyon, ICBMS, UMR 5246, CNRS, France, [9]Department of Experimental Medicine, University of Rome Tor Vergata, Italy, [10]Sanford Burnham Prebys Medical Discovery Institute, United States, [11]Key Laboratory for Advanced Materials and Joint International Research Laboratory of Precision Chemistry and Molecular Engineering, Feringa Nobel Prize Scientist Joint Research Center, East China University of Science and Technology, China, [12]Institute of Fine Chemicals, School of Chemistry & Molecular Engineering East China University of Science & Technology, China, [13]Departamento de Química, Faculdade de Filosofia, Ciências e Letras de Ribeirão Preto da Universidade de São Paulo (FFCLRP-USP), Brazil

Matrix vesicles (MVs) of 100-300 nm diameter are released by mineralization competent cells to initiate formation of apatite. Among proteins present in MVs, annexin A6 (AnxA6) is the largest member of the annexin family of proteins. To define functions of AnxA6 during mineralization, we determined its localization in MVs. MVs were extracted from bone femurs of chicken embryos. Western blot on extracts of MV membranous fractions, indicated that AnxA6 is found in the MV-lumen, as a MV-transmembrane, on the internal and external leaflets of the MV bilayer. AnxA6 is selectively recruited by cholesterol in MVs as probed by the addition of methyl-β-cyclodextrin. Thermodynamics analysis on monolayers and proteoliposomes composed of either dipalmitoylphosphatidylcholine (DPPC) to mimic the outer leaflet of the MV or a 9:1 DPPC:dipalmitoylphosphatidylserine (DPPS) mixture to mimic the inner leaflet, confirmed that AnxA6 interacted differently with each class of phospholipids. AnxA6-lipid interaction was also Ca2+-dependent, as evidenced by the increase in surface pressure of negatively charged 9:1 DPPC:DPPS monolayers and a decrease in enthalpy in 9:1 DPPC:DPPS proteoliposomes caused by the addition of AnxA6 in the presence of Ca2+ compared to DPPC zwitterionic bilayers. Protrusion of the protein at the surface of DPPC proteoliposomes observed by AFM suggested that AnxA6, in the polymeric form, interacted with the vesicle membrane. A decrease in pH inside MVs during apatite formation was observed. We hypothesized that acidification may render the protein hydrophobicity facilitating its insertion into the bilayer of MVs, which was monitored with fluorophore N-4-hydroxyphenyl-N'-phenyl dihydrodibenzo[a,c]phenazine. Addition of Anx6 to either DMPC at both pHs 7.4 and 5.4, or DMPC: DPPS (9:1) at pH 7.4 decreased membrane fluidity, consistent with AnxA6 interactions with the surface of bilayer. In contrast, AnxA6 addition to DMPC: DPPS (9:1) at pH 5.4 increased the fluidity of the liposome membrane, suggesting insertion of AnxA6 into the bilayer, accompanied by changes in the protein secondary structure as observed by CD during acidification. Distinct localization of AnxA6 during apatite formation may reflect several steps of mineralization process, formation of nucleation core with AnxA6 on the internal leaflet of MVs, apatite-formation inducing AnxA6 translocation, and MV binding to collagen with AnxA6 at the external leaflet of MVs.

***Disclosures: Ekeveliny Amabile Veschi**, None*

P-333

Prrx1-CreAlplfl/fl mice, a model for further investigations into the pathophysiological changes in hypophosphatemia *Victoria DeMambro[1], Jennifer Daruszka[1], Daniel Brooks[2], Mary Bouxsein[2], Cliff Rosen[1]. [1]Maine Medical Center Research Institute, United States, [2]Center for Advanced Orthopaedic Studies, Beth Israel Deaconess Medical Center, United States

Hypophosphatasia (HPP) is caused by loss of function mutations in the tissue-nonspecific alkaline phosphatase (TNSALP) gene (Alpl) resulting in rickets, osteomalicia, bone fragility and lean body mass in severe childhood forms. In vitro, inhibition of TNSALP leads to decreased lipid accumulation suggesting TNSALP, an enzyme known for its mineralizing properties, may be pro-adipogenic. TNSALP may play a role in bone marrow mesenchymal stem cell (BMMSC) lineage determination between osteoblasts and adipocytes. Alpl-/- mice die postnatally, therefore, to further delineate TNSALP's role in bone homeostasis and adipogenesis we are utilizing a Prrx1-Cre driver mated with to an Alplflfl (CreAlplflfl) mouse line. Male and female CreAlplflfl and control mice were evaluated for body composition and areal bone mineral density (aBMD) at 8, 16 and 24wks of age by DXA analysis (n=10/geno/gender). Metabolic cage analysis was performed at 24wks of age (n=8/geno/gender). At sacrifice body weights, serum, inguinal fat depots (IWAT) and long bones were isolated for MicroCT/histological analysis and gene expression. In vitro BMMSCs were differentiated into osteoblasts and adipocytes as well as the stromal vascular fraction (SVF) from the inguinal fat (IWAT) depot to query osteoblastic and adipogenic capacity in CreAlplflfl cells. At 8, 16 and 24wks of age CreAlplflfl mice exhibited significantly reduced body weight and femoral aBMD compared to controls. CreAlplflfl fat mass was reduced at 8 and 16wks however, by 24wks there were no differences relative to controls. Alpl expression was reduced by 70% in CreAlplflfl IWAT depots coupled with a reduction in adipocyte size. CreAlplflfl femurs had reductions in length, cortical thickness, area and BMD with increases in marrow area. MicroCT imaging revealed an extremely disorganized growth plate as well as reduced trabecular bone mass, thickness, number in CreAlplflfl femurs. Metabolically, male CreAlplflfl mice exhibited decreased energy expenditure relative to controls, correlating with decreased activity levels. Preliminary BMMSCs cultures had decreased osteoblast mineralization coupled with increased adipogenesis in CreAlplflfl cells. Conversely, CreAlplflfl IWAT SVF cultures exhibited reductions in lipid accumulation. In sum, ongoing studies of Prrx1-CreAlplflfl mouse model will help elucidate probable intracellular actions of TNSALP and aid in a greater understanding of the pathophysiological changes that occur in bone and fat in HPP.

***Disclosures: Victoria DeMambro**, None*

P-334

UK Biobank GWAS Reveals Influence of Parathyroid-Bone-Kidney Axis on Serum Calcium and Phosphate Concentrations *Taha Elajnaf[1], Fadil Hannan[1], Mark McCarthy[2], Diane Smelser[3], Juho Asteljoki[1], Xin Meng[1], William Rayner[1], Gerda Breitwieser[4], David Carey[3], Richard Eastell[5], Anubha Mahajan[2], Rajesh Thakker[1]. [1]University of Oxford, United Kingdom, [2]Genentech, United States, [3]Weis Center for Research, Geisinger, United States, [4]Florida Atlantic University, United States, [5]University of Sheffield, United Kingdom

Mineral metabolism is tightly coordinated by interactions between the parathyroid glands, bone and kidneys. We further characterized the genetic determinants influencing this process by undertaking a genome-wide association study (GWAS) of serum calcium and phosphate concentrations, which are heritable traits, in >308,000 adult individuals of European ancestry from the population-based UK Biobank cohort. Individuals with vitamin D deficiency (25-hydroxyvitamin D <30nmol/L) or low estimated glomerular filtration rate (eGFR, <60 ml/min/1.73m2) were excluded, and serum calcium was adjusted for alterations in serum albumin. Directly genotyped and imputed variants were assessed using a linear mixed model adjusted for age, sex, array, and relatedness in samples and population structure. Genome-wide significance was defined at p140,000 individuals. These findings demonstrate that variants in genes encoding key components of the parathyroid-bone-kidney axis influence both serum calcium and phosphate concentrations. Identification of these genetic determinants may help elucidate the pathophysiological basis of calcitropic disorders and highlight targets for the therapeutic modulation of mineral homeostasis.

***Disclosures: Taha Elajnaf**, None*

P-335

A novel GNAS duplication associated with loss-of-methylation restricted to exon A/B causes pseudohypoparathyroidism type Ib (PHP1B) *Monica Reyes[1], Masayo Kagami[2], Dirk Schnabel[3], Maki Fukami[2], Harald Jueppner[4]. [1]Massachusetts General Hospital, United States, [2]National Research Institute for Child Health and Development, Japan, [3]Pädiatrische Endokrinologie und Diabetologie Charitè, Universitätsmedizin Berlin, Germany, [4]Massachusetts General Hospital and Harvard Medical School, United States

Pseudohypoparathyroidism type Ib (PHP1B) is characterized by resistance to parathyroid hormone (PTH) leading to hypocalcemia and hyperphosphatemia, and in some cases resistance towards additional hormones. Patients affected by this disorder all share a loss-of-methylation at the differentially methylated GNAS exon A/B, which reduces expression of the stimulatory G protein α-subunit (Gsα) from the maternal allele. In the proximal renal tubules, the paternal GNAS allele does not contribute significantly to expression of this signaling protein. Thus LOM at the maternal exon A/B leads to little or no Gsα thereby causing PTH-resistance in that portion of the kidney. We now describe a PHP1B patient with a de novo genomic GNAS duplication of approximately 88-kb, which is associated with LOM restricted to exon A/B. Multiplex ligation-dependent probe amplification (MLPA), comparative genomic hybridization (CGH) and whole genome sequencing (WGS) established that the added DNA fragment extends from GNAS exon AS1 (telomeric breakpoint) to a small region between two imperfect repeats just up-stream of LOC105372695 (centromeric breakpoint). Our novel duplication is considerably shorter than previously described duplications/triplications in that portion of chromosome 20q13 and it does not affect methylation at exons AS and XL. Based on these and previous findings, it appears plausible that the identified genomic abnormality disrupts in cis the actions of a transcript that is required for establishing or maintaining exon A/B methylation. Our findings extend the molecular causes of PHP1B and provide additional insights into the structural GNAS features that are required for maintaining maternal Gsα expression and for preventing PTH-resistance.

***Disclosures: Monica Reyes**, None*

P-336

An overview of the etiology, clinical manifestations, management strategies and complications of hypoparathyroidism from the Canadian National Hypoparathyroidism Registry *Hajar Abu Alrob[1], Sharjil Hussain [2], Mihai Romanovschi[2], Rafik El Werfalli[2], Hisham Al Kassem[1], Manoela Braga[1], Tayyab S Khan [3], Adam Miller[4], Zubin Punthakee[1], J.E.M Young[1], Muhammad Shrayyef[1], Aliya Khan[1]. [1]McMaster University, Canada, [2]Bone Research and Education Centre, Canada, [3]Western University, Canada, [4]University of Toronto, Canada

Objective(s):The Canadian National Hypoparathyroidism Registry was formed in 2014, with an aim to• identify the etiology and presenting symptoms of patients with hypoPTH.• evaluate current treatment practice in Canada.• assess differences in presentation based on etiology of the disease.• compare parameters of calcium homeostasis amongst those developingcomplications of nephrolithiasis or nephrocalcinosis versus those withoutcomplications.• assess fracture risk and microstructure in Canadian patients with hypoPTH.Material and Methods:• Prospective observational registry of 130 patients >18 years of age. • The inclusion criteria:1. Chronic HypoPTH (low PTH in the presence of low serum calcium [total or ionized] for at least 6 months prior to enrolment)2. HypoPTH (including post-surgery) requiring calcium/calcitriol replacement to maintain normal calcium (total or ionized) level for at least 6 months prior to enrolment3. Pseudohypoparathyroidism with elevated PTH and low serum calcium (total or ionized), normal vitamin D and hyperphosphatemia•Exclusion criteria:1. Transient hypoPTH which resolved within <6 months of treatment.•We reviewed etiology, initial clinical presentation, laboratory investigations, management strategies, markers of skeletal health including fractures, bone mineral density (BMD), and complications including nephrolithiasis/nephrocalcinosis, and basal ganglia calcification. Fracture risk was determined using the Canadian Association of Radiologists and Osteoporosis Canada (CAROC) toolResults: 70% (91/130) of patients had postsurgical hypoparathyroidism, 25% had idiopathic/autoimmune disease (31/130) and 3% had pseudohypoparathyroidism (4/130). The mean age of onset was 41.8 years. All patients were on calcium supplements, 85% were on calcitriol (N=111), 30 patients were on PTH(1-34) and 3 patients were on PTH(1-84). Nephrocalcinosis or nephrolithiasis was observed in 27% (n=14/52) of patients with postsurgical disease and 17% (n=4/24) of patients with nonsurgical hypoparathyroidism. Among patients with postsurgical hypoparathyroidism, 15% (n=5/34) has basal ganglia calcification and among patients with nonsurgical hypoparathyroidism, 37% (n=7/19) had basal ganglia calcification. Approximately 44 patients (34.0%) required hospitalization at initial presentation. Patients with idiopathic/autoimmune disease were twice as likely to be hospitalized compared to those with postsurgical disease. Conclusion:1. HypoPTH is associated with a significant disease burden and leads to hospitalizationin a large number of patients.2. Renal complications of nephrocalcinosis and nephrolithiasis were present in 22.1% of treated patients and were more commonly seen in those with hypercalciuria.3. Fracture risk was low in the absence of traditional osteoporosis risk factors among these patients.

***Disclosures: Hajar Abu Alrob**, None*

P-337

Bone Marrow Fat in Women with Post-Surgical Hypoparathyroidism *Davide Diacinti[1], Cristiana Cipriani[2], Antonio Iannacone[3], Endi Kripa[3], Martina Orlandi[4], Jessica Pepe[5], Luciano Colangelo[5], Valentina Piazzolla[5], Daniele Diacinti[4], Salvatore Minisola[5]. [1]Department of Oral and MaxilloFacial Sciences, Umberto I Hospital, University Sapienza, Rome, Italy; Department of Diagnostic and Molecular Imaging, Radiology and Radiotherapy, University Tor Vergata, Rome, Italy, Italy, [2]Department of Clinical, Internal, Anesthesiological and Cardiovascular Sciences, "Sapienza" Rome University, Rome, Italy, Italy, [3]Department of Radiological Sciences, Oncology and Anatomo-Pathology, University Sapienza, Rome, Italy, Italy, [4]Department of Radiological Sciences, Oncology and Anatomo-Pathology, University Sapienza, Rome, Italy., Italy, [5]Department of Clinical, Internal, Anesthesiological and Cardiovascular Sciences, "Sapienza" Rome University, Rome, Italy., Italy

Introduction:Hypoparathyroidism (HypoPT) is characterized by reduced bone remodeling with average normal or high normal values of bone mineral density (BMD).There are instead no definitive data on prevalence of fragility vertebral fractures in HypoPTpatients or on possible risk factors.Among its several actions on bone metabolism, parathyroid hormone (PTH)stimulates commitment of bone marrow mesenchimal stem cells to osteoblasts, thus suppressing adipogenesis. An increased adipogenesis may therefore be hypothesized in HypoPT.Purpose: To assess lumbar spine Bone Marrow Fat (BMF) content in post-menopausal women with chronic post-surgical HypoPT using Magnetic Resonance Spectroscopy and evaluate how it could be related to vertebral fragility.Materials and methods: We studied 29 post-menopausal women with post-surgical HypoPT (mean age 66 +/- 6.8 SD years) and 20 healthy age-matched women. In all subjects we assessed: lumbar spine (L1-L4),femoral neck (FN) and total hip (TH) BMD by dual X-ray absorptiometry (Hologic QDR 4500A, USA); Trabecular Bone Score (TBS) on the L1-L4 images by the TBS-iNsight software; Vertebral Fracture Assessment (VFA) by iDXA (Lunar, GE, USA).BMF was measured by 3 Tesla L1-L5 MRI with application of the PRESS spectroscopy sequences on L3 vertebral body. Results:HypoPT subjects had significantly higher mean BMD values than controls (1.044 vs 0.956 g/cm^2; $p < 0.01$), andlower TBS values (1.218 vs 1.273; $p < 0.01$). Vertebral fractures by VFA were observedin 6/29 (20%) of HypoPTvs 2/20 (10%) of healthy subjects.Mean BMF values were significantly higher in HypoPT compared to healthy subjects: 79% vs 60% ($p<0.05$). The percentage of unsaturated, residual and saturated BMF in the HypoPTgroup were: 5%, 6% and 68%; in healthy subjects: 9%, 3%, 48%, respectively. We observed statistically significant negative correlationsbetween BMF values and both BMD (R=0.517; $p < 0.03$) and TBS (R=0.767; $p < 0.03$)in the HypoPT group.When only patients with vertebral fractures were compared, BMF was higher in HypoPT than in healthy subjects (62% vs 78%; $p<0.05$).Conclusion:BMFassessed by Magnetic Resonance Spectroscopy at the lumbar spine is increased in postmenopausal women with chronic post-surgicalHypoPT and is associated with increased prevalence of fragility fractures at this level.Hence, adipogenesis may be stimulated in the trabecular bone in the absence of PTH and associated with skeletal fragility.Keywords: Bone Marrow Fat; Hypoparathyroidism;MRI

***Disclosures: Davide Diacinti**, None*

P-338

Cpne7 Contributes to the Maintenance of Odontoblast Viability Under Stress Condition *Song Yi Roh[1], Joo-Cheol Park[1]. [1]Seoul National University, Republic of Korea

Precise regulation of epithelial-mesenchymal interaction (EMI) is critical during dentinogenesis. Cpne7, a member of calcium dependent phospholipid-binding copine family, was previously identified in the preameloblast conditioned medium (PA-CM). Cpne7 is believed to be secreted from dental epithelium and induce the differentiation of ectomesenchymal cells into preodontoblast and eventually into mature odontoblasts with odontoblast processes. Although the precise function of Cpne7 and detailed mechanisms regarding its role remain to be elucidated, accumulating evidence suggests Cpne7 as a key molecule that contributes to the formation of tubular tertiary dentin. Preliminary study showed that wild type mice formed reactionary dentin when dentin was slightly exposed with a high speed hand piece. On the other hand, Cpne7 deficient mice formed reparative dentin, in which odontoblast processes were absent and cell bodies were entrapped within bone-like dentin matrix. When recombinant CPNE7 protein was treated on the exposed dentin of Cpne7 KO mice, reactionary dentin was formed just as in WT mice. The goal of this study is to investigate the detailed mechanism of how Cpne7 contributes to the maintenance of odontoblast viability and reactionary dentin formation under stress condition. One hypothesis is that Cpne7 deficient cells are more vulnerable to stress therefore more likely to undergo apoptosis and die even under mild stress, and reparative dentin is formed as a result. The other hypothesis is that cpne7 deficiency disturbed odontoblast differentiation, leading to the loss of cell integrity and eventually, cell death. To test these hypothesis, the expression of the apoptosis related molecules was examined by western blotting, IF, IHC, and qPCR. Cpne7 knockdown upregulated the protein expression of p53 and pro-apoptotic factors, including BAX and BID in MDPC-23 cells. Anti-apoptotic factors such as Bcl-2 and Mcl-1, however, were upregulated as well. Bcl-2/Bax ratio did not show any significance. These results indicate that Cpne7 deficiency altered the expression of apoptotic factors but was insufficient to

Posters

cause cell death when no stress was applied. Further study is needed to examine the effects of Cpne7 in odontoblast differentiation and viability under stress.

***Disclosures: Song Yi Roh**, None*

P-339

NaQuinate, a Vitamin K Catabolite, is Found in Blood after Oral Vitamin K1 Administration and Reduces Osteoclast Activity Without Effecting Osteoclast Number in Culture *Isabel Orriss[1], Elizaveta Igumnova[2], Lars Ytrebo[2], Andrew Pitsillides[1], Ole-Martin Fuskevaag[2], Stephen Hodges[1]. [1]Royal Veterinary College, United Kingdom, [2]Tromso University Hospital, Norway

Background: High dose vitamin K is used as a clinical therapeutic for osteoporosis. Much of the development for this was predicated on gamma-carboxylation of vitamin K-dependent bone proteins. We contended that the doses that are used are substantially more than required for complete gamma-carboxylation of these proteins and that the active agent for any skeletal benefits may be derived from a minor catabolite of vitamin K, a 7-carbon, branched-chain carboxylic acid derivative, NaQuinate. However, the presence of NaQuinate in blood after ingestion of vitamin K has not previously been measured. In vivo bone formation effect of NaQuinate has been found, but the effects of NaQuinate on osteoclasts has not been demonstrated.Methods 1: In a preliminary experiment, blood was collected into EDTA vacutainers over 8h from a single volunteer under clinical supervision after taking a single dose of 20mg vitamin K1 in 100mL milk under local North Norway ethics (Ref: 2015/1378/REK nord). NaQuinate was measured in whole blood (200uL) and plasma (200uL) by LC-MS/MS methods using C13 NaQuinate stable isotope as an internal standard.Methods 2: Primary osteoclasts were isolated from the bone marrow of C57BL-6 mice and cultured on dentine discs for up to 9 days in the presence of 150ng/ml M-CSF, 3ng/ml RANKL and NaQuinate (1nM-10mM). Osteoclast formation and bone resorption were assessed by bright field and reflective light microscopy, respectively.Results: High dose vitamin K ingestion releases NaQuinate into blood and appears to partition into the cell fraction before appearing in plasma.The generation of osteoclasts by MCSF and RANKL on a dentine matrix is unchallenged by NaQuinate. In repeat experiments NaQuinate reduces total resorption and resorption per osteoclast by <=45% (P<0.05). Cultures exposed at initiation show the greatest effects, although it is interesting that replacing NaQuinate early, after 3days with fresh media, or introducing NaQuinate later (day 7) result in the inhibition of osteoclast activity. Conclusion: NaQuinate, as the free acid, is generated from a single high dose vitamin K, suggesting it would be available to bone. In whole blood its presence is seen earlier and may suggest that there may be a specific cell transporter for NaQuinate. Cultured osteoclasts respond to NaQuinate through reduced activity, while cell number remains unchanged. The observation of early cell exposure at different times implies that the cells have memory of exposure.

***Disclosures: Isabel Orriss**, Haoma Medica Ltd, Grant/Research Support*

P-340

Investigations to Identify Regulators of Phosphate Sensing *Lauren Surface[1], Chang Liu[1], Michael Mannstadt[1]. [1]Endocrine Unit, Massachusetts General Hospital, Harvard Medical School, United States

Organismal phosphate (Pi) homeostasis is tightly controlled to maintain a consistent serum Pi level, disruption of which can have major consequences for the body. One of the primary regulators of this homeostasis is FGF23, a protein released by bone cells in response to changing serum Pi levels. How these cells are sensing these changes in Pi remains an outstanding question in endocrinology. Using cell-based approaches, we seek to identify factors in osteogenic cells responsible for sensing and responding to changes in extracellular Pi concentration. We initially temporally profiled the transcriptional response of MC3T3-E1 and OCY454 cells to increases in extracellular Pi using RNA-seq and qRT-PCR following exposure to high Pi media for 30 minutes, 6hr, 24hr, and 48hr, and detected clear transcriptional response signatures. We observed an initial induction of immediate early response genes within 30 min, including Egr1, Fos, and Ier2. This was followed by a late phase response at 24-48 hours that included increased expression of EGF and MAPK signaling components (including Areg, Ereg and Dusp6, Spry4), as well as osteogenic genes, such as Dmp1, Spp1, and Enpp1. We find that the late phase response requires consistent exposure to elevated Pi, as a 3 hour pulse of elevated Pi followed by incubation in normal Pi media failed to induce expression of these genes. Consistent with previous publications, inhibition of MEK/ERK signaling using the small molecule U0126 was sufficient to block the early transcriptional response to Pi and blunt the late phase response. Using these findings, we have developed a fluorescent reporter system for the cellular response to increases in Pi. With this reporter, we are utilizing genome-wide screens to find genes that impact the sensing and response of osteogenic cells to changes to extracellular phosphate.

***Disclosures: Lauren Surface**, None*

P-341

Increased Expression of Dentin Matrix Proteins and Connexin43 is Associated to Reactionary Dentin Formation in Fluoride Exposed Rats *Pablo A. Fontanetti[1], Victoria Interlandi[1], Rubén H Ponce[2], Raquel Gallara[1], Viviana Centeno[2]. [1]Universidad Nacional de Córdoba. Facultad de Odontología. Departamento de Biología Bucal., Argentina, [2]Universidad Nacional de Córdoba. Facultad de Odontología. Departamento de Biología Bucal, Argentina

Excessive fluoride (F-) intake may increase the body burden of the ion and induce acute and chronic F- toxicity, osteo-dental fluorosis. Connexin 43, (Cx43), the most abundant member of the connexin family in the dental pulp complex, controls cellular growth and differentiation; however, its function in dental pulp tissue in response to F- exposure has not been fully investigated. Previously, we showed that chronic intake of water with micro-molar concentrations of F- increased Cx43 and Hsp25 (Heat shock protein 25) expression in dental pulp and this effect appears to be associated with the secretory status of incisor odontoblasts. We evaluated if the expression of Cx43 and dentin matrix molecules is associated with the reactionary dentine formation in response to chronic exposure to a high dose of F- in rat incisors. Twelve male Wistar rats drank water with different F- concentrations in form of NaF during 8 weeks: a) control (n=6), 0.3 mg/L F- and b) F- exposed (n=6), 22 mg/L F- (50 mg/L NaF). The jaws were resected for histological processing and to obtain incisor pulp tissue. Cx43 protein expression was analyzed on buccolingual serial sections using immunohistochemistry. Number of odontoblasts/µm and nucleus/cytoplasm ratio were analyzed on digital photomicrographs. Total RNA was extracted from pulp tissue, and gene expression of Cx43, osteocalcin (OCN) and dentin sialophosphoprotein (DSPP) was analyzed by RT-PCR. Data were analyzed by Student t test, setting a p-value <0.05 for significant differences. Immunoreactivity of Cx43 was higher in odontoblasts from F-exposed animals than in those from controls. The dose of 22 mg/L of F- did not alter the number of odontoblast/µm neither the predentin width. However, it increased odontoblast differentiation, which was evidenced by the decrease in nucleus/cytoplasm ratio (NaF: 0.150 +/- 0.003 vs. Control: 0.177 +/- 0.007; p<0.05). The animals in F- exposed group showed histomorphological alterations in lower incisor dentin, as well as a significant increase in OCN and DSPP expression as compared to controls. In summary, these data show that high levels of F- in drinking water produce an alteration in dentin mineralization pattern. The molecular mechanism triggered by F- seems to involve events to promote an increase in the rate of extracellular matrix secretion resulting in the formation of reactionary dentin. These events apparently are associated with the status of odontoblast differentiation.

***Disclosures: Pablo A. Fontanetti**, None*

P-342

Abaloparatide, A Novel Selective Agonist of PTH/PTHrP Receptor, Increases Lumbar, Total Hip and Femoral Neck BMD in Japanese Patients with Osteoporosis -A Phase III Randomized Clinical Trial (ACTIVE-J)- *Toshio Matsumoto[1], Teruki Sone[2], Satoshi Soen[3], Toshitsugu Sugimoto[4], Sakae Tanaka[5], Maki Mihoya[6], Tetsuo Inoue[7]. [1]Fujii Memorial Institute of Medical Science, Tokushima University, Japan, [2]Department of Nuclear Medicine, Kawasaki Medical School, Japan, [3]Soen Orthopaedic Clinic, Japan, [4]Eikokai Ono Hospital, Japan, [5]Department of Orthopedic Surgery, the University of Tokyo, Japan, [6]Clinical Development Administration Department, Teijin Pharma Limited, Japan, [7]Aoyama General Hospital, Japan

Background and Objectives: Abaloparatide (ABL) is a selective PTH/PTHrP receptor agonist that significantly increased lumbar and hip bone mineral density (BMD) and reduced new osteoporotic fractures in the multinational phase 3 ACTIVE trial. The objective of this randomized, double-blind, placebo-controlled, multicenter trial in Japan (ACTIVE-J) was to evaluate the efficacy and safety of ABL treatment for 18 months in Japanese patients with osteoporosis. Methods: Patients aged 55 or older with lumbar spine (LS) BMD less than T-score -1.77 and one or more vertebral fractures, BMD T-score less than -3.0 without fractures, or aged 65 years or older with BMD less than T-score -2.5 were randomly assigned to receive daily subcutaneous injection of 80 µg ABL or placebo (PBO) in a 2:1 ratio. The primary endpoint was percent change from baseline in LS BMD. The secondary endpoints included percent changes in total hip (TH) and femoral neck (FN) BMD, changes in bone turnover markers (BTM) and new vertebral and non-vertebral fractures. Results: After 18 months, LS BMD increased 16.33% in ABL group [postmenopausal women (PMO) 122, male 14], and 3.78% in PBO group [PMO 64, male 6] (p<0.001). TH and FN BMD increased by 4.66% and 5.13%, respectively, in ABL group, and 0.45 and 0.91%, respectively in PBO group (p<0.001). In male patients, ABL treatment resulted in similar increases in LS, TH and FN BMD as observed in the PMO patients. With ABL, serum PINP rapidly increased by over 200%, gradually decreased after 6 months and remained above PBO through 18 months. Serum CTX increased by over 130% at 6 months then decreased and was not different from PBO after 15 months. The incidence of new vertebral fractures was 4.3% in PBO group, but none in ABL group. New non-vertebral fractures occurred in 2.2% of ABL and 2.9% of PBO groups. During the 18 months of treatment, the safety profile was similar to that observed in the ACTIVE trial. Discussion and Conclusion: In Japanese patients with osteoporosis, ABL treatment robustly increased LS, TH and FN BMD and rapidly and markedly increased PINP with a gradual and less prominent increase in CTX, with a good safety profile. Although there is a limit for assessing the reduction in non-vertebral fracture due to the small number of patients, separate analyses on hip structure (HSA) and QCT demon-

strated improvements in bone geometry and microstructure, suggesting that bone strength was also improved by ABL.

***Disclosures: Toshio Matsumoto**, Astellas, Consultant, Amgen, Consultant, Daiichi-Sankyo, Consultant, Chugai, Speakers' Bureau, Daiichi-Sankyo, Speakers' Bureau, Amgen, Speakers' Bureau, Asahi-Kasei Pharma, Consultant, Astellas, Speakers' Bureau, Teijin Pharma, Consultant, Chugai, Consultant*

P-343

Fibroblast growth factor-23 and bone microarchitecture in ovariectomized rats with induced hyperthyroidism *Keunyoung Kim[1], In-Joo Kim[1], Kyoungjune Pak[1], Yun Kyung Jeon[1], Seong-Jang Kim[1]. [1]Pusan National University Hospital, Republic of Korea

Purpose: We evaluated the effect of a thyroid stimulating hormone (TSH)-suppressive dose of levothyroxine (LT4) on bone mass and bone metabolism in ovariectomized (OVX) rats. Materials and Methods: Bilateral OVX and sham operations (Sham) were performed in female Sprague-Dawley virgin rats at 7 weeks of age. Rats were divided into four experimental groups as follows: 1) Sham (n=6), 2) Sham+LT4 (n=6), 3) OVX (n=8), and 4) OVX+LT4 (n=8). After 6 weeks of treatment, the areal bone mineral density (aBMD) and volumetric BMD (vBMD) of the second lumbar spine were measured ex vivo using high-resolution DXA and μCT. Bone microarchitecture and histomorphologic analyses were also performed. Serum TSH, free thyroxine, fibroblast growth factor (FGF)-23, calcium, phosphate, osteocalcin, collagen Type-1 C-Telopeptide (CTX), and intact parathyroid hormone (iPTH) levels were compared among the four experimental groups. The proinflammatory cytokines including interleukin (IL)-6, IL-10, IL-17, monocyte chemoattractant protein (MCP) -1 and tumor necrosis factor-α were compared. Spearman rank correlation was used to analyze the relationships between BMD, bone microarchitecture, and serum components, including FGF-23. Results: Significant microarchitecture deterioration in the OVX+LT4 group was found in the trabecular thickness. The OVX+LT4 group had solely elevated levels of FGF-23, osteocalcin and iPTH compared with other groups. There was no significant difference in phosphate as well as reduced calcium levels. The serum levels of IL-6 and IL-10 was increased in OVX rats, regardless of LT4 treatment. The rats with OVX+LT4 showed increased levels of IL-17 and MCP-1 among the evaluated proinflammatory cytokines compared with other rats. FGF-23 was positively correlated with parameters of microarchitectures, aBMD, vBMD, phosphate and IL-6 in OVX+LT4 group. Conclusion: This study affirmed that OVX+LT4 treatment was the significant contributor to the deterioration of bone microarchitecture and suggests that the serum levels of FGF-23 are significantly correlated with both bone loss and IL-6.

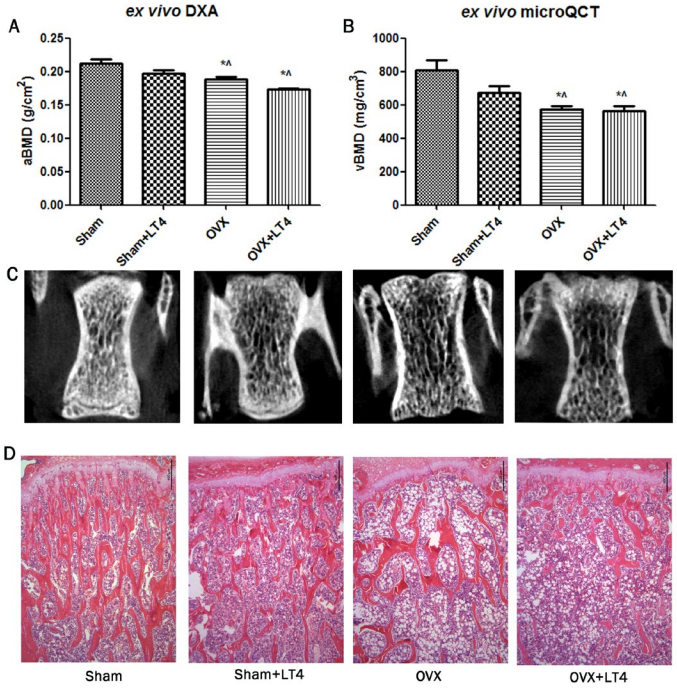

***Disclosures: Keunyoung Kim**, None*

P-344

THE LEVELS OF VITAMIN D IN THE SPONDYLARTHRITIS. DOES THE DEFICIT CORRESPOND TO THE INFLAMMATORY ACTIVITY? *David Castro Corredor[1]. [1]General University Hospital of Ciudad Real, Spain

Background: Spondyloarthritis is a group of chronic inflammatory diseases with involvement of the axial skeleton (mainly), and also of peripheral joints. Patients with spondyloarthritis have a significant prevalence of vitamin D levels below normal and that would correlate with the degree of activity of the disease.Objectives: To determine the association between vitamin D deficiency and the degree of activity of the disease (inflammatory activity) in a cohort of patients with spondyloarthritis.Methods: Case-control type analytical observational study. We propose a retrospective review of the database of patients with spondyloarthritis (according ASAS2010 criteria) who were treated in the outpatient clinics of the Rheumatology Service of the General University Hospital of Ciudad Real during June 2018 to June 2019. Patients with the data will be selected. necessary for the analysis of the variables under study. The numerical variables of normal distribution evaluated will be described using measures of frequency and measures of central tendency / dispersion as appropriate. To assess the association between vitamin D levels and activity index, the odds ratio (OR) is calculated, with a 95% confidence level and the T-student for related samples. Results: The final results of the study are presented. 115 patients were analyzed, of which 64 were men and 51 women, with an average age of 45.97 years (+/- 13.41 DE). 47% were ankylosing spondylitis, 21% psoriatic arthropathy, 16% undifferentiated spondyloarthritis, 7% spondyloarthropathy associated with inflammatory bowel disease and 9% were spondyloarthropathy associated with inflammatory bowel disease. The average of the activity was a BASDAI of 4.57 (+/- 2.35 SD) and measured by DAPSA was 12.61 (+/- 6.76 SD). 63 and 14 patients had activity measured by BASDAI and DAPSA, respectively. 49.56% patients presented an elevation of acute phase reactants. Vitamin D levels were 23.81 (+/- 10.5 SD). 77.4% presented figures of vitamin D deficiency or insufficiency. When performing the association analysis, the vitamin D deficit / insufficiency presented an OR 10 (95% CI: 3.66-27.29, p=<0.0001) with the degree of activity measured with BASDAI and DAPSA and against the elevation of RCP it was 3.63 (95% CI 1.43-9.25, p = 0.0092) and against the elevation of ESR it was 2.76 (95% CI 1.09-7, 0, p = 0.0438). Regarding the comparative analysis of means between vitamin D deficiency/insufficiency and BASDAI/DAPSA it was +3.29 (95% CI: 1.34-8.09, p=0.0084).Conclusion: Patients with spondyloarthritis, as in other autoimmune diseases, vitamin D deficiency is associated with increased inflammatory activity (BASDAI, DAPSA, RCP and ESR), measured in different time periods. Therefore, an optimization of vitamin D levels can imply an improvement in the patient's clinical situation, measured by both BASDAI and DAPSA, as well as by RCP and ESR.

***Disclosures: David Castro Corredor**, None*

P-345

Regular Strength and Sprint Training Counteracts Bone Aging: a 10-year Follow-up in Male Masters Athletes *Tuuli Suominen[1], Markku Alén[2], Ari Heinonen[3], Hans Degens[4], Jörn Rittweger[5], Timo Törmäkangas[1], Harri Suominen[3], Marko Korhonen[1]. [1]Gerontology Research Center, Faculty of Sport and Health Sciences, University of Jyväskylä, Finland, [2]Department of Medical Rehabilitation, Oulu University Hospital and Center for Life Course Health Research, University of Oulu, Finland, [3]Faculty of Sport and Health Sciences, University of Jyväskylä, Finland, [4]Musculoskeletal Science and Sports Medicine Research Centre, Department of Life Sciences, Manchester Metropolitan University, United Kingdom, [5]Institute of Aerospace Medicine, German Aerospace Center, Germany

According to cross-sectional and interventional studies, high-intensity strength and impact-type training provide a powerful osteogenic stimulus even in old age. Longitudinal evidence on the ability of high-intensity training to attenuate age-related bone deterioration is currently lacking, however. This follow-up study assessed the role of continued strength and sprint training on bone aging in 40- to 85-year-old male sprinters (n=69) with long-term training background. pQCT-derived bone structural, strength and densitometric parameters of the distal tibia (5% distal-proximal tibia length) and tibial midshaft (50% length) were assessed at baseline and after 10 years. The groups of well-trained (actively competing, sprint training including strength training >=2 times/wk; n=36) and less-trained (<2 times/wk, no strength training, switched to endurance training; n=33) athletes were defined based on the self-reports at follow-up. The association of continued strength and sprint training with longitudinal changes in bone traits was assessed using an interaction term (group*time) in linear mixed models. Over the 10-year period, the mid-tibia showed a significant group*time interaction in cortical cross-sectional area, cortical thickness, total BMC, and BMC at the anterior and the posterior sites (polar mass distribution analysis) ($p<0.05$, raw values). At distal tibia, there was a significant interaction in total BMC, trabecular vBMD and compressive strength index ($p<0.05$, raw values). After adjustment for multiple comparisons, mid-tibia posterior BMC and distal tibia trabecular vBMD remained significant ($p<0.05$). Overall, the mean differences in changes in the bone traits in well-trained compared to less-trained ranged from 2 to 6%. These were reflected as improved (mid-tibia) or maintained (distal tibia) bone properties in well-trained and decreased in less-trained athletes over the 10-year period. The structural improvements at mid-tibia tended to be more pronounced among older (65-85-yr) well-trained, whereas the densitometric properties were best preserved among younger (40-64-yr) well-trained. In conclusion, our longitudinal findings indicate that con-

tinued strength and sprint training is associated with maintained or even improved tibial properties in middle-aged and older male sprint athletes, suggesting that regular, intensive exercise counteracts bone aging.

***Disclosures: Tuuli Suominen**, None*

P-346

Colchicine improves muscle function, enhances bone formation, and reduces white adipose tissue in aged mice but not young mice. *Jenna Leser[1], Nicole Gould[1], Gouli Shi[1], Nathalie Spita[2], Makenzy Mull[1], Ryan Riddle[2], Christopher Ward[1], Joseph Stains[1]. [1]University of Maryland Baltimore, United States, [2]Johns Hopkins School of Medicine, United States

The cycle of frailty is a feed forward mechanism during aging in which mechano-responsive tissues, bone and skeletal muscle, acquire a diminished capacity to respond to mechanical stimuli, becoming osteopenic and sarcopenic respectively, leading to reduced strength, mobility, and physical activity. Optimally, osteopenia and sarcopenia need to be addressed simultaneously to restore musculoskeletal deficits in the elderly. We have described parallel mechano-transduction pathways with shared components in responsive, young adult mouse bone and muscle. Mechano-sensitivity in this pathway is tuned by cytoskeletal stiffness, specifically detyrosinated microtubules. With advancing age, we observed increased abundance of detyrosinated microtubule in muscle and bone, consistent with an attenuated mechano-response, pinpointing a potential therapeutic target to treat both tissues concurrently. Not only does this pathway affect muscle and bone, the mechano-responsive bone derived protein, sclerostin, increases white adipose tissue (WAT) accumulation in addition to inhibiting bone formation. We hypothesized increased detyrosinated microtubules contribute to age dependent defects in muscle function and bone mechano-responsiveness, leading to sarcopenia and osteopenia, and accumulation of WAT. We treated 16-week (young) and 78-week (aged) C57BL/6 male mice with colchicine (a microtubule destabilizing drug) 1mg/L in drinking water for 8 weeks, anticipating that targeting microtubules might restore mechano-transduction to increase bone formation, improve muscle function, and reduce WAT accumulation in aged mice. Consistent with our hypothesis, colchicine treated aged mice showed significantly increased bone formation on the cortical surface (300% increase, p=0.0496) and decreased bone derived sclerostin. Additionally, these mice exhibited improved in vivo muscle contraction velocity (40% increase, p=0.0106) and power (20% increase, p=0.0058). Finally, colchicine treated aged mice lost body mass (p=0.0146), showed reduced WAT mass (50% reduction of inguinal fat, p=0.0199, 60% reduction of gonadal fat, p=0.0038) and adipocyte size (30% reduction, p<0.0001). In contrast, young colchicine treated mice, which do not have an over-abundance of detyrosinated microtubules, had no significant effects on bone, muscle or WAT. These data show that targeting the aging microtubule network restores mechano-responsiveness to improve aging dependent sarcopenia, osteopenia and diminish WAT.

***Disclosures: Jenna Leser**, None*

P-347

A natural small molecule targeting miR487b-Wnt5a interaction to promote myogenic potential in vitro *Zhenjian Zhuo[1], Youyan Wan[2], Shuaijian Ni[2], Zongkang Zhang[2], Ning Zhang[1], Yuanyuan Yu[2], Aiping Lu[2], Ge Zhang[2], Bao-Ting Zhang[1]. [1]The Chinese University of Hong Kong, Hong Kong, [2]Hong Kong Baptist University, Hong Kong

A natural small molecule targeting miR487b-Wnt5a interaction to promote myogenic potential in vitro Zhenjian Zhuo1,4, Zong-Kang Zhang1, Youyang Wan2,3,4, Shuaijian Ni2,3,4, Ning Zhang1, Ge Zhang2,3 & Bao-Ting Zhang11School of Chinese Medicine, Faculty of Medicine, The Chinese University of Hong Kong, Hong Kong SAR, China,2Law Sau Fai Institute for Advancing Translational Medicine in Bone & Joint Diseases, School of Chinese Medicine, Hong Kong Baptist University, Hong Kong SAR, China,3Institute of Integrated Bioinformedicine and Translational Science, School of Chinese Medicine, Hong Kong Baptist University, Hong Kong SAR, China,4Aptacure Therapeutics Limited, Kowloon, Hong Kong SAR, China Sarcopenia, age-related loss of skeletal muscle mass and strength, is associated with serious health consequences. However, there is no clinically established therapy for sarcopenia to date. MicroRNAs (miRNAs) play key roles in a series of pathological processes by interacting with their specific target mRNAs for translation repression. We previously reported that miR487b, which elevated during aging and inhibited the expression of an important myogenic regulator Wnt5a, thereby contributed to sarcopenia development during aging. Mir487b could be a potential therapeutic target for sarcopenia. Using our recently developed virtual screening model targeting Argonaute (AGO)-mediated miRNA-mRNA interactions (Zhuo et al. 2020), 10 natural small molecules (MA-1 to MA-10) specifically targeting miR487b-Wnt5a mRNA interaction were selected (F-1). The binding between the four candidates (MA-1 to MA-4) and synthesized miR487b-Wnt5a loop was confirmed, respectively, by streptavidin pull down assay and liquid chromatography-mass spectrometry (LC-MS) (F-2a). AgomiR487b (a miR487b agonist) treatment could suppress Wnt5a expression and inhibit cell differentiation in C2C12 cells. Among the above four small molecule candidates, MA-4 elevated Wnt5a protein level (F-2b), but not Wnt5a mRNA level (F-2c) in agomiR487b-treated C2C12 cells. Moreover, MA-4 elevated the expression of myogenic marker (MyoD) (F-2d) and enhanced myotube formation (F-2e,f) in agomiR487b-treated C2C12 cells. To further validate the interaction between MA-4 and miR487b-Wnt5a loop, the interaction site in miR487b-Wnt5a loop were mutated. MA-4 could only bind with wild-type miR487b-Wnt5a loop, instead of mutated miR487b-Wnt5a loop in vitro (F-3a). In addition, the MA-4-incubation-induced enhancement in the Wnt5a protein, MyoD, and myotube formation in agomiR487b-treated C2C12 cells could be abolished by wild-type miR487b-Wnt5a loop, whereas no significant change was found in mutated miR487b-Wnt5a loop transfection group (F-3b-f). Taken together, MA-4 could be a potential agent to block miR487b-Wnt5a interaction to promote myogenic potential in vitro (F-4). The current study could provide a novel natural small molecule drug candidate to promote myogenic potential. Acknowledgments: This study was supported by the Innovation & Technology Fund (UIM/328) and General Research Fund (14108816 and 14100218). Reference: Z Zhuo et al. A Loop based and AGO incorporated Virtual Screening Model Targeting AGO mediated miRNA-mRNA Interactions for Drug Discovery to Rescue Bone Phenotype in Genetically Modified Mice. Adv. Sci., 2020. DOI: 10.1002/advs.201903451.

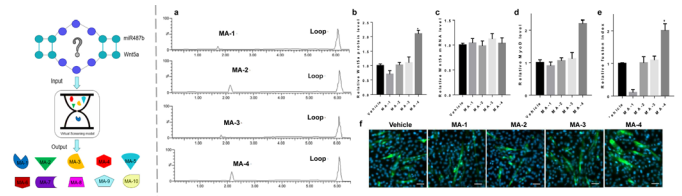

F-1. Schematic of virtual screening model

F-2. Biological function of candidates in agomiR487b-treated C2C12 cells. (a) LC-MS. (b,d) Western blot. (e) RT-PCR. (e,f) Immunostaining for MHC (green) and DAPI (blue). *P<0.05 vs. Vehicle.

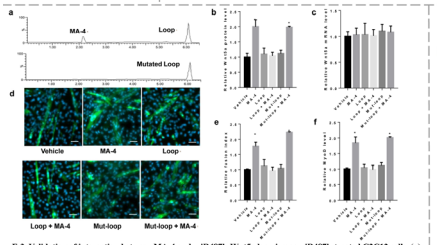

F-3. Validation of interaction between MA-4 and miR487b-Wnt5a loop in agomiR487b-treated C2C12 cells. (a) LC-MS. (b,f) Western blot. (e) RT-PCR. (d,e) Immunostaining for MHC (green) and DAPI (blue). *P<0.05 vs. Vehicle.

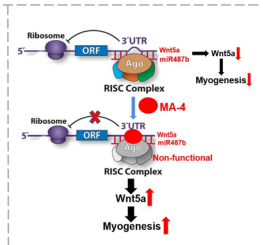

F-4. Schematic of MA-4 targeting miR487b-Wnt5a interaction to promote myogenic potential *in vitro*.

***Disclosures: Zhenjian Zhuo**, None*

P-348

Musculoskeletal and cardiac defects in the Presenilin-1 (PSEN1) L166P KI mouse model of Alzheimer Disease. *Vidyani Suryadevara[1], Amy Sato[2], Anuradha Valiya Kambrath[1], Teresita Bellido[2], Monte Willis[3]. [1]Indiana Center for Musculoskeletal Health, Department of Pathology & Laboratory Medicine, Indiana University School of Medicine, Indianapolis, IN 46202, United States, [2]Department of Anatomy Cell Biology and Physiology, Indiana University School of Medicine, Indianapolis, IN 46202, United States, [3]Indiana Center for Musculoskeletal Health, Department of Pathology & Laboratory Medicine, Krannert Cardiology Institute, Department of Internal Medicine, Indiana University School of Medicine, Indianapolis, IN 46202, United States

Alzheimer Disease (AD) is the 6th leading cause of death in the US and a leading cause of disability and poor health. Beyond memory deficits, the systemic nature of AD has emerged with patients demonstrating significantly more skeletal muscle weakness, bone loss, and heart failure compared to age-matched controls without AD. There is currently an unmet need for translational models that exhibit clinically relevant muscle defects and the hallmark neurological characteristics of AD. We investigated skeletal and cardiac muscle dysfunction in a mouse knock-in model with a mutation in PSEN1 known to cause early-onset AD in humans (PSEN1 L166P) at ages that Abeta accumulates intracellularly in the mouse brain (>6 mos). Skeletal and cardiac muscle function was assessed by in vivo DXA, plantarflexion torque, and echocardiography, respectively, in PSEN1 KI and strain-, sex-, and age-matched wildtype (WT) mice at 12 months of age (N=16-18). DXA analysis identified a reduction in whole-body bone mineral density (BMD) in female, but not male, PSEN KI mice (0.0482+/-0.002, p<0.05) compared to WT control mice (0.05+/-0.001, p<0.05). PSEN1 KI mice demonstrated skeletal muscle weakness compared to WT mice, as detected by decreased plantarflexion torque and muscle contraction energy for stimulation frequencies 25-300Hz (normalized by lean body mass). The time required for PSEN1 KI skeletal muscle to relax was significantly decreased when stimulated at 125-275 Hz, consistent with altered re-establishment of calcium equilibrium post-contraction. Echocardiography of the heart identified significant increases in left ventricular (LV) anterior and posterior wall thickness and LV Mass (5.6+/-0.3 vs. 4.3+/-0.2 mg/g, normalized to body weight, p<0.01). No changes in systolic function (e.g., ejection fraction) were detected in PSEN1 KI mice. Doppler analysis of the mitral valve (MV) to identify measure diastolic function by determining MV E and A wave measurements. The PSEN1 KI mice had a significantly lower E/A ratio (0.7+/-0.2) compared to controls (2.3+/-0.3, p<0.05), revealing cardiac relaxation defects consistent with diastolic heart failure. These results are the first description of the early onset AD PSEN1 L166P mutation causing cardiac and musculoskeletal defects at an age that neurological defects are present. Since PSEN1 is a protein involved in neuronal

Notch and Wnt signaling, future studies will define how PSEN1 mutations alter these pathways in the tissue level.

***Disclosures: Vidyani Suryadevara**, None*

P-349

The gut microbiota of old mice reduces lean mass in young mice *Lina Lawenius[1], Carrie Cowardin[2], Julia M. Scheffler[1], Karin L. Gustafsson[1], Cecilia Engdahl[1], Jianyao Wu[1], Liesbeth Vandenput[1], Ulrika Islander[1], Jeffrey I. Gordon[2], Klara Sjögren[1], Claes Ohlsson[1]. [1]Centre for Bone and Arthritis Research, Institute of Medicine, Sahlgrenska Academy at University of Gothenburg, Gothenburg, Sweden, Sweden, [2]The Edison Family Center for Genome Sciences and Systems Biology, Washington University in St. Louis, St. Louis, MO, USA, United States

Aging is associated with an increased risk of sarcopenia and osteoporosis. Decreases in gut microbiota (GM) diversity have been associated with aging. Moreover, studies have demonstrated that manipulation of GM composition can influence both lean body mass and bone mass. Therefore, we hypothesized that changes in GM composition may contribute to the reduced lean and/or bone mass observed in old compared to young mice. The aim of the present study was to determine if transplanting GM from old versus young conventionally-raised C57BL/6 donor mice to young versus old recipient C57BL/6 germ-free (GF) mice transfers the observed decreased lean and/or bone mass.As expected, old (21-month-old) female GM donors had reduced relative lean mass (lean %; -29.1+/-2.0%, p<0.001) and trabecular bone volume fraction (BV/TV in tibia; -37.7+/-6.3%, p<0.001) compared with young adult (5-month-old) female GM donors.To investigate whether the age of the recipients would influence responses to colonization, old or young adult GM was used to colonize 5-, 11- or 17-week-old germ-free (GF) recipient mice (n=12/group). 16S rDNA amplicon sequencing was performed on fecal samples collected at sacrifice five weeks after transplantation. Lean mass percentage was determined by quantitative magnetic resonance analyses at baseline and after five weeks of colonization.The gut microbial communities of recipient animals were similar to the original donors. GM transplantation from old donors reduced the lean mass percentage in recipient mice relative to GM transplantation from young donors (Figure 1). Interestingly, this effect was observed in young growing (colonized at 5 weeks or 11 weeks of age) but not in adult (colonized at 17 weeks of age) recipients. Two-way ANOVA revealed a significant interaction effect between the age of the donors and the age of the recipients (Figure 1). Thus, the effect of the age of the donor mice on lean mass percentage in recipient mice was modulated by the age of the recipient. In contrast, no significant effect of the age of the donor mice on bone mass parameters were observed, regardless of recipient age.Conclusions - Old mice had a low relative lean mass and this phenotype could be transferred to young mice by GM transplantation. This effect was dependent on the age of the recipient mice, suggesting that gut communities from old mice have the capacity to transfer this phenotype to young, growing but not to older, mature mice.

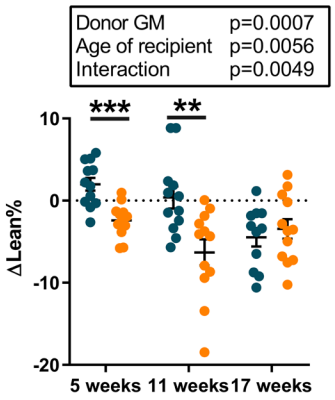

Figure 1. GM from old or young adult donor mice was transplanted to GF mice of different ages. Body composition was determined at colonization and after 5 weeks using qMR to calculate difference in lean mass percentage (ΔLean%). Values are given as mean ± SEM. The overall effect of age of donor mice (adult vs old), age of recipient mice (GF mice) and their interaction were calculated using two-way ANOVA including an interaction term. Student's t-test was used to analyze differences between adult GM and old GM at the specific age of recipient mice. ***p≤0.001 and **p≤0.01

***Disclosures: Lina Lawenius**, None*

P-350

Musculoskeletal and cardiac defects in the microtubule associated protein Tau (MAPT) P301S Tg+ mouse model of Frontotemporal Dementia. *Anuradha Valiya Kambrath[1], Vidyani Suryadevara[1], Amy Sato[2], Teresita Bellido[2], Monte Willis[3]. [1]Indiana Center for Musculoskeletal Health, Department of Pathology & Laboratory Medicine, Indiana University School of Medicine, Indianapolis, IN 46202, United States, [2]Department of Anatomy Cell Biology and Physiology, Indiana University School of Medicine, Indianapolis, IN 46202, United States, [3]Indiana Center for Musculoskeletal Health, Department of Pathology & Laboratory Medicine, Krannert Cardiology Institute, Department of Internal Medicine, Indiana University School of Medicine, Indianapolis, IN 46202, United States

Frontotemporal dementia (FTD, aka Pick's Disease) is a group of disorders caused by progressive nerve cell loss in the frontal or temporal lobes of the brain. In contrast to Alzheimer Disease, FTD has distinctive symptoms of losing the ability to understand or formulate words or characterized by hesitant, labored, or ungrammatical speech. Changes in motor function have been identified in FTD patients, but underlying causes are not clear. We investigated the MAPT P301S transgenic (MAPT Tg+) FTD mouse model with the human disease-causing mutation at time points neurological involvement (which starts at 1-3 months) was present. mCT analysis of MAPT Tg+ femurs revealed a reduction in the cortical properties at 12 months of age (vs. WT?, males>females). Three-point bending tests revealed that the femur mechanical properties were reduced in MAPT Tg+ before the yield point compared to controls. However, several mechanical properties were increased after the yield point in a sex-dependent manner. Since human FTD is associated with muscle weakness and dementias with increased heart failure and EKG changes, we next investigated skeletal muscle and cardiac function. MAPT Tg+ mice had significantly decreased grip strength (160.6+/-16.7g) compared to WT (194.3+/-12.4g, p<0.0001). Similarly, plantarflexion torque detected increased time to maximum in MAPT Tg+ mice (for 125, 175-300Hz), indicating impairment in neuromuscular and/or motor unit recruitment. MAPT Tg+ mice exhibited a decreased half relaxation time and plantarflexion torque (for 125-300 Hz). MAPT Tg+ hearts had significantly reduced systolic function (ejection fraction: 76.2+/-1.0%) compared to WT (85.2+/-1.0, p<0.0001). ECG analysis of cardiac electrophysiology identified lower heart rates (749.6+/-10.0 vs. 772.2+/-2.6, p<0.01), increased heart rate variability (HRV) (20.6+/-1.8 vs. 10.0+/-1.6 bpm), and an elongated QT interval (25.05+/-1.06 vs. 19.8+/-1.0 ms, p<0.05) in MAPT Tg+ mice. These studies identify the first extraneuronal FTD phenotypes, including cardiac autonomic dysfunction (increased HRV), muscle weakness, and systolic heart failure at an age when neurologic and bone defects occur. These findings illustrate the systemic involvement of the musculoskeletal system in the pathogenesis of FTD, along with clinical features not previously investigated in patients (e.g., arrhythmogenic long QT, bone loss) that may contribute to the hypotension and increased falling risks reported in FTD patients.

***Disclosures: Anuradha Valiya Kambrath**, None*

P-351

Aminobutyric Acids: Potential Biomarkers for Musculoskeletal Health during Exercise and Aging? *Zhiying Wang[1], Chenglin Mo[1], Charalampos Lyssikatos[2], Ziyue Liu[2], Stuart Warden[2], Lynda Bonwald[2], Marco Brotto[1]. [1]Bone-Muscle Research Center, College of Nursing and Health Innovation, University of Texas-Arlington, United States, [2]Indiana Center for Musculoskeletal Health, ICMH, School of Medicine, Indiana University, United States

Exercise contributes to musculoskeletal (MSK) health. MSK decline during aging creates synergistic negative effects between inactivity and aging. Healthy aging interventions require the identification of serum biomarkers that inform on MSK health. We reported that β-aminoisobutyric acid (BAIBA) and γ-aminobutyric acid (GABA) have the potential use for early detection of osteoporosis and MSK health during aging (Wang et. al, Commun Biol 2020).We determined serum levels of aminobutyric acids in subjects from the ICMH-Clinical Research Center FitCore Program. Human serum samples from 80 white non-Hispanic individuals aged 20-85 years were used in these studies. 40 women and 40 men were classified as "low performers" (LP) or "high performers" (HP), according to performance on grip strength, repeat chair stand test, six-minute walk test (6MWT), etc. Serum concentrations of isomeric aminobutyric acids including α-aminobutyric acid (AABA), BAIBA, and GABA in serum samples were quantified using a recently customized method at the Bone Muscle Research Center, University of Texas-Arlington (Wang et al, 2020).The concentrations for D-BAIBA and L-BAIBA were 1.52 +/- 0.73 μM and 0.037 +/- 0.030 μM, respectively. Serum GABA levels, ranging from 0.09-0.25 μM, significantly correlated with age (Spearman's correlation coefficient (ρ) 0.392, p < 0.001). Moreover, subjects in the HP group showed relatively higher serum GABA levels, irrespective of gender but especially in aged women. Serum GABA levels were 0.177 +/- 0.040 μM in HP women (age 50-65 years) and 0.149 +/- 0.040 μM in age-matched LP women, suggesting modulations by both exercise and aging. L-AABA (7.5-41.8 μM), rarely reported in bone and exercise studies, was significantly and positively associated with different physical performance measures, including usual gait speed (ρ = 0.272, p = 0.015) and 6MWT (ρ = 0.322, p = 0.046, males). Positive associations were also observed between L-AABA and bone mineral density (BMD) in males, including femoral neck BMD (ρ = 0.378, p = 0.016) in male subjects aged 20-85 years and spine BMD (ρ = 0.492, p = 0.028) in young male subjects aged 20-50 years.These

findings suggest that serum levels of aminobutyric acids have important relationships with bone and muscle health during aging. Exercise may modulate these metabolites and it will be important to determine if they mediate the positive effects of exercise on aging in addition to serving as biomarkers of physical performance.

***Disclosures: Zhiying Wang**, None*

P-352

Elimination of Senescent Osteocytes Prevents Age-Related Bone Loss *Joshua Farr[1], Madison Doolittle[1], Brittany Eckhardt[1], Jennifer Rowsey[1], Daniel Fraser[1], Parinya Samakkarnthai[1], Yuji Ikeno[2], Laura Niedernhofer[3], Paul Robbins[3], Robert Pignolo[1], Nathan LeBrasseur[1], Tamar Tchkonia[1], James Kirkland[1], David Monroe[1], Sundeep Khosla[1]. [1]Mayo Clinic, United States, [2]University of Texas Health San Antonio, United States, [3]University of Minnesota, United States

Diverse forms of stress converge to cause a cell to enter an essentially irreversible permanent growth arrest, termed "senescence". The key senescence mediator, p16Ink4a, increases with aging in several tissues, including osteocytes among other bone-resident cell types. Eliminating senescent cells across tissues in old mice using p16-ATTAC, an inducible "suicide" transgene driven by the p16Ink4a promoter activated upon administration of a synthetic drug (AP20187 [AP]), or with "senolytics" – drugs that selectively kill senescent cells, improves healthspan. In addition, both approaches prevent age-related bone loss in old mice by reducing bone resorption and having favorable effects on formation. Here we describe a novel Cre-loxP mouse, termed p16-LOX-ATTAC, engineered to carry a construct where the p16Ink4a promoter drives 3 SV40 poly(A) transcription termination sequences (3xSTOP) flanked by loxP sites upstream of ATTAC. In the un-recombined state (no Cre), transgene harboring mice do not express ATTAC; however, when crossed with a Cre, the 3xSTOP is removed, resulting in ATTAC expression in a senescent cell-specific manner. Importantly, the combination of the Cre and AP permits attaining both cell-specific and temporal (in old mice) control of senescent cell elimination. To determine whether clearance of senescent osteocytes in old mice is sufficient to prevent age-related bone loss, we crossed p16-LOX-ATTAC mice with 8 kb Dmp1-Cre mice (thereby limiting suicide transgene expression to Dmp1-expressing osteocytes), and at 20-months of age, randomized the mice to four months of vehicle (VEH) or AP treatments. We found, using real-time qPCR, significantly reduced p16Ink4a mRNA expression (by -1.6-fold, $p<0.05$; Figure Panel A) in osteocyte-enriched samples of VEH- vs AP-treated mice, but no difference between groups in other tissues (Figure Panel A). Micro-CT revealed significantly improved spine trabecular bone volume fraction (BV/TV; by 42%, $p<0.01$; Figure Panel B) and femur cortical thickness (Ct.Th; by 13%, $p<0.05$; Figure Panel C) in AP- vs VEH-treated mice. Collectively, by specifically clearing senescent osteocytes, these data establish that osteocyte senescence is causally implicated in age-related bone loss and build a framework for developing and translating senolytics that target senescent osteocytes with superior specificity and efficacy for the prevention of osteoporosis.

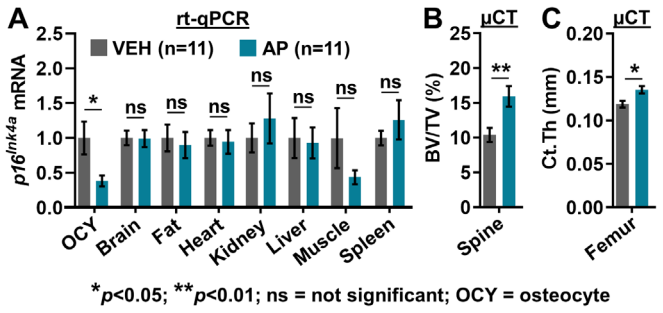

***Disclosures: Joshua Farr**, None*

P-353

Pregnancy-related change in pQCT and bone biochemistry in a population with habitually low calcium intake *Mícheál Ó Breasail[1], Kate Ward[2], Landing Jarjou[3], Sophie Moore[4], Ann Prentice[1]. [1]MRC Nutrition and Bone Health Research Group, United Kingdom, [2]MRC Lifecourse Epidemiology Unit, University of Southampton, United Kingdom, [3]MRC Unit The Gambia, London School of Hygiene and Tropical Medicine, Gambia, [4]Department of Women and Children's Health, King's College London, United Kingdom

In pregnancy, changes in maternal calcium (Ca) economy occur to satisfy fetal Ca demand. Whether maternal mineral reserves facilitate these requirements in a population with habitually low Ca intake (~400mg/day) is difficult to quantify and no data exist from sub-Saharan Africa. The aim was to determine skeletal changes using pQCT and bone biochemistry between early second and third trimesters. Pregnant rural Gambians aged 18-45 years (n=467) participating in a trial of antenatal nutritional supplements (ISRCTN49285450) were invited for longitudinal measurements: pQCT radius/tibia 4% total vBMD, trabecular vBMD, total CSA; 33%/38% radius/tibia cortical vBMD, BMC, total CSA; biochemistry serum collagen type 1 cross-linked β-C-telopeptide (CTX), type 1 procollagen N-terminal (P1NP), parathyroid hormone (PTH), and 1,25(OH)2D. Supplements were iron folic acid (IFA; standard care), multi-micronutrient (MMN), protein energy (PE), and PE+MMN. Independent t-tests tested whether within-group and pooled change differed significantly from 0. Multiple regression adjusting for age and supplement tested if between-visit change differed significantly from the IFA group. Data for change are expressed as mean[SEM]%. Visits occurred at mean(SD) 14 (3) and 31 (1) weeks of pregnancy. Radius trabecular and cortical vBMD, and BMC increased by 1.15 [0.30]%, 0.41 [0.09]%, and 0.47 [0.11]% respectively (all $p<0.001$). At the tibia, total and trabecular vBMD increased by 0.34 [0.10]% and 0.46 [0.14]% ($p<0.001$,$p<0.01$), while cortical vBMD and BMC increased by 0.35 [0.04]% and 0.55[0.07]% (both $p<0.001$). At the radius change in cortical vBMD in MMN and PE was 0.54 [0.24]% and 0.73[0.24]% lower vs IFA ($p<0.05$, $p<0.01$ respectively). Change in tibia total vBMD was 0.76 [0.28]% greater in PEMNN vs IFA ($p<0.01$). Between visits CTX, PTH, and 1,25(OH)2D increased by 23.0 [3.64%], 13.2 [2.78]%, and 21.0 [1.65]% respectively (all $p<0.001$). P1NP decreased by 32.4 [2.30]% ($p<0.001$). Changes in biochemistry did not differ significantly from the IFA group. Between-visit changes in BTMs suggest pregnancy-related changes in maternal bone mineral homeostasis. No evidence of bone mobilisation was observed in the peripheral skeleton, nor were consistent differences found by supplement group. It remains possible that mobilisation occurs at axial sites. In this population, with habitually low Ca intakes, the peripheral skeleton is not mobilised as a Ca source for the fetus.

***Disclosures: Mícheál Ó Breasail**, None*

P-354

Lipid Signaling Mediators regulates myogenesis with ageing *Ahmed Al Saedi[1], Gustavo Duque [2], Marco Brotto[3], Zhiying Wang[4]. [1]Department of Medicine – Western Health, The University of Melbourne, Australia, [2]Australian Institute for Musculoskeletal Science (AIMSS), The University of Melbourne and Western Health, St. Albans, Australia, [3]Bone-Muscle Research Center, College of Nursing and Health Innovation, The University of Texas-Arlington, United States, [4]bone, United States

Aging is associated with a progressive decline in muscle mass and function. Altered lipid metabolism contribute to age-related muscle atrophy and muscle weakness, and are responsible for significant disability in older persons. Accumulating evidence indicates that lipid mediators (LMs) regulate skeletal muscle mass and function, and potentially influence muscle wasting, metabolism, and functional status in response to various pathological conditions. Individual eicosanoid species [e.g., prostaglandins (PGs) and Arachidonic acid (AA)-derived eicosanoids (e.g. polyunsaturated fatty acid (PUFA)] emphasize the biosynthesis, metabolism, and signaling pathways of many tissues and organs. The course to determine the molecular components that lead to mass/strength decrements in the aged skeletal muscle is still evolving. In this study we hypothesized that LMs play an important role in the regulation of basic cellular processes and thereby pathophysiological actions in skeletal muscle and ageing, particularly its association with bone muscle crosstalk. Profiling of 29 Lipid Signaling Mediators (LMs) and quantification was performed in gastrocnemius muscles obtained from young (6 weeks) and (28 weeks) C57BL6 mice. We found gender- and/or age- related differences are present for 20 LMs identified in this study. 28 weeks old male and female showed relatively higher LM levels [including prostaglandins (PGs), PGs2α (p=0.036), PGsα, Arachidonic acid (AA)(p=0.042), Eicosapentaenoic acid (EPA) (p=0.0057) and anandamide (AEA) (p=0.023)] than the younger mice. Similarly, with AA/EPA ratio (p=0.005), while AA derivatives (e.g. Lipoxin B4, a strong muscle regulator) showed significantly lower values compared to the young mice in both genders (p= 0.0092). Furthermore, Docosahexaenoic acid (DHA) autoxidation products (20-HDoHE, 11-HDoHE, 7-HDoHE, 4-HDoHE and platelet-activating factor) were significantly higher in older mice than younger mice (p=0.003, p=0.020, p=0.025, p=0.045 respectively). In conclusion, even at relatively young age of about 6 months, a noted increase in pro-inflammatory LMs can be detected in female mice. These results suggest that LMs could play an earlier and long-term role in modulating musculoskeletal function during aging, which might relate to osteoporosis. Application of these principles will help advance the understanding of skeletal muscle pathophysiology to study the role of LMs in health and disease.

***Disclosures: Ahmed Al Saedi**, None*

P-355

pQCT Muscle Density Predicts Hip Fractures Independent of FRAX, Falls and BMD in the Osteoporotic Fractures in Men (MrOS) Study: a Meta-Analysis *Nicholas Harvey[1], Eric Orwoll[2], Jane Cauley[3], Timothy Kwok[4], Magnus Karlsson[5], Björn Rosengren[5], Eva Ribom[6], Peggy Cawthon[7], Kristine Ensrud[8], Enwu Liu[9], Kate Ward[1], Cyrus Cooper[1], John Kanis[10], Mattias Lorentzon[11], Claes Ohlsson[11], Dan Mellström[12], Helena Johansson[10], Eugene McCloskey[10]. [1]MRC Lifecourse Epidemiology Unit, University of Southampton, United Kingdom, [2]Oregon Health & Science University, United States, [3]Graduate School of Public Health, University of Pittsburgh, United States, [4]Department of Medicine & Therapeutics and School of Public Health, The Chinese University of Hong Kong, China, [5]Clinical and Molecular Osteoporosis Research Unit, Department of Clinical Sciences Malmo, Lund University and Department of Orthopedics, Skane University Hospital, Sweden, [6]Department of Surgical Sciences, University of Uppsala, Sweden, [7]Research Institute, California Pacific Medical Center, United States, [8]Medicine and Epidemiology & Community Health, University of Minnesota, United States, [9]Mary MacKillop Institute for Health Research, Australian Catholic University, Australia, [10]Centre for Metabolic Bone Diseases, University of Sheffield, United Kingdom, [11]Institute of Medicine, Sahlgrenska Academy, Sahlgrenska University Hospital, Sweden, [12]Centre for Bone and Arthritis Research (CBAR), Sahlgrenska Academy, University of Gothenburg, Sweden

Muscle size decreases and muscle adiposity increases with ageing, both changes being associated with adverse health outcomes. DXA-measured appendicular lean mass has limitations as a predictor of incident hip fracture (HF), so we wished to examine the predictive performance of peripheral quantitative computed tomography (pQCT) measures of both calf muscle size (cross sectional area, CSA) and muscle density (an established surrogate for muscle adiposity) for hip fracture. pQCT (Stratec XCT2000/3000) measurements at the tibia were undertaken in the MrOS US, Hong Kong (HK) and Swedish Gothenburg (SW) cohorts. Analyses were undertaken for each cohort and merged by meta-analysis. The predictive value for incident HF, using an extension of Poisson regression adjusted for age and follow-up time, was expressed as gradient of risk (GR=hazard ratio per SD increase in the exposure). Further analyses controlled for BMD, FRAX 10-year fracture probability and prior falls (y/n, in the preceding 12 months).We studied 1008 (US), 1662 (HK), 581 (SW) men, mean (SD) age 77.0 (5.1), 73.9 (4.9), 80 (3.4) years, followed for a mean (SD) 7.9 (2.2), 8.1 (2.3), 4.4 (1.6) years, with 31, 47, and 34 incident HF respectively. Both greater muscle CSA and greater density (suggesting lower muscle adiposity and higher muscle quality) were associated with a lower risk of incident HF [GR: 0.79 (95% CI:0.65,0.96) and 0.83 (95%CI:0.69,0.99) respectively]. The pattern of relationships was not materially changed by adjustment for prior falls or FRAX probability. In contrast, after inclusion of femoral neck BMD T-score, the association for muscle CSA was attenuated [GR: 0.97 (95%CI:0.80,1.19)], whereas that for muscle density was not materially changed [GR: 0.74 (95%CI:0.62,0.89)].In conclusion, pQCT measures of greater muscle area and density were both associated with lower incidence of hip fractures, but only lower muscle density remained an independent risk factor for fracture after accounting for femoral neck BMD T-score. These findings demonstrate a complex interplay between measures of bone, and muscle size and quality, in determining fracture risk.

***Disclosures: Nicholas Harvey**, None*

P-356

Renal-bone axis: Vitamin D status and supplementation in older adults *Marilena Christodoulou[1], Terence Aspray[2], Isabelle Piec[1], Christopher Washbourne[1], Jonathan Tang[1], William Fraser[1], Inez Schoenmakers[1]. [1]University of East Anglia, Medical school, Norwich, UK, United Kingdom, [2]University of Newcastle upon Tyne, Freeman hospital, Bone Clinic, UK, United Kingdom

Bone and renal metabolism are regulated by common factors and there is extensive cross-talk between these organs. Ageing is associated with a decrease in estimated glomerular filtration rate (eGFR) and reduced tissue sensitivity to regulating hormones. We investigated the influence of renal function on plasma concentrations of vitamin D metabolites, regulators of bone and mineral metabolism and their response to vitamin D supplementation in older people. Associations with vitamin D status were also investigated.Samples collected at baseline and after 12 months of supplementation from a randomised dose-ranging vitamin D intervention trial (VDOP; 12000, 24000, 48000IU vitamin D3/month); (n=376; >70y; CKD<G4) were analysed for plasma 25(OH)D (LC-MS/MS), 1,25 (OH)2D (Diasorin, Liaison XL), Klotho (ELISA IBL Int.), PTH (Immulite 2000, SIEMENS), SOST, DKK1 (Biomedica), cFGF23 and iFGF23 (Immutopics, Gen 2 ELISA). eGFR was calculated according to 4-variable MDRD and were pragmatically split by eGFR <60 and >=60 ml/min/1.73m2. Group differences were tested by ANCOVA, with vitamin D dose as a co-variate for post-supplementation data. ANOVA followed by regression analyses was used to test associations with category of 25(OH)D concentration (<=25, 25.1-50, 50.1-75, >75nmol/L).At baseline, 25(OH)D, 1,25(OH)2D, Klotho, DKK1 were significantly lower and PTH, SOST, cFGF323, iFGF23, c:iFGF23 ratio higher in the group with the lower eGFR (Table). Plasma 25(OH)D was negatively associated with PTH (β -0.143; p<0.001), cFGF23 (β -0.085; p<0.01) and c:iFGF23 ratio (β -0.126; p<0.001).After 12 months of supplementation, mean plasma concentrations of 25(OH)D, 1,25(OH)2D and cFGF23 dose-dependently increased and PTH decreased (all p<0.05). There were no differences by eGFR group in 25(OH)D, 1,25(OH)2D and Klotho, while DKK1 was significantly lower and PTH, SOST, cFGF23, iFGF23 and the c:iFGF23 ratio higher (p<0.05; Table). Vitamin D dose was not significant in these models with eGFR. After supplementation, plasma 25(OH)D was negatively associated with plasma PTH (β -0.201; p<0.001).Even with a moderate decline in eGFR, markers associated with bone catabolism were elevated at baseline. Vitamin D supplementation reduced PTH, but increased cFGF23 and there were no effects on Klotho, SOST, DKK1 and iFGF23. Between eGFR group differences in 25(OH)D, 1,25(OH)2D and Klotho were no longer detectable. This might suggest a benefit of vitamin D supplementation on the renal-bone axis.

	BASELINE					12 MONTHS	
Biomarkers	Mean	SD	eGFR category[a]	Mean	SD	Mean	SD
Age (years)	74.9	1.1	≥60	74.5	4.0	75.6	4.1
			<60	77.1	4.1	77.8	4.4
MDRD-4 creatinine (mL/min per 1.73 m²)*†	72.4	15.2	≥60	76.9	12.5	77.5	12.2
			<60	51.7	6.6	52.2	7.0
25(OH)D (nmol/L)*	39.99	20.06	≥60	41.27	20.56	66.45	18.10
			<60	34.30	16.88	66.40	17.64
1,25(OH)₂D (pmol/L)*	94.50	28.99	≥60	97.99	28.05	101.04	30.92
			<60	79.65	28.08	104.72	28.51
Klotho (pg/ml)*	512.06	1.53	≥60	526.83	1.56	512.57	1.52
			<60	450.39	1.34	502.28	1.42
PTH (pg/ml)*†	43.91	1.58	≥60	42.00	1.56	36.94	1.61
			<60	52.47	1.59	44.07	1.68
SOST (pmol/L)*†	44.52	1.54	≥60	42.32	1.52	43.20	1.56
			<60	54.59	1.48	55.01	1.51
DKK1 (pmol/L)*†	31.23	16.46	≥60	32.36	16.61	38.06	18.27
			<60	26.28	15.04	32.27	17.29
cFGF23 (RU/ml)*†	71.72	1.53	≥60	67.45	1.48	74.01	1.42
			<60	95.56	1.61	100.55	1.44
iFGF23 (pg/ml)*†	54.99	1.65	≥60	52.80	1.66	61.67	1.51
			<60	65.98	1.57	75.80	1.52
c:iFGF23 ratio*†	1.98	1.81	≥60	1.93	1.81	1.83	1.61
			<60	2.27	1.78	2.11	1.70

*eGFR <60 (n=68) and ≥60 (n=309) ml/min/1.73m²
Significant difference (p<0.05) between eGFR categories at baseline* or after 12 months of supplementation†

***Disclosures: Marilena Christodoulou**, None*

P-357

Validation of a novel musculoskeletal image analysis software (Tissue CompassTM) *Mahdi Imani[1], Gustavo Duque[1], Ebrahim Bani Hassan[1]. [1]Department of Medicine, Western Health and the Australian Institute for Musculoskeletal Science (AIMSS), Melbourne Medical School, The University of Melbourne, St Albans, Melbourne, VIC, Australia., Australia

Purpose: Accurate quantification of bone, muscle and their components (e.g. infiltrated fat) is still an unmet need in the musculoskeletal field, especially in newly emerging areas such as osteosarcopenia. Indeed, quantifying tissue volumes on 3D images using the existing software is labor-intensive and time-consuming. Hence, we developed and validated a software for semi-automated to automated segmentation and quantification of musculoskeletal tissues, which includes muscle, fat, hematopoietic marrow (HBM) and bone.Methods: Tissue Compass™ is a standalone software developed on MATLAB 2019b (MathWorks). To validate the software, slices of quantitative CT images (QCTs) (n=100 men) were used to quantify bone, HBM and marrow adipose tissue (MAT) in L1 vertebral body and left hip using Tissue Compass and the leading commercial software (SliceOmatic, TomoVision, CA) as a comparator. Using the same software, QCT slices of 50 men were used to quantify psoas muscle volumes and their intramuscular fat (IMF) and fat-infiltrated muscle (FIM). Mean difference and limits of agreement were calculated using Bland Altman plots. Also, Pearson's correlation coefficients and intra-class correlation coefficient were calculated to study the agreement between both techniques.Results: Semi-automated and automated segmentation techniques (that to our knowledge are unique to Tissue Compass™) accelerated tissue analyses by up to 10 times. Tissue Compass™ also provided a 3D visualization of segmented ROI with different transparency levels, making it ideal for investigating interior geometry and proximities of tissues by seeing them through each-other (Fig 1a & 1b).The two softwares showed excellent to perfect correlations (R=0.99 to 1.00) in quantification of all tissues.Bland Altman mean difference (limits of agreement) for hip and L1 showed excellent agreement between the two software: 0.03 (-0.13, 0.20) for MAT-hip, 0.05 (-0.08, 0.18) for HBM-hip, and 0.05 (-0.24, 0.34) for bone-hip; and -0.02 (-0.34, 0.31) for MAT-L1, -0.14 (-0.44, 0.17) for HBM-L1, and -0.29 (-0.62, 0.05) cm3 for bone-L1.Same excellent agreements were observed for psoas muscle measurements: -0.004 (-0.013, 0.006) for IMF, -0.045 (-0.133, 0.043) for FIM, and 0.020 (-0.326, 0.366) cm3 for muscle.Conclusion: Presented software using its semi-automatic segmentation and automatic quantification techniques provides a faster and easier tool to study musculoskeletal tissues and their components.

Posters

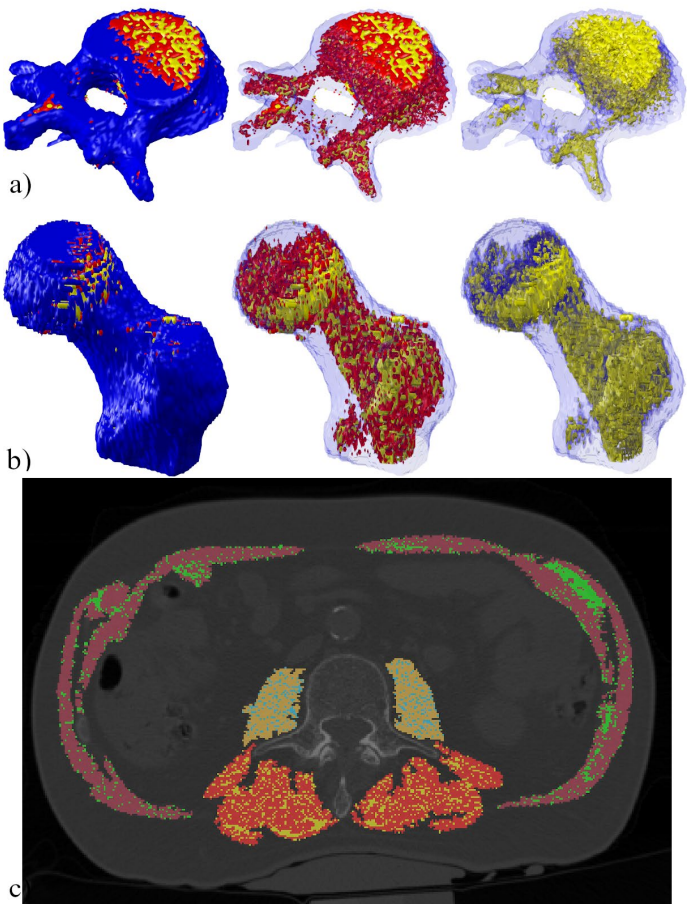

***Disclosures: Mahdi Imani**, None*

P-358

Bone loss with aging is independent of age-related gut microbiome dysbiosis in mice *Xiaomeng You[1], Jing Yan[1], Jeremy Herzog[2], Ross Campbell[3], Allison Hoke[4], Rasha Hammamieh[5], R. Balfour Sartor[2], Melissa A. Kacena[6], Nabarun Chakraborty[7], Julia F. Charles[8]. [1]Department of Orthopedic Surgery, Brigham and Women's Hospital, Harvard Medical School, Boston, MA, USA, United States, [2]National Gnotobiotic Rodent Resource Center, University of North Carolina at Chapel Hill, Chapel Hill, NC, USA, United States, [3]The Geneva Foundation, Walter Reed Army Institute of Research, Silver Spring, MD, USA; Medical Readiness Systems Biology, Walter Reed Army Institute of Research, Silver Spring, MD, USA, United States, [4]Medical Readiness Systems Biology, Walter Reed Army Institute of Research, Silver Spring, MD, USA; ORISE, Walter Reed Army Institute of Research, Silver Spring, MD, USA, United States, [5]Medical Readiness Systems Biology, Walter Reed Army Institute of Research, Silver Spring, MD, USA, United States, [6]Department of Orthopaedic Surgery, Indiana University School of Medicine, IN, USA; Richard L. Roudebush VA Medical Center, IN, USA, United States, [7]The Geneva Foundation, Walter Reed Army Institute of Research, Silver Spring, MD, USA; Medical Readiness Systems Biology, Walter Reed Army Institute of Research, Silver Spring, MD, USA, United States, [8]Department of Orthopedic Surgery, Brigham and Women's Hospital, Harvard Medical School, Boston, MA, USA; Division of Rheumatology, Brigham and Women's Hospital, Harvard Medical School, Boston, MA, USA, United States

Emerging evidence suggests an important role of the microbiome in bone health. The microbiome sustains a dynamic status that constantly adapts to the host physiology and fitness. During the aging process, the microbiome integrates and responds to aging signals from the host, which in turn impacts host health. However, it is unclear whether microbial dysbiosis with aging contributes to age-related bone loss.Here, age-specific microbial signatures were characterized and their roles in age-related bone loss were investigated in a murine model. 16s rRNA gene sequencing of fecal community samples from 3- and 24-month old CB6F1 males indicated an age-dependent shift towards a Firmicutes-dominant community with an alteration in energy and nutrient metabolism potential. Muscipirillum, a pathobiont associated with host inflammation, was increased in the aged microbiome. An integrative analysis of 16s predicted metagenome function and LC-MS fecal metabolome revealed enrichment of amino acid biosynthesis pathways in aged mice. Microbial methionine and S-adenosyl methionine metabolism were increased in the aged mice, which have previously been associated with the host aging process. Collectively, aging caused microbial taxonomic and functional dysbiosis in mice. We tested whether the young vs old microbiome differentially impacts bone turnover by colonizing 4 or 8-week old germ-free (GF) mice by fecal transplant from 3- or 24-month old specific-pathogen-free (SPF) mice. We assessed trabecular and cortical bone by micro-computed tomography 1 and 6 months after colonization. The effect of microbial colonization on bone phenotypes was independent of the microbiome donor age. To assess if the gut microbiome was required for age-related bone loss, we compared the trabecular and cortical bone structure of 24-month old CB6F1 GF female mice compared to that of littermates colonized at 8-weeks of age. The 24-month old bone phenotype was indistinguishable between colonized and GF mice. We next examined bone loss from 3 to 24 months in CB6F1 GF compared to SPF mice. Neither female nor male GF mice were protected from age-related bone loss. In conclusion, our study indicates age-related bone loss occurs independent of age-related gut microbial dysbiosis.

***Disclosures: Xiaomeng You**, None*

P-359

Longitudinal Evaluation of Saturated and Unsaturated Vertebral Marrow Adipose Tissue (MAT) Over 3 Years in Older Men and Women *Trisha Hue[1], Ann Schwartz[1], Susan Ewing[1], Kaipin Xu[2], Thomas Link[1], Sigurdur Sigurdsson[3], Thomas Lang[1], Deborah Kado[4], Gina Woods[4], Eric Vittinghoff[1], Clifford Rosen[5], Tamara Harris[6], Anne Schafer[1], Vilmundur Gudnason[3], Xiaojuan Li[7]. [1]University of California, San Francisco, United States, [2]Suzhou Niumag Analytical Instrument Corporation, China, [3]Icelandic Heart Association, Iceland, [4]University of California, San Diego, United States, [5]Maine Medical Center Research Institute, United States, [6]NIH-National Institute on Aging, United States, [7]Cleveland Clinic, United States

Marrow adipose tissue (MAT) increases with age and several investigations have identified higher MAT as a potential risk factor for worse bone and metabolic health outcomes. However, few studies have been conducted to evaluate longitudinal changes in MAT. Thus, we aimed to characterize total, saturated and unsaturated vertebral MAT change over approximately 3 years and assess the impact of vertebral lesions on measurements in a cohort of older men and women in the Bone Marrow Adiposity Follow-Up (BMAF) study. BMAF is a longitudinal ancillary study to Age Gene/Environment Susceptibility-Reykjavik (AGES-Reykjavik), a population-based cohort in Iceland. After excluding those who reported current bone-active medication use (n=65), a total of 143 men (mean age: 82.7 years +/- SD 4.3) and 140 women (mean age: 81.0 years +/- 4.3), with both baseline and follow-up MAT measures, were included in this analysis. Vertebral (L1-L4) MAT content was measured with single voxel proton magnetic resonance spectroscopy (1.5T MRS) and seven-peak Voigt model quantification. Total, saturated, and unsaturated MAT were defined as the ratio of total lipids (6 lipid peaks), saturated lipid (1.3 ppm peak), and unsaturated lipid (5.3 ppm peak) to total marrow contents, respectively. As part of the quality control process, spectra were graded for relative relationship between vertebral lesions (e.g., bone marrow edema and microfractures) and MRS volume of interest (VOI) box: grade 0=no lesion, 1=lesion outside of box, 2=partial lesion within box; 3=entire lesion within box. Additionally, a grading system was developed for evaluating the visual resolution of unsaturated lipids from water peak: grade 0=well resolved; 1=partially resolved; 2=not resolved. Mean changes in total MAT were +0.16 % per year for men and -0.046 % per year for women, with a wide range of values. When we excluded vertebral levels with grade 3 lesions, there was little effect on the mean or SD for change in total, saturated, or unsaturated MAT. Change in unsaturated MAT also did not differ when we excluded vertebral levels with low unsaturated lipid resolution (grade 2). Excluding vertebra with grade 3 lesions and/or poor spectral resolution of unsaturated lipids did not significantly change the results and therefore, may not be necessary in future studies. After approximately 3 years of follow-up, changes in saturated and unsaturated MAT were small and similar between older men and women.

	Change in Total L1-L4 MAT[a] (%/year)				Change in Saturated MAT[b] (%/year)				Change in Unsaturated MAT[c] (%/year)					
	ALL		Excluding vertebra with lesions grade 3		ALL		Excluding vertebra with lesions grade 3		ALL		Excluding vertebra with lesions grade 3		Excluding vertebra with lesions grade 3 AND/OR unsaturated lipid resolution grade 2	
	N	Mean ± SD	N	Mean ± SD	N	Mean ± SD	N	Mean ± SD	N	ALL	N	Mean ± SD	N	Mean ± SD
MEN F/U Time (yrs)	143	2.7 ± 1.5												
MEN change in BMF (%) per year	143	0.16 ± 3.01	131	0.11 ± 3.06	143	0.17 ± 2.17	131	0.17 ± 2.12	143	0.23 ± 0.37	131	0.23 ± 0.41	130	0.24 ± 0.42
WOMEN F/U Time (yrs)	140	3.2 ± 1.5												
WOMEN change in BMF (%) per year	140	-0.046 ± 2.06	130	-0.011 ± 2.26	140	0.14 ± 1.51	130	0.19 ± 1.62	140	0.25 ± 0.32	130	0.27 ± 0.34	127	0.27 ± 0.33

[a]Total L1-L4 MAT = [saturated lipid (1.3 ppm peak) + unsaturated lipid (5.3 ppm peak) + 4 other lipid peaks] / total marrow contents*
*NOTE: total marrow contents = water + 6 lipid peaks
[b]saturated MAT = saturated lipid (1.3 ppm peak) / total marrow contents
[c]unsaturated MAT = unsaturated lipid (5.3 ppm peak) / total marrow contents

***Disclosures: Trisha Hue**, None*

P-360

An Aging-Related Bone Loss through Activation of Succinate Receptor1 *yuqi guo[1], Xin LI[2]. [1]NYU College of Dentistry, United States, [2]NYU COLLEGE OF DENTISTRY, United States

Mitochondrial succinate dehydrogenase (SDH) deficiency was reported to directly contribute to aging. But the underlying mechanism is unknown. The deficient SDH activity unavoidably leads to the accumulation of succinate, an intermediate metabolite in tricarboxylic acid cycle. We have observed a significant elevation of succinate, in bone cells from old subjects and sera from aged mice. The elevated succinate can be released to act as an extracellular signaling mediator through the succinate specific receptor (SUCNR1). SUCNR1 is a G protein-coupled receptor and Succinate/SUCNR1 signaling has provided a new paradigm for the mechanism of cell stress response in organs. We have investigated on the role of elevated succinate and SUCNR1 activation in age-related bone loss. Our hypothesis is targeting succinate receptor activation attenuates the accelerated bone loss in aging. We have demonstrated that succinate directly stimulates osteoclastogenesis and osteoclast activity through SUCNR1 in vitro and in vivo. We compared the effects of extracellular succinate action through SUCNR1 on bone resorption in WT and SUCNR1 KO littermate mice at various ages. Vehicle or succinate treated Young (1-month-old, 6-month-old), Mid-Aged (12-month-old), and Aged (18- month-old) male and 6-month-old sham and ovariectomized female mice were examined. Femur bone samples were isolated for computed tomographic (micro-CT) analysis. Serum levels of succinate and bone turn-over markers were measured with blood collected via cardiac puncture. The results revealed an age-associated decline of SDH activity in marrow cells, succinate elevation in aged mice and a significant reduction of age-related bone loss in SUCNR1 KO mice. Importantly, succinate elevation leads to an increase of pro-inflammatory cytokine expression and augments myelopoiesis. Our study underscores the potential benefits of further investigation into the SUCNR1 receptor as a possible therapeutic target to delay age-related skeletal degeneration.

***Disclosures: yuqi guo**, None*

P-361

Population-Based, 3-Dimensional Analysis of Age- and Sex-Related Femur Geometry Changes *Ik Jae Jung[1], Eun Jung Choi[2], Byung Gook Lee[3], Ji Wan Kim[4]. [1]University of Ulsan, College of Medicine, Republic of Korea, [2]Asan Medical Center, Republic of Korea, [3]Dongseo University, Republic of Korea, [4]Asan Medical Center, Universitu of Ulsan, Republic of Korea

The changes in femur geometry that occur with aging and lead to fragility or insufficiency fracture remain unclear. The role of the lower limb geometry, including the femur and femoral bowing, has become a point of discussion, especially in atypical femur fracture. This study aimed to analyze femur geometry using 3-dimensional skeletonization. We acquired computed tomography images of both femurs obtained. A total of 1400 age- and sex-stratified participants were enrolled and were divided into subgroups according to age (by decade) and sex. The computed tomography images were used to produce 3-dimensional samplings of anatomical elements of the human femur using reconstruction and parametrization from these datasets. The process of skeletonization was conducted to obtain compact representation of the femur. With the skeletonization, we were able to compare all parameters according to age and sex. The femur length was 424.4 +/- 28.6 mm and were longer in men ($P < 0.001$). The minimum diameter of the medullary canal was 8.9 +/- 2.0 mm. The radius of curvature (ROC) was 906.9 +/- 193.3mm. Men had a larger femur length, femur outer diameter, and the narrowest medullary diameter ($P < 0.001$, respectively). Women had significantly smaller ROC ($P < 0.001$). ROC decreased by 19.4% in men and 23.6% in women between the ages of 20 to 89 years. Femur width increased over life by 11.4% in men and 24.5% in women. Between the ages of 50 and 89 years, the medullary canal appears to have increased by 32.7% in women. This geometry analysis demonstrated that femoral bowing and femoral width increased related to aging, and that the medullary canal widened after the age of 50 years in women. This study revealed important age- and sex-related changes in femur geometry that occur with aging and osteoporosis.

***Disclosures: Ik Jae Jung**, None*

P-362

Body-composition reference ranges in healthy Australian adults: The Australian Body Composition (ABC) Study *Ben Kirk[1], Ebrahim Bani Hassan [1], Sharon Brennan Olsen[2], Stefanie Bird[1], Sara Vogrin[1], Jesse Zanker[1], Steven Phu[1], Gustavo Duque [1]. [1]Australian Institute for Musculoskeletal Science (AIMSS), The University of Melbourne and Western Health, St Albans, Melbourne, VIC, Australia., Australia, [2]School of Health and Social Development, Deakin University, Geelong Waterfront, Geelong, VIC, Australia. d. Institute for Health Transformation, Deakin University, Geelong, VIC, Australia., Australia

Purpose: To develop age- and sex-specific reference ranges for body-composition parameters using data from Hologic dual energy x-ray absorptiometry (DXA) machines in Australian adults. Methods: Cross-sectional analyses of healthy community-dwelling adults (>=18 years) who underwent a DXA scan at one of three health and wellness sites (Mobile DXA Pty Ltd; DXA Melbourne Pty Ltd; and EC Group Pty Ltd) in Australia. Whole-body scans were carried out on Hologic Discovery and Horizon machines (Hologic, Inc., Bedford, MA). Adult participants with a maximum height of 190cm were included. LMS method was used generate sex-specific, age-dependent centile curves for body-composition parameters [lean body mass (LBM), total body fat (TBF), appendicular lean mass (ALM), appendicular fat mass (AFM), ALM/BMI, ALM/height(h)2, ALM/AFM, android fat, gynoid fat]. A subset of reference range (ALM/h2, ALM/BMI, TBF) results are shown here. Results: A total of 15479 Caucasian adults (54% men) with a median age of 33 years (interquartile range: 28, 42) were included. ALM/h2 remained stable until the 5th decade after which this parameter started to decline in both sexes (Figure 1). The reference values (3rd, 97th percentiles) were 7.84-13.06 kg for men (M) and 5.89-9.99 kg for women (W) at 30 years, 7.95-12.82 kg (M) and 5.93-10.16 kg (W) at 40 years, 7.83-12.47 kg (M) and 5.84-10.14 kg (W) at 50 years and 7.42-11.82 kg and 5.57-9.74 kg, respectively, at 60 years. ALM/BMI showed a steady decline from 20 years onwards in both sexes (Figure 1), the reference values were 0.90-1.45 kg/m2 (M) and 0.62-1.13 kg/m2 (W) at 30 years, 0.87-1.42 kg/m2 (M) and 0.59-1.10 kg/m2 (W) at 40 years, 0.85-1.38 kg/m2 (M) and 0.55-1.05 kg/m2 (W) at 50 years and 0.80-1.32 kg/m2 and 0.51-0.98 kg/m2, respectively, at 60 years. TBF tended to increase with age in both sexes (Figure 1), the reference values were 7.1-37.5 kg (M) and 8.7-43.7 kg (W) at 30 years, 7.9-40.9 kg (M) and 8.8-48.2 kg (W) at 40 years, 8.7-40.6 kg (M) and 9.1-52.0 kg (W) at 50 years and 9.2-41.2 kg and 10.9-49.9 kg, respectively, at 60 years. Conclusions: These findings will facilitate clinicians and researchers in identifying body-composition abnormalities involved in various pathological states (i.e., obesity, cachexia, sarcopenia, frailty) using the most widely used DXA machine (Hologic). Adjusting ALM for BMI versus h2 also produced different trends, which may be clinically relevant for diagnosis of sarcopenia and obesity.

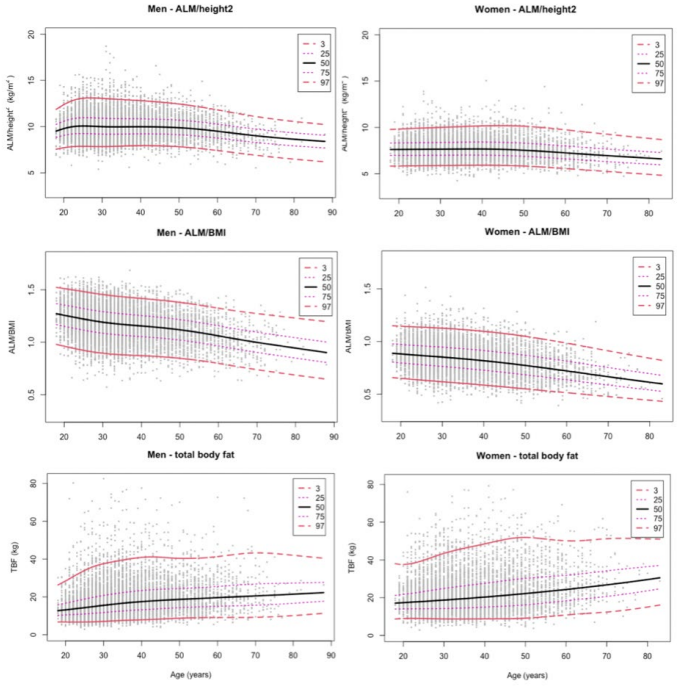

***Disclosures: Ben Kirk**, None*

P-363

Prevalence of radiographic lumbar spondylosis and its association with osteoporosis in an elderly Brazilian population of the community: São Paulo Ageing & Health (SPAH) Study *Ricardo Fuller[1], Thaysa Passalini[1], Rosa Pereira[1]. [1]University of Sao Paulo, Brazil

Purpose: to evaluate the relationship between the radiographic lumbar spondylosis (LS) and osteoporosis (OP) in a representative population of Brazilian elderly. Methods: Cross-sectional evaluation of 616 (385 woman and 235 man) Brazilian elderly people of the community (65 years or older) from a cohort São Paulo Ageing & Health (SPAH) Study. Lateral spine radiographs (L1 to L5) were analyzed using the Kellgren & Lawrence index to determine: presence of spondylosis (KL> = 2 in at least one intervertebral level), KL total score (L1-L2 to L4-L5) and presence of vertebral fractures. Bone mineral density was assessed by dual energy X-ray absorptiometry (DXA) of the lumbar spine and femur. Osteoporosis was defined as a BMD 2.5 standard deviations or more below the mean value for young adults (T score<−2.5). Results: Lumbar spondylosis was present in 76.64% in women and 92.34% in men (p=0.000). The prevalence of LS was lower in women with vs without osteoporosis (respectively 69.2% vs 81.9%, p = 0.005); there was no difference for men (90.2% vs 91.4%, p = 0.744). There was no difference in the prevalence of LS in women with vs without fragility fractures (respectively 73.5% vs 75%, p = 0.763), and men (respectively 94.6% vs 89.4%, p = 0.198). There was also no difference in the prevalence of LS when

vertebral and non-vertebral fractures were analyzed separately, for both women and men. Conclusions: The prevalence of LS was very high in elderly people of the community. The LS was less prevalent in women with osteoporosis

***Disclosures: Ricardo Fuller**, None*

P-364

Blood borne bone: Circulating Osteoprogenitors Associated with Bone and Muscle quality. *Jack Feehan[1], Cassandra Smith[2], Alexander Tacey[2], Ahmed Al Saedi[1], Gustavo Duque[1], Itamar Levinger[2]. [1]The University of Melbourne, Australia, [2]Victoria University, Australia

Circulating osteoprogenitor (COP) cells, found within the peripheral blood, express characteristics of mesenchymal stem cells (MSCs) with the capacity to proliferate and differentiate into bone, muscle and fat. While some aspects of their in vitro and in vivo behaviour as mesenchymal progenitors has been established, much remains unknown about their role in age-related musculoskeletal diseases such as osteoporosis and sarcopenia. In this study, our aim was to identify if a relationship exists between COP cells and important muscle and bone parameters.Thirty-eight healthy older people [mean age 72 (+/-6yrs), mean BMI 28.4] were recruited from the community. Exclusion criteria included recent history of fracture, or initiation of osteoporosis medication, type 2 diabetes mellitus, haematological, myelodysplastic or myeloproliferative disorders. Participants underwent a series of assessments including a blood sample, anthropometry and body composition analysis via densitometry. Peripheral blood samples were analysed for via flow cytometry, with COP cells defined as peripheral blood mononuclear cells (PBMCs) co-expressing the CD45 and osteocalcin markers. COP cell number is expressed as a percentage of the total PBMC population. Regression analysis was used to identify relationships between variables.Increased COP cell number was associated with increased femoral (r=0.442, p=0.008,) and total BMD (r=0.376, p=0.025) and tended to correlate with appendicular lean mass (r=0.314, p=0.06). These results remained consistent after adjustment for age and BMI.COP cell number is linked to bone and muscle parameters in vivo. This suggests the hypothesis that COP cells have a role in the maintenance and cross talk between these tissues. Future studies should evaluate whether COP cells can be used as a novel biomarker for diseases such as osteosarcopenia.

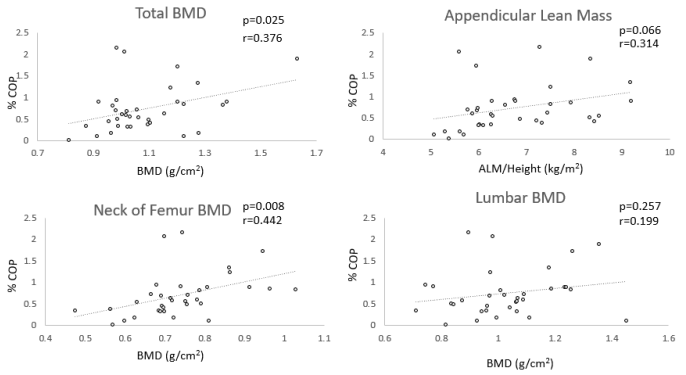

***Disclosures: Jack Feehan**, None*

P-365

Predictors of change in the peripheral skeletons of older adults in rural Gambia *Mícheál Ó Breasail[1], Camille Parsons[2], Ayse Zengin[3], Landing Jarjou[4], Ann Prentice[1], Kate Ward[2]. [1]MRC Nutrition and Bone Health Research Group, United Kingdom, [2]MRC Lifecourse Epidemiology Unit, University of Southampton, United Kingdom, [3]Department of Medicine, School of Clinical Sciences at Monash Health, Monash University, Australia, [4]MRC Unit The Gambia, London School of Hygiene and Tropical Medicine, Gambia

Growing aging populations across Sub-Saharan Africa (SSA) will lead to increases in osteoporosis and other chronic musculoskeletal conditions, data are required to understand musculoskeletal aging in the region. No longitudinal studies to date describe changes in bone in SSA. Repeat measures were acquired from rural Gambians (n=322, 52.5% female) aged 40-92 (mean(SD) 60(12)) years. pQCT outcomes were total area (TotA), total (TotBMD) and trabecular vBMD (TrBMD) from the 4% distal radius and tibia. Height (cm), weight (kg) and BMI (kg/m2) were recorded. Muscle function was assessed by handgrip dynamometry (max grip, N/kg) and jumping mechanography (relative force (kN/kg) and max relative power (kW/kg)). Bone turnover markers (BTM), serum collagen type 1 cross-linked β-C-telopeptide (CTX) and type 1 procollagen N-terminal (P1NP), were measured. Percentage annual change for pQCT outcomes was calculated. Univariate analysis was performed to explore if baseline age, BMI, BTMs, or muscle function predicted bone change. Models were repeated with a sex adjustment. Results are presented as β (95% CI) where β is the percentage change per year per unit of the independent variable. Mean(SD) time to follow up was 1.8(0.3) years. At all sites Tot and TrBMD decreased and TotA increased except tibia TotA. Baseline age was predictor of change in radius TotBMD (-0.06(-0.10,-0.02)) and TotA (0.07(0.01,0.10)), and tibia TrBMD (-0.04(-0.07,-0.01)). Greater baseline grip strength was associated with less decrease in tibia TotBMD (0.003(0.001,0.006)) and TrBMD (0.006 (0.002,0.009)). Similarly greater force was associated with less decrease in radius TotBMD (0.16(0.03,0.29)) and power with less decrease in tibia TrBMD (0.04(0.01,0.08)), and radius TotBMD (0.07(0.02,0.12)). Greater force and power were associated with less change in radius TotA (-0.17(-0.31,-0.02);-0.06(-0.11,-0.01)); whereas at the tibia greater power was associated with greater change in TotA (0.02(0.01,0.05)). BTMs did not predict change. Adjustment for sex had no material effect, except for max relative power which no longer predicted tibia TotA change. These novel data suggest that increasing age is the main predictor of decreases in BMD in the peripheral skeleton. Better muscle function was associated with lower decline in vBMD. At the trabecular-rich distal radius and tibia no discernible sex-specific differences in change were found. These data provide important insight into musculoskeletal ageing in SSA.

***Disclosures: Mícheál Ó Breasail**, None*

P-366

Association of regional body composition and physical function using the Short Physical Performance Battery among Peruvian women with HIV *Diego Cabrera[1], Mijahil Cornejo[2], Yvette Pinedo[2], Patricia Garcia[3], Evelyn Hsieh[4]. [1]Universidad Peruana Cayetano Heredia - Yale University, Peru, [2]Hospital Nacional Arzobispo Loayza, Peru, [3]Universidad Peruana Cayetano Heredia, Peru, [4]Yale University, United States

Background: The musculoskeletal (MSK) system is significantly affected by HIV and its treatment. Changes in body composition can reflect important changes in bone and MSK health, particularly among populations at risk for developing fat redistribution syndromes, like HIV-positive women (HpW). Although more than half of HIV-infected population worldwide are women, there are limited data about characteristics of women aging with HIV in Latin American and the Caribbean (LAC). No studies from LAC have focused on the relationship between body composition changes and physical function among these individuals. We aimed to explore the scope of this problem among Peruvian women aging with HIV. Methods: We enrolled HpW and HIV-negative women (HnW) >=40 years of age receiving care at a large HIV clinic in Lima, Peru. Dual X-ray absorptiometry (DXA) was used to measure trunk and limb lean mass (LM) and fat mass (FM). Physical performance was assessed with the well-established Short Physical Performance Battery (SPPB) and physical strength with the grip strength test (GST) using a hand dynamometer. We used linear regression to model associations between HIV status, body composition and physical test scores.Results: 104 HpW and 212 HnW were enrolled with a mean age of 52.4+/-8.2 and 56.4+/-8.8 years (p<0.001) and BMI of 26.4+/-5.1 and 27.6+/-4.1 kg/m2 (p=0.03), respectively. Among HpW, the mean years since HIV diagnosis was 11.8+/-6 and everyone was on antiretroviral treatment (9.9+/-5.3 years). Fat mass index (FMI) was 9.6+/-3 vs 10.9+/-2.7 kg/m2 (p<0.001) between HpW and HnW, respectively. Overall mean SPPB score was 9.9 vs 10.8 between HpW and HnW, respectively (p<0.001). Mean grip strength was 19.9+/-5.9 vs 19.8+/-5.4 kg (p=0.83) between HpW and HnW, respectively. In multivariate models adjusted by age and HIV status, increased trunk FM was independently associated with decreased SPPB score (p<0.001), increased arm LM was independently associated with increased GST(p<0.001) and increased arm %fat was independently associated with decreased GST (p<0.001).Conclusions: In this study, trunk FM and arm LM were independent predictors for the physical performance and function tests described, and HIV status was independently associated with SPPB score. Larger prospective studies are needed among PWH in LAC to help identify individuals at high risk for declines in physical function, and to inform prevention guidelines.

Overall SPPB Scores and Subscores and Grip Strength test between HIV-positive and HIV-negative women in Lima, Peru

Characteristics	HIV-positive women N= 104	HIV-negative women N = 212	P-value
SPPB			
Overall score, *mean (SD)*	9.99 (1.4)	10.81 (1.12)	**<0.001**
score <8 *N(%)*	3 (2.9)	5 (2.4)	0.464
score ≥8 *N(%)*	101 (97.1)	207 (97.6)	**<0.001**
Balance test, *mean (SD)*	3.68 (0.51)	3.86 (0.36)	**0.0003**
Gait test, *mean (SD)*	3.56 (0.55)	3.71 (0.48)	**0.0116**
Chair stand test, *mean (SD)*	2.75 (0.71)	3.14 (0.77)	**<0.001**
Grip Strength Test			
Score (kg), *mean (SD)*	19.93 (5.91)	19.78 (5.44)	0.8251

SPPB: Short Physical Performance Battery

Overall SPPB score, balance test, gait test, chair stand test and grip strength score were tested using two independent samples T-test; proportion SPPB <8 and ≥8 were tested using Fisher's exact test

***Disclosures: Diego Cabrera**, None*

P-367

Maresin 1 resolves macrophage inflammation to improve aged bone fracture healing *Rong Huang[1], Linda Vi[2], Xiaohua Zong[1], Gurpreet Baht[1]. [1]Department of Orthopaedic Surgery, Duke University, United States, [2]Division of Physical Medicine and Rehabilitation, University of Toronto, Canada

Inflammaging is associated with the poor tissue regeneration observed in advanced age. Here, we investigated the efficacy of using Maresin 1 to improve aged fracture healing by resolving inflammation after acute bone injury. 24-month-old mice underwent tibial fracture surgery and were either treated with vehicle (Veh) or Maresin 1 (MaR1). Healing bones from MaR1-treated mice displayed increased bone deposition, increased structural stiffness, and increased force to fracture in the later stages of repair. In the early stages, MaR1 treatment decreased the number of pro-inflammatory macrophages within the fracture callus and decreased the level of inflammatory biomarkers in circulation. In tissue culture models, MaR1 treatment of macrophages derived from the bone marrow of aged mice induced secretion of an osteoinductive secretome, able to enhance osteoblast differentiation. Our findings here identify resolution of inflammation, and MaR1 itself, to be a point of intervention to improve age bone healing.

***Disclosures: Rong Huang**, None*

P-368

Aging delays epimorphic regeneration in mice *Regina Brunauer[1], Ian Xia[1], Shabistan Asrar[1], Lindsay Dawson[1], Connor Dolan[1], Ken Muneoka[1]. [1]Texas A&M University, United States

Regenerative decline is one of the most striking effects of aging. Currently available studies exploring age effects on regeneration typically investigate a single tissue type and focus on stem cell function. Amputation of the distal mouse digit tip transects nail and skin epidermis, bone and connective tissue and induces an epimorphic regeneration response hallmarked by formation and patterned differentiation of a blastema and de novo morphogenesis of all involved tissues, but the effects of aging on this process are unknown. We find that the state of epidermal wound closure, which depends on osteoclast-dependent bone resorption, determines the pace of blastema maturation and bone formation, and is postponed in aged digits. This delay is not due to a scarcity of progenitor cells, but a drastically reduced mineralization rate in aged digits. We conclude that with aging, blastema formation is intact, and the blastema is fully capable of regeneration, but crucial intermediate steps are temporally inhibited, resulting in a significantly delayed completion of regeneration, reminiscent of delayed fracture healing in aged bone. This study is the first report about the effects of aging on mammalian epimorphic regeneration, highlighting the importance of the spatiotemporal regulation of cell function in regeneration, and our findings will be instructive to identify aging mechanisms that hamper homeostatic and reparative tissue regeneration.

***Disclosures: Regina Brunauer**, None*

P-369

Smad-dependent BMP signaling in cranial neural crest cells directs their cell fate towards chondrogenic lineage through chromatin structural changes to cause midline craniosynostosis *Yuji Mishina[1], Hiroki Ueharu[2], Jingwen Yang[1]. [1]University of Michigan School of Dentistry, United States, [2]University of Michigan School of Dentisrty, United States

Neural crest cells (NCC) are pluripotent cell populations that differentiate into numerous derivatives in the vertebrate body. We previously generated a craniosynostosis mouse model via conditionally express a constitutively active form of BMP type IA receptor (caBmpr1a) in a neural crest cells (caBmpr1a;P0-Cre). The mutant mice showed premature fusion of the anterior frontal (AF) suture associated with increased BMP-Smad signaling. Ectopic cartilages were identified in the AF suture before its fusion. These facts prompted us to hypothesize that increased BMP signaling in cranial NCC alters cell fate towards chondrogenic lineage to generate ectopic cartilage at the AF suture, thus inducing its premature fusion through endochondral ossification.To get mechanistic insights of how increased BMP signaling alters cell fate of NCCs, we used a similar model to activate BMP-Smad signaling via ACVR1, another type 1 receptor for BMPs (caAcvr1;P0-Cre), since this model develops massive endochondral ossification during craniofacial development. In vivo treatment with LDN-193189, a selective inhibitor of BMP type I receptor kinases, rescued ectopic cartilage formation, when treated at E11.5, but not E12.5. Single-cell ATAC sequence using cells from the first branchial arch (BA1) of E10.5 embryos demonstrated that chromatin of Sox6, a gene essential for chondrogenesis, is more accessible in mutants than controls, while those of Sp7 (osteogenesis), Pax7 (myogenesis) and Zfp423 (adipogenesis) are less accessible in mutants. These results strongly suggest that increased BMP signaling in cranial NCCs around E10.5-11.5 alters cell fate towards chondrogenesis.We set up an unbiased screening to identify key genes for cell fate specification by comparing cranial NCCs and trunk NCCs between controls and mutants, since there was no ectopic cartilage in the mutant trunk region despite increased BMP signaling. Single-cell RNA sequence followed by QRT-PCR and in situ validations revealed increased expression of expected BMP targets such as Dkk1 and Sox9. Interestingly, we found reduced expression of Efnb1, which encodes Ephrin B1 and is a causative gene for craniofacial malformations. We will discuss updated bioinformatics analyses to understand downstream events of increased BMP signaling in cranial NCCs for cell fate specification. These findings would provide a potential target for the prevention of premature fusions of cranial sutures caused by endochondral ossification.

***Disclosures: Yuji Mishina**, None*

P-370

Phlpp1 and Phlpp2 differentially regulate endochondral ossification and chondrogenesis *Samantha Weaver[1], Shannon Flanary[1], Elizabeth Zars[1], Earnest Taylor[1], Jennifer Westendorf[1]. [1]Mayo Clinic, United States

Endochondral ossification is controlled by a coordinated network of signaling cascades. Phlpp1 and Phlpp2 are protein phosphatases that negatively regulate anabolic signaling in chondrocytes and other cell types. Phlpp1 and Phlpp2 variants are associated with height phenotypes in GWAS studies. Phlpp1-/- mice have shorter femurs and tibiae and lower bone volume than WT mice. Immature articular chondrocytes (IMCs) cultured from Phlpp1-/- mice are more chondrogenic, with greater production of glycosaminoglycans and increased signaling of anabolic enzymes pAKT, pPKC, and pERK, among others. Phlpp2 targets similar signaling cascades, but prefers AKT1 over AKT2/3. Here, we report that Phlpp2 has similar chondrogenic effects as Phlpp1 in vitro, but not in vivo. At four weeks of age, femur and tibiae lengths in Phlpp2-/- mice were similar to WT mice. The epiphyseal growth plates of Phlpp2-/- mice did not have increased proliferative cell number, as previously reported in Phlpp1-/- mice. However, Phlpp2-/- IMCs plated in micromass had increased Alcian blue staining and Col2a1, Sox9, and pAKT signaling as well as elevated production of AP-1 transcription factors JunB and FosB. Both Phlpp1-/- and Phlpp2-/- chondrocytes were more proliferative than WT cells in vitro, as evaluated by a growth assay over 48 hours. To examine the discrepancy between the in vitro and in vivo phenotypes, Phlpp1-CKOCol2a1 and Phlpp2-CKOCol2a1 mice were generated to conditionally delete Phlpp1 or Phlpp2 only in Col2a1-expressing cells. No growth phenotype was observed in mice from either of these genotypes at four weeks of age, but IMCs from both genotypes were more chondrogenic in vitro than WT-Col2a1Cre+ controls. These data suggest that: 1) Phlpp1 is the main regulator of endochondral ossification in vivo and may have a compensatory effect over Phlpp2 deletion in the murine growth plate and 2) the reduced growth phenotype evident in Phlpp1-/- mice is not due solely to Phlpp1 expression in Col2a1-expressing cells such as chondrocytes and bone marrow cells. Thus, Phlpp1 and Phlpp2 have complementary but non-redundant roles in chondrocytes and endocrine factors may control endochondral growth in Phlpp1 deficient mice.

***Disclosures: Samantha Weaver**, None*

P-371

Impairment of Limb Development by Genetic Ablation of Cobra1 *Chao Tu[1], Bin Yuan[2], Huiliang Yang[3], Rui Hua[1], Sumin Gu[1], Wentian Yang[3], Rong Li[2], Jean X Jiang[1]. [1]Department of Biochemistry and Structural Biology, The University of Texas Health Science Center, San Antonio, TX 78229, USA, United States, [2]Department of Biochemistry and Molecular Medicine, School of Medicine and Health Sciences, The George Washington University, Washington, DC 20037, USA, United States, [3]Department of Orthopaedics, Brown University Alpert Medical School and Rhode Island Hospital, Providence, RI 02903 USA., United States

Background: Osteochondral progenitors (OCPs) are mesenchymal precursors that could differentiate into chondrocytes and osteoblasts, and thus exert important function in limb development. COBRA1, also known as NELF-B, is a pleiotropic transcriptional cofactor that regulates RNA polymerase II pausing and transcription elongation, and subsequently controls cell survival and growth in diverse developmental processes. However, the function of Cobra1 in lineage commitment of OCPs remains largely unknown. In this study, we aimed to investigate the role of COBRA1/NELF-B in early limb development by conditional deletion of Cobra1 in OCPs of the limb bud mesenchyme. Methods: We generated Prx1-cre; Cobra1flox/flox conditional knockout mice (cKO) and their control littermates. The lengths of long bones were measured. The skeletal structure and formation of newborn limbs were grossly and histologically evaluated by whole-mount skeletal staining, H&E, and Safranin-O staining. TUNEL assay was performed to detect the apoptotic cells. Quantitative real-time PCR, western blotting, and RNAscope-based in situ hybridization were utilized to determine the mRNA- and protein-level expression of genes related to osteogenesis and chondrogenesis. Results: Cobra1 cKO mice exhibited severe skeletal defects after birth, including shortened length in long bone and decreased cortical thickness. Histological analysis revealed remarkable reduced bone mass density, disorganized chondrocyte column of growth plate, scattered distribution and compromised terminal differentiation of chondrocytes, as well as impaired endochondral ossification. These characteristics manifested severely restrained chondrogenesis and osteogenesis. In addition, Cobra1 cKO exhibited increased apoptotic chondrocytes. Moreover, expression levels of osteogenic markers (Col1a1, Ibsp1), chondrogenic markers (Acan, Col2a1), and hypertrophic markers (Col10a1, Mmp13) were significantly downregulated in Cobra1 deficiency mice. Importantly, SOX9, a key regulator of chondrogenesis, was also markedly decreased in Cobra1 cKO mice compared to control. Conclusions: This study unveils a previously unrecognized role of Cobra1 in regulation of limb development, likely in part by regulating the chondrogenesis and osteogenesis of OCPs.

***Disclosures: Chao Tu**, None*

P-372

Combinatorial CRISPR/Cas9 approach to elucidate the role of WNT16 in regulating bone development in zebrafish *zhen liu[1], weiwei liu[1], xing su[1], ying wang[2], lijun tan[1], yun deng[3], xiang-ding chen[1]. [1]Laboratory of Molecular and Statistical Genetics, College of Life Sciences, Hunan Normal University, Changsha, Hunan 410081, China, China, [2]The National and Local Joint Engineering Laboratory of Animal Peptide Drug Development, College of Life Sciences, Hunan Normal University, Changsha, 410081, Chin, China, [3]The Center for Heart Development, Key Lab of MOE for Development Biology and Protein Chemistry, College of Life Sciences, Hunan Normal University, Changsha, 410081, Hunan, China, China

Human genetic studies demonstrate that WNT16 plays important role in the regulation of bone mineral density, cortical thickness, bone flexion rate, bone mass and ultimately fracture risk. However, the underlying mechanism is not yet fully understood. In this study, the role of WNT16 in skeletal development and metabolism were evaluated on a WNT16 null mutant in zebrafish through CRISPR/Cas9-mediated gene knockout. As the result, the homozygous mutants exhibited mortality rate over 15% in an early embryonic stage. 20% of homozygous juveniles showed curved vertebra, upturned tail, lengthened jawbone, enlarged abdomen, slenderized caudal fin and lost caudal fin. In addition, most of them died at 19 days post fertilization. Further Micro-CT studies revealed that the bone mineral density of WNT16 -/- zebrafish showed a distinct reduction compared with wild type, which is similar to the phenotypes of the human osteoporosis. ALP staining and TRAP staining data suggested that WNT16 deficiency increase osteoclast activity but inhibit osteoblast activity. In summary, WNT16 is involved in the early embryonic development and the regulation of bone formation and resorption in zebrafish. It indicated that WNT16 might be a target for therapeutic interventions to improve osteoporosis treatment.

***Disclosures: zhen liu**, None*

P-373

Fam210a Alters Long Bone Development Through its Action in Mesenchymal Stem Cells and Chondrocytes *Loan Nguyen-Yamamoto[1], Aimee-Lee Luco[1], Takeshi Shimoide[1], Rene St Arnaud[2], David Goltzman[1]. [1]Research Institute of the McGill University Health Centre, Canada, [2]McGill University and Shriner's Hospital for Children, Canada

Purpose: FAM210a, a nuclear-encoded mitochondrial protein has been associated with osteoporosis in humans, and we previously reported that, although Fam210a is not expressed in mature osteoblasts, global deletion of Fam210a in mice reduced BMD and bone formation, altered microarchitecture and decreased bone biomechanical strength, at least in part through its action in muscle. This suggested that Fam210a has a crucial role in regulating bone structure and function. In this study, we examined the role of Fam210a in early long bone development and endochondral bone formation.Methods: We employed Fam210a flox/flox mice, and Prx1-Cre or Col2-Cre mice to generate mice with specific deletion of Fam210a in mesenchymal stem cells (MSC) or chondrocytes (Chon) respectively. We examined male and female mice at 2 months of age; because mice with homozygous deletion of Fam210a die shortly after birth, we studied heterozygous Fam210a MSC+/- and Fam210a Chon+/- mice. Prx1 cre- and Col2 cre- mice were used as controls, respectively. We examined femoral BMD, and microarchitectural changes in femurs by μCT analysis-Results: Compared to control mice, heterozygous female Fam210a MSC+/- mice showed significantly reduced BMD and femur length, and μCT analysis of femurs showed increased cortical BV/TV, reduced cortical porosity, reduced trabecular BV/TV, and reduced trabecular thickness and trabecular number. Significant changes were not, however, seen in male mice. In contrast, heterozygous male Fam210a Chon+/- mice showed significantly reduced BMD and femur length compared to control mice, with a trend toward increased cortical BV/TV and lower cortical porosity, and reduced trabecular BV/TV, trabecular thickness and trabecular number. Female mice, however showed no change in BMD and less reduction in femur length. Thus, female mice with haploinsufficency of Fam210a in osteoblast precursors and/or immature osteoblasts were more severely affected than males, whereas male mice with haploinsufficiency of Fam210a in chondrocytes were more severely affected than females. Conclusions: Fam210a plays an important role in long bone development through its action in mesenchymal stem cells and chondrocytes. This role may manifest features of sexual dimorphism. Further studies are ongoing to understand the mechanisms underlying these observations.

***Disclosures: Loan Nguyen-Yamamoto**, None*

P-374

Differential sensitivity to TGFβ signaling and regulatory changes to the Mmp13 promoter underlie species-specific variation in bone resorption and jaw length *Spenser Smith[1], Daniel Chu[1], Tiange Qu[1], Goutam Krish[1], Richard Schneider[1]. [1]University of California, San Francisco, United States

Precise regulation of jaw length is essential for species-specific adaptation and survival. Jaws are often affected by size-related birth defects like hypoplasia, retrognathia, asymmetry, and clefting. The jaw skeleton is derived from neural crest mesenchyme (NCM), and our prior work has shown that NCM governs species-specific jaw length through a variety of mechanisms, including embryonic regulation of bone resorption. By comparing jaw development in Japanese quail and white Pekin duck, we have identified Matrix metalloproteinase 13 (Mmp13) as a key determinant of jaw length. We have found that Mmp13 is expressed at substantially higher levels in the jaw primordia of quail than duck, that Mmp13 expression and bone resorption are NCM-mediated as revealed through quail-duck chimeras, and that inhibiting Mmp13 and bone resorption can lengthen the jaw. Here, we investigate molecular mechanisms that lead to differential regulation of Mmp13 and the ability of NCM to control bone resorption and jaw length. We focus on the TGFβ pathway, a known regulator of Mmp13 and bone resorption. We find significantly higher levels of TGFβ ligands, receptors, and effectors in the jaws of quail versus duck, indicating that quail have elevated TGFβ signaling. By treating jaw primordia from quail and duck with TGFβ1, we also discover intrinsic species-specific differences in sensitivity to TGFβ, with quail showing much stronger induction of intracellular effectors (SMADs), Mmp13, and other targets like Runx2. To ascertain mechanisms underlying species-specific differences in TGFβ sensitivity and levels of Mmp13 expression, we analyze the Mmp13 promoter in quail and duck. We find that the Mmp13 promoter contains RUNX2 and SMAD binding sites that affect Mmp13 expression. We generate species-specific reporter constructs with or without these binding sites. The endogenous quail Mmp13 promoter responds to TGFβ1, whereas the duck promoter does not. Removing the SMAD binding site reduces the response in quail but adding it to the duck increases activity. We also identify single nucleotide polymorphisms (SNPs) adjacent to the RUNX2 binding site that distinguish quail from duck. Swapping these SNPs plus the SMAD site between species abolishes the TGFβ1 response with quail promoters but adds a response to duck. Overall, our results suggest that multiple levels of gene regulation in the TGFβ signaling pathway mediate bone resorption, and ultimately species-specific variation in jaw length.

***Disclosures: Spenser Smith**, None*

P-375

Loss of Hypoxia-Inducible Factor-1a in the Presomitic Mesoderm Impairs Somitogenesis and Causes Spine and Rib Abnormalities Reminiscent of Jarcho-Levin Syndrome *Zachary Tata[1], Qing Yao[1], Matthew Anderson[2], Christophe Merceron[1], Frances Farley[1], Mark Lewandoski[2], Ernestina Schipani[3]. [1]Department of Orthopedic Surgery, School of Medicine, University of Michigan, United States, [2]Genetics of Vertebrate Development Section, Cancer and Developmental Biology Lab, National Cancer Institute, National Institutes of Health, United States, [3]Department of Orthopedic Surgery, School of Medicine, University of Michigan; Department of Medicine, Division of Endocrinology and Department of Cell and Developmental Biology, University of Michigan Medical School, United States

Jarcho-Levin Syndrome is a disease characterized by congenital scoliosis, abnormally shortened trunk length, and numerous costal and vertebral defects. Approximately 25% of cases of Jarcho-Levin Syndrome are secondary to loss of function mutations in genes of the Notch Signaling Pathway. Notch signaling plays a critical role in somitogenesis, the periodic segmentation of somites from the presomitic mesoderm (PSM) during embryonic axis extension, and these somites give rise to both the vertebrae and ribs in the fully developed organism. It has previously been reported that gestational hypoxia is sufficient to disrupt the oscillatory Notch Signaling expression normally required in the PSM for somitogenesis. Interestingly, hypoxia occurs naturally in embryos before the establishment of the mammalian circulatory system. The key mediator of the hypoxic response in mammals is the transcription factor Hypoxia-Inducible factor-1a (HIF1), which regulates expression of genes involved in a variety of processes including survival, differentiation and reprogramming of metabolism. Hypoxia increases the stability and transcriptional activity of HIF1 protein. However, the role of HIF1 in both somitogenesis and spinal development has yet to be investigated. To address this gap in knowledge, we conditionally inactivated HIF1 in the PSM using the T- (brachyury) Cre. Mutant mice displayed an abnormal curvature of the spine, as well as costal and vertebral defects which closely resemble those observed in Jarcho-Levin Syndrome. Loss of HIF1 did not affect cellular survival but led to dysregulation of the Notch signaling pathway in the PSM of mutant embryos. Additionally, inactivation of HIF1 in segmented somites or later developmental stages did not duplicate the phenotype seen with loss of HIF1 in the PSM. These results demonstrate that HIF1 plays a specific developmental role for the spine and ribs in the PSM and acts upstream of the Notch signaling pathway in the regulation of somitogenesis, offering new insight into the potential etiology of Jarcho-Levin Syndrome. In particular, we are currently testing the hypothesis that loss of HIF1 in the PSM increases local hypoxia by reprogramming metabolism and augmenting mitochondrial respiration, which could explain why either gestational hypoxia or loss of HIF1 in the PSM may cause a Jarcho-Levine Syndrome phenotype.

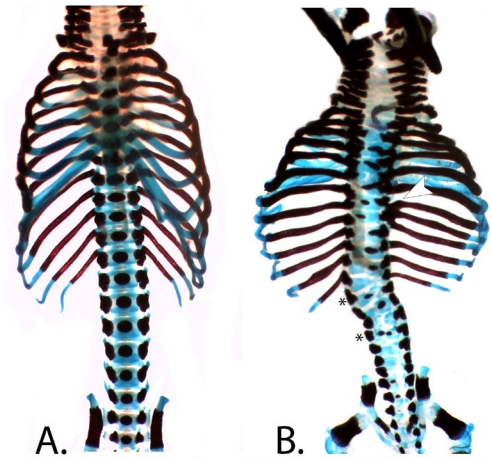

Wholemount alcian blue/alizarin red staining of E18.5 control (A) and mutant (B) embryos. Note the normal morphology seen in the ribs and lumbar region of the control embryo and the presence of fused ribs (white arrow) and hemi- and butterfly vertebrae (asterisks) in the mutant contributing to an abnormal scoliosis of the spine.

***Disclosures: Zachary Tata**, None*

P-376

METTL3-mediated m6A mRNA Methylation Modulates Tooth Root Formation *Rui Sheng[1], Yunshu Wu[1], Jun Wang[1], Shiwen Zhang[1], Qiwen Li[1], Danting Zhang[1], Xingying Qi[1], Qingyue Xiao[1], Shuang Jiang[1], Quan Yuan[1]. [1]Sichuan University, China

Purpose:N6-methyladenosine (m6A), one of the most abundant eukaryotic mRNA epigenetic modification catalyzed by methyltransferase-like 3 (Mettl3), influences various RNA processing events in RNA metabolism. However, the role of Mettl3-mediated m6A modification in tooth development has not been revealed. In this study, we aim to reveal the function of m6A modification regulated by METTL3 during tooth root formation.Methods:we established Sp7-Cre; Mettl3fl/fl and Gli1-CreERT2;Mettl3fl/fl mice to investigate that how deletion of Mettl3 affected the development of mandibular first molar root. Next, we silenced METTL3 in human dental pulp cells (hDPCs) to study the influence of METTL3 on odontogentic differentiation. Mechanically, we performed m6A MeRIP-Seq and analysis other published data to identify the critical m6A targets.Results:METTL3 was highly and prevalently expressed, during the stage of tooth root development, especially in dental papilla and dental pulp near the HERS. The Sp7-Cre; Mettl3fl/fl mice which especially knockout Mettl3 in dental pulp cells and odontoblasts showed the anomalous odontogenesis during tooth root formation, including short root anomaly and thinner root dentin. H&E staining sections and double labelling assay indicated decreasing pre-dentin secreting and mineral apposition rate of dentin. In addition, acid-etched SEM showed sparse odontoblast-processes in root area. Furthermore, The capacity of reparative dentin formation was impaired in Sp7-Cre; Mettl3fl/fl mice, while it was enhanced in Sp7-Cre; Mettl3KI/KI mice. The Gli1-CreERT2; Mettl3fl/fl mice also showed abnormal phenotype, including short molar root and decreased bone mass of alveolar bone. Depletion of METTL3 in hDPCs also crippled the ability of proliferation and mineralization. Mechanically, we revealed that specific and enriched m6A peak near translation stop codon of NFIC. Moreover, software prediction using published m6A-seq data from other cells also confirmed that NFIC was modified. Deletion METTL3 impaired the protein translation of NFIC, and the defect partially rescued by NFIC overexpression. These evidences suggested that METTL3 was crucial for tooth root development. Conclusion:In conclusion, we demonstrated m6A modification in odontogenetic cells regulated by METTL3 could affect NFIC translation and modulate odontogenesis or mineralization during tooth root formation.

***Disclosures: Rui Sheng**, None*

P-377

Opposite Effects of Cntnap4 Knockout in Cranial Neural Crest Cells of Cranial Base and Vault *Pin Ha[1], Chenshuang Li[2], Samantha Lee[1], Nuo Dong[1], Zhong Zheng[1], Kang Ting[1], Chia Soo[3], Xinli Zhang[1]. [1]Division of Growth and Development, School of Dentistry, University of California, Los Angeles, United States, [2]Department of Orthodontics, School of Dental Medicine, University of Pennsylvania, United States, [3]Department of Orthopaedic Surgery and the Orthopaedic Hospital Research Center, University of California, Los Angeles, United States

Contactin-associated protein-like 4 (Cntnap4), a member of the neurexin superfamily of transmembrane molecules that have critical functions in neuronal cell communication, has been identified as a specific receptor of an osteogenic protein, Nell-1 for osteogenesis. This opens up a new revenue for Cntnap4 functional studies beyond its putative roles in brain. Our previous reports showed that Cntnap4flox/flox; Wnt1-Cre (Cntnap4Wnt1KO) mice and Nell-1flox/flox; Wnt1-Cre (Nell-1Wnt1KO) mice developed very similar craniofacial dysplasia phenotype, which includes frontonasal, maxilla and mandibular bone defects, premature ossification/fusion of the intrasphenoidal synchondrosis (ISS), and an obvious increased incidence of postnatal hydrocephalus. To unravel the cellular and molecular mechanisms of a contradictory craniofacial skeletal phenotype of vault and base, primary Cntnap4-deficient cranial neural crest cells (CNCCs) were isolated separately from both frontonasal bones and cranial base sphenoidal bones. Cntnap4-deficient CNCCs from cranial vault (cvCNCC) demonstrated a significant reduction in osteogenic differentiation and non-responsive to Nell-1's stimulation compared to wild-type (WT) cells. Surprisingly, Cntnap4-deficient CNCCs from cranial base (cbCNCC) presented the opposite effects with significant increase in osteogenic differentiation, but without significant further augmentation by Nell-1 protein. Since ISS premature ossification/fusion and hydrocephalus of Cntnap4Wnt1KO mice usually occur at week-3 old, tissue sections of cranial base were obtained at this stage for histology and immunostaining. Coincidently, these in vivo analyses demonstrated that a significant accelerated ossification at both ISS and spheno-occipital synchondrosis (SOS) with elevated levels of Col 1, Col10 and OCN, along with tremendously increased cell proliferation in the bone marrow of pre- and basi-sphenoid bones in Cntnap4Wnt1KO over WT mice. Mechanistically, the differential activations of Wnt/β-catenin and Ihh signalings were observed in Cntnap4-deficient cvCNCCs and cbCNCCs that are responsible for intramembranous and endochondral type of bone formations, respectively. In aggregate, Cntnap4 was not only a novel key regulator of CNCCs, but also executing a striking opposite effect on cbCNCCs from cvCNCCs, which underscores the unique craniofacial phenotypes of calvarial hypoplasia and premature ossification of synchondrosis in Cntnap4Wnt1KO mice (see Fig. A-C).

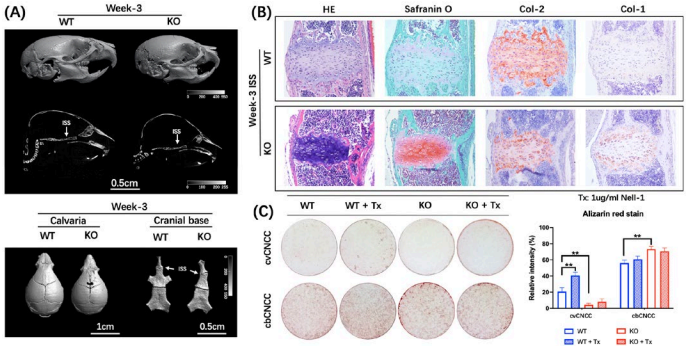

***Disclosures: Pin Ha**, None*

P-378

Evaluating the Role(s) of Wnt Receptor Frizzled 2 in Limb and Craniofacial Development *Megan Michalski[1], Cassandra Diegel[1], Alex Zhong[1], Gabrielle Foxa[1], Bart Williams[1]. [1]Van Andel Institute, United States

Heterozygous mutations in Frizzled 2 (FZD2), a Wnt ligand receptor, are associated with two syndromes which present with limb reductions and craniofacial anomalies: Robinow syndrome and autosomal dominant omodysplasia. We utilized two Fzd2 mouse models to study the role of Fzd2 in craniofacial and limb development: Fzd2tm1.1Nat (global knockout) and Fzd2FloxMOR (conditional-ready). While homozygosity for the Fzd2tm1.1Nat allele results in partial penetrance of cleft palate and delayed neonatal growth (consistent with previous reports), we did not note limb reductions. We found that the Fzd2tm1.1Nat allele retains a small fragment of the CDS encoding the Fzd2 C-terminus and noted an in-frame ATG, associated with a strong Kozak sequence near the 5' end of this FZD2 fragment that could drive expression of a 531bp in-frame CDS. We found this FZD2 fragment to retain signaling function. Conditional heterozygous deletion of the Fzd2FloxMOR allele using Prx1-cre and Wnt1-cre2 resulted in limb reductions and craniofacial anomalies respectively. The Fzd2FloxMOR allele was thought to contain loxP sites surrounding the protein coding sequence of Fzd2. However, cre-mediated recombination of the Fzd2FloxMOR allele did not result in significant loss of FZD2 protein or mRNA. We carried out whole genome sequencing of Fzd2FloxMOR mice and found that this allele contains two copies of the Fzd2

gene, exogenous bacterially-derived sequence, and duplication of endogenous sequence. Due to the unexpected issues noted in the above models, we have recently generated a new floxed allele of Fzd2 (Fzd2Flox-VAI) by injecting 2-cell embryos with purified Cas9-streptavidin fusion protein and biotinylated repair templates designed to incorporate loxP sites surrounding the Fzd2 gene. From 85 potential founders, we identified 4 containing loxP sites incorporated into both the 5' and 3' sites. After crossing these animals to C57Bl/6J mice, both the 5' and 3' loxP sites were transmitted in cis within the germline. Our preliminary data shows successful cre-mediated recombination when crossed with CMV-cre. Overall, we successfully simultaneously inserted 2 loxP sites using this method and significantly reduced the cost and time burden to generate floxed mice. Fzd2 is likely an important mediator of craniofacial and limb development and we are in the process of utilizing our new mouse model to gain a deeper understanding of the mechanism by which Fzd2 controls development of these structures.

***Disclosures: Megan Michalski**, None*

P-379

Hydrolyzed collagen and vitamin D3 accelerate bone regeneration in adult zebrafish *Nili Vasserman[1], Chen Shochat Carvalho[1], David Karasik[1]. [1]Bar Ilan university, Israel

Bone regeneration is an important process that allows healing of bone tissue after trauma, fractures, or surgical removal. There are clinical cases in which bone regeneration is needed in large quantity. Therefore, there is a need to develop novel, more potent, drugs, especially of anabolic nature. Due to its fast bone regeneration, zebrafish (Danio rerio, ZF) is a popular in-vivo model for such a study.Our aim was to assess the in-vivo and in-vitro effect of a collagen hydrolysate (CH) and 1α,25-Dihydroxyvitamin D3 (VitD) supplementation on bone regeneration, using ZF jawbone model. After bone resection, 6-mo-old ZF were fed fish food supplemented with low, medium, or high dose of either CH or VitD (Table 1). Jaw bone gap at resection site was measured by microCT scans and averaged (n=4) to estimate bone regeneration rate. The smallest gap, i.e. fastest regeneration rate, was observed at 14 and 28 days post resection, at low dose of VitD, while at 35 days post resection, the smallest gap was observed with CH treatments compared to VitD and control (Table 1). In addition to the gap's closure there was an overgrowth of the new bone. After 60 days, in the highest dose of CH, the shape of the mandible resembled that of a wild type ZF.In-vitro: the effect of 3 doses of CH and VitD was studied on MC3T3-E1 osteoblast and RAW264.7 osteoclast cell lines by cell-specific staining and functional assays. The expressions of osteogenic and osteoclastogenic genes were measured by qPCR. The medium dose of CH increased osteoblast proliferation and calcium deposition and decreased the size of osteoclasts, while VitD in all doses increased ALP activity but not ALP gene expression. Additionally, CH increased osteoblast expression of RUNX2, while the expression of all 3 osteoclast genes, RANKL, TRAP and CTSK was increased by VitD and CH.Our results indicate that CH and VitD have an anabolic therapeutic potential in bone regeneration. Gap closure after resection was similarly accelerated by CH and VitD treatments even after 2 weeks of feeding, but in the long term, it was more significant with CH treatment. Our findings demonstrate that CH can upregulate osteoblast and osteoclasts activity (the latter activity is necessary to remodeling process). In conclusion, we suggest that CH could represent a promising treatment for bone healing, but at the same time, the effect of combining both treatments should be examined.

***In-vivo* (D. rerio)**		Vitamin D (mg/kg)			collagen hydrolysate (mg/kg)		
	Control	0.05	0.5	1.25	40	80	160
	Resection gap width (μm)						
Day 14	238	139	218	203	212	177	148
Day 28	144	59	123	80	96	78	96
Day 35	53	54	82	51	50	35	39
In-vitro*		Vitamin D (nM)			Collagen hydrolysate (mg/ml)		
MC3T3-E1 cells		100	500	5000	0.25	0.5	1.0
Proliferation for 72 hours		↑↑	↑	↑	↑↑↑	↑	↑
alizarin red staining	7d	~	~	~	~	↑↑	~
	14d	↑↑	~	~	~	↑	↓
	21d	↑↑	~	↓	↑↑	↑↑	↓
ALP activity	7d	↓↓	↑	↑	~	~	~
	14d	↑↑	↑↑↑	↑↑	↓↓↓	↓↓	~
	21d	↑	↑	↓↓	↓↓	↑	↑↑
gene expression at day 14 (R= RUNX2; A= ALP)		R↓ A↓↓	R↓ A↓	R↑ A~	R↑↑ A↓	R↑ A↓	R↑ A~
RAW 264.7 cells							
TRAP staining at day 6		~	↑	↑	~	↓	↑
Gene expression at day 6 (R=RANKL, T=TRAP, C=CTSK)		R↑ T↑ C~	R↑ T~ C↑	R~ T↑ C↑	R↑↑ T↑↑ C↓	R↑↑↑ T↑↑ C↑↑↑	R↑ T↑ C~
* compared to control: ↑ - increased, ↓ - decreased, ~ - similar to control							

***Disclosures: Nili Vasserman**, None*

P-380

Global deficiency of chaperone mediated autophagy leads to low cancellous bone mass in young mice *Nisreen Akel[1], Milena Dimori[1], Ryan Macleod[2], Stuart Berryhill[1], Julie Crawford[1], Melda Onal[1]. [1]University of Arkansas for Medical Sciences, United States, [2]university of Arkansas for Medical Sciences, United States

Chaperone-mediated autophagy (CMA) is a protein degradation pathway that eliminates soluble cytoplasmic proteins that are damaged, incorrectly folded, or targeted for selective proteome remodeling. CMA has been proposed to contribute to DNA repair, cellular reprograming, and the cellular stress response. However, the role of CMA in skeletal remodeling under physiological and pathophysiological conditions is unknown. To determine whether CMA contributes to skeletal homeostasis, we deleted the CMA receptor Lamp2a from the mouse genome, thereby producing mice that lack CMA in all tissues. MicroCT analysis at five-weeks-of age revealed that female LAMP2A global knockout (L2AgKO) mice had lower vertebral cancellous bone mass compared to wild type (WT) controls. Bones of female CMA-deficient mice exhibited higher mRNA levels of the osteoclast marker genes Trap and Cathepsin K compared to controls. Unlike the female mice, bone mass of five-week-old male L2AgKO mice was not different from controls. Previous studies by others have shown that in young mice lack of CMA in liver tissue is partially compensated for by an increase in other proteostasis mechanisms. However, this partial compensation has been shown to dissipate as mice mature and leads to a premature aging phenotype in this tissue. Consistent with this, our ex vivo studies showed that CMA-deficient osteoblasts exhibited a slight increase in the ubiquitin-proteasome system. To determine whether a functional role of CMA for bone tissue becomes more pronounced as mice mature, we analyzed the skeletal phenotype of young adult mice at eighteen weeks of age. MicroCt analysis revealed that both male and female L2AgKO mice had lower vertebral cancellous bone mass compared to WT controls. At this age, gene expression analysis performed at the whole bone level did not show any significant differences in mRNA levels of osteoclast or osteoblast marker genes. However, ex vivo analysis of bone marrow progenitors showed that CMA deficient progenitors have an increased ability to produce osteoclasts and a decreased ability to form alkaline phosphatase-positive osteoblast colonies compared to WT progenitors. Whether these ex vivo changes are the underlying cause of the low bone mass phenotype of L2AgKO mice needs to be determined. Taken together our results suggest that CMA gains importance as mice mature and that lack of CMA leads to low vertebral cancellous bone mass in young adult mice.

***Disclosures: Nisreen Akel**, None*

P-381

Sex Differences in the Skeletal Phenotype of the African Spiny Mouse (Acomys cahirinus) *Kirby Sherman[1], Alyssa Falck[1], Shannon Huggins[1], Lindsay A Dawson[1], Ken Muneoka[1], Dana Gaddy[1], Malcolm Maden[2], Larry J Suva[3]. [1]Texas A&M University, United States, [2]Univeristy of Florida, United States, [3]Department of Veterinary Physiology and Pharmacology, United States

Although similar in appearance to mice of the genus Mus, "African spiny mice" of the genus Acomys are distinct and have unusually stiff guard hairs and possess brittle, easily torn skin allowing the animals to escape predators by discarding extensive patches of skin. In response to such profound injuries, Acomys completely regenerate hair follicles, sebaceous glands, dermis and fur with no evidence of scarring, unlike Mus. Based on the profound regenerative capabilities of Acomys, and an absence of skeletal data, the baseline Acomys bone phenotype was determined. Tibiae and femurs were harvested from adult male and female 2 and 4-6 month old Acomys as well as from 3-to-6-month-old Mus (C57/Bl6). The baseline Acomys skeletal phenotype were ascertained using microCT, histology, and immunohistochemistry. Interestingly in younger Acomys, females had significantly higher BV/TV, Tb.Th, and decreased Tb.Sp. than age-matched male Acomys. Cortical bone analysis revealed that female Acomys have significantly increased Ct.Th. and larger cortical CSA than males. Interestingly, these significant differences between male and female bone microarchitecture and geometry were not maintained in the older Acomys, perhaps indicative of earlier attainment of peak adult bone mass in females. Indeed, although young female Acomys had higher BV/TV than age-matched young males, no significant differences were noted when either young or old females were compared to older males. This supports the idea that female Acomys attain peak adult bone mass earlier than males. Acomys females at all ages have significantly greater BV/TV than either 3 or 6 month old male C57/Bl6 mice. Histologically, Acomys bone marrow demonstrates different cellular organization relative to Mus, with Acomys having significantly fewer bone marrow adipocytes, distinct cuboidal-like morphology of marrow cells, robust cell proliferation along bone surfaces, prominent megakaryocytes, and large osteoclasts decorating the Acomys' growth plate. The significantly increased bone volume, microarchitecture and altered geometry in adult female Acomys likely provides an evolutionary advantage to the females, who are typically more aggressive and dominant compared to their male counterparts. Our ongoing efforts seek to accurately define the Acomys bone and bone marrow phenotype and identify the molecular pathways controlling bone regeneration in order to enhance mammalian regenerative capabilities.

***Disclosures: Kirby Sherman**, None*

P-382

LepR-expressing stem cells are essential for alveolar bone regeneration *Shiwen Zhang[1], Danting Zhang [1], Jun Wang[1], Qiwen Li[1], Quan Yuan[1]. [1]State Key Laboratory of Oral Diseases & National Clinical Research Center for Oral Diseases, West China Hospital of Stomatology, Sichuan University, Chengdu, China, China

Purpose: Stem cells play a critical role in alveolar-bone repair. Several populations of skeletal stem cells (SSCs) have been identified in the long bone, while their identity and function in alveolar bone remain poorly understood, due to the lack of specific in vivo markers. Previously, we found that LepR+ cells were expressed in the alveolar bone and stayed quiescent, but activated and differentiated into osteoblasts in response to tooth extraction. In this study, we sought to find out whether LepR+ cells represent a population of alveolar bone SSCs and investigate the role and mechanism of LepR+ SSCs regulating alveolar bone regeneration.Methods:LepR-Cre;tdTomato;Col2.3-GFP reporter mice was generated and the mandible was collected at different time points to follow the fate of LepR+ lineage cells. Next we created a tooth extraction model in LepR-Cre;tdTomato;Col2.3-GFP mice and LepR-Cre;tdTomato;iDTR mice to investigate the contribution of LepR+ cells to alveolar bone regeneration through mirco-CT, frozen section and double labeling. Further, we generated parabiosis models to investigate whether LepR+ cells in the extraction sockets are derived from peripheral blood circulation. In order to explore the potential mechanism that regulates LepR+ cell response, we performed RNA-Seq through sorting the LepR+ cells from the tooth sockets and injured alveolar bone and found a high expression of Pth1r gene. Then we created LepR-Cre;Pth1rfl/fl;tdTomato mice to further study PTH/PTH1R signaling regulating LepR+ cells.Results:Tracing data showed that LepR+ cells gradually differentiated to osteoblasts with age in alveolar bone. LepR+ cells were maintained in a quiescent state, but activated in response to tooth extraction and generated most of the new bone. By post-tooth extraction day 28, 47.84% of Col2.3-GFP+ osteoblasts were tdTomato+, whereas only 13.29% of double positive cells in the uninjured controls. Micro-CT and double labeling results demonstrated that ablation of LepR+ cells suppressed extraction socket healing. Intermittent PTH treatments significantly induced LepR+ cells increasing and differentiating into osteoblasts both in physiology condition as well as in injured model. In addition, conditional knockout Pth1r in the LepR+ cell lineage resulted in impaired bone healing. Conclusions:we demonstrate LepR+ cells, a postnatal SSCs population, are essential for alveolar bone regeneration, which is regulated by PTH/PTH1R signaling.

***Disclosures: Shiwen Zhang**, None*

P-383

A Positive Feedback Loop Between PTH1R and ZFP467 Mediates the Linage Allocation in the Bone Marrow Niche *Hanghang Liu[1], Phuong Le[1], Lama Alabdulaaylly[2], Yosta Vegting[3], Isabella Calle[1], Francesca Gori[2], Beate Lanske[2], Roland Baron[2], Clifford Rosen[1]. [1]Maine Medical Center Research Institute, Maine Medical Center, United States, [2]Harvard School of Dental Medicine, United States, [3]University of Amsterdam, Amsterdam UMC, Meibergdreef 9, Netherlands

We previously reported that deletion of Pth1r in mesenchymal progenitors reduced osteoblast differentiation and bone mass while enhancing adipogenesis and bone marrow adipose tissue. Mechanistically, we found that PTH suppressed the expression of Zfp467, a pro-adipogenic zinc finger transcription factor. Consequently, Pthr1 deficiency in mesenchymal progenitors leads to increased Zfp467 expression. Based on these observations, we hypothesized that genetic loss of Zfp467 would lead to an increase in bone mass by shifting marrow progenitor cell fate towards osteogenesis. To test this hypothesis, we generated Zfp467-/- mice. At 16wks of age, Zfp467-/- mice (-/-) were significantly smaller than Zfp467+/+ mice (+/+). µCT of tibial trabecular (Tb.) bone showed that Tb.BV/TV, Tb.BMD, Tb.N, and Conn.D were significantly higher in -/- vs. +/+ ($p<0.002$) with lower SMI ($p=0.005$). Cortical (Ct.) parameters showed smaller Ma.Ar and higher Ct.Ar/Tt.Ar in -/- ($p<0.03$). Additionally, Ct. Porosity was significantly lower in -/- vs. +/+ ($p=0.003$). Histomorphometry showed higher structural parameters of Tb.BV/TV, Tb.N, and Tb.Th in -/- ($p<0.0175$). Furthermore, MS/BS, MAR, and BFR/BV were higher in -/- vs. +/+ ($p<0.005$). Oc.S/BS was significantly higher in -/- ($p<0.05$). Femoral gene expression including Alpl, Sp7, and Acp5 were increased in -/- ($p< 0.018$). Adiponectin, Cebpa, Lepr, and Ppra? mRNA were lower in -/- vs. +/+ ($p<0.01$). Similarly, Fabp4 and Lep in the inguinal depot were also decreased in -/- ($p<0.05$). Marrow adipocyte numbers were reduced in -/- ($p=0.0074$). In vitro, COBs and BMSCs-/- showed more positive ALP and Alizarin Red staining and a decrease in ORO droplets. Interestingly, Pth1r and Creb mRNA and protein levels were increased in -/- COBs and BMSCs ($p<0.05$). Additionally, -/- COBs exhibited enhanced endogenous levels of cAMP vs. control cells ($p=0.0003$), and the pro-osteogenic effect of Zfp467-/- could be blocked by a PKA inhibitor ($p<0.01$). Furthermore, Zfp467-/- cells showed greater glycolytic activity vs. control cells ($p<0.05$), but no differences in mitochondrial respiration. Taken together, these results show that global deletion of Zfp467 leads to increase osteogenesis and bone mass and decreased adipogenesis in female mice as well as an increased basal level of PTH1R expression in osteoblasts. These data support a critical role for Zfp467 in early lineage allocation and provide a novel potential mechanism by which PTH acts in an anabolic manner.

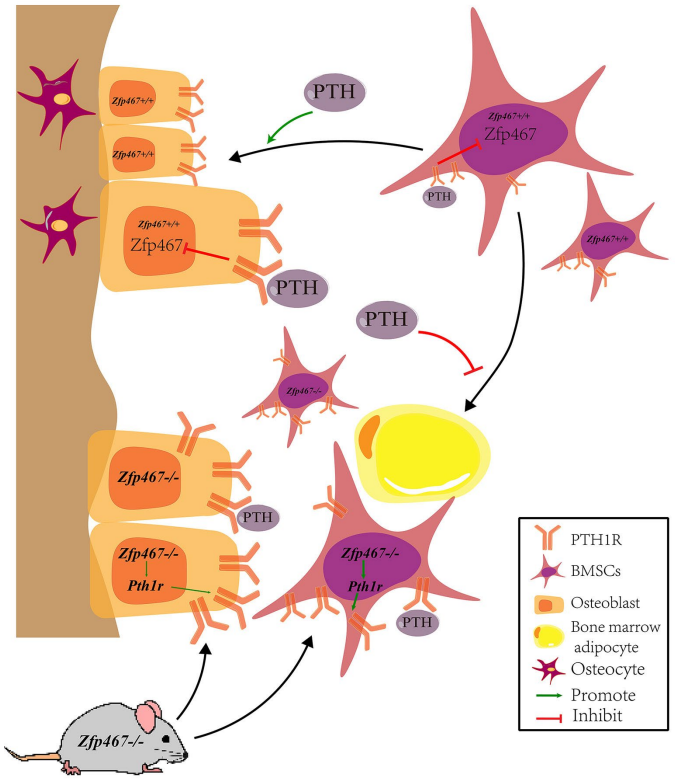

***Disclosures: Hanghang Liu**, None*

Posters

P-384

Chondrocyte Dedifferentiation: An Alternate Fate For Hypertrophic Chondrocytes *Jason Long[1], Abigail Leinroth[1], Yihan Liao[1], Anthony Mirando[1], Yinshi Ren[2], Deepika Sharma[1], Colleen Wu[1], Courtney Karner[1], Kathryn Cheah[3], Matthew Hilton[1]. [1]Duke University, United States, [2]Texas Scottish Rite Hospital, United States, [3]The University of Hong Kong, China

Skeletal stem and progenitor cells (SSPCs) have the capacity to become osteoblasts, chondrocytes, and adipocytes during normal bone development, aging, and regeneration. SSPCs reside within the periosteum surrounding cortical bone and the intramedullary bone marrow. However, whether these SSPCs have a distinct origin and/or function remains to be determined. Recent in vivo lineage tracing and genetic reporter studies determined that many marrow associated osteoblasts are derived from hypertrophic chondrocytes of the growth plate cartilage, thereby raising questions as to whether these cells undergo trans-differentiation to directly generate committed osteoblasts or rather a de-differentiation process to generate SSPCs that ultimately give rise to osteoblasts and/or other cell types. Using similar lineage tracing and reporter analyses (Col10a1Cre; R26-tdTomato and Col10a1CreERT2; R26-tdTomato), we determined that hypertrophic chondrocytes undergo de-differentiation to generate SSPCs that likely give rise to osteoblasts, osteocytes, and adipocytes within the marrow during skeletal development. Colony forming unit – fibroblast (CFU-F) assays performed using the bone marrow harvested from these reporter mice indicate that as many as 50% of the CFU-Fs (a general measure of SSPCs) may be derived from the growth plate, and bulk RNA-sequencing of tdTomato positive and negative colonies demonstrated uniquely expressed genes within these populations, suggesting alternative origins and/or functions. Further, single cell RNA-sequencing of marrow associated tdTomato+ cells from reporter mice determined that hypertrophic chondrocytes give rise to two osteoblast populations, while also generating at least 3 populations of SSPCs that share common markers but also exhibit uniquely expressed genes. Ongoing studies are aimed at determining the spatial and functional significance of these unique bone marrow associated SSPC populations.

***Disclosures: Jason Long**, None*

P-385

Mfap4 Expression Marks Mesenchymal Cells in the Mouse Calvaria *Didem Goz Ayturk[1], Eun Sung Suh[1], Ugur M Ayturk[1]. [1]Hospital for Special Surgery, United States

Bone tissue-resident macrophages (also referred to as osteomacs) regulate fracture healing and osteoblast differentiation (Chang et al., J Immunol, 2008; Batoon et al., Biomaterials, 2019). We recently described osteomacs, along with osteoblasts and their precursors in the neonatal mouse calvaria with single cell RNA-seq (Ayturk et al., J Bone Miner Res, 2020). We found that primary calvarial cells consist of multiple, transcriptionally distinct cell populations, predominantly including osteoblasts (Bglap+) and a population resembling osteoblast-precursors (Bglap-, Col1a1+, Mfap4+), as well as a small group of macrophages (F4/80+, less than 5% of all cells). In the present study, our goal was to determine the spatial locations of macrophages and osteoblast-lineage cells in vivo, and identify and validate genetically modified mice that could be useful in studying osteoprogenitors in the mouse calvaria. Our single cell RNA-seq data indicated that Mfap4-expression distinctly marks osteoprogenitors among calvarial cells. We therefore obtained the Tg(Mfap4-EGFP)HF313Gsat reporter mouse (i.e. Mfap4.eGFP, GENSAT) and imaged calvarial tissue in this mouse strain at P5 and P16. We detected strong and comprehensive GFP expression in all layers of the calvarial periosteum and endosteum, except for the bone-lining layers that presumably consist of mature osteoblasts (Figure 1). To determine if GFP+ cells include any non-mesenchymal populations, we performed FACS and immunohistochemistry analyses for CD45, F4/80 and CD31 expression, but found no overlap between these markers and GFP-expression. In contrast, we found that Mfap4-driven GFP expression is limited to connective tissue (such as the patellar tendon and cruciate ligaments) and hematopoietic populations of the bone marrow in the limbs. When we stained calvariae of Mfap4.eGFP mice for macrophage markers F4/80 or CD169, we found that labeled macrophages were positioned immediately adjacent to Mfap4-expressing cells in the periosteum endosteum (Figure 1). Our data indicate that Mfap4-expression marks periosteal and endosteal cells (that are likely osteoprogenitors) in the calvaria but not the long bones. Furthermore, these cells are intertwined with macrophages that might be required for bone formation; future experiments might reveal mechanisms of signaling between the two cell types.

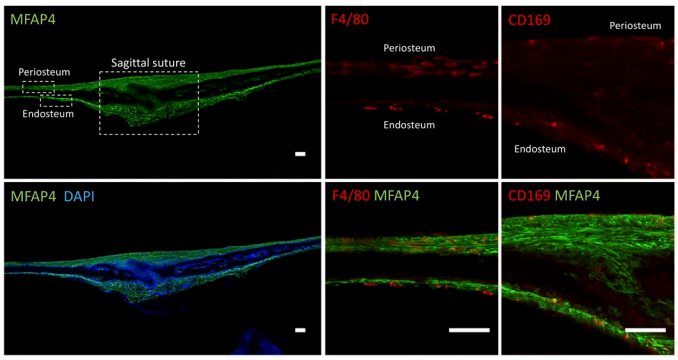

Figure 1: Mfap4.eGFP-expressing cells are abundantly present in the periosteum and endosteum of mouse calvaria at P5 (left). F4/80- (center) and CD169-expressing macrophages (right) are positioned in both

***Disclosures: Didem Goz Ayturk**, None*

P-386

Biglycan Regulates Structural Integrity and Bone Regeneration *Reut Shainer[1], Vardit Kram[1], Tina M. Kilts[1], Li Li[1], Andrew Doyle[2], Carl G. Simon Jr[3], Liliana Schaefer[4], Marian F. Young[1]. [1]Molecular Biology of Bones and Teeth Section, NIDCR, NIH, United States, [2]Cell Biology Section, NIDCR, NIH, United States, [3]Biosystems and Biomaterials Division, NIST, United States, [4]Institut für Allgemeine Pharmakologie und Toxikologie, Goethe University, Germany

Bone healing involves a complex sequence of physiological events starting with an inflammatory response at the fracture site, followed by activation and proliferation of skeletal stem cells in the periosteum. To identify new factors that further control bone regeneration, immunohistochemistry and RNA analysis were performed and showed that Biglycan (Bgn), an extracellular matrix proteoglycan, is greatly enhanced in the periosteum in response to injury. Here, we used WT and Bgn deficient (KO) mice in order to examine the role of Bgn in the bone.µCT analysis showed that compared with WT bones, Bgn KO bones had a reduction in cortical thickness and trabecular number. The structural integrity of the Bgn KO bones was found to be compromised as second harmonic generation microscopy demonstrated irregular structure and spacing between the collagen fibers of the Bgn KO bones. This molecular structural change was coupled with a reduction in the hardness of the Bgn KO bones.Next, we examined bone regeneration by fracturing the bones. Bgn KO mice showed reduced inflammation and macrophage infiltration around the fracture site. In addition, RNAseq analysis showed an enhanced expression of genes involved in suppressing inflammation. The periosteum of Bgn KO did not expand to the same extent as WT after fracture, leading to reduced callus formation, which regained its original (pre-fracture) shape faster. Since periosteal-derived cells (PDCs) have an important role in fracture healing, we decided to investigate whether they can be used to enhance or improve the healing process. We isolated and cultured PDCs from the long bones of WT mice, using a 3D system to mimic the native environment of the cells. We found that PDCs create a distinct microenvironment that favors cartilage formation in vitro. When the 3D scaffolds containing PDCs were transplanted subcutaneously into mice, they differentiated into calcified cartilage. Finally, we cultured WT PDCs in the 3D scaffold and wrapped it around the fracture site in WT and Bgn KO mice. Here we show that the 3D scaffolds with PDCs enhanced the recovery of the fractured bone in both WT and Bgn KO mice.Overall our results demonstrate that Bgn deletion impairs bone formation and fracture repair, and highlight the importance of biglycan and periosteal cells in skeletal tissue in both homoeostasis and during bone healing.

***Disclosures: Reut Shainer**, None*

P-387

Periosteal cells labeled by VEGFR2 (KDR) and CCR5 are a subset of long-term repopulating adult skeletal stem cells in mouse and human *Youngjae Jeong[1], Laura Ortinau[1], Kevin Lei[1], Lorenzo Deveza[1], Dongsu Park[1]. [1]Baylor College of Medicine, United States

Skeletal stem cells (SSCs) are heterogeneous in population and have multipotent capacity to differentiate into bone, adipocyte, cartilage and marrow stromal cells. In particularly, they continuously supply chondrocytes and osteoblasts for cartilage and bone formation, respectively, during skeletal development and bone regeneration/repair process throughout lifetime. Due to the limited number, heterogeneity, and wide tissue distribution of SSC population in adult bones, it is challenging to identify and characterize the selective markers to distinguish rare periosteal (ourter surface of bone) SSCs in vivo. Recent advancement in SSC fields allowed discovery of a few molecular markers that specifically define subsets of population, and yet their functional roles are not still clear. Especially, common selective markers for periosteal SSCs in both mouse and human and their differential function compared to bone marrow SSCs (BM-SSCs) are largely unknown. In the following study, we have used Prx1CreER-EGFP mouse model to demonstrate that VEGFR2 (KDR) is selective-

ly expressed in endogenous periosteal SSCs (CD45-CD31-Ter119-CD150+CD140a+GFP+) by flow cytometry. Immunofluorescent imaging analysis showed Prx1-GFP+ periosteal cells in the femoral periosteum were KDR positive. From our recent study, we revealed that the combination of Mx1 and αSMA-GFP can selectively label endogenous periosteal SSCs in mouse models. These cells highly express CCR5, a chemokine receptor for CCL5, and have migratory function toward the injury site upon bone defect. In the current study, flow cytometry analysis demonstrated Prx1-GFP+ endogenous periosteal SSCs express both KDR and CCR5. We also defined that human periosteal cells express KDR and CCR5. Notably, the expression of CCR5 appeared in early post-natal periosteal SSCs and their expression sustained in adult bones, implicating that periosteal SSCs acquire their unique markers and function postnatally and the KDR and CCR5 combination can distinguish both mouse and human periosteal SSC subsets that preserve long-term repopulating capability. Identifying and understanding the functional mechanism of periosteum-resident SSC subsets constitutes a promising therapeutic approach to develop more effective treatment for degenerative bone disease and bone defects.

***Disclosures: Youngjae Jeong**, None*

P-388

Phagocytosis by mesenchymal stromal cells: A facultative process that induces senescence *Emily Quarato[1], Allison Li[1], Charles Smith[1], Roman Eliseev[1], Laura Calvi[1]. [1]University of Rochester, United States

Mesenchymal stromal cell (MSC) dysfunction is implicated in multiple settings including age-induced bone loss, radiation injury, and dysfunction of the hematopoietic stem cell niche in hematologic malignancies. Our laboratory studies the supporting role of MSCs and macrophages within the hematopoietic system and recently reported their role in the aged microenvironment. Aged marrow macrophages were found to be expanded but defective in their ability to phagocytose apoptotic cells (efferocytosis), resulting in increased inflammatory signals and expansion of dysfunctional MSCs. Since MSCs have previously been reported to be facultative phagocytes during embryonic development when macrophages are defective, we hypothesized that MSCs possess efferocytic capacity that impairs their function and fate determination. In vivo, we observed the phagocytic activity of MSCs and quantified efferocytosis of fluorescently labeled apoptotic neutrophils to be 5%. Notably, all phagocytic activity in MSCs was increased in aged mice and in a murine model of myeloid malignancy. Through in vitro assays utilizing a murine bone marrow stromal cell line (ST2) we analyzed the extent of phagocytic and efferocytic capabilities in MSCs given both biological and non-biological cargo and determined the consequences to fate determination post a phagocytic event. We observed that 2μm carboxylated beads were phagocytosed by most MSCs, while, with senescent neutrophils, 5% of the MSCs actively conduct efferocytosis in vitro, similar to the rate observed in vivo. In the MSCs that are actively engulfing, there was a significant increase to the rate of senescence over controls and their non-engulfing counterparts, and we observed global depression in differentiation potential to the osteoblastic and adipocytic lineages. As both phagocytosis and MSC differentiation are accompanied by changes in mitochondrial dynamics, we sought to determine if increased phagocytosis in MSC is a result of mitochondrial changes. Utilizing in vitro culture, MSCs' oxidative and glycolytic functions were decreased by phagocytosis and efferocytosis. Collectively, these data support the hypothesis that efferocytic activity by MSCs compromises their function and fate determination with disruption of mitochondrial activity, and therefore may serve as a therapeutic target to mitigate MSC damage in the setting of aging, radiation and hematologic malignancies.

***Disclosures: Emily Quarato**, None*

P-389

Identification of a novel population of stem cells in mouse muscle: potential for bone regeneration *Yu Liu[1], Louis Gerstenfeld[2], Beth Bragdon[1]. [1]Boston University School of Medicine, Department of Orthopaedic Surgery, United States, [2]Boston University School of Medicine, Department of Orthopaedic Surgery, United States

Acquired heterotopic bone, which is bone formation within the musculature in response to injury, implies the existence of stem cells with osteogenic potential in the muscle. Published work and our studies showed the paired related homeobox gene1 (Prx1) expressing cells connote a postnatal skeletal stem cell (SSC) population that contributes to bone homeostasis and wound repair. While Prx1 is widely expressed in mesenchymal tissues, questions remain whether Prx1+ muscle cells can contribute to bone formation and whether stem cells from different locations are functionally the same.To address this, 8-10 week old Prx1CreER;Rosa26tdTomato ;Rag mice received two doses of tamoxifen in 72 hours to induce fluorescent labeling of the Prx1 cells. 2 days after injection, bone marrow, periosteum and muscle were harvested and processed for fluorescence-activated cell sorting. Antibodies for CD45 (hematopoietic), CD105 and CD200 were used to isolate SSC (Prx1+ CD105-CD200+ CD45-) and two progenitor populations1 (CD105- CD200- and CD105+). Cells were then cultured and differentiated toward the osteo-, adipo- and chondro-genic lineages to directly characterize and compare the sub-populations of Prx1.Results showed the highest percentage of Prx1+ cells were found in the muscle followed by periosteum, while the bone marrow showed the least. Percentage of SSC within the non-hematopoietic population from muscle, periosteum and bone marrow were 3.73+/-0.72%, 0.79+/-0.30%, 0.05+/-0.02% respectively (Figure A). Muscle SSCs showed greater proliferative capacities and tri-lineage differentiation potentials than periosteal SSCs, while bone marrow SSCs were not able to form colonies even when plated at high density (Figure B). Bulk RNA-sequencing analysis demonstrated SSC populations were distinct from their progenitors while tissue source had a lesser influence on the uniqueness of stem cells.These results suggest that the Prx1 population consists of both stem and progenitor cells. The high percentage and regenerative potential of muscle SSCs indicate that mesenchymal tissues consist of multiple distinct pools of stem cells. The identification of the novel population of muscle-derived stem cells raises the possibility that it may serve as a promising source for bone regeneration. 1. Debnath, S. et al. Discovery of a periosteal stem cell mediating intramembranous bone formation. Nature 562, 133–139 (2018).

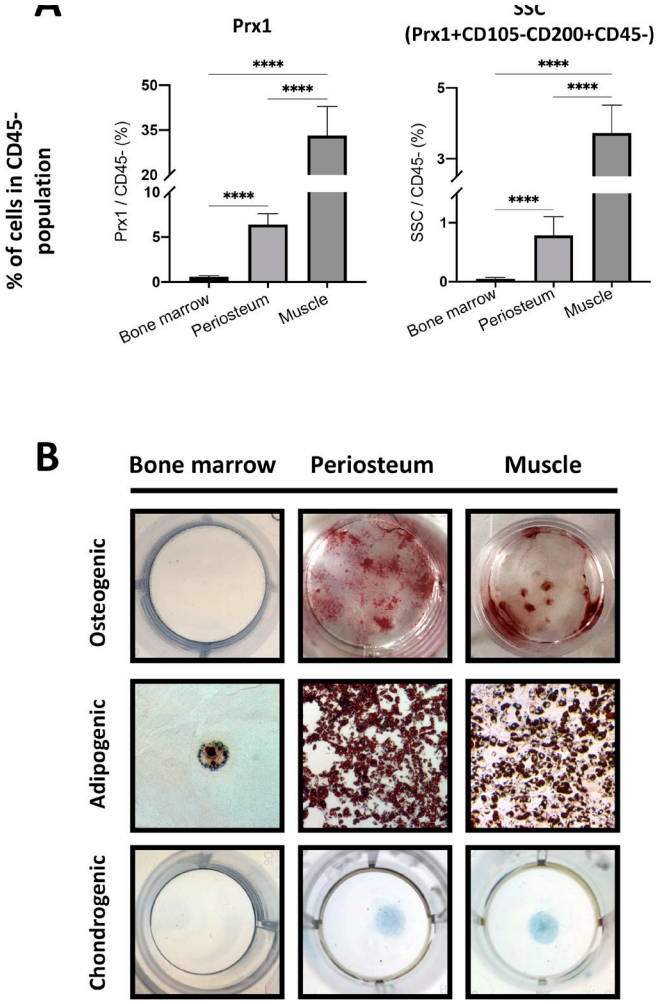

***Disclosures: Yu Liu**, None*

P-390

A Subset of Osteocytes Contribute to Intramedullary Bone Formation during Fracture Repair *Yongmei Wang[1], Anna Celli[2], Sun Hee Won Kim[1], Daniel Bikle[1]. [1]Endocrine Unit, University of California, San Francisco/ San Francisco VA Health Care System, United States, [2]Laboratory for Cell Analysis Core Facility, Helen Diller Family Comprehensive Cancer Center, University of California, San Francisco, United States

Fracture (Fx) repair is a complex process including intramembranous bone formation (BF), endochondral BF and intramedullary BF. Intramedullary bone formation (IMBF) occurs within the marrow of the ends of fractured bones, and the mechanisms of its repair remain unknown. To address this issue, we investigated the origin of the progenitors and mechanism of progenitor differentiation involved in IMBF by histology, lineage tracing and multi-photon microscopy. A unilateral closed mid tibial Fx was made in 12 wks old wild type mice by 3 point-bending. Histological staining showed that at day 5 (D5) post Fx, only granulation tissues appeared in the intramedullary (IM) area; neither bone nor cartilage had yet formed in this area. No Sox2 positive cells were observed in the area as well. At D10 post Fx, bone formed in the IM area, accompanied by vascular invasion, as indicated by CD31 and VEGF expression, and marrow space formation within the newly formed bone. At D28 post Fx, no trabecular bone was observed at the IM area, indicating the transient nature of IMBF during Fx repair. We then determined progenitors contribute to IMBF by tracing the

cell fate of type II collagen (Col2) expressing cells in the mice by crossing tamoxifen (tam) regulated tam regulated Col2 cre-recombinase (Col2 cre) with Rosa TdTomato (TdT) expressing mice. Tam was given 1 day prior to Fx. At D10 post Fx, TdT labeled cells appeared in the IM area as well as in the cortical bone (CB) of the fractured bone ends (FBE) as osteocytes. Immunohistochemistry (IHC) identified that in the CB, TdT labeled osteocytes continuously expressed Col2 and co-expressed the stem cell marker Sox2, while in the IM area, the TdT labeled cells no longer expressed Sox2, but expressed the osteoblastic gene osteocalcin and osteocytic gene DMP-1. Multi-photon microscopy (Zeiss LSM780, Carl Zeiss microscopy), reconstructed 3D images demonstrated that TdT labeled cells were located inside the lacunae in the CB of the FBE and on the bone surface in the IM area. Interestingly, blood vessels originating from the lacunae containing TdT labeled cells crossed the CB and connected to the newly formed IM bone with the TdT labeled cells. Our data indicate that during Fx repair, IMBF is a transient process, Col2 expressing osteocytes from the broken bone ends appear to reprogram, migrate to the intramedullary area via the cortical vessel network, differentiate into osteoblasts, and contribute to IMBF.

***Disclosures: Yongmei Wang**, None*

P-391

Nox4 is critical for early but not late stages of osteoblastic stem cell renewal *Jin-Ran Chen[1], Oxana P. Lazarenko[1], James Watt[2], Martin J. Ronis [2]. [1]1Department of Pediatrics, University of Arkansas for Medical Sciences, and 2Arkansas Children's Nutrition Center, United States, [2]3Department of Pharmacology and Experimental Therapeutics, Louisiana State University Health Sciences Center, United States

Reactive oxygen species (ROS) can be generated by several sources, the tightly controlled and cell-specific NADPH-oxidases (Nox) represent one of the major sources of ROS signaling molecules, including superoxide, hydrogen peroxide, and hydroxyl radicals in many cell types. We have previously identified that osteoblastic cells do not express Nox3 but do express Nox 1, 2 and 4, with isoforms 4 and 2 being relatively abundant. We have characterized the role of Nox2 in bone cells during bone development by using a mouse model in which its co-factor p47phox was knocked out. In contrast, Nox4 has never been examined to determine if it plays a role during osteoblast self-renewal, proliferation and postnatal bone development. We have generated systemic Nox4 gene deletion mouse model (Nox4-/-), osteoblast specific Nox4 gene deletion mouse model (Nox4flox/flox/Prx1-Cre+, CKO) and control mouse model (Nox4flox/flox). Using these mouse models, we investigated the role Nox4 in osteoblast stem cell renewal and late stage cell proliferation and postnatal bone development. Bone marrow stromal cells and non-adherent hematopoietic cells were isolated from 18 weeks old above three genotypic mouse groups (n=3). We found colony forming units-fibroblasts (CFU-F) were significantly lower in samples from CKO (56.0+/-12.3) and Nox4-/- (59.7+/-4.7) compared with those from Nox4flox/flox control (76.0+/-5.0). This was accompanied by significantly lower osteoblast stromal cell proliferation and senescence associated β-galactosidase activity in CKO and Nox4-/- groups compared Nox4flox/flox control group. We have passaged and re-cultured those osteoblast stromal cells and repeated assays for more than 12 times. We found that after 9 passages, those suppressed osteoblast stem self-renewal and proliferation in CKO and Nox4 groups caught up to control group. In passage 10, there were no differences on cell proliferation among groups, CKO (2.64+/-0.1 cells/well x 104) and Nox4-/- (2.67+/-0.1 cells/well x 104) compared with Nox4flox/flox control (2.61+/-0.2 cells/well x 104). Osteoclastogenesis assays showed no differences among groups, however, β-Catenin mRNA expression in osteoclast progenitors was lower in CKO and Nox4-/- groups compared Nox4flox/flox control group. We have collected bone samples from 3 weeks old, 13 weeks old and 32 weeks old of all genotypic groups (at least 6 per group), bone growth and bone mass in tibia and spine are under assessment using micro-CT and peripheral quantitative computerized tomography (pQCT) and histologic methods. These data suggested that Nox4 expression in bone osteoblastic cells might play different roles during osteoblast differentiation, maturation and proliferation. This study was supported by NIH grant R37 AA18282 to MJR.

***Disclosures: Jin-Ran Chen**, None*

P-392

Knockdown of Zbtb40 disrupts mesenchymal differentiation and likely acts as a cell fate determination gene *Madison Doolittle[1], Robert D Maynard[2], Dana A Godfrey[2], Charles R Farber[3], Cheryl L Ackert-Bicknell[2]. [1]Center for Musculoskeletal Research, University of Rochester, United States, [2]Departament of Orthopedics, University of Colorado, United States, [3]Center for Public Health Genomics, University of Virginia, United States

Zinc Finger and BTB Domain containing 40 (Zbtb40) is an under-characterized DNA binding protein that has been implicated in the regulation of bone mineral density (BMD) by genome-wide association studies (GWASs). We previously showed that knockdown of Zbtb40 in vitro reduces mineralized nodule formation in MC-3T3 cells subjected to osteoblast differentiation and mice homozygous for a Zbtb40 truncation mutation have decreased trabecular bone volume in the vertebrae. Other members of the ZBTB gene family act as regulators of stem cell differentiation. In this work we sought to determine if Zbtb40 played a role in mesenchymal stem cell (MSC) differentiation. In MC-3T3 cells ZBTB40 was bound to the promoter of the early MSC differentiation factor Msx2, suggesting that indeed Zbtb40 may act to impact the three main MSC lineages. To test if ZBTB40 impacted chondrogenesis we knocked down Zbtb40 in C3H10T ½ cells via siRNA and subjected these cells to DMEM:F12 media and 100ng of BMP-2. Knockdown of Zbtb40 resulted in decreased expression of Sox9 ($p<0.05$), but interestingly expression of Col2a1 was increased ($p<0.001$) at day 3 post differentiation, compared to cells treated with scramble siRNA. At day 7 we saw an increase in Col10a1 ($p<0.01$) and Acan (Aggrecan, $p<0.01$). Next, we tested if Zbtb40 was involved in adipocyte differentiation. We knocked-down expression of this gene in C3H10T ½ cells, but this time treated them with high glucose DMEM, 1uM dexamethasone 0.5uM IMBX and 10 ug/ml of insulin. We saw a reduction in mRNA levels for Pparg ($p<0.01$), but no change in PPARG protein. We observed a reduction of Fabp4 mRNA ($p<0.01$) and substantial reduction of FABP4 protein ($P<0.0001$), which may in part explain the lack of reduction of PPARG protein levels. ZBTB40 did bind to the promoter of Pparg. Further, Oil Red O staining was reduced in the Zbtb40 knockdown cells relative to the scramble siRNA treated cells after 8 days of differentiation. These data suggest ZBTB40 may be an inhibitor of chondrogenesis and activator of adipogenesis. If these data are taken together with our previous work where we showed that knockdown or mutation of Zbtb40 impacted osteoblastogenesis, these data collectively suggest that ZBTB40 plays a role in early MSC commitment and or differentiation. Future studies will be needed to determine how ZBTB40 impacts adipose and cartilage formation in vivo.

***Disclosures: Madison Doolittle**, None*

P-393

Physiological And Nutrition-related Effects On Bone Marrow Adipocyte Formation *George Soultoukis[1], Marina Leer[2], Charlotte Rinne[2], Nicole Dittberner[2], Katharina Schmidt-Bleek[3], Tim Julius Schulz[2]. [1]Leibniz Association, Germany, [2]German Institute of Human Nutrition, Germany, [3]Charité - Universitätsmedizin Berlin Julius Wolff Institut, Germany

IntroductionBone marrow fat comprises of adipocytes that are important components of the regenerative niche in bone. Unlike the more traditional brown and white adipose depots throughout the body, marrow fat can expand in response to both nutrient shortage (e.g. caloric restriction) and nutrient excess (e.g. high fat diet). Marrow adipocytes are formed by a distinct population of committed adipogenic progenitor cells which in turn arise from a specialized population of the cellular stroma of the bone marrow. Under normal physiological conditions long-bone derived mesenchymal stromal cells appear to mainly play a regulatory role, but they also increasingly undergo adipogenic lineage commitment under pathological conditions (e.g. obesity) and with age. However, the precise transcriptional and niche changes modulating these events are not fully understood. This work aims to elucidate these phenomena further. MethodsWe use a mouse model and immortalized murine bone-derived stem cell lines to investigate how bone regeneration is influenced by aging, nutrition, and sitagliptin. We perform single-cell RNA-sequencing analysis, and profile the defined stem/progenitor cell populations to trace lineage commitment as a function of age and diet. We validate our findings through in vitro and in vivo analyses targeting identified candidate genes found to modulate cellular fate determination. ResultsWe find that adipogenic lineage fate determination is highly sensitive to specific nutrition-related signals. We show that distinct nutrients, alone or in conjunction with Bone Morphogenetic Protein (BMP) signaling, regulate osteogenic and adipogenic progenitor cell specialization, while related molecules promote the expansion of ectopic marrow fat. Commited adipogenic lineage cells highly express the protease DPP4, and inhibition of DPP4 by its antagonist sitagliptin abolishes its negative effects on bone healing mineralization via modulation of osteogenic progenitor cells. Finally, we also uncover a novel regulatory role of the alarmin cytokine IL-33. ConclusionsOur results expose critical changes in the bone marrow niche and elucidate novel mechanisms modulating bone regeneration as a function of age and diet. Loss of appropriate stem and progenitor cell formation contributes to the age- and diet-related loss of bone tissue integrity and regenerative capacity, and targeting molecules secreted by adipogenic progenitor cells can reverse these detrimental processes.

***Disclosures: George Soultoukis**, None*

P-394

Horizontal fissuring at the osteochondral interface: a novel and unique pathological feature in patients with obesity-related osteoarthritis *Lianzhi Chen[1], Christopher Mitchell[1], chriswjones@health.wa.gov.au Jones[2], Minghao Zheng[1]. [1]University of Western Australia, Australia, [2]Fiona Stanley Hospital, Australia

Obesity is a well-recognized risk factor for osteoarthritis (OA). We aim to investigate if obesity is the causal antecedent of early joint replacement in patients with OA and characterize the body mass index (BMI)-associated pathological changes in the osteochondral unit. We analyzed the impact of BMI on the age at which patients undergo total knee replacement (TKR). 616,469 cases of TKR from the Australian Orthopaedic Association National Joint Replacement Registry (AOANJRR) and the British National Joint Registry (NJR) were assessed. It revealed that there was a significant progressive reduction in the age at which patients with increased BMI underwent TKR. The mean age of TKR in obese class III patients was 8 years younger than normal-weight patients. We then investigated the effect of BMI on pathological changes of the knee joint in a representative subset of 88 cases undergoing TKR. Histopathological examination revealed, for the first time, that horizontal fissuring at the osteochondral interface (Figure 1) was the major pathological feature of obesity-related

OA. The frequency of horizontal fissure was strongly associated with increased BMI in the predominant compartment. An increase in one unit of BMI (1 kg/m2) increased the odds of horizontal fissures by 14.7%. Over 80% of the horizontal fissures were attributable to obesity. Reduced cartilage degradation and alteration of subchondral bone microstructure were also associated with increased BMI. In conclusion, obesity is strongly associated with a younger age of TKR. Due to differences in the mechanical properties of cartilage, calcified cartilage and subchondral bone, secondary shear stress generated by high body weight in obesity-related OA induces horizontal fissures at the osteochondral interface. This key pathological feature may be the cause of earlier TKR in patients with obesity. This finding will draw considerable attention to the osteochondral interface as a therapeutic target for obesity-related OA.Figure 1. Osteochondral interface of patients with normal weight (A), cartilage is firmly attached to calcified cartilage. In patients with obese class III (B), a horizontal fissure is observed at the osteochondral interface between the articular cartilage (AC) and subchondral bone (SCB). Free bone debris (black arrowhead) and cartilage erosion (empty arrow) are presented within the fissure.

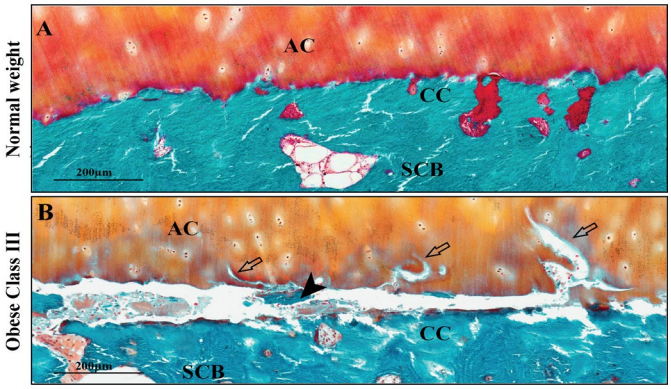

***Disclosures: Lianzhi Chen**, None*

P-395

Effect of Denosumab on Osteoclast Activity within Osteolytic Lesions after Total Hip Arthroplasty: A Proof of Concept Trial *Mohit M Mahatma[1], Raveen L Jayasuriya[1], David Hughes[2], Simon C Buckley[2], Andrew Gordon[2], Andrew J Hamer[2], M Wassim Tomouk[2], Robert M Kerry[2], J Mark Wilkinson[1]. [1]University of Sheffield, United Kingdom, [2]Sheffield Teaching Hospitals NHS Foundation Trust, United Kingdom

Osteolysis, leading to aseptic loosening, causes recurrent pain and disability after total hip arthroplasty (THA), and for which there are no established pharmacological alternatives to revision surgery. In this phase 2 clinical trial (EudraCT 2011-000541-20) we examined the effect of denosumab versus placebo on osteolytic lesion activity in patients undergoing revision surgery after THA. Men and women >= 30 years old scheduled for revision surgery for symptomatic, radiologically-confirmed osteolysis were randomised (1:1) to receive either denosumab 60mg or placebo subcutaneously eight weeks prior to operation. At surgery, biopsies from the osteolytic membrane-bone interface were taken for histomorphometric analysis of osteoclast number, the primary outcome measure. Secondary outcome measures included other static histomorphometric indices and systemic bone turnover markers. Adverse events and patient-reported clinical outcome scores were recorded as safety endpoints. Of the 24 subjects enrolled, 22 completed the study (10 denosumab) and comprise the per-protocol analysis. There were no differences in baseline characteristics and bone turnover markers between groups (p>0.05). The denosumab group had 78% fewer osteoclasts at osteolytic lesion sites (95% CI -61 to -95, P=0.011), 81% lower osteoclast surface (-70 to -95, P=0.009), and 73% lower eroded surface (-54 to -92, P=0.020) compared to the placebo group. Number of osteoblasts and osteoblast surface were also reduced by 81% (-62 to -100, p=0.021) and 82% (-64 to -101, p=0.017), respectively. Immunocytochemistry for cell proliferation (Ki67) and apoptosis (Caspase 3) identified no differences between the groups (p>0.05). At surgery, serum CTX-I, TRAP5b and PINP were 80% (-65 to -95, p<0.001), 65% (-40 to -90, p<0.001), and 53% (-41 to -65, p0.05). In this phase 2 clinical trial, a single dose of denosumab reduced osteoclast activity within osteolytic lesions and was safe to administer. These data provide a biological basis for a definitive phase 3 clinical trial using clinical outcomes of pain, function and prosthesis survival as the study endpoints.

***Disclosures: Mohit M Mahatma**, None*

P-396

Mitigation of Osteoarthritis Progression by Inhibiting Connexin Hemichannels *Rui Hua[1], Yi Tian[1], Manuel Riquelme[1], Liang Ma[1], Sumin Gu[1], Jean X. Jiang[1]. [1]Department of Biochemistry and Structural Biology, UT Health San Antonio, United States

Osteoarthritis (OA) is a joint disease characterized by degeneration of articular cartilage, subchondral bone remodeling and synovial inflammation, which causes pain and limited mobility. Connexin43 (Cx43) acts as a vital homeostatic regulator in the musculoskeletal system and its expression is increased in the cartilage and synovial tissue of OA patients. Emerging evidence suggests that Cx43 contributes to the production of catabolic and inflammatory factors and exacerbates joint destruction. Cx43 forms hemichannels (HCs) that mediate the release of small molecules, such as ATP and prostaglandin E2 (PGE2), into the extracellular environment. The open probability of HCs is low under physiological conditions, while their activation is regulated by multiple factors, including proinflammatory cytokines. We have developed a monoclonal antibody, which specifically inhibits the activity of Cx43 HCs. In primary mouse chondrocytes, ethidium bromide dye uptake assay indicated that this antibody blocked the IL-1β treatment induced HCs opening. To investigate its function in OA progression, post-traumatic OA model was induced in male C57BL/6 mice by surgically destabilization of the medial meniscus (DMM). Antibody or saline was administered by intraperitoneal injection twice during 8 weeks post-surgery. Cartilage degradation and synovial inflammation were analyzed by histology and immunohistochemistry. Compared to saline group, Cx43 antibody treatment significantly improved cartilage integrity as quantified by the OARSI scoring system, decreased degree of synovitis, along with reduction of Mmp13 and Collagen X levels. Microcomputed tomography (μCT) of subchondral bone sclerosis showed a decrease in BV/TV, Tb.Th and an increase in Tb.Sp after inhibition of Cx43 HCs. In addition, Von Frey filament and open-field tests exhibited ameliorated OA associated pain symptoms in DMM mice with antibody treatment, while no difference was observed between saline and antibody treated sham mice. We found the antibody was primarily localized to the synovium region, and the signal was detectable even at 2 weeks after antibody administration. In vivo dye uptake and immunofluorescence assay further validated the role of antibody in blocking OA induced HCs opening in synoviocytes that express Cx43. Taken together, our study suggests that targeting Cx43 HCs is a potential, novel therapeutic strategy to mitigate the catabolic and inflammatory environment of the joint during OA progression.

***Disclosures: Rui Hua**, None*

P-397

Mechanosensitive Control of Articular Cartilage and Subchondral Bone Homeostasis Requires Osteocytic TGFβ Signaling *Karsyn Bailey[1], Jeffrey Nguyen[2], Cristal Yee[1], Neha Dole[1], Alexis Dang[1], Tamara Alliston[1]. [1]University of California, San Francisco, United States, [2]California State University, Long Beach, United States

Osteoarthritis (OA) is characterized by the irreversible disruption of multiple joint tissues including articular cartilage and subchondral bone. While cartilage degeneration and subchondral bone changes are established hallmarks of OA, the causal mechanisms driving the coordinated loss of homeostasis in these two tissues remains unclear. The transforming growth factor beta (TGFβ) signaling pathway is known to play a complex tissue-specific and non-linear role in OA. The chondrocytic- and MSC-intrinsic contributions of TGFβ signaling to OA have been studied, but the role of osteocyte-intrinsic TGFβ signaling in joint homeostasis is unknown. Recent evidence demonstrates a new role for osteocytes in human and mouse OA, and we sought to identify the osteocytic contributions of TGFβ signaling to OA.We used male and female mice (n = 7-11 mice per group) with an osteocyte-intrinsic ablation of TGFβ type II receptor (DMP1Cre+; TβRIIfl/fl abbreviated as TβRIIocy-/-) and their control littermates (DMP1Cre-; TβRIIfl/fl), and assessed defects in cartilage degeneration, subchondral bone plate (SBP) thickness, and SBP sclerostin expression. To further investigate these mechanisms in male mice, we perturbed joint homeostasis using the medial meniscal/ligamentous injury (MLI) model, which preferentially disrupts the mechanical environment of the joint on the medial side to induce OA. In all contexts, independent of sex, genotype, or medial or lateral joint compartment, increased SBP thickness and SBP sclerostin expression were spatially associated with cartilage degeneration. Male TβRIIocy-/- mice, but not female TβRIIocy-/- mice, have significantly increased cartilage degeneration, increased SBP thickness, and higher levels of SBP sclerostin relative to Cre- controls, demonstrating that the role of osteocytic TGFβ signaling on joint homeostasis is sexually dimorphic. With changes in joint mechanics due to injury, injured Cre- control mice significantly increase SBP thickness, subchondral bone volume, and SBP sclerostin expression. TβRIIocy-/- mice, however, are insensitive to subchondral bone changes with injury, suggesting that mechanosensation at the SBP requires osteocytic TGFβ signaling. Our results provide new evidence that osteocytic TGFβ signaling is required for a mechanosensitive response to injury, and that osteocytes control SBP homeostasis to maintain cartilage health, uncovering osteocytic TGFβ signaling as a novel therapeutic target for OA.

***Disclosures: Karsyn Bailey**, None*

Posters

P-398

Tibial Bone Quality in Former Bariatric Surgery Patients with Knee Osteoarthritis *Breanne S. Baker[1], Chantelle C. Bozynski[1], Emily V. Leary[1], Richard J. Sherwood[2], James A. Keeney[1], James L. Cook[1], Dana L. Duren[2]. [1]Department of Orthopaedic Surgery and Thompson Laboratory of Regenerative Orthopaedics, Missouri Orthopaedic Institute – University of Missouri, Columbia, MO, United States, [2]Department of Orthopaedic Surgery and Thompson Laboratory of Regenerative Orthopaedics, Missouri Orthopaedic Institute – University of Missouri, Columbia, MO and Department of Pathology and Anatomical Sciences – University of Missouri, Columbia, MO, United States

The recent rise in bariatric weight loss surgery poses a unique set of challenges for orthopaedic surgeons. While bariatric surgery can be an effective means for rapid weight loss prior to procedures such as total knee arthroplasty (TKA) for severely overweight patients, it can also be associated with substantial bone resorption, potentially jeopardizing TKA prostheses fixation and/or ingrowth. This study sought to determine if TKA patients with history of bariatric surgery exhibit different subchondral bone quality compared to matched controls. Approval for this study was granted by the University of Missouri Institutional Review Board and was in accordance with the Declaration of Helsinki. Former bariatric surgery patients (BS n=12) and sex-, age-, weight-, height-, and BMI-matched controls (CON n=10) completed Patient-Reported Outcomes Measurement Information System (PROMIS) surveys and underwent elective TKA at the Missouri Orthopaedic Institute. Tibial plateau osteochondral tissues that would otherwise be discarded were recovered after standard of care surgical resection and immediately processed. The central portions of the medial and lateral tibial plateaus were cut into 1 x 2 cm samples. These samples were scanned using microCT at 10.007–10.060 µm and analyzed using ImageJ and BoneJ software. Next, the same medial and lateral specimens underwent plastic embedding of undecalcified bone in methyl methacrylate. Two sections from each specimen were prepared for histologic sectioning, stained with Goldner's trichrome, and histomorphometric measures of bone quality were analyzed using Clemex Vision PE software. Paired t-tests with a Bonferroni correction were performed and effect sizes (ES) were calculated for all measures between groups. BS patients reported more pain interference with daily tasks (p=0.044, ES=0.98) and poorer physical function (p=0.013, ES=1.28) compared to CON (see Figure 1). No differences were found between BS and CON patients when comparing microCT (all p>0.195, all ES0.239, all ES<0.58). These results suggest that despite reporting greater difficulties with pain and physical function than control peers, former bariatric surgery patients who presented with endstage knee osteoarthritis requiring TKA did not exhibit altered bone microarchitecture or histomorphometry.

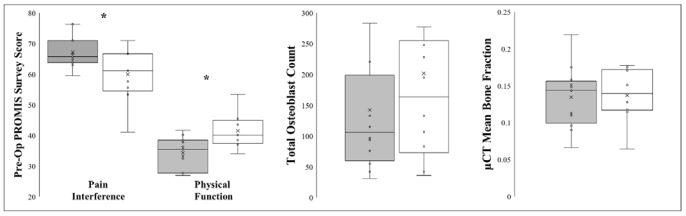

Figure 1. Former bariatric patients (■ BS n=11) report greater pain and difficulties with physical function than controls (□ CON n=9) but do not present with altered bone properties including osteoblast count or bone fraction.

***Disclosures: Breanne S. Baker**, None*

P-400

Identification of Gli1 as A Progenitor Cell Marker for Meniscus Development and Injury repair *Yulong Wei[1], Ling Qin[1], Tao Gui[1]. [1]University of Pennsylvania, United States

Meniscal tears, the most common injury of the knee, are associated with a high risk of osteoarthritis (OA). Stem cell transplantation has been proposed to repair injured meniscus. However, meniscus-specific progenitors remained largely unknown. Gli1, an effector of hedgehog (Hh) pathway, was recently recognized as a mesenchymal progenitor marker in bone. In this study, we constructed Gli1-CreER Tomato (Gli1ER/Td) mice for lineage tracing studies. Td did not label meniscus in newborn pups. In 2-wk-old mice, Td initially labeled the entire anterior horn and gradually concentrated at the superficial cells by 8 wk of age. Td started to label posterior horn in 4-wk-old mice and later also focused on superficial cells. In adult mice, Td+ cells only occurred in the superficial layer of meniscal horns and long-term tracing did not detect their expansion. Td+ cells were co-stained with mesenchymal progenitor markers (Sca1, CD90, CD200, and PDGFRα) and lubricant Prg4. Sorted Td+ meniscal cells generated 2.6-fold more CFU-Fs and grew much faster than Td- cells. They also differentiate better into osteoblasts, chondrocytes, and meniscal cells than Td- cells in vitro. Hh activator (Purmorphamine, Pur) stimulated proliferation, migration, and differentiation of meniscus progenitors, while inhibitor (GANT-61) suppressed them. After transection of meniscal anteriomedial horn, Td+ cells quickly emerged at the injury ends and proliferated. This is line with human degenerated meniscus, in which Gli1 appeared in cell clusters with Ki67+ staining. Normally, the two ends of mouse meniscus remained separated 3 mo later (Repair score, RS: 3.9, n=8/group). However, injection of Td+ cells, but not Td- cells, from Gli1ER/Td meniscus into the joint capsule of WT mice right after injury resulted in the reconnection of two ends within 1 mo (4.8, n=8/group). Intraarticular injection of Pur also exhibited a strong repair effect (4.9, n=7/group). Knee OA develops 2 mo later after meniscus injury. Strikingly, injection of Td+ cells or Pur right after injury greatly reduced cartilage degeneration and attenuated OA-related pain (Mankin Score: veh 6.9, Gli1+ cells 4.5, and Pur 3.3; n=8/group, p<0.001). Taken together, our work establishes Gli1+ cells as a novel progenitor population contributing to meniscus development and injury response and indicates a new therapeutic target for repairing injured meniscus and preventing OA propagation.

***Disclosures: Yulong Wei**, None*

P-401

Understanding causal pathways between bone mineral density, body mass index and osteoarthritis using bidirectional and multivariable Mendelian randomization *April Hartley[1], Eleanor Sanderson[1], Raquel Granell[1], Lavinia Paternoster[1], Jie Zheng[1], George Davey Smith[1], Lorraine Southam[2], Konstantinos Hatzikotoulas[2], Cindy G Boer[3], Joyce van Meurs[3], Eleftheria Zeggini[2], Celia L Gregson[1], Jon H Tobias[1]. [1]University of Bristol, United Kingdom, [2]Institute of Translational Genomics, Helmholtz Zentrum Munchen, Germany, [3]Erasmus Medical College, Netherlands

Objectives: Observational and Mendelian randomization (MR) analyses suggest that high Bone Mineral Density (BMD) is a risk factor for osteoarthritis (OA); however, it is unclear whether this represents a direct causal effect or shared aetiology. Moreover, confounding by body mass index (BMI) might contribute to this relationship, due to causal effects on both OA and BMD. We performed bidirectional MR to elucidate causal pathways between BMD, BMI and OA, and multivariable (MV)MR to determine if the causal pathway from BMD to OA is BMI-independent.Methods: One-sample (1S)MR estimates were generated by two-stage least-squares regression, adjusted for sex, genotyping chip and 10 principal components. Unweighted allele scores instrumented each exposure. Two-sample (2S)MR estimates were generated using inverse-variance weighted fixed-effects meta-analysis. Steiger filtering was performed prior to 2S analysis to remove SNPs explaining a greater proportion of variation in the outcome than the exposure. 1S MVMR, including BMD and BMI instruments in the same model, determined the BMI-independent causal pathway from BMD to OA. Instruments used for each analysis are summarized in Table 1. Latent causal variable (LCV) analysis, using weight-adjusted femoral neck BMD and hip/knee OA summary statistics, determined whether genetic correlation explained the causal effect of BMD on OA.Results: 1SMR provided strong evidence that higher eBMD causes hip and knee OA (ORhip=1.28[1.05,1.57], ORknee=1.40[1.20,1.63], OR per SD increase). 2SMR effect sizes were consistent in direction (Table 1). 1SMR suggested that causal pathways between eBMD and OA were bidirectional (βhip=1.10[0.36,1.84], βknee=4.16[2.74,5.57], β=SD increase per doubling in risk). BMI was strongly causally related to both hip & knee OA and eBMD in both 1S and 2SMR, but a causal effect of eBMD on BMI was not observed (Table 1). MVMR identified a BMI-independent causal pathway between eBMD and hip & knee OA (ORhip=1.26[1.03,1.54], ORknee=1.36[1.16,1.59]). LCV suggested that genetic correlation (i.e. shared genetic aetiology) did not fully explain causal effects of BMD on hip & knee OA.Conclusions: Our results provide evidence for a BMI-independent causal effect of BMD on OA. Despite evidence of bidirectional effects, the effect of BMD on OA did not appear to be fully explained by shared genetic aetiology, suggesting a direct action of bone on joint deterioration.

Analysis	Exposure	Outcome	Instrument(s)	Beta	95% CI	*p* value
1S	eBMD	Knee OA	Unweighted allele score using GEFOS FN-BMD SNPs	1.40[OR]	1.20, 1.63	$3x10^{-5}$
2S	eBMD	Knee OA	349 eBMD SNPs from GEFOS	1.04[OR]	1.00, 1.09	0.068
MV[a]	eBMD	Knee OA	Unweighted allele score using GEFOS FN-BMD SNPs Unweighted allele score using GIANT BMI SNPs	1.36[OR]	1.16, 1.59	$1x10^{-4}$
1S	eBMD	Hip OA	Unweighted allele score using GEFOS FN-BMD SNPs	1.28[OR]	1.05, 1.57	0.016
2S	eBMD	Hip OA	346 eBMD SNPs from GEFOS	1.09[OR]	1.03, 1.16	0.002
MV[a]	eBMD	Hip OA	Unweighted allele score using GEFOS FN-BMD SNPs Unweighted allele score using GIANT BMI SNPs	1.26[OR]	1.03, 1.54	0.027
2S	eBMD	BMI	267 eBMD SNPs from GEFOS	0.01[SD]	-0.01, 0.03	0.472
1S	BMI	Knee OA	Unweighted allele score using GIANT BMI SNPs	2.01[OR]	1.76, 2.29	$<2x10^{-16}$
2S	BMI	Knee OA	61 BMI SNPs from GIANT	1.69[OR]	1.48, 1.93	$1x10^{-14}$
MV[b]	BMI	Knee OA	Unweighted allele score using GIANT BMI SNPs Unweighted allele score using GEFOS FN-BMD SNPs	1.93[OR]	1.62, 2.30	$3x10^{-13}$
1S	BMI	Hip OA	Unweighted allele score using GIANT BMI SNPs	1.60[OR]	1.35, 1.91	$7x10^{-8}$
2S	BMI	Hip OA	58 BMI SNPs from GIANT	1.56[OR]	1.31, 1.87	$8x10^{-7}$
MV[b]	BMI	Hip OA	Unweighted allele score using GIANT BMI SNPs Unweighted allele score using GEFOS FN-BMD SNPs	1.49[OR]	1.19, 1.87	$5x10^{-4}$
2S	BMI	eBMD	51 BMI SNPs from GIANT	0.13[SD]	0.09, 0.17	$7x10^{-10}$
1S	Knee OA	eBMD	Unweighted allele score using knee OA SNPs from the GO consortium meta-analysis (excluding UK Biobank)	4.16[SD]	2.74, 5.57	$8x10^{-9}$
2S	Knee OA	eBMD	3 knee OA SNPs from the GO consortium meta-analysis (excluding UK Biobank)	0.13[SD]	0.03, 0.23	0.010
1S	Knee OA	BMI	Unweighted allele score using knee OA SNPs from the GO consortium meta-analysis (excluding UK Biobank)	8.44[SD]	6.65, 10.23	$<2x10^{-16}$
2S	Knee OA	BMI	6 knee OA SNPs from UK Biobank/arcOGEN	0.00[SD]	-0.03, 0.03	0.995
1S	Hip OA	eBMD	Unweighted allele score using hip OA SNPs from the GO consortium meta-analysis (excluding UK Biobank)	1.10[SD]	0.36, 1.84	0.003
2S	Hip OA	eBMD	9 hip OA SNPs from the GO consortium meta-analysis (excluding UK Biobank)	0.02[SD]	-0.01, 0.05	0.117
1S	Hip OA	BMI	Unweighted allele score using knee OA SNPs from the GO consortium meta-analysis (excluding UK Biobank)	0.54[SD]	0.01, 1.07	0.048
2S	Hip OA	BMI	17 hip OA SNPs from UK Biobank/arcOGEN	0.02[SD]	0.00, 0.04	0.120

Table 1: summary of results for one-sample, two-sample and multivariable Mendelian randomization analyses
Abbreviations: 1S: one-sample MR; 2S: two-sample MR; eBMD: estimated bone mineral density; BMI: Body Mass Index; HD: hospital-diagnosed; FN-BMD: femoral neck bone mineral density; OA: osteoarthritis
[OR]beta=odds ratio per SD increase in exposure
[SD]beta= standard deviation increase per standard deviation increase in exposure (for continuous exposure) or per doubling in risk of exposure (binary exposures)
[a]estimating the direct causal pathway, independent of BMI
[b]estimating the direct causal pathway, independent of eBMD

***Disclosures: April Hartley**, None*

P-402

Image-Based Bone Remodeling in Patients Achieving a Favourable Clinical Response to Biologic Therapies *Scott C Brunet[1], Justin J Tse[1], Micheal T Kucynski[1], Steven K Boyd[1], Cheryl Barnabe[2], Sarah L Manske[1]. [1]McCaig Institute for Bone and Joint Health, Biomedical Engineering Graduate Program, and Department of Radiology; Cumming School of Medicine, University of Calgary, Canada, [2]McCaig Institute for Bone and Joint Health, Department of Community Health Sciences, Department of Medicine; Cumming School of Medicine, University of Calgary, Canada

Purpose: High resolution-peripheral quantitative computed tomography (HR-pQCT) imaging of patients with rheumatoid arthritis (RA) has suggested that biologic therapies may lead to the repair of bone damage in the hands, but this has not been assessed using a quantitative image-based bone remodeling analysis. The purpose of this study was to use HR-pQCT to assess bone formation and resorption for patients that demonstrated a good clinical response to biologic therapy, and to examine if there are differences in bone remodeling across different biologic mechanisms of action.Methods: Ninety participants who met the 2010 ACR/EULAR classification for RA and achieved a moderate or good EULAR response within 3 months of initiating biologic therapy were recruited. HR-pQCT images of the 2nd and 3rd metacarpophalangeal (MCP) joints were obtained at the time of their EULAR response achievement and again 9 months later. After registering the follow-up image to the baseline, image-based bone remodeling analysis of the metacarpal head was performed to calculate bone formation (BF/TV) and resorption fractions (BR/TV), as well as net change (BF/TV – BR/TV). The average BF/TV and BR/TV across both joints were compared. We assessed differences in BF/TV and BR/TV by biologic therapy mechanism of action (anti-TNF, anti-IL6, or T-cell co-stimulatory inhibitor).Results: Image-based bone remodeling analysis was successfully performed in at least one MCP joint of 46 patients. Thirty-three participants were lost to follow-up and 11 were excluded due to motion or inability to register in both joints. BR/TV was significantly higher (0.57%) than BF/TV (0.47%) (p0.05). Conclusions: This study demonstrates that biologic therapy results in minimal levels of bone remodeling in the metacarpal head of RA patients over the course of 9 months. This suggests that biologic therapy stabilizes bone remodeling but does not necessarily lead to systemic bone formation. There is visual evidence of local change in some patients (Figure 1), but the relationship with biologic therapy is unclear at this time. Future research should investigate local bone remodeling in eroded regions to determine if biologic therapy can lead to the local repair of RA erosions.

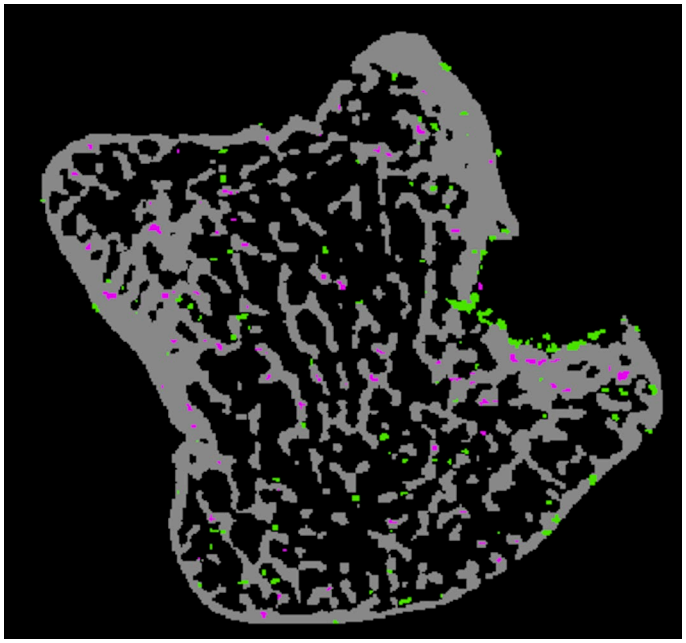

***Disclosures: Scott C Brunet**, None*

P-403

Association Between Serum Vitamin D Level and Osteoarthritis in Korean Elderly Population *Hee Sook Lim[1], Kyo Il Suh[2], Dong Won Byun[2], Hyeong Kyu Park[2], Hye Jeong Kim[2], Sang Joon Park[2]. [1]Department of Food and Nutrition, Yeonsung University, Republic of Korea, [2]Division of Endocrinology and Metabolism, Department of Internal Medicine, Soonchunhyang University College of Medicine, Republic of Korea

Background and Purpose: Vitamin D is important in bone health and its relationship with osteoarthritis has been reported. Osteoarthritis (OA) and osteoporosis are common diseases in the elderly and are known to be negatively associated, but their relationships in Koreans are not known. This study aimed to assess the risk of osteoarthritis by vitamin D and bone mineral density (BMD) status using a nationally representative database. Method: A total of 3,156 participants aged >=60 years were selected from the Korean National Health and Nutrition Examination Survey 2010-2013. We classified into two groups (normal: 2,431, OA: 725) according to arthritis presence. Radiographic osteoarthritis defined as Kellgren-Lawrence (KL) grade >=2. Bone health was classified according to T-score for osteoporosis or in tertiles. Socio-economic factors and health behaviors were compared into two groups. Results: The prevalence of osteoarthritis was 41.6% in males and was 58.4% in females. Subjects with osteoarthritis regardless of site tended to be older, have lower income, lower education level, higher BMI, lower strength exercise frequency. Quality of life (EQ-5D) was also significantly lower in the osteoarthritis group. Medium vitamin D status was associated with a lower compared to those with higher vitamin D status both males and females. In BMD tertiles, osteoarthritis was lower in those with BMDs of T1 compared to T3 at the total femur and lumbar spine in females. Conclusion: Vitamin D level and bone mineral density were positively associated with osteoarthritis in elderly people.

***Disclosures: Hee Sook Lim**, None*

P-404

Possibities of Trabecular Bone Score to Reflect Activity and Progression of Ankylosing Spondilitis in Young Patients *Konstantin Kolpakov[1], Julia Ubshaeva[1], Vitaly Omelchenko[1], Maxim Korolev[1]. [1]RICEL - Branch of IC&G SB RAS, Russian Federation

I. INTRODUCTION Ankylosing spondylitis (AS) is a systemic inflammatory disease, with primary lesion of spine. Inflammation is developing mainly in lumbar vertebrae, leading to its degradation. Meanwhile, it is proliferating in AS resulting in syndesmophytes formation. Dual-energy X-ray absorptiometry (DXA) is used to measure bone mineral density (BMD), but it is invalid in AS, because of osteophytosis. Trabecular bone score (TBS) is another tool to evaluate bone properties. While BMD represents quantity of the bone tissue, TBS represents its quality. So, TBS does not lose its value in the presence of syndesmophytes. The aim of this work is to investigate TBS correlation with BMD, clinical and laboratory disease activity and structural progression of AS in the males before 50. II. MATERIALS AND METHODS 21 AS male patients before 50 were included in investigation. The following parameters were collected: age, duration of the disease, BASDAI and

ASDAS scores, consumption of corticosteroids, smoking status, history of fractures. Erythrocyte sedimentation rate (ESR), C-reactive protein (CRP) and fibrinogen were also evaluated. The degree of structural progression of AS was determined by the stage of sacroiliitis according to Kellgren. BMD was measured in the lumbar spine, right and left femurs and femoral necks. TBS in the lumbar spine was determined using an iNsight software package. All the results are presented as Median (Me) +/- Standard Deviation (SD). The relationships between variables were studied using Spearman correlation analysis. III. RESULTS The median age is 36+/-6.8 years, the BASDAI index is 2.3+/-0.9. Two patients had a history of vertebral fractures. 19.0% of patients have stage 2 sacroiliitis, 33.3% have stage 3 and 47.7% have stage 4. The median TBS in the group was 1.407+/-0.131, BMD in the lumbar spine - 1.184+/-0.136, in the right and left femurs - 1.012+/-0.127 and 1.006+/-0.126, respectively, in the right and left necks of the femur - 0.980+/-0.152 and 0.957+/-0.132, respectively. A negative correlation was revealed between the stage of sacroiliitis and TBS values (r=-0.49; p<0.05). There was no correlation between either TBS or stage of sacroiliitis and age. Patients with a history of vertebral fractures had the lowest TBS values in the entire group (1.167 and 1.121). No one parameter of AS activity correlated with TBS or BMD. IV. CONCLUSION TBS, unlike BMD, reflects structural progression of AS, but do not correlate with clinical or laboratory activity.

***Disclosures: Konstantin Kolpakov**, None*

P-405

Development of a precision medicine-based therapeutic strategy forrheumatoid arthritis *Chao Liang[1], Duoli Xie[1]. [1]Hong Kong Baptist University, Hong Kong

Bone erosion is a central feature of rheumatoid arthritis (RA). Traditional concept holds that chronic inflammation causes bone erosion in RA. Thus, most of the anti-RA drugs are designed for targeting inflammation to attenuate bone erosion. Among these drugs, Leflunomide has been used for almost twenty years. However, only 40-50% RA patients show good response to Leflunomide in attenuating bone erosion.Recently, we found that RA patients with either good or limited response to Leflunomide in attenuating bone erosion had equivalent basal inflammation. Surprisingly, these two subgroups of patients showed comparable immunosuppression after Leflunomide treatment. C-reactive protein (CRP) is synthesized by liver and commonly considered as an inflammation marker. However, emerging evidences reveal that there are large genetic variations of CRP, which are irrelevant to inflammation status in RA. Further, it has been reported that CRP could directly regulate osteoclastic activity. We found that RA patients with good response to Leflunomide showed relatively low basal serum CRP (CRPlow), whereas the others with limited response demonstrated high basal CRP (CRPhigh). We observed the similar relationship between the high basal CRP and the limited response to Leflunomide in established collagen-induced arthritis (CIA) rats. CRP silencing compensated the limited efficacy of Leflunomide, leading to adequate attenuation of bone erosion in the CRPhigh CIA rats. We concluded that in addition to inflammation, high CRP was another factor responsible for inducing bone erosion in CRPhigh RA.CRP has two isoforms: native CRP (nCRP) and monomeric CRP (mCRP). nCRP is normally present as a pentamer of five identical subunits in serum, which is inefficient for osteoclastic activity. However, nCRP dissociates into monomeric CRP (mCRP) upon entering inflammatory sites. Studies have shown that mCRP directly induces osteoclastic differentiation in vitro. We found that there was excessive mCRP in both CRPlow and CRPhigh RA patients and CIA rats. 1,6-bis(phosphocholine)-hexane has been reported to be a small molecular CRP inhibitor, which could suppress dissociation of nCRP to mCRP. In vitro proper inhibition of nCRP dissociation by 1,6-bis-PC decreased osteoclastic differentiation. Combination of 1,6-bis-PC with Leflunomide could compensate the limited efficacy of Leflunomide, leading to adequate attenuation of bone erosion in CRPhigh CIA rats.This study would present a precision medicine-based therapeutic strategy for RA. Combination of Leflunomide with 1,6-bis-PC will be a promising approach for adequately attenuating bone erosion in CRPhigh RA. This study was supported by grants from the Natural Science Foundation Council of China (81700780 and 81922081).

***Disclosures: Chao Liang**, None*

P-406

Conditional Knockout of SHP2 in Mice Reveals Its Indispensable Role in Osteogenic Maturation and Bone Mineral Homeostasis *Huiliang Yang[1], Lijun Wang[1], Jiahui Huang[1], Douglas Moore[1], Wentian Yang[1]. [1]Brown University Alpert Medical School and Rhode Island Hospital, United States

Purpose: The maturation and function of osteoblasts (OBs) heavily rely on the reversible phosphorylation of signaling proteins. To date, most of the work on OBs has been focused on phosphorylation by protein kinases, whereas little has been studied on dephosphorylation by protein tyrosine phosphatases (PTPase). SHP2 (encoded by Ptpn11) is an ubiquitously expressed PTPase. Previous studies show that SHP2 mutations are associated with human Noonan syndrome (NS) and metachondromatosis (MC); both display bone and cartilage manifestations. The role of SHP2 in skeletal cells remains incompletely understood. To investigate whether and how SHP2 functions in skeletal cells, we generated OB-specific SHP2 deficient mutant mice.Methods: OB-specific SHP2 deficient mice (SHP2KOBglap) and littermate controls (SHP2CTRBglap) were generated by crossing mice bearing Ptpn11 floxed allele to Tg(Bglap-Cre) mice. Tg(Rosa26ZsG) allele served as a Cre reporter. Mice were sacrificed at the indicated time points and underwent X-ray, μ-CT, histological, biochemical, and biological analyses per the protocols approved by IACUC. Results: SHP2KOBglap mice appeared normal and indistinguishable from the SHP2CTRBglap mice up to 10 weeks. However, the mobility of SHP2KOBglap mutants became progressively restricted as they aged. Analysis of skeletal morphology with radiographs revealed a striking skeletal phenotype in SHP2KOBglap mutants featuring scoliosis, reduced bone mineral density, and growth of osteochondromas and enchondromas adjacent to the metaphysis of multiple joints. Further phenotypic studies showed that SHP2 deletion in OBs leads to significant osteopenia in both trabecular and cortical bones (Fig.1A, 1B) due to failed bone cell maturation and function (Fig. 1C), and enhanced osteoclast activity (Fig. 1D). SHP2 deficient but Bglap+ chondrocytes were found to contribute to the onset of enchondromas and osteochondromas in old mice. Mechanistically, SHP2 was found to promote osteoblastic differentiation by promoting RUNX2/OSTERIX signaling and suppress osteoclastogenesis by inhibiting STAT3-mediated RANKL production by osteoblasts and osteocytes.Conclusions: Our study uncovered an indispensable role for SHP2 in regulating OB maturation and function, local osteoclastogenesis, and bone mineral homeostasis. These findings also explain why the skeletal system is compromised in NS and MC patients and inform the development of novel therapeutics to combat skeletal disorders.

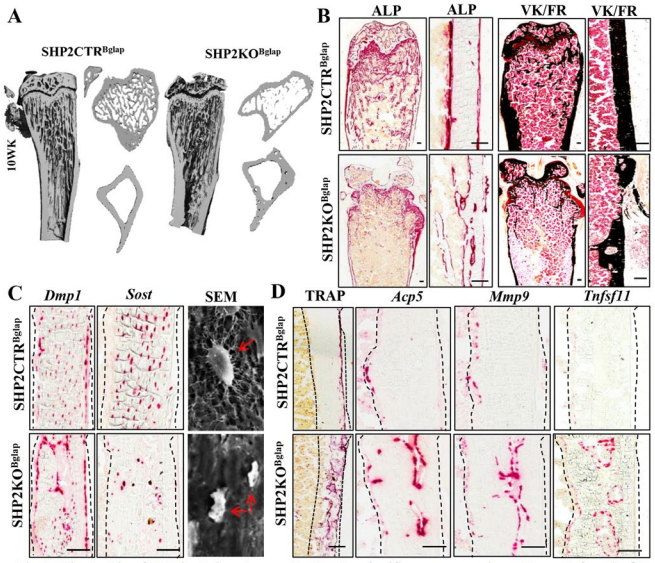

Fig.1 Mice lacking SHP2 in *Bglap+* bone cells develop significant osteopenia and have defects in OB maturation. μ-CT radiograph and Von Kossa staining of tibia frozen sections revealed decreased mineralization of both trabecular and cortical bone in 13-wk-old SHP2 mutants but not controls (A, B). RNAscope® analysis revealed decreased and increased expression of osteogenic (C) and osteoclastogenic (D) genes respectively in the cortical bone of SHP2 mutants. SEM images demonstrate a significant reduction in the numbers of dendrites and canalicular network of osteocytes in the cortical bone of SHP2 mutants (C).

***Disclosures: Huiliang Yang**, None*

P-407

SLC1A5 regulates osteoblast differentiation by providing glutamine used for de novo amino acid synthesis. *Deepika Sharma[1], Guo-fang Zhang[1], Yilin Yu[2], Courtney Karner[1]. [1]Duke University, United States, [2]duke University, United States

Osteoblasts are bone forming cells whose primary function is to synthesize and secrete Type I Collagen and other proteins that comprise the bone matrix. A constant supply of amino acids is required to sustain high rates of protein synthesis associated with bone anabolism. To meet this requirement, osteoblasts must maximize the production or acquisition of amino acids. Indeed, recent reports have linked the regulation of amino acid uptake and metabolism to osteoblast function and bone formation. For example, osteoblast progenitors increase glutamine uptake and metabolism necessary for osteoblast differentiation. However, little is known about specific amino acid transporters mediating glutamine uptake, nor their regulation during osteoblast differentiation. Here we identify the amino acid transporter Slc1a5 as the primary glutamine transporter in osteoblasts. To determine the role of Slc1a5 during bone development, we generated a novel floxed Slc1a5 allele (Slc1a5fl) using homologous recombination to insert lox P sites flanking exon 2. Deletion of Slc1a5 in specified osteoblasts using Sp7Cre significantly reduced glutamine uptake and resulted in defective intramembranous and endochondral ossification. Sp7Cre;Slc1a5fl/fl animals were characterized by reduced protein expression of both Osterix (encoded by Sp7) and Type I Collagen despite normal Sp7 and Col1a1 mRNA expression. Consistent with this, inhibiting Slc1a5 dependent glutamine uptake reduced the rate of general protein synthesis as well as collagen synthesis in vitro. Mechanistically, Slc1a5 dependent glutamine uptake is critical to maintain intracellular amino acid homeostasis. Stable isotopomer analysis indicated that glutamine carbon and nitrogen are used for de novo synthesis of many amino acids including glutamate, proline and aspartate which are directly incorporated into newly synthesized protein. Importantly, inhibiting glutamine catabolism significantly reduced the concentration

of glutamine derived amino acids as well as protein and collagen synthesis. Collectively, our data indicates Slc1a5 provides osteoblasts with glutamine used for de novo synthesis of amino acids that are rapidly incorporated into protein to support bone matrix production. Thus, our data strongly suggest that manipulation of Slc1a5 activity may provide a therapeutic approach for normalizing deranged bone anabolism associated with human bone diseases.

***Disclosures: Deepika Sharma**, None*

P-408

FAK promotes early osteoprogenitor cell proliferation by enhancing mTORC1 signaling *Shuqun Qi[5], Xiumei Sun[5], Han Kyoung Choi[5], Jinfeng Yao[5], Li Wang[5], Guomin Wu[5], Yun He[5], Jian Pan[3], Jun-lin Guan[4], Fei Liu[5]. [5]Department of Biologic & Materials Sciences and Prosthodontics, University of Michigan School of Dentistry, Ann Arbor, MI 48109, USA, China, [5]Department of Biologic & Materials Sciences and Prosthodontics, University of Michigan School of Dentistry, Ann Arbor, MI 48109, USA, Republic of Korea, [3]Department of Oral and Maxillofacial Surgery, West China Hospital of Stomatology, Sichuan University, Chengdu, Sichuan 610041, China, China, [4]Department of Cancer Biology, University of Cincinnati College of Medicine, Cincinnati, OH 45267, USA, United States, [5]Department of Biologic & Materials Sciences and Prosthodontics, University of Michigan School of Dentistry, Ann Arbor, MI 48109, USA, United States

Focal adhesion kinase (FAK) is an intracellular non-receptor tyrosine kinase and a major mediator of signal transduction by integrins. The goal of this study was to determine the impact and mechanism of FAK inhibition in osteoblast lineage cells on bone homeostasis. μCT and histomorphometry analyses showed that mice lacking FAK in Dermo1-expressing cells exhibited low bone mass and decreased osteoblast number. By generating compound mice using Ai14 fluorescence reporter mice, we were able to specifically analyze the effect of Fak deletion on the Dermo1-expressing bone marrow stromal cells (BMSCs). Our data showed that Dermo1-targeted FAK-deficient early osteoprogenitor cells had decreased proliferation and reduced colony formation ability. Mechanistically, FAK-deficient early osteoprogenitor cells had significantly reduced mammalian/mechanistic target of rapamycin complex 1 (mTORC1) signaling, a central regulator of cell growth and proliferation, shown by a significant decrease in the levels of phospho-mTOR and phospho-S6 by western blot and immunofluorescence analyses. Furthermore, our data showed that the pharmacological inhibition of FAK kinase function alone was sufficient to decrease the proliferation and compromise the mineralization of early osteoprogenitor cells in vitro. In contrast to the Fak deletion in early osteoprogenitor cells, FAK loss in Col3.6 Cre-targeted osteoblasts did not cause bone loss, and Fak deletion in osteoblasts did not affect proliferation, differentiation, and mTORC1 signaling but increased the level of active proline-rich tyrosine kinase 2 (PYK2), which belongs to the same non-receptor tyrosine kinase family as FAK. Importantly, if FAK kinase was inhibited in BMSCs at the early osteogenic differentiation stage, mTORC1 signaling was reduced without any change in active PYK2 level and mineralization was compromised. In contrast, if FAK kinase was inhibited at a later osteogenic differentiation stage, mTORC1 signaling was not affected but active PYK2 was upregulated, however, the concomitant inhibition of both FAK kinase and PYK2 kinase reduced mTORC1 signaling and mineralization. In summary, our data suggest that FAK promotes early osteoprogenitor cell proliferation by enhancing mTORC1 signaling via its kinase-dependent function and the loss of FAK in osteoblasts can be compensated by the upregulated active PYK2. Together with previous work, we conclude that FAK has differential roles in osteoblast lineage cells (Fig 1).

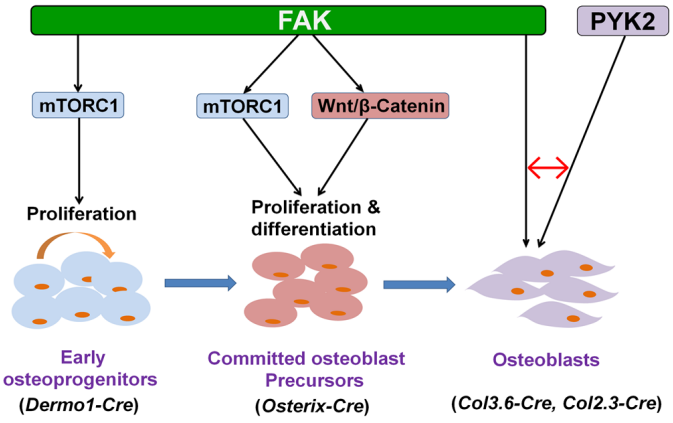

Fig 1. Schematic model of the differential roles of FAK in the cells of osteoblast lineage. The model depicts the mechanisms of FAK action at three distinct stages of osteoblast lineage in which the roles of FAK have been addressed by genetic and pharmacological approaches (this study) as well as the respective *Cre* transgenes used to delete *Fak*, including *Dermo1-Cre* (this study), *Osterix-Cre* (*Sun C et al, JBMR, 2016*), *Col3.6-Cre* (this study) and *Col2.3-Cre* (*Kim JB et al, Bone, 2007*). Red ↔ indicates that the loss of FAK in osteoblasts can be compensated by the upregulated active PYK2.

***Disclosures: Shuqun Qi**, None*

P-409

Slc38a2 provides proline to fulfill energetic and biosynthetic demands associated with osteoblast differentiation and bone formation *Leyao Shen[1], Yilin Yu[2], Guo-Fang Zhang[3], Courtney Karner[1]. [1]Department of Orthopaedic Surgery, Department of Cell Biology, Duke University, United States, [2]Department of Orthopaedic Surgery, Duke University, United States, [3]Duke Molecular Physiology Institute, United States

Osteoblasts are the chief bone forming cell responsible for producing and secreting the Type I Collagen rich extracellular matrix. Protein synthesis is very demanding from an energetic and biosynthetic standpoint, requiring copious amounts of ATP and amino acids amongst other metabolites. Thus, bone matrix production is predicted to burden osteoblasts with unique biosynthetic and energetic demands to maintain high rates of protein synthesis associated with bone anabolism. To understand how osteoblasts fulfill these metabolic demands, we devised a computational method to predict important amino acids and how amino acid demand changes during osteoblast differentiation. This method identified proline as a potentially important amino acid whose demand increases during osteoblast differentiation. For example, proline is significantly enriched in important osteoblast proteins including RUNX2, OSX, COL1A1 and OCN. Consistent with this, proline uptake increases concomitantly with induction of these proteins during differentiation indicating proline may be a critical regulator of osteoblast differentiation. Unfortunately little is known about how osteoblasts obtain or utilize proline. Here we identify the amino acid transporter Slc38a2 as the primary proline transporter in osteoblasts. Conditional deletion of a floxed allele of Slc38a2 (Slc38a2fl) in either mesenchymal progenitors using Prx1Cre or preosteoblasts using Sp7Cre resulted in defects in both intramembranous and endochondral ossification due to defective osteoblast differentiation highlighted by a specific reduction of proline enriched proteins (e.g. OSX and COL1A1). Mechanistically, Slc38a2 provides proline to support osteoblast differentiation via two major modes. First, stable isotopomer analysis indicates proline is directly incorporated into nascent protein and does not contribute to amino acid biosynthesis or TCA cycle anaplerosis. Second, proline oxidation provides electrons to the electron transport chain to fuel ATP production necessary for cellular activity. Collectively, these data highlight a bipartite mechanism by which proline fulfills the energetic and biosynthetic demands associated with osteoblast differentiation and bone matrix production.

***Disclosures: Leyao Shen**, None*

P-410

Runx2 defines the osteoblast chromatin landscape in skeletal development *Hironori Hojo[1], Taku Saito[1], Shoko Onodera[2], Toshifumi Azuma[2], Ung-il Chung[1], Masahide Seki[1], Yutaka Suzuki[1], Andrew McMahon[3], Shinsuke Ohba[4]. [1]The University of Tokyo, Japan, [2]Tokyo Dental College, Japan, [3]University of Southern California, United States, [4]Nagasaki University, Japan

Runx2 is an essential transcription factor for both osteoblast specification and chondrocyte hypertrophy. At the 2019 ASBMR annual meeting, we presented our finding that Runx2 acted on accessible chromatin regions in a cell-type-distinct manner in osteoblasts and chondrocytes. However, it remains to be clarified whether Runx2 is involved in the establishment of the chromatin accessibility. To address this question in an in vivo setting, we generated Sp7-GFP::Cre;Runx2fl/fl;R26Rtdtomato compound mice. This mouse line

enabled us to perform both conditional ablation of Runx2 and genetic marking with Td-tomato in the Runx2-deficient cells simultaneously upon CRE expression driven by Sp7 activation. As Runx2 is genetically upstream of Sp7, Runx2 was transiently expressed in osteoblast progenitors, but was ablated at Sp7-positive stage in the Runx2-deficient cell lineage. We confirmed that skeletal formation was severely impaired in the conditional Runx2 homozygous-knockout mice (Runx2 cKO) at E18.5 as previously reported (Takarada T. et al., Development 143, 2016). We performed ATAC-seq with the Tdtomato positive cells purified from E18.5 Runx2 cKO calvaria. The assay revealed that chromatin accessibility was significantly decreased in 2,643 genomic regions in Runx2 cKO cells compared to the Runx2 heterozygous-knockout cells. Gene ontology analysis, de novo motif analysis and integrative analysis with a Runx2-DNA binding profile revealed that the Runx2-dependent accessible regions were primarily bound by Runx2 through a Runx consensus motif, and were highly associated with genes related to skeletal development. Next, to identify Runx2-mediated functional enhancers, we conducted a CROP-seq assay (Datlinger P. et al., Nat Methods 14, 2017). In this assay, multiplexed CRISPR-based enhancer knockout was combined with single-cell RNA-sequencing, giving both the genotype as guide RNA sequence and the phenotype as transcriptome at single-cell resolution. This assay identified a functional osteoblast enhancer called Enh-Ob. Reporter assays and EMSA confirmed that Runx2 transactivated the Enh-Ob through a Runx motif. Finally, a reporter transgenic assay and enhancer knockout study revealed that the Enh-Ob was specifically activated in skeletal tissues and was required for normal osteogenesis. Collectively, these results suggest that Runx2 is required for maintenance of chromatin accessibility at osteoblast cis-regulatory modules, which underlies osteoblast specification.

***Disclosures: Hironori Hojo**, None*

P-411

Aromatase Deficiency in Osteoblasts Causes Decrease Bone Mass Accrual in Young Mice *Amber Sherwood[1], Katie Rubitschung[1], Orhan K. Öz[1]. [1]UT Southwestern Medical Center Department of Radiology, United States

Estrogens have a regulatory role in bone metabolism. Peripheral estrogen synthesis is thought to be important in post-menopausal women and men. Using a novel transgenic mouse model, we evaluate changes in bone mineral density by DXA in young osteoblast specific aromatase knockout mice (ObArKO).The ObArKO model was generated using a conditional Cre recombinase driven by the Col1a1-2.3 promoter1 and a floxed Cyp19a1 Exon 2 allele. Homozygous floxed (Aromfl/fl) female mice were bred to hemizygous Col2.3-Cre Aromfl/fl males. Mice were maintained on a C57BL/6J background and fed a normal chow diet. DXA imaging was performed on male and female ObArKO and Aromfl/fl littermates at 4, 8, 12, and 16 weeks of age. Animal weight and nose-anal length were recorded at each time point. Upon sacrifice, gonads were characterized to assess ectopic Cre expression. There were at least n=8/group.Uterine weight and testicular weights were not different between groups. Nose-anal length and body fat % were comparable to controls. Significant decreases in whole body BMD were observed in female ObArKO mice at 4, 8, 12, and 16 weeks of age (p=0.014 or better). Spinal BMD was also significantly decreased in ObArKO females at 4 and 8 weeks, but was comparable to controls thereafter. ObArKO females showed decreased femoral BMD at 4, 8, 12, and 16 weeks (p=0.001, 0.0002, 0.002, and 0.120). ObArKO females displayed significantly abated body weight at 4, 8, and 12 weeks (p=0.016 or better). The differences were resolved at 16 weeks. Male ObArKO mice exhibited low whole body BMD only at 8 weeks of age (p=0.017). Spinal and femoral BMD was reduced at 4 weeks (p=0.014 and p=0.005) and 8 weeks (p=0.011 and p=0.010, respectively), although no differences were seen at 12 or 16 weeks. Nose-anal length was less in male ObArKO at 8 weeks (p=0.037). Body fat % was similar between groups.Here we present a reproductively sound mouse model to facilitate investigation into the role of osteoblast derived estrogen in bone metabolism. Male and female ObArKO mice demonstrated significant decreases in BMD compared to control littermates, suggesting that estrogen synthesized by osteoblasts is necessary for early bone mass accrual in mice. The normal % body fat and uterine weights are distinct from the global aromatase knockout. Underlying mechanisms of impaired bone mass accrual warrant further examination.1Liu F. et al. (2004). Int J Dev Biol. 48:645–653.

***Disclosures: Amber Sherwood**, None*

P-412

Overexpressing miR-125b in Osteoblasts Confers a Significant Survival Benefit in Mice with Bone Metastasis *Shohei Kohno[1], Nushrat Sarmin[1], Tomoko Minamizaki[1], Yuji Yoshiko[1]. [1]Department of Calcified Tissue Biology, Graduate School of Biomedical & health Sciences, Hiroshima University, Japan

We have previously shown that miRNAs encased in matrix vesicles (MVs) budding from osteoblasts accumulate in bone matrix. Of these, miR-125b inhibits osteoclast formation by downregulating its target Prdm1, a transcription repressor, resulting in increased expression of anti-osteoclastogenesis factors including MAFB and IRF8. Transgenic (Tg) mice overexpressing miR-125b by using human osteocalcin promoter exhibit high bone mass with a decreased number of osteoclasts. Taken together with the fact that miR-125b is known to act as a tumor suppressor, these results lead us to determine whether miR-125b as MV cargo abrogates osteolytic bone metastasis. First, we treated cancer cell lines (the human prostate cancer PC-3 and breast cancer MCF-7 and the murine mammary carcinoma Py8119) with mouse MVs, resulting in suppression of cancer cell proliferation, migration and invasion in vitro. These effects were mimicked by ectopic overexpression of miR-125b in cancer cells. To determine whether miR-125b as a MV cargo can suppress cancer metastasis in vivo, Py8119 cells tagged with luciferase (Py-Luc cells) were injected into wild-type (WT) and Tg mice via the caudal artery. In vivo imaging demonstrated that Luc activity was detected in femurs as early as 17 days post-injection (pi) and then spread across multiple sites in WT mice and only in femurs in Tg mice at 21 days pi. Micro-CT could detect bone loss in the proximal femurs as early as 10 days pi. Concomitant with these, less severe bone defects in the metastatic lesions were histologically proven in Tg vs WT mice. A large number of TRAP-positive multinuclear cells (osteoclasts) could be detected in the interface between bone and metastatic Py-Luc in both genotypes, and ROI analysis revealed that the number of osteoclasts in Tg mice was less than that in WT mice. To assess whether overexpression of miR-125b in osteoblasts show a significant survival benefit, Tg mice and WT mice injected with and without Py-Luc cells were grown under normal conditions. All WT mice received Py-Luc cells died by 28 days pi, while some of Tg mice with Py-Luc cells survived more than 40 days. In this study, we demonstrated that overexpression of miR-125b in osteoblasts suppress bone metastasis via its possible dual actions by inhibiting osteoclastogenesis and blocking cancer cell activities. Our findings may provide a potential therapeutic strategy for osteolytic bone metastasis.

***Disclosures: Shohei Kohno**, None*

P-413

Cell Trafficking and Regulation of Osteoblastogenesis by Extracellular Vesicle Intralumenal Bone Morphogenetic Protein-2 *Saigopalakrishna Yerneni[1], Juraj Adamik[2], Lee Weiss[3], Phil Campbell[1]. [1]Department of Biomedical Engineering, Carnegie Mellon University, United States, [2]Department of Hematology/Oncology, School of Medicine, University of Pittsburgh, United States, [3]The Robotics Institute, Carnegie Mellon University, United States

Extracellular vesicles (EVs), which are found in all body fluids as well as immobilized within the tissue extracellular matrix, contain a wide array of both surface-bound and intralumenal signaling cargo, including growth factors. Whereas EV surface-bound growth factors can directly access their receptors on target cell surfaces, the cell signaling mechanism(s) associated with intraluminal EV growth factor regulation of cell function remains unknown. To help gain insight into this mechanism, we investigated trafficking and regulation of osteoblastogenesis by bone morphogenetic protein-2 (BMP2), as a paradigm growth factor, loaded directly into the lumen of J774A.1-derived EVs (BMP2-EVs) using sonification or indirectly collected as an EV product of BMP2 recycling experiments with C2C12 cells. Bioactivity of BMP2-EVs was then assessed using C2C12 cell culture. ‘Free’ uncomplexed BMP2 was used as a control. Trafficking studies were performed using 125I-BMP2 or 125I-EVs. Both were readily internalized by C2C12 cells, with similar intracellular and cell surface-bound fractions of ~90% and ~10%, respectively. Recycling experiments to determine the fate of internalized BMP2 and EVs showed rapid externalization of both BMP2 and EVs in as little as 2 min, with an eventual release of 23-40% of internalized BMP2 or EVs by 30 min. Recycled BMP2 or EVs were minimally proteolytically degraded, with 10% of each being retained on the cell surface and 90% being released into the extracellular microenvironment. Approximately 65% of recycled BMP2 was associated with EVs, whereas ~75% of recycled EVs remained intact and capable of cell signaling. Based on gene and protein expression experiments, BMP2-EVs regulated osteoblastogenesis similarly to free BMP2. Finally, cell culture experiments with added noggin, an inhibitory BMP2 extracellular binding protein, demonstrated that BMP2-EVs could still regulate osteoblastogenesis via intracellular signaling since any recycled, extracellular free BMP2 did not play a significant role in inducing osteoblastic differentiation. Collectively, these experiments show that EV intraluminal BMP2 can bypass BMP2 cell surface receptors and deliver BMP2 directly into the intracellular compartment via EV internalization processes where BMP2 signaling is apparently initiated from within the cell. It also raises the question do other EV intralumenal growth factors utilize similar cell signaling processes?

***Disclosures: Saigopalakrishna Yerneni**, None*

P-414

Analysis of BMP2-dependent Gene Regulatory Network Revealed New Perspective of Klf4 as a Novel Transcription Factor Governing Osteoblast Differentiation *Shuaitong Yu[1], Huan Liu[1], Zhi Chen[1]. [1]School of Stomatology Wuhan University, China

Transcription factors turn on/off the expression of target genes, which, in turn, allow for changes in cell morphology or activities needed for cell fate determination and differentiation. BMP signaling have been widely regarded as one of the most important topics in vertebrate skeletal biology, of which BMP2 is a potent inducer governing osteoblast differentiation of bone marrow stromal cells (BMSCs). However, how BMP2 initiate its downstream transcription factor to determine differentiation direction remain largely unknown. Here, we used RNA-seq, ATAC-seq and animal models to illustrate BMP2-dependent gene regulatory network governing osteoblast lineage commitment. We firstly generated Bmp2f/fSp7-Cre mice (Bmp2-cKO). We did not observe any significant difference between Bmp2-cKO and their siblings in newborn mice. However, as early as 2 weeks of age, these mice were small in size compared with control. Micro-CT analyses revealed Bmp2-cKO mice exhibited decreased bone density. Histological analyses also found obvious defects in the number of osteoblasts. In vitro experiment showed BMSCs isolated from Bmp2-cKO mice exhibiting

impacted osteoblast differentiation. BMSCs were harvested from Bmp2f/f (Bmp2-WT) and Bmp2-cKO mice and induced with osteogenic medium for 7 days, which were then subjected to RNA-seq and ATAC-seq analysis to reveal BMP2-dependent gene regulatory network governing osteoblast differentiation. Combined with previous reported H3K27Ac ChIP-seq for osteoblast differentiation, we identified xxx chromatin regions of active enhancers were closed with the loss of BMP2 resulting the down-regulation of 2352 genes and up-regulation of 2231 genes. We further identified over 80% of these cis-regulatory elements were directly targeted by Runx2, Dlx5, Mef2c, Oasis and Klf4. We further chose Klf4 as a novel research target and also generated Klf4f/fSp7-Cre mice to investigate the role of KLF4 in osteoblast differentiation of mBMSCs. However, most of Klf4f/fSp7-Cre mice (Klf4-cKO) died after birth, Klf4f/+Sp7-Cre (Klf4-Het) survived to adulthood and exhibited smaller body size accompanied by defective incisors like Bmp2-cKO mice. In addition, histology and cytobiology analyses showed Klf4-Het had fewer osteoblasts and lower osteogenic ability. In conclusion, our current work outlined a comprehensive BMP2-dependent gene regulatory network in which Klf4 was a novel transcription factor specifically governing osteoblast differentiation of Sp7+ lineage.

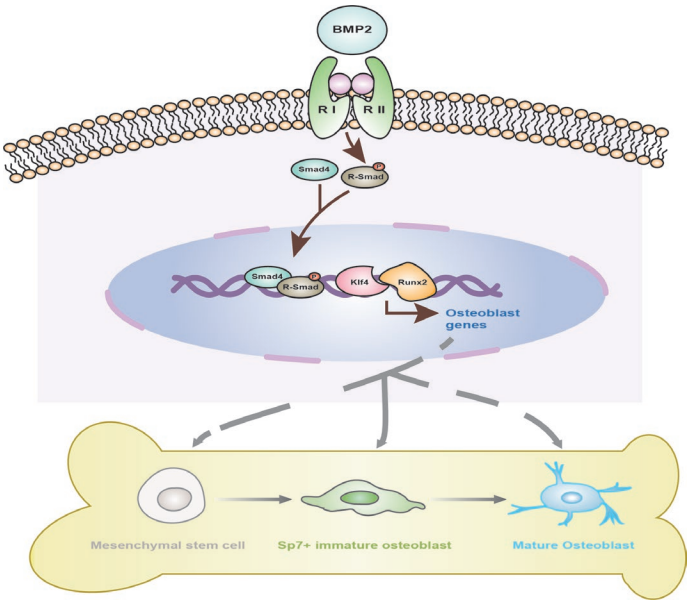

***Disclosures: Shuaitong Yu**, None*

P-415

MicroRNA-101, which Inhibits the Epigenetic Suppressor Ezh2, Increases Trabecular Bone Volume in Male Mice *Sofia Jerez[1], Amel Dudakovic[1], Janet Denbeigh[1], Padmini Deosthale[2], Christopher Paradise[1], Martina Gluscevic[1], Pengfei Zan[1], Oksana Pichurin[1], Farzaneh Khani[1], Roman Thaler[1], Lilian Plotkin[2], Andre van Wijnen[1]. [1]Mayo Clinic, United States, [2]Indiana University, United States

High-throughput microRNA sequencing was used to identify novel miRs that regulate osteoblast differentiation. We established that miR-101, which targets the epigenetic enzyme Ezh2, is highly up-regulated in differentiated MC3T3 cells (~7 fold) and robustly expressed in primary mouse calvarial osteoblasts. We have shown previously that loss of Ezh2 function enhances osteogenic differentiation in vitro and bone formation in vivo. Thus, we tested the attractive mechanistic model that increased miR-101 expression may suppress Ezh2 expression to stimulate osteogenesis and bone formation. Indeed, transient miR-101 over-expression suppresses Ezh2 protein levels and also reduces tri-methylation on lysine 27 of histone 3 (H3K27me3), a heterochromatic mark catalyzed by Ezh2. Importantly, over-expression of miR-101 stimulates osteogenic differentiation of MC3T3 cells as quantified by alizarin red staining. Therefore, we examined transgenic doxycycline-inducible miR-101 expressing mice that permit robust induction of miR-101 by an order of magnitude. Experimental control and mir-101 over-expressing mice were exposed to doxycycline during pregnancy and postnatal stages (phenotyping at 8 weeks) to maximize penetrance of skeletal phenotypes. Our analyses revealed that miR-overexpressing male mice are bigger as measured by total body weight and exhibit an increase in long bone length. These mice exhibit significant increases in trabecular bone volume fraction, trabecular number, trabecular thickness, as well as a reduction in trabecular spacing based on microCT analysis. Histomorphometric examination established a significant reduction in osteoid volume to bone volume and osteoid surface to bone surface. These findings suggest that the enhancement in trabecular bone may be due to accelerated bone mineralization in miR-101 over-expressing male mice. Remarkably, while female mice exhibit a significant increase in bone length, no significant changes were noted by microCT (trabecular bone parameters) and histomorphometry (osteoid parameters). We conclude that miR-101 upregulation during osteoblast maturation enhances trabecular bone parameters in male mice. Thus, miR-101 and Ezh2 may form part of an intricate epigenetic feed-forward mechanisms that controls bone formation.

***Disclosures: Sofia Jerez**, None*

P-416

Discoidin Domain Receptor 2 is a Novel Inducer of Bone Regeneration *Chunxi Ge[1], Abdulaziz Binrayes[1], Fatma Mohamed[2], Kenneth Kozloff[2], Renny Franceschi [2]. [1]University of Michigan, United States, [2]University of Michigan, United States

Bone loss caused by trauma, neoplasia, congenital defects or periodontal disease is a major cause of disability and human suffering. Skeletal progenitor/stem cell:extracellular matrix (ECM) interactions are critical for bone regeneration. This project will focus on discoidin domain receptor 2 (DDR2), an understudied, but important bone-associated collagen receptor. Ddr2 loss-of-function mutations in humans and mice cause severe craniofacial and skeletal defects. In this study, we examine the role of DDR2 in bone regeneration. Calvarial subcritical-size defects and tibial fractures were generated in Ddr2 deficient mice. For calvarial defects, complete bridging, seen in wild type (WT) mice at 4 weeks post-surgery, was not observed in Ddr2 deficient mice, which failed to heal defects even after 12 weeks. For tibial fractures, complete union was observed after 6 weeks in WT mice, but was severely reduced in Ddr2-deficient animals. This was manifested as significant reductions in callous volume and modified radiographic union scoring tibial fracture (mRUST) score. Ddr2 expression, measured by LacZ activity in Ddr2+/LacZ mice, was restricted to periosteal surfaces of uninjured calvarial bone and tibia. Within 2 days of injury, expression expanded into regeneration areas and continued throughout the healing process. Lentiviral mediated overexpression of DDR2 and shRNA knockdown of DDR2 were performed in a mesenchymal cell line (ST2 cells). We found that overexpression of DDR2 increased osteoblast differentiation while knockdown of DDR2 was inhibitory. Furthermore specific triple helical peptides containing DDR2 or b1 integrin binding regions of fibrillar collagens were synthesized and used to coat tissue culture surfaces. DDR2 peptide strongly stimulated osteoblast differentiation as measured by induction of mineralization and osteoblast marker mRNAs. b1 integrin peptide was also stimulatory, but to a lesser extent than the DDR2 peptide. Most interestingly, the combination of both peptides synergistically enhance osteoblast differentiation and activation of DDR2 and integrin signals. This study shows DDR2 is required for bone regeneration in surgically-induced bone defect models. Stimulation of DDR2 activity either by overexpression or activation with DDR2-binding peptides may provide novel strategies for bone regeneration.

***Disclosures: Chunxi Ge**, None*

P-417

Egr1 Regulates Prx1 Expression through CXCL12 Signaling in Fracture Repair *Alessandra Esposito[1], Mariana Lima-Miranda[2], Lily Yu[3], Anna Spagnoli[1]. [1]Rush University Medical Center, United States, [2]Rush University Medical Centerq, United States, [3]Rush University medical Center, United States

Studies, including from our laboratory, have reported that Paired Related Homeobox 1 (Prx1) regulates mesenchymal stromal cells differentiation and is postnatally expressed within the periosteum and endosteum. Our in vitro and in vivo studies have previously reported that Prx1 is a downstream target of CXCL12 signaling during BMP2-induced fracture healing, and a downregulation of Prx1 is required for osteoblast differentiation. However, little is known about the mechanism of such regulation. Notably, studies have been reported that Egr-1 (Early growth response gene 1) plays a key role in differentiation and angiogenesis and loss of Egr1 results in impaired endochondral bone repair. Here, we hypothesize that BMP2-CXCL12 axis regulates Prx1 expression during osteoblast differentiation through Egr1 expression in fracture. For in-vivo experiments, BMP2flox/flox mice were crossed with Prx1-Cre transgenic males to generate BMP2cKO/+ mice. For treatment with AMD3100, mice were i.p.-injected with 2.5 mg/g AMD3100-PBS solution twice per day, 2 days once prior to fracture and then 6 times beginning 2 days after fracture (day 2 through day 7) followed by harvest at 14 days postfracture (PFD). Tibias were dissected at 1, 3, 7, 10, 14, and 21 PFD and subjected to immunofluorescence (IF). For in vitro experiments, BMP2cKO/+ mice were crossed with BMP2flox/flox mice to produce BMP2cKo/cKO. Endosteal cells were isolated from the bone marrow of tibias and femurs of BMP2cKo/cKO. Osteoblastic differentiation was carried out using StemXVivo osteogenic base media and supplement. For in vitro AMD3100 treatment of confluent endosteal cells, beginning on day 7, 400 µM of AMD3100 dissolved in water was added to the cells every 3 days until day 14 when cells were harvested. To support our hypothesis, we found that mice haploinsufficient for BMP2 in Prx1 expressing cells (BMP2cKO/+), that have impaired fracture healing, have increased Egr1, as well as Prx1, mRNA levels and such increase positively correlated with increased levels of CXCL12. Furthermore, in WT fractured calluses Egr1 mRNA expression, as well as Prx1's, increased rapidly right after fracture and decline by day 21. Impaired fracture healing of BMP2cKO/+ mice was rescued when mice were systemically treated with AMD3100, an inhibitor of CXCL12 signaling, that led to a downregulation of CXCL12 and Prx1 mRNA expressions, as well as Egr1's. Isolated endosteal cells from BMP2cKO/cKO mice failed to differentiate into osteoblasts and showed increased Egr1 mRNA levels, as well as Prx1 and CXCL12; AMD3100 treatment restored osteogenic differentiation and normalized their mRNA expressions. Our findings unveil a novel role of Egr1 in regulating Prx1 expression

through CXCL12 signaling that is critical in fracture healing. Studies are in progress to further characterize the nature of such regulation.

***Disclosures: Alessandra Esposito**, None*

P-418

The effect of SNP rs2887571 (located in an estrogen receptor α binding site) on WNT5B function in bone *Sarocha Suthon[1], Gustavo A. Miranda-Carboni[1], Susan A. Krum[1]. [1]UTHSC, United States

Osteoporosis is a bone metabolic disease in which there is a loss of bone mineral density (BMD). WNTs, including WNT5A, promote osteogenesis; in contrast, WNT5B shows the opposite effect as high-throughput knockout of Wnt5b increased BMD in mice (Brommage et al., 2014). Expression levels of WNT5B continuously increase during osteogenesis (Kemp et al., 2014), suggesting that WNT5B has a role in osteoblasts. A GWAS revealed SNP rs2887571 is associated with lower BMD (Estrada et al., 2012). This SNP showed overlap with an estrogen receptor alpha (ERα) binding site from ChIP-sequencing (Krum et al., 2008) and is located 45 kilobases upstream of WNT5B. However, the relationship between SNP rs2887571 and WNT5B is unclear, as is the function of WNT5B in bone. We hypothesize that SNP rs2887571 alters ERα binding to suppresses level of WNT5B which inhibits osteogenesis. 110 samples of human osteoblasts (hOBs) were genotyped for SNP rs2887571 and compared to the expression of nearby genes (WNT5B, ERC1 and FBXL14). The correlation between genotypes and gene expression was plotted and homozygous AA had significantly higher expression than homozygous GG for only WNT5B. 10 nM E2 decreased mRNA and protein expression of WNT5B in hOBs, human osteosarcoma U2OS-ERα cells and mouse osteoblasts (mOBs), as well as ovariectomized mice showed higher WNT5B levels compared to sham operated mice by IHC. ERα directly represses WNT5B, as ERα bound at SNP rs2887571 and H3K27 was tri-methylated when treated with E2 in U2OS-ERα cells. Therefore, a decreased amount of WNT5B due to the GG allele or decreased E2 is correlated with lower BMD. Mechanistically, WNT5B functions through a β-catenin-independent signaling pathway by activating phospho-JNK and repressing β-catenin. Mouse mesenchymal stem cells were treated with 50 ng/mL recombinant mouse WNT5B and showed that WNT5B increased proliferation and adipogenesis, while it inhibited osteogenesis. Although WNT5B did not affect proliferation and migration in pre-osteoblasts, WNT5B inhibited osteoblast differentiation and mineralization by suppressing levels of Alpl and Bglap (osteocalcin) expression. WNT5B also suppressed E2-induced osteoblast differentiation in mOBs and U2OS-ERα cells by recruiting SIN3A, which is part of the histone deacetylase complex, to ALPL enhancers. Taken together, this data reveal the mechanistic functions of SNP rs2887571 and WNT5B on bone mineral density.

***Disclosures: Sarocha Suthon**, None*

P-419

Irisin Downregulates the Senescent Marker p21 in Osteoblasts in vitro and its Serum Levels Positively Correlates with a Lower Rate of Age-Related Osteoporosis *Graziana Colaianni[1], Lorenzo Sanesi[1], Angela Notarnicola[2], Monica Celi[3], Roberta Zerlotin[1], Giuseppina Storlino[1], Patrizia Pignataro[2], Mariella Errede[2], Vito Pesce[2], Umberto Tarantino[3], Biagio Moretti[2], Maria Grano[1]. [1]Department of Emergency and Organ Transplantation,University of Bari, Italy, [2]Department of Basic Medical Sciences, Neuroscience and Sense Organs, University of Bari, Italy, [3]Department of Orthopedics and Traumatology, Tor Vergata University of Rome, Italy

Irisin is a myokine produced by skeletal muscle during exercise in both mice and humans. We previously showed that Irisin treatment ameliorates disuse-induced osteoporosis and muscular atrophy in mice. Data in humans showed a positive association between Irisin and bone mineral density in athletes and a population of healthy children. However, the role of this myokine regarding the state of muscle and bone in the same population remained to be determined.For this purpose, 62 patients (age 68.71+/- 12.31 years) undergoing total hip or knee replacement were recruited. Our results showed that irisin serum levels negatively correlated with age ($r=-0.515$; $p<0.001$) and positively correlated with femoral bone mineral density (BMD) ($r=0.619$; $p<0.001$) and vertebral BMD ($r=0.201$; $p<0.001$). Irisin was also positively associated with Fndc5 mRNA in muscle biopsies ($r=0.248$; $p<0.01$), as well as with Osteocalcin (Ocn) mRNA in bone biopsies ($r=0.708$; $p<0.001$). In skeletal muscle, FNDC5 positive fibers positively correlate with BMD of the total femur ($r=0.765$; $p<0.001$) and BMD of the femoral neck ($r=0.575$; $p<0.05$). Interestingly, by analyzing patients divided by their T score, we found lower irisin levels ($p<0.01$) in patients with osteopenia/osteoporosis (OP) compared to healthy controls matched for age and sex. By analyzing the senescence marker p21, we found a significant increase in its mRNA expression in the bone biopsies of OP patients compared to control ones. Therefore, we investigated in vitro whether rec-irisin had a direct effect on this senescence marker, showing that p21 mRNA expression was significantly down-regulated in osteoblasts by the treatment with irisin.Overall, these results indicate that higher irisin levels are associated with a lower rate of age-related osteoporosis and that irisin could be effective in delaying the osteoblast aging process, suggesting a potential senolytic action of this myokine.

***Disclosures: Graziana Colaianni**, None*

P-420

Dio3os influences neighboring Dio3 gene expression and in trans regulates osteoblastogenesis *QUAMARUL HASSAN[1], Yuechuan Chen[2], Benjamin Wildman[1], Delores Stacks[1], Mohammad Rehan[1]. [1]School of Dentistry, University of Alabama, United States, [2]School of Dentistry, University of Alabama, Birmingham AL, United States

LncRNAs are classified as a unique class of long RNA transcripts, lack of translational potential, and influence the chromatin state of protein-coding genes. A few of these lncRNAs have been shown to regulate osteoblastogenesis. In the current research we have studied lncRNA Dio3os to decipher a molecular regulation that is unique for thyroid hormone metabolism and osteogenesis. Human LncRNA library was screened with murine osteoblast cDNA to identify unique lncRNAs specific for bone formation. CRISPR-Cas9/dCAS9-CRAB technologies were used to knock-out exons and suppress expression. ChIP and promoter activity assays were used to study the transcriptional status of the chromatin state. RNA-IP was used to study lncRNA-protein interactions. We uncovered a novel lncRNA named Dio3os in the proximity of iodothyronine deiodinase 3 (Dio3) gene and its expression is significantly decreased during osteoblast differentiation. The bi-directional Dio3 promoter initiates transcription of Dio3os in opposite direction. T4 and Vitamin D significantly activate Dio3/Dio3os bidirectional promoter activity. ChIP and promoter activity assays indicated HIF1a and HDAC1 directly binds and induced, however RUNX2, BRG1 repressed both Dio3 and Dio3os transcription. Dio3os overexpression activates neighboring Dio3 expression, while inhibits osteoblast progression and maturation in trans. Transcriptional repression of Dio3os by dCAS9-KRAB negatively regulates the expression of immediate neighbor Dio3 gene while increased osteogenesis. CRISPR Knockdown of Dio3os exons 1, 2 and 3 decreased Dio3 however increased osteoblast gene expression to support osteoblast differentiation. Taken together, these findings directly suggest that the local control of Dio3 chromatin state by lncRNA Dio3os linked to T4 inactivation which results in inhibition osteoblast differentiation.

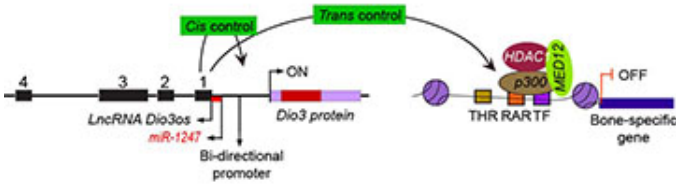

***Disclosures: QUAMARUL HASSAN**, None*

P-421

miR-199a-5p located at the Osteoporosis GWAS Implicated DNM3 Loci Regulates Human Osteoblast Differentiation *Yadav Wagley[1], Alessandra Chesi[2], Matthew E. Johnson[2], Solomon Chang[1], James A. Pippin[2], Andrew D. Wells[2], Struan F. A. Grant[2], Kurt D. Hankenson[1]. [1]University of Michigan, United States, [2]Children's Hospital of Philadelphia, United States

By intersecting genome-wide promoter focused Capture C and ATAC-seq data derived from differentiating human osteoblasts, we recently reported consistent contacts between multiple candidate causal variants underpinning GWAS-implicated BMD loci and putative target effector gene promoters. Functional assays using siRNA knockdown led to identification of ING3 (at the 'CPED-WNT16' locus) and EPDR1 (at the 'STARD3NL' locus) as effector genes during human osteoblastogenesis. Here, we explored the 'DNM3' locus which harbors DNM3OS and the embedded MIR199A2 as candidate target genes. Bone morphogenetic protein-2 (BMP2) stimulation of human mesenchymal stem cells (hMSCs) reduced DNM3OS and corresponding MIR199A2 expression in a time-dependent fashion. Of the two mature microRNAs, miR-199a-5p and miR-199a-3p, both of which are expressed from MIR199A2, we elected to focus on the miR-199a-5p in this study. As observed with the MIR199A2 precursor, significant reduction of the mature miR-199a-5p was observed after 24 hours of BMP2 stimulation in hMSCs, suggesting that its downregulation coincides with osteoblast commitment. hsa-miR-199a-5p mimetic was introduced into hMSCs and cells were stimulated with BMP2. Interestingly, cells overexpressing miR-199a-5p mimetic revealed a unique morphological change, along with failure to efficiently undergo mineralization despite having no effect on ALPL expression compared to control cells. Immunoblot analysis revealed that miR-199a-5p mimetic overexpressing cells had higher levels of the osteoblastic transcription factor RUNX2 after BMP2 stimulation, whilst Osterix protein levels did not significantly differ from the control cells. Given the morphological change observed after miR-199a-5p mimetic overexpression, we hypothesized that the mimetic was inducing differentiation to a chondrogenic fate. Expression levels of ACAN, COMP and COL10A1 were significantly higher in cells overexpressing the microRNA mimetic, with further increases following BMP2 stimulation. Additionally, in control cells, the levels of chondrocyte specific transcription factor SOX9 was transiently upregulated in response to BMP2 and returned to baseline within 72 hours; however, in contrast, SOX9 protein levels remained elevated in cells overexpressing miR-199a-5p. Since BMP signaling intersects with the Notch pathway to induce hMSC osteoblast differentiation and SOX9 harbors an antagonistic relation with the Notch pathway, we examined whether Notch processing is altered after miR-

199a-5p mimetic overexpression. As suspected, Notch processing was reduced upon BMP2 stimulation of miR-199a-5p mimetic overexpressing cells. Exposing miR-199a-5p mimetic overexpressing cells to immobilized Jagged1 rescued the mineralization defect within 10 days. Taken together, while miR-199a-5p impedes BMP-induced osteoblast differentiation, promoting a chondrogenic fate over osteoblastogenesis, Notch signaling bypasses the miR-199a-5 inhibition of osteoblast differentiation.

***Disclosures: Yadav Wagley**, None*

P-422

Identification of Molecular Players in Phosphate-Induced Signaling Cascade Initiating the Mineralization Process. *Dobrawa Napierala[1], Sana Khalid[1], Mairobys Socorro[1], Juan Taboas[1]. [1]University of Pittsburgh School of Dental Medicine, United States

Phosphate (Pi) is a signaling molecule that supports osteogenic differentiation of skeletal and dental progenitor cells and stimulates formation of mineralized extracellular matrix (ECM) by differentiated cells. The importance of Pi for the development and homeostasis of all mineralizing tissues is underscored by bone, cartilage, dentin and periodontal complex pathologies in genetic and acquired disorders affecting Pi availability. However little is known about Pi-induced signaling cascade in cells producing mineralizing ECM, and the key players, such as Pi receptors/sensors, kinases transmitting the Pi signal inside the cell and transcription factors regulating gene expression in response to Pi are largely unknown. The goal of our research is to delineate the signaling cascade that initiates mineralization in response to extracellular Pi. 17IIA11 and MLO-A5 committed osteogenic cell lines were used as two different models of cells supporting mineralization. Activation and inhibition of specific molecules was accomplished either by genetic modification of model cells or pharmacologically. Using ChIP assay, we detected that Pi changes binding of the mineralization-regulating transcription factor Trps1 to its target regulatory elements. On the other hand, Trps1 deficiency results in loss of activation of extracellular signal-regulated kinase Erk1/2 in response to Pi. Gene expression analyses detected significantly decreased expression of parathyroid hormone/ parathyroid hormone related protein receptor1 (Pth1r) in Trps1-deficient 17IIA11 cells. Furthermore, the depletion of Pth1r from either 17IIA11 or MLO-A5 cells was sufficient to abolish activation of Erk1/2 and expression of classic Pi-responsive genes Dmp1 and Spp1 (Opn). Analyses of signaling cascades downstream of Pth1r identified phospholipase C (PLC) and protein kinase C (PKC) as mediators of Pi signaling in osteogenic cells. In conclusion, we identified Pth1r/PLC/PKC signaling pathway and the Trps1 transcription factor as new players in the Pi-induced signaling cascade in cells producing mineralized ECM.

***Disclosures: Dobrawa Napierala**, None*

P-423

Zinc Finger Homeobox 3 (ZFHX3) Transcription Factor is a Novel Negative Regulator of Osteoblast Differentiation *Gustavo Gomez[1], Weirong Xing [1], Sheila Pourteymoor[1], Jasmine Lau[1], Subburaman Mohan[1]. [1]VALLHS, United States

Bone formation is the fundamental process of skeletal development in vertebrates that is strictly regulated by a complex transcriptional network which is incompletely understood. Based on the established importance of homeobox transcription factors in bone formation, we tested a role for a zinc finger homeobox (Zfhx) protein about which nothing is known. Zfhx3, also known as AT motif binding factor 1 (ATBF1), was originally identified as a tumor suppressor as loss of heterozygosity at Zfhx3 locus frequently occurs in gastric cancer. By immunohistochemistry, we found that Zfhx3 was predominantly expressed in Osterix (Osx) expressing chondrocytes and osteoblasts at the primary and secondary spongiosa of long bones of mice. In vitro studies revealed that Zfhx3 is highly expressed in pre-osteoblasts and that its expression remained unchanged during ascorbic acid-induced osteoblast differentiation, as measured by real time RT-PCR. To evaluate the role of Zfhx3, we overexpressed PCDNA 3.1 vector containing the full length cDNA clone of human Zfhx3 or GFP control by electroporation in MC3T3-E1 osteoblasts and confirmed nearly 100-fold overexpression by real time PCR using primers that are specific to human Zfhx3. Overexpression of Zfhx3 caused a two-fold increase in cell proliferation (P<0.001) vs PCDNA 3.1-GFP control. In contrast, expression levels of osteoblast differentiation markers, ALP and BSP were decreased by 70% and 65% (both P<0.01) respectively, compared to GFP control. To determine the mechanism for negative effect of Zfhx3 on osteoblast differentiation, we measured expression levels of Runx2, Osx, β-catenin, Dlx3, Dlx5 and Dlx6 by real RT-PCR in Zfhx3 overexpressing and GFP control MC3T3-E1 cells. We found that while expression of Osx and Dlx5 were reduced by 37% and 17% (both P<0.05) respectively, expression levels of other transcription factors were not affected by Zfhx3 overexpression. Based on these data, we propose that ZFHX3 is a negative regulator of osteoblast differentiation that mediates its effects in part via regulating Osx expression.

***Disclosures: Gustavo Gomez**, None*

P-424

Functional evidence of bone regulation of WNT16 through upstream enhancers within CPED1 *Núria Martínez-Gil[1], Neus Roca-Ayats[1], Carlos Herrera[1], Nicola Gritti[2], Nerea Ugartondo[1], Natàlia Garcia-Giralt[3], Diana Ovejero[3], Xavier Nogués[3], Jordi Garcia-Fernandez[1], Daniel Grinberg[1], Susanna Balcells[1]. [1]Department of Genetics, Microbiology and Statistics, Faculty of Biology, Universitat de Barcelona, CIBERER, IBUB, IRSJD, Barcelona, Spain., Spain, [2]European Molecular Biology Laboratory (EMBL) Barcelona, 08003 Barcelona,Spain, Spain, [3]Musculoskeletal Research Group, IMIM (Hospital del Mar Medical Research Institute), Centro de Investigación Biomédica en Red en Fragilidad y Envejecimiento Saludable (CIBERFES), ISCIII, Barcelona, Spain, Spain

WNT16 stands up as an essential gene of bone homeostasis due to its role in regulation of cortical bone and its consistency as a bone mineral density (BMD) GWAS signal. Here, we present new evidences through in vitro functional experiments, of two WNT16 variants: a common CT insertion (rs142005327) associated with BMD and a rare variant (rs190011371) found only in three women of the BARCOS cohort (n = 1490), all three with BMD below the 50th percentile (Martínez-Gil, N. et al. Sci Rep. 8:10951, 2018). The rs142005327 variant is located in a proximal region of intron 2 containing chromatin enhancer/promoter marks in osteoblasts (ENCODE). Through a 4C chromatin conformation analysis in 3 bone cell lines (Saos2, hFOB and MSC), we identified physical interactions between this intron 2 region and several putative regulatory regions within the CPED1 gene known to be active in osteoblasts (Genehancer database; Maynard RD et al. Gene 674:127-133, 2018). Moreover, luciferase assays indicated that a region close to the variant exhibited promoter activity in Saos2 cells (See figure 1). Analysis of previously published RNA-seq data from hFOB cells showed expression of a region located downstream of this promoter, which would be a novel transcript of the gene. Regarding the 3'UTR-variant rs190011371, by means of a reporter assay we described the partial loss-of-function for the minor allele, which is in agreement with the low BMD phenotype of the carriers of the rare variant. Our results confirm the role of WNT16 in BMD determination and suggest a novel regulatory mechanism of WNT16 in bone, mediated by physical interaction with various enhancer regions within CPED1.Figure 1. Relative luciferase activity of different intron 2 fragments cloned into the pGL3-basic vector: PFull, Pins, P1, P2, Pvar, Pcons, Ppic. For reference, the structure of WNT16 exon2, intron 2 and exon 3 is depicted, above the graph where the asterisk marks the position of SNP rs142005327. Values are normalized to the activity of the empty vector, arbitrarily set at 1. ****p<0.0001 and ***p<0.001. Error bars indicate s.d.

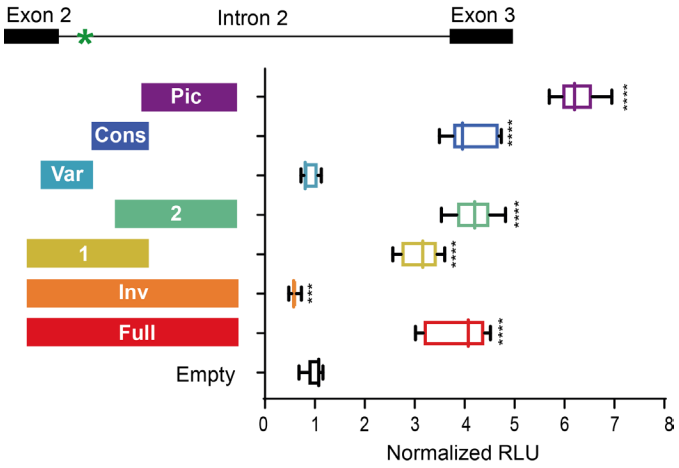

***Disclosures: Núria Martínez-Gil**, None*

P-425

The evaluation of bone union activity of freeze-dried platelet-rich plasma *Hideyuki Kinoshita[1], Sumihisa Orita[1], Kazuhide Inage[1], Yasuhiro Shiga[1], Seiji Ohtori[1]. [1]Department of Orthopaedic Surgery, Graduate School of Medicine, Chiba University, Japan

Fresh platelet-rich plasma (PRP) accelerates bone union in rat model. However, fresh PRP has a short half-life. We suggested freeze-dried PRP (FD-PRP) prepared in advance and investigated its efficacy in vivo. Spinal posterolateral fusion was performed on 8-week-old male Sprague-Dawley rats divided into six groups based on the graft materials (n = 10 per group): sham control, artificial bone (A hydroxyapatite–collagen composite) –alone, autologous bone, artificial bone + fresh-PRP, artificial bone + FD-PRP preserved 8 weeks, and artificial bone + human recombinant bone morphogenetic protein 2 (BMP) as a positive control. At 4 and 8 weeks after the surgery, we investigated their bone union–related characteristics including amount of bone formation, histological characteristics of trabecular bone at remodeling site, and biomechanical strength on 3-point bending. Comparable radiological

bone union was confirmed at 4 weeks after surgery in 80% of the FD-PRP groups, which was earlier than in other groups ($p < 0.05$). Histologically, the trabecular bone had thinner and more branches in the FD-PRP. Moreover, the biomechanical strength was comparable to that of autologous bone. FD-PRP accelerated bone union at a rate comparable to that of fresh-PRP and BMP by remodeling the bone with thinner, more tangled, and rigid trabecular bone. Next, we evaluated the pharmacological activity of growth factors (GFs) in FD-PRP in vitro after storage for four weeks. The platelet counts in both the fresh-PRP and FD-PRP samples were approximately 10-fold higher than those in peripheral blood samples. The phosphorylation and activation of platelet-derived growth factor (PDGF) receptor and extracellular signal-regulated kinase (ERK) were evenly induced by fresh-PRP and FD-PRP stimulation. Both fresh-PRP and FD-PRP significantly induced osteoblast proliferation in MTT cell viability assays. Furthermore, osteoblast PDGF receptor knockdown attenuated the downstream ERK activation by fresh PRP and FD-PRP. In conclusion, we demonstrated that FD-PRP promoted bone union in vitro and in vivo. If FD-PRP is clinically applicable, it could be used to promote bone fusion in bone fracture surgery and induce interbody fusion with the appropriate scaffold in spine surgery without intraoperative blood collection.

***Disclosures: Hideyuki Kinoshita**, None*

P-426

Agrin drives osteoblast differentiation through Wnt and BMP signaling modulation *Alann Thaffarell Portilho de Souza[1], Fabiola Singaretti de Oliveira[2], Denise Weffort[2], Helena Bacha Lopes[2], Gileade Pereira Freitas[2], Maria Paula Oliveira Gomes[2], Roger Rodrigo Fernandes[2], Adalberto Luiz Rosa[2], Marcio Mateus Beloti[2]. [1]Bone Research Lab, School of Dentistry of Ribeirao Preto, University of Sao Paulo / Baron-Gori Lab, Department of Oral Medicine, Infection and Immunity, Harvard School of Dental Medicine, Brazil, [2]Bone Research Lab, School of Dentistry of Ribeirao Preto, University of Sao Paulo, Brazil

The extracellular matrix protein Agrin has been detected in chondrocytes and endosteal osteoblasts but its function in osteoblast differentiation has not been investigated yet. Thus, we hypothesized that Agrin regulates osteoblast differentiation and, due to Agrin and wingless-related integration site (Wnt) sharing the same receptor, transmembrane low-density lipoprotein receptor–related protein 4 (Lrp4), and the crosstalk between Wnt and bone morphogenetic protein (BMP) signaling, both pathways could be involved in this regulation. To show if and how the expression of Agrin occurs during osteoblast differentiation, the temporal gene expression of Agrin and osteocalcin (Oc) as well as of Agrin receptors Lrp4 and α-dystroglycan (Dag1) was evaluated by real-time PCR in mouse pre-osteoblastic cell line MC3T3-E1 subclone 14, mouse osteoblasts differentiated from bone marrow-derived mesenchymal stromal cells and mouse calvarial-derived osteoblasts, cultured under osteogenic conditions. Moreover, protein expression of AGRIN was detected by immunofluorescence labeling. To determine the influence of Agrin on osteoblast differentiation, Agrin was knocked down in MC3T3-E1 cells by transfection with small interfering RNA (siRNA). Then, the Agrin silencing effects were evaluated on gene expression of Agrin receptors and the bone markers runt-related transcription factor 2 (Runx2), osterix, alkaline phosphatase (Alp), bone sialoprotein, Oc and α-1 type I collagen, as well as on protein expression of RUNX2 and ALP activity. In addition, genes related to Wnt and BMP signaling pathways were evaluated in order to explore the possible mechanisms involved in the Agrin-mediated osteoblast differentiation. We have shown that Agrin and its receptors Lrp4 and Dag1 are expressed during osteoblast differentiation in the three well-established cell culture models. Moreover, the disruption of Agrin by siRNA impaired the expression of its receptors and inhibited osteoblast differentiation evidenced by the downregulation of the bone markers RUNX2 and ALP activity. Furthermore, Agrin knockdown also downregulated the expression of genes related to Wnt and BMP signaling pathways. In conclusion, our data uncover the role of Agrin in regulating osteoblast differentiation and suggest that an Agrin-Wnt-BMP circuit is involved in this process. These findings make Agrin a candidate as a target for developing new therapeutic strategies to treat bone-related diseases and injuries.

***Disclosures: Alann Thaffarell Portilho de Souza**, None*

P-427

In Vitro Bone Tissue Model in a Well Plate Capture Molecular Regulation of Bone Remodeling *Yongkuk Park[1], Jungwoo Lee[1]. [1]University of Massachusetts Amherst, United States

Bone is dynamic tissue undergoes repeated bone remodeling for the maintenance of bone integrity throughout the lifetime, which include bone-forming osteoblasts and bone-resorbing osteoclasts. This process is under the regulation of local growth factors and cytokines by interaction between bone cells. However, one of the main limitations is difficult to study the detailed mechanism of molecular and cellular process of bone remodeling due to anatomical inaccessibility of the inner bone surface. It is necessary to develop relevant experimental model for in vitro bone biology study. Here, we report a new class of in vitro bone tissue model using a demineralized bone slice that retains intrinsic complexity of bony extracellular matrix with semi-optical transparency. We devised sequential method to fabricate (10-20 μm) sectioned demineralized bone matrix from a bovine femur. The bone pieces in 1.2 M hydrochloric acid were located in the hydrostatic pressure chamber at 4-bar to accelerate the demineralization step. Next, a demineralized bone block was cryosectioned and tailored in a circular shaped to be fit in multi-well plates. Primary osteogenic progenitors and marrow hematopoietic cells were retrieved from transgenic DsRed and eGFP mice. Demineralized bone slice directed osteoblasts to develop structurally mineralized bone tissue and subsequently acquire a resting state bone lining cell phenotype with gap junction. Vitamin D3 and prostaglandin E2 stimulation reverted lining cells to activated osteoblasts, which can induce differentiation of bone marrow mononuclear cells into mature osteoclasts. The functions of bone cells on the bone slice were confirmed by the real-time imaging and enzyme immunoassay. Finally, we created tissue-inspired trabecular bone model in a well plate by co-layering stimulated and resting bone tissue surface together, reproducing cellular connection and communication between osteoblast and osteoclast. We envision that the established bone tissue model will facilitate to pursue a better understanding in bone remodeling biology with high experimental control and access.

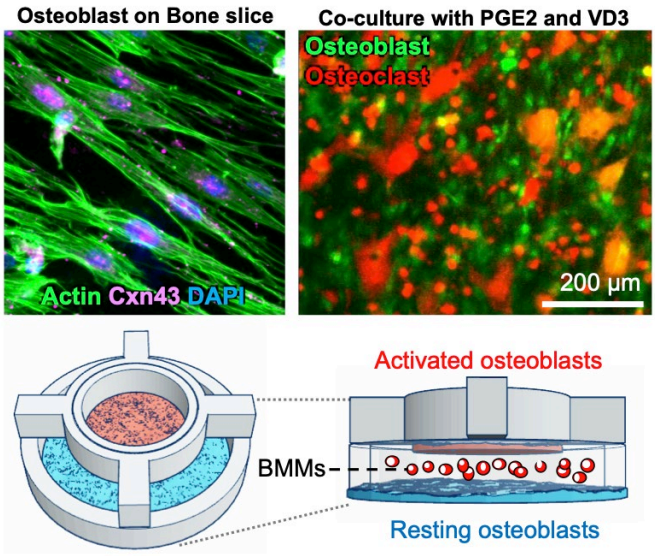

***Disclosures: Yongkuk Park**, None*

P-428

Dullard/Ctdnep1 negatively regulates Smad2/3 protein level and TGF-β signaling in osteoblastic cells. *Iori Nozawa[1], Yasuhiro Arasaki[1], Takuro Akiya[1], Masafumi Inui[2], Masaki Noda[3], Yoichi Ezura[4], Tadayoshi Hayata[1]. [1]Department of Molecular Pharmacology, Graduate School of Pharmaceutical Sciences and Faculty of Pharmaceutical Sciences, Tokyo University of Science, Japan, [2]Laboratory of Animal Regeneration Systemology, Department of Life Sciences, School of Agriculture, Meiji University, Japan, [3]Department of Molecular Pharmacology, Medical Research Institute, Tokyo Medical & Dental University (TMDU), Japan, [4]Department of Judo Therapy, Faculty of Medical Technology, Teikyo University, Japan

Transforming growth factor-β (TGF-β) is a pivotal cytokine that controls behavior and fate of many different types of cells. In early skeletal development, TGF-β signaling is required for sternum formation, perichondrium development, and joint morphogenesis. Importantly, TGF-β signaling is suppressed or terminated by various phosphatases and ubiquitin ligases after the onset of TGF-β signaling. We previously showed that the phosphatase Dullard (Ctdnep1) is an important negative regulator of TGF-β signaling during endochondral ossification. However, the role of Dullard in the regulation of TGF-β signaling during osteoblast differentiation remains elusive. In this study, we wished to study relationship between Dullard and TGF-β signaling using osteoblastic MC3T3-E1 cells and HEK293T cells as model systems. Western blot analysis showed that siRNA-mediated knockdown of Dullard mRNA resulted in increased Smad2/3 protein level in MC3T3-E1 cells, whereas overexpression of Dullard reduced Smad2/3 protein level. To examine whether Dullard physically interact with the components of TGF-β signaling pathway, we conducted co-immunoprecipitation assay using HEK293T cells. However, interaction of Dullard with Smad2, SMAD4 and TGF-βRII was not detected. Overexpression of Dullard suppressed TGF-β-responsive (CAGA)12-luciferase reporter activity induced by TGF-β1 treatment, whereas Dullard knockdown upregulated the reporter activity in MC3T3-E1 cells. Regarding osteoblast differentiation, Dullard knockdown impaired osteoblast differentiation as revealed by the alkaline phosphatase and mineralization assay. These data suggest that Dullard/Ctdnep1 negatively regulates TGF-β signaling pathway, at least in part, by downregulating Smad2/3 protein level and is required for osteoblast differentiation.

***Disclosures: Iori Nozawa**, None*

P-429

NMUR1 is not required for Neuromedin U (NMU)-mediated regulation of bone remodeling *Kelli Jestes[1], Tara Zukosky[2], Maria Squire[2], Julia Hum[1], Corinne Metzger[3], Matthew Allen[3], Jonathan Lowery[1]. [1]Marian University, United States, [2]University of Scranton, United States, [3]Indiana University School of Medicine, United States

Neuromedin-U (NMU) is an evolutionarily conserved peptide that regulates varying physiologic effects including blood pressure, stress and allergic responses, metabolic and feeding behavior, pain perception, neuroendocrine functions. Recently, several lines of investigation implicate NMU in regulating bone remodeling. For instance, global loss of NMU expression in male and female mice leads to high bone mass due to elevated bone formation rate with no alteration in bone resorption rate or observable patterning defect. Additionally, NMU treatment reduces osteoblastic differentiation of bone marrow stromal cells in vitro. Taken together, these findings suggest that targeting the NMU pathway may be a beneficial strategy for increasing bone mass. It is unclear at present, however, which receptor is utilized by NMU to mediate bone-specific effects as it signals via two G-protein-coupled receptors (GPCRs), NMU Receptor 1 (NMUR1) and NMU Receptor 2 (NMUR2), and both are expressed in the postnatal skeleton. Here, we tested the hypothesis that NMUR1 is required for the NMU-mediated regulation of bone remodeling by examining bone mass in global Nmur1 mutant mice. These results reveal that bone mass in femora and tibiae of twelve-week-old male Nmur1 mutants is unchanged compared to controls with no defects observed in osteoblast or osteoclast-related histological parameters. These results suggest that 1) the effects of NMU on bone remodeling in vivo are accomplished via NMUR2 or 2) the absence of NMUR1 is compensated by NMUR2. Future studies are required to distinguish between these possibilities and determine the downstream pathway utilized by NMU to regulate bone remodeling in vivo.

***Disclosures: Kelli Jestes**, None*

P-430

METTL7A Promotes Cell Survival and Enhances Osteogenic Differentiation *Eugene Lee[1], Juyoung Kim[1], Tae-kyung Kim[1], Gun-Il Im[1]. [1]Dongguk University, Republic of Korea

In transplanting adult stem cells for the treatment of bone disease, in the case of extensive loss of damaged blood vessels, the expected effect is not obtained because the transplanted cells do not receive blood supply and are mostly necrotic in the early stage of transplantation. To increase the effectiveness of stem cell transplantation, the survival of transplanted stem cells must be considered, and the problem found consistently in many studies is that the most of transplanted cells are hypoxic, inflammatory, oxidative stress, and no glucose is supplied. Cells are exposed to these environments, fail to engraft in the early stage, die at least 90% in the early stage, and disappear. To date, little is known about cell survival in the clinical microenvironment that occurs during bone healing. This study suggests that glucose can be the key factor to stem cell survival and bone differentiation. To support this, an in vitro mimics was created in which the microenvironmental stress of glucose deficiency, which cells may be exposed to during transplantation, was previously regulated. Furthermore, the METTL7A gene, bone regeneration marker, has been newly discovered by genetic analysis of the model. In this study, bone marrow stem cells induced by overexpression of the METTL7A gene were applied to a bone-deficient animal model, and the problem of early necrosis of stem cell transplantation could be alleviated by regulation of methylation. Finally, this study is the first study revealing the association and mechanism of METTL7A gene and bone regeneration signaling pathway, and confirmed the potential as a new model for improving cell survival and bone differentiation in stem cell transplantation therapy.

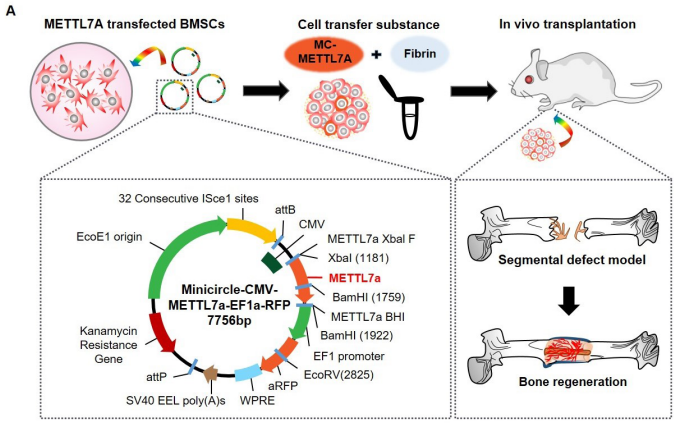

***Disclosures: Eugene Lee**, None*

P-431

Effects of mesenchymal stromal cells from healthy rats on the impaired osteoblast differentiation of mesenchymal stromal cells from osteoporotic and diabetic rats *Alann Thaffarell Portilho de Souza[1], Gileade Pereira Freitas[2], Helena Bacha Lopes[2], Denise Weffort[2], Fabiola Singaretti de Oliveira[2], Letícia Faustino Adolpho[2], Márcio Mateus Beloti[2], Adalberto Luiz Rosa[2]. [1]Bone Research Lab, School of Dentistry of Ribeirao Preto, University of Sao Paulo / Baron-Gori Lab, Department of Oral Medicine, Infection and Immunity, Harvard School of Dental Medicine, Brazil, [2]Bone Research Lab, School of Dentistry of Ribeirao Preto, University of Sao Paulo, Brazil

Osteoporosis and diabetes mellitus are systemic diseases that impaired osteoblast differentiation of mesenchymal stromal cells (MSCs). Considering the cell therapy applications to treat bone defects under osteoporotic and diabetic conditions, where MSCs from healthy donors (HE-MSCs) interact with MSCs from osteoporotic (ORX-MSCs) and diabetic (DM-MSCs) receptors, we hypothesized that HE-MSCs would counteract the deleterious effects of these diseases on the ability of ORX-MSCs and DM-MSCs to differentiate into osteoblasts. Thus, the aim of this study was to evaluate the influence of HE-MSCs on the osteoblast differentiation of both ORX-MSCs and DM-MSCs, using an indirect co-culture model. Osteoporosis and diabetes mellitus were induced in rats by orchiectomy surgery and streptozotocin injection, respectively. Then, MSCs were isolated and cultured from bone marrow of healthy, osteoporotic and diabetic rats. HE-MSCs were co-cultured with ORX-MSCs (HE-MSCs→ORX-MSCs) or DM-MSCs (HE-MSCs→DM-MSCs) under osteogenic conditions, and Runx2 gene expression (n = 3) and alkaline phosphatase (ALP) activity (n = 5) were evaluated on day 10 and extracellular matrix mineralization (n = 5), on day 14. Co-cultures of MSCs at the same condition (HE-MSCs→HE-MSCs, ORX-MSCs→ORX-MSCs or DM-MSCs→DM-MSCs) were used as controls. The data were compared by ANOVA ($p <= 0.05$). In osteoporosis, the gene expression of Runx2 was HE-MSCs→ORX-MSCs > HE-MSCs→HE-MSCs > ORX-MSCs→ORX-MSCs ($p = 0.001$), ALP activity was HE-MSCs→HE-MSCs > HE-MSCs→ORX-MSCs > ORX-MSCs→ORX-MSCs ($p=0.001$) and mineralization was HE-MSCs→HE-MSCs = HE-MSCs→ORX-MSCs > ORX-MSCs→ORX-MSCs ($p = 0.001$). In diabetes, the gene expression of Runx2 was HE-MSCs→HE-MSCs HE-MSCs→DM-MSCs > DM-MSCs→DM-MSCs ($p = 0.001$) (Figure). Together, the data indicated that MSCs derived from healthy rats partially recover the osteogenic potential of MSCs from rats with osteoporosis and diabetes mellitus. These findings suggest that the use of MSCs from healthy donors may be an interesting strategy in cell therapy approaches to repair bone tissue under osteoporotic and diabetic conditions.

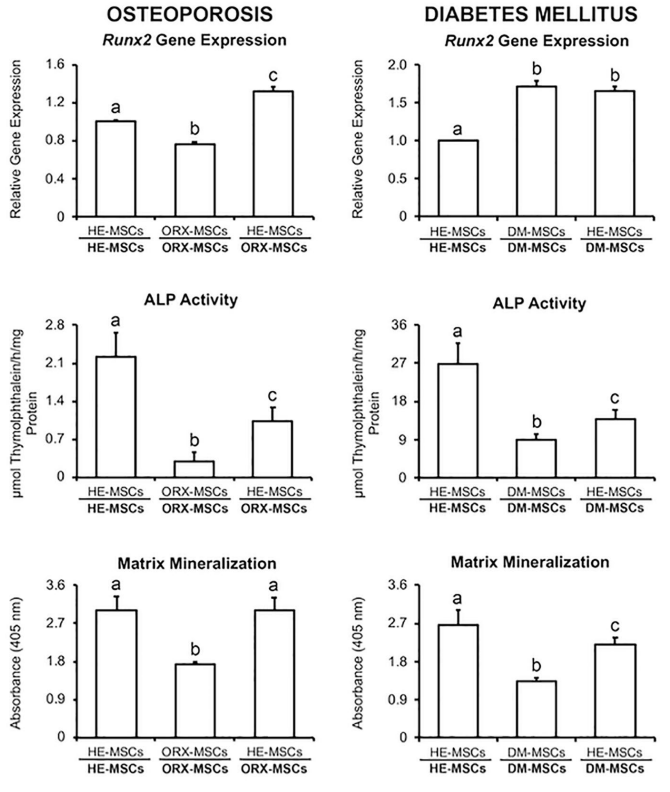

***Disclosures: Alann Thaffarell Portilho de Souza**, None*

Posters

P-432

Gprc5a is a novel target gene of teriparatide involved in osteoblastic cell proliferation. *Kosuke Kato[1], Yasuhiro Arasaki[1], Takuro Akiya[1], Masaki Noda[2], Yoichi Ezura[3], Tadayoshi Hayata[1]. [1]Department of Molecular Pharmacology, Graduate School of Pharmaceutical Sciences and Faculty of Pharmaceutical Sciences, Tokyo University of Science, Japan, [2]Department of Molecular Pharmacology, Medical Research Institute, Tokyo Medical & Dental University (TMDU), Japan, [3]Department of Judo Therapy, Faculty of Medical Technology, Teikyo University, Japan

Objective. Osteoporosis is caused by an imbalance between bone formation by osteoblasts and bone resorption by osteoclasts. Teriparatide is one of the therapeutic drugs for osteoporosis that promotes bone formation. However, its mechanism of action is not fully understood. In an exhaustive search for teriparatide target genes, we focused on Gprc5a, one of the G protein-coupled receptors (GPCRs) considering the effectiveness of GPCR in drug discovery. In this study, we wished to characterize function of Gprc5a in osteoblastic cells. Methods & Results. Gene expression analysis revealed that treatment of rat osteosarcoma ROS17/2.8 cells and mouse osteoblastic MC3T3-E1 cells with 100 nM teriparatide for 1 hour resulted in a significant increase in Gprc5a expression. Gprc5a expression was also significantly increased in femurs of 4-week-old rats 1 hour after injection of teriparatide (80 μg/kg body weight). Time-course experiment using MC3T3-E1 cells revealed that Gprc5a expression was maximized at the 1-hour time point after 100 nM teriparatide treatment and then attenuated. To examine the subcellular localization of Gprc5a, Gprc5a-HA expression plasmid was transfected into MC3T3-E1 for immunofluorescence study. The results showed that the localization pattern of Gprc5a-HA was consistent with plasma membrane localization pattern. We also examined the effects of Gprc5a siRNA transfection in MC3T3-E1 cells on cell proliferation, and we found that siRNA-mediated knockdown of Gprc5a significantly reduced the cell proliferation.Conclusion. These findings suggest that Gprc5a is one of the possible target genes of teriparatide, responsible for osteoblastic cell proliferation.

***Disclosures: Kosuke Kato**, None*

P-433

Effect of Fucoidan, a Sulfated Polysaccharide, Extracted from the Algae Macrocystis pyrifera, Sargassum muticum, and Undaria pinnatifida on Bone Remodeling *Brenda Iduarte[1], Jessica Landeros[1], Enrique Hernández[2], Rodrigo Beas[3], Pierrick Fournier[1], Patricia Juárez[1]. [1]CICESE, Mexico, [2]CRIAP-Ensenada, Mexico, [3]UABC, Mexico

Bone is a dynamic tissue that is in constant repair and remodeling, however, the imbalance in this process causes bone diseases such as osteoporosis. In this work, we experimented if the sulfated polysaccharides of the Macrocystis pyrifera, Sargassum muticum and Undaria pinnatifida algae from Todos Santos Island, BC, can modulate the bone remodeling process. Sulfated polysaccharides were extracted by the acid hydrolysis method. Extract characterization was performed using in vitro and ex vivo tests to study cell proliferation and differentiation in order to evaluate the modulatory effect of sulfated polysaccharides at different stages of bone development. At an early stage, osteoblast precursors (MC3T3-E1 cells) were treated with different concentrations of sulfated polysaccharides demonstrating a dose-dependent proliferation inhibitory effect. Differentiation assays with MC3T3-E1 cells treated with sulfated polysaccharides stimulated osteoblast cells to produce areas of bone mineralization. These results were consistent with osteoblastogenesis studies using ex vivo bone marrow assays of Balb/c mice, while in osteoclastogenesis they maintained an inhibitory effect, demonstrating that these compounds have the ability to stimulate differentiated and undifferentiated cells to mineralize bone. Furthermore, gene expression assays of MC3T3-E1 treated with the sulfated polysaccharides indicated significant expression of Osteoprotegerin (OPG), a RANKL antagonist protein. Our results suggest that sulfated polysaccharides from the marine algae studied are compounds capable of promoting bone formation demonstrating their potential as an anabolic therapeutic agent.

***Disclosures: Brenda Iduarte**, None*

P-434

κ-Carrageenan-Functionalization of Octacalcium Phosphate-Coated Titanium Discs Enhances Pre-Osteoblast Behavior and Osteogenic Differentiation *Wei Cao[1], Gang Wu[2], Nathalie Bravenboer[3], Marco N. Helder[4], Engelbert A.J.M. Schulten[4], Jianfeng Jin[1], Lester Geonzon[5], Shingo Matsukawa[5], Rommel G. Bacabac[6], Christiaan M. ten Bruggenkate[4], Jenneke Klein-Nulend[1]. [1]Department of Oral Cell Biology, Academic Centre for Dentistry Amsterdam (ACTA), University of Amsterdam and Vrije Universiteit Amsterdam, Amsterdam Movement Sciences, Netherlands, [2]Department of Oral Implantology and Prosthetic Dentistry, Academic Centre for Dentistry Amsterdam (ACTA), University of Amsterdam and Vrije Universiteit Amsterdam, Amsterdam Movement Sciences, Netherlands, [3]Department of Clinical Chemistry, Amsterdam University Medical Centers, Vrije Universiteit Amsterdam, Amsterdam Movement Sciences, Netherlands, [4]Department of Oral and Maxillofacial Surgery/Oral Pathology, Amsterdam University Medical Centers and Academic Centre for Dentistry Amsterdam (ACTA), Vrije Universiteit Amsterdam, Amsterdam Movement Sciences, Netherlands, [5]Department of Food, Science & Technology, Tokyo University of Marine Science & Technology, Japan, [6]Department of Physics, Medical Biophysics Group, University of San Carlos, Philippines

Introduction: A highly bioactive coating is promising to improve osteointegration and long-term prognosis of dental implants. Carrageenan is highly hydrophilic and biocompatible seaweed-derived sulfated-polysaccharide. Whether carrageenan can be used to functionalize octacalcium phosphate (OCP)-coatings to enhance osseointegration of titanium dental implants is unclear.Purpose:To characterize carrageenan-functionalized biomimetic OCP-coated titanium, and to test the effect of carrageenan on pre-osteoblast behavior and osteogenic differentiation.Method:Preparation and characterization of k-carrageenan-functionalized OCP-coating: OCP-solution containing k-carrageenan at 0.125, 0.25, 0.5, 1, and 2 mg/ml was used to precipitate OCP-coating onto titanium discs. Characterization was performed using SEM, EDX, XRD, Raman spectroscopy, and contact angle measurements. MC3T3-E1 pre-osteoblast behavior: Cell adhesion and spreading were determined using fluorescent staining (1,2 h), and cell metabolic activity by PrestoBlue® assay, and proliferation by CyQuant® cell proliferation assay kit (day 1,2,3).Osteogenic differentiation: Alkaline phosphatase activity, osteogenic gene expression, and matrix mineralization alizarin red staining) were determined.Statistics: ANOVA (n=3-5), statistical significance: $p<0.05$. Results:k-Carrageenan (all concentrations) in OCP-coating changed the titanium disc coating's morphology/microstructure by decreasing porosity compared to controls. k-Carrageenan (2 mg/ml only) increased OCP interplanar crystal distance (~1.5-fold). k-Carrageenan did not affect hydrophilicity. k-Carrageenan (0.5 and 2 mg/ml) significantly increased (6-7-fold) cell adhesion and spreading. All concentrations tested dose-dependently increased proliferation (max. 1.3-fold, day 3), metabolic activity (max. 1.5-fold, day 3), alkaline phosphatase activity (max. 1.8-fold, day 4), and matrix mineralization (max. 2.6-fold, day 28). Conclusions:k-Carrageenan modified morphology and microstructure of OCP-coating, and enhanced pre-osteoblast metabolic activity, proliferation, and osteogenic differentiation. This suggests that k-carrageenan might improve dental implant osseointegration in vivo. Figure 1. k-Carrageenan dose-dependently stimulates metabolic activity (day 3), alkaline phosphatase activity (day 4), and mineralized nodule formation (alizarin red; day 28) of MC3T3-E1 pre-osteoblasts.

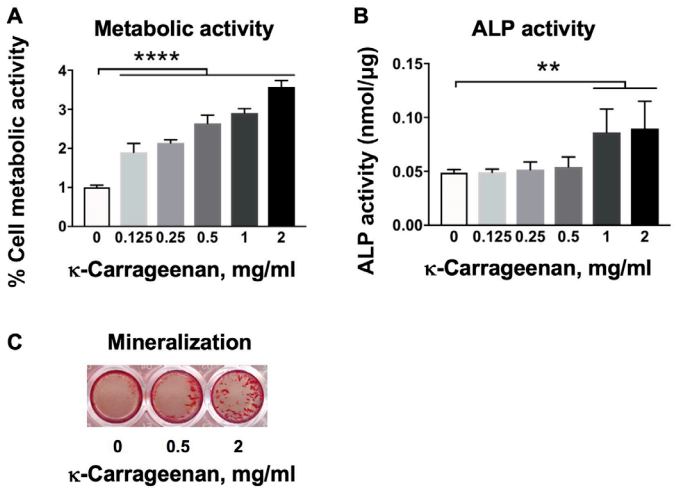

***Disclosures: Wei Cao**, None*

P-435

Osteoblastic cell differentiation and the quest for energy for calcium synthesis *Claudia Medeiros[1], Joseph Wallace[1]. [1]IUPUI, United States

Bone quality is essential for proper bone function. The quality of bone tissue is measured by material properties, geometry, and mass. Bone is a flexible tissue that can withstand mechanical loading by dynamic processes of modelling and remodeling as a mechano-response to stress. Therefore, the more we exercise, the more we improve bone content and function. Over time, disease states alter bone matrix composition and compromises bone's ability to resist fracture. Bone diseases have been associated with altered bone metabolism. Energy production is mitochondria's main role. Mitochondria is also responsible for calcium homeostasis. Calcium is an important component of bone function found in the mineral phase formed during osteoblast deposition. Osteoblastic cells are known to utilize both glycolysis and oxidative phosphorylation for energy production. However, as it differentiates, the metabolic needs shift to accommodate the demands required for mineralization. Here, we investigate the energy metabolism during osteoblast differentiation. Through Alizarin staining, we detected calcium accumulation by microscopy (Fig.1A) and quantitative analysis (Fig.1B). Using molecular analyses, we determined relative mitochondrial DNA (mtDNA) content during mineral synthesis. Mitochondrial copy number increased as mineralization accumulated in the matrix, suggesting that differentiated osteoblastic cells require more energy. Additional work is needed to characterize expression of key components of tricarboxylic acid (TCA) cycle, the central metabolic pathway in mitochondria, during osteoblast maturation. Further analysis of biochemical TCA markers is underway.

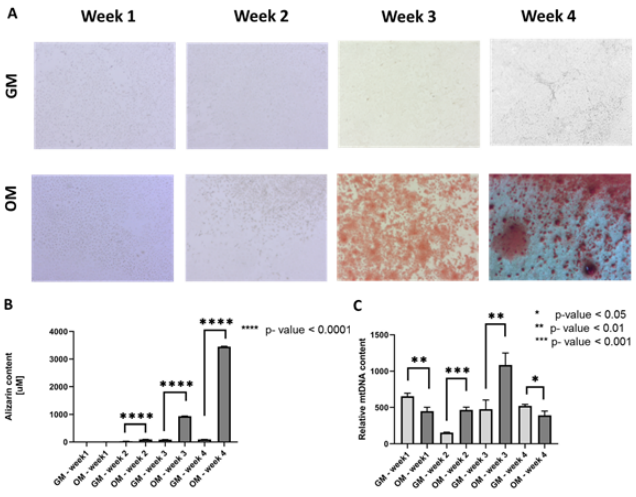

Figure 1. Characterization of mineral layer formation. A) Microscopic analysis of calcium deposition using Alizarin assay (5x magnification).GM (growth medium); OM (osteogenic medium). B) Quantitative analysis of calcium deposition using Alizarin assay (one experiment in triplicates). C) Relative mtDNA content during mineralization (three independent experiments in triplicates). A Student t-test was used to determine significance.

***Disclosures: Claudia Medeiros**, None*

P-436

Prostate transmembrane protein androgen induced-1 and Nedd4 Regulate Bone Resorption by Promoting Proton Production in Osteoclasts *Hirohito Hirata[1], Xianghe Xu[2], Masatoshi Murayama[1], Makoto Shiraki[1], Toshio Kukita[3], Masaaki Mawatari[4], Akiko Kukita[2]. [1]Department of Pathology and Microbiology, Department of Orthopedic Surgery, Faculty of Medicine, Saga University, Japan, [2]Department of Pathology and Microbiology, Faculty of Medicine, Saga University, Japan, [3]Department of Molecular Cell Biology & Oral Anatomy, Faculty of Dentistry, Kyushu University, Japan, [4]Department of Orthopedic Surgery, Faculty of Medicine, Saga University, Japan

Prostate transmembrane protein androgen induced 1 (Pmepa1), is a binding protein with Nedd4 family of E3 ubiquitin ligases, which is mainly localized to vesicle membrane, and is involved in regulation of cell proliferation, metastasis, autophagy, and lysosomal stability in cancer cells. We have previously reported that Pmepa1 is highly expressed in osteoclasts on bone and is involved in bone resorption. In this study, we investigated the role and the regulatory mechanism of bone resorption via Pmepa1 using Pmepa1 mutant mice and involvement of Nedd4 in bone resorption. Mutant mice which lack membrane and cytoplasmic Nedd4 binding domains of Pmepa1 were generated by CRISPR/Cas9 system. Micro CT Analysis revealed that bone volume was relatively increased in Pmepa1 mutant mice compared to wild type (WT). Bone histomorphometry of lumbar vertebrae showed Pmepa1 mutation slightly increased osteoblast numbers, but significantly decreased osteoclast numbers on bone surface and decreased erosion depth of osteoclasts. In vitro culture of bone marrow macrophages with RANKL showed that there was no difference in osteoclastogenesis between Pmepa1 mutant and WT mice, whereas bone resorption activity of Pmepa1 mutant osteoclasts was markedly decreased. The proton produced by osteoclasts was analyzed using an acid-sensitive fluorescent probe. Analysis by confocal laser microscopy showed proton production of Pmepa1 mutant osteoclasts was significantly decreased. In the previous study, we found Pmepa1 was localized to lysosome, but intracellular localization and role of Nedd4 in osteoclasts has not been investigated. Analysis by immunofluorescence with Airyscan super resolution microscopy showed that Nedd4 is localized to lysosome with V0a3 or V0d2 subunits of V-ATPase, and Pmepa1 was highly colocalized with Nedd4 in osteoclasts. In addition, knockdown of Nedd4 expression in osteoclasts markedly reduced bone resorption and proton production of osteoclasts. Finally, analysis by genomewide expression of osteoclasts showed that regulatory genes involved in vesicular trafficking was decreased in Pmepa1 mutant osteoclasts in comparison with those in WT osteoclasts. Collectively, our data show that both Pmepa1 and Nedd4, which are localized to lysosome with components of V-ATPase regulate bone resorption by affecting proton production. Our results show that together with Pmepa1, Nedd4 is a possible target for bone resorption.

***Disclosures: Hirohito Hirata**, None*

P-437

TAF12, a Member of TFIID Transcription Factor Complex, Contributes to Osteoclast Differentiation and Bone Resorption In Vivo *Kazuaki Miyagawa[1], Yasuhisa Ohata[1], Jumpei Teramachi[1], Jiro Miura[2], Mark A Subler[3], John M Chirgwin[3], Jolene J Windle [3], G. David Roodman[1], Noriyoshi Kurihara[4]. [1]Division of Hematology and Oncology, Department of Medicine, Indiana University, United States, [2]Division for Interdisciplinary Dentistry, Osaka University, Japan, [3]Department of Human and Molecular Genetics, Virginia Commonwealth University, United States, [4]Division of Hematology and Oncology, Department of Medicine, Indiana University, United States

We reported that TAF12 is expressed at higher levels in osteoclasts (OCLs) than osteoblasts (OBs), and contributed to OCL formation, particularly in OCLs of patients with Paget's disease (Cell Metab,2012). However, TAF12's role in normal bone remodeling is unclear, in part because global knockout of TAF12 is embryonic lethal in mice. Therefore, we generated mice with targeted heterozygous deletion of Taf12 (Taf12flox/- mice), using CRISPR/Cas9 technology and bred them to Trap-Cre mice to generate Trap-Cre/Taf12flox/- mice with targeted deletion of Taf12 in the OCL lineage. TAF12 protein levels in highly purified OCLs from Trap-Cre(+)/Taf12flox/- (TC(+)/Taf12) mice were decreased by 60% compared to OCLs from 8-month-old Trap-Cre(-)/Taf12flox/- (TC(-)/Taf12) and WT mice . Histomorphometric analysis of femurs revealed that BV/TV in 8-month-old TC(+)/Taf12 mice was increased 1.6-fold compared to TC(-)/Taf12 mice. OCLs number and surface were also decreased by 20% in TC(+)/Taf12 mice compared to TC(-)/Taf12 mice, while OB numbers and surface were unchanged. These findings suggested that targeted deletion of TAF12 in OCLs enhances bone volume due to the inhibition of OCL formation/ resorption during bone-remodeling. Consistent with these results, OCL formation and bone resorption induced by RANKL in cultures of TC(+)/Taf12 bone marrow were reduced by 40% and 60% respectively, compared to OCL of TC(-)/Taf12 mice. Further, expression levels of NFATc1 and Cathepsin K (CTSK) in OCLs from TC(+)/Taf12 mice were decreased by 50% and 75% respectively, compared with TC(-)/Taf12. CTSK expression in OCLs in bone sections of TC(+)/Taf12 mice was similarly decreased. Since autophagy regulates bone resorption and secretion of proteases to the ruffled border in OCLs (DeSelm CJ et al, Dev Cell, 2011), we examined the effects of loss of TAF12 on autophagic molecule expression in OCLs. We found that syntaxin17 expression, which is involved in autophagosome formation, was significantly lower on Western blots and by immunohistochemistry of OCLs from TC(+)/Taf12 mice vs. TC(-)/Taf12 mice . Transmission electron microscopy of OCLs resorbing bone showed that the ruffled borders of OCLs from TC(+)/Taf12 mice were poorly formed compared to TC(-)/Taf12 mice. These results suggest that TAF12 contributes to OCL differentiation, bone resorption, and CTSK secretion in vivo and may be a novel target for blocking bone resorption.

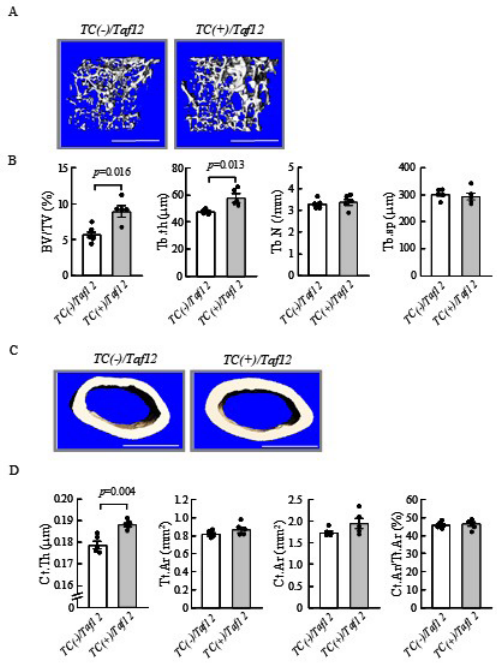

Figure 2. Bone structure and remodeling in *TC(-)/Taf12* and *TC(+)/Taf12* mice. (A) Representative 2D μCT images of femurs (Sagittal section). The scale bar is 1 mm. (B) Representative 3D μCT images of femurs. The scale bar is 1 mm. (C) Bone volume and structural parameters of trabecular bone in vertebrae. Results are expressed as the mean ± SEM for *TC(-)/Taf12* (5 male, 8 months old) and *TC(+)/Taf12* (5 male, 8 months old). The data were analyzed using two-tailed Welch's *t*-test. (D) Representative 3D μCT images of the femur (Horizontal section). The scale bar is 1 mm. (E) Cortical bone parameters. Results are expressed as the mean ± SEM for *TC(-)/Taf12* (5 male, 8 months old) and *TC(+)/Taf12* (5 male, 8 months old). The data were analyzed using two-tailed Welch's t-test. Results in panels B and D were analyzed by similar representative mice.

***Disclosures: Kazuaki Miyagawa**, None*

P-438

Sterol Regulatory Element Binding Transcription Factor 2 (SREBF2) Negatively Regulates Osteoclastogenesis and Pathological Bone Erosion *Haemin Kim[1], Seyeon Bae[2], Sehwan Mun[2], Steven Zeng[2], Kyung-Hyun Park-Min[1]. [1]Hospital for Special Surgery/Weill Cornell Medical College, United States, [2]Hospital for Special Surgery, United States

Osteoclasts are the sole bone resorbing cells, and their dysregulation leads to pathological bone destruction. Recently, the importance of metabolic reprogramming in osteoclast differentiation and bone remodeling is increasingly appreciated and is an emerging area of research. However, its role in osteoclasts remains to be determined. Lipids, including cholesterol and fatty acids, have greatly impacted on skeleton and bone cells. Previously, the close correlation between plasma lipids and bone mineral density has been well established. SREBFs are a key transcription factor for regulating lipid biosynthesis and are sensors for intracellular lipids. To investigate the role of SREBF2-mediated lipid metabolism in osteoclasts, we generated osteoclast-specific SREBF2 deficient mice (SF2 cKO). Strikingly, SF2 cKO mice exhibit reduced bone mass compared to control mice and show accelerated osteoclastogenesis. Consistent with data from mouse osteoclasts, SREBF2 knockdown by siRNAs in human osteoclasts promotes osteoclastogenesis, and overexpression of SREBF2 completely suppresses osteoclast differentiation, suggesting that SREBF2 is a negative regulator of both human and mouse osteoclastogenesis. During the osteoclastogenesis, the levels of intracellular cholesterol significantly increase in a time-dependent manner, and the genes associated with cholesterol biosynthesis are induced during receptor activator of NF-κB ligand (RANKL)-mediated osteoclastogenesis. Nuclear SREBF2 is also highly induced by RANKL. However, SREBF2 mediated regulation of osteoclast differentiation is independent of intracellular cholesterol. Small molecule inhibitors targeting SREBF2 activation also enhance osteoclastogenesis. Moreover, SREBF2 deficiency accelerates pathological bone erosion in a murine inflammatory arthritis model. Using ChIP sequencing and RNA sequencing, we revealed that SREBF2 regulates osteoclastogenesis in part by targeting the interferon signaling pathway. Taken together, our findings have elucidated the effect of lipid metabolism and SREBFs on osteoclastogenesis and bone homeostasis and also open up a new avenue to therapeutically target pathological bone destruction.

***Disclosures: Haemin Kim**, None*

P-439

Cellular Origin and Functions of Osteoclast Progenitors in Inflammatory Arthritis *Christian Jacome-Galarza[1], Julia Charles[1]. [1]Brigham and Women's Hospital, United States

Inflammatory arthritis (IA) is an autoimmune disease targeting multiple joints resulting in osteoclast (OC) mediated bone and cartilage destruction, leading to physical disability. However, the precise cellular origins of OC and the mechanisms that regulate their formation in IA are poorly understood. Myeloid lineages including OC can derive from either hematopoietic stem cells (HSC) or erythro-myeloid progenitors (EMP). Previous studies suggest that, in IA, HSC-derived monocytes differentiate into OC and others showed that macrophages (macs) can form OC under the influence of inflammatory cytokines in vitro. We hypothesized that EMP-derived macs and HSC-derived monocytes can independently contribute to the formation of OC in IA. To test this hypothesis, we used Flt3Cre;Rosa26LSL-YFP mice to label HSC-derived cells and Cx3cr1CreERT2;Rosa26LSL-tdTomato mice, pulsed with tamoxifen at E9.75, to label EMP-derived cells. We harvested ankle joints and examined synovium and periosteal bone by histology and confocal microscopy to detect fluorescent proteins (lineage-tracer), OC and macs. Histology of ankle joints from healthy Flt3Cre;Rosa26LSL-YFP embryos at E16.5, newborn at P0 and 8 week-old mice showed that ~7 % of synovial F4/80+ or CD68+ cells were of HSC origin, suggesting that EMPs are the major source of synovial macs. We confirmed, using Cx3cr1CreERT2;Rosa26LSL-tdTomato mice, that numerous F4/80+ synovial macs were TdTomato+, showing for the first time an EMP-origin. To test the HSC origin of OC in IA, adult Flt3Cre;Rosa26LSL-YFP mice were treated with K/BxN arthritogenic serum and ankle joints were harvested at day 10 (peak inflammation). Unexpectedly, we found that only 56% of OC were YFP-positive, indicating that a large proportion of synovial OC are not HSC-derived. Further, we identified CD68+TRAP+ cells localized to periosteal surfaces as candidate progenitors of synovial OC. Consistent with the dual origin of synovial OC, CD68+TRAP+ progenitors derive from both HSC (27%) and non-HSC (73%) lineages.We are currently confirming the EMP-origin of OC in arthritic mice, more precisely defining the phenotype of OCPs and investigating their transcriptional profile by scRNA sequencing. A better understanding of the transcriptional mechanisms that regulate OC formation in IA will allow us to decipher pathogenic mechanisms and identify cell specific molecules to develop new therapeutic targets to inhibit OC formation and prevent bone and cartilage erosions.

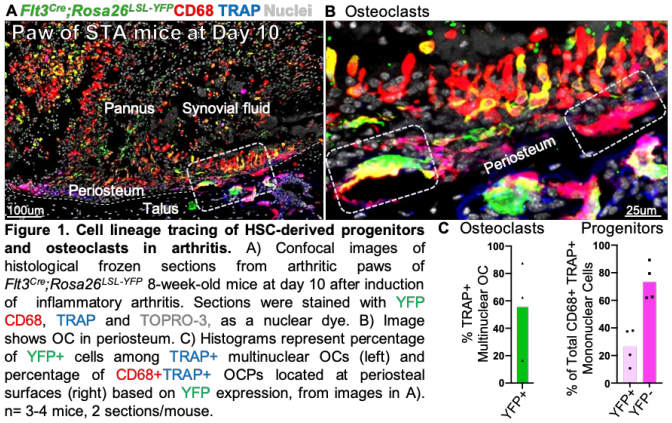

Figure 1. Cell lineage tracing of HSC-derived progenitors and osteoclasts in arthritis. A) Confocal images of histological frozen sections from arthritic paws of *Flt3Cre;Rosa26LSL-YFP* 8-week-old mice at day 10 after induction of inflammatory arthritis. Sections were stained with YFP CD68, TRAP and TOPRO-3, as a nuclear dye. B) Image shows OC in periosteum. C) Histograms represent percentage of YFP+ cells among TRAP+ multinuclear OCs (left) and percentage of CD68+TRAP+ OCPs located at periosteal surfaces (right) based on YFP expression, from images in A). n= 3-4 mice, 2 sections/mouse.

***Disclosures: Christian Jacome-Galarza**, None*

P-440

β-adrenergic Receptors in Osteoclasts Regulate Differentiation and Resorption Activity in vitro *Audrey Bergeron[1], Audrie Langlais[1], Deborah Barlow[2], Karen Houseknecht[2], Katherine Motyl[1]. [1]Maine Medical Center Research Institute, United States, [2]University of New England, United States

Sympathetic nervous system (SNS) signaling via β-adrenergic receptors (βAR) leads to uncoupled remodeling and bone loss. Therefore, βAR antagonists (β-blockers, BB) may be used to treat or prevent osteoporosis. Our recent finding that the non-selective β-blocker propranolol (Pro) prevents resorption in vivo without influencing RANKL suggests that βARs play a direct role in osteoclasts (OCLs).Therefore, we hypothesized that βAR signaling directly promotes OCL differentiation/function. To test this, we injected 3 mg/kg sc of the βAR agonist salbutamol (Sal) daily for 4 wks in BL/6 female mice. Both μCT and ELISA showed striking Sal-induced bone resorption in vivo with marked trabecular bone loss in the distal femur (BV/TV was reduced by 35% compared to veh, p<0.001) and L5 vertebra. Sal increased serum levels of CTx (137%, p<0.001) without changing P1NP

levels (p=0.9), suggesting enhanced resorption but no changes in formation. Next, using RNAscope, we were able to detect both Adrb1 and Adrb2 transcripts in femur. Importantly, both Adrb1 and Adrb2 transcripts colocalize with Acp5 positive cells lining trabecular bone surfaces, indicating that both are expressed in OCLs in vivo. In vitro, we further confirmed low levels of Adrb1 gene expression (Ct values >30) and moderate Adrb2 gene expression in primary bone marrow stromal cells and RAW264.7 cells differentiated to OCLs (Ct values = 29.8/26.3, respectively). We observed β1AR and β2AR protein in OCL cultures using IHC (but not in OCLs from Adrb1/2 global KO mice). We next treated primary OCLs with Pro or Sal at concentrations comparable to those achieved in vivo in the bone marrow of dosed mice; 1 μM Pro inhibited OCL differentiation (# TRAP positive multinucleated cells) by 18% (p=0.005) and reduced resorption (OsteoAssay Surface) by 45% (p=0.05) while 1 μM Sal enhanced OCL differentiation by 51% (p<0.0001) and increased resorption by 139% (p=0.03). Consistent with this, Pro inhibited mid-to-late stage differentiation markers while Sal enhanced these markers (including Acp5, Fam102a, Fos, and Nfatc1). Interestingly, in OCLs derived from Adrb1/2 global KO mice, Pro reduced OCL numbers (but to a lesser degree than in WT cells) while Sal did not increase OCL numbers; indicating that Pro may exhibit β1AR and β2AR-independent effects on OCL differentiation while Sal targets βARs more specifically. In summary, these data suggest that BB may serve as a therapy targeting OCLs in bone pathologies.

***Disclosures: Audrey Bergeron**, None*

P-441

Regulation of Osteoclast Differentiation by MEF2A *Andrew Norton [1], Nicholas Blixt[1], Brian Spencer[1], Cory Baumann[1], Dawn Lowe[1], Kim Mansky[1]. [1]University of Minnesota, United States

Osteoclasts are large multinuclear cells that are responsible for breaking down bone. Myocyte enhancer factor 2 (MEF2) is a family of transcription factors, Mef2a, b, c and d, that regulate gene transcription in multiple cell types. Research from other groups has demonstrated that MEF2 regulates chondrocytes, osteoblasts and osteocytes; however, little work to date has been done to demonstrate if MEF2 plays a role in regulating osteoclast differentiation. We initially determined that MEF2A, C and D are expressed during osteoclast differentiation. To study MEF2A's role in regulating osteoclast differentiation, we created a conditional mouse model of MEF2A in which Mef2a floxed mice (A-WT) were bred to mice expressing c-Fms-Cre (A-cKO). At three months of age, femurs from female A-cKO mice have increased BV/TV and decreased CTX and decreased number of osteoclasts compared to female A-WT mice. We did not observe a skeletal phenotype or change in bone biomarkers in the male mice that were conditional for Mef2a. In vitro cultures of osteoclasts from male or female A-cKO mice form smaller and less active osteoclasts compared to A-WT mice. MEF2C has been shown to regulate expression and activity of the estrogen receptor in cardiac cells via the interaction of class IIA HDACs with MEF2C. Thus, we hypothesize that sex specific effects on osteoclasts that we measure in female A-cKO mice is due to changes in the expression and/or activity of the estrogen receptor. We measured a 3-fold increase in Esr1, the gene for estrogen receptor-alpha, in A-cKO osteoclasts. We sham-operated or ovariectomized (OVX) 8 to 10-week old female A-WT or A-cKO female mice. We measured approximately a 45% reduction in the BV/TV of femurs from A-WT OVX vs. A-WT sham mice. BV/TV of A-cKO OVX mice was reduced 55% compared to A-cKO sham mice. Additionally, BV/TV of the A-cKO OVX mice was not significantly different than A-WT sham mice supporting the hypothesis that dysregulation of estrogen signaling is the mechanism for the increased BV/TV in female A-cKO mice. Lastly, we measured a 3-fold increase in Mef2c expression and a 3-fold decrease in Hdac9 expression in osteoclasts from A-cKO mice suggesting that MEF2A may regulate estrogen receptor expression and activity thorough modulation of Mef2c and Hdac9 expression.

***Disclosures: Andrew Norton,** None*

P-442

Hem1 Promotes Osteoclast Fusion and Bone Resorption in Mice *Xiaoyan Wang[1], Lijian Shao[2], Nukhet Aykin-Burns[1], Daohong Zhou[3], Maria Almeida[1], Ha-Neui Kim[1]. [1]University of Arkansas for Medical Sciences, United States, [2]University of Illinois Chicago, United States, [3]University of Florida, United States

Hem1 (Hematopoietic protein 1), a hematopoietic cell-specific member of the Hem family of cytoplasmic adaptor proteins, is essential for lymphopoiesis and innate immunity via actin polymerization as well as the transition of fetal liver hematopoiesis to the bone marrow. Hem1 is indispensable for the Arp2/3 complex-induced cell migration and the accompanying enhanced mitochondrial function in yeast, but little is known about Hem1 regulation of mitochondrial function in mammalian cells. Here we report that Hem1 contributes to the fusion of pre-osteoclasts in mice. Five-week-old male or female mice with global deletion (KO) of Hem1 gene had higher cancellous bone volume and BMD in femur than wild-type littermate controls (WT). This change was due to an increase in trabecular number and a decrease in trabecular spacing while trabecular thickness was not affected as determined by micro-CT. The high bone mass phenotype was associated with decreased CTx levels in the serum. To examine the cellular mechanisms responsible for the decrease in bone resorption, we used bone marrow-derived macrophage (BMM) cultures and induced osteoclast formation with RANKL. In the cells from WT mice, Hem1 mRNA and protein levels were greatly increased during the transition of BMMs to mature osteoclasts in the presence of RANKL. Osteoclast progenitors from Hem1 KO mice differentiated normally into TRAP-positive osteoclasts albeit with impaired resorptive function due to defects in actin ring formation. Osteoclasts lacking Hem1 exhibited a striking decrease in oxygen consumption rate and mitochondrial ATP production as compared to osteoclasts from WT mice. Osteoclast resorbing activity was increased in BMM cultures from wild-type C57BL6 mice transduced with retroviral vectors expressing the murine Hem1. Hem1 overexpression increased RANKL-induced DC-stamp and ATP6v0d2, known osteoclast fusion markers, suggesting that, consistent with its polymerization properties of actin, Hem1 promotes osteoclastogenesis by regulating actin ring organization. Transplantation of Hem1 KO mice with normal hematopoietic cells (Lin-CD45+) restored cancellous bone volume and microarchitecture in the distal femur, as well as the levels of serum CTx and actin ring formation in osteoclasts. Taken together, these results indicate that Hem1 activation in mice stimulates osteoclast fusion and its resorbing activity, most likely by promoting mitochondrial function; and thereby decreases bone mass.

***Disclosures: Xiaoyan Wang**, None*

P-443

Genetic and pharmacological activation of Hedgehog signaling suppresses osteoclastogenesis and hinders titanium particle-induced osteolysis via inhibiting the JNK/c-Fos-NFATc1 cascade *Liwei Zhang[1], Yanjun Yang[1], Zirui Liao[1], Meng Li[1], Xinhaun Lei[2], Chiting Yuan[2], Jianquan Chen[1]. [1]Department of Orthopaedics, the First Affiliated Hospital of Soochow University, China, [2]Orthopedic Department, Taizhou Hospital Affiliated to Wenzhou Medical University, China

Aseptic loosening is a major long-term complication after total joint arthroplasty and has become the first cause for further revision surgery. Proinflammatory cytokines release resulting from engulfing implant debris by macrophages and subsequent stimulation of osteoclast differentiation and bone resorption are considered as the mechanism of periprosthetic osteolysis (PPO). Thus, therapeutic approaches of suppressing osteoclast formation and activity are considered to be of great potential to prevent and treat this osteolytic disease. Hedgehog (Hh) signaling has been shown to play a critical role in skeletal development and metabolism with promoting osteoblast differentiation and inhibiting adipogenesis. While Hh signaling is also implicated in regulating osteoclastogenesis indirectly, whether it can inhibit osteoclast differentiation and bone resorption remains controversial. In this study, we explored the cell-autonomous role of Hh signaling in regulating osteoclastogenesis and its therapeutic potential in preventing wear particle-induced osteolysis.Hh signaling activation in macrophages was resulted from conditional ablation of negative regulator suppressor of fused (Sufu) using LysM-Cre or Smo-agonist purmorphamine (PM) treatment. Firstly, RANKL-induced osteoclast formation and bone resorption were strongly inhibited after Hh signaling activation detected by TRAP staining, F-actin ring immunofluorescence and scanning electron microscope. Meanwhile, the down-regulated expressions of osteoclast-specific genes including Nfatc1, c-Fos, Ctsk, Dcstamp, Acp5, Oscar, Atp6v0a3, and Atp6v0d2 were assessed by RT-qPCR. Ti particle-induced osteolysis models were established to assess osteoclastogenesis and bone resorption in vivo and the samples were analyzed using Micro-CT and histomorphometry, which confirmed the protective effect of Hh signaling activation on osteolysis. The mechanistic study by western blot revealed that activation of Hh signaling suppressed RANKL-induced JNK phosphorylation and downregulated protein levels of two key osteoclastic transcriptional factors, c-Fos and its downstream target NFATc1.Hh signaling activation caused by Sufu ablation and PM treatment inhibited osteoclastogenesis and Ti particle-induced osteolysis through suppressing JNK/NFATc1/c-Fos signaling, indicating it may serve as a novel candidate for therapeutic intervention in PPO and other osteolytic diseases.

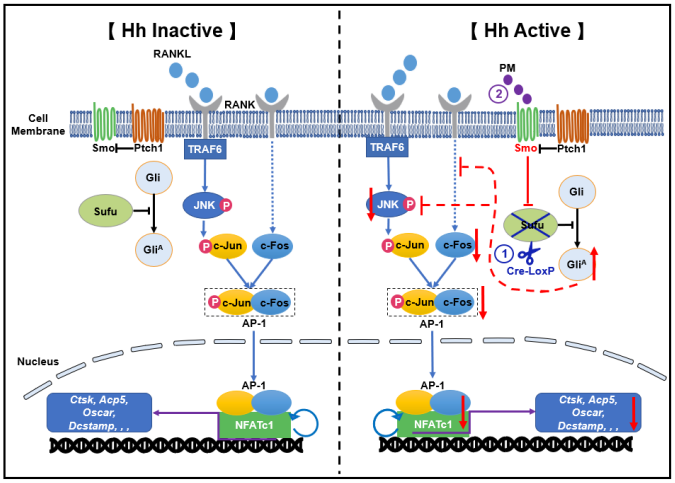

***Disclosures: Liwei Zhang**, None*

Posters

P-444

STAT3 controls osteoclast differentiation and bone homeostasis by regulating NFATc1 transcription *Yang Yiling[1], Jiang Lingyong[1], Dai Qinggang[1], Zhou Siru[1]. [1]Shanghai Jiaotong University School of Medicine, China

The transcription factor Signal Transducer and Activator of Transcription 3 (STAT3) plays a central role in cell survival and function. STAT3 has been demonstrated to participate in maintenance of bone homeostasis in osteoblasts, but its role in osteoclasts in vivo remains poorly defined. Here we generated a conditional knockout mouse model in which Stat3 was deleted in osteoclasts using a Cathepsin K-Cre (Ctsk-Cre) driver. We observed osteoclast-specific Stat3 deficiency caused increased bone mass in mice, which we attributed to impaired bone catabolism by osteoclasts. Stat3-deficient bone marrow macrophages (BMMs) showed decreased expression of nuclear factor of activated T cells, cytoplasmic 1 (NFATc1) and reduced osteoclast differentiation determined by decreases in osteoclast number, TRAP activity and expression of osteoclast marker genes. Enforced expression of NFATc1 in Stat3-deficient BMMs rescued the impaired osteoclast differentiation. Mechanistically, we revealed that STAT3 could drive the transcription of NFATc1 by binding to its promoter. Furthermore, preventing STAT3 activation using an inhibitor of upstream phosphorylases, AG490, also impaired osteoclast differentiation and formation in a similar way to gene deletion of Stat3. In summary, our data provide the first evidence that STAT3 is significant in osteoclast differentiation and bone homeostasis in vivo, and may be identified as a potential pharmacological target for the treatment of bone metabolic diseases through regulation of osteoclast activity.

***Disclosures: Yang Yiling**, None*

P-445

F-actin mediates suppression of bone resorption and prevention of ovariectomy-induced bone loss by a C-glycoside isoflavonoid *Ling Li[1], Zuocheng Qiu[1], Xinluan Wang[1]. [1]Translational Medicine R&D Center, Institute of Biomedical and Health Engineering, Shenzhen Institutes of Advanced Technology, Chinese Academy of Sciences, China

Given the limitations of current anti-resorption agents for postmenopausal osteoporosis, there is a need for alternatives without impairing coupling crosstalk between bone resorption and bone formation. In this study, we evaluated the effects of puerarin, a natural C-glycoside isoflavonoid, on bone resorption using an ovariectomized (OVX)-rat model and further investigated its underlying molecular mechanism of action in vitro. Puerarin significantly inhibited F-actin ring formation and bone resorption, without affecting osteoclastgenesis or apoptosis. In terms of mechanism, it down-regulated c-Fos, TRAP and CAII gene expression, but not suppressed osteoclastogenesis-related proteins TRAF6, NFATc1 and p-NF-kappa B (p65), decreased protein of integrin-beta 3 and phosphorylations of Src, Pyk2 and Cbl, but not inhibited Src kinase activity. Oral administration of 150 mg/kg/day of puerarin prevented OVX-induced trabecular bone loss of proximal tibia and significantly improved bone strength of femur diaphysis in rats. Moreover, puerarin significantly decreased TRAP-positive osteoclast numbers and serum TRAP-5b, CTx, without affecting bone formation rate. Taken together, we present novel findings that puerarin prevents the bone loss in OVX rat through suppression of osteoclast activation and bone resorption, by disrupting F-actin ring formation of osteoclast via inhibiting integrin-beta3-Pyk2/Cbl/Src signaling pathway, without affecting osteoclasts formation or apoptosis. These results demonstrate the unique mechanism of puerarin on bone metabolism and provide a novel natural C-glycoside isoflavonoid as potential agent for prevention of postmenopausal osteoporosis.

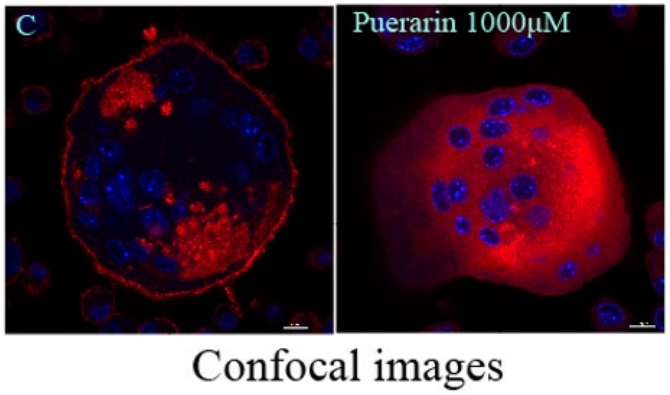

Confocal images

***Disclosures: Ling Li**, None*

P-446

Deletion of Sirt3 increases bone mass and alleviates estrogen deficiency-induced bone loss through suppressing osteoclast activity *Qiangqiang LI[1], Haixing WANG[2], Jiajun Zhang[1], Alice Pik Shan KONG[3], Tsz-ping LAM[1], Wayne Yuk Wai LEE[1]. [1]Department of Orthopaedics and Traumatology, SH Ho Scoliosis Research Laboratory, The Chinese University of Hong Kong, Hong Kong, [2]Department of Orthopaedics and Traumatology, The Chinese University of Hong Kong, Hong Kong, [3]Department of Medicine & Therapeutics, The Chinese University of Hong Kong, Hong Kong

Purpose: Sirt3 is a NAD+-dependent deacetylase and plays important roles in mitochondrial function and energy homeostasis. Osteoclasts (OC) consist of large amounts of mitochondria owing to high energy demand for bone-resorption activity. Previous study demonstrated the regulatory effect of Sirt3 on OC formation in vitro only. In this study, we aimed to study the biological function of Sirt3 in OC activity in aging and ovariectomy (OVX)-induced osteoporosis mice models.Methods: First, Sirt3 expression was investigated during OC differentiation in vitro by using primary bone marrow-derived macrophages (BMM), and in fresh bone tissue and bone marrow cells collected from ovariectomized mice and sham group. Next, we knockdown Sirt3 expression in RAW264.7 cell line to determine its effect on osteoclast differentiation. Moreover, female mice with global deletion (KO) of Sirt3 gene were used for the characterization of bone phenotypes at different ages (5 weeks, 3 months and 6 months old). Finally, the impact of Sirt3 deficiency on OVX-induced bone loss was investigated. Results: Cellular study demonstrated that Sirt3 mRNA level was greatly increased during the differentiation of BMMs to mature OCs and inhibition of Sirt3 significantly decreased osteoclastogenesis. Sirt3 mRNA in bone tissue and bone marrow cells was also significantly increased following OVX in wildtype (WT) mice. Compared to WT mice, Sirt3 deletion in KO mice resulted in increased femoral cortical thickness and higher trabecular bone mineral density in femur, which could be attributed to lower OC activity following Sirt3 deletion as indicated by suppressed osteoclastogenic differentiation and decreased serum level of TRACP-5b level. Finally, we observed OVX markedly depleted bone mass in WT mice but this decline was less obvious in Sirt3 KO mice. TRAP staining and ELISA assay showed that OC activities was markedly enhanced in the WT OVX group when compared to WT sham group, while no significant difference was observed in bone resorption parameters between Sirt3 KO sham group and Sirt3 KO OVX group. Conclusion: Sirt3 has important roles in the bone homeostasis and estrogen deficiency-induced bone loss by modulating OC activity, suggesting that inhibiting Sirt3 and its downstream targets might be novel therapeutic targets to modulate osteoresorptive disorders.

***Disclosures: Qiangqiang LI**, None*

P-447

Specific role of Hh signaling pathway in bone resorption *Ryuma Haraguchi[1], Yukihiro Kohara[1], Riko Kitazawa[2], Yuuki Imai[3], Sohei Kitazawa[1]. [1]Department of Molecular Pathology, Ehime University Graduate School of Medicine, Japan, [2]Department of Diagnostic Pathology, Ehime University Hospital, Japan, [3]Proteo-Science Center, Ehime University, Japan

The functional role of the Hedgehog (Hh) signaling pathway has been widely investigated in bone physiology/development. Previous studies have, however, focused primarily on Hh functions in bone formation, while its effects on bone resorption have not been fully elucidated. Here, we found that cyclopamine (Smoothened [Smo] inhibitor), GANT-58 (GLI1 inhibitor) or GANT-61 (GLI1/2 inhibitor), significantly inhibited RANKL-induced osteoclast differentiation of bone marrow-derived macrophages. Although the inhibitory effects were exerted by cyclopamine or GANT-61 treatment over 0-48 h (early-stage of osteoclast differentiation) or 48-96 h (late-stage of osteoclast differentiation) after RANKL stimulation, GANT-58 suppressed osteoclast formation only during the early stage. These results suggest that the Smo-GLI1/2 axis mediates the whole process of osteoclastogenesis, and that GLI1 activation is requisite only during early cellular events of osteoclastogenesis. Additionally, macrophage/osteoclast-specific deletion of Smo in mice was found to attenuate the aging phenotype characterized by trabecular low bone mass, suggesting that blockage of the Hh signaling pathway in the osteoclast lineage plays a protective role against age-related bone loss. Our findings reveal a specific role of the Hh signaling pathway in bone resorption, and highlight that its inhibitors show potential as therapeutic agents that block osteoclast formation in the treatment of senile osteoporosis.

***Disclosures: Ryuma Haraguchi**, None*

P-448

Sexual dimorphism in early osteoclasts demonstrates enhanced inflammatory pathway activation in female cells *Se Hwan Mun[1], Sandra Jastrzebski[2], Judy Kalinowski[3], Steven Zeng[1], Seyeon Bae[1], Eugenia Giannopoulou[1], Nazir M Khan[4], Hicham Drissi[4], Bongjin Shin[3], Sun-Kyeong Lee[3], Joseph Lorenzo[3], Kyung-Hyun Park-Min[1]. [1]Hospital for Special Surgery, United States, [2]University of Connecticut Health Center, United States, [3]University of Connecticut Health, United States, [4]Emory University, United States

Sexual dimorphism of the skeleton is well-documented. At maturity, the male (M) skeleton is larger and has a higher bone density than the female (F). However, the underlying mechanisms for these differences remain incompletely understood. We examined sexual dimorphism in the formation of osteoclasts (OC) between cells from F and M mice. In vivo we found that the number of OC in bones was greater in F (typically 2.5-3 x greater, $p<0.01$). Similarly, in vitro osteoclast differentiation and pit formation were accelerated in cultures of F highly purified osteoclast precursor (OCP) cells or bone marrow macrophages, treated with M-CSF and RANKL (typically ~ 1.5 - 2 x greater in F, $P<0.01$). To further characterize sex differences between F and M early OC, we performed unbiased RNA-sequencing analysis of cultured, murine bone marrow OCPs, which were treated for 3 days with M-CSF and RANKL. We found 125 differentially expressed genes (DEGs) that were significantly regulated in a sex-dependent manner. Only 9 DEGs were located on sex chromosomes. Transcriptional sexual dimorphism was found to be predominately mediated by genes involved in innate immune and inflammatory response pathways. Gene set enrichment analysis (GSEA) showed that the pathways related to inflammatory response, allograft rejection, IL6_JAK_STAT3 signaling, UV-response up, and interferon gamma response were enriched in sex-dimorphic genes in early OCs. Upstream regulator analysis of Ingenuity Pathway Analysis also showed that the responses to inflammatory mediators were higher in F early OCs compared to M early OCs. We then used GSEA to identify transcription factor-binding motifs that are enriched in the promoters of sex-dimorphic genes. The binding motifs for Ets2, PU.1, EN1, NF-?B, and NFATc1 were significantly enriched in the promoters of sex-dimorphic genes. Although both RANK expression and the proximal RANKL-signaling pathways were comparable between females and males, accumulation of both nuclear p65 and NFATc1 was significantly increased in female OCPs compared to male OCPs on day 1 after RANKL stimulation, which partially explains the differences in transcriptomic sexual-dimorphism in OCs. Collectively, our findings identify a sex-dependent intrinsic difference in early osteoclasts, which results from an altered response to osteoclastogenic stimulation. In humans, these differences could contribute to the lower peak bone mass and increased risk of osteoporosis of females relative to males.

***Disclosures: Se Hwan Mun**, None*

P-449

Dectin-2, a Fc receptor gamma-harboring receptor, regulates foreign body reaction by interfering with intracellular calcium oscillation. *Hiroyuki Okada[1], Hiroshi Kajiya[2], Yasunori Omata[3], Koji Okabe[2], Takeshi Miyamoto[4], Sakae Tanaka[3]. [1]Center of Disease Biology and Integrative Medicine, Faculty of Medicine, the University of Tokyo, Japan, [2]Department of Physiological Science and Molecular Biology, Fukuoka Dental College, Japan, [3]Department of Orthopaedic Surgery, The University of Tokyo, Japan, [4]Department of Orthopaedic Surgery, Faculty of Life Science, Kumamoto University, Japan

Dectin-2, a mannose receptor expressed in dendritic cells and macrophages, is coupled with Fc receptor gamma (FcRγ), an immunoreceptor tyrosine-based activation motif (ITAM) adaptor. Dectin-2 has an important role in host defense against Candida and Mycobacterium. Recent report showed that Dectin-2 in tissue macrophage has a crucial role in the pathogenesis of aortitis. However, the role of Dectin-2 in the differentiation of osteoclasts (OCs) and foreign body giant cells (FBGCs) remains unknown.Methods: OCs were induced from murine bone marrow macrophages (BMMs) by four-day treatment with M-CSF and RANKL, and FBGCs by three-day treatment with GM-CSF and IL-4. Gene expression of Dectin-2 was evaluated by RT-PCR. Intracellular localization of Dectin-2 was confirmed by immunocytochemistry. The role of Dectin-2 on osteoclastogenesis in vivo was examined by bone densitometry, and the role in FBGCs was histologically examined using an intraperitoneal sponge grafting model. Finally, calcium oscillation in BMMs, a downstream signal of ITAM receptors, was analyzed using calcium indicator Fura-2. BMMs form Dectin-2 KO and FcRγ KO mice were also used.Results and Discussion: Expression of Dectin-2 was increased in both OCs and FBGCs, especially in FBGCs, during the course of their differentiation. Dectin-2 was colocalized with FcRγ on the plasma membrane. BMD of Dectin-2 KO and FcRγKO mice was not changed compared to wild type mice. In contrast, foreign body reaction caused by intraperitoneal sponge grafting was reduced in Dectin-2 KO and FcRγKO mice. Finally, the analysis of frequency of calcium oscillations in BMMs showed that slow waves were increased in FcRγ KO BMMs before GM-CSF and IL-4 stimulation, and in Dectin-2 KO mice after stimulation with cytokines.In this study, we found that Dectin-2 was localized on cellular membrane and interfered with downstream calcium oscillations. Dectin-2 had an important role especially in the differentiation of FBGCs and foreign body reaction.

***Disclosures: Hiroyuki Okada**, None*

P-450

Acetylcholinesterase in osteoclastogenesis and osteoporosis via ACh-independent pathway *Xiaohe LUO[1], Chunyi WEN[1]. [1]The Hong Kong Polytechnic University, Hong Kong

PurposeAcetylcholinesterase (AChE), originally known as an enzyme to hydrolyze ACh, has been demonstrated to regulate skeletogenesis via both cholinergic[1] and non-cholinergic pathways[2]. Recent research claims that cholinergic activity favors bone mass by inhibiting AChE[3]. However, AChE in bone regulation via ACh-independent pathway remains largely unknown. Moreover, osteoclasts-mediated bone resorption plays a pivotal role in bone homeostasis and diseases. Compared to osteogenesis and bone development, AChE in osteoclastogenesis and bone degeneration is still poorly understood.Here, we aimed to investigate the expression pattern of endogenous AChE during osteoclastogenesis; the effects of exogenous AChE/heat-inactivated AChE in osteoclastogenesis; the pharmaceutical inhibition of AChE both in vitro and in vivo.Methods15 ng/ml soluble RANKL was used to induce osteoclastogenesis of RAW 264.7 cells. Recombinant AChE, AChE inhibitors Donepezil and Galantamine were added during osteoclastogenesis respectively. Sham/OVX Balb/C mice were treated with Donepezil. Quantitative RT-PCR of TRAP, RANK, MMP9 and ACHE; TRAP and IF staining were performed.Results and ConclusionDuring differentiation, mRNA and protein levels of endogenous AChE first increased (Fig.A,B), sharing a same trend of mRNA expression of osteoclast-markers (TRAP, RANK and MMP9), suggesting AChE may play an emerging role in regulating osteoclastogenesis.By TRAP staining, larger size osteoclasts were observed in AChE/heat-inactivated AChE groups, indicating the non-enzymatic effect of AChE in osteoclastogenesis. Higher concentration of AChE/heat-inactivated AChE were associated with increased nuclear NO. in single TRAP+ cell and mRNA levels of cell-cell fusion markers (OC-STAMP, DC-STAMP), pointing that AChE may contribute to cell-cell fusion of OCs (Fig.D-F).AChE inhibitor Donepezil could inhibit osteoclastogenesis in vitro, decreased NO. of OCs was observed in Donepezil-treated OVX mice, indicating the potential therapeutics of osteoporosis by inhibiting AChE. (Fig.G,H) Donepezil but not Galantamine inhibited osteoclastogenesis in vitro. Donepezil binds to both catalytic and peripheral site of AChE, while Galantamine only binds to the catalytic site, suggesting the peripheral site may contribute to cell-cell fusion of OCs. (Fig.I,J)References1.Eimar, H., J Musculoskelet Neuronal Interact, 2013.2.Spieker, J., PLOS one, 2016. 3.Ma, Y. & F. Elefteriou, J Bone Miner Res, 2020.

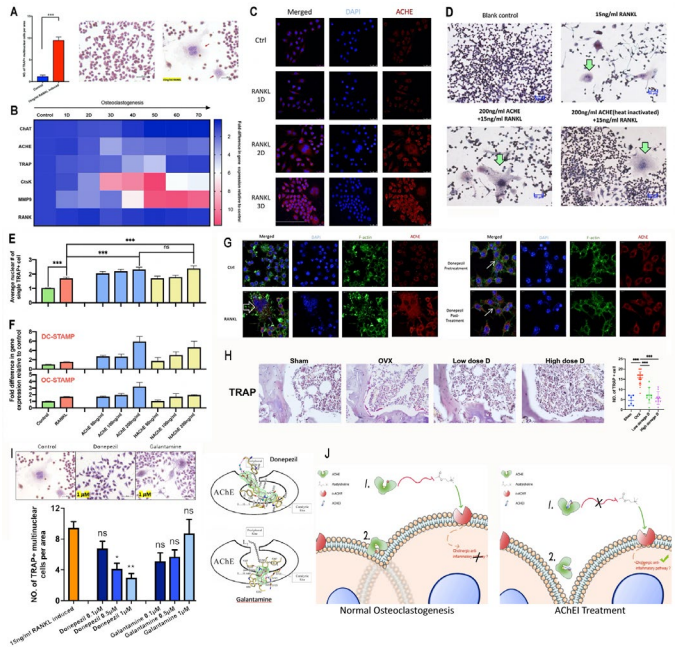

***Disclosures: Xiaohe LUO**, None*

P-451

Regulatory network mediated by RBP-J/NFATc1-miR182 controls inflammatory bone resorption. *Kazuki INOUE[1], Xiaoyu Hu[2], Baohong Zhao[1]. [1]HOSPITAL FOR SPECIAL SURGERY, United States, [2] Institute for Immunology and School of Medicine, Tsinghua University, China

Bone resorption is a severe consequence of inflammatory diseases associated with osteolysis, such as rheumatoid arthritis (RA), often leading to disability in patients. In physiological conditions, the differentiation of bone-resorbing osteoclasts is delicately regulated by the balance between osteoclastogenic and anti-osteoclastogenic mechanisms. Inflammation has complex impact on osteoclastogenesis and bone destruction, and the underlying mechanisms of which, especially feedback inhibition, are underexplored. Here, we identify

Posters

a novel regulatory network mediated by RBP-J/NFATc1-miR182 in TNF-induced osteoclastogenesis and inflammatory bone resorption. This network includes negative regulator RBP-J and positive regulators, NFATc1 and miR182, of osteoclast differentiation. In this network, miR182 is a direct target of both RBP-J and NFATc1. RBP-J represses, while NFATc1 activates miR182 expression through binding to specific open chromatin regions in the miR182 promoter. Inhibition of miR182 by RBP-J servers as a critical mechanism that limits TNF-induced osteoclast differentiation and inflammatory bone resorption. Inflammation, such as that which occurs in RA, shifts the expression levels of the components in this network mediated by RBP-J/NFATc1-miR182-FoxO3/PKR (previously identified miR182 targets) towards more osteoclastogenic, rather than healthy conditions. Treatment with TNF inhibitors in RA patients reverses the expression changes of the network components and osteoclastogenic potential. Thus, this network controls the balance between activating and repressive signals that determine the extent of osteoclastogenesis. These findings collectively highlight the biological significance and translational implication of this newly identified intrinsic regulatory network in inflammatory osteoclastogenesis and osteolysis.

***Disclosures: Kazuki INOUE**, None*

P-452

Zoledronic acid is not equally potent on osteoclasts generated from different individuals – osteoclasts from smokers are less sensitive *Anaïs MJ Møller[1], Jean-Marie Delaisse[2], Jacob B Olesen[2], Troels Bechmann[3], Jonna S Madsen[4], Kent Søe[2]. [1]Clinical Cell Biology, University Hospital of Southern Denmark, Dept. of Regional Health Research, University of Southern Denmark, Denmark, [2]Clinical Cell Biology, Odense University Hospital, Dept. of Clinical Research, University of Southern Denmark, Denmark, [3]Dept. of Oncology, Lillebaelt Hospital, University Hospital of Southern Denmark, University of Southern Denmark, Denmark, [4]Dept. of Immunology and Biochemistry, Lillebaelt Hospital, University Hospital of Southern Denmark, University of Southern Denmark., Denmark

Zoledronic acid is a bisphosphonate, commonly used to treat bone diseases such as osteoporosis and cancer induced bone disease. However, patients show a variable sensitivity to zoledronic acid and the reason remains unclear. The objective of this study was to obtain more knowledge in this regard. We hypothesized that osteoclasts generated from different individuals will show a variable sensitivity to zoledronic acid in vitro. Osteoclasts were generated using monocytes from 46 healthy female blood donors (40-66 years). Matured osteoclasts were reseeded onto bone slices pre-coated with different concentrations of zoledronic acid and e.g. IC50 and maximum inhibition values were determined based on the eroded bone surface after 3 days of resorption. We found that the IC50 for inhibition of osteoclastic bone resorption varied from 0.06 to 12.57 µM zoledronic acid (median of 0.26 µM) and the dose for maximum inhibition varied from 0.3 to 50 µM (median of 2 µM), thus a more than 200- and 167-fold difference, respectively, in sensitivity to zoledronic acid among osteoclasts from different healthy individuals. Multiple linear regression analyses showed that the determined IC50 correlated with: 1. smoking habits – osteoclasts from smokers were less sensitive than those of non-smokers; 2) the average number of nuclei per osteoclast in vitro – more nuclei made osteoclasts less sensitive. Further analyses showed that: 3. increasing protein levels of mature cathepsin K in osteoclast cultures rendered the osteoclasts less sensitive to zoledronic acid; 4. surprisingly, neither gene nor protein expression of farnesyl diphosphate synthase was found to correlate with the sensitivity to zoledronic acid; 5. in 1/3 of the cultures, zoledronic acid had no negative impact on the metabolic activity neither at IC50 nor at maximum inhibition; 6. trench-forming osteoclasts were found to be more sensitive to zoledronic acid than those making pits in the same cell culture; Thus, we conclude that there indeed is a high degree of variation in the potency of zoledronic acid on osteoclasts when generated from different individuals. We propose that these findings may explain at least some of the variance observed in patients. These findings may therefore be of clinical importance, which is currently being investigated in a clinical trial combining in vitro and in vivo investigations.

***Disclosures: Anaïs MJ Møller**, None*

P-453

Galectin-8 is Involved in Osteoclastic Formation and Activity *Michèle ROY[1], Elizabeth STEPHENS[1], Sophie BOUHOUR[1], Sophie ROUX[1]. [1]Sherbrooke University, Canada

Introduction: The best characterized functions of galectin-8, a β-galactoside-binding lectin encoded by LGALS8, are performed extracellularly, where it binds glycans to modulate cell-matrix interactions and triggers signaling cascades mediated by integrin and organization of the cytoskeleton. The functions of intracellular galectin-8 are less well known, but cytosolic galectin-8 is a danger recognition receptor, which has been implicated in selective autophagy. While an increase in osteoclastogenesis and bone resorption has been reported in transgenic mice overexpressing galectin-8 secondary to an increase in RANKL production by osteoblasts (Vinik et al, 2015), we wondered if galectin-8 could have a direct impact on osteoclasts, in particular by modulating the processes associated with vesicle trafficking such as autophagy or bone resorption. Indeed, we have previously demonstrated a differential expression of galectin-8 splicing variants in the osteoclasts of Paget's disease of bone characterized by overactivity of these cells.Methods: Using human osteoclasts generated in vitro from cord blood monocytes, this study was aimed to characterize galectin-8 involvement in osteoclastic formation, bone resorbing activity and basal autophagy. All experiments were performed after specific knock-down of LGALS8 expression using DsiRNA transfected in mature osteoclasts.Results: Inhibiting galectin-8 expression was associated with a significant decrease in the bone resorption area, and in the number of multinucleated cells (MNCs) compared to cells transfected with a negative control (bone resorption: -58%; MNCs -45%, both $p<0.05$), or to non-transfected cells. By immunoblots, we also evaluated LC3II/LC3I ratio, a reliable marker of autophagic vesicles, and observed a significant increase in this ratio in basal conditions in LGALS8 knock-down cells compared to cells transfected with a negative control (+52%, $p<0.05$), and in non-transfected cells as well. This increased in basal autophagy could be due to the inactivation of mTORC1, as a trend to decrease in 4EBP1 phosphorylation, a well-known substrate of mTOR, was also observed in the same conditions (-55%, LGALS8 DsiRNA vs negative control, ns).Conclusion: Galectin-8 appears as a new player in human osteoclast biology that could be involved in the regulation of osteoclast formation and bone resorption. Galectin-8 might impact osteoclastic activity through mTOR signaling, although mechanisms remain to be elucidated.

***Disclosures: Michèle ROY**, None*

P-454

Senescence-dependent increase of CpG methylation at receptor activator NF-κB (RANK) gene promoter impairs osteoclastogenesis by decreasing RANK-positive osteoclast precursors *Riko Kitazawa[1], Ryuma haraguchi[2], Yukihiro Kohara[2], Sohei Kitazawa[2]. [1]Ehime University Hospital, Division of Diagnostic Pathology, Japan, [2]Ehime University Graduate School of Medicine, Department of Molecular Pathology, Japan

Receptor activator of NF-κB (RANK) is a member of the tumor necrosis factor receptor (TNFR) family expressed in osteoclast precursors, and RANK-RANK ligand (RANKL) signaling plays a central role in differentiation, activation and survival of osteoclasts. The 5'-flanking region of the mouse RANK gene lacks canonical TATA-box but contains four continuous Sp-1 binding sites with clustered CpG-loci (CpG-island) around the transcription and translation start sites. In this study, the passage-dependent and age-related change in osteoclastogenesis and RANK expression relative to the methylation status of its gene promoter was investigated. Quantitative RT-PCR disclosed that the steady-state expression of RANK mRNA of RAW cells was lower at passage 40 (P40) than at P18; also, RANKL-induced osteoclastogenesis as well as the expression of TRACP and CTSK mRNA was significantly lower at P40 than at P18. Mirroring the passage-dependent reduction in osteoclastogenesis, both methylation-specific PCR and bisulfite mapping of the CpG-island region (-150 /+110, adjacent to transcription and translation start sites) showed a higher frequency of CpG methylation at P40 than at P18. Morphologic detection of sequence-specific methylated cytosine by the newly established ICON-probe technique revealed that the number of cells positive for RANK gene promoter methylation increased significantly at P40. Conversely, pre-treatment with demethylating agent 5-Aza-dC restored the expression of RANK gene and RANKL-induced osteoclastogenesis at P40. Reflecting the in vitro passage-dependent increase of CpG methylation of the cultured RAW cells, RANK gene promoter methylation in mono-nucleated cells of mouse spleen and bone marrow tissue disclosed a higher rate of methylation-positive and RANK-negative populations in 12-month-old mice than in 10.5-week-old ones. These data suggest that DNA methylation at CpG-island in the RANK gene promoter occurs in an age-related manner (the so-called type-A methylation), which may explain, in part, the impairment of bone resorption activity by reduced osteoclastogenesis, namely impairment of the coupling of bone resorption and bone formation, in the elderly.

***Disclosures: Riko Kitazawa**, None*

P-455

An Uncommon Cause of Toothache: A New Perspective on Eagle Syndrome *Sanne Treurniet[1], Jeroen Jansen[2], Leo van Ruijven[3], Ton Langeveld[2], Tim Forouzanfar[4], Nathalie Bravenboer[5], Elisabeth Eekhoff[1]. [1]Department of Internal Medicine, Amsterdam University Medical Center, location VUmc, Amsterdam Movement Sciences, Amsterdam, The Netherlands, Netherlands, [2]Department of otolaryngology, Leiden University Medical Center, Leiden, The Netherlands, Netherlands, [3]Department of Oral Cell Biology and Functional Anatomy, ACTA-University of Amsterdam and VU University, Amsterdam Movement Sciences, Amsterdam, The Netherlands, Netherlands, [4]Department of Oral and Maxillofacial Surgery/Pathology, Amsterdam University Medical Centers, location VUmc, Vrije Universiteit Amsterdam, Amsterdam, The Netherlands, Netherlands, [5]Department of Clinical Chemistry, Bone and Calcium Metabolism Lab, Amsterdam University Medical Centers, location VUmc, Amsterdam Movement Sciences, Amsterdam, The Netherlands, Netherlands

Introduction. A 44-year old woman presented with pain and nerve compression in the face due to Eagle syndrome. Eagle syndrome was diagnosed after many years of unexplained toothache, pain in the neck and hearing loss. The Eagle syndrome is due to elongation of the styloid process or calcification of the stylohyoid ligament. In this patient, Eagle syndrome was diagnosed on both sides of the neck, which is very rare. Previously performed surgery, at the age of 39, to relieve complaints was not successful. At the age of 42, a second surgery

took place to remove calcified tissue matching with Eagle syndrome on the right side of the neck. Two years later, surgical removal of the calcified tissue on the left side of the neck was performed successfully.Purpose. Follow-up of the clinical symptoms and analysis of the removed tissue from the neck.Method. A [18F]NaF PET/CT scan was conducted preoperatively. Histologic examination and microCT was performed on the removed tissue.Results. Prior to surgery an [18F]NaF PET/CT scan showed no increased uptake of [18F]NaF in the styloid hyoid region, indicating no active bone formation at this site. The tissue removed during surgery is classified as calcified tissue. Histologic examination and microCT revealed cortical and trabecular bone and some areas of cartilage tissue.Conclusion. The molecular mechanism leading to calcification in the styloid region in Eagle syndrome is still unknown. This case-report suggested an endochondral process of bone formation. Further examination of the calcified tissue will take place to investigate the properties of this material.

***Disclosures: Sanne Treurniet**, None*

P-456

RNA-binding protein Cpeb4 is required for osteoclastogenesis. *Masamichi Li[1], Yasuhiro Arasaki[1], Takuro Akiya[1], Iori Nozawa[1], Yoichi Ezura[2], Tadayoshi Hayata[1]. [1]Department of Molecular Pharmacology, Graduate School of Pharmaceutical Sciences and Faculty of Pharmaceutical Sciences, Tokyo University of Science, Japan, [2]Department of Judo Therapy, Faculty of Medical Technology, Teikyo University, Japan

It has been shown that useful therapeutic agents such as an anti-RANKL antibody denosumab could be developed from the identification of osteoclast differentiation factors. As one of the possible factors regulating the osteoclast differentiation, we previously reported that expression of Cytoplasmic polyadenylation element binding protein 4 (Cpeb4), an RNA-binding protein, is increased during osteoclast differentiation. Cpeb4 is involved in various biological aspects and pathogenesis including cancer, fatty liver, erythroid cell differentiation. Cpeb4 mis-splicing is also related to autism-like phenotype. However, the function of Cpeb4 in osteoclast differentiation is unknown. In this study, we aimed to elucidate the function of Cpeb4 in osteoclast differentiation. First, to determine which transcript variants are expressed in RAW264.7 cells, we performed RT-PCR experiment using primer set to amplify exons 2 to 5. We found that variant 2 and variant 3 were expressed out of 4 variants and variant 2 was expressed more abundantly than variant 3. Next, we attempted to generate a stable cell line expressing short hairpin RNA (shRNA) against Cpeb4 using mouse macrophage cell line RAW264.7. We successfully generated a stable cell line expressing Cpeb4 shRNA with approximately 37% reduction of Cpeb4 expression compared to that expressing control shRNA. To determine the function of Cpeb4 during osteoclast differentiation, we treated those cells with RANKL. TRAP staining experiment revealed that depletion of Cpeb4 resulted in a dramatic decrease in osteoclast numbers. Gene expression study also demonstrated that knockdown of Cpeb4 strongly repressed the mRNA induction of Atp6v0d2, Cathepsin K, Dcstamp, Nfatc1, RANK and Acp5 (TRAP) by RANKL, supporting a role of Cpeb4 in RANKL-induced osteoclast formation. Thus, our findings suggest that Cpeb4 is a novel essential regulator for osteoclastogenesis.

***Disclosures: Masamichi Li**, None*

P-457

Role of Lrp1 in RAW264 cells on osteoclast differentiation *Yukihiro Kohara[1], Ryuma Haraguchi[1], Riko Kitazawa[2], Sohei Kitazawa[1]. [1]Department of Molecular Pathology, Ehime University Graduate School of Medicine, Japan, [2]Department of Diagnostic Pathology, Ehime University Hospital, Japan

Low density lipoprotein receptor-related protein 1 (LRP1; also known as CD91), a member of the low-density lipoprotein receptor family, functions as a receptor for several ligands such as α-2 macroglobulin, Apolipoprotein E and tissue plasminogen activator. In human studies, LRP1 single nucleotide polymorphism (SNP) is associated with bone mineral density. While LRP1 is thought to be a suppressor of osteoclast differentiation at late stages, its function at early stages remains unclear. In this study, we generated Lrp1 gene-stable knockdown macrophage cell line RAW264 cells by the lentiviral short hairpin RNA (shRNA) vector to gain insight into the function of Lrp1 in osteoclast precursors. Lrp1 gene stable knockdown RAW264 cells inhibited RANKL-induced osteoclast formation and osteoclastic master transcription factor Nfatc1 mRNA expression as assessed by quantitative RT-PCR. Furthermore, to investigate osteoclast-osteoblast interactions, the conditioned-medium (CM) from Lrp1 knockdown RAW264 cells was harvested during 48-96 h after RANKL stimulation and used in bone marrow stromal cell line ST2 cultures. Surprisingly, the CM of Non-Mammalian shRNA RAW264 cells inhibited alkaline phosphatase (ALP) activity induced by ascorbic acid and β-glycerophosphate compared with the untreated control, whereas the CM of Lrp1 knockdown RAW264 cells nullified the inhibitory effects on ALP activity, suggesting that osteoclast-derived humoral factors inhibit osteoblast differentiation, and that the expression or secretion of these factors is mediated by LRP1. Thus, we propose that LRP1 in macrophages mediates both differentiation into osteoclasts and osteoclast-osteoblast interactions.

***Disclosures: Yukihiro Kohara**, None*

P-458

RNA-binding protein Cpeb4 is localized in nuclei during osteoclast differentiation. *Yasuhiro Arasaki[1], Masamichi Li[1], Takuro Akiya[1], Iori Nozawa[1], Yoichi Ezura[2], Tadayoshi Hayata[1]. [1]Department of Molecular Pharmacology, Graduate School of Pharmaceutical Sciences and Faculty of Pharmaceutical Sciences, Tokyo University of Science, Japan, [2]Department of Judo Therapy, Faculty of Medical Technology, Teikyo University, Japan

Little attention has been paid to the mechanism of osteoclast differentiation by post-transcriptional regulation such as splicing, stability or translation of mRNA. Here we focused on RNA-binding protein Cpeb family consisting of Cpeb1, Cpeb2, Cpeb3 and Cpeb4 as one of the possible factors regulating the osteoclast differentiation through post-transcriptional mechanisms. Quantitative RT-PCR analysis revealed that only Cpeb4 expression out of 4 members was upregulated two days after RANKL stimulation in RAW264.7 cells. Immunofluorescence analysis revealed that Cpeb4 was localized in cytoplasm in untreated RAW264.7 cells, whereas Cpeb4 was localized in nuclear bodies by RANKL stimulation in addition to the cytoplasm. Similar results were also obtained for RANKL-stimulated mouse bone marrow macrophages. To determine the property of the nuclear bodies where Cpeb4 is localized, we performed immunofluorescence analysis using antibodies identifying the nuclear speckle and Cajal bodies. However, Cpeb4 was not colocalized in either of them. Time-course experiment revealed that nuclear localization of Cpeb4 was detected at least 9 hours after RANKL stimulation. Finally, we investigated the downstream pathway of RANKL signaling that may contribute to nuclear localization of Cpeb4 using various inhibitors. The results showed that PI3K-Akt signaling and Nfatc1 activation are important for the localization. Thus, these results suggest that Cpeb4 may be involved in post-transcriptional regulation of differentiating osteoclasts in the nuclei.

***Disclosures: Yasuhiro Arasaki**, None*

P-459

Deletion of the Matrix-Degrading Enzymes MMP13 and Cathepsin K in Osteocytes Regulates Osteocytic Osteolysis and Bone Mass, Protecting the Skeleton in Lactating Mice *Yinbo Niu[1], Jiaming Zhang[1], Ai Orimoto[1], Shuang Liang[1], Dorothy Hu[1], Pamela Dann[2], Daniel Brooks[3], Mary L. Bouxsein[3], John Wysolmerski[4], Francesca Gori[5], Roland Baron[6]. [1]Division of Bone and Mineral Research, Harvard School of Dental Medicine;, United States, [2]Endocrine Section, Yale School of Medicine, United States, [3]Dept of Orthopedics, Beth Israel Deaconess Hospital, United States, [4]: Endocrine Section, Yale School of Medicine, United States, [5]Division of Bone and Mineral Research, Harvard School of Dental Medicine, United States, [6]Division of Bone and Mineral Research, Harvard School of Dental Medicine;, United States

Cathepsin K (Ctsk) and MMP13 are extra-cellular matrix-degrading enzymes secreted by osteocytes (Ocy) in the peri-lacunar space. We showed that targeted deletion of Ctsk in Ocy (Ctskocy) prevented lacunae (Lac) enlargement and bone loss during lactation but did not affect the skeleton at steady state. Since MMP13 is up-regulated by Ctskocy deletion and by lactation, we generated: 1) MMP13ocy mice and 2) MMP13:Ctskocy mice to delete Ctsk from the MMP13ocy mice (Ctsk may compensate for the lack of MMP13). We explored Ocy osteolysis (Olysis), bone remodeling, skeletal homeostasis and Ocy gene expression at steady state (12 wk old females) and in response to 12 days of lactation. μCT and dynamic histomorphometry showed that MMP13ocy mice exhibited a pronounced increase in Tb BV/TV but no changes in bone formation or resorption, suggesting changes that occurred earlier. In contrast, the cortex showed only a marked increase in Ocy Lac area (LacA, p30μ2, $p< 0.01$) by back scattered electron microscopy, but no changes in Ocy canalicular organization by silver stain. Cortical bone qRT-PCR showed a significant decrease in OPG with unchanged RANKL. Bone strength was increased and, importantly, MMP13ocy mice were protected from bone loss during lactation. Deletion of Ctsk in the MMP13ocy mice resulted in a further increase in Tb BV/TV compared to MMP13ocy mice ($p<0.0001$). In contrast to MMP13ocy mice, MMP13:Ctskocy mice had larger cortical volume, thickness and total area, suggesting enhanced periosteal bone formation. Importantly, Ocy LacA and the number of large Lac, both increased in MMP13ocy mice, returned to normal after deletion of Ctsk, suggesting a role of Ctsk in the Lac enlargement observed in MMP13ocy mice. In contrast with the lack of changes observed in MMP13ocy mice, MMP13:Ctskocy mice showed a significant increase in MAR ($p<0.01$) and decrease in osteoclasts ($p<0.05$). Like Ctskocy and MMP13ocy, MMP13:Ctskocy mice were protected from bone loss during lactation, despite a significant increase in serum PTH. MMP13ocy RNA Seq analysis of Ocy identified changes in several signaling pathways known to affect bone cells and remodeling. These results suggest that in Ocy, MMP13 and Ctsk are involved in the regulation of Olysis but also of bone homeostasis. Deleting these enzymes in the Ocy micro-environment prevents peri-lacunar matrix degradation, favors bone mass and prevents the loss of bone induced by lactation.

***Disclosures: Yinbo Niu**, None*

Posters

P-460

Kalirin regulates Osteocyte Dendrite Connectivity and Function *Jung Min Hong[1], Kornchanuk Joy Wayakanon[1], Loan Do[1], Tehrune Tyler[1], Sung-Kyung Kin[2], Kawak Stephanie[2], Su Huang[1], Angela Bruzzaniti[1]. [1]Indiana University School of Dentistry, United States, [2]Indiana University, United States

Communication among bone cells, especially osteocytes, is important for the maintenance of bone mass. However, the intracellular proteins that control the morphology and function of osteocytes, and their ability to communicate with other bone cells are still unknown. Kalirin is a multi-domain GDP/GTP-exchange factor protein that activates the Rho GTPases. A rare missense mutation in the Kalirin gene (KALRN) in female and male siblings was shown to cause short stature and delayed bone age, among other abnormalities. Previously, we found that lack of Kalirin (Kal-KO) leads to the loss of trabecular and cortical bone mass, consistent with the human findings. In addition to its expression in osteoblasts and osteoclasts, our data revealed Kalirin expression in osteocytes, where it was localized to the perinuclear region and to the dendritic processes. Moreover, mRNA expression of Dmp1, Sost, Phex and RANKL was decreased in Kal-KO long bones (marrow flushed). Based on the possible role of Kalirin on the morphology and function of osteocytes, we examined the role of Kalirin in regulating osteocyte connectivity and the mechanism of osteocyte dendritic elongation. Analysis of the lacunar-canalicular system with basic fuchsine staining revealed shorter canaliculi in Kal-KO mice, compared to wild-type (WT), although lacunar density was similar between genotypes. Ex vivo analysis of osteocytes from collagenase-digested long bones also revealed shorter and fewer dendrites in Kal-KO osteocytes, which was associated with a dramatic decrease in both ERK levels and RhoA activation, compared with WT osteocytes. We identified the GTP-exchange factor domain 1 (GEF1) of Kalirin as the predominate dendrite-lengthening domain. Overexpression of GEF1 caused dendrite elongation in MLO-Y4 cells via activation of ERK and RhoA, while chemical inhibition of these pathways led to dendrite shortening. Overall, these results suggest that Kalirin controls osteocytic connectivity and function in part by regulating cytoskeletal remodeling through the activity of ERK and RhoA. Consequently, Kalirin may control the bone remodeling cycle by regulating osteocyte signaling to osteoclasts and osteoblasts.

***Disclosures: Jung Min Hong**, None*

P-461

Deletion of Gata4 from cells of the osteoblast lineage increases bone mass in mice and blunts the stimulation of RANKL expression by pro-senescence signals *Ha-Neui Kim[1], Aaron Warren[1], Elisabeth Ferreira[1], Wen Ling[1], Srividhya Iyer[2], Charles O'Brien[1], Maria Almeida[1]. [1]University of Arkansas for Medical Sciences, United States, [2]University of Colorado School of Medicine, United States

As in humans, aging in mice leads to cortical thinning and increased cortical porosity associated with increased bone remodeling. Production of the osteoclastogenic cytokine RANKL by osteocytes increases with age in mice and is essential for the loss of cortical bone and increase in cortical porosity. The age-related increase in RANKL expression is associated with increased markers of cellular senescence in osteocyte-enriched cortical bone, including increased levels of Gata4, a transcription factor that mediates expression of the senescence associated secretory phenotype (SASP). However, the molecular mechanisms responsible for the increased RANKL expression and osteoclast number in cortical bone with age are unclear. To determine whether cellular senescence can stimulate RANKL production, we examined the ability of several well-established inducers of senescence, such as irradiation, etoposide, and H2O2, to stimulate RANKL expression in cultured osteoblastic cells and osteocyte-enriched organ cultures. Induction of cellular senescence increased RANKL production in each of these murine culture models as well as in human fibroblasts, suggesting a potential explanation for elevated RANKL levels with age. The increase in RANKL was associated with higher protein levels of Gata4 and elements of the SASP. Moreover, over-expression of Gata4 stimulated RANKL expression in primary cultures of murine osteoblastic cells. To determine whether Gata4 in osteocytes is required for the senescence-induced expression of RANKL, we generated mice lacking Gata4 in the entire osteoblast lineage using Osx1-Cre (Gata4ΔOsx1). Irradiation of femoral shaft organ cultures from 3-month-old Osx1-Cre control littermate mice increased RANKL protein levels but this effect was prevented in organ cultures from Gata4ΔOsx1 mice. Three-month-old female Gata4ΔOsx1 mice had higher femoral and spinal BMD than Osx1-Cre littermates as determined by DXA. In contrast, Gata4ΔOsx1 male mice had no changes in BMD. Micro-CT analysis of L5 vertebra and femur from female mice revealed increased BV/TV associated with increase trabecular number and trabecular thickness. Overall, these findings support the working hypothesis that Gata4 in osteocytes stimulates RANKL expression to promote bone remodeling during growth and aging.

***Disclosures: Ha-Neui Kim**, None*

P-462

Increased bone mass, bone formation, and bone resorption caused by adult onset compound deletion of Sik2 and Sik3 in mice *Marc Wein[1], Christian D Castro Andrade[1], Kathy Cheng-Chia Tang[1], Daniel J Brooks[1], Janaina da Silva Martins[1], Marc Foretz[2], Mary L Bouxsein[1]. [1]Massachusetts General Hospital, Harvard Medical School, United States, [2]Université de Paris, Institut Cochin, France

Background:Salt inducible kinases (SIK) control parathyroid hormone action in osteocytes downstream of cAMP and protein kinase A. Previous work by our lab demonstrated that in vivo combined deletion of Sik2 and Sik3 in osteocytes and osteoblasts using DMP1-Cre showed dramatic increase in bone mass, increased bone turnover, and gene expression changes similar to those seen with constitutive PTH signalling. These results suggest that SIK2/3 inhibitors may represent a new class of PTH-like small molecules. However, the organism-wide consequences of deleting these kinases in postnatal mice remains to be determined. Here, we addressed this problem by breeding Sik2/3 floxed mice to ubiquitin-CreERt2 animals to achieve ubiquitous deletion of these kinases in a tamoxifen-dependent manner.Methods:6 week old control (Sik2f/f ; Sik3f/f) or Sik2/3 DKO (Sik2f/f ; Sik3f/f ; ubiquitin-CreERt2) mice were treated with tamoxifen (1 mg, IP, Q48H, 3 doses total). Animals were sacrificed 21 days after the first tamoxifen injection and skeletal phenotypes were assessed by micro-CT, histology, histomorphometry, and serum bone turnover markers. Results:Combined Sik2/3 deletion in adult mice led to a dramatic increase in trabecular bone mass and growth plate expansion by micro-CT (Figure) without causing overt health effects. Fasting serum turnover biomarkers showed accelerated bone turnover with elevated P1NP (bone formation, p<0.0001) and CTX (bone resorption, p=0.00017) levels in Sik2/3 DKO mice. Other skeletal parameters such as Trabecular BV/TV (p=0.0012), trabecular number (Tb.N) (p=0.0001), trabecular thickness (Tb.Th) (p=0.0148), trabecular spacing (Tb.Sp) (p=0.00089) and cortical porosity (p=0.0185) are also significantly higher in Sik2/3 mutants versus tamoxifen-treated control mice. Also, elevated tartrate-resistant acid phosphatase (TRAP) staining was observed in the mutant mice compared to tamoxifen-treated control animals, consistent with increased bone resorption. Furthermore, histomorphometry analysis showed significant higher numbers of osteoblasts (N.Ob/T.Ar) (p=0.0006) and osteoclasts (N.Oc/T.Ar) (p=0.001) per tissue area. Bone formation rate (BFR/TV) (p=0.0053) and fibrocyte volume (Fb.V/TV) (p=0.0012) per tissue volume are also significantly increased in Sik2/3 DKO mice versus tamoxifen-treated controls. Finally, serum analysis of Sik2/3 DKOs showed elevated levels of alkaline phosphatase (p<0.0001) and calcium (p=0.0245) without affecting phosphorus levels.Conclusion:Global loss of Sik2 and Sik3 in vivo using the tamoxifen-induced CreERt2 under the control of ubiquitin promoter led to significantly increased bone mass, bone formation and bone resorption. Differences at the level of bone resorption exist between genetic Sik2/3 deletion and our previous results using pharmacologic SIK inhibitors, supporting sthe notion that Sik2/3 inhibitors may represent a promising new class of pharmacologic agents for osteoporosis treatment.

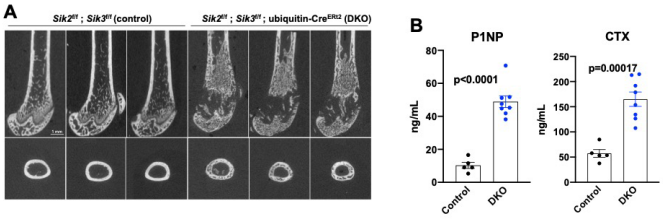

Figure 1. (A) Micro-CT of the femur of mice 3 weeks after tamoxifen treatment. Compound *Sik2/3* mutants show increased growth plate expansion, trabecular bone mass, and cortical porosity versus tamoxifen treated control mice. (B) Fasting serum analysis shows increased P1NP (left) and CTX (right) levels in *Sik2/3* DKO mice versus controls.

***Disclosures: Marc Wein**, Galapagos NV, Grant/Research Support, Radius Health, Inc, Grant/Research Support*

P-463

PTH protects osteocytes from oxidative stress-induced death and senescence *Yuhei Uda[1], Roberto Santos[1], Alejandro Kochen[1], Carly Newell[1], Anna Tse[1], Paola Divieti Pajevic[1]. [1]Henry M. Goldman School of Dental Medicine, Boston University, United States

Osteoporosis, one of the major skeletal disorders during aging, is characterized by uncoupled osteoblast and osteoclast activities. Parathyroid hormone (PTH) is widely used in the clinic to treat osteoporosis due to its anabolic actions on bone, which require signaling via the PTH receptor (PPR). PPR is highly expressed in cells of the osteoblastic lineage, including osteocytes. Osteocytes are the most abundant cells in bone and serve as a key regulator of bone remodeling. Despite the significant role of PPR signaling in skeletal homeostasis, its function during aging remains unclear. Preliminarily, we have demonstrated that mice lacking PPR in osteocytes (Dmp1-PPRKO) display marked age-related bone loss driven by increased bone resorption and suppressed bone formation. In these mice, with aging, there is a significant decrease in osteoprogenitors and an increase in bone marrow

adiposity, reminiscent of skeletal senescence. We hypothesized that PPR signaling protects osteocytes from senescence and oxidative stress. To test this hypothesis, we designed an in vitro approach and established an osteocytic cell line in which the PPR expression was ablated using CRISPR/Cas9 technique. Ocy454-PPRKO and Ocy454-PPRCtrl cells were used to examine whether PTH protects osteocytes from oxidative stress. Cells were treated with PTH prior to exposure to hydrogen peroxide (H2O2) and cell viability was measured by resazurin-based assays. PTH treatment significantly suppressed the increase in H2O2-induced death in PPRCtrl cells. As expected, the protective effect of PTH was not observed in PPRKO cells. High levels of reactive oxygen species (ROS), including hydrogen peroxide, promote protein and DNA oxidation, resulting in cell death. We analyzed the production of ROS using a fluorescent probe and found that PTH treatment significantly reduced the increase in ROS levels induced by H2O2 treatment, suggesting an antioxidant function of PTH in osteocytes. Oxidative stress is one of the causes of senescence. To further investigate if PTH prevents osteocytes from oxidative stress-induced senescence, we examined senescence-associated (SA) β-galactosidase activity in cells treated with PTH and exposed to low doses of H2O2. Compared to untreated and PPRKO groups, treatment with the hormone significantly decreased the number of SA-βgal positive cells, demonstrating that PPR signaling protects osteocytes, and possibly other osteoblastic cells, from H2O2-induced cellular senescence.

***Disclosures: Yuhei Uda**, None*

P-464

PPARG in Osteocytes Regulates Sclerostin Expression, Bone Mass and Marrow Adiposity *Sudipta Baroi[1], Piotr Czernik[1], Amit Chougule[1], Patrick Griffin[2], Beata Lecka-Czernik[1]. [1]University of Toledo, College of Medicine and Life Sciences, United States, [2]The Scripps Research Institute, United States

Peroxisome proliferator activated receptor gamma (PPARG) is a transcription factor known for regulating energy metabolism and insulin sensitivity; however, its role in regulation of osteocyte function is largely unknown. In this study, we report that PPARG is abundantly expressed in osteocytes, as compared to endosteal osteoblasts, and is transcriptionally essential for sclerostin production. Mice lacking PPARG primarily in osteocytes (γOTKO) have increased bone mass and decreased marrow fat, and there is an excellent correlation of sclerostin protein level in osteocytes with the level of PPARG deletion. This is paralleled by increased WNT signaling and bone forming activity of endosteal osteoblasts. Moreover, osteocyte conditioned medium depleted of sclerostin decreases adipogenesis in recipient bone marrow stromal cells consistent with decreased marrow adiposity in γOTKO mice. Examination of 8 kb sequence upstream of Sost gene transcription start site (TSS), using position weighted matrix prediction for transcription factors binding sites (JASPAR), revealed multiple PPARG binding elements (PPREs). Two of them, with highest scores for consensus PPARG binding sequence, were chosen for further analysis. Chromatin immunoprecipitation assays (ChIP) showed that PPARG binds to both PPREs. Interestingly, pharmacologic modulation of PPARG activity with full agonist rosiglitazone increases PPARG binding to both PPREs and increases sclerostin mRNA and protein expression. Consistently, γOTKO mice are at least partially resistant to the negative effects of rosiglitazone on bone. These findings indicate that transcriptional activities of PPARG are essential for sclerostin expression in osteocytes and support consideration of targeting PPARG activities with selective modulators to treat osteoporosis.

***Disclosures: Sudipta Baroi**, None*

P-465

ABT263 attenuate irradiation-induced bone loss in mice through cleaning senescent osteocytes and inhibiting SASP production *Qinghe Geng[5], Shen Wang[2], Han Huan[3], Juan Zhai[1], Huabei Sun[0], Yilong Guo[0], Ke Heng[4], Hanjun Guo[5], Huaiyuan Zhai[6], Hongwei Li[0], Guangliang Su[7], Qing Zhang[5], Junnian Zheng[0]. [5]Central Lab, Pizhou Hospital, Xuzhou Medical University, China, [2]Guangxi Medical Universtiy, China, [3]Nanjing University of Chinese Medicine, China, [1]Central Lab, Pizhou Hospital, Xuzhou Medical University, China, [0]Central Lab, Pizhou Hospital, Xuzhou Medical University, China, [4]Changzhou Second Hospital, Nanjing Medical University, China, [5]Xuzhou Medical University, China, [6]Ruidong Hospital of Nanjing, China, [0]Xuzhou Medical University, China, [7]Yongcheng City Hospital, Henan, China

Radiotherapy widely treats life-threatening cancers effectively in clinic, but also injuries neighboring healthy tissues, in which skeletal system is usually involved. Cellular senescence of osteocytes and senescence-associated secretory phenotype (SASP) plays a causative role in pathogenesis of radiation-induced osteoporosis, suggesting great benefits of senolytic drugs in preventing radiation-induced bone loss through clearance of senescent cells. To determine the effects of ABT263, a specific inhibitor of anti-apoptotic protein BCL-2 and BCL-xL, on senescent osteocyte clearance and radiation-induced bone loss, 2-m-old C57 mice were irradiated focusing on femoral metaphyseal region with a single dose of 24 Gy and treated with vehicle or ABT263, and followed by molecular, histomorphometric and biomechanical tests 8 weeks after focal radiation treatment (FRT). We found that senescence-associated beta-galactosidase (SA-β-gal) activity, cellular senescence markers, including p16Ink4a, p21, and p53, and SASP factors were significantly higher in irradiated femoral bone tissue of irradiated mice than non-irradiated control mice, while bone mineral density (BMD) and trabecular bone mass were lower than non-irradiated control mice, suggesting success establishment of FRT mouse model. Notably, the irradiated mice treated with ABT263 had reduced senescent-cell burden, including fewer SA-β-gal+ osteocytes and lower expression of senescence markers (p16Ink4a, p21 and p53) and SASP factors, and higher BMD than that of vehicle-treated irradiated mice. Consist with this, biomechanical tests of irradiated femora revealed that maximum load, yield load, ultimate displacement, yield displacement, stiffness, and energy absorption of femora were lower in irradiated mice than non-irradiated mice. While this decrease was significantly reversed in ABT263-treated irradiated mice than vehicle-treated mice. Therefore, our data indicate a radioprotective role of ABT263 in radiation-induced osteoporosis through clearing senescent osteocytes and inhibiting SASP production.

***Disclosures: Qinghe Geng**, None*

P-466

Late Osteoblast- and Osteocyte-Derived NOTUM Regulates Cortical Bone Mass in Mice *Karin H. Nilsson[1], Petra Henning[1], Maha Abdelghaffar[1], Jianyao Wu[1], Ulf H. Lerner[1], Claes Ohlsson[1], Sofia Movérare-Skrtic[1]. [1]Centre for Bone and Arthritis Research, Institute of Medicine, Sahlgrenska Academy at University of Gothenburg, Gothenburg, Sweden, Sweden

Osteoporosis is a common skeletal disease, leading to increased risk of fractures. Current osteoporosis treatments primarily reduce risk of fracture in the vertebrae, mainly dependent on trabecular bone, while most fractures occur at non-vertebral bone sites, mainly dependent on cortical bone. WNT signaling is a crucial regulator of bone homeostasis. The activity of WNTs is inhibited by NOTUM, which is a secreted WNT lipase highly expressed by osteoblast lineage cells in the cortical bone. We previously demonstrated that conditional inactivation of NOTUM in all osteoblast lineage cells using the Runx2-Cre mouse model specifically increased the cortical bone thickness, with an unchanged trabecular bone phenotype(1). To determine if NOTUM with an impact on cortical bone is mainly derived from osteoblast precursors/early osteoblasts or from late osteoblasts/osteocytes, we developed a mouse model where NOTUM is inactivated only in late osteoblasts/osteocytes expressing the dentin matrix protein 1 (Dmp1) promoter. We observed a specific increase in cortical bone area and thickness in both femur and tibia, but no change in trabecular bone volume fraction (BV/TV) in adult female Dmp1-creNotumflox/flox mice as compared to control mice. In conclusion, NOTUM expressed by late osteoblasts and osteocytes regulates the cortical bone mass, and we suggest that NOTUM inhibition might be an interesting pharmacological target for increasing cortical bone mass.1. Moverare-Skrtic S, Nilsson KH, Henning P, et al. Osteoblast-derived NOTUM reduces cortical bone mass in mice and the NOTUM locus is associated with bone mineral density in humans. FASEB J: 2019;33(10):11163-79.

***Disclosures: Karin H. Nilsson**, None*

P-467

Piezo1 expression in both osteoblasts and osteocytes contributes to bone homeostasis *Xuehua Li[1], Jacob Kordsmeier[1], Jinhu Xiong[1]. [1]University of Arkansas for Medical Sciences, United States

Mechanical loading plays an essential role in bone growth and homeostasis. The identity of the cells responsible for directly sensing changes in mechanical loading of the skeleton is unclear. Although osteocytes are commonly thought to perform this function, in vitro evidence suggested that osteoblasts are also sensitive to mechanical stimulation and produce the same molecules in response as osteocytes, such as prostaglandins. Therefore, both osteoblasts and osteocytes are potential mechanosensors in bone. In recent studies, deletion of Piezo1, a mechanosensitive ion channel, from Dmp1-Cre-targeted cells decreased cancellous and cortical bone mass and blunted the response of the skeleton to mechanical stimulus, demonstrating the important role of Piezo1 in skeletal mechanotransduction. However, in addition to osteocytes, the Dmp1-Cre transgene used in our work also causes recombination in mature osteoblasts. To determine whether Piezo1 promotes bone formation via its expression in osteoblasts, osteocytes, or both, we deleted the Piezo1 gene using Sost-Cre transgenic mice, which express the Cre recombinase in osteocytes but not in osteoblasts. Mice lacking the Piezo1 gene in SOST-Cre expressing cells, hereafter referred to as SOST-Cre;Piezo1f/f mice, exhibited normal body weight but low bone mineral density at 12 weeks of age compared to littermate controls. Micro-CT analysis revealed decreased cancellous bone mass in the femur and vertebra of 12-week-old male and female SOST-Cre;Piezo1f/f mice. Cortical thickness in the femur was also significantly decreased in SOST-Cre;Piezo1f/f mice at 12 weeks of age. Longitudinal femoral length was not affected by the Piezo1 deletion. In contrast to Dmp1-Cre;Piezo1f/f mice, periosteal and endocortical circumferences in the midshaft of femur were unaltered in SOST-Cre;Piezo1f/f mice. In addition, the decreases in cancellous bone mass and cortical thickness in SOST-Cre;Piezo1f/f mice were not as large as those observed in Dmp1-Cre;Piezo1f/f mice. These results suggest that Piezo1 expression in both osteoblasts and osteocytes contributes to the maintenance of bone mass, and that osteoblasts, in addition to osteocytes, sense changes in mechanical loading in vivo.

***Disclosures: Xuehua Li**, None*

P-468

Osteocytic Wnt protects unloading-induced bone loss via increased endochondral ossification *Xiaolin Tu[1], Saima Khan[1], Syed Zain Azher[1], Teresita Bellido[2], Wei Huang[3]. [1]Chongqing Medical University, China, [2]Indiana University, United States, [3]The First Affiliated Hospital of Chongqing Medical University, China

Osteocytes, the terminal stage cells of osteoblast differentiation orchestrates Wnt anabolic action even with upregulated expression of Sost/sclerostin (PNAS 2015, 112:E478). We hypothesized that osteocytic Wnt protects bone loss induced by unloading (unL), independent of Sost/sclerostin. This study aims to examine the consequence of unL in mice with dominant activation of Wnt/β-catenin signaling in osteocytes (daβcatOt). Mice were generated by a cross of DMP1-Cre mice with Catnb lox (ex3) mice. UnL was performed by tail suspension in 12-wk-old mice with 30 degree of head-down tilted body and cage surface for 2 wks. Bone mass was gained in daβcatOt mice with more lumbar vertebral BMD by unL than normal loading (NL, 13.7% versus 4.2%), not like control mice (-15.1% versus 8.6%). daβcatOt mice robust raised femoral BMD by 10.3% via unL, equivalent to that done by NL in either daβcatOt (11.1%, n.s.) or control (9.8%, n.s.) mice. As expected, control mice dramatically lost femoral BMD by unL (-8.3%). Both X-ray radiography and μCT imaging displayed significant loss of cancellous bone by unL under primary spongiosa only in controls; however, this did not happen in daβcatOt mice. In control mice, unL decreased BV/TV about 7-fold, lowered Tb.N but increased Tb.Sp about 2-fold each without changes in Tb.Th as compared to NL counterparts; however, in daβcatOt mice, unL didn't change any of these parameters. Neither NL nor unL changed cortical bone area in any mice. Bone histomorphometry further confirmed such changes in cancellous bone microarchitecture. UnL lowered osteoblasts lining on the trabeculae of control mice, but not in daβcatOt mice with even higher N.Ob/Tr. Serum bone formation marker, osteocalcin level was maintained in daβcatOt mice, which was lower in controls of unL compared to NL. The expression of osteoblast genes Alp, Ocn, Col1, Runx2, and Osx behaved as the changes of bone mass. TRAPase-staining revealed increase in N.Oc/BS and Oc.S/BS only in control unL mice as compared to NL; whereas such alternations were shown between daβcatOt groups. Serum CTX-level was robust increased by 46.1% in the controls before and after unL, much higher than that in NL control (2.5%). However, there is no significant difference in serum CTX levels between daβcatOt groups, unL versus NL. Conclusion: osteocytic Wnt 100% protects unL-induced bone loss possibly by the enhancement of endochondral ossification.

***Disclosures: Xiaolin Tu**, None*

P-469

Naproxen affects the osteocyte dendritic network and perilacunar remodeling in mouse bone *Alexandra Ciuciu[1], Ryan Tomlinson[2]. [1]Thomas Jefferson University, United States, [2]Thomas Jefferson University, United States

Osteocytes orchestrate mechanosensation, bone remodeling, and mineral homeostasis by acting through a complex network of dendritic projections that connect them to each and other bone cells, known as the lacunocanalicular system. Our lab recently reported that regular administration of the non-steroidal anti-inflammatory drug (NSAID) naproxen to mice for two weeks significantly decreased femoral bone toughness, consistent with clinical reports of increased fatigue injuries in patients taking NSAIDs. However, our understanding of the mechanisms by which NSAIDs, such as naproxen, may reduce bone toughness is limited. Since previous mouse models of diminished bone toughness have illustrated alterations in the osteocyte dendritic network, we hypothesized that NSAIDs diminish bone toughness by actions on the lacunocanalicular system. Here, naproxen sodium (10.9 mg/kg) or vehicle control (DI water) was administered through drinking water for 15 days to adult mice. Two days before the last day of treatment, mice were injected with calcein (10 mg/kg). Both femurs, tibias, and forelimbs, were harvested and fixed with 10% NBF overnight. One group was decalcified in 14% EDTA at 4ºC, sunk in 30% sucrose, and embedded in OCT before sectioning. Osteocyte dendrites were visualized using phalloidin-stained 20 μm thick sections imaged by confocal microscopy (Zeiss LSM800) at 40x magnification. Quantification of dendrite number and length using FIJI revealed that naproxen-treated osteocytes had a lower average number of dendrites and a greater variance in dendrite length, as compared to control osteocytes (Figure 1). Immunohistochemistry against MMP13 on 10 μm thick sections showed significantly fewer MMP13-positive osteocytes in naproxen-treated osteocytes as compared to control (p=0.0004). Separately, a group of undecalcified bones was dehydrated in graded ethanol, embedded in MMA, and sectioned at 100 μm using a low speed saw. Each section was imaged using confocal microscopy (Zeiss LSM800) at 20x. These images revealed significantly fewer calcein labeled osteocytes in bones harvested from mice treated with naproxen as compared to vehicle control (p=0.042). In summary, our results reveal that naproxen significantly alters the osteocyte dendritic network and diminishes perilacunar remodeling. These observations provide new insight into the mechanisms by which naproxen affects bone toughness and increases stress fracture risk.

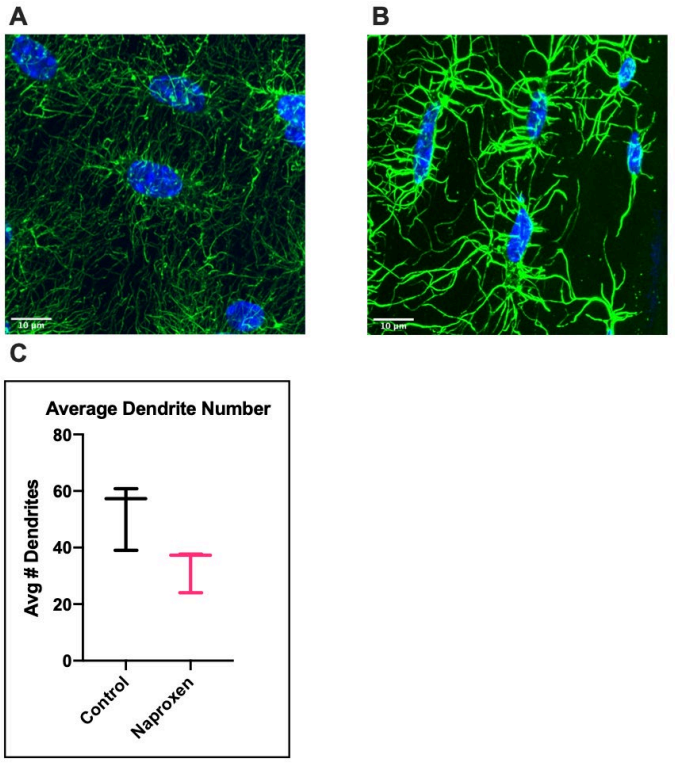

***Figure 1:** Phalloidin-stained 20 μm-thick sections of Control (A) or Naproxen (B) mouse bones analyzed for dendrite number in the cortical mid-bone region (p=0.076)*

***Disclosures: Alexandra Ciuciu**, None*

P-470

TGFβ activates canonical Wnt signaling in osteocytes: Regulation via miR-100 *Neha Dole[1], Jihee Yoon[1], David Monteiro[1], Courtney Mazur[2], Jason Yang[3], Cassandra Belair[1], Tamara Alliston[1]. [1]UCSF, United States, [2]Massachusetts General Hospital, Harvard, United States, [3]UC Berkley, United States

Skeletal responses to loading and unloading are tightly calibrated by the mechanosensory function of osteocytes. We and others have shown TGFβ and Wnt signaling to be key in mediating mechanotransduction; however, how these distinct molecular networks converge to fine-tune osteocyte responses remains elusive. Our previous studies implicated post-transcriptional mechanisms in coupling TGFβ and Wnt pathways to mechanical load. Since, microRNAs (miRs), are known to post-transcriptionally regulate multiple signaling cascades simultaneously, we aimed to identify mechanosensitive miRs that integrate TGFβ and Wnt signaling in osteocytes.Using an unbiased small RNA-seq detecting miR transcriptomal changes in OCY454 osteocytic cells with fluid shear stress (FSS, 10 dynes/cm2, 2-hours), we revealed 60 differentially expressed mechanosensitive miRs. Of these, miR-100 was shown to mediate crosstalk between TGFβ and Wnt pathways in hematopoietic cells. This led us to focus on candidate miR-100 and unravel its function in integrating TGFβ and Wnt signaling during osteocyte mechanotransduction.Using primary BMSCs and MC3T3E1 cells, we showed that miR-100 is suppressed during osteogenic differentiation due to its inhibitory activity on the expression of osteogenic markers Runx2, osteocalcin, and bone sialoprotein. In osteocytes, FSS caused a 40% reduction in miR-100 expression, while inducing TGFβ, Wnt, and load responsive genes (i.e. Serpine1, Tcf4, Ptgs2). This load-induced repression of miR-100 in osteocytes was also confirmed in vivo in C57BL/6 mouse bones subjected to hindlimb loading (3.5N, 600 cycles, 1Hz, one load session).We then studied the cooperation between TGFβ, miR-100, and Wnt pathways in OCY454 osteocytes. We found that TGFβ signaling repressed miR-100 expression while augmenting Wnt signaling. Inhibition of miR-100 increased expression of Wnt-responsive genes Ctnnb1 and Tcf4 and enhanced active β-catenin protein levels. Using a Wnt-luciferase reporter (TOPFlash) we found that inhibiting miR-100 activity amplifies Wnt signaling by 5-fold. Inhibition of Wnt signaling by miR-100 was attributed to its direct binding and repression of Wnt receptors, frizzled (FZD)-4, -5, and -8 in osteocytes, shown by luciferase- 3'UTR constructs, gene expression, and protein analyses. Overall, our study identifies a novel mechanism by which TGFβ activates canonical Wnt signaling by suppressing miR-100, a negative regulator of the Wnt pathway, during mechanotransduction.

***Disclosures: Neha Dole**, None*

P-471

Osteocytes as main responders to Low Intensity Pulsed Ultrasound for the treatment of fracture healing *Tatsuya Shimizu[1], Fujita Naomasa[2], Sato Mari[3], Tsuji-Tamura Kiyomi[3], Kitagawa Yoshimasa[1], Fujisawa Toshiaki[2], Tamura Masato[3]. [1]Oral Diagnosis and Medicine, Department of Oral Pathobiological Science, Faculty of Dental Medicine and Graduate School of Dental Medicine, Hokkaido University, Japan, [2] Dental Anesthesiology, Department of Oral Pathobiological Science, Faculty of Dental Medicine and Graduate School of Dental Medicine, Hokkaido University, Japan, [3]Oral Biochemistry and Molecular Biology, Department of Oral Health Science, Faculty of Dental Medicine and Graduate School of Dental Medicine, Hokkaido University, Japan

Skeletal tissue is known to respond to mechanical stress. Ultrasound stimulation is one of mechanical stress and low intensity pulsed ultrasound (LIPUS) devices have been clinically utilized to promote the fracture healing. However, it is still not clear which skeletal cells mainly respond to LIPUS and how they contribute to fracture healing. To examine that, we utilized medaka and zebrafish as an in vivo model for fracture healing. Medaka are known to have bones without embedded osteocytes, while zebrafish are known to have bones with embedded osteocytes. To investigate whether osteocytes are necessary for fracture healing in response to LIPUS, the tail bones of medaka and zebrafish were fractured and given LIPUS until fracture have been completely recovered. Interestingly, fracture healing was accelerated by ultrasound stimulation in zebrafish but not in medaka. Thus, osteocytes are important to receive the ultrasound stimulation and modulate fracture healing. Next, to examine the molecular events induced by LIPUS in osteocyte, we performed RNA-sequencing analysis in the murine MLO-Y4 cells exposed to LIPUS. Among 16,476 genes, 179 genes were significantly changed by LIPUS. Since most of bone-related genes were not changed, LIPUS may contribute to fracture healing through not direct effect on osteogenic genes. As a result of functional annotation analysis, annotation such as “Immunity”, “Antiviral defense”, “Cytoplasm”, “Secreted”, “Extracellular matrix”, “Transcription” were included in top ranks. Furthermore, the same tendency was observed in the clustering analysis. These results suggest that osteocytes respond to LIPUS with these 179 genes and may affect fracture healing via regulation of neighbor tissues/cells with secreted factors and/or control inflammatory immune response partially regulated by transcriptional factors. To examine whether genes contained in above three clusters are also modulated by LIPUS in vivo, we isolated RNA from zebrafish tail given bone fracture and measured the gene expression.” Although Secreted factors were not altered, inflammatory genes Ptgs2 and four transcriptional genes such as Egr1, Egr2, Nr4a1 and Fosb were significantly changed by LIPUS in zebrafish tail. Taken together, bone-embedded osteocytes[KT1] are necessary to respond to LIPUS and give effects on fracture healing probably through osteocyte-derived factors induced by Egrs, Nr4a1 and Fosb and control of inflammation.

***Disclosures: Tatsuya Shimizu**, None*

P-472

Increased Glycolytic Flux is Associated With Extracellular Matrix Mineralization and Acquisition of a Mature Osteocyte-Like Phenotype *Matthew Prideaux[1], Yukiko Kitase[1], Lynda Bonewald[1], Tom O’Connell[1]. [1]Indiana University, United States

The differentiation of osteoblasts into osteocytes is accompanied by dramatic changes in cell morphology, extracellular matrix mineralization and the expression of osteocyte marker genes. However, whether changes in energy metabolism regulate osteocyte differentiation remains unexplored. To investigate this, we used the IDG-SW3 cell line, which differentiate from osteoblasts into mature osteocyte-like cells in long term culture. An untargeted NMR-based metabolomics approach was applied on cell extract and culture media taken at days representing the early osteoblast (d4), osteoid osteocyte (d9), mineralizing osteocyte (d18) and mature osteocyte (d28). Changes in metabolites were correlated with gene expression profiles by RNA Seq.Glycolysis was the most strongly upregulated metabolic pathway during differentiation, with a 3-fold increase in glucose consumption and 2-fold increase in lactate secretion between day 9 and 18 ($P<0.001$). This glycolytic flux was accompanied by increased mRNA expression of key enzymes for glycolysis (Hk2, Pfkfb3, Pgam1/2, Pkm) (2-22 fold increase), lactate production and transport (Ldha, Pdk1, Slc16a3) (2.5-110 fold) and osteocyte markers (Dmp1, Sost, Mepe) (120-500 fold) ($P<0.001$). Quantitative PCR analysis on cells harvested every 3 days of differentiation identified a key time period between day 12 and 18 where the onset of mineralization correlated with increased glucose utilization, lactate secretion, and elevated expression of glycolytic enzymes and osteocyte markers.To confirm the role of this glycolytic flux, 50-500 μM 2-Deoxy-D-Glucose (2DG) or 1-20 μM of the Pfkfb3 inhibitor PFK158 was used to inhibit glycolysis in IDG-SW3 cells between day 9 and 21 of differentiation. Both inhibitors significantly decreased mineralization ($P<0.001$), as well as Alpl mRNA expression by 3-4 fold ($P<0.001$). Both inhibitors dose dependently inhibited the mRNA expression of glycolytic/lactate enzymes Hk2 (2-3 fold), Pkm (2-fold), Ldha (2-3 fold), Pdk1 (2.5-fold) and Slc16a3 (50-fold) ($P<0.001$). Furthermore, 500 μM 2DG strongly inhibited the late osteocyte markers Sost (6-fold) and Mepe (14-fold) ($P<0.001$). Therefore, our data suggests that osteocytes, unlike most other cell types, use glycolysis rather than the more efficient oxidative phosphorylation as the predominant energy source during differentiation. Current therapeutic strategies to inhibit glycolysis in diseases such as cancer may thus have detrimental effects on bone health.

***Disclosures: Matthew Prideaux**, None*

P-473

Bone Loss is Associated with Direct Effects of Progranulin on Osteoblast Lineage Cells *Liping Wang[1], Robert Nissenson[1]. [1]San Francisco VA Health Care System, United States

Progranulin (PGRN) is a cytokine that can display either pro- or anti-inflammatory properties depending on the tissue context. We recently reported that macrophage-derived PGRN uncouples bone turnover in aging female mice by promoting bone resorption and suppressing bone formation. Treatment of primary cultures of osteoblasts or macrophages with PGRN (500 ng/ml) significantly increased the expression of proinflammatory genes including Nlrp3, Il-1, and TNF-α. Since osteocytes serve as master regulators of bone resorption and bone formation, we tested whether PGRN might have direct effects on gene expression in Ocy454 cells (Ocys). We compared these effects with those of PTH which (like PGRN) is pro-osteoclastogenic but (unlike PGRN) is anti-anabolic. KEGG analysis demonstrated that PGRN treatment for 4 hrs was associated with altered expression of genes associated with osteoclast differentiation ($p=1.7x10-4$). PGRN increased Rankl (3.1-fold), Ccl2 (10.3-fold), and Csf1 (2.2-fold). By comparison, treatment with 100 nM PTH(1-34) for 4 hrs increased the expression of Rankl (16.4-fold), Ccl2 (1.9-fold), and Csf1 (1.8-fold). The most significant pathway association identified by KEGG analysis of PGRN-treated Ocys was the TNF signaling pathway ($p=8.1x10-12$). Of the 23 genes in this pathway that were affected by PGRN, 22 were up-regulated. Among the noteworthy proinflammatory genes induced by PGRN were serum amyloid A3 (Saa3, 26-fold), lipocalin2 (Lcn2, 11-fold), proteoglycan4 (Prg4, 17-fold), Cxcr6 (13-fold), and Steap4 (20-fold). These results suggest that PGRN may inhibit bone formation through a direct TNF-α-like effect on osteoblast lineage cells (OBLs). Treatment of Ocys with PGRN for 24 hrs altered the expression of genes associated with Wnt signaling (KEGG analysis, $p=8.5x10-4$). PGRN down-regulated the expression of Wnt4 (-2.3-fold), Wnt7b (-2.9-fold), Tcf7 (-1.9-fold), and Axin2 (-1.6-fold). Furthermore, comparison of WT to PGRN KO mice indicated that the loss of PGRN increased the exprssion of Wnt4 (1.3-fold, $p<0.05$) and decreased the expression of Saa3 (8-fold, $p<0.05$), Prg4 (63-fold, $p<0.05$), Cxcr6 (2.2-fold, $p<0.05$), Lcn2 (2.6-fold, $p=0.09$), and Steap4 (4.6-fold, $p<0.01$) in 6 month old female mouse bone. These results suggest that direct effects of PGRN on OBLs may contribute to its bone resorption action and that PGRN may inhibit bone formation by producing proinflammatory TNF-α-like effects on OBLs resulting in the suppression of Wnt signaling.

***Disclosures: Liping Wang**, None*

P-474

Conditional Deletion of CaMKK2 Alters the Osteocyte Secretome to Promote Bone Accrual in a Sex-Dependent Manner *Uma Sankar[1], Justin Williams [1]. [1]Indiana University School of Medicine, United States

One in two women and one in four men will experience osteoporotic fractures. Anabolic therapies that stimulate bone accrual are in high clinical demand. Ca2+/CaM-dependent protein kinase kinase 2 (CaMKK2) is a potent regulator of bone remodeling and fracture healing. Genetic ablation or pharmacological inhibition of CaMKK2 elicits a profound bone anabolic response by stimulating osteoblast-mediated bone formation and inhibiting osteoclast-mediated bone resorption. CaMKK2 inhibition protects female mice from ovariectomy-induced osteoporosis, and reverses age-associated bone loss and accelerates bone healing in male mice. The aim of our current work is to determine the cell-intrinsic role of CaMKK2 in osteocytes (OCY), the most abundant cell type in bone. Our recent studies indicate that deletion of CaMKK2 from osteocytes results in enhanced bone microarchitecture only in female mice by modulating osteoblasts and osteoclasts. Moreover, female CaMKK2-deficient osteocytes expressed significantly reduced Sost and enhanced Opg mRNA, and their conditioned media reduced WT OC function in vitro. Based on these findings we hypothesized that deletion of CaMKK2 from osteocytes alters their secretory profile to promote bone accrual in a sex dependent-manner. Conditional deletion of CaMKK2 from OCYs was accomplished by generating dentin matrix protein1 (Dmp1-8kb)-Cre+::Camkk2fl/fl (Camkk2OCY) mice and Dmp1-8kb-Cre+::Camkk2+/+ (CtlOCY) littermates were used as controls. We performed label-free quantitative proteomics on serum-free osteocyte CM from 12 w/o Camkk2OCY and CtlOCY mice (n=3/group/sex) using liquid chromatography coupled with tandem mass spectrometry (LC-MS/MS). Approximately 1140 extracellular proteins were identified using SEQUEST HT, with a false discovery rate of <1%. LC-MS/MS data was cross-referenced with the Uniprot mouse proteome using the FASTA database and all samples were normalized to total peptide amount to account for random errors. Functional annotation analysis was performed using DAVID. Proteins of interest were selected based on the relative abundance ratio of Camkk2OCY and CtlOCY osteocyte CM collected from either sex. Our top candidates were selected based on at least a 10-fold (maximum of 100-fold) increase or decrease in CaMKK2-deficient female osteocyte CM relative to control CM, while observing no change in abundance among CM from male osteocytes. Currently we are validating the top 10 factors using ELISA-based approaches.

***Disclosures: Uma Sankar**, None*

P-475

Role of primary cilia and parathyroid hormone (PTH) receptor type 1 (PTH1R) in osteocyte- osteoclast communication. *Irene Tirado-Cabrera[1], Eduardo Martín-Guerrero[1], Sara Heredero-Jiménez[1], Irene Buendia[1], Juan A. Ardura[1], Arancha R Gortazar[1]. [1]Bone Physiopathology laboratory, Applied Molecular Medicine Institute (IMMA), Universidad San Pablo-CEU, CEU Universities, Campus Monteprincipe, Spain

Primary cilia have been described as potential mechanosensors in bone cells, such as osteocytes and mesenchymal osteoprogenitors. Certain osteogenic responses induced by fluid flow in vitro are decreased by primary cilia inhibition in MC3T3 osteoblastic cells and MLO-Y4 osteocytes. The parathyroid hormone receptor type 1 (PTH1R) is expressed along the osteoblast lineage and controls several bone cell functions during the process of bone remodeling and homeostasis. PTH1R modulates osteoblast, osteoclast and osteocyte effects during bone remodeling upon activation by PTH or PTH-related protein (PTHrP). We and others have described that some actions of PTH1R can be triggered directly by mechanical stimulation in a ligand independent manner. We hypothesize that PTH1R forms a signaling complex in the primary cilium that is essential for mechanotransduction in osteocytes and affects osteocyte-osteoclast communication. We aim to describe the role of primary cilia and PTH1R on the secretion of osteoclastic precursor recruiting signals by mechanically-stimulated osteocytes.MLO-Y4 osteocytes were mechanically stimulated with fluid flow (FF) or with PTHrP(1-37). PTH1R and primary cilia signaling were inhibited using PTH1R or primary cilia specific siRNAs, respectively. Conditioned media (CM) and total protein extracts were collected. CM-induced migration of the murine monocyte/macrophage cell line RAW 264.7 was analyzed. The expression of monocyte pro-migratory MCP-1 and RANTES chemokines was studied by western blot. Proteomic analysis of CM obtained from MLO-Y4 cells in static conditions (SC) or stimulated with FF with or without PTH1R silencing was performed.CM obtained from mechanically- or PTHrP-stimulated MLO-Y4 cells decreased RAW 264.7 cell migration compared to CM from MLO-Y4 kept under SC. However, these effects were inhibited in primary cilia- and PTH1R-silenced conditions. Furthermore, both mechanical stimulation and PTHrP(1-37) inhibited MCP-1 and RANTES protein expression and secretion in MLO-Y4 cells. Proteomic analysis of the secretomes revea1ed secretion of 1.323 proteins. Comparing SC and FF secretomes 27 proteins increased while a total of 37 proteins decreased. If we compare SC with SC and PTH1R-silenced secretomes, 28 proteins increased, and 15 proteins decreased. Comparing secretomes of mechanical stimulus with PTH1R-silenced and FF conditions, 10 proteins increased and 5 decreased. Regarding, PTH1R-silenced and SC with mechanical stimulus conditions, 40 proteins showed a significant increase and 1 protein a decrease. Twenty-two proteins were related to inflammatory processes or to recruitment of osteoclast precursors, such as Serum amyloid A-3 protein, Complement C3, and Dickkopf-related protein 3. Our results indicate that mechanisms dependent of PTH1R and primary cilia in osteocytes are involved in the recruitment of osteoclast precursors.

***Disclosures: Irene Tirado-Cabrera**, None*

P-476

Connexin 43 Deficiency Inhibits Osteocyte Differentiation and Sclerostin Secretion *Evan Buettmann[1], Gabriel Hoppock[2], Aaron Vincent[1], Michael Friedman[2], Yue Zhang[1], Henry Donahue[2]. [1]Virginia Commonwealth University, United States, [2]Virginia Commonwealth University, United States

Mutations in Connexin 43 (Cx43) result in various clinical skeletal abnormalities. Preclinical studies have shown that loss of osteocytic Cx43 in vivo leads to increased periosteal bone apposition and decreased SOST expression. Although these effects are largely attributed to the significant osteocyte apoptosis occurring, few studies have directly investigated the role of Cx43 in osteocyte differentiation and sclerostin secretion in vitro. We hypothesized that Cx43 deficiency directly inhibits osteocytic differentiation and soluble sclerostin production.Wildtype (WT) Ocy454 cells (from Boston University, Pajevic Lab) and Cx43 knockout (Cx43 KO) cells generated by CRISPR were seeded into collagen coated 3D Alvetex inserts (500,000 cells/insert; Reprocell). The osteocytes were cultured at 37°C in αMEM (10% FBS) to induce differentiation and harvested at 3, 6, 10 and 14 days. Osteocyte apoptosis (Ddit3 expression) and differentiation (Dmp1 expression) were assessed by qPCR. Proliferation was quantified by PicoGreen DNA Assay (Invitrogen). Soluble sclerostin was assayed from conditioned media by ELISA (R&D Systems). Data were analyzed by 2-way ANOVA with Tukey's post-hoc test ($p<0.05$).WT osteocytes demonstrated no significant increases in Ddit3 expression or proliferation throughout differentiation (Figure 1A-C). In contrast, Cx43 KO osteocytes showed significantly higher Ddit3 expression, relative to WT osteocytes, at days 10 and 14. Concurrent with this increased Ddit3 expression, Cx43 KO osteocytes showed significantly increased cell proliferation compared to WT osteocytes. Dmp1 expression significantly increased in WT and Cx43 KO osteocytes until day 6 but expression was significantly lower in Cx43 KO osteocytes at all timepoints (Figure 1B). Soluble sclerostin levels were significantly elevated from baseline at day 14 in WT osteocytes and 4-fold greater than levels in Cx43 KO osteocytes (Figure 1D).Our results support our hypothesis and demonstrate that osteocyte differentiation and soluble sclerostin production are significantly inhibited with Cx43 deficiency. Furthermore, these changes occurred despite no significant decreases in cell number in Cx43 KO osteocytes. These novel in vitro results indicate that the enhanced periosteal bone formation in Cx43 deficient mice may not simply be simply due to a loss of osteocytes, but also due to a potent inhibition of osteocytic differentiation, thereby causing a decrease in sclerostin secretion.

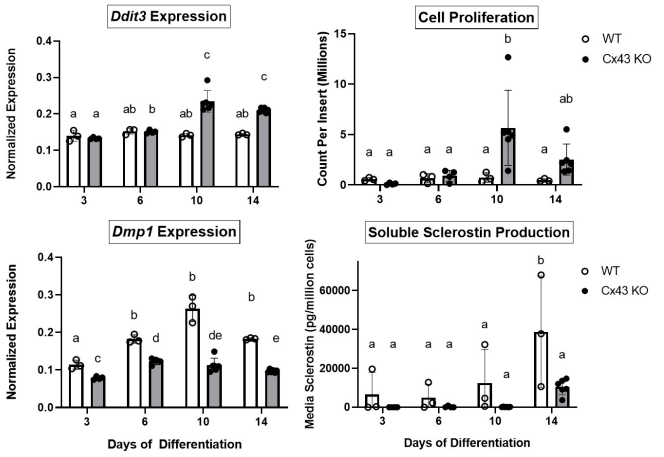

Figure 1. A-B) Gene expression normalized to reference genes GAPDH and β-Actin. **C)** Cell number calculated from DsDNA PicoGreen Assay **D)** Sclerostin ELISA from conditioned media normalized to cell number. Columns with different letters are statistically significant by 2-way ANOVA with Tukey post-hoc. Data presented as Mean ± SD.

***Disclosures: Evan Buettmann**, None*

P-477

Serum Vitamin-D Levels and Osteocyte Lacunar Properties in Postmenopausal Women *Mohammed Akhter[1], Sue Bare[1], Joan Lappe[1], Robert Recker[1]. [1]Creighton University, United States

The serum vitamin-D (25OHD(2) and 25OHD(3)) levels have been shown to be a factor in skeletal health. The project presents data with regards to osteocyte lacunar properties as a function of low and high levels of serum vitamin-D in healthy postmenopausal women. Our work continues to understand the bone tissue's intrinsic properties that may also be affected by other factors that include serum level vitamin-D status. The overall objective is to examine features/causes of osteoporosis-related skeletal fragility in humans by obtaining additional information concerning the intrinsic properties of bone tissue (including osteocyte lacunar properties) to develop better treatments for osteoporosis. This preliminary project used the MicroXCT-200 (Carl Zeiss) system to quantify osteocyte lacunar properties in transilial bone biopsy specimens from healthy post-menopausal women representing Low level (n=3, Low 53.9+/-5.7 ng/mL) and high serum vitamin-D (n=3, High 148.1+/-11.5 ng/mL). Each biopsy specimen was prepared with a maximum thickness of 0.4mm for optimal image quality. Two cortical [Cort] and trabecular [Trab] sites (2 nodal regions) were selected for 0.6μm pixel resolution (PR) scanning (Figure-1). The field of view (FOV) was 0.6mmx0.6mm (1000x1000 pixels). Avizo (9.1 FEI, MA) software was used to segment the lacunar voids. Using the one-way ANOVA, (SPSS), the serum vitamin D status (Low vs High) related differences were analyzed. An average of 3000 segmented lacunae/specimen in the cortical region and 1500 lacunae/specimen in the trabecular region were analyzed (Figure-2). While osteocyte lacunar volume (LcV) and surface area (LcSA) for cortical bone were significantly smaller, and for trabecular bone, they tended to be smaller in Low than High vitamin-D group (Table-1). The lacunar density (LcD) was not different between the two groups both in cortical and trabecular bone tissue. These preliminary data (Table-1) suggest that osteocyte lacunae are smaller in women with low serum vitamin-D (Low) than those with high vitamin-D levels (High). These are the first preliminary data looking into the relationship between osteocyte lacunar properties and serum vitamin-D levels. Larger sized lacunae may provide increased heterogeneity and better intrinsic mechanical strength properties. Further investigation with additional data is needed to better understand the effects of various health conditions on bone intrinsic properties.

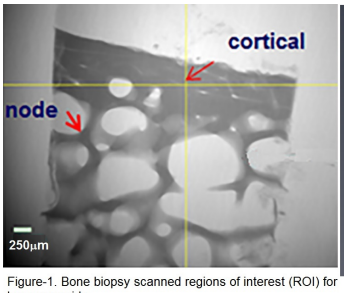

Figure-1. Bone biopsy scanned regions of interest (ROI) for lacuanar voids

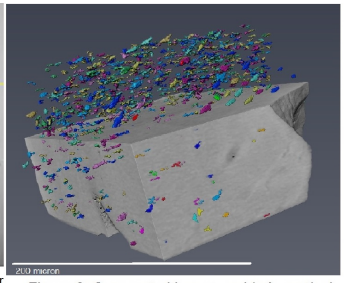

Figure-2. Segmented lacunar voids in cortical bone tissue.

Table-1. Osteocyte Lacunar Properties and Serum Vitamin-D Levels in postmenopausal women

	Volume (μm^3)-L_cV	Surface Area (μm^2) L_cSA	Density (#/mm^3) L_cD
Cortical			
Vit-D Low	155.4±11.3 [a]	218.9±2.4 [a]	37660±7946
Vit-D High	227.5±21.2	271.8±19.4	22803±2375
Trabecular			
Vit-D Low	185.6±11.0 [b]	257.8±13.6 [b]	34228±6627
Vit-D High	219.4±15.8	269.2±9.4	20817±1399

Mean±sem; Differences; Low vs High Serum Vitamin-D Level (ng/mL); [a] P<0.05, [b] P<0.1)

***Disclosures: Mohammed Akhter**, None*

P-478

Hyperglycemia and Collagen Glycation Alter Gene Expression of Sclerostin and RANKL in Osteocytes *Rachana Vaidya[1], Jacob Aaronson[1], Paola Pajevic[2], Lamya Karim[1]. [1]Department of Bioengineering, University of Massachusetts Dartmouth, United States, [2]2Department of Translational Dental Medicine, Boston University, Boston, MA, United States

Patients with type 2 diabetes (T2D) have 3X higher fracture risk than healthy adults despite having normal or high bone density. One contributing factor to poor bone tissue quality in T2D are the changes in bone cell functions induced by hyperglycemia and increased non-enzymatic glycation of the collagen matrix. Osteocytes secrete sclerostin and receptor activator of nuclear factor-κB (RANKL), two proteins that aid in bone resorption and formation. We hypothesized exposure of osteocytes to high glucose and glycated collagen would alter SOST and RANKL expression to indicate an imbalance in remodeling.The osteocytic cell line Ocy454 was grown 1) in complete α-MEM media with 5.56mM(Control), 14mM (2X), or 22mM (4X) glucose with 25mM HEPES to maintain pH, or 2) on glycated vs non-glycated collagen substrate. For glycation, rat tail type I collagen was treated with 257mM methylglyoxal in 100mM sodium phosphate, pH 7.4, for 6h at 22°C and dialyzed against 0.02M acetic acid at 4°C. Collagen (glycated and non-glycated) was used to coat six well plates at a concentration of 5 µg/cm2. Cells were grown for 12 days before measurement of gene and protein expression. RT-qPCR for SOST and RANKL was performed using SYBR green and β-actin was used as housekeeping gene. Protein expression was determined in cell supernatants using ELISA kits.After 12 days in culture, SOST expression was significantly upregulated in 14mM glucose (p<=0.05), with a similar trend in 22mM glucose (p=0.069) relative to control, with a corresponding increase in sclerostin protein expression (p<=0.05) in the medium. There was no change in RANKL gene or protein expression after 12 days in 14mM or 22mM glucose. RANKL expression was significantly increase after 5 days of exposure to glycated collagen (p<=0.05) (Figure 1) whereas SOST expression was unaffected. Moreover, both sclerostin and RANKL protein expression were unchanged upon exposure to glycated vs non-glycated collagen.High sugar treatments changed the expression of sclerostin, but glycated collagen treatment only effected RANKL gene expression. These results suggest that Ocy454 cells are modified by conditions representative of T2D. Their altered behavior has the potential to cause disruptions in the bone remodeling cycle, causing a deterioration in the bone tissue quality that may contribute to increased fracture risk. Further work is needed to clarify how bone remodeling signaling factors from Ocy454 changes in T2D.Acknowledgements: The Ocy454 cell line was provided by the MGH Center for Skeletal Research P30 Core (P30AR066261). This study was funded by NIH-NIAMS (K01AR069685) and the ASBMR Rising Star Award.

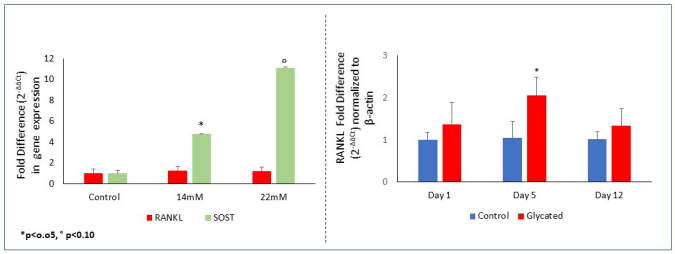

***Disclosures: Rachana Vaidya**, None*

P-479

Connexin 43 Deficiency in Osteocytes Promotes Bone Catabolism but Makes Osteocytes More Sensitive to Anabolic Effects of Mechanical Loading *Michael Friedman[1], Yue Zhang[1], Evan Buettmann[1], Henry Donahue[1]. [1]Virginia Commonwealth University, United States

Introduction: Anabolic mechanical loading increases bone mass, strength, and quality. Osteocytes are the main mechanosensing cells in bone that transduce mechanical signals into changes in bone metabolism. The gap junction protein Connexin 43 (Cx43) is part of bone's mechanosensing mechanism. Deletion of Cx43 in osteoblasts and osteocytes decreases bone volume but increases responsiveness to mechanical loading in mice1. It remains unclear how loading results in a greater anabolic response in Cx43-deficient bone. We hypothesized that loss of Cx43 in osteocytes exposed to loading in vitro via oscillating fluid flow would increase expression of genes responsible for bone anabolism.Methods: Mouse osteocytic OCY454 cells had the Cx43 gene deleted by CRISPR. Wildtype (WT) and Cx43-deficient (Cx43KO) cells were seeded on glass slides at 15,000 cells/slide and incubated in alpha-MEM media at 33°C for 3 days of proliferation. The cells were then transferred to 37°C for 10 days of differentiation. Cells were exposed to 2 hours of oscillating fluid flow (1Hz, 10 dyne/cm2) using a Flexcell Streamer and Osci-Flow controller. Static control cells were placed into the streamer without fluid flow. Then, cells were incubated in fresh media for 2 hours. Cells were harvested, and gene expression was analyzed by RT-qPCR. Conditioned media samples from the post-flow incubation were analyzed by ELISA for RANKL, OPG, and sclerostin. Two-Way ANOVAs with Tukey's tests were used to determine significance ($p<0.05$). Results: Gene expression of RANKL and RANKL/OPG ratio were significantly increased in Cx43KO cells compared to WT cells under static and flow conditions (Fig 1). Sclerostin gene expression was not affected. Conditioned media from Cx43KO cells had increased sclerostin and decreased OPG compared to conditioned media from WT cells. Fluid flow decreased media sclerostin and OPG only in Cx43KO cells.Discussion: Cx43 deficiency alone increased signals leading to osteoclastogenesis and decreased signals leading to osteoblastogenesis in vitro. Mechanical signals decreased the catabolic marker sclerostin but only in Cx43KO cells. These results support the observed phenotype in Cx43KO bones which have low bone mass, increased turnover and increased sensitivity to loading. Our results suggest Cx43 regulates bone metabolism and responsiveness to mechanical loading. Cx43 may be a novel target to increase bone mass.Reference: 1. Bivi et al. J Orthop Res 2013.

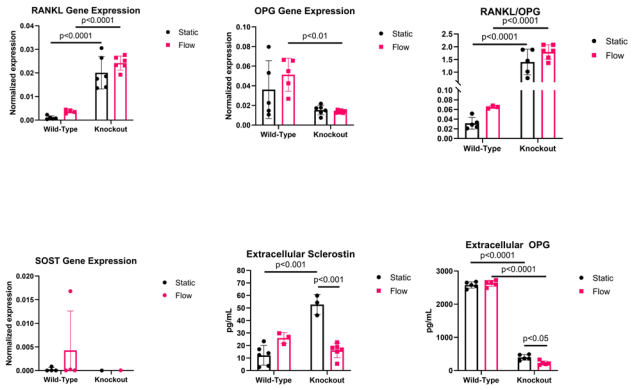

Figure 1. Gene expression (mean ± SD) and conditioned media concentrations of RANKL, OPG, and sclerostin from wild-type and Cx43-deficient osteocytes 2 hours after exposure to 2 hours of fluid flow in vitro. *Significant group difference (p<0.05). #Significant main effect of loading. ^Significant main effect of genotype.

***Disclosures: Michael Friedman**, None*

P-480

A mathematical and computational model of an osteocyte immersed in flow with experimental validation *Jared Barber[1], Luoding Zhu[1], Sungsoo Na[1], Hiroki Yokota[1]. [1]Indiana University-Purdue University Indianapolis, United States

In order to produce a tool that can be used to better understand osteocyte mechanics, a three-dimensional mathematical and computational model for an osteocyte in viscous flow is developed. The initial model consists of a membrane, cytoskeleton, and nucleus and is modeled by an interlinked viscoelastic fiber network. The network is created by constructing a triangularization of the cell's surface, using a meshing tool to convert that triangularization into a tetrahedralization of the cell's volume, and then using the edges of the tetrahedra to define the interlinked network of linearly viscoelastic elements or fibers (dashpots and springs in parallel). The fiber size and various mechanical properties (e.g. viscosity and elasticity) for the membrane, cytoskeleton, and nucleus are adjusted to match results from literature and experiment. The lattice Boltzmann equations (the D3Q19 model) are used to model the viscous incompressible flow. Forces due to the cellular structures are estimated using the

Posters

principal of virtual work combined with bending and elongational elastic energy estimates, volume and surface area conservation associated energies, and viscous energy dissipation. The immersed boundary (IB) method framework models the interaction between the fluid and osteocyte structures. By developing the model using an idealized ellipsoidal geometry, the numerical and physiological capabilities are initially assessed. The model uses methods that are highly parallelizable and the model can be run on multiple cores simultaneously in order to produce simulations in a feasible amount of time. The model is also capable of producing cell motions qualitatively similar to those seen in experiment as well as force estimates, which can be more difficult to obtain from experiment. Additional simulations using more realistic cell shapes and cytoskeletal networks further support the model's capability to produce reasonable cell motions and force distributions. These results suggest that this three-dimensional model is a tool capable of providing insight into more realistic scenarios. Such scenarios include in vitro laboratory experiments involving varying shear flow rates, the problem of in vivo strain amplification in bone (whereby microscale geometry amplifies small macroscopic strains into large microscopic strains), and osteocyte-cancer cell interactions, all subjects for future work.

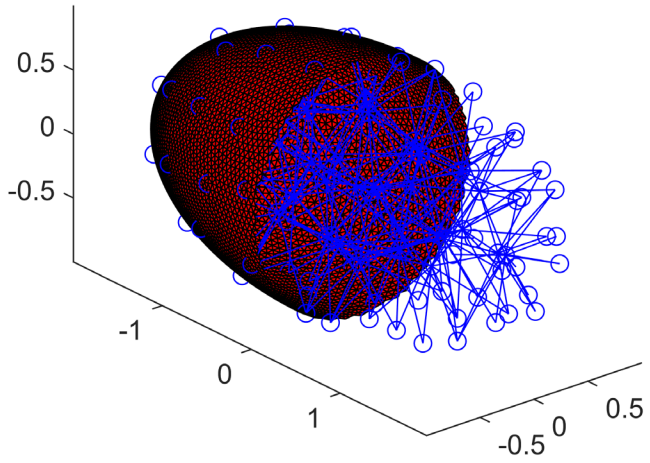

***Disclosures: Jared Barber**, None*

P-481

Effect of Yerba Mate (Ilex paraguariensis) on Osteocytic Cells *Florencia D`Andrea[1], Natasha Sanz [1], Mercedes Lombarte [1], María J Rico[2], Viviana Rozados [2], O. Graciela Scharovsky [2], Verónica E Di Loreto [1], Lilian I Plotkin[3], Lucas Ricardo BRUN[1]. [1]Bone Biology Laboratory. School of Medicine. Rosario National University., Argentina, [2]Instituto de Genética Experimental. School of Medicine. Rosario National University, Argentina, [3]Department of Anatomy, Cell Biology & Physiology, Indiana University School of Medicine, United States

Yerba mate (YM) infusion is frequently drank in several Latin American countries. Several active phytochemicals including caffeine and polyphenols have been identified in YM solution. Whereas caffeine has shown a negative impact on BMD in healthy postmenopausal women in particular when it is associated with low calcium diet, polyphenols have shown positive bone effects due to their antioxidant properties. In addition, we found that YM significantly increased MC3T3E1 osteoblastic cells viability in vitro and positive effect on BMD, trabecular bone biomechanical properties, and alkaline phosphatase levels in vivo. However, whether the infusion also affects osteocytes is not known. To examine this possibility, we evaluate the effect of YM components on MLO-Y4 osteocytic cells in vitro. Cell viability (Cell Proliferation Reagent WST-1, Roche) was evaluated before exposing cells (48 hours) to YM components (caffeine and two polyphenols: rutin and chlorogenic acid) in two different experiments: 1. caffeine (C 0.66, 1.66 and 3.33 µg/ml), chlorogenic acid (AC 1, 5 and 10 µg/ml) and their combinations (n=8/group). 2. caffeine (C 0.66, 1.66 and 3.33 µg/ml), rutin (R 1, 5 and 10 µg/ml) and their combinations (n=8/group). A qualitative analysis of the cell morphology according to treatment was made. Differences between groups were analyzed using one-way ANOVA test and it was considered significant if $p<0.05$. No apparent changes in cell morphology were observed with the treatments. A significant increase in osteocytic cells viability was observed with low rutin concentration (R1 µg/ml = 114.3+/-5.1% vs. control) and highest caffeine concentrations (C1.66 µg/ml = 120.2+/-7.4%, C3.33 µg/ml = 113.3+/-5.4% vs. control). All rutin/caffeine combinations showed a positive effect on cell viability, in particular, the combination R10/C0.66 (118%) that has the normal ratio polyphenols/caffeine (15/1) found in YM. On the other hand, chlorogenic acid did not show any effect on cell viability. We conclude that caffeine and rutin -components of YM- individually and in combination have a positive effect, increasing osteocytic viability in cell culture. Chlorogenic acid individually or combined with caffeine has no effect on osteocytic cells, suggesting an inhibitory effect of the polyphenol on the survival effect of caffeine. Our data suggests that the positive effects of YM at the bone level previously described, could be -at least in part- due to the increased survival of osteocytes.

***Disclosures: Florencia D`Andrea**, None*

P-482

Development of an Electrical Stimulation Environment for Osteocytes *Taylor deVet[1], Roshan Bashar[1], Hubert deBruin [1], Gregory Wohl[1]. [1]McMaster Univeristy, Canada

Bone remodelling is a relatively well-understood process. However, there is debate over the mechanisms of activation and communication of the cells, specifically osteocytes. The hypothesis is that osteocytes sense mechanical stimuli and generate a biochemical response to control remodelling. Studies have shown that the application of direct electrical current has positive effects on osteogenesis, indicating that bone cells are sensitive to an electrical environment. However, this is currently under-researched, specifically in the case of osteocytes. The goal of our work is to improve our understanding of how osteocytes respond to electrical stimulation.To investigate osteocytes in vivo, we developed a miniaturized electrical stimulation device that fits into a 12-well cell culture plate. Platinum electrodes were used to characterize the electrical properties of the cell culture media to try and maximize cellular stimulation while minimizing changes to the media. A DC current was applied with an increasing magnitude from 100 to 800 µAmps using a constant current. We measured the resistance of the medium in two commonly used cell media – McCoy's and DMEM.Our results show that electrical stimulation of culture media causes changes in the media that increase with the applied current. There are changes to the pH of the medium instantaneously upon the application of current visible through the media's built in pH indicator. The pH change depends on the polarity of the electrode with the positive electrode creating a basic environment and the negative electrode creating an acidic one. This separation disperses between 60-120 minutes. There are also changes in the resistance of the media depending on the stimulating current and the amount of time stimulation occurs.To probe the field strength across the stimulation field, we are developing an electrode array on the base of each cell culture well consisting of more platinum electrodes. This will allow us to measure the amount of stimulation that is getting to the cells in the bottom of the well.These experiments have given insight into the stability of cell culture medium with the introduction of direct electrical stimulation which will allow us to decipher if the behaviour of osteocytes under electrical stimulation is coming from the stimulation or the electrochemical reactions in the culture media. This is a first step into creating a stable electrical environment for osteoblast and osteocyte cells in culture.

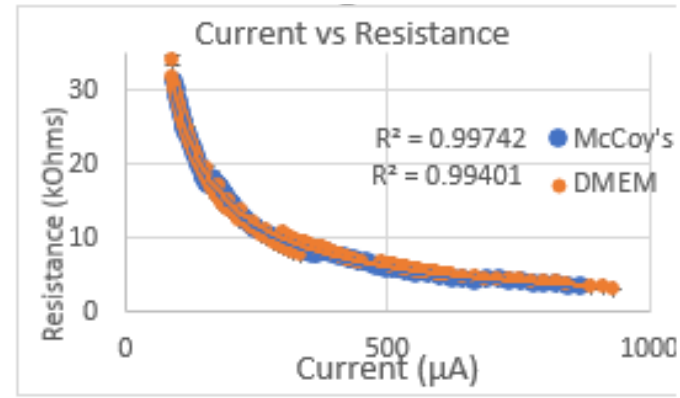

Figure 1: A) Current vs Resistance trend of DMEM and McCoy's Cell Culture Media **B)** View of L shaped Stimulating Electrodes and probing array in cell culture well **C)** pH Separation of stimulated culture media

***Disclosures: Taylor deVet**, None*

P-483

General Comorbidity Indicators Contribute to Fracture Risk Independent of FRAX: A Registry-Based Cohort Study. *William Leslie[1], Suzanne Morin[2], Lisa Lix[1], Eugene McCloskey[3], Helena Johansson[3], Nicholas Harvey[4], John Kanis[3]. [1]University of Manitoba, Canada, [2]McGill University, Canada, [3]University of Sheffield, United Kingdom, [4]University of Southampton, United Kingdom

BACKGROUND: FRAX® estimates 10-year fracture probability from osteoporosis-specific risk factors. General comorbidity indicators are associated with fracture risk and can be assessed at the population level using easily-obtained administrative healthcare information. Whether these general indicators contribute to fracture risk independently from those included in FRAX is uncertain.OBJECTIVE: To examine the associations between two general comorbidity indicators (Johns Hopkins Aggregated Diagnosis Groups™, ADGs® or the number of hospitalizations in the preceding 3 years) and the risk of major osteoporotic fracture (MOF) and hip fracture (HF) outcomes adjusted for FRAX probability without/with competing mortality.METHODS: We used the population-based Manitoba Bone Mineral Density (BMD) Program registry to identify women and men age 40 years or older with at least 3 years of prior health care data undergoing baseline BMD assessment with FRAX scores. Using linked population-based administrative healthcare information, we constructed ADG scores and tabulated the total number of hospitalizations in the prior 3 years for each individual. We identified subsequent incident MOF and HF, and performed Cox regression analysis to determine associations between increasing ADG score (mildly increased=3-5, moderately increased 6-8, markedly 9+ increased vs low=0-2) or number of hospitalizations (1, 2, 3+ vs 0) and fracture outcomes. There was no evidence of collinearity therefore both indicators were included in the final models.RESULTS: The study population included 83,461 individuals (mean age 64.6 years, 90% women) with 8,416 MOF and 2,665 HF during average follow up 9 years. ADG score was low in 18.9%, mildly increased in 44.1%, moderately increased in 26.3%, and markedly increased in 10.8%. Hospitalizations in the previous 3 years were distributed as none in 79.9%, 1 in 8.4%, 2 in 7.1% and 3+ in 4.6%. Increasing ADG score and number of hospitalizations showed a gradient of increasing MOF and HF risk adjusted for age and sex (TABLE). ADG score was unaffected by adjustment for FRAX and when competing mortality was considered. Hospitalizations were partially attenuated by adjustment for FRAX and no longer significant when competing mortality was considered.CONCLUSIONS: A general comorbidity indicator (Johns Hopkins ADG score) but not the number of hospitalizations in the preceding 3 years was a FRAX-independent risk factor for incident MOF and hip fracture.

Adjusted for:	HR for MOF (95% CI)	HR for MOF (95% CI)	HR for HIP (95% CI)	HR for HIP (95% CI)
Model 1: Age/sex	ADG score	Hospitalizations	ADG score	Hospitalizations
Mildly increased	**1.16 (1.09-1.24)**	**1.20 (1.12-1.30)**	**1.19 (1.05-1.34)**	0.99 (0.86-1.13)
Moderately increased	**1.40 (1.31-1.50)**	**1.32 (1.22-1.43)**	**1.37 (1.20-1.56)**	**1.26 (1.11-1.44)**
Markedly increased	**1.67 (1.54-1.82)**	**1.56 (1.42-1.70)**	**1.43 (1.22-1.67)**	**1.21 (1.03-1.41)**
Model 2: FRAX with BMD				
Mildly increased	**1.17 (1.10-1.25)**	**1.10 (1.02-1.19)**	**1.28 (1.13-1.45)**	1.02 (0.89-1.16)
Moderately increased	**1.42 (1.33-1.53)**	**1.26 (1.16-1.36)**	**1.55 (1.36-1.76)**	**1.36 (1.19-1.55)**
Markedly increased	**1.67 (1.54-1.82)**	**1.32 (1.20-1.44)**	**1.68 (1.43-1.96)**	**1.23 (1.05-1.44)**
Model 3: FRAX with competing mortality				
Mildly increased	**1.13 (1.06-1.20)**	1.01 (0.93-1.09)	**1.20 (1.06-1.36)**	0.89 (0.77-1.02)
Moderately increased	**1.31 (1.23-1.41)**	**1.12 (1.04-1.21)**	**1.37 (1.20-1.56)**	**1.14 (1.00-1.30)**
Markedly increased	**1.47 (1.35-1.60)**	1.06 (0.97-1.16)	**1.38 (1.18-1.61)**	0.91 (0.78-1.07)

ADG scores mildly=3-5, moderately 6-8, markedly 9+ (vs 0-2). Hospitalizations mildly=1, moderately=2, markedly=3+ (vs 0).

***Disclosures: William Leslie**, None*

P-484

Identifying Patients at High Risk of Hip Fracture — Combining CT-based Vertebral Fracture Assessment and Biomechanical Computed Tomography Analysis *Tony M. Keaveny[1], David C. Lee[2], Heidi Fischer[3], Annette L. Adams[3], David L. Kopperdahl[2]. [1]University of California, Berkeley, United States, [2]O.N. Diagnostics LLC, United States, [3]Kaiser Permanente Southern California, United States

Addressing the need to identify more patients at high and very high risk of hip fracture, here we investigated hip fracture discrimination in a real-world setting via combining CT-based Vertebral Fracture Assessment (VFA) with hip BMD T-scores and femoral strength from Biomechanical Computed Tomography analysis (BCT), all measured from the same CT scan. Using a case-cohort design sampled from 111,694 Kaiser patients (both sexes) aged 65 or older who had a hip-containing CT scan for any indication, a DXA within 3 years of the CT, and no prior hip fracture, we compared those with subsequent hip fracture with randomly selected sex-stratified controls and analyzed their CT scans blinded to all other data. For BCT, we investigated two binary classifications: patients with either a hip BMD T-score <= -2.5 or with femoral strength less than the threshold for fragile bone strength ("or" logical, oBCT); or patients testing positive for both criteria ("and" logical, aBCT). For VFA, we investigated three binary classifications: presence of any vertebral fracture (Genant grade 1–3); presence of any moderate or severe vertebral fracture (grade 2–3); or a total fracture grade of 4 or more, summed over all vertebrae. The VFA and BCT binary classifications were then combined using "or" or "and" logicals. The outcome was an incident hip fracture after any imaging; DXA (spine or hip osteoporosis) without any VFA was used as a reference. Overall, combining VFA with BCT did not improve the BCT prediction but did provide various levels of competing sensitivity and specificity (Table). For the women, the presence of at least one vertebral fracture of any grade performed at least as well as spinal osteoporosis by DXA; when combined using an "or" logical with oBCT, it identified patients at slightly higher risk of hip fracture than did clinical osteoporosis by DXA (age- BMI- and race/ethnicity-adjusted Hazard Ratio 3.53 vs. 2.04; diagnostic odds ratio 4.33 vs. 2.77) and with high sensitivity (80%) but modest specificity (53%); and when combined using an "and" logical with aBCT, it identified patients at over two-fold higher risk of hip fracture than did clinical osteoporosis by DXA (HR 4.84 vs. 2.04; diagnostic odds ratio 7.25 vs. 2.77) and at high specificity (95%) but low sensitivity (29%). Similar trends occurred for the men but required the presence of a moderate or severe vertebral fracture. We conclude that combining VFA with BCT may have clinical utility.

Binary Classification	Hip Fracture Discrimination in Women					
	Number Hip Fx	Sens	Spec	DOR	Hazard Ratio	(95% Conf Int)
DXA						
Clinical osteoporosis (hip or spine)	437	59%	65%	2.77	2.04	(1.47–2.83)
Hip osteoporosis	437	51%	77%	3.56	2.69	(1.89–3.83)
Spine osteoporosis	437	41%	77%	2.32	*1.27*	*(0.88–1.82)*
VFA						
Any Fracture **(AF)**	382	49%	72%	2.54	2.07	(1.44–2.98)
Any Moderate or Severe Fracture **(AMSF)**	382	29%	88%	2.95	1.86	(1.15–2.99)
Sum of Fracture Grades ≥ 4 **(SFG4)**	382	15%	96%	4.49	2.21	(1.12–4.36)
Hip BCT						
Fragile bone strength *or* hip osteoporosis **(oBCT)**	382	65%	70%	4.37	3.65	(2.58–5.16)
Fragile bone strength *and* hip osteoporosis **(aBCT)**	382	49%	83%	4.95	3.87	(2.66–5.63)
VFA & Hip BCT Combined						
AF *or* oBCT	382	80%	53%	4.33	3.53	(2.46–5.08)
AMSF *or* oBCT	382	72%	63%	4.47	3.36	(2.37–4.76)
SFG4 *or* oBCT	382	68%	69%	4.68	3.36	(2.38–4.74)
AF *and* oBCT	382	35%	90%	4.64	3.37	(2.13–5.32)
AMSF *and* oBCT	382	22%	94%	4.78	2.90	(1.62–5.20)
SFG4 *and* oBCT	382	13%	97%	5.37	3.50	(1.61–7.62)
AF *and* aBCT	382	29%	95%	7.25	4.84	(2.76–8.50)
AMSF *and* aBCT	382	20%	96%	6.00	4.37	(2.29–8.33)
SFG4 *and* aBCT	382	11%	98%	7.17	3.69	(1.51–9.02)

Number Hip Fx = number of hip-fracture cases within 5 years of imaging; Sens = sensitivity; Spec = specificity
DOR = Diagnostic Odds Ratio = ratio of (odds of testing positive and fracturing) to (odds of testing positive and not fracturing)
5 years of follow up (from imaging) required for the sensitivity/specificity/DOR analysis; no time limit for the HR analysis
Hazard Ratio is adjusted for age, BMI, and race/ethnicity; five years of follow up not required (thus had a larger sample size)
Italicized values for the Hazard Ratio are not statistically significant (p>0.05)

***Disclosures: Tony M. Keaveny**, Amgen, Consultant, O.N. Diagnostics, Other Financial or Material Support, Bone Health Technologies, Consultant*

P-485

Independent Performance Evaluation of the Garvan Fracture Risk Calculator: A Registry-Based Cohort Study. *William Leslie[1], Tuan Nguyen[2], Suzanne Morin[3], Lisa Lix[1], John Eisman[2]. [1]University of Manitoba, Canada, [2]Garvan Institute of Medical Research, Australia, [3]McGill University, Canada

BACKGROUND: Absolute risk estimation is the preferred approach for assessing fracture risk and treatment decision making, but the optimal model remains controversial. The Garvan Fracture Risk Calculator (FRC) is a simple prediction model derived from the Dubbo Osteoporosis Study (DOES) cohort from Australia.OBJECTIVE: To evaluate the predictive performance of the Garvan FRC in a large clinical registry from Manitoba, Canada. METHODS: Using the population-based Manitoba Bone Mineral Density (BMD) registry, we identified women and men age 50-95 years undergoing baseline BMD assessment from September 1, 2012 onwards, with registry linkage and self-reported falls in the prior 12 months. 5-year Garvan FRC predictions were generated from clinical risk factors (CRFs) without BMD and again with femoral neck BMD. We identified subsequent non-traumatic incident osteoporotic fractures (OF, any fracture excluding craniofacial, hand/foot, ankle) and hip fractures (HF) from population-based healthcare data sources to March 31, 2018. Overall risk stratification was assessed from area under the receiver operating characteristic curve (AUROC). Cox regression analysis and calibration ratios (5-year observed / predicted) was assessed for risk quintiles. All analyses were sex stratified.RESULTS: The study population consisted of 16,682 women (mean age 66.6 +/- SD 8.7 years) and 2,839 men (mean age 68.7 +/- SD 10.2 years). During mean observation time of 2.6 years there were incident OF in 681 women and 140 men; incident HF in 199 women and 22 men. AUROC showed significant fracture risk stratification with the Garvan FRC; predictions from the tool using CRFs were better than from age or weight alone, predictions the tool with BMD were better than age and BMD alone (TABLE). Garvan FRC used with BMD was better than predictions from CRFs, especially for HF prediction (AUROC 0.86 in women, 0.82 in men). There was a strong gradient of increasing risk for Garvan FRC quintiles (highest vs lowest, hazard ratios women 5.75 [95% CI 4.32-7.76] and men 3.43 [1.95-6.04] for any OF; women 101.6 [14.2-727.5] for HF, insufficient numbers for men). Calibration differences were noted with Garvan FRC both over- and underestimating risk.CONCLUSIONS: A simple fracture risk prediction model, Garvan FRC, outperformed clinical risk factors or BMD alone for fracture risk stratification, particularly for hip fractures, but may require recalibration for accurate predictions in this population.

Posters

	Any OF	HF
Women	AUROC (95% CI)	AUROC (95% CI)
Age	0.56 (0.54-0.59)[ab]	0.80 (0.75-0.85)[ab]
Weight (decreasing)	0.57 (0.54-0.59)[ab]	0.66 (0.61-0.70)[ab]
Hip T-score (decreasing)	0.64 (0.62-0.66)	0.81 (0.77-0.85)
Garvan FRC, CRFs	0.63 (0.60-0.65)[b]	0.84 (0.81-0.88)
Garvan FRC, BMD	0.67 (0.64-0.69)[a]	0.86 (0.83-0.89)
Men	AUROC (95% CI)	AUROC (95% CI)
Age	0.57 (0.52-0.62)[b]	0.68 (0.56-0.81)[b]
Weight (decreasing)	0.51 (0.46-0.57)[b]	0.58 (0.46-0.70)[b]
Hip T-score (decreasing)	0.61 (0.56-0.66)	0.79 (0.71-0.88)
Garvan FRC, CRFs	0.59 (0.54-0.64)[b]	0.71 (0.60-0.81)[b]
Garvan FRC, BMD	0.61 (0.57-0.66)[a]	0.82 (0.74-0.89)[a]

[a] $p \leq 0.05$ vs Garvan FRC CRFs; [b] $p \leq 0.05$ vs Garvan FRC BMD.

***Disclosures: William Leslie**, None*

P-486

Assessment of machine-learning technologies for predicting major osteoporotic fracture in 25,772 postmenopausal women with genomic and phenotypic data *Qing Wu[1]. [1]University of Nevada, Las Vegas, United States

The performance of existing fracture risk assessment tools in fracture prediction remains suboptimal. But recent innovations in genomic data and machine learning (ML) technologies have shown great potential in improving fracture prediction performance. Artificial neural networks (ANN) and support vector machines (SVM) are widely used ML approaches in prediction research; however, their performance for fracture prediction, especially with genomic data, has been rarely studied. This study aimed to develop ANN and SVM models from genomic and phenotypic data, determine if these ML models perform better than conventional logistic regression, and ascertain which method performs the best in fracture prediction. We used genomic and phenotypic data from the Women's Health Initiative Clinical Trial and Observational Study (N=25,772) as the data source and conducted genotype imputation at the Sanger Imputation Server. We identified 1,103 associated SNPs from the genomic data and derived the corresponding genetic risk score (GRS) for each participant. Major osteoporotic fractures (MOF) was used as the outcome variable, and clinical fracture risk factors were included in the modeling. The data were normalized and then randomly split into a training set (70%) and a validation set (30%). The model was built using ANN, SVM, and logistic regression separately. For the model training, the adaptive synthetic oversampling technique was used to account for the low fracture rate in the data, and the 10-fold stratified cross-validation was employed for hyper-parameters optimization. The fracture prediction performance of each model was assessed by area under the ROC curve (AUC) and accuracy in the testing set. We found that the performance of ANN in predicting fracture was the best, with an accuracy of 0.752 and an AUC of 0.830. The performance of SVM and logistic regression in MOF prediction was similar. SVM and logistic regression had an accuracy of 0.705 and 0.708, and both methods had AUC of 0.750. The performance of ANN remained the best in MOF prediction in sensitivity analyses when we limited the study sample to the control or interventional group in the data. We also observed that GRS is a significant predictor of MOF, and GRS significantly improved the accuracy and AUC of each ML method. Therefore we concluded that ANN performed the best for the prediction of MOF in postmenopausal women, and genomic variants can significantly improve fracture prediction.

***Disclosures: Qing Wu**, None*

P-487

Comparison of Short-Term and 10-year Probabilities to Characterise Fracture Risk After a Recent Sentinel Fracture *Helena Johansson[4], John A Kanis[4], Nicholas C Harvey[2], Vilmundur Gudnason[3], Gunnar Sigurdson[3], Kristin Siggeirsdottir[3], Mattias Lorentzon[4], Enwu Liu[4], Liesbeth Vandenput[4], William D Leslie[5], Eugene V McCloskey[6]. [4]Mary McKillop Institute for Health Research, Australian Catholic University, Australia, [2]MRC Lifecourse Epidemiology Unit, University of Southampton, United Kingdom, [3]Icelandic Heart Association Research Institute, Iceland, [4]Mary McKillop Institute for Health Research, Australian Catholic University, Iceland, [5]Department of Medicine, University of Manitoba, Canada, [6]Centre for Integrated research in Musculoskeletal Ageing, Mellanby Centre for bone research, Department of Oncology and Metabolism, University of Sheffield, United Kingdom

Purpose The recency of a prior fracture affects subsequent fracture risk (imminent risk), leading some to suggest that short term probability calculations might be more useful than 10-year probabilities to identify patients for treatment. The aim of this analysis was to quantify the effect of a recent sentinel fracture, by site, on future fracture probability expressed over periods of 2, 5 and 10 years.Methods The Reykjavik Study fracture register prospectively captured all fractures at all skeletal sites in a large sample of the population of Iceland. Fracture probabilities were determined after a sentinel fracture (humeral, clinical vertebral, forearm and hip fracture), occurring within the previous two years, and probabilities for a prior osteoporotic fracture irrespective of recency. The probability ratios were used to adjust fracture probabilities calculated over 2-, 5- and 10-year time horizons.Results Probability ratios to adjust probabilities of a hip or major osteoporotic fracture (MOF) following a sentinel fracture were age dependent, decreasing with age in both men and women, and varied according to the site of sentinel fracture. For the outcome of MOF the ratio was 1.09 if the sentinel fracture was a forearm fracture (for a woman aged 70 for 10-year probability) and 1.50 if the sentinel fracture was a vertebral fracture. While probability ratios for a sentinel fracture were higher with a shorter time horizon, particularly over 2 years, the final absolute fracture probability was much lower (Figure). The ratios between probability with sentinel and any previous fracture for a woman aged 70 years were 1.50 for 10-year probability, 1.99 for 5-year and 2.55 for 2-year probability. At all ages, the 10-year probability was much higher than the 2-year probability, ranging from 3.8-fold at the age of 40 to 1.7-fold at the age of 90. The 5-year probability gave intermediate values.Conclusion Probability ratios provide adjustments to conventional FRAX estimates of fracture probability for recent sentinel fractures. Ten-year probability of fractures captures the impact of recency of fracture with magnitudes of change and final probability that can readily inform clinical decision making. Figure. 10-year, 5-year and 2-year probability of major osteoporotic fracture (MOF) in women from Iceland with a recent vertebral fracture.

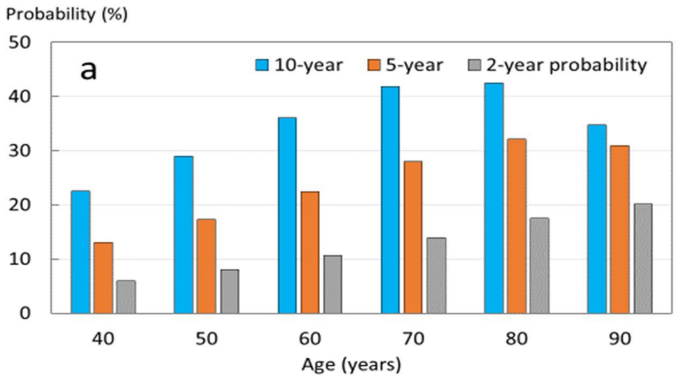

***Disclosures: Helena Johansson**, None*

P-489

Predicting Mortality and Re-fracture Following an Initital Fracture *Thao P. Ho-Le[2], Thach S. Tran[2], Hanh M. Pham[2], Steven A. Frost[2], Jacqueline Center[2], John A. Eisman[2], Tuan V. Nguyen[2]. [2]Healthy Aging Theme, Garvan Institute of Medical Research, Australia, [2]Healthy Aging Theme, Garvan Institute of Medical Research, Viet Nam

Background and Aim. An initial fracture signifies increased risks of subsequent fracture andmortality. There is, however, a large variation between individuals in terms of adverse healthstates following a fracture. This study sought to define the pattern of, and determinants for, thetransition between fracture, refracture, and mortality.Methods. This cohort study involved 2046 women and 1205 men, aged 60 years and olderwhose fracture status and health outcomes had been continuously monitored for up to 20 years. Fragility fractures were ascertained using X-ray report and circumstance of fracture. The incidence of mortality was ascertained from the state birth, death and marriage registry. Femoral neck bone mineral density (BMD, GE-Lunar Prodigy) was measured at baseline. A multistate Markov style of the Cox's proportional hazards model was used to estimate the transition probabilities and transition time between 5 statuses (ie no fracture, initial fracture,second fracture, third fracture, and mortality).Results. Approximately 22.4% of women and 9.2% of men had osteoporosis (FN BMD T-scores <= -2.5). Among women without a fracture, approximately 51% would remain fracture-free during the study time; 12% would suffer a fracture, and 1% went on to re-fracture. Amongmen without a fracture, 52% would remain fracture-free during the study period; 5.6% wouldsuffer a fracture, and 3.4% went on to re-fracture. Five-year probability of transition from nofracture to initial fracture was 6% and 13.9% for a woman without and with osteoporosis,respectively. For a man without and with osteoporosis, the respective five-year risk was 3.5%and 8.3%.Conclusion. Individuals with an initial fracture have an increased risk of subsequent fractureand mortality, and the risk of fracture-associated mortality in men is greater than in women.The predictive model developed here can aid patients and doctors to reach an informed decision concerning treatment in individuals with an initial fracture to reduce fracture and mortality inthe general population.

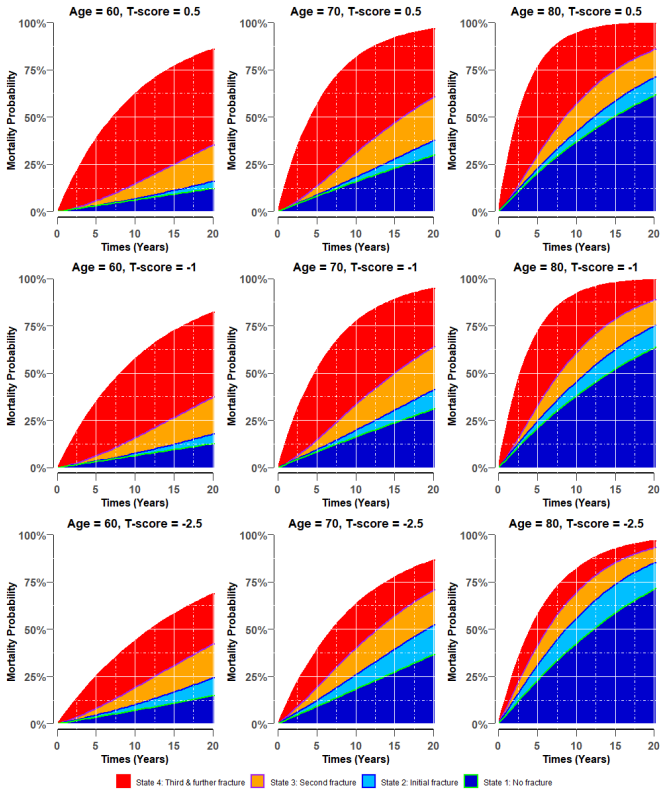

***Disclosures: Thao P. Ho-Le**, None*

P-490

Automated Workflow for Vertebral Deformity Measurements on CT and MRI Scans Using Artificial Intelligence *Abhinav Suri[1], Grace Ng[1], Brandon Jones[1], Nancy Anabaraonye[1], Patrick Beyrer[1], Grace Choi[1], Nikita Bastin[1], Thomas Leichner[1], Sungho Kim[1], Amanda Jankelovits[1], Helene Chesnais[1], Andy Chen[1], Alisha Agarwal[1], James Parente[1], Jacquelyn Golden[1], Samantha Turner[1], Alexandra Rizaldi[1], Emily Tu[1], Lauren Rodio[1], Nima Missaghian[1], Eusha Hasan[1], Chamith Rajapakse[1]. [1]University of Pennsylvania, United States

PURPOSEVertebral fractures comprise almost 50% of osteoporotic fractures in the United States. Vertebral deformity fractures can be classified as wedge, biconcave, or crush, depending on the anterior (Ha), middle (Hm), and posterior (Hp) heights of each vertebral body. However, determining these measurements is time-consuming and resource intensive. Artificial Intelligence algorithms offer the ability to automatically determine Ha, Hm, and Hp and segment vertebral bodies for 3D bone quality assessment. We report the development and testing of a deep learning neural network implementation for analyzing sagittal spine CT and MR images. METHODSSagittal spine MR (T1) and CT scans (MR = 998 subjects, age 67 +/- 11yrs; CT = 35 subjects, age 64 +/- 3yrs; all female) were used to train two networks (Fig.1). A key-point detection network was trained with 4622 labeled vertebral bodies--augmented to 5667 vertebrae (4398 MR, 1269 CT)--to find relevant points for height calculations. A 3D segmentation network was trained with labelled scans (68 MR, 35 CT) to extract volumes of vertebral bodies and discs. Accuracy of the neural networks were measured using two parameters: 2D/3D Dice score (ranges from 0 to 1 where 1 means predicted segmentation = labelled ground truth) and error distance (distance of predicted key-point location to true location). Each network was evaluated with 238 MR and 15 CT scans. RESULTSThe network was able to predict relevant key-points and segmentation masks. The neural network achieved an overall 2D Dice coefficient of 0.97, 3D Dice coefficient of 0.94, and error distance of 0.97 mm. Mean percent error in Ha, Hm, and Hp height calculations was 0.13%. Each scan slice was processed by the neural network with a mean time of 0.973 seconds. CONCLUSIONSThe neural network was able to determine morphometric measurements for detecting spinal deformities with high accuracy on sagittal MR and CT images. Additionally, it was able to extract 3D volumes for vertebral bodies and discs. Thus we were able to show AI algorithms are able to automatically extract measurements for rapid quantification of vertebral bone health. This approach could simplify the screening, detection of changes, and surgical planning in patients with vertebral deformities and fractures by reducing the burden on radiologists who have to do these measurements manually.

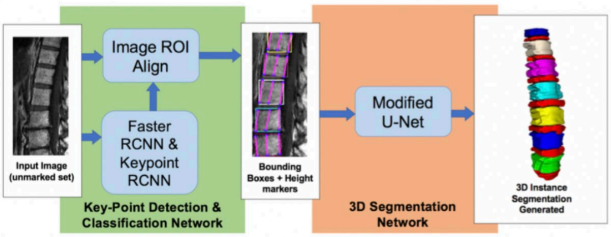

Figure 1: Basic overview of the Neural Network layout. Picture shown for MRI series. Different colors in 3D instance segmentation represent distinct vertebral body volume outputs from algorithm. RCNN stands for recurrent convolutional neural network. A U-Net is a type of CNN (convolutional neural network).

Metric	MR	CT
2D DICE Coefficient (0 to 1; 1 = best)	0.98	0.96
3D DICE Coefficient Vertebral Bodies (0 to 1; 1 = best)	0.93	0.96
3D DICE Coefficient Vertebral Discs (0 to 1; 1 = best)	0.92	-
Mean Distance (mm; lower = better)	0.69	1.28
Mean % error in Height calculations	0.09%	0.17%

Table 1: Performance statistics of neural network on MR and CT. Vertebral discs not visible in CT scans, hence no 3D Dice Score for that value.

***Disclosures: Abhinav Suri**, None*

P-491

Adjusting Fracture Probability for the Effects of Recent Fracture: A Registry-Based Cohort Study. *William Leslie[1], Suzanne Morin[2], Lisa Lix[1], Eugene McCloskey[3], Helena Johansson[3], Nicholas Harvey[4], John Kanis[3]. [1]University of Manitoba, Canada, [2]McGill University, Canada, [3]University of Sheffield, United Kingdom, [4]University of Southampton, United Kingdom

BACKGROUND: FRAX® estimates 10-year fracture probability from multiple risk factors, including prior fracture. Prior fracture in FRAX does not consider fracture site or time since fracture, and has been reported to underestimate fracture risk after recent fractures (less than 2 years) and some fracture sites (especially vertebral and hip). Site-specific multipliers to adjust FRAX for the effect of a recent fracture were developed in the Icelandic population but have not been validated in other populations.OBJECTIVE: To examine the effect of recent fracture (less than 2 years) on fracture risk predictions from FRAX and the validity of adjusting predictions with the Icelandic risk multipliers.METHODS: Using the population-based Manitoba Bone Mineral Density (BMD) Program registry, we identified women and men age 40 years or older with a major osteoporotic fracture (MOF) in the prior two years, baseline FRAX assessments (without and with BMD), and fracture outcomes. We estimated calibration ratios for observed 10-year cumulative MOF and hip fracture probability (with competing mortality) versus conventional FRAX predictions, and compared these with the Icelandic multipliers for recent fracture.RESULTS: The study population included 5,056 women (mean age 66.8 years) and 963 men (mean age 68.8 years) with MOF in the prior 2 years. MOF Icelandic multipliers decreased with advancing age for women (from mean 2.79 age 40-49 to 1.03 age 80+ years) and men (from mean 2.77 age 40-49 to 1.05 age 80+ years). This paralleled the age-related decrease in the calibration ratios for empirically observed 10-year cumulative MOF probability and unadjusted FRAX predictions (Table). There was corresponding improved MOF prediction for women ages 40-49 and 50-59 and men ages 40-49, 50-59, 60-69 and 70-79 with adjusted compared with conventional FRAX scores. The multipliers were numerically smaller for women age 60 years or older and did not significantly improve risk prediction. When analyzed by prior fracture site, the multipliers showed the largest improvement in MOF prediction following recent vertebral and humerus fracture. Assessment of hip fracture was limited by smaller numbers and wide confidence intervals, but the multipliers improved hip fracture prediction in women age 50-59 years and men ages 60-69 and 70-79.CONCLUSIONS: Risk multipliers for recent fracture meaningfully improved prediction of 10-year fracture risk in some age subgroups of women and men.

WOMEN	Age 40-49	Age 50-59	Age 60-69	Age 70-79	Age 80+	All ages
Icelandic multiplier MOF	2.79	1.48	1.32	1.18	1.03	1.34
Observed ratio MOF, no BMD	2.63 (1.68-3.58)[a]	1.41 (1.17-1.64)[a]	0.92 (0.78-1.07)[b]	0.94 (0.83-1.06)[b]	0.71 (0.61-0.81)[ab]	0.96 (0.89-1.02)[b]
Observed ratio MOF, BMD	2.36 (1.50-3.21)[a]	1.34 (1.11-1.56)[a]	0.96 (0.81-1.11)[b]	1.10 (0.96-1.23)	0.94 (0.80-1.07)	1.08 (1.00-1.16)[ab]
Icelandic multiplier HIP	1.80	1.61	1.49	1.22	1.00	1.39
Observed ratio HIP, no BMD	1.04 (0-3.06)	1.74 (0.95-2.53)	0.95 (0.58-1.33)[b]	0.75 (0.57-0.93)[ab]	0.77 (0.60-0.94)[ab]	0.85 (0.73-0.98)[ab]
Observed ratio HIP, BMD	0.64 (0-1.90)	1.60 (0.87-2.33)	1.12 (0.68-1.56)	1.01 (0.77-1.24)	1.35 (1.06-1.64)[ab]	1.20 (1.03-1.37)[ab]
MEN	Age 40-49	Age 50-59	Age 60-69	Age 70-79	Age 80+	All ages
Icelandic multiplier MOF	2.77	1.57	1.46	1.35	1.05	1.42
Observed ratio MOF, no BMD	4.05 (0.70-7.39)	2.31 (1.46-3.16)[a]	1.78 (1.13-2.44)[a]	1.48 (0.99-1.97)	1.07 (0.69-1.45)	1.56 (1.29-1.83)[a]
Observed ratio MOF, BMD	2.79 (0.49-5.10)	1.92 (1.22-2.63)[a]	1.62 (1.03-2.22)[a]	1.56 (1.04-2.08)[a]	1.42 (0.91-1.93)	1.63 (1.35-1.91)[a]
Icelandic multiplier HIP		2.36	1.90	1.42	1.03	1.73
Observed ratio HIP, no BMD	Insufficient#s	1.61 (0-3.95)	2.00 (0.30-3.70)	1.30 (0.51-2.09)	1.05 (0.44-1.66)	1.27 (0.81-1.73)[b]
Observed ratio HIP, BMD		0.77 (0-1.88)[b]	1.51 (0.23-2.80)	1.44 (0.56-2.31)	1.69 (0.71-2.68)	1.44 (0.92-1.96)

a = Observed calibration ratio differ from unity (P<0.05); b = Icelandic multiplier differs from observed ratio (P<0.05). 95% CI intervals are shown.

***Disclosures: William Leslie**, None*

Posters

P-492

Risk of fragility fractures in patients with Type 1 diabetes mellitus may be associated with diabetes-specific clinical parameters *Pavithra Natarajan[1], Jacob Mather[1], Saifuddin Kassim [2], Rebecca Sagar[2], Afroze Abbas[2]. [1]University of Leeds, United Kingdom, [2]Leeds Teaching Hospitals Trust, United Kingdom

Background: Type 1 Diabetes Mellitus (T1DM) is associated with impaired bone health and increased risk of fragility fractures. The pathophysiology of this is considered to be multi-factorial. However, clinical management guidelines for T1DM rarely mention bone health, and the suspicion is that fracture risk is underestimated in this cohort. This study aims to assess and stratify fracture risk in patients with T1DM, within a UK tertiary hospital setting.Methods: A retrospective analysis of 497 patients aged 50 to 98 with T1DM was conducted. Data were collected including; demographics, medications, biochemistry, fracture history, bone mineral density, microvascular complications (neuropathy, retinopathy & microalbuminuria) and HbA1c levels. The validated Fracture Risk Assessment tool (FRAX) was used to calculate 10-year major osteoporotic and hip fracture risk, respective risk categories according to National Osteoporosis Guidelines Group (NOGG) recommendations were also recorded. Relevant statistical analysis was performed using Prism version 8.3.1. Results: As expected, results showed that 10-year major osteoporotic and hip fracture risk was significantly greater in females ($p<0.001$) and increased with age ($p<0.001$). Fracture risk was greater with a lower eGFR ($p<0.001$) and fell with rising BMI (p78mmol/mol), the proportion requiring investigation for osteoporosis or active treatment was significantly higher than those with better glycaemic control ($p=0.04$). Mean fracture risk was positively correlated with an increasing number of microvascular complications (major osteoporotic; $p= 0.009$, hip; $p=0.004$). Patients with microalbuminuria had greater FRAX risk than those with no complications (major osteoporotic; $p= 0.04$, hip; $p=0.007$), those with retinopathy and neuropathy were not found to have a significantly increased risk. Conclusion Our findings demonstrate the potential for diabetes-specific clinical risk factors (elevated HbA1c, low eGFR, presence of multiple microvascular complications and presence of microalbuminuria) to be used alongside conventional risk factors for fracture (e.g. age, sex, BMI) to effectively identify patients with T1DM who may be most at risk of fracture. This has implications for clinical practice in the future management of patients with T1DM, which may help to reduce the risk of fragility fractures in this group.

***Disclosures: Pavithra Natarajan**, None*

P-493

Crystal Bone: Personalized, Short-term Fracture Risk Prediction With Natural Language Processing Methods *Yasmeen Almog[1], Angshu Rai[1], Anirban Mishra[1], Amanda Moulaison[1], Ross Powell[1], Kerry Weinberg[1], Celeste Hamilton[1], Mary Oates[1], Eugene McCloskey[2], Steven R. Cummings[3]. [1]Amgen Inc., United States, [2]University of Sheffield, United Kingdom, [3]University of California San Francisco, United States

Fractures due to osteoporosis are common and associated with significant clinical, personal, and economic burden; however, osteoporosis remains widely underdiagnosed and undertreated. Common fracture risk assessment tools, such as FRAX and Garvan, confer risk over the long-term but do not provide short-term risk estimates necessary to identify very high-risk patients likely to fracture in 1–2 years. Further, these tools use cross-sectional data representing a subset of all available clinical risk factors for risk prediction. These methods are generalized across patient populations and may not fully utilize patient histories commonly found in electronic health records (EHRs) that contain temporal information for thousands of unique features.We used the Optum® de-identified EHR dataset (2007–2018) to develop Crystal Bone, a method that applies machine learning techniques commonly used in natural language processing to the temporal nature of patient histories to predict fracture risk over a 1–2-year timeframe. We repurposed deep-learning models typically applied to language-based prediction tasks which learn the meanings of words and sentences to classify them. Crystal Bone uses context-based embedding techniques to learn an equivalent "semantic" meaning of various medical events. Similar to how language models predict the next word in a given sentence or the topic of an overall document, Crystal Bone can predict that a patient's future trajectory may contain a fracture or that the "signature" of the patient's overall journey is similar to that of a typical fracture patient.We applied Crystal Bone to two datasets, one enriched for fracture patients and one representative of a typical hospital system. In both datasets, when predicting likelihood of fracture in the next 1–2 years, Crystal Bone had an area under the receiver operating characteristic (AUROC) score ranging from 72%–83% on a test (hold-out) dataset. These results suggest performance similar to that of FRAX and Garvan, which have 10-year fracture risk prediction AUROC scores of 64.4% +/– 3.7%.Our results suggest it is possible to use each patient's unique medical history as it changes over time to predict patients at risk for fracture in 1–2 years. Furthermore, it is theoretically possible to integrate a model like Crystal Bone directly into an EHR system, enabling "hands-off" fracture risk prediction, which could lead to improved identification of patients at very high risk for fracture.

***Disclosures: Yasmeen Almog**, Amgen Inc., Other Financial or Material Support*

P-494

Hip Fracture Risk Modeling using DXA and Artificial Intelligence *Yannik Glaser[1], Peter Sadowski[2], Thomas Wolfgruber[3], Li-Yung Lui[4], Steven Cummings [4], John Shepherd[3]. [1]Information and Computer Sciences University of Hawai'i at Mānoa, United States, [2]Information and Computer Sciences University of Hawai'i at Mānoa, United States, [3]University of Hawai'i Cancer Center, United States, [4]University of California, San Francisco Coordinating Center, United States

Bone density and geometry measures of the hip from Dual-Energy X-ray absorptiometry (DXA) scans are highly predictive of hip fracture. However, these approaches are limited to using specific bone regions and features without consideration of surrounding tissues. In this study, we ask if deep learning can enable us to use DXA scans to better predict fracture risk and eliminate quality problems associated with ROI placement. We model four clinical-relevant scenarios with increasing a priori risk information: from none to the equivalent of the FRAX model.We trained and evaluated our model on patient data from the Health, Aging and Body Composition study (Health ABC), a prospective cohort study of 3075 white and black men and women aged 70 to 79 years; Health ABC DXA scans were collected using a Hologic system (Hologic Inc., MA). Participants were separated into training (70%) and validation (10%) sets for model tuning, and a test (20%) data set for final evaluation. Neural networks were trained for each of the following scenarios: 1-Opportunistic Screening: only demographic information used without imaging data; 2-Advanced Screening: demographic information and low-energy DXA image to approximate populations with only demographics and a clinical femur X-ray scan; 3-Full Diagnostic Workup without DXA (17 additional data-fields per patient including blood markers, disability status, and general indicators of fitness); 4-Full Diagnostic with DXA: model 3 with both low and high energy DXA images, femur-neck bone mineral density (BMD). For each model, the neural network fracture predictions are probabilistic, with the network output parameterizing an exponential distribution from which we can derive a risk score and estimate time-to-fracture.We used 4197 DXA hip scans from all 3075 participants followed up for 15-years period . On the test data, the opportunistic model achieved an AUROC of 0.70 using demographic variables only. The Advanced Screening model marginally improved performance with inclusion of the low-energy DXA images (AUROC = 0.71). The full diagnostic model without and with the full DXA scans achieved AUROC values of 0.73 and 0.77 respectively.We conclude that deep learning can improve hip fracture prediction models that already include demographic, bone density, and clinical risk factors. Further, deep learning can be applied to DXA images without post acquisition analysis eliminating a major error source for DXA hip scans.

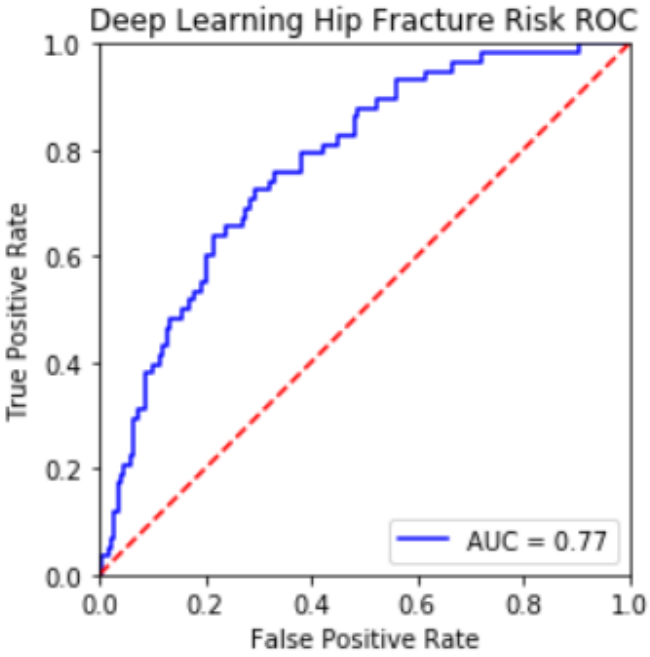

***Disclosures: Yannik Glaser**, None*

P-495

Replication of a Novel Hip Structural Assessment Measure for Incident Hip and Other Fractures in the Study of Osteoporotic Fractures Cohort

*BCC Khoo[1], JR Lewis[2], J Schousboe[3], K Brown[4], RL Prince[1], K Ensrud[5]. [1]University of Western Australia, Australia, [2]Edith Cowan University, Australia, [3]Park Nicollet Osteoporosis Centre and HealthPartners Institute, United States, [4]Mindways Software Inc, United States, [5]University of Minnesota, United States

The internal distribution of bone within the proximal femur is known to be related to resistance to fracture. However areal bone density (aBMD) only assesses total bone in the scanned area. We have developed a four variable analytical method for hip DXA images termed Minimal Analysis (MA) measured at 1cm sections through the Femoral Neck (FN), Trochanter (TR) and Shaft (S) regions of the hip(1). The MA has two internal structural variables, Sigma, related to bone distribution and Delta, the difference between the geometric and mineral mass centres, in addition to aBMD and bone Width of the cross sections (1). Previous analysis of data from the Perth Longitudinal Study of Ageing in Women (PLSAW) identified predictive benefit from the addition of the MA variable TRSigma to age and proximal femur aBMD (THaBMD) on net reclassification improvement (NRI) (2). We now replicate the evaluation of MA in prediction of hip fracture in the SOF cohort based on a prespecified analytical protocol. The analytical approach was to firstly test the additional benefit of TRSigma only and secondly all 12 MA variables in improving hip fracture prediction in addition to age and THaBMD, using logistic and Cox proportional hazard regression and ROC.The participants were 7330 women, mean baseline age 73.3 (5.06) Mean (SD) years, 854 of whom sustained a hip fracture in the15 years after baseline. In the first logistic analysis, when added to age and THaBMD, TR sigma significantly improved AUC-ROC for hip fracture (C-statistic 0.70 and 0.72, P<0.001). To illustrate effect size of TRSigma tertiles were created and compared in Cox regression. Compared to the lowest tertile of the HR (95% CI) for hip fracture in the second and third tertile were 1.61 (1.24 – 2.08) and 2.66 (2.09 – 3.37) respectively. In the second logistic analysis when compared to age and THaBMD alone (C-statistic 0.70) the addition of forward stepwise regression identified seven of the 12 MA variables (Table) that contributed to improved prediction (C-statistic 0.73, P<0.001). These data identify additional clinical benefit of using structural data related to the internal distribution of bone in predicting resistance to hip fracture In addition, software is available for current DXA machines to allow reporting of the Minimal Analysis variables and thus a potentially improved hip fracture risk for individuals.(1) Khoo et al. J Clin Densitom. 201417(1): 38-46(2) Khoo et al. Osteoporos Int. 2016; 27(1): 241-8

Table The logistic regression for hip fracture

							95% C.I. for Exp(B)	
Variables	B	S.E.	Wald	df	Sig.	Exp(B)	Lower	Upper
Age_SD	0.199	.036	30.084	1	.000	1.220	1.137	1.310
THaBMD_SD	0.151	.122	1.535	1	.215	1.163	0.916	1.476
NNaBMD_SD	-0.442	.086	26.758	1	.000	0.642	0.543	0.760
ITaBMD_SD	-0.432	.118	13.325	1	.000	0.649	0.515	0.819
ITWidth_SD	-0.283	.104	7.322	1	.007	0.754	0.614	0.925
NNSigma_SD	-0.129	.050	6.537	1	.011	0.879	0.796	0.970
NNDelta_SD	0.118	.041	8.453	1	.004	1.126	1.039	1.219
ITSigma_SD	0.539	.102	28.006	1	.000	1.715	1.404	2.094
ITDelta_SD	0.103	.040	6.430	1	.011	1.108	1.024	1.200
Constant	-3.716	.888	17.530	1	.000	.024		

***Disclosures: BCC Khoo**, None*

P-496

HIGH RESOLUTION PERIPHERAL QCT (HR-pQCT) PREDICTS FRACTURES FOR ALL AGE GROUPS IN OLDER ADULTS – THE BOMIC CONSORTIUM

*Pawel Szulc[1], Mary Bouxsein[2], Steven Boyd[3], Emmanuel Biver[4], Roland Chapurlat [1], Serge Ferrari[4], David Goltzman[5], Marian Hannan[6], Sundeep Khosla[7], Elisabeth Sornay-Rendu[1], Douglas Kiel[8], Elizabeth Samelson[9]. [1]INSERM UMR1033, University of Lyon, Hospices Civil de Lyon, France, [2]Beth Israel Deaconess Medical Center, Harvard Medical School, United States, [3]University of Calgary, Canada, [4]Geneva University Hospital and Faculty of Medicine, Switzerland, [5]McGill University, Canada, [6]HSL Marcus Institute for Aging Research and Harvard Medical School, United States, [7]Mayo Clinic College of Medicine, United States, [8]Harvard Medical School, Hinda and Arthur Marcus Institute for Aging Research, Hebrew SeniorLife, United States, [9]Hebrew SeniorLife, Harvard Medical School, United States

Areal bone mineral density (aBMD) is used to assess fracture risk; however, its predictive value may decrease with age. Our aim was to determine if the association of HRpQCT indices with fracture risk varies by age.Participants included 6,836 men and women aged 40-96 yrs from 7 cohorts (Framingham, CaMos, Mayo, QUALYOR, GeRiCo, OFELY, STRAMBO). We used Cox models to estimate age-specific hazard ratios (HRs) and 95%CIs for associations between incident fracture and HR-pQCT bone indices, adjusted for age, sex, weight, height, cohort and femoral neck (FN) aBMD. We evaluated two fracture outcomes, all osteoporotic fractures and major osteoporotic fractures (MOF). We repeated the analyses adjusting for FRAX corrected for FN aBMD and cohort.During the median follow-up of 49 months, 719 individuals had incident fragility fractures. Distal radius trabecular volumetric BMD (Tb.vBMD) and number (Tb.N) were associated with similar increases in fracture risk in all the age groups (Table). After adjustment for FRAX corrected for FN aBMD and cohort, distal radius Tb.vBMD and Tb.N remained associated with a similar increase in fracture risk across age groups. In the analyses limited to 369 MOF, the patterns were similar in both the statistical models, e.g. distal radius Tb.vBMD was associated with higher fracture risk similarly in all the age groups. HRpQCT indices varied in their associations with the fracture risk (those at distal radius being more predictive than those at distal tibia), but each of them showed similar associations across age groups (interactions with age p>0.05).Thus, in a large group of men and women followed up prospectively, the link between HRpQCT indices and fracture risk did not vary across age groups. The patterns were similar regardless of the skeletal site of the scan, HRpQCT measure, statistical model and type of fracture. Our data show that above and beyond aBMD and FRAX, trabecular density and microarchitecture provides important fracture prediction information for all age groups.

Association between distal radius indices and all fracture risk stratified by age

Age quintiles (years)	Tb.vBMD HR per SD (95% CI)*	Tb.N HR per SD (95% CI)*
<62	1.44 (1.11 – 1.85)	1.43 (1.11 – 1.84)
62–66	1.21 (0.97 – 1.52)	1.20 (0.97 – 1.50)
>66–69	1.41 (1.12 – 1.77)	1.36 (1.10 – 1.68)
>69–75	1.52 (1.18 – 1.97)	1.31 (1.04 – 1.64)
>75	1.33 (1.10 – 1.60)**	1.23 (1.04 – 1.46)**

* adjusted for age, sex, weight, height, cohort and FN aBMD
** All tests for age-by-HR-pQCT trait interaction, p>0.05

***Disclosures: Pawel Szulc**, None*

P-497

Clinical characteristics of patients with wrist fracture attending a Bone Health Unit in Ireland

*Maire Rafferty[1], Nessa Fallon[2], Georgina Steen[2], Niamh Maher[2], Claire O Carroll[2], James Bernard Walsh[2], Kevin McCarroll[2]. [1]Sj James Hospital, Ireland, [2]St James Hospital, Ireland

IntroductionFragility fracture of the wrist is the most common osteoporotic fracture. Identifying patients at risk for wrist and other fractures is central to the assessment of older adults and fracture liaison services. The aim of this study was to identify retrospectively the baseline characteristics of patients presenting to our bone health service with wrist fractures. In particular, we aimed to explore parameters of bone health including US heel and also establish the point prevalence of osteoporosis/osteopenia using standard DXA criteria.MethodsData regarding all patients attending our service with a wrist fracture between 2014-2018 were obtained from a database at our unit. This included demographic details and clinical characteristics at the time of their presentation such as a results of blood tests, DXA with Vertebral Fracture Assessment (VFA) and US heel. Statistical analysis were performed using SPSSv26.Results1724 patients were identified and 86% were female. Mean age was 67.6+/-13.1 and BMI 25.6+/-5.0. 15.2% had a history of hip fracture. 36% were taking >5 medications with about one third (36.1%) on anti-resorptives or anabolic therapy at the time of their first visit. The majority (70.2%) had a 25(OH)D level > 50 nmol/l and 17.2% had an eGFR <60 ml/min. Based on DXA, 57.9% had osteoporosis and 33.2% osteopenia with 24.7% having a vertebral fracture on VFA. US heel correctly identified 57.5% of those with osteoporosis. Those with a diagnosis of osteoporosis were more likely to be female (p<0.001), older

(p<0.001) and have a lower BMI (p<0.001), worse eGFR (p=0.015) and a previous fracture (p=0.001). Predictors of osteoporosis treatment included being female (p<0.001) and having lower T scores at all sites (p<0.001).ConclusionsAbout 60% of those with wrist fracture had osteoporosis which is similar to other international studies. Importantly a high proportion had a history of other fractures including hip (15.2%) and vertebral fracture (24.7%) highlighting the importance of targeting future fracture prevention in this group. In particular, those with wrist fractures who had lower BMD (and thereby at higher risk of future fracture) were older, female, had a previous fracture and had lower BMI and worse renal function. US of heel did not identify a substantial number who had osteoporosis by DXA criteria.

***Disclosures: Maire Rafferty**, None*

P-498

The reversal-resorption phase is further extended in glucocorticoid-induced osteoporosis compared to postmenopausal controls and osteoporotic patients *Lisbeth Koch Thomsen[1], Majken I Kejser[1], Line L Sørensen[1], Pia R Jensen[2], Ellen-Margrethe Hauge[3], Jens Bollerslev[4], Lene W T Boel[5], Jean-Marie Delaissé[1], Christina M Andreasen[1], Thomas L Andersen[1]. [1]Clinical Cell Biology, Department of Clinical Pathology, Odense University Hospital & Research Unit of Pathology, Department of Clinical Research, Department of Molecular Medicine, University of Southern Denmark, Denmark, [2]Department of Clinical Cell Biology (KCB), Vejle Hospital, IRS, University of Southern Denmark, Denmark, [3]Department of Rheumatology, Aarhus University Hospital, Denmark, [4]Section of Specialized Endocrinology, Medical Clinic B, Oslo University Hospital, Norway, [5]Faculty of Medicine, University of Oslo, Norway

Studies have shown an age-induced increased cortical porosity due to an accumulation of eroded type 2 pores (remodeling of existing pores) reflecting an extended reversal-resorption phase. The present study addresses the histomorphometric changes in cortical bone remodeling within postmenopausal osteoporosis (PMO) and glucocorticoid-induced osteoporosis (GIO) compared to controls.In this study we analysed 7-µm-thick Goldner-Masson trichrome stained sections from transiliac bone biopsies from i) postmenopausal women with GIO (n=19, age 71+/-5 years), ii) women with PMO, but no prior glucocorticoid treatment (n=17, age 71+/-6 years), and iii) postmenopausal women with no prior osteoporosis diagnosis (controls, n=21, age 71+/-7 years).We found statistically significantly thinner cortices (~40%) in both GIO and PMO relative to controls (p<0.001). Only in controls cortical thickness decreased with age (rp=-0.49, p<0.05, -0.02% per year), while GIO and PMO showed no significant age correlation. In the remaining cortices, PMO had a borderline significantly decreased cortical porosity compared to controls (p=0.054) and GIO (p=0.066). In all three groups the cortical porosity correlated with mean pore diameter (GIO: rp=0.88, p<0.0001, PMO: rp=0.93, p<0.0001, controls: rp=0.54, p<0.05), but not pore density. The percentage of cortical porosity reflecting non-quiescent pores was high in all three groups, but even higher in PMO (88.2%, p=0.051) and GIO (89.2%, p<0.05) compared to controls (79.5%). Most of the porosity from non-quiescent pores was due to a higher prevalence of eroded pores. Especially in GIO, a significant higher percentage of the porosity is reflecting eroded pores compared to PMO (p<0.05) and controls (p<0.01). On the other hand, GIO had a significantly lower percentage of porosity reflecting eroded-formative pores than in PMO (p<0.05). Moreover, the pore diameter of quiescent osteons was lower in PMO (p<0.001) and GIO (p=0.053) compared to controls, suggesting an improved BMU balance. Interestingly, none of the investigated parameters in GIO showed a significant correlation with dosage or treatment-time, possibly due to the late stage in GC-treatment at biopsy collection (6.0 +/- 5.1 years).In conclusion, GIO and PMO have a very pronounced cortical thinning, and the cortical porosity of the remaining cortices reflects cortical remodelling with an extended reversal-resorption phase in all groups, but especially in GIO – not a negative BMU balance.

***Disclosures: Lisbeth Koch Thomsen**, None*

P-499

External Validation of FREM in 74,828 Patients from Manitoba, Canada: A Registry-Based Cohort Study. *William Leslie[1], Sören Möller[2], Michael Skjødt[3], Lin Yan[1], Bo Abrahamsen[2], Lisa Lix[1], Eugene McCloskey[4], Helena Johansson[4], Nicholas Harvey[5], John Kanis[4], Katrine Rubin[2]. [1]University of Manitoba, Canada, [2]University of Southern Denmark and Odense University Hospital, Denmark, [3]Holbæk Hospita, Denmark, [4]University of Sheffield, United Kingdom, [5]University of Southampton, United Kingdom

BACKGROUND: FREM is a tool developed from Danish public health registers (hospital diagnoses) to identify individuals over age 45 years at high imminent risk of major osteoporotic fractures (MOF) and hip fracture (HF). The tool was internally validated within the Danish population, but generalizability to other populations and robustness with respect to non-hospital data sources has not been reported.OBJECTIVE: To examine the ability of FREM to identify individuals at high imminent fracture risk in women and men from Manitoba, Canada.METHODS: Using the population-based Manitoba Bone Mineral Density (BMD) Program registry, we identified women and men age 45 years or older undergoing baseline BMD assessment with 2 years of follow up data (1996-2016). From linked population-based data sources we constructed FREM scores using up to 10 years of prior healthcare information (full 10 years available in >93% of the population). Scores were based upon hospitalization diagnoses alone (FREM-H), physician claims diagnoses alone (FREM-P) or both sources (FREM-HP). We identified subsequent incident MOF and HF over 1- and 2-years, and assessed risk stratification (area under the curve, AUC) and calibration (observed vs predicted for 1-year outcomes). We used age alone as a minimum lower bound comparator and FRAX® with BMD as the optimal upper bound comparator. All analyses were sex-stratified.RESULTS: The study population comprised 74,828 subjects (67,930 women, mean age 65.1 years; 6,898 men, mean age 67.4 years. Over the 2 years of observation there were 1,612 incident MOF and 299 incident HF. The TABLE shows significant fracture risk stratification for all FREM scores, with performance better than age alone but still below that from FRAX® with BMD. The inclusion of physician claims data (FREM-HP and FREM-P) gave slightly better performance than hospitalization data alone (FREM-H). Overall calibration for 1-year MOF prediction was reasonable (observed/predicted ratios FREM-HP 0.88, FREM-H 1.09, FREM-P 0.93) but HF prediction was underestimated (observed/predicted ratios FREM-HP 0.36, FREM-H 0.48, FREM-P 0.39).CONCLUSIONS: The FREM algorithm showed significant fracture risk stratification when applied to an independent clinical population from Manitoba, Canada. Physician claims data enhanced the performance of FREM in this population. Calibration for MOF prediction was good but HF risk was systematically underestimated indicating the need for recalibration.

WOMEN	AUC (95% CI) MOF 1 year	AUC (95% CI) HF 1 year	AUC (95% CI) MOF 2 year	AUC (95% CI) HF 2 year
FREM-HP	0.664 (0.644: 0.684)[ab]	0.846 (0.816: 0.877)[b]	0.666 (0.651: 0.680)[ab]	0.832 (0.808: 0.856)[ab]
FREM-H	0.656 (0.636: 0.677)[ab]	0.845 (0.816: 0.874)[b]	0.661 (0.646: 0.676)[ab]	0.821 (0.796: 0.846)[ab]
FREM-P	0.656 (0.636: 0.676)[ab]	0.847 (0.816: 0.877)[b]	0.660 (0.645: 0.674)[ab]	0.829 (0.805: 0.853)[ab]
Age	0.639 (0.618: 0.659)[b]	0.835 (0.801: 0.869)[ab]	0.647 (0.632: 0.662)[b]	0.807 (0.780: 0.833)[ab]
FRAX	0.703 (0.684: 0.721)[a]	0.900 (0.880: 0.919)[ab]	0.700 (0.686: 0.714)[a]	0.869 (0.851: 0.887)[ab]
MEN	AUC (95% CI) MOF 1 year	AUC (95% CI) HF 1 year	AUC (95% CI) MOF 2 year	AUC (95% CI) HF 2 year
FREM-HP	0.640 (0.592: 0.688)[a]	0.667 (0.547: 0.787)[b]	0.644 (0.603: 0.685)[a]	0.662 (0.568: 0.755)[b]
FREM-H	0.586 (0.533: 0.639)[b]	0.657 (0.519: 0.795)[b]	0.596 (0.551: 0.641)[ab]	0.647 (0.549: 0.746)[b]
FREM-P	0.632 (0.582: 0.681)[a]	0.666 (0.545: 0.787)b	0.633 (0.591: 0.675)[a]	0.643 (0.546: 0.739)[b]
Age	0.565 (0.512: 0.618)[b]	0.664 (0.529: 0.799)[ab]	0.562 (0.517: 0.607)[b]	0.613 (0.512: 0.715)[ab]
FRAX	0.642 (0.595: 0.689)[a]	0.774 (0.698: 0.850)[ab]	0.649 (0.610: 0.688)[a]	0.774 (0.700: 0.849)[ab]

a, P<0.05 vs age; b, P<0.05 vs FRAX.

***Disclosures: William Leslie**, None*

P-500

Phenotypic cluster analysis of HR-pQCT parameters for assessment of fragility fracture risk *Danielle Whittier[1], Elizabeth Samelson[2], Marian Hannan[2], Emmanuel Biver[3], Pawel Szulc[4], Roland Chapurlat[4], David Goltzman[5], Sundeep Khosla[6], Serge Ferrari[3], Mary Bouxsein[7], Doug Kiel[2], Steven Boyd[1]. [1]McCaig Institute for Bone and Joint Health, University of Calgary, Canada, [2]Marcus Institute for Aging Research, Hebrew SeniorLife, Harvard Medical School, United States, [3]Division of Bone Diseases, Geneva University Hospitals and Faculty of Medicine, University of Geneva, Switzerland, [4]INSERM UMR1033, Université de Lyon, Hôpital Edouard Herriot, France, [5]Department of Medicine, McGill University and McGill University Health Centre, Canada, [6]Mayo Clinic College of Medicine and Science, United States, [7]Department of Orthopedic Surgery, Harvard Medical School, Center for Advanced Orthopedic Studies, Beth Israel Deaconess Medical Center, United States

Purpose: Previous studies have found that HR-pQCT measures provide additive predictive power to DXA for evaluating fracture risk. However, improvement is limited, and distinguishing fracture risk remains a challenge. There are reoccurring patterns of microarchitectural features that appear in a population, but are not explicitly captured with individual HR-pQCT measures. Unsupervised machine learning is capable of identifying clusters in complex data, and when applied to HR-pQCT imaging, it may provide insight into bone phenotypes. This study applies machine learning to HR-pQCT to identify bone "phenotypes" in the population and determines the associated fracture risk.Methods: A total of 5,780 individuals (71% women, mean age of 68 +/- 9 years) from the Bone Microarchitecture International Consortium (BoMIC) across 7 cohorts were included. Participants had HR-pQCT (XtremeCT, Scanco Medical AG) scans of the distal radius and tibia, and were followed for incident major osteoporotic fractures (wrist, hip, spine, humerus) over an average 4.7 +/- 2.4 years. Parameters used for cluster analysis included total, cortical and trabecular BMD; cortical and trabecular microarchitecture; and estimated failure load, from the tibia and radius. Clusters were identified separately for each sex using hierarchical agglomerative clustering. Model tuning parameters and number of clusters were chosen from dendrogram diagrams and optimizing for the silhouette coefficient. Hazard ratios (HRs) for association between cluster and fracture were estimated using Cox models, adjusted for age and cohort.Results: We identified 3 female and 2 male clusters. Female clusters revealed unique phenotypes that we designated as "healthy bone", "osteoporotic trabecular bone", and "osteoporotic cortical bone". The osteoporotic clusters had significantly higher fracture risk relative to the healthy cluster; HR of 2.03 (95% CI: 1.40, 2.93) and 3.19 (2.05, 4.96) for osteoporotic trabecular and cortical clusters, respectively. One male cluster had worse HR-pQCT measures overall and significantly higher fracture risk relative to the other healthier male cluster; HR of 2.91 (1.51, 5.59).Conclusion: We identified unique bone phenotypes in a large prospective multi-center study, and demonstrated relevance to fracture risk. Grouping the population into bone phenotypes using cluster analysis is a novel method that may be more effective than using individual HR-pQCT measures for assessing fracture risk.

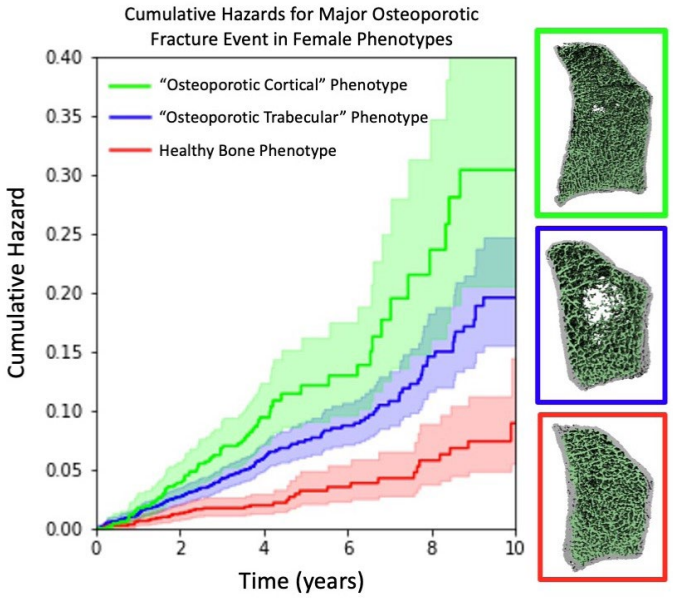

***Disclosures: Danielle Whittier**, None*

P-501

Biochemical Markers of Bone Turnover in Postmenopausal Women with and without Atypical Femur Fracture Following Long-term Bisphosphonate Therapy: A Nested Case-Controlled Study *Ruban Dhaliwal[1], Bernard Cook[2], Elizabeth Warner[2], Shijing Qiu[2], Sudhaker Rao[2]. [1]Division of Endocrinology, State University of New York Upsate Medical University, United States, [2]Henry Ford Health System, United States

Purpose: Atypical femur fracture (AFF), a rare but serious complication of long-term bisphosphonate (BP) therapy, is considered to be a consequence of severe suppression of bone turnover thereby compromising bone biomechanical properties.Methods: We compared serum bone formation markers [osteocalcin (OC) and N-terminal propeptide (PINP)] and bone resorption marker, C-terminal telopeptide of type 1 collagen (CTX) in a nested case control, age-, sex- and race matched postmenopausal women on long term BP therapy: 17 non-AFF and 17 with AFF.Results: The Mean age was 67.2 +/- 7.4 years in non-AFF group compared to 67.5 +/- 7.7, $p > 0.05$). Mean duration of BP use was 7.3 +/- 4.7 years in non-AFF group compared to 11.1 +/- 5.0 ($p < 0.05$). The mean level of serum PINP was 31.6 +/- 19.8 pg/L in the non-AFF group and 64.2 +/- 48.5 pg/L in the AFF group ($p=0.015$); serum CTX was 257.5 +/- 192.7 ng/L vs 265.8 +/- 137.3 ng/L; and serum OC was 15.4 +/- 6.6 vs 16.2 +/- 7.2 respectively. There were no between group differences in CTX or OC.Conclusion: Our preliminary data suggest no differences in circulating levels of bone turnover markers (BTMs) between AFF and non-AFF postmenopausal women on long term BP therapy. However, despite a major fracture (AFF) there was no expected increase in BTMs, implying that bone turnover might have been much lower in AFF patients before the fracture than in non-AFF patients. Additionally, the lack of difference between groups may be related to the duration of BP therapy and baseline levels of BTMs prior to BP therapy, which we did not have. Further studies in larger number of patients with and without AFF are needed to fully understand the role of BTMs in monitoring BP therapy and for surveillance of AFF.

***Disclosures: Ruban Dhaliwal**, None*

P-502

A novel non-ionizing technology for bone densitometry and fracture risk prediction *Francesco Conversano[1], Delia Ciardo[1], Fiorella Lombardi[1], Paola Pisani[1], Sergio Casciaro[1]. [1]National Research Council, Institute of Clinical Physiology, Italy

Purpose The aim is to present the available data concerning a novel non-ionizing application in the context of osteoporosis diagnosis, fracture risk prediction and bone strength assessment, named Radiofrequency Echographic Multi-Spectrometry (REMS) technology. Methods The available literature, including full papers, reviews and abstracts about REMS technology published before May 25th 2020 has been reviewed. Results REMS novelty relies on a non-ionizing approach, based on the automatic processing of the raw unfiltered signals obtained by an ultrasound scan of reference sites, i.e. femoral neck and lumbar spine [1]. It has been clinically validated through the comparison of the bone mineral density (BMD) and T-score values calculated by REMS with the corresponding dual X-ray absorptiometry (DXA) ones. This study, involving over 1900 women, demonstrated the high accuracy, sensibility and specificity in the identification of osteoporotic/non-osteoporotic patients as well as high repeatability and reproducibility of REMS [1]. A multicenter clinical study on over 1300 patients has shown the ability of T-score values calculated by REMS to predict incident fragility fractures, with comparable performance to DXA in case of femoral neck analysis and superior than DXA in case of lumbar spine [2]. Other studies have shown that REMS is able to evaluate BMD with higher accuracy than DXA in particular conditions, i.e. patients with arthrosis, vertebral collapses, vertebroplasty, presence of artifacts, etc. [3,4]. Recently, this technology has been object of a consensus paper by the European Society for Clinical and Economic Aspects of Osteoporosis, Osteoarthritis and Musculoskeletal Diseases (ESCEO), that underlined the validity of REMS for osteoporosis diagnosis and fracture risk prediction, in view of an improved management for osteoporotic patients [5]. Conclusion REMS allows to overcome the main drawbacks of DXA, measuring the BMD value and giving insight of the bone micro-architecture using a non-ionizing approach. The demonstrated performance allows for the application of REMS in short-term monitoring, widespread access to early diagnosis and evaluation in specific populations of patients, such as pregnant women and paediatrics. References1. Osteoporos Int 2018;30:391–402 2. Bone 2020 May;134:115297 3. Exp Ther Med 2019;18(3):1661-68 4. Abstract accepted for oral presentation at ISCD 2020 Annual Meeting 5. Aging Clin Exp Res 2019;31(10):1375–89

***Disclosures: Francesco Conversano**, None*

P-503

Visceral Fat Metabolic Activity Evaluated by 18F-FDG PET/CT Predicts Osteoporosis in Healthy Postmenopausal Korean Women *Kisoo Pahk[1], Yeongkeun Kwon[1], Sungsoo Park[1], Sungeun Kim[1]. [1]Korea University Anam Hospital, Republic of Korea

Purpose: Traditionally, obesity is believed to be protective against osteoporosis. However, recent accumulating evidences suggest that visceral obesity increases the risk of osteoporosis and obesity-driven dysfunctional metabolic activity in visceral adipose tissue (VAT) is considered as a possible underlying mechanism for the development of obesity-related osteoporosis. 18F-fluorodeoxyglucose positron emission tomography/computed tomography (18F-FDG PET/CT) is an established method to assess the degree of VAT metabolic activity. We aimed to investigate the predictive role of VAT metabolic activity evaluated by 18F-FDG PET/CT for osteoporosis in healthy postmenopausal Korean women.Materials and methods: A total of 115 postmenopausal women who underwent routine health check-up between January 2016 and December 2018 were enrolled in this study, retrospectively. They all underwent dual-energy X-ray absorptiometry and 18F-FDG PET/CT. Osteoporosis was defined as bone mineral density (BMD) T-score <= -2.5 at either lumbar spine or femoral neck. Metabolic activity of VAT was defined as the maximum standardized uptake value (SUVmax) of VAT divided by the SUVmax of subcutaneous adipose tissue (V/S ratio).Results: The participants with osteoporosis showed significantly higher V/S ratio than the participants without osteoporosis. V/S ratio of 1.33 was proposed as an optimal cut-off value for predicting osteoporosis (sensitivity; 93%, specificity; 43.1%, area under the curve; 0.716, $p < 0.001$). Furthermore, V/S ratio was significantly associated with osteoporosis in postmenopausal woman by uni-and multivariate analyses. Interestingly, V/S ratio showed significant positive correlation with high sensitivity C-reactive protein, which is a surrogate marker of systemic inflammatory condition.Conclusions: VAT metabolic activity as measured by V/S ratio predicts osteoporosis in healthy postmenopausal Korean women.

***Disclosures: Kisoo Pahk**, None*

P-504

Bone Material Properties are Related to Accumulation of Advanced Glycation Endproducts whereas Cortical Porosity is Related to Microvascular Disease in Type 2 Diabetes Mellitus Patients *Parinya Samakkarnthai[1], Jad Sfeir[1], Elizabeth J. Atkinson[1], Sara J. Achenbach[1], Paul W. Wennberg[1], Peter J. Dyck[1], Amanda J. Tweed[1], Tammie L. Volkman[1], Shreyasee Amin[1], Joshua N. Farr[1], Adrian Vella[1], Matthew T. Drake[1], Sundeep Khosla[1]. [1]Mayo Clinic, United States

Reduced bone material strength index (BMSi) and increased cortical porosity (CtPo) have emerged as potentially contributing to fragility fracture risk in type 2 diabetes mellitus (T2DM), as these patients generally have normal DXA BMD and preserved trabecular bone microarchitecture. However, data are conflicting regarding whether BMSi or CtPo are consistently altered in T2DM. Thus, we sought to identify determinants of BMSi and CtPo in T2DM by relating them to conventional diabetic complications, thereby potentially identifying subsets of T2DM patients with reduced BMSi or increased CtPo. We recruited an age-stratified, random sample of 171 T2DM patients (75 postmenopausal women and 96 men >= 50 yrs) and age-matched controls (63 women and 45 men) who underwent extensive phenotyping: BMSi using in vivo microindentation (OsteoProbe®); skin advanced glycation endproducts (AGEs) using autofluorescence (AGE Reader®); HRpQCT at the distal radius and tibia; and, in the T2DM patients, detailed assessment of diabetic microvascular complications including urine microalbuminuria, retinopathy, neuropathy, and vascular disease (ankle brachial index [ABI], and transcutaneous oxygen tension [TcPO2]). All analyses were adjusted for age, sex, and BMI.In this cohort, BMSi did not differ between T2DM (mean+/-SEM, 74.8+/-0.8) and control (75.0+/-1.0; $p = 0.843$) subjects, but AGEs were significantly (+17%; $p < 0.001$) higher in the T2DM patients versus controls. Of note, skin AGEs were negatively correlated with BMSi in both T2DM ($r= -0.30$, $p < 0.001$) and control ($r= -0.23$, $p=0.020$) subjects. In relating diabetic complications to CtPo, we found that

Posters

T2DM patients with clinically significant peripheral vascular disease (TcPO2 <= 40 mm Hg on the dorsum of the foot) had significantly higher (+21.0%, p = 0.031) CtPo at the distal tibia as compared to controls; in these subjects, CtPo was negatively correlated with TcPO2 at both the distal tibia (r = -0.39, p = 0.041) and radius (r = -0.41, p = 0.029).Our findings thus demonstrate that BMSi is related to AGE accumulation, regardless of diabetes status, while CtPo in T2DM is linked to TcPO2, a measure of peripheral microvascular blood flow. These data may explain the conflicting findings regarding whether these measures differ between T2DM and control subjects, as only those T2DM patients with high AGEs may have reduced BMSi, whereas only those T2DM patients with significant peripheral microvascular disease may have increased CtPo.

***Disclosures: Parinya Samakkarnthai**, None*

P-505

Longitudinal evolution of bone microarchitecture and strength in type 2 diabetic postmenopausal women with and without history of fragility fractures - a 5-year follow-up study using HR-pQCT *Ursula Heilmeier[1], Gabby B. Joseph[2], Pasco Courtney[3], Julio Carballido-Gamio[4], Nhan Dinh[3], Soheyla Torabi[3], Karin Darakananda[3], Jiwon Youm[3], Andrew J. Burghardt[3], Thomas M. Link[3], Galateia Kazakia[3]. [1]University of California San Francisco, Musculoskeletal Quantitative Imaging Group, United States, [2]University of California, San Francisco, Musculoskeletal Quantitative Imaging Research Group, United States, [3]University of California San Francisco, Musculoskeletal Quantitative Imaging Research Group, United States, [4]Department of Radiology, University of Colorado Anschutz Medical Campus, United States

Introduction: Type 2 diabetic (T2D) bone disease is characterized by an increased fragility fracture risk that cross-sectional clinical studies partly attribute to severe deficits in cortical bone quality such as a higher cortical porosity. However, the temporal evolution of bone microarchitecture, strength and particularly of cortical porosity in diabetic bone disease is still unknown. Here, we aimed to prospectively characterize via high resolution peripheral quantitative computed tomography (HR-pQCT) the 5-year changes in bone microarchitecture, cortical porosity and strength seen in T2D postmenopausal women with (DMFx, n=12) and without history of fragility fractures (DM, n=10) and to compare those to nondiabetic fracturefree controls (Co, n=10). Methods: 32 postmenopausal women underwent a baseline HR-pQCT scan of the ultradistal tibia and a FU-scan 4-5 years after. Cortical parameters including cortical porosity (Ct.Po), pore volume (Ct.Po.V), tissue mineral density (Ct.TMD-an inverse marker for subresolution microporosity) and bone strength estimates via µFEA were calculated for each timepoint and annualized. GLM were run for intergroup comparisons. Results: All 3 groups were similar in age (60+/-1 y) and BMI (27+/-0.8 kg/m2). At baseline, DMFx exhibited the highest macroporosity of the 3 groups (71.9% greater Ct.PoV, p=0.02, 66.3% greater Ct.Po%, p=0.02 than DM), and had a significantly higher cortical microporosity (inverse Ct.TMD) than DM (p=0.037). Longitudinally, both micro- (inverse Ct.TMD) and macroporosity (Ct.Po) increased significantly over time (0.012<p<0.004) in all 3 groups and at similar annual rates, while bone strength indices decreased yearly 14x (failure load F) and 22x (stiffness K) more in DMFx versus Co (0.017<=p<=0.004) and 4x (F) and 6.7x (K) more in DMFx versus DM (0.025<=p<=0.010). Conclusion: Our data suggest that despite different baseline levels in cortical porosity, T2D women with and without fractures exhibited long-term porosity increases at a rate similar to non-diabetics. However, the annual loss in bone strength was by far strongest in T2D women with history of a fragility fractures. This suggests a potentially non-linear course of cortical porosity development in T2D: major porosity development may occur rather early in the course of disease, followed by a smaller steady annual increase in porosity which in turn can still have a detrimental effect on bone strength - depending on the amount of early cortical predamage.

***Disclosures: Ursula Heilmeier**, None*

P-506

Clinical Utility of TBS versus Lumbar DXA at a Single Academic Center Osteoporosis Clinic *Sophie Cannon[1], Jian Shen[1], Reema Patel[1], David Wing[1], Lauren Claravall[1], Jeanne Nichols[1], Deborah Kado[1]. [1]University of California San Diego, United States

Trabecular Bone Score (TBS) is a validated independent tool for analyzing lumbar bone microarchitecture and assessing fracture risk, but it is not widely used in U.S. clinical practice. The current gold standard for analyzing bone mass and fracture risk is DXA BMD. While each independently predicts fracture, TBS and DXA are not strongly correlated with each other (r ~ 0.30).Thus, at a single academic institution, we investigated how DXA with TBS testing may add value to the diagnosis and management of patients referred to an osteoporosis clinic. Using a convenience sample of the first 121 patients referred for TBS testing (5/2016-2/2019), we conducted a cross-sectional analysis of DXA BMD versus TBS in association with clinical characteristics of age, sex, BMI, history of fracture at >50 years, medication use, health behaviors, and chronic medical conditions obtained from the electronic medical record.Patients were a mean age of 62.4 (SD = 10.9, range 22-94) and had an average BMI of 23.6 kg/m2 (SD = 4.2). One hundred (83%) were female, 103 (85%) were Caucasian, 14 (12%) Asian, 3 (2.5%) Hispanic, and one listed Other. Most had been prescribed osteoporosis medications (74.4%) and 58 (48%) reported a fracture at age > 50, of which 23 (19%) had a spine fracture, and 5 (4%) had a hip fracture. The mean TBS score was 1.30 (SD = 0.11, range 0.94-1.53). After adjusting for age and BMI, the Spearman Partial Correlation Coefficient (r) was 0.23 (p = 0.01) between TBS and lumbar spine BMD. After excluding patients under age 50 (n = 14) and stratifying by history of fracture at age >50, in those with a fracture history, r was only 0.22 (p = 0.12) compared to those with no fracture history (r = 0.37, p = 0.003) (Figure). The mean TBS score was lower in those with a fracture history vs not (1.27 vs. 1.30, p = 0.02), but this difference was no longer significant after adjusting for age and BMI (p = 0.20). Lumbar spine DXA values were no different between those who did and did not report a fracture (p = 0.35). Of the other clinical measures, there were significant correlations between TBS and 24-hour urinary calcium excretion (r = -0.26, p = 0.03) and PTH (r = 0.23, p = 0.02), findings not seen with other DXA BMD measures. In conclusion, compared to traditional spine DXA, TBS score was more strongly correlated with a history of fracture and other fracture risk factors, suggesting that TBS testing adds clinical utility in the real-world setting.

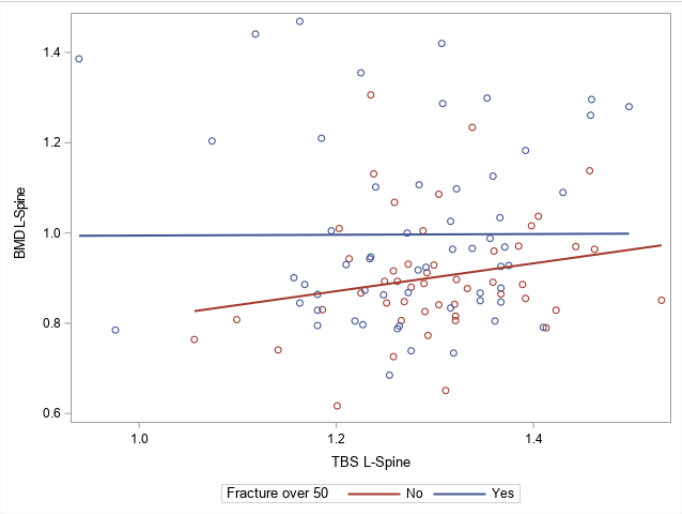

***Disclosures: Sophie Cannon**, None*

P-507

Longer Duration of Type 2 Diabetes Mellitus Associated with Poor Bone Microarchitecture Assessed by Trabecular Bone Score (TBS) *Mohammed Almohaya[1], Abdullah Almuqawed[1], Alwaleed Alaskar[1], Uhoud Almohareb[1], David Kendler[2]. [1]King Fahad Medical City, Saudi Arabia, [2]University of British Columbia, Canada

Type 2 diabetes mellitus (T2DM) is associated with increased osteoporotic fractures with the greatest fracture risk observed in those with T2DM longer than 10 years. Lumber spine areal bone mineral density (LS-BMD) is paradoxically increased compared to non-diabetics. TBS estimates trabecular microarchitecture, which is an independent predictor of fracture in patients with T2DM. Data concerning the effect of T2DM duration on TBS is lacking. We retrospectively reviewed consecutive patients older than 50 years and in whom Lumbar Spine Bone Mineral Density (LS-BMD) and TBS data were available at a tertiary referral center in Riyadh, Saudi Arabia. Individuals were categorized as with T2DM or without diabetes (no-DM). The T2DM group was subdivided based on duration of diabetes to those were diagnosed within 4 years (New-DM), moderate duration between 4 to 10 years (Mod-DM) and longer duration of more than 10 years (LT-DM). Patients were considered to have very poor glycemic control if hemoglobin A1C (HgbA1c) was over 9.5% (very poor-control T2DM), poorly-controlled T2DM when HgbA1c was 7.5% to 9.5% and well-controlled T2DM when HgbA1c was below 7.5%. A total of 211 patients were included (195 females, 16 males), mean age was 65.4 +/- 9.1years. There were 104 patients diagnosed with T2DM (49.2%) of whom 64 patients were LT-DM. LS-BMD was significantly higher in T2DM (mean 0.934 g/cm2 in T2DM vs. 0.881 g/cm2 in no-DM; p = 0.01). Mean TBS trended lower in T2DM (1.264 in T2DM vs. 1.290 in non-T2DM; p = 0.11). T2DM had higher BMI (32.4 vs. 28.8; p <0.001). Within T2DM, age, BMI and prior fractures were similar; HgBA1c in LT-DM was higher compared to New-DM (mean +1.65%). TBS was significantly lower in subjects with LT- DM compared to New-DM (-0.085, p 0.02) and no-DM (-0.056, p 0.01). 78% of LT-DM had TBS < 1.320 (degraded). Poor-control T2DM was associated with lower TBS compared to New-DM and no-DM (decreased by average of 0.007 and 0.092 respectively, both p <0.005). TBS positively correlated with BMD (Pearson r= 0.45) but negatively correlated with duration of T2DM (r= -0.14) and HgbA1c (r= -0.26). Since TBS is a marker for vertebral trabecular architecture, these data indicate that there is greater architectural deterioration in individuals with LT-DM and poor control T2DM. Such changes are independent of changes in LS-BMD. This may help explain the increased fracture risk at higher BMD in T2DM patients and in particular those with longer and poor control T2DM.

***Disclosures: Mohammed Almohaya**, None*

P-508

Comparison of hip structure analysis and 3D-SHAPERTM images in post-kidney transplant recipients with denosumab treatment. *Yasumasa Yoshino[3], Eisuke Tomatsu[1], Sahoko Sekiguchi-Ueda[1], Megumi Shibata[1], Takeshi Takayanagi[1], Hiroshi Toyama[0], Renaud Winzenrieth[0], Atsushi Suzuki[1], Yohei Asada[1]. [3]Department of Endocrinology and Metabolism, Fujita Health University, Japan, [1]Department of Endocrinology and Metabolism, Fujita Health University, Japan, [0]Department of Radiology, Fujita Health University, Japan, [0]Galgo Medical S.L. Barcelona, Spain

Background: 3D-SHAPERTM Software generates a 3D QCT model from a patient's hip DXA scan, and measures separately cortical and trabecular bone density. We have previously reported that 3D-SHAPERTM could give us more precise information in post-kidney transplantation (KTx) patients treated with denosmab (Dmab), an anti-RANKL antibody. In this study, we further analyze 2D-DXA image in these patients and compare the change of 3D bone measurements and hip structure analysis (HSA) data.Methods: Novel KTx patients were recruited (n=35, M/F=22/13, age=53.6 +/- 2.3 years). All patients were treated with glucocorticoids (GCs) during the study period. Dmab was administrated every 6 months during first year after KTx in 28 cases regardless of BMD at the time of KTx. Among them, 24 cases (Dmab-C) stopped Dmab, and 4 cases (Dmab-D) were continuously administered Dmab for 3 years. 7 other patients received no anti-osteoporosis medicine during the study period (Control). BMD at total femur (TF BMD) was measured using a Discovery A densitometer (Hologic, Inc., MA, USA) after KTx, at 6, 12, 24 and 36 months and total femur DXA image was analyzed retrospectively using 3D-SHAPERTM software (v2.9, Galgo Medical, Spain), and by the parameters of HSA from same DXA images.Results1. 3D-ShaperTM analysis: Control showed continuous decline of both cortical surface BMD (Cort sBMD) (-6.2%) and trabecular volumetric BMD (Tb vBMD) (-15.8%). On the contrary, Dmab-D showed the increase of both Cort sBMD (+8.0%) and Tb vBMD (+5.2%). Dmab-C showed transient increase of Cort sBMD at total femur at 12 months and returned to baseline at 36 M (+0.4%), while its Tb vBMD decreased (-6.4%).2. HSA: Both Dmab-C and Dmab-D maintained baseline levels of CSA, CSMI and Z modules at femoral neck. At intertrochanteric region, all parameters showed positive changes in Dmab-D but not in Dmab-C. Control patients showed decrease of all parameters at any site.Discussion: KTx patients with GCs exhibited rapid decrease of BMD. 12 months of Dmab is protective enough to balance with GCs negative effect on the cortical bone at femoral neck and intertrochanteric region at 36 months but does not compensate the trabecular loss linked to GCs.Conclusion: New imaging technologies, such as 3D-SHAPERTM, in accordance with HSA, seems to give us more precise assessment of bone structure in KTx patients.

***Disclosures: Yasumasa Yoshino**, None*

P-509

Fracture Risk Assessment (FRAX) without BMD and Risk of Major Osteoporotic Fractures in Adults with Type 1 Diabetes *Viral Shah[1], Anagha Champakanath[1], Amena KESHAWARZ[1], Janet Snell-Bergeon[1]. [1]Barbara Davis Center for Diabetes, United States

Purpose: The risk for major osteoporotic fractures (MOF) in people with type 1 diabetes (T1D) is three- to four-fold higher compared to adults without diabetes and cannot be explained by DXA-measured bone mineral density (BMD) alone. Fracture risk assessment tool (FRAX) underreports fracture probability in patients with type 2 diabetes who are also at increased risk for fractures. There are no studies to verify FRAX applicability in T1D population and therefore, we aimed to evaluate the predictability of FRAX without BMD for MOF risk in a prospective cohort of adults with T1D compared to adults without diabetes.Methods: Participants were enrolled into the Coronary Artery Calcification in Type 1 Diabetes (CACTI) study between 2000-2002, and were followed prospectively over three visits: 3, 6 and 14 years later. At the 14-year follow-up examination, participants reported the age and location of all fractures they had sustained. FRAX scores were calculated at the 6-year examination, using race-specific FRAX tools. Native Americans and those with missing race information but non-Hispanic ethnicity had FRAX scores calculated using the Caucasian tool. Individuals younger than 40 were entered into the FRAX tool with their age set to 40, since the calculator does not include younger ages. New MOF were defined as fractures to the hip, forearm, humerus, or spine occurring between the 6- and 14-year visits. Risk for MOF was examined using Cox proportional hazards survival analysis.Results: 346 T1D (mean age 43.3 +/- 9, BMI 26.4 +/- 5, diabetes duration 29.4 +/- 8.6 years, A1c 7.8 +/- 1.1) and 411 controls (mean age 46.9 +/- 9 years, BMI 26.3 +/- 5 kg/m2, A1c 5.5 +/- 0.4) were analyzed in this study. T1D was a significant predictor of new MOF [unadjusted HR 1.8 (95% CI 1.0-3.3)], even after adjusting for age and sex [HR 2.0 (1.1-3.8), p=0.02]. However, T1D was not a significant predictor of new MOF after adjusting for FRAX without BMD [HR 1.5 (0.8-2.8), p=0.2] or after adjusted for age, sex and FRAX without BMD [HR 1.6 (0.8-3.0, p=0.2)] [Figure]. A sensitivity analysis excluding people under 40 years of age showed similar results.Conclusion: FRAX without BMD accurately identified individuals at higher risk of MOF in adults with T1D and its clinical use would facilitate therapeutic decision-making in this population.

Figure 1: Effect of Type 1 Diabetes on New Major Osteoporotic Fractures

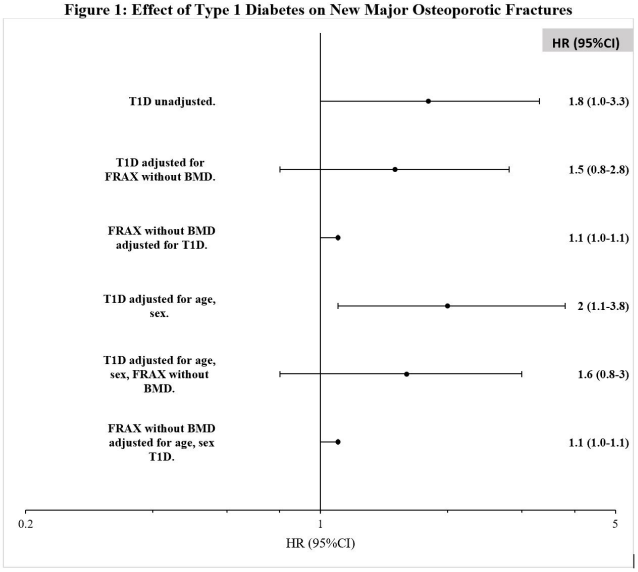

Statistics presented are in Hazard Ratios and 95% Confidence Interval (HR (95% CI)) and X-axis is labeled on logarithmic scale. MOF; Major osteoporotic fractures, T1D; Type 1 Diabetes; FRAX; fracture risk assessment tool, BMD; bone mineral density.

***Disclosures: Viral Shah**, None*

P-510

Pelvic Bone Density is Lower than Proximal Femur Bone Density in Postmenopausal Women *Mahshid Mohseni[1], Shannon Stum[1], Bridgett Toennies[1], Seth Eisen[2], Roberto Civitelli[1]. [1]Divison of Bone and Mineral Diseases, Washington University School of Medicine, United States, [2]Divison Rheumatology, Washington University School of Medicine, United States

Pelvic fractures represent 7% of all fragility fractures and are commonly (> 50%) associated with loss of independence in the elderly. The incidence of pelvic fractures has increased significantly over the past 3 decades; however, little is known about the relationship between bone mineral density (BMD) and pelvic fractures. We conducted a pilot, cross-sectional study to establish a method of measuring pelvic BMD and to correlate BMD of the pelvis with BMD at other skeletal sites. Postmenopausal women without a history of pelvis and hip fragility fractures were enrolled. Hip, spine, and pelvis DXA scans were obtained using a Hologic DXA machine. Pelvic BMD was calculated using Hologic Research Software from 3 areas of the pelvis (R1: public symphysis, R2: inferior pubic ramus, and R3: superior pubic ramus), corresponding to common fracture locations. Pelvis BMD was the average of the 3 pelvis sites. 104 postmenopausal women were enrolled in the study. Precision error was calculated using the root mean square method, as recommended by International Society of Clinical Densitometry. BMD precision error was 0.011g/cm2 which is slightly lower than the precision total hip BMD at our center (0.007 g/cm2). BMD of R1, R2, and R3 pelvic areas were measured as 0.44+/-0.15, 0.41+/- 0.15, and 0.62 +/-0.19 g/cm2, respectively. Notably, BMD of R3 was significantly higher than the other 2 areas (P<0.001, ANOVA). Pelvic BMD (0.49+/-0.14 g/cm2) was significantly lower than BMD of femoral neck (0.72+/- 0.16 g/cm2), total proximal femur (0.86+/-17 g/cm2) and spine (0.97+/- 19 g/cm2) (P <0.001). Pelvic BMD correlated with BMD of proximal femur (R2:0.73), femoral neck (R2: 0.51), and spine (R2:0.64). Women with osteoporosis in both spine and hip areas had significantly lower BMD of pelvis but osteoporosis at one location (only spine or hip) was not associated with lower pelvic BMD. Type 2 DM was associated with increase BMD of spine and total hip but not with increased pelvic BMD. In summary, we report a precise method of measuring BMD of commonly fractured areas of the pelvis. Pelvis BMD is lower than hip, femoral neck, and spine. Bone density of the pelvis correlates most with BMD of total proximal femur. The results of this pilot study can be used for future studies to determine whether pelvic BMD could help identify patients at risk for pelvic fragility fractures better than proximal femur BMD, which may change how osteoporosis is defined based on DXA tests.

***Disclosures: Mahshid Mohseni**, None*

Posters

P-511

Performance of the Garvan Fracture Risk Calculator in Individuals with Diabetes: A Registry-Based Cohort Study. *William Leslie[1], Tuan Nguyen[2], Suzanne Morin[3], Lisa Lix[1], John Eisman[2]. [1]University of Manitoba, Canada, [2]Garvan Institute of Medical Research, Australia, [3]McGill University, Canada

BACKGROUND: The Garvan Fracture Risk Calculator (FRC) is a simple prediction model derived from the Australian Dubbo Osteoporosis Study (DOES) cohort. Diabetes increases fracture risk and also falls risk. The Garvan FRC includes prior falls as an input variable. Whether the Garvan FRC captures diabetes-associated fracture risk is uncertain. OBJECTIVE: To evaluate the performance of the Garvan FRC in individuals with versus without diabetes.METHODS: Using the population-based Manitoba Bone Mineral Density (BMD) registry, we identified women and men age 50-95 years undergoing baseline BMD assessment from September 1, 2012 onwards with registry linkage, diagnosed diabetes, and self-reported falls in the prior 12 months. 5-year Garvan FRC predictions were generated from clinical risk factors (CRFs) without BMD and again with femoral neck BMD. We identified subsequent non-traumatic incident osteoporotic fractures (OF, any fracture excluding craniofacial, hand/foot, ankle) and hip fractures (HF) from population-based healthcare data sources to March 31, 2018 (mean observation time of 2.6 years). Overall risk stratification was assessed from area under the receiver operating characteristic curve (AUROC). Cox regression analysis was performed to examine the effect of diagnosed diabetes on fracture outcomes adjusted for Garvan FRC predictions (log-transformed to correct for a skewed distribution). All analyses were sex stratified.RESULTS: The study population consisted of 2,618 women with and 14,064 women without diabetes; 636 men with and 2,201men without diabetes. The Garvan FRC provided significant OF and HF risk stratification in women with diabetes, similar to those without diabetes (TABLE). Analyses of OF in men were limited by smaller numbers but did not show a significant difference between those with and without diabetes (insufficient HF in men for analysis). Cox regression showed that OF risk was 23% greater in women with diabetes adjusted for Garvan FRC including BMD (hazard ratio 1.23, 95% confidence interval [CI] 1.01-1.49) suggesting that the Garvan FRC slightly underestimated risk. An increased point estimate was also seen for diabetes-related HF risk in women (hazard ratio 1.37, 95%CI 0.88-2.15) but this was not statistically significant. CONCLUSIONS: The Garvan FRC shows similar fracture risk stratification in individuals with vs without diabetes, but may underestimate this risk.

	WITH DIABETES	WITHOUT DIABETES	
WOMEN – OSTEOPOROTIC fracture	AUC (95% CI)	AUC (95% CI)	p-value
Garvan FRC, without BMD	0.66 (0.61-0.71)	0.62 (0.59-0.65)	0.131
Garvan FRC, with BMD	0.70 (0.66-0.75)	0.66 (0.63-0.68)	0.072
WOMEN - HIP fracture	AUC (95% CI)	AUC (95% CI)	p-value
Garvan FRC, without BMD	0.82 (0.75-0.89)	0.85 (0.82-0.88)	0.426
Garvan FRC, with BMD	0.86 (0.80-0.93)	0.86 (0.82-0.90)	0.930
MEN - OSTEOPOROTIC fracture	AUC (95% CI)	AUC (95% CI)	p-value
Garvan FRC, without BMD	0.57 (0.46-0.67)	0.60 (0.54-0.65)	0.615
Garvan FRC, with BMD	0.60 (0.50-0.70)	0.62 (0.56-0.67)	0.759

p-value for AUROC, with vs without diabetes.

***Disclosures: William Leslie**, None*

P-512

Non-linear FE is more predictive of femoral fractures in the AGES RS cohort than aBMD or linear FE *Ingmar Fleps[1], Halldór Pálsson[2], Alexander Baker[1], William Enns-Bray[1], Hassan Bahaloo[2], Navrag Singh[1], William R. Tayler[1], Stephen J. Ferguson[1], Sigurdur Sigurdsson [3], Vilmundur Gudnason[3], Benedikt Helgason[1]. [1]Institute for Biomechanics, ETH Zürich, Switzerland, Switzerland, [2]School of Engineering and Natural Sciences, University of Iceland, Reykjavik, Iceland, Iceland, [3]The Icelandic Heart Association Research Institute, Kopavogur, Iceland, Iceland

Hip fractures in the elderly are a major socioeconomic burden. Clinical fracture risk assessment based on areal bone mineral density (aBMD) is known to only identify about 50% of individuals that will later fracture their hip. Finite element models (FEMs) based on CT scans are more predictive of ex-vivo measured proximal femoral strength than aBMD. However, improved hip fracture risk assessment with FEMs in clinical cohorts using only information gathered at baseline has not been demonstrated. Only studies that used data collected post-fracture [1] or with biased cohorts that do not include subjects with normal bone T-score [2] have found FEMs to be significantly better at assessing fracture risk than aBMD. In this study, we compare the ability of FEMs to classify hip fractures to that of aBMD in the AGES Reykjavik Study (RS) cohort.CT-based FEMs were built for 602 subjects (362 females and 239 males) of the AGES RS. Of these subjects, 201 suffered a hip fracture during the subsequent 5-7 year follow up period. Material properties were assigned to the FEMs based on CT grey scale values [3]. Each femur was loaded under 12 sideways fall impact alignments (Figure 1). Simulations were performed with linear (FEMsLinear) and with non-linear (FEMsNonlin) material properties. Classification of hip fractures was assessed with the area under the receiver-operator curve (AUC). Non-parametric bootstrapping was used to test for significance and a Benjamini-Hochberg correction procedure for multiple hypotheses testing was applied. Squared Spearman's coefficient of correlation (RS2) was used to quantify the variance in ranking for hip fracture classification depending on loading alignments.The AUC based on FEMsNonlin was found to be significantly higher than for aBMD for all 12 loading conditions (Figure 1). FEMsNonlin were significantly more predictive of hip fractures than FEMsLinear. The rankings based on femoral strength FEMsNonlin and FEMsLinear were highly correlated RS2 = 0.76-0.86. Using only baseline information from a large clinical cohort, we have shown a significant improvement in AUC for FEM-derived proximal femur strength compared to aBMD. This study adds credibility to the use of FEM-based hip fracture risk assessment in clinical settings. These models can be valuable for future development of in-silico selection of personalized preventive treatment options. Quasim et al, Osteoporos Int, 27:2815-2822, 2016.Sarvi et al, J Biomech, 88:64-71, 2019.

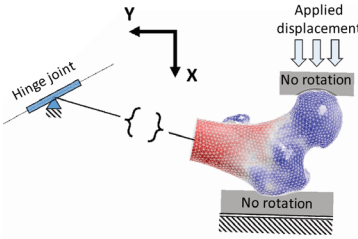

	Male N = 239	Female N = 362	All N = 573
aBMD	0.719	0.686	0.714
$FEMs_{Nonlin,10/30}$	0.777*+	0.740*+	0.760*+
$FEMs_{Nonlin,min}$	0.773*	0.737*	0.757*
$FEMs_{Linear,-5/0}$	0.742	0.710	0.729
$FEMs_{Linear,\ min}$	0.720	0.678	0.709

Figure 1 (left) Boundary conditions for the FEMs. (right) AUC values for female, male and pooled subjects. 10/30 indicates a loading alignment of 10 degrees adduction and 30 degrees internal rotation; min indicates that the minimum femoral strength across the 12 loading alignments was used. * indicate significance with respect to aBMD based AUC and + indicates significance with respect to the $FEMs_{Linear}$ results

***Disclosures: Ingmar Fleps**, None*

P-513

Biomechanical CT predicts vertebral stiffness in a cohort of Chinese cadavers *Wentian Feng[1], Yi Wei[2], Zuchang Li[0], Haisheng Yang[1]. [1]Department of Biomedical Engineering, Beijing University of Technology, China, China, [2]Beijing Jishuitan Hospital, China, China, [0]Beijing Jishuitan Hospital, China, China

Introduction: Osteoporotic spine fracture is a global issue affecting a great percentage of elderly population, and it is particularly serious in China which has the largest aging population and the fastest speed of aging. Accurate fracture risk prediction is the key for preventing osteoporotic vertebral fractures. Currently, bone mineral density (BMD) measurement based on dual-energy X-ray absorptiometry (DXA) is the clinical standard for vertebral strength (or related fracture risk) assessment [1]. While BMD works well for the hip at fracture risk prediction, it is far less successful for the spine. The biomechanical CT (i.e. QCT-based finite element (FE) analysis), which measures facture-related mechanical characteristics of the vertebra, has shown improved results in predicting vertebral fracture risk over BMD [2]. However, there is little evidence on its application in Chinese population. Thisstudy was motivated to develop a QCT-FE model to predict the vertebral stiffness for a cohort of Chinese cadavers and evaluate the accuracy of the FE predictions by comparing with mechanical testing results.Methods: QCT scans were taken for 13 vertebral bodies excised from 6 cadavers (T10–L4; age: 72-98 years; Male=4, Female=2). BMD of each vertebra was measured from the QCT scans. Each vertebral specimen was tested in compression until failure. The stiffness and strength of the vertebrae were measured from the load-displacement curves. FE models were created with voxel-based hexahedron elements and assigned with BMD-based heterogeneous material properties. Linear elastic FE analyses were performed. Results: Results showed high correlations (R^2=0.83, $p<0.05$) between FEA-predicted and experimentally measured stiffness values. The correlation between BMD and the measured stiffness was sightly lower, (R^2=0.76, $p<0.05$). The correlation between FEA-predicted stiffness and experimentally measured strength (R^2=0.52) was also stronger than that between BMD and experimental strength (R^2=0.39).Conclusion: These results show the effectiveness of QCT-FEA in assessing mechanical properties of vertebrae in Chinese and could provide support for future application of biomechanical CT for risk prediction of osteoporotic spine fractures in Chinese population.References: [1] Allaire B T et al., 2018, Osteoporosis International. [2] Keaveny T M et al., 2020, Osteoporosis International.Acknowledgement: BJNSF (7202003), NSFC (11702008).

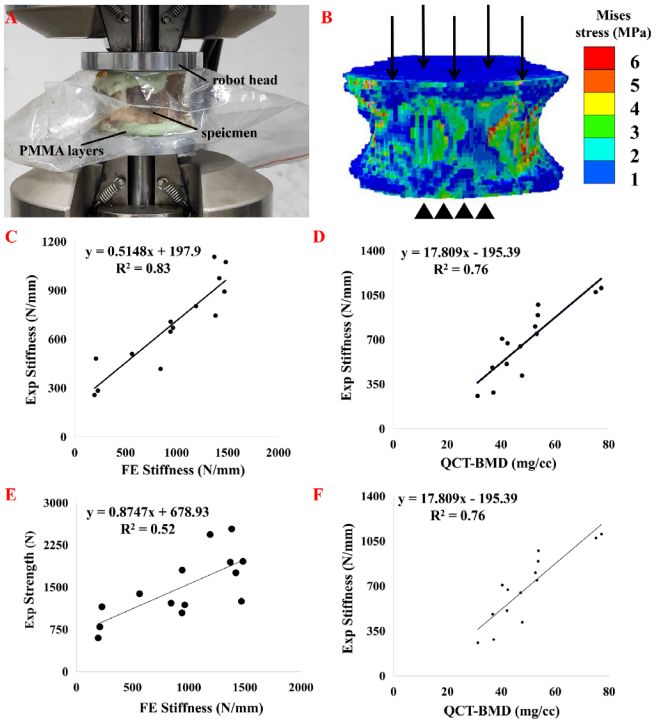

Fig. 1: (A) Experimental setup for uniform compression testing of the vertebral cadaver. The inferior and superior ends of the vertebra was filled with PMMA and cut in parallel. (B) von Mises stress distributions in the QCT-FEA model of a vertebra loaded in compression. (C-F) Correlations between experimental measurements (stiffness and strength) and FE-predicted stiffness or QCT-based BMD. For all analyses, n=14 specimens

***Disclosures: Wentian Feng**, None*

P-514

Defining incident vertebral compression fractures: comparison of three CT-derived and DXA-derived morphometric approaches *WING P. CHAN[1], Ai-Ling Hsu[1]. [1]Department of Radiology, Wan Fang Hospital, Taipei Medical University, Taiwan, Province of China

Defining incident vertebral compression fractures: comparison of three CT-derived and DXA-derived morphometric approaches*Wing P. Chan and Ai-Ling Hsu, Department of Radiology, Wan Fang Hospital, Taipei Medical University, Taiwan.Background: We hypothesized that the lowest parts of vertebral body heights cannot be obtained by two- dimensional vertebral fracture assessment (VFA) images from dual-energy X-ray absorptiometry (DXA) scans. The aim of this study was to assess the discrepancies between DXA-derived and series of thin-cut sagittal CT-derived images in measuring and classifying vertebral compression fractures using Genant's grade.Methods: We recruited 35 patients aged over 50 years (13 men, mean age 71.2+/-10.8; 22 women, 72.7+/-9.4) who had routine CT including lumbar spine and DXA scans. Patients who received spinal surgery or had metallic implants or scoliosis were excluded. A CT radiological technologist reformatted axial images into mid-sagittal views with a slice thickness of 2.50 mm, resulting in 235 sagittal reformatted slices of the vertebral columns. A radiologist with 28 years of experience in spine imaging manually marked 6 points on vertebral inner square corner (excluding cortical bone) of each mid-sagittal reformatted CT image, and the Genant's grade were automatically measured and calculated. We compared the "consistent / inconsistent" ratios of the CT-derived and DXA-derived morphometric approaches for each vertebral body. To classify each vertebral fracture grade, the CT scan of each patient was categorized by 3 methods: 1) Classical Method: Select the mildest grade from a series of images on a CT scan; 2) Consensus Method: Select the most prevalent grade from a series of images on a CT scan; and 3) Global Search Method: Select the most severe grade from a series of images on a CT scan.Results: In total, 165 vertebrae (T12 to L4) were analyzed. There was no statistically significant difference between the results of the DXA method and those of the CT-derived Classical Method (p = 0.069), but the DXA results were different from those of the other two CT-derived methods (p <0.001). The classification of compression fractures of Genant's grades 0, 1, 2, and 3 were75.8%, 6.1%, 9.1%, and 9.1%, respectively, for DXA; 69.1%, 7.9%, 11.5%, and 11.5%, respectively, for the CT-derived Classical Method; 44.2%, 21.8%, 17.0%, and 17.0%,respectively, for the CT-derived Consensus Method; and 22.4%, 26.7%, 29.1%, and 21.8%, respectively, for the CT-derived Global Search Method.Conclusion: The DXA method was unable to capture the lowest parts of vertebral body heights as defined by series of thin-cut sagittal CT-derived images, thereby underestimating the severity of vertebral compression fractures.***Disclosures:*** The authors declare that they have no competing interest.

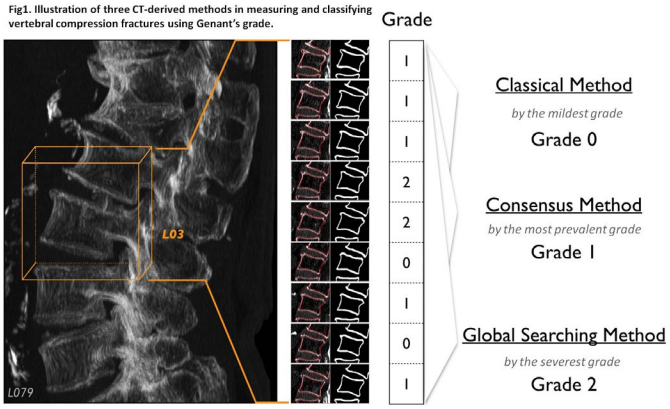

***Disclosures: WING P. CHAN**, None*

P-515

Development of Spine Radiography-Based Fracture Prediction Model Using Convolutional Neural Network *Sung Hye Kong[1], Jung Hee Kim[1], Jae Won Lee[2], Byeong Uk Bae[2], Jin Kyeong Sung[2], Kyu Hwan Jung[2], Chan Soo Shin[3]. [1]Department of Internal Medicine, Seoul National University College of Medicine, Republic of Korea, [2]Vuno Inc, Republic of Korea, [3]Seoul National University College of Medicine, Republic of Korea

Traditionally, bone mineral density has been used to define osteoporosis and to predict the risk of osteoporotic fractures. Deep-learning techniques from images have been rapidly developing, which may give us a novel insight into the bone quality, along with density. Therefore, we aimed to develop a spine radiography-based fracture prediction model using deep-learning methods. From 2012 to 2019 at Seoul National University Hospital, 2450 participants aged 50-75 years who had at least 2 lumbosacral radiographs without fracture at the baseline were included. Among them, 742 participants with radiographs inappropriate for the analysis and 113 followed up for < 6 months were excluded, which leaves 1595 participants in the final analyses. Positive cases were defined as participants who developed osteoporotic fractures during follow-up, and negative cases as those who did not. Two models using a convolutional neural network (CNN) and one model using naïve-Bayes were trained using the baseline radiographs, to predict the occurrence of osteoporotic fracture. The first CNN model used a key-point detection network to extract a region of interest of L1-5 vertebral bodies, which gives a bounding box of the whole lumbar spine. The second CNN model used segmented areas of each vertebral body to minimize the effect of confounders, such as aortic calcification or bowel gas. A naïve-Bayes model was trained using the information of age and sex of the participants. The performance was evaluated using the area under the receiver operating curves (AUCs) with 5-fold cross-validation. In a total of 1595 participants, 1188 were women, and the mean age was 60.5 years. The mean follow-up duration was 40.7 months, and there were 120 positive cases. The AUCs were 0.72+/-0.02, 0.80+/-0.03, and 0.72+/-0.02, and the sensitivities were 0.61, 0.74, and 0.65 in the first, second model of CNN, and the naïve-Bayes model, respectively. The specificities were 0.77 in all models. The CNN model using segmented images showed the highest AUC and sensitivity among models (both p<0.001). In conclusion, the CNN model with segmented vertebral images outperformed the CNN model with non-segmented images and naïve-Bayes model in predicting osteoporotic fractures using baseline lumbosacral radiographs.

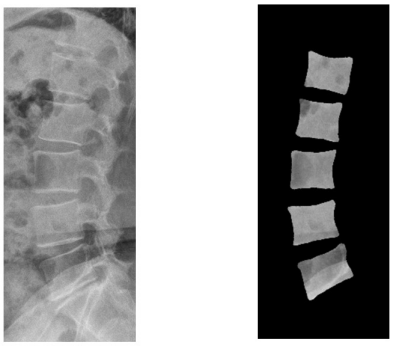

A) CNN Model 1 with non-segmented image

B) CNN Model 2 with segmented image

***Disclosures: Sung Hye Kong**, None*

Posters

P-516

Classification of Motion Artifact Severity in High-Resolution Peripheral Quantitative Computed Tomography Using Deep Convolutional Neural Network *Jin Long[1], Jessica Whalen[1], Derek Yang[1], Ariana Strickland[1], Kyla Kent[1], Saeed Seyyedi[2], Mary Leonard[1], Andrew Burghardt[3]. [1]Department of Pediatrics, Stanford University, Stanford, CA, United States, [2]Department of Radiology, Stanford University, Stanford, CA, United States, [3]Department of Radiology & Biomedical Imaging, University of California San Francisco, San Francisco, CA, USA, United States

In vivo bone imaging techniques, including conventional and high-resolution peripheral quantitative computed tomography (HR-pQCT), are susceptible to motion artifacts, particularly in fidgety pediatric populations. While some attempts have been made to implement motion correction in lower resolution peripheral cone beam CT, these techniques have not been adapted to HR-pQCT specifically. Visual inspection is widely used to subjectively categorize scans into 5 grades of motion artifact severity, from completely acceptable (1) to completely unusable (5), following the scaling method by Pialat et al. The scoring scale has been adopted in recent consensus guidelines; however, it is time-consuming, highly subjective and operator dependent. We report an innovative deep learning method to classify motion artifact severity in HR-pQCT scans of the metaphyseal and diaphyseal tibia and radius obtained in children and adolescents. A total of 10,000 2D images were randomly sampled from 5627 3D scans (168 images/scan) performed in 320 participants and randomized into training (60%), validation (20%) and testing (20%) datasets. Annotations using the standard 5-grade scale were performed by one highly-experienced observer and used as the ground truth. To give each motion grade an equal chance for the machine to learn, scans with grades 4 and 5 were oversampled from the scan pool to create 5 equally distributed samples. Multiple unique images were sampled from each scan. Neural networks are good at dealing with this within-scan correlation by processing each input image independently (e.g. flipping, distorting and randomly cropping). To avoid the use of correlated data across training, validation, and testing datasets, randomization at the scan level was used. The initial results in 1,000 annotated images demonstrated the best performance for a 161-layer DenseNet model that was pretrained on ImageNet and then further trained and tuned on our HR-pQCT data. This transfer learning classifier achieved an overall accuracy of 93% (kappa=0.94), with high accuracy across motion grades 1 to 3 (grade 1: 85%; grade 2: 78%; grade 3: 96%). Notably, the accuracy of the classifier was 100% for the grades 4 and 5, which are conventionally excluded from analyses. Deep convolutional neural networks can provide rapid automated classification of motion artifact severity, representing an important tool for operational efficiency and quality in multi-center clinical studies.

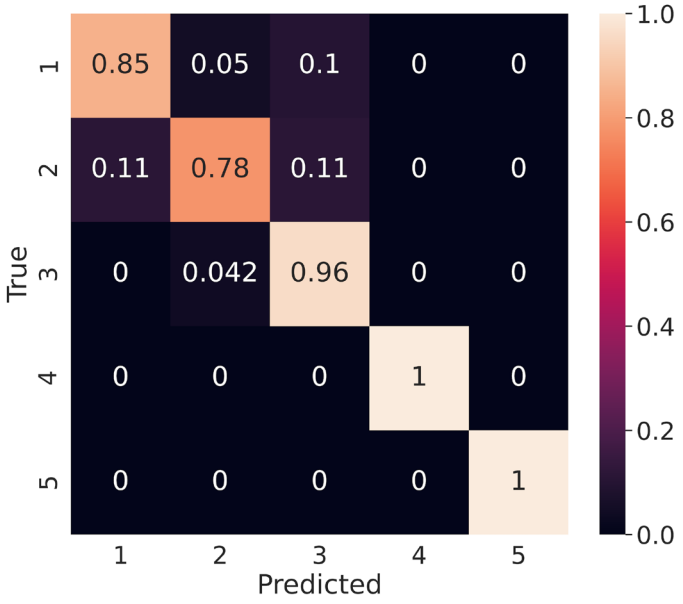

***Disclosures: Jin Long**, None*

P-517

Rapid Detection of Vertebral Deformities and Lumbar Scoliosis from Spine DXA Scans *Abhinav Suri[1], Sisi Tang[1], Ashley Terry[1], Anjali Gupta[1], Iman Fathali[1], Charis Ma[1], Abigail Manion[1], Anita Kalluri[1], Winnie Xu[1], Anna Feng[1], Elyse Migdal[1], Eric Ji[1], Christian Fernandes[1], Uchechi Nwogwugwu[1], Soomin Lee[1], Vikram Balasubramanian[1], Kelly Moyer[1], Devna Chopra[1], Albert Chen[1], Elijah Li[1], Chamith Rajapakse[1]. [1]University of Pennsylvania, United States

PURPOSELumbar spinal deformities are highly prevalent among older patients with osteoporosis and other degenerative bone diseases. Furthermore, these deformities cause a curvature of the spine (scoliosis), leading to a higher risk of fracture and pain in patients. Currently, DXA scans report vertebrae specific BMD scores; however, they do not report vertebral deformities or presence of lumbar curvature. We report the development of a computer vision algorithm for rapid automated morphometric measurement of Spine DXA scans. METHODSSpine DXA reports (1282 subjects, age 64.5+/-10.7yrs, female) were processed to isolate the relevant DXA image. From the DXA scan, lines were detected using Hough Line transforms (similar lines were consolidated using K-Means clustering on endpoints) and intersections were found between reconstructed lines and the contour of the spine outline (Fig 1). From these intersection points, corner points for each vertebral body (n=6410) were isolated, allowing for the measurement of vertebral body lateral heights (right lateral vs left lateral height) and Cobb angles in the coronal plane. The algorithm was evaluated using a key-point error distance metric that measures distance of predicted corner points to manually marked corner points of vertebral bodies.RESULTSThe algorithm was able to detect relevant corner points rapidly and with high accuracy. On a set of 1000 scans, each scan was processed in an average of 0.035 +/- 0.012 seconds. Average key-point error distance was 0.13mm when evaluated on a testing set of 100 manually annotated scans (age 64.3+/-5.3yrs, female).CONCLUSIONSThe computer vision algorithm was able to determine morphometric measurements for detecting vertebral body corner points with high accuracy on DXA images. Additionally, it was able to do so quickly. These corner points can be used to calculate vertebral deformities and Cobb angles for scoliosis grading. Thus, we were able to show this algorithm is able to automatically extract measurements for rapid quantification of vertebral bone health and potential risk of fracture. This automated approach could simplify the screening, detection of changes, further cross-sectional imaging workup, and surgical planning in patients with vertebral deformities and fractures by reducing the burden on radiologists who have to do these measurements manually.

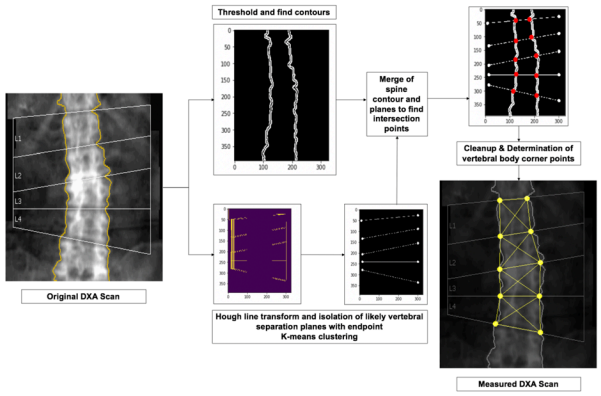

Figure 1: Basic overview of the computer vision algorithm pipeline. First DXA scan is converted to byte array and thresholded to find spine outline contours. Additionally, line annotations are extracted using Hough line transform and endpoints are determined from the resulting candidate lines using K Means clustering (10 clusters). The resulting key-points are joined to form line segments and are merged with contour image to find intersection points. Intersection points are isolated and vertebral heights (and other measurements) are determined.

***Disclosures: Abhinav Suri**, None*

P-518

Interval Bone Mineral Density Loss in Osteopenic Patients: A Limitation of FRAX *Charles Intenzo[1], Aishwarya Gulati[1], John Bilezikian[2]. [1]Thomas Jefferson Univ., United States, [2]Columbia Univ., United States

Background:Bone mineral density (BMD), considered to be a gold standard for the diagnosis of osteoporosis, is most commonly measured by dual-energy x-ray absorptiometry (DXA). For patients with osteopenia, the Fracture Risk Assessment Tool (FRAX) incorporates acknowledged other risk factors to assess overall fracture risk, and aid in patient management. If the FRAX score in in an osteopenic patient predicts a 10-year fracture risk of >20% for a major osteoporotic fracture, or >3% for a hip fracture, pharmacologic therapy is indicated.. However, FRAX does not include an assessment of a significant decline in BMD

over time.Methods:Our goal was to determine the frequency with which BMD declines in patients with osteopenia by DXA, but whose FRAX score coninues to be below treatment thresholds.Results:Over a 2-year interval, 1,112 (15.59%) of 7,133 patients with osteopenia by DXA experienced a significant decrease in BMD, but had FRAX scores remain in the subtherapeutic range.Conclusion:Since a decline in BMD is, by itself, a clinical risk factor, FRAX assessment may therefore potentially underestimate true fracture risk if a significant decline in BMD is measured.

***Disclosures: Charles Intenzo**, None*

P-519

New technology REMS demonstrated good accuracy for the diagnosis of osteoporosis defined by DXA, in Brazilian adult women. *Débora Meira Ramos Amorim[1], Eliane Naomi Sakane [1], Sérgio Setsuo Maeda[1], Marise Lazaretti Castro[1]. [1]Federal University of Sao Paulo, Brazil

Background: Dual energy X-ray absorption (DXA) is the standard method used to define osteoporosis, according to the criteria created by the World Health Organization in 1995. However, DXA has some limitations that other new methodologies try to overcome. A new technology is the Radiofrequency Echographic Multi Spectrometry(REMS), which uses sound waves instead of ionizing radiation, in addition to the advantages of portability and lower cost. To better understand the utility of this method, we compared bone mass density (BMD) measured using both REMS and DXA in Brazilian women recruited at the School-Hospital's DXA Service in Sao Paulo, Brazil. The short-term intra-operator and inter-operator CV% were also performed. Results: A total of 343 patients were included. Due to poor quality on acquisitions, we had to exclude 67 lumbar spines and 63 femoral neck from the REMS exams, and 41 lumbar spines and 31 proximal femurs from the DXA exams. In addition, 22 exams were excluded for other technical reasons. In the resulting dataset (227 spines and 238 femurs) there were high correlations between both methodologies for BMD values (r=0,75, p<0.001 for lumbar spine and r=0.78, p<0.001 for femoral neck). The comparison between REMS outcomes and DXA showed that the average difference in BMD (expressed as bias +/- 1.96 SD) was -0.026 +/- 0.1758 g/cm2 for the spine and -0.027 +/- 0.1525 for the femoral neck.The good correlation between the two methods also is showed by standard error of the estimate (SEE) of 8.3% for the spine and 10.3% for the femur. RMS-CV% was 0.33% for spine and 0.29% for femoral neck. For the diagnosis of osteoporosis in women older than 40 years, REMS approach effectively discriminated the osteoporotic patients from the non-osteoporotic for both lumbar spine(sensitivity = 84%, specificity=94.6%) and femoral neck (sensivitity= 92.6%,specificity 93.5%), by accepting a 0.3 tolerance on T-score value of "borderline" patients. Evaluating REMS precision by CV-RMS%,the result was 0.943 for BMD lumbar spine and 1.175 for BMD femoral neck. With regard to REMS repeatability by CV-RMS%, it resulted in 0.671 for BMD lumbar spine and 0,706 for BMD femoral neck. Conclusions: The REMS approach can be used for non-ionizing osteoporosis diagnosis directly on the lumbar spine and femoral neck with a good level of accuracy and precision.

***Disclosures: Débora Meira Ramos Amorim**, None*

P-520

Bone Fragility Parameters do not Fiffer Significantly in Patients with Primary and Subsequent Distal Radius Fracture *Jongjin Lee[1], Young Ho Shin[1]. [1]Department of Orthopedic Surgery, Asan Medical Center, University of Ulsan College of Medicine, Republic of Korea

Purpose: The characteristics of patients who experienced subsequent distal radius fracture (DRF) after initial DRF have not been determined. The purpose of this study was to investigate the characteristics of patients with subsequent DRF and to compare bone fragility parameters of patients with primary and subsequent distal DRF.Methods: We compared demographic characteristics and bone fragility parameters, including bone mineral density (BMD), trabecular bone score (TBS), hip geometry parameters, and bicortical thickness (BCT) of the distal radius in 215 patients with primary and 26 with subsequent DRF. To reduce bias, patients with subsequent DRF were propensity score matched in a 1:2 manner with patients with primary DRF and additional comparison was done.Results: The mean time to subsequent DRF after initial DRF was 121.9 mo +/- 85.3 mo (range, 1 to 240 mo). Subsequent DRF group was older than primary DRF group, but it was not statistically significant (p=0.077). The portion of patients exposed to osteoporosis medications was significantly higher in the subsequent DRF group (38.5% vs. 19.1%, p=0.022).Bone fragility parameters, including BMDs, TBS, hip geometry parameters and BCT did not differ significantly in the two groups. Similar results were observed in comparison between propensity score matched primary and subsequent DRF group.Conclusions: Despite patients in the subsequent DRF group being older, bone fragility parameters did not differ significantly in patients with primary and subsequent DRF. These findings suggest that the occurrence of subsequent DRF is due to multiple factors, not to bone fragility alone.

***Disclosures: Jongjin Lee**, None*

P-521

Deep Learning for Rapid High-Resolution Proximal Femur MRI Scans *Brandon Jones[1], Carlos Osuna[1], Srikant Iyer[1], Olivia Sandvold[1], Nicholas Josselyn[1], Matthew MacLean[1], Gregory Chang[2], Walter Witschey[1], Hee Kwon Song[1], Felix Wehrli[1], Chamith Rajapakse[1]. [1]University of Pennsylvania, United States, [2]New York University, United States

Introduction:Hip fractures affect one in six postmenopausal women during their lifetime and cause the greatest mortality and morbidity among fractures, with the one-year mortality rate reaching 20%. While existing osteoporotic medications have been shown to reduce fracture risk by half, they are not prescribed to everyone who would benefit from them. As such, there is a clear need for improved methods for clinical assessment of bone quality-both in terms of diagnostic accuracy and cost. In recent years, MRI has shown strong potential for quantifying hip fracture risk due to its ability to image both trabecular and cortical microarchitecture in vivo. One of the existing MRI protocol for microstructural imaging of the proximal femur involves a 16-minute Spoiled Gradient Recalled Echo (SPGR) sequence which is too long to be clinically viable. Therefore, the present abstract investigated feasibility of reducing this scan time through the application of deep convolutional neural networks (CNNs) for Compressed Sensing.Methods: A Monte Carlo algorithm retrospectively subsampled k-space data in 2D from fully sampled MR images of the proximal femur. The subsampled k-space was then naïvely Fourier transformed with zero padding and the resultant artefactual image was used as input to the CNN. We employed a 2D U-Net with 9 layers consisting of 4 feature contracting and 4 feature expanding segments, each with a series of convolutions followed by Rectified Linear Unit (ReLU). The network was trained for 500 epochs at 5 times acceleration factor (AF), which means only 102 lines of k-space frequency encoding was included out of 512 total, but was evaluated for both AF of 3 and 5. We used a custom loss defined as the sum of the mean squared error (MSE) in image space, the MSE between the measured and predicted k-space within the MC mask, and the MSE of horizontal gradients.Results: Reconstructed images are shown in Fig 1. The CNN removes the majority of artefacts are both acceleration factor (AF) of 3x and 5x. At 5x AF, the CNN improved the structural similarity index, normalized root-mean-squared error, and peak SNR (p<0.0001 for all).Discussion:The present abstract comprises the first preliminary results that CNNs can reconstruct high-resolution bone MRI scans which are sampled below the Nyquist criterion. Ongoing work will develop a concurrent model which to interpolate missing data in k-space, as well as extend the models to work for 3-D and parallel imaging.

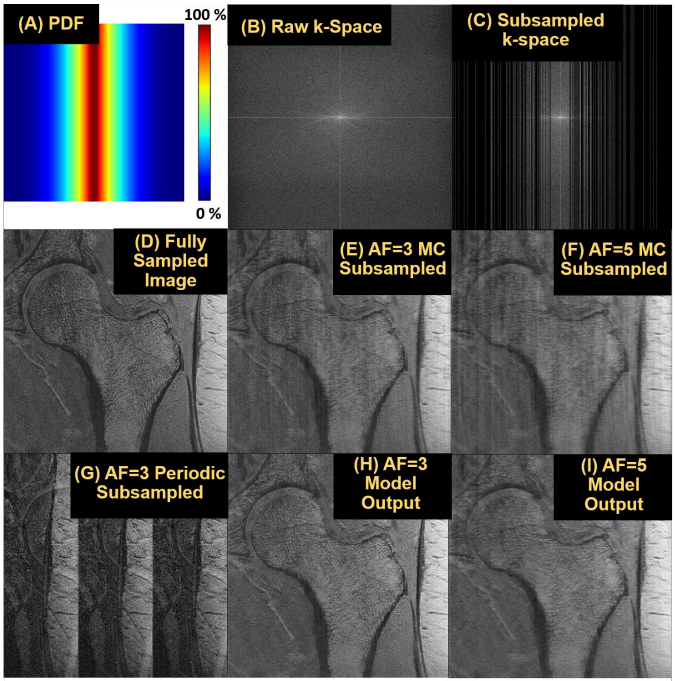

Figure 1: (A) Probability density function for creating pseuorandom k-space mask. **(B)** Raw k-space for a single SPGR image slice. **(C)** Monte Carlo subsampled k-space. **(D)** Fully sampled image used as network label. **(E)** and **(F)** are the Monte Carlo subsampled images accelerated 3x and 5x. **(G)** is an image with periodic 3x acceleration. The reconstructed images from the CNN shown in **(H)** and **(I)** correspond to the inputs from **(E)** and **(F)**.

***Disclosures: Brandon Jones**, None*

Posters

P-522

Assessment of Gender Differences in Bone Metabolism Using [18F]NaF PET/CT in the Spine *Helene Chesnais[1], Sylvia Rhodes[1], Poul Høilund-Carlsen[2], Abass Alavi[1], Chamith Rajapakse[1]. [1]Penn Medicine, United States, [2]Odense University, Denmark

Structural imaging modalities such as DXA are currently used to assess bone quality in osteoporosis but may lack the sensitivity to detect changes in metabolic activity. The use of [18F]NaF PET/CT is increasing as a marker of bone metabolism. The purpose of this study was to analyze gender differences in the lumbar and thoracic spines of healthy males and females as measured by [18F]NaF PET/CT. This retrospective study included136 participants (68 females and 68 males, ages 21-75) that had undergone [18F]NaF PET/CT. The operator guided computer software PMOD software (PMOD Technologies LLC, Switzerland) was used to segment individual vertebra, and calculate SUV. Bone metabolism of the thoracolumbar spine, lumbar spine and thoracic spine was compared using linear regressions with age and BMI in all subjects, then stratified by gender, and by Young (<50) and Old (>=50) age categories. In females but not males, bone metabolism was negatively correlated with age (r=-0.51, P<.001). In females but not males, bone metabolism was positively correlated with BMI (r=0.44, P<.001).Bone metabolism was correlated with BMI in young and old females, but not young and old males, Figure 1. Bone metabolism as measured by SUV demonstrated more consistent trends with age and BMI in females than in males. This can inform the analysis of future healthy, mixed-age and mixed-BMI cohorts for [18F]NaF PET/CT.

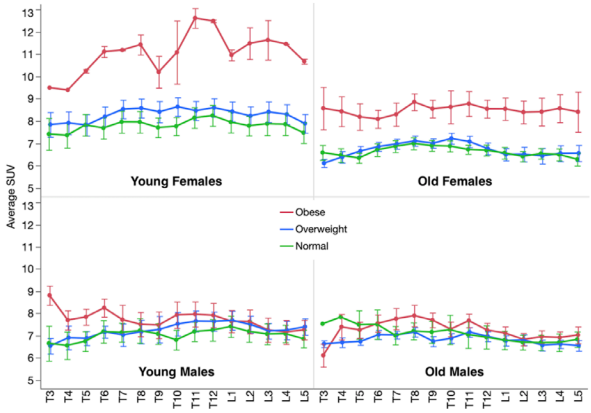

Figure 1. Mean Average SUV by BMI Categorization. Each error bar is constructed using 1 standard error from the mean.

***Disclosures: Helene Chesnais**, None*

P-523

Towards explainable AI: Can Visualizations via Saliency Maps Support Understanding a Neural Network's Decision on 3D CT Vertebral Fracture Discrimination? *Eren Bora Yilmaz[1], Alexander Oliver Mader[2], Tobias Fricke[3], Jaime A. Peña[4], Carsten Meyer[5], Claus-Christian Glüer[4]. [1]Department of Computer Science, Kiel University, Germany, [2]Institute of Computer Science, Kiel University of Applied Sciences, Kiel, Germany, Germany, [3]Klinik für Radiologie und Neuroradiologie des Universitätsklinikums Schleswig-Holstein, Campus Kiel, Germany, [4]Section Biomedical Imaging, Dept. of Radiology and Neuroradiology, University Hospital Schleswig-Holstein (UKSH), Campus Kiel, Germany, [5]Kiel University of Applied Sciences, Institute of Computer Science, Kiel, Germany AND Kiel University, Faculty of Engineering, Department of Computer Science, Kiel, Germany AND Philips Research, Department of Digital Imaging, Hamburg, Germany, Germany

Automated evaluation of vertebral fracture status on computed tomography (CT) scans acquired for various purposes (opportunistic CT) may substantially enhance vertebral fracture detection rate. Deep neural networks (NNs) have shown promising performance in a number of classification tasks but their black box nature may hinder acceptance by radiologists and clinicians. We aim: (a) to develop and evaluate a convolutional NN architecture for osteoporotic vertebral fracture discrimination based on 3D CT data as part of a pipeline localizing (Mader et al., MICCAI 2019) and classifying individual vertebrae with regard to their fracture status and (b) to compute saliency maps to visualize areas that majorly influence the network's decision. Low-dose CT images of 159 patients (136 female), typically T5–L4, from 7 participating centers were annotated with vertebral coordinates and per-vertebra fracture status by a trained radiologist. A total of 132 of 1,943 vertebrae in the dataset showed osteoporotic fractures based on the Genant classification method. Experiments were conducted using a VGG-like network with 4 convolutional layers and 5.6 million trainable parameters. The network was trained in a random four-fold cross-validation setup for the task of osteoporotic fracture discrimination, based on 3D image patches containing a single vertebra, using the cross-entropy loss (plus additional regularization terms taking into account the radiologist's vertebral height gradings). Saliency maps were computed using the Grad-Cam and Guided BackProp algorithms. As proposed by Adebayo et al., NIPS 2019, the maps were qualitatively compared to those of models with randomly initialized weights and those of models trained on random labels to ensure meaningfulness of the maps. After training for less than 30 minutes on a high-end GPU the vertebra level models achieved areas under the ROC curve (AUC) between 0.966 and 0.999 across different folds. Thus, CT-based NN permit highly accurate discrimination of osteoporotic vertebral fracture status of individual vertebrae. Saliency maps (see figure) seem to highlight vertebral end plates and borders, i.e., fracture-relevant features, but were qualitatively found to depend on the model architecture (not shown) and the algorithm used to compute the maps. Thus, more research is needed on the calculation and interpretation of saliency maps as a means to visualize the complex decision process of a NN.

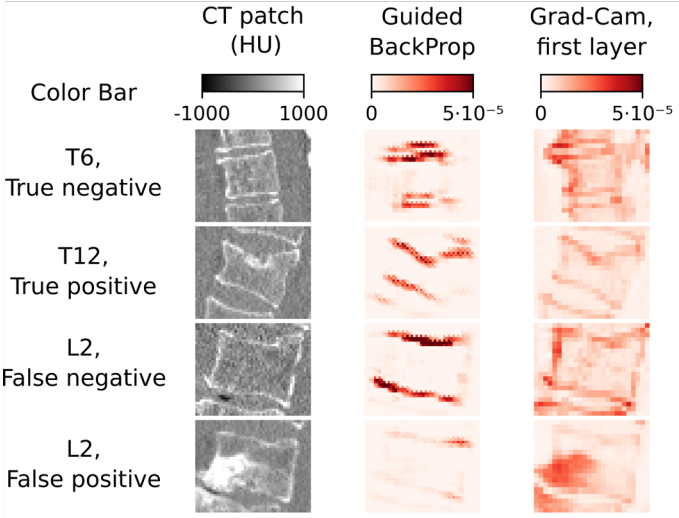

Figure: Central sagittal slices of vertebral patches and saliency maps

***Disclosures: Eren Bora Yilmaz**, None*

P-524

Impact of Trabecular Bone Score on Fracture Risk in Postmenopausal Women With Type 2 Diabetes Compared to Those Without Type 2 Diabetes *Shamsuddin Shaik[1], Ibtehal Shamleffer[2], M Raihan Azad[3], Diann Jones[4], Shemra Rizzo[5], Fiona Cook[4]. [1]Lehigh Valley Health Network, United States, [2]LeBauer Endocrinology, United States, [3]Physicians East Endocrinology, United States, [4]East Carolina University, United States, [5]Independent Researcher, United States

BackgroundRecent literature indicates that patients with Type 2 diabetes (T2DM) have higher fracture risk despite higher bone mineral density (BMD) than non-diabetic patients and that this involves adverse effects of T2DM on bone quality. Trabecular Bone Score (TBS) is a noninvasive test of bone quality. Previous studies have found an association with T2DM and lower TBS. Our aim was to compare the impact of adding TBS to the calculation of 10-year fracture risk (FRAX) in post-menopausal (PM) women with or without T2DM. MethodsRecords of 1,504 women of age>55 on the same DXA machine within the preceding 10 years were systematically screened. Those with BMD of the femoral neck and at least 2 valid lumbar vertebrae and lowest T score -2.5 were included. TBS was analyzed on valid vertebrae. Information on fracture risk factors and diabetes was found in medical records. Patients with GFR <30 ml/min, causes of secondary osteoporosis, or use of drugs affecting bone metabolism were excluded. A validated calculator (www.sheffield.ac.uk/FRAX) was used to determine major osteoporotic (MOP) and hip FRAX for each eligible case. Logistic regression was used to assess the association of T2DM status with having an increased FRAX score when including TBS.ResultsThe study included 109 patients with T2DM and 112 without DM. Significant differences were found in age, BMI, and race between the groups. The DM group was 63% African American (AA), with mean age 69 and mean BMI 33. The non DM group was 66% Caucasian (W), with mean age 67 and mean BMI 31. In unadjusted models, inclusion of TBS was more likely to increase MOP FRAX and hip FRAX in the T2DM than the non DM group. This finding lost significance after adjustment for age, race, and BMI. In the adjusted model, inclusion of TBS was more likely to increase MOP FRAX and hip FRAX in AA than W and less likely to increase MOP FRAX and hip FRAX with increase in BMI. Inclusion of TBS was less likely to increase hip FRAX with increase in age. (see Table)ConclusionThis study does not clarify the impact of TBS on FRAX in PM women with osteopenia and T2DM due to age, race, and BMI differences between the groups. However, the study does demonstrate that age, race, and BMI significantly influence the impact of TBS on FRAX. Since T2DM is prevalent in AA and Hispanic patients, it will

be important to consider race in future studies investigating the reasons for the association of T2DM with increased fracture risk.

Table. Logistic regression models of having larger 10-year probability of fracture risk after adding TBS.

A. MOP Fracture Risk

	Non-adjusted model			Adjusted model		
	OR	95% CI	p-value	OR	95% CI	p-value
Type 2 Diabetes						
Yes	1.81	(1.06, 3.11)	0.030	1.55	(0.80, 2.99)	0.188
No	---	---	---	---	---	---
Race						
White	---	---	---	---	---	---
Black	---	---	---	6.07	(3.12, 11.8)	<0.001
BMI	---	---	---	0.90	(0.86, 0.94)	<0.001
Age	---	---	---	0.97	(0.92, 1.02)	0.285

B. Hip fracture risk

	Non-adjusted model			Adjusted model		
	OR	95% CI	p-value	OR	95% CI	p-value
Type 2 Diabetes						
Yes	1.90	(1.09, 3.27)	0.022	1.52	(0.79, 2.93)	0.208
No	---	---	---	---	---	---
Race						
White	---	---	---	---	---	---
Black	---	---	---	2.16	(1.13, 4.13)	0.020
BMI	---	---	---	0.91	(0.86, 0.96)	<0.001
Age	---	---	---	1.13	(1.07, 1.20)	<0.001

***Disclosures: Shamsuddin Shaik**, None*

P-525

Effects of Risedronate on Trabecular and Cortical Volumetric Bone Density of the Hip after Sleeve Gastrectomy: a Pilot Randomized Controlled Trial *Katelyn Greene[1], Kylie Reed[2], Kristen Beavers[2], Daniel Beavers[1], Adolfo Fernandez[3], Jamy Ard[3], Sarah Wherry[4], Ashley Weaver[1]. [1]Wake Forest School of Medicine, United States, [2]Wake Forest University, United States, [3]Wake Forest Baptist Health, United States, [4]University of Colorado Anschutz Medical Campus, United States

Purpose: Bone mineral density (BMD) loss and increased fracture risk following bariatric surgery indicate a need for effective strategies to minimize bone loss, particularly at the hip. Bisphosphonates may be effective in mitigating surgical weight loss-associated bone loss, which can comprehensively assess bone in each compartment using quantitative computed tomography (QCT).Methods: This 6-month pilot randomized controlled trial (NCT03411902) enrolled 24 older sleeve gastrectomy (SG) patients to examine the efficacy of 150 mg once monthly risedronate (versus placebo) in the prevention of surgical weight loss-associated bone loss. Helical QCT scans of the left hip were performed at baseline (prior to SG) and at 6 months post-SG with a bone calibration phantom (Mindways Inc.). Trabecular and cortical volumetric BMD (vBMD) of the total hip, femoral neck, and trochanter were measured using QCT Pro v6.1. Group treatment effects were estimated using a general linear model adjusted for baseline values of each outcome.Results: Of 24 participants randomized, 20 (n=7, risedronate; n=13, placebo) completed baseline QCT testing and 17 completed 6-month QCT testing. At baseline, average age was 57+/-7 years, 85% were female (65% postmenopausal), and 15% were black. Compared to the placebo group, the risedronate group had a higher baseline body mass index (46.6+/-8.0 vs 41.9+/-3.8 kg/m2) and osteopenia incidence (2 vs 0). No statistically significant differences were observed in any vBMD outcomes between treatment groups. However, the directionality of treatment effect estimates suggests preserved trabecular vBMD in the risedronate group versus placebo at the total hip [mean (SE): -7.3 (5.1) vs -9.3 (3.3) mg/cm3] and femoral neck [3.7 (6.8) vs -5.0 (4.4) mg/cm3], but not at the trochanter [-5.5 (2.0) vs -4.5 (1.3) mg/cm3]; (see Figure 1). Treatment effect estimates suggest a trend in the opposite direction for cortical vBMD, with higher losses in the risedronate group vs placebo at the total hip [-5.0 (13.5) vs 21.0 (8.5) mg/cm3], femoral neck [-109.6 (50.9) vs -15.5 (32.7) mg/cm3], and trochanter [14.7 (51.5) vs 21.7 (31.7) mg/cm3].Conclusion: Data from this pilot study do not show risedronate treatment significantly affects compartmental vBMD change following SG. However, the direction and magnitude of change observed suggest risedronate may minimize short-term trabecular vBMD loss at the hip and femoral neck, but not necessarily protect against cortical vBMD loss.

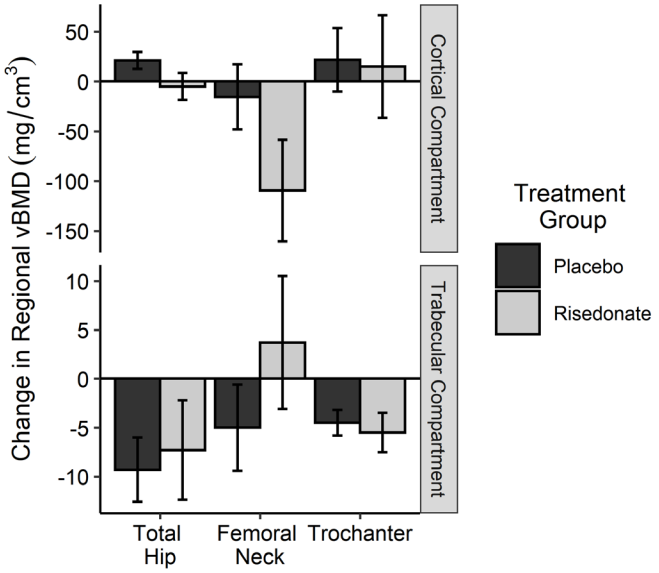

***Disclosures: Katelyn Greene**, None*

P-526

Towards a Generalized Convolutional Neural Network for Automated Identification of Vertebral Compression Fractures: The Manitoba Bone Mineral Density Registry *Barret A. Monchka[1], Douglas Kimelman[1], Lisa M. Lix[1], William D. Leslie[1]. [1]University of Manitoba, Canada

Background: Automated identification of vertebral compression fractures with accuracy comparable to human experts is possible through the use of convolutional neural networks (CNNs). Due to technical differences between GE dual-energy (DE) vertebral fracture assessment (VFA) images and Hologic single-energy (SE) VFA scans, CNNs trained on one scan mode may not generalize well to another.Aim: To evaluate the ability of CNNs to generalize between DE and SE VFA scan modes.Methods: 12,742 VFAs were obtained from the Manitoba Bone Mineral Density Program between 2010 and 2017 (GE Lunar Prodigy and iDXA). VFAs were classified by expert readers as fracture present vs. absent using the modified algorithm-based qualitative (ABQ) method. Scans were randomly divided into independent training (60%), validation (10%), and test (30%) sets. Three CNN models were constructed by training separately on DE only, SE only, and a composite dataset comprised of both SE and DE VFAs. All three trained CNN models were separately evaluated against both SE and DE test datasets (6 combinations). Accuracy, sensitivity, specificity, and area under the receiver operating characteristic curve (AUC) were used to evaluate predictive performance compared with the human reference.Results: Good performance was seen for CNNs trained and evaluated on the same scan mode. DE scans used for both training and evaluation achieved accuracy 87.5%, sensitivity 87.9%, specificity 87.4%, AUC 0.94. SE scans used for both training and evaluation achieved accuracy 87.4%, sensitivity 79.4%, specificity 89.0%, AUC 0.91. Conversely, CNNs performed poorly when evaluated on scan modes that differed from their training sets (DE-trained model evaluated against SE VFAs AUC=0.58; SE-trained model evaluated against DE VFAs AUC=0.58). However, a composite CNN trained simultaneously on both SE and DE VFAs gave performance comparable to DE/DE; and significantly better than SE/SE, DE/SE, and SE/DE, whether evaluated against DE VFAs (accuracy=92.3%, sensitivity=82.4%, specificity=94.3%, AUC=0.95) or SE VFAs (accuracy=90.6%, sensitivity=82.2%, specificity=92.3%, AUC=0.94).Conclusion: CNNs for vertebral fracture identification are highly sensitive to scan mode and do not generalize when trained on only one scan mode. Training CNNs on a composite dataset, comprised of both DE and SE VFAs, allows CNNs to generalize to both scan modes and improves automated fracture identification in SE VFA scans.

Training dataset	Evaluation dataset	Accuracy	Sensitivity	Specificity	AUC
Dual-energy	Dual-energy	87.5%	87.9%	87.4%	0.94
Dual-energy	Single-energy	60.4%	47.4%	63.1%	0.58
Single-energy	Dual-energy	70.4%	30.3%	78.6%	0.58
Single-energy	Single-energy	87.4%	79.4%	89.0%	0.91
Composite	Dual-energy	92.3%	82.4%	94.3%	0.95
Composite	Single-energy	90.6%	82.2%	92.3%	0.94

AUC = area under the receiver operating characteristic curve.
Composite = dataset comprised of both single-energy and dual-energy vertebral fracture assessments.

***Disclosures: Barret A. Monchka**, None*

Posters

P-527

Global impact of COVID-19 on osteoporosis management: A retrospective, longitudinal descriptive analysis of access to online FRAX fracture risk assessments. *Eugene McCloskey[1], Nicholas Harvey[2], Helena Johansson[3], Mattias Lorentzon[4], Liesbeth Vandenput[5], Enwu Liu[5], John Kanis[3]. [1]Centre for Integrated research in Musculoskeletal Ageing, University of Sheffield, United Kingdom, [2]MRC Lifecourse Epidemiology Unit, University of Southampton, United Kingdom, [3]Centre for Metabolic Bone Diseases, University of Sheffield, United Kingdom, [4]Sahlgrenska Academy, University of Gothenburg, Sweden, [5]Mary McKillop Health Institute, Australian Catholic University, Australia

The COVID-19 pandemic and its management is impacting on the care of patients with osteoporosis. We have quantified the international impact by examining changes in the usage of online fracture risk assessments before and after the declaration of the COVID-19 pandemic on March 11th.A retrospective, longitudinal analysis using GoogleAnalytics data on daily sessions on the FRAX® fracture risk calculator website from November 2019 to April 2020, based on country of origin (IP address location) and a comparison with the same period in 2019. The main outcome was change in session number between the months of February, March and April 2020. Detailed results are presented for 66 countries comprising 98% of all sessions. During the 3-month period, the FRAX website recorded 460,495 sessions from 184 countries, with 210,656 sessions recorded in February alone. In March and April, the number of sessions fell by 23.1% and 58.3% respectively (Figure). No such pattern was observed over the same period in 2019. There were smaller reductions in Asia than elsewhere, partly related to earlier and less-marked nadirs in some countries (China, Taiwan, Hong Kong, South Korea and Vietnam). In Europe, the majority of countries (24/31, 77.4%) reduced usage by at least 50% in April. Seven countries showed smaller reductions (range -2.85% to -44.1%) including Poland, Slovakia, Czech Republic, Germany, Norway, Sweden and Finland. There was no significant relationship between the reduction in FRAX usage and measures of disease burden such as deaths per million of the population.This study documents a marked impact of the COVID-19 pandemic on the management of osteoporosis using a globally applicable assessment. The impact appears unrelated to the burden of disease, suggesting that it may relate more to the societal and healthcare measures taken to ameliorate the pandemic.

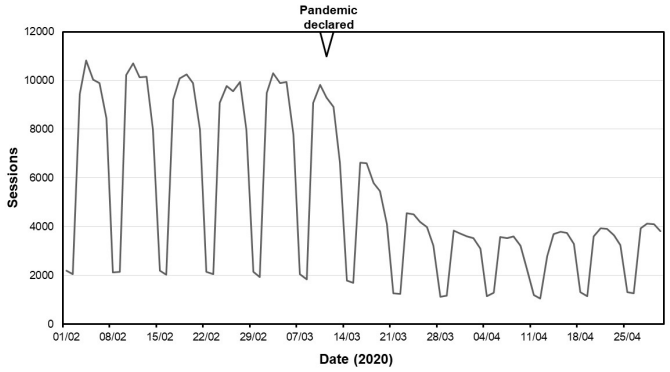

***Disclosures: Eugene McCloskey**, None*

P-528

The correlation between bone mineral density/trabecular bone score and body mass index, height, and weight *Jin Hwan Kim[1]. [1]Department of Orthopaedics, Ilsan Paik Hospital of Inje University, Republic of Korea

Objectives: This study investigated the correlation between bone mineral density (BMD)/trabecular bone score (TBS) and body mass index (BMI), height and weight in Korean adults.Methods: We enrolled 2555 female participants in their 20s - 80s and 1631 male participants in their 20s - 70s. Participants with history of previous vertebral surgeries or current vertebral diseases were excluded. Female and male participants were divided into osteoporosis group (n = 136 and n= 31, respectively), osteopenia group (n = 822 and n = 460, respectively), and normal group (n = 1596 and n = 1140, respectively) based on their BMD T-score. Dual-energy X-ray absorptiometry image analysis and linear regression analysis were conducted on each participant in each group to determine the P value and the correlation between BMD T-score/TBS T-score and BMI, weight, and height.Results: We found a significant correlation between BMI and TBS in both male and female participants. In the male participants, the correlation coefficient increased progressively from the normal group to the osteoporosis group. In the female group, we observed a significant positive correlation between height and TBS, and in the male group a significant negative correlation between weight and TBS was observed.Conclusions: BMI and weight are closely correlated to body fat content. BMD was positively correlated to BMI and weight, while TBS was negatively correlated to BMI and weight. Therefore, although BMI causes an increase in BMD, it appears to be negatively affecting bone quality.

***Disclosures: Jin Hwan Kim**, None*

P-529

REMS technology a new diagnostic approach in patients with spine artifacts *Maria Dea Tomai Pitinca[1], Carla Caffarelli[1], Stefano Gonnelli[1]. [1]Department of Medicine, Surgery and Neuroscience. University of Siena, Italy

Bone Densitometry performed by DEXA technology is the Gold Standard in the evaluation of BMD. It is well known that some conditions (arthrosis, vertebral collapses, vertebroplasty) can result in an overestimation of the spinal BMD measured by DEXA.The purpose of this work is to evaluate the REMS (Radiofrequency Echographic Multi-Spectrometry) technology in patients with alterations of the spine (osteophytes, vertebral fractures, vertebroplasty). 86 female patients (mean age 70.44 +/- 9.1), with vertebral alterations that could affected the spine BMD were considered.Patients, after obtaining informed consent, underwent DEXA and REMS examination on the reference sites (proximal femur and Lumbar vertebrae). The bone mineral density assessed by REMS technology showed lower values ??in the spine compared to the densitometric test performed with DEXA technology for both the BMD (0.772 +/- 0.065 vs 1.067 +/- 0.210) and the T-score (-2.5 +/- 0.6 vs 0.2 +/- 1.8). The BMD and T-score values ??measured with REMS and DEXA at ??the femoral site were highly correlated and this correlation reached statistical significance ($p < 0.01$). Furthermore, a high correlation was shown between the BMD and the T-score measured with the DEXA technology at the femoral sites (FN and TH) and those measured at the lumbar site with the REMS method ($p < 0.01$).The high correlation between the values ??of femoral BMD, T-score FN and T-score TH in the two methods confirms that the REMS technology is a highly reliable examination in the evaluation of BMD and fracture risk. Furthermore the data obtained on lumbar scans shows that REMS technology is able to evaluate BMD more accurately than DEXA in patients with conditions that can make the DEXA exam less reliable. These data open new possible scenarios from both research and clinical point of view and for fracture prevention.

***Disclosures: Maria Dea Tomai Pitinca**, None*

P-530

Radiofrequency Echographic Multi Spectrometry (REMS) technology: repeatability and precision assessment for short-term monitoring application *Paola Pisani[1], Fiorella Lombardi[1], Delia Ciardo[1], Francesco Conversano[1], Sergio Casciaro[1]. [1]National Research Council, Institute of Clinical Physiology, Italy

PURPOSE The assessment of bone health through densitometric techniques is based on the evaluation of bone mineral density (BMD) at reference axial sites, i.e. femur or lumbar spine. In a setting of patients (pts) undergoing pharmacological treatments with non-physiological BMD reduction as a side effect, the evaluation of BMD loss must be accurately performed with repeated examinations over time. The aim is to review the intra-operator (i.e. short-term precision), inter-operator and inter-device repeatability of Radiofrequency Echographic Multi-Spectrometry (REMS), a non-ionizing approach for osteoporosis diagnosis [1], in view of short-term BMD monitoring in breast cancer (BC) pts undergoing aromatase inhibitors (AIs) with or without Denosumab administration. METHODS Following the indications of the ISCD [2], the parameters of interest were assessed on groups of 30-patient each. All subjects underwent 2 REMS scans at lumbar spine or femoral neck, performed by the same operator (for intra-operator repeatability) or by 2 different operators (for inter-operator repeatability) or by the same operator using 2 different devices (for inter-device repeatability). The results are expressed as percentage coefficient of variation (RMS-CV) and least significant change for a 95% confidence level (LSC). The performance of lumbar spine REMS scans for the short-term monitoring of the effect of AIs with/without denosumab in BC pts has been evaluated. RESULTS The results, obtained from a literature review [3,4], have shown a high precision of REMS for both axial sites, with intra- and inter-operator RMS-CV lower than 0.55%. These results correspond to an LSC lower than 1.3% for femoral neck and 1.6% for lumbar spine. As concerning the inter-device repeatability, RMS-CV in the range 0.4%-0.6% were observed, with corresponding LSC of 1.1%-1.5%. The assessment of bone health-related parameters by REMS in BC pts every 6 months from the onset of the therapies, showed a statistically significant increasing trend of BMD in pts assuming AIs and Denosumab and a decreasing trend for patients undergoing AIs only. CONCLUSION The high repeatability and precision, with the low LSC values, associated with the non-ionizing approach, show that REMS is eligible for short-term monitoring of BMD. REFERENCES1. Aging Clin Exp Res 2019;31(10):1375–89 2. Osteoporos Int 2019; 30:3–44. 3. Osteoporos Int 2018;30:391-402 4. Ann Rheum Dis 2020; 79, S1:1826.

***Disclosures: Paola Pisani**, None*

P-531

Hip Spine Discordance in Bone Mineral Density: Prevalence and Significance in Indian Patients *Amulya yalamanchi[1], Karthik balachandran[2], Adlyne Reena Asirwatham[3], Shriraam Mahadevan[3], Krishna Mori[3], Sathish Kumar[3]. [1]Sri ramachandra medical college, India, [2]Sri ramachandra medical college, India, [3]Sriramachandra medical college, India

Abstract: Introduction: The WHO recommends that osteoporosis be diagnosed based on the lowest T score in hip, spine or distal 33% radius. Indian guidelines also emphasize T score based diagnosis and treatment of osteoporosis. One of the reasons for measuring bone

density is to account for differences in bone density between sites. The data on discordance in bone density between the hip, spine and distal radius is scarce in India - despite DXA scanning being available in India for the last 20 years. If there's a significant discordance between hip and spine, this can potentially have impact on the diagnosis of osteoporosis. Objective: To study the prevalence of hip and spine discordance in BMD and its predictors in Indian patients. Materials and Methods: This was a retrospective study in which individuals who underwent BMD measurement and FRAX scoring at Sri Ramachandra Medical Centre, Chennai during the time period July 2016 to July 2018 were included. Those who have already received treatment with US Food and Drug Administration (USFDA) approved drugs for osteoporosis were excluded. Results: The study included 808 adults, both men and women, above the age of 50. The mean age(sd) was 58.7 (6.2) years. The group had 56.8% men. None of the patients were taking any osteoporosis medications. 41.9% of patients tend to have discordance between their hip and spine, regardless of the normative data used for classification. discordance is minor in 39.9% minor and major in 2% . Conclusions: Discordance between hip and spine classification by DXA is common (roughly 4 out of 10 patients) while major discordance is rare(2 out of 100 patients). Optimizing vertebral fracture detection and choice of anti-osteoporosis therapy are clinically significant implications of hip spine discordance, which need to be explored in future prospective studies. Keywords: Hip spine discordance, Bone mineral density, T score, DXA, Indian patients.

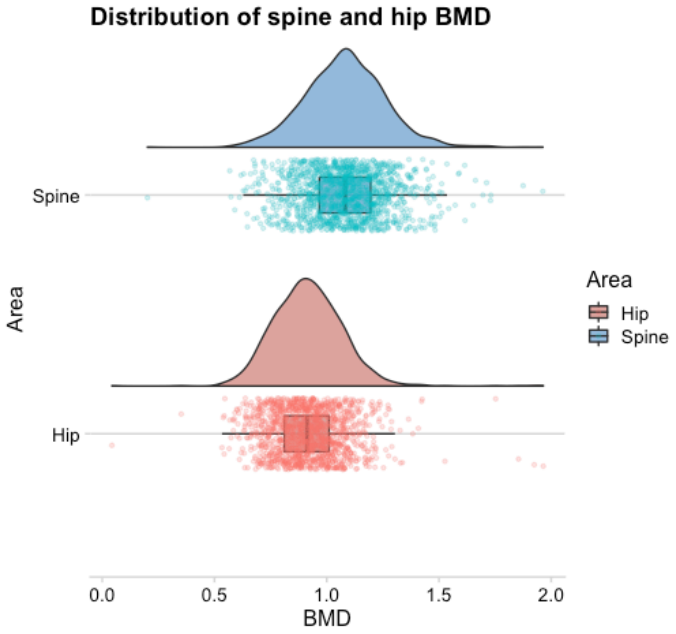

***Disclosures: Amulya yalamanchi**, None*

P-532

Phthalates and bone mineral density change in the Women's Health Initiative *KATHERINE REEVES[1]. [1]University of Massachusetts Amherst, United States

BackgroundPhthalates are endocrine-disrupting chemicals, often used in food packaging materials and other consumer goods, that could disrupt normative physiologic function, triggering detrimental impacts on bone. Longitudinal associations between phthalate exposure and bone mineral density (BMD) have not been explored.MethodsWe evaluated associations between urinary phthalate biomarkers and BMD in postmenopausal women participating in the prospective Women's Health Initiative (WHI). WHI participants who were enrolled in the BMD substudy (N=11,020) and were included in a nested case-control study of phthalates and breast cancer (N=1257, 419 cases and 838 matched controls) were included in these analyses. We measured thirteen phthalate biomarkers and creatinine in 2-3 urine samples per participant collected over 3 years, when all participants were cancer-free. Total hip and femoral neck BMD were measured at baseline and year 3, concurrent with the time of urine collection, via dual energy x-ray absorptiometry (Hologic QDR 2000, 2000+ or 4500). We fit multivariable generalized estimating equation models and linear mixed effects models to estimate cross-sectional and longitudinal associations, respectively, between phthalate biomarkers and BMD measures, with stratification on postmenopausal hormone therapy (HT) use.ResultsIn multivariable cross-sectional analyses urinary concentrations of mono-benzyl phthalate, mono-3-carboxypropyl phthalate, and the sum of di-isobutyl phthalate metabolites were inversely associated with total hip BMD among women not using HT, but not among HT users. Multivariable longitudinal analyses showed greater declines in total hip BMD among women not using HT and with highest concentrations of mono-carboxyoctyl phthalate (MCOP) (-1.48%, 95% CI -2.45 – -0.51%) or mono-carboxynonyl phthalate (MCNP) (-1.45%, 95% CI -2.35 – -0.55%); similar associations were observed with femoral neck BMD in this group. Among women using HT, phthalate biomarkers were not associated with total hip or femoral neck BMD change.ConclusionsWe report, for the first time, that MCOP and MCNP are associated with greater percent decreases in total hip and femoral neck BMD. Phthalate exposure may have clinically important effects on BMD, and potentially fracture risk.

***Disclosures: KATHERINE REEVES**, None*

P-534

Cross-sectional associations between visceral adipose tissue and bone mineral density in the UK Biobank Imaging Study *Victoria Bland[1], Yann Klimentidis[1], Jennifer Bea[1], Denise Roe[1], Scott Going[1]. [1]University of Arizona, United States

While the strong positive relationship between body mass, particularly lean mass, with areal bone mineral density (aBMD) in adults is well established, the relationship between aBMD and adipose tissue distribution is not well understood. Consequently, our aim was to characterize the association of MRI-derived abdominal visceral adipose tissue (VAT) with DXA-derived whole body (WB), lumbar spine (LS), and femoral neck (FN) aBMD in males, premenopausal females, and postmenopausal females. We used data from 3177 individuals aged 44-77 years old from the UK Biobank who took part in the imaging study and had available DXA and abdominal MRI data. Linear regression analysis was used to assess the relationship between abdominal VAT (liters) and aBMD (g/cm2), controlling for age, race, DXA total body lean mass, height, BMI class (normal weight: < 25 kg/m2, overweight: >= 25 and < 30 kg/m2, obese: >= 30 kg/m2), physical activity, smoking, and oral contraceptive/hormone replacement therapy use (females only). In postmenopausal females, VAT was positively associated with WB (β: 0.013, p = 0.009), LS (β: 0.030, p < 0.0001), and FN aBMD (β: 0.016, p = 0.003). In males and premenopausal females, a significant interaction (p < 0.05) between VAT and BMI class was identified for WB aBMD and LS aBMD bone outcomes. In males, the interactions showed a positive relationship between VAT and aBMD in normal weight men, but a negative relationship between VAT and aBMD in obese men. In premenopausal females, the interaction indicated a positive relationship between VAT and aBMD in normal weight women, but a negative relationship in overweight and obese women. No significant relationship between VAT and FN aBMD was identified in males (p = 0.63), but VAT was positively associated with FN aBMD in premenopausal females (β: 0.024, p = 0.007). These results indicate that VAT may positively influence aBMD in normal weight individuals, likely due to a mechanical influence on bone, but could be detrimental to bone density in overweight and obese individuals, especially among males and premenopausal females. Future analyses are needed to determine if there is a threshold at which VAT might become detrimental to aBMD.

***Disclosures: Victoria Bland**, None*

P-535

Does Serial Bone Density Measurement Meaningfully Improve Incident Fracture Risk Prediction in Postmenopausal Women? Results from the Women's Health Initiative Observational Study and Clinical Trials *CAROLYN CRANDALL[1], Joseph Larson[2], Nicole Wright[3], Deepika Laddu[4], Marcia Stefanick[5], Andrew Kaunitz[6], Nelson Watts[7], Jean Wactawski-Wende[8], Catherine Womack[9], Karen Johnson[10], Laura Carbone[11], Rebecca Jackson[12], Kristine Ensrud[13]. [1]University of California, Los Angeles, United States, [2]Fred Hutchinson Cancer Research Center, United States, [3]University of Alabama at Birmingham, United States, [4]University of Illinois, United States, [5]Stanford University School of Medicine, United States, [6]University of Florida College of Medicine, United States, [7]Mercy Health Osteoporosis and Bone Health Services, Cincinnati, United States, [8]University at Buffalo, the State University of New York, United States, [9]The University of Tennessee Health Science Center, United States, [10]University of Tennessee Health Science Center, Memphis, United States, [11]Medical College of Georgia at Augusta University, United States, [12]The Ohio State University, Columbus, OH, United States, [13]University of Minnesota and Veterans Affairs Health Care System, Minneapolis, United States

Background. Whether repeated osteoporosis screening improves fracture prediction is controversial. Objectives. To determine whether a second BMD measurement an average of 3 years after the initial assessment adds to the prediction of fracture risk beyond baseline BMD measurement alone. Design. Women's Health Initiative (WHI), a prospective observational study, mean 12.1 years follow-up Setting. 3 clinical centers Participants. Postmenopausal women aged >=50 years (n = 7,419). Measurements. BMD was measured at baseline and 3 years later Methods. We calculated area under the receiver operating characteristic curve (AUC) for baseline BMD, absolute change in BMD, and the combination of baseline BMD and change in BMD to predict incident hip fracture or major osteoporosis fracture (MOF) during follow-up. Results. During follow-up, 139 hip fractures and 732 MOF occurred. For prediction of hip fractures, AUC values were 0.79 (95% confidence interval [CI] 0.75, 0.82) for baseline total hip BMD, 0.77 (0.74, 0.81) for change in total hip BMD, and 0.79 (0.76, 0.83) for the combination of baseline total hip BMD and change in total hip BMD. Femoral neck and lumbar spine BMD predicted hip fracture in a similar manner. For prediction of MOF, AUC values were 0.67 (0.65, 0.69) for baseline total hip BMD, 0.66 (0.64, 0.68) for change in total hip BMD, and 0.67 (0.65, 0.69) for the combination

of baseline total hip BMD and change in total hip BMD. Femoral neck and lumbar spine BMD predicted MOF in a similar manner. Limitations. Observational design, self-reported fractures. Conclusion. A second BMD measure after 3 years does not meaningfully improve the prediction of hip or major osteoporotic fracture beyond baseline BMD alone. Funding. National Institutes of Health.

Receiver Operating Characteristic Curves for Prediction of Hip & MOF

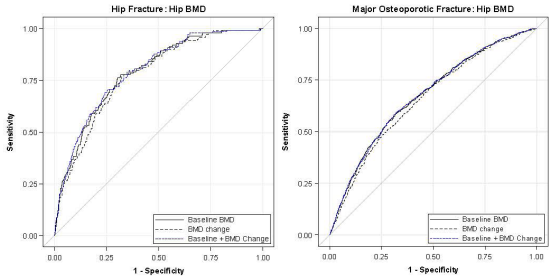

Area under the Curve of models adjusted for baseline BMD, absolute yearly change (g/cm²), or their combination, overall and by age group, in prediction of incident fracture[1]

Hip Fracture	Baseline	BMD Change	Baseline + BMD Change
BMD Site	*AUC (95% CI)*	*AUC (95% CI)*	*AUC (95% CI)*
Total Hip			
Overall	0.79 (0.75, 0.82)	0.77 (0.74, 0.81)	0.79 (0.76, 0.83)
<65	0.77 (0.65, 0.88)	0.77 (0.66, 0.88)	0.79 (0.68, 0.90)
65-74	0.72 (0.67, 0.78)	0.70 (0.65, 0.76)	0.72 (0.67, 0.78)
≥75	0.73 (0.67, 0.79)	0.73 (0.67, 0.80)	0.75 (0.69, 0.82)
Major Osteoporotic Fracture	Baseline	BMD Change	Baseline + BMD Change
BMD Site	*AUC (95% CI)*	*AUC (95% CI)*	*AUC (95% CI)*
Total Hip			
Overall	0.67 (0.65, 0.69)	0.66 (0.64, 0.68)	0.67 (0.65, 0.69)
<65	0.67 (0.64, 0.71)	0.66 (0.62, 0.69)	0.67 (0.64, 0.71)
65-74	0.67 (0.64, 0.70)	0.65 (0.62, 0.68)	0.67 (0.64, 0.70)
≥75	0.69 (0.65, 0.73)	0.70 (0.65, 0.74)	0.70 (0.66, 0.74)

[1] Adjusted for current hormone use (Yes/No), Women's Health Initiative Study component (Clinical Trial/Observational Study), age, race/ethnicity, history of fracture, physical activity, physical function, and number of falls in the last year. Major osteoporotic fractures include: hip, spine, lower arm/wrist, upper arm/shoulder.

***Disclosures: CAROLYN CRANDALL**, None*

P-536

Major osteoporotic fracture to hip fracture incidence rate ratios: a systematic review of observational studies. *Marlene Chakhtoura [1], Hiba Dagher[1], Sima Lynn Sharara[1], Ziyad Mahfoud[1], Jane Cauley[2], Ghada El Hajj Fuleihan[1]. [1]American University of Beirut - Lebanon, Lebanon, [2]University of Pittsburgh, United States

BackgroundThe Fracture Risk Assessment Tool (FRAX) is central to many osteoporosis guidelines. Country specific FRAX calculators are made possible with country specific hip fracture incidence and life expectancy data. The calculator provides 10-year probabilities for hip and major osteoporotic fracture (MOF), and uses MOF/hip fracture incidence rate ratios (IRR) from Malmo Sweden for the latter, in most countries. However, the risk of osteoporotic fractures varies by age, gender, and geography.AimEvaluate the IRR [and 95% confidence interval (CI)] of MOF/hip fractures, by gender and age categories, in studies extending >1 year, across continents.MethodsWe conducted a systematic search in 3 databases targeting observational studies on MOF (forearm, vertebral, proximal humerus, hip) and hip fractures in men and women >50 years (CRD42019129259). We used relevant MeSh terms/keywords, and did not apply language nor time restriction until May 2018. One reviewer completed title/abstract and full text screening, and 2 reviewers completed duplicate and independent data abstraction. We assessed studies quality based on population representativeness, study design, definition of ethnicity and fracture. We calculated the MOF/hip IRR and its 95% CI using incident fractures, by gender and age category, using Rothman's formula (1).ResultsWe included 27 studies, from Europe (15), US and Canada (7), Asia (3) and Australia (2). Calculations were done for four countries, awaiting needed data from authors of other studies. The MOF/hip IRR is higher in younger age categories, and higher in women compared to men, across all countries. This is driven by low hip fracture incidence at young ages. The IRR at 50-54 years is 3-12 folds higher than the IRR at 85+ years in women, and 2.3-10.3 folds higher in men. The difference between men and women is larger at younger ages, and varies across countries. The IRR is 1.3-3.3 folds higher at 50-54 years in women compared to men. At ages 85-90+, the IRR in both genders become almost similar, with few exceptions. The MOF/hip IRR vary across countries; differences are larger at younger ages (see Table for selected countries from different continents).ConclusionThe variability in the MOF/hip fracture IRR may affect the 10-year MOF fracture risk prediction in FRAX using ratios from Malmo Sweden ratios. This would depend on the impact of observed differences on derived FRAX estimates. Further research is needed to elucidate the clinical implication of our findings.(1)Rothman 2008

MOF/Hip Fracture Incidence Rate Ratios and 95% Confidence Interval in Women and Men from Various Continents

Age (years)	50-54	55-59	60-64	65-69	70-74	75-79	80-84	85-89	90+
Women									
Canada	22.7 (16.6;31.0)	15.9 (12.6;20.0)	11.1 (9.1;13.4)	6.6 (5.7;7.7)	5.5 (4.9;6.2)	3.6 (3.3;3.9)	2.8 (2.6;3.1)	2.3 (2.1;2.4)	1.9 (1.7;2.0)
Japan	-	6 (1.3;26)	-	7.8 (3.3;18.3)	5.5 (3.0;10.2)	4.8 (3.1;7.5)	4 (2.8;5.6)	2.8 (2.2;3.6)	-
Italy	14.7 (14;15.4)	13.0 (12.5;13.5)	9.7 (9.4;9.9)	6.4 (6.2;6.5)	4.2 (4.0;4.2)	3.2 (3.0;3.6)	2.3 (2.2;2.3)	1.8 (1.7;1.8)	1.5 (1.4;1.5)
Australia	22 (3;163)	8.2 (2.9;23.2)	13.7 (4.2;44.1)	5.7 (3.4;9.8)	4.5 (3.0;6.7)	2.9 (2.1;3.2)	2.2 (1.6;2.8)	1.5 (1.1;2.0)	1.7 (1.2;2.4)
Men									
Canada	11.0 (8.5;14.3)	8.8 (6.9;11.3)	5.6 (4.5;7.0)	4.6 (3.7;5.6)	3.9 (3.3;4.6)	2.8 (2.4;3.2)	2.4 (2.1;2.8)	1.9 (1.6;2.1)	1.6 (1.4;1.8)
Japan	-	9 (1.1;71)	2.7 (0.7;10)	2.7 (0.8;8.6)	4 (1.5;10.0)	3.5 (1.7;7.1)	4.3 (1.8;9.7)	2.45 (1.4;4.1)	-
Italy	13.4 (12.8;14.1)	10.7 (10.3;11.2)	8.1 (7.9;8.4)	5.7 (5.5;5.9)	3.7 (3.6;3.9)	2.8 (2.7;2.9)	2.0 (2.0;2.1)	1.6 (1.6;1.7)	1.4 (1.3;1.5)
Australia	3.7 (1.0;13.1)	4.6 (1.7;12.1)	4.7 (1.6;14)	2.8 (1.0;7.8)	2.2 (1.2;4.0)	1.7 (0.9;3)	1.9 (1.0;3.7)	1.4 (0.9;2.4)	1.4 (0.7;2.8)

***Disclosures: Marlene Chakhtoura,** None*

P-537

Associations between Seasonal Influenza, Fractures and Fall Injuries - a National Retrospective Cohort Study *Kristian Axelsson[1], Henrik Litsne[1], Mattias Lorentzon[1]. [1]Geriatric Medicine, Institute of Medicine, Sahlgrenska Academy, University of Gothenburg, Sweden

Background: Fractures and fall injuries often lead to disability, increased morbidity and mortality. Older adults are at higher risk of influenza related complications such as pneumonia, cardiovascular events and deaths, but the risk of fractures and fall injuries is unclear. The primary objective of this study was to investigate if the risk of fractures and fall injuries is increased in older patients diagnosed with seasonal influenza compared to propensity score matched controls.Methods: In this retrospective cohort study of 6 692 older adults (70 years or older) with seasonal influenza diagnosed at Swedish hospitals (from December 1st, 2015 to December 31st, 2017) and 6 692 propensity score matched controls derived from the general population, the risk of fracture or fall injury was investigated.Results: The mean (SD) age of the 6 692 influenza patients was 82.3 (7.1) years, 50.9% were women and the mean (SD) Charlson Comorbidity Index was 2.2 (2.3). During the first 14 days after baseline, there were 217 fractures or fall injuries among the patients with influenza and 32 among the propensity score matched controls corresponding to incident rates of 900 (95% CI, 788-1028) and 127 (95% CI, 90.1-180) fractures or fall injuries per 1000 person-years, respectively, translating to an increased risk of fracture or fall injury in a logistic regression model (odds ratio 6.98 (95% CI, 4.81-10.13)) in influenza patients. The incidence among the influenza patients was higher also in the subsequent period (day 15 to 60) than in the controls, with incident rates of 195 (95% CI, 165-230) and 112 (95% CI, 90.4-138), respectively, corresponding to an increased risk in influenza patients in a Cox model (hazard ratio 1.74 (95% CI, 1.33-2.28)).Conclusions: Among older adults with influenza diagnosis, the risk of fracture or fall injury was increased substantially, providing additional evidence to support the prevention of influenza and of injurious falls in those affected by the disease.

Incidence of fracture or fall injury during first year after influenza diagnosis

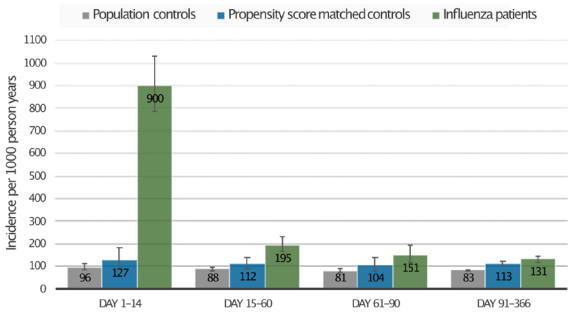

	DAY 1–14	DAY 15–60	DAY 61–90	DAY 91–366
Population controls				
At risk	66 920	64 581	61 032	59 987
Events	242	689	401	3171
Propensity score matched controls				
At risk	6692	6390	5921	5782
Events	32	86	50	405
Influenza patients				
At risk	6692	5989	5344	5158
Events	217	137	65	416
OR* / HR for influenza vs populations controls	9.23 (7.67–11.11)	2.22 (1.85–2.67)	1.87 (1.44–2.43)	1.58 (1.42–1.75)
OR* / HR for influenza vs propensity score matched controls	6.98 (4.81–10.13)	1.74 (1.33–2.28)	1.45 (1.00–2.10)	1.16 (1.01–1.33)

***Disclosures: Kristian Axelsson**, None*

P-538

Treat-to-Target in Osteoporosis: Total Hip BMD T-Score as an Indicator of Fracture Risk in Bisphosphonate-Treated Postmenopausal Women from Real-World Data *Gustaf Ortsäter[1], Jonas Banefelt[1], Emma Söreskog[1], Jen Timoshanko[3], Alireza Moayyeri[3], Kristina Åkesson[4], Anna Spångéus[5], Östen Ljunggren[6], Cesar Libanati[3]. [1]Quantify Research, Sweden, [3]UCB Pharma, United Kingdom, [3]UCB Pharma, Belgium, [4]Lund University, Skåne University Hospital, Sweden, [5]Linköping University Hospital, Sweden, [6]Uppsala University Hospital, Sweden

PurposeThe association between bone mineral density (BMD) and fracture (fx) risk is well established. The importance of total hip (TH) BMD T-score in determining fx risk observed in recent studies has reignited discussion on whether a BMD target could be suitable in a treat-to-target approach in patients (pts) with osteoporosis (OP).1,2 We use real-world data to extend the evidence confirming a relationship between TH T-score and fx risk in postmenopausal women with prior bisphosphonate (BP) treatment (tx).MethodsIn this retrospective cohort study, all women aged >=55 years (yrs) with >=1 TH T-score measured between 2006–2013 at 1 of 3 Swedish OP clinics with prior BP tx and without Paget's disease or malignancy were identified. Pt data were linked to fx and BP tx data from national health registers.The index date was set to the first BMD measurement; cumulative incidence of any clinical and non-vertebral (NV) fx was assessed 12 and 24 months following this date. The association between T-score and fx risk was estimated using proportional hazards regression; restricted cubic splines were added to illustrate any potential non-linear relationship. 4 subgroups were considered: any prior BP tx; BP tx for >=3 yrs; any prior BP tx but no dispensations during the last yr; and any prior BP tx with >=1 dispensation in the last yr.ResultsOf 3,422 included pts, the mean (SD; range) age was 71.5 (8.6; 55–98) yrs and median (IQR; range) TH T-score was –1.7 (1.4; -7.7–3.0). 22.6% had a TH BMD<=-2.5; 34.4% had a prior fx. At 12 and 24 months respectively, cumulative incidence (95% CI) of any clinical fx was 4.44% (3.79–5.17) and 8.39% (7.49–9.35), and NV was 3.83% (3.22–4.51) and 7.31% (6.47–8.21). In women with prior BP tx, TH T-score was inversely related with 12-month clinical and NV fx incidence [Figure]; the association was similar at 24 months. This relationship was maintained overall and similar across subgroups.ConclusionsIn BP-treated women, TH T-score is associated with 12- and 24-month fx risk, similar to that reported from clinical trials with other therapeutic agents.1,3 These real-world data provide additional evidence supporting the use of BMD in a treat-to-target approach for pts at increased fx risk receiving OP tx.References1. Ferrari S. JBMR 2019;34:1033–40; 2. Cummings SR. JBMR 2016;32:3–10; 3. Cosman F. JBMR 2018;33(Suppl 1):25.AcknowledgementsThis study was funded by UCB Pharma and Amgen Inc. Medical writing services were provided by Costello Medical.

Figure. Risk of fracture within 12 months in patients with any history of bisphosphonate treatment

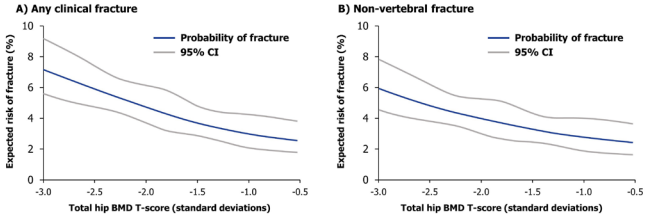

BMD: bone mineral density; CI: confidence interval

***Disclosures: Gustaf Ortsäter**, Quantify Research, Other Financial or Material Support*

P-539

Height Loss in Old Age and Hip Fracture Risk Among Men in Late Life: Findings from the Osteoporotic Fractures in Men (MrOS) Study *Kristine Ensrud[1], John Schousboe[2], Allyson Kats[3], Tien Vo[3], Brent Taylor[1], Peggy Cawthon[4], Jane Cauley[5], Nancy Lane[6], Andrew Hoffman[7], Lisa Langsetmo[3]. [1]VA Health Care System / University of Minnesota, United States, [2]HealthPartners Institue / University of Minnesota, United States, [3]University of Minnesota, United States, [4]California Pacific Medical Center Research Institute, United States, [5]University of Pittsburgh, United States, [6]University of California - Davis, United States, [7]Stanford University, United States

Height loss in older adults is associated with a higher risk of all-cause mortality. Thus, the competing risk of mortality (unrelated to hip fracture) may modify the relationship of height loss with hip fracture risk, especially in late life. To determine the association of height loss in old age with subsequent risk of hip fracture in men late in life while accounting for the competing risk of mortality, we used data from 3498 men (mean [SD] age 79.2 [5.2] years) participating in the Year 7 (Y7) MrOS exam. Height was measured at the baseline and Y7 exams with a Harpenden stadiometer. Height loss (cm) was expressed as a categorical variable (<1 cm [referent group], >=1 and <2 cm, >=2 and <3 cm, and >=3 cm). Men were contacted every 4 months after Y7 to ask about hip fractures (confirmed by radiographic reports) and ascertain vital status (deaths verified by death certificates). Cumulative incidence was estimated considering mortality as competing risk. Hazard ratios (HR) were calculated using Fine-Gray models accounting for death as a competing risk. Mean (SD) height loss between baseline and Y7 exam was 1.4 (1.4) cm. During a maximum follow-up of 10 years after Y7, 158 (4.5%) men experienced a hip fracture and 1418 (40.6%) died before experiencing this event. The absolute probability of hip fracture at 10 years steadily increased with greater height loss; the probability (95% CI) was 2.7% (1.9-3.7%) among men with height loss <1 cm increasing to 11.6% (7.9-16.0%) among men with height loss >=3 cm. After adjusting for age, race and enrollment site, hip fracture risk after Y7 increased in a graded manner with greater height loss between baseline and Y7 (subdistribution HR 1.61 among men with loss >=1 cm and <2 cm, 1.95 among men with loss >=2 cm and <3 cm, and 3.45 among men with loss >=3 cm) (Model 1, Table). The association was somewhat attenuated but persisted after further adjustment for fall history, multimorbidity, baseline height, weight change between baseline and Y7 exam and FN BMD (Model 2). Additional adjustment for incident radiographic vertebral fracture between baseline and Y5 exam did not alter the results (Model 3). In conclusion, height loss of 3 cm or more in old age is a strong risk factor for hip fracture in men in late life, even after accounting for traditional risk factors and considering the competing risk of mortality.

Table 1. Fine-Gray Competing Risk Models for Association of Height Loss in Old Age and Risk of Hip Fracture (Entire Cohort N=3498)

	Subdistribution Hazard Ratio (95% CI)			
	<1 cm	≥1 and <2 cm	≥2 and <3 cm	≥3 cm
	N=1268	N=1448	N=528	N=254
Model 1*	(referent)	1.61 (1.07-2.43)	1.95 (1.20-3.18)	3.45 (1.98-6.01)
Model 2†	(referent)	1.46 (0.97-2.19)	1.50 (0.92-2.45)	1.94 (1.05-3.56)
Model 3‡	(referent)	1.46 (0.97-2.19)	1.52 (0.93-2.48)	1.98 (1.07-3.66)

*adjusted for age, race and enrollment site
†adjusted for age, race, enrollment site, fall history, multimorbidity, baseline height, weight change and FN BMD
‡adjusted for age, race, enrollment site, fall history, multimorbidity, baseline height, weight change, FN BMD and new radiographic vertebral fracture

***Disclosures: Kristine Ensrud**, None*

P-540

Frailty Phenotype and Risk of Fracture Among Women Late in Life: Impact of Traditional Risk Factors and Competing Mortality *John Schousboe[1], Lisa Langsetmo[2], Allyson Kats[2], Tien Vo[2], Deborah Kado[3], Stone Katie[4], Brent Taylor[2], Kristine Ensrud[2]. [1]HealthPartners Institute, United States, [2]University of Minnesota, United States, [3]University of California, San Diego, United States, [4]California Pacific Medical Center, United States

Frailty phenotype is traditionally defined as frail, pre-frail, or robust by five Cardiovascular Health Study (CHS) criteria (slow gait speed, low grip strength, poor energy, weight loss, low physical activity). Alternatively, three Study of Osteoporotic Fractures (SOF) criteria (weight loss, low energy, inability to rise from a chair 5 times without use of the arms) have been proposed to identify frailty status in the busy clinical practice setting. CHS and SOF Frailty phenotypes are associated with increased fracture risk, but competing risk of mortality may mitigate this risk, especially in the very old.Our objective was to estimate the associations of the frailty phenotype with hip and non-spine fracture risks over 5-years of follow-up in women >80 years using Cox proportional hazards models and Fine-Gray subdistribution hazards models to account for competing mortality. Models were adjusted for age and race, followed by adjustment for traditional risk factors (e.g. femoral neck BMD, prior clinical fracture, prevalent radiographic vertebral fracture, body mass index, fall history, parental hip fracture, current smoking) with a cut-off p-value <0.10. The referent group in the analyses was robust women.Among 2638 women at the SOF year 16 visit (mean age 83.2 years), 187 (7.1%) had a subsequent hip fracture, 439 (16.6%) had a non-spine fracture, and 430 (16.3%) died without having a fracture over the 5-years of follow-up. Adjusted for age and race, SOF defined frailty was associated increased risks of hip and non-spine fractures, and CHS defined frailty was associated with a higher risk of non-spine fracture (Table). These associations were similarly attenuated after considering competing mortality or after adjusting for traditional risk factors. After adjusting for both competing mortality and traditional risk factors, these associations were further attenuated and no longer significant. In contrast, femoral neck BMD remained strongly associated and prevalent vertebral fracture or self-reported falls were moderately associated with hip and non-spine fractures, regardless of competing mortality.In conclusion, after accounting for competing mortality risk and traditional risk factors, frailty defined by phenotypic criteria is not a strong fracture risk factor in late life women. BMD, vertebral fracture and fall history retained significance, confirming the importance of identifying and appropriately treating those with osteoporosis and falls.

Table: Associations of Frailty Phenotype Components with Incident Fracture Over 5 years

HIP FRACTURE				
Predictor	**No Competing Mortality Adjustment***		**Competing Mortality Adjustment†**	
	Model 1^ HR (95% CI)	Model 2‡ HR (95% CI)	Model 1^ SHR (95% CI)	Model 2‡ SHR (95% CI)
CHS Phenotype[a]				
Robust	Reference	Reference	Reference	Reference
Pre-Frail	1.20 (0.51, 2.78)	1.17 (0.50, 2.74)	1.18 (0.51, 2.74)	1.15 (0.49, 2.69)
Frail	1.57 (0.68, 3.64)	1.39 (0.59, 3.24)	1.46 (0.63, 3.38)	1.27 (0.55, 2.98)
SOF Phenotype[b]				
Robust	Reference	Reference	Reference	Reference
Pre-Frail	0.82 (0.53, 1.29)	0.78 (0.50, 1.22)	0.81 (0.51, 1.26)	0.76 (0.48, 1.19)
Frail	**1.60 (1.04, 2.47)**	1.39 (0.90, 2.15)	1.46 (0.94, 2.26)	1.25 (0.80, 1.96)
NON-SPINE FRACTURE				
Predictor	Model 1^ HR (95% CI)	Model 2ϕ HR (95% CI)	Model 1^ SHR (95% CI)	Model 2ϕ SHR (95% CI)
CHS Phenotype				
Robust	Reference	Reference	Reference	Reference
Pre-Frail	1.40 (0.88, 2.21)	1.36 (0.85, 2.15)	1.38 (0.87, 2.20)	1.33 (0.84, 2.12)
Frail	**1.66 (1.05, 2.64)**	1.49 (0.94, 2.36)	1.56 (0.98, 2.49)	1.37 (0.86, 2.19)
SOF Phenotype				
Robust	Reference	Reference	Reference	Reference
Pre-Frail	1.22 (0.95, 1.56)	1.14 (0.89, 1.46)	1.19 (0.93, 1.52)	1.10 (0.86, 1.41)
Frail	**1.54 (1.19, 2.00)**	**1.37 (1.06, 1.78)**	**1.42 (1.10, 1.84)**	1.25 (0.97, 1.62)

Statistically significant associations are in **bold**
*Estimated with Cox Proportional Hazards Models †Estimated with Fine-Gray Subdistribution Hazards Models
^Adjusted for age, race, study enrollment site
‡Incident Hip Fracture Model 2 covariates: Model 1 plus femoral neck BMD, prevalent radiographic vertebral fracture, BMI, one or more falls prior 12 months
ϕIncident Non-Spine Fracture Model 2 covariates: Model 1 plus femoral neck BMD, prevalent radiographic vertebral fracture, prior clinical fracture, current smoking, one or more falls prior 12 months, parental history of hip fracture
[a]CHS Phenotype: Robust; no frailty component Pre-Frail; 1-2 frailty components Frail: ≥3 frailty components
[b]SOF Phenotype: Robust; no frailty component Pre-Frail; 1 frailty component Frail: ≥2 frailty components

***Disclosures: John Schousboe**, None*

P-541

FRAX probabilities generally do not change much over time. A prospective analysis from the OFELY cohort. *elisabeth SORNAY-RENDU[1], francois DUBOEUF[1], Roland Chapurlat[1]. [1]INSERM UMR1033 and Université de Lyon, France

Introduction: The Fracture Risk Assessment Tool (FRAX) identifies the probability of Major Osteoporotic Fractures (MOF) and/or Hip Fractures (HF) in the next 10 years, but the evolution of FRAX has not been evaluated so far.Materials and Methods: We have collected incident fracture in 579 women (mean age, 67 +/- 11 years) from the 14th to the 20th annual follow-up visit of the OFELY prospective study and calculated the change in FRAX probabilities over these 6 years. We examined whether the change in FRAX would predict incident fracture. Fragility fractures, all confirmed by radiographs, were prospectively registered.Results: The FRAX probabilities were highly correlated 6 years apart with a Spearman coefficient between 0.90 and 0.97 for MOP and HF with and without BMD. The median (interquartile range [IQ]) variation of FRAX probabilities expressed in absolute difference was 1.7 [0.1-4.3] for MOP FRAX with BMD, 0.7 [0.1-1.9] for MOP FRAX without BMD, 1.7 [0.5-3.5] for HF FRAX with BMD and 1.7 [0.2-4.3] for HF FRAX without BMD.The highest increases in FRAX probabilities (e.g., highest quartile of absolute difference for MOP without BMD) were moderately associated with older age with an OR [95%CI] of 1.24 [1.19-1.30] per year and lower BMI (0.93 [0.89-0.98] per unit), and strongly with Fx sustained since the prior evaluation of FRAX 6 years earlier (22.2 [8.4-58.6]). During a median (interquartile range [IQ]) of 7.0 years (6.9–7.3 years) of follow-up, 104 women sustained incident fragility fractures including 14 HF, 28 vertebral Fx and 63 nonHipnonVert Fx. Using a Cox model, the highest quartile of absolute difference for MOP FRAX without BMD (6.5-54) was associated with an increased risk of incident Fx with an Hazard Ratio (95%CI) of 2.5 (1.7-3.7), p<0.0001. Among 502 women below the French intervention threshold for the MOP FRAX with BMD, only 20 women (4%) were above the threshold 6 years later. Conclusions: Over 6 years, the FRAX tracks for most women. Incident fragility fracture is the main predictor of increasing FRAX probabilities. Without incident fracture, recalculating FRAX after 6 years will not change treatment decision in most instances.

***Disclosures: elisabeth SORNAY-RENDU**, None*

P-542

Geographic Variations in Bone Mineral Density and Prevalent Fractures in Canada *Nazila Hassanabadi[1], Claudie Berger[2], Alexandra Papaioannou[3], Angela M Cheung[4], Elham Rahme[1], William D Leslie[5], David Goltzman[1], Suzanne N Morin[1]. [1]McGill University, Canada, [2]Research Insitute of the McGill University Health Centre, Canada, [3]McMaster University, Canada, [4]University of Toronto, Canada, [5]University of Manitoba, Canada

Purpose: The prevalence of osteoporosis and fractures differs across countries and regions. We aimed to describe sex-specific bone mineral density (BMD) and prevalent fracture patterns across geographical regions in Canada.Methods: We used baseline data of 27,244 Canadians (13,828 women and 13,416 men) aged 50 years+ participating in the Canadian Longitudinal Study of Aging from 7 provinces across the country (2012-15). We created linear and logistic regression models to determine associations between province of residence and total hip BMD and prevalent self-reported major osteoporotic fractures (MOF) stratified by sex adjusting for age, body mass index (BMI), height, vitamin D level, comorbidities and physical performance measures. Results: The mean (SD) age of participants was 64.4 (9.4) years in women and 64.8 (9.4) in men. Mean BMI was lowest (27.4 kg/m2 [5.1]) in British Columbia (BC) and highest (29.0 kg/m2 [6.1]) in Manitoba (MB). The mean total hip BMD was lowest in BC (0.908 g/cm2 [0.141]) and highest in Newfoundland and Labrador (NL) (0.944 g/cm2 [0.149]) and Ontario (ON) (0.936 g/cm2 [0.145]). The overall prevalence of osteoporosis (T-score £-2.5 femoral neck) was 7.0% in women and 1.5% in men and of MOF was 4.6%; ranging from 3.1% in BC to 5.8% in MB. The mean (SD) FRAX score was 10% (7) in women and 6% (3) in men, and was noted to be 4% lower in women from BC and between 4 to 11 % lower in men from BC, MB, NS and NL compared to women and men from ON. Alberta (AB) (12.3%) and Quebec (QC) (12.0%) had the highest proportion of participants reporting falls (previous 12 months), while MB (8.6%) had the fewest.Adjusted linear regressions demonstrated significant differences in total hip BMD across provinces; women and men from BC and AB, and women from MB and NS had lower BMD than ON (Table). Adjusted Odds Ratios (OR) for prevalent MOF were significantly lower in women (OR 0.56; 95% CI: 0.40- 0.79) and men (OR 0.35; 95% CI 0.21- 0.58) from BC and men from NS, (OR 0.52; 95% CI: 0.28-0.98) compared to ON. Results were similar when restricting the analyses to participants of White ancestry only. Conclusion: Though prevalence of osteoporosis and MOF was low in this cohort, significant geographic variations in total hip BMD and fractures were observed. Future work will examine the determinants of these variations and how they have evolved over time by contrasting our results with those published by the Canadian Multicenter Osteoporosis Study.

Table: Associations of province of residence with total hip BMD and prevalent major osteoporotic fractures in Canadian women and men

	Total Hip BMD g/cm² Estimate (95% CI)		**Prevalent MOF** Odds Ratio (95% CI)	
	Women[1]	Men[2]	Women[3]	Men[4]
British Columbia (n=5696)	**-0.021 (-0.028, -0.014)**	**-0.018 (-0.026, -0.010)**	**0.52 (0.37, 0.74)**	**0.34 (0.21, 0.56)**
Manitoba (n=2836)	**-0.014 (-0.022, -0.006)**	0.004 (-0.005, 0.014)	1.05 (0.75, 1.46)	1.28 (0.85, 1.92)
Newfoundland and Labrador (n=1978)	-0.003 (-0.013, 0.007)	0.007 (-0.004, 0.018)	0.95 (0.62, 1.45)	0.73 (0.41, 1.28)
Nova Scotia (n=2779)	**-0.015 (-0.024, -0.006)**	**0.013 (0.003, 0.023)**	1.32 (0.92, 1.88)	**0.52 (0.28, 0.98)**
Alberta (n=2703)	**-0.020 (-0.029, -0.012)**	**-0.022 (-0.032, -0.013)**	0.72 (0.49, 1.07)	0.70 (0.43, 1.15)
Quebec (n=5416)	-0.005 (-0.012, 0.002)	0.001 (-0.008, 0.009)	0.79 (0.57, 1.09)	0.75 (0.50, 1.12)
Ontario (n=5836)	**Reference**			

[1] adjusted for age, height, body mass index (BMI), life space index, smoking, education, hormone replacement therapy (HRT), physical performance measures and comorbidities

[2] adjusted for age, height, body mass index (BMI), life space index, smoking, education, vitamin D level, hormone replacement therapy (HRT), physical performance measures and comorbidities

[3] adjusted for age, height, body mass index (BMI), life space index, vitamin D level, history of corticosteroid use, history of hip fractures in parents, number of falls in the past 12 months, history of calcium usage in previous month, physical performance measures, comorbidities and femoral neck BMD

[4] adjusted for age, height, body mass index (BMI), level of income, history of calcium usage in previous month, physical performance measures, comorbidities and femoral neck BMD

***Disclosures: Nazila Hassanabadi**, None*

P-543

Increase in C-reactive Protein is Associated with Increased Rate of Bone Loss: Study of Women's Health Across the Nation (SWAN) *Arun Karlamangla[1], Nicholas Jackson[1], WeiJuan Han[1], Mei-Hua Huang[1], Jane Cauley[2], Carrie Karvonen-Gutierrez[3], Gail Greendale[1]. [1]UCLA, United States, [2]University of Pittsburgh, United States, [3]University of Michigan, United States

Purpose: Greater levels of inflammation marker, C-reactive protein (CRP), have been associated with less BMD in some investigations, but longitudinal studies of the association between CRP and bone loss are lacking. We set out to determine whether within-woman change in serum CRP in midlife, before, during, and after the menopause transition (MT), is related to within-woman change in BMD decline rate. Methods: We measured serum CRP level and BMD by DXA every 1-2 years over a 21-year period, in 2365 women, starting at age 42–52 when they were in premenopause or early perimenopause. We excluded CRP values significantly higher than the woman's CRP in other visits, since these likely represent acute, not chronic, inflammation. We censored women when they started hormone therapy. 1431 women had 2 or more visits (total, 7700 visits) with valid CRP and BMD measured

concurrently, and a follow up BMD measurement 1.5-3.5 years following each such visit (for BMD decline rate calculation). To eliminate all confounding by woman-specific, time-fixed characteristics (even those not measured) and focus exclusively on within-woman changes, we used individual fixed effects (IFE) models to estimate the association of log CRP with BMD decline rate over the following 1.5–3.5 years. We included the following time-varying covariates: MT stage (1: pre or early perimenopause, 2: late peri- or early postmenopause, 3: late postmenopause), BMI, diabetes, smoking, alcohol, and medication use. Results: Mean BMD decline rate over all visits was 0.76% per year at the LS and 0.67% per year at the FN. The geometric mean of CRP over all visits was 1.53 mg/L. CRP was greater in MT stage 2 than in 1 ($p<0.001$), but not different in stages 2 vs. 3. BMD decline at both LS and FN was faster in MT stage 2 than both other stages (all $p < 0.001$). In unadjusted IFE models, every within-woman doubling of CRP was associated with 0.13% per year faster decline in FN BMD but was not associated with LS BMD decline. In adjusted IFE models, MT stage modified this relationship (interaction p value < 0.05, stage 1 vs. 2, 2 vs 3; LS and FN). Each within-woman doubling of CRP was associated with 0.09% faster decline per year in FN BMD in MT stages 1 and 3, and 0.10% faster decline in LS BMD in MT stage 3 only (Table).Conclusions: Within-woman increase in CRP is associated with faster BMD decline before and after the MT, but not during the MT when bone loss may be primarily driven by sex hormone changes.

Table: Associations Between Within-Woman Doubling in Serum CRP and Within-woman Increase in Annualized BMD Decline Rate (% per year) by Menopause Transition Stage; Results of Individual Fixed Effects Analysis

		Menopause Transition (MT) Stage					
		Stage 1: Premenopause through Early Perimenopause		Stage 2: Late Perimenopause through Early Postmenopause		Stage 3: Late Postmenopause	
Bone Site	Model	Effect size (95% CI)	P	Effect size (95% CI)	P	Effect size (95% CI)	P
Lumbar Spine	Unadjusted	0.03 (-0.02, 0.08)	0.2	-0.04 (-0.11, 0.03)	0.3	**0.11** (0.04, 0.18)	0.002
	Adjusted 1	0.03 (-0.03, 0.08)	0.3	-0.05 (-0.12, 0.03)	0.2	**0.10** (0.03, 0.17)	0.007
	Adjusted 2	0.03 (-0.03, 0.08)	0.3	-0.05 (-0.12, 0.03)	0.2	**0.10** (0.02, 0.17)	0.009
	Adjusted 3	0.03 (-0.03, 0.08)	0.3	-0.05 (-0.12, 0.03)	0.2	**0.10** (0.03, 0.17)	0.007
Femoral Neck	Unadjusted	**0.13** (0.07, 0.19)	< 001	0.05 (-0.03, 0.13)	0.2	**0.15** (0.07, 0.23)	< 001
	Adjusted 1	**0.08** (0.02, 0.15)	0.007	-0.01 (-0.09, 0.08)	0.9	**0.09** (0.01, 0.17)	0.03
	Adjusted 2	**0.09** (0.02, 0.15)	0.005	-0.00 (-0.09, 0.08)	0.9	**0.09** (0.00, 0.17)	0.04
	Adjusted 3	**0.09** (0.02, 0.15)	0.006	-0.00 (-0.09, 0.08)	0.9	**0.09** (0.01, 0.17)	0.03

Adjusted Model 1: Adjusted for MT stage, BMI, diabetes, smoking, alcohol use

Adjusted Model 2: Model 1 + Bone Positive Meds, Bone Negative Meds, corticosteroids, NSAIDs, Aspirin

Adjusted Model 3: Model 2 + supplemental Calcium and Vitamin D

***Disclosures: Arun Karlamangla**, None*

P-544

Geographic Variation in Prevalence of Osteoporosis Diagnosis and Utilization of Anti-Osteoporosis Therapies Among Commercially Insured Women Aged 50 Years and Older with Fragility Fractures in the United States *Andrea J. Singer[1], E. Michael Lewiecki[2], Pallavi B. Rane[3], Xin Wang[4], Timothy Hill[4], Kainan Sun[4], Rolin L. Wade[4], Michele McDermott[3], Shravanthi R. Gandra[3]. [1]MedStar Georgetown University Hospital, United States, [2]University of New Mexico Health Sciences Center, United States, [3]Amgen Inc, United States, [4]IQVIA, United States

Background: There is limited real-world evidence on geographic variation in fragility-fracture related outcomes among commercially insured women in the US.Objective: To describe geographic variation in distribution of fragility fractures among commercially insured women aged >=50 years in the US, and in rates of osteoporosis diagnosis and treatment in these women.Methods: This retrospective cohort study utilized a nationally representative commercial claim database (IQVIA). Women aged >=50 years were identified on the first occurrence of a fragility fracture of hip, vertebra, or non-hip non-vertebral in inpatient or outpatient setting, between Jan 2015 - Aug 2018. Fracture-related age-standardized measures in the 1-year period preceding and following the fracture, including diagnosis of osteoporosis (identified using ICD9/10 diagnosis codes for osteoporosis), use of anti-resorptive or anabolic agents, and subsequent fracture events were described at the sub-national level.Results: 40,377 commercially insured women were identified who met study eligibility criteria and had >=1 fragility fracture. Their mean[SD] age was 63.4[9.6] years, 33.9% were from southern regions and their mean[SD] Charlson comorbidity index score was 2.3[2.6]. Their most common index fracture type was non-hip non-vertebral (54.4%), followed by vertebral (32.5%) and hip (13%); with 36.6% of all index fractures reported in an inpatient setting. In the 1-year pre-index period, 10.7% women had received a bone mineral density test, 13.4% had a diagnosis of osteoporosis, and 8.6% were receiving any anti-resorptive or anabolic agents. Despite experiencing fragility fractures, these values later increased to 21.1%, 27.4%, and 15.9%, respectively; and 11.9% of women had a subsequent fragility fracture (with 53% presenting with a hip fracture) in the 1-year following the fracture. There was geographic variation across the different states for fracture related measures as described in Table 1.Conclusion: Osteoporosis is an underdiagnosed and undertreated condition among commercially insured women with fragility fractures in the US, who remain at risk for subsequent fractures. There is geographic variation across different states in the US for osteoporosis diagnosis and treatment.

Fracture Related Measure	1-Year Pre-fracture State Average (Lowest to Highest)	1-Year Post-fracture State Average (Lowest to Highest)
% women with osteoporosis diagnosis	5.2% (New Hampshire) to 21.6% (Florida)	20.7% (South Carolina) to 48.1% (Iowa)
% women with any osteoporosis treatment	4.0% (Wyoming) to 17.3% (Iowa)	6.7% (New Hampshire) to 32.7% (Iowa)

***Disclosures: Andrea J. Singer**, Amgen Inc., Consultant*

P-545

Estimated glomerular filtration rate (eGFR) based on cystatin C predicts fragility fractures better than eGFR based on creatinine in women but not in men: The Tromsø Study *Sofie Karoliina Nordvåg[1], Frida Igland Nissen[1], Tove Tveitan Borgen[2], Camilla Andreasen[3], Ragnar Martin Joakimsen[1], Toralf Melsom[1], Martin Dahl Solbu[1], Åshild Bjørnerem[1]. [1]UiT The Arctic University of Norway, Tromsø, Norway, [2]Vestre Viken Hospital Trust, Drammen Hospital, Norway, [3]UiT The Arctic University of Norway, Tromsø, Norway

Patients with end-stage kidney disease have a higher fracture risk than the general population. Previous studies on whether early kidney dysfunction is associated with low bone mineral density and increased fracture risk have yielded ambiguous results. The results of these studies may have been confounded by the use of creatinine based estimates of the glomerular filtration rate (eGFRcre), because creatinine levels correlates with muscle mass, an important risk factor for fractures. Moreover, few population-based prospective studies have reported the importance of reduced eGFR and risk of fracture other than hip fracture. We tested the hypothesis that decreased eGFR based on serum cystatin C (eGFRcys) or both cystatin C and creatinine (eGFRcrecys) predict fractures better than eGFR based on creatinine (eGFRcre).At baseline in the Tromsø Study in 1994-95, a total of 3016 women and 2836 men aged 50-94 years were included in this study. eGFRcre, eGFRcys and eGFRcrecys were estimated using the Chronic Kidney Disease Epidemiology Collaboration equations. Hazard ratio (HR) was calculated in Cox's proportional hazards models and adjusted for age, height, body mass index, bone mineral density, diastolic blood pressure, smoking, physical activity, previous fracture, diabetes and cardiovascular disease. During a median of 14.6 years follow-up, and 34,851 person-years, 232, 135, 394 and 669 of 3016 women suffered incident hip, proximal humerus, wrist and fragility fractures (hip, proximal humerus and/or wrist). During 33,442 person-years, 118, 35, 65 and 201 of 2836 men suffered incident hip, proximal humerus, wrist and fragility fractures. In women, lower eGFRcre did not predict any type of fracture. A 1 SD lower eGFRcys increased the risk for hip, proximal humerus and fragility fracture (HR 1.36; 95% CI 1.16-1.60, HR 1.33; 95% CI 1.08-1.63 and HR 1.12; 95% CI 1.02-1.23), respectively. A 1 SD lower eGFRcrecys increased the risk for hip and proximal humerus fracture (HR 1.25; 95% CI 1.08-1.45 and HR 1.30; 95% CI 1.07-1.57), respectively. Women with eGFRcys in the lowest quartile had doubled risk of hip fracture compared with those in the upper quartile (HR 2.09; 95% CI 1.15-3.78). In men, lower eGFRcre, eGFRcys or eGFRcrecys did not predict any fracture. In conclusion, lower eGFR based on cystatin C increased the risk of hip, proximal humerus and fragility fracture in women. Neither eGFR based on cystatin C, creatinine or both, predicted any type of fracture in men.

***Disclosures: Sofie Karoliina Nordvåg**, None*

P-546

Concomitant Use of Oral Glucocorticoids and Proton Pump Inhibitors and Risk of Osteoporotic Fractures among Patients with Rheumatoid Arthritis: A Population-based Cohort Study *Shahab Abtahi[1], Johanna H.M. Driessen[1], Andrea M. Burden[2], Patrick Souverein[3], Joop P. van den Bergh[4], Tjeerd van Staa[3], Annelies Boonen[4], Frank de Vries[1]. [1]Department of Clinical Pharmacy and Toxicology, MUMC+, Netherlands, [2]Institute of Pharmaceutical Sciences, Department of Chemistry and Applied Biosciences, ETH-Zurich, Switzerland, [3]Division of Pharmacoepidemiology and Clinical Pharmacology, Utrecht. Institute for Pharmaceutical Sciences, Netherlands, [4]Department of Internal Medicine, Division of Rheumatology, MUMC+, Netherlands

Background and Purpose: Patients with rheumatoid arthritis (RA) commonly use oral glucocorticoids (GCs) and proton pump inhibitors (PPIs). Both drugs are associated with osteoporotic fractures, where the underlying biological mechanism is known for oral GCs but not yet understood for PPIs. We investigated the association between concomitant use of oral GCs and PPIs and the risk of osteoporotic fractures among patients with RA.Methods: This was a retrospective cohort study including all RA patients aged 50+ from the Clinical Practice Research Datalink (CPRD) between 1997-2017. Exposure to oral GCs and PPIs was stratified into current (1 year), based on the time since the most recent prescription. Current use was further stratified by average daily and cumulative dose and duration of use. Time-dependent Cox proportional-hazards models estimated risk of osteoporotic fractures (included hip, vertebrae, humerus, forearm, pelvis, or ribs) in RA patients with concomitant current use of oral GCs and PPIs versus non-use. The analyses were statistically adjusted for lifestyle parameters, comorbidities and comedications.Results: Among 12,351 patients with RA (mean age 68 years, 69% females), 1411 osteoporotic fractures were observed. Concomitant current use of oral GCs and PPIs was associated with a 1.6-fold increased risk of osteoporotic fracture compared with non-use (adjusted hazard ratio 1.60, 95%CI 1.35-1.89, Table

1). This was statistically different from a 1.2-fold increased osteoporotic fracture risk associated with oral GC or PPI use alone. Most individual fracture sites were significantly associated with concomitant use of oral GCs and PPIs. Among concomitant users, fracture risk was not increased with higher daily dose or longer duration of PPI use. Current PPI use was associated with 1.3-fold increased risk of osteoporotic fractures versus non-use.Conclusions: Concomitant use of oral GCs and PPIs was associated with a 1.6-fold elevated risk of osteoporotic fracture compared with non-use. This increased risk seems to emerge from separate mechanisms of action of GCs and PPIs on bone or falling risk, since the observed HRs with oral GC or PPI use alone seem to be additive. Considering the increasing life expectancies and high consumption of PPIs among elderly patients, these findings may be clinically relevant in RA patients treated with oral GCs in combination with PPIs.

Table 1. Osteoporotic fracture risk by concomitant use of oral glucocorticoids and proton pump inhibitors in patients with rheumatoid arthritis.

By recency of use	Number of OP fractures (N=1411)*	IR per 1,000 Pys	Age/Sex adjusted Hazard Ratio (95%CI)	Fully adjusted Hazard Ratio† (95%CI)
Non-use of GCs and PPIs	325	10.5	Reference	Reference
Current use‡				
GCs and PPIs concomitantly	264	24.4	**1.93 (1.65-2.27)**	**1.60 (1.35-1.89)**
GCs alone	178	15.5	**1.34 (1.12-1.59)**	**1.23 (1.03-1.47)**§
PPIs alone	324	16.7	**1.32 (1.14-1.54)**	**1.22 (1.05-1.42)**§
Recent GC use‡ ‖	34	11.0	0.87 (0.62-1.23)	0.82 (0.58-1.16)
Recent PPI use‡ ‖	49	16.0	1.21 (0.90-1.62)	1.17 (0.87-1.57)
Past GC use‡ ‖	339	15.6	**1.16 (1.01-1.33)**	1.13 (0.98-1.29)
Past PPI use‡ ‖	219	13.5	0.96 (0.82-1.13)	0.94 (0.80-1.10)

Abbreviation: OP, osteoporotic; IR, incidence rate; Pys, person years; GCs, glucocorticoids; PPIs, proton pump inhibitors.
Statistically significantly increased hazard ratios are shown in bold.
* 1411 osteoporotic fracture events among all included RA patients. The number of events in exposure groups do not sum to this total due to overlap between recent and past use of GCs and PPIs.
† Adjusted at baseline for sex, body mass index, smoking status and alcohol use, and during follow-up for age, a history of ankylosing spondylitis, chronic obstructive pulmonary disease, dementia, falls (in the past 7-12 months), inflammatory bowel disease, and the use in the past 6-months of antidepressants, paracetamol, non-selective non-steroidal anti-inflammatory drugs, cyclooxygenase-2 selective inhibitors, tramadol, opioids, conventional synthetic disease modifying antirheumatic drugs.
‡ Current, recent and past use refer to the last prescription within 6 months, 7-12 months, and >12 months before a period, respectively.
§ Statistically different from concomitant GC and PPI use, Wald test p < 0.05.
‖ Regardless of the use of the other drug.

***Disclosures: Shahab Abtahi**, None*

P-547

High Prevalence of Osteoporosis in Older Male Veterans Receiving Hip-Containing Computed Tomography Scans *Polly Fu, MD[1], Janet Chiang, MD[1], Anne Schafer, MD[1], Preeti Sukerkar, MD PhD[2], Tony Keaveny, PhD[3], Daniel Bikle, MD PhD[1]. [1]Division of Endocrinology and Metabolism, University of California, San Francisco; Endocrine Research Unit, San Francisco Veterans Affairs Health Care System, United States, [2]Departments of Radiology and Biomedical Imaging, University of California, San Francisco, United States, [3]Departments of Mechanical Engineering and Bioengineering, University of California, Berkeley, United States

Osteoporosis care in men is suboptimal due to low rates of DXA testing. Biomechanical computed tomography analysis (BCT) can be applied "opportunistically" to prior hip-containing CT scans to measure femoral bone strength using finite-element analysis and DXA-equivalent femoral neck BMD, both of which are independently associated with incident hip fracture in men. In this study, we used BCT in older male Veterans with prior abdominal/pelvic CT performed for unrelated indications to investigate their prevalence of osteoporosis, as defined by either hip BMD (T-score <= -2.5) or fragile bone strength (<= 3500 N). Additionally, we identified which clinical parameters are associated with osteoporosis in these men.Out of 4,209 abdominal/pelvic CT scans performed between 2017 and 2019 in men age >= 65 in the San Francisco Veterans Affair Health Care System, 625 de-identified CT scans were randomly selected for BCT analysis, stratified by age. Scans were excluded if the femoral coverage or image quality was insufficient. Blinded from the BCT analysis, data from the electronic health record were collected on demographics, medical history, prescriptions, labs, and prior imaging. These data were then associated with osteoporosis using multivariate logistic regression.After exclusions, we obtained BCT results from 557 men. Mean age was 77.2 +/- 7.6 years; 69.1% were white; mean BMI was 26.9 +/- 5.4 kg/m2. Most CTs were performed in an outpatient setting (62.1%); cancer (47.8%), chronic kidney disease (36.6%), and diabetes (30.3%) were the most common comorbidities. As expected, prevalence of osteoporosis increased with age (Fig 1). In those with osteoporosis, 42.6% had a history of major osteoporotic fracture, 38.0% had a prior DXA ever, and 18.6% had received antiresorptive/anabolic therapy. In those without a prior osteoporosis diagnosis or treatment (n = 482) and after adjusting for age, BMI, race, and inpatient vs. outpatient CT, osteoporosis was associated with end stage renal disease (OR 7.4 [95%CI 2.3-23.8], p=0.001), COPD (OR 2.2 [1.2-4.0], p=0.009), exposure to high-dose inhaled steroids (OR 3.7 [1.2-11.8, p=0.03), and presence of bone metastasis (OR 3.0 [1.1-8.6], p=0.04).These results suggest that performing BCT in men with prior CT would be valuable in identifying those at high risk of hip and major osteoporotic fractures, particularly those with specific risk factors such as advanced age, end stage renal disease, COPD, or high-dose inhaled steroid use.

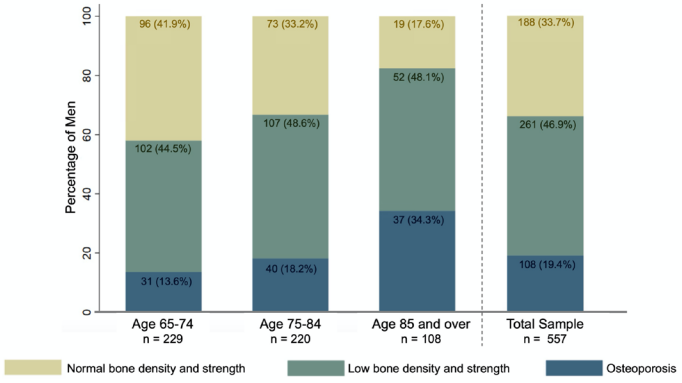

Figure 1. Prevalence of osteoporosis (OP) assessed by biomechanical tomography (BCT) increases with age.
Normal bone density is defined as femoral neck BMD T-score ≥ -1.0. Normal bone strength is defined as femoral bone strength ≥ 5000 N. Low bone density is defined as femoral neck BMD T-score < -1.0 and > -2.5. Low bone strength is defined as femoral bone strength > 3500 N and < 5000 N. OP is defined as femoral neck BMD T-score ≤ -2.5 or femoral bone strength ≤ 3500 N. Results in bar graphs are presented as n (%).

***Disclosures: Polly Fu, MD**, None*

P-548

Racial Differences in Musculoskeletal Health in Elderly Population from the WHICAP cohort *Sanchita Agarwal[1], Carmen Germosen[1], Nayoung Kil[1], Mariana Bucovsky[1], John Williams[1], Marcella Walker[1]. [1]Division of Endocrinology, Department of Medicine, Columbia University, United States

There are racial differences in risk of fracture that are not explained by differences in Bone Mineral Density (BMD) by Dual X-ray Absorptiometry (DXA). Fracture rates are higher in White vs. Black men and women. Some data suggest intermediate fracture risk in Hispanics, while other work shows rates similar to Whites, a finding that may be skeletal site-specific. We enrolled adults >= age 65 from a multi-ethnic (34% Black, 25% White, 41% Hispanic) population-based study in New York City. Bone health was assessed using DXA, High Resolution peripheral Quantitative Computed Tomography (HRpQCT), Trabecular Bone Score (TBS), Vertebral Fracture Assessment (VFA) and grip strength in 265 participants (mean age 76+/-6 yrs). Weight was higher in Black vs. White and Hispanic women while Hispanic women and men were shorter vs. the other groups (all p<0.05). Calcium intake was lower in Black vs. White and Hispanic women and Hispanic vs. White men (all p<0.05), while vitamin D intake did not differ. White women had twice as many historical fractures vs. both groups (both p<0.05), but no difference in vertebral fracture by VFA (p=0.85). Age and weight-adjusted BMD by DXA was higher at the femoral neck and radius in Black vs. White women (all p<0.05). In contrast at the spine, adjusted BMD was higher in White and Black vs. Hispanic women (all p<0.05), while adjusted TBS was higher in White vs. Hispanic women only (p<0.05). By HRpQCT, adjusted cortical indices tended to be lower in White vs. Hispanic and Black women at both sites, while White women had more trabeculae and lower separation vs. Hispanic women (both p<0.05). Differences resulted in higher adjusted stiffness in Black vs. white women at radius (p<0.05). In contrast, age and weight-adjusted HRpQCT trabecular indices tended to be deteriorated in Hispanic men at both sites, while Black men had lower indices at the tibia vs. white men, but there were no differences in cortical indices or stiffness. Falls, body composition and physical activity did not differ by race, but grip strength was lower in Hispanic vs. Black women (p<0.01). In summary, White women had cortical bone loss while Hispanic women had trabecular deterioration leading to higher stiffness in Black women. Non-white men, particularly Hispanic men, tended to have trabecular deterioration vs. White men. Sex, site, and compartment-specific racial differences in microstructure may contribute to racial differences in fracture rates.

Table: Racial difference in demographics, nutrition, DXA and HR-pQCT data separated by Sex. Values are shown as Mean (SD). Statistical significance tested by ANOVA with post-hoc Tukey's HSD.
a: p<0.05 Black vs Hispanic; b: p<0.05 Black vs White; c: p<0.05 Hispanic vs White.
* p<0.05 Adjusted p-value using ANCOVA using age and weight as covariates with post-hoc Tukey's HSD.

SEX	FEMALES				MALES			
RACE	Black (N=66)	Hispanic (N=74)	White (N=37)	p-value	Black (N=23)	Hispanic (N=37)	White (N=28)	p-value
Age (years)	75.98 (5.98)	76.56 (7.07)	76.7 (5.11)	0.81	73.3 (4.77)	74.97 (6.79)	77.13 (4.63)	0.06
Ethnicity (% Hispanic)	15	99	16		0	97	14	
Height (inches)	63.27 (2.29)	60.74 (2.68)	62.13 (2.99)	**p<0.01 a,c**	68.87 (2.82)	65.74 (2.31)	68.01 (2.37)	**p<0.01 a,c**
Weight (pounds)	170.2 (33.74)	153.62 (32.43)	146.85 (35.5)	**p<0.01 a,b**	184.28 (43.45)	170.3 (27.41)	182.34 (28.75)	0.19
BMI (kg/m2)	29.9 (5.7)	29.25 (5.88)	26.84 (5.51)	**p<0.05 b**	27.17 (5.6)	27.87 (3.99)	27.66 (3.7)	0.9
Calcium intake (mg/day)	1043 (588)	1292 (587)	1385 (573)	**p<0.01 a,b**	1013 (657)	951 (454)	1311 (523)	**p<0.05 c**
Vitamin D intake (IU/day)	1608 (1946)	1411 (1742)	1615 (1766)	0.77	881 (704)	1161 (1488)	1454 (913)	0.22
Falls in past 12 months(N)	1.83 (1.23)	1.33 (0.66)	1.5 (0.76)	0.23	1 (0)	2.86 (3.48)	1.4 (0.55)	0.54
Prior fractures (N)	1.25 (0.44)	1.27 (0.55)	2.08 (1.44)	**p<0.01 b,c**	1.22 (0.67)	1.84 (2.29)	1.47 (1.07)	0.62
Physical activity score	78.48 (39.55)	86.55 (43.35)	95.48 (40.34)	0.13	89.45 (46.96)	84.74 (50.03)	91.3 (40.82)	0.84
Grip strength (kg force)	18.36 (5.89)	14.75 (5.41)	16.01 (3.96)	**p<0.01 a**	26.88 (10.7)	27.02 (7.27)	27.52 (8.18)	0.96
DXA								
LS Total T-score	0.03 (1.76)	-1.19 (1.45)	-0.36 (1.54)	**p<0.01 a*,c***	0.52 (2.26)	0 (1.79)	0.66 (1.72)	0.34
Femoral Neck T-score	-1.05 (1.17)	-1.6 (0.86)	-1.81 (1.01)	**p<0.01 a,b***	-0.94 (1.05)	-1.06 (0.95)	-0.83 (0.96)	0.67
Total Hip T-score	-0.66 (1.09)	-1.11 (0.83)	-1.22 (1.07)	**p<0.01 a,b**	-0.57 (1.12)	-0.46 (0.88)	-0.3 (0.91)	0.61
Radius 1/3 T-score	-0.67 (1.45)	-1.25 (1.33)	-1.59 (1.19)	**p<0.01 a,b***	-0.36 (2.01)	-1.23 (1.54)	-1.37 (1.28)	0.06
Subtotal % Fat	39.16 (6.73)	39.42 (5.57)	37.9 (6.31)	0.49	27.13 (8.48)	28.54 (6.28)	28.7 (5.19)	0.66
Subtotal % Lean	60.84 (6.73)	60.58 (5.57)	62.1 (6.31)	0.49	72.87 (8.48)	71.46 (6.28)	71.3 (5.19)	0.66
VFA compression fx (%)	9	19	16	0.85	4	19	7	**p<0.01 a,b**
TBS	1.17 (0.15)	1.15 (0.12)	1.23 (0.13)	**p<0.01 c***	1.27 (0.13)	1.21 (0.15)	1.29 (0.13)	0.11
HR-pQCT Radius (4% Relative offset)								
Tot.vBMD (mgHA/ccm)	249.21 (61.83)	230.99 (50.59)	223.36 (59.22)	0.06	260.79 (66.9)	276 (51.03)	277.48 (59.03)	0.55
Tb.vBMD (mgHA/ccm)	136.27 (41.47)	121.05 (33.63)	126.71 (39)	0.07	143.64 (31.81)	157.58 (31.07)	165.76 (37.53)	0.08
Tb.N (1/mm)	1.29 (0.23)	1.21 (0.24)	1.28 (0.24)	0.15	1.38 (0.22)	1.35 (0.18)	1.48 (0.2)	**p<0.05 c**
Tb.Th (mm)	0.23 (0.03)	0.23 (0.02)	0.22 (0.01)	0.06	0.23 (0.01)	0.24 (0.01)	0.23 (0.01)	**p<0.05 a***
Tb.Sp (mm)	0.77 (0.18)	0.84 (0.28)	0.78 (0.2)	0.18	0.71 (0.14)	0.71 (0.12)	0.64 (0.11)	**p<0.05**
Ct.vBMD (mgHA/ccm)	807.28 (68.8)	802.65 (62.15)	779.29 (73.84)	0.13	828.85 (97.21)	825.66 (78.15)	811.78 (57.03)	0.7
Ct.Po (%)	1.2 (0.63)	1.04 (0.77)	1.22 (0.95)	0.38	1.02 (0.52)	1.49 (0.87)	1.49 (0.72)	0.05
Ct.Th (mm)	0.83 (0.2)	0.78 (0.15)	0.69 (0.14)	**p<0.01 b*,c**	0.95 (0.26)	0.98 (0.21)	0.94 (0.2)	0.72
Stiffness (N/mm)	50621 (16717)	43468 (11190)	37768 (8771)	**p<0.01 a,b***	64670 (21436)	74767 (20247)	67271 (14040)	0.21
HR-pQCT Tibia (7.3% Relative offset)								
Tot.vBMD (mgHA/ccm)	244.91 (56.43)	230.35 (52.2)	234.8 (46.8)	0.26	265.88 (58.72)	274.36 (46.59)	286.51 (40.76)	0.31
Tb.vBMD (mgHA/ccm)	146.85 (43.28)	138.18 (37.93)	156.54 (32.36)	0.06	146.02 (44.76)	162.56 (31.68)	186.23 (31.18)	**p<0.01 b*,c**
Tb.N (1/mm)	1.23 (0.24)	1.16 (0.26)	1.32 (0.18)	**p<0.01 c***	1.26 (0.28)	1.23 (0.18)	1.38 (0.17)	**p<0.05 c**
Tb.Th (mm)	0.25 (0.02)	0.25 (0.02)	0.25 (0.02)	0.19	0.25 (0.02)	0.26 (0.02)	0.26 (0.02)	0.16
Tb.Sp (mm)	0.82 (0.22)	0.89 (0.25)	0.74 (0.15)	**p<0.01 c***	0.81 (0.19)	0.8 (0.12)	0.69 (0.11)	**p<0.01 b*,c***
Ct.vBMD (mgHA/ccm)	799.16 (76.11)	795.12 (69.22)	754.74 (82.54)	**p<0.01 b*,c***	853.2 (101.77)	841 (64.77)	807.92 (56.48)	0.07
Ct.Po (%)	4.17 (1.47)	3.81 (1.5)	4.14 (1.34)	0.3	3.63 (1.91)	3.8 (1.71)	4.44 (1.72)	0.21
Ct.Th (mm)	1.26 (0.34)	1.16 (0.23)	1.07 (0.23)	**p<0.01 b***	1.54 (0.36)	1.45 (0.32)	1.46 (0.22)	0.51
Stiffness (N/mm)	158985 (37358)	141581 (29124)	135476 (30423)	**p<0.01 a,b**	189252 (53341)	207004 (43807)	223589 (36505)	0.11

***Disclosures: Sanchita Agarwal**, None*

P-549

The association of tea intake with BMD and fractures in White women and men of the Canadian Multicentre Osteoporosis Study (CaMos) *Suzanne N Morin[1], Claudie Berger[2], Weiyi Liu[1], Jerilynn C Prior[3], Angela M Cheung[4], David A Hanley[5], Steven K Boyd[5], Andy KO Wong[4], Alexandra Papaioannou[6], Elham Rahme[1], David Goltzman[1]. [1]McGill University, Canada, [2]Research Institute of the McGill University Health Centre, Canada, [3]University of British Columbia, Canada, [4]University of Toronto, Canada, [5]University of Calgary, Canada, [6]McMaster University, Canada

Purpose: Previous reports support the beneficial effect of tea consumption on BMD and hip fracture in women. Data are lacking on its impact on BMD change over time, on incident fractures, and in men. Methods: We included 7398 White participants aged 50+ (5355 women, 2043 men) from the population-based longitudinal cohort study CaMos at baseline (1995-97), among which 4386 women and 1561 men had a 5-year follow-up. Daily tea intake was categorized: no tea (NoT), moderate <= 2cups (MoT), and high >2 cups (HiT). Incident major osteoporotic fractures (MOF) were assessed yearly. We used regression models to study the association between tea intake and baseline total hip BMD (linear), %-change in total hip BMD over 5 years (linear), prevalent MOF (logistic) and 5-year incident MOF (logistic).Results: The median daily tea intakes were 1.6 cups (IQR: 0.0-2.6) in women and 1.4 cups (IQR: 0.0-2.0) in men. The distribution of daily tea intake (with caffeinated tea representing 87%) was 22.3% in NoT, 51.1% in MoT and 26.6% in HiT for women, and was 27.7% in NoT, 51.4% in MoT and 21.0% in HiT in men. Compared to NoT, HiT consumers were older (67.8 years [SD=9.2] vs. 65.8 years [9.4]), smoked less (13% vs. 21%) and exercised more regularly (56% vs. 51%). The average baseline total hip BMD was lowest in HiT (0.867g/cm2 [0.157]) and highest in MoT consumers (0.889g/cm2 [0.161]). The prevalence of MOF was 13.6% in women and 8.3% in men and did not differ by group of tea intake. In the subsample of participants with a 5-year follow-up, the total hip BMD decreased by 1.9% (5.2) over 5 years in HiT compared to 1.2% (4.8) in NoT. The proportion of incident MOF was 5.0% in women and 1.7% in men and differed by tea intake groups only in women. Adjusted linear regression models (Table) demonstrated that compared to NoT consumers, women with MoT intake had a higher baseline BMD (+ 0.013g/cm2 (95% confidence interval: 0.005; 0.021); however, those with a HiT intake showed a greater BMD loss and a higher incidence of MOF. In men, we also noted a greater loss in adjusted total hip BMD in HiT vs NoT consumers at 5 years. Conclusion: Our results support a favorable effect of moderate tea consumption in men and women. However, more than 2 cups of tea per day was associated with greater BMD loss over time in both men and women, and with increased risk for incident MOF in women.

Table: Baseline and % change over 5-year estimates (95% C.I.) in total hip BMD and Odds Ratios (OR) with 95% CI for prevalent and 5-year incident MOF for moderate and high tea drinkers compared to no-tea drinkers, in white men and women aged 50+

Sex	WOMEN		MEN	
Daily tea intake **Reference level = NoT**	>0 but ≤ 2 cups/day (MoT)	>2 cups/day (HiT)	>0 but ≤ 2 cups/day (MoT)	>2 cups/day (HiT)
Baseline Total hip[1] (g/cm^2)	**0.013 (0.005; 0.021)**	0.007 (-0.003; 0.016)	0.004 (-0.010; 0.019)	-0.008 (-0.026; 0.010)
% total hip BMD change over 5 year[1]	-0.12 (-0.56; 0.32)	**-0.71 (-1.21; -0.20)**	-0.08 (-0.63; 0.47)	**-0.76 (-1.46; -0.07)**
Prevalent MOF[2] (OR, 95% CI)	1.20 (0.96; 1.49)	1.16 (0.91; 1.48)	1.04 (0.71; 1.51)	0.87 (0.54; 1.41)
5-year incident MOF[3] (OR, 95% CI)	1.28 (0.86;1.91)	**1.56 (1.02; 2.39)**	0.78 (0.33; 1.83)	0.73 (0.24; 2.19)

Bold are significant values

1 cup of tea = 6oz
MOF= major osteoporosis fracture
[1]Adjusted for age (polynomials up to 3 degrees), height, BMI, prevalent low trauma fracture, participation in a regular activity, smoking status, alcohol intake, use of calcium supplements.
[2]Adjusted for age, height, BMI, diagnosis of osteoporosis (in women only), participation in a regular activity, smoking status, use of calcium supplements.
[3]Adjusted for age, height, BMI, participation in a regular activity (women only), smoking status (women only), use of calcium supplements (women only)

***Disclosures: Suzanne N Morin**, None*

P-550

Current, but not Past Smoking, is Associated with Sex-Specific Skeletal Deficits *Sanchita Agarwal[1], Carmen Germosen[1], Nayoung Kil[1], Mariana Bucovsky[1], Natalie Cusano[2], John Williams[1], Marcella Walker[1]. [1]Division of Endocrinology, Department of Medicine, Columbia University, United States, [2]Division of Endocrinology, Department of Medicine, Lenox Hill Hospital, United States

Smoking is a risk factor for fracture. The mechanism by which smoking increases fracture risk and its effect on skeletal microstructure is unclear. We compared musculoskeletal health in current, past and non-smokers from a population-based multiethnic cohort of older adults in New York City, the Washington Heights-Hamilton Heights-Inwood Columbia Aging Project. Of N=265 subjects, most smokers were non-White (42% Black, 38% Mixed). Dual X-ray Absorptiometry (DXA), High Resolution peripheral Quantitative Computed Tomography (HRpQCT), Trabecular Bone Score (TBS), Vertebral Fracture Assessment (VFA), and grip strength were assessed. Participants mean age was 76+/-6 years, mostly female (67%) with a mean smoking exposure of 22+/-21 pack-years. In men, weight and calcium intake were 18% and 49% lower in current (n=8) vs. past (n=39) smokers, respectively (both p<0.05). Age and weight-adjusted BMD by DXA did not differ at any site. Current male smokers had 11 % lower age and weight-adjusted TBS compared to past and non-smokers (both p<0.05). By HRpQCT, age and weight-adjusted trabecular (Tb) volumetric BMD was 28-30% lower and Tb separation was higher by 22% in male current vs. past and non-smokers at the radius (all p<0.05). Tb number and thickness were 16% and 8% lower in current vs. never smokers (both p<0.05). There were no differences in cortical indices. There were similar findings at the tibia. Additionally, age and weight-adjusted tibial stiffness was 25% lower in current vs. non-smokers (p=0.01). Grip strength was lower in current smokers vs. past and non-smokers (p<0.05). There were no between-group differences in age, physical activity, vitamin D intake, falls, or vertebral fractures by VFA in men. In women (n=177), current smokers were younger than both groups and non-smokers were shorter than past smokers (p<0.05). There were no differences by DXA, but cortical porosity by HRpQCT was twice as high in current (n=8) vs. past and non-smokers at the radius and 40% higher vs. non-smokers at the tibia (both p<0.05). There was no difference in Tb indices in women. Pack-years was not associated with skeletal indices. In summary, current but not past smoking, is associated with trabecular skeletal microstructural deficits at the spine and peripheral skeleton in men and cortical deficits in women. Smoking may have sex-specific effects. The association with current, but not past smoking, suggests that effects of tobacco use may be reversible with smoking cessation.

Posters

Table: Difference in demographics, nutrition, DXA and HR-pQCT data by smoking status and sex. Values are shown as Mean (SD). Statistical significance tested by ANOVA with post-hoc Tukey's HSD.

a: p<0.05 Past vs Non-Smokers ; b: p<0.05 Past vs Current Smokers ; c: p<0.05 Non vs Current Smokers.

* p<0.05 Adjusted p-value using ANCOVA using age and weight as covariates with post-hoc Tukey's HSD.

SEX	FEMALES				MALES			
SMOKING	Past (N=62)	Never (N=107)	Current (N=8)	p-value	Past (N=39)	Never (N=41)	Current (N=8)	p-value
Age (years)	76.27 (5.4)	76.85 (6.71)	70.71 (3.54)	**p<0.05 b,c**	75.63 (6.09)	75.22 (5.74)	73.21 (4.74)	0.57
Race (% Black)	50	29	50	**p<0.05**	26	22	50	0.29
Ethnicity (% Hispanic)	37	58	50	**p<0.05**	54	37	50	0.31
Height (inches)	62.71 (2.63)	61.61 (2.89)	61.19 (2.83)	**p<0.05 a**	67.42 (3.23)	67.25 (2.59)	66.74 (1.22)	0.82
Weight (pounds)	165.03 (37.71)	153.71 (32.15)	169.44 (37.08)	0.08	188.22 (34.82)	172.34 (28.67)	154.81 (29.04)	**p<0.05 b**
BMI (kg/m2)	29.42 (6.02)	28.48 (5.76)	31.56 (4.91)	0.26	28.99 (4.27)	26.75 (3.9)	24.46 (4.67)	**p<0.01 a,b**
Calcium intake (mg/day)	1195 (657)	1247 (574)	1022 (430)	0.55	1187 (668)	1076 (406)	601 (309)	**p<0.05 b**
Vitamin D intake (IU/day)	1655 (1889)	1521 (1831)	626 (401)	0.32	1084 (768)	1281 (1350)	1145 (1741)	0.75
Falls in past 12 months(N)	1.73 (1.12)	1.46 (0.85)	2 (0)	0.53	1.71 (1.5)	2.67 (3.61)	1 (0)	0.75
Prior fractures (N)	1.41 (1.01)	1.6 (0.94)	1 (0)	0.6	1.82 (2.4)	1.42 (0.97)	1.5 (1)	0.74
Physical activity score	86.14 (40.59)	84.82 (43.1)	87.57 (31.47)	0.97	82.33 (42.28)	93.26 (51.64)	89.35 (32.37)	0.57
Grip strength (kg force)	17.71 (4.95)	15.47 (5.57)	16.21 (7.5)	0.06	29.3 (8.72)	26.24 (8)	20.61 (7.41)	**p<0.05**
DXA								
LS Total T-score	-0.49 (1.61)	-0.58 (1.7)	-0.91 (1.96)	0.79	0.89 (1.52)	0.09 (2.13)	-1.01 (1.57)	**p<0.05 b**
Femoral Neck T-score	-1.28 (1.12)	-1.57 (1.03)	-0.95 (0.61)	0.09	-0.64 (0.84)	-1.17 (1.05)	-1.48 (0.76)	**p<0.05 a**
Total Hip T-score	-0.87 (0.98)	-1.07 (1.02)	-0.33 (0.92)	0.09	-0.11 (0.8)	-0.65 (1.03)	-0.97 (0.78)	**p<0.01 a,b**
Radius 1/3 T-score	-1.04 (1.38)	-1.19 (1.38)	-0.46 (1.45)	0.33	-0.72 (1.63)	-1.19 (1.67)	-1.86 (1.23)	0.15
Subtotal % Fat	39.38 (6.41)	38.73 (6.1)	40.24 (4.81)	0.69	30.72 (5.96)	26.68 (6.39)	23.45 (7.15)	**p<0.01 a,b**
Subtotal % Lean	60.62 (6.41)	61.27 (6.1)	59.76 (4.81)	0.69	69.28 (5.96)	73.32 (6.39)	76.55 (7.15)	**p<0.01 a,b**
VFA compression fx (%)	15	15	13	0.6	10	12	13	**p<0.01 b,c**
TBS	1.15 (0.15)	1.19 (0.12)	1.09 (0.13)	**p<0.05**	1.26 (0.15)	1.27 (0.13)	1.12 (0.12)	**p<0.05 b*,c***
HR-pQCT Radius (4% Relative offset)								
Tot.vBMD (mgHA/ccm)	231.74 (51.47)	236.86 (61.53)	270.87 (39.4)	0.23	273.35 (49.99)	281.39 (63.09)	226.05 (41.57)	**p<0.05 c**
Tb.vBMD (mgHA/ccm)	126.33 (36.51)	126.93 (38.95)	158.49 (35.95)	0.1	158.76 (27.38)	163.58 (34.29)	113.26 (32.14)	**p<0.01 b*,c***
Tb.N (1/mm)	1.25 (0.2)	1.26 (0.26)	1.34 (0.29)	0.6	1.41 (0.16)	1.43 (0.22)	1.2 (0.19)	**p<0.05 b,c***
Tb.Th (mm)	0.23 (0.02)	0.23 (0.03)	0.24 (0.01)	0.43	0.24 (0.01)	0.24 (0.02)	0.22 (0.02)	**p<0.05 c***
Tb.Sp (mm)	0.79 (0.15)	0.81 (0.28)	0.73 (0.16)	0.64	0.67 (0.09)	0.68 (0.13)	0.83 (0.17)	**p<0.01 b*,c***
Ct.vBMD (mgHA/ccm)	793.96 (69.02)	803.35 (67.07)	797.33 (69.83)	0.69	827.81 (71.42)	817.5 (86.12)	818.36 (55.68)	0.84
Ct.Po (%)	1.21 (0.74)	1.03 (0.72)	2 (1.03)	**p<0.01 b*,c***	1.37 (0.90)	1.41 (0.69)	1.25 (0.46)	0.86
Ct.Th (mm)	0.79 (0.17)	0.77 (0.18)	0.88 (0.16)	0.25	0.95 (0.2)	0.98 (0.24)	0.89 (0.18)	0.56
Stiffness (N/mm)	46432 (14158)	44189 (14335)	51619 (8738)	0.48	74819 (21213)	69675 (19240)	59059 (8720)	0.17
HR-pQCT Tibia (Relative offset)								
Tot.vBMD (mgHA/ccm)	234.07 (50.24)	236.58 (55.01)	258.93 (43.37)	0.46	271.01 (41.04)	289.4 (53.44)	231.78 (17.81)	**p<0.01 c***
Tb.vBMD (mgHA/ccm)	144.61 (40)	144.08 (38.65)	165.93 (43.95)	0.32	165.79 (31.1)	174.18 (41.87)	122.53 (19.96)	**p<0.01 b,c***
Tb.N (1/mm)	1.19 (0.24)	1.23 (0.24)	1.3 (0.26)	0.39	1.32 (0.2)	1.28 (0.23)	1.13 (0.18)	0.08
Tb.Th (mm)	0.25 (0.02)	0.25 (0.02)	0.26 (0.02)	0.27	0.25 (0.02)	0.26 (0.02)	0.24 (0.02)	**p<0.05 c**
Tb.Sp (mm)	0.85 (0.26)	0.82 (0.21)	0.77 (0.23)	0.49	0.74 (0.12)	0.77 (0.16)	0.88 (0.13)	**p<0.05 b,c**
Ct.vBMD (mgHA/ccm)	779 (78.21)	794.25 (76.33)	778.36 (58.28)	0.43	837.56 (73.33)	831.3 (81.15)	826.79 (60.23)	0.9
Ct.Po (%)	4.23 (1.48)	3.79 (1.41)	5.24 (1.33)	**p<0.01 c***	3.71 (1.78)	4.15 (1.84)	4.21 (1.48)	0.5
Ct.Th (mm)	1.19 (0.28)	1.16 (0.29)	1.28 (0.22)	0.48	1.44 (0.3)	1.54 (0.31)	1.32 (0.21)	0.1
Stiffness (N/mm)	150216 (34020)	144878 (34154)	152722 (33802)	0.67	215469 (44929)	210416 (44900)	157115 (16340)	**p<0.01 b,c***

***Disclosures: Sanchita Agarwal**, None*

P-551

Gut microbiota and bone status in postmenopausal women – pilot study *Pawel Szulc[1], Victoria Meslier[2], Christian Morabito[2], Nathalie Galleron[2], Mamadou Gabou Thiam[2], Nicolas Pons[2], Stanislav Dusko Ehrlich[2], Joël Doré[2], Roland Chapurlat[1], Hugo Roume[2], Philippe Wagner[3]. [1]INSERM UMR 1033, University of Lyon, Hospices Civils de Lyon, France, [2]Université Paris-Saclay, INRAE, Metagenopolis, France, [3]INSERM UMR1033 University of Lyon, Hospices Civils de Lyon, France

Data from clinical and experimental studies show that gut microbiota is involved in the regulation of bone loss after menopause in women and after ovariectomy in mice. Our aim was to assess cross-sectionally the association between bone status and gut microbiota composition in postmenopausal women. Four groups of volunteer postmenopausal women aged 60 and over were examined:A – 38 women aged 70+/-6 years with normal bone mineral density (BMD) defined by T-score> –1.5 at the lumbar spine, total hip and femoral neck (all three),B – 38 women aged 71+/-5 years with normal BMD and fractures (at least one prevalent vertebral fracture on a lateral DXA scan or self-reported prior fragility fracture),C – 38 women aged 69+/-6 years with osteoporosis (T-score< –2.5 at one skeletal site at least) without fracture,D – 38 women aged 71+/-6 years with osteoporosis and fractures. BMD measurementss and lateral scans were obtained using a Hologic Discovery A device. Microbial diversity and composition of the gut microbiota were assessed by standardized quantitative metagenomic pipeline. Metagenomic Species was used to identify and quantify microbial species by comparing to the 10.4 IGC2 gene reference catalogue.At the order rank, Christensenellales were less abundant and Burkholderiales were more abundant in Group B vs. other groups (p<0.05). Victivallales and Oscillospirales were more abundant in women with osteoporotic BMD vs. those with normal BMD (p<0.01).At the rank of Metagenomic Species, Akermansia muciniphila was most abundant in Group A and, somewhat unexpectedly, in Group D. Allisonella histaminiformans was enriched in Group B vs. other groups (p<0.005). Anaerostipes hadrus was enriched in women with osteoporotic BMD vs. those with normal BMD (p<0.01). One unclassified Methanomethylophilaceae species was enriched in Group D vs. other groups (p<0.001).Our preliminary data suggest that, in postmenopausal women, BMD and fracture status seem to be associated with specific components of gut microbiota. Further studies are needed to better characterize potential pathways underlying these associations, e.g. good general health status (Akermansia muciniphila, Christensenellales), leanness (Oscillospirales, Victivallales), inflammation (Allisonella histaminiformans, Methanomethylophilaceae), synthesis of short chain fatty acids (Akermansia muciniphila, Anaerostipes hadrus), high dietary fiber and protein intake (Christensenellales).

***Disclosures: Pawel Szulc**, None*

P-552

A Prospective Observational Study of Bone Mineral Density in Premenopausal Women with Uterine Fibroids *Michael R. McClung[1], Arthur Santora[2], Ayman Al-Hendy[3], Juan Camilo Arjona Ferreira[4], Yulan Li[4], Laura McKain[4], Rachel B. Wagman[4]. [1]Oregon Osteoporosis Center, United States, [2]Kinexum Services LLC, United States, [3]Department of Obstetrics and Gynecology, University of Illinois/Chicago, United States, [4]Myovant Sciences Inc., United States

Purpose: Uterine fibroids (UF) may cause heavy menstrual bleeding (HMB) and negatively impact daily living and quality of life. Gonadotropin-releasing hormone (GnRH) agonists and antagonists treat UF-associated bleeding but are associated with bone loss. The aim of this prospective study was to characterize longitudinal bone mineral density (BMD) in untreated premenopausal women with UF over a 52-week observational period and to evaluate factors correlated with changes in BMD.Methods: Premenopausal women aged 18–50 years with ultrasound-confirmed UF, were enrolled contemporaneously at a subset of sites conducting trials assessing the efficacy and safety of relugolix combination therapy (relugolix 40 mg, a GnRH antagonist, estradiol 1 mg and norethindrone acetate 0.5 mg) for women with HMB associated with UF (Al-Hendy, 2019). HMB was not a requirement for inclusion. BMD was measured by dual energy X-ray absorptiometry at the lumbar spine (LS), total hip (TH), and femoral neck (FN) at screening, Weeks 24 and 52. Mean % change in BMD from baseline was summarized by anatomic location. Trends for age, body mass index (BMI), and racial subgroups were examined.Results: A total of 262 participants, mean age 41.8 (SD: 5.5) years, were enrolled in the United States; 58% were Black/African American; 37% were White. Mean BMI was 31.6 kg/m2 (SD: 8.0). Baseline mean BMD at the LS was 1.21 g/cm2 (SD: 0.18) and the mean % changes from baseline (95% CI) were 0% (–0.32%, 0.31%) and –0.41% (–0.77%, –0.05%) at Weeks 24 and 52, respectively. Baseline mean BMD was 1.05 g/cm2 (SD: 0.15) at TH and 0.97 g/cm2 (SD: 0.19) at FN with similar minimal changes observed over 52 weeks. A histogram of % change from baseline LS BMD at Week 52 showed a symmetrical distribution with women who both gained and lost bone mass. Evaluation of subgroups, BMI < 30 kg/m2 vs >= 30 kg/m2 or Black/African American vs White, showed consistent results with the overall population. In the youngest women (age 18–34 years subgroup), gains in BMD were observed through Week 52, while no change or non-significant decline was observed in other age subgroups (Figure).Conclusion: In this novel set of longitudinal data in premenopausal women with UF, BMD changes over 52 weeks were consistent with results of cross-sectional studies of BMD in women of reproductive age. Although age-related differences were observed, race and BMI did not influence BMD over time.

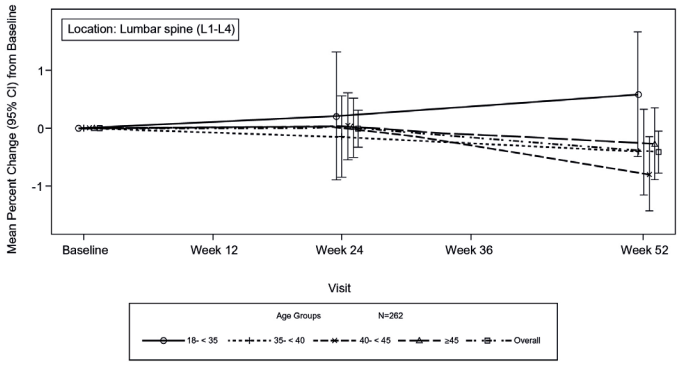

***Disclosures: Michael R. McClung**, Amgen, Speakers' Bureau, Amgen and Myovant, Consultant*

P-553

Effects of Vitamin D Analogues on Fracture Incidence in Chronic Kidney Disease: A Systematic Review and Meta-Analysis of Randomized Clinical Trials *Nada Khelifi[1], Louis-Charles Desbiens[2], Aboubacar Sidibé[2], Fabrice Mac-Way[2]. [1]CHU de Quebec Research Center, Faculty and Department, Canada, [2]CHU de Quebec Research Center, Faculty and Department of Medicine, Laval University, Quebec City, Canada, Canada

Background: We performed a systematic review and meta-analysis of randomized clinical trials (RCTs) to evaluate the effect of vitamin D analogues on fracture incidence and bone mineral density (BMD) in adult patients with chronic kidney disease (CKD).Methods: We searched MEDLINE, EMBASE, CENTRAL, ClinicalTrials.gov, and the WHO's International Clinical Trials Registry Platform databases from inception to October 16, 2019. Two reviewers independently screened all identified references in order to include RCTs comparing active vitamin D analogues, alone or in combination, to placebo or another medication, in adults with CKD requiring or not dialysis. Trials involving kidney transplant recipients and/or comparing vitamin D analogues to anti-resorptive or anabolic bone therapy were excluded. Primary outcome was fracture at any anatomical site (total fractures). Secondary outcomes were BMD at femoral neck, lumbar spine, and/or total hip. Pre-specified sub-

group analyses were conducted according to baseline demographics, overall risk of bias and follow-up time. Risk of bias was assessed with the Cochrane Risk of Bias tool. Meta-analysis was conducted with random-effects models.Results: From 6 293 references retrieved, 9 RCTs were eligible (1 615 participants), 7 of which were used in the meta-analyses. All of these studies used placebo as comparator. Vitamin D analogues were not associated with a significant reduction in total fractures (RR= 0.92 [95% CI 0.45, 1.86], I2= 0%, 7 trials, 1 553 patients) in overall and in pre-specified subgroup analyses. Only two trials reported BMD thus, a meta-analysis could not be performed. Eight RCTs were at high risk of bias, notably due to incomplete outcome data and pharmaceutical funding.Conclusions: Current evidence from RCTs is insufficient to associate vitamin D analogues with bone protection in CKD. Additional large and long-term studies specifically designed to evaluate the efficacy of vitamin D analogues on bone outcomes are thus required.Registration: CRD42020154915

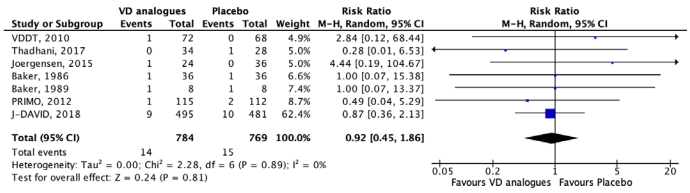

***Disclosures: Nada Khelifi**, None*

P-554

Sex-specific differences in bone mass are maintained following spinal cord injury *Courtney Mazur[1], W. Brent Edwards[2], Ifaz Haider[2], Ying Fang[3], Leslie Morse[4], Thomas Schnitzer[5], Karen Troy[6]. [1]Massachusetts General Hospital, United States, [2]University of Calgary, Canada, [3]University of Northern Arizona, United States, [4]University of Minnesota Medical School, United States, [5]Northwestern University, United States, [6]Worcester Polytechnic Institute, United States

Spinal cord injuries (SCI) cause rapid, severe bone loss in the distal femur and proximal tibia and increase risk of low-impact fracture. The rate of bone loss and the affected sites are distinct from osteoporosis following menopause or aging, so SCI-induced bone loss requires specific attention. While women are at higher risk of osteoporosis than men, current studies of SCI-induced bone loss do not enroll enough women to discern sex-specific patterns following SCI. We analyzed QCT scans from four clinical trials with nearly identical imaging protocols to test the hypothesis that there are sex-specific differences in bone loss following SCI.In this cross-sectional study of 137 people (31 female) with varying duration of SCI, we used baseline QCT scans from four clinical trials. Protocols were approved by the IRB at each study site, and all participants provided informed consent. Scans were segmented to include all tissue inside the periosteal boundary of the proximal tibia or distal femur (0.15 g/cm2 threshold). Regions of interest (epiphysis, metaphysis, diaphysis) were assigned as successive 10% bone length sections.As in prior analyses, we found that integral bone volume (BV) in both bones and all regions does not change after SCI, while bone mineral content (BMC) rapidly declines until reaching a plateau approximately 3 years post-injury. In all regions of interest, female BV was 72-77% of that in males (Fig 1A, p<0.0001). The decline in BMC over time in each region of interest was well described by separate single-phase exponential decay curves for each sex (Fig 1B, p<0.001), which were primarily determined by lower mean values for females in the early (3 years post-SCI) phases. From the early to the plateau phase, BMC in the epiphysis, metaphysis and diaphysis was reduced by approximately 63%, 54%, and 40%, respectively, for both sexes. The number of female subjects between 0.5-2 years post-SCI was insufficient to detect sex-specific changes in the rate of BMC change. As expected with lower BV and BMC, the bending strength index (BSI) in female bones was significantly lower than in males over time, particularly in the metaphysis and diaphysis (Fig 1C, p<0.001). These data suggest that the magnitude of SCI-induced bone loss is similar in males and females, but due to consistently lower BV, BMC, and BSI, special attention should be paid to female patients to prevent low-impact fractures.

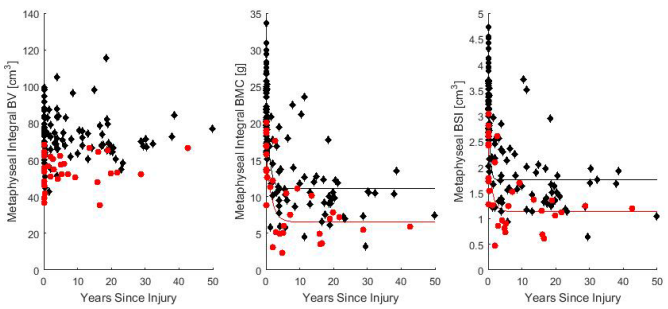

Figure 1: QCT outcomes in the distal femoral metaphysis of men (♦) and women (●) following spinal cord injury.

***Disclosures: Courtney Mazur**, None*

P-555

Incidence and Risk Factors for Osteoporotic Non-vertebral Fracture in Low-Income Community-dwelling Elderly: a Population-based Prospective Cohort Study in Brazil. The São Paulo Ageing & Health (SPAH) Study. *Diogo Souza Domiciano[1], Luana Gergeim Machado[1], Camille Pinto Figueiredo[1], Valéria Caparbo[1], Ricardo M Oliveira[2], Paulo Rossi Menezes[3], Rosa Maria Rodrigues Pereira[1]. [1]Bone Metabolism Laboratory, Rheumatology Division, Faculdade de Medicina da Universidade de São Paulo., Brazil, [2]RDO Diagnósticos Médicos, Brazil, [3]3Department of Preventive Medicine, Faculdade de Medicina da Universidade de São Paulo., Brazil

Introduction. No data on incidence of osteoporotic non-vertebral fracture have been reported in low- income countries where the population's aging has been faster. Even in developed countries, currently available prospective data on major fractures rates beyond hip are scarce. Thus, we sought describe the incidence and risk factors for non-vertebral fracture in a longitudinal prospective Brazilian population-based elderly cohort.Methods. 707 older adults (449 women, 258 men) were evaluated at baseline and after a mean follow-up of 4.3+/-0.8 years. Clinical questionnaire, bone mineral density (BMD) and laboratory tests were performed at baseline. New non-vertebral fracture (hip, proximal humerus, rib, forearm) was determined during the follow-up. Multivariate Poisson regression models were used to identify independent predictors of fracture.Results. The age-standardized incidence of non-vertebral fracture was 1706.1/100,000 person-years (pyr) in women and 632.8/100,000 in men. Concerning to hip fractures, the incidence was 421.2/100,000 pyr in women and 89.9/100,000 in men. In a multivariate analysis, age (RR 2.07, 95% CI 1.13-3.82, p=0.019, per each 10-year increase), prior non-vertebral fracture (RR 3.08, 95% CI 1.36-6.95, p=0.007) and total hip BMD (RR 1.68, 95% CI 1.11-2.56, p=0.015, per each 1 SD decrease) were predictors of new non-vertebral fracture. In men, fitting a model of risk factors for fracture was prevented by the limited number of events in male sample.Conclusion. This is the first population-based study to ascertain the incidence of major non-vertebral fractures in elderly Latin Americans, confirming the high frequency of the disorder. Age, prior fracture and hip BMD were predictors of the short-term incidence of fracture.

***Disclosures: Diogo Souza Domiciano**, None*

P-556

How do risk factors for incident fracture differ in obese and non-obese community-dwelling older men? The Concord Health and Ageing in Men Project *David Scott[1], Markus Seibel[2], Robert Cumming[2], Vasi Naganathan[2], Fiona Blyth[2], David Le Couteur[2], David Handelsman[2], Benjumin Hsu[2], Louise Waite[2], Vasant Hirani[2]. [1]Monash University, Australia, [2]University of Sydney, Australia

Background: Obese older adults have higher bone mineral density (BMD) than non-obese counterparts but other characteristics of obesity, including increased falls risk, metabolic disorders and hypogonadism, may predispose these individuals to fracture. Furthermore, high body mass index (BMI), which is generally used to define obesity, is associated with better BMD and reduced fracture risk, whereas high fat mass per se may not be. The primary aim of this study was to compare clinical risk factors for incident fracture in community-dwelling older men with and without obesity, defined according to body fat percentage.Methods: BMI and body fat percentage were assessed at baseline by anthropometry and dual-energy X-ray absorptiometry, respectively, in 1,625 community-dwelling men aged >=70 years. Categories for non-obese and obese were <30kg/m2and >=30kg/m2 for BMI, and <30% and >=30% for body fat percentage. Sociodemographic, medical, physical function and blood biochemistry parameters were collected at baseline. Self-reported incident fractures of any type and cause (excluding pathological fractures and fractures of hands, fingers, feet, toes and the skull) were confirmed by radiographic reports and recorded up to 9 years. Hip fractures were also followed for 14 years using data linkage.Results: Prevalence of obesity was lower when defined according to BMI (27%) than when defined according to body fat percentage (44%). There were no differences in incidence of any fracture between non-obese and obese men by BMI (10.7 vs 9.3%, respectively; P>0.05) or body fat percentage (10.2 vs 10.6%, respectively; P>0.05). When obesity was defined according to body fat percentage, significant interactions were observed demonstrating that prevalent dementia at baseline increased hazard for incident any and hip fracture in non-obese men (adjusted hazard ratio 7.08; 95% CI 3.27-15.36 and 8.36; 3.13-22.31, respectively) but not for obese men. Past-year falls increased hazard for any fracture in obese men (2.86; 95% CI 1.60-5.10) but not for non-obese men, while higher luteinizing hormone concentrations reduced hazard for hip fracture in obese men (0.91; 0.85-0.97 per IU/L) but not for non-obese men.Conclusions: Community-dwelling older men with obesity, regardless of the definition applied, do not demonstrate reduced risk for incident fracture compared with non-obese counterparts. Assessments of falls history and gonadotrophin levels, in addition to established clinical risk factors for fracture, may contribute to improvements in fracture prediction in obese older men.

***Disclosures: David Scott**, None*

Posters

P-557

Long-Term Changes in Bone Mineral Density and Trabecular Bone Score among Chinese Patients with HIV on Antiretroviral Therapy *Wenmin Guan[1], Wei Pan[2], Wei Yu[3], Xiaojing Song[2], Yanling Li[2], Taisheng Li[2], Evelyn Hsieh[4]. [1]Department of Radiology, Peking Union Medical College Hospital, Chinese Academy of Medical Sciences and Peking Union Medical College, China, [2]Department of Infectious Diseases, Peking Union Medical College Hospital, Chinese Academy of Medical Sciences, China, [3]Department of Radiology, Peking Union Medical College Hospital, Chinese Academy of Medical Sciences, China, [4]Rheumatology, Yale School of Medicine, United States

PurposeAntiretroviral therapy (ART) has been associated in several studies with low bone mineral density (BMD) in persons with HIV (PWH). However, BMD measured by dual-energy X-ray absorptiometry (DXA) only provides information about bone mineral quantity. Trabecular bone score (TBS) is a textural index that estimates bone microarchitecture from lumbar spine DXA images. Few studies have reported long-term changes in TBS in PWH.Materials and MethodsWe conducted a retrospective chart review of adult PWH receiving care at a large tertiary care center in Beijing. Patients were included in this analysis if they had a DXA scan prior to ART initiation and at least one follow-up DXA after ART initiation. We collected information regarding demographic and clinical history, HIV treatment, BMD and TBS information.ResultsA total of 459 PWH were included in this analysis (mean age: 36.1+/-11.3 years). Among 391 patients <50 years of age, 10 (2.6%) had a BMD below the expected range for age (Z score <=-2.0). Among 68 patients >=50 years, low bone density (-2.5< T score <-1) was diagnosed in 15 (22.1%) and only 1 (1.5%) had osteoporosis (T score <=-2.5). TBS of 107 patients (23.3%) and 6 patients (1.3%) were partially degraded (1.200< TBS <1.350) and degraded (TBS <=1.200), respectively. Mean percent change in lumbar spine BMD from 0 to 48 weeks (-3.0%) was larger than the percent change observed from 0 to 96, 144, and 192 weeks (-2.4%, -1.1%, and -1.3%, respectively, p<0.002). The mean percent change from 0 to 240 weeks was not statistically significant. Femoral neck BMD decreased by -3.5% from 0 to 48 weeks, and by -4.6% from 0 to 96 weeks. Thereafter the percent change from baseline remained stable (p=0.595). The percent change in total hip BMD was similar to that of femoral neck BMD at each timepoint. In terms of TBS, the largest percent change was observed from 0 to 48 weeks (-1.6%), compared with -1.1% to -1.2% change observed between week 0 and subsequent timepoints (Figure 1).ConclusionAt baseline, among PWH with normal BMD, 20%-40% of them were identified as having partially degraded or degraded TBS respectively. After three years of ART, the percent change from baseline in BMD and TBS remained stable. Lumbar spine BMD returned to baseline levels at 240 weeks, but femoral neck / total hip BMD and TBS did not recover.

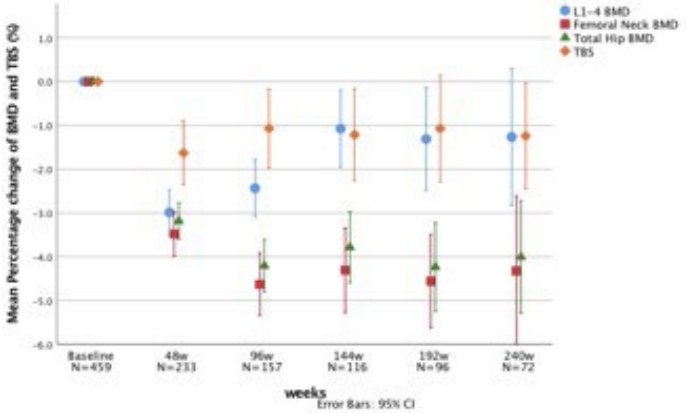

***Disclosures: Wenmin Guan**, None*

P-558

Osteoporotic Fractures in the Arab region A Systematic Review *Maya Barake[1], Rozana El Eid[2], Marlene Chakhtoura[2], Lokman Meho[3], Tala Mahmoud[4], Jessica Atieh[3], Abla Mehio SIbai[5], Sara Ajjour[2], Ghada El Hajj Fuleihan[2]. [1]Clemenceau Medical Center, Lebanon, [2]American University of Beirut Medical Center, Lebanon, [3]American University of Beirut, Lebanon, [4]University of Balamand, Lebanon, [5]American University of Beirut, Lebanon

Asia is projected to account for the largest proportion of the rising burden of osteoporotic fractures worldwide. Data from the Middle East is scarce. We performed a systematic review on the epidemiology of vertebral and hip osteoporotic fractures in 22 Arab League countries, using Scopus, Pubmed and Embase. We identified 64 relevant publications, of which 37 were in Q1 Scopus-rated journals, mostly of fair quality. Of the 17 eligible hip fracture studies, only 6 provided hip fracture incidence data. Mean age of hip fractures patients was 70-74 years, female to male ratio was 1.2-1.35. Age-standardized incidence rates, to the UN 2010 population, were 200 to 300/100,000 for women from Kuwait and Lebanon, and lower in Morocco. Risk factors included lower BMD or BMI, taller stature, intake of anxiolytics and sleeping pills. Most patients were not tested nor treated, and mortality 1-2 years post-fracture varied between 12-47%. Of the 18 Q1 papers on vertebral fractures, 14 based on 10 cohorts presented data on prevalent fractures. In women, the prevalence of morphometric vertebral fractures varied, possibly due to differences in population selection, patients' mean age or fracture detection. Excluding grade I fractures, 7.9-25.6% of women, from Lebanon and Morocco, mean age 58-74 years, had prevalent vertebral fractures; and 12-14% of men from the same countries, mean age of 62-74 years, had. Risk factors included age, gender, smoking, multiparity, years since menopause, low BMD, bone markers, high sclerostin, low IgF1, hypovitaminosis D, Abdominal Aortic Calcification (AAC) score and Vitamin D Receptor (VDR) gene polymorphisms. Vertebral fracture incidence in women from Saudi Arabia, mean age 61 years, with low baseline risk, was 6.3% at 5 years. Prospective population-based studies on incidence and prevalence, predictive models, and fracture outcomes from Arab countries are lacking. They are the key for addressing the staggering osteoporosis burden and closing the care gap of this deadly disease.

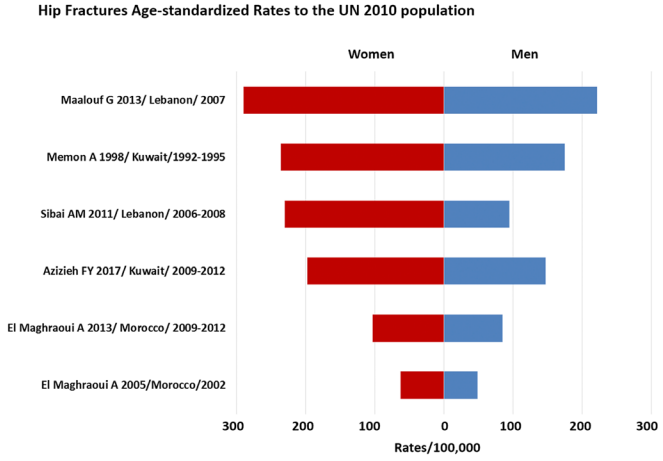

***Disclosures: Maya Barake**, None*

P-559

Associations Between Lipid Concentrations and Bone Mineral Density in a Cohort of Patients With History of Fractures. *Charilaos Chourpiliadis[1], Evangelos Karvounis[2], Harikleia Hourpiliadi[1], Dionysios Papachristou[3], Georgia Antoniou[4], Juan Jaume[5], Rodis Paparodis[5]. [1]Private Practice, Greece, [2]Department of Endocrine Surgery, EuroclinicGeneral Hospital, Greece, [3]University of Patras School of Medicine, Greece, [4]Department of Orthopaedics, Evaggelismos General Hospital, Greece, [5]Center for Diabetes and Endocrine Research, University of Toledo, United States

Purpose: Population-based studies identified an association between serum HDL concentrations and bone mineral density (BMD). We designed this study to examine all lipids association with BMD in a population with a history of fractures.Methods: We prospectively enrolled adult subjects of both genders with history of fracture(s) (anytime during their lifetime), not on lipids-altering medications, at our practice in Patras, Greece, between 2014-2018. We recorded patients' age, menopause status and tobacco use. We performed a fasting lipid panel and BMD measurements at >=2 sites, with a GE Lunar DEXA device. We split our subjects' BMD, based on the lowest T/Z-score in "Normal" (>-1.0), "low bone mass" (LBM) (-2.5) and "Osteoporosis" (OST) (<=-2.5). We classified them according to gender, smoking status, age and lipids concentrations. Ratios were compared with $\chi 2$ test; continuous variables were compared with one-way ANOVA; correlations were estimated with Spearman's rank correlation coefficient; p<0.05 was deemed significant.Results: We screened 3596 consecutive patients and enrolled 332 subjects with history of fractures; 70.5% of them had abnormal BMD (OST or LBM). Subjects with BMI>=25kg/m2 had higher mean T/Z score compared to those with BMI<25kg/m2 in men >50 years old and in all women's subgroups. HDL correlated negatively with the lowest T/Z score (r=-0.19, p=0.01) and this association remained significant independent of tobacco use (smokers: r=-0.20, non smokers: r=-0.15, p=0.03 for both). Individuals with OST had the highest mean HDL-C concentration (p=0.04) compared to LBM and Normal BMD. In subjects of age >50, the lowest T/Z score correlated positively with LDL (r=0.17, p=0.02) and triglycerides (r=0.22, p=0.002) concentrations. Triglycerides were higher in those with normal, compared to those with abnormal BMD (p=0.001). OST was more prevalent in subjects with normal compared to those with elevated triglycerides [p=0.004, OR 2.7(1.4-5.4)]. Lower triglycerides were found in individuals with recurrent fractures, compared to those with one fracture (p=0.03). LDL-C was higher in postmenopausal women with normal T/Z score compared to those with abnormal BMD (p=0.003). Total cholesterol concentration was higher in individuals >50 with history of hip fracture, compared to those with other fracture sites.Conclusions: Our analysis identified a strong association between bone mass and lipids concentrations, implying that these metabolic parameters might play a - yet not fully elucidated - role in

bone metabolism and BMD. Since the interactions between the liver, adipose and skeletal metabolism are very complex, further studies are required to address this issue.

***Disclosures: Charilaos Chourpiliadis**, None*

P-560

A Tailored Education Program Can Increase Bone Health Knowledge in Older Black Adults *Nicole Wright[1], Ventrice Shillingford-Cole[1], Ama Lee[2], Ann Wingate[3], Kathleen Cody[3]. [1]University of Alabama at Birmingham, United States, [2]BonesNBalance, United States, [3]American Bone Health, United States

Purpose: Previous studies report that osteoporosis and bone health knowledge is lower in Black and other women of color compared to White women. However, osteoporosis educational efforts have infrequently targeted populations of color, taken place in their communities, or have been led by someone from the community. Our study evaluated if a peer-educator led bone health educational program tailored for Black women increases osteoporosis knowledge. Methods: We tailored an American Bone Health community presentation for Black women to increase knowledge and awareness about bone health, osteoporosis, and fractures. The 60-minute program, "Why Healthy Bones Matter" covered the importance of the musculoskeletal system, data about bone health in the Black community, and provided four elements designed to encourage action including: understanding baseline bone health, identifying factors that increase bone loss, engaging in protective bone health activities, and becoming proactive about bone health. Participants completed a pre- and post-survey, including the Osteoporosis & You Knowledge scale, which we evaluated pre and post program. Results: To date, 16 participants with a mean (SD) age of 61.1 (13.5) years attended one virtual session. Three (19%) of the participants had a prior fracture, but only one reported having a DXA scan. When asked what the greatest obstacle was in taking care of their bones, the majority reported that they rarely thought about bone health (42.9%) or were more concerned with other health issues (42.9%). The mean (SD) pre-osteoporosis knowledge score was 7.6 (2.0) out of 10, which increased to 9.4 (0.70) post program. The greatest change pre- and post- program was observed in the "bones cannot be rebuilt once they thin from osteoporosis" question. Similar results were seen among those with pre- and post- data (n=9). All participants (100%) said that they planned to make changes in their life based on something they learned from the program.Conclusions: Despite global circumstances resulting in a virtual format, in our sample of community-dwelling Black adults, we observed increases in bone health knowledge with a tailored educational program. Given where the largest change was observed and the reports of plans to change, our program indicates an intention to act around bone health. This is the first step needed to see if increasing knowledge leads to activation and changes in behaviors regarding bone health in Black women.

***Disclosures: Nicole Wright**, Amgen, Grant/Research Support, Pfizer, Other Financial or Material Support*

P-561

A RETROSPECTIVE OBSERVATIONAL STUDY TO ESTIMATE PREVALENCE OF FRAGILITY FRACTURES IN SPANISH PRIMARY CARE (PREFRAOS STUDY): INTERIM ANALYSIS *Cristina Carbonell[1], Daniel Martínez-Laguna[2], José-Carlos Bastida[3], Milagros González[4], Rafael M Micó-Pérez[5], Francisco Vargas[6], Mónica Balcells-Oliver[7], Laura Canals[7]. [1]1 Health Center Vía Roma, Barcelona. 2 GREMPAL Investigation Group, IDIAP Jordi Gol, Spain, [2]2 GREMPAL Investigation Group, IDIAP Jordi Gol.3. Health Center Sant Martí de Provençals, Barcelona 4. CIBERFes 3, Spain, [3]5. Health Center of Marín, Pontevedra, Spain, [4]6 Health Center of Montesa, Madrid, Spain, [5]7. Health Center of Fontanars dels Alforins, EAP Ontinyent, Valencia, Spain, [6]8. Health Center Dr. Guigou, Santa Cruz de Tenerife, Spain, [7]9. Medical Department, Amgen Europe, Spain

Purpose: Some studies suggest underdiagnosis and inadequate treatment of osteoporosis (OP) among elderly patients in Spanish Primary Care (PC) settings. Recent data on the prevalence of fragility fractures in this population is lacking. The purpose of this study was to estimate the prevalence of fragility fractures among subjects >=70 years old seen in Spanish PC centers and describe the main characteristics of OP in subjects with at least one fragility facture.Methods: This is an observational, retrospective chart review in Spanish PC centers. The study is divided into two phases (A and B). Phase A comprises subjects >=70 years old listed in the participating center´s medical records from November 2018-February 2020. Phase B includes approximately 20 consecutive consented subjects per center with a recorded fragility (osteoporotic) fracture (defined as a 'low energy' trauma) and prior consultation at the center for any reason. Phase A will estimate the prevalence of fragility fractures in the PC setting and Phase B will describe the main characteristics of OP (risk factors, diagnosis and non-pharmacological /pharmacological interventions) in subjects with at least one fragility facture. We report data from an interim analysis of Phase A (data cut-off dated February 26,2020).Results: 32 PC centers across 15 Spanish Regions participated. Of 47,472 medical records reviewed in Phase A, 20.2% (9,586) subjects were >=70 years old. The majority of these eligible patients were female (5,731/9,586 [59.8%]). The prevalence of fragility fractures is summarised in Table 1.Conclusions: Prevalence of fragility fractures in subjects >=70 years old seen in Spanish PC centers is 17.1%, being higher in women (23.4% had at least one fragility fracture) and vertebral the most common fracture type. The prevalence of fragility fractures in all locations assessed was higher among women compared with men.

Table 1. Prevalence of fragility fractures in patients aged ≥70 years

	Men (N=3,855)	Women (N=5,731)	Overall (N=9,586)
Any fragility fracture, n (%)	297 (7.7)	1,340 (23.4)	1,637 (17.1)
Vertebral	92 (2.4)	374 (6.5)	466 (4.9)
Wrist/forearm	58 (1.5)	291 (5.1)	349 (3.6)
Hip/femur	71 (1.8)	275 (4.8)	346 (3.6)
Humerus	33 (0.9)	192 (3.4)	225 (2.4)

n (%), number (%) of patients with at least one fracture recorded

***Disclosures: Cristina Carbonell**, AMGEN Europe, Consultant*

P-562

Pelvic Ring Fragility Fractures: A Debilitationg Fracture Occurring in Elderly Ambulatory Patients with Monoclonal Gammopathy of Uncertain Significance, Pernicious Anemia, Hyponatremia, and Associated with High Mortality *Michael Lovy[1]. [1]Desert Oasis Healthcare, United States

PURPOSE: To study the clinical characteristics and course of a cohort of patients presenting with pelvic ring fragility fractures(PFF).METHODS: A retrospective chart review of 43 patients with PFF seen over a 4 year period in a community based outpatient fracture clinic was conducted. A complete history and physical, review of medical records and x-rays, CBC, chemistry profile, TSH, urinalysis, vitamin B12, 25-OH vitamin D, PTH, and immunofixation(IMF) was done in all patients. Antiparietal cell(APA) and intrinsic factor(IF) antibody and SPE was done in select cases. Comorbidity including history of solid tumor, diabetes, COPD, cardiac and neurologic disorder were tabulated.RESULTS: There were 38 females and 5 males ranging in age 55-95 years(mean 82.3). 23 patients had a previous major osteoporotic fracture and 8 a total hip replacement. 17 had received previous osteoporosis treatment. 40 patients were living at home and 22 were still driving within 3 months prior to the fall causing the PFF. 13 were using ambulatory aids. Patients had 0-3(mean 0.93) comorbid conditions: COPD-11, cardiac-11, cancer-7, neurologic-6, and diabetes-5. 2 patients had previous radiation therapy to the pelvic area. The BMI was 20< in 9 patients and 19 had peripheral neuropathy(PN). CT or MRI confirmed the PFF in 37 patients and showed fractures of the sacrum-17, acetabulum-7, and both sacrum and acetabulum-5 in addition to the pelvic rami. Monoclonal protein was found with IMF in 17(42%) patients: IgG-7, IgG-6, and light chains-4. M-spike was found in 8. 5(14%) patients had low vitamin B12 and either APA or IF. 3 patients had vitamin D levels 20<ng/ml and 7 had hyponatremia. Alkaline phosphatase was elevated in 12 patients. 29 patients required rehabilitation in a nursing home. During follow up (mean 20.7 months) 12(31%) patients died,10 within 1 year after PFF from causes unrelated to the fracture.CONCLUSIONS: PFF occurs predominantly in female, elderly, independent and active patients with few comorbid conditions and is associated with significant morbidity. PFF may be a prelude to mortality within 1 year of occurrence. CT or MRI scans are necessary to define the full extent of injury to the pelvis. Although the clinical characteristics may differ between PFF, hip, and vertebral fracture patients, they all share age related conditions such as low BMI, PN, MGUS, pernicious anemia and hyponatremia that predispose to falling and bone fragility.

***Disclosures: Michael Lovy**, None*

P-563

VERTEBRAL FRACTURES IN LIVING DONOR LIVER TRANSPLANT: STUDY FROM A TERTIARY CARE CENTRE IN INDIA *Shalin Shah[1], Beena Bansal[1], Sunil Kumar Mishra[1], Mohammad Shafi Kucchay[1], A S Soin[1], Jai Prakash Sharma[1], Ambrish Mithal[1]. [1]Medanta The Medicity, India

Objective:To determine the prevalence of radiological vertebral fractures in living donor liver transplant recipients. Methods:84 consecutive patients visiting the liver transplant clinic from December 2017 to October 2018, aged >18 years, were included in the study. These patients had undergone liver transplant between 2010 to 2017. Vertebral fractures were assessed semi-quantitatively from lateral spine X-rays using Genant scoring. Results:The mean age of the patients was 50.7+/-10.1 years with 76 males and 8 females. The median duration from liver transplantation was 5 months (range 1.4-96.1 months). Vertebral fractures were recorded in 39/84 (46.4%) patients, out of which only one was symptomatic. Thoracic fracture was seen in 22 (26.2%) patients (Grade 1- 14.3 %, Grade 2- 8.3%, Grade 3- 3.6 %) and lumbar fractures in 24 (28.6%) patients (Grade 1- 22.6%, Grade 2- 4.8%,

Posters

Grade 3- 1.2%). There was a significant difference in the age of the patients with and without fracture, with fracture rates being highest in patients aged more than 60 years. There was no significant difference in the prevalence of fracture in patients with history of diabetes, smoking, alcohol, previous history of vertebral or upper limb fractures or those receiving calcium and vitamin D supplementation. Serum levels of calcium (9.73 vs 9.69 mg/dl), phosphorus (3.54 vs 3.57 mg/dl), PTH (50.8 vs 58.5 pg/ml) and 25 (OH) D (21.2 vs 20.4 ng/ml) were not different between the two groups. We looked at the relationship of vertebral fractures with the etiology of chronic liver disease (CLD). Vertebral fractures were found in 8/10 patients with NAFLD (Non Alcoholic Fatty Liver Disease), 8/14 patients with hepatitis B associated CLD, 15/30 patients with alcoholic liver disease, 2/6 patients with autoimmune CLD, 3/11 patients with cryptogenic CLD, and 1/6 patients with HCV CLD. No fractures were found in patients with Wilson's disease (0/4) and Budd-Chiari syndrome (0/3).Vertebral fractures were more prevalent in patients who had undergone transplant in the previous one year. Conclusions:Asymptomatic vertebral fractures are a common occurrence in living donor liver transplant recipients in India. Liver transplant recipients should be evaluated for vertebral fractures prior and within one year after transplantation. Strategies to optimize bone mass prior to transplant and prevention of further bone loss in the early post-transplant period need to be implemented uniformly.

***Disclosures: Shalin Shah**, None*

P-564

Changes in Bone Mineral Density and Trabecular Bone Score in Chinese HIV-Infected Individuals One Year after Initiation of Antiretroviral Therapy *Wenmin Guan[1], Wei Pan[2], Wei Yu[3], Xiaojing Song[2], Yanling Li[2], Taisheng Li[2], Evelyn Hsieh[4]. [1]Department of Radiology, Peking Union Medical College Hospital, Chinese Academy of Medical Sciences & Peking Union Medical College, China, [2]Department of Infectious Diseases, Peking Union Medical College Hospital, Chinese Academy of Medical Sciences, China, [3]Department of Radiology, Peking Union Medical College Hospital, Chinese Academy of Medical Sciences, China, [4]Rheumatology, Yale School of Medicine, United States

PurposeHIV infection and antiretroviral therapy (ART) have been associated with reduced bone mineral density (BMD) in persons with HIV (PWH). BMD measured by dual-energy X-ray absorptiometry (DXA) provides information only about bone mineral quantity but not bone microarchitecture. Trabecular bone score (TBS) is a noninvasive tool that estimates bone microarchitecture from lumbar spine DXA images. No prior studies have measured changes in TBS among Chinese PWH.MethodsWe conducted a retrospective chart review of adult Chinese PWH seen at a large tertiary care hospital. Patients with a DXA scan prior to ART initiation, and again 48 weeks later were included. Information regarding demographic and clinical history, HIV treatment history, BMD and TBS were collected. We analyzed differences in BMD and TBS over 48 weeks in the overall group, and by exposure to three types of antiviral drugs [tenofovir disoproxil fumarate (TDF), lopinavir/ritonavir (LPV/r) and efavirenz (EFV)]. Associations between key risk factors and changes in BMD and TBS were analyzed using linear regression.ResultsOur study included 233 PWH (mean age = 36.6+/-11.1 years). Patients treated with regimens containing TDF (Figure 1) or LPV/r showed greater percent decreases in BMD than those on regimens without those agents. The differences in TBS were not significant in any of the groups. Higher baseline HIV viral load and TDF exposure were associated with larger decreases in BMD at each site. The use of LPV/r was only associated with decreased total hip BMD [β (95% CI): -0.213 (-0.373, -0.053), p=0.009]. Lower BMI [0.250 (0.008, 0.492), p=0.043] and higher baseline CD4+ cell count [-0.005 (-0.010, 0.000), p=0.032] were associated with larger decreases in TBS. No associations were found between TBS changes and specific antiretroviral exposure.ConclusionBoth BMD at each site and TBS decreased one year after ART initiation. Although BMD decreases were observed in patients treated with TDF- and PI-containing regimens, change in TBS was not statistically significant. Lower BMI and higher baseline CD4+ cell count were associated with greater declines in TBS.

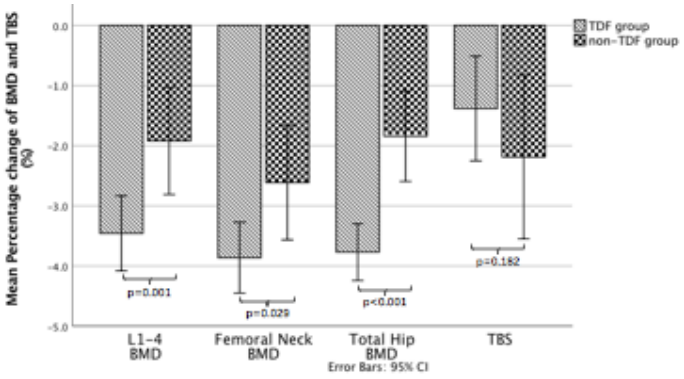

***Disclosures: Wenmin Guan**, None*

P-565

Dentists'knowledge about osteoporosis and the ability to identify the disease *Renato Ferreira[1], Suely Roizenblatt[1], Vera Szejnfeld[1]. [1]UNIFESP/Escola Paulista de Medicina, Brazil

Objective: to evalute the knowledge of general dentists about osteoporosis and verify their ability to identify these patients by applying mandibular cortical width (MCW) and mandibular cortical index (MCI) on panoramic dental radiographs using a simple visual method. Methods: A questionnaire regarding the diagnosis and prevention of osteoporosis was administered via e-mail to 20773 dentists. These proofessionals indication was obtained from the database provided by the Regional Council of Dentistry of the State of Sao Paulo. The dentists who completed the questionnnaire were selected and, after receiving mandibular radiomorphometric training via internet, analysed MCI and MCW of 114 panoramic radiographs of postmenopausal women who were submitted to both panoramic radiograph and bone densitometry of the spine and femur. Based on radiomorphometric indices, and without knowledge of densitometry results, the dentists decided if they would or not indicate bone density for these patients. Results: Overall, 485 dentists completed the questionnaire, and 50 evaluated panoramic radiographs using MCW and MCI. Although all of them answered that they had some knowledge about osteoporosis, 41.6% responded that osteoporosis is "lack of calcium in bones", demonstrating the misleading concept of the disease. About 90%reported minimal or no access to this information during graduation and only 27% had adequate exposure to the theme during postgraduate training. About 70.7% expressed the desire to learn more about osteoporosis prevention and 99% expressed interest in learning how to apply the radiomorphometric indices on panoramic radiographs. The application of the MCW and MCI indices by dentists resulted in 52.9% sensitivity and 64% specificity for the detection of low mineral density. Conclusions: Dentists have insufficient knowledge about osteoporosis and their ability to detect osteopenia or osteoporosis, by applying radiomorphometric indices, is lower than described in the literature.

***Disclosures: Renato Ferreira**, None*

P-566

The study of risk factors for fractures in sports veterans *Elena Tenyaeva[1], Elena Turova[2], Golovach Albina[2], Irina Articulova[2]. [1]Turova E.A., Golovach A.V., Articulova I.N., Russian Federation, [2]membership, Russian Federation

The purpose of the study was to research the metabolic parameters of bone metabolism in sports veterans depending on the type of physical activity and their relationship with the probability of developing osteoporotic fractures.Metabolic parameters of bone metabolism were studied in 50 sports veterans aged 51 to 82 years, the average age of athletes was 67 years. Athletes previously engaged in such sports as swimming, cross-country skiing, cycling, jumping, light and heavy athletics, football, hockey, speed skating, figure skating, and martial arts. Of the examined sports veterans, 9 people (in 18% of cases) had fractures of the radius, hip neck or spine.Statistical analysis showed a significant negative correlation of vitamin D level with age (r= -0.25, p<0,05), parathyroid hormone level (r= -0.23,p<0,05), probability of fracture development (r= -022,p<0,05) and positive with body mass index (r=0.32, p<0,05), osteocalcin level (r=0.16,p<0,05) and testosterone (r=0.22, p<0,05). The probability of developing fractures did not depend on the level of osteocalcin and b-cross-laps.There was a negative correlation of testosterone levels, regardless of the gender of athletes, with the probability of developing fractures (K= -0.27,p<0,05) and also a negative correlation of insulin levels with the probability of developing fractures (r= -0.23, p<0,05). When analyzing sports depending on the Olympic classification, it was found that sports veterans who were engaged in cyclical and speed-power sports had lower levels of testosterone, vitamin D and osteocalcin than athletes who were previously engaged in martial arts and weightlifting (p<0,05), which is probably due to high levels of bone and muscle mass under these sports loads.Thus, it was found that sports veterans who previously engaged in martial arts or weightlifting, the probability of osteoporotic fractures is lower than in cyclic, game and speed-power sports, due to higher levels of vitamin D, testosterone and higher muscle mass

***Disclosures: Elena Tenyaeva**, None*

P-567

The Silent Wreck – Prevalence and risk factors of Atraumatic Osteoporotic Vertebral Compression Fractures *Saikrishna Gadde[1], Sudhir Ganesan[1], Ajay Gowtham[1], Shriraam Mahadevan[1], Adlyne Reena Asirvatham[1], Vignesh Jeyabalan[1], Karthik Kailash Kannan[1]. [1]Sri Ramachandra Medical College and Research Institute, India

Background: Osteoporosis emerged to be a major contributor for the rise in morbidity among elderly population along with other chronic medical diseases. It is a skeletal disorder characterised by compromised bone strength, predisposing a person to an increased risk of fragile fractures. The presentation of a vertebral compression fracture may vary from being asymptomatic to complete paraplegia and disability. These fragile vertebral compression fractures are not always caused due to trauma, shifting the focus over to the concept of skeletal endocrinology.Purpose: The main purpose of this study is to find the prevalance and risk factors associated with atraumatic vertebral compression fractures of thoracolumbar spine in an emerging country where the socioeconomic conditions do not encourage aggressive

screening.Methodology: This is a cross sectional study conducted on 700 individuals aged above 50 years at Sri Ramachandra Medical Centre, Chennai from 2017-2019 and their plain radiographs of the thoracolumbar spine were assessed. Reduction in the vertebral height of more than 25% was considered as a fracture. Patients with history of previous spinal surgery and deformities were excluded. Questionnaire containing information regarding age, gender, height, weight, Body Mass Index, comorbid conditions, chronic drug usage, vision problems, previous and family history of fragile fractures were filled by them. Data was assessed using FRAX scoring system and statistical analysis was done. Bone Mineral Density was not calculated.Results: 19% of the subjects had vertebral compression fractures and 9.4% of the study population had atraumatic vertebral compression fractures. 45.28% of the subjects are at increased risk of hip fractures and 19.98% are at increased risk of major osteoporotic fractures.Conclusion: Old age, female gender, history of fragile fracture are major risk factors contributing to sustain a new fracture. There need not always be a history of trauma for fractures to occur. These risk factors identification may target prevention of these fractures, early diagnosis and intervention in order to reduce the disability, morbidity and mortality due to osteoporotic atraumatic vertebral compression fractures.Keywords: Osteoporosis, Atraumatic Vertebral Compression fractures, FRAX scoring system

***Disclosures: Saikrishna Gadde**, None*

P-568

Estimation of Bone Fracture Risk Using FRAX Model in Two Regions of Jalisco (México) *Jose Francisco Torres-Naranjo[1], Edgar Saul Tejeda Chavez[7], Martha Yadira Perez Avalos[0], Roberto Gabriel González-Mendoza[4], Hugo Gutiérrez-Hermosillo[5], Claudia Martinez-Cordero[6], Juan Ricardo López-Taylor[4], Ricardo Garcia Gaeta[0]. [1]Centro de Investigación Ósea y de la Composición Corporal, CIO, Mexico, [7]Servicios de Salud Jalisco, Centro Universitario del Norte de la Universidad de Guadalajara, Mexico, [0] Centro Universitario del Norte de la Universidad de Guadalajara Profesor de Tiempo Completo del Centro Universitario del Norte de la Universidad de Guadalajara, Mexico, [4]Institute of Applied Sciences for Physical Activity and Sport, Department of Human Movement Sciences, Education, Sport,Recreation and Dance, University Health Sciences Center, University of Guadalajara, Mexico, [5]Hospital Aranda de la Parra, Mexico, [6]HRAEB Hospital Regional de Alta Especialidad del Bajio, Mexico, [0]Departamento de Medicina Preventiva de los Servicios de Salud Jalisco, Mexico

Purpose: To estimate the absolute risk of major osteoporotic and hip fractures in an urban and rural population of some Jalisco regions using Mexico-specific FRAX® model.Material and methods: Representative samples of the population without social security from an urban and a rural community included 693= Mexican residents (505 women and 188 men) aged 50-80 years (mean age 70.84 +/- 7.92 years). The absolute risk of fractures was calculated without BMD using the batch processing of data. High fracture risk fracture was fixed to a probability of 20% a 3% for MOF and HF, respectively. Results: The average absolute risk of major osteoporotic fractures (MOF) was 12.81% (14.78% in women and 7.52% in men, p=0,0001), hip fractures (HF) 5.36% (6.12% in women and 3.31% in men, p=0.0001). The absolute risk of MOF and HF increased with age both in men and women. In women, the absolute risk of MOF and HF was higher in all age groups across than in men. There were significant differences in the absolute risk of fracture between urban and rural populations. MOF 10.54% and 20.70%; HF 3.97% and 10.17%, in urban and rural populations, respectively, p=0.0001). The proportion of individuals who reported a previous fragility fracture was 13.56%, and only 57% of them were classified as high-risk of fracture using the prespecified cut off points. Conclusion: The absolute risk of MOF and HF increased with age and were significantly higher among the female population. Differences were observed between urban and rural scenarios. Only a proportion of participants with previous fragility fractures were classified as high fracture risk of fracture, according to FRAX, which may imply a low sensibility for those patients.

***Disclosures: Jose Francisco Torres-Naranjo**, None*

P-569

Prevalence of Osteoporosis in Armenia and Relationship to Vitamin D Level *Nicholas Hutchings[1], Varta Babalyan[4], Annemieke Heijboer[3], Sisak Baghdasaryan[4], Mushegh Qefoyan[4], Mariëtte T Ackermans[3], Arus Ivanyan[5], Anna Formenti[6], Andrea Giustina[6], John P Bilezikian[7]. [1]University of California, Irvine, United States, [4]Osteoporosis Center of Armenia, Armenia, [3]Vrije Universiteit Medisch Centrum, Netherlands, [4]Osteoporosis Center of Armenia, United States, [5]Yerevan State Medical University, Armenia, [6]Università Vita-Salute San Raffaele, Italy, [7]Columbia University, United States

Osteoporosis is a leading cause of morbidity among older women. The prevalence and thus the burden of the disease in Armenia is unknown. In addition, the relationship between vitamin D level, as measured by 25-hydroxyvitamin D (25-OH D), and bone mineral density (BMD) remains a matter of discussion. This study sought to identify the prevalence of osteoporosis and characterize the relationship between 25-OH D and T-score in post-menopausal community dwelling adults in Armenia. As part of a larger study investigating vitamin D insufficiency in the country, 265 participants underwent BMD testing, from a roughly geographically proportional distribution. BMD was evaluated by DXA of the lumbar spine, femoral neck, total hip, and forearm. Osteoporosis, as determined by a T-score < -2.5, in at least one of the anatomical regions evaluated, was detected in 46% of participants. Osteopenic values were detected in 31%. Only 23% had normal T-scores throughout. The mean 25-OH D levels of osteoporotic and osteopenic individuals were not significantly different from those without abnormal BMD. However, we noted a trend towards lower 25-OH D in association with lower T-scores: participants in the lowest tertile of 25-OH D had lower mean T-scores in all regions than the other tertiles. We conclude that osteoporosis and osteopenia are prevalent in Armenia, and, given its high morbidity, addressing this disease should remain a high priority for clinicians and public health programs. The extent to which vitamin D deficiency is playing a role, given its high prevalence in the population, remains to be elucidated.

***Disclosures: Nicholas Hutchings**, None*

P-570

Low Awareness of and Knowledge About Osteoporosis Among Women in Armenia *Nicholas Hutchings[1], Varta Babalyan[2], Sisak Baghdasaryan[2], Mushegh Qefoyan[2], Arus Ivanyan[3], Annemieke Heijboer[4], Mariëtte T Ackermans[4], Anna Formenti[5], Andrea Giustina[5], John P Bilezikian[6]. [1]University of California, Irvine, United States, [2]Osteoporosis Center of Armenia, Armenia, [3]Yerevan State Medical University, Armenia, [4]Vrije Universiteit Medisch Centrum, Netherlands, [5]Università Vita-Salute San Raffaele, Italy, [6]Columbia University, United States

Assessing current knowledge of osteoporosis and understanding of the disease among the population is necessary in order to design programs to increase awareness. Such programs to disseminate knowledge are the first steps towards implementing proactive measures to prevent the disease. To that end, we conducted an assessment of knowledge and attitudes towards osteoporosis among post-menopausal women in Armenia. As part of a larger study investigating vitamin D in the country, 591 postmenopausal women (mean age 63) completed questionnaires about osteoporosis, a subset not different from the larger population. A majority of the participants had heard little about osteoporosis. In addition, the majority could not identify characteristics of or risk factors for the disease. Overall, participants from Armenia scored markedly worse than participants of a 2006 survey of women in North America and Europe. The results of this survey reveal a substantial knowledge gap among those most at risk for developing osteoporosis. This information should serve as an impetus for country-wide programs to be established among clinicians and public health officials to raise awareness of the disease and improve community-wide preventive measures.

***Disclosures: Nicholas Hutchings**, None*

P-571

The Fragility Hip Fracture: Not only a Marked Burden of Disease, but also a Significant Predictor of Subsequent Hip Fracture Risk *Emil Schemitsch[1], Jonathan D. Adachi[2], Jacques P. Brown[3], Jean-Eric Tarride[4], Natasha Burke[5], Thiago Oliveira[5], Lubomira Slatkovska[5]. [1]Division of Orthopaedics, Department of Surgery, Western University, Canada, [2]St Joseph's Healthcare, McMaster University, Canada, [3]CHU de Québec Research Centre, Laval University, Canada, [4]Department of Health Research Methods, Evidence and Impact, McMaster University, Canada, [5]Amgen Canada Inc., Canada

Purpose: Hip fracture is one of the most common and burdensome fragility fractures caused by osteoporosis. We describe the contribution of hip fractures to fragility fracture burden in older adults in Ontario, Canada.Method: This retrospective observational study used de-identified health services data generated from the publicly funded healthcare system in Ontario, Canada. The cohort included men and women aged >65 years with an index fragility fracture between January 1, 2011 and March 31, 2015, identified using ICD-10 codes from hospital admissions, emergency and ambulatory care. Patients were followed to a cutoff date of March 31, 2017. Results: The cohort consisted of 115,776 patients with an index fragility fracture. The median age (interquartile range) was 81 (74–87) years and 72.3% were female. Hip fracture was the most common index fracture (27.3%, n=31,613), and 32.4% (n=10,254) of index hip fractures occurred in patients <=80 years of age. Proportion of index fractures that were hip fractures by age was: ages 66-70, 12.1% (n=2,179); ages 71-75, 17.3% (n=3,092); ages 76-80, 24.2% (n=4,983); ages 81-86, 31.2% (n=7,524); and ages 86+, 39.3% (n=13,835). Hip fracture was also the most common second fracture (27.8%, n=5,745). It occurred as the second fracture in >=19% of cases for all index fracture sites examined; occurring most often after hip (33.0%) or pelvic (32.3%) index fractures, and least often after tibia/fibula/knee (23.3%) or radius/ulna (19.4%) index fractures. Among patients requiring surgery related to their index fracture (n=44,949) and those experiencing complications 30 days post-surgery (n=8,868), respectively, 64.1% and 71.9% had a hip fracture. One-year mortality (due to any cause) was 26.2% after hip index fracture and 15.9% in the entire cohort; hip fracture had the highest mortality rate of all index fracture sites examined, followed by femur (21.9%). Total mean (+/- standard deviation) healthcare cost per patient (in 2017 Canadian dollars) in the first year after index fracture was the second highest for hip index fracture ($62,793 +/- 44,438), after femur index fracture ($65,490 +/- 54,116). Conclusion: These data highlight the significant morbidity, mortality and financial burden of hip fragility fractures in adults aged >65 and the urgent need to initiate secondary fracture

prevention measures after a fragility fracture occurring at any site to help reduce subsequent hip fracture and associated burden.

***Disclosures: Emil Schemitsch**, Amgen; Biocomposites; Smith & Nephew, Grant/ Research Support, Acumed, LLC; Amgen; Implants for Trauma Surgery; Pentopharm; Sanofi-Aventis; Smith & Nephew; Stryker; Swemac, Consultant, DePuy; Saunders/Mosby-Elsevier; Smith & Nephew; Springer; Stryker; Zimmer, Other Financial or Material Support*

P-572

Associations Between Health Service Use and Quality of Life 12-Months Following a Non-Hip Osteoporotic Fracture: Analyses of the International Costs and Utilities Related to Osteoporotic Fractures Study (ICUROS) *Jason Talevski[1], Kerrie Sanders[1], Ljoudmila Busija[2], Alison Beauchamp[2], Catherine Connaughton[1], Gustavo Duque[3], Karen Lim[4], Fredrik Borgström[5], John Kanis[6], Axel Svedbom[7], Amanda Stuart[8], Sharon Brennan-Olsen[8]. [1]The University of Melbourne, Australia, [2]Monash University, Australia, [3]Australian Institute for Musculoskeletal Science (AIMSS), Australia, [4]Australian Catholic University, Australia, [5]Quantify Research, Sweden, [6]University of Sheffield, United Kingdom, [7]ICON Plc, Sweden, [8]Deakin University, Australia

Objectives: While it is well-documented that hip fractures are the most severe type of fracture, imposing the greatest burden on health-related quality of life (HRQoL) and physical disability, fractures at other osteoporotic sites – vertebrae, wrist and humerus – are also associated with a significant burden on patients and the healthcare system. There is limited knowledge of which types of health services are associated with improved HRQoL in older adults after a non-hip major osteoporotic fracture (MOF). This study aimed to identify specific combinations of health service use that facilitate the recovery of HRQoL 12-months following non-hip MOF.Methods: The analyses included 2,469 adults aged >=50 years with a non-hip MOF participating in the International Costs and Utilities Related to Osteoporotic Fractures Study (ICUROS) – a multinational observational study (Australia, Austria, France, Italy, Lithuania, Mexico, Russia, Spain, UK). HRQoL at pre-fracture and 12-months post-fracture was measured using the EQ-5D-3L survey. Health service use data was collected by patient interviews and medical record reviews including in-hospital care; outpatient care; community services and medication use. The data analyses involved two stages: 1) latent class analyses to identify different combinations of health service use ("classes"); and 2) logistic regression to assess effects of classes on HRQoL recovery (adjusted and unadjusted analyses).Results: Overall, 1,439 participants (58.3%) recovered to their pre-fracture HRQoL at 12-month follow-up. The number of classes ranged from two to five across countries. We identified several distinct, country-specific classes that were associated with improved HRQoL recovery across individual countries. Across all countries, increased odds of HRQoL recovery at 12-months was commonly characterized by a combination of emergency department presentations without hospitalization; outpatient department visits; general practitioner or primary care centre visits; allied health visits (e.g. physiotherapy, occupational therapy); vitamin D/calcium supplementation; and/or non-opioid analgesic use.Conclusion: Understanding country-specific health services that are associated with greater recovery of HRQoL, and that are not routinely accessed in other countries, could improve post-fracture care on a global scale. Future research should focus on determining the cost-utility of these care pathways.

***Disclosures: Jason Talevski**, None*

P-573

A prospective cohort study of patient characteristics, bone health measures and clinical outcomes following low trauma wrist fracture *Maire Rafferty[1], James Bernard Walsh[2], Kevin McCarroll[1]. [1]St James Hospital, Ireland, [2]Sj James Hospital, Ireland

IntroductionPatients with lower BMD are at increased risk of fragility fracture. We aimed to explore characteristics of patients with wrist fractures and to identify whether bone health parameters might also influence patient reported outcome measures (PROMs). MethodsPatients aged > 50 years who had a new x-ray diagnosis of a low trauma wrist fracture were recruited into our study between January and October 2018. Assessments were performed within 12 weeks and at 6 and 12 months. Data were collected regarding patient characteristics and results of DXA, Clinical Frailty Scale (CFS) and PROMs including the Short Form 12, Patient Rated Wrist Evaluation (PRWE) and Disabilities of the Arm, Shoulder and Hand (DASH). Statistical analysis was performed using SPSS v26.Results133 patients attended for initial assessment and 113 had at least one follow up visit. 91.9% were female and median age was 69.0. The majority (68.9%) were not frail (CFS <4) and were on <5 medications (59.7%). The biggest risk factor for fracture was a history of previous fracture (45.9%) followed by premature menopause (39.3%) (<45 yrs), low dietary calcium (39.3%), a family history of osteoporosis (29.6%), recurrent falls (23.0%) and smoking (17.8%). 41% had osteoporosis using DXA criteria. Better outcomes in PCS12 (p=0.046), PRWE (p<0.001) and DASH (P=0.001) were identified within the first 12 weeks. There were continued improvements in PCS-12 (P<0.001), MCS-12 (P<0.001), PRWE (P<0.001) and DASH (P<0.001) over 12 months. We also found that lower BMD at the spine was associated with poorer scores on the PRWE (p=0.006) and DASH (p=0.018) at 6 months, which remained at 12 months for PRWE (p= 0.043) and also present for MCS12 (p=0.02). Similarly there were associations at 12 months between neck of femur BMD and PRWE (p=0.008) and DASH (p=0.018).Other factors shown to negatively impact outcomes included dominant hand fracture (all measures) and gender (DASH) though there was no affect of age on disability or function (DASH or PRWE).ConclusionsThis study shows an association between lower BMD and poorer patient reported outcomes following wrist fractures. This is to our knowledge the first time this finding has been reported though associations have been found between BMD and radiographic features of severity and other clinical outcomes. Age did not affect disability or function suggesting that other factors independent of age such as frailty are more important.

***Disclosures: Maire Rafferty**, None*

P-574

Joining Forces for Bone Health: Lessons from a Bone Health Campaign with Susan G. Komen *Kathleen Cody[1], Lisa Qualls[2]. [1]kathleen@americanbonehealth.org, United States, [2]American Bone Health, United States

Objective:To extend the reach of bone health messages beyond a traditional audience by collaborating with a larger advocacy organization in a mutually beneficial education and awareness campaign.Methods and Materials:The campaign was designed to 1) determine the extent of participants' bone health knowledge, and 2) empower walkers with information to develop a personal bone health plan as measured by post-event surveys and focus groups. American Bone Health provided content, tools and resources for use by Susan G. Komen, the world's leading breast cancer charity, at its 3-Day walks and races. The material was used to educate and empower participants to take steps to protect their bone health, particularly during and after treatment for breast cancer. This educational campaign included:- A digital phase of emails, blog posts and online articles about a variety of bone health topics.- An onsite phase with learning experiences. The races included a personal bone health quiz and the American Bone Health Fracture Risk Calculator, and the 3-Day walks also had an interactive game.Results:Total Reach: >58,000 digital; 17,050 onsiteTotal Activations:Digital: 292• Those 292 users account for 532 sessions on the landing pages.• The average duration of sessions was 434% longer than the average session on American Bone Health webpages during the same time.• The largest traffic spike corresponds with the blog post and email around the topic of exercise and bone health.Onsite: 1,157• 798 people (age 45+) used the American Bone Health Fracture Risk Calculator to learn their risk in the next 10 years: with 39% being at moderate or high risk.• 359 (people under 45) people took Bone Health Quiz. Conclusion:Collaborating with a larger advocacy organization can amplify bone health messages and provide bone health awareness to an audience not traditionally reached.

***Disclosures: Kathleen Cody**, None*

P-575

Stronger Together: The Asia Pacific Fragility Fracture Alliance (APFFA) *Yoonah Choi[1], Angie Roddick[2], Kirsten Bruce[3], Ding-Cheng (Derrick) Chan[4], Jacqueline Close[5], Joon Kiong Lee[6], Paul Mitchell[7], Robert D Blank[8]. [1]Evidencia Medical Communications Pty Ltd, Australia, [2]APFFA Secretariat, New Zealand, [3]Viva! Communications Pty, Australia, [4]National Taiwan University Hospital ChuTung Branch, Taiwan, Province of China, [5]Prince of Wales Hospital, University of New South Wales, Australia, [6]Beacon Hospital, Petaling Jaya, Malaysia, [7]Synthesis Medical NZ Ltd, New Zealand, [8]Garvan Institute of Medical Research, Australia

The Asia Pacific Fragility Fracture Alliance (APFFA) is a collaborative forum for Asia Pacific regional organisations and global organisations that focus on osteoporosis and fractures. APFFA was launched in November 2018 and comprises the following member organisations: Asian Federation of Osteoporosis Societies, Asia-Oceanian Society of Physical and Rehabilitation Medicine, Asia Pacific Geriatric Medicine Network, Asia Pacific Orthopaedic Association, Fragility Fracture Network, International Osteoporosis Foundation and International Society for Clinical Densitometry.The primary purpose of APFFA is to drive policy change, improve awareness and change political and professional mindsets to facilitate optimal fragility fracture management across the Asia Pacific region. Aligned with the Global Call to Action, the clinical focus of APFFA is to improve acute care for people in the Asia Pacific region who sustain fragility fractures, and optimise subsequent rehabilitation and secondary fracture prevention.To actualize the mission and vision of APFFA, three working groups have been established and a strategic plan has been developed, which includes a detailed communications plan.The Hip Fracture Registry Working Group aims to:provide practical tools and resources that outline key steps in setting-up and rolling-out national hip fracture registries in each countryraise awareness of the problems relating outcomes of hip fracture across the regionadvocate for national professional organizations to collaborate to establish national quality improvement initiatives, and lobby governments for policy change and fundingThe Education Working Group aims to:identify a range of educational resources from member organisations that will be shared through an Education Directorycreate new resources to fill the gaps for key stakeholder groupsdevelop an approach to distribute the educational content, including use of conference presentationscustomise educational content to address differing concerns of distinct segments of our audienceThe Evidence Generation Working Group aims to:identify evidence gaps relating to the vision and mission of APFFAdesign research collaborations with partners to use real-world data share the new understanding through publication and other knowledge-sharing activitiesidentify and promote

any findings that would be considered practice-changing to improve patient outcomesFurther information at: https://apfracturealliance.org

***Disclosures: Yoonah Choi**, Amgen, Other Financial or Material Support*

P-576

Calcifediol Soft Gelatin Capsules Have a Superior Efficacy and a More Rapid Response than Cholecalciferol for the Management of Vitamin D Deficiency in Postmenopausal Women: Calcifediol Must be Considered in Therapeutic Guidelines *Jose Luis Pérez-Castrillón[1], Antonio Dueñas-Laita[2], Carlos Gómez-Alonso[3], Gonzalo Hernández-Herrero[4], Nieves Fernández-Hernando[4], Sandra Pamela Chinchilla[4]. [1]Hospital Universitario Río Hortega, Internal Medicine Department, Spain, [2]Hospital Universitario Río Hortega, Clinical Toxicology Unit, Spain, [3]Hospital Universitario Central de Asturias, Bone Mineral Metabolism Department, Spain, [4]Faes Farma, R&D and Innovation Department, Spain

BackgroundVitamin D deficiency has a high prevalence worldwide, with relevance in specific diseases and stages of life. Few guidelines assess the optimal dosing in the general population however, levels above 20 ng/mL are necessary to obtain benefits on bone metabolism.ObjectiveTo assess the efficacy of calcifediol in the treatment of vitamin D deficiency, compared with therapeutic guidelines recommendations for cholecalciferol in postmenopausal women.MethodsPhase III-IV, double blind, randomised, controlled, multicentre superiority clinical trial. Postmenopausal women with baseline levels of 25(OH)D < 20 ng/mL were randomised to three arms: 266 mcg of calcifediol/month for 4 or 12 months (approved SmPC and test regimes), or to cholecalciferol 25000 IU/month for 12 months (as per therapeutic guidelines).Main analysis performed upon completion of 4 months of treatment are presented and reported without unblinding study treatments (interim analysis).The trial has been approved by ethics committees and national competent authorities.Results298 women were included in the ITT analysis. The average age was 63.4 +/- 8.2 years, mean BMI 29.3 +/- 6 kg/m2 and received treatment, 25% of the population had 25(OH)D levels <10ng/mL. All demographic characteristics and risk factors for osteoporosis were balanced amongst groups.13.5% and 35% of women in the calcifediol group reached values of 25(OH)D > 30ng/mL at 1 and 4 months, respectively, compared to 0% and 8.2% in the cholecalciferol group (p<.0001). Calcifediol achieved target levels more rapidly (Figure 1, highlights 20ng/mL which is a widely accepted minimum therapeutic level). Mean increase in 25(OH)D levels in calcifediol v. cholecalciferol arms were 9.7 ng/mL v. 5.1 ng/mL; p<.0001 (month 1) and 14.9 ng/mL v. 9.9 ng/mL; p<.0001(month 4).No relevant safety issues were reported for the present analysis.ConclusionsCalcifediol shows a greater efficacy and a more rapid effect than cholecalciferol regime (as recommended in therapeutic guidelines), for the treatment of vitamin D deficiency in postmenopausal women, which could impact osteoporosis treatment. Cholecalciferol fails to achieve 25(OH)D recommended levels in a significant proportion of this population.AcknowledgementsPrincipal investigators and their teams: F Cereto, ML Brandi, E Jodar, J del Pino-Montes, JM Quesada-Gómez, JM Olmos-Martínez, MA Colmenero-Camacho, R Alhambra, B Galarraga

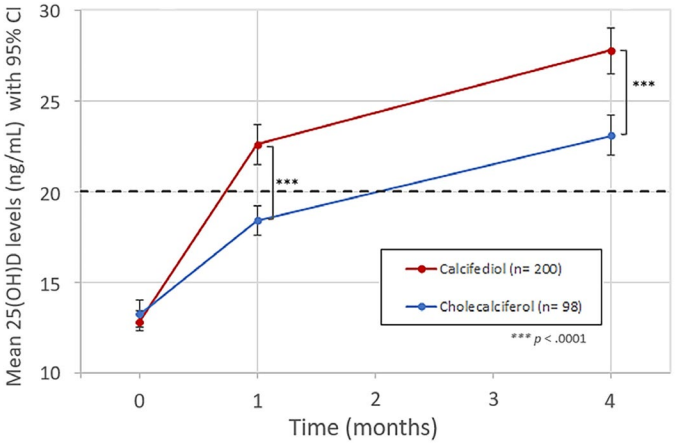

***Disclosures: Jose Luis Pérez-Castrillón**, Faes Farma S.A., Consultant, Faes Farma S.A., Grant/Research Support*

P-577

The impact of vitamin D supplementation on fractures: an umbrella review of systematic reviews and meta-analyses of randomized controlled trials *Marlene Chakhtoura[1], Charbel Gharios[1], Sara Ajjour[1], Mariam Assaad[1], Dania Saleh Bacha[1], Yara Jabbour[1], Francesca Kahale[1], Aya Bassatne[1], Stephanie Antoun[1], Elie A Akl[1], Ghada El-Hajj Fuleihan[1]. [1]American university of Beirut, Lebanon

Introduction: Despite recent conflicting evidence on the benefits of vitamin D supplementation on skeletal outcomes, calcium and vitamin D (CaD) provide the basis for most primary and secondary fracture prevention recommendations. We reviewed all systematic reviews of randomized controlled trials assessing the effect of vitamin D supplementation on the risk of fractures in adults.Methods: We searched MEDLINE, PubMed, Embase, and Cochrane databases (2010 -2020). Two independent reviewers assessed studies against the following eligibility criteria: 1) meta-analyses of randomized controlled trials, 2) comparing vitamin D, alone or in combination with calcium (CaD), 3) to placebo or control, 4) in adults >= 50 years old, and 5) reporting fracture as an outcome. We assessed the quality of the systematic reviews in duplicate and independently using the AMSTAR-2 tool. Registration: CRD42019129540.Results: Out of 13,621 captured citations, we included 22 eligible meta-analyses. Four were of moderate quality, 6 were of low quality, and the remaining 12 were of critically low quality. Seven out of 13 meta-analyses reported a significant reduction in the risk of hip fractures with CaD supplementation (400-800 UI/d + 0.5-1.2 mg/d); risk reduction range 16-39% (Figure). Similarly, CaD significantly reduced the risk of fractures at any skeletal site, by 5-19%, in 7 out of 14 meta-analyses. Vitamin D alone did not reduce the risk of hip nor any other fractures in any meta-analysis. In one review of moderate quality, subgroup analysis by residency found that the relative risk of hip and of any fracture with CaD was significantly lower in institutionalized individuals but not in community dwelling individuals. This finding was not consistent in lower-quality meta-analyses performing the same subgroup analysis. Meta-analyses that only included trials of community dwelling individuals did not show any significant fracture risk reduction.Conclusion: Supplementation with CaD, but not vitamin D alone, most consistently decreased the risk of hip and of any fractures, in several meta-analyses. Assessment of the overlap in trials included, of statistical methods used, and a focus on higher quality meta-analyses, may identify the patients who would benefit the most from CaD supplementation (by baseline fracture and vitamin D status).

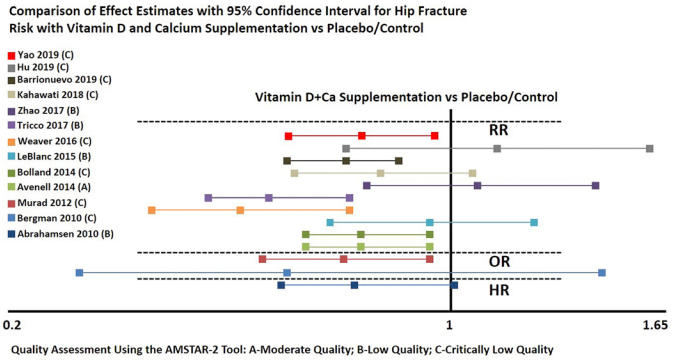

***Disclosures: Marlene Chakhtoura**, None*

P-578

The effect of exercise intensity on postmenopausal BMD: a meta-analysis *Melanie Fischbacher[1], Benjamin K Weeks[1], Beck Belinda R [1]. [1]Menzies Health Institute Queensland, Griffith University, Gold Coast campus, Gold Coast, Queensland, Australia, Australia

Background: Previous reviews have concluded that exercise has only modest effects on aBMD in postmenopausal women. Despite the well-recognised strong positive relationship between load magnitude and bone response observed from animal research, the majority of human trials have examined the effects of only low to moderate intensity exercise on bone. We speculated that meta-analysing according to intensity may reveal a more potent exercise effect at higher intensity.Objectives: To determine the effects of low, moderate and high intensity exercise on aBMD at the spine and hip in postmenopausal women.Methods: Electronic databases and reference lists were searched for RCTs that examined the effect of exercise compared to control on DXA-derived lumbar spine, femoral neck or total hip aBMD in healthy postmenopausal women. Interventions were classified as low, moderate or high intensity and pooled based on classification. Mean differences (MD) were calculated using random effects models and a risk of bias analysis was undertaken.Results: Fifty-one trials, testing 61 interventions (17 low, 38 moderate, 5 high intensity) were included. At the lumbar spine, high intensity exercise yielded greater aBMD effects (MD = 0.025 g/cm2 95% CI [0.007, 0.043], p = 0.007) than moderate (MD = 0.013 g/cm2 95% CI [0.008, 0.018], p < 0.001) and low intensity (MD = 0.010 g/cm2 95% CI [0.005, 0.015], p < 0.001). Low and moderate intensity exercise was equally effective at the femoral neck (low: 0.012 g/cm2 95% CI [0.006, 0.017], p < 0.001; moderate: 0.011 g/cm2 95% CI [0.007, 0.016], p < 0.001), but

no effect of high-intensity exercise was observed. Moderate intensity exercise increased total hip BMD (0.007 g/cm2 95% CI [0.003, 0.010], p < 0.001), but low intensity did not. There were insufficient data to meta-analyse the effect of high intensity exercise at the total hip. Risk of bias was mainly low or unclear due to insufficient information reported.Conclusion: High intensity exercise is a more effective stimulus for lumbar spine aBMD than low or moderate intensity, but not the femoral neck, however, the latter may be due to lack of power. While data from high-intensity exercise interventions are limited, the current comprehensive meta-analysis demonstrates the same positive relationship between load magnitude and bone response in humans as observed from animal research. Findings have implications for optimal exercise prescription for osteoporosis in postmenopausal women.

***Disclosures: Melanie Fischbacher**, None*

P-579

Influence of race/ethnic background on tibial bone microarchitecture changes following 8 weeks of US Army Basic Combat Training *Kristin Popp[1], Julie Hughes[1], Kathryn Taylor[1], Katelyn Guerriere[1], Nathaniel Smith[1], Susan Proctor[1], Stephan Foulis[1], Mary Bouxsein[2]. [1]Military Performance Division, United States Army Research Institute of Environmental Medicine, United States, [2]Center for Advanced Orthopedic Studies, Beth Israel Deaconess Medical Center, United States

Risk of stress fracture (SF) increases during periods of heightened physical activity, such as U.S. Army Basic Combat Training (BCT), with highest incidence rates among those of White racial/ethnic background. We previously showed bone adaptation, which may mitigate SF risk, in both men and women in response to BCT. However, it is unknown whether these changes differ according to race/ethnicity. PURPOSE: To determine whether changes in tibial bone microarchitecture following 8 weeks of BCT differ by racial/ethnic background. METHODS: In an on-going prospective study of risk factors for SF among Army trainees, we will enroll 4,000 subjects and measure cortical (Ct) and trabecular (Tb) bone density and microarchitecture by HR-pQCT of the distal tibia pre- and post-BCT. Here, we present data from 995 men and 525 women who completed BCT. Subjects were of White non-Hispanic (WNH: 466M, 173W), White Hispanic (WH: 112M, 63W), Black non-Hispanic (B: 215M, 164W) and Other/mixed (176M, 110W) racial/ethnic backgrounds. We used linear mixed models to determine, within each sex: 1) pre- to post-BCT differences in bone parameters controlling for age, height, and weight and 2) whether changes differ by race/ethnic groups controlling for age, height, weight, and baseline bone values. RESULTS: Men (21.0+/-3.8yrs) and women (20.3+/-3.5) were of similar age. Ct.thickness, Tb.thickness, Tb.BV/TV, and total, Ct. and Tb.vBMD increased significantly from baseline (all p<0.001) in both men and women. Tb.separation decreased among both sexes (p<0.001), whereas Tb.number increased among men (p=0.002), but not women. Changes were largely similar among race/ethnic groups, with few meaningful differences. B men had slightly greater increases in total (0.88%) and Tb. (0.80%) vBMD compared to WNH men (0.64%, 0.58%, respectively; p<0.05). WNH women had greater decreases in Tb.separation compared to B women (p=0.02). B women, however, had a greater increase in total vBMD (1.12%) than WNH women (0.87%; p=0.08), though these differences were not statistically significant. There were no other differences between racial/ethnic groups for men or women. CONCLUSION: Eight weeks of BCT led to significant changes in bone density and microstructure in both men and women. Overall, bone changes in response to BCT did not vary markedly by race/ethnic group, suggesting that mechanisms beyond differential adaptive response to BCT contribute to racial/ethnic disparities in SF risk during BCT.

***Disclosures: Kristin Popp**, None*

P-580

Accelerometer-measured physical activity in relation to bone mineral density: a Mendelian randomization study *Ruizhuo Li[1], Pengfei Wu[2], Bing Wang[3], Kun Xia[2]. [1]Fifth Affiliated Hospital of Sun Yat-sen University, China, [2]School of Life Sciences, Central South University, China, [3]Second Xiangya Hospital, Central South University, China

Background: The potential beneficial effect of physical activity in improving bone mineral density (BMD) has long been postulated. Emerging observational studies and randomized controlled trials have yielded inconsistent results. Traditional physical activity measurement based on self-report exercise patterns is prone to be confounded or biased, leading to unconvincing conclusions.Methods: We conducted a two-sample Mendelian randomization (MR) analysis to infer the causal effects of physical activity on BMD in the European ancestry. To identify instrumental variables associated with objectively measured physical activity, we selected 5 genetic variants reaching genome-wide significance ($P < 5 \times 10\text{-}8$) from the largest meta-analysis of 91,105 UK Biobank participants. Summary statistics for BMD based on dual-energy X-ray absorptiometry scans, incorporating lumbar spine (n = 28,498), femoral neck (n = 32,735), forearm (n = 8143), and total body BMD (n = 66,628) were released by the Genetic Factors for Osteoporosis consortium. The inverse-variance weighted MR was employed as the primary analysis, while MR-PRESSO, weighted median, and MR-Egger test were implemented in sensitivity analyses. Effects were expressed as standard deviation (SD) changes in BMD per 1-SD increment in physical activity (~8 milligravities per 5-second-epoch). All statistical analyses were performed in R version 3.6.1. Statistical significance was set at Bonferroni corrected P = 0.0125.Results: MR results did not support a role for genetically-proxied higher physical activity in the BMD accrual. In the main MR analyses, 1-unit increase in accelerometer-measured physical activity was not causally associated with lumbar spine (-0.42, 95% confidence interval [CI]: -0.88 to 0.04; P = 0.07), femoral neck (-0.06, 95% CI: -0.59 to 0.48, P = 0.84), forearm (-0.05, 95% CI: -0.62 to 0.52, P = 0.86), or total body BMD (0.17, 95% CI: -0.11 to 0.45, P = 0.24). No evidence of horizontal pleiotropy was detected by MR-Egger regression; consistency and robustness of primary results were verified through sensitivity analyses.Conclusion: This study suggests that genetically predicted physical activity is not causally associated with BMD. Provided that genetic structures and molecular mechanisms for BMD regulation are still largely unraveled, further studies are warranted to shed verify whether the physical activity should be promoted as an effective strategy for improving bone health.

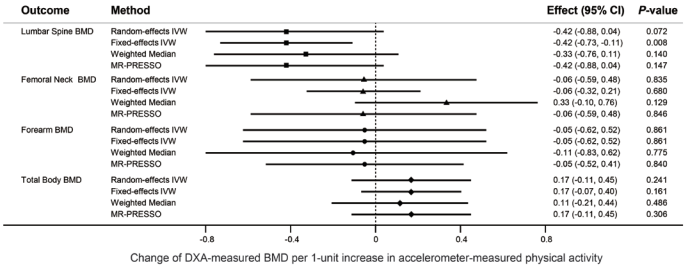

Figure 1. Mendelian randomization estimates for the causal effect of physical activity on BMD. Effect estimates represented SD changes in DXA-measured BMD per 1-SD higher average acceleration in genetically predicted physical activity (~8 milligravities per 5-second-epoch, i.e., 75-minute moderate activity like fast walking in place of sedentary behavior each day). *BMD*, bone mineral density, *CI*, confidence interval; *DXA*, dual-energy X-ray absorptiometry; *IVW*, inverse-variance weighted; *MR-PRESSO*, Mendelian randomization pleiotropy residual sum and outlier.

***Disclosures: Ruizhuo Li**, None*

P-581

Feasibility, safety and effectiveness of a pilot 16-week home-based, high-impact exercise intervention in post-menopausal women with low bone mineral density *Carrie-Anne Ng[1], Lachlan McMillan[1], Ludovic Humbert[2], Peter Ebeling[1], David Scott[1]. [1]Department of Medicine, School of Clinical Sciences at Monash Health, Monash University, Australia, [2]Musculoskeletal Unit, Galgo Medical, Barcelona, Spain, Spain

OBJECTIVE: High-impact exercise may improve bone health, but the feasibility and efficacy of home-based exercise in postmenopausal women with low bone mineral density (BMD) is unclear. We aimed to determine feasibility and safety, and changes in BMD, bone microarchitecture, physical function, and bone turnover markers, following a pilot 16-week home-based, high-impact exercise intervention in postmenopausal women with low BMD. METHODS: 50 community-dwelling postmenopausal women with BMD T-scores < -1.0 participated in 16-weeks of home-based high-impact exercise progressively increasing to 50 multi-directional unilateral hops on each leg for 7 days a week. Bone density and structure was assessed by lumbar spine and total hip dual-energy X-ray absorptiometry (DXA), 3D modelling algorithms (3D-SHAPER) of hip DXA scans, and distal tibial high-resolution peripheral quantitative computed tomography scans (HR-pQCT). Physical performance was assessed by repeated chair stand time and stair climb time. RESULTS: 44 women (mean+/-SD age 64.5+/-7.5 years) completed the intervention, with adherence to exercise sessions of 84.7+/-18.0%. Six (12%) women did not complete the study due to related soreness (n=2), unrelated injury (n=1) and loss of interest (n=3). Femoral neck areal BMD significantly increased by 1.13+/-3.76% (p=0.048). Trabecular volumetric BMD of the total hip and femoral neck estimated by 3D-SHAPER significantly increased (2.27+/-7.03%; p=0.038 and 3.20+/-5.39%; p<0.001, respectively). Additionally, femoral neck integral (trabecular plus cortical) volumetric BMD increased by 1.81+/-4.33% (p=0.010). At the distal tibia, total volumetric BMD significantly increased by 0.32+/-0.88% (p=0.032) and cortical cross-sectional area significantly increased by 0.55+/-1.54% (p=0.034). Chair stand and stair climb time significantly improved by 2.3+/-1.88s (p<0.001) and 0.27+/-0.49s (p<0.001), respectively. CONCLUSION: A pilot 16-week home-based, high-impact exercise intervention was both feasible and effective in improving femoral neck areal BMD, total hip and distal tibial volumetric BMD, and physical function in postmenopausal women. Home-based, high-impact exercise interventions may reduce risk factors for fracture in older populations with limited access to clinic- or gym-based exercise programs.

***Disclosures: Carrie-Anne Ng**, None*

P-582

Longitudinal population vitamin D sufficiency is increasing and associated with less BMD loss over 10 years *Michael Thompson[1], Graeme Jones[1], Saliu Balogun[2], Dawn Aitken[1]. [1]Menzies Research Institute Tasmania, Australia, [2]Australian National University, Australia

IntroductionVitamin D deficiency is a prevalent, modifiable determinant of osteoporotic fracture risk. Efforts to improve population vitamin D have intensified. There are limited data that examine the longitudinal change in population 25-hydroxyvitamin D (25OHD) and none that evaluate the skeletal outcomes of longitudinal vitamin D sufficiency. Meth-

odsCommunity-dwelling adults aged 50-80 years had 25OHD assessed by radioimmunoassay at baseline (n=1096), 2.5 (n=870) and 10 (n=565) years. Sun exposure was quantified by questionnaire, supplement use at clinic review, BMD by DXA and physical activity by pedometer. 25OHD <50nmol/L was considered deficient. ResultsOver 10 years 25OHD increased (52.4+/-18.7 vs 62.5+/-23.5 nmol/L, p<0.001) and the percentage of vitamin D deficient participants decreased (45.4% vs 31.0%, p<0.001). Participants with baseline deficiency had larger 25OHD increases than baseline sufficient participants (19.2+/-25.3 vs 1.6+/-23.3 nmol/L, p<0.001). Longitudinal change in 25OHD was associated with vitamin D and calcium supplement use, baseline and change in BMI, physical activity and sun exposure. The proportion of participants taking vitamin D (2.3% vs 37.1%, p<0.001) and calcium (7.3% vs 18.8%, p<0.001) supplements increased. Longitudinal vitamin D sufficiency was associated with less BMD loss at lumbar spine (-0.016+/-0.08 vs 0.012+/-0.09 g/cm2, p=0.006), total hip (-0.054+/-0.08 vs -0.034+/-0.07 g/cm2, p=0.046), femoral neck (-0.031+/-0.08 vs -0.012+/-0.06 g/cm2, p=0.034) and total body (-0.013+/-0.06 vs 0.005+/-0.10 g/cm2, p=0.047).ConclusionsCohort 25OHD concentration increased over 10 years and longitudinal vitamin D sufficiency was associated with less BMD loss. This suggests population vitamin D status can improve and that persistent sufficiency may ameliorate age-related BMD loss.

***Disclosures: Michael Thompson**, None*

P-583

Plasma Vitamin C Sufficiency is Related to Higher Bone Mineral Density: The Boston Puerto Rican Osteoporosis Study *Kelsey Mangano[1], Sabrina Noel[1], Bess Dawson-Hughes[2], Katherine Tucker[1]. [1]University of Massachusetts, Lowell, United States, [2]Jean Mayer USDA Human Nutrition Research Center on Aging, United States

There is evidence that vitamin C is important for bone health, but few studies have evaluated plasma vitamin C status. The purpose of this study was to investigate the relation of bone mineral density (BMD) with 1) dietary vitamin C (diet and supplements) and 2) plasma vitamin C (an established biomarker) among Puerto Rican adults. In this cross-sectional study of 902 adults aged 46-78y, from the Boston Puerto Rican Osteoporosis Study (BPROS), BMD was measured using DXA at the hip and spine. Usual dietary intakes and supplement use were assessed with a food frequency questionnaire. The association between dietary, supplemental (yes/no) and plasma vitamin C with BMD was assessed by multivariable linear regression. Least squares mean BMD was compared across energy adjusted tertile categories of dietary vitamin C (median intake: 36 mg/d (lowest); 64 mg/d; 106 mg/d (highest)) and plasma vitamin C status (deficiency (<20 µmol/dL, 20% of sample); subclinical deficiency (20-50µmol/dL, 36%); adequate status (>=50 µmol/dL, 44%)). Interactions by sex and smoking status (never, former, current) were examined, but not significant. Covariates included age, sex, education, menopause, smoking status, alcohol consumption, physical activity score, height, BMI, calcium intake, plasma vitamin D (ng/mL), C-reactive protein (mg/dL) and diabetes (yes/no). Greater vitamin C from dietary intake was not associated with BMD at any site (P-range=0.34-0.90). Supplemental vitamin C intake approached a positive association with BMD at the femoral neck (FN, P=0.07) and total femur (TF, P=0.08). A significant linear association between plasma vitamin C and BMD was observed at the trochanter (TR, β=0.0004, P=0.05) and the association approached significance at the TF (β=0.0004, P=0.08). Mean TR and TF BMD among individuals with vitamin C deficiency (0.820+/-0.012g/cm2, 1.022+/-0.013g/cm2 respectively) was significantly lower than among those vitamin C sufficient (0.847+/-0.010g/cm2, P=0.02; 1.050+/-0.011g/cm2, P=0.03). In this sample, Puerto Rican adults with plasma vitamin C concentration below 20 µmol/dL had significantly lower BMD at the hip compared to those with sufficient plasma vitamin C, after controlling for confounders. Replication in other cohorts is needed to confirm these results and to develop dietary recommendations of vitamin C sufficiency for optimal bone health among older adults. This is important, as a large percentage of the population may not meet these guidelines.

Table. Adjusted least squares means bone mineral density (g/cm²) at the hip and spine across groups of plasma vitamin C status in 902 men and women from the Boston Puerto Rican Health Study[1].

	Plasma Vitamin C <20 µmol/L	Plasma Vitamin C 20-50 µmol/L	Plasma Vitamin C ≥50 µmol/L	P-Trend
Femoral Neck BMD	0.9339 ± 0.0119	0.9487 ± 0.0103	0.9523 ± 0.0098	0.15
Trochanter BMD	0.8204 ± 0.0115[a]	0.8289 ± 0.0099	0.8472 ± 0.0095[b]	0.01
Total Femur BMD	1.0222 ± 0.0128[a]	1.0326 ± 0.0110	1.0496 ± 0.0106[b]	0.02
Lumbar Spine BMD	1.1659 ± 0.0163	1.1828 ± 0.0140	1.1910 ± 0.0136	0.13

[1] ab superscript indicate statistically significant differences in BMD values between groups (trochanter BMD p=0.02; total femur BMD p=0.03).

***Disclosures: Kelsey Mangano**, None*

P-584

Muscle Strength and Muscle Area Independently Predict Bone Strength at the Tibia and Radius in Women at Risk of Fracture *Suelen M. Goes[1], Bradley Bigsby[1], Philip Chilibeck[1], James D. Johnston[2], Saija Kontulainen[1]. [1]University of Saskatchewan - College of Kinesiology, Canada, [2]University of Saskatchewan - Department of Mechanical Engineering, Canada

Background/Purpose: Muscle size and strength, physical function and physical activity can contribute to fracture prediction by reducing fall risk; however, their role in determining bone strength and areal bone mineral density (aBMD) in women at high risk of fracture is unknown. Our objective was to assess if muscle size and strength, physical performance, daily moderate-to-vigorous physical activity (MVPA), and impact counts would independently predict bone strength and aBMD in women at risk of fracture.Methods: We included 45 women (mean age 74, SD 8.6y) with osteoporosis, hyperkyphosis, or history of vertebral fracture. We estimated bone strength to resist compression (BSIc) at the distal sites and torsion (SSIp) at the shaft sites of tibia and radius and recorded muscle area at the lower leg and forearm using pQCT. We measured aBMD at the femoral neck and lumbar spine as well as total body lean mass using DXA, physical performance by 30-second sit-to-stand and grip strength tests, and daily minutes of MVPA and impact counts using tri-axial accelerometers over seven days. We performed hierarchical linear regression (adjusted for body mass index and age) to assess if muscle outcomes (muscle area and total lean mass), physical performance, daily MVPA, and daily impacts would independently predict bone strength and aBMD.Results: Lower leg muscle area was an independent predictor of BSIc at the distal tibia [β=0.01, CI95% 0.001;0.02, p<0.05]. However, when the 30-second sit-to-stand performance was added to the model, this muscle strength measure took place as an independent predictor of BSIc at the distal tibia [β=1.9, CI95% 0.05;3.9, p<0.05]. Forearm muscle area was an independent predictor of SSIp at the radial shaft [β=0.07, CI95% 0.03;0.13, p0.05). Daily MVPA and impact counts did not independently predict bone strength or aBMD at any site (p>0.05).Conclusion: These findings suggest that muscle size and strength measures, rather than time spent in MVPA or number of daily impact counts, might be critical for maintaining bone strength at the tibia and radius in women at risk of fracture.

***Disclosures: Suelen M. Goes**, None*

P-585

In a clinical trial of vitamin D there was no effect on physical performance *Lynette Smith[1], J Chris Gallagher[2]. [1]University Nebraska Medical center, United States, [2]Creighton University, United States

Introduction: The effect of vitamin D supplementation on physical performance is controversial. Longitudinal cohort studies show very low levels of serum 25OHD (< 15- 20ng/ml) are associated with lower physical performance. There are few clinical trials of the effect of vitamin D on physical performance and results are mixed.Design: 163 independent living women entered a 12-month double blind randomized dose ranging study of daily vitamin D,400,800,1600,2400,3200,4,000,4800IU or placebo together with calcium supplement as needed for a total intake ~1200mg and mean diet vitamin D of 114 IU. Inclusion criteria: total serum 25OHD <= 20ng/ml (Diasorin RIA); no known disease or drugs affecting calcium or bone metabolism. Physical performance tests were performed at baseline and end as described in the Short physical performance battery (SPPB) that included Balance, Timed walk, Chair rising test. Additional tests included Timed up and Go, Grip strength and Balance (Biodex). Fall history was recorded at baseline and at 3-monthly visits. Serum 25OHD was measured by Diasorin RIA and LCMS,Free 25OHD was measured by Elisa (Future Diagnostics).Changes in physical performance and fallers were analyzed by dose groups and by quintiles of serum 25OHD(46 ng/ml). This was a secondary analysis using Intent to treat and statistical analysis used Chi square and ANOVA for association between dose, quintiles and tests.Results: Age range 57-87 years, mean age 66.2 years (SD 7.3), mean BMI 30.3 kg/m2 (SD 5.9). Compliance, measured every 3 months, was 94% for vitamin D and 91% calcium. 147 women completed study. There was no significant effect of vitamin D dose on any physical performance test. When data was examined according to serum total or free 25OHD quintiles there was no association between serum levels of 25OHD and change in any physical performance test. The relation between vitamin D dose and serum 25OHD and falls followed a U-shaped curve as previously published with a 45 percent reduction in fallers in the serum middle quintile 32-41ng/ml compared to quintiles 1 and 5, p<0.001 (1).Conclusions: There was no effect of vitamin D on physical performance. There was a U-shaped response on vitamin D with a significant reduction in falls in the serum 25OHD range 30-40ng/ml.There is no correlation between physical performance, fallers and non- fallers.1Smith LM, Gallagher JC, Suiter C. J Steroid Biochem Mol Biol. 2017 Oct; 173:317-322.

***Disclosures: Lynette Smith**, None*

Posters

P-586

Moderate Blueberry Consumption Increased Net Bone Calcium Retention in Healthy Postmenopausal Women: A Randomized Crossover Trial *Joanna K. Hodges[1], Sisi Cao[1], Pamela J. Lachcik[2], Munro Peacock[3], George P. McCabe[4], Linda D. McCabe[4], Dennis P. Cladis[4], Mario G. Ferruzzi[5], Berdine R. Martin[4], Connie M. Weaver[4]. [1]The Ohio State University, United States, [2]Bioanalytical Systems, Inc., United States, [3]Indiana University School of Medicine, United States, [4]Purdue University, United States, [5]North Carolina State University, United States

Objectives: Preclinical studies suggest that blueberry consumption is associated with improved bone health. This study quantified changes in urinary excretion of the long-lived calcium radioisotope 41Ca to assess the effect of blueberries on bone loss in postmenopausal women. We hypothesized that blueberry consumption would reduce bone loss in a dose-dependent manner.Methods: Healthy women at least 4 years past menopause were dosed with 41Ca and completed a 5-mo equilibration period for 41Ca deposition in bone, a 6-wk control period, and 3 alternating rounds of 6-wk intervention and washout periods. During the interventions, participants consumed a low (17.5 g/d), medium (35 g/d), or high (70 g/d) dose of freeze-dried blueberry powder equivalent to 0.75, 1.5, or 3 cups of fresh blueberries. The blueberry powder was consumed daily as part of granola bars, spread, and drinks. Urinary 41Ca:Ca ratio was measured by accelerator mass spectrometry in 24-h urine collected weekly during intervention and every 3 wk during washout periods. Serum bone biomarkers (P1NP, CTX, OPG, RANKL, and Sclerostin) and urinary polyphenols were measured at the end of control and each intervention period. Serum 25-hydroxyvitamin D and calcium concentrations were measured prior to each intervention. Data were analyzed using a linear mixed model and repeated measures ANOVA.Results: Fourteen healthy non-osteoporotic (baseline mean bone mineral density t-score: -1.3) women completed the study. Net bone calcium retention increased by 6% during the low ($p < 0.01$) and 4% during the medium ($p < 0.05$) dose intervention compared with the control and washout periods. The high dose had no significant effect on net bone calcium retention ($p = 0.19$). Serum RANKL was significantly lower during the medium dose intervention ($p < 0.05$), while serum P1NP was significantly lower during the low and medium dose interventions ($p < 0.01$) compared with the control period. Urinary excretion of hippuric acid was significantly higher during the high dose intervention compared with the control period ($p < 0.01$). No significant changes were found in serum 25-hydroxyvitamin D or calcium during the study.Conclusions: A hormetic response was observed, whereby daily consumption of foods containing 17.5-35 g, but not 70 g, of freeze-dried blueberry powder increased net bone calcium retention. Moderate consumption of blueberries may be an effective strategy to attenuate bone loss in healthy postmenopausal women.

***Disclosures: Joanna K. Hodges**, None*

P-587

Bovine colostrum improves bone microstructure in ovariectomized and orchidectomy rats via VEGFA signaling *Eirini Kydonaki[1], Laura Freitas[1], Bruno Fonseca[1], Henrique Reguengo[1], Carlos Simón[2], Ana Bastos[3], Raphaël Canadas[3], Joaquim Oliveira[4], Vitor Correlo[4], Rui Reis[4], Yiannis Koutedakis[5], Rui Pinto[6], Franklim Marques[1], Tânia Amorim[1]. [1]UCIBIO/REQUIMTE, Faculty of Pharmacy, University of Porto, Porto, Portugal, Portugal, [2]Centro de Estudios Superiores de la Industria Farmacéutica (CESIF, SA). Madrid, Spain, Spain, [3]3B's Research Group, I3Bs - Research Institute on Biomaterials, Biodegradables and Biomimetics, University of Minho, Guimarães, Portugal; ICVS/3B's, Braga/Guimarães, Portugal, Portugal, [4]The Discoveries Centre for Regenerative and Precision Medicine, University of Minho, Guimarães, Portugal., Portugal, [5]Faculty of Education, Health and Wellbeing, University of Wolverhampton, Walsall, United Kingdom; School of Sports and Exercise Sciences, University of Thessaly, Trikala, Greece, Greece, [6]iMed.UL, Faculty of Pharmacy, University of Lisbon, Lisbon, Portugal; JCS, Dr. Joaquim Chaves, Miraflores Algés, Portugal, Portugal

IntroductionResearch has shown that components of bovine colostrum (BC), as lactoferrin, induce bone anabolic effects. However, the effects of BC supplementation as a whole in bone microarchitecture and the mechanisms through which BC may induce bone anabolic effects is relatively unclear. The aim of this study was to evaluate the effects of different BC doses supplementation in ovariectomized (OVX) and orchidectomy (ORX) rat-models and to identify the pathways that may mediate the action of BC on bone.MethodsAfter baseline measurements of bone microarchitecture (µCT), twenty-seven-month-old female (OVX, n=32) and male (ORX, n=32) Wistar rats were randomly assigned to the following groups: a) placebo b) BC dose 1 (0.5g/day/females; 1.0g/day/males), c) BC dose 2 (1g/day/females; 1.5g/day/males) and d) BC dose 3 (1.5g/day/females; 2g/day/males). After 4 months of supplementation, bone microarchitecture was re-assessed. Gene expression of VEGFA, FGF2, TATA, OPG, RANK and RANKL were measured by qRT-PCR. The study was approved by the National Ethics Committee for the Use of Animals in Research.ResultsRegarding male rats, BC dose 1 significantly improved bone microarchitecture, as these rats not only revealed significantly less cortical porosity (41.9%, $p<0.05$) and cortical pore size (25.7%, $p<0.05$) compared to placebo group, but also significantly increased cortical volume (89.7%, $p<0.05$), cortical BMD (134.9%, $p<0.01$), trabecular thickness (37.3%, $p<0.01$), trabecular volume (24.6%, $p<0.001$) and trabecular BMD (7.5%, $p<0.01$). BC dose 2 induced the same effects as dose 1 for male rats, and significantly reduced trabecular porosity (8.1%, $p<0.01$), while dose 3 reduced trabecular separation (29.3%, $p<0.05$). As for female rats, BC dose 1 did not induce positive effects on bone microarchitecture. However, BC dose 2 and 3 decreased cortical porosity (placebo: 65.75+/-4.22; dose 2: 25.16+/-8.83; dose 3: 25.22+/-8.54%, $p<0.01$) and improved trabecular thickness (placebo: 12.22+/-0.99; dose 2: 21.11+/-3.28; dose 3: 18.39+/-2.45µm, $p<0.01$) compared to placebo. BC dose 3 significantly increased mRNA expression of VEGFA (2.37+/-1.83, $p<0.05$).ConclusionBC preserves bone mass of OVX and ORX rats by stimulating bone formation. Indeed, as bone is a high vascularized organ and VEGFA plays important roles in vascular development and angiogenesis, it seems that VEGFA is influencing skeletal development and osteogenesis in OVX and ORX rats.

***Disclosures: Eirini Kydonaki**, None*

P-588

The Impact of Exercise on Bone Health in the Transmenopause Period: Helpful or Harmful? *Laura Flores[1], Nancy Waltman[2], Kevin Kupzyk[1], Joan Lappe[3], Laura Bilek[4]. [1]University of Nebraska Medical Center, United States, [2]University of Nebraska Medical Center College of Nursing- Lincoln Division, United States, [3]Creighton University, United States, [4]University of Nebraska Medical Center- College of Allied Health Professions, United States

Introduction: Transmenopause, the period immediately following menopause, is a time of rapid bone loss. The most rapid decline in bone mineral density (BMD) is seen early following menopause with a modest decline thereafter. These changes increase osteoporosis risk and should be mitigated. Interventions including vitamin D and calcium supplementation and weight-bearing exercise are often recommended for maintenance of bone health. As transmenopause is a time of tremendous bone loss, establishing appropriate and timely interventions is necessary to prevent osteoporosis. Thus, we evaluated the effect of time since onset of menopause on change in BMD of the spine and hip in persons participating in lifestyle interventions for bone health.Methods: Data are from postmenopausal women with low bone mass who completed the Heartland Osteoporosis Prevention Study and were randomized to 12 months of control [Ca and vit D] or exercise + Ca and vit D. BMD of the total hip and lumbar spine were assessed at baseline and 12 months using DXA. Women within 6 years of menopause diagnosis with 12 month data were included in analysis. Time from menopause was self-reported, and groups were divided into 24 months since the last menstrual cycle (Late Menopause). The within group (exercise and control) and between group effect of time from menopause on BMD were analyzed.Results: There were 72 women (22 Early Menopause; 50 Late Menopause) in the exercise group with a mean age of 54.7(3.0). The control group had 77 (18 Early Menopause, 59 Late Menopause) women with an average age of 54.3(3.3). In the exercise group, within group analysis demonstrated a significant difference in lumbar spine BMD between early and late menopause groups ($p=0.021$) with those in the early menopause group having greater bone loss relative to those the late menopause group. A similar trend was observed for hip BMD within the exercise group ($p=0.06$). There were no significant differences in BMD changes of the hip or spine between women of early and late menopause in the control group.Conclusion: While lifestyle (exercise, calcium and vitamin D supplementation) for bone health is important, the ability of these interventions to maintain BMD may depend on the time elapsed since a women's last menstrual cycle. This result should be evaluated further in terms of bone strength and structure.

Table 1: Change in BMD over 12 months in Exercise Group		N	Mean (SD)	P value
Change in Hip BMD	Early Menopause	22	-0.0030 (0.01987)	**p=.060**
	Late Menopause	50	0.0085 (0.02476)	
Change in Lumbar Spine BMD	Early Menopause	22	-0.0093 (0.03235)	**p=.021**
	Late Menopause	50	0.0069 (0.02400)	

***Disclosures: Laura Flores**, None*

P-589

Vitamin D level and functional recovery after hip fracture *Sneha Mohan[1], Pam Holte[1], Brandon Yuan[1], Andrew Sems[1], Ann Kearns[1]. [1]Mayo Clinic, United States

Background: Vitamin D deficiency is common in patients presenting with low energy hip fractures. The relationship between Vitamin D levels at the time of a fracture and long term functional outcomes has not been studied. Identifying a benefit to recovery with adequate vitamin D would support supplementation in elderly patients at risk for hip fracture. Methods: A retrospective cohort of patients >/= 50 years, who were treated surgically for low energy hip fracture between July 1 2016 and June 30 2018 were identified. The correlation between Vitamin D levels and functional recovery, assessed using the time up and go (TUG) test, survival at 3 months and 1 year, and readmission within 3 months was examined. The Charlson comorbidity index (CCI) at baseline was also assessed.Results: A total of 216 patients were treated for a hip fracture. A majority was female (134, 62%), mean age 80 years (+/-12) and mean CCI 5.98 (+/- 2.6). 52 (24%) individuals died within a year of surgery, among whom 23 (44.2% of 52) passed away within 3 months. 45 (20.8%) were readmitted within 3 months of surgery and 20 (9.2%) sustained a second fracture within a year.174 patients had Vitamin D level measured at presentation and were included for analysis. Vitamin

D <20 ng/ml was seen in 39 (22.4%) patients and all received appropriate supplementation. The correlation of Vitamin D levels, taken as a continuous variable, to outcomes, was analyzed using logistic regression. No significant relationships between higher Vitamin D and death within 3 months (OR=0.995, p=0.8), death within 1 year (OR=1.008, p=0.62), readmission within 3 months (OR=1.001, p=0.96), second fracture within 1 year (OR=1.017, p=0.33) and failure to recover (OR=1.002, 0.86). After adjusting for age, gender and CCI, Vitamin D levels were non-significantly inversely associated with both TUG 1 and TUG2, with every 1 unit higher Vitamin D associated with a TUG lowered by 0.15 seconds, p=0.42 and 0.44. Vitamin D was poorly correlated to CCI with correlation coefficient of 0.02, p = 0.71.Conclusions: Our results indicate that Vitamin D levels at the time of a hip fracture do not correlate with patients' functional outcomes. It is possible that replacing vitamin D eliminated the possible negative impact on functional recovery.

***Disclosures: Sneha Mohan**, None*

P-590

The Impact of a Nutritional Intervention on Indices of Bone Health in Exercising Women with Menstrual Disturbances *Mary Jane De Souza[1], Emily Southmayd[1], Rebecca Mallison[1], Nancy Williams[1]. [1]Penn State University, United States

Exercising women with low energy availability (EA) and menstrual dysfunction are at risk for poor bone health. REFUEL was a 52-wk randomized controlled trial designed to improve energy status, restore menses, and improve bone health in exercising women with menstrual disturbances. Women (n=62, 18-30 yrs) with oligo/amenorrhea were randomized to increase energy intake 20-40% above baseline energy requirements (+Cals, n=32) or maintain baseline energy intake (Control, n=30) for 52 weeks. Bone mineral density (BMD, total body (TB), lumbar spine (LS), femoral neck (FN), and total hip (TH)) was assessed by DXA at baseline, wk21, and wk53 (post). Markers of bone formation (P1NP) and resorption (sCTx) were measured at baseline and weeks 5, 9, 21, 33, and 53 to assess bone formation index, resorption index, and balance (formation index/resorption index). The impact of group, time, and group*time for BMD and bone turnover were assessed with linear mixed models. Twenty-nine women completed the intervention (+Cals, n=15; Control, n=14). Percent changes described below include only those that completed. Energy intake (EI) increased +448 kcal/day (24%) and body weight increased 3.0 kg (5.6%) by wk53 in the +Cals group compared with a change in EI of -42 kcal/day and BW of 0.5 kg in the Control group (p<0.05). Women in the +Cals group were more likely to experience menses compared with the Control group (p0.05). In exercising women with low EA and menstrual dysfunction, a modest increase in energy intake for 53 weeks increased body weight and improved menstrual regularity but was not sufficient to significantly improve BMD. Sustained and/or more substantial increases in energy intake that improve bone formation relative to resorption are likely needed to improve BMD in oligo/amenorrheic exercising women.

***Disclosures: Mary Jane De Souza**, None*

P-591

Assessing the Efficacy of Herbal Teas on Bone Health in an Osteopenic Population: OsTea *Fahima Munmun[1], Alyssa Linden[2], Sa'ed Al-Olimat[2], Jacquelyn Madler[2], Hunter Hanlon[2], Hannah Enderby[3], Paula Witt-Enderby[1]. [1]Duquesne University Graduate School of Pharmaceutical, Administrative and Social Sciences, United States, [2]Duquesne University School of Pharmacy, United States, [3]Duquesne University Bayer School of Natural and Environmental Sciences, United States

The purpose of the OsTea (Herbal Teas on Bone Health in an Osteopenic Population; NCT03480126) RCT was to assess the efficacy of herbal teas (tulsi, rooibos, oolong) compared to placebo (coriander) in an osteopenic population. In this study, the effects of these teas were assessed on markers of bone health, inflammation, melatonin, and the microbiome . Quality of life was also assessed using validated questionnaires and diary logs. Participants were asked to drink 3 cups of tea per day for 90 days. Mechanistic studies were also performed on hMSC to determine tea effects on viability and osteoblast differentiation. Overall, it was observed that out of the four groups, rooibos and tulsi demonstrated the most significant effects. Specifically, rooibos consumption significantly decreased urinary CTX levels and this was associated with a decrease in urinary bone turnover marker activity (i.e., decreased P1NP:CTX ratio); an increase (p=0.06) in nocturnal melatonin levels; an increase in the morning: evening salivary cortisol ratio; a decrease in serotonin-producing microbes in the gut; a trend (p=0.09) towards an improvement in emotional parameters in QUALIOST; and a significant increase in the hMSC differentiation into osteoblasts under normal and oxidative stress conditions revealed through alizarin red staining. For tulsi, consumption primarily affected subjective measures related to stress, anxiety, and bone health. Specifically, consumption of tulsi over 3 months significantly improved scores of PSS, STAI-trait anxiety and osteoporosis/osteopenia-related parameters in QUALIOST. These improvements in subjective measures were associated with an increase in the morning: evening salivary cortisol ratio; and a decrease in urinary bone turnover marker activity (i.e., decreased P1NP:CTX ratio). Tulsi tea also protected hMSC viability (i.e., significantly increased osteoblast differentiation) under oxidative stress conditions. Although no clinical effects of oolong were observed, oolong tea was found to protect hMSCs under oxidative stress conditions reflected by an increase in hMSC viability and osteoblast differentiation, similar to tulsi. These findings provide both clinical and mechanistic support for the use of herbal teas, particularly rooibos and tulsi, for improving quality of life and bone health.

***Disclosures: Fahima Munmun**, None*

P-592

Vitamin D Insufficiency is Widespread in Armenia *Nicholas Hutchings[1], Varta Babalyan[2], Annemieke Heijboer[3], Sisak Baghdasaryan[2], Mushegh Qefoyan[2], Mariëtte T Ackermans[3], Arus Ivanyan[4], Anna Formenti[5], Andrea Giustina[5], John P Bilezikian[6]. [1]University of California, Irvine, United States, [2]Osteoporosis Center of Armenia, Armenia, [3]Vrije Universiteit Medisch Centrum, Netherlands, [4]Yerevan State Medical University, Armenia, [5]Università Vita-Salute San Raffaele, Italy, [6]Columbia University, United States

Vitamin D plays a critical role in skeletal development and in its maintenance. Thus, vitamin D sufficiency is an important goal for public health programs. Given the absence of any foods fortified in vitamin D in the land-locked country of Armenia, we hypothesized that vitamin D insufficiency would be widespread. To test this hypothesis, we conducted a random modified cluster model survey of vitamin D status of women in the country. We employed a dried blood spot (DBS) assay, a convenient and accurate method which lends itself to representative sampling throughout a country like Armenia: sampling entails obtaining a small volume of blood, applying it to filter paper, and then transporting it to the laboratory for LC/MS analysis. We also utilized a questionnaire to assess lifestyle factors which may influence vitamin D levels. In summer, we sampled 1206 participants from 40 randomly selected communities in Armenia, covering the entire country. Mean 25-hydroxyvitamin D (25-OH D) level among women aged 18-24 was 19.63 ng/mL (SD 7.61); among women aged 25-64 was 20.76 ng/mL (SD 7.39); and among women > 65 was 18.39 ng/mL (SD 7.51). The country-wide mean of the entire population was 19.76 ng/mL (SD 7.55). A majority of the population (> 54%) had 25-OH D levels < 20 ng/mL with nearly 13% having 25-OH D levels < 12 ng/mL. Participants who reported calcium, vitamin D, or multivitamin supplementation had statistically higher levels of 25-OH D (p-values 0.004, 0.0002, and 0.03 respectively) as did pre- vs post-menopausal women (p = 0.01), pregnant vs non-pregnant women (p = < 0.0001) and women who had experienced a sunburn in the past year (p = 0.004). There was no statistically significant relationship between the 25-OH D level and acknowledged smoking, alcohol use, sun exposure, physical activity, or dietary intake of foods rich in vitamin D. In Armenia, the results show a strikingly high prevalence of vitamin D insufficiency, providing much-needed data to inform and bolster public health directives to address this pervasive threat to optimal skeletal health.

***Disclosures: Nicholas Hutchings**, None*

P-593

Different impact of running, soccer and rugby trainings on diaphyseal tibia and fibula architecture, with different dependence on cortical tissue mineralization. *Sergio Luscher[1], Leandro Pisani[2], Nicolas Pilot[2], Leandro Mackler[1], Joern Rittweger[3], Alex Ireland[4], Jose Luis Ferretti[1], Ricardo Francisco Capozza[1], Gustavo Roberto Cointry[1]. [1]Center for P-Ca Metabolism Studies (CEMFoC), Natl Univ of Rosario and Arg NRC (CONICET), Argentina, [2]Unit of Musculoskeletal Biomechanics Studies (UDEBOM), CUADI, Universidad del Gran Rosario, Argentina, [3]Institute of Aerospace Medicine, German Aerospace Center (DLR); Department of Pediatrics and Adolescent Medicine, University of Cologne, Germany, [4]School of Healthcare Science, Manchester Metropolitan University, United Kingdom

Some differences between pQCT indicators of cortical tibia and fibula design between athletes trained in disciplines involving a different use of the foot with respect to untrained controls have been observed. This study aims to analyze these differences and assess their possible dependence on cortical tissue deformability (a relevant feature to mechanostat control of bone design). To that purpose, we compared the pQCT-assessed, anterior-posterior and lateral bending moments of inertia (xMI, yMI) in 18 serial scans taken at every 5% of the dominant-tibia length of 13 long-distance runners (LDR, in whom the foot is not trained in rotation/eversion), 28 soccer players and 19 rugbiers (S,R, in which foot rotation/eversion are intensively solicited), and 15 untrained controls (C). We correlated both MI values with the cortical vBMD (vCtD) at every site as a surrogate of bone tissue stiffness.Tibia MIs were significantly but moderately larger in R, S and LDR that in C, in that decreasing order (p<0.001), especially in the proximal region. In contrast, in the fibulae, xMI was much larger in R, S and DLR than in C (p<0.001) throughout, and yMI was similar to C in LDR and much higher in R and S (p<0.001), with differences increasing proximally. The vCtD was significantly but mildly lower in R, S and LDR tan in C, with differences increasing proximally. The negative, hyperbolic MI/vCtD relationships for both MI's were more significant in the tibiae (r=0.61-0.81, always p<0.001) than in the fibulae (r=0.11-0.39, not always significant) in all groups.Results show a contrasting behavior of both MI's between both bones and disciplines. In the tibiae, the MI's varied 'canonically' (significantly larger values in LDR, S or R than in C throughout), regardless of foot behavior. In the fibulae, however, the MI's varied in parallel with the degree of predominance of foot rotation/eversion on training and showed some site-specificity. Moreover, in the tibiae, the MI/vCtD relationships followed the 'natural', negative relationship observed in previous studies, while in

the fibulae they were much less significant if any. This suggests that the strikingly larger MI (especially, yMI) values in R and especially F than in LDR or C should have taken place 'despite of' the natural limitations of mechanostat input imposed by the intrinsic stiffness of cortical tissue. These observations are consonant with some phylogenetical features related to Natural Selection of leg bones.

***Disclosures: Sergio Luscher**, None*

P-594

Blueberry Polyphenols do not Improve Bone Mechanical Properties in Ovariectomized Rats *Dennis P Cladis[1], Elizabeth A Swallow[2], Matthew R Allen[2], Kathleen M Hill Gallant[1], Mario G Ferruzzi[3], Connie M Weaver[4]. [1]Department of Nutrition Science, Purdue University; Department of Food Science and Nutrition, University of Minnesota, United States, [2]Department of Anatomy, Cell Biology, and Physiology, Indiana University School of Medicine, United States, [3]Plants for Human Health Institute, North Carolina State University, United States, [4]Department of Food Science, Purdue University, United States

Postmenopausal women are at increased risk of osteoporosis and osteoporotic fractures. Bisphosphonates are commonly prescribed to mitigate osteoporotic bone loss, but some are hesitant to use them because of potential side effects. In light of this, alternative treatment options have been sought, including the use of fruit and vegetable-derived polyphenols. Previous in vitro experiments have demonstrated beneficial effects of polyphenols on bone health, leading to the increased use of polyphenol-rich herbal and botanical dietary supplements for bone health. We examined the efficacy of this strategy using blueberry polyphenols in a rat model of postmenopausal bone loss. Five-month old, ovariectomized, Sprague-Dawley rats (n=10/gp) were orally gavaged for 90 days with either a purified extract of blueberry polyphenols (0, 50, 250, or 1000 mg total polyphenols/kg bw/d) or lyophilized blueberries (50 mg total polyphenols/kg bw/d, equivalent to 1-2 cups fresh blueberries/d in humans). Upon completion of the dosing regimen, right femur, right tibia, and L1-L4 vertebrae were harvested. Bone mineral density (BMD) was assessed at all three sites by PIXImus. Micro-architecture and mechanical properties of femora were determined using micro-CT and three-point bending, respectively, with standard equations used to calculate material properties. Total polyphenol content of lyophilized blueberries and the purified extract were 3.5% and 27% (w/w), respectively. No differences were observed in BMD at any of the sites analyzed. Bone mechanical properties, including ultimate force, total displacement, stiffness, and total work, were not different across treatment groups. For material-level biomechanical properties, ultimate stress was higher in the 1000 mg group as compared to the 250 mg group (p=0.042), although no other differences were noted across treatment groups for total strain, modulus, or toughness. These results indicate that consuming blueberry polyphenols in the whole fruit or as an extract had little impact on BMD or bone mechanical properties in an animal model of estrogen deficiency-induced bone loss.

***Disclosures: Dennis P Cladis**, None*

P-595

The Dried Blood Spot Assay: Successful Application of a Methodology to Conduct a Country-Wide Survey of Vitamin D Status *Nicholas Hutchings[1], Annemieke Heijboer[2], Varta Babalyan[3], Sisak Baghdasaryan[3], Mushegh Qefoyan[3], Mariëtte T Ackermans[2], Anna Formenti[4], Andrea Giustina[4], John P Bilezikian[5]. [1]University of California, Irvine, United States, [2]Vrije Universiteit Medisch Centrum, Netherlands, [3]Osteoporosis Center of Armenia, Armenia, [4]Università Vita-Salute San Raffaele, Italy, [5]Columbia University, United States

Information about nutrients throughout a population is critical not only to quantify nutritional status but also to establish a foundation for public health recommendations and interventions. Obtaining reliable and robust data for a large and geographically diverse population is a major challenge of conducting such studies. In our country-wide survey of vitamin D nutrition in Armenia, we developed and applied a replicable and accurate method for randomized, representative participant selection and sampling. Using citizen registration data from the Ministry of Health in Armenia, we randomly selected 40 health clinics and then randomly selected 35 individuals registered to each clinic in a representative age distribution. From 1206 participants, using a finger prick, we obtained a drop of blood which was applied to and dried on filter cards (dried blood spot [DBS] cards). We also obtained point-of-care hematocrit and questionnaires. DBS cards were subsequently analyzed for 25-OH D via liquid chromatography mass spectrometry (LC-MS/MS). This well-standardized LC-MS/MS method shows a strong correlation between DBS and serum-obtained measurements of 25-OH D (R = 0.98) and DBS measurements were calibrated against serum measurements, thereby assuring the accuracy of the data. The results, provided in another abstract, represent the most comprehensive survey of any similarly important health index among the population of Armenia. The DBS methodology can be adapted to the measurement of other nutrients in Armenia or other countries. Using dried blood spots, such studies can be conducted conveniently, accurately, and in a cost-effective manner.

***Disclosures: Nicholas Hutchings**, None*

P-596

Correlations between dietary patterns of Mediterranean-type and Dietary Approaches to Stop Hypertension style and bone health status in adults *Yi-Chin Lin[1], Jia-Yu Lin[1]. [1]Department of Nutrition, Chung Shan Medical University, Taiwan, Province of China

Osteoporosis is an asymptomatic disease characterized by low bone mass and microarchitectural deterioration that would consequently increase bone fragility and the risk of fracture. According to the results from 2013-2016 Nutrition and Health Survey in Taiwan (NAHSIT), the prevalence rates of osteoporosis in those aged 50 years and older were 8.6% in men and 15.5% in women, respectively, and the prevalence increases with age. Previous studies have shown that both DASH (Dietary Approaches to Stop Hypertension) diet and the Mediterranean diet are associated with improved health. We thus hypothesized that adults with higher adherence to these diets would have better bone health status. The subjects were 289 adults (141 males and 148 females) aged 20 years and older who were originally recruited for two independent observational studies on adult bone health. Adherence to DASH diet was assessed by calculating the Mellen's index based on the intake of 9 nutrients according to the 24-h dietary recalls of the subjects, whereas the adherence to the Mediterranean diet was assessed by calculating the MMDS (modified Mediterranean Diet score) according to the intake of 5 beneficial components (vegetables, fruits and nuts, legumes, cereals, and fish) and 2 components presumed to be detrimental (meat and poultry products, and dairy products). These diet scores were then evaluated for the association with bone health measurements, including BMC and BMD at total body, lumbar spine and femoral neck.The results showed that only low to fair adherence to both diets in the subjects though the adherence to DASH diet seemed to increase with age ($p<0.0001$ for both genders). There were positive correlations, of borderline significance, between MMDS and BMC at total body ($b=70.22$; $p=0.0591$), lumbar spine ($b=2.98$; $p=0.0585$), and femoral neck ($b=0.15$; $p=0.0559$) and between MMDS and BMD at lumbar spine ($b=0.04$; $p=0.0759$) in males aged 65 years and older. DASH diet score, however, was negatively correlated with BMD in males and females, but positively correlated with lean mass in males ($b=4.26$; $p=0.0264$). It appears that adhere to DASH diet may be beneficial for maintaining lean mass in males, whereas higher adherence to diet of Mediterranean type may be associated with better bone health status in males aged 65 years or older.

***Disclosures: Yi-Chin Lin**, None*

P-597

Time Restricted Eating for 12 Weeks Does Not Adversely Alter Bone Mineral Content and Bone Metabolism in Overweight Adults *Andrea Lobene[1], Satchindananda Panda[2], Douglas Mashek[3], Kathleen Hill Gallant[4], Lisa Chow[5]. [1]Department of Nutrition Science, Purdue University, United States, [2]Salk Institute for Biological Studies, United States, [3]Department of Biochemistry, Molecular Biology and Biophysics and Department of Medicine, Division of Diabetes, Endocrinology and Metabolism, University of Minnesota, United States, [4]Department of Nutrition Science, Purdue University; Department of Food Science and Nutrition, University of Minnesota, United States, [5]Department of Medicine-Division of Diabetes, Endocrinology, and Metabolism, University of Minnesota, United States

Time-restricted eating (TRE), shortening the daily eating window to 8-10 hours, has been investigated as a potential strategy for weight loss and improving cardiometabolic health. However, the effect of TRE on bone health has not yet been determined. The aim of our study was to assess the effect of TRE on bone mineral content and bone metabolism. This study was a secondary analysis of a feasibility study which assessed the effect of TRE on weight, body fat, and cardiometabolic outcomes (Chow et al. Obesity 2020). Overweight and obese participants with a documented eating window >=14 hours (age=45+/-12 years) were randomly assigned to either TRE (n=11) or non-TRE (n=9). TRE participants were instructed to maintain a self-selected 8-hour ad libitum window for the 12-week intervention period, while non-TRE participants maintained their usual eating habits. Total body bone mineral content (BMC) and bone mineral density (BMD) were assessed pre- and post-intervention by DXA. Pre- and post-intervention serum samples were used to assess NTX and P1NP by ELISA, and intact PTH by EIA. Data were non-normally distributed and were log-transformed. Bone outcomes did not differ between groups at baseline. Linear mixed model analyses were conducted to assess the effect of time, treatment, and the interaction between treatment and time on the measured bone-related outcomes. There was an interaction between treatment and time for BMC ($p=0.02$) such that BMC increased in the TRE group but decreased in the non-TRE group over the 12 weeks, though the changes were <20g each. P1NP decreased in both treatment groups ($p=0.04$) with a larger decrease in the non-TRE group such that the interaction between treatment and time approached significance ($p=0.07$). PTH increased in both groups, though the change did not reach statistical significance ($p=0.09$). There were no significant differences in BMD or NTX over time or between groups. Changes in bone outcomes were not correlated with changes in weight or BMI in either group. Our results suggest 12 weeks of TRE does not negatively affect BMC, BMD, or markers of bone metabolism. Given the prevalence of overweight/obesity, and the importance of implementing weight-loss interventions in this population, it is important to understand the impacts on long-term bone health. Therefore, future studies should include a longer intervention period with clinically important measures such as site-specific BMD, bone microarchitecture, or fracture risk.

Bone Outcomes in the TRE and Non-TRE Groups Over 12-Weeks Values are means ± SD					P-values		
	Pre-Intervention	Post-Intervention	Absolute Change	% Change	Treatment	Time	Treatment x Time
BMC, g							
TRE	2852 ± 573	2866 ± 561	13.4 ± 28.5	0.55 ± 1.11	0.80	0.05	0.02
Non-TRE	2802 ± 476	2784 ± 476	-17.8 ± 23.8	-0.64 ± 0.95			
BMD, g/cm^3							
TRE	1.33 ± 0.1	1.33 ± 0.1	0.002 ± 0.035	0.17 ± 2.51	0.13	0.82	0.94
Non-TRE	1.25 ± 0.1	1.25 ± 0.1	0.001 ± 0.015	0.08 ± 1.25			
NTX, pg/mL							
TRE	1074 ± 372	1231 ± 422	28.3 ± 203.0	6.01 ± 18.98	0.13	0.30	0.83
Non-TRE	1780 ± 1540	1722 ± 982	-57.9 ± 711.7	9.88 ± 26.96			
P1NP, ng/mL							
TRE	18.7 ± 4.4	23.9 ± 18.7	-0.22 ± 2.82	-0.37 ± 14.60	0.57	0.04	0.07
Non-TRE	28.8 ± 26.4	24.7 ± 24.6	-4.07 ± 4.05	-15.3 ± 18.58			
PTH, pg/mL							
TRE	45.0 ± 22.9	56.4 ± 20.6	7.30 ± 9.90	70.7 ± 160.9	0.09	0.10	0.64
Non-TRE	62.8 ± 24.7	75.2 ± 30.4	12.34 ± 40.63	40.6 ± 71.1			

***Disclosures: Andrea Lobene**, None*

P-598

Predominant Effects of Inducible Deletion of ERα in Osteocytes as Compared to Osteoclasts in Reducing Bone Mass in Adult Female Mice *David Monroe[1], Madison Doolittle[1], Joshua Farr[1], Megan Weivoda[2], Jennifer Rowsey[1], Brittany Eckhardt[1], Daniel Fraser[1], Sundeep Khosla[1]. [1]Mayo Clinic, United States, [2]University of Michigan, United States

The skeleton has long been recognized as a major target for estrogen (E) action, however major gaps still exist in our fundamental knowledge of how E and E receptors (ERs) regulate bone metabolism. Previous studies have shown that global deletion of ERα (ERα-KO) results in increased bone mass, however this is confounded by high circulating E levels. Specific osteocyte/osteoblast ERα-KO resulted in conflicting findings, perhaps confounded by ERα effects on growth and development versus on the adult skeleton. By contrast, specific osteoclast ERα-KO throughout life has fairly consistently resulted in decreased bone mass through an increase in osteoclasts. Thus, in order to directly evaluate E effects on the adult skeleton, we developed two novel mouse models that express the tamoxifen-inducible Cre deleter, CreERT2, in either osteocytes or osteoclasts using the Dmp1(8kb) and Ctsk promoters, respectively. We crossed these models with an ERα-flox mouse and treated with tamoxifen using a predetermined regimen at 4 months of age to create the ERαΔOcy/CreERT2 and ERαΔOcl/CreERT2 adult-deleted models and analyzed the bone phenotype at 5 months. Female, but not male, ERαΔOcy/CreERT2 mice exhibited a significant decrease in trabecular BV/TV (-20.1%, P = 0.004; Panel A) and Tb.Th (-9.7%, P = 0.014) at the spine, clearly establishing a key role for osteocytic ERα in regulating the skeleton in adult female mice. Periosteal expansion (+65.6%, P = 0.004) and endocortical resorption (+64.1%, P = 0.003) were higher in ERαΔOcy/CreERT2 mice compared to control mice at the tibial diaphysis, with no change observed in Ct.Th., demonstrating an action of E through ERα to inhibit periosteal apposition and promote endocortical formation. An increase in Sdf1/Cxcl12 mRNA (1.38-fold, P = 0.002) was observed in trabecular bone at the spine, as well as an increase in the Wnt-inhibitor Sost (2.1-fold, P = 0.015), consistent with previous reports that E suppresses Sost levels in mice and humans. Interestingly, a decreasing trend in trabecular BV/TV (-10.2%, P = 0.084; Panel B) was observed in the female ERαΔOcl/CreERT2 adult-deleted model, along with a concomitant increase in serum Ctx (2.1-fold, P = 0.005). These findings thus establish that osteocytic ERα, and to a lesser extent osteoclastic ERα, is critical for E action in female, but not male, adult bone metabolism and that these effects may differ from mechanisms of E action during early growth and development.

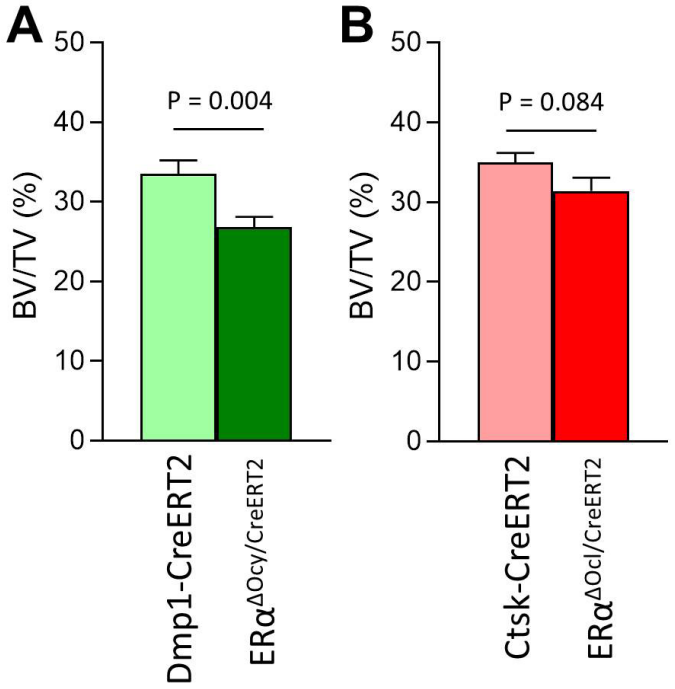

***Disclosures: David Monroe**, None*

P-599

Identification of a new circulating cellular biomarker from patients with postmenopausal osteoporosis *Kaichi Kaneko[1], Deniece Menez[1], Steven Zeng[1], Peter Sang Park[1], Haemin Kim[1], Hao Chen[1], Seyeon Bae[1], Sehwan Mun[1], Eugenia Giannopoulou[1], Emily Stein[2], Richard Bockman[2], Linda A Russell[3], Joseph Lane[4], Jessica Starr[2], Patricia Donohue[2], Kyung-Hyun Park-Min[1]. [1]Arthritis and Tissue Degeneration Program, David Z. Rosensweig Genomics Research Center, Hospital for special surgery, United States, [2]Endocrine Service, Hospital for Special Surgery, United States, [3]Rheumatology, Hospital for Special Surgery, United States, [4]Orthopedic surgery, Hospital for Special Surgery, United States

Osteoporosis is a metabolic bone disorder characterized by compromised bone mass, quality, and strength, resulting in an increased risk of fracture. More than 25% of the middle-age population has low bone mass and most remain unaware of their growing risk for fracture. Although considerable work has been done to improve diagnostic standards and tools to identify low bone mass, early detection of the predicate causes of osteoporosis does not exist. Therefore, discovering new diagnostic markers that closely correlate with early osteoporosis disease activity is imperative. Here, we describe a new cellular marker that closely correlates with increased osteoclast activity, a prime underlying cause responsible for pathological bone loss.We describe a new circulating cell population from human blood—osteoclast-enhancing cells (OECs). OECs enhance human osteoclastogenesis and express essential osteoclast-specific receptors such as CSF1R and RANK, but do not express CD66b, CD3, and CD19. OECs also express CD14, but the morphology of OECs differs from CD14+monocytes. To further characterize OECs, we performed RNA-sequencing and identified that the expression of 2697 genes was significantly (p 1.5) changed between OECs and monocytes. Ingenuity Pathway Analysis identified that the differentially expressed genes are enriched in key regulatory pathways for osteoclastogenesis including oxidative stress and interferon signaling pathways.We then hypothesized that the number of circulating OECs could act as a marker for increased osteoclastic activity in bone. To test this, we determined the frequency of OECs in blood from postmenopausal women with no treatment and compared the number of OECs with lumbar spine and total hip bone mineral density (BMD) from DXA and serum bone turnover markers. Of the 44 participants, 16 women (36%) had osteoporosis (mean age +/- SD: 67.3 +/- 8.8), 19 (43%) had osteopenia (66.8 +/- 8.8), and 9 (20%) had normal BMD (66.1 +/- 9.5). Correlation analysis showed a significant correlation between the number of OECs and BMD (p = 0.0008, r = -0.4960), and between the number of OECs and CTX (p = 0.0185, r = 0.4585). In summary, a circulating population of OECs with high osteoclastogenic activity is described and significantly increased OECs have been found in subjects with the lowest BMD values. We conclude that OECs could potentially serve as a prognostic marker for patients with low and falling bone mass.

***Disclosures: Kaichi Kaneko**, None*

P-600

The Role of Tmem263 in the Regulation of Bone Mass and Micro-architecture in Mice *Imranul Alam[1], Rita Gerard-O'Riley[1], Dena Acton[1], Sara Hardman[1], Madeline Murphy[1], Caylin Billingsley[1], Michael Econs[1]. [1]Indiana University School of Medicine, United States

Previously, several genome-wide association studies (GWAS) discovered a list of genes important in genetic variation of BMD and risk of fracture. One locus on chromosome 12q23.3 harboring the gene TMEM263 was strongly associated with hip BMD ($p<9.6x10-10$). Recently, we discovered a unidirectional allelic imbalance in TMEM263 mRNA expression in human bone. Also, we found Tmem263 mRNA was highly expressed in osteoblasts and osteocytes compared to osteoclasts. These data suggest that Tmem263 might play important roles in bone homeostasis predominantly through osteoblasts. Currently, very little is known about the TMEM263 gene as it is not part of an established protein family and most publications about this gene document the identification of open reading frame or cDNA sequences. To further identify the role of Tmem263 in bone biology, in this study, we created osteoblast-specific conditional Tmem263 knockout male and female mice using 2.3-kb α1 type 1 collagen promoter (Col2.3-α1-Tmem263) and measured bone density and micro-architecture, evaluated serum biochemistry and biomarkers of bone metabolism in growing (8 weeks) and adult (16 and 24 weeks) age. We found that Col2.3-α1-Tmem263 mice were smaller in size compared to their WT and heterozygote littermates at 8, 16 and 24 weeks of age. In addition, compared to WT and heterozygote mice, Tmem263 knockout mice exhibited significantly lower whole body aBMD and BMC in growing and adult age, and significantly lower femur and spine (L1-5) aBMD and BMC at 24 weeks of age in both male and females (Figure 1). Micro-CT analysis of trabecular bone at distal femur also revealed lower BV/TV in male and female Tmem263 knockout mice at all time points compared to the age-matched WT and heterozygote mice (Figure 1). Cortical analysis at femur midshaft showed lower cortical area and thickness in the Tmem263 homozygote knockout mice compared to the other genotypes at 24 weeks of age in female. In addition, we did not observe any significant differences for serum biochemistry (Ca, P, BUN and Creatinine) at any age as well as no differences for serum CTX, TRAP and P1NP levels at 24 weeks of age among different genotypes. Further, only Tmem263 knockout mice displayed spontaneous tail fractures at various ages. Our study demonstrates that Tmem263 plays a critical role in the regulation of bone mass and micro-architecture in mice.

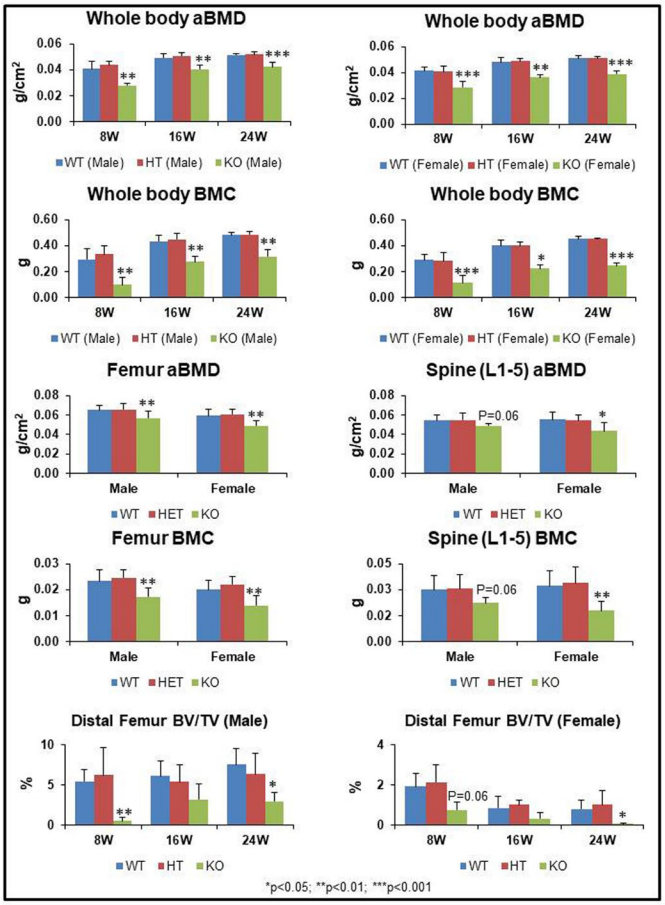

***Disclosures: Imranul Alam**, None*

P-601

ENPP1 regulates bone mass via an unidentified catalytically independent mechanism *Demetrios Braddock[1], Ralf Oheim[2], Kristin Zimmerman[1], Simon v. Kroge[2], Paul Stabach[1], Dillon Kavanagh[1], Steven Tommasini[3], Thomas Carpenter[4]. [1]Yale University, Department of Pathology, United States, [2]Department of Osteology and Biomechanics, University Medical Center Hamburg-Eppendorf, Germany, [3]Department of Orthopædics and Rehabilitation, Yale University School of Medicine, United States, [4]Department of Pediatrics at Yale University School of Medicine, United States

Heterozygous ENPP1 deficiency is associated with early onset osteoporosis, a phenotype faithfully reproduced in murine models. ENPP1 hydrolyzes extracellular nucleotide triphosphates to generate nucleotide monophosphates and pyrophosphate (PPi), however the mechanism of ENPP1 associated osteoporosis is not readily apparent given that PPi is a strong inhibitor of mineralization. Current murine models reduce both Enpp1 catalytic activity and protein expression via disruption of protein folding and stability. A single catalytic site, a Threonine at position 238 in Enpp1, is responsible for the hydrolysis of the high-energy nucleoside phosphate bond via an SN2 reaction mechanism. Accordingly, we converted the Threonine nucleophile to an Alanine in C57BL/6 mice using Crispr/Cas techniques to eliminate Enpp1 catalytic activity without disrupting protein folding or expression, and compared the skeletal and tissue mineralization phenotype in Enpp1T238A/T238A mice with WT sibling pairs, and to Enpp1asj/asj mice which exhibit disrupted protein expression and catalysis. Similar to Enpp1asj/asj mice, Enpp1T238A/T238A mice exhibited markedly decreased plasma PPi (13% of WT), increased intact FGF23 (180% of WT), phosphate wasting (70% of WT), and increased extra-skeletal calcifications in the soft tissues and joints. Of note, bone mass in Enpp1T238A/T238A mice was better preserved than in Enpp1asj/asj mice at both 10 and 23 wks of age, with normal trabecular bone volume and trabecular number (by both microCT and histomorphometry). Moreover, Enpp1T238A/T238A mice had a consistently more favorable biomechanical profile (stiffness, maximum load, and total work in tibias on 4-point bending) than Enpp1asj/asj mice. Furthermore, in contrast to Enpp1asj/asj mice, Enpp1T238A/T238A mice exhibited no evidence of osteomalacia – MAR and MLT were normal at both 10 and 23 weeks. Finally, similar to Enpp1asj/asj mice, qBEI analysis demonstrated decreased osteocyte lacunar area at both time points. Overall, this constellation of findings suggests that Enpp1 contributes to skeletal mass through an unidentified mechanism independent of its catalytic activity.

***Disclosures: Demetrios Braddock**, Inozyme Pharma, Grant/Research Support*

P-602

A decrease in NAD+ contributes to the loss of osteoprogenitors and bone mass in aged mice *Ha-Neui Kim[1], Filipa Ponte[1], Aaron Warren[1], Maria Almeida[1]. [1]University of Arkansas for Medical Sciences, United States

Age related osteoporosis results in part from a deficit in osteoblasts. The forkhead box O (FoxO) transcription factors attenuate Wnt/β-catenin signaling and thereby decrease bone formation. The NAD+ dependent Sirtuin 1 (Sirt1) deacetylates FoxOs and β-catenin in osteoblast progenitors and increases bone mass. NAD+ is recycled from nicotinamide via activity of nicotinamide phosphoribosyltransferase (Nampt). Although the number of osteoblast progenitors greatly decrease with age, it remains unknown whether dysregulation of the Sirt1/FoxO/β-catenin pathway contributes to this effect and to age-related bone loss. We found that the levels of NAD+ decrease in osteoblast progenitor cultures from old mice, associated with increased acetylation of FoxO1 and with decreased levels of Nampt – a critical enzyme of the NAD salvage pathway. Addition of the NAD+ precursor nicotinamide riboside (NR) to the cultures abrogated FoxO1 and β-catenin acetylation and increased the osteoblastogenic capacity of cells from old mice. We next administered NR (via the drinking water) to 12 month-old C57BL/6 female mice or TdRFP;Osx1-Cre mice, to achieve a dose of 400 mg/kg of body weight/day, for 8 months. NR administration increased the levels of NAD+ in liver and fat, and in cultured bone marrow-derived stromal cells. The number of TdRFP;Osx1 osteoprogenitors, present in the bone marrow, was also increased as determined by flow cytometry. Furthermore, NR attenuated the loss of cortical bone as determined by micro-CT in femur. This was associated with increased mineralizing surface while osteoclast numbers were unaffected. We next examined whether a decrease in NAD in bone cells could mimic the effects of aging. To this end, we generated mice haploinsufficient for Nampt in the mesenchymal lineage targeted by Prx1-Cre (Namptfl/+;Prx1-Cre). At 2 mo Namptfl/+;Prx1-Cre mice had no detectable bone phenotype but at 8 mo had decreased cortical thickness when compared to Namptfl/+ littermate controls, as determined by micro-CT. In addition, bone marrow derived osteoblastic cell cultures from Namptfl/+;Prx1-Cre mice had decreased NAD+ and increased FoxO1 and β-catenin acetylation, and decreased levels of β-catenin and osteoblastogenic capacity. Together, these findings suggest that the decrease in bone formation with old age is due to a decrease in NAD+ and dysregulated Sirt1/FoxO/β-catenin pathway in osteoblast progenitors.

***Disclosures: Ha-Neui Kim**, None*

P-603

Loss of Osteogenic Dickkopf-1 Ameliorates Cortical and Trabecular Bone Loss by Suppressing Bone Resorption in Male Mice With Type 1 Diabetes Mellitus *Souad Daamouch[1], Juliane Coldtitz[1], Nick Hildebrandt[1], Sylvia Thiele[1], Lorenz C. Hofbauer[1], Martina Rauner[1]. [1]Department of Medicine III and Center for Healthy Aging, Technische Universität, Germany

Patients with type 1 diabetes mellitus (T1D) have decreased bone mass and increased susceptibility to fractures. The underlying molecular mechanisms, however, remain incompletely understood. Studies have shown that patients suffering from T1D have an increased expression of Dickkopf-1 (Dkk-1), a potent inhibitor of the pro-osteogenic Wnt signaling pathway. Here, we investigated the role of Dkk1 in a mouse model of T1D-induced bone loss.T1D was induced in 10-week-old male mice with Dkk1-deficiency in osteoblasts/osteocytes (Dkk1f/f; Dmp1-Cre, cKO) by 5 subsequent injections of streptozotocin (40 mg/kg). Control groups received citrate buffer. Four weeks later, the bone phenotype was analyzed using µCT and dynamic histomorphometry. Each group contained 8-10 mice. We measured the blood glucose level and body weight twice per week throughout the experiment. Further, a glucose tolerance test (GTT) was performed.During the experiment, diabetic mice did not gain body weight compared to control mice and further lost their perigonadal and subcutaneous fat pads. There were no differences between Dkk1-cKO and control mice. Diabetic mice had highly elevated serum glucose levels and impaired glucose tolerance; however, this was regardless of Dkk1.T1D led to a 36% decrease in trabecular bone volume in control animals, whereas Dkk1 cKO mice only lost 16% of bone volume. Moreover, trabecular number was decreased and trabecular separation increased in T1D control mice, whereas it remained unchanged in T1D Dkk1 cKO mice. Moreover, Dkk1 cKO mice were completely protected from T1D-induced cortical bone loss. T1D suppressed the bone formation rate, the number of osteoblasts in trabecular bone, and serum levels of P1NP in both, Dkk1-deficient and sufficient mice. This may be explained by the increase in serum sclerostin levels in both genotypes. In contrast, the number of osteoclasts and TRAP serum levels only increased in diabetic control mice, but not in Dkk1 cKO mice.In summary, Dkk1 derived from osteogenic cells does not influence the development of T1D, but plays a crucial role in T1D-induced bone loss in male mice by regulating osteoclast numbers.

***Disclosures: Souad Daamouch**, None*

P-604

Cathepsin D regulates bone mass through distinct mode of actions in the autophagy pathway in osteoblasts and osteoclasts *Chao Wan[1], Fengjie Zhang[1], Wing Pui Tsang[1], Qiling He[2]. [1]Key Laboratory for Regenerative Medicine, Ministry of Education, School of Biomedical Sciences, Faculty of Medicine, The Chinese University of Hong Kong, Hong Kong SAR, China., Hong Kong, [2]Department of Microbiology, University of Alabama at Birmingham, AL 35294, USA., United States

Insufficiency in nutrient and oxygen availability, oxidative stress, and autophagy failure are fundamental factors for the decline of bone mass and strength with aging. Accumulating evidence indicates that these factors affect normal autophagosomal or lysosomal activities which are the major force in clearance of aggregated or damaged proteins. Cathepsin D (CtsD), the principal lysosomal aspartate protease and a main endopeptidase, functions in the normal activity of autophagosome and lysosome. It is indicated that CtsD exists in the skeletal tissue during development or injury. However, the molecular and cellular mechanisms of CtsD mediated autophagosome or lysosome function in the skeletal homeostasis remain unclear. In the present study, we showed that global knockout of CtsD dramatically decreased bone mass in the 3-week old mutant mice compared with their control littermates as indicated by decreased BV, BV/TV, BS, trabecular number, trabecular thickness and increase trabecular separation in the microCT analysis. Histomorphometry analysis revealed that the phenotype was characterized by decreased osteoblast numbers, osteoblast surface/bone surface and mineral apposition rate, increased osteoclast numbers, osteoclast surface/bone surface and erosion surface/bone surface. At molecular level, siRNA medicated inactivation of CtsD in MC3T3E1 cells attenuated osteoblastic differentiation and downregulated LC3B expression, which was accompanied by decreased levels of P62, p-Akt and p-GSK-3beta in osteoblasts. Intriguingly, inactivation of CtsD in RAW264.7 cells increased osteoclast differentiation with decreased LC3B expression but upregulated P62 level. This was accompanied by alterations in the formation of autophagosome and differential gene profiles associated with the autophagy pathway during the differentiation of osteoblasts and osteoclasts. The results suggest that CtsD mediated autophagy pathway plays important roles in regulation of bone mass and homeostasis through distinct mode of actions in osteoblasts and osteoclasts, fine tuning of CtsD activity may serve as a potential therapeutic target for the maintenance of bone mass.

***Disclosures: Chao Wan**, None*

P-605

Glycosaminoglycan and Pyridinoline content at forming trabecular surfaces are strongly associated with fracture incidence independent of clinical diagnosis and estimated fracture risk based on BMD. *Eleftherios P. Paschalis[1], Sonja Gamsjaeger[1], Stamatia Rokidi[1], David Dempster[2], Hua Zhou[2], Elizabeth Shane[2], Adi Cohen[2], John P. Bilezikian[2], Mishaela Rubin[2], Carolina Moreira[3], Vicente F.C. Andrade[3], Socrates Papapoulos[4], Erik F. Eriksen[5], Klaus Klaushofer[1]. [1]Ludwig Boltzmann Institute of Osteology at the Hanusch Hospital of WGKK and AUVA Trauma Centre Meidling, 1st Medical Department, Hanusch Hospital, Vienna, Austria, Austria, [2]Medicine and Pathology, College of Physicians and Surgeons of Columbia University, New York, New York, USA, United States, [3]Endocrinology Division (SEMPR), Federal University of Parana, Curitiba, Brazil, Brazil, [4]Center for Bone Quality, Leiden University Medical Center, Leiden, The Netherlands, Netherlands, [5]Oslo University Hospital and Institute of Clinical Medicine, University of Oslo, Oslo, Norway, Norway

Background: Bone fragility is attributed to low BMD as well as altered structure and material properties. In the present work we tested the hypothesis that organic matrix quality at actively forming trabecular surfaces is associated with fragility fracture incidence (Fx) independent of BMD and clinical diagnosis.Methods: We used Raman microspectroscopy to analyze iliac crest biopsies from females who belonged any of three groups: 1. Healthy (HC; ages 1.5 – 59 yrs, N = 124) 2. Women sustaining Fx irrespective of clinical diagnosis and BMD (Fx; ages 2 – 74 yrs, N = 92) 3. Women with altered BMD values but without Fx (NC; ages 23-74 yrs, N = 79). The measured indices were: mineral/matrix (MM; affecting stiffness and brittleness), glycosaminoglycan (GAG; negative modulators of mineral homeostasis; involved in collagen fibrilogenesis), and pyridinoline (Pyd; associated with fiber stiffness, ultimate stress and post-yield energy and strength, and bending strength) contents at forming cancellous surfaces. Spectra were obtained between the second fluorescent label and the mineralizing front (TA1), between the two labels (TA2), and right behind the first label (TA3). Individual patient data were considered as a function of patient- and tissue-age. Additionally, lumbar spine (LS) and femoral neck (FN) Z-scores were available for all subjects except healthy females aged 1-19 years. LS, FN, and total hip (TH) T-scores were available for all subjects except healthy females aged 1-19 years, as well as children diagnosed with mild osteogenesis imperfecta.To evaluate differences in BMD, and bone quality related spectroscopic parameters between the 3 groups, 2-way analysis of covariance (ANCOVA) was applied with age as a continuous covariate and tissue age as categorical cofactor. Sidák´s post-hoc test was used for pairwise comparisons amongst levels of skeletal health status. Differences were considered significant at $p<0.05$.Findings: ANCOVA indicated that BMD Z- and T-scores discriminated between HC and either Fx or NC groups but not between Fx and NC. On the other hand, unlike MM, GAGs and Pyd contents discriminated between patients in the 3 groups (Table 1).Interpretation: The results indicate that GAG and Pyd contents identify patients sustaining fragility fractures irrespective of clinical diagnosis and commonly employed clinical screening tools. Thus, they provide new insight into the pathogenesis of skeletal diseases characterized by fragility fractures.

Table 1: Results of the ANCOVA of spectroscopic parameters at actively bone forming trabecular surfaces

Pairwise Comparisons			
Dependent Variable: MM			
(I) HEALTH	(J) HEALTH	Mean Difference (I-J)	p values
HC	Fx	-0.001	1
	NC	0.027	0.427
Fx	NC	0.027	0.449
Dependent Variable: GAGs			
(I) HEALTH	(J) HEALTH	Mean Difference (I-J)	p values
HC	Fx	-.036*	<0.0001
	NC	0.018	0.312
Fx	NC	.054*	<0.0001
Dependent Variable: Pyd			
(I) HEALTH	(J) HEALTH	Mean Difference (I-J)	p values
HC	Fx	-.007*	<0.0001
	NC	.002*	0.002
Fx	NC	.009*	<0.0001

***Disclosures: Eleftherios P. Paschalis**, None*

Posters

P-606

Exaggerated Bone Microarchitecture Defects and Osteopenia After Splenectomy in a Thalassemia Mouse Model *Hui Sun[1], Ling Wang[2], Matthew Sherrier[1], Mark Gladwin[2], Hongshuai Li[1]. [1]Musculoskeletal Growth & Regeneration Laborotary, Department of Orthopaedics Surgery, University of Pittsburgh, United States, [2]Pittsburgh Heart, Lung, and Blood Vascular Medicine Institute, Department of Medicine, University of Pittsburgh, United States

Thalassemia bone disease (TBD) is a common and severe complication in β-thalassemias for which there is limited prevention or treatment options. Clinical manifestations of TBD include osteoporosis, fragility fractures, and pain. The etiology of low bone mass is multifactorial with ineffective erythropoiesis, iron overload, chelation, and endocrine dysfunction all being implicated. Splenectomy, a common surgical procedure to help maintain hemoglobin levels, is strongly correlated with increased risk of osteoporosis in thalassemic patients. However, little is known about the mechanism of TBD progression after splenectomy. In this study, we characterize the effects of splenectomy on bone abnormalities in a thalassemic mouse model and explore the possible mechanisms. A heterozygous mouse model of β0-thalassemia (Hbbth3/+), which demonstrates moderate anemia and severe splenomegaly was used. Th3/+ mice were found to have cranial bone enlargement, decreased BV/TV, Tb. N, and Tb. Th on trabecular bone of spine and proximal tibia, decreased cortical bone thickness, bone area, and increased marrow area (mid-shaft femur) when compared to WT controls. Osteopenia and bone microstructural defects were present in both male and female th3/+ mice, although more severe in males. Splenectomy at age 4 weeks significantly worsened the geometric parameters in trabecular and cortical bone in both male and female th3/+ mice when compared with th3/+ sham surgery controls. Splenectomy had no significant influence on bone geometric parameters in WT controls. Histomorphometric analyses demonstrated decreased bone formation and increased resorption in th3/+ mice, which was exaggerated after splenectomy. To explore the mechanism, iron metabolism was tested. When compared to WT controls, Pearl's staining in th3/+ mice revealed progressive iron accumulation in liver and spleen, but less so in bone marrow. Following splenectomy in th3/+ mice, there was a significant increase in hepatic iron accumulation but significantly decreased iron content in bone marrow. This study demonstrates accelerated bone loss after splenectomy in a thalassemic animal model, which represents clinical observations seen in human patients. The worsened bone loss after splenectomy is due to further decreased bone formation and increased bone resorption. Splenectomy exaggerates the hepatic iron overload and conversely causes iron deficiency in the bone marrow, which may accelerate the progression of the bone abnormalities in thalassemia.

***Disclosures: Hui Sun**, None*

P-607

Abaloparatide Promotes Bone Repair of Vertebral Defects in an Ovariectomized Rat Model of Osteoporosis *Akito Makino[1], Tomoka Hasegawa[2], Hideko Takagi[1], Yoshimasa Takahashi[1], Naoki Hase[1], Norio Amizuka[2]. [1]Pharmacology Research Department, Teijin Pharma Limited, Japan, [2]Developmental Biology of Hard Tissue, Graduate School of Dental Medicine, Hokkaido University, Japan

Objective: Osteoporotic vertebral fractures (OVF) are associated with morbidity and mortality. This study was examined to investigate the effects of abaloparatide, a bone anabolic agent for the treatment of severe osteoporosis, on bone repair in ovariectomized (OVX) rats with vertebral defects.Material and Methods: Female Sprague-Dawley rats (7-8 weeks old) were subjected to OVX or sham surgery. After 32 +/- 4 days of bone depletion period, bone defects were created in OVX animals at L4-L6 vertebral bodies using a 1.5 mm diameter dental drill. OVX animals were given once-daily subcutaneous injection of abaloparatide at a dose of 30 μg/kg or vehicle for maximum 6 weeks from the day of the vertebral defect surgery (Day 0). Animals weresequentially sacrificed at Day 3, Week 1, Week 2, Week 4, and Week 6, followed by collecting defected (L4-L6) and non-defected (L3) vertebrae. Bone mass and trabecular structural parameters (BV/TV, Tb.Th, Tb.N, and Tb.Sp) of the vertebrae were measured by DXA and micro-CT. Bone strength was measured by a vertebral body compression test.Results: OVX animals showed significantly lower lumbar BMD than sham animals at the end of the bone depletion period. At the defected site of vertebrae, abaloparatide showed significantly higher BMC than vehicle at Week 2, Week 4, and Week 6. Trabecular structure parameters were significantly improved by abaloparatide administration after Week 2. Abaloparatide showed significantly greater increases in bone strength of defected vertebrae than vehicle at Week 2, Week 4, and Week 6. Histological analysis revealed that alkaline phosphatase and cathepsin K positive cells were abundant on the surface of new bone by abaloparatide administration, suggesting that bone remodeling is highly promoted at the defected site. Abaloparatide also showed significantly higher BMD and bone strength at non-defected vertebrae. There was no significant change in serum calcium concentrations by abaloparatide during the administration period.Conclusion: Abaloparatide promoted bone repair of defected vertebrae with an increase in bone strength in OVX rats. Abaloparatide also improved BMD and bone strength at non-defected vertebrae. These results suggest that abaloparatide is a promising therapeutic option for the treatment of severe osteoporosis with OVF.

***Disclosures: Akito Makino**, None*

P-609

Loss of glucocorticoid rhythm induces an osteoporotic phenotype in mice *Maaike Schilperoort[1], Jan Kroon[2], Sander Kooijman[2], Kathrin Mletzko[3], Leo vanRuyven[4], Felix Schmidt[3], Bjorn Busse[3], Alberto Pereira[2], Natasha Appelman-Dijkstra[5], Nathalie Bravenboer[6], Patrick Rensen[2], Onno Meijer[2], Elizabeth Winter[5]. [1]Department of Medicine, Division of Endocrinology, Einthoven Laboratory for Experimental Vascular Medicine, Netherlands, [2]Department of Medicine, Division of Endocrinology, Einthoven Laboratory for Experimental Vascular Medicine, Netherlands, [3]Department of Osteology and Biomechanics (IOBM), University Medical Center Hamburg-Eppendorf, Germany, [4]Department of Functional Anatomy, Academic Centre for Dentistry Amsterdam (ACTA), Netherlands, [5]Department of Medicine, Division of Endocrinology, Center for Bone Quality, Einthoven Laboratory for Experimental Vascular Medicine, Netherlands, [6]4Department of Clinical Chemistry, Vrije Universiteit Amsterdam, Amsterdam Movement Sciences, Netherlands

Glucocorticoid (GC)-induced osteoporosis is a widespread health problem that is accompanied with increased fracture risk. Detrimental effects of GC therapy on bone have been ascribed to the excess in GC exposure, but it is unknown whether disruption of the endogenous GC rhythm inherent to GC therapy also plays a role. To investigate this, we subcutaneously implanted female C57Bl/6J mice with either vehicle pellets or slow-releasing corticosterone (CORT) pellets to blunt CORT rhythm without inducing hypercortisolism (n=10 mice/group). This experiment was approved by the Central Animal Experiments Committee. Flattening of the CORT rhythm for 7 weeks reduced cortical and trabecular bone volume (-8.1%, P=0.0009 and -25.5%, P=0.017 respectively), cortical and trabecular thickness (-6.9%, P<0.0001 and -8.7%, P=0.03 respectively), and cortical BMD (-3.4%, P=0.032), as determined by micro-CT analysis. Furthermore, TRAP levels were increased (+42%, P=0.008) while P1NP levels were decreased (-37%, P<0.0001) in plasma of mice with a flattened CORT rhythm compared to vehicle, indicative of a negative balance in bone remodelling. Double calcein labeling of bone in vivo revealed a reduced bone formation, as reflected by a reduced mineral apposition rate (MAR; -20%, P=0.018), mineralizing surface per bone surface (MS/BS; -23%, P=0.014) and bone formation rate per bone surface (BFR/BS; -39%, P=0.002). Collectively, these perturbations in bone turnover and structure decreased bone strength (-14.7%, P=0.003) and stiffness (-11.1%, p=0.003), as determined by mechanical testing. In conclusion, we demonstrate for the first time that flattening of the GC rhythm results in an osteoporotic phenotype in mice. Our findings indicate that at least part of the fracture risk associated with GC therapy may be the consequence a disturbed GC rhythm, rather than an excess in GC dose alone.

***Disclosures: Maaike Schilperoort**, None*

P-610

The bone Quality Index of Mineral Maturity / Crystallinity at forming trabecular surfaces and its potential role in the bone mineral loss evident in postmenopausal osteoporosis *Sonja Gamsjaeger[1], Klaus Klaushofer[1], Eleftherios Paschalis[1]. [1]Ludwig Boltzmann Institute for Osteology, Austria

Bone formation consists of two phases: the initial formation of mineral crystals and the subsequent mineral accumulation.In the present study, we used Raman microspectroscopic analysis of iliac crest biopsies from healthy females (HC; N = 108) and postmenopausal osteoporosis patients (PMOP) receiving placebo (N = 66) to test the hypothesis that at forming trabecular surfaces, mineral maturity / crystallinity (MMC) of the youngest crystallites associates with the amount of subsequent mineral accumulation. Surfaces were chosen based on the presence of fluorescent double labels, allowing measurements at three tissue ages: between the second label and the mineralizing front, between the two labels, and right behind the first one.The mineral content was estimated from the ratio of the v2PO4 band (410–460 cm−1) integrated area to the spectral slice 494-509 cm-1 (PMMA). MMC was approximated from the inverse of the full width at half height (FWHH) of the v1PO4 (930–980 cm−1) band.Individual patient values were considered as a function of age and tissue age. To evaluate differences in bone mineral content and MMC between the levels of skeletal health status, 2-way analysis of covariance (ANCOVA) was applied with biological age as continuous covariate and tissue age as categorical cofactor, followed by Sidák´s post-hoc test. Differences were considered significant at p<0.05.The results (Fig. 1) indicated that there were no differences in amount of initial mineral formed between healthy females and postmenopausal osteoporosis patients, while PMOP had larger crystallites and decreased mineral content compared to healthy females at the two older tissue ages considered.This can affect bone as follows:i) affect the mechanical properties of bone as larger crystallites have been shown to result in compromised mechanical attributes.ii) increased homogeneity in the distribution of MMC values.iii) larger crystallites grow slower compared to smaller ones due to decreased crystallite specific surface area. Thus, it is conceivable that the decelerated mineral accumulation in PMOP is in part due to the larger crystallites that are initially formed, compounding the bone mineral loss due to increased bone resorption in PMOP patients.In conclusion, the results of the present analysis indicate that increased MMC of the youngest formed mineral may contribute to the bone mineral loss evident in PMOP and the accompanying increased fracture risk independently of bone turnover rate.

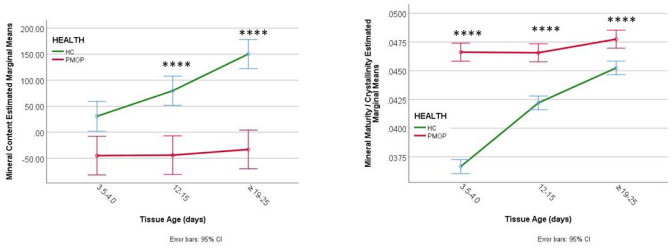

***Disclosures: Sonja Gamsjaeger**, None*

P-611

Bilirubin increases the viability of osteoclasts: An in vitro study *Susana Jurado[1], Núria Guañabens[2], Pilar Peris[2], Andreu Combalia[2], Ana Monegal[2], Albert Pares[2]. [1]CIBERehd, Spain, [2]Hospital Clinic, University of Barcelona, Spain

Introduction Osteoporosis is a complication of primary biliary cholangitis (PBC), a liver disease resulting in cholestasis with increased circulating bile acids and bilirubin. Bilirubin and litocholic acid (LCA) have harmful effects on osteoblasts and osteocytes in vitro. Ursodeoxycholic acid (UDCA), which is used in the treatment of PBC patients, neutralizes these deleterious actions. The effects of bilirubin and LCA on osteoclasts have not been analyzed, although there is evidence of increased bone resorption, especially in cholestatic end-stage disease. Objective To analyze the effects of bilirubin, LCA and UDCA on the viability of osteoclast cells obtained from differentiated RAW 264.7 cells. Methods The murine macrophage cell line RAW 264.7 was seeded in 96 well plates at a density of 8,000 cells per well and cultured in α-MEM with 10% FBS and 30 ng/mL of RANKL for 7 days. Differentiation into osteoclasts was assessed by TRAP stain. FBS in media was reduced to 2% and cells were treated for 24 hours with: bilirubin (10 µM, 50 µM and 100 µM), LCA (10 µM, 100 µM and 500 µM) and UDCA (10 µM, 100 µM and 500 µM), as well as combinations of LCA 10 µM and/or bilirubin 50 µM with UDCA 10 µM or 100 µM. Controls were an untreated group and a positive control group treated with Camptothecin (CAM, 0.5 µM) to potentiate cell death. Cell viability was measured using the WST-1 assay. In each experiment, three replicates were made per condition and experiments were performed 6 times. Results Treatment with bilirubin increased osteoclast viability when compared with the untreated control group. Although there was a slight decrease in cell viability at 10 µM (10%), a progressive increase was observed at bilirubin concentrations of 50 µM (35%) and 100 µM (80%; p<0.007). By contrast, cell viability decreased significantly with CAM, LCA and UDCA (500 µM) (59%, 53% and 77%). Combination treatments showed that bilirubin 50 µM with UDCA 10 µM or LCA 10 µM increased viability by 37% and 60%, respectively. LCA 10 µM plus UDCA 100 µM decreased cell viability by 35%. Conclusions Bilirubin increases viability of differentiated osteoclasts from RAW 264.7 cells. This effect of bilirubin counteracts the deleterious actions of litocholic and ursodeoxycholic acids, favoring viability even in the presence of these substances. Therefore, bilirubin at concentrations found in patients with severe cholestasis may contribute to increased bone resorption and the development of osteoporosis.

***Disclosures: Susana Jurado**, None*

P-612

The Regulatory Role of PiRNA-63049 in Pathogenesis of Osteoporosis via Targeting Wnt2b *Gaoyang Chen[1], Shang Wang[1], Songlin Peng[1]. [1]The Second Clinical Medical College of Jinan University, China

Purpose: Osteoporosis is an age-related metabolic osteopathy, which leads to bone fragility and increased risk of fracture. The bone marrow stromal cells (BMSCs) play critical roles in the process of osteoporosis. However, the osteogenic differentiation ability of osteoporotic BMSCs was significantly decreased, leading to the decrease of bone formation. Recent studies have shown that piwi-binding RNA (piRNA) was involved in the occurrence of diseases at post transcriptional level. However, to the best of our knowledge, the role and regulatory mechanism of piRNA in bone and joint diseases remains unclear.Methods: The differential expression profile of piRNA in BMSCs of osteoporotic rats was detected using RNA sequencing, and then verified by quantitative real time PCR. The piRNA-mRNA networks were conducted to predict the potential targets of differentially expressed piRNAs. The hub piRNA-mRNA axis was screened out based on bioinformatics analysis and correlation analysis. The luciferase report gene assay was carried out to verify the binding sites of piR-63049 and Wnt2b. PiR-63049 mimics and inhibitor were transfected into BMSCs to evaluate the effect of knocking-down and over-expressing piR-63049 on osteogenic differentiation of BMSCs. Antagomir of piR-63049 was used to evaluate the effect of piR-63049 on prevention and treatment of osteoporosis via the tail vein injection in ovariectomized rats.Results: Our study showed a novel non-coding RNA, piR-63049, may play important roles in bone metabolism in osteoporosis. The expression of piR-63049 was significantly increased in of osteoporotic rats and peripheral blood mononuclear cells of patients with osteoporosis, while negative linear with the osteogenic differentiation of BMSCs. The further bioinformatics and luciferase study showed that Wnt2b was the potential target of piR-63049. Furthermore, Wnt2b is a positive regulator in Wnt/beta-catenin signaling during bone formation. Over-expressing piR-63049 could attenuate the osteogenic differentiation of BMSCs, while knocking down piR-63049 could promote the osteogenic differentiation of BMSCs. In vivo experiment further verified the stimulating effect of knocking-down piR-63049 on bone formation.Conclusion: Our study revealed the differential expression profile of piRNA in osteoporotic BMSCs and screened out piR-63049 as the hub piRNA, which might play critical role in osteogenic differentiation of BMSCs and bone metabolism in osteoporosis via targeting Wnt2b.

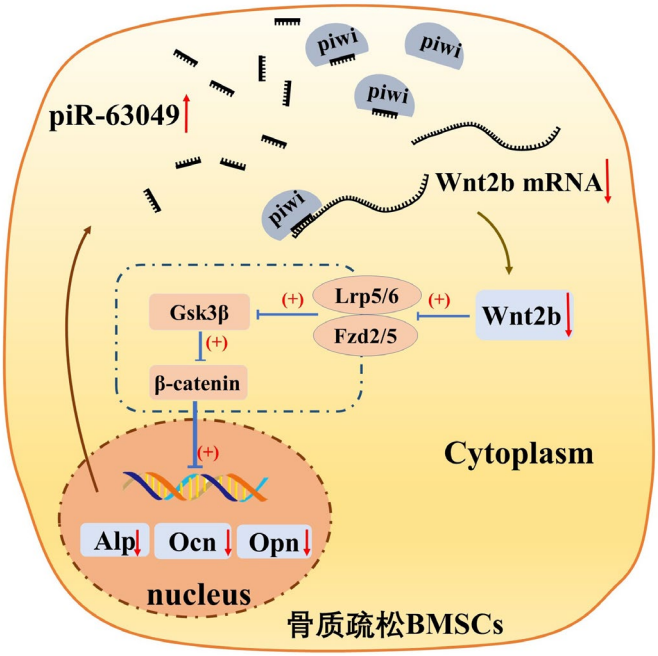

***Disclosures: Gaoyang Chen**, None*

P-613

Alendronate suppresses initiation of bone formation in cortical bone in postmenopausal osteoporosis *Xenia G Borggaard[1], Jean-Paul Roux[2], Jean-Marie Delaisse[1], Pascale Chavassieux[2], Christina M Andreasen[1], Thomas L Andersen[1]. [1]Molecular Bone Histology Team, Clinical Cell Biology, Research Unit of Pathology, Dept. of Clinical Research, University of Southern Denmark and Dept. of Pathology, Odense University Hospital, Denmark, [2]INSERM UMR 1033, Université de Lyon, France

In cortical bone, the age-induced and osteoporosis-related porosity is attributed to accumulation of enlarged eroded pores, reflecting a delayed bone formation. This study focus on the cortical effect of alendronate treatment within postmenopausal osteoporotic (PMO) women. Intracortical pores were measured and categorized according to their surface (eroded, eroded-formative, formative or quiescent) on 89 transiliac biopsies obtained from the International Phase III study of alendronate. Biopsies collected from PMO women after either two years of treatment with alendronate (n = 9) or placebo (n = 26) or after three years of treatment with alendronate (n = 15) or placebo (n = 39) were investigated as pooled (placebo vs. treatment). The cortical porosity (%) and pore density (#/T.Ar) was unaffected by alendronate treatment in PMO. Cortical porosity, but not pore density, correlated positively with pore diameter in both alendronate and placebo (r2=0.77, p<0.0001 and r2=0.74, p<0.0001, respectively) and mainly reflected non-quiescent pores. In alendronate compared to placebo a significantly higher percentage of the cortical porosity reflected eroded pores (p<0.001) and a significantly lower percentage reflected eroded-formative pores (p0.01). This was evident, although fractions (%) of eroded and eroded-formative pores did not change with treatment. Interestingly, although the contribution of eroded and eroded-formative pores correlates negatively and positively (respectively) with the degree of porosity in placebo, these correlations disappear upon alendronate treatment. Additionally, the prevalence of formative pores and their contribution to cortical porosity decreased significantly in the alendronate treatment compared to placebo ($p < 0.01$ and $p < 0.05$, respectively), whereas pore size and mean wall thickness did not change significantly.Overall, the ratio between eroded pores and pores with initiated formation was significantly higher for alendronate treatment ($p < 0.001$), while the wall thickness reflecting the magnitude of bone previously formed in quiescent osteons was not statistically different comparing alendronate and placebo. Collectively, this study shows that alendronate further inhibit the initiation of bone formation in cortical bone, rather than affecting the magnitude of bone formed when initiated.

***Disclosures: Xenia G Borggaard**, None*

Posters

P-614

Effects of Spaceflight on Cancellous and Cortical Bone in Proximal Femur in Rats *Lara Sattgast[1], Amanda Gamboa[1], Dawn Olson[1], Adam Branscum[2], Urszula Iwaniec[1], Russell Turner[1]. [1]Skeletal Biology Laboratory, Oregon State University, United States, [2]Oregon State University, United States

Bone loss is common in astronauts during long-duration spaceflight missions with severe bone loss often occurring in the proximal femur, a region not typically investigated in animal models. We recently evaluated bone microarchitecture in the femoral head in rapidly growing male Sprague Dawley rats subjected to a 4-day spaceflight aboard STS-41. Compared to ground controls, cancellous bone volume fraction (bone volume/tissue volume, BV/TV) was dramatically lower in the flight animals. Because the effects of spaceflight on the rodent skeleton can vary with age, duration of flight, and potentially strain and sex, we evaluated bone in the femoral head from two additional missions: a 10-day mission (STS-57) using growing male Fisher rats, and a 14-day mission (STS-62) using growing ovariectomized (ovx) Fisher 344 rats. Cancellous microarchitecture and cortical thickness were assessed using microcomputed tomography. In male rats, BV/TV was lower in flight animals compared to flight controls but differences were not significant compared to baseline, suggesting that osteopenia was due in part to reduced bone accrual. In ovx rats, BV/TV was lower in flight animals compared to flight controls and tended to be lower (p=0.06) compared to baseline. Whereas BV/TV was lower in flight animals compared to flight controls in all studies, changes in bone microarchitecture (connectivity density, trabecular thickness, number, and separation) in response to spaceflight were not uniform among studies. Cortical thickness did not differ among groups in any of the studies. Taken together, these findings support the conclusion that spaceflight results in cancellous osteopenia in femoral head of growing rats. Fractures in humans occur at several locations in the femoral neck, including intertrochanteric, transcervical neck, subcapital neck, and subtrochanteric region. Fractures occurring through the femoral head are more commonly associated with trauma and are particularly difficult to manage. That being said, traumatic injury would be the most likely cause of a fracture during a spaceflight mission and a microgravity-induced reduction in bone volume fraction at this site would likely reduce the magnitude of trauma required for fracture. We therefore conclude that future studies performed in more skeletally mature animals should carefully evaluate this site.

***Disclosures: Lara Sattgast**, None*

P-615

Synthesis and in vitro evaluation of a bispecific aptamer targeting both Sclerostin and Dickkopf-1 *Zhenjian Zhuo[1], Shuaijian Ni[2], Zongkang Zhang[1], Ning Zhang[1], Yuanyuan Yu[2], Aiping Lu[2], Ge Zhang[2], Bao-Ting Zhang[1]. [1]The Chinese University of Hong Kong, Hong Kong, [2]Hong Kong Baptist University, Hong Kong

Synthesis and in vitro evaluation of a bispecific aptamer targeting both Sclerostin and Dickkopf-1Zhenjian Zhuo1,5*, Shuaijian Ni2,3,4,5*, Zongkang Zhang1, Ning Zhang1, Yuanyuan Yu2,3,4, Aiping Lu2,3,4, Ge Zhang2,3,4 & Bao-Ting Zhang11School of Chinese Medicine, Faculty of Medicine, The Chinese University of Hong Kong, Hong Kong SAR, China,2Law Sau Fai Institute for Advancing Translational Medicine in Bone & Joint Diseases, School of Chinese Medicine, Hong Kong Baptist University, Hong Kong SAR, China,3Institute of Integrated Bioinformedicine and Translational Science, School of Chinese Medicine, Hong Kong Baptist University, Hong Kong SAR, China,4Guangdong-Hong Kong-Macao Greater Bay Area International Research Platform for Aptamer-based Translational Medicine and Drug Discovery, Hong Kong, China,5Aptacure Therapeutics Limited, Kowloon, Hong Kong SAR, China*Contributed equally.Abstract: Sclerostin antibody treatment has been reported to promote bone formation, whereas the promotion wanes over time due to the increased Dickkopf-1 as a negative feedback. It is desirable to co-inhibit both Sclerostin and Dickkopf-1. However, immunogenicity, production, and stability are the major concerns of antibody. Aptamers are non-naturally oligonucleotides with high specificity and affinity to proteins without the above concerns. We have obtained an aptamer against Sclerostin, and an aptamer against Dickkopf-1 from published study. We first synthesized bispecific aptamer candidates targeting both Sclerostin and Dickkopf-1 by coupling of 5' an amine-functionalized aptamer1 with N-hydroxysuccinimide-activated PEG (PEG3/PEG6/PEG9/PEG24) and 3' a thiol-functionalized aptamer2 with maleimide bound to the other end of bivalent PEG (PEG3/PEG6/PEG9/PEG24) linker (F-1). Aptbis03, aptbis04, aptbis07 and aptbis08 with higher binding specificity to Sclerostin and Dickkopf-1 were chosen for affinity characterization (F-2). Aptbis03 and aptbis07 with low nM level of affinity to both Sclerostin and Dickkopf-1 were chosen for activity characterization (F-3). The inhibition potency of the aptamer candidates on antagonistic effects of both Sclerostin and Dickkopf-1 in Wnt signaling in vitro was further examined. Aptbis03 with the best inhibition potency was identified (F-4). This work develops a bispecific aptamer targeting both Sclerostin and Dickkopf-1. Acknowledgments: This study was supported by the Innovation & Technology Fund (UIM/328) and General Research Fund (14108816).

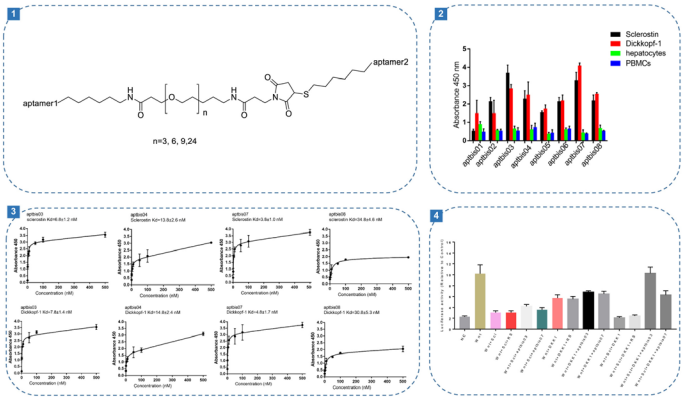

Figure 1 Schematic diagram of synthesizing bispecific aptamers using fragment condensation by bis-functionalized PEG linkers with a maleimide group. **Figure 2 The specificity characterization of the bispecific aptamer candidates.** Bispecific Aptamer candidates aptbis03, aptbis04, aptbis07 and aptbis08 with higher binding specificity to sclerostin and Dickkopf-1 were chosen for the following affinity characterization. **Figure 3 Affinity characterization of the bispecific aptamer candidates.** The binding curves was plotted and fitted by non-linear fitting and the KD value for each candidate was calculated. Aptbis03 and aptbis07 which showed low nM level of affinity to both sclerostin and Dickkopf-1 were chosen for the following activity characterization. **Figure 4 Inhibition potency of the optimal aptamer candidates to Sclerostin's and Dickkopf-1's antagonistic effect on Wnt signaling**.

***Disclosures: Zhenjian Zhuo**, None*

P-616

Kynurenine Promotes Age-Related Bone Loss via Upregulating RANKL–Induced Osteoclastogenesis and Inhibiting Bone Marrow Mesenchymal Stem Cells Osteogenesis *Nada Eisa[1], Sakamuri Reddy[2], Ahmed Elmansi[3], Galina Kondrikova[1], Dmitry Kondrikov[3], Xing-Ming Shi[4], Chad Novince[5], Mark Hamrick[6], Meghan McGee-Lawrence[7], Carlos Isales[8], Sadanand Fulzele[9], William Hill[3]. [1]Dept. Pathology, Medical University of South Carolina, United States, [2]Dept. Pediatrics, Medical University of South Carolina, United States, [3]Dept of Pathology, Medical University of South Carolina, United States, [4]Department of Neuroscience and Regenerative Medicine, Augusta University, United States, [5]College of Dental Med / Oral Health Sciences, Medical University of South Carolina, United States, [6]Dept of Cellular Bio & Anatomy, Augusta University, United States, [7]Dept Cellular Bio & Anatomy, Augusta University, United States, [8]Sec Endocrinology, Augusta University, United States, [9]Dept of Orthopedic Surgery, Augusta University, United States

Aging is associated with a decrease of bone mass that increases the risk for osteoporosis and fractures to the spine and extremities. While accumulating evidence from diverse studies show the involvement of kynurenine (KYN) - an oxidized, or IDO-1, tryptophan metabolite - in aging related bone loss, the direct effect of KYN on osteoclast formation has not been studied. We have previously reported that KYN contributes to aging-related bone loss via reducing in vivo and in vitro osteogenic differentiation potential of bone marrow mesenchymal stem cells. Further, we showed that in vivo treatment with KYN significantly increased the number of osteoclasts on bone surfaces suggesting that in addition to inhibiting bone formation it could drive increased bone resorption. Here, we report the direct effect of KYN on receptor activator of nuclear factor kappa B ligand (RANKL)-induced in vitro osteoclastogenesis. We show that treating RAW 264.7 macrophages cells with KYN results in dose dependent enhancement of RANKL-induced osteoclast differentiation. This was evident by the significant increase in number of multinucleated TRAP positive osteoclasts, significant increase in hydroxyapatite bone resorptive activity and significant upregulation of osteoclast differentiation genes including c-Fos, CTSK and DC-STAMP. Mechanistically the aryl hydrocarbon receptor (AhR), which is a known KYN receptor, is a negative regulator of bone mass. Indeed, our results show that treating RAW 264.7 cells with 3′,4′-dimethoxyflavone [DMF] (an AhR inhibitor) significantly decreased KYN mediated enhancement of osteoclastogenesis as evident by significant decrease in number of multinucleated TRAP positive osteoclasts. Altogether, our results suggest that KYN can act as positive regulator of RANKL-mediated osteoclast differentiation. Whether kynurenine acts solely via direct activation of AhR or through additional pathways, or downstream metabolites, needs to be further investigated. Due to the dual activity of KYN on both osteogenic and osteoclastogenic differentiation in bone, it could provide a potential clinical intervention target for prevention and treatment of osteoporosis.

***Disclosures: Nada Eisa**, None*

P-617

Bone mineral density and shifts in plasma estradiol concentrations throughout the menstrual cycle in young female oral contraceptive users versus non-users *Jenna Laughlin[1], Mark Kern[2], Shirin Hooshmand [1]. [1]San Diego State University, United States, [2]San Diego State University, United States

Purpose: Oral contraceptives (OCs) may negatively affect bone health of young women. One potential mechanism of this is suppressed endogenous estrogen levels. The objective of

this study was to compare bone mineral density (BMD) and hormone concentrations during the menstrual cycle between oral contraceptive users and non-users. Methods: Sixteen women, aged 18-25 y, either taking oral contraceptives (n=8) or not taking any hormones (n=8) were recruited. Women in the OC group were required to have used their current regimen consistently for at least 1 year prior to starting the study. Anthropometric measurements, Block Food Frequency Questionnaire (FFQ), physical activity and habitual calcium and vitamin D intake were evaluated at baseline to detect any differences between groups. Bone density scans were performed at baseline including lumbar spine (L1-L4), hip, forearm, and whole body BMD using DXA. Plasma estradiol levels were evaluated from samples collected on menstrual cycle days 1, 4, 11, and 21. Results: The groups did not significantly differ in height, weight, and body mass index (BMI), which is important as excess body fat can impact estrogen levels. Intake of calcium and vitamin D, two important nutrients for bone metabolism were nearly identical between the two groups. BMD measurements and T-scores for each group were similar and in the normal range. There was a significant main effect of cycle day on plasma estradiol level ($p<.05$) and a significant interaction between group (OC vs. non-OC) and cycle day ($p<.5$) with estradiol increasing throughout the menstrual cycle in non-users and remaining relatively unchanged in users. The largest difference between groups occurred on cycle day 21 ($p<.05$). Conclusion: Women taking OCs maintain relatively static estradiol concentrations across the menstrual cycle while women not taking any hormonal contraceptives experience fluctuations in estradiol levels across the menstrual cycle. These results confirm that taking OCs interferes with estrogen levels, which according to some research may have negative effects on bone health, predisposing young women to osteopenia or osteoporosis.

***Disclosures: Jenna Laughlin**, None*

P-618

CT-derived bone mineral density is the main determinant of prevalent vertebral fractures in cirrhotic patients awaiting liver transplantation.

*Clément Nachef[1], Valérie Bousson[2], Nadia Belmatoug[3], Martine Cohen-Solal[4], Valérie Vilgrain[5], François Durand[6], Thomas Funck-Brentano[1]. [1]Department of Rheumatology, Hôpital Lariboisière, APHP.Nord, Université de Paris, France, [2]Department of Radiology, Hôpital Lariboisière, APHP.Nord, Université de Paris, France, [3]Department of internal medicine, Hôpital Beaujon, APHP.Nord, Université de Paris, France, [4]Bioscar INSERM U1132, Université de Paris, Paris, France, France, [5]Department of Radiology, Hôpital Beaujon, APHP.Nord, Université de Paris, France, [6]Department of Hepatology, Hôpital Beaujon, APHP.Nord, Université de Paris, France

Background: Candidates for liver transplantation (LT) with cirrhosis are at high risk of fragility fractures. However, screening for osteoporosis may be suboptimal due to limited access to DXA and lack of awareness. The primary objective of the study was to identify the determinants of vertebral fractures using opportunistic CT screening at candidates' registration on OLT waiting list. The secondary objective was to identify the determinants of CT-derived bone mineral density (CT-derived BMD).Methods: Consecutive cirrhotic patients placed on waiting list for LT in an academic center from March 2004 to June 2018 were included in the study. Prevalent vertebral fractures (VF) were identified on sagittal and coronal reconstructions of thoraco-abdominal CT scans performed at evaluation. CT-derived BMD (mean Hounsfield unit) was measured in an elliptic region of interest of an axial section of the vertebral body of L1. Skeletal muscle index (SMI) was defined as the axial psoas muscle area divided by height squared.Results: Among the 381 consecutive candidates, 376 had available thoraco-abdominal CT scans, and were included in the final analysis (75% males; mean age 55 +/- 8 years; mean BMI 26.3 +/- 4.6 kg/m²; 42% alcoholic cirrhosis, 40% viral hepatitis cirrhosis). A total of 139 VF in 55 (14.6%) patients were identified. The prevalence of VF was greater in alcoholic (22.6%) and non-alcoholic steatohepatitis cirrhosis (19.0%) compared to viral hepatitis cirrhosis (7.9%). Patients with VF were older (56.9 55 +/- 7.2 vs 54.3 +/- 8.5 years, P=0.034) and had lower CT-derived BMD (86.3 +/- 30.3 vs 137.6 +/- 40.2 HU, P<0.001). In logistic regression models including age, sex, BMI and alcoholic cirrhosis, low CT-derived BMD was the only determinant of prevalent VF (for each SD decrease, OR=6.76 95%CI[3.94 to 11.63]; AUC for ROC curve = 0.86, Figure). A CT-derived BMD < 100 HU was associated with increased prevalence of VF (OR=8.7 95%CI[4.5 to 16.6]). The association between SMI and CT-derived BMD was significant, but the correlation was modest (Pearson's coefficient=0.30; variance explained r2=9%). In linear regression models, determinants of low CT-derived BMD were high age, alcoholic cirrhosis and low SMI (P<0.001 for all).Conclusions: Low CT-derived BMD is the major determinant of vertebral fractures in cirrhotic patients awaiting LT and should be routinely assessed to screen patients at high risk of fragility fractures.

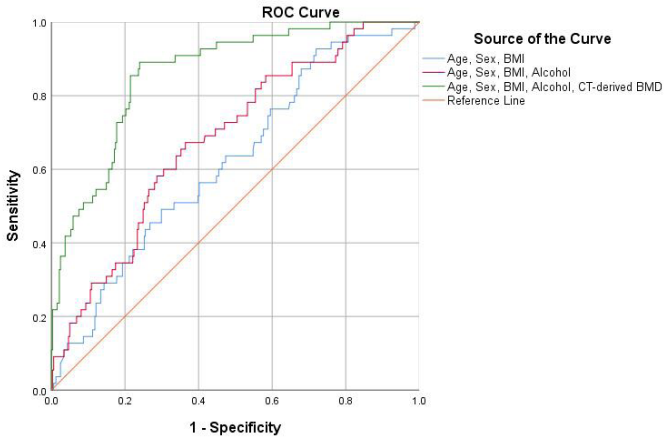

***Disclosures: Clément Nachef**, None*

P-619

Effects of Zoledronic Acid and Ambulation on Hip Bone Mineral Density after Acute Spinal Cord Injury: Year 1 of a Randomized Controlled Trial

*Ifaz Haider[1], Narina Simonian[2], Joana Barroso[3], W. Brent Edwards[1], Thomas Schnitzer[2]. [1]University of Calgary, Canada, [2]Northwestern University Feinberg School of Medicine, United States, [3]Universidade do Porto, Portugal, Portugal

Spinal cord injury (SCI) is associated with a significant decline in bone mineral density (BMD) and increased risk of fracture at sublesional locations. Losses in BMD occur rapidly after SCI, plateauing 2 to 5 years after injury [1]. Zoledronic acid (ZOL) has been shown to effectively attenuate bone loss in individuals with recent SCI [2]. However, the durability of treatment is unclear, as are the effects of potential covariates such as ambulation. Here, we report results from the first year of a prospective double-blind clinical trial (NCT02325414), assessing the durability of ZOL for the prevention of bone loss in individuals with acute SCI (i.e., < 4 months post-injury). Sixty individuals were randomized to receive an IV infusion of placebo (PBO; n=30) or 5 mg ZOL (n=30). Areal bone mineral density (aBMD) at the total hip (TH) and femoral neck (FN) was measured at baseline and after 6 and 12 months of treatment as was ambulation ability using the Walking Index for Spinal Cord Injury II (WISCI). Linear mixed modeling analysis was applied with baseline aBMD, visit and WISCI score as covariates to examine the effects of treatment group on % change from baseline in total hip (TH) and femoral neck (FN) aBMD. Interaction effects for treatment group*visit and treatment group*WISCI score were also included. There were no significant differences in age, gender, BMI, WISCI, or ASIA scores between treatment groups at baseline. Significant differences were found for % change in TH and FN aBMD between groups at both the 6 mo and 12 mo time points, $p<0.001$ for all. (TH data shown in Fig.1: ZOL and PBO groups LS means % change +/-SE in aBMD at 6 months and 12 months; -1.3+/-1.4 vs -10.4+/-1.4 and -3.0+/-1.4 vs -14.9+/-1.4, respectively, $p<0.001$ for both comparisons). WISCI had a significant effect on % change in both TH and FN aBMD, $p=0.004$ and 0.028, respectively. Although both treatment and WISCI had a positive effect on % change in aBMD, the interaction term between these variables was not significant. Further analyses of this cohort, over 2 years of treatment, is ongoing and will include assessment of treatment durability and computed tomography of bone mineral at the knee. However, these initial data support the notion that one-year treatment with ZOL can effectively attenuate bone loss after SCI, with benefits of treatment observed regardless of ambulatory ability. [1] Haider, Osteoporosis Int. 2018. [2] Goenka, Spinal Cord. 2018.

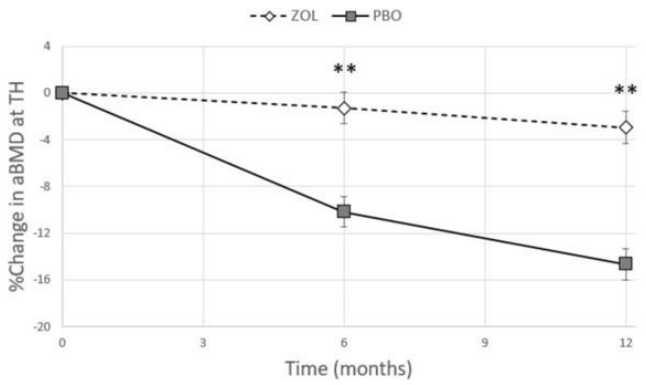

Fig. 1. %Change of aBMD at TH over 12 months, for ZOL and PBO treatment groups.
** P < 0.001 for pairwise comparison between groups.

***Disclosures: Ifaz Haider**, None*

P-620

Aromatase Inhibitor Induced Bone Loss in Postmenopausal Women with Breast Cancer: A Systematic Review and Meta-analysis of Randomized Controlled Trials *Abir Bou Khalil[1], Aya Bassatne[1], Marlene Chakhtoura[1], Asma Arabi[1], Catherine Van Poznak[2], Ghada El-Hajj Fuleihan [1]. [1]American University of Beirut, Lebanon, [2]University of Michigan, United States

Aromatase inhibitors (AIs) suppress estrogen levels, leading to accelerated bone loss and fractures. In this systematic review and meta-analysis of randomized controlled trials (RCTs), we assess the effect of anti-resorptive therapy in postmenopausal women with early breast cancer (BCa), receiving AIs, on Bone Mineral Density (BMD), fracture risk and bone turnover markers (BTM). We conducted the search in 4 databases from inception until December 6, 2019. We completed title/abstract and full text screening in duplicate and independently. The primary outcome is % change at lumbar spine (LS) or total hip (TH) BMD at 12 months and secondary outcomes include % change in BMD, fracture incidence and change in BTM, at different intervals. For BMD we report the % change mean weighted differences, and for any fracture we report the risk ratio (RR), with corresponding 95% CI. Only trials with data on BMD and estimated standard deviations were analyzed. Analysis of BTM is ongoing. We identified 19 RCTs. Participants had mean age of > 55 years, mean BMI of 23.08-31 kg/m2, and were followed up to 5 years. The mean weighted difference in LS BMD in patients on intravenous zoledronate (ZOL) with placebo, when combining 3 trials (N=2194), were 5.30 [4.36, 6.24], 7.27 [6.13, 8.42] and 8.03 [6.92, 9.13], at 1, 2 and 3 years respectively. Similarly, the % mean weighted difference at LS in 4 ZOL trials (N= 2745) was 9.43 [8.85, 10.00] at 5 years. Corresponding numbers at the TH were 3.33 [3.09, 3.57], 4.65 [4.35, 4.94], 5.06 [4.71, 5.42] and 6.37 [5.68, 7.07], at 1, 2, 3 and 5 years. Combining data from 4 oral bisphosphonate trials, N=383, revealed % mean weighted differences at LS of 3.05 [1.03, 5.07] and 4.78 [3.83, 5.73], and at TH of 2.36 [0.81, 3.90] and 3.75 [2.85, 4.65], at 1 and 2 years respectively. There was a decrease in clinical fracture, RR 0.93 [0.50, 1.70], 0.90 [0.59, 1.39], and 0.89 [0.61, 1.30] with ZOL vs. placebo at 1, 2 and 3 years, respectively. In 1 trial, denosumab decreased clinical fracture with a RR of 0.47 [0.36, 0.61] vs. placebo at 3 years. Combining parenteral data from ZOL and denosumab trials showed a RR of 0.68 [0.41, 1.13], vs. placebo at 3 years. I2 in 5 out of 6 of LS BMD analyses was > 50% and <50% in 4 out of 6 of TH BMD analyses. Use of anti-resorptive therapy in women with early BCa receiving AIs is effective at preventing bone loss and decreasing fracture risk.

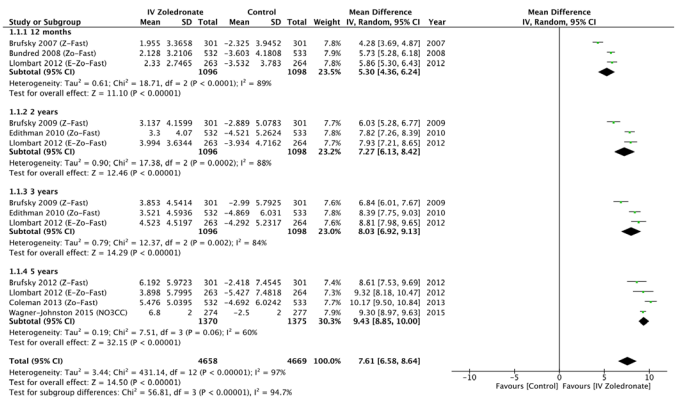

***Disclosures: Abir Bou Khalil**, None*

P-621

Androgen Deprivation Therapy Differentially Impacts Bone and Muscle in the Short Term in Physically Active Men with Prostate Cancer *Naim Maalouf[1], Orhan Oz[1], Avneesh Chhabra[1], Dwight Towler[1], Jason Zafereo[1], Ross Querry[1], Joseph Frankl[1], May Xac[1], Craig Rubin[1]. [1]University of Texas Southwestern Medical Center, United States

Background: Androgen Deprivation Therapy (ADT) is a cornerstone of therapy in advanced prostate cancer (PCa). Its use is associated with a loss of bone mineral density (BMD) and a greater risk of falls and osteoporotic fractures. Androgen receptors are expressed on myocytes, and ADT-related fall and fracture risk may be in part due to early changes in muscle and body composition. The well-described crosstalk between bone and muscle led us to test the hypothesis that a decline in muscle strength precedes the decline in bone strength in men initiating ADT for PCa.Methods: Men with PCa were enrolled and evaluated at 3 time points: immediately before (Week 0), and 6 and 24 weeks after ADT initiation. Study measures included fasting blood (for markers of muscle and bone metabolic activity), MRI and QCT imaging (for muscle volume and composition, and bone density and architecture), and validated clinical tests of muscle strength and gait.Results: Sixteen men (13 Caucasian,3 African American) completed all study visits. At baseline, median (25th, 75th percentile) age was 67 (65, 68) years, BMI 29.8 (27.9, 31.3) kg/m2, and PSA 4.6 (0.9, 7.3) ng/ml. The men were considered physically active, exercising a median of 3 (2, 6) times/week throughout the duration of the study, but still experienced weight gain (+2.2 kg at week 24 vs. week 0, p=0.004). Biochemically, all men sustained dramatic reductions in sex hormones at 6 weeks post-ADT that persisted at 24 weeks, along with a progressive and significant increase in serum CTX (by +88% at week 24 vs. week 0). There was a trend for rise in serum sclerostin (p=0.09) and IL-6 (p=0.08), but no significant change in serum myostatin (p=0.99). Volumetric BMD by QCT declined significantly at the femoral neck (-4.4% at week 24 vs. week 0), particularly at the trabecular compartment (-5.7% at week 24 vs. week 0). On MRI, there were no significant changes in gluteal and thigh muscle volume or fat fraction. On physical testing, men developed weaker grip strength, but no change in lower extremity and lumbar spine muscle strength (Hip abduction/adduction, and hip/knee/lumbar flexion/extension), or functional tests of gait (step velocity and length at self-selected and fast speed).Conclusions: In physically active men, ADT for 24 weeks results in a significant increase in bone turnover and reduction in BMD, but no significant change in pelvic/thigh muscle volume and quality (on imaging) or strength and gait (on functional testing).

***Disclosures: Naim Maalouf**, None*

P-622

Feasibility of Risedronate to Prevent Bone Loss after Sleeve Gastrectomy: a Pilot Randomized Controlled Trial *Kristen Beavers[1], Daniel Beavers[2], Aldofo Fernandez[2], Ashley Weaver[2], Jamy Ard[2]. [1]Wake Forest University, United States, [2]Wake Forest School of Medicine, United States

Purpose: Mounting evidence implicates bariatric surgery in increased skeletal fragility and fracture risk. Bisphosphonate therapy reduces osteoporotic fracture risk and may be effective in minimizing bone loss associated with bariatric surgery.Methods: The main objective of this pilot randomized controlled trial (RCT; NCT03411902) was to determine the feasibility of recruiting, treating, and following 24 older sleeve gastrectomy (SG) patients in a 6 month RCT examining the efficacy of 150 mg once monthly risedronate (versus placebo) in the prevention of surgical weight loss associated bone loss. Feasibility was defined as: (1) >30% recruitment yield; (2) >80% retention; (3) >80% pills taken; (4) 80% participant satisfaction. Secondary outcomes include 6 month change in dual energy x-ray absorptiometry (DXA) acquired regional bone mineral density (BMD) and trabecular bone score (TBS). Primary outcomes were estimated using descriptive measures, and secondary group treatment effects were estimated using a general linear model adjusted for baseline values of each outcome. Sensitivity analyses included stratification by menopausal status and adjustment for total weight change.Results: 70 participants were referred, with 24 randomized (34% yield) to risedronate (n=11) or placebo (n=13). Average age was 56+/-7 years, 83% were female (75% postmenopausal), and 21% were black. The risedronate group had a higher baseline body mass index than placebo (48.1+/-7.2 vs 41.9+/-3.8 kg/m2). 10-year fracture risk was low (6.0% major osteoporotic fracture, 0.4% hip fracture); however, three individuals (12%, all risedronate group) were osteopenic at baseline. 21 participants returned for 6 month follow up testing (88% retention) with all (n=3) loss to follow up occurring in the risedronate group. Average pills taken among completers was 5.9+/-0.4 and 6.0+/-0.0 in risedronate and placebo groups, respectively (p=0.21), with all active participants taking >80% of allotted pills. Four AEs (134 contacts; 3% AE rate) were reported; one definitely related, one possibly related, and none serious. All participants reported being highly satisfied with participation in the study. Treatment effect estimates revealed preserved BMD at all sites in the risedronate group versus placebo, with significant effects observed at the femoral neck [mean: 0.005 (95% CI: -0.028, 0.038) vs -0.043 (-0.069, -0.017) g/cm2] and lumbar spine [0.024 (-0.007, 0.055) vs -0.028 (-0.052, -0.005) g/cm2]; both p<=0.03 (see Figure 1). BMD results did not differ when stratified by menopausal status or after adjusting for total weight change. No differences in TBS were observed.Conclusion: Risedronate treatment in the 6 months following SG appears feasible. Preliminary treatment effects suggest risedronate use minimizes short-term BMD loss, particularly at weight bearing sites, following SG.

Figure 1. Six Month Change in Regional BMD by Treatment Group.

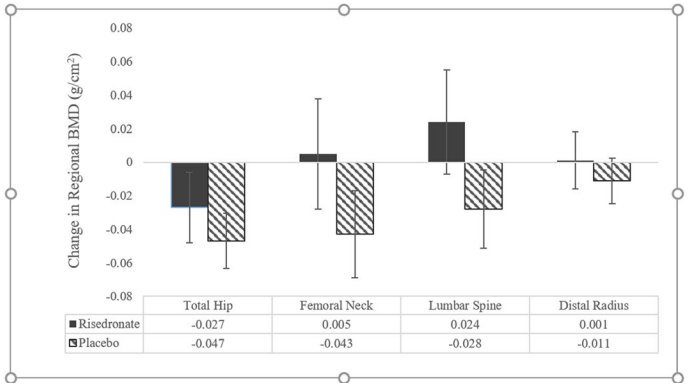

	Total Hip	Femoral Neck	Lumbar Spine	Distal Radius
Risedronate	-0.027	0.005	0.024	0.001
Placebo	-0.047	-0.043	-0.028	-0.011

***Disclosures: Kristen Beavers**, None*

P-623

Bone Quality is Associated with Fragility Fracture in Patients with Hemoglobinopathies *Ellen Fung[1], Lisa Calvelli[1], Melissa Cervantes[1], Kaylianna Cadena[1], Ashutosh Lal[1]. [1]UCSF Benioff Children's Hospital Oakland, United States

Introduction: Low bone mass has been described in up to 70% of adults with thalassemia (Thal) and sickle cell disease (SCD). DXA assessment is part of routine clinical practice, though bone quality has been inadequately characterized. Trabecular bone score (TBS), a textural analysis of bone quality from spine DXA scan, is predictive of fracture in adults without hemoglobinopathies. We evaluated the prevalence of abnormal bone quality and its relationship to fracture in patients with Thal or SCD. Methods: A retrospective chart review was conducted in patients with Thal or SCD who weighed >40 kg and had >1 spine bone mineral density (BMD) scan performed on a Hologic Horizon scanner in the past 10 yrs. The most recent scan was reanalyzed for bone quality using TBS Insight (Medimaps v 3.0.2, Geneva, CH) and abnormal bone quality was defined as TBS <1.20. Fracture prevalence was determined by patient report at time of DXA. TBS results were compared with data obtained from healthy controls. Statistical analysis was performed using STATA, v16. Results: Data from 352 individuals with mean (SD) 28+/-13 years of age were abstracted that included 58% female and 62% were over 21 years. There were 131 patients with Thal, 154 with SCD, and 67 controls. Thal group had greater deficits in spine BMD Z-score (-2.2+/-1.2, range 1.3 to -5.7), compared with SCD (-1.4+/-1.5, 4.8 to -4.9) and control (-0.1+/-0.8) groups (p<0.01). There was a higher prevalence of abnormal TBS (25%) in Thal compared with SCD (10%), or control (5%, p<0.01). More Thal had hypogonadism (31% vs. 1% in SCD) and diabetes (9% vs. 3% in SCD); however, there was no difference in fracture prevalence between the two groups. TBS was positively correlated with BMD (r=0.7) and negatively with age (r=-0.3). After controlling for age and hypogonadism, abnormal TBS was associated with a Thal diagnosis (p=0.01). Although abnormal TBS was not related to overall fracture prevalence, it was associated with fragility type fracture, regardless of diagnosis (RR: 8.9, p=0.013). Conclusions: These data support the relationship between reduced bone mass and bone quality in adolescent and adult patients with hemoglobinopathies. TBS may be a valuable tool in differentiating risk of fragility fractures in this group of inactive patients with extremely low BMD. There is a need to develop models that include both BMD and TBS for prediction of fracture risk in patients with hemoglobinopathies who might benefit from anti-resorptive therapies.

***Disclosures: Ellen Fung**, None*

P-624

Low Serum Osteocalcin Levels are Associated with the Presence of Diabetes Mellitus in Glucocorticoid Treated Patients *Helena Florez[1], José Hernández-Rodríguez [2], Josep Lluis Carrasco[3], Sergio Prieto-González [2], Xavier Filella[4], Ana Monegal[1], Núria Guañabens[1], Pilar Peris[1]. [1]Metabolic Bone Diseases Unit. Department of Rheumatology. Hospital Clinic, University of Barcelona, Spain, [2]Vasculitis Research Unit, Department of Autoimmune Diseases, Hospital Clínic, University of Barcelona, Institut d'Investigacions Biomèdiques August Pi i Sunyer (IDIBAPS), Barcelona, Spain., Spain, [3]Biostatistics, Department of Basic Clinical Practice, University of Barcelona, Barcelona, Spain., Spain, [4]Biochemistry and Molecular Genetics Department. Hospital Clinic, University of Barcelona, Spain

Increasing evidence indicates that osteocalcin (OC) is involved in the regulation of glucose homeostasis. Glucocorticoid (GC) treatment is associated with impaired osteoblast function and decreased OC levels and also with the development of CG-induced diabetes mellitus (GIDM). However, whether decreased OC levels in GC-treated subjects contribute to GIDM is not well known.Purpose: To analyse whether OC levels in GC-treated patients are associated with the presence of GIDM.Methods: 127 patients (aged 62+/-18years, 63% women) on GC treatment for autoimmune diseases (>=5mg/day,>3 months) were included. Clinical and anthropometric data were analysed, including the GC dose and treatment duration, presence of GIDM, fragility fractures, densitometric osteoporosis and bone formation (OC, bone alkaline phosphatase [BAP], PINP) and resorption markers (urinary NTX, serum CTX). The cut-offs of each bone marker for the presence of GIDM were estimated and optimized with the Youden index and included in the logistic regression analysis (adjusted for BMI, age and GC doses).Results: 17.3% of patients presented GIDM. Diabetic subjects were older (70.5+/-12.2 vs. 59.6+/-18.4, p=0.001) and had a higher BMI than non-diabetics (30+/-5.2 vs. 26+/-4.2, p=0.002). No differences were observed in GC dose, disease duration or in the presence of vertebral fractures. Diabetics showed lower levels of OC (7.57+/-1.01 vs. 11.56+/-1; p<0.001), PINP (21.48+/-1.01 vs. 28.39+/-1; p=0.0048), NTx (24.91+/-1.01 vs. 31.7+/-1; p=0.036) and CTX (0.2+/-1.01 vs. 0.3+/-1; p=0.0016) with similar BAP values. The best discriminating cut-offs for GIDM presence were: <9.25ng/mL for OC, <24ng/mL for PINP, <27.5nMol/mM for NTX and <0.25ng/mL for CTX. On multivariate analysis OC (<9.25) was the only marker related to the presence of GIDM (OR 6.1; CI95% 1.87-19.89; p=0.001).Conclusions: Decreased OC levels in GC-treated patients are associated with an increased risk of GIDM, a finding that was not observed with other bone turnover markers, further confirming the involvement of OC in the glucose homeostasis regulation in this entity.

***Disclosures: Helena Florez**, None*

P-625

Bone Mineral Density, Trabecular Bone Score and proximal Femur 3D-DXA Analysis in Psoriatic Diseases. *Eric Toussirot[1], Renaud Winzenrieth[2], Maxime Desmarets[3], Francois Aubin[4], Gilles Dumoulin[5]. [1]INSERM CIC-1431 CHU de Besançon, France, [2] Galgo Medical, Spain, [3]INSERM CIC-1431 CHU de Besançon, France, [4]Dermatologie CHU de Besançon, France, [5]Biochimie Médicale CHU de Besançon, France

Purpose: current data regarding areal bone mineral density (aBMD) in patients with psoriasis (PsO) or psoriatic arthritis (PsA) are conflicting. Results on Trabecular Bone Score (TBS) in these patients are lacking. 3D-analysis of cortical and trabecular bone from hip DXA is a new method for non-invasive bone structure assessment, providing separate assessment of the cortical layer and trabecular macrostructure. Patients and methods: Case-control study (NCT02849795) in which 52 PsO and 52 PsA cases (CASPAR criteria) were each paired to a control subject matched for age, sex and body mass index (BMI). aBMD measurements at (L2-4) lumbar spine (LS), femoral neck (FN) and total hip (TH) were performed using DXA, Lunar GE. TBS was calculated from antero-posterior L2-L4 BMD image using TBS iNsight V1.8 (Med-Imaps, Pessac, France). 3D-SHAPER software (version 2.10, Galgo Medical S.L, Barcelona, Spain) was used to derive a 3D analysis from the hip DXA scans. Results: LS and TH aBMD measurements did not differ between patients with PsO or PsA and their respective controls (Table 1). Left FN BMD was higher in patients with PsO compared to controls (p = 0.028), a difference not observed on the right FN. TBS was similar in PsA patients and their controls while decreased values were observed in PsO patients (p = 0.04). In 3D analysis, none of the parameters differed between patients with PsA and their controls. For patients with PsO, no difference was found with the controls for 3D-DXA parameters from the right FN, while total hip cortical surface BMD (sBMD) of the left FN was higher in PsO compared to their controls (p = 0.037). Similarly, cortical thickness (Cth) of the intertrochanteric and shaft regions of the left FN was also higher in PsO (p = 0.032 and p = 0.033). Finally, analysis by region (neck, intertrochanteric and shaft) showed higher values for cortical sBMD from each region of the left FN in the patients with PsO (all p <0.05).Conclusion: Our results showed comparable aBMD, TBS and 3D proximal femur parameters in patients with PsA and controls. This supports that PsA population is not at increased risk of osteoporosis. In patients with PsO, while LS bone microarchitecture seems impaired, FN displayed better cortical parameters than the controls. Although these results seem marginal, they support the fact that patients with PsO are not at high risk for osteoporosis and hip fracture.

	PsA (N = 52)	PsA controls (N = 52)	PsO (N = 52)	PsO controls (N = 52)
Age (years)	52.5 ± 11.7	52.8 ±11.1	50.5 ± 12.8	50.7 ± 12.8
Sex (M/F)	25/27	25/27	38/14	36/15
Menopausal women	18 (67%)	16 (59%)	5 (36%)	8 (50%)
BMI (Kg/m^2)	27.4 ± 5.9	27.7 ± 6.4	28.4 ± 5.8	28.2± 6.1
PASI	2.4 ± 4.1		8.4 ± 4.9	
CPDAI	7.4 ± 3.3			
ESR (mm/h)	19.8 ± 16.6 ***	6.9 ± 5.8	10.7 ± 8.8 ***	6.4 ± 6.4
CRP (mg/L)	10.5 ± 11.7 ***	3.9 ± 4.8	5.9 ± 9	4.7 ± 5.4
LS (L2-4) aBMD (g/cm^2)	1.27 ± 0.49	1.2 ± 0.2	1.25 ± 0.2	1.2 ± 0.18
FN aBMD (g/cm^2) right left	0.96 ± 0.12 0.96 ± 0.16	0.94 ± 0.14 0.93 ± 0.12	0.98 ± 0.15 1.0 ± 0.14 *	0.98 ± 0.15 0.97 ± 0.13
TH aBMD (g/cm^2)	1 ± 0.16	1 ± 015	1.11 ± 0.22	1.06 ± 0.2
L2-L4 TBS	1.32 ± 0.1	1.32 ± 0.15	1.23 ± 0.15 *	1.3 ± 0.16
Cortical sBMD (left FN) (mg/cm^2)	169.7 ± 32.8	163.05 ± 29.7	182.0. ± 30.9 *	173.4 ± 30.3
Cth intertrochanteric (left FN) (mm)	1.91 ± 0.2	1.94 ± 0.2	2.03 ± 0.23 `	1.97 ± 0.2
Cth shaft (left FN) (mm)	2.98 ± 0.31	3.01 ± 0.3	3.19 ± 0.3 *	3.09 ± 0.3
cortical sBMD (left FN) (mg/cm^2) neck intertrochanteric shaft cort	135.27 ± 26.9 162.32 ± 31.1 269.2 ± 49	129.67 ± 21.9 155.3 ± 29.3 257.1 ± 47.3	140.29 ± 24.2 * 171.39 ± 29.1* 286.2 ± 47.5 *	134.6 ± 22.5 163.1 ± 28.9 272.7 ± 45.2

Table 1:

patients' clinical characteristics, areal bone mineral density (lumbar spine, femoral neck, total hip), trabecular bone score and proximal femur DXA-derived 3D analysis in patients with psoriatic arthritis and their paired controls and in patients with psoriasis and their paired controls
PsA : psoriatic arthritis ; PsO : psoriasis ; M: male; F : female; BMI: body mass index; PASI : psoriasis area severity index ; CPDAI : composite psoriatic disease activity index ; ESR : erythrocyte sedimentation rate ; CRP : C-reactive protein ; aBMD : areal bone mineral density ; LS: lumbar spine; FN : femoral neck ; TH: total hip; TBS: trabecular bone score; sBMD : surface bone mineral density; Cth : cortical thickness.
Quantitative data are mean ± standard deviation.
* and *** : paired *t* test comparing patients with psoriatic arthritis or psoriasis alone to their respective controls.
* p < 0.05; *** p < 0.001.

***Disclosures: Eric Toussirot**, None*

P-626

Association of bone and plasma microRNA levels in patients with Cushing's disease. *Zhanna Belaya[1], Tatiana Grebennikova[1], Alexey Nikitin[2], Alexandr Solodovnikov[3], Andrey Grigoriev[1], Galina Melnichenko[1]. [1]The National Medical Research Centre for Endocrinology, Russian Federation, [2]Federal Research and Clinical Center FMBA of Russia, Russian Federation, [3]Ural State Medical Academy, Russian Federation

MicroRNA (miR) are considered promising osteoporosis biomarkers but current understanding of the relationship between miR levels in bone tissue and circulation is limited.Objective: to estimate if there is an association between miR levels in bone and plasma samples of patients with active Cushing's disease (CD).Methods: Bone and plasma samples were obtained from patients with clinically and biochemically-evident CD. Morning fasting blood samples were collected and centrifugated twice at a temperature of +5C at 3000 rpm. Plasma samples were frozen and stored at -80C. Bone samples were obtained during transsphenoidal adenomectomy from the base of the sella turcica. Differences between miR levels in bone samples of CD vs control group were previously estimated [1] in the following miRs : miR- 100-5p; miR-10b-5p; miR-122-5p; miR-125b-5p; miR-133a-5p; miR-135a-5p; miR-148a-3p; miR-155-5p; miR-188-3p; miR-199a-5p; miR-203a-5p; miR-21-3p; miR-21-5p; miR-211-5p; miR-22-3p; miR-26a-5p; miR-27a-3p; miR-27a-5p; miR-31-5p; miR-320a; miR-328-3p; miR-34a-5p; miR-550a-5p; miR-550b-2-5p; miR-7g-5p; miR-9-5p; miR-96-5p. These miRs were measured in plasma samples by qPCR on the same patients with CD. Twenty-four hours urine free cortisol (24hUFC) was measured by an immunochemiluminescence assay on a Vitros ECi.Results: Patients with Cushing's disease (n=14 (13 females and 1 male); age 38 (95%CI 32-44) years) had elevated levels of 24hUFC – 1230 (95%CI 748-1711) nmol/24h (reference range 60-413 nmol/24h). We observed statistically significant correlations between three miRs levels in bone and plasma samples: miR-203a-5p ρo = 0.555 p=0.047; miR-21-3p ρo = -0.635 p = 0.015 and miR-96-5p ρo = -0.63 p = 0.021. MiR-203a-5p, miR-21-3p were previously shown to be upregulated whereas miR-96-5p was unchanged in bone samples of patients with CD [1]. Plasma levels of miR- 203a-5p (ρo = 0.560 p=0.046), miR-96-5p (ρo = 0.786 p=0.001); and miR-35-5p (ρo = 0.703 p=0.007) correlated with 24hUFC levels.Conclusions: Hypercortisolism due to CD changes miR levels both in bone and circulation. The plasma levels of MiR-203a-5p and miR-96-5p are associated with their levels in bone and with 24hUFC. 1) Belaya ZE, Grebennikova TA, Melnichenko GA, Nikitin AG, Solodovnikov AG, Brovkina OI, Grigoriev AU, Rozhinskaya LY, Dedov II. Effects of endogenous hypercortisolism on bone mRNA and microRNA expression in humans. Osteoporos Int. 2018 Jan;29(1):211-221. doi: 10.1007/s00198-017-4241-7

***Disclosures: Zhanna Belaya**, None*

P-627

Anti-depressant Use is Associated with Cortical Bone Deficits and Reduced Physical function *Carmen Germosen[1], Sanchita Agarwal[1], Mariana Bucovsky[1], John Williams[1], Mishaela Rubin[1], Elizabeth Shane[1], Marcella Walker[1]. [1]Columbia University Irving Medical Center, United States

Recent work suggests anti-depressants, particularly selective serotonin reuptake inhibitors, are associated with an increased risk of fracture. The mechanism is unclear and may be due to effects on bone metabolism, muscle strength, falls or other factors. We compared musculoskeletal health between anti-depressant (ever) users vs. never users from a population-based multiethnic cohort study of adults >= 65 yrs old in New York, the Washington Heights-Inwood Community Aging Project. Musculoskeletal health was assessed using dual x-ray absorptiometry (DXA), trabecular bone score (TBS), vertebral fracture assessment (VFA), high resolution peripheral quantitative computed tomography (HRpQCT), body composition, grip strength and impact microindentation (IMI). The analysis was limited to women (n=195, mean age 76.3+/-6.1 yrs). The cohort was 35.6% black, 22.3% white and 42.1% mixed race. Anti-depressant users were more likely to be white than non-white (OR 3.6, 95% CI 1.6-8.2) and were shorter vs. non-users, but there was no difference in age, weight, BMI, physical activity, calcium/vitamin D intake, falls or self-rated health. There was a trend toward more historical fractures in users vs. non-users (62.1% vs. 42.9%, p=0.07), particularly pelvic fractures. Age- and weight-adjusted T-score by DXA was lower in users at the 1/3-radius (-1.8+/-1.4 vs. -1.0+/-1.3, p=0.006), but not other sites. There was no difference in TBS (p=0.09), the frequency of vertebral fractures by VFA (p=0.77) or fat/lean mass by DXA, but grip strength was 14.4% lower in users vs. non-users (p=0.03). By HRpQCT, age- and weight-adjusted cortical (Ct.) volumetric BMD (vBMD) was 5.9% lower in users vs. non-users at the 4% radius (p=0.006), but stiffness in a subset (n=49) did not differ (p=0.13). There were no differences in trabecular indices, tibial microstructure, or IMI in a subset (n=10). When the analysis was limited to non-white women (n=153), results were similar. Age- and weight-adjusted 1/3-radius T-score (-1.7+/-1.4 vs. -0.9+/-1.2, p=0.03), Ct. vBMD (754+/-66 vs. 808+/-66 mgHA/cm3, p=0.001), Ct. thickness (0.712+/-0.16 vs. 0.806+/-0.16 mm, p=0.03) at the radius and grip strength were lower in users vs. non-users. In summary, anti-depressant use was associated with cortical, but not trabecular, skeletal microstructural deficits and reduced physical function. These findings indicate that taking anti-depressants may contribute to the increased risk of fracture in older adults.

Musculoskeletal Health in Anti-depressant Users vs. Never Users

	Never N=165	Ever N=30	p-value
Age (years)	76.4±6.2	76.2±5.6	0.83
Race			0.01
White (%)	17.6%	43.3%	
Black (%)	37.6%	23.3%	
Mixed Race (%)	44.9%	33.3%	
Ethnicity (% Hispanic)	51.5%	46.7%	0.69
Weight (pounds)	159.1±35.7	154.6±27.9	0.51
Height (inches)	62.1±2.8	60.8±2.4	0.02
BMI (kg/m²)	29.0±5.9	29.5±5.7	0.64
Physical activity score	86.5±42.4	76.4±37.4	0.22
Calcium intake (mg/day)	1206±605	1207±514	0.99
Vitamin D intake (IU/day)	1530±1805	1232±1477	0.39
Fall in last year (%)	31.5%	43.3%	0.21
Self-rated health	3.0±0.98	2.9±1.0	0.44
Historical fracture (%)	42.9%	62.1%	0.07
Trabecular bone score	1.186±0.13	1.142±0.13	0.09
% with vertebral fracture by VFA	14.9%	17.9%	0.77
DXA			
Lumbar Spine T-score	-0.6±1.7	-0.8±1.3	0.44
Femoral Neck T-score	-1.4±1.0	-1.7±1.1	0.26
1/3 radius T-score	-0.9±1.4	-1.8±1.3	0.006*
Lean mass (%)	60.6±6.3%	61.4±5.4%	0.62
Fat mass (%)	39.4±6.3%	38.6±5.4%	0.62
Other Skeletal parameters			
Grip strength (kgs force)	16.7±5.3	14.3±4.7	0.04*
Bone material strength index by impact microindentation (n=10)	78.2±1.6	73.7±5.4	0.14
HRpQCT – 4% Radius			
Tb. vBMD (mgHA/ccm)	127.9±37.0	132±42.7	0.58
Ct. vBMD (mgHA/ccm)	806.8±63.5	758.1±81.8	0.0006*
Tb. Number (1/mm)	1.251±0.23	1.304±0.28	0.29
Tb. Thickness (mm)	0.227±0.02	0.237±0.05	0.54
Tb. Spacing (mm)	0.798±0.19	0.805±0.39	0.93
Ct. thickness (mm)	0.787±0.17	0.715±0.16	0.005
Ct. porosity (%)	1.1±0.8	1.2±0.8	0.81
Stiffness (N/mm)	48234±16242	37412±7535	0.006

Values represent mean ± SD or percentages; *p<0.05 after adjusting for age and weight; VFA=vertebral fracture assessment; Tb=trabecular; Ct=cortical; vBMD=volumetric bone mineral density

***Disclosures: Carmen Germosen**, None*

P-628

Association Between Sleep Duration and Bone Mineral Density in Midlife Women *Christine Swanson[1], Patrick Blatchford[1], Wendy Kohrt[1], Kenneth Wright, Jr.[2], Howard Kravitz[3], Ellen Gold[4], Katie Stone[5], Martica Hall[6], Jane Cauley[6]. [1]University of Colorado, United States, [2]University of Colorado at Boulder, United States, [3]Rush University Medical Center, United States, [4]University of California Davis, United States, [5]University of California, San Francisco, United States, [6]University of Pittsburgh, United States

Accelerated bone mineral density (BMD) loss occurs across the menopausal transition when sleep disturbance often occurs, but the rate of loss varies between individuals, and reasons for more rapid bone loss are largely unknown. Self-reported short and long sleep durations have been associated with lower BMD in women, but the association between objectively assessed sleep duration and BMD in women across the menopausal transition is unknown. We used objective measures of sleep duration (wrist actigraphy) and BMD (DXA) from the Study of Women's Health Across the Nation (SWAN) Sleep Study to determine the cross-sectional association between sleep duration and BMD in midlife women. Sleep duration was analyzed as both a continuous and dichotomous variable using NIH sleep duration recommendations to categorize women as recommended (7-8 h/night, N = 18) or short (<6 h/night, N = 92) sleepers. Covariates were incorporated into adjusted models if their group differences were either clinically or statistically significant. Three linear regression models were used. Model A was unadjusted. Model B adjusted for age, race, BMI and clinical site. Model C additionally adjusted for calcium/vitamin D use, depressive symptoms, self-reported health, menopausal status, hormone use and days between actigraphy and DXA visit. On average, women were 52.6 +/- 2.37 years old, with a BMI of 29.0 +/-6.67 kg/m2, and 43.6% were Caucasian. Menopausal status included: unknown due to hormone use (8.2%), pre- (6.4%), peri- (73.6%), and postmenopausal (11.8%). In the unadjusted model only, femoral neck BMD was higher in short sleepers compared to women with the recommended sleep duration (p = 0.027). This was likely driven by BMI differences as it was not significant in the minimally and fully adjusted models. BMD at the L-spine or total hip did not differ significantly between recommended and short sleepers in any model (all p >= 0.15). When sleep duration was analyzed as a continuous variable (N = 183), BMD at the femoral neck and total hip were non-significantly lower in women with shorter sleep duration in the fully adjusted model only (total hip BMD 0.013 g/cm2 higher for each hour of sleep, p = 0.21). In conclusion, BMD was not associated with objectively-determined sleep duration in midlife women. However, the cohort was small, actigraphy and BMD were obtained, on average, 92 +/- 62 days apart, and sleep durations >=7 h/night were under-represented.

Table 2: BMD (g/cm²) in Peri-menopausal Women with the Recommended (7-8 hours/night) vs. Short (<6 hours/night) Sleep Duration Using Objective (Actigraphy) Sleep Durations. Data are presented as adjusted means (95%CI).

Objective Nocturnal Sleep Duration, Determined by Actigraphy									
	Model A (Unadjusted)[a]			Model B (Minimally Adjusted)[b]			Model C (Fully Adjusted)[c]		
	Recommended Sleep Duration	Short Sleepers	Difference (Recommended - Short) in g/cm²	Recommended Sleep Duration	Short Sleepers	Difference (Recommended - Short) in g/cm²	Recommended Sleep Duration	Short Sleepers	Difference (Recommended - Short) in g/cm²
N	18	92		18	92		18	90	
L-spine	1.035 (0.950, 1.119)	1.095 (1.062, 1.128)	-0.061 p = 0.15	1.052 (0.968, 1.136)	1.064 (0.997, 1.131)	-0.012 p = 0.76	1.002 (0.774, 1.230)	1.039 (0.812, 1.266)	-0.037 p = 0.39
Total Hip	0.950 (0.884, 1.016)	0.979 (0.946, 1.013)	-0.029 p = 0.47	1.008 (0.940, 1.076)	0.979 (0.924, 1.034)	0.029 p = 0.36	1.008 (0.827, 1.189)	1.000 (0.820, 1.180)	0.008 p = 0.81
Femoral Neck	0.790 (0.742, 0.839)	0.855 (0.824, 0.886)	**-0.065 p = 0.027**	0.845 (0.781, 0.909)	0.854 (0.803, 0.905)	-0.009 p = 0.76	0.803 (0.630, 0.976)	0.821 (0.649, 0.993)	-0.018 p = 0.58

Table 3: Association Between BMD and Nocturnal Sleep Duration (Continuous Variable) Determined by Actigraphy. Data are presented as the change in BMD (g/cm²) per additional hour of sleep (β), p-value, (95%CI).

Objective Nocturnal Sleep Duration, Determined by Actigraphy			
	Model A - Unadjusted[a] (N = 183)	Model B - Minimally Adjusted[b] (N = 183)	Model C - Fully Adjusted[c] (N = 179)
L-spine	-0.020, p = 0.13 (-0.045, 0.006)	-0.001, p = 0.94 (-0.025, 0.023)	0.001, p = 0.93 (-0.024, 0.026)
Total Hip	-0.013, p = 0.29 (-0.037, 0.011)	0.007, p = 0.47 (-0.012, 0.026)	0.013, p = 0.21 (-0.007, 0.033)
Femoral Neck	-0.017, p = 0.14 (-0.040, 0.006)	0.004, p = 0.67 (-0.014, 0.022)	0.011, p = 0.26 (-0.008, 0.031)

[a] Model A = Unadjusted
[b] Model B = Minimally adjusted: age, race, clinical site, and BMI
[c] Model C = Fully adjusted: age, race, clinical site, BMI, calcium/vitamin D use, depression (as assessed by CES-D), self-reported overall health status, number of days between sleep visit and SWAN core visit, hormone use, menopausal hormone status.

***Disclosures: Christine Swanson**, None*

P-629

Assessment of bone mineral density, cortical bone thickness and bone marrow fat at the proximal femur in HIV-infected subjects *Julio Carballido-Gamio[1], Magdalena Posadzy[2], Po-Hung Wu[2], Thomas Link[2], Phyllis Tien[3], Roland Krug[2], Galateia Kazakia[2]. [1]Department of Radiology, University of Colorado Anschutz Medical Campus, United States, [2]Department of Radiology and Biomedical Imaging, University of California, San Francisco, United States, [3]Department of Medicine, University of California, San Francisco, United States

Purpose. Increased fracture risk is increasingly recognized as a significant comorbidity of HIV infection and treatment. While low bone mineral density and deteriorated bone quality has been reported at the extremities in HIV-infected individuals, data at the proximal femur –an important anatomical site for fracture– is limited. The purpose of this work was to quantify differences in volumetric bone mineral density (vBMD), cortical bone thickness, and bone marrow fat content (BMF) between HIV-infected patients and uninfected controls. Methods. Forty HIV-infected patients and 26 age-matched uninfected controls were included in this study. Using quantitative computed tomography (QCT) and quantitative magnetic resonance imaging (MRI), proximal femur maps of volumetric bone mineral density (vBMD), cortical bone thickness (Ct.Th), and BMF were generated. Using linear regression, differences in vBMD, Ct.Th. and BMF between HIV-infected patients and uninfected controls were investigated for different volumes of interest: total hip, femoral head, femoral neck and trochanter. The linear models were adjusted for age, body mass index (BMI), sex and race.Results. There were no significant differences in age and BMI between HIV-infected patients (58+/-5 years and 26+/-4 kg/m2) and uninfected controls (58+/-5 years and 25+/-4 kg/m2). Thirty percent in the HIV-infected group, and 54% in the uninfected control group were females; and 65% of the participants were white in both groups. Significantly lower values were identified in HIV-infected patients compared to uninfected controls for: 1) integral (cortical + trabecular) vBMD at the total hip, femoral neck and trochanter (P<0.05); and 2) trabecular vBMD at the femoral neck and trochanter (P<0.006). Significantly higher BMF values were identified in HIV-infected patients compared to uninfected controls at the femoral neck (P<0.007). Cortical vBMD and cortical bone thickness were not significantly different between the two groups. Discussion. Results of this study indicate that the trabecular bone and not the cortical bone is compromised in HIV-infected patients at the proximal femur. Lower vBMD at the femoral neck and trochanter, and higher BMF at the femoral neck –both fracture prone regions– are indicators of lower bone strength, partly explaining the higher risk of fracture in HIV-infected patients.

***Disclosures: Julio Carballido-Gamio**, None*

P-630

Characterization of bone involvement in early Parkinson's Disease patients: a pilot cross-sectional study *Antimo Moretti[1], Sara Liguori[1], Marco Paoletta[1], Matteo Bertone[1], Giovanni Iolascon[1]. [1]Department of Medical and Surgical Specialties and Dentistry, University of Campania "Luigi Vanvitelli", Naples, Italy, Italy

PurposeBone involvement in early stages of Parkinson's disease (PD) is poorly investigated. We aim to evaluate the qualitative and quantitative alteration of bone in patients with early PD and the associations among BMD, Trabecular Bone Score (TBS), and physical performance in the same population.MethodsIn our cross-sectional study, we enrolled PD patients with Hoehn & Yahr stage <=2 without fragility fracture. In this population, we assessed the following outcomes: BMD of left femoral neck (l-FN), lumbar spine (LS) measurement by GE Lunar i-DXA, and TBS by TBS iNsight™ software; muscle performance using Short Physical Performance Battery (SPPB) to identify a "poor performance" group A (SPPB score <= 8), and "high performance" group B (SPPB >8). Distribution of all variables was tested using Shapiro-Wilk test. All variables were normally distributed; intergroup comparisons were made using t-test for independent variables. Continuous variables are presented as mean +/- standard deviation (SD), and categorical variables as counts and percentage (%).ResultsWe included 13 PD patients (7 men, 6 women) aged 65.8 +/- 6.1 years, with a BMI of 27.6 +/- 3.9 kg/m2 and duration of PD 4.2 +/- 1.2 years.The DXA examination showed the following results: L1-L4 BMD = 1.19 +/- 0.160 g/cm2, T-score =-0.67 +/- 1.23 SD; l-FN BMD=0.825 +/- 0.134 g/cm2, T-score =-1.62 +/- 1.04 SD. The mean value of TBS was 1.311 +/- 0.14. Bone microarchitecture was degraded in 4 patients (30.8%) and partially degraded in 3 patients (23.1%). Age was not statistically significant associated with low BMD (<-1 SD at LS or l-FN, p=0.337), whereas it was statistically significant associated with low TBS (<1.350, p=0.032). The SPPB mean score was 8.8 +/- 2.3. Five patients (38.5%) included in group A and 8 patients (61.5%) in group B. For densitometric values, there are no statistically significant differences between the two groups (BMD LS vs SPPB p=0.587; BMD l-FN vs SPPB p=0.958); otherwise, for the qualitative evaluation, statistically significant between-group difference is observed (p <0.0063).ConclusionOur data suggest that TBS might identify bone involvement earlier than BMD in initial stages of PD, confirming the experimental findings of an early bone microarchitectural alteration due to dopaminergic depletion regardless of motor impairment. On the other side, it seems that the worsening of physical performance is associated with poor bone microarchitecture instead of low bone density in early PD patients.

***Disclosures: Antimo Moretti**, None*

P-631

Changes in Bone and Fat derived hormones are correlated with BMD and Body Fat at 12 months after initiation of antiretroviral therapy in men with HIV. *Arnold Olali[1], Ryan Ross[1], Elizabeth Shane[2], Michael Yin[2]. [1]Rush University Medical Center, United States, [2]Columbia University Medical Center, United States

Low bone mineral density (BMD) is commonly observed in people living with HIV (PLWH), especially after initiation of combination antiretroviral therapy (cART). cART initiation is also associated with lipodystrophy, which is characterized by body fat redistribution. Although previous studies have reported an association between cART initiation and change in bone and fat mass, the mechanisms remain unclear. There is growing evidence that bone and fat cells produce hormones that influence the function of one another. Therefore, in the current study, we tested the hypothesis that cART initiation induces changes in the circulating levels of the bone-derived hormones, undercarboxylated osteocalcin (ucOCN), and lipocalcin-2 sclerostin, and the fat-derived hormones, leptin and adiponectin, and that these changes are associated with BMD and fat mass. Serum samples were collected from a small cohort of men with HIV (n=15) initiating fixed dose tenofovir disoproxil fumarate/em-

tricitabine/efavirenz at baseline, prior to cART initiation, and at 12-months after initiation. BMD at the lumbar spine (LS) and femoral neck (FN), as well as, trunk fat was evaluated using dual energy x-ray absorptiometry (DXA) 12 months after initiation. Serum ucOCN, sclerostin, leptin, adiponectin and lipocalcin-2 were measured using enzyme-linked immunosorbent assays (ELISAs). Baseline and 12-month hormones levels were compared using paired t-test or a Wilcoxon rank test. The correlation between change in hormone levels and BMD and body fat was evaluated using Spearman's rank order correlation analysis. There was a significant reduction in LS BMD ($p<0.05$) and FN ($p=0.003$). There was a significant increase in lipocalin-2 ($p=0.012$), and no significant changes in ucOCN, leptin, adiponectin, and sclerostin between baseline and 12-months. Change in sclerostin between baseline and 12-months was positively associated with LS ($r=0.649$, $p=0.012$) and FN BMD ($r=0.548$, $p=0.043$). Change in ucOCN was negatively associated with trunk fat ($r=0.538$, $p=0.047$) and change in adiponectin was negatively associated with LS BMD ($r=-0.600$, $r=0.023$). Our findings support previously published work demonstrating the association between circulating sclerostin and bone mass . The associations noted between the bone-derived hormone, ucOCN, and trunk fat and the fat-derived hormone, adiponectin, and lumbar spine BMD are supportive of bone-fat hormonal cross-talk in PLWH treated with ART.

***Disclosures: Arnold Olali**, None*

P-632

Hip Fracture risk in Type 2 Diabetes in an elderly population of three Communities of Central Spain **Federico Hawkins[1], Guillermo Martínez Díaz-Guerra[1], David Lora[1], Felix Bermejo Pareja[1]. [1]Research Institute i+12,University Hospital 12 de Octubre, Spain

Background.Type 2 Diabetes (T2D) affects approximately one-third of those aged 65 and older. Data on Hip Fracture (HF) risks in T2D are inconsistent.The reported risk factors(RFs) for these fractures are under discussion. We have performed a study to analyze RFs in elderly patients with and withoutHF and T2D.Design and Methods.We have studied the association ofHFwithT2D in the NEDICES cohort survey.Subjects were selected by the local census. A questionnary and a detailed face-to-face interview for the evaluation of T2D was performed in people aged >=65 years from three areas:1)Lista (professional class);2) Las Margaritas (workingarea);3) Arévalo (agriculture zone).This areas were selected because there were approximately 2000 inhabitants, facilities of computer-based registry medical data, and represented different socioeconomic geographic communities of central Spain. Results. There were initially 5278 screening patients, 42.3%were men and 67.6% women.Of these 874 were T2D; prevalence of T2D was higher in women respect men (18.5% vs. 1.4%). Age was similar in T2D (74+/-6 yrs) and non-DM (74.4+/-7). HF was present in 21 T2D (2.4%)and in 145 non-diabetics (3.3%).BMI was significantly higher in T2D vs.non-DM(28.2+/-8 vs. 27.2+/-5,p<0.001). Smoking(12.4%vs.9.6%),alcohol ingestion (35.1%vs.24.3%),p=<0.001)were higher in non-DM, while diagnosis of osteoporosis and serum cholesterol levels were similar.Hypertension was significantly higher in T2D (63% vs. 48%, p=<0.001).Other RFs were cataracts (39.9%vs.29%,p<0.001),CVD (14.5% vs.9.2%, p<0.001).Patientswith HF were older and there were more females (81%) and mostly diagnosed of osteoporosis (46.9 vs,15%,p<0.001).T2D was not significantly different in patients with/without HF. Charlson and Carey indexes were higher in areas 2 and 3(p<0.001).There was a higher percent of illiterates and lower higher studies in T2D and in patients with HF.Percentage of HF was lower in zone 3(rural) compared with 1 and 2 (22.3%,39.2% & 38.5%, p<0.001).Conclusions. Our study provides information regard the associations of HF and T2D in a large cohort of community-dwelling elderly subjects. Cataracts, hypertension, CVD, comorbidites, and lower cultural levels are more frequent in T2D, while in patients with HF, osteoporosis, cataracts,female sex and differences in socioeconomic areas has to be considered.

***Disclosures: Federico Hawkins**, None*

P-633

Is Hypocitraturia Associated with Reduced Bone Mineral Density? *Anusha Veeravanallur Appuswamy[1], Frederick Hance[2], Stephen Knohl[3], Donald Cibula[4], Scott Wiener[5], Ruban Dhaliwal[6]. [1]Division of Endocrinology, Diabetes and Metabolism - SUNY Upstate Medical Univeristy, United States, [2]College of Medicine, SUNY Upstate Medical University, United States, [3]Division of Nephrology, SUNY Upstate Medical Univeristy, United States, [4]Department of Public Health and Preventative Medicine, SUNY Upstate Medical University, United States, [5]Division of Urology- SUNY Upstate Medical Univeristy, United States, [6]Division of Endocrinology, Diabetes and Metabolism - SUNY Upstate Medical Univeristy, United States

Purpose:Hypercalciuria is a known risk factor for bone mineral density (BMD) loss. Hypocitraturia (HC), a metabolic alteration that facilitates the formation of kidney stones, is commonly observed with hypercalciuria. The objective of this study was to determine the effect of hypocitraturia on bone mineral density as an independent risk factor and in the presence of hypercalciuria. Methods:In total, 211 patients were included in the study of four groups: group A – 42 patients with HC without hypercalciuria, group B – 98 patients with hypercalciuria without HC, group C – 40 patients with HC and hypercalciuria, and group D – 31 controls. Parameters of phospho-calcium metabolism, bone metabolism and bone densitometry were assessed. The intergroup differences in BMD were analyzed by one-way ANOVA with multiple comparisons. Hochberg's T2 comparisons were used for variables with homogeneous variance among groups; Games-Howell comparisons were used when the equal variance assumption was not met.Results:Baseline characteristics (weight, body mass index, serum intact parathyroid hormone and 25-hydroxy vitamin D levels) were similar between groups. Mean age was lower in group C compared to group D (44.7 +/- 13.7 vs 53.9 +/- 14.2 years, $p<0.05$). Twenty-four-hour urine calcium was higher in groups B and C (subjects with hypercalciuria) than in groups A or D ($p<0.05$). Twenty-four-hour urine citrate was lowest in group A compared to all other groups (all p values <0.05). Mean lumbar spine BMD was lower in group C (1.074 +/- 0.144) compared to groups A, B and D (1.102 +/- 0.160, 1.113 +/- 0.198 and 1.118 +/- 0.180 respectively), but did not differ significantly between groups ($p=0.67$). Adjusting for age had no effect on this comparison.Conclusion:Despite younger age of patients in group C (with hypocitraturia and hypercalciuria), this group had the lowest BMD. The lack of statistical significance was likely a consequence of small sample size. Hypocitraturia, similar to hypercalciuria, may be a risk factor for bone loss, independent of age. Hypocitraturia may also accentuate bone loss in the presence of hypercalciuria. Larger studies are needed to ascertain whether individuals with hypocitraturia and hypercalciuria have a higher risk of osteopenia and osteoporosis.

***Disclosures: Anusha Veeravanallur Appuswamy**, None*

P-634

Factors Contributing to Fracture in Pernicious Anemia Patients Presenting with Symptomatic Subacute Vertbral Compression Fractures *Nir Ben-Shlomo[1], Michael Lovy[2]. [1]University of Iowa Medial School, United States, [2]Desert Oasis Healthcare, United States

PURPOSE: Pernicious anemia has been associated with both low spine BMD and increased fracture risk in retrospective cohort studies. The cause of these observations is obscure. The purpose of this study is to describe and compare the clinical details of a cohort of pernicious anemia patients who presented with subacute vertebral compression fractures (SVCF) to one without pernicious anemia.METHODS: A retrospective cohort study was conducted from a population of 173 patients presenting with SVCF to an outpatient fracture clinic. The clinical characteristics of 38 pernicious anemia patients diagnosed at the time of presentation, based low vitamin B12 levels and either intrinsic factor (IF) or antiparietal cell antibodies (APCA), was compared to the remaining 135 without pernicious anemia. A complete history and physical exam including review of past medical records and current and past radiographs was performed. CBC, sedimentation rate, chemistry profile, TSH, urinalysis, vitamin B12, PTH, 25-OH vitamin D, and serum protein electrophoresis was done in all patients.RESULTS: There were 27 female and 11 male pernicious anemia patients, ranging in age from 66-96 (mean 79.5 years) with a BMI of 15-31 (mean 25.3). 17 patients were taking thyroid hormone and 16 were on protein pump inhibitors (PPIs) . 19 had previous fractures. Fractures occurred after falling in 28, lifting in 3, and were spontaneous in 6. The location of the fracture was between T-11 and L-2 in 58% of cases and 10 patients presented with multiple fractures. 31 out of the 38 patients had evidence of peripheral neuropathy. IF was present in 21 patients, APCA in 7, and 10 had both. 25-OH vitamin D was 65 pg/ml in 10. A monoclonal gammopathy of undetermined significance (MGUS) was found in 7. There was an increased incidence of peripheral neuropathy ($p<0.0001$), 25-OH vitamin D <20ng/dl ($p< 0.0003$), use of PPIs (p 65 ng/dl ($p=0.00001$), thyroid disease ($p=0.04$), and MGUS ($p=0.064$) in the patients with pernicious anemia. Age, gender, previous fractures, diabetes, BMI, fracture location, mechanism of fracture, and occurrence multiple fractures did not differ between the two cohorts.CONCLUSIONS: This cohort of SVCF patients with pernicious anemia had a higher incidence of peripheral neuropathy, vitamin D deficiency, hyperparathyroidism, thyroid disease and MGUS than SVCF patients without pernicious anemia. These observations may explain the higher incidence of fractures and low BMD found in previous studies of pernicious anemia patients.

***Disclosures: Nir Ben-Shlomo**, None*

P-636

Denosumab for preoperative management of severe hypercalcemia due to primary hyperparathyroidism *Anna Eremkina[1], Julia Krupinova[1], Ekaterina Bibik[1], Anna Gorbacheva[1], Natalia Mokrysheva[1]. [1]Endocrinology Research Centre, Moscow, Russian Federation

Intoduction: Denosumab is widely used and approved for hypercalcemia of malignancy. But data on its applying in patients with primary hyperparathyroidism (PHPT) is limited.Aim: We present 2 cases of PHPT patients that received denosumab prior to surgery. Material and methods. The values are: «albumin-adjusted» serum calcium (Ca, RR 2.15-2.55 mmol/l), phosphate (P, RR 0.74-1.52 mmol/l), intact parathyroid hormone (iPTH, RR 15-65 pg/ml) concentrations, glomerular filtration rate (GFR, ml/min/1.73m2); dual energy X-ray absorptiometry (DXA).Case 1. Female 40-year old patient with no significant past medical history presented with pathological fracture of the femur and osteoporosis on DXA (total hip –3.9 SD, total radius –5.4SD, L1-L4 -1.2SD in Z-score). Laboratory data revealed Ca 3.99 mmol/l, P 0.56 mmol/L, GFR 68, iPTH 1120 pg/ml. Considering the increase in neurological symptoms, the denosumab 60 mg was administred in combination with cinacalcet 30 mg and rehydration therapy. Normocalcemia (2.46 mmol/l) was achieved on the 9th day, cinacalcet was discontinued. After curative parathyroid surgery Ca dropped to 1.75 mmol/l. Active vitamin D and calcium supplements were prescribed. Histopathological examination confirmed parathyroid adenoma.Case 2. 61 year-old man with previous history of PHPT,

osteoporosis (total hip -2.5SD, total radius -4.5SD, no change in L1-L4 in T-score), chronic cardiovascular and kidney disease (GFR 13) presented with severe hypercalcemia: Ca 4.11 mmol/l, P 1.18 mmol/l, iPTH 2146 pg/ml. To prevent the hypercalcemic crisis and stabilize renal function denosumab 60 mg, saline infusion and cinacalcet 120 mg were administred. Follow-up Ca levels were: day 3rd– 3.5 mmol/l, 7th – 2.82 mmol/l with complete normalization on the 10th day, then cinacalcet was gradually discontinued . Right lower (55 mm) and upper left (15 mm) parathyroid glands tumors were removed, Ca decreased to 1,72 mmol/l the day after resection. The histological examination confirmed parathyroid carcinomas. The therapy with active vitamin D and calcium supplements was carried out to manage postoperative hypocalcemia.Conclusion. Denosumab interferes with RANKL signaling, inhibits bone resorption and thereby reduces calcium level. Thus, it could be useful to control severe hypercalcemia in patients with PHPT and bone impairment before surgery. Benefits include no restrictions of Denosumab use in patients with concomitant CKD.

***Disclosures: Anna Eremkina**, None*

P-637

Infection among Denosumab and Alendronate Users for Osteoporosis *Jiannong Liu[1], Haifeng Guo[1], kimberly Niewan[1]. [1]Hennepin Healthcare Research Institute, United States

Denosumab (Prolia, DEN) was approved to treat osteoporosis with a warning of serious infection risk. Studies on infection risk for DEN have been conducted based on clinical trial data or case reports. We assessed serious infection risk for DEN, compared with alendronate (ALN), in real-world practice.We used 2011-2017 Medicare 20% database and included patients who initiated DEN or ALN for osteoporosis 2012-2016, were aged >=66 years and covered by Medicare for >=1 year pre-initiation; patients with cancer were excluded. Patients were followed from medication initiation to the earliest of death, Medicare coverage loss, 90 days after medication discontinuation, or 12/31/2017. Outcomes included any serious infection (hospitalization due to cellulitis, infectious endocarditis, gastroenteritis, diverticulitis, labyrinthitis, osteomyelitis, urinary tract infection, or respiratory infection) and cause-specific serious infections (hospitalization due to one of the above). Adjusted 2-year infection probability was calculated for DEN users and ALN users separately to compare infection risk between DEN and ALN use; the probability was adjusted for patient demographics, previous zoledronic acid use, and previous infections (serious and mild [non-hospitalized], separately). Analysis was also performed separately for men and women.In total, 73,750 DEN and 103,790 ALN users were included. DEN users were older (mean age 78.1 vs 76.7 years); more were female (93.3% vs 89.7%) and white (87.2% vs 80.5%). Previous serious infection rates were similar (8.7% vs 8.8%), but DEN users had more previous mild infections (59.1% vs 53.9%,). During the mean follow-up of 20.9 and 19.2 months for DEN and ALN users, respectively, 5.9% of DEN and 4.9% of ALN users had serious infections. Adjusted 2-year infection probability was 6.8% (95% CI: 6.50-7.05) for DEN vs 6.3% (95% CI: 6.13-6.55) for ALN users. Adjusted probability of cause-specific serious infection varied by cause (Table 1). Due to a small number/percent of male users, results for women were almost identical to those for all and estimates for men are not stable. We found low serious infection risk among DEN and ALN users. Estimate of adjusted infection probability was slightly higher for DEN users, but the difference was not clinically significant and varied slightly by cause. As with other observational studies, despite adjustment for demographics and previous infection, results might be biased due to unmeasured confounders.

Table 1. Percentages of Patients with Serious Infection in the Baseline and Follow-up Periods and Adjusted 2-Year Serious Infection probability with 95% Confidence Interval among Denosumab and Alendronate Users

Infections	Baseline Period		Follow-up Period			
	Percent of Infection		Percent of Infection		Adjusted 2-Year Infection Probability*	
	Alendronate	Denosumab	Alendronate	Denosumab	Alendronate	Denosumab
Any Infection	8.70	8.76	4.87	5.94	6.34 (6.13,6.55)	6.77 (6.50,7.05)
Cellulitis	0.91	0.83	0.66	0.74	0.85 (0.77,0.93)	0.87 (0.76,0.98)
Endocarditis	0.05	0.07	0.01	0.02	0.02 (0.01,0.03)	0.03 (0.00,0.05)
GI*	1.63	1.75	0.60	0.88	0.78 (0.70,0.86)	0.98 (0.87,1.09)
Diverticulitis	0.88	1.06	0.20	0.31	0.26 (0.22,0.31)	0.37 (0.30,0.44)
Labyrinthitis	0.02	0.03	0.01	0.02	0.01 (0.00,0.02)	0.01 (0.00,0.02)
Osteomyelitis	0.05	0.03	0.04	0.05	0.04 (0.03,0.06)	0.07 (0.04,0.11)
UTI**	4.52	4.36	1.47	1.63	1.96 (1.84,2.08)	1.86 (1.71,2.01)
Respiratory	3.21	3.14	2.20	2.75	2.96 (2.81,3.11)	3.14 (2.95,3.34)

*Adjusted for demograophics, previous zoledronic acid use, and previous infections. Alendronate users was the reference cohort.
**GI=gastroenteritis; UTI=urinary tract infection

***Disclosures: Jiannong Liu**, None*

P-638

Factors associated with vertebral fractures after Denosumab. A retrospective study of 797 cases. *Olivier Lamy[2], Peter Burckhardt[0], Thierry Buclin[1], Mohamed Faouzi[3], Daniel Aeberli[4], Fabio Cattaneo[4], Jean Dudler[4], markus Felder[4], Diana Frey[4], paul hasler[4], Hans Jörg Häuselmann[4], Sigrid Jehle-Kunz[4], Ina Krull[4], Thomas Lehmann[4], Kurt Lippuner[4], Christian Meier[4], Urs Moser[4], Martin Oehri[4], Andreas Rohrer[4], Franco Tanzi[4], Martin Toniolo[4], Brigitte Ubelhart[4], Lukas Wildi[4], Dagmar Wildpaner[4]. [2]University Hospital CHUV, Switzerland, [0]Clinique Hirslanden, Switzerland, [1]University Hospital CHUV, Switzerland, [3]university, Switzerland, [4]Swiss Denosumab Study Group, Switzerland

PURPOSE: Search of factors influencing the occurrence of vertebral fractures (VF) after Denosumab Treatment (DMAB).METHODS: 22 specialists in Switzerland collected data of 861 randomly chosen women, in whom DMAB was interrupted, by a questionnaire for the periods before, during and after DMAB.RESULTS: We excluded 64 cases with missing data, and analyzed 797 cases (134 breast cancer). Mean age was 65.3 years (27-92). 91 patients experienced VF after discontinuation of DMAB, in average 2.6 VF (1-5), 15.6 months (median 12) after the last dose of DMAB. DMAB was given for +35 months (5-120) and the follow-up after DMAB was +25.7 months (1-78). The incidence of VF was 19.8% before, 2.3% during, and 11.4% after DMAB. Lumbar spine BMD (T-score) increased sign. by 26% during DMAB, and decreased sign. by 14% thereafter. Fem. neck and total hip BMD changed accordingly. TBS improved sign.by 4.0% during DMAB, and did not decline thereafter.Patients with VF after DMAB discontinuation had no higher resorption markers (ResM) measured before DMAB than those without VF. But they had more previous VF (HR=1.8, p=0.009) and were less often previously treated with bisphosphonates (BP) (HR=0.35, p<0.001). Their total hip BMD was lower before DMAB (HR=0.71, p=0.06), during DMAB (HR=0.62, p=0.004), and after DMAB (HR=0.69, p=0.01). After DMAB, their femoral neck BMD was lower (HR=0.61, p=0.005), and their ResM were higher (HR=1.71, p<0.001). They experienced sign. more non-vertebral fractures after DMA discontinuation (6.6% vs 1.4%).Patients without VF after DMAB discontinuation received more often BP after DMAB than women who fractured (68.7% vs 48.3%, IRR=0.41, p<0.001), and BP were given earlier: 9.1 mos after the last DMAB dose vs 16.5 mos (HR=1.06, p<0.0001).The number of VF after DMAB discontinuation (NbVF) did not correlate with risk factors for osteoporosis, neither with the number of DMAB injections, nor with the pre-DMAB lumbar spine and femoral neck BMD. But it correlated negatively with total hip and femoral neck BMD after DMAB (both p=0.02), and positively with ResM measured after DMAB (IRR=2, p=0.001). It was decreased by a treatment with BP before DMAB (IRR=0.26, p<0.001), and after DMAB (IRR=0.52, p=0.03). The changes in BMD during and after DMAB had no sign. influenceCONCLUSION: This retrospective study describes the factors favoring an increase of VF after DMAB cessation, esp. prevalent VF, low BMD, high resorption markers, no treatment with bisphosphonates.

***Disclosures: Olivier Lamy**, None*

P-639

Evaluation of Relugolix Combination Therapy to Maintain Bone Mass in Women with Uterine Fibroids Through 52 Weeks: LIBERTY Long-Term Extension Study *Michael R. McClung[1], Arthur Santora[2], Ayman Al-Hendy[3], Laura McKain[4], Yulan Li[4], Rachel B. Wagman[4]. [1]Oregon Osteoporosis Center, United States, [2]Kinexum Services LLC, United States, [3]Department of Obstetrics and Gynecology, University of Illinois/Chicago, United States, [4]Myovant Sciences Inc., United States

Purpose: Relugolix combination therapy (Rel-CT), a once-daily, orally active, non-peptide, gonadotropin-releasing hormone (GnRH) receptor antagonist, estradiol (E2), and norethindrone acetate (NETA), reduced menstrual blood loss and pain in women with uterine fibroids and was well tolerated with preservation of bone mineral density (BMD) through 24 weeks (Al Hendy, 2019). We assessed the effects of Rel-CT on BMD for up to 52 weeks of treatment in the LIBERTY extension study.Methods: Patients with heavy menstrual bleeding associated with uterine fibroids who were enrolled in 24-week double-blind, placebo-controlled LIBERTY 1 and 2 trials were randomized to receive Rel-CT, delayed Rel-CT (relugolix 40 mg monotherapy for 12 weeks followed by Rel-CT for 12 weeks), or placebo. Women who completed those trials who met all entry criteria were eligible to enroll in a 28-week study extension in which all women received once-daily treatment with open-label Rel-CT. BMD was assessed by dual-energy X-ray absorptiometry of the lumbar spine (L1–L4) and proximal femur at baseline, at Weeks 12 and 24 in LIBERTY, and Weeks 36 and 52 in the extension. Percent change from LIBERTY baseline was summarized by location according to original treatment assignment using a mixed-effect model with repeated measures adjusted for region, visit, and selected baseline characteristics.Results: Of the 610 women who completed LIBERTY 1 and 2 studies, 477 (78%) were enrolled in the extension, of which 363 (76%) completed. Least squares mean % change BMD from baseline to Week 52 in lumbar spine and total hip for Rel-CT was –0.80% and –0.15%, respectively (Figure). These values were relatively unchanged from Week 12 and were similar to values for the placebo group that transitioned to Rel-CT at Week 24. In the delayed Rel-CT group, which showed significant bone loss after 12 weeks of relugolix monotherapy, BMD remained stable upon transitioning to Rel-CT through 52 weeks. Similar patterns of change in total hip BMD were observed.Conclusion: The combination of relugolix with E2/NETA maintained BMD

through 52 weeks of treatment. Rel-CT represents a potential long-term treatment for women with symptomatic uterine fibroids, providing therapeutic benefit while preserving BMD.

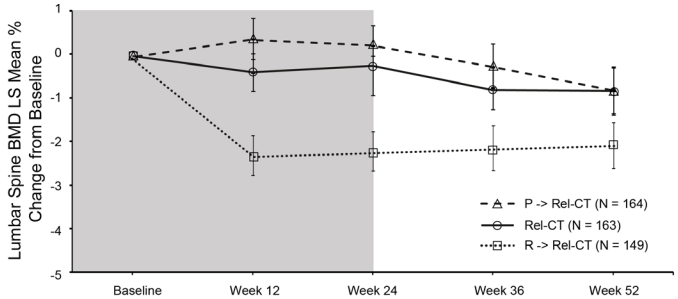

No. of patients					
P → Rel-CT	164	146	156	138	120
Rel-CT	163	145	153	145	132
R → Rel-CT	149	137	144	120	108

BMD = bone mineral density; LS = least squares; N = number of patients in the parent study treatment group; P = placebo; R = Relugolix; Rel-CT = Relugolix Combination Therapy. Note: LS means are generated separately for each treatment group and are based on a mixed-effect model with visit, region, baseline menstrual blood loss volume (<225 mL, ≥225 mL), age at baseline, body mass index at baseline, BMD at baseline, and race included as fixed effects. The multiple visits for each patient were the repeated measures as random effect within each patient and an unstructured covariance. Error bars represent 95% confidence intervals.

***Disclosures: Michael R. McClung**, Amgen, Speakers' Bureau, Amgen and Myovant, Consultant*

P-640

Cardiovascular Risk in Patients Treated with Romosozumab: Disproportional Meta-Analysis *Abdulhafez Selim[1], Omar Selim[2], Paula Karabelas[3]. [1]PCOM, United States, [2]University of Maryland, Baltimore, United States, [3]Independent Scientist, United States

Background: Osteoporosis and cardiovascular (CV) diseases are closely correlated. Wnt signaling pathway is implicated in the pathogenesis of both osteoporosis and CV diseases. Romosozumab (ROMO), a sclerostin inhibitor, was FDA-approved in 2019 for the treatment of osteoporosis in postmenopausal women at high risk for fracture. Romosozumab works through Wnt signaling manipulation via the anti-sclerostin antibody mechanism. Sclerostin inhibition may enhance CV risk by increasing arteriosclerosis through boosted mineralization as well as lipid accumulation. We, therefore, aimed to investigate the risk of CV outcomes in patients with primary osteoporosis treated with ROMO.Methods: MEDLINE's PubMed, Cochrane Library, and EMBASE commercial databases were systematically searched from the inception dates to March 18, 2020. We included randomized clinical trials comparing ROMO versus active comparators (alendronate or teriparatide) or placebo for at least 6 months, in patients diagnosed with primary osteoporosis or osteopenia. Two investigators independently extracted data for study characteristics and outcomes of interest in accordance with PRISMA guidelines. For data analysis, we used the approach of disproportional analysis, which is a known tool to generate hypotheses on possible causal relations between drugs and adverse effects. We examined the following endpoints: composite CV outcome; three-point major adverse CV event (3P-MACE); 4P-MACE; myocardial infarction (MI); stroke; heart failure (HF); death or CV death; congestive heart disease (CHD); and atrial fibrillation (AF).Results: Six relevant studies with a total of 12,219 subjects were included. These subjects were as follows: 6,116 ROMO; 3,770 placebo (PBO); 268 teriparatide (TERI); and 2,065 alendronate (ALEN). A Disproportional analysis comparing ROMO subjects (6,116) to all other treatments combined (6,103 subjects) showed numerically higher risk ratios (mean and median values) in all endpoints (Table 1). However, statistical significance was only seen in 4P-MACE endpoint (Risk Ratio: 1.4 with 95.0% CI of 1.002 to 1.928).Conclusion: These data demonstrated a trend of higher rates in CV events in patients treated with ROMO. Additionally, a statistically significant risk was seen in the 4P-MACE endpoint. This causal relationship appears likely considering these data, as well as the biological plausibility. These findings highlight the importance of weighing risk versus benefits when treating patients with osteoporosis who have pre-existing CV risk factors. Additionally, our data demonstrated the need for extensive post-marketing studies aiming CV risk assessment.

Endpoint	Mean	SD	2.5%	Median	97.5%
Death or CV death	1.4265	0.5283	0.7404	1.3048	2.7636
AF	1.2575	0.5465	0.5525	1.1180	2.6693
CHF	1.6143	0.4529	0.9506	1.5542	2.6835
HF	1.3068	0.4427	0.7046	1.2041	2.4064
Stroke	1.4553	0.4170	0.8718	1.3888	2.4365
MI	1.3693	0.4673	0.7439	1.2673	2.5408
4P MACE	1.4056	0.2383	1.0020	1.3851	1.9288
3P MACE	1.4313	0.2750	0.9895	1.4054	2.0413
Composite	1.2769	0.1912	0.9636	1.2609	1.6952

***Disclosures: Abdulhafez Selim**, None*

P-641

Relugolix Combination Therapy Preserves Bone Mass in Patients with Uterine Fibroids: Results from Phase 3 LIBERTY Program *Michael R. McClung[1], Arthur Santora[2], Ayman Al-Hendy[3], Laura McKain[4], Yulan Li[4], Rachel B. Wagman[4]. [1]Oregon Osteoporosis Center, United States, [2]Kinexum Services LLC, United States, [3]Department of Obstetrics and Gynecology, University of Illinois/Chicago, United States, [4]Myovant Sciences Inc., United States

Purpose: Relugolix is a once-daily, orally active, non peptide gonadotropin releasing hormone (GnRH) receptor antagonist being developed in combination with estradiol (E2) and norethindrone acetate (NETA) for the treatment of heavy menstrual bleeding (HMB) associated with uterine fibroids (UF). The purpose of adding E2 to relugolix is to prevent the bone loss anticipated with relugolix monotherapy. The efficacy and safety of treatment was evaluated in replicate Phase 3 LIBERTY 1 and 2 trials. Relugolix combination therapy (Rel-CT [once-daily relugolix 40 mg, E2 1 mg, NETA 0.5 mg]) significantly reduced menstrual blood loss and pain in women with UF and was well tolerated (Al-Hendy, 2019). In these studies, we assessed the effects of Rel-CT vs relugolix monotherapy on bone mineral density (BMD).Methods: Premenopausal women (age 18–50 years) with HMB were randomized 1:1:1 to receive Rel-CT for 24 weeks, relugolix 40 mg alone for 12 weeks followed by Rel-CT for 12 weeks (delayed Rel-CT), or placebo for 24 weeks. BMD was assessed by dual-energy X-ray absorptiometry of the lumbar spine (L1–L4), total hip and femoral neck at baseline, and Weeks 12 and 24. Treatment comparisons were performed on pooled data from the LIBERTY 1 and 2 studies. Percent change from baseline was summarized by location for each treatment group using a mixed-effect model with repeated measures adjusted for region, visit, and selected baseline characteristics.Results: Evaluation included 768 patients. Least squares (LS) mean percent changes from baseline to Week 12 and 24 in lumbar spine BMD were comparable for Rel-CT vs placebo (Week 12: –0.63% vs 0.34%; Week 24: –0.23% vs 0.18%, respectively) (Figure). For patients who received 12 weeks of relugolix alone, % change from baseline at Week 12 was –1.96%, which stabilized with transition to Rel-CT at –1.97% at Week 24. Rel-CT was statistically superior to relugolix alone at Week 12 with a difference of 1.34% ($p < 0.0001$). Findings at the proximal femur were consistent with those at the lumbar spine and comparable between Rel-CT and placebo groups.Conclusion: Compared with relugolix alone, Rel-CT prevented bone loss over 12 weeks of treatment: this benefit was maintained over 24 weeks. Initiating treatment for with relugolix combined with E2/NETA represents a potential method for preserving BMD while providing therapeutic benefit for women with symptomatic UF.

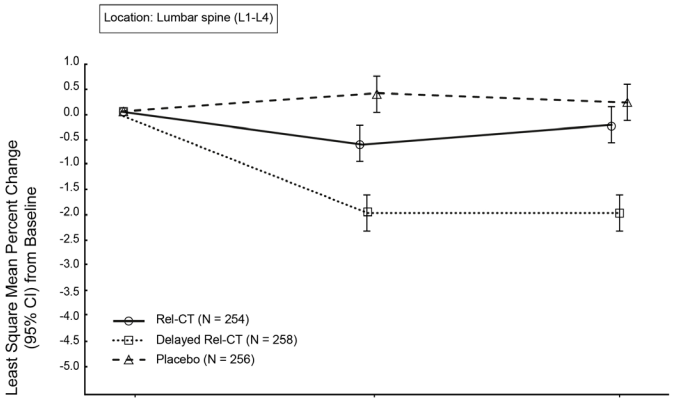

No. evaluable patients		Visit	
Rel-CT	254	204	195
Delayed Rel-CT	258	198	194
Placebo	256	207	197

***Disclosures: Michael R. McClung**, Myovant, Consultant, Amgen, Speakers' Bureau, Amgen, Consultant*

P-642

Romosozumab After Denosumab Improves Lumbar Spine and Maintains Total Hip Bone Mineral Density in Postmenopausal Women with Low Bone Mass *MR McClung[1], MA Bolognese[2], JP Brown[3], J-Y Reginster[4], BL Langdahl[5], N Ruiz-Santiago[6], Y Shi[6], M Rojeski[6], J Timoshanko[7], C Libanati[7], H Kassahun[6], M Oates[6]. [1]Oregon Osteoporosis Center, United States, [2]Bethesda Health Research Center, United States, [3]Laval University and CHU de Québec (CHUL) Research Centre, Canada, [4]University of Liège, Belgium, [5]Aarhus University Hospital, Denmark, [6]Amgen Inc., United States, [7]UCB Pharma, Belgium

Objective: Romosozumab, an anti-sclerostin antibody that increases bone formation while decreasing bone resorption, reduces fracture risk within 12 months. Here we evaluate the effects of transitioning from denosumab to romosozumab in treatment-naïve patients.

Materials and Methods: This phase 2 trial (NCT00896532) enrolled postmenopausal women with a lumbar spine, total hip, or femoral neck T-score <= –2.0 and >= –3.5. Patients were randomized to placebo or various doses of romosozumab monthly or every 3 months from baseline to month (M) 24, were rerandomized to 12 months of denosumab 60 mg every 6 months or placebo (M24–36), and then all were to receive romosozumab 210 mg monthly for 12 months (M36–48). Results for the overall population have been previously published (McClung et al, J Bone Miner Res 2018; Kendler et al, Osteoporos Int 2019). Here we present data from a subset of patients who were randomized to placebo for 24 months, denosumab (n = 16) or placebo (n = 12) for 12 months, and then romosozumab for 12 months.Results: In patients who were randomized to placebo followed by denosumab, romosozumab treatment for 12 months maintained BMD gained during denosumab treatment at the total hip (mean change from end of denosumab treatment, 0.9%) and further increased BMD gains at the lumbar spine (mean change from end of denosumab treatment, 5.3%) (Table). As expected, P1NP and CTX levels decreased with denosumab. Upon transition to romosozumab (M36–48), P1NP levels initially increased and gradually returned to baseline by M48 while CTX gradually increased to baseline levels.In patients who transitioned to romosozumab after 36 months of placebo, BMD increased at the lumbar spine and total hip (Table). P1NP levels initially increased with romosozumab and gradually returned to baseline by M48 while median CTX level remained below baseline with romosozumab treatment.Conclusions: BMD response in the placebo to romosozumab group was similar to that observed in other studies. Transitioning to romosozumab after 12 months of denosumab further improves lumbar spine BMD and maintains total hip BMD.

Table

Treatment from M0–24:	Placebo	Placebo
Treatment from M24–36:	Placebo	Denosumab 60 mg Q6M
Treatment from M36–48:	Romosozumab 210 mg QM	Romosozumab 210 mg QM
	N = 12	N = 16
Bone Mineral Density, mean % change (95% CI)		
Lumbar spine		
M0–24	2.7 (0.2, 5.1)	–0.8 (–2.8, 1.1)
M24–36	–0.4 (–2.1, 1.4)	5.5 (3.6, 7.4)
M36–48	9.1 (6.1, 12.1)	5.3 (3.2, 7.4)
M24–48	8.9 (5.5, 12.4)	11.5 (8.8, 14.3)
Total hip		
M0–24	–2.2 (–3.6, –0.8)	–1.6 (–2.7, –0.5)
M24–36	–0.3 (–1.4, 0.8)	2.8 (2.1, 3.6)
M36–48	4.6 (2.7, 6.4)	0.9 (–0.1, 1.8)
M24–48	4.7 (2.7, 6.7)	3.8 (2.6, 5.0)
Bone Turnover Marker, median (Q1, Q3)		
P1NP, µg/L		
M0	37.0 (33.8, 41.0)	52.6 (44.9, 59.2)
M24	38.2 (30.0, 55.6)	50.0 (40.0, 56.0)
M36	35.9 (30.3, 55.5)	17.4 (11.2, 21.4)
M39	49.5 (36.3, 79.9)	43.1 (31.6, 55.6)
M48	36.2 (29.2, 48.2)	64.6 (54.2, 72.5)
β-CTX, ng/L		
M0	372.0 (306.0, 415.5)	503.5 (392.5, 635.5)
M24	534.0 (433.5, 692.0)	626.0 (466.0, 833.0)
M36	376.0 (305.0, 533.5)	162.5 (95.5, 268.0)
M39	348.0 (282.0, 438.5)	311.0 (239.0, 385.0)
M48	321.0 (276.5, 407.0)	532.0 (378.0, 661.0)

β-CTX = β-isomer of the C-terminal telopeptide of type I collagen, CI = confidence interval, M = month, P1NP = procollagen type 1 N-terminal propeptide, Q1 = quartile 1, Q3 = quartile 3, QM = monthly, Q6M = every 6 months.

Disclosures: MR McClung*, Myovant, Consultant, Amgen Inc., Speakers' Bureau, Amgen Inc., Consultant*

P-643

Heterogeneity in the Cortical Response to Abaloparatide and Teriparatide in the Proximal Femur by DXA-Based 3D Modeling *Renaud Winzenrieth[1], Michael S. Ominsky[2], Yamei Wang[2], Ludovic Humbert[1], Richard J. Weiss[2]. [1]Galgo Medical, Barcelona, Spain, Spain, [2]Radius Health, Inc., Waltham, MA, United States

Differences in the effects of abaloparatide (ABL) and teriparatide (TPTD) on cortical bone density were previously reported based on 3D modeling of proximal femur DXA images. These changes were further examined in the femur neck (FN), intertrochanteric (IT), and shaft (S) subregions to determine heterogeneity and impact on bone strength indices. Baseline, 6 month (M), and 18 M hip DXA scans from 750 patients, 250 in each group (PBO, ABL, TPTD), from the ACTIVE trial were subjected to DXA-based 3D modeling (3D-SHAPER v2.10.1, Galgo Medical, Spain). Changes from baseline were calculated for each subregion for cortical thickness (Ct.Th), cortical volumetric BMD (Ct.vBMD), cross-sectional moment of inertia (CSMI), and section modulus (Z). Regions in the proximal femur that lost vBMD from baseline during treatment were further evaluated to quantify the % of total volume and average vBMD loss. Comparisons to baseline were made using paired t-tests; pairwise group comparisons were made for % change from baseline data using P-values derived from contrast tests based on an MMRM model.For each subregion at 18 M, ABL and TPTD similarly increased Ct.Th from baseline (1.4-2.1%; all P<0.05), while only ABL significantly increased Ct.vBMD from baseline (1.4-1.8%; all P<0.05). Ct.vBMD improvement with ABL was associated with greater increases in the density-weighted strength indices CSMI and Z than with TPTD, particularly at the more cortical subregions (FN: 7.2-7.7% vs 4.5-5.0%; S: 2.7-3.2% vs 0.4-0.5%, all P<0.001 ABL vs TPTD). Analysis of the anatomical distribution of average changes in vBMD revealed areas within the proximal femur where vBMD decreased at 6 and 18 M, as shown in the Figure. At 6 M, treatment with TPTD, and to a lesser extent ABL, resulted in focal declines in vBMD, primarily in the cortical shaft. At 18 M, the % volume with vBMD decline was persistent in the TPTD group (6.11%) but mostly reversed in the ABL group (0.14%).Both ABL and TPTD resulted in increased positive changes in Ct.Th and bone strength indices across the proximal hip by DXA-based 3D modeling after 18 M. The greater ABL-mediated increases in Ct.vBMD were associated with lesser focal losses than with TPTD, with vBMD losses having resolved after 18 M of ABL. Future research may investigate the mechanisms by which these differences in cortical vBMD occur and estimate their impact on hip strength.

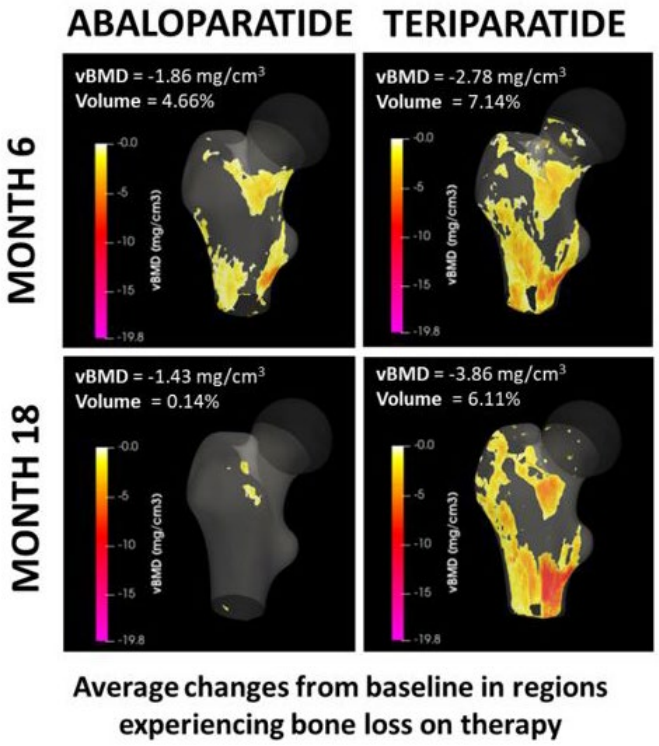

Disclosures: Renaud Winzenrieth*, Galgo Medical, Other Financial or Material Support, Radius Health, Consultant*

P-644

Geographic Variation in Prevalence of Osteoporosis Diagnosis and Utilization of Anti-Osteoporosis Therapies in United States Female Medicare Fee-for-Service Beneficiaries with Fragility Fractures *E. Michael Lewiecki[1], Andrea J. Singer[2], Pallavi B. Rane [3], Anne Shah[4], Allison Petrilla[4], Kris Norris [4], Michele McDermott[3], Shravanthi R. Gandra[3]. [1]University of New Mexico Health Sciences Center, United States, [2]MedStar Georgetown University Hospital, United States, [3]Amgen Inc., United States, [4]Avalere Health, United States

Background: There is limited real-world evidence on geographic variation in prevalence of fragility fractures among postmenopausal women in the US, and in osteoporosis diagnosis or treatment rates in such women.Objective: To describe geographic variations in distribution of fragility fractures among female Medicare Fee-for-Service (FFS) beneficiaries at the sub-national level, and to describe osteoporosis diagnosis and treatment rates among these women.Methods: This retrospective cohort study utilized the 100% Medicare FFS Part A, B, & D claims data. Female beneficiaries aged >=66 years were identified on the first occurrence of a fragility fracture of hip, vertebra, or non-hip non-vertebral in the hospital or outpatient setting (based on diagnosis and procedure codes on medical claims), between Jan 1, 2011 – Dec 31, 2017. Fracture-related measures in the year preceding and following fracture included: diagnosis of osteoporosis (medical claim with ICD9/10 diagnosis code for age-related or other osteoporosis), use of anti-resorptive or anabolic agents, receipt of bone mineral density (BMD) testing, and subsequent fracture events.Results: Among the 26,104,783 women who met study eligibility criteria, 1,026,295 (3.9%) had >=1 fragility fractures (mean[SD] age= 82.2[8.5] years; 91.2% were Caucasian and 38.8% were from southern regions, with mean[SD] Charlson comorbidity index score= 1.9[2.3]). The most commonly occurring index fracture were hip (38.2%), followed by non-hip non-ver-

tebral (37.0%), and vertebral (24.8%), with 74.6% of all index fractures reported in a hospital setting. In the 1-year pre-index fracture period, 10.2% of women received a BMD test, 15.2% had a diagnosis of osteoporosis, and 17.5% were receiving any anti-resorptive or anabolic agents. Despite having sustained fractures, these values increased to 12.8%, 36.2%, and 20.3%, respectively; and 10.0% of women had a subsequent fragility fracture in the 1-year follow-up period. There was geographic variation in different US states for fracture-related measures as described in Table 1; Hawaii had the lowest prevalence of fracture and subsequent fracture and the highest utilization of anti-resorptive or anabolic agents. Conclusion: Osteoporosis is underdiagnosed and undertreated in elderly US women with fragility fractures, and geographic variation is observed across different states in the US for fragility-fracture related measures.

Table 1. Geographic variation in fracture events, osteoporosis diagnosis and treatment

Fracture Related Measure	National Average	State Average (Lowest to Highest)
% Female Medicare FFS beneficiaries aged 66+ with ≥1 fragility fracture, 2011-2017	3.9%	1.9% (HI) to 8.5% (ND)
Events in women with ≥1 fragility fracture		
% with osteoporosis diagnosis in 1-year baseline period	15.2%	10.0% (DC) to 23.1% (ME)
% with osteoporosis diagnosis in 1-year follow-up period	36.2%	29.5% (DC,GA) to 45.8% (MT)
% with use of anti-resorptive or anabolic agents in 1-year baseline period	17.5%	13.7% (AL) to 28.7% (HI)
% with use of anti-resorptive or anabolic agents in 1-year follow-up period	20.3%	16.9% (AL) to 35.3% (HI)
% with a subsequent fragility fracture in 1-year follow-up period	10.0%	7.7% (HI) to 12.9% (VT)

AL=Alabama; CA=California; DC=Washington, DC; GA=Georgia; HI=Hawaii; MD=Maryland; ME=Maine; MT = Montana; ND=North Dakota; NJ=New Jersey; SD=South Dakota; VT=Vermont

***Disclosures: E. Michael Lewiecki**, Amgen Inc., Consultant*

P-645

Spaceflight-Induced Osteoporosis in Non-Weight-Bearing Bone and Treatment with BP-NELL-PEG *Timothy Liu[1], Diana-Beatrix Velicu[2], Stella Dong[2], Luan Tran[2], Shahin Setoudeh Maram[2], Josiah Low[1], Jiayu Shi[2], Kang Ting[2], Chia Soo[1], Jin Hee Kwak[2]. [1]David Geffen School of Medicine, University of California, Los Angeles, United States, [2]School of Dentistry, University of California, Los Angeles, United States

Purpose: Spaceflight induces osteoporosis by mechanical unloading. Interestingly, recent studies report that microgravity directly affects osteoblasts (OB) and osteoclasts (OC) in vitro, by upregulating OC activity and disrupting the OB cytoskeleton. Non-weight-bearing bones, such as those in the temporomandibular joint (TMJ), provide important insight into cellular-level effects of microgravity in vivo. NELL-1 is a novel osteogenic growth factor, which upon PEGylation (NELL-PEG) demonstrates enhanced pharmacokinetics and promising potential as a systemic therapy for osteoporosis in mice. To test NELL-PEG systemic therapy in spaceflight-induced osteoporosis, we have collaborated with CASIS and NASA through the Rodent Research 5 (RR-5) mission. This study is a branch of the RR-5 mission and, for the first time, focuses on the TMJ to investigate how space microgravity and NELL-1-based treatment affect non-load-bearing bones in vivo. Methods: To meet the mission's technical demands, we conjugated NELL-PEG with bioinert bisphosphonate as a bone-targeting molecule (BP-NELL-PEG, or 'BP-NP') to enhance NELL-PEG's pharmacokinetics and safety. Eight-month-old female BALB/c mice (n=10/group) were randomly assigned to 4 groups: (1) Flight + PBS, (2) Flight + BP-NP, (3) Ground + PBS, and (4) Ground + BP-NP. Flight and Ground groups were housed in the International Space Station and the Kennedy Space Center, FL, respectively, for 9 weeks. Mice received 10mg/kg BP-NP or PBS via intraperitoneal injection every 2 weeks. At 9 weeks, TMJ were analyzed with micro-CT and histology. Results: Micro-CT of subchondral bone of mandibular condyle showed increased porosity and decreased bone mineral density in Flight + PBS, compared to Ground + PBS. BP-NP treatment showed significantly increased subchondral bone in both Ground and Flight groups. Histology revealed significant changes in condylar cartilaginous zones (Fig. 1). Polymorphic zone thickness was significantly decreased in Flight + PBS compared to Ground + PBS. Strikingly, BP-NP treatment showed a 3-fold increase in thickness of the calcified hypertrophic zone in Ground and Flight groups. Treatment also showed an increased mature zone thickness in Flight group. Conclusion: Spaceflight induces osteoporotic changes in the TMJ, a non-weight-bearing joint, suggesting that microgravity has direct effects on OB and OC. In addition, BP-NP systemic therapy has demonstrated potent chondrogenic and osteogenic effects in the TMJ.

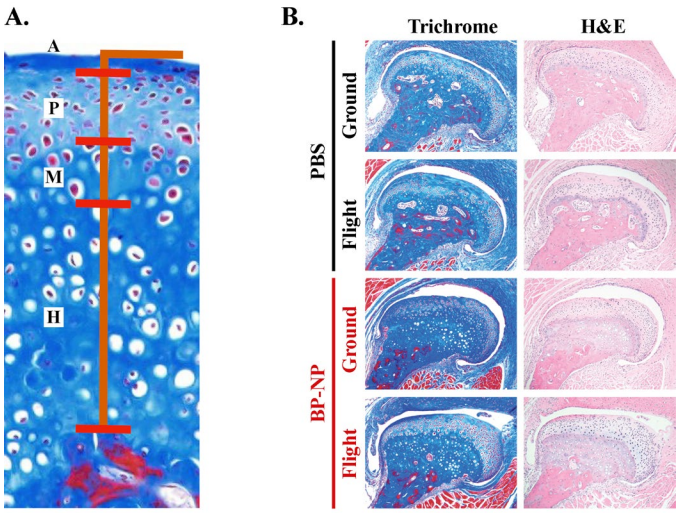

Figure 1. Histology. (A) Cartilaginous zones include A = Articular zone, P = polymorphic zone, M = mature zone, H = hypertrophic zone. (B) Representative images.

***Disclosures: Timothy Liu**, None*

P-646

Estimating Relative Fracture Reduction of Romosozumab versus Teriparatide for Postmenopausal Osteoporosis Using Bone Mineral Density Outcomes *Benjamin Johnson[1], Michael McClung[2], Stuart Silverman[3], Shravanthi Gandra[4], Jennifer Timoshanko[5], Björn Stollenwerk[6]. [1]Amgen Ltd, United Kingdom, [2]Oregon Osteoporosis Center, United States, [3]Cedars Sinai, United States, [4]Amgen Inc., United States, [5]UCB Pharma Ltd, United Kingdom, [6]Amgen GmbH, Switzerland

Introduction: When modelling the cost-effectiveness of osteoporosis therapies, relative treatment efficacy is typically informed by fracture outcomes. However, for the comparison of romosozumab versus teriparatide, no direct evidence exists on relative fracture incidence. Indirect comparisons of these treatments would require synthesis of studies with substantial heterogeneity in trial populations, sequential therapies, and follow-up times. Consequentially, estimates obtained would be prone to uncertainty and bias. Therefore, the aim of this study was to use direct bone mineral density (BMD) outcomes for romosozumab versus teriparatide to estimate relative risks (RRs) of fracture in postmenopausal women with osteoporosis. The approach is justified by the significant linear relationship between percentage total hip BMD change from baseline and RRs of hip and vertebral fracture on the log scale shown by a meta-regression conducted by the Foundation for the National Institutes of Health (FNIH). Methods: The STRUCTURE trial provides a 3.4% difference in total hip BMD change from baseline at 12 months for romosozumab versus teriparatide in patients previously treated with bisphosphonates. This value was translated into RRs of hip, vertebral, and nonvertebral fracture using slopes from the FNIH meta-regression. Uncertainty around resulting estimates was derived by error propagation. As a sensitivity analysis, BMD efficacy for romosozumab versus teriparatide was taken from a phase II trial (2.8% difference in total hip BMD change from baseline) to explore outcomes for a treatment-naïve population.Results: In the base case, RRs of fracture (with 95% confidence intervals) for romosozumab versus teriparatide were 0.75 (0.60 to 0.95), 0.53 (0.37 to 0.76), and 0.90 (0.78 to 1.03) for hip, vertebral, and nonvertebral fracture, respectively. The sensitivity analysis using phase II trial data yielded RRs of 0.79 (0.64 to 0.97), 0.59 (0.43 to 0.82), and 0.91 (0.81 to 1.03) for hip, vertebral, and nonvertebral fracture. Validation of the approach using romosozumab trials reporting both BMD and fracture outcomes at 12 months (FRAME, ARCH) showed consistency between BMD-predicted and observed RRs of fracture.Conclusion: Results indicate that the BMD benefit of romosozumab versus teriparatide translates into clinically meaningful fracture reductions for bisphosphonate pre-treated and treatment naïve patients.

***Disclosures: Benjamin Johnson**, Employee: Amgen, Other Financial or Material Support, Amgen, Major Stock Shareholder*

P-647

Sequential Therapy with Denosumab After Teriparatide Leads to Large Increases in Spine and Hip BMD in Premenopausal Women with Idiopathic Osteoporosis (IOP) *Adi Cohen[1], Stephanie Shiau[2], Mafo Kamanda-Kosseh[1], Mariana Bucovsky[1], John M. Williams[1], Sanchita Agarwal[1], Robert R. Recker[3], Joan M. Lappe[3], Julie Stubby[3], Jennifer Larsen[3], Elizabeth Shane[1]. [1]Columbia University Irving Medical Center, United States, [2]Rutgers School of Public Health, United States, [3]Creighton University Medical Center, United States

We have previously reported that teriparatide (TPTD; 20 mcg daily for 24 months) is associated with substantial increases in BMD at the lumbar spine (LS), total hip (TH) and femoral neck (FN) in premenopausal women with IOP (PreMenIOP), all severely affected with low trauma vertebral and/or non-vertebral fractures and/or very low BMD.After completing TPTD, 33 women enrolled in an open label, FDA-funded phase 2b study of denosumab (Dmab; 60mg SC q6M) and 32 completed 12M of Dmab. BMD was measured annually and bone turnover markers (BTMs) at baseline, 3, 6 and 12M: osteocalcin (OC), N-terminal propeptide of type I procollagen (PINP), C-telopeptide (CTX). On average, these 32 women had experienced large BMD increases on TPTD of 14.2+/-8.1% at LS, 5.3+/-4.3% at the TH and 5.1+/-5.2% at the FN, while BMD declined by -2.2+/-3.1% at the distal radius (DR; all p<0.001). Three were TPTD NonResponders (12M change in LS BMD <0.026g/cm2).After 12M of Dmab, BMD increased a further 5.2+/-2.6% at the LS, 2.9+/-2.4% at the TH, 3.0+/-3.8% at the FN (all p<0.001) and 0.9+/-2.5% at the DR (p<0.05). BMD increases on Dmab were similar in TPTD-Responders and NonResponders at all sites (p=NS). BTMs decreased by 75-80% from baseline by 3M and remained suppressed (Figure). Change in TH BMD at 12M was inversely related to change in all BTMs at all timepoints (r=-0.44-0.63; p<=0.01 for all). Change in FN BMD was inversely related to change in OC at 6 and 12M and CTX at 6M (r=-0.37-0.38; p200 pg/mL after 6M of Dmab, the 12M BMD response to Dmab did not differ from the rest of the group. Increases after 24M of TPTD + 12M of Dmab totaled 20.1+/-7.5% at the LS, 8.4+/-5.3% at the TH and 8.3+/-6.2% at the FN (all p<0.0001). DR remained below baseline by -1.4+/-3.2% (p<0.05).In summary, a 12M course of Dmab after a 24M course of TPTD led to further BMD gains in PreMenIOP, even those in whom BMD did not increase on TPTD. The substantial gains in TH BMD after 24M of TPTD + 12M of Dmab are encouraging, as change in BMD at this site has been recently reported to be the strongest predictor of fracture risk reduction in postmenopausal women. We conclude that sequential therapy with TPTD followed by Dmab markedly improves spine and hip BMD in severely affected premenopausal women with IOP.

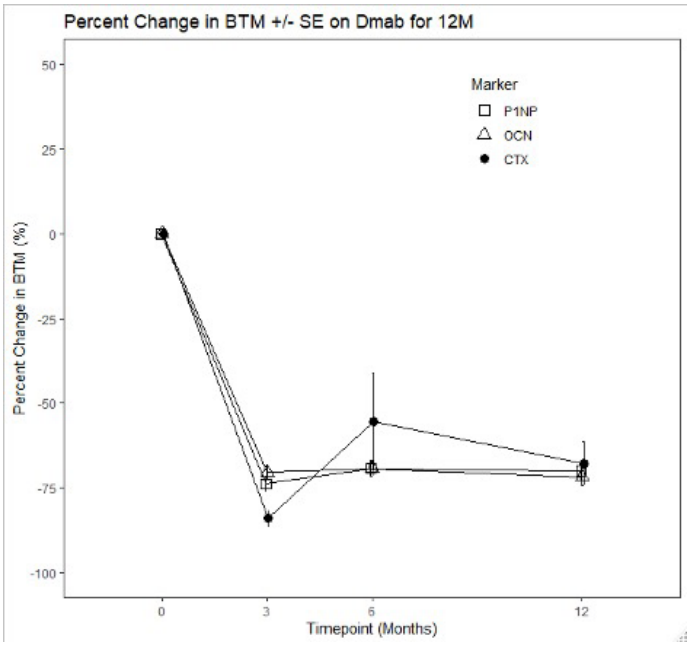

***Disclosures: Adi Cohen**, None*

P-648

Hormone therapy reduces the risk of fracture regardless of baseline FRAX probability or prior falls – results from the Women's Health Initiative hormone therapy trials *Mattias Lorentzon[1], Helena Johansson[2], Nicholas Harvey[3], Enwu Liu[4], Liesbeth Vandenput[5], Carolyn Crandall[6], Eugene McCloskey[7], John Kanis[8]. [1]Geriatric Medicine, Institute of Medicine, Sahlgrenska Academy, University of Gothenburg, Gothenburg, Sweden and Mary McKillop Institute for Health Research, Australian Catholic University, Melbourne, Australia, Sweden, [2]Mary McKillop Institute for Health Research, Australian Catholic University, Melbourne, Australia and Centre for Metabolic Bone Diseases, University of Sheffield, Sheffield, UK, Australia, [3]MRC Lifecourse Epidemiology Unit, University of Southampton, Southampton, UK and NIHR Southampton Biomedical Research Centre, University of Southampton and University Hospital Southampton NHS Foundation Trust, Southampton, UK, United Kingdom, [4]Mary McKillop Institute for Health Research, Australian Catholic University, Melbourne, Australia, Australia, [5]Mary McKillop Institute for Health Research, Australian Catholic University, Melbourne, Australia and Geriatric Medicine, Institute of Medicine, Sahlgrenska Academy, University of Gothenburg, Gothenburg, Sweden, Australia, [6]Department of Medicine, David Geffen School of Medicine at the University of California, Los Angeles, US, United States, [7]Mellanby Centre for bone research, Department of Oncology and Metabolism, University of Sheffield and Centre for Integrated research in Musculoskeletal Ageing (CIMA), Mellanby Centre for Bone Research, University of Sheffield, Sheffield, UK, United Kingdom, [8]Mary McKillop Institute for Health Research, Australian Catholic University, Melbourne, Australia and Centre for Metabolic Bone Diseases, University of Sheffield, Sheffield, UK, Australia

Objective The objective of the present analysis was to determine if the anti-fracture efficacy of menopausal hormone therapy (HT) was dependent on baseline falls history or FRAX fracture probability in a combined analysis of the two Women's Health Initiative (WHI) HT trials.Material and methods25,389 postmenopausal women aged 50-79 years were randomized to receive HT (n=12,739) or matching placebo (n=12,650). At baseline, questionnaires were used to collect information on falls history, within the last 12 months, and clinical risk factors. FRAX 10-year probability of major osteoporotic fracture (MOF) was calculated without BMD. Incident clinical fractures, other than fractures of the skull, face, fingers, toes, ribs, sternum, and cervical vertebrae, were verified using medical records. An extension of Poisson regression was used to investigate the relationship between treatment and fractures in 1) the whole cohort; 2) those with prior falls; and 3) those without prior falls. The effect of baseline FRAX probability on efficacy was investigated in the whole cohort. ResultsOver 4.3+/-2.1 years (mean+/-SD), in the whole population, HT (vs. placebo) significantly reduced the risk of any clinical fracture (Hazard Ratio [HR] 0.72 [95% CI, 0.65-0.78]), MOF (HR 0.60 [95% CI, 0.53-0.69]) and hip fracture (0.66 [95% CI, 0.45-0.96]). Treatment was effective in reducing the risk of any clinical fracture (Figure 1), MOF and hip fracture in women regardless of baseline FRAX MOF probability, with no evidence of an interaction between HT and FRAX (p>0.30 for the interaction term for all fracture outcomes). Similarly, there was no interaction (p>0.30) between HT and prior falls. HT was effective in reducing the risk of any clinical fracture and MOF both in those with prior falls (any fracture HR 0.74 [95% CI, 0.63-0.85] and MOF HR 0.57 [95% CI, 0.46-0.70]) and in those without prior falls (any fracture HR 0.70 [95% CI, 0.62-0.79] and MOF HR 0.62 [95% CI, 0.53-0.73]).ConclusionsHT reduces fracture risk regardless of FRAX probability and falls risk in postmenopausal women. FundingThe National Heart, Lung, and Blood Institute, National Institutes of Health, U.S. Department of Health and Human Services through contracts HHSN268201600018C, HHSN268201600001C, HHSN268201600002C, HHSN268201600003C, and HHSN268201600004C. WHI project:3572

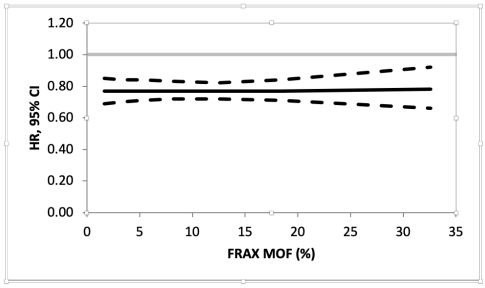

Figure 1. Effect of HT on the risk of any clinical fracture according to FRAX MOF probability.

***Disclosures: Mattias Lorentzon**, None*

Posters

P-649

Efficacy of low dose Denosumab in maintaining bone mineral density in postmenopausal women with osteoporosis: a real world, prospective observational study *Aliya Khan[1], Hajar Abu Alrob[1], M'Hiri Iman[2], Hosay Said[1], Romanovschi Mihai[2], Sharjil Hussain [2], Heather Zariffeh[2], Ismail Hweija[1], Salman Iqbal [2], Shawn Davison[3]. [1]McMaster University, Canada, [2]Bone Research and Education Centre, Canada, [3]Trilogy Writing & Consulting, Canada

Introduction: Denosumab, a fully human monoclonal antibody to RANK-ligand, has been shown to increase bone mineral density (BMD) and reduce the risk of hip, vertebral and non-vertebral fractures in postmenopausal women with osteoporosis (1,2). Varying doses of denosumab including 30mg/3months have demonstrated a decrease in bone remodelling in a dose-dependent manner (3,4,5). The primary objective of this study is to evaluate the efficacy of low dose denosumab (30mg/6 months) in postmenopausal women with osteoporosis who are reluctant to consider or continue the full dose of denosumab due to adverse events (AE) or concerns of potential AE.Methods: Following informed consent, postmenopausal women with a T-score of <= -2.5 at the lumbar spine (LS) or at the total hip (TH) received denosumab 30mg/6months. Patients with an additional skeletal disorder, prior fragility fracture, or on oral steroids (daily in the past 12 months) were excluded. The primary endpoint was the percent change in BMD at the lumbar spine (LS), total hip (HP), femoral neck (FN) and 1/3 radius (1/3R) at 12 months. Secondary outcomes were 1) percent change in BMD at the LS, TH, FN, and 1/3R at 24 months and 2) AE.Results: We enrolled 183 patients. The mean age was 69 years (SD= 7.07), 80% of patients had a moderate fracture risk (CAROC tool), 3% were current smokers and 9% consumed alcohol daily. 14.4% of patients were on SSRI/SNRI, 9.6% were on PPI, and no patient was on an aromatase inhibitor. At 12 months (n=125), the mean BMD significantly increased by +2.0% (95% CI 2.8%-1.3%) at the LS (p<0.001). There was no significant change in BMD at the FN, TH, or 1/3R site. At 24 months (n=65), the percent change in BMD was +3.4% (95% CI 4.8%-2.0%: p<0.001) at the LS, +1.5% (95% CI 2.9%-0.15%: p=0.031) at the FN, +1.9% (95% CI 3.5%-0.24%: p=0.025) at the 1/3R. There was no significant change in BMD at the TH.Conclusion: Low dose denosumab appears to be effective in maintaining BMD in postmenopausal women with a moderate fracture risk and may be of benefit in individuals who are experiencing side effects or have concerns of side effects. This may also be a potential treatment option following 10 yrs of denosumab therapy.

***Disclosures: Aliya Khan**, Shire, Grant/Research Support, Ultragenyx, Speakers' Bureau, Amgen, Grant/Research Support, Alexion, Grant/Research Support*

P-650

Randomized Study to Evaluate a Secondary Prevention Program for Women with Osteoporotic Fractures *Cori Blauer-Peterson[1], Alon Yehoshua[2], Maureen Carlyle[1], Valery Walker[1], Shravanthi Gandra[2]. [1]Optum, United States, [2]Amgen Inc., United States

Purpose: To assess the impact of an intensive outreach program in post-menopausal osteoporosis patients (pts) over 3, 6, and 12 months (mos).Methods: Medicare Advantage female members (age 67–85y) with pharmacy and medical coverage and evidence of a fragility fracture (fx) (index date=date of fx) from 15 Apr 2016–27 Jan 2017 and 23 Oct 2017–27 Nov 2017 were eligible. Pts had no history of fx 60 days pre-index and continuous enrollment 12 mos pre-index. Pts with BMD test during 24 mos pre-index, osteoporosis medication 12 mos pre-index, Paget's, or fxs of finger, toe, and skull were excluded. Randomization was to a current health plan program (standard-of-care [SOC]), or an intensive outreach intervention designed to increase post-fx care coordination and communication between pts and providers. In addition to SOC, it included an educational mailing to pts, post–heel scan follow-up phone calls to pts and providers, and an informational fax and phone call to providers. Study endpoints were: 1) composite of DXA monitoring and/or osteoporosis medication fill, 2) DXA monitoring, 3) osteoporosis medication fill, and 4) subsequent fxs. Endpoints 1–3 were evaluated at 3, 6, and 12 mos, and endpoint 4 at 12 mos. Results:The 12-mo follow-up included 3,720 pts (1,847 intervention; 1,873 SOC). Only 98 (5.3%) pts and 678 (36.7%) providers were eligible for phone outreach and successfully contacted. The results were consistent across mos 3, 6, and 12. At 12 mos, the intervention group had a statistically significant greater proportion of DXA monitoring and/or osteoporosis medication fill vs. SOC (32.7% vs. 29.5%; p=0.036) and a greater proportion of DXA monitoring alone vs. SOC (29.9% vs. 26.1%; p=0.009). No significant differences between intervention and SOC were found for medication fill alone (10.5% vs. 10.1%, respectively; p=0.759) or subsequent fxs (21.0% vs. 21.7%; p=0.591). The overall osteoporosis medication fill for all pts was 6.8% within 6 mos and 10.3% within 12 mos. Further, 21.4% of all pts experienced an additional fx, and 4.4% experienced multiple fxs.Conclusion: An intensive outreach program increased post-fx DXA monitoring vs. SOC, with no differences between groups in medication fill or subsequent fxs. Addressing the barriers encountered in this study to increase contact with pts and providers may be needed to increase osteoporosis monitoring and use of osteoporosis medication and reduce subsequent fxs during post-fx care.

***Disclosures: Cori Blauer-Peterson**, Optum, Other Financial or Material Support*

P-651

A simple-to-use nomogram for identifying individuals at high risk of denosumab-associated hypocalcemia in postmenopausal osteoporosis: a real-world cohort study *Kyoung Jin Kim[1], Namki Hong[1], Seunghyun Lee[1], Yumie Rhee[1]. [1]Department of Internal Medicine, Severance Hospital, Endocrine Research Institute, Yonsei University College of Medicine, Republic of Korea

Denosumab, a fully-humanized monoclonal antibody against receptor activator of nuclear factor-kappa B ligand (RANKL), has been increasingly prescribed based on its potent anti-resorptive action. Although denosumab-associated hypocalcemia was infrequent in previous randomized trials, data on incidence and risk factors of hypocalcemia in the general population is limited. This study was aimed to identify risk factors and develop a helpful nomogram for identifying individuals at risk for hypocalcemia after denosumab injection. In this retrospective cohort, 790 consecutive female patients received denosumab 60 mg between November 2016 and September 2017 were analyzed after excluding patients with metastatic cancer, liver cirrhosis, or hypoparathyroidism. Mild hypocalcemia and moderate hypocalcemia were defined as albumin-corrected serum calcium levels of <8.5 mg/dL and <8.0 mg/dL and observed in 8.2% (65; range 5.4-8.4 mg/dL) and 1.0% (8; range 5.4-7.9 mg/dL) patients, respectively. The median time to hypocalcemia was 6.3 months (interquartile range 5.3 to 7.4). Patients who developed mild hypocalcemia had lower baseline cCa (8.9 vs. 9.3 mg/dL), lower estimated glomerular filtration rate (eGFR; 75.0 vs. 83.2 mL/min/1.73m2), and more frequent loop diuretics use (10.8% vs. 4.4%; p<0.05 for all). In a multivariate model, low baseline cCa (OR 0.78, 95% CI: 0.72-0.84) and chronic kidney disease stage 4-5 increased the risk of mild and moderate hypocalcemia (OR 4.27, 95% CI: 1.55-11.80 and OR 13.56, 95% CI:2.28-80.71, respectively). The use of loop diuretics was associated with modest hypocalcemia (OR 2.61, 95% CI: 1.11-6.18 and OR 12.43, 95% CI:2.86-54.07) independent of baseline cCa and CKD stage. Based on these three independent risk factors, we constructed a nomogram for predicting the probability of denosumab induced hypocalcemia in Korean female patients with osteoporosis. A nomogram approach identified four risk groups: 1) cCa < 8.5 mg/dL; 2) cCa 8.5-8.9 mg/dL with loop diuretics use or 3) with CKD 4-5; 4) cCa 9.0-9.4 mg/dL with CKD 4-5. In conclusion, the incidence of moderate hypocalcemia after denosumab injection was low in real world-settings, which was reassuring. This simple-to-use nomogram identified high-risk groups for hypocalcemia after denosumab treatment in postmenopausal osteoporosis, which may enable the individualized monitoring strategy.

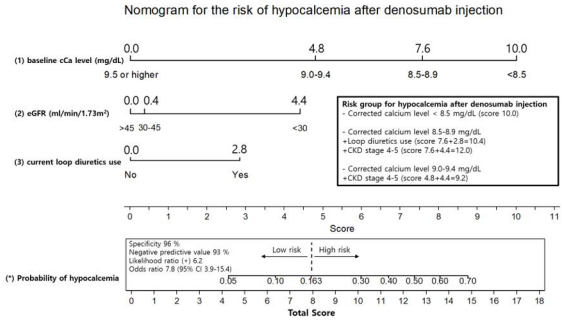

Figure1. Nomogram for predicting the risk of hypocalcemia after denosumab injection. Instruction for usage: (1) Mark the baseline cCa level of an individual on the "baseline cCa level" axis and check the point. (2),(3) Repeat the process for each additional risk factor (eGFR and current loop diuretics use). (*) Sum the points of three risk factors. Total score higher than 8 indicates high risk group for hypocalcemia with specificity 96%, positive likelihood ratio 6.2, and odds ratio 7.8.

***Disclosures: Kyoung Jin Kim**, None*

P-652

Bisphosphonate protects cortical bone at key locations of the femur in aromatase-inhibitor associated bone loss: a 3D cortical bone mapping study *Namki Hong[1], Graham Treece[2], Kyungjin Kim[1], Seunghyun Lee[1], Heajeong Park[1], Yumie Rhee[1]. [1]Yonsei University College of Medicine, Republic of Korea, [2]University of Cambridge, United Kingdom

Aromatase inhibitor treatment in hormone-sensitive breast cancer is associated with accelerated bone loss and increased risk of fracture. Bisphosphonates (BP) are the mainstay treatment of aromatase inhibitor associated bone loss (AIBL), which might improve femoral bone at key locations prone to fracture. To test this hypothesis, we performed 3D cortical bone mapping based on QCT scans in postmenopausal women with early breast cancer receiving aromatase inhibitors. In Severance Hospital early breast cancer cohort, Korea, data of subjects who had both baseline and at least one time of follow-up QCT between 2005 and 2015 were analyzed (BP user, n=93; non-user, n= 203). After excluding BP users with low medication persistence (proportion of days covered 0.05 for all). At follow-up, BP use prevented AIBL in LSvBMD (+7.2% vs. -3.8%, p<0.001), FNaBMD (+1.3% vs. -2.7%, p<0.001), and THaBMD (-0.3% vs. -2.5%, p=0.024). BP had protective effect on cortical parameters of femoral bone: estimated cortical thickness (CTh), +3.3% vs. +0.1%, p=0.007; cortical mass surface density (CMSD, cortical mass per unit surface area calculated by multiplying cortical BMD × CTh), +3.4% vs. -0.3%, p<0.001. CMSD increased by up to 15% at key locations including superior part of femoral neck and lateral femoral trochanter. BP

prevented the thinning of average CTh of femoral neck (-1.4% vs. -6.1%, p<0.001), particularly at superior anterior quadrant of femoral neck (absolute difference +12.8% vs. non-users in linear regression model with the adjustment for age and baseline BMD). Compared to non-users, BP users had improved cross-sectional moment of inertia (+4.4% vs. -0.7%, p=0.001) and less increase in buckling ratio (+1.3% vs. +7.5%, p<0.001). BP use prevented cortical bone loss in AIBL at key locations of proximal femur.

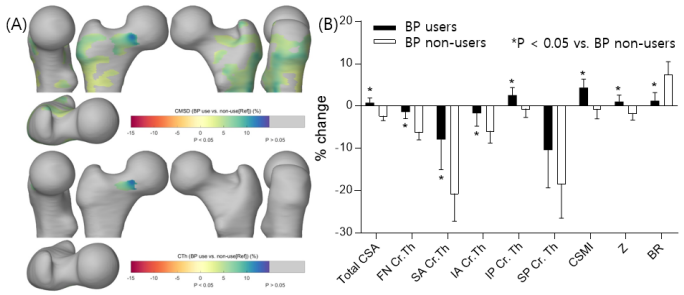

***Disclosures: Namki Hong**, None*

P-653

Overcoming the adherence gap through specialized osteological care - Data from the DVO Osteoporosis Registry *Christina Westphal[1], Lars Joeres[2], Tanja Heidbrede[2], Hans-Christof Schober[3], Alexander Defèr[4]. [1]Max-Planck-Institut für demografische Forschung, Germany, [2]UCB Pharma GmbH, Germany, [3]Klinikum Südstadt Rostock, Germany, [4]Outpatient Centre for bone diseases, Germany

Introduction: Osteoporosis and associated fractures are serious health issues.Even though effective therapy options are now available, there are still significant deficits in the care of outpatients and compliance to osteoporosis medications has been shown to be poor after 2 years (S. Morell 2017; J. Morley, 2019). Moreover, the question if specialized osteological care improves the intake of medication compared to standard care has not yet been clarified. This study assessed persistence in patients using osteoporosis medications within the DVO registry, a German patient registry assessing clinical outcomes and reflecting specialized care, and in a German-wide prescription database provided by Insight health, reflecting standard care.Methods: Selected patients from the DVO registry had at least 2 observations and documented continuous treatment with the respective drugs. From the prescription database, patients with initiation of respective medications (index date) from 01.01.2017 – 30.06.2017 and with a medication free period of 12 months prior to index date were selected. Age and gender matched distribution per respective medication groups according to the distribution provided by DVO registry was applied. Persistence was calculated as being still on treatment with the respective drug on month 12 and month 24, divided by all patients starting the respective treatment.Results: The DVO registry contains data from approx. 17.000 patients, where of 6.346 were selected according to the selection parameters. (ALN: 2.698, RIS: 1.548, ZOL: 239, TPD: 30, IBN: 601, DNB:1230). 11.64% of patients were male; 88.35% female. Persistence overall after 12/24 months was 98.11% and 92.70% respectively. The Insight health prescription dataset covers around 60 million patients, which equals to 77% of the German statutory insured population. Of those 96.459 patients were prescribed with medication according to the selection parameters (ALN: 46.704, RIS: 14.896, ZOL: 4.451, TPD: 164, IBN: 6.725, DNB: 23.519). 12.76% of patients were male; 87.23% female. Persistence overall after 12/24 months was 48.69% and 33.46%, respectively.Conclusion: A continuous, specialized osteological care leads to a considerable improvement in therapy persistence. 92,7% of patients from the DVO registry still followed the prescription after two years. Only 33,46% of patients in standard care did ex aequo to the Morley work. Limiting is the lack of diagnosis codes in the prescription database.

***Disclosures: Christina Westphal**, None*

P-654

Clinical Features of 99 Patients with Vertebral and Non-Vertebral Fractures after Denosumab Discontinuation: an International Cohort *Elena Gonzalez Rodriguez[1], Maria Belen Zanchetta[2], Pilar Peris[3], Elisa Fernández Fernández[4], Stergios A Polyzos[5], Maria Carolina Ballarino[2], José Luis Mansur[6], Polyzois Makras[7], Helena Florez[3], Pilar Aguado Acin[4], Berengere Aubry-Rozier[1], Athanasios D Anastasilakis[8], Olivier Lamy[1]. [1]Center of Bone Diseases, Bone and Joint Department, University of Lausanne and Lausanne University Hospital, Switzerland, [2]Cátedra de Osteología y Metabolismo Mineral, Universidad del Salvador, Argentina, [3]Department of Rheumatology. Hospital Clinic, University of Barcelona, Spain, [4]Servicio de Reumatología, Hospital Universitario La Paz, Spain, [5]First Laboratory of Pharmacology, School of Medicine, Aristotle University of Thessaloniki, Greece, [6]Centro de Endocrinologia y Osteoporosis La Plata, Argentina, [7]Department of Endocrinology and Diabetes and Department of Medical Research, 251 Hellenic Air Force & VA General Hospital, Greece, [8]Department of Endocrinology, 424 General Military Hospital, Greece

PurposeDenosumab (DMAb) discontinuation (DD) induces an increase of bone turnover above baseline for up to 2 years and a loss of the BMD gain, associated with an 1 to 10% of spontaneous clinical vertebral fractures (SCVF). Risk factors for SCVF and the incidence of other fractures are not known.MethodsBetween Mars 2013 and November 2018, 99 women were evaluated in 5 international tertiary hospitals because of new fractures attributed to DD. We report the anthropometric, clinical and biological characteristics obtained from clinical records.ResultsWomen were 68.7+/-9.0 years and had received 6.6+/-2.7 (2 to 14) DMAb doses; in 14 cases it was given for aromatase-inhibitor (AI) bone-loss prevention. DMAb was mostly omitted (26), delayed (14) or stopped (13) by the patients themselves. Ninety-eight women developed SCVF [of which 11 also had non-vertebral fractures (Non-VF)], and one no SCVF but 4 Non-VF. They had 3.4+/-2.3 (range: 1-13) SCVF, and 2.0+/-1.4 (range: 1-4) Non-VF, following 11.6+/-4.0 months from the last DMAb injection. At the time of SCVF 3 women were under bisphosphonates (BP) for 2 to 14 months, and 1 had a DMAb dose 1 month before. Mean serum ß-crosslaps (sCTX) value was 1034+/-564 g/l (Normal < 573). Following SCVF, 20 women had 3.4+/-1.8 vertebroplasties, and 6 of them presented 1 to 8 new SCVF.In the 2 years prior DMAb initiation, 23 women had received a BP, and 10 other anti-osteoporotic agents. From the 47 (47.5%) women with prevalent fractures, 31 had vertebral ones (mean 1.8+/-1.3). During DMAb treatment, 3 women suffered a VF and 7 a Non-VF.SCVF number was not associated with treatment in the 2 previous years, prevalent or incident fractures, or any T-score value at DMAb initiation or at the time of fractures. SCVF number was inversely correlated with age at DMAb initiation, and at the time of fracture, with more SCVF in younger patients (4.2+/-2.8 vs 2.8+/-1.8, 65 years, p=0.004), but was not correlated with CTX values at the time of fracture. The higher the number of DMAb doses, the higher the CTX at SCVF (R2=0.14, p=0.01), and the shorter the time to fracture (R2=0.04, p=0.04). There was no factor associated to Non-VF occurrence.ConclusionFractures occur in patients who discontinue DMAb mostly for non-medical reasons. About 10% of patients also develop Non-VF. The number of SCVF is higher in younger patients, and they occur earlier in patients with longer treatment. A close follow-up for 2 years after DD is necessary. Further studies are needed to improve the identification of patients at risk for SCVF and the most adequate transition treatment after DD.

***Disclosures: Elena Gonzalez Rodriguez**, None*

P-655

Potential cases of missed hypophosphatasia in an Osteoporosis Clinic? Low ALP as a signal for hypophosphatasia *Elisabeth Ng[1], Claudia Ashkar[1], Shoshana Sztal-Mazer[1]. [1]Alfred Health, Australia

Purpose: To evaluate alkaline phosphatase (ALP) levels in patients referred to an Osteoporosis Clinic and describe the prevalence of subnormal values which may signal low ALP enzymatic activity and, potentially, hypophosphatasia (HPP).Background: HPP is a rare condition that can masquerade as osteoporosis. Caused by impaired tissue-non-specific alkaline phosphatase (TNSALP) production, it can manifest at any age with varying clinical severity and can be mild in adults such that it evades suspicion. Fragility fractures and low bone mineral density are common to both adult HPP and osteoporosis, hence HPP can be misdiagnosed as the latter, more prevalent condition. The risk of this is use of bisphosphonate therapy, which is first line in osteoporosis but harmful in HPP due to the effect of excess pyrophosphate in the setting of ALP deficiency, which can further inactivate TNSALP and impair mineralization, posing a heightened fracture risk. Furthermore, atypical femoral fractures, a hallmark of adult HPP, can occur in long term bisphosphonate therapy, confounding the misdiagnosis. Diagnosis is confirmed with DNA sequencing, but reduced ALP enzymatic activity can be a clue to potential underlying HPP.Methods: We retrospectively audited all adult patients seen in the Osteoporosis Clinic of a metropolitan tertiary center from its inception in 2012 up until 2020. Pathology results from 2008 onwards were reviewed and clinical notes interrogated in those with an ALP level below the lower limit of normal, 30 IU/L. Results: 1866 patients were identified, and 27 excluded due to no recorded ALP level (see Figure 1). 168 patients (9.1%) had an ALP level < 30 IU/L, with the median number of tests per patient being 76. 158 of these patients (94%) had at least 20 ALP tests, with a median ALP of 56 IU/L. Seven (4.2%) patients had over 50% of their ALP levels < 30 IU/L, with the median ALP in this group being 25 IU/L. Two had already undergone ALPL genetic testing confirming a pathogenic variant. The other five patients will receive further workup for HPP.

We also evaluated circumstances surrounding transiently low ALP values.Conclusion: Adult HPP should not be forgotten as a differential diagnosis in those presenting with fractures and osteoporosis. We highlight the value of testing and analyzing the ALP level in individuals referred for osteoporosis management to ensure consideration of HPP before antiresorptive therapy is initiated.

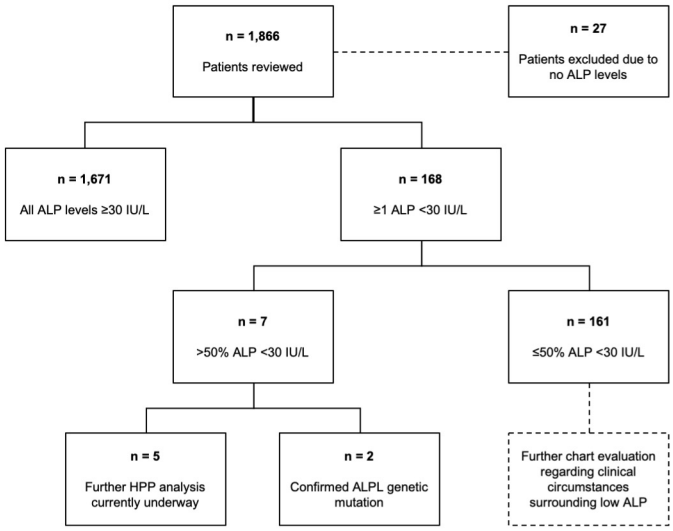

***Disclosures: Elisabeth Ng**, None*

P-656

KER-012, A NOVEL ACTIVIN RECEPTOR TYPE II LIGAND TRAP INCREASES BONE IN MICE VIA A UNIQUE MECHANISM OF ACTION

*Keith Babbs[1], Christopher Materna[1], ffolliott Fisher[1], Jasbir Seehra[1], Jennifer Lachey[1]. [1]Keros Therapeutics, United States

Osteoporosis is a bone disorder affecting over 200 million people worldwide and is characterized by low bone mineral density, reduced bone strength, deterioration of bone, and high risk of bone fracture leading to increased mortality. TGFß superfamily ligands, including activin A and B, are negative regulators of bone remodeling suppressing bone growth. KER-012 is a modified Activin receptor II ligand trap designed to bind and inhibit activins and SMAD 2/3 signaling. Our aims were to test the efficacy of KER-012 in increasing bone and to investigate the mechanism of action of KER-012 in mice. To investigate the mechanism of KER-012's effects, adult male mice (n=10/grp) were administered 20 mg/kg KER-012 or vehicle (VEH) twice weekly for 5 weeks. Ex vivo analysis demonstrated that, relative to VEH-dosed mice, KER-012-dosed mice had 82.0% greater bone volume ($p<0.001$), 28.8% higher bone volume fraction ($p<0.001$), and 33.5% greater trabecular number ($p<0.01$). Additionally, in KER-012 treated mice, relative to VEH, we observed reductions in trabecular eroded surface ratio (-42.2%; $p<0.001$) and osteoclast number (-45.8%; $p<0.01$), as well as increased mineralizing surface (+63.4%; $p<0.01$), mineral apposition rate (+29.9%; $p<0.05$), and bone formation rate (+107.7%; $p<0.01$), suggesting attenuated catabolism and enhanced anabolism. Together, these results suggest that KER-012 potentially acts through a differentiated mechanism to increase bone in mice by reducing bone resorption and enhancing formation. This suggests that KER-012 could potentially treat conditions resulting in bone loss.

***Disclosures: Keith Babbs**, Keros Therapeutics, Grant/Research Support*

P-657

Sclerostin loop3: a potential target for developing a next generation sclerostin inhibitor for bone anabolic therapy with low cardiovascular concern

*Yuanyuan Yu[1], Luyao Wang[2], Shuaijian Ni[1], Zhenjian Zhuo[3], Hang Yin Chu[4], Ning Zhang[3], Dijie Li[1], Jin Liu[1], Aiping Lyu[1], Bao Ting Zhang[3], Ge Zhang[1]. [1]Law Sau Fai Institute for Advancing Translational Medicine in Bone and Joint Diseases (TMBJ), School of Chinese Medicine, Hong Kong Baptist University, Hong Kong, [2]Guangdong-Hong Kong-Macao Greater Bay Area International Research Platform for Aptamer-based Translational Medcine and Drug Discovery, Hong Kong, [3]School of Chinese Medicine, Faculty of Medicine, The Chinese University of Hong Kong, Hong Kong, [4]Aptacure Therapeutics Limited, Hong Kong

Sclerostin is an antagonist of bone anabolic Wnt signaling pathway. Antibody against sclerostin for postmenopausal osteoporosis has been approved by US FDA, with a boxed warning for potential cardiovascular risk. Therefore, it is desirable to develop a next generation sclerostin inhibitor with low cardiovascular concern.Sclerostin has a protective role in cardiovascular system by inhibiting the proinflammatory cytokines to prevent aortic aneurysm and atherosclerosis development in ApoE-/- mice induced by angiotensin II (AngII). Sclerostin has three loops within its central region. We found sclerostin regulated skeletal and cardiovascular system via different loops (Fig 1a). Loop2 and/or loop3 played important roles in inhibiting Wnt signaling and osteogenic potential in MC3T3-E1 cells (Fig 1b). Either loop2&3 deficiency by genetic truncation or loop2&3 inhibition by sclerostin antibody could attenuate the suppression effects of sclerostin on the expression of inflammatory cytokines and chemokines in macrophages and VSMCs, whereas loop3 deficiency by genetic truncation maintained the above suppression effects of sclerostin in macrophages and VSMCs with AngII infusion in vitro (Fig 1c&d). Therefore, we hypothesized that specifically targeting sclerostin loop3 could promote bone formation and maintain sclerostin loop3-independent cardiovascular protective effect. We have tailored screened an ssDNA aptamer aptscl56 which selectively targeting human sclerostin loop3 by using full length sclerostin as the positive target, and loop3 deficient sclerostin as the negative target (Fig 2). The aptamer had a high inhibition effect to sclerostin's antagonistic effect on Wnt signaling in vitro, but had no effect on the expression of inflammatory cytokines and chemokines in macrophages and VSMCs, with AngII infusion in vitro (Fig 1&2). Furthermore, by mutation studies, we found residues R114, Q116, R117, V118, Q119, E126, P128, K132, V133, and R134 on sclerostin loop3 were the functional sites in antagonizing Wnt signaling.Residues D111, R112, Y113, L120, L121 and C122 on loop3, and nucleotides T13C14G15, C23T24T25 and T30G31G32 on the aptamer could be the binding sites between sclerostin and the aptamer. This study could help to understand the functional mechanism of sclerostin and provide a strong basis for the development of the next generation sclerostin inhibitor specifically targeting loop3 to promote bone formation with a low cardiovascular concern.

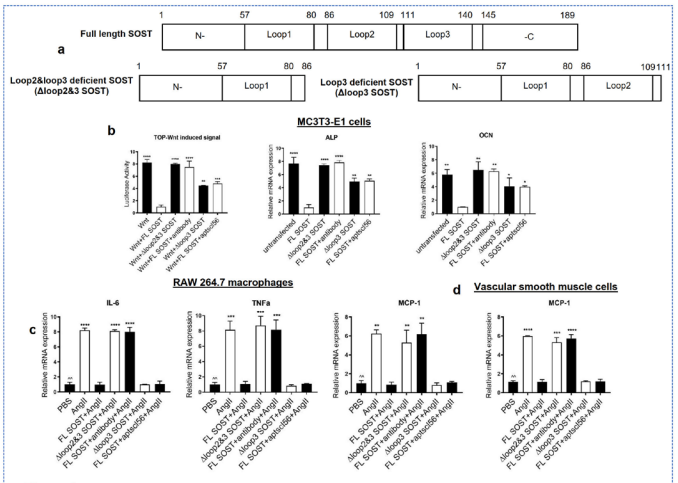

Figure 1 Effects of sclerostin loops in regulating inflammatory cytokines and chemokines in macrophages, inflammatory chemokines, contractile phenotype loss and apoptosis in vascular skeletal muscle cells, as well as Wnt signaling and osteogenic potential in MC3T3-E1 cells *in vitro*.

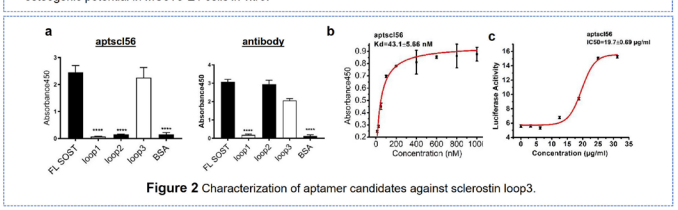

Figure 2 Characterization of aptamer candidates against sclerostin loop3.

***Disclosures: Yuanyuan Yu**, None*

P-658

Six-month Study of Early Clinical Effects and Drug Interactions in Romosozumab Treatment

*Ayako Tominaga[1], Keiji Wada[1], Ken Okazaki[1], Yoshiharu Kato[2]. [1]Tokyo Women's Medical University, Japan, [2]Kita Shinagawa 3rd Hospital, Japan

Purpose: Romosozumab first appeared as a new osteoporosis medication in Japan in 2019. This drug is an anti-sclerostin antibody that increases bone formation and suppresses bone resorption. We aimed to assess its actual clinical effects and whether other anti-osteoporosis pre-treatments affect romosozumab treatment.Methods: We analyzed 185 patients treated with romosozumab for six months. We measured bone mineral density (BMD) before and after six months of romosozumab treatment. We also performed blood tests before romosozumab treatment and after one, three, and six months. We set tartrate-resistant acid phosphatase 5b (TRACP-5b) as the bone resorption marker and type ? procollagen N-terminal propeptide (P1NP) as the bone formation marker. We grouped patients according to anti-osteoporosis treatment before romosozumab, as follows: non pre-treatment group (Non, n = 71), change from Teriparatide group (TPD, n = 35), change from denosumab G1 group (DMAB G1, n = 13), change from denosumab G2 group (DMAB G2, n = 21), and change

from bisphosphonate group (BIS, n = 39). As denosumab is a long-acting drug, we named the group that started romosozumab within three months after using denosumab for G1 and the group that started after four months for G2.Results: There were no new fractures during treatment. As the percent changes in spine and total hip BMD from the baseline were 6.34% and 1.53% after six months of treatment (Figure 1A), this treatment was effective on spine osteoporosis. In terms of spine BMD with pre-treatment, all groups showed a therapeutic effect that was higher than the least significant change. Compared with the anabolic windows provided by bone resorption and formation markers (Figure 1B–F), the anabolic windows in the Non and TPD group were closed after six months of treatment with romosozumab, whereas in the DMAB G1 and BIS groups, the windows remained open after six months of treatment. DMAB G2 had a much narrower anabolic window than did other groups.Conclusion: Romosozumab was effective in preventing fractures and useful for increasing spine BMD. At present, no significant difference in spine BMD was observed, but the anabolic window had characteristic movements for each anti-osteoporosis pre-treatment before romosozumab treatment. The effect may be diminished if romosozumab is started more than four months after the last denosumab treatment.

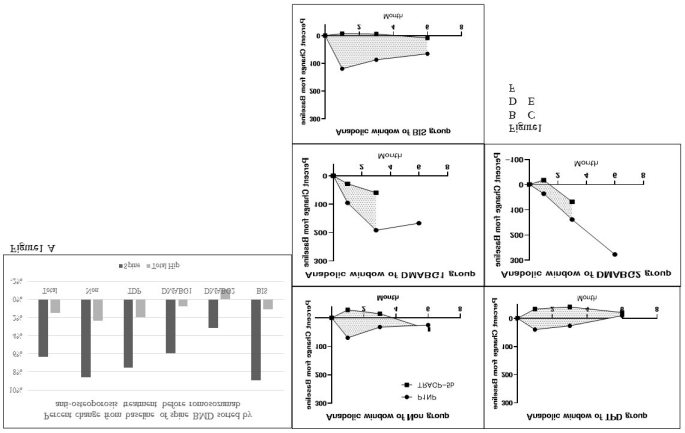

Disclosures: Ayako Tominaga*, None*

P-659

Comparison of the therapeutic effects of teriparatide and denosumb in distributing lumbar spine bone mineral density: Differing effects using QCT and finite element analysis *Soji Tani[1], Koji Ishikawa[1], Koki Tsuchiya[1], Takako Negishi-Koga[1], Takashi Nagai[1], Tomoaki Toyone[1], Katsunori Inagaki[1]. [1]Department of Orthopaedic Surgery, Showa University School of Medicine, Japan

IntroductionTeriparatide and denosumab are promising treatments for patients with osteoporosis who have a high risk of fractures. The anabolic agent teriparatide stimulates osteoblasts while denosumab targets osteoclast-mediated bone resorption. Despite these drugs having opposite effects on the bone, their effects on fracture reduction of the lumbar spine are equal.The aim of this study was to determine the effects of osteoporosis medications teriparatide and denosumab on the distribution of lumbar spine bone density.MethodIn this study, we retrospectively analyzed with postmenopausal osteoporosis who were initially treated with either teriparatide (n = 14) or denosumab (n = 14). Between the two groups, the mean age, mean lumbar spine bone mineral density (LS-BMD) at baseline, and mean percent change of LS-BMD after treatment were compares. At baseline and at 12 months, we divided the lumbar body into eight sections and measured the volumetric BMD (vBMD) using quantitative computed tomography. The compression forces of the lumbar vertebrae were also measured using computed tomography-based finite element analysis.ResultIn the teriparatide group, the vBMD was significantly increased in all sections of the vertebral body. In contrast, in the denosumab group, limited sections of the vBMD were increased. The percent change of vBMD at the vertebral body was greater in the teriparatide group than in the denosumab group. However, the compression forces of both groups were significantly increased. No significant difference was noted between two groups.ConclusionThe present study revealed that teriparatide was more effective on the trabecular bone than was denosumab. Both treatments, however, reduced the risk of vertebral fractures. These results suggested that the effect of fracture prevention was different for teriparatide and denosumab.

Disclosures: Soji Tani*, None*

P-660

Romosozumab Treatment Lowers The Incidence Of New Vertebral Fractures Across All Fracture Severity Grades Among Postmenopausal Women With Osteoporosis *Robert Feldman[1], Piet Geusens[2], Mary Oates[3], Thierry Thomas[4], Polyzois Makras[5], Franz Jakob[6], Bente Langdahl[7], Wenjing Yang[3], Maria Rojeski[3], Cesar Libanati[8]. [1]Senior Clinical Trials, Inc, United States, [2]Maastricht University Medical Center, Netherlands, [3]Amgen Inc., United States, [4]Department of Rheumatology, Hôpital Nord, CHU Saint-Etienne, France, [5]Department of Endocrinology & Diabetes, 251 Hellenic Air Force General Hospital, Greece, [6]University of Würzburg, Germany, [7]The Department of Endocrinology and Diabetes, Aarhus University Hospital, Denmark, [8]UCB, Belgium

Vertebral fractures (VFx) are the most common fracture in postmenopausal osteoporosis (PMO), carry the highest subsequent fracture rate of fragility fractures, and are associated with significant morbidity regardless of severity. Genant grading classifies VFx as mild (grade 1), moderate (grade 2), or severe (grade 3), based on the degree of compression visible on spinal x-rays. Here, we assessed the incidence of new VFx by Genant grading in the romosozumab (Romo) vs placebo (Pbo) or alendronate (ALN) arms of the FRAME and ARCH studies, respectively.In FRAME, 7180 women with PMO were randomized 1:1 to Romo 210mg or Pbo SC QM (12 months) followed by denosumab (DMAb) 60mg Q6M (Romo→DMAb or Pbo→DMAb) (12 months). In ARCH, 4093 women with PMO and >=1 fracture were randomized 1:1 to Romo 210mg QM or ALN 70mg PO QW (12 months) followed by ALN 70mg PO QW (Romo→ALN or ALN→ALN) (>=12 months). In both studies, lateral spinal radiographs were assessed by Genant grading for the presence and severity of VFx at baseline,12, and 24 months post-treatment.In both studies, incidence of new VFx was significantly lower among patients who received Romo. Over 12 months, incidence of new VFx was 0.5% Romo vs 1.8% Pbo (P<0.001) in FRAME and 3.2% Romo vs 5.0% ALN (P=0.008) in ARCH. Over 24 months, incidence of new VFx was 0.6% Romo→DMAb vs 2.5% Pbo→DMAb (P<0.001) in FRAME and 4.1% Romo→ALN vs 8.0% ALN→ALN (P<0.001) in ARCH. Fewer new VFx were observed in the Romo arm of both studies across severity grades. In FRAME, incidence of mild VFx was 0.2% Romo vs 0.4% Pbo (12 months) and 0.2% Romo→DMAb vs 0.6% Pbo→DMAb (24 months); incidence of moderate VFx was 0.1% Romo vs 0.9% Pbo (12 months) and 0.2% Romo→DMAb vs 1.4% Pbo→DMAb (24 months); and incidence of severe VFx was 0.2% Romo vs 0.5% Pbo (12 months) and 0.2% Romo→DMAb vs 0.6% Pbo→DMAb (24 months). In ARCH, incidence of mild VFx was 0.5% Romo vs 1.0% ALN (12 months) and 0.4% Romo→ALN vs 1.4% ALN→ALN (24 months); incidence of moderate VFx was 1.3% Romo vs 2.1% ALN (12 months) and 1.8% Romo→ALN vs 3.4% ALN→ALN (24 months); and incidence of severe VFx was 1.5% Romo vs 1.9% ALN (12 months) and 1.9% Romo→ALN vs 3.3% ALN→ALN (24 months). Thus, Romo administered over 12 months to women with PMO resulted in VFx reduction across severity grades compared with Pbo and standard-of-care ALN. This effect continued after transitioning to an antiresorptive agent. These data may foster treatment decisions in postmenopausal women at high risk for VFx.

Disclosures: Robert Feldman*, Amgen, Biogen, AB Biogenesis, GSK, TTP, Grant/Research Support, Amgen, Consultant, Amgen, Other Financial or Material Support, Amgen, Merck, Speakers' Bureau*

P-661

Smad4-dependent transforming growth factor-β family signaling regulates the differentiation of dental epithelial cells in adult mouse incisors *Aiko Machiya[1], Sho Tsukamoto[2], Satoshi Ohte[3], Mai Kuratani[2], Naoto Suda[4], Takenobu Katagiri[2]. [1]Division of Oral Rehabilitation of Sciences, Department of Restorative and Biomaterials Sciences, Meikai University School of Dentistry, Japan, [2]Division of Biomedical Sciences, Research Center for Genomic Medicine, Saitama Medical University, Japan, [3]Microbial Chemistry Laboratory, Graduate School of Pharmaceutical Sciences, Kitasato University, Japan, [4]Division of Orthodontics, Department of Human Development and Fostering, Meikai University School of Dentistry, Japan

Teeth consist of two major tissues, enamel and dentin, which are formed during development by epithelial and mesenchymal cells, respectively. Rodent incisors are useful experimental models for studying the molecular mechanisms of tooth formation because they are simultaneously growing in not only embryos but also adults. Members of the transforming growth factor-β (TGF-β) family regulate epithelial-mesenchymal interactions through an essential coactivator, Smad4. In the present study, we established Smad4 conditional knockout (cKO) mice and examined phenotypes in adult incisors. Smad4 cKO mice died with severe anemia within one month. Phosphorylated Smad1/5/9 and Smad2/3 were detected in epithelial cells in both control and Smad4 cKO mice. Disorganized and hypoplastic epithelial cells, such as ameloblasts, were observed in Smad4 cKO mice. Moreover, alkaline phosphatase expression and iron accumulation were reduced in dental epithelial cells in Smad4 cKO mice. These findings suggest that TGF-β family signaling through Smad4 is required for the differentiation and functions of dental epithelial cells in adult mouse incisors.

Disclosures: Aiko Machiya*, None*

Posters

P-662

Effects of Denosumab, Alendronate, or Denosumab after Alendronate on Humeral Bone Mineral Density and Finite Element Predicted Strength in Ovariectomized Cynomolgus Monkeys *Ifaz Haider[1], Paul Kostenuik[2], Steven Boyd[1], W. Brent Edwards[1]. [1]University of Calgary, Canada, [2]Amgen Inc; University of Michigan (Adjunct), United States

Proximal humeral fragility fractures are common in older women with postmenopausal osteoporosis (PMO) and are associated with high health care costs, disability, and a reduction in perceived health status1,2. Denosumab was recently shown to reduce the rate of humeral fractures in this population3. Several studies show that denosumab increases radius BMD in postmenopausal women who are treatment-naïve or transitioning from bisphosphonate therapy, but there are no human or nonclinical data on the effects of denosumab on humeral BMD. We therefore assessed BMD in harvested humeri from ovariectomized cynomolgus monkeys after 12 monthly injections of s.c. vehicle (VEH; n = 10), s.c. denosumab (DMAb; 25 mg/kg, n = 9), or the bisphosphonate alendronate i.v. (ALN; 50 µg/kg, n = 10). Other groups received 6 months of VEH followed by 6 months of DMAb (VEH-DMAb; n = 7) or 6 months of ALN followed by 6 months of DMAb (ALN-DMAb; n = 9). Harvested humeri were imaged with computed tomography (CT) to quantify integral, trabecular, and cortical bone mineral density (Int.vBMD, Tb.vBMD, Ct.vBMD) at the ultra-proximal and proximal regions and Ct.vBMD at the 1/5 proximal and midshaft regions, as defined by fixed percentages of humeral length (Fig). CT-based finite element (FE) models were used to predict stiffness and strength in axial compression, torsion, and 3-point bending. Bone was modeled as an elastic perfectly-plastic, transversely isotropic material, with elastic moduli based on apparent density. Ct.vBMD at the ultra-proximal region was significantly higher with DMAb and ALN-DMAb vs. VEH ($p <= 0.014$; Fig). Ct.vBMD at the 1/5 proximal, region and midshaft were higher in all active treatment groups vs. VEH ($p <= 0.011$). There were no significant between-group differences for ultra-proximal and proximal Int.vBMD and Tb.vBMD. FE predictions of stiffness and strength were not significantly different between groups (Fig). In summary, antiresorptive treatments were associated with higher Ct.vBMD in most humeral regions, and 12 months of denosumab or 6 months of denosumab after 6 months of alendronate was associated with higher Ct.vBMD in all humeral regions. These findings support the hypothesis that BMD gains in the humeral cortex contribute to reduced humeral fracture rates in denosumab-treated women with PMO3.1. van Eck, Ann Joint 2019; 2. Calvo, J Shoulder Elbow Surg 2011; 3. Bilezikian Osteoporos Int 2019.

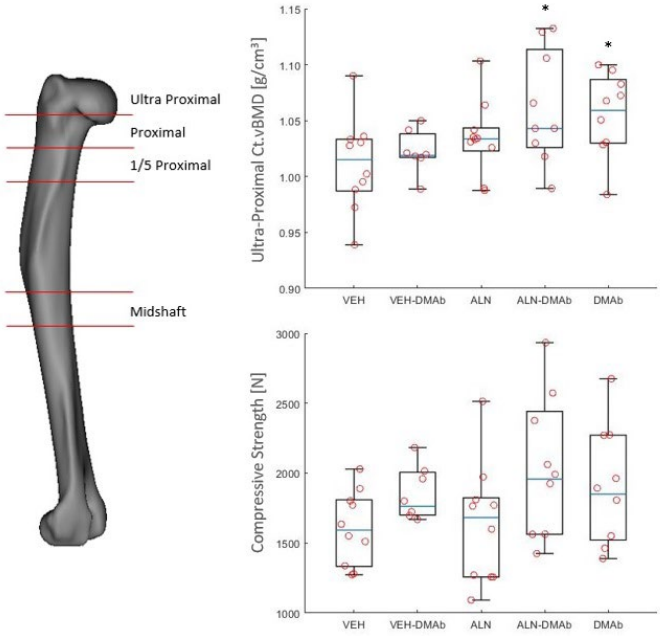

***Disclosures: Ifaz Haider**, Amgen, Grant/Research Support*

P-663

Probability of Achieving T-scores Goals Above -2.5 With Alendronate or Romosozumab Followed by Alendronate or Denosumab *Steven Cummings[1], Cesar Libanati[2], Celeste Hamilton[3], Zhigang Yu[3], Wenjing Yang[3], Serge Ferrari[4], Jens-Erik Beck Jensen[5], Pilar Peris Bernal[6], Francesco Bertoldo[7], Eric Lespessailles[8], Eric Hesse[9], Felicia Cosman[10]. [1]San Francisco Coordinating Center, United States, [2]UCB Pharma, Belgium, [3]Amgen Inc., United States, [4]Geneva University Hospital, Switzerland, [5]Copenhagen University Hospital, Denmark, [6]University of Barcelona, Spain, [7]University of Verona, Italy, [8]Centre Hospitalier Régional d'Orléans, France, [9]University Hospital, Ludwig-Maximilians-University, Germany, [10]Columbia University, United States

Background: Increases in bone mineral density (BMD) reduce fracture risk in patients receiving treatment for osteoporosis. Goal-directed Treatment (also called 'Treat-to-Target') recommends that selection of initial treatment (anti-resorptive agent or bone-forming agent) for patients with a T-score <−2.5 should be based on the probability of achieving a goal BMD T-score >=−2.5.Objective: To compare the probability of achieving a T-score of >=−2.5 at the total hip or lumbar spine after 3 years of treatment with alendronate (ALN) only; or the treatment sequences of 12 months of romosozumab (ROMO) followed by 2 years of ALN (ROMO/ALN) or denosumab (ROMO/DMAB).Methods: Female participants in the ARCH trial received ALN for 3 years or ROMO for 1 year followed by ALN for 2 years. Those in the FRAME trial received ROMO for 1 year followed by DMAB for 2 years. For participants with initial BMD T-scores <–2.5 at total hip or spine, we calculated the probability of achieving a T-score >=–2.5 with the three treatments.Results: The probabilities of achieving a T-score >=–2.5 depended on baseline T-score and treatment. At year 3, those with baseline spine T-scores of >=–3.0 had a >=55.3% probability with ALN, >=80.7% with ROMO/ALN and >=92.8% with ROMO/DMAB. Participants with a spine T-score of –3.5 had a 11.2% probability with ALN, 46.3% with ROMO/ALN, and 68.1% with ROMO/DMAB. The probabilities of reaching a T-score >=–2.5 were lower for the total hip but trended similarly by treatment sequence. While >=50% of participants with an initial T-score of >=–2.7 achieved a T-score >=–2.5 with any of the treatments at both sites, those with a hip T-score of >=–3.0 had a >=10.2% probability with ALN, >=39.2% with ROMO/ALN, and >=62.1% with ROMO/DMAB. Participants with a total hip T-score of –3.5 had a very low probability of reaching a T-score >=–2.5 after 3 years of any treatment.Conclusion: Women with a baseline T-score >=–3.0 at the spine or >=–2.7 at the hip have at least a 50% chance to achieve a T-score >=–2.5 with any of the three regimens. In contrast, those with a T-score below –3.0 at the spine, or –2.7 to –3.5 at the total hip, have a substantially greater probability of achieving T-scores >=–2.5 when using a bone-forming agent first (i.e. ROMO/ALN or ROMO/DMAB vs. ALN alone). Those with hip T-scores <=–3.5 may require more than 3 years of treatment that continues to improve BMD. These probabilities should be considered when selecting initial treatment.

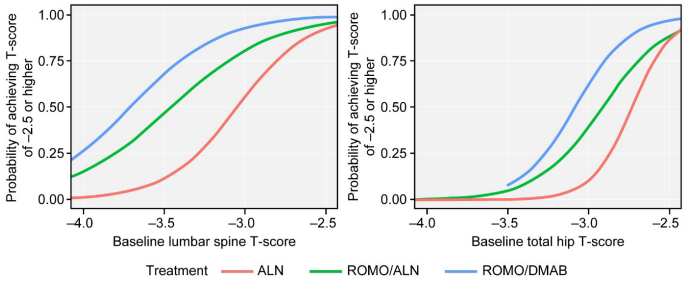

***Disclosures: Steven Cummings**, Amgen, Radius, Myovant, Consultant, Amgen, Grant/Research Support*

P-664

The Effect of Teriparatide Treatment on the Risk of Clinical Fragility Fractures in Postmenopausal Women with Osteoporosis: Results from the Asian and Latin America Fracture Observational Study (ALAFOS) *Huilin Yang[1], Nadia Al Ali[2], Lale Altan[3], Joao Borges[4], Alan Brnabic[15], Noemi Casas[6], Chung-Hwan Chen[7], Abdulaziz Elsalmawy[8], Sirel Gurbuz[15], Sophia Ish-Shalom[10], Seung-Jae Lim[11], Fernando Marin[15], Thomas Moll[15], Imre Pavo[15], Sandra Florez[15]. [1]Department of Orthopedics, The First Affiliated Hospital of Soochow University, Suzhou, People's Republic of China, China, [2]Endocrinology Unit, Amiri Hospital, MOH, Kuwait, Kuwait, [3]Department of Physical Medicine and Rehabilitation, Uludağ University School of Medicine, Bursa, Turkey, Turkey, [4]Faculty of Medicine, Universidade Católica de Brasília, Brasilia, Brazil, Brazil, [15]Eli Lilly and Company, Australia, [6]Riesgo de Fractura CAYRE, Bogotá, Colombia, Colombia, [7]Department of Orthopedics and Orthopedic Research Center, Kaohsiung Municipal Ta-Tung Hospital and Kaohsiung Medical University Hospital, College of Medicine, Kaohsiung Medical University, Kaohsiung City, Taiwan, Taiwan, Province of China, [8]Department of Trauma and Orthopedic Surgery, Al Noor Specialized Hospital, Makkah, Saudi Arabia, Saudi Arabia, [15]Eli Lilly and Company, United States, [10]Lin Endocrine Research Center, Haifa, Israel, Israel, [11]Department of Orthopedic Surgery, Samsung Medical Center, Sungkyunkwan University School of Medicine, Seoul, South Korea, Republic of Korea, [15]Eli Lilly and Company, Spain, [15]Eli Lilly and Company, Switzerland, [15]Eli Lilly and Company, Austria, [15]Eli Lilly and Company, Colombia

Purpose: To evaluate new clinical vertebral and nonvertebral fragility fractures in relation to time on teriparatide therapy, up to 24 months, in real-world clinical practice. Methods: Prospective, site-based, observational study in postmenopausal women with osteoporosis from 20 countries across Asia, Latin America, the Middle East, and Russia. Teriparatide was initiated according to local prescription practices. Fractures were collected at each follow-up visit. Generalized linear models, adjusted for clinically relevant baseline covariates, were used to assess the rate of patients with one or multiple fractures over 6-month intervals. Odds ratios (OR), incident rate ratios (IRR), and 95% confidence intervals (95% CI) are presented.Results: In total, 3098 postmenopausal patients (mean [SD] age 72.4 [10.4] years) recruited at 152 sites were analyzed. At baseline, 63.2% had at least one pre-existing osteoporotic fracture, with 28.8% having >=2. Mean (SD) bone mineral density T-scores at baseline were -3.07 (1.39) and -2.59 (1.05) at the lumbar spine and femoral neck, respectively. For those 3054 patients who started teriparatide therapy, median treatment duration was 18.7 months, and treatment adherence at 12, 18 and 24 months was 68.2%, 53.5% and 31.0%, respectively. Over the 24-months, 111 patients (3.6%) sustained 126 clinical fractures (2.98 fractures/100 patient-years; 39 vertebral and 87 nonvertebral, including 25 hip fractures). Of these 111 patients, 97 sustained a single fracture while 13 patients sustained 2 fractures and 1 patient 3 fractures. In the adjusted analyses, compared with the first 6-month treatment period, the rate of new clinical fragility fractures decreased by 37% (IRR 0.63; 95% CI: 0.40-0.99; p=0.0434), 64% (IRR 0.36; 95% CI: 0.20-0.65; p6-12, >12-18 and >18-24-month treatment periods, respectively. After adjustments, odds of first fracture was also statistically significantly reduced at every time period compared with the first 6 months (Table 1). Similar results were obtained in the unadjusted analyses. Conclusions: Results from this observational study suggest that postmenopausal women with osteoporosis, treated with teriparatide up to 24 months in standard clinical practice across a broad geographic area, experience a greater reduction of osteoporotic fractures over time.

Table 1 Risk of first incident clinical fracture in relation to time on treatment with teriparatide

Observational period (months)	Number of patients	Total number of fractures	Fracture rate per 100 patient years	Patients with ≥1 fracture, *n (%)*[a]	Odds Ratio vs. 0-6 months (95% CI)	p value
Adjusted						
0-6	3054	65	4.81	60 (2.0)	-	-
>6-12	2410	33	2.95	29 (1.2)	0.62 (0.39-0.96)	0.0321
>12-18	2072	15	1.62	14 (0.7)	0.35 (0.20-0.63)	0.0004
>18-24	1616	13	1.92	11 (0.7)	0.39 (0.20-0.73)	0.0036

[a]Adjusted model by age, body mass index, ethnicity, geographic region, tobacco use, prior use of osteoporosis medications or patient support program, and history of fragility fractures after age 40, glucocorticoid-induced osteoporosis, diabetes (type I or II) or number of falls in the past year

***Disclosures: Huilin Yang**, None*

P-665

Dual-target effect of tanshinone IIA sulphate on osteoclast-osteoblast activity: A time-lapse study *PREETY PANWAR[1], Jean-Marie Delaisse[2], Kent Soe[2], Dieter Bromme[1]. [1]UBC, Canada, [2]University of Southern Denmark, Denmark

Bone homeostasis is maintained by osteoclasts (OCs) and osteoblasts (OBs) in a coupling process. In this study, we used specific markers and time-lapse analyses to monitor the action of antiresorptive and anabolic compounds. OCs were generated from human CD14+ peripheral blood monocytes, while OBs were outgrowths obtained from human trabecular bone specimens. We compared the efficacy of bisphosphonate (zoledronic acid) (BP), odanacatib (ODN, active site cathepsin K inhibitor), tanshinone IIA sulphate (T06, ectosteric cathepsin K inhibitor), and cladrin (anabolic compound) in in-vitro cell assays. In accordance with OC mono culture time-lapse results, we found under control conditions elongated trenches generated by OCs moving rapidly over the bone surface while resorbing. However, clusters of small round pits reflecting intermittent bone resorption were observed during T06 and ODN treatments. Bisphosphonate abolished the resorption by targeting OCs, however, cladrin showed only minor effect on resorption by interrupting the formation of longer trenches. More interestingly, in co-culture between OCs and OBs, BP, T06, and ODN significantly reduced the release of the cathepsin K-specific collagen type I degradation marker, CTx1, but only T06 and cladrin enhanced the deposition of mineralized matrix as seen by EDX analysis and corroborated by increased alkaline phosphatase (ALP) activity in OBs. In addition, time-lapse results of human OC/OB co-cultures revealed a higher affinity of OBs towards pits compared to trenches. Here, significantly more OBs approached the pits and occupied these cavities for longer periods of time under T06 treatment when compared to their length of stay in trenches under untreated conditions where rapid migration of OBs was common. Immunofluorescence microscopy analysis of OC and OB morphology in terms of nuclei, actin fibres and actin-ring formation was not changed during T06 treatment. In conclusion, T06 showed both antiresorptive and anabolic properties and is acting as a dual-targeting compound and may represent a novel and more effective approach to treat osteoporosis.

***Disclosures: PREETY PANWAR**, None*

P-666

The Case for Limiting Teriparatide Treatment to One Year *Clay Larkin[1], Florence Lima[1], Margaret Lund[1], Madhumathi Rao[1]. [1]University of Kentucky, United States

Background: Treatment with anabolic agents such as teriparatide is generally recommended for 18-24 months, and not to exceed the latter. However, emerging data suggests that the maximal effect on bone formation is seen in the first year. In this study we compared the effect of teriparatide in the first and second years of treatment on bone density (BMD), trabecular bone scores (TBS) and bone turnover markers (BTM) - serum levels of bone specific alkaline phosphatase, n-telopeptide and osteocalcin, to assess the incremental value of the second year of treatment vs risk of forearm bone loss. Patients and methods: We studied 117 patients receiving teriparatide for treatment of osteoporosis who underwent serial bone density measurements of the axial skeleton, as well as forearm measurements. Time trends of BMD and BTM changes were analyzed using repeated measures ANOVA. Results: The mean age of patients at onset of therapy was 62+/-11 years and 84 % were female. Lumbar spine (LS) BMD increased by 7.1%, forearm BMD declined by 4.4%, (p<0.01 for both) and TBS did not change significantly during treatment. The increase in LS BMD was significantly higher during year 1 than year 2 (p=0.03); the decline in forearm BMD did not differ significantly between years 1 and 2 of treatment (p=0.11) (figure 1). BMD did not change significantly at other axial sites. All three BTMs showed a uniform increase over the first year with either decline or plateau in the second year, despite continued treatment with teriparatide (p value for interaction <0.05) (figure 1). Conclusions: Teriparatide induces gains in axial BMD that are maximal in the first year with non-significant incremental value in the second year. This observation is consistent with the downtrend in BTMs during the second year despite continued treatment with teriparatide, suggesting a less evident effect on bone turnover. Decline in forearm BMD appears to continue monotonically during the second year of treatment. These observations suggest that treatment could potentially be limited to one year, potentially as a basis for cyclic therapy with anti-resorptive agents or allowing the opportunity for later use of anabolic therapy if the need arose.

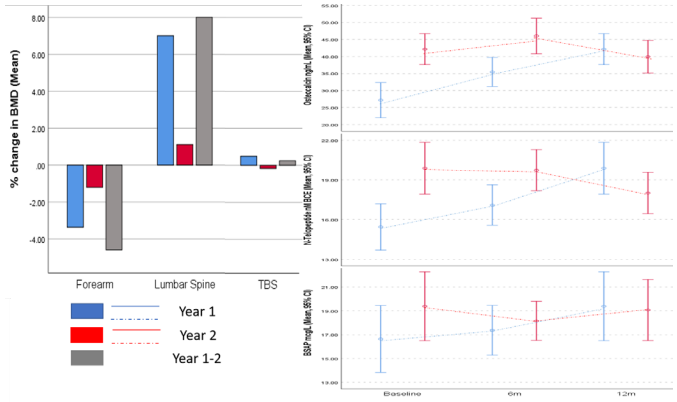

***Disclosures: Clay Larkin**, None*

Posters

P-667

Safety and efficacy of zoledronic acid for prevention of bone loss after gastric bypass: pilot study *Yi Liu[1], Michael Cheney[2], Maya Cote[2], Katherine Lindeman[2], Claire Rushin[2], Elaine Yu[2]. [1]Lahey Hospital and Medical Center, United States, [2]Endocrine Unit, Massachusetts General Hospital, United States

Purpose: Roux-en-Y gastric bypass (RYGB) inadvertently causes bone loss and increased fracture risk. To date, there have been no studies examining whether pharmacologic treatments can prevent bone loss after RYGB. We sought to examine the preliminary safety and efficacy of zoledronic acid (ZOL) to suppress bone turnover markers and prevent declines in bone mineral density (BMD) after RYGB.Methods: Postmenopausal women older than 50 years with obesity who were planning RYGB were recruited for this open-label pilot study (n=4). A single dose of ZOL 5 mg was given intravenously prior to RYGB. BMD was obtained at the spine and hip by dual-energy x-ray absorptiometry and at the trabecular spine by quantitative CT at baseline and 24 weeks. Serum bone biochemistries including C-telopeptide (CTX) were measured. Results were compared against pre-operative baseline and against historical RYGB controls (n=10).Results: Baseline characteristics of ZOL and control groups were similar (mean +/-SD: age 59 +/-9 years, BMI 42 +/-4 kg/m^2), and post-RYGB weight loss at 24 weeks was similar in both groups (59 +/- 22 lbs). By 24 weeks after RYGB, participants receiving ZOL had a significant increase in CTX above pre-operative baseline (+0.228 +/-0.117 ng/dL, p=0.030) but this CTX rise was less than that observed in the controls (+0.601 +/-0.307 ng/dL, p=0.042 between groups). There was a suggestion that the ZOL group was protected against trabecular spine volumetric bone loss as compared to the control group (+4.8+/-8.0% vs. -5.9+/-7.0%, p=0.075 between groups). Despite ZOL, participants had significant areal BMD loss at the total hip as compared to pre-operative baseline (-4.2+/-1.5%, p=0.012) that was similar in magnitude to total hip BMD loss in the controls (-5.5+/-3.9%, p=0.005). Serum calcium, 25-hydroxyvitamin D, and parathyroid hormone did not change in either group. No hypocalcemia, change in renal function, or significant adverse events were observed after ZOL.Conclusion: In patients receiving RYGB, zoledronic acid was safe and appeared to mitigate but not fully prevent high bone turnover in the acute postoperative period. Our preliminary data suggest that ZOL may preserve trabecular bone density at the spine, but was not sufficient to prevent bone loss at the hip at 24 weeks. Prospective controlled studies are needed to confirm our findings and to identify the best strategies for preventing bone loss and lowering fracture risk in this bariatric population.

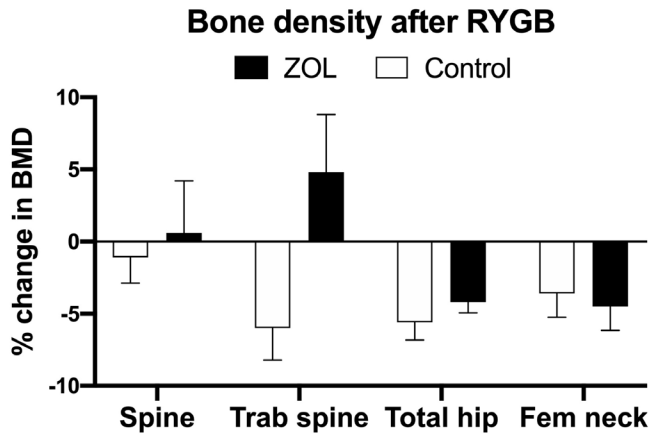

***Disclosures: Yi Liu**, None*

P-668

Generation of humanized RANKL mice to study rebound resorption after discontinuation of Denosumab *Qiang Fu[1], Cecile Bustamante-Gomez[1], Anveshi Guha[1], Igor Gubrij[1], Charles O'Brien[1]. [1]University of Arkansas for Medical Sciences, United States

Discontinuation of long-term administration of Denosumab results in a dramatic decrease in bone mass unless anti-resorptive treatment is resumed. After discontinuation, bone resorption increases to levels above those observed prior to Denosumab treatment, a phenomenon that has been referred to as rebound resorption. The molecular mechanisms responsible for rebound resorption are unknown, therefore we sought to develop a murine model to study it. Because murine RANKL is not inhibited by Denosumab, the region of the protein bound by the antibody must be replaced using the human sequence. Amgen had previously accomplished this by replacing the coding region of exon 5 of the Tnfsf11 gene, which encodes RANKL, with the coding sequence of the human gene. Because these mice are not widely available, we used gene-editing in mice to change exon 5 to match the human sequence only in the region encoding the epitope bound by Denosumab, which was recently identified. We tested the ability of Denosumab to inhibit resorption in these mice by weekly injection of 10 mg Denosumab/kg body weight for 3 weeks into adult males homozygous for the humanized gene. Wildtype C57BL/6 mice were injected as controls. Seven days after the final injection, blood was collected and markers of bone resorption were quantified. Denosumab had no effect on CTX-1 or TRAP5b in wildtype mice but potently suppressed these markers in humanized RANKL mice. We next determined whether discontinuation of Denosumab would lead to rebound resorption in these mice. Adult mice homozygous for the humanized gene were injected once per week with vehicle or Denosumab for 10 weeks. Blood was collected at day 0, on the last day of injection, and at 2 and 4 weeks after the last injection. Analysis of BMD by DXA 2 weeks after final injection revealed that bone mass was elevated in Denosumab-treated mice versus vehicle-treated mice. Consistent with this, circulating TRAP5b was much lower after 10 weeks of Denosumab injection compared with vehicle injection. However, 2 weeks after the last injection, TRAP5b levels were similar in both groups and 4 weeks after the last injection, they were much higher in Denosumab-treated mice versus vehicle-treated mice. These results demonstrate that discontinuation of Denosumab in our humanized RANKL mice leads to rebound resorption that mimics the human condition. These mice should be useful in identifying the molecular mechanisms underlying rebound resorption.

***Disclosures: Qiang Fu**, None*

P-669

Cost-effectiveness of Romosozumab versus Teriparatide for Severe Postmenopausal Osteoporosis in Japan *Hiroshi Hagino[1], Kiyoshi Tanaka[2], Michael McClung[3], Stuart Silverman[4], Shravanthi Gandra[5], Mata Charokopou[6], Kenji Adachi[7], Benjamin Johnson[8], Björn Stollenwerk[9]. [1]Tottori University, Japan, [2]Kobe Gakuin University, Japan, [3]Oregon Osteoporosis Center, United States, [4]Cedars Sinai, United States, [5]Amgen Inc., United States, [6]UCB BioPharma SPRL., Belgium, [7]Amgen K.K., Japan, [8]Amgen Ltd., United Kingdom, [9]Amgen GmbH, Switzerland

Objective: To assess the cost-effectiveness of romosozumab versus teriparatide, both sequenced to alendronate, for the treatment of severe postmenopausal osteoporosis from the perspective of the Japanese healthcare system.Methods: A published Markov cohort cost-effectiveness model was adapted to a Japanese setting using country-specific data. 12 months of romosozumab was compared with 24 months of teriparatide, with both treatments sequenced to alendronate to make up a total treatment duration of 60 months. The population comprised postmenopausal women with severe osteoporosis (T-score <= -2.5 and a history of fragility fracture) with a mean age of 78 years. The analysis used a Japanese public healthcare and long-term care system perspective, a lifetime horizon, and a discount rate of 2% per annum for costs and health outcomes. Direct osteoporosis-related healthcare costs and costs of long-term institutional care were included. Based on the bone mineral density (BMD) superiority of romosozumab compared with teriparatide, two scenarios were assessed: a scenario where the BMD advantage of romosozumab was translated into fracture reduction benefits, and a conservative scenario where it was assumed that both regimens were equally efficacious. Costs were assessed in 2019 US dollars and Japanese yen, and health outcomes in quality-adjusted life years (QALYs).Results: Romosozumab/alendronate dominated teriparatide/alendronate (i.e. it was cost saving and more or equally effective). Cost savings were $4,961 (¥533,491) and $4,401 (¥473,270) under the superior and equal efficacy scenarios, respectively, with 0.042 QALYs gained in the superior efficacy scenario. Conclusion: Cost-effectiveness model outcomes indicate that treating women with severe postmenopausal osteoporosis with 12 months of romosozumab produces a greater number of QALYs at a lower cost than 24 months of teriparatide, when both treatments are sequenced to alendronate.

***Disclosures: Hiroshi Hagino**, Asahi Kasei Pharma, Astellas, Chugai, Eisai, Mitsubishi Tanabe Pharma, Pfizer Japan, Taisho Toyama, Teijin Pharma, Grant/Research Support, Speaking Fees : Astellas-Amgen, Asahi Kasei Pharma, Astellas, Chugai, Eisai, Eli Lilly Japan, Mitsubishi Tanabe Pharma, Mochida, MSD, Pfizer Japan, Taisho Toyama, Teijin Pharma, UCB Japan, Other Financial or Material Support, Asahi Kasei Pharma, Consultant*

P-670

Relative Potency of Calcifediol vs Cholecalciferol *Salvatore Minisola[1], Jessica Pepe[1], Luciano Colangelo[1], Luciano Nieddu[2], Franco Mazzei[3], Cristiana Cipriani[1]. [1]Department of Clinical, Internal, Anesthesiologic and Cardiovascular Sciences, Sapienza University of Rome, Italy, [2]Faculty of Economics, UNINT University of Rome, Italy, [3]Department of Chemistry and Technology of Drugs, Sapienza University of Rome, Italy

There is a long standing debate on the relative potency of calcifediol versus cholecalciferol. We analyzed investigations in which calcifediol was utilized to reach vitamin D sufficiency and compared with most recent and important studies that utilized cholecalciferol to reach sufficiency. There were two main "a priori" selection criteria: the first was represented by basal 25(OH)D values less than 30 ng/mL; the second was the duration of treatment of at least 10 weeks. Since there are many more studies with cholecalciferol than with calcifediol, we chose the most recent and the most cited. A total population of 402 subjects for calcifediol studies and 1086 subjects for cholecalciferol investigations, was included.Concerning the rise in serum 25(OH)D as a function of daily oral input, we found significant correlations for both calcifediol and cholecalciferol (r=0.788, p<0.001 ; r=0.779, p<0.001, respectively). However, the slope values of the correlations between the daily dose ingested and the final 25(OH)D value was steeper for calcifediol (1.59 +/- 0.32) compared to cholecalciferol

(0.25+/-0.01) and significantly different (p<0.001). This observation is confirmed, considering the average values of the induced metabolic effect for the same dose concentration ranges (as daily mcg) used in the administration of the two drugs (Figure 1). Furthermore, the difference of calcifediol potency in respect to cholecalciferol increases as a function of daily oral input.No correlations were found between the delta, final minus basal 25(OH) D value, for each study and initial 25(OH)D values considering all studies and those with calcifediol or cholecalciferol, separately. However, the slope of the curve (albeit not significantly different) was positive considering cholecalciferol studies and negative taking into account calcifediol studies.Considering mean BMI of the population studied and the delta of 25(OH)D values adjusted for the treatment period, we found statistical significance correlations considering studies as a whole (r=-0.404, p=0.013) and no statistical significance with cholecalciferol data; in contrast, data pertaining calcifediol were significant (r=-0.528, p=0.029).We showed on a large data base that 1) calcifediol has a variable greater relative potency in respect to cholecalciferol depending on the dose administered; 2) the inverse correlation found between BMI and calcifediol suggests that fat mass might be negatively involved in the CYP2R1 regulation.

Figure 1. Correlations between the daily dose of calcifediol and cholecalciferol and 25(OH)D value

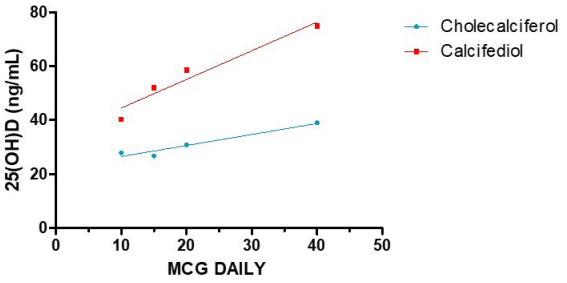

***Disclosures: Salvatore Minisola**, Abiogen, Amgen, Bruno Farmaceutici, Diasorin, Eli Lilly, Shire, Sandoz, Takeda, Speakers' Bureau, Abiogen, Kyowa Kirin, Pfizer, UCB, Other Financial or Material Support*

P-671

Abaloparatide, A Novel Selective Agonist for PTH/PTHrP Receptor, Effectively Improved Hip Geometry and Biomechanical Properties Assessed by Hip Structural Analysis in Elderly Osteoporotic Patients - Results of the Japanese Phase 3 Trial (ACTIVE-J)- *Teruki Sone[1], Kazuhiro Ohnaru[2], Maki Mihoya[3], Tetsuo Inoue[4], Toshio Matsumoto[5]. [1]Department of Nuclear Medicine, Kawasaki Medical School, Japan, [2]Department of Orthopedic Surgery, Kawasaki Medical School, Japan, [3]Clinical Development Administration Department, Teijin Pharma Limited, Japan, [4]Aoyama General Hospital, Japan, [5]Fujii Memorial Institute of Medical Science, Tokushima University, Japan

Background and Objectives: Abaloparatide (ABL) is a selective agonist for PTH/PTHrP receptor, which significantly increased bone mineral density (BMD) and lowered the risk of osteoporosis-related vertebral and non-vertebral fractures in the international phase 3 ACTIVE trial. In Japan, ABL also demonstrated potent increases in BMD at the lumbar spine, total hip, and femoral neck, in a randomized, double blind, multi-center, placebo-controlled phase 3 trial, ACTIVE-J. To evaluate the effect of ABL on hip geometry and biomechanical properties, hip structural analysis (HSA) was performed based on dual-energy X-ray absorptiometry (DXA) scans from ACTIVE-J. Subjects: A total of 213 patients (193 postmenopausal women and 20 men) aged 55 or older with lumbar spine (LS) BMD less than T-score -1.77 and one or more vertebral fractures, BMD T-score less than -3.0 without fractures, or aged 65 years or older with BMD less than T-score -2.5 were randomly assigned to daily subcutaneous injection of 80 µg ABL or placebo (PBO) for 18 months in a 2:1 ratio. Methods: Hip DXA scans were performed at baseline, 3, 6, 12 and 18 months. Cross-sectional geometrical parameters at the narrowest segment of the femoral neck (NN), the intertrochanteric region (IT), and the proximal shaft (PS) were analyzed using APEX 3.0 software (Hologic, Inc.). Geometrical parameters and derived strength indices included average cortical thickness (CT), bone cross-sectional area (CSA), cross-sectional moment of inertia (CSMI), section modulus (SM), and buckling ratio (BR). Change from baseline in these indices in the ABL group were compared with PBO at the NN, IT and PS regions. Results: Compared with the PBO group (n=65) after 18 months, the ABL group (n=128) showed higher CT, CSA, CSMI, and SM at both the NN and IT regions. And lower BR was observed in the ABL group at the IT region. No expansion of periosteal diameter was observed at these regions. There were no differences in CSMI and BR at the PS region. Conclusion: These results indicate that overall structural strength in the proximal femur increased compared to placebo, suggesting that 18-months of ABL treatment effectively reverses changes in hip geometry and strength with aging.

	CT [% (95%CI)]	CSA [% (95%CI)]	CSMI [% (95%CI)]	SM [% (95%CI)]	BR [% (95%CI)]
NN	4.48 (1.67-7.29)	5.46 (3.65-7.26)	6.68 (3.83-9.54)	6.07 (3.34-8.81)	-3.52(-7.82- 0.78)
IT	5.34 (3.48-7.21)	4.70 (2.97-6.43)	3.63 (0.36-6.91)	4.50 (1.56-7.44)	-5.85(-7.62- -4.08)

***Disclosures: Teruki Sone**, Teijin Pharma, Consultant, Shimadzu Corporation, Consultant, Teijin Pharma, Grant/Research Support*

P-672

Real-world bone turnover marker use: Impact on treatment decisions and fracture *Nancy E. Lane[1], Kenneth Saag[2], Tyler J. O'Neill[3], Megan Manion[4], Roma Shah[3], Ursula Klause[5], Richard Eastell[6]. [1]Department of Internal Medicine, UC Davis Health, United States, [2]Department of Medicine, Division of Clinical Immunology and Rheumatology, University of Alabama at Birmingham, United States, [3]Data Science and Services, Diagnostics Information Solutions, Roche Diagnostics, United States, [4]Roche Diagnostics, United States, [5]Roche Diabetes Care, Roche Diagnostics, United States, [6]Department of Oncology and Metabolism, University of Sheffield, United Kingdom

Purpose: 1) To characterise bone turnover marker (BTM) testing patterns in patients with osteoporosis in a large, heterogeneous practice setting using a retrospective claims database. 2) To estimate potential BTM clinical utility in treatment decision-making and fragility fracture risk following BTM use.Methods: Data from patients aged >=50 years with newly diagnosed osteoporosis enrolled in the Truven MarketScan® Commercial Claims and Encounters and Medicare Supplemental and Co-ordination of Benefits databases from 1 Jan 2008–30 Jun 2018 were included. Osteoporosis was ascertained by explicit claims, or fragility fracture events associated with osteoporosis, or prescribed anti-resorptive or anabolic therapy. Patients with metabolic or genetic diseases associated with low bone mineral density and those with neoplasia were excluded. Eligible BTMs (osteocalcin, bone-specific alkaline phosphatase, collagen cross-links) tested patients were 1:1 propensity score matched to those untested following diagnosis. Generalised estimating equation models with logit links and independent correlation structures were performed to estimate odds ratios (ORs) and 95% confidence intervals (CIs) for testing versus no testing on both treatment decision-making (categorised following a BTM test according to days of coverage or supply) and fragility fracture.Results: Of 457,829 patients with osteoporosis, 6,075 were identified with >=1 BTM test claims on/following diagnosis; of these patients, 1,345 had a unique treatment decision made <=30 days of BTM testing. During the study period, the proportion of patients receiving BTM tests increased significantly each year (average annual % change=+8.1%; 95% CI=5.6–9.0; p=0.01) despite a stable average testing of 2.2 tests (standard deviation [SD]=2.0) per patient (Figure). On matching 6,075 BTM tested to 6,075 untested patients, those tested were significantly more likely to have a treatment decision (OR=1.14; 95% CI=1.13–1.15), and testing was associated with lower odds of fracture, versus those untested (OR=0.87; 95% CI=0.85–0.88).Conclusions: In this large, heterogeneous population of presumed osteoporotic patients, BTM testing was associated with treatment decision-making, likely leading to fragility fracture reduction following use. Further investigation is needed to validate our findings and understand what drives test ordering, but our evidence provides further value of monitoring osteoporotic patients with BTMs.Figure: Annual period prevalence (per 100 persons) of bone turnover marker testing and average testing per patient among osteoporotic patients enrolled in Truven MarketScan® Commercial Claims and Encounters and Medicare Supplemental and Co-ordination of Benefits databases, 2008–2018.

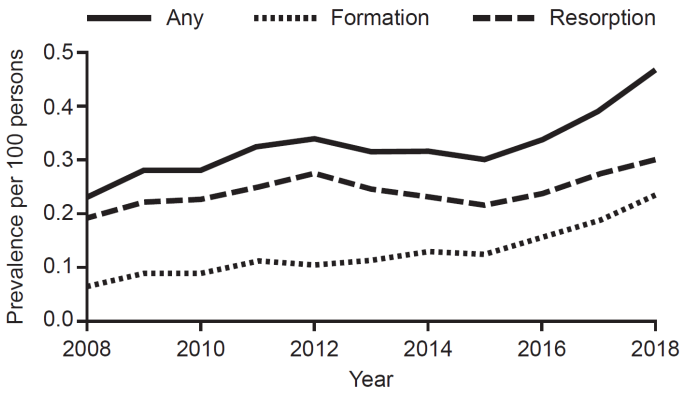

***Disclosures: Nancy E. Lane**, Roche, Consultant*

Posters

P-673

Factors associated with adherence to osteoporosis medications among male Veterans *Nicole Sagalla[1], Richard Lee[1], Richard Sloane[1], Kenneth Lyles[1], Cathleen Colón-Emeric[1]. [1]Duke University, United States

Purpose: To determine adherence rates and factors associated with adherence to osteoporosis medications among male Veterans. Methods: We conducted a secondary analysis of a national cohort of male Veterans with a prescription for an oral bisphosphonate or Calcitonin between 2000-2010. We identified demographic, comorbid and fracture-related risk factors by their ICD9 and CPT codes and used multivariable logistic regression to evaluate their association with adherence as measured by medication possession ratio (MPR) over 5 years starting at the time of their first prescription during the study period and censoring at death or end of study period. Results: Of 135,306 men identified with at least 1 prescription for an osteoporosis medication during the study period, 90,406 (67%) were non-adherent (MPR < 0.80). The median duration of therapy was 3.2 years (IQR=1.7, 5.0). In the fully adjusted model, the odds of adherence were lower in those < 65 years (OR=0.87; 95% CI: 0.84,0.89), with no copay (OR=0.78; 0.76,0.80), dementia (OR=0.87; 0.83,0.91), anxiety/depression (OR=0.93; 0.90,0.95), tobacco use (OR=0.91; 0.89,0.94), alcohol abuse (OR=0.91; 0.89,0.94), rheumatoid arthritis (OR=0.91; 0.87,0.96), and on androgen deprivation therapy (OR=0.89; 0.83,0.95). The odds of adherence were higher in whites (OR=1.14; 1.11,1.17), with a prior screening colonoscopy (OR=1.12; 1.09, 1.15), on Alendronate vs. other agents (OR=1.60; 1.55,1.66), with a DXA (OR=1.14; 1.11,1.17), and on glucocorticoids (OR=1.08; 1.02,1.14). Conclusion: Adherence to oral bisphosphonates/Calcitonin for osteoporosis/osteopenia is poor, with particular subgroups at greatest risk. These findings may help tailor approaches for supporting adherence in men prescribed osteoporosis medications.

***Disclosures: Nicole Sagalla**, None*

P-674

Sclerostin Mutant with Selective Binding to LRP4 Activates Wnt Pathway and Promotes Bone Anabolic Functions *Svetlana Katchkovsky[1], Niv Papo[1], Noam Levaot[1]. [1]Ben Gurion University of the Negev, Israel

The Wnt signaling pathway plays an essential role in bone homeostasis and is finely tuned by a complex interplay between Wnt ligands, receptors, activators and inhibitors. Wnt induction of bone formation is inhibited upon binding of sclerostin, a glycoprotein produced by osteocytes, to the Wnt receptors LRP5/6. Binding of sclerostin to additional receptor LRP4 is required to facilitate optimal inhibition. Herein, we show that a sclerostin mutant (sclerostinN93A) with high binding affinity to LRP4 but not LRP5/6 antagonizes wild-type sclerostin (sclerostinWT) inhibition of Wnt signaling pathway in vitro in osteoblast cultures. In order to increase retention of sclerostinN93A we fused the Fc domain of immunoglobulin G to the C-terminal of sclerostinN93A (sclerostinN93AFc). We show that this modification does not interfere with its ability to antagonize sclerostinWT. Finally, we show that bi-weekly subcutaneous injections of sclerostinN93AFc for two weeks significantly increase trabecular volumetric bone fraction and bone length in developing mice. Our data suggest that compounds that target sclerostin LRP4 binding interface could serve as a potential strategy to promote bone anabolic functions.

***Disclosures: Svetlana Katchkovsky**, None*

P-675

Autonomy begets adherence: Patients stick with their decisions to initiate osteoporosis pharmacotherapy after attending an osteoporosis group 'educonsult' program which emphasizes shared decision-making *Maddie Wilton-Clark[1], Lynn Feasel[2], Greg Kline[1], Emma Billington[1]. [1]University of Calgary, Canada, [2]Alberta Health Services, Canada

Many individuals recommended for osteoporosis pharmacotherapy do not start treatment, and persistence at one year is only 50% among those who do. Patients do not always agree with physician-set treatment thresholds, and low uptake and persistence may reflect lack of confidence in the treatment recommendations provided by physicians. In this prospective study, we assessed patterns in pharmacotherapy use in patients who attended a group 'educonsult' program for osteoporosis that focuses on shared decision-making. Participants were women referred to our specialty clinic for age-associated osteoporosis who attended a 2-hour group educonsult in lieu of one-on-one specialist consultation. The educonsult is facilitated by a specialist physician and nurse, and involves estimation of ten-year major osteoporotic fracture risk (FRAX) and extensive education regarding fracture consequences and potential advantages and disadvantages of pharmacotherapy. Post-consult, patients make autonomous decisions regarding treatment intent and follow-up with their primary care provider to enact their preferred plan. We assessed treatment intent post-consult, and treatment status 3 and 12 months later. Treatment status at 3 months was considered to reflect each individual's final treatment decision, and treatment status at 12 months indicated congruence with the final (3 month) decision. Persistence was defined as the proportion of treated participants at 3 months who remained treated at 12 months. Among 101 participants, mean(SD) age was 62.7(5.8) years, and median(IQR) FRAX 10.7(8.3-17.6)%; 18 patients (17.8%) were considered high-risk using a common physician-set threshold (FRAX >=20%). Treatment status at 3 and 12 months is shown in Figure 1. Immediately post-consult, 27 intended to initiate treatment. At 3 months, 23 (22.8%) were on treatment and 25 (24.8%) were on treatment at 12 months. At 12 months, treatment status was congruent in 94 (93.1%), and 21/23 (91.3%) were persistent with therapy. Of 94 respondents to a 3 month survey, 80 (85.1%) reported being confident in their final treatment decision, and 85/89 (95.5%) respondents reported confidence at 12 months. When individuals with age-associated osteoporosis are encouraged to make autonomous decisions regarding pharmacotherapy use, final treatment decisions may differ from initial intentions, but these decisions are made with high confidence and result in much better persistence than previously reported in the literature.

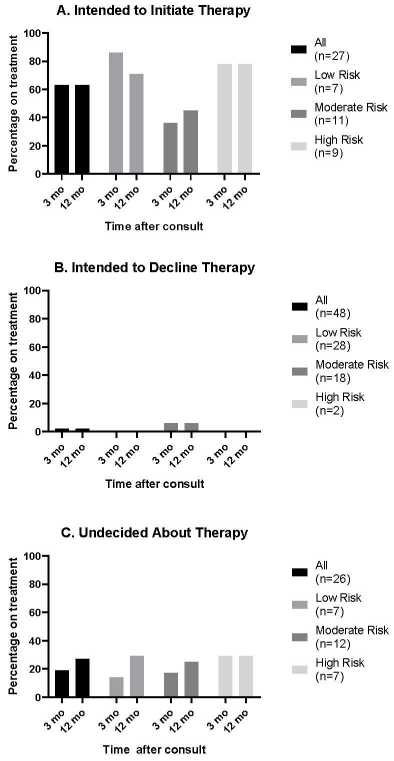

Figure 1. Patterns of pharmacotherapy use in women with age-associated osteoporosis who attended a group 'educonsult' for osteoporosis and either A) intended to initiate therapy, B) intended to decline therapy, or C) were undecided about therapy immediately post-consult. Treatment status is stratified by ten-year risk of major osteoporotic fracture risk (low risk: <10.0%, moderate risk 10.0-19.9%, high risk ≥20.0%).

***Disclosures: Maddie Wilton-Clark**, None*

P-676

Effect of bisphosphonates for secondary prevention of fracture in frail older adults *Sarah Berry[1], Dae Kim[1], Gahee Oh[2], Natalia Gouskova[2], Douglas Kiel[1]. [1]Hebrew SeniorLife & BIDMC, United States, [2]Hebrew SeniorLife, United States

Background: Osteoporosis treatment is often withheld in frail, older adults after the occurrence of a hip fracture given the uncertainty as to whether these drugs are safe and effective in this vulnerable population. Our objective was to determine whether the effect of oral bisphosphonates on secondary fracture prevention differed in frail, older adults.Methods: To minimize between-person confounding, we conducted a nested case-control study using an augmented 5% sample of Medicare beneficiaries in 2014-2015. Using Part A claims, we identified subjects aged >= 65 yrs with a hospitalized incident hip fracture (7/2014-12/2015). We excluded subjects with a claim for Hospice or any osteoporosis medication in the 6 months before fracture (remaining n=16,725). Cases were subjects with a second hip fracture at least 100 days following the incident hip fracture and through 12/2016. We matched four controls for each case using risk-set sampling and based on age, sex, and date of incident hip fracture. Exposure was duration of oral bisphosphonate use (no more than 30 days versus > 30 days) following the incident fracture and ascertained by Medicare Part D claims. A frailty index (range 0-1 with 1 most frail) was calculated using a validated algorithm from Medicare claims in the 6 months before the incident hip fracture. An index of >=0.2 was defined as frail. Conditional logistic regression was used to calculate the odds ratio and 95% confidence intervals of second hip fracture according to bisphosphonate exposure. In adjusted models, we included the number of medications in the model. Models were stratified by frailty status.Results: Cases included 752 subjects with a second hip fracture (mean age 82yrs, 76% female) and 3,008 matched controls. 396 cases were frail prior to the incident hip fracture. Only 26.7% of BP users received 6 months or more of the drug. As shown in the table, bisphosphonate use appeared to decrease the risk of second fracture in non-frail persons,

whereas it had no effect in frail persons; however, none of the odds ratios were statistically significant. Conclusions: Although our results were not significant, our findings suggest the efficacy of bisphosphonates may differ according to frailty status.

	Non-frail			Frail		
Oral bisphosphonate exposure	Cases N (%)	Controls N (%)	OR (95% CI)	Cases N (%)	Controls N (%)	OR (95% CI)
None or no more than 30 days	343 (96.3)	1,348 (94.7)	REF	383 (96.7)	1,534 (97.3)	REF
> 30 days	13 (3.7)	76 (5.3)	0.67 (0.37, 1.23)	13 (3.3)	50 (3.2)	1.02 (0.54, 1.92)

***Disclosures: Sarah Berry**, None*

P-677

Compliance with the Administration of Denosumab Injections during COVID-19 Pandemic. *Ejaz Mahmood[1], Alexis Richardson[2], Maria Meirzon[1], Catherine Anastasopoulou[1]. [1]Einstein Medical Center, United States, [2]Department of Endocrinology, Einstein Medical center., United States

Purpose: Denosumab is a monoclonal antibody to the receptor activator of nuclear factor kappa-B ligand (RANKL). It inhibits osteoclast formation which decreases bone resorption, increases bone mineral density and reduces the risk of fracture. It has been established that stopping or omitting Denosumab is associated with increased fracture risk.[1] Its administration is approved to be provided by a healthcare professional.[2] Our study aims to assess the compliance with Denosumab injection during COVID-19 pandemic when elective services were limited.Methods:A retrospective chart review of all the patients with osteoporosis who were due to receive Denosumab Injection in an endocrine practice between 03/01/2020 and 05/22/2020 was conducted. The patients who received the scheduled Denosumab were categorized based on the type of visit.Results:A total of 89 patients were identified. 14 patients (15.7%) refused to get Denosumab injection during this pandemic. 2 patients (2.3%) had to be rescheduled due to logistic needs of infusion center. 73 patients (82%) received scheduled dose of Denosumab in different ways; 23 patients (25.8%) attended a scheduled office visit to get the injection, 46 patients (51.7%) received the medication on a home visit by a registered nurse of the practice and 4 patients (4.5%) also got their injections by the registered nurse via a drive through arrangement.Conclusion:The current COVID-19 pandemic has a significant effect on the health care facilities by limiting direct access to non-emergent care to the patients. It also has an impact on patients' behavior of utilizing the medical services and on their perception of how they want to get their care delivered in a safe manner. Continuation of Denosumab injection is time sensitive and delay in administration is associated with worse outcomes. By actively identifying the patients and offering them different options of logistics including office visits, home visits or drive through injections, a high percentage of adherence to the scheduled Denosumab was achieved during the early phase of the COVID-19 pandemic. References:Cummings SR, Ferrari S, Eastell R, et al. Vertebral Fractures After Discontinuation of Denosumab: A Post Hoc Analysis of the Randomized Placebo-Controlled FREEDOM Trial and Its Extension. J Bone Miner Res. 2018;33(2):190-198. doi:10.1002/jbmr.3337Johnson, Gretchen L. "Denosumab (prolia) for treatment of postmenopausal osteoporosis." Am Fam Physician 2012; 85(4): 334-336

***Disclosures: Ejaz Mahmood**, None*

P-678

Trends in Medication Prescribing for Primary Osteoporosis Using the Korea National Health Insurance Database, 2006-2015 *Nami Lee[1], Jaeyong Shin[1], Yong Jun Choi[1], Yunhwan Lee[1], Dae Jung Kim[1], Yoon-Sok Chung[1]. [1]Ajou University School of Medicine, Republic of Korea

Osteoporosis has emerged as a significant health problem, contributing to socioeconomic burdens due to the rapidly growing elderly population worldwide, including South Korea [1, 2]. However, adherence to medications for osteoporosis is relatively low because there are seldom symptoms until the patient develops osteoporotic fractures, leading to increased morbidity and mortality [3-5]. We investigated the prescribing pattern of anti-osteoporotic drugs (AODs) with government health insurance reimbursement guideline, especially bisphosphonates and selective estrogen receptor modulators (SERMs), in South Korea during the recent ten-year period.We used the Korea National Health Insurance Service – National Sample Cohort (NHIS-NSC) data from January 1, 2006 to December 31, 2015. We selected patients 50 years of age or older, diagnosed with osteoporosis.The mean age at the time of diagnosis for osteoporosis was 69.9 years (means +/- SD; 61.3~78.6 years). The proportion of women among total osteoporotic patients was 88%. One-half of osteoporotic patients received AOD prescriptions.Over the 10-year period, oral bisphosphonates (oral BP, 90.2%) were the most frequently prescribed AOD in South Korea (Table 1). The proportion of oral BP prescription decreased steadily from about 95% to 77.9%, though it still was the most commonly used AOD. In the mid-2000s, the intravenous bisphosphonates (IV BP) were scarcely prescribed, but it gradually increased to 12.1% in 2015. Moreover, this trend stood out at 24.9% among hospitalized patients in 2015. SERMs were prescribed 6.2% in 2006, but as of 2011, its proportion decreased to 2.9%. After that, the prescription of SERMs increased to 9.9% in 2015.Bisphosphonate was still the mostly preferred AOD, a pattern similar to that of other countries. However, the prescription pattern has changed according to the administration route of bisphosphonates. The proportion of IV BP increases while oral BP decreases. This trend is probably due in part to patient's medication adherence. SERMs are approved drug to treat osteoporosis only for women in several Asian countries, including South Korea. It is the relatively preferred AOD mainly because of the safety concern. More recently since 2016, the prescription of denosumab and teriparatide has increasing due to advanced osteoporosis observed in aged patients.

Table 1. Annual Trends of Anti-osteoporotic Drug Prescription and Adherence from the Korea NHIS-NSC Database [Unit : %]

Year		2006	2007	2008	2009	2010	2011	2012	2013	2014	2015	Weighted mean
Prescription	AOD*											
Total drug	Oral BP†	93.8	95.4	96.0	95.8	95.2	94.6	92.2	88.7	84.1	77.9	90.2
	IV BP‡	0.0	0.0	0.4	1.0	1.4	2.4	3.4	5.0	8.5	12.1	4.2
	SERM§	6.2	4.6	3.6	3.2	3.3	2.9	4.4	6.4	7.5	9.9	5.6
Inpatient drug	Oral BP	95.5	95.7	93.5	91.9	89.8	87.0	79.7	75.2	68.4	64.8	83.4
	IV BP	0.0	0.2	1.8	5.7	7.2	10.8	14.9	18.3	22.5	24.9	11.3
	SERM	4.5	4.1	4.6	2.4	3.0	2.1	5.4	6.5	9.1	10.3	5.3
Outpatient drug	Oral BP	93.8	95.4	96.1	96.0	95.4	94.9	92.6	89.2	84.5	78.3	90.5
	IV BP	0.0	0.0	0.3	0.8	1.2	2.1	3.0	4.5	8.1	11.8	3.9
	SERM	6.2	4.6	3.6	3.3	3.4	3.0	4.3	6.3	7.4	9.9	5.6

*Anti-osteoporotic drug, †Oral bisphosphonate, ‡Intravenous bisphosphonate, §Selective Estrogen Receptor Modulator

***Disclosures: Nami Lee**, None*

P-679

Comparison of Femoral Neck Shortening and Outcomes between In Situ Fixation and Fixation after Reduction for Severe Valgus Impacted Femoral Neck Fractures *Youngchang Park[1], Kyuhyun Yang[2]. [1]Catholic Kwandong University, Republic of Korea, [2]Yonsei university, Republic of Korea

Purpose: To compare femoral neck shortening (FNS) and outcomes between in situ fixation and fixation after reduction for severe valgus impacted femoral neck fractures (AO/OTA classification 31-B1.1) in patients aged 65 years or younger. Methods: This retrospective study included 55 patients who underwent internal fixation with three parallel screws for severe valgus impacted femoral neck fracture between January 2006 and December 2018. Twenty-eight patients were treated with in situ fixation (in situ group), and 27 underwent fixation after reduction (reduction group). In the reduction group, reduction using lateral traction with a Schanz pin was performed before internal fixation. The independent t-test and chi-square or Fisher exact test were used for data analysis. Results: Bone union was achieved in all patients; avascular necrosis occurred in two patients each in both groups. There was no significant difference in the preoperative characteristics between the groups. FNS at 1 year postoperatively was significantly smaller and FNS >5 mm was significantly less in the reduction group than in the in situ group (11% versus 75%). The mean Harris Hip Score (HHS) at 1 year postoperatively was significantly higher in the reduction group than in the in situ group. FNS and HHS were negatively correlated; the mean HHS was significantly higher in none/mild shortening (<5 mm) than in moderate/severe shortening (>=5 mm). Conclusion: In patients aged 65 years or younger, internal fixation after reduction for severe valgus impacted femoral neck fractures is safe and effective for restoring the femoral neck length and achieving successful bone union.

***Disclosures: Youngchang Park**, None*

P-680

Short-term of clinical efficacy of romosozumab in patients with rheumatoid arthritis and primary osteoporosis *Yasuhide Kanayama[2], Taichi Tsuji[0], Naohisa Futamura[0], Kyotaro Ota[0], Yui Adachi[0], Ryosuke Sugimoto[0], Kei Terasawa[0], Kento Maeda[0]. [2]Orthopedic Surgery and Rheumatology, Toyota Kosei Hospital, Japan, [0]Orthopedic Surgery, Toyota Kosei Hospital, Japan

[Background] Romosozumab (ROM), a monoclonal antibody that binds sclerostin, increases bone formation and decreases bone resorption.And although it is a novel therapeutic agent for osteoporosis, which has shown high effects of increasing bone density and inhibiting fragile fracture in overseas clinical trials. However the clinical efficacy in daily clinical practice is unknown.[Objectives] To evaluate the early clinical efficacy of ROM in patients with osteoporosis between rheumatoid arthritis (RA-OP) and primary osteoporosis (P-OP) for 6 months.[Methods] RA patients diagnosed according to the 2010 ACR/EULAR criteria. RA-OP and P-OP patients met at least one of the following criteria were eligible; a bone mineral density T score of -2,5 or less at the lumber spine or total hip and either one or more moderate or severe vertebral fractures or two or more mild vertebral fractures. All patients were initiated ROM from between March and September, 2019. The total number of patients was 26 cases, including 11 RA-OP and 15 P-OP. All patients received continuous ROM therapy more than 6 months. The ROM dose was 210mg at once every 1 months. In all cases native or activated vitamin D has been used. We reviewed the results for 6 months about the increase and decrease of bone mineral density (BMD) of lumbar spine(LS) and total hip(TH) by DEXA and bone turnover markers, intact n-terminal propeptide type I procollagen(PINP) and tartrate-resistant acid phopshatate form 5b(TRACP-5b).[Results] The gender was 25 female and 1 male. The mean age was 70.7 +/- 11.2; disease duration of RA-OP patients was 19.4 +/- 15.0 years; the body mass index was 19.4 +/- 3.6 and the FRAX was 31.1 +/- 15.3. Clinical findings related to RA-OP at baseline were as follows; CRP 1.51 +/- 1.73; DAS-CRP 3.57 +/- 0.98; HAQ 1.60 +/- 1.03 in RA-OP patients and in the all patients, bone turnover markers and bone mineral density at baseline were as follows ; P1NP 57.6 +/- 42.3;

TRACP-5b 434 +/- 232 ; LS-BMD and T-score 0.81 +/- 0.17 g/cm2 and -2.62 +/- 1.13 and TH-BMD 0.57 +/- 0.08 g/cm2 and -3.07 +/- 0.62 g/cm2. The rate of increased P1NP from baseline to 1, 3 and 6 months were each 119.8 +/- 90.0% at 1 month, 108.4 +/- 98.6% at 3 month and 79.4 +/- 133.6% at 6 month and decreased TRAC-5b were -17.5 +/- 23.8% at 1 month, -49.9 +/- 44.9% at 3 month and 0.5 +/- 53.1% at 6 month. The rate of increased LS-BMD from baseline to 6 months were 9.3 +/- 7.1% and TH-BMD were 4.4 +/- 4.5%. [Conclusion] Short-term of clinical efficacy of ROM for RA-OP and P-OP was extremely effective and has the high potential to be an important option in the treatment of osteoporosis.

***Disclosures: Yasuhide Kanayama**, None*

P-681

Evaluation of a Multidisciplinary Team Approach to Improve Osteoporosis Management *Violet Lagari[1], Gracielena Rodriguez[1], Maribel Garcia[1], Sue Kwok[1], Martha Salazar[1], Silvina Levis[1]. [1]Miami VA Healthcare System, United States

The Veterans Health Administration (VHA) provides care for 9 million veterans, of which 64% are men older than 55. In 2012, the Office of the Inspector General determined that 42% of veterans with osteoporotic fractures received appropriate evaluation and treatment. We evaluated the impact of a multidisciplinary team on osteoporosis management at one of the largest VA facilities.The multidisciplinary team (3 clinical pharmacists and 2 endocrinologists) began working in May 2015 to compare outcomes prior to program implementation (5/2014 – 5/2015) and after implementation (11/2017 - 11/2018). Abnormal bone mineral density (BMD) test results were defined as either 1) T-score diagnosis of osteoporosis, 2) Osteopenia with high fracture risk as determined by FRAX score, 3) history of a low-trauma fracture noted on the BMD intake. Thirty days after abnormal BMD results were reported to the ordering physician, a clinical pharmacist performed a chart review to identify patients who did not receive an appropriate prescription for an osteoporosis medication. Recommendations included 1) a follow-up phone call to obtain more information, 2) patient referral for further work-up in the endocrinology clinic, or 3) anti-osteoporosis therapy initiation. The primary outcome was osteoporosis management as defined by initiation of anti-osteoporosis medications, endocrinology referral or patient contact for osteoporosis management discussion.The pre-intervention group consisted of 89 patients and intervention group consisted of 176 patients. Baseline characteristics were similar between groups. Osteoporosis management was provided to 53.9% of patients in the pre-intervention group and to 95.5% of patients in the intervention group. Anti-osteoporosis medications were initiated/continued in 44.9% of patients in the pre-intervention group, and in 72.2% of patients in the intervention group. Of the patients in the pre-intervention group, 44% had sustained a low-trauma fracture and, of those, 46% had received osteoporosis management. In the intervention group, 22% had sustained a low trauma fracture and, of those, 89% received osteoporosis management.A greater proportion of patients received osteoporosis management, inclusive of anti-osteoporosis medications, in the intervention group. Having a multidisciplinary team approach that includes clinical pharmacists as part of a multidisciplinary team-based approach improves osteoporosis management.

***Disclosures: Violet Lagari**, None*

P-682

The urgent need of strategies to improve secondary fracture prevention in Spain: A call to action *Cristina Carbonell[1], José Carlos Bastida[2], Josep Blanch[3], Enrique Casado[4], José Luis Pérez Castrillón[5], Laura Canals[6], Luis Lizán[7]. [1]Primary care, Catalan Health Institute (ICS), Spain, [2]Family Medicine, Marín Health Centre, Spain, [3]Department of Rheumatology, Hospital del Mar, Spain, [4]Department of Rheumatology, Hospital Universitari Parc Taulí (UAB), Spain, [5]Department of Internal Medicine, Hospital Universitario "Rio Hortega", Spain, [6]Amgen (Europe) GmBH, Spain, [7]Outcomes'10, Spain

PurposeSeveral scientific organizations have called for an improvement in fragility fracture management to prevent subsequent fractures. This study aims to establish a consensus among health professionals regarding the strategies to promote secondary prevention of osteoporotic fractures in Spain.MethodsA literature review and a working group with experts (n=12) were performed to identify the main barriers for secondary fracture prevention. Twenty improvement strategies were compiled in a 43-item questionnaire, reviewed by a committee (2 rheumatologists, 2 primary care (PC) physicians, 1 internist physician). Questions were approached from 3 perspectives: current (C: current situation), desire (D: what is wanted to happen) and prognosis (P: what will really happen in 5 years); and rated on a 7-point scale (1=total disagree; 7=total agree). A total of 102 professionals from 14 scientific societies were invited to participate in a 2-round Delphi consultation. Consensus was established (D and P perspectives) when at least 75% of the answers were in the range of disagreement (points 1-3) or agreement (points 5-7). Items that did not reach consensus in the 1st round were included in the 2nd round.ResultsA total of 75 and 69 multidisciplinary healthcare professionals participated in the 1st and 2nd rounds, respectively. All the strategies reached consensus from D perspective and 58.1% from P perspective. Secondary prevention strategies identified as not widespread and requiring improvement, but with low probability of implementation, were (% of agreement): clinical report standardization (C:8.0%, D:93.3%, P:33.3%), PC-hospital communication via case manager (C:8.0%, D:92.0%, P:47.8%) or telephone/e-mail (C:13.3% D:85.3% P:47.8%), quality of life questionnaires use (C:9.3%, D:81.3%, P: 18.8%), treatment compliance monitoring (C:13.3%, D:96.0%, P:55.1%), health managers involvement in educational campaigns (C:9.3%, D:92.0%, P:23.2%), treat-to-target strategy application (C:12.0%, D:78.7%, P:53.6%), and social support promotion (C:17.3%, D:90.7%, P:43.5%).ConclusionsA multidisciplinary panel of healthcare experts has reached consensus on the strategies to improve secondary prevention of fragility fractures in Spain. Although all the strategies proposed were considered necessary, some of them are considered difficult to implement in the mid-term. Greatest attention should focus on those strategies with the largest divergences between the D and P perspectives.

***Disclosures: Cristina Carbonell**, Amgen, Rubió, Consultant*

P-683

The Florence Text Messaging System Can Improve Patient Concordance with Osteoporosis Medications and Treatment Plans *Eamonn Brankin[1], Margaret Yates[2], Anne Lickrish[2], Morag Hearty[3], Robin Munro[2]. [1]NHS Lanarkshire Osteoporosis Service / University of Glasgow/ Glasgow Caledonian University, United Kingdom, [2]NHS Lanarkshire Osteoporosis Service, United Kingdom, [3]NHS Lanarkshire Technology Enabled Care Team, United Kingdom

Florence (Flo) is a novel telehealth text messaging service evolving in the UK National Health Service (NHS) which sends patients reminders and health ideas tailored to their individual situation. It was named after Florence Nightingale, the founder of modern nursing practice. The NHS Lanarkshire telehealth monitoring service has been funded by a Scottish Government initiative called Technology Enabled Care which aims to increase the number of people receiving telehealth at home.Health Care professionals can adjust the settings on Flo for each patient, deciding when to send messages, what information is being asked for and how the system should respond. With appropriate patient consent, Flo then sends regular text messages to patients as an aide to help them to monitor their own health, sharing any information sent back by the patient with the health professional managing their care. Patients receive instruction on and leaflets about how the system works.This system was introduced as a pilot to the NHS Lanarkshire Osteoporosis service in autumn 2019 as an aid to medication concordance and to identify those who may therefore benefit from 2nd line treatments. Text questions ascertain if the patient is currently taking their bisphosphonate, if they are taking it correctly on an empty stomach and avoiding other food/medications, if the patient is experiencing any side effects from this and if the patient leaves 4hrs between their weekly bisphosphonate and calcium and vitamin D supplements. It allows for patients to flag and discuss any concerns. It has run over a 9 month period so far.In the first 9 months, so far 95 patients have opted into the system, 37 have not responded and been removed and 83 are in regular touch with the system. 250 e-mails have been generated to/from patients subsequent to their involvement and patient care updated as required. Appropriately identified patients are referred for an updated DEXA scan then review by an osteoporosis nurse specialist or physician and alternative therapy offered as required. By adding in this text facility to the fracture liaison service (FLS) we have improved medication concordance, improved communication with patients otherwise currently disengaged from the service and offered them further opportunities to discuss their disease and treatment and with improvements in appropriately taken treatment, reduced their risk of further fragility fracture in a more patient centred way.

***Disclosures: Eamonn Brankin**, None*

P-684

Clinical Utility of Trabecular Bone Score (TBS) *Stuart Silverman[1], Alan Chien[2]. [1]Cedars-Sinai Medical Center, David Geffen School of Medicine at UCLA, OMC Clinical Research Center, United States, [2]OMC Clinical Research Center, United States

Purpose: The Trabecular Bone Score or TBS is a clinical risk factor for fracture, which is partially independent of areal bone density (aBMD) at the lumbar spine/proximal femur, and the FRAX® algorithm. We assessed the clinical utility of TBS in determining osteoporosis (OP) treatment in a retrospective chart review. Methods: We performed a retrospective chart review on 100 consecutive patients seen 2018 and 2019 for whom FRAX and trabecular bone score (TBS) was ordered in a bone clinic with institutional affiliation. The mean age was 64 years old. Nineteen of the 100 patients were male. We recorded indications for TBS use, BMD of spine and hip, FRAX score before and after TBS adjustment, and patient willingness to take medication for osteoporosis after discussion of the TBS adjusted FRAX score with a clinician. Results: TBS was ordered for one of five reasons: 21% of the orders were to decide if therapy was needed, 60% to help choose an appropriate therapy (anabolic or antiresorptive), 10% to optimize bone health prior to surgery, 2% to explain a fracture in the setting of normal bone density, and 7% to decide if medications should be continued by comparing TBS scores to baseline. Twenty-one percent of patients had a TBS score in the top third (TBS>=1.3), 41% of the patients in the middle third (1.2<TBS<1.3), and 38% of patients in the bottom third (TBS<=1.2). Of the patients with TBS in the top third, 43% (9/21) did not receive therapy. Nineteen percent (4/21) received an oral bisphosphonate. Of the patients with TBS in the bottom third, 47% (18/38) of patients received an anabolic. In this group, 11% (4/38) of patients deferred starting osteoporosis therapy. Conclusion: TBS may have clinical utility for an osteoporosis clinician to help choose a therapy, decide whether a therapy is needed, or optimize bone health. Some patients, at high risk of fracture by FRAX with a TBS in the bottom third, were still not willing to take OP medication. These patients,

despite being informed about their OP risk, chose to defer OP therapy. We recognize patients may choose to defer therapies based on their perception of risks and benefits. While TBS risk information is understood by clinicians, it is not clear how well it is understood by patients. Further prospective research is needed to fully understand whether TBS information increases osteoporosis prescription fulfillment and/or adherence.

***Disclosures: Stuart Silverman**, None*

P-685

Improving Access with Nurse-Led Telephone Follow-up after Bisphosphonate Initiation: Saving time and travel *Kathryn Dinh[1], Magdalena Wojtowicz[2], Katherine Wysham[3], Radhika Narla[1]. [1]Division of Metabolism, Endocrinology, and Nutrition, Department of Medicine, University of Washington School of Medicine, United States, [2]Geriatric Research, Education, and Clinical Center (GRECC), Veteran Affairs Puget Sound Health Care System, United States, [3]Department of Rheumatology, Veteran's Affairs Puget Sound Health Care System, United States

Purpose: Veterans Administration's (VA) Puget Sound Health Care System has a multi-disciplinary osteoporosis clinic aimed at fracture prevention, serving all of Washington state. An expanding referral base and aging population has increased demand for tailored bone health care resulting in lengthy wait for new referrals and limited follow-up availability. With the goals of optimizing clinic access, ensuring medication adherence, and decreasing Veteran travel, we implemented a nurse (RN)-led telephone initiative to provide three-month follow-up in place of a physician (MD) visit for patients initiated on a bisphosphonate.Method: Patients started on bisphosphonate therapy from 5/1-12/31/2019 were enrolled for a RN telephone visit in three months and MD follow-up in 12 months. The call assessed adherence to bisphosphonate and prescribed supplements, side effects, new falls, and changes in clinical status. MDs were alerted to patient or RN concerns, and face-to-face visits were scheduled when necessary. Distance Veteran travels to clinic, comorbidities, therapy referrals, and patient reported mobility changes were also recorded.Results: Five patients on alendronate (ALN) and nine patients on zoledronic acid (ZA) had telephone follow-up with the Osteoporosis Clinic RN by 5/1/2020. The patients were majority male (71%) and 93% had Charlson comorbidity index higher than 3 (average 5.1) which was numerically higher in the ZA group (5.7 vs 4.0). Adherence was 100% for ALN and all patients received ZA as prescribed. One patient on ZA had a fracture (11%) and four had new falls (44%); no falls or fractures occurred in those on ALN. MD was alerted to side effects, patient questions, or mobility changes for seven patients (50%) while clinic visits were needed for only three patients (21%), all on ZA. This intervention saved 11 follow-up visits and spared Veterans, on average, $40 USD and 96 minutes in travel. The average call took 17 minutes, ranging from 12-25.Conclusion: In a VA Osteoporosis Clinic, RN-led telephone follow-up at three months for Veterans initiated on a bisphosphonate increased clinic access, identified patients with side effects, new falls or fractures necessitating MD evaluation while allowing for five new consultations and preserving Veteran travel costs. This intervention appears to balance principles of high-quality care delivery, even in patients with significant comorbidities, while improving clinic availability and saving Veteran time.

Table 1: Summary of Veteran demographic, call outcomes, and Veteran travel estimates

	All N=14	Alendronate N=5	Zoledronic Acid N=9
Age (years)	71.5 (57-83)	68.4 (57-77)	73.2 (59-83)
Female Sex	4 (29%)	3 (60%)	1 (11%)
Charlson Comorbidity Index*	5.1 (2-8)	4.0 (2-6)	5.7 (4-8)
Dental Concerns	5 (36%)	1 (20%)	4 (44%)
Falls Identified, self-reported	4 (29%)	0 (0%)	4 (44%)
New Fracture	1 (7.1%)	0 (0%)	1 (11%)
Change in Mobility, self-reported	5 (36%)	0 (0%)	5 (56%)
MD Alerted	7 (50%)	1 (20%)	6 (67%)
MD follow-up needed	4 (29%)	0 (0%)	4 (44%)
Early Appointment Scheduled	3 (21%)	0	3 (33%)
MD follow-up visit saved	11 (78%)	5 (100%)	6 (67%)
Average distance to VA (round trip, miles)	68.4	92.8 (20-186)	54.9 (4-138)
Average cost to VA ($0.58 USD/mile, round trip)**	$ 39.69	$ 53.82 ($11.60-107.88)	$ 31.84 ($2.32-80.04)
Average time to VA, (minutes)	96	122 (36-214)	82 (16-272)
Total miles saved	958	464	494
Total Money saved (USD)	$555.64	$ 269.12	$ 286.52
Total time saved (minutes)	1344	610	734

*Charlson comorbidity Index is a composite score classifying comorbid conditions that alter risk of 10-year mortality

**calculated from the IRS deduction per mile drive in 2019 ($0.58)

***Disclosures: Kathryn Dinh**, None*

P-686

Results of a Multidisciplinary Clinic to Prevent Second Fragility Fracture *Nariman Saba Khazen[1], Miri Steier[2], Ronit Wollstein[3]. [1]Carmel and Lin Medical Center, Haifa, Israel, Israel, [2]Carmel and Lin Medical Center, Israel, [3]NYU School of Medicine, United States

Purpose: Identifying and treating patients with fragility fractures may be effective in prevention of consequent fractures since a first fragility fracture predicts a second fracture. Since fracture liaisons have been shown to be effective in preventing fracture occurrence, a multidisciplinary anti-osteoporotic clinic designed for patients with prior distal radius fragility fractures (DRF) was formed. The purpose of this study was to evaluate the outcome of this clinic. We hypothesized that targeting this early fracture may be effective in prevention of a second fracture.Methods:A retrospective case-control study. Cases included patients treated surgically for a DRF fragility fracture, assigned to a tertiary, multidisciplinary, fracture prevention clinic. Controls constituted a series of similarly treated patients in the same health system that did not attend the clinic. Our main outcome was a second fracture during the follow-up period.Results:Average follow-up period was 42 months in the treated group and 85 months in the untreated group. The treated group was treated significantly more for osteoporosis than the control group. There was one new fracture in the treated group, and 6 new fractures in the control group. Using multivariate analysis, follow-up period was not a significant factor in new fracture occurrence. There was no significant difference in fracture occurrence between the groups.Conclusion:The evidence from this study supports implementation of the multidisciplinary anti-osteoporotic clinic in treating osteoporosis but not in reducing subsequent fractures. Despite a significant difference in treatment, there was no difference in fracture occurrence. Though it is possible that we were underpowered to detect a difference in fracture incidence and that longer follow-up is needed, it is also possible that our treatment is not effective enough.

***Disclosures: Nariman Saba Khazen**, None*

P-687

Extent of and Reasons for Osteoporosis Medication Non-Adherence Among Veterans and Feasibility of a Pilot Text Message Reminder Intervention *Nicole Sagalla[1], Richard Lee[1], Kenneth Lyles[1], Julie Vognsen[2], Cathleen Colón-Emeric[1]. [1]Duke University, United States, [2]Durham VA, United States

Purpose:To evaluate the extent of and reasons for non-adherence to oral bisphosphonates among Veterans and to assess the acceptability and feasibility of a pilot text message reminder application. Methods:We surveyed 105 Veterans initiating oral bisphosphonates for osteoporosis/osteopenia within the prior 18 months utilizing a validated self-report measure adapted for osteoporosis. Additionally, we conducted a pilot text message reminder application for 12 patients who were initiating or were currently non-adherent to oral bisphosphonates. Patients were surveyed on their experience/satisfaction. Medication adherence measured with MPR (medication possession ratio) was an exploratory outcome. Results:Of the 43 (40.9% response rate) completed surveys, the most common reasons for non-adherence were "I forgot" (37.5%), "I had other medications to take" (20.5%), "my bones are not weak" (18.4%), "I felt well" (18.4%), and "I worried about taking them for the rest of my life" (17.9%). Median MPR for the 49 (46.7%) non-adherent (MPR< 0.80) veterans was 0.35 (IQR 0.21-0.64). Of patients offered a weekly automated text message reminder, 12 (50%) accepted. Nine of these 12 patients reported the text message reminders did "very well" at reminding them to take their medication and would recommend the application to other patients/family/friends. The median 6-month MPR for the reminder group was 0.96 (IQR 0.54 – 1.00) and median 3 to 9-month MPR for the comparison group was 0.67 (0.39–1.00), p = 0.50. Conclusion:Half the patients in our sample were taking insufficient doses of oral bisphosphonates to attain the full benefit of fracture risk reduction. Reasons for poor adherence included forgetfulness, polypharmacy, and misconceptions about osteoporosis. A pilot text message reminder intervention targeted to the most commonly cited reason was found to be acceptable and feasible among veterans.

***Disclosures: Nicole Sagalla**, None*

P-688

Treatment with Zoledronic Acid in Patients with Osteoporosis who Have Various Characteristics: Results in 12 months *Yuji Hirano[1], Jyunya Hasegawa[2], Hironobu Kosugiyama[3], Daisuke Kihira[3], Kyosuke Hattori[3]. [1]Rheumatology, Toyohashi Munucipal Hospital, Japan, [2]Rheumatology, Toyohashi Municipal Hospital, Japan, [3]Orthopaedic Surgery, Nagoya University, Japan

Background : Zoledronic acid (ZOL) is an intravenous bisphosphonate administered yearly. Although ZOL was permitted for clinical use to treat osteoporosis (OP) in the United States and Europe in 2006, it was permitted in Japan only in 2016. Hence, data on the efficacy and safety of ZOL in Japanese clinical practice is still insufficient. Patients with OP have various backgrounds, comorbidities, and concomitant drugs. Differences in such characteristics could affect the effect and safety of ZOL. Objectives: The aim of this retrospective study was to investigate the efficacy of ZOL in daily clinical practice in patients with OP who have various characteristics. Methods: This retrospective study included 53 women with OP who were treated with ZOL for >12 months. The time courses of bone mineral density (BMD) in

the lumbar spine (LSBMD) and total hip (THBMD) and of bone turnover markers (BTM) and the frequency of acute phase reaction (APR) were investigated. The patients were classified by disease (OP background; category 1) and by the drug used before ZOL for OP treatment (category 2). In category 1, we compared patients with rheumatoid arthritis (RA) without taking prednisolone (PSL) (RAOP-N), patients with RA taking PSL (RAOP-GC), patients with postmenopausal OP (PMOP), and patients with glucocorticoid-induced OP (GIOP). In category 2, we compared patients with bisphosphonate pretreatment (BP), patients without pretreatment apart from vitamin D (DN), and patients with denosumab pretreatment (DMB). Results: The mean age of all the patients was 72 years, and 43% of them had a history of a previous fracture. The number of patients categorized in each group was as follows: category 1 RAOP-N (n = 23), RAOP-GC (n = 6), PMOP (n = 19), and GIOP (n = 5); category 2 BP (n = 26), DN (n = 19), DMB (n = 7). In all the patients, LSBMD and THBMD increased significantly by +3.8% and +1.1%, respectively, at 12 months, whereas BTM decreased significantly. At 12 months, LSBMD and THBMD increased by +4.9% and +1.9% in RAOP-N, +3.9% and +1.4% in RAOP-GC, +2.8% and +0.0% in PMOP, and +2.3% and +0.4% in GIOP, respectively, in category 1 and by +3.6% and +0.7% in BP, +5.1% and +2.8% in DN, and +0.1% and −2.0% in DMB, respectively, in category 2; most APRs were mild. Conclusions: ZOL was comparatively effective for RAOP-N, PMOP, BP, and DN with respect to LSBMD and for RAOP-N and DN with respect to THBMD. BMD decreased with DMB, and most APRs were mild but frequent.

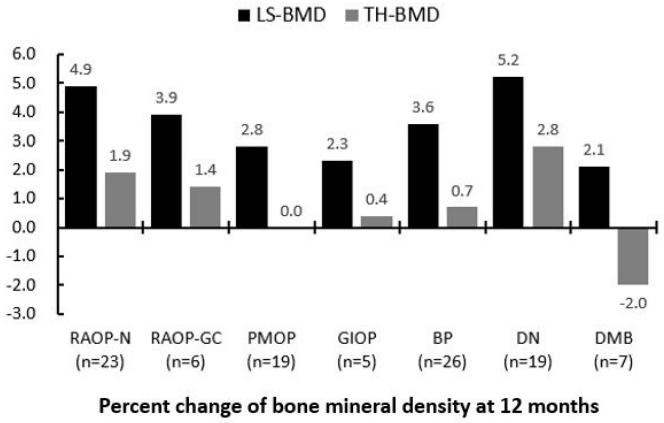

Percent change of bone mineral density at 12 months

***Disclosures: Yuji Hirano**, None*

P-689

Bone metabolism markers change in the initial 4 months after switching from Denosumab to Romozosumab *yoichi kishikwa[1]. [1]kishikawa orthopedic clinic, Japan

Backgrounds Romozosumab(RZMb) is a biological antibody which suppresses Sclerostin. It promotes Wint /β catenin signals, and makes strong bones by means of activating bone formation and suppressing bone resorption. On the other hand, Denosumab(DSMb) has a problem of bone metabolismovershoot when it is discontinued. It has been reported that switching from DSMb to Teriparatide results in a loss of BMD in the femoral neck, a very undesirable affect. To date, there has been no report of the effect on bone metabolism when switching from DSMb to RZMb. Purpose and method In cases where no increase of BMD or incidence of new fractures occurred under administration of DSMb, I chose to switch from DSMb to RZMb in 25 subjects. I compared these 25 subjects to 21 subjects, whom I switched from bisphosphonates(BPs) to RZMb. Subjects were retrospectively observed and statistically demonstrated from the point of bone metabolism markers (TRACP5b, OC, ucOC) and BMD (Femoral neck and total) for 4 months after switching to RZMb. The initial blood samples were taken 6 months after the last administration of DSMb. Results OC, ucOC, ucOC/ OC increased significantly in both groups after 4 months of switching from BPs or DSMb(P<0.001). TRACP5b decreased when switching from BPs (P<0.001), but increased when switching from DSMb(P<0.001). When looking at the data on an individual subject basis, TRACP5b decreased in 2 cases when initial TRACP5 were high above 700 mu/dl although in the other 20 cases it increased when initial TRACP5 were under 500 mu/dl. This phenomenon might mean an overshoot of bone metabolism overrides the original effect of RZMb when DSMb is discontinued. Further careful observation must be needed to investigate how bone metabolism markers change after 12 months when switching from DSMb to RZMb. BMD didn't change significantly in either group after 4 months. It is said that Serum Calcium may drop down no less than 8 mg/ml after 2 weeks upon administration of RZMb. This phenomenon was not observed under concordant use of activated vitamin D in any of these cases. Discussion When switching from DSMb to RZMb, bone formation is activated as OC increased (P<0.001), but bone resorption is activated too as TRACP5b increased DSMb(P<0.001) after 4 months.

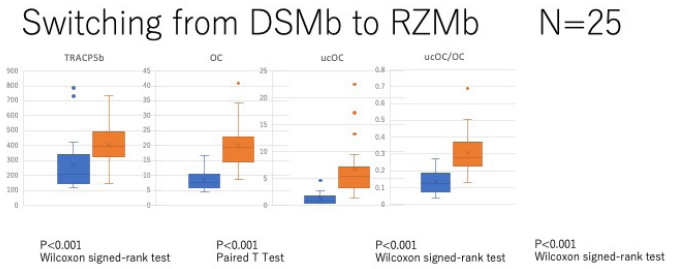

***Disclosures: yoichi kishikwa**, None*

P-690

Pearls for Creating and Sustaining a Successful Fragility Fracture Liaison Program *Susan Williams-Judge[1], Teresa Sherman[1], Julie L. Carkin[1]. [1]University of Washington Northwest, United States

Osteoporosis remains a silent, underappreciated and under-treated disease. One of the most successful ways to break the fragility fracture cycle is to implement fragility fracture liaison programs; yet there are a dearth of programs nationwide, and many programs fail due to a plethora of issues including program costs, personnel retention and recruitment, and addressing critical issues and therapy disconnections in a timely manner.Five years into establishing a successful fragility fracture liaison program, the Strong Bones Program at the University of Washington Medical Center Northwest campus in Seattle, Washington felt it was important to share major pearls that will serve as a basis for implementation and sustainment in creating a successful fragility fracture program regardless of geographic or clinical service boundaries. Information will include the four stages of creating a successful interdisciplinary program, how to avoid common pitfalls and major roadblocks, creating and sustaining a successful, well-balanced inpatient and outpatient referral center at no extra cost to the institution, and with considerable benefit to the aging community in preventing potential future fractures resulting in an improved quality of life.

***Disclosures: Susan Williams-Judge**, None*

P-691

Denosumab (Dmab): Long Inter-Injection Interval (III) without Apparent Adverse Effects *Elliott Schwartz[1], Patricia Schwartz[1], Clinten P. Edmondson[2]. [1]Northern California Institute for Bone Health, Inc., United States, [2]Northern California Institute for bone Health, Inc, United States

Dmab is a fully human monoclonal antibody to the receptor activator of nuclear factor Kβ ligand (RANKL) that inhibits development and activity of osteoclasts. Dmab was approved in the US in 2009 utilizing data from 30 clinical trials and 12,000 subjects.Results of "rebound" phenomena in bone turnover markers (BTM) after discontinuing indicated increased bone resorption (BR), bone loss and VCFxs. At the 6-month mark, BR should return to 45 % of baseline (BSL) from its nadir at 1 month. Subsequently, reports of a "crisis" or "gap" in treatment of OP became prominent. Patients were concerned with increased AEs where decrease in bone turnover (BTO) may play a role. In order to monitor BTO more closely, we began a program consisting of BSL BTM, BTM 1 month post-injection (post-Prolia lab), BTM at 6 months post -injection (pre-Prolia lab) and BTM at subsequent 3 month intervals if the patient was deemed "not ready" for their next dose by the 45 % "rule." We followed 17 patients who, because of different issues (persistent decrease in BTM, dental work, non-compliance, etc.) had long III (shortest 11 months, longest 56 months). No VCFxs occurred monitored by VFA or other imaging.Additional risk factors for the occurrence or non-occurrence of VCFxs after Dmab discontinuation need to be explored and may include persistent decrease in BTM.

***Disclosures: Elliott Schwartz**, None*

P-692

Molecular and cellular analyses of BMP-dependent coupling signals between osteoclasts and osteoblasts during bone remodeling *Maiko Omi[1], Laura Ortinau[2], Dongsu Park[0], Yuji Mishina[1]. [1]Department of Biologic and Materials Sciences & Prosthodontics, University of Michigan School of Dentistry, United States, [2]Department of Molecular Human Genetics, Baylor College of Medicine, United States, [0]Department of Molecular Human Genetics, Baylor College of Medicine, United States

The balance between bone resorption and bone formation is regulated by a mechanism called coupling that includes communication between osteoclasts (OCLs) and osteoblasts (OBs). We reported that OCL-specific disruption of a BMP receptor encoded by Bmpr1a (Bmpr1afx/fx;Ctsk-Cre) leads to increased bone mass associated with increased bone formation. In vitro studies have shown that conditioned media from Bmpr1a mutant OCLs promote OB mineralization compared to those from control OCLs, while OCLs inhibit OB differentiation in a direct co-culture system, suggesting that OCLs regulate OB activity via two distinct modes. Interestingly, OCLs physically interact with OBs thorough tunneling nanotubes (TNTs), actin-based long cell protrusions, and Bmpr1a mutant OCLs exhibit a decrease in TNT-mediated OCL-to-OB interaction, suggesting that TNT-mediated cellular communication is a downstream event of BMP signaling. In this study, we further investigated how TNT-mediated OCL-to-OB interaction contributes to OB-mediated bone formation both in vitro and in vivo.The in vitro studies showed that (1) OBs co-cultured with OCLs exhibited increased Annexin V expression. In addition, (2) OBs interacted with OCLs via TNTs displayed typical morphological changes of cells undergoing apoptosis, and (3) those OBs highly expressed Bax, a proapoptotic marker, suggesting that OCLs induce OB cell death through TNTs. To address the in vivo function of TNTs, we established an intravital imaging system of mouse calvaria tissues, in which bone marrow cells from Ctsk-Cre/tdTomato mice were transplanted into sublethally irradiated Osteocalcin-GFP mice. Using intravital microscopy, we were able to show that (4) OCLs physically interact with OBs via TNTs in live calvaria. Additionally, (5) OBs interacted with OCLs via TNTs exhibited abnormal cell shape in the fixed femur samples, suggesting that OCLs may regulate cell death of OBs via TNTs.Taken together, our data suggest that OCLs have two distinct functions during bone remodeling; OCLs induce OB cell death via TNTs when and where they resorb bone matrix, while they promote OB activity via secreted factors to initiate subsequent bone formation, which may be important for regulating spatial and temporal coupling of bone formation and bone resorption. Our findings also suggest that those direct and indirect OCL-to-OB interaction are the potential targets of BMP signaling providing new therapeutic opportunities for bone mass-related diseases.

***Disclosures: Maiko Omi**, None*

P-693

Mmp13 deletion in cells of the mesenchymal lineage decreases osteoclast number, increases cortical and trabecular bone mass, and may attenuate the cortical bone loss caused by estrogen deficiency in mice *Filipa Ponte[1], Ha-neui Kim[1], Srividhya Iyer[1], Aaron Warren[1], Li Han[1], Erin Mannen[1], Horacio Gomez-Acevedo[1], Maria Almeida[1], Stavros Manolagas[1]. [1]UAMS, United States

Estrogens attenuate the resorption of trabecular and cortical bone via estrogen receptor alpha (ERα), mediated actions on cells of the hematopoietic and mesenchymal lineages, respectively. To identify estrogen target genes that regulate osteoclast number via actions on cells of the mesenchymal lineage, we performed microarray analysis of GFP-sorted Osx1+ cells without or with ERα, derived from the calvaria of ERαDGFP:Osx1mice or GFP:Osx1-Cre controls. Among 510 up-regulated transcripts in ERα deleted cells (cut off p=0.01) the highest, 9-fold increase, encoded the matrix metalloproteinase 13 (MMP13). The microarray findings were confirmed by qPCR and reproduced in ERα-deleted Prx1 cells derived from the calvaria of ERαDPrx1. Additionally, the protein levels of the active form of MMP13 were 4-fold higher in the BM plasma of ovariectomized C57BL/6J mice, as compared to sham controls. To obtain functional evidence for the role of mesenchymal cell-derived MMP13 in bone resorption we next generated mice with Mmp13 deletion in Prx1 expressing cells (Mmp13DPrx1). Mmp13f/f control littermates and Mmp13DPrx1 mice where either ovariectomized (OVX) or sham-operated at 5 months of age and euthanized 1 month later. Relative Mmp13 mRNA expression in femur shafts of Mmp13DPrx1 mice was decreased by 50-fold, as compared to the controls. Total body and uterine weight were no different, but femur and tibia length was decreased. Cortical thickness at the distal metaphysis and diaphysis, trabecular bone volume and trabecular number and thickness in the femur and tibia, measured by micro-CT, as well as bone strength (yield, ultimate stress and modulus of elasticity) were increased in the sham-operated female Mmp13DPrx1 mice. These phenotypic changes were accompanied by a decrease in osteoclast number, as determined by dynamic histomorphometry of undecalcified endocortical sections. Mineral apposition rate, mineralizing surface, and bone formation rate, on the other hand, were unaffected by the Mmp13 deletion. OVX decreased both femoral and tibia cortical thickness in the control mice and this effect was attenuated in the Mmp13DPrx1 mice; whereas the effect of OVX on cancellous bone was not affected by the Mmp13 deletion. These findings suggest an important role of mesenchymal cell–derived MMP13 on osteoclast number, bone resorption, and bone mass; as well as a contributory role in the cortical, but not trabecular, bone loss caused by estrogen deficiency.

***Disclosures: Filipa Ponte**, None*

P-694

Stem Cell Marker and Wnt-associated Protein Lgr6 is Dispensable for Development and Intramembranous Bone Formation but Required for Endochondral Fracture Healing *Laura Doherty[1], Daniel Youngstrom[1], Sanja Novak[1], Kurt Hankenson[2], Ivo Kalajzic[1], Archana Sanjay[1]. [1]UConn Health, United States, [2]University of Michigan, United States

Because of its essential role in osteoblast function, the Wnt pathway is a current target of clinical trials to treat bone diseases including osteoporosis. Leucine-rich repeat-containing G protein-coupled receptor 6 (Lgr6) potentiates Wnt signaling and has been identified as a putative osteochondral stem cell marker in vitro and in vivo. However, its function in the context of fracture healing is undefined. Hypothesizing a requirement for Lgr6 in bone regeneration, we ablated endogenous Lgr6 expression using homozygous knock-in Lgr6EGFP-ires-CreERT2 mice (Lgr6-null). In contrast to Lgr5-null and Lgr4-null mice, which exhibit severe skeletal abnormalities and neonatal lethality, Lgr6-null mice develop normally with no overt skeletal phenotype. We performed femoral fractures in Lgr6-null mice and wild-type controls, and analyzed the calluses at 14 and 28 days post-fracture. Lgr6-null mice experience significant delays in mineralization during repair. While overall callus size at 14 days post-fracture is comparable among groups, Lgr6-null bones have significantly reduced callus bone volume relative to controls (46% reduction in BV/TV, p=0.038). The calluses are characterized by large unmineralized voids shown by μCT, and retain significant amounts of cartilage as shown by safranin O staining, suggesting a defect in endochondral bone healing. 28 days post-fracture, Lgr6-null calluses display aberrant morphology compared to controls, with significantly higher retained callus volume (115% larger callus TV, p=0.033), and fewer, thinner areas of newly formed cortical bone. Periosteal progenitors isolated from Lgr6-null mice show significant delays in in vitro mineralization compared to controls following 21 days of exposure to differentiation media, further validating in vivo results. To understand the role of Lgr6 in intramembranous ossification as opposed to endochondral ossification, we performed bone marrow ablation studies, and analyzed the intramedullary femur 7 days post-injury. Strikingly, Lgr6-null mice regenerate significantly more trabecular bone following marrow ablation compared to controls (158% increased BV/TV 7 days post-ablation, p=0.003). Our results suggest that Lgr6 is an essential, yet context-specific, component of skeletal regeneration. Its divergent function in endochondral and intramembranous bone formation, including cellular and molecular mechanisms within the broader context of Wnt signaling, are the subject of ongoing investigation.

***Disclosures: Laura Doherty**, None*

P-695

Role of Sfrp4-dependent Non-canonical Wnt Regulation in Bone Repair and Regeneration *Chiho Ahn[1], Ruiying Chen[1], Kun Chen[1], Shawn Berry[1], Roland Baron[2], Francesca Gori[1]. [1]Division of Bone and Mineral Research, Harvard Medical School and Harvard School of Dental Medicine. Department of Oral Medicine, Infection and Immunity, Harvard School of Dental Medicine., United States, [2]Division of Bone and Mineral Research, Harvard Medical School and Harvard School of Dental Medicine. Department of Oral Medicine, Infection and Immunity, Harvard School of Dental Medicine. Endocrine Unit, Massachusetts General Hospital., United States

Sfrp4 (Secreted Frizzled Receptor Protein 4) functions as a decoy receptor for the Wnt ligands and, differently from other well-known Wnt antagonists, such as sclerostin (Sost) that binds to Lrp5/Lrp6 and block canonical (c)Wnt signaling, Sfrp4 suppresses both cWnt and non-cWnt cascades. Loss of function mutations in SFRP4 are the cause of Pyle's disease, a rare skeletal disease that leads to limb deformity and fragility fractures. Sfrp4 deletion in mice causes skeletal deformities closely mimicking those seen in individuals with Pyle's disease: long bones with wide metaphyses, increased trabecularization and thin cortex. Using these mice, we uncovered that cortical thinning is due to decreased periosteal bone formation as well as uncoupled remodeling on the endosteal surface, largely due to the activation of the non-cWnt/Jnk cascade. Given that the periosteum contains a niche of stem cells which contributes to the response to injury to support new bone formation, we asked whether activation of both cWnt and non-cWnt signaling (Sfrp4-/- mice) may alter bone repair and regeneration. To this end, we created both calvarial critical-sized defects (which don't heal spontaneously) and subcritical-sized defects (which heal spontaneously). We used Sost-/- mice as a model for cWnt signaling activation. We demonstrated that while cWnt signaling is equally activated in calvarial bones of Sost-/- and Sfrp4-/- mice, the non-cWnt cascade is activated only in Sfrp4-/- calvarial bones. Confirming previous findings, activation of cWnt signaling (Sost deletion) favors bone regeneration (measured as BV/TV%) within the initial critical defect (14%+1.7 in wt vs 29%+12.4 in Sost-/- mice, p<0.01) 6 wk after surgery. In contrast, deletion of Sfrp4 did not (13%+1.1 in wt vs 13.1%+0.44 in Sfrp4-/- mice, NS). In the subcritical defects, while activation of cWnt signaling (Sost-/- mice) led to accelerated bone regeneration (38.3%+7.7 in wt vs 57.5%+3 in Sost-/- mice, p<0.05), Sfrp4-/- mice showed only a response similar to wt mice (31.5%+2 in wt vs 31.2%+2.3 in Sfrp4-/- mice, NS). These findings demonstrate once again how Wnt signaling fine-tuning is critical to achieve proper bone responses. Given that activation of cWnt signaling in the calvaria is similar in both Sost and Sfrp4 null mice, we hypothesize that activation of non-cWnt signaling might be responsible for improper function of stem cells within the sutures and/or progenitors in the periosteum.

***Disclosures: Chiho Ahn**, None*

Posters

P-696

Interleukin-6 Trans Signaling Enhances the Chondrogenic Response of Human Bone Marrow Stromal Cells to Bone Morphogenetic Proteins

*Landon Gatrell[1], Hong Wu[1], Elisabeth Ferreira[2], Ryan Porter[2]. [1]University of Arkansas for Medical Sciences, Department of Internal Medicine, United States, [2]University of Arkansas for Medical Sciences, Departments of Internal Medicine and Orthopaedic Surgery, United States

Bone fractures typically heal through endochondral ossification, involving formation and remodeling of a cartilaginous callus. For larger defects, this endochondral repair pathway is compromised. Preclinical studies have demonstrated that cartilage templates engineered in vitro from bone marrow-derived mesenchymal stem/stromal cells (BMSCs) can stimulate the repair of large bone defects. Directing BMSC chondrogenesis within the bone injury site would be a more practical alternative to tissue engineering; however, pro-inflammatory cytokines upregulated in response to skeletal injury have been shown to inhibit BMSC chondrogenesis induced by transforming growth factor (TGF)-β. Less has been reported about chondroinduction by BMPs, which have distinct potency on BMSCs compared to the TGF-β isoforms. When screening pro-inflammatory cytokines for their impact on BMSC chondrogenesis using a differentiation-conditional luciferase reporter, interleukin (IL)-6 was observed to enhance reporter activity in response to BMPs, in contrast to the other cytokines tested. This effect required co-stimulation with the soluble IL-6 receptor (i.e., trans signaling), though sIL-6R had negligible independent effects. IL-6 trans signaling enhanced proteoglycan deposition and chondrogenic gene expression stimulated by BMPs -2, -4, and -7, but not TGF-β1. Cell sorting demonstrated that the CD146-positive subpopulation of BMSCs was responsive to IL-6 enhancement of BMP-induced chondrogenesis. Gene expression analysis of the TGF-β superfamily and related signaling mediators revealed minimal effects of IL-6/sIL-6R – as opposed to IL-1β challenge. Instead, members of the Wnt signaling pathway were differentially expressed by IL-6 trans signaling in a pattern suggesting enhanced canonical Wnt signaling. These data demonstrate that the pro-inflammatory cytokines are not uniformly refractory to BMSC chondrogenesis; rather, IL-6 through a trans signaling pathway can potently enhance their chondroinductive response to multiple bone morphogenetic proteins known to promote endochondral bone formation.

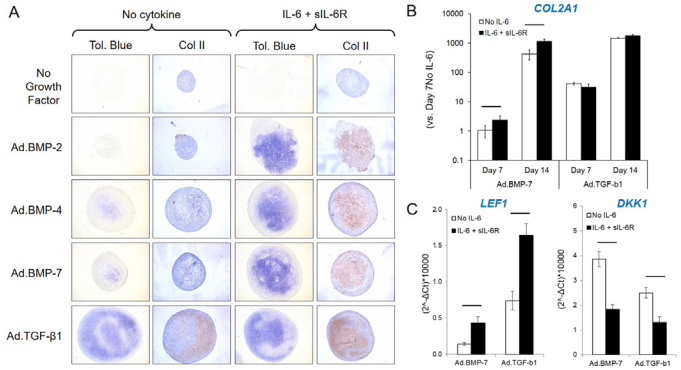

Figure 1. IL-6 trans signaling enhances BMSC chondrogenesis induced by BMPs but not TGF-β1. (A) Toluidine Blue staining or type II collagen immunostaining of human BMSC aggregates after 28 days in culture. (B) Fold induction in *COL2A1* expression (log scale) within BMSC pellets after 7 or 14 days in culture. (C) Relative *LEF1* or *DKK1* expression in BMSC pellets after 4 days in culture. Horizontal lines indicate p<0.05 for comparison of means by two-tailed t-test.

***Disclosures: Landon Gatrell**, None*

P-697

PDGF Regulation of BMP2-Mediated Osteogenesis

*Josip Madunic[1], Laura Shum[1], MIlan Vucetic[1], Sanja Novak[1], Ivo Kalajzic[1]. [1]UConn Health, United States

Bone healing consists of complex cell interactions regulated by growth factors. Recombinant BMP2 is used in orthopedic treatments to induce bone formation. However, the supraphysiological doses used can cause serious side-effects. PDGF, a mitogenic growth factor highly expressed during bone healing, has also been used to induce bone formation in some clinical applications. Despite the individual abilities of PDGF and BMP2 to induce bone, our previous work showed that PDGF inhibits BMP2-induced osteogenesis in periosteal progenitor cells in vitro. The purpose of the current study was to determine the in vivo role of PDGF on BMP2-mediated osteogenesis. We used critical-sized long bone defects in αSMA9/Col2.3GFP transgenic mice. These mice express the red reporter tdTomato in αSMA+ mesenchymal progenitor cells allowing for analysis of progenitor expansion. Col2.3GFP is expressed in mature osteoblasts and is an indicator of osteogenesis. Critical-sized femoral defects (3 mm) stabilized by external fixation were made in 5-month-old male mice. Growth factors PDGF-BB (2 μg) and BMP2 (0.5 μg or 5 μg), individually or in combination, were applied on the collagen-based material "Infuse" in the defect. αSMA-driven Cre activity was induced by injecting tamoxifen. We assessed defect healing at 2 and 9 weeks using histological analyses. μCT-based morphometry was quantified 9 weeks after defect surgeries. We observed expansion of αSMA+ progenitor cells into the defect following BMP2 treatment and a more pronounced effect with the higher dose. This effect was significantly decreased when the higher dose of BMP2 was combined with PDGF, as quantified by αSMA+ area ($p<0.01$). At 9 weeks of healing, PDGF and BMP2 individually stimulated osteoblast differentiation, as evidenced by the increase in Col2.3GFP signal corresponding to the areas of new bone formation. However, these effects were inhibited when the growth factors were combined. Although 5 μg BMP2 had biggest impact on bone bridging and bone volume within the defect area, PDGF treatment alone also increased bone volume. Furthermore, μCT data showed that PDGF had inhibited BMP2-induced bone formation, demonstrated by the decrease in bone volume in the defect area ($p<0.01$). Our in vivo data shows evidence that individual treatments by BMP2 and PDGF-BB induced bone formation, while PDGF exerted negative effects on the osteogenic action of BMP2.

***Disclosures: Josip Madunic**, None*

P-698

ENDOTHELIAL CELL PHYSIOLOGY IN A MICROFLUIDIC DEVICE AND THEIR RESPONSE TO MESENCHYMAL STROMAL CELLS

*Shuang Zhang[1], Bastiaan Tuk[2], Marijke Koedam[1], Pouyan E. Boukany[3], Georg Pesch[3], Gert-Jan Kremers[4], Johan W. van Neck[2], Johannes P.T.M. van Leeuwen[1], Bram C.J. van der Eerden[1]. [1]Internal Medicine, Erasmus University Medical Center, Netherlands, [2]Plastic and Reconstructive Surgery, Erasmus University Medical Center, Netherlands, [3]Chemical Engineering, Delft University of Technology, Netherlands, [4]Optical Imaging Center, Erasmus University Medical Center, Netherlands

Introduction: Fracture healing involves a complex sequence of physiological events. A functional vascular system is a prerequisite for bone repair as disturbed angiogenesis often causes nonunions. Paracrine factors derived from bone mesenchymal stromal cells have angiogenic effects on endothelial cells. However, whether this paracrine step participates in blood flow dynamics within bone capillaries remains poorly understood.Objective: Study the effect of human bone marrow-derived mesenchymal stromal cells (hBMSCs) secretome on endothelial cell behaviour in blood capillary physiology-mimicking microfluidic models. Methods: Conditioned medium was collected from hypoxic hBMSCs (hBMSC-CM), and cytokines were detected by angiogenic protein array. The effect of hBMSC-CM on endothelial cell proliferation (Ki-67 immunostaining) was monitored in a microfluidic model under physiological shear stress. A second microfluidic wound-healing model was generated to mimic endothelial cell disruption following injury-induced hypoxia. Differently sized fluorescence-labelled dextrans were used to mimic chemotactics of proteins in the hBMSC-CM. By analyzing wound healing over time, the mechanotactic effect of shear stress and chemotactic effects of hBMSCs on endothelial cell migration were evaluated.Results: Different angiogenic-related factors including platelet-derived growth factor (PDGF-BB; 10-fold) and vascular endothelial growth factor (VEGF; 15-fold), were elevated in hBMSC-CM versus control medium. hBMSC-CM introduction in the microfluidic single channel model induced endothelial cell proliferation (2-fold) as assessed by ki67 staining and cell number counts. In the microfluidic-based endothelium rupture model, a wound was generated by introducing three parallel fluid streams in the channel, of which the middle one contained the protease trypsin. A stable diffusion gradient of differently sized dextrans was measured in the channel implicating that chemotactics takes place in the model. Indeed, hBMSC-CM infusion at physiologically relevant shear stress-inducing flow rates increased the endothelial cell migration rate (1.5-fold) versus control medium.Conclusion: Trophic factors released by hBMSCs enhanced angiogenic properties in microfluidic models mimicking endothelial cell physiology including injury, hypoxia, shear stress and chemotaxis. This platform provides a novel in vivo-like microenvironmental approach to study fracture healing-related processes.

***Disclosures: Shuang Zhang**, None*

P-699

Muscle-derived lumican stimulates bone formation via integrin α2β1 and the downstream ERK signal

*Jin Young Lee[1], So Jeong Park[1], Da Ae Kim[1], Beom-Jun Kim[2]. [1]Asan Institute for Life Sciences, Asan Medical Center, University of Ulsan College of Medicine, Republic of Korea, [2]Division of Endocrinology and Metabolism, Asan Medical Center, University of Ulsan College of Medicine, Republic of Korea

Skeletal muscle and bone are highly interrelated, and previous proteomic analyses suggest that lumican is one of muscle-derived factors. To further understand the role of lumican as a myokine affecting adjacent bone metabolism, we investigated the effects of lumican on osteoblast biology. Lumican expression was significantly higher in the cell lysates and conditioned media (CM) of myotubes than those of undifferentiated myoblasts, and the known anabolic effects of myotube CM on osteoblasts were reduced by excluding lumican from the CM. Lumican stimulated preosteoblast viability and differentiation, resulting in increased calvaria bone formation. The expression of osteoblast differentiation markers was consistently increased by lumican. Lumican increased the phosphorylation of ERK, whereas ERK inhibitors completely reversed lumican-mediated stimulation of Runx2 and ALP activities in osteoblasts. Results of a binding ELISA experiment in osteoblasts show that transmembrane integrin α2β1 directly interacted with lumican; and an integrin α2β1 inhibitor attenuated the stimulation of ERK and ALP activities by lumican. Taken together, the results indicate that

muscle-derived lumican stimulates bone formation via integrin α2β1 and the downstream ERK signal, indicating that this is a potential therapeutic target for metabolic bone diseases.

***Disclosures: Jin Young Lee**, None*

P-700

Fluoxetine Exposure during the Peripartal Period Has Sex-Specific Impacts on Adult Bone Health in Mice *Hannah Fricke[1], Chandler Krajco[1], Celeste Sheftel[1], Julia Charles[2], Laura Hernandez[1]. [1]University of Wisconsin - Madison, Department of Animal and Dairy Sciences, United States, [2]Harvard Medical School, Department of Orthopedic Surgery, United States

Selective serotonin reuptake inhibitors (SSRIs) are the most commonly prescribed class of antidepressants during pregnancy and lactation. SSRIs decrease bone mineral density (BMD) across all ages and sexes. Lactation is also characterized by increased bone resorption to mobilize calcium and achieves this via a serotonin-induced hormonal cascade. This serotonin-mediated bone loss is normally restored after weaning but is persistent when an SSRI is administered during the peripartum period. Previous research in our lab has shown that peripartal fluoxetine (FLX) exposure is associated with increased serum serotonin content, decreased femoral length, lower BMD, and lower trabecular bone volume/tissue volume (BV/TV) in the exposed offspring at weaning. We hypothesize that peripartal FLX exposure has a negative impact on long bone growth and BMD that persists into adulthood. Female C57BL/6J between 6-8 weeks of age were randomized to receive the SSRI fluoxetine hydrochloride (20 mg/kg) or saline daily via intraperitoneal (IP) injection from the beginning of pregnancy (E0) through the end of lactation (D21). At weaning, the offspring were then separated into the following groups: Saline-exposed female (SF) and male (SM) and FLX-exposed female (FF) and male (FM). Dual-energy X-ray absorptiometry (DEXA) was used to measure a baseline BMD at 6 weeks of age, and a baseline weight was taken as well. BMD was measured periodically, and daily weights were taken until 12 weeks of age. At 12 weeks, all groups were euthanized, and the femurs were collected for gene expression analysis via RT-PCR. The total body BMD of the FM group was significantly lower than SM across the treatment period ($p=0.0119$), but there was no difference between the SF and FF ($p=0.4991$) groups. There was an increase in the ratio of gene expression between RANKL and OPG in the FLX groups ($p=0.0287$) and an increase in RANK expression in FM compared to SM ($p=0.0364$). There was no difference in weight gain between 6 and 12 weeks of age between the SF and FF ($p=0.8699$) groups or the SM and FM ($p>0.9999$) groups. Bone microarchitecture will be measured via micro-computed tomography (micro CT) to further analyze the impact of developmental FLX exposure. We conclude that peripartum FLX exposure has a sex-dependent impact on adult bone health in mice.

***Disclosures: Hannah Fricke**, None*

P-701

Effects of Peripartal Sertraline on Maternal and Fetal Bone Health *Celeste M. Sheftel[1], Luma C. Sartori[1], Robbie Manuel[1], Hannah Fricke[1], Julia Charles[2], Laura L. Hernandez[1]. [1]University of Wisconsin-Madison, United States, [2]Harvard Medical School, United States

Lactation is taxing on mothers' bone health, causing them to lose up to 10% of their bone mass to supply milk calcium. Selective serotonin reuptake inhibitor antidepressants (SSRIs) are commonly used during pregnancy and lactation but decrease maternal bone mass independent of lactation. We have previously demonstrated that both maternal and offspring bone densities were compromised by maternal treatment with the SSRI fluoxetine throughout pregnancy and lactation.In this study, we examined whether sertraline would similarly compromise maternal and offspring bone like observations with treatments of fluoxetine. Female C57BL/6 dams (n=20/group) were treated with sertraline (10mg/kg/d) or a vehicle (DMSO) from pregnancy day 1 through 21 (weaning). Pups were euthanized at weaning. Dams were euthanized at weaning (n=10/group) or three months post-weaning (n=10/group) for analysis.Compared to control, sertraline treatment reduced the expression of parathyroid hormone related protein, ($p<0.1$), and the calcium transport proteins Orai1 and Serca2 ($p<0.05$) in the mammary gland at weaning. However, circulating calcium was not altered during lactation in either group. Circulating procollagen type I N-terminal propeptide, a marker of bone formation, was not altered in sertraline-treated dams on the first day of lactation or at weaning, contrary to results observed due to fluoxetine treatment. Sertraline treatment altered gene expression in maternal femoral bone, with a tendency towards increased Mmp13 expression at weaning ($p<0.1$), and an increase in Mcp1, a bone resorption gene, at three months postpartum ($p<0.05$); however, no other bone resorption or formation marker was affected at either timepoint. Circulating calcium was similarly unaffected in the pups at weaning, suggesting an adequate supply of calcium in the milk from the dam. In utero exposure to sertraline reduced litter size (5.4 vs 6.8 pups/dam, $p<0.01$) and increased pup mortality (20% vs 5% dead pups/litter, $p<0.01$) during the first 24 hours postpartum compared with controls.These data suggest that sertraline has a milder impact on maternal bone and calcium trafficking than fluoxetine but may induce a failure to thrive in the offspring. Bones will be analyzed by micro-computed tomography to measure sertraline-mediated changes to maternal bone microarchitecture at weaning and 3 months post-weaning in the dams and in the offspring at weaning.

***Disclosures: Celeste M. Sheftel**, None*

P-702

Very low doses of sclerostin and Dkk1 neutralizing antibody are strongly anabolic if administered at the optimal ratio *Roy Choi[1], Alexander Robling[1]. [1]Indiana University School of Medicine, United States

Sclerostin is an attractive target for targeted bone therapies due to its selectivity to bone cells and its prominent effects on bone mass. Recently, sclerostin antibody(Evenity™) was approved for clinical use in the US to treat bone disorders. Curiously, targeting other Wnt inhibitors such as Dkk1 fails to induce significant osteoanabolic response. However, Dkk1 antibody(Dkk1-mAb) is highly osteoanabolic in Sost KO mice, suggesting that Sost might restrain the otherwise anabolic action of Dkk1 inhibition. Moreover, co-treatment of both sclerostin antibody(Scl-mAb) and Dkk1-mAb showed synergistic osteoanabolic action, where the anabolic response was greater than either, Scl-mAb or Dkk1-mAb alone, and well beyond additive effects. The strength of the response promoted us to explore whether the proportions of Scl-mAb and Dkk1-mAb could be optimized to elicit maximal osteoanabolic activity. At a previous ASBMR meeting, we presented that a 3:1 ratio was found to be the optimal formulation. In the current experiments, we sought to determine the minimal total dose of 3:1 antibody treatment that could maintain equal efficay as the Scl-mAb alone at 25mg/kg, or 25,19,12, or 6mg/kg of 3:1 antibody mixture. The 25mg/kg 3:1 mixture was able to generate significantly increased cancellous properties in the both distal femur and lumbar spine compared to 25mg/kg Scl-mAb alone, with stepwise reduction according to total dose. However, the loweset 3:1 dose (6.2mg/kg), was able to generate similar bone anabolic action as the 25mg/kg Scl-mAb alone group, at roughly one quarter of the total dose. In conclusion, the optimal 3:1 ratio of Scl-mAb and Dkk1-mAb can significantly increase cancellous bone properties and provide equal anabolic action as 4X the amount of Scl-mAb alone.

***Disclosures: Roy Choi**, None*

P-703

Prophylactic treatment of rapamycin ameliorates naturally developing and episode - induced heterotopic ossification in mice expressing human mutant ACVR1 *Hirotsugu Maekawa[1], Shunsuke Kawai[1], Sanae Nagata[1], Nishio Megumi[2], Yonghui Jin[2], Hiroyuki Yoshitomi[3], Shuichi Matsuda[3], Junya Toguchida[1]. [1]Department of Cell Growth and Differentiation, Center for iPS Cell Research and Application, Kyoto University, Japan, [2]Department of Regeneration Sciences and Engineering, Institute for Frontier Life and Medical Sciences, Kyoto University, Japan, [3]Department of Orthopaedic Surgery, Graduate School of Medicine, Kyoto University, Japan

Fibrodysplasia ossificans progressiva (FOP) is a rare autosomal-dominant disease characterized by heterotopic ossification (HO) in soft tissues and caused by a mutation of the ACVR1A/ALK2 gene, which encodes a type I receptor for bone morphogenetic protein (BMP). Activin-A is a key molecule for initiating the process of HO via the activation of mTOR, while rapamycin, an mTOR inhibitor, effectively inhibits the Activin-A-induced HO. However, few reports have verified the effect of rapamycin on FOP in clinical perspectives.We investigated the effect of rapamycin for different clinical situations by using mice conditionally expressing human mutant ACVR1A/ALK2 gene (FOP-ACVR1 mice). We also compared the effect of rapamycin between early and episode-initiated treatments for each situation.First of all, we investigated the effect of rapamycin on spontaneous HO which developed without any known triggers in FOP-ACVR1 mice. Continuous, episode-independent administration of rapamycin reduced the incidence and severity of HO in the natural course of FOP-ACVR1 mice. In addition, rapamycin also improved the survival rate of FOP-ACVR1 mice during observation period.Next, we evaluated the effect of rapamycin on HO induced by a physical skeletal muscle damage in FOP-ACVR1 mice. To imitate the clinical situation, FOP-ACVR1 mice received pinch-injury to lower hindlimbs. Pinch-injury induced HO in FOP-ACVR1 mice not only at the injured sites, but also in the contralateral limbs and provoked a prolonged production of Activin-A in inflammatory cells. Although both early and injury-initiated treatment of rapamycin suppressed HO in the injured sites, the former was more effective at preventing HO in the contralateral limbs. In addition, we confirmed that rapamycin suppressed infiltration of inflammatory cell at the injured site in the inflammatory stage of HO.Finally, we investigated whether rapamycin can suppress the recurrent HO formation after resection. Rapamycin was also effective at reducing the volume of recurrent HO after the surgical resection of injury-induced HO, for which the early treatment was more effective.Our study suggested that rapamycin inhibit HO formation not only at chondrogenic stage but also at inflammatory stage and prophylactic treatment will be a choice of method for the clinical application of rapamycin for FOP.

***Disclosures: Hirotsugu Maekawa**, None*

P-704

Small molecule inhibition of TGFβ-activated kinase (TAK1) results in reduced heterotopic ossification *Amy Strong[1], Philip Spreadborough[2], Chase Pagani[1], Ryan Haskins[2], Devaveena Dey[2], Patrick Grimm[2], Keiko Kaneko[1], Simone Marini[1], Amanda Huber[1], Charles Hwang[1], Kenneth Westover[3], Yuji Mishina[1], Matthew Bradley[4], Benjamin Levi[1], Thomas Davis[4]. [1]University of Michigan, United States, [2]Uniformed Services University of the Health Sciences, United States, [3]University of Texas Southwestern Medical Center, United States, [4]Uniformed Services University of the Health Sciences, United States

Heterotopic ossification (HO) is defined as ectopic bone formation around joints and in soft tissue following trauma, particularly blast-related extremity injury or thermal injury, or following orthopedic surgery or neurological injury, leading to increased pain and diminished quality of life. Current treatment options include non-steroidal anti-inflammatory drugs, radiotherapy, or surgical excision, but these treatments have limited efficacy and have associated complication profiles. In contrast, small molecule inhibitors have been shown to have more favorable specificity and less systemic cytotoxicity. Previous studies have shown that downstream non-canonical BMP signaling of TGF-β activated kinase-1 (TAK1) contributes to HO. In the current study, small molecule inhibition of TAK1 (NG-25) was evaluated for its efficacy in limiting ectopic bone formation following a rat blast lower extremity injury model and a murine burn tenotomy injury model. A significant decrease in total HO volume in the rat blast injury model was observed by microCT, with no systemic complications following NG-25 therapy. Furthermore, rat tissue-resident mesenchymal progenitor cells (MPCs) harvested from animals treated with NG-25 demonstrated decreased proliferation, osteogenic differentiation capacity, and reduced gene expression of Tac1, Col10a1, Ibsp, Smad3, and Sox2. Single cell RNA-sequencing of murine cells harvested from the injury site in a burn tenotomy injury model showed increased expression of these genes in murine MPC during stages of chondrogenic differentiation. Additional in vitro cell cultures of murine tissue-resident MPCs and osteochondrogenic progenitor cells (OCPs) treated with NG-25 demonstrated reduced chondrogenic differentiation by 10.2-fold and 133.3-fold, respectively as well as associated reduction in chondrogenic gene expression. Induction of HO in Tak1 knockout mice demonstrated a 7.1-fold and 2.7-fold reduction in chondrogenic differentiation in murine MPCs and OCPs, respectively, with reduced chondrogenic gene expression. Together, our in vivo models and in vitro cell culture studies demonstrate the importance of TAK1 signaling in chondrogenic differentiation and HO formation and suggest that small molecule inhibition of TAK1 is a promising therapy to limit the formation and progression of HO.

***Disclosures: Amy Strong**, None*

P-705

Nerve modulation therapy: targeting galectin-1 expression from dorsal root ganglia alleviates osteoarthritis *Jingtian Mei[1], Feng Zhou[1], Hanjun Li[1], Tingting Tang[1]. [1]Shanghai Key Laboratory of Orthopaedic Implants, Department of Orthopaedic Surgery, Shanghai Ninth People's Hospital, Shanghai Jiao Tong University School of Medicine, Shanghai, PR China, China

Osteoarthritis (OA) is the most common and debilitating type of arthritis, causing a large societal and economic burden. During OA development, all joint components are affected, resulting in significant subchondral bone remodelling and osteochondral neovascularisation that occur prior to articular cartilage degeneration [1]. In this process, pathological sensory nerve sensitation and its innervation into normally aneural tissues mostly causes pain. Tanezumab, the β nerve growth factor (β NGF) targeting drug, has been proven efficaciously in reducing pain for OA patients, while data demonstrated increased incident of rapidly progressive OA (RPOA) with dose and duration [2]. It suggests the significant role of peripheral nerve in the progression of OA. In addition, sensory nerves of dorsal root ganglia (DRG) in OA innervating into bone and synovium mediate joint pain and may affect other joint components by secreting neurotrophic factor. Here, RNA-Seq screened out the up-regulated Galectin-1 (Gal-1) in primary DRG cells within inflammatory environment. We found that DRG-derived Gal-1 promoted angiogenesis and osteoclastogenesis, which was further examined in experimental OA rats as the local injection of lentiviral vectors expressing Gal-1 short hairpin RNA significantly attenuated articular cartilage degeneration, subchondral bone angiogenesis, and remodelling. Also, Gal-1 levels in subchondral bone were higher in patients with more severe osteoarthritis. Subsequently, we screened the most effective small molecular compound Kaempferol (Kae) that could suppress Gal-1 expression both in DRG cell bodies and peripheral nerve fibres via inhibiting the NF-κB, JNK and ERK pathways, thereby inhibiting downstream c-Fos, c-Jun, and ΔFosB expression as well as AP-1 binding activity to the Gal-1 promoter. Nerve fibres of less Gal-1 expression innervated the subchondral bone, consequently exerting a protective effect on OA including less cartilage degeneration, ameliorated hypersensitivity, reduced subchondral bone remodelling and H-type angiogenesis. These results suggest a more intimate connection between the nervous system and OA progression mediated by DRG-derived Gal-1. Thus, targeting up-regulated Gal-1 expression in DRG by Kae provides novel insights for future OA research in both disease modifying and pain alleviation.1, Chen Y, et al. Bone Research. 5: 17034,2017.2, Schnitzer TJ, et al. Ann Rheum Dis. 74: 1202,2015.

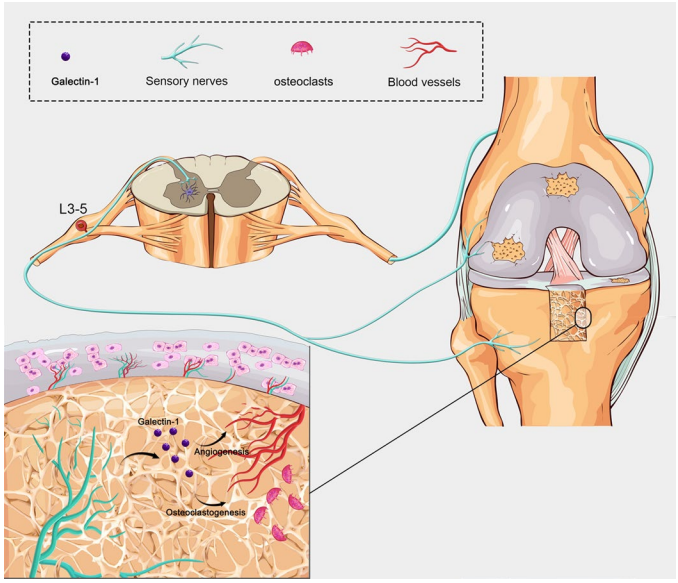

***Disclosures: Jingtian Mei**, None*

P-706

Blocking CCN2 Preferentially Inhibits Osteoclastogenesis Induced by Repetitive High Force Bone Loading *Mary F Barbe[1], Mamta Amin[1], Anne Gingery[2], Alex G Lambi[3], Steven N Popoff[1]. [1]Lewis Katz School of Medicine, Temple University, United States, [2]Mayo Clinic, United States, [3]University of California, Los Angeles David Geffen School of Medicine, United States

We recently found that blocking CCN2 signaling using a monoclonal antibody (FG-3019, from Fibrogen, Inc) may be a novel therapeutic strategy for reducing overuse-induced tissue fibrosis. Since CCN2 plays roles in osteoclastogenesis, and persistent performance of a high repetition high force (HRHF) lever pulling task results in a loss in trabecular bone volume in the radius, our aim was to determine if blocking CCN2 signaling would reduce the early catabolic effects of performing a HRHF task for 3 weeks. The experiment was approved by the the Institutional Animal Care and Use Committee in compliance with NIH guidelines for the humane care and use of laboratory animals. Studies were conducted on 40 young adult, female, Sprague-Dawley rats. Twenty-five rats were randomly chosen to undergo an initial operant shaping period for 6 wks to learn a high force lever pulling task, before then going on to perform an operant HRHF lever pulling task for 3 weeks (pulling a lever bar at 50% of their maximum pulling force, 1.27 Newtons, 4 reaches/min for a food reward, for 2 hrs/day, in 30 min intervals with 1.5 hr rest breaks between, 3 days/wk) HRHF rats were randomly divided into subcohorts that were untreated (HRHF Untreated), treated with an anti-CCN2 monoclonal antibody (HRHF+FG-3019, 40 mg/kg body wt, i.p.; 2x per wk for 2 wks), or with a human IgG as a vehicle control (HRHF+IgG),), while continuing to perform the task. Non task control rats (n=15) were left untreated. In distal metaphyseal trabeculae of the radius, HRHF Untreated rats showed increased osteoblast numbers and other indices of bone formation, compared to controls, yet decreased trabecular bone volume, increased osteoclast numbers, and increased serum CTX-1 (a serum biomarker of bone resorption). HRHF+FG-3019 rats also showed increased osteoblast numbers and bone formation, but in contrast to HRHF Untreated rats, showed higher trabecular bone volume, and reduced osteoclast numbers and serum CTX-1 levels (statistically similar to Control levels). In conclusion, HRHF loading increased bone formation in each task group, yet blocking CCN2 dampened trabecular bone catabolism by reducing osteoclast numbers and activity.

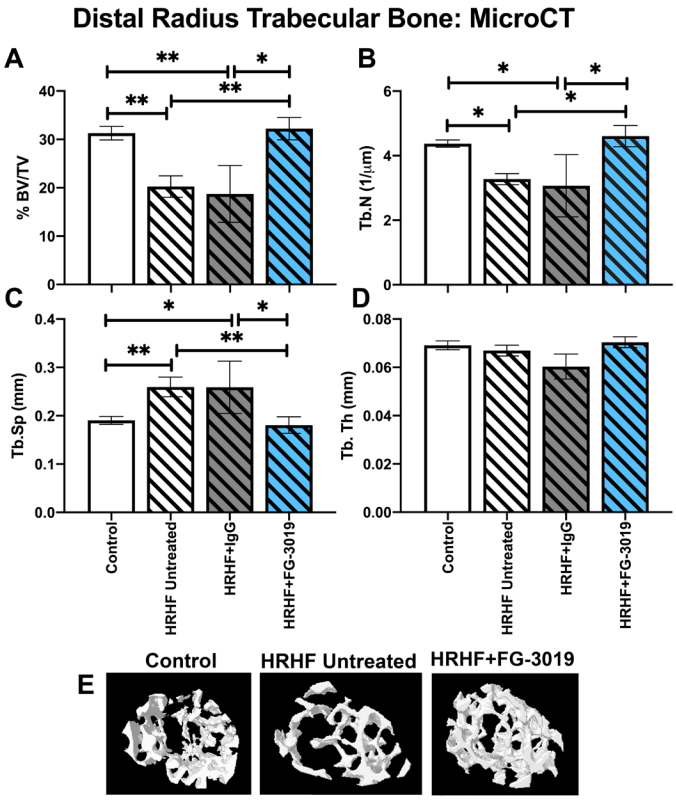

***Disclosures: Mary F Barbe**, None*

P-707

Abaloparatide is more effective than PTH in restoring bone formation, but both agents correct the impaired bone structural and material properties and citrate content in mice with Type 1 Diabetes *Serra Ucer Ozgurel[1], Amy Y. Sato[2], Kevin McAndrews[3], David Halladay[3], Meloney Cregor[3], Alma Villasenor [4], Maricruz Marmani-Huanca[5], Coral Barbas[4], Arancha Gortazar[6], Teresita Bellido[2]. [1]Department of Anatomy, Cell Biology and Physiology, Indiana University School of Medicine, Richard L. Roudebush Veterans Administration Medical Center, Indianapolis, IN, United States, [2]Department of Anatomy, Cell Biology and Physiology, Indiana University School of Medicine, Indianapolis, IN, Richard L. Roudebush Veterans Affairs Medical Center, Indianapolis, IN, United States, [3]Department of Anatomy, Cell Biology and Physiology, Indiana University School of Medicine, Indianapolis, IN, Richard L. Roudebush Veterans Administration Medical Center, Indianapolis, IN, United States, [4]Centre for Metabolomics and Bioanalysis (CEMBIO), Faculty of Pharmacy, Universidad San Pablo-CEU, CEU Universities, Campus Monteprincipe, 28925 Alcorcón, Madrid, Spain, [5]4Centre for Metabolomics and Bioanalysis (CEMBIO), Faculty of Pharmacy, Universidad San Pablo-CEU, CEU Universities, Campus Monteprincipe, 28925 Alcorcón, Madrid, Spain, [6]Bone Physiopathology laboratory, Applied Molecular Medicine Institute (IMMA), Universidad San Pablo-CEU, CEU Universities, Campus Monteprincipe, 28925 Alcorcón, Madrid, Spain

Pharmacologic approaches to treat skeletal fragility induced by diabetes are needed. We compared the effects on bone of 12 pmoles/g/d of hPTH(1-34) (PTH, 50ng/g/d) or abaloparatide (ABL, 47.5ng/g/d, Radius Health), FDA approved bone anabolic agents. Agents or vehicle (veh) were administered for 28d to 19wk old C57BL/6J male mice with established bone disease induced by streptozotocin, a preclinical model of type 1 diabetes (T1D). We showed earlier that ABL was superior than PTH in increasing or restoring bone mass (BMD and μCT) in control (C) or T1D mice, respectively, and that ABL induced a longer-lasting increase in bone remodeling compared to PTH. We now report that T1D mice exhibited reduced trabecular (t) and periosteal (p) bone formation rate (BFR) (38% and 49% below C, respectively). ABL increased t and pBFR to a greater extent than PTH under physiologic and T1D conditions. Thus, ABL increased tBFR 70% and 194% over veh, and pBFR 110% and 372% over veh in C and T1D mice, respectively. In contrast, PTH did not significantly alter BFR in C mice; and increased tBFR only 92% over veh and did not increase pBFR in T1D mice. We next evaluated bone strength by femoral 3-point-bending. Structural (extrinsic) bone indexes: ultimate force and energy to failure were decreased in T1D. Only ABL increased ultimate force in C and T1D mice. T1D mice treated with ABL or PTH exhibited similar ultimate force and energy to failure when compared to respective C mice, indicating bone strength restoration. Material (intrinsic) properties: toughness and Young's modulus were decreased or increased, respectively, in T1D mice vs C; whereas no differences were detected between T1D and C mice treated with ABL/PTH, indicating restoration. In addition, though T1D mice did not exhibit changes vs C in ultimate stress, another intrinsic property, both agents increased it in T1D mice. We next measured by capillary electrophoresis/MS bone content of citrate, an innate component of hydroxyapatite crystals that imparts nanocrystal stability, bone strength, and resistance to fracture. Bones from T1D mice displayed 46% less citrate than C mice; and, similar to the effects on toughness, bones from T1D mice treated with ABL or PTH displayed similar citrate content to their corresponding C mice. In conclusion, ABL is more effective than PTH in restoring bone formation, but both ABL and PTH have the ability to correct the impaired bone extrinsic and intrinsic properties in T1D mice.

***Disclosures: Serra Ucer Ozgurel**, None*

P-708

Genotypic and Phenotypic Characterization of CRISPR/Cas9 Mediated Fluorescent Osteoclast Reporter Mice *Dilara Yilmaz[1], Yannick Fischer[2], Ralph Müller[2], Esther Wehrle[2]. [1]ETH Zurich, Switzerland, [2]ETH Zurich, Switzerland

Several transgenic BAC or Cre based fluorescent mouse models have been developed to understand the function of bone cells during adaptation and regeneration, however, these methods remain ineffective and costly. By employing CRISPR/Cas9 genome editing, our lab recently developed fluorescent osteoclast reporter mice. To validate the model, we aimed to identify fluorescent osteoclasts and by combining single-cell mechanomics, we will track them dynamically in mouse bone and investigate the molecular response to changes in mechanics in their 3D local in vivo environment (LivE). Osteoclasts were labeled linking mCherry with acid phosphatase type 5 (Acp5). PCR genotyping and Sanger sequencing were performed. Specific endogenous signals of osteoclasts were confirmed with fluorescent (ELF-97) and histological TRAP stainings. Bone histomorphometry parameters such as the number of osteoclasts per bone surface (N.Oc/BS) were assessed and data were expressed as mean+/-standard deviation (SD). Unpaired Student's two-tailed t-test was used to evaluate statistical differences. Wild type mice were used as a control to confirm the specificity of fluorescent protein expression in osteoclasts. Our results displayed complete integration of all targets at the intended loci through PCR and Sanger sequencing. We observed distinct fluorescence signals around the resorption pits in femurs and vertebrae of 4 and 20 week-old homozygous mice (Acp5-mCherry). This was confirmed by co-localization of endogenous mCherry signals with histological and fluorescent osteoclast specific TRAP stainings. Moreover, mean N.Oc/BS was quantified (n=4) as 4.43+/-0.89/mm for homozygous and 4.61+/-0.43/mm for wild type mice. Statistical analysis did not reveal a significant difference between the groups (p=0.716). Furthermore, sequential stainings and imaging enabled us to co-localize fluorescent (Calcein Blue) and histological (Toluidine Blue) signals from a single section (Fig.1).In this study, we generated fluorescent reporter mice through CRISPR/Cas9 technology to identify osteoclasts fluorescently and validated the function of the fluorescent protein through genotyping, sequencing, and histology. Furthermore, by combining fluorescent and histological stainings, we were able to obtain extensive molecular information from the same section. In the near future, these fluorescent reporter mice will serve to investigate spatially resolved in vivo single-cell mechanomics of bone adaptation and regeneration.

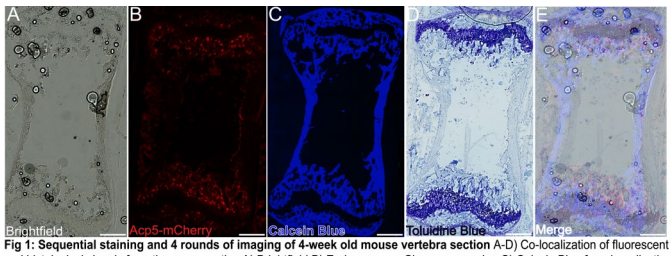

Fig 1: Sequential staining and 4 rounds of imaging of 4-week old mouse vertebra section A-D) Co-localization of fluorescent and histological signals from the same section A) Brightfield B) Endogenous mCherry expression C) Calcein Blue for mineralization D) Toluidine Blue for highlighting tissue architecture. E) Composite image stack. Images are taken with 20X magnification. Scale bar: 200μm

***Disclosures: Dilara Yilmaz**, None*

Posters

P-709

A Simultaneous Bone and Muscle Surgical Injury Model Reveals Age/Gender Differences in Musculoskeletal Healing *Claudia Cristina Biguetti[1], Ana Claudia Rodrigues Silva[6], João Shindo[3], Marco Antonio Hungaro Duarte[3], Jesus Carlos Andreo[3], Lynda Bonewald[4], Zhiying Wang[1], Marco Brotto[5], Mariza Matsumoto[6]. [1]Bone-Muscle Research Center, CONHI, The University of Texas at Arlington, United States, [6]School of Dentistry, São Paulo State University, UNESP, Brazil, [3]School of Dentistry, University of São Paulo, USP, Brazil, [4]Indiana Center for Musculoskeletal Health, Indiana University, United States, [5]Bone-Muscle Research Center, CONHI,The University of Texas at Arlington, United States, [6]School of Dentistry, São Paulo State University, UNESP, United States

Most if not all in vivo models of musculoskeletal (MSK) injury, evaluate recovery from injury in only one tissue at a time. We created a new tool for bone-muscle and MSK crosstalk studies, using a simultaneous surgical injury in the vastus lateralis (VA) muscle and the femuri of 129/SvEv mice. Mice were ethically anesthetized, and a 1mm micro punch was used to create a muscle defect to a depth of 1.5mm until reaching the femoral bone, which was drilled using a 0.50mm drill to produce a subjacent monocortical bone defect in a maximum depth of 1mm. Only subcutaneous tissue was sutured to allow natural healing. After one day of surgery, male (M) and female (F), young (3 months), and aged (18 months) mice were able to properly ambulate. Mice were euthanatized at 7 and 14 days post-surgery to evaluate MSK healing, utilizing microCT, histology, and immunohistochemistry for MuRF1 and MyoD. Non-injured skeletal muscles were used for targeted lipidomics analyses. Data were evaluated for statistical significance ($p<0.05$) by two-way ANOVA followed by Bonferroni correction. At 7 days, a decreased bone formation (BV/TV, %) was observed in the femurs of aged M and F mice (7.7+/-4.1 and 5.6+/-2.4) compared to young M and F (22+/-1.8 and 25+/-1.9). At day 14, the aged F group presented increased inflammation compared to young F, in both injured tissues; adipose and connective tissue was observed in the central area of muscle injury in both M and F aged mice, while young controls displayed myoblasts surrounded by connective tissue fibers. At day 14, a decreased cross-sectional area (μm2) of muscle fibers was noted adjacent to the injury in aged F (505+/-101) compared to the young F (1127+/-446). At day 7, MuRF1 was significantly increased in injured muscles of aged animals, while MyoD was significantly higher in young mice, with no gender differences. Lipidomics revealed that 6-keto-PGF1α was increased in aged F compared to young F mice, while the levels of 11,12-EET were increased in aged F compared to aged M. We conclude that MSK healing is influenced by age and gender, with major changes observed in aged F. Changes in skeletal muscle levels of AA derived lipid mediators may contribute to MSK healing differences in older females. We are now employing pharmacological and molecular-genetic approaches to investigate mechanisms contributing to these differences in older females. Our new model will be useful to advance the understanding of bone-muscle crosstalk with injury during aging.

***Disclosures: Claudia Cristina Biguetti**, None*

P-710

Dyrk1a-Related Down Syndrome Bone Defects Abrogated by Temporally-Targeted Pharmacological Intervention *Jonathan LaCombe[1], Matthew Blackwell[1], Kourtney Sloan[1], Randall Roper[1]. [1]IUPUI, United States

All individuals with Down syndrome (DS) have skeletal defects and experience an earlier onset of osteoporosis as compared to the general population. Skeletal abnormalities characteristic of DS emerge early and are developmental in nature. Trisomy of chromosome 21 (T21) causes a gene dosage imbalance of almost 300 genes, leading to negative effects on skeletal development, maturity, and maintenance. Of the many genes triplicated in T21, DYRK1A has been shown to have pathogenic effects in Alzheimer's disease, neural development, and skeletal maintenance. The Ts65Dn mouse model is the most studied model of DS. It has a extra freely segregating chromosome containing about 50% of the genes homologous to human chromosome 21, including Dyrk1a, and recapitulates the skeletal phenotype of DS. Genetic normalization of Dyrk1a in otherwise trisomic Ts65Dn male mice improved trabecular bone measure at six weeks of age, suggesting that trabecular phenotypes are related to Dyrk1a overexpression and pharmacological inhibition of DYRK1A may improve trabecular bone measures. Gene expression and microcomputed tomography (μCT) analysis revealed that Dyrk1a overexpression at P24 precedes the emergence of trabecular deficits at P30 in male Ts65Dn mice. We hypothesized that pharmacologically targeting the overexpression of Dyrk1a in a critical developmental window would prevent the emergence of Dyrk1a-related skeletal defects. Male Ts65Dn mice were treated with a DYRK1A inhibitor from P21-P29. Femurs were obtained at P30 and subjected to μCT analysis. In DS model mice receiving treatment, pharmacological intervention improved percent bone volume, trabecular separation, and trabecular number, similar to measurements observed in euploid controls. These data suggest that a pharmacological intervention during a developmental window that is sensitive to Dyrk1a overexpression prevents the emergence of Dyrk1a-related skeletal phenotypes and suggests that other Dyrk1a-related phenotypes can be targeted in a similar manner. Future experiments aim to determine the molecular mechanisms that Dyrk1a overexpression dysregulates to produce characteristic Dyrk1a-related appendicular skeletal phenotypes. This work will contribute to improving the overall health, quality of life, and longevity of individuals with DS.

***Disclosures: Jonathan LaCombe**, None*

P-711

Single-cell RNASeq analysis of developing bones in a G610C mouse model of osteogenesis imperfecta *Laura Gorrell[1], Elena Makareeva[1], Shakib Omari[1], Sergey Leikin[1]. [1]NICHD, NIH, United States

Abnormal osteoblast differentiation and function have been reported in several mouse models of osteogenesis imperfecta (OI). We previously introduced and characterized a G610C mouse model, in which a Gly610 to Cys substitution in the triple helical region of the α2(I) chain causes a moderately severe OI. We demonstrated that accumulation of misfolded procollagen in the osteoblast ER caused cell stress and resulted in osteoblast malfunction, but the molecular mechanisms of the cell stress and osteoblast adaptation to it remained unclear. To identify these molecular mechanisms, here we performed single-cell RNASeq analysis of calvaria, femur, and tibia in E18.5 embryos of wild type, heterozygous and homozygous G610C mice. We found that the mutation significantly affects gene expression only in hypertrophic chondrocytes and osteoblasts. We confirmed our earlier qPCR findings of significant cell stress, which was not accompanied by activation of canonical unfolded protein response (UPR). Instead of increased Hspa5 and Atf4 transcription expected in UPR, scRNASeq revealed upregulation of their paralogs Hspa9 and Atf5 in mature osteoblasts and Atf3 in hypertrophic chondrocytes, indicating activation of unexpected cell stress pathways, which we are currently investigating. In mature osteoblasts, most changes occurred in mRNA transcripts of genes involved in regulating different aspects of cellular homeostasis and osteoblast function. However, we also observed significant changes in transcription of some extracellular matrix proteins, e.g. decorin and several types of collagen. Overall, our findings not only support the concept of osteoblast cell stress and malfunction as an important factor in OI pathophysiology but also reveal underlying molecular pathways and potential therapeutic targets.

***Disclosures: Laura Gorrell**, None*

P-712

The role of osteoblasts in skeletal abnormalities of Down syndrome male and female mice *Jared Thomas[1], Randall J. Roper[1]. [1]IUPUI, United States

Individuals with Down syndrome (DS) have lower bone mineral density (BMD) that is present in adolescence and persists until adulthood. In adults with DS, here is an age-related decline in BMD in individuals with DS leading to an increased risk of osteoporosis and fracture. Trisomy 21 is the cause of DS and increased gene dosage disrupts bone development and homeostasis and occurs in both males and female, but at different times. Skeletal anomalies observed postnatally may be the result of a cellular defect, resulting in reduced bone formation and/or low bone turnover. DYRK1A is found in three copies in humans with DS and Ts65Dn DS model mice, and has been linked to cognitive impairments and skeletal abnormalities. Previous studies in Ts65Dn male mice at 6 weeks revealed decreased osteoblast number, activity and significantly decreased bone formation. Reduction of Dyrk1a copy number to normal levels from conception in all cells in otherwise trisomic mice rescues postnatal skeletal abnormalities and cellular deficits. We hypothesized reduction of Dyrk1a copy number in osteoblasts would improve osteoblast proliferation, activity and mineralization thereby normalizing trabecular architecture, cortical geometry and mechanical strength in Ts65Dn mice.Ts65Dn mice with a floxed Dyrk1a gene (Ts65Dn, Dyrk1afl/+) were bred to Osx1-GFP::Cre+ mice to generate Ts65Dn animals with a reduced copy of Dyrk1a in mature osteoblast cells. Our preliminary data indicate that Ts65Dn,Dyrk1a+/+/+ and Ts65Dn,Dyrk1a+/+/-male and female mice display significant defects in both trabecular and cortical architecture. Ultimate force was reduced in female trisomic animals, suggesting whole bone and tissue level properties are not adversely affected by Dyrk1a copy number in female trisomic mice. Based on our preliminary data, trisomic Dyrk1a may not alter osteoblast cellular activity in a cell-autonomous manner in trisomic animals. Three copies of Dyrk1a could influence cellular signaling pathways involved in bone remodeling, mineralization, and proliferation independent of osteoblast expression of Dyrk1a. Alternatively, Dyrk1a expression in osteoclasts could highlight cell autonomous or non-cell autonomous mechanisms related to skeletal defects and possible alterations in DS bone homeostasis. Identifying the genetic and developmental etiology of skeletal phenotypes associated with DS could help to design therapies to rescue skeletal deficiencies seen in DS.

***Disclosures: Jared Thomas**, None*

P-713

Support for a new therapeutic approach of using a low-dose FGFR tyrosine kinase inhibitor (infigratinib) for achondroplasia *Benoit Demuynck[1], Justine Flipo[1], Gary Li[2], Carl Dambkowski[2], Laurence Legeai-Mallet[1]. [1]Université de Paris, Imagine Institute, INSERM UMR, France, [2]QED Therapeutics Inc., United States

Background: Fibroblast growth factor receptor 3 (FGFR3) plays a crucial role in bone elongation, demonstrated by FGFR3 gain-of-function mutations in individuals with achondroplasia (ACH). We evaluated a therapeutic strategy targeting all pathways downstream of FGFR3, hypothesizing that a very low dose of the oral selective FGFR1–3 tyrosine kinase inhibitor (TKI) infigratinib (BGJ398) could improve defective bone elongation and have greater potency at lower concentrations in a human chondrocyte cell line than a C-type Natriuretic Peptide (CNP) analog (vosoritide).Methods: A mouse model (Fgfr3Y367C/+)

mimicking ACH was treated with subcutaneous infigratinib daily (0.2 or 0.5 mg/kg/d) or intermittently (1 mg/kg q3d) for 15d (PND1–15). In vivo results were compared with vehicle-treated mutant mice. TAN 4-18-chondrocytes, a human chondrocyte line expressing a heterozygous Y373C FGFR3 mutation, were treated with multiple concentrations of infigratinib and vosoritide and MAPK levels were measured.Results: We observed a significant improvement of the upper (humerus +7%, ulna +11%) and lower (femur +11%, tibia +16%) limbs at 0.5 mg/kg/d, and improvement in the foramen magnum. The effect of infigratinib on bone elongation was reduced with a lower dose (0.2 mg/kg), confirming a dose-response relationship. With intermittent injections of infigratinib (1 mg/kg q3d), gain of growth was significant for all long bones (+7%) and foramen magnum size was increased. Modification of the growth plate structure, displaying better organization, was also seen. Compared with FGF18-treated TAN 4-18-chondrocytes, infigratinib at 10-6M to 10-10M led to statistically significant ($p<0.05$) improvements. With vosoritide, a concentration of 10-4M led to statistically significant improvements vs FGF18-treated chondrocytes ($p<0.05$), although this was not seen at 10-5M.Conclusions:In vitro data demonstrate that infigratinib has superior activity over a CNP analog, suggesting that inhibition of multiple key pathways downstream of FGFR3 controlling either proliferation or differentiation of the chondrocytes leads to better efficacy vs MAPK inhibition alone. In vivo data demonstrate that low, as well as intermittent, doses of infigratinib promote growth in this ACH mouse model. No apparent toxicity of infigratinib was observed. These results suggest that, at low doses, infigratinib has the potential to be a valuable and relevant therapeutic option for children with ACH.

***Disclosures: Benoit Demuynck**, None*

P-714

Effects of Alzheimer's Disease on Bone Quality in the 5xFAD Transgenic Mouse Model *Joan LLabre[1], Blanca Barquera[2], Bernard Possidente[3], Deepak Vashishth[4]. [1]Department of Biomedical Engineering, Rensselaer Polytechnic Institute, United States, [2]Department of Biological Sciences, Rensselaer Polytechnic Institute, United States, [3]Department of Biology, Skidmore College, United States, [4]Center for Biotechnology and Interdisciplinary Studies, Rensselaer Polytechnic Institute, United States

Alzheimer's disease (AD), an irreversible brain disorder that occurs with aging is one of the most common causes of dementia affecting an estimated 35 million people worldwide. Interestingly, skeletal fragility has been found to be a comorbidity of AD with patients exhibiting reduced mineralization, increased risk of osteoporosis, and a 2-fold risk for fragility fractures. Here we used the established 5xFAD transgenic mouse model to better understand the effects of AD on bone quality. Five-week old 5xFAD mice (34840-JAX, The Jackson Laboratory) and their wildtype (WT) littermate controls (n=10/group; 50% Female/50% Male) were used in this study. 5xFAD mice overexpress mutant human Abprecursor protein (APP695) with the Swedish (K670N, M671L), Florida (I716V), and London (V717I) familial AD (FAD) mutations, along with human PS1 harboring 2 FAD mutations, M146L and L286V. As an indicator of cognitive ability, their nesting behavior was assessed throughout the study. This behavior was quantified by measuring the weight of a cotton roll before and after being placed atop the mice cages for 5 days. 5xFAD mice showed a statistically significant and consistent decline in their ability to build nests by 6 months onwards (Fig. 1A). To measure bone quality, femoral samples were harvested (age 12 months) and analyzed via μCT (VivaCT40, Scanco) with high-resolution scans (70kVp, 114mA, 10.5mm voxel size, 301ms integration time). μCT analysis of the femoral mid-diaphysis revealed significant decreases in cortical thickness (9.6%), BMD (12.4%, Fig. 1B), and cortical bone area fraction (12.8%, Fig. 1C) in 5xFAD female mice compared to WT. Similarly, analysis of the distal femoral epiphysis revealed a decrease in BV/TV (8.5%), trabecular number (16.8%, Fig. 1D), as well as an increase in trabecular separation (12.5%), trabecular thickness (10.4%), and SMI (3.2%) in 5xFAD female mice compared to WT. These results suggest degradation of bone quality for female 5xFAD mice as the reduction in trabecular number correlates to an 80% loss strength. However, as the male 5xFAD mice did not show these same findings it is likely that the results seen here are attributable to genotype and gender interactions. Overall, 5xFAD female mice showed poorer bone quality and typical signs of osteoporosis compared to WT.

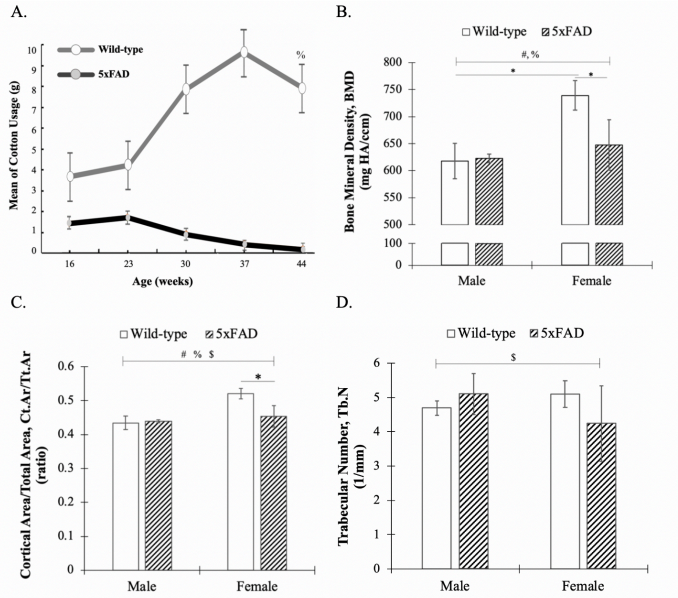

Figure 1. Effects of Alzheimer's Disease on Bone Quality in the 5xFAD Transgenic Mouse Model. A. Nesting behavior of mice. B. Mineralization, shown by BMD. C. Cortical morphology, shown by Ct.Ar./Tt.Ar. ratio. C. Trabecular morphology, shown by Tb. N. All data displayed as mean +/- SD. #gender effects, %genotype effects, $genotype x gender interaction effects, and * individual differences determined by Two-Factor ANOVA with Replication (p-value < 0.05).

***Disclosures: Joan LLabre**, None*

P-715

Association between endogenous oxidative stress and muscle atrophy in the elastase-induced pulmonary emphysema mouse model *Yosuke Mano[1], Manabu Tsukamoto[1], Ke-Yong Wang[3], Kenji Kosugi[1], Takafumi Tajima[1], Yoshiaki Yamanaka[1], Eiichiro Nakamura[1], Tamiji Nakashima[0], Quian Zhou[4], Kagaku Azuma[4], Yun-shan Li[5], Kazuaki Kawai[5], Kazuhiro Yatera[6], Akinori Sakai[1]. [1]Department of Orthopaedic Surgery, University of Occupational and Environmental Health, Japan, Japan, [3]Shared-Use Research Center, University of Occupational and Environmental Health, Japan, Japan, [0]Department of Human, Information and Life Sciences, University of Occupational and Environmental Health, Japan, Japan, [4]Department of Anatomy, University of Occupational and Environmental Health, Japan, Japan, [5]Department of Environmental Oncology, University of Occupational and Environmental Health, Japan, Japan, [6]Department of Respiratory Medicine, University of Occupational and Environmental Health, Japan, Japan

Background; Chronic obstructive pulmonary disease (COPD) causes skeletal muscle atrophy. Although exogenous oxidative stress (OS) due to smoking and endogenous OS due to chronic inflammation are considered as the factors of muscle atrophy, the details are not clear. In a previous study, bone loss and type I muscle fiber atrophy were observed in elastase-induced pulmonary emphysema (PE) mice, and we hypothesized that endogenous OS was involved in the phenotype. The purpose of this study was to investigate the relationship among PE, endogenous OS, and muscle atrophy.Methods; 12-week-old male mice were treated with intratracheal administration of 0.1 U porcine pancreatic elastase (PPE group) dissolved in saline or saline alone (control group). We analyzed the percentage of low-attenuation area (%LAA) in the lungs as the PE parameter on micro CT images. Mice were euthanized 12 weeks after administration, and the lungs and leg muscles were obtained. 8-hydroxy-2'-deoxyguanosine (8-OHdG) levels in the urine, lung and muscle tissues were analyzed. We measured the muscle weight and examined mRNA/protein expression levels in the muscle. Morphological evaluations were also performed on the muscle.Results; We obtained the following four findings. First, the OS marker in PE mice was elevated systemically. In the urine, lung and muscle tissues, the 8-OHdG levels in the PPE group were significantly higher than those in the control group. In addition, 8-OHdG levels in each tissue were positively correlated with the %LAA. Second, mitochondrial dysfunction due to OS was suggested in PE mice. Mitochondrial swelling, which are signs of mitochondrial dysfunction, were observed in the PPE group using electron microscopy. Furthermore, the mitochondria-specific superoxide dismutase levels were significantly lower. Third, the mRNA/protein expression levels of phospho-MKK3/6, phospho-p38, and FoxO1, which are the muscle atrophy-related signaling pathways caused by OS, were elevated in the muscles of PE mice. Fourth, PE mice showed significant muscle weight loss in only the soleus, in which type I muscle fibers are richly contained.Conclusion, In PE mice, OS was elevated in the muscle, resulting in mitochondrial dysfunction and activation of muscle atrophy-related signaling pathways caused by OS. Since PE mice showed dominantly type I muscle fiber

atrophy, endogenous OS may be strongly involved in COPD-related skeletal muscle atrophy, especially type I muscle fiber atrophy.

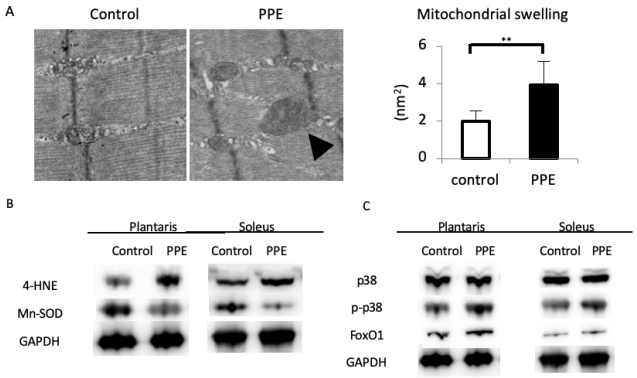

Figure 1. Mitochondrial dysfunction and activation of muscle atrophy-related signaling pathway caused by oxidative stress in pulmonary emphysema mice.
(A) Electron microscopy findings in the both groups. Mitochondrial swelling in the muscle tissue (black arrow). **p<0.01. (B-C) Western blotting analysis. (B) 4-hydroxynonenal (4-HNE) levels in the muscles were elevated, and the mitochondria-specific superoxide dismutase (Mn-SOD) levels were lower in the PPE group. (C) Protein expression levels of phospho-p38 and FoxO1, which are the muscle atrophy-related signaling pathways caused by oxidative stress, were elevated in the muscles of pulmonary emphysema mice.

***Disclosures: Yosuke Mano**, None*

P-716

Characterization of a Pediatric Lateral Meningocele Syndrome Mouse Model *Haydee Torres[1], Ashley VanCleave[2], Tania Rodezno[2], Malini Mukherjee[3], Jennifer Westendorf[4], Jianning Tao[5]. [1]Cancer Biology & Immunotherapies Group at Sanford Research; Department of Chemistry and Biochemistry, South Dakota State University, United States, [2]Cancer Biology & Immunotherapies Group at Sanford Research, United States, [3]Functional Genomics and Bioinformatics Core at Sanford Research, United States, [4]Department of Orthopedic Surgery, Mayo Clinic, Rochester, MN, USA; Department of Biochemistry & Molecular Biology, Mayo Clinic, Rochester, MN, USA, United States, [5]Cancer Biology & Immunotherapies Group at Sanford Research; Department of Pediatrics at Sanford School of Medicine at the University of South Dakota; Department of Biomedical Engineering, University of South Dakota, United States

Notch signaling is an evolutionarily conserved signaling pathway involved in cell fate decisions and cell renewal of multiple systems, including skeletal and muscle homeostasis. Recently, whole exome sequencing of family-related or unrelated patients with Lateral Meningocele Syndrome (LMS) revealed truncating mutations in the last exon of NOTCH3. To understand the gap in our knowledge of LMS and NOTCH3, we are characterizing a mouse model (N3LMS) of the human disease, specifically the causing role of NOTCH3 activation in osteosclerosis and kyphosis, a phenotype resulting from changes of either bone shape (e.g. abnormal thoracic vertebrae) or muscle integrity (e.g. truncal hypotonia). Our central hypothesis is that NOTCH3 gain-of-function (GoF) perturbs either osteoblast or myocyte differentiation, inducing the osteosclerosis and other abnormal characteristics of LMS in our model. We performed Sanger Sequencing, revealing that the heterozygous N3LMS mice contain a G to A point mutation (G to A) in the first base pair of the splice donor site in intron 31 of Notch3, which mimics truncating NOTCH3 mutations found to occur in human LMS patients. The homozygous N3LMS mutant mice developed kyphosis by 5 weeks of age, and we observed a difference in their weights at p14. qRTPCR analysis shows mutant mRNA is highly expressed in N3LMS mice. Preliminary trabecular bone MicroCT analysis of N3LMS homozygous mice indicates that these mutant mice may exhibit osteosclerosis by 2 months. On the other hand, mutant mice show a decrease in TA muscle weight and lower gripping strength in our behavior analysis of N3LMS mice, the latter suggesting normal embryonic muscle development but dramatic defects in postnatal muscle growth and function. Ongoing studies, including BASEscope and RNA-seq transcriptomic analysis on bone and muscle, will further elucidate gene expression pattern and potential pathways that lead to disease. Because there is currently no treatment available, a thorough biological understanding of this novel mouse model may point to new treatments to reduce the morbidity of LMS patients.

***Disclosures: Haydee Torres**, None*

P-717

Congenic myostatin (GDF8) deficiency increases skeletal bone volume in Col1a2 G610C osteogenesis imperfecta mouse model. *Catherine Omosule[1], Victoria Gremminger[1], Ashley Aguillard[1], Youngjae Joeng[1], Ferris Pfeiffer[1], Laura Schulz[1], Charlotte Phillips[1]. [1]University of Missouri, United States

Bone fragility is a hallmark of osteogenesis imperfecta (OI), a rare genetic connective tissue disorder with no known cure. OI is phenotypically and clinically heterogeneous and occurs due to greater than 1500 known mutations. Mild to moderate human OI is modeled in the established G610C (Col1a2tm1.1Mcbr) OI mouse model that is due to a glycine to cysteine substitution in the Col1a2 gene.Muscle and bone cross-talk reflect both physical and biochemical reciprocity. Myokines like myostatin, a TGF-β superfamily member, potently regulate muscle. The absence of myostatin results in increases in muscle fiber number and size in mice. We had previously shown that congenic myostatin deficiency in mild heterozygous OI murine (Col1a2oim/+) mice (due to a functional null of Col1a2 gene) improved skeletal phenotype in adulthood. Ligands which trap myostatin (sActRIIB) have also successfully increased muscle mass and bone integrity in heterozygote G610C (+/G610C) mice, while improving muscle mass but not skeletal integrity in Col1a2oim/oim or Col1a-1Jrt/+ mouse models of OI. In addition, sActRIIB, which binds multiple additional ligands, caused adverse effects in humans.To further delineate how the loss of myostatin impacts skeletal integrity in OI, we generated double heterozygous myostatin and G610C mice (+/mstn +/G610C, Dbl.Het) and compared their musculoskeletal properties to those of their littermates [wildtype (Wt), +/mstn, +/G610C, Dbl.Het] at 16 weeks of age. The +/G610C mice had inferior femoral biomechanical properties and reduced body weights relative to Wt offspring. Myostatin deficiency was verified in the Dbl.Het offspring and they showed 32.7% and 14.3% decreases in circulating myostatin relative to Wt and +/G610C, respectively. Dbl.Het offspring were substantially heavier, with increases in muscle mass relative to +/G610C mice and rivaling +/mstn offspring weights. Femoral cortical and trabecular bone microarchitecture was significantly improved in Dbl.Het compared to +/G610C although biomechanical strength was unaffected.Our study further confirms myostatin's regulatory role in muscle. We are unable to confirm whether the improved microarchitecture in the Dbl.Het offspring is a result of mechanosensation via increased muscle loading or direct biochemical signaling on bone. However, our results suggest that increasing muscle mass by decreasing circulating myostatin can improve bone microarchitecture and may improve skeletal integrity in OI.

***Disclosures: Catherine Omosule**, None*

P-718

Skeletal and Systemic Phenotype of a Combined Model of Type 1 Diabetes and Chronic Kidney Disease in Mice *John Damrath[1], Corinne Metzger[2], Jennifer Hatch[3], Elizabeth Swallow[2], Matthew Allen[2], Joseph Wallace[3]. [1]Purdue University, United States, [2]Indiana University School of Medicine, United States, [3]Indiana University - Purdue University at Indianapolis, United States

INTRODUCTION: Chronic Kidney Disease (CKD) affects 15% of Americans and dramatically increases fracture risk. However, 45% of CKD patients have diabetes listed as their primary cause of CKD, another condition that alters bone strength and quality. While these conditions have been studied independently, there is a great clinical need to understand the interactive effects of these diseases on the skeleton. Here, we report a rodent model, combining type 1 diabetes (T1D) and CKD, that demonstrates the effects of these conditions on bone microarchitecture.METHODS: Eight-week old male C57BL/6 mice (n=4) received daily streptozotocin injections (STZ, 50 mg/kg) for 5 days to induce T1D with blood glucose (BG) analyzed weekly. T1D was defined as BG >= 250 mg/dl. At 10 weeks of age, STZ-injected mice were fed a casein-based diet (0.9% P, 0.6% Ca) with 0.2% adenine diet (AD) to induce CKD. At 16 weeks of age, STZ+AD mice were switched to a casein control diet with maintained calcium and phosphorus ratios. A control cohort without T1D or CKD (n=4) was fed the casein control diet. All mice were sacrificed at 20 weeks. At harvest, serum was collected for biochemistries while femora and vertebrae were collected to assess microarchitecture and bone mineral density. Data were analyzed by Student's t-test.RESULTS: STZ+AD mice demonstrated varying degrees of T1D based on glucose tolerance tests performed one day before sacrifice. Blood urea nitrogen (BUN) was 170% higher and parathyroid hormone (PTH) was 506% higher in STZ+AD mice vs. control. BUN was highest in the most diabetic animal. Micro-CT of the femur demonstrated 3,355% higher cortical porosity with 40% lower cortical thickness (Ct.Th) in STZ+AD mice. In femora, trabecular bone volume fraction (BV/TV) and trabecular thickness (Tb.Th) were 39% and 26% lower, respectively. In vertebrae, trabecular BV/TV, Tb.Th, trabecular number (Tb.N), and tissue mineral density (TMD) were 46%, 16%, 36%, and 10% lower, respectively ($p < 0.05$ for all). Ct.Th, BV/TV, and Tb.Th were lowest in the most diabetic animal.DISCUSSION: This study demonstrated that a spectrum of T1D can be induced in mice alongside CKD. Importantly, we found that biochemical and skeletal outcomes that are typically abnormal in CKD, such as BUN and cortical geometry/porosity are preserved with T1D. Future studies will incorporate larger cohorts to investigate the independent and combined effects of T1D and CKD on the skeleton.

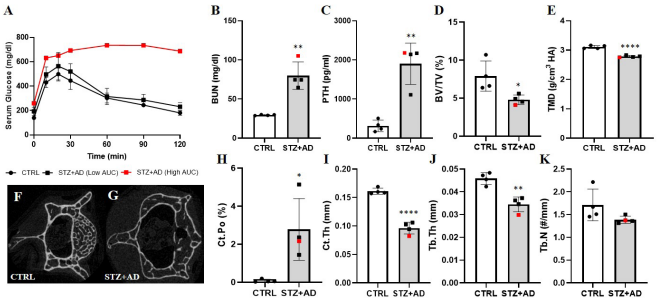

Figure 1: Effects of Combined T1D and CKD on Biochemical and Skeletal Properties. Glucose tolerance testing was performed by administering 1 g/kg of glucose per mouse and measuring blood glucose across a 2-hour window, revealing three mice with slight glucose intolerance and one with high glucose intolerance, as determined by the area under the curve (A). Blood urea nitrogen (B) and parathyroid hormone (C) levels were measured in serum taken at the end of the study. Microcomputed tomography was performed on right femora and vertebrae and analyzed for geometric properties and tissue mineral density (D-K). In all plots, the most glucose intolerant mouse is represented by a red data point (*$p < 0.05$, **$p < 0.01$, ***$p < 0.001$, ****$p < 0.0001$). AUC – area under curve; BUN – blood urea nitrogen; PTH – parathyroid hormone; BV/TV – bone volume/total volume; TMD – tissue mineral density; Ct.Po – cortical porosity; Ct.Th – cortical thickness; Tb.Th – trabecular thickness; Tb.N – trabecular number.

***Disclosures: John Damrath**, None*

P-719

Mechanical Ventilation-Induced Myopathy is Accompanied by Significant Trabecular Bone Loss *Zbigniew Gugala[1], Gordon Klein[1], Lars Larsson[2]. [1]University of Texas Medical Branch, United States, [2]Karolinska Institutet, Sweden

Mechanical ventilation is the mainstay treatment for critically ill patients with respiratory distress. However, through the course of ventilator therapy, these patients routinely develop severe muscle wasting with preferential loss of myosin not attributable to immobility. Systemic inflammation triggered by lung mechanical injury with subsequent cytokine storm and upregulation of catabolic pathways likely contribute to this myopathy, although the exact mechanisms are unknown. We have developed a rat model of ventilator-induced muscle wasting and established its feasibility and clinical validity. This model involves pharmacologic muscle paralysis, parenteral nutrition, and continuous mechanical ventilation up to 10d, and represents the respiratory setup used clinically, In this study we hypothesized that deterioration of skeletal muscle on mechanical ventilation is accompanied by bone changes. The aim was to determine the rate, nature and extent of changes in the femora and spines of rats subjected to ventilator for 0 (control), 2,5,8, and 10d. (N=20). In addition to routine muscle analyses, we performed microCT and bone biomechanical tests. Following ventilator exposure,animals were euthanized at the designated time points. MicroCT demonstrated progressive decline in femoral trabecular bone volume (p=0.0001-.0077), mineral density (p=0.0071-.0086), trabecular number (p=0.002-.011), connectivity density (p=0.0012-.0043), and increased porosity (p=0.0009-.018), beginning at day 8 of mechanical ventilation and correlated with loss of muscle mass and myosin/actin ratio (r2=0.64, p<0.0001). Biomechanical 3 point bending revealed a decrease in flexural stiffness (p=0.0078) and strength (p=0.0383) at day 10, coincidental with muscle decline. The femoral cortical bone and the trabecular bone of the lumbar vertebrae did not show statistically significant changes. Results indicate that mechanical ventilation leads to quantitative and qualitative deterioration of distal femoral trabecular bone correlating with severe skeletal muscle loss and involving reduction in bone mechanical integrity. Simultaneous loss of muscle and bone provide a fracture risk for survivors of ventilator therapy. Preventing or impeding this loss maylty improve post-ventilator functional recovery. Our rat model of ventilator-induced muscle and bone loss allows us to gain insight into muscle-bone interactions and to establish therapeutic targets to combat post-ventilator frailty and bone loss

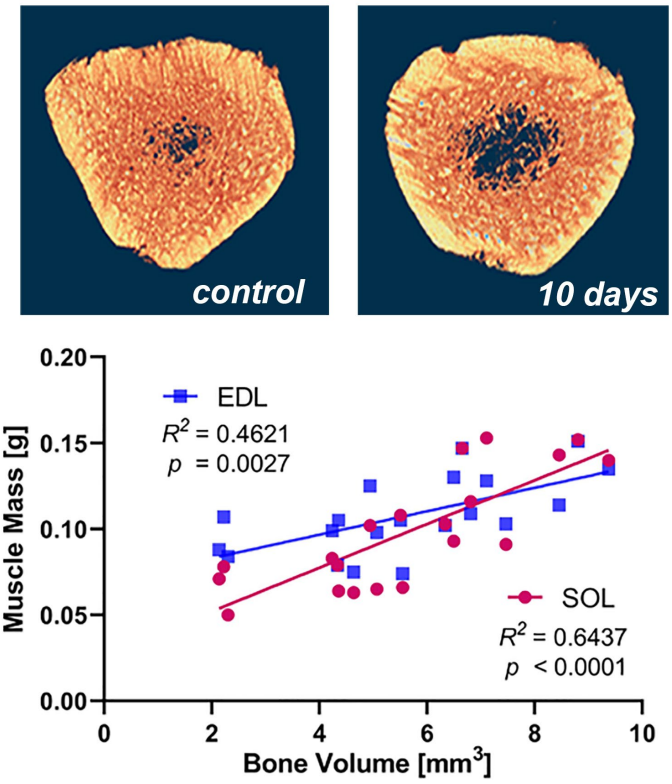

***Disclosures: Zbigniew Gugala**, None*

P-720

Thrombopoietic Agents Improve Angiogenesis during Fracture Healing *Ushashi Dadwal[1], Paul Childress[1], Jeffery Nielsen[2], Aamir Tucker[1], Alexander Brinker[1], Kelli Jestes[3], Krista Jackson[0], Rachel Blosser[1], Roman Natoli [1], Stewart Low[4], Philip Low[2], Todd McKinley[1], Jonathan Lowery [0], Melissa Kacena [1]. [1]Department of Orthopaedic Surgery, Indiana University School of Medicine, IN, USA, United States, [2]Departments of Medicinal Chemistry and Molecular Pharmacology, Purdue University, West Lafayette, Indiana, USA, United States, [3]Division of Biomedical Science, Marian University College of Osteopathic Medicine, Indianapolis, Indiana, USA, United States, [0]Division of Biomedical Science, Marian University College of Osteopathic Medicine, Indianapolis, Indiana, USA, United States, [4]Department of Chemistry, Purdue University, West Lafayette, Indiana, USA, United States

Achieving bone union remains a significant clinical dilemma. Osteoinductive agents such as BMPs are used clinically, but have significant side effects. Thus, identifying novel bone healing agents is critical. First, we demonstrate the robust bone healing capabilities of the main megakaryocyte growth factor, thrombopoietin (TPO) and/or second generation TPO agents in mice, rats, and pigs. This bone healing activity is shown by X-ray, µCT, histology, and biomechanical testing in two fracture models (critical sized defect and closed fracture) and with local or systemic administration. Second, we began to dissect the mechanisms by which TPO improves bone healing. To accomplish this, we treated collagenase digested bone cells and bone marrow from mouse femurs with BMP-2 (100ng/mL), TPO (200ng/mL), or saline for 48 hours and collected total RNA for microarray analysis. Our data revealed that TPO treatment resulted in the upregulation of more growth factors and cytokines than BMP-2 treatment, implicating enhanced angiogenesis. To test the effect of TPO on endothelial cells (ECs), we examined several cellular parameters using validated 2D culture assays. TPO significantly increased proliferation and the length of vessel-like structures from human cord blood-derived ECs. Additionally, TPO-treated mice had increased numbers of ECs within the fracture callus. Next, we completed multianalyte phospho-profiling arrays of protein from the fracture callus of mice treated with saline, TPO (5µg), or BMP-2 (5µg). Our data revealed broader regulation of effector phosphorylation status with TPO as compared to BMP-2, with increased expression of proteins important in regulation of actin cytoskeletal dynamics and motility as well as cytokines and growth factors, including Angiopoietin 1. We then determined TPO treatment of megakaryocytes significantly increased Angiopoietin 1 mRNA expression (3.4-fold increase). Together, our data suggest that TPO acts to increase angiogenesis at the fracture site, improving fracture healing. Although additional preclinical safety studies are required before the FDA would approve use of thrombopoietic agents for bone healing in humans, our rodent and pig studies

are promising. Thus, expanding the therapeutic potential of this axis to include bone healing is an attractive possibility.

***Disclosures: Ushashi Dadwal**, None*

P-721

Improved Bone Fracture Repair through Targeted Delivery of Angiogenic Agents *Jeffery Nielsen[1], Stewart Low[1], Philip Low[1], Chris Chen[1], Ephriam Mbachu[1]. [1]Purdue University, United States

PURPOSE: Delayed fracture healing is a major health issue, and strategies to improve repair will improve patient outcomes and lower healthcare costs. Revascularization of fracture is an essential step in fracture healing, low vascularization delays healing. Our lab has developed a system based on acidic oligopeptides whereby a targeted therapeutic agent can be administered SC distally and it will accumulate on the exposed hydroxyapatite at the bone fracture. We sought to develop a new class of bone fracture targeted angiogenic drug to improve bone fracture healing. These would be able to stimulate a targeted revascularization of the tissue adjacent to the exposed mineral surface of the bone fracture and thus providing oxygen, nutrients, progenitor cells, and minerals for cell survival and proliferation in order to result in successful healing.METHODS: Targeted conjugates of anabolic fragments or memetics of VEGF(QK)1, SPARC (SPARC 113)2, and PDGF-BB(PBA2-1c)3 were synthesized using standard Fmoc solid-phase peptide synthesis. Once the activity of the conjugates was confirmed, they were tested in an Einhorn method midshaft-stabilized femur fracture model in 12-week-old Swiss Webster mice with and without STZ induced type 1 diabetes. The mice(n=10) were dosed SC daily for 3 weeks. Healing was assessed using µCT. Fractured femurs were tested for strength in a four-point bend to failure. Statistical analysis was performed using a one-way ANOVA (α=0.05). All animal experiments were performed in accordance with protocols approved by Purdue University's Institutional Animal Care and Use Committee.RESULTS: Targeted angiogenic fragments demonstrated significant improvements in bone fracture healing both structurally and mechanically. The VEGF memetic QK had the greatest improvement with a 180% increase in callus BV/TV, and a 242% increase in max load after 17 days of treatment. No side effects were observed, even at very high doses. Significant healing responses were seen in both healthy and in slow healing diabetic mice.CONCLUSIONS:The targeted angiogenic agents rapidly improved fracture healing and, and the attachment of a targeting ligand allowed angiogenic agents to be noninvasively administered. QK shows promise as a future drug as it significantly improved the healing of bone fractures in repeated in vivo models of normal and delayed healing by promoting earlier revascularization. This could reduce the time a patient spends suffering with immobility

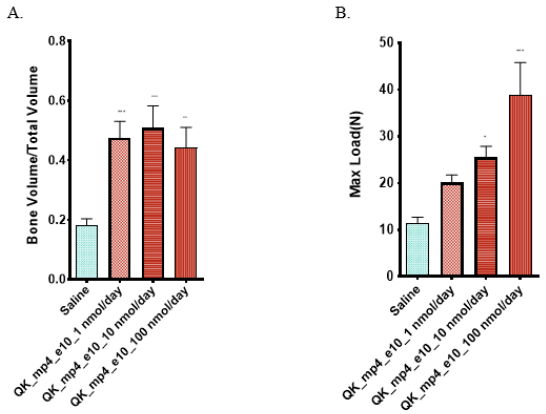

Figure 1: *In vivo* fracture healing efficacy of QK_mp4_e10 conjugate in Swiss Webster fracture-bearing mice (n=5) after 17 days as measured by micro-CT assessment of the widest 100 slices of the fracture callus. The healed fractured femurs were refractured in a postmortem 4-point bend biomechanical analysis A) BV/TV represents the bone volume of the total volume of the fracture callus and is a measure of bone density at the site of fracture repair. B) "Max load" represents the maximum force the healed femur withstood before it refractured. 1 nmol, 10 nmol, and 100 nmol of the conjugate were delivered daily by subcutaneous injection.

***Disclosures: Jeffery Nielsen**, None*

P-722

Effects of Treatment with Bone-Targeted Prostaglandin E2 Receptor 4 Agonist prodrug, C3 (Mes-1007), in a Mouse Model of Severe Osteogenesis Imperfecta *Iris Boraschi-Diaz[1], Jonathan Polak[2], Gang Chen[2], Robert N Young[2], Frank Rauch[1]. [1]Shriners Hospital for Children-Canada, Canada, [2]Department of Chemistry, Simon Fraser University, Canada

Osteogenesis imperfecta (OI) is a heritable bone fragility disorder that is typically caused by mutations in COL1A1 or COL1A2, the genes encoding collagen type I. Bisphosphonates are widely used to decrease fracture rate but are only partially effective. Prostaglandin E2 (PGE2) and PGE2 receptor 4 (EP4) agonists have been shown to be bone anabolic in vivo and treatment with EP4 agonists may bring additional benefits. In this study, we tested a novel bone-targeted EP4 agonist prodrug, C3 (Mes-1007), in Jrt mice, a model of severe OI. Male 8-week old wild-type and OI mice were randomly assigned to 4 weeks of three intraperitoneal injections per week with C3 (5 or 25 mg/kg body weight), control injections, zoledronate (5 µg/kg), and a combination treatment of zoledronate (5 µg/kg) and C3 (25 mg/kg). MicroCT analysis at the distal femoral metaphysis showed that treatment with zoledronate alone or with both C3 and zoledronate led to a significant increase in trabecular bone volume. C3 had an additive effect on trabecular bone volume in zoledronate-treated wild type mice that was due to increased trabecular thickness. In OI mice, C3/zoledronate combination treatment was associated with higher trabecular thickness but the difference in bone volume was not significant. At the femoral midshaft, C3/zoledronate combination treatment increased cortical thickness in both genotypes and led to higher periosteal diameter in OI mice. Three-point bending tests of femurs showed that zoledronate increased the stiffness in wild type but not in OI mice. L4 vertebral body microCT revealed that C3/zoledronate combination treatment had an additive effect on trabecular bone volume, which in OI mice was due to an increase in both trabecular number and thickness. Trabecular bone volume in OI mice that received combination treatment was similar to untreated wild type mice (p-value = 0.25). In conclusion, adding C3 to zoledronate amplified the effect of zoledronate in this severe model of OI.

***Disclosures: Iris Boraschi-Diaz**, None*

P-723

The role of nonhuman primates as a model for diabetes pathophysiology *Roberto J. Fajardo[1], Todd L. Bredbenner[2], Ellen E. Quillen[3]. [1]Clinical and Applied Science Education, University of the Incarnate Word School of Osteopathic Medicine, United States, [2]Department of Mechanical and Aerospace Engineering, University of Colorado Colorado Springs, United States, [3]Section on Molecular Medicine and Center for Precision Medicine, Wake Forest School of Medicine, United States

In vivo associations between glycemic control and skeletal characteristics in humans and animal models remain unclear. At the cellular level, hyperglycemia decreases bone formation. However, identifying relationships between HbA1c and systemic indicators of bone health, such as bone mineral density (aBMD) and bone biomarkers, such as osteoprotegerin (OPG), osteocalcin (OCN), sclerostin (SOST), and parathyroid hormone (PTH), remain somewhat elusive. We investigated the relationship between HbA1c, imaging, and serum based skeletal health indicators in a baboon animal model. Due to pathophysiologic similarity with humans, nonhuman primates represent an ideal model of obesity and diabetes progression, but almost nothing is known about how bone traits co-vary with glycemic control in this animal model. To evaluate the relationship between diabetes and bone traits, we evaluated 17 female baboons, 18-27 years of age (54-81 human-equivalent years) with elevated HbA1c levels (>5%) for several years prior to death and 17 age- and weight-matched healthy controls. Weight-matching was included to minimize the influence of obesity on bone. Panels of circulating bone biomarkers were run in triplicate using the Milliplex MAP Human Bone Magnetic Bead Panel. L2 vertebral bodies were imaged using microCT (53 mm), and tissue mineral density (TMD), vertebral shell thickness (VS.t), and thickness of the pedicle (cortical) shell (PS.t) were determined. HbA1c ranged between 3.2% and 6.1%. Linear regression indicated that HbA1c was positively associated with PS.t (adj R2 = 0.185, p=0.006) and OPG levels (adj R2 = 0.098, p=0.051, Figure 1). OCN and PTH showed non-significant inverse relationships with HbA1c (p=0.154 and p=0.186, respectively). TMD, aBMD, and SOST were not significantly related to HbA1c, despite approximately a two-fold variation in the sample, suggesting ample dynamic ranges. While our results support a role for OPG and cortical shell thickness in increased fracture risk among individuals with poorer glycemic control and diabetes, the mechanisms that underlie these associations and metrics that reliably predict diabetic fracture risk are unclear. Although nonhuman primates are an excellent model of human obesity and diabetes pathophysiology, more needs to be learned about the relationship between glycemic control and skeletal traits in these animals.

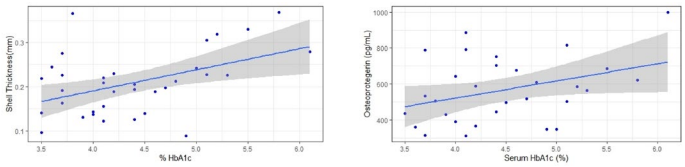

***Disclosures: Roberto J. Fajardo**, None*

P-724

Effect of TNFα Inhibition on Synovial Joint Inflammation and Subchondral Bone Healing Following Intraarticular Fracture in a Rat PTOA Model *Michael Valerio[1], Sarah Franco[1], Connor Dolan[1], Naveena Janakarim[1], Benjamin (Kyle) Potter[2], Christopher Dearth[1], Stephen Goldman[1]. [1]1 DoD-VA Extremity Trauma & Amputation Center of Excellence, Fort Sam Houston, TX 2 Department of Surgery, Uniformed Services University of the Health Sciences & Walter Reed National Military Medical Center, Bethesda, MD, United States, [2]2 Department of Surgery, Uniformed Services University of the Health Sciences & Walter Reed National Military Medical Center, Bethesda, MD 3 Department of Orthopaedic Surgery, Walter Reed National Military Medical Center, Bethesda, MD, United States

Intraarticular fractures (IAF) lead to a particularly aggressive form of post-traumatic osteoarthritis (PTOA) occurring primarily in younger populations, costing the healthcare systems billions of dollars annually. TNFα, an early acting pro-inflammatory cytokine, has been implicated in the development of PTOA and has been shown to persist in traumatized synovial joints well past the inflammatory phase of healing. Infliximab (INX), a monoclonal antibody against TNFα, inhibits its action and may protect against the development of PTOA. The aim of this study was to test the effects of TNFα inhibition via INX on inflammation and long-term osteochondral healing. IAF were induced in male Lewis rats via a 5J blunt impact to the lateral aspect of the left hindlimb knee. Osmotic pumps delivering INX at rate of 10mg/kg/day or saline (control) were implanted for 2 weeks. Blood was drawn at days -1, 0, 1, 3, 7, 14, 28 and 56 relative to injury. At days 14 and 56 post-injury, hindlimbs were imaged and synovial fluid (SF) and limbs were harvested. Multiplex and target-specific ELISA kits were used to detect relevant soluble factors and INX from serum and SF. μCT analysis was conducted on cortical and trabecular regions from isolated tibial plateau head, femoral head and proximal tibial bones. IAF were mainly classified as full articular fractures (41C, 33C), with some extra-articular avulsion (41A, 33A) and were mostly comminuted. Serum [INX] was shown to increase after pump implantation and remained elevated (>2500ng/mL) through Day 28. Plasma soluble factor analysis showed that at Day 14, TNFα, IL-1β and IL-13 values were reduced by ~ 42, 53, and 49% respectively, in the INX treated group vs control (n=3/group). Analysis of SF at 14 days showed a near six-fold reduction in inflammatory cytokines;TNFα, IFNγ, IL1α, IL1β, IL2, IL12, IL13 and IL17A ($p<0.001$, each) and chemokines; IP10 and MCP3 ($p<0.01$) in the INX treated group compared to control. μCT analysis revealed no differences in subchondral bone morphometry between groups but increased bone mineral density (BMD, $p<0.02$) in INX treated relative to control. These results suggest that INX effectively damps the local pro-inflammatory microenvironment following IAF which is associated with an increased BMD of the subchondral bone. As such, INX represents a clinically available therapy that may have additional utility for mitigating the particularly aggressive form of PTOA that typically follows IAF.Acknowledgements: This study was aided by a grant from the Orthopaedic Trauma Association (Grant#2819). Disclaimer: The contents of this publication are the sole responsibility of the author(s) and do notnecessarily reflect the views, opinions or policies of Uniformed Services University of the HealthSciences (USUHS), the Department of Defense (DoD), the Departments of the Army, Navy, or Air Force.Mention of trade names, commercial products, or organizations does not imply endorsement by the U.S.Government.

***Disclosures: Michael Valerio**, None*

P-725

Novel Osteomyelitis Model Development Utilizing Clinical Isolates of Staphylococcus aureus *Philip Roper[1], Linda Cox[1], Yael Alippe[1], Gabriel Mbalaviele[1], Deborah Veis[1]. [1]Washington University School of Medicine, United States

Osteomyelitis (OM) is the debilitating infection of bone, and Staphylococcus aureus is the predominant causative organism. We developed two separate OM models in our laboratory - an intratibial injection model mimicking direct deposition of bacteria after injury or surgery and a tail vein injection model mimicking hematogenous OM more common in children - employing 5 clinical isolates from pediatric OM. All isolates were transformed with a Lux operon to become bioluminescent. Infected mice were monitored for four or five weeks, during which bioluminescent imaging (BLI) was performed to longitudinally track bacterial burden, followed by microCT and histological analyses of femora and tibiae. All 5 isolates produced an infection by BLI, and in all cases, once an infection developed, it persisted without much change to the BLI intensity, suggesting a balance between host and pathogen. We also found that BLI signal correlated with the extent of trabecular bone loss as measured by microCT. There were, however, differences in the infectivity of isolates as measured by the percentage of infected legs by BLI. Two isolates that best highlight this difference are 6416W and 6473W2, as they consistently had the lowest and highest infection incidence, respectively, across trials and models. This suggested an inherent difference in these isolates, which was borne out by histology. 6416W consistently had a predilection for producing a joint centered infection with 100% of bioluminescent legs showing joint inflammation in the intratibial model, and 75% in the hematogenous model. Conversely, 6416W only displayed bone involvement in 25% and 37% of bioluminescent legs in the respective models, and any bone involvement seemed to be secondary to the joint infection, occurring exclusively in the epiphyses. 6473W2 predominantly localized to the long bones, primarily femurs, producing abscesses in metaphysis and/or diaphysis, often associated with bacterial colonies. Bony changes with 6473W2 included loss of trabeculae in the metaphysis, sometimes extending through the growth plate into the epiphysis.In bioluminescent legs, 6473W2 produced bone centered infection in 80% of hematogenous and 87% of intratibial samples, with only 18% of hematogenous samples displaying minor joint inflammation. These distinct mouse models of S. aureus bone infection initiated by hematogenous spread and direct deposit will catalyze further study of OM pathogenesis and treatment.

***Disclosures: Philip Roper**, None*

P-726

Fibroblast growth factor receptor (FGFR)-selective tyrosine kinase inhibitors (TKI), such as infigratinib, show potency and selectivity for FGFR3 at pharmacologically relevant doses for the potential treatment of achondroplasia (ACH) *Katherine Dobscha[1], Ge Wei[1], Carl Dambkowski[1], Daniela Rogoff[1]. [1]QED Therapeutics Inc., United States

Background: Germline mutations in FGFR genes 1–3 can cause skeletal dysplasias and craniosynostoses. ACH, the most common form of disproportionate short stature, is caused primarily by an autosomal dominant G380R substitution in FGFR3. Infigratinib (BGJ398), a potent and selective FGFR1–3 TKI, demonstrated preclinical efficacy at low doses in an ACH mouse model. The objective of this analysis is to evaluate the dose dependency and toxicity profiles of FGFR-selective TKIs like infigratinib in preclinical skeletal dysplasia models.Methods: A review of the literature was performed to investigate non-clinical data from studies of infigratinib and other FGFR-selective TKIs relevant to FGFR-driven skeletal dysplasias. Major databases (e.g. PubMed, Medline [NLM Catalog]) were searched for relevant articles from the past 10 years and conference archives (e.g. ENDO, ESPE, ISDS, ASHG, ASBMR) for relevant abstracts from the past 5 years. Full text was included where possible. Keywords included in the searches were: achondroplasia, FGFR inhibition, infigratinib, BGJ398, AZD4547, PD173074, tyrosine kinase inhibitor.Results: Of the 683 publications identified, 10 relevant articles and 2 abstracts were selected for review. Due to direct relevance, 2 additional articles were included (total 14 publications). Infigratinib was the most commonly identified TKI. In vitro data showed inhibition of FGFR1–3 activity at concentrations of 5 to 100 nM, including reversal of established growth arrest in chondrocytes at 7 nM. In vivo studies revealed dose-dependent improvements in foramen magnum and long bone length in Fgfr3Y367C/+ mice at doses of 0.2–2 mg/kg/day. No studies reported a survival disadvantage and one showed a significant survival advantage for infigratinib-treated mice. For other FGFR TKIs, one study showed that AZD4547 decreased survival in mice treated at doses of 1x106 to 2x106 nM; another showed limb malformation in chicken embryos treated with PD173074 at doses of 1x106 to 50x106 nM. While one study suggested toxicity with FGFR-selective TKIs, the results were not generated at pharmacologically relevant doses for ACH, nor were they replicated in the literature. Furthermore, in vivo mice studies with low doses of infigratinib did not result in any of the abnormal findings observed in this study.Conclusions: Given the totality of evidence, low-dose infigratinib appears to be a potentially safe option for further development in children with ACH.

***Disclosures: Katherine Dobscha**, QED Therapeutics Inc., Other Financial or Material Support*

P-727

Mutant Mouse BMD Phenotypes for 509 Genes from the Mouse Mutant Informatics (MGI) Database *Robert Brommage[1]. [1]BoneGenomics, United States

Mouse models of human skeletal diseases contribute to understanding mechanisms and developing therapies for osteoporosis and rare human genetic skeletal diseases. Skeletal analyses of mutant mice often include dual-energy X-ray absorptiometry (DXA) measurements of bone mineral density (BMD).The Mouse Genome Database (MGD; http://www.informatics.jax.org) of the Mouse Genome Informatics (MGI) resource summarizes mutant mouse phenotypes . Data are derived from published papers and direct data submissions from the International Mouse Phenotyping Consortium (IMPC). The April 2020 database (MGI 6.15) provides 62,884 mutant alleles in 14,823 genes. Alleles showing BMD phenotypes include QTL loci (72), transgenes (24), spontaneous mutations (32), radiation-induced mutants (2), ENU chemical mutagenesis mutants (51), and engineered mutations employing gene-targeting (505), gene trap (11), and CRISPR/Cas9 (64) technologies. There are three long noncoding RNAs and two microRNAs.There are certainly unidentified false-positive phenotypes. Low body BMD is frequently observed in small-sized mice (often unhealthy from pleiotropic gene actions) and a limitation of body DXA scans is that measured body BMD is artifactually reduced in obese mice. BMD phenotypes can result from disrupting genes having pleiotropic actions in multiple tissues or from genes acting specifically in bone cells.These BMD mutant alleles comprise 509 unique genes, with 350 low BMD, 147 high BMD and 12 complex BMD phenotypes. Mutations in 61 homologous human genes result in human genetic skeletal disorders characterized by the International Skeletal Dysplasia Society. The IMPC high-throughput body BMD screen (http://www.mousephenotype.org) identified 173 low BMD and 81 high BMD mutant lines, with 2 lines showing opposite BMD phenotypes in males and females. Phenotypes consistent with small body size were present in 117 (68%) of the IMPC low BMD mutants. Elevated lean body mass occurs in 21 (26%) of the high BMD lines. The MGD also provides links to mutants having various skeletal structural abnormalities, including osteomalacia, osteopetrosis, osteogenesis imperfecta, craniofacial defects and spontaneous fractures. This summary provides a 2020 snapshot of

our knowledge and ignorance on the genetics of BMD and skeletal abnormalities in mouse models of human diseases.

***Disclosures: Robert Brommage**, None*

P-728

Low-dose infigratinib treatment does not lead to changes in phosphorus in preclinical animal studies *Maribel Reyes[1], Uma Sinha[2], Gary Li[1], David Martin[1]. [1]QED Therapeutics Inc., United States, [2]BridgeBio Pharma, United States

Background: Infigratinib (BGJ398) is a potent and selective FGFR1–3 inhibitor under evaluation for the treatment of achondroplasia (ACH), the most common form of disproportionate short stature. Low doses of infigratinib were effective in improving skeletal abnormalities in a mouse model of ACH [Demuynck et al. 2019; Komla-Ebri et al. 2016]. At higher doses in adults (e.g. 10–100-fold the dose shown to have efficacy in preclinical models of achondroplasia), infigratinib appears to be associated with elevation in phosphorus, an effect known to be associated with FGFR1 inhibition. Specifically, FGFR1 inhibition leads to decreases in FGF23 which, in turn, leads to decreased excretion of phosphate by the kidneys. We sought to understand the relationship between lower doses of infigratinib and changes in phosphorus in preclinical animal models.Methods: Changes in phosphorus were tested at multiple doses in three different species – mouse, rat, and dog – across five different studies. Infigratinib was given orally at doses ranging from 0.03 mg/kg to 30 mg/kg. Both PK and PD (i.e., phosphorus) data was available in all species. Measurement days ranged from day 10 to week 12, although PK/PD measurements occurred within 1 day of each other. All animals were treated in accordance with AVMA guidelines.Results: No significant dose-phosphorus relationship was observed in animals treated with doses of infigratinib ranging from 0.03 mg/kg to 5 mg/kg. A dose-phosphorus and exposure (AUC0-24)-phosphorus relationship was observed at doses of infigratinib >=10 mg/kg across transgenic mouse, rat, and dog studies. At low doses, the exposure (AUC0-24)-phosphorus relationship showed a shallow slope with linear regression analysis in rats and mice.Conclusions: These findings from five studies in three different species indicate that the exposure-phosphorus relationship is consistent. Importantly, no relationship was observed between dose and phosphorus levels in rats and mice treated with infigratinib at or below 5 mg/kg (human equivalent dose of 0.41 mg/kg based on mouse to human conversion). Despite hyperphosphatemia being an early on-target toxicity expected with infigratinib, this study suggests that low doses of infigratinib (shown previously to improve skeletal abnormalities in an ACH mouse model) do not result in meaningful changes in phosphorus. Infigratinib (planned dose of 0.016 mg/kg) will be evaluated in global clinical studies in children with ACH in 2020.

***Disclosures: Maribel Reyes**, QED Therapeutics Inc., Other Financial or Material Support, BridgeBio, Major Stock Shareholder, QED Therapeutics Inc., Major Stock Shareholder, Gilead Sciences, Major Stock Shareholder*

P-729

Characterization of Brittle Mechanical Phenotype in Amish G610C Model of Osteogenesis Imperfecta *Rachel Kohler[1], Carli Tastad[2], Amy Creecy[2], Joseph Wallace[2]. [1]Purdue University, United States, [2]Indiana University Purdue University Indianapolis, United States

Osteogenesis imperfecta (OI) is a hereditary bone disease where gene mutations affect collagen formation resulting in osteopenia and increased fracture risk. There are several established mouse models of OI, but these are often severe, resulting in spontaneous fractures or early animal death leading to significant specimen loss in preclinical studies. The Amish G610C mouse model is a newer, more moderate OI model that shows potential for use in intervention studies including those applying external mechanical loading. One limitation of this model to date is that it has been bred on several different inbred mouse strains so the data available in the literature regarding its bone phenotype are inconsistent. This study is the first comprehensive mechanical and architectural characterization of the bone quality of Amish mice based on a pure C57BL/6 inbred strain, and will provide a baseline for future treatment studies. Male and female wild-type (WT) and heterozygous (G610C) mice were euthanized at 10 and 16 weeks (n = 13-16). Harvested tibiae, femurs, and L4 vertebrae were scanned via micro-computed tomography (10 mm resolution), and analyzed for cortical and trabecular architectural properties. Right femurs and tibiae were then tested to failure in 3 or 4-point bending, respectively. G610C mice were found to have less bone but more highly mineralized cortical and trabecular tissue than their sex- and age-matched WT counterparts, with cortical cross-sectional area, thickness, and mineral density, and trabecular bone volume, mineral density, spacing and number all differing significantly as a function of genotype (2 Way ANOVA with main effects of sex and genotype at each age). In addition, mechanical yield force, ultimate force, displacement, strain, and toughness were all significantly lower in G610C vs. WT, resulting in a highly brittle phenotype. Importantly, there were no spontaneous fractures noted in any bones harvested from the Amish mice. This characterization demonstrates that despite being a moderate OI model, the Amish G610C mouse model maintains a distinctly brittle phenotype and is well-suited for use in treatment, loading, and mechanical analysis studies.

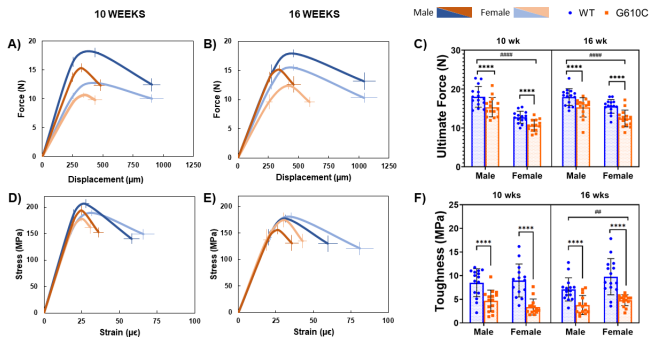

Figure 1. Mechanical properties of right tibiae. **A)** Average force-displacement plot for 10-week mice, showing weaker G610C bones. **B)** The strength disparity continued with the 16-week bones as quantified by **C)** the ultimate or maximum force. **D)** Average stress-strain plots for 10-week mice show how G610C bones break much quicker than WT bones. **E)** This brittle phenotype continued in the 16-week bones and can be quantified by **F)** bone toughness. (2-way ANOVA performed with main effects of sex and genotype at each age. ****, #### = p≤0.0001; ## = p≤0.01)

***Disclosures: Rachel Kohler**, None*

P-730

Mild Traumatic Brain Injury (TBI) in Mice-induces Releases of Osteogenic Growth Factors into Serum: A Potential Mechanism for Neurological Heterotopic Ossification *Subburaman Mohan[1], Chandrasekhar Kesavan [1]. [1]VALLHS, United States

Heterotrophic ossification (HO) is a serious disorder of an extra-skeletal bone formation in soft connective tissues that occurs as a common complication of trauma or in rare genetic disorders. It is now well established that patients who suffered from bone fracture combined with TBI are at significantly increased risk of HO (exceeds 50%). Although the pathophysiology of HO after TBI is poorly understood, recent findings of central nervous system control of bone mass by factors such as leptin, serotonin and neuropeptide Y suggest an important role for humoral factors from injured brain in contributing to peripheral osteogenesis at HO sites. To test for the hypothesis that TBI induces release of osteogenic molecules into serum, we tested the biological activity of serum samples collected from mice that were subjected to mild TBI or control anesthesia. Eight-week-old mice were subjected to mild TBI using an established weight drop model for four consecutive days and serum collected 24 hours after the last impact. Control mice were subjected to sham anesthesia without an injury to the brain. The effects of TBI and control sera on proliferation and differentiation of osteogenic cells were tested under serum-free conditions. We found that TBI serum promoted cell proliferation to a greater extent (20%, P<0.05) than control sera in both established mouse osteoblast cell line, MC3T3-E1, as well as primary cultures of osteoblasts-derived from calvaria of 7-day old mice. To determine if TBI-induced factors promoted differentiation, we measured alkaline phosphatase activity, a measure of osteoblast differentiation, after treatment with sera from mild TBI and control mice. We found that sera from TBI mice increased ALP activity by 50-100% (P<0.05) compared to control sera in MC3T3 and in ST2 stromal cell lines. In conclusion, our in vitro data demonstrate that TBI induced factors in serum stimulate both proliferation and differentiation of osteoblast lineage cells, thereby providing a potential mechanism for neurological HO.

***Disclosures: Subburaman Mohan**, None*

P-731

Assessment of bone microarchitecture and mineralization changes in an animal model of inflammatory bowel disease using high-resolution synchrotron-based microCT *Damian Myers[1], Christopher Hall[2], Ahmed Al Saidi[3], Ali Ghasem Zadeh[1], Shilpa Sharma[3], Sara Vogrin[3], Rhiannon Filippone[4], Anton Maksimenko[2], Daniel Häusermann[5], Kulmira Nurgali[6], Gustavo Duque[1]. [1]University of Melbourne and the Australian Institute for Musculoskeletal Science, Australia, [2]Australian Nucelar Science Technology Organisation, Australia, [3]University of Melbourne, Australia, [4]Victoria University, Australia, [5]Australian Synchrotron, Australia, [6]Victoria University and the Australian Institute for Musculoskeletal Science, Australia

Background: The Winnie-muc2 mouse (C57BL/6 background) exhibits pathophysiology of inflammatory bowel disease and other organ system changes, providing an opportunity to study bone loss related to malabsorption and other factors. We hypothesized that both bone microstructure and mineralization may differ in Winnie-muc2 mice so performed temporal studies using high-resolution synchrotron-based microCT (HR-S-μCT).Aim: To characterize cortical and trabecular metrics in Winnie-muc2 vs C57BL/6 mice including bone volume (BV), bone mineral density (BMD) and other ultrastructural parameters.Methods: Male and female animals (4-7/group) were euthanized after cardiac perfusion (4% PFA) at 6, 14 and 24wks and tibiae harvested then stored in 10% formol saline. MicroCT images were acquired at the Australian Synchrotron (25keV beam, 1800 projections, 6.82 μ3 isotropic volumes, at 2-3 mm below condyls). Volumes were reconstructed using XTRACTTM (CSIRO), trimmed using Image-J and processed using the BMA module in Analyze14.0 (Mayo Clinic).Results:• In Winnie-muc2 males (vs C57BL/6), whole BV was 26% lower

at 24 wks (0.99 mm3, IQR 0.82-1.16 vs 1.34 mm3, IQR 1.28-1.39 p=0.021) and in Winnie-muc2 females (vs C57BL/6 females) whole BV was less at 14 and 24wks (21%, p=0.11 and 9%, p=0.021, respectively) with both female groups decreasing over time.• Tb vBMD was sustained over time for all groups but Tb Tissue vBMD (Tb+IntraTb) was lower at 14 and 24 wks in Winnie-muc2 males (vs C57BL/6 males, p=0.047 and 0.021) and at 14 wks in females (vs C57BL/6 females; p=0.033).• Tb Tissue BMD in Winnie-muc2 males (vs C57BL/6 males) was 21% less at 14 wks (155 mg/cc, IQR 131-173 vs 203 mg/cc, IQR 175-215 p=0.043) and 32% less at 24 wks (116 mg/cc, IQR 105-128 vs 174 mg/cc, IQR 168-175 p=0.021). In females, both C57BL/6 and Winnie-muc2 showed similar temporal decreases over 6 to 24 wks (both p=0.021).• Whilst Tb BMD was sustained in Winnie-muc2 and C57BL/6 males, C57BL/6 females showed an increase from 6 to 24 wks (p=0.021), however, the Winnie-muc2 group did not change over time (p>0.05), indicating compromised mineralization of trabeculae in female Winnie-muc2.Conclusion: HR-S-µCT analysis reveals microarchitectural and BMD changes in the Winnie-muc2 that highlight the value of this model to study bone microarchitecture. This model exhibits severe bone loss and altered mineralization and will aid in the study of mechanisms and potential treatments for bone lytic diseases.

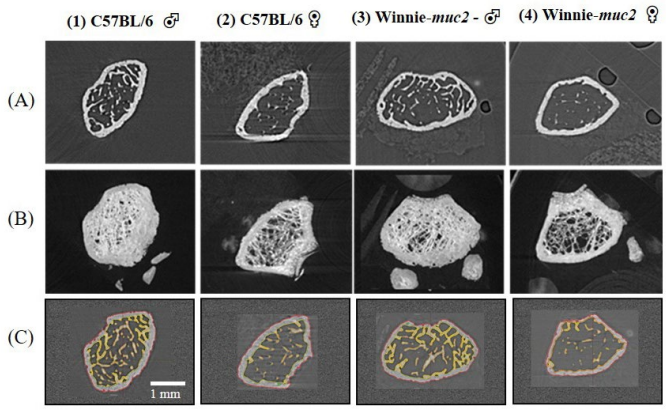

High-resolution synchrotron-based microtomography (HR-S-µCT) of tibiae. These panels show representative images from analysis of tibiae from Control (C57BL/6), and IBD (Winnie-*muc2*) groups at age of 14 weeks. These are axial orientation HR-S-µCT images of one slice (A) or a projection image of 10 slices (B); each from a of 160 slice bone. The lower panels (C) are representative images from the analysis of tibiae from control (C57BL/6; 1=Male and 2=Female) and IBD (Winnie-*muc2*; 3=Male and 4=Female) groups at age of 14 wks. (A) Single 6.82 micron slices (of 160 slices) from each of the samples; total acquisition was 1 mm thickness of tibia at a distance 2 mm proximal from the condyls; (B) Projection images of 10 slices with a total thickness of 68.2 microns; and, (C) Image frames from Analyze14 BMA analysis of single slices (6.82 microns) that demonstrate segmentation of samples into Cortex (red), Trabeculae (Yellow) and low-attenuation Trabecular Tissue (Orange=low mineralization).

***Disclosures: Damian Myers**, None*

P-732

Direct Four-Dimensional Assessment of Cortical Bone Basic Multicellular Unit Longitudinal Erosion Rate in PTH-Dosed Rabbits: A Novel Synchrotron X-Ray Imaging Approach *Kim Harrison[1], Erika Sales[1], Beverly Hiebert[1], Arash Panahifar[2], Ning Zhu[2], Terra Arnason[3], Peter Pivonka[4], Kurtis Swekla[5], David Cooper[1]. [1]Department of Anatomy, Physiology, and Pharmacology, College of Medicine, University of Saskatchewan, Canada, [2]BioMedical Imaging and Therapy Beamline, Canadian Light Source, Canada, [3]Department of Medicine, College of Medicine, University of Saskatchewan, Canada, [4]School of Mechanical, Medical, and Process Engineering, Queensland University of Technology, Australia, [5]Research Services and Ethics Office, Office of the Vice-President of Research, University of Saskatchewan, Canada

Basic Multicellular Units (BMUs) remodel cortical bone through the creation of secondary osteons via spatio-temporal coupling of osteoclastic and osteoblastic activities. Current understanding of BMU behavior has been developed largely from fluorochrome-based 2D histomorphometry. While effective at measuring bone formation, this approach cannot directly assess resorption rates, including the progression of the resorptive phase (cutting-cone) of BMUs - their Longitudinal Erosion Rate (LER). LER has only been inferred in classical studies of dogs from the rate at which the formative phase (closing-cone) of BMUs advance (~39 µm/day). A 3D imaging approach deployed longitudinally (4D) would, for the first time, enable direct measurement of LER; though, radiation dose and resolution limitations have presented significant challenges. Synchrotron-based X-ray phase contrast micro-CT presents an opportunity to overcome these challenges through superior detection of cortical porosity with improved radiation dose efficiency. Our objective was to develop and deploy a method for direct 4D measurement of LER in a rabbit model of elevated cortical bone remodeling induced by Parathyroid Hormone (PTH). In-line X-ray phase contrast micro-CT at the Canadian Light Source synchrotron was used to detect BMU-related resorption spaces (13 µm voxel size), in vivo, in the right tibiae of New Zealand White rabbits (n=5/group) at approximately 1, 2.5 and 5 Gy, 2 weeks after the initiation of PTH dosing (30 µg/kg/day). After 2 more weeks of PTH dosing, post-mortem ex vivo desktop micro-CT (5 µm voxel size) scans were performed and co-registered with the in vivo scans to directly assess LER via 3D landmarking. 3D (cortical porosity, canal diameter and cortical thickness) and 2D (total area, marrow area and cortical area) parameters compared between the irradiated and non-irradiated limbs revealed no differences, suggestive of no significant radiation impacts for all dose groups. LER was successfully assessed from 186 BMUs from 12 rabbits (4/group, ~ 12.4 BMUs/rabbit) and did not vary significantly by dose group. Pooled LER was 23.79 +/- 1.83 um/day. This study represents the first direct assessment of LER in 4D in an animal model. Imbalanced BMU activity is the root of osteoporotic bone loss and thus this novel platform holds great promise in the study of remodeling regulated bone adaptation and disease including consideration of BMU 4D spatio-temporal behavior.

***Disclosures: Kim Harrison**, None*

P-733

Altered Endochondral Ossification and Primary Cilia in a Hypothyroid Swine Model *Ashley Mohrman[1], Erica Reber[2], Fayez Safadi[2], Mark Adamczyk[1]. [1]Akron Children's Hospital, United States, [2]Northeast Ohio Medical University, United States

Hormonal defects in children are known to affect bone development, and specifically hypothyroidism (HypoTH) delays lengthening at the physis. A reversible, experimental HypoTH swine model was used to study primary cilia and differentiation of chondrocytes during endochondral ossification. Six male Sinclair mini-swine age 10 wk were evenly split into HypoTH and control (CTL) groups. HypoTH mini-swine were dosed orally with propylthiouracil for 15 wk while CTL animals received a placebo. Hindlimb endochondral samples were split for multiple analyses. Decalcified paraffin slides were stained with Safranin O and IHC staining for collagen type II (Col2) and type X (ColX) is underway. Individual zones and total growth plate (GP) height were quantitated using ImageJ. Thicker sections were dual-stained for acetylated tubulin and a cilia surface marker. Measures of primary cilia length and angle of emergence are underway. RNA was extracted and reverse transcribed from gene expression samples. Real-time PCR was used to assay markers of GP regulation (Col2; ColX; Sox9; aggrecan, Acan; matrix metalloproteinase 13, Mmp13; vascular endothelial factor, Vegf) as well as hedgehog signaling (Indian hedgehog, Ihh; patched; Gli transcription factor 2, Gli2). Differences between GP organization and cellularity are easily observed between CTL and HypoTH mini-swine (Figure 1A). Glycosaminoglycan staining did not demonstrate qualitative differences in matrix composition; however, trabeculae distal to the physes appear thicker in HypoTH samples than CTL and contained more undigested cartilage matrix. HypoTH physes have a significantly smaller hypertrophic fraction compared to CTL ($p<0.5$) (Figure 1B,C). Cilia have been identified in the GP of both groups, and measures of the angle of emergence and primary cilia length are underway. PCR results of key physeal regulators are shown in Figure 1D. Col2 and Ihh mRNA are significantly decreased in HypoTH physes compared to CTL. Though ColX mRNA appears greatly reduced in the HypoTH group, it is not statistically significant between groups. Lack of Ihh may indicate disruption of signaling through primary cilia. The hedgehog receptor, patched, and Gli2 will be assayed by PCR to confirm signaling deficits in the Ihh pathway. HypoTH physes showed reduced hypertrophy and Ihh expression, which is expected to correlate with reduced primary cilia function.

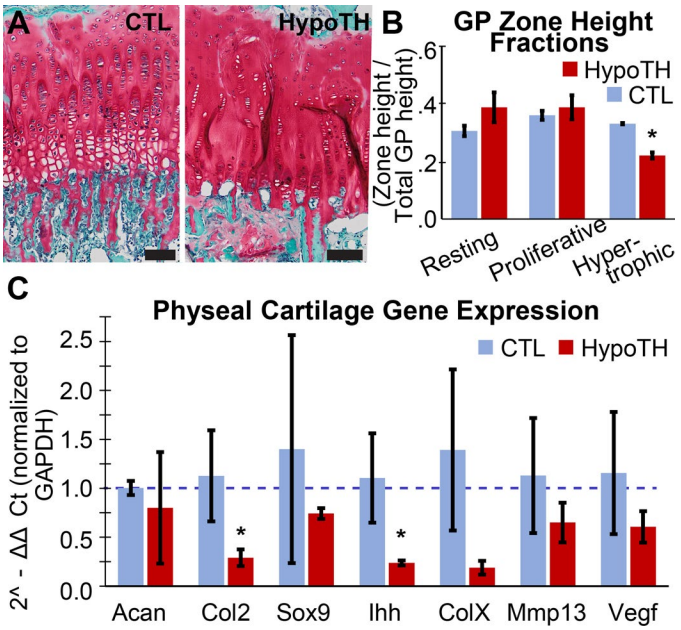

***Disclosures: Ashley Mohrman**, None*

Posters

P-734

NaQuinate Protects Against Ovariectomy-Induced Changes in Cortical Bone Mass and Architecture Through a Regionally Targeted Mechanism *Amy Lock[1], Stephanie Gohin[1], Behzad Javaheri[1], Mark Hopkinson[1], Ruby Chang[1], Robin Soper[2], Andrew Pitsillides[1], Stephen Hodges[1]. [1]Royal Veterinary College, United Kingdom, [2]Haoma Medica Ltd, United Kingdom

Background: Current therapies for osteoporosis have limited long-term use and create a gap for new anti-osteoporosis agents with greater safety margins. NaQuinate, a naphthoquinone carboxylic acid, increases cortical cross-sectional area (CSA) in the tibia of ovariectomized (OVX) rats. These beneficial effects on bone mass were targeted to specific cortical regions, modifying architecture to increase predicted resistance to torsion (J). A minimum effective NaQuinate dose of 250ug/Kg/day for tibial skeletal changes and 1500ug/Kg/day for increased femoral fracture resistance have been determined. The mechanism by which NaQuinate acts remains to be determined.Aims: To gain further insight into the skeletal mass and architectural effects of NaQuinate at the minimum effective dose in rat tibia of OVX rats in a confirmatory study by improved whole-bone, high-resolution micro-computed tomography analysis.Methods: Sham-operated (SO) and OVX rats were dosed daily (ip) for 6wks with either vehicle (5% EtOH in PBS) or NaQuinate (250µg/Kg/day). Whole tibiae were scanned by ex-vivo high-resolution micro-CT (9um resolution), manually segmented into whole-bone trabecular and cortical compartments and analysed along the entire tibial length for mass and architectural bone parameters.Results: NaQuinate exerted minimal changes in mass and architecture along the tibia in SO rats. In contrast, NaQuinate increased midshaft regional cortical CSA and J in OVX rats, confirming earlier findings and extending to a wider spatial range. There was an increase in CSA from 30-60% ($P<0.05$) and 80-90% ($P<0.05$) of the tibial length, indicating both diaphyseal mid-shaft and distal beneficial effects. There was an increase in cortical thickness in the midshaft tibial region of OVX rats (48-60%; $P<0.05$), with increases in the second moment of area around minor (Imin) and major axes (Imax) as well as J suggesting an increase in resistance to torsion. Both Imin and Imax were also significantly greater in the distal region (65-90%; $P<0.05$), again culminating in an overall increase in predicted resistance to torsion.Conclusions: Highly targeted and regional tibial increases in bone mass and shape in OVX rats by NaQuinate treatment were confirmed in this study. The findings have been extended to show changes in previously unexplored regions of the tibial cortex, suggesting that the observed skeletal changes may hold clues to a novel mechanism of action.

***Disclosures: Amy Lock**, None*

P-735

3D volumetric analysis is more sensitive than 1D linear analysis to detect bone loss in the ligature-induced periodontitis model. *Mizuho Kittaka[1], Marcus Levitan[2], Tetsuya Yoshimoto[1], Yasuyoshi Ueki[1]. [1]Department of Biomedical Sciences and Comprehensive Care, Indiana University School of Dentistry, Indianapolis, United States, [2]Indiana University School of Dentistry, Indianapolis, United States

The ligature-induced periodontitis model in mice is widely used to study the mechanism of bone loss in periodontitis. In this model, the distance between cementoenamel junction (CEJ)-alveolar bone crest (ABC) is preferentially used to assess the bone loss. This preference is based on the assumption that ABC is the primary site for osteoclastic bone resorption. However, many previous reports show that the induction of TRAP-positive osteoclasts occurs in more in-depth and broader areas of the alveolar bone beyond ABC. Therefore, we hypothesized that bone reduction is a 3-dimensional (3D) volumetric event rather than a 1-dimensional (1D) linear event in periodontitis and that sensitivity for detecting bone loss is different between 1D and 3D analysis.The maxillary left second molar of 10-week-old C57BL/6 mice was ligated with a silk suture to induce periodontitis. The right second molar was left un-ligated to serve as a control. After 5, 7, and 10 days maxilla was CT-scanned. Bone erosion was evident at all time points, but we observed periosteal reaction suggesting bone formation at day 7 and 10. Therefore, we performed a microCT analysis on day 5 to exclude the influence of bone formation. In the 1D analysis, total CEJ-ABC distance underneath the four cusps of the second molar was measured. To determine the net increase in the CEJ-ABC distance, we subtracted an increase in the periodontal ligament width at the apical root from the CEJ-ABC distance. In the 3D analysis, bone volume (BV/TV) between two buccal roots of the second molar, which is 140 µm of width, was measured.The CEJ-ABC measurement identified 10.7 +/- 7.0 and 19.0 +/- 8.5% differences, while the BV/TV measurement identified 28.6 +/- 9.6 and 26.3 +/- 8.5% differences in males and females, respectively, suggesting that the difference in BV/TV is more significant than that in CEJ-ABC. Furthermore, the BV/TV analysis detected the restoration of bone loss by antibiotics treatment in both genders, while the CEJ-ABC analysis failed to detect it.In conclusion, the 3D volumetric analysis showed superior sensitivity to the 1D linear analysis in detecting a bone loss in the ligature-induced periodontitis model. Measurement and assessment of multiple parameters will be required to prevent overlooking site- and stage-specific delicate alveolar bone loss.

***Disclosures: Mizuho Kittaka**, None*

P-737

Locally applied basic fibroblast growth factor promotes osseointegration of loosely inserted screw in rodent long bone: A preliminary study for salvage of failed screw fixation *Chikara Ushiku[1], Soki Kato[1], Hisashi Hashimoto[1], Masataka Okabe[1], Kazuhito Morioka[2], Shoshi Akiyama[1], Mitsuru Saito[1]. [1]The Jikei University School of Medicine, Japan, [2]University of California, San Francisco (UCSF) Orthopaedic Trauma Institute (OTI) Zuckerberg San Francisco General Hospital and Trauma Center (ZSFG), United States

Background:Screw fixation is a frequently used technique in orthopaedic and dental surgery, but one of the most common troubles that may occur with this fixation method is intraoperative screw loosening, in other word, iatrogenic loosening. Despite the widespread use of screw fixation in the management of fracture treatment, very few papers have looked at revision screw strategies. Purpose:To evaluate the local reaction of the screw hole which become bigger than screw size induced by basic fibroblast growth factor (bFGF) released from a gelatin hydrogel put on the top of screw for the purpose of osseointegration for salvage of a failed screw in the long bone. Methods:8-12-weeks-old female Sprague–Dawley rats were used. A hole was made in the tibia diaphysis with a 14G needle (outer diameter, 2.1 mm) as the screw hole. A stainless screw with 1.43 mm outer diameter of threads and 3.0 mm of the screw head was installed in the hole. Gelatin-based hydrogel contained either saline (control group) or 10 µg bFGF (bFGF group) was applied onto the top of the screw head. Samples were examined histologically at 1 and 6 weeks after surgery. Results:A gap between the screw and bone was not filled with a new bone at 1 week in the both control and bFGF groups. Six weeks after the surgery, in the bFGF group, massive new bone formation was found in the area adjacent to the screw where the gap between screw and bone was originally seen. The mean bone implant contact ratio in the control group at 6 weeks was 17.543% +/- 4.241%, whereas it was 19.745 +/- 4.722% in the rh-FGF2 group at 6 weeks. Conclusion:We investigated whether local application of gelatin-hydrogel contained bFGF might improve osseointegration in a developed rat model of screw loosening. Histological observations indicated that new bone formation at the area close to the screw was higher in the bFGF group compared to the control group.

***Disclosures: Chikara Ushiku**, None*

P-738

In Vitro Osteoclast Assay as a Predictor of Zoledronate Response In Vivo *Jukka Rissanen[1], Katja Fagerlund[1], ZhiQi Peng[1], Jukka Morko[1]. [1]Pharmatest Services, Finland

Bisphosphonates (BP) are used to treat a number of bone diseases including osteoporosis, cancer bone metastases and rare bone diseases such as osteogenesis imperfecta. Preclinical evaluation of drug candidates for treating bone diseases often utilize clinically used drug, such as BP's, as a reference compound to demonstrate in vitro or in vivo test system potency. However, there is no universal conversion formula from in vitro to in vivo dose and, therefore, dose conversion is determined based on experimental data. In this study, dose-response of a nitrogen containing bisphosphonate zoledronate (ZOL) was determined in in vitro human osteoclast assay and obtained dose-response was used as a predictor of ZOL response in vivo in adult ovariectomized (OVX) rat model of human postmenopausal osteoporosis. In the osteoclast assay, human CD34+ osteoclasts were cultured on bovine bone slices in the presence of ZOL (1-1000 µM). C-terminal cross-linked telopeptides of type I collagen (CTX-I) was measured from the culture medium to quantitate bone resorption. Based on the EC50 value in osteoclast assay 20 µg/kg dose was selected for in vivo study with 6-month-old female OVX rats. The selected 20 µg/kg (sc) ZOL single dose completely prevented OVX induced osteopenia in trabecular bone as assessed by peripheral quantitative computed tomography (pQCT) and histomorphometry during 8-week follow-up period. By using ZOL as an example of commonly used bone disorder drug, this study demonstrated dose conversion of ZOL from in vitro osteoclast assay to in vivo rat OVX model and typical effective doses in those studies.

***Disclosures: Jukka Rissanen**, None*

P-739

Greater Activation of Modeling-Based Bone Formation and Improvement in Bone Microarchitecture by Intermittent PTHrP vs. PTH in Ovariectomized (OVX) Rats *Tala Azar[1], Wenzheng Wang[1], Wei-Ju Tseng[1], Hongbo Zhao[1], Nathaniel Dyment[1], Xiaowei Sherry Liu[1]. [1]University of Pennsylvania, United States

Similar to parathyroid hormone (PTH), PTH-related protein analog (PTHrP), an FDA approved treatment for postmenopausal osteoporosis, exhibits anabolic effect when administered intermittently. However, the effects of PTH and PTHrP at the trabecular level, including microarchitecture and types of bone formation (BF) induced, have not been compared. Modeling-based BF (MBF - BF on quiescent surfaces) and remodeling-based BF (RBF - BF coupled with resorption by osteoclasts), are important mechanisms by which anabolic agents improve bone mass. We hypothesized that different levels of MBF and RBF induced by PTHrP vs. PTH may lead to different degrees of improvement in bone microarchitecture. We injected calcein (green, G), alizarin complexone (red, R), and tetracycline (yellow, Y)

fluorochrome labels in a G-R-Y-G sequence on days -2, 5, 12, and 19 (treatment initiated on day 0) with euthanasia on day 21 in 5-mo-old OVX rats. In VEH-, PTH- (20 µg/kg), and PTHrP-treated (20 µg/kg) samples (n=6/group, Fig A-C), fluorochrome labels and cement lines on cryo-sections of tibial trabecular bone were used to identify MBF (smooth cement line, Fig D) or RBF (scalloped cement line, Fig E) sites. Compared to VEH, both PTH and PTHrP groups had significantly greater MBF- and RBF-induced mineralizing surface (MS/BS), mineral apposition rate (MAR), and bone formation rate (BFR/BS, Fig F-H). Compared to PTH, PTHrP activated 55% and 50% greater MBF-induced MS/BS and BFR/BS, respectively. MAR did not differ between PTH and PTHrP, indicating similar rates of mineral deposition at each BF site. Conversely, there were similar increases of RBF-induced MS/BS, MAR, and BFR/BS in response to PTH vs. PTHrP.In vivo µCT at wks 0 and 3 (Fig I) demonstrated that PTH and PTHrP (40 µg/kg, n=7-9/group) improved bone volume fraction (BV/TV), thickness (Tb.Th), and number (Tb.N) of tibial trabecular bone, and yielded more plate-like trabeculae indicated by reduced structure model index (SMI, Figs J-M). Compared to PTH, PTHrP led to greater improvement in BV/TV (78% vs. 54%), more plate-like trabeculae (-0.8 vs. -0.6 in SMI), and less reduction in Tb.N (-1% vs. -14%). Increases in Tb.Th did not differ between PTH and PTHrP.In conclusion, compared to PTH, PTHrP treatment better improved trabecular bone volume and microarchitecture in estrogen deficient rats. This may be due to greater activation of new MBF sites that most efficiently enhance structural integrity of the trabecular network.

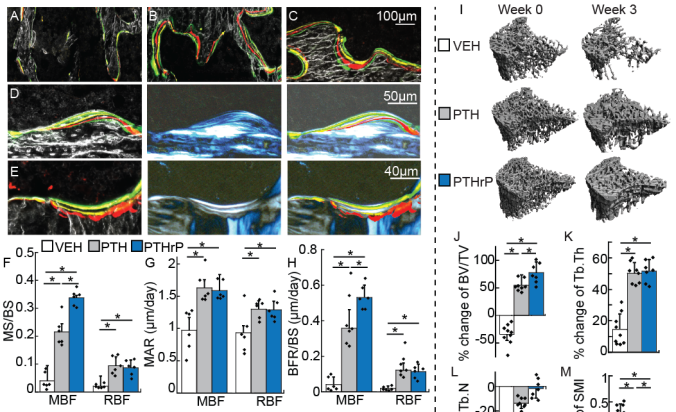

(A-C) Representative images of bone dynamics of (A) VEH, (B) PTH, and (C) PTHrP groups. (D-E) Representative images of (D) MBF sites and (E) RBF sites where MBF sites were identified by smooth cement lines and uniform collagen fiber alignment indicated by polarized images while RBF sites were identified by scalloped cement lines with interrupted collagen fiber alignment. (F) MS/BS, (G) MAR, and (H) BFR/BS of MBF and RBF. (I) Representative trabecular bone images at weeks 0 and 3. (J-M) % change in (J) BV/TV, (K) Tb.Th, (L) Tb.N, and (M) raw change in SMI from registered scans. *p< 0.05 by one-way ANOVA.

***Disclosures: Tala Azar**, None*

P-740

A synbiotic treatment protects from ovariectomy-induced trabecular bone loss and correlates with microbiome pathway enrichment for fiber degradation, and SCFA and vitamin K2 production *Lina Lawenius[1], Karin L. Gustafsson[1], Jianyao Wu[1], Karin H. Nilsson[1], Sofia Movérare-Skrtic[1], Eric M. Schott[2], Maria J. Soto-Giron[2], Gerardo V. Toledo[2], Klara Sjögren[1], Claes Ohlsson[1]. [1]Centre for Bone and Arthritis Research, Institute of Medicine, Sahlgrenska Academy at University of Gothenburg, Gothenburg, Sweden, Sweden, [2]Solarea Bio, Cambridge, Massachusetts, USA, United States

As fear of side effects of current osteoporosis therapeutics have led to low treatment rates and adherence to medication, a safer, more natural alternative is needed. Recent reports have shown that certain strains of Lactobacillus can protect against bone loss induced by estrogen deficiency in both rodents and humans. To date, no study has shown whether a combinatorial effect of a synbiotic product (probiotic bacteria and prebiotic fibers), or other microbes including fungi could expand available bone-sparing probiotics.The aim with this project was to develop a novel synbiotic intervention at an optimal dose to prevent bone loss in ovariectomized (ovx) mice. We hypothesized that microbes naturally occurring in fresh or fermented fruits and vegetables might provide beneficial health effects. To test this, we isolated and sequenced the genomes of >4,000 bacterial and fungal strains from these food sources. Using genomic, ecological, and functional insights, we prioritized the synbiotic consortium SBD111, with the greatest capacity to produce short chain fatty acids (SCFA) from plant fibers and code for vitamin K2 biosynthesis compared to other combinations. SBD111 consists of lactic acid bacteria, gammaproteobacteria, yeast, and prebiotic plant fibers.To determine if SBD111 protects from ovx-induced bone loss, 10 week-old-mice were ovx and treated by daily oral gavage with vehicle, the prebiotic fibers of SBD111 or three doses of SBD111 (low 5x108; medium 5x109; or high 1.5x1010 total CFU/dose) with prebiotic fibers for 4 weeks. Both the medium (trabecular BMD, +14.1%; p<=0.01) and high (+17.1%; p<=0.01) dose of SBD111 protected from ovx-induced trabecular bone loss in the distal femur compared to vehicle treatment. Both the low (trabecular BMD, +9.9%; p<=0.01) and medium (+11.4%; p=0.01) dose protected from ovx-induced trabecular bone loss in vertebra L5 and a similar trend was observed for the high dose (+7.2%; p=0.06). No effect of the prebiotic fiber alone was observed. To connect the bone protective phenotype with functional changes in the microbiome, fecal samples were analyzed using shotgun metagenomics. We observed an enrichment in the relative gene abundance of pathways related to fiber degradation, and SCFA and vitamin K2 production in SBD111-treated ovx mice.In conclusion, using a novel strategy targeting specific pathways within the microbiome, we have developed a synbiotic treatment that protects from bone loss caused by estrogen deficiency.

***Disclosures: Lina Lawenius**, None*

P-741

Effects of Teriparatide and Low-Intensity Aerobic Exercise on Osteopenia and Muscle Atrophy in Type 2 Diabetes Mellitus Model Rats *Kazunobu Abe[1], Naohisa Miyakoshi[1], Yuji Kasukawa[1], Koji Nozaka[1], Hiroyuki Tsuchie[1], Chiaki Sato[1], Hikaru Saito[1], Ryo Shoji[1], Yoichi Shimada[1]. [1]Akita university graduate school of medicine, Japan

Purpose: In patients with type 2 diabetes mellitus (T2DM), bone fragility and sarcopenia increase the risk of fractures and falls. Teriparatide (TPTD) increases bone strength by promoting bone formation. On the other hand, exercise therapy has been shown to increase bone mineral density (BMD), prevent falling, and promote muscle remodeling and hypertrophy effects. However, there have been few reports on their combined effects on bone and skeletal muscle. In this study, we examined the effects of TPTD and exercise therapy on bone and skeletal muscle in T2DM rats. Methods: Thirty-week-old T2DM model rats (Otsuka Long-Evans Tokushima Fatty) were divided into four groups: Control (vehicle-treated, sedentary, hereafter referred to as Cont), TPTD (30 µg/kg subcutaneously injected, 3 times/week), Exercise (treadmill exercise, 10 m/min, 60 min/day, 5 times/week, hereafter referred to as Exe), and Combined (TPTD-treated and treadmill exercise combined, hereafter referred to as Comb) groups. Long-Evans Tokushima Otsuka (LETO) rats were used as a nondiabetic control (n=9-10 per group). At 5 weeks after treatment, blood glucose levels, BMD of the lumbar spine and the femur, bone strength of the middle shaft and the distal metaphysis of the femur, and wet weight of the tibialis anterior (TA) and soleus muscles were assessed. Results: Blood glucose levels in the Cont group were significantly higher in the T2DM model rats than in the LETO rats ($p < 0.01$), but there was no significant difference between the four intervention groups. BMDs of the lumbar spine and the femur were significantly higher ($p < 0.01$) only in the Comb group compared to the Cont group. In the three-point bending test of the middle shaft of the femur, the maximum load in the Comb group was significantly higher than in the Cont and Exe groups ($p < 0.01$). In the compression test of the distal metaphysis of the femur, the maximum loads in the TPTD and Comb groups were significantly higher than in the Cont and Exe groups ($p < 0.01$). On the other hand, the wet weight of the TA and soleus muscles in the Cont group was significantly lower than in the LETO rats (respectively $p < 0.001$ and $p < 0.01$), but neither were significantly different among the four intervention groups. Conclusions: The combination of TPTD and treadmill exercise increased BMD and bone strength of the lumbar spine and the femur in T2DM model rats. On the other hand, there was no effect on muscle wet weight in either the TA or the soleus.

***Disclosures: Kazunobu Abe**, None*

P-742

Effects of Low and High Dietary Phosphorus and Acute High Dietary Phosphorus on Intestinal Phosphorus Fractional Absorption in Nephrectomized Male Rats *Kendal Schmitz[1], Dennis Cladis[1], Colby Vorland[2], Ying Dong[3], Meryl Wastney[3], Sharon Moe[4], Kathleen Hill Gallant[1]. [1]Department of Nutrition Science, Purdue University; Department of Food Science and Nutrition, University of Minnesota, United States, [2]Department of Applied Health Science, Indiana University School of Public Health-Bloomington, United States, [3]Department of Nutrition Science, Purdue University, United States, [4]Department of Medicine-Division of Nephrology, Indiana University School of Medicine, United States

Dietary phosphorus (P) restriction and phosphate binder medications are common therapies for patients with chronic kidney disease (CKD). The goal of these therapies is to reduce intestinal P absorption to slow the development of CKD-mineral and bone disorder. However, bouts of non-adherence to these interventions could cause unintended consequences of spikes in P absorption and serum P due to increased intestinal P absorption efficiency. This has been observed in healthy rats using in vitro methods for assessing intestinal P uptake but has not been evaluated in CKD rats nor with in vivo absorption testing methods. This study aimed to determine the effects of dietary P level in CKD and normal rats using a 2x3 factorial design. Male Sprague-Dawley rats with 5/6 nephrectomy (n=36) or sham operation (n=36) were block randomized to one of three diets: low P (LP, 0.1%), high P (HP, 1.2%), or low P followed by acute high P (LPHP, 0.1% then 1.2%) (n=12/group) and were fed for 4h/d for 7 days. LPHP rats were fed the LP diet on days 1-6 and the HP diet on day 7. Following the final feeding period, rats underwent an in vivo intestinal P absorption test using 33P radioisotope administered either by oral gavage or IV. Fractional P absorption was determined from the ratio of area under the oral and IV plasma 33P curves (AUCPO/AUCIV)

from serial blood draws over 2 hours. A linear mixed model was used to determine main effects of diet and disease and the interaction. Results show a main effect of diet (p=0.03), no effect of disease (p=0.31), and no interaction effect (p=0.98). LP rats had higher fractional P absorption (0.13 +/- 0.01) compared to HP rats (0.08 +/- 0.01, p(diff)=0.046) or LPHP rats (0.08 +/- 0.01, p(diff)=0.049). Fractional P absorption was not different between HP and LPHP (p(diff)=0.999). These results are consistent with prior studies using in vitro methods showing an increase in P uptake efficiency with P restriction. The lack of statistical difference for P absorption efficiency between CKD and sham rats aligns with other emerging reports that CKD does not reduce P absorption efficiency. Importantly, these results show a rapid response to reduce intestinal P absorption efficiency when an acute high P load is given following a week of dietary P restriction. This is evidence against the notion that dietary P restriction causes an unintended harm of increased absorption efficiency during dietary non-adherence.

***Disclosures: Kendal Schmitz**, None*

P-743

Reconstitution of the Host Holobiont Acutely Increases Bone Growth of the Gnotobiotic Rat *Piotr Czernik[1], Rachel M Golonka[1], Saroj Chakraborty[1], BengSan Yeoh[1], Saha Piu[1], Abdullah Ahmed[1], Blair Mell[1], Y Tian[2], AD Patterson[0], Bina Joe[1], Matam Vijay-Kumar[0], Beata Lecka-Czernik[3]. [1]University of Toledo, Microbiome Consortium, College of Medicine and Life Sciences, Dept. Physiology and Pharmacology, United States, [2]The Pennsylvania State University, Dept. Veterinary and Biomedical Sciences, United States, [0]The Pennsylvania State University, Dept. Veterinary and Biomedical Sciences, United States, [0]University of Toledo, Microbiome Consortium, College of Medicine and Life Sciences, Dept. Physiology and Pharmacology, United States, [3]University of Toledo, College of Medicine and Life Sciences, Dept. Orthopaedic Surgery, United States

In recent years there has been growing evidence regarding the influence of microbiota on the skeletal growth and homeostasis in humans and rodents. Here we present for the first time an accelerated longitudinal and radial bone growth in response to short-term exposure of germ-free rats to newly established gut microbiota. In our study, 7 week-old germ-free male rats were colonized with microbiota through co-housing with conventional rats of the same sex and age. Changes in bone mass and structure were analyzed 10 days post colonization and revealed unprecedented acceleration of bone accrual in cortical and trabecular compartments, increased bone tissue mineral density, improved proliferation and hypertrophy of growth plate chondrocytes, bone lengthening, and preferential deposition of periosteal bone in tibia diaphysis. It is widely accepted that short-chain fatty acids (SCFA, e.g. acetate, propionate and butyrate) produced by gut microbiota act as regulatory metabolites, and affect bone growth through a variety of molecular mechanisms. The observed changes in bone status were paralleled with a dramatic increase in cecal concentration of all three SCFA and increased hepatic Igf-1 expression implicating an involvement of the somatotropic axis. Increased serum levels 25-OH vitamin D and alkaline phosphatase pointed towards active process of bone formation. Our studies demonstrate that gut microbiotal metabolic products can deliver powerful signals to the skeleton and accelerate bone expansion resembling adolescent growth spurt. Our findings may help in developing microbiota-based therapeutics to combat bone related disorders resulting from the microbiotal dysbiosis-associated with hormonal defects and malnutrition in children.

***Disclosures: Piotr Czernik**, None*

P-744

The effects of a phosphate-enriched diet on the progression of chronic kidney disease in an experimental 5/6-nephrectomy model in C57BL/6 mice *Judith Radloff[1], Nejla Latic[1], Ulrike Pfeiffenberger[1], Claudia Bergow[1], Reinhold Erben[1]. [1]Veterinary University of Vienna, Austria

Surgical removal of functional kidney mass is a commonly used experimental model to study pathophysiological processes in chronic kidney disease (CKD). C57Bl/6 mice are known to be rather resistant to the development of CKD after 5/6-nephrectomy (NX). Because it is known that increased phosphate intake aggravates the progression of renal injury, we sought to characterize the development of CKD and its cardiac and skeletal sequelae during the first three months after experimental CKD induction in C57Bl/6 mice on a phosphate-enriched diet. CKD was surgically induced by two-step 5/6-nephrectomy in 12-week-old male C57BL/6 mice. Age- and sex-matched animals underwent Sham surgery. All mice were maintained on a diet enriched with phosphate, calcium and lactose. Intra-arterial blood pressure measurements were performed 4, 8 and 12 weeks post-surgery. Serum concentrations of aldosterone, intact FGF23 and intact PTH were measured by immunoassays. Skeletal phenotyping included bone histomorphometry and assessment of bone mass by peripheral quantitative computed tomography (pQCT) in lumbar vertebrae and tibiae. Picrosirius red staining of renal and cardiac paraffin sections was performed to assess fibrosis. Serum creatinine and urea levels significantly increased in NX mice when compared to Sham controls. Serum levels of aldosterone, FGF23 and PTH were increased in NX mice at all time points. In line with decreased volumetric bone mineral density in lumbar vertebrae and tibiae, serum alkaline phosphatase activity as well as osteoclast numbers and mineralization lag time were increased in NX mice. Furthermore, cortical thickness of the tibial shaft was decreased in NX mice at 12 weeks after 5/6-Nx, relative to Sham controls. Histological assessment of kidney paraffin sections revealed increasing interstitial fibrosis with time postsurgery in NX mice. Moreover, NX mice showed elevated mean arterial pressure and pulse pressure, relative to Sham mice at 12 weeks after 5/6-Nx, but not at earlier time points. Collectively, our data show that 5/6-Nx in BL/6 mice on a phosphate-rich diet leads to increased serum creatinine and urea levels, tubulointerstitial fibrosis, progressive cortical bone loss, impaired bone mineralization, and the development of hypertension, all hallmarks of clinical CKD. Therefore, our model may be useful for gaining further insights into the pathophysiology of cardiovascular and bone disorders associated with CKD.

***Disclosures: Judith Radloff**, None*

P-745

Treatment with a Chimeric Long-Acting CSF1 Molecule Enhances Fracture Healing *Lena Batoon[2], Susan Millard[2], Kyle Williams[2], Wenhao Sun[2], Cheyenne Sandrock[2], Andy Wu[3], Martin Wullschleger[4], Katharine Irvine[2], Vaida Glatt[5], Liza Raggatt[2], David Hume[2], Allison Pettit[2]. [2]Mater Research Institute-The University of Queensland, Australia, [2]Mater Research Institute-The University of Queensland, Singapore, [3]Translational Research Institute, Australia, [4]Gold Coast University Hospital, Australia, [5]University of Texas Health Science Center San Antonio, United States

Macrophage colony-stimulating factor 1 (CSF1) controls the proliferation, differentiation and function of osteoclasts and macrophages. Exogenous CSF1 has been shown to have anabolic effects on multiple tissues, including the ability to promote bone repair. Clinical and pre-clinical CSF1 applications have been constrained by its short circulating half-life. This limitation was overcome by engineering a chimeric CSF1 molecule, CSF1-Fc, to bypass renal clearance, facilitating a more potent and long-acting CSF1-receptor signaling. We tested weekly and biweekly CSF1-Fc treatment regimens over a 4-week period in adult 12-16-week-old female and male mice. Histomorphometric analysis showed F4/80+ osteal macrophage number was unchanged after either regimen, while TRAP+ osteoclast surface/trabecular bone surface was significantly increased only after biweekly CSF1-Fc treatment (p=0.0071) irrespective of gender. Hence, weekly CSF1-Fc treatment had minimal impact on bone-related myeloid cell populations under homeostatic conditions. To assess whether this non-myeloproliferative CSF1-Fc regimen primed regenerative mechanisms, we investigated the therapeutic potential in bone regeneration using the MouseFix internally plated femoral fracture model. Weekly CSF1-Fc treatment for 4 weeks post-fracture significantly increased bone marrow macrophages as examined by flow cytometry (p<0.0001) but did not alter osteoclast surface/trabecular bone surface on the contralateral/unfractured limb. Torsional strength testing of the fractured femora revealed CSF1-Fc treatment significantly increased fracture maximum torque (+44%). Collectively, our results indicate that targeting macrophages using a weekly CSF1-Fc treatment regimen is a promising fracture therapeutic to promote bone regeneration.

***Disclosures: Lena Batoon**, None*

P-746

Iron deficiency does not impact femoral bone properties in young female rats following 12-weeks of high-intensity running *Jonathan Scott[1], Yasmin Mejia-Guevara[2], Elizabeth Swallow[3], Corinne Metzger[3], Alexander Stacy[3], Matthew Allen[3], Heath Gasier[4]. [1]Department of Military and Emergency Medicine, Uniformed Services University, United States, [2]Henry M. Jackson Foundation f or the Advancement of Military Medicine, United States, [3]Department of Anatomy and Cell Biology, Indiana University School of Medicine, United States, [4]Department of Anesthesiology, Duke University, United States

Purpose: Up to 20% of females sustain stress fractures during initial military training, and ~1/3 of female recruits who finish training develop iron deficiency. Iron is a cofactor in bone collagen formation, thus we hypothesized iron deficiency is contributing to altered bone structure and mechanics during periods of increased mechanical loading.Methods: Three-week old female Sprague-Dawley rats were assigned to one of four groups (n = 10/group): iron adequate sedentary (IAS), iron deficient sedentary (IDS), iron adequate exercise (IAE), and iron deficient exercise (IDE). IDS and IDE rats consumed a modified AIN-93G diet containing no added iron, whereas IAS and IAE consumed a control diet. Energy and macronutrient composition were similar between diets. IAE and IDE rats performed 54 min of high-intensity running three times/week. After 12-weeks, rats were euthanized and blood and whole femora were collected. Blood and serum were used to measure iron status and biomarkers of bone formation and resorption. Microcomputed tomography was used to measure cortical geometry and cancellous microarchitecture. Four-point bending tests were used to measure mechanical properties. All animal procedures were approved by the Uniformed Services University Institutional Animal Care and Use Committee. Analyses were completed using a two-way repeated measures ANOVA.Results: Body weight was similar between groups at the end of the 12-weeks. An iron deficient diet led to reductions in Hemoglobin (Hb), hematocrit, mean corpuscular Hb (MCH), MCH concentration, and red cell distribution width. Iron deficiency increased tartrate-resistant acid phosphatase 5b (TRAcP 5b) (11%) and CTx (50%) levels compared to IAS rats. Exercise (IAE + IDE) increased CTx (51%) and osteocalcin (14%) levels compared to IAS rats. IDE increased the levels of TRAcP 5b (17%) and P1NP (6%) compared to IAS rats. Independent of diet, exercise

increased Ct.Th (5%), BV/TV (22%), and Tb.Th (9%) and maximum load (7%) compared to sedentary rats.Conclusion: These data show femoral bone geometry and mechanics are unaffected by diet-induced iron deficiency during 12-weeks of high-intensity running in young growing female rats.

***Disclosures: Jonathan Scott**, None*

P-747

Analysis of bone and muscle in a adenine-induced chronic kidney disease model rats *Hikaru Saito[1], Miyakoshi Naohisa[1], Yuji Kasukawa[1], Koji Nozaka[1], Hiroyuki Tsuchie[1], Chiaki Sato[1], Kazunobu Abe[1], Ryo Shoji[1], Yoichi Shimada[1]. [1]Department of Orthopedic Surgery, Akita University Graduate School of Medicine, Japan

[Background]Patients with chronic kidney disease (CKD) are at increased risk of falls and fractures due to decreased bone and muscle strength. However, there is insufficient evidence about how bone loss and muscle weakness progresses in patients with advanced CKD. In the present study, we generated adenine-induced CKD model rats and examined the changes in bone and muscle.[Methods]Eight-week-old male Wistar rats were treated with a 0.75% adenine diet for 4 weeks, followed by a regular diet to generate CKD model rats (CKD group). The CKD and Sham groups were sacrificed at 12, 16, and 20 weeks of age, and the following parameters were evaluated. Bone was evaluated by bone mineral density (BMD) of whole body by dual energy X-ray absorptiometry, bone strength testing by the three-point bending test of femoral shaft and compression test of distal femoral metaphysis, and bone structural analysis and BMD of the distal femur using micro-computed tomography (micro-CT). Muscle wet weights of the tibialis anterior and soleus muscles were measured to assess the muscle. Blood urea nitrogen (BUN), serum creatinine (Cre), phosphorus (P), and calcium (Ca) were measured as serologic assessments. Renal tissue sections were stained with Elastica Masson to evaluate the kidney and the area of fibrotic interstitium was measured.[Results]In the CKD group, whole body BMD was reduced at 12, 16 and 20 weeks of age ($P < 0.05$). In addition, micro-CT at 20 weeks of age in the CKD group showed decreased trabecular BMD, cortical BMD, cortical bone area, and cortical bone thickness ($P < 0.05$). Breaking energy and maximum load by the bone strength testing in the CKD group were significantly decreased compared with the sham group at 20 weeks of age ($P < 0.05$). At 20 weeks of age in the CKD group, tibialis anterior and soleus muscle wet weights were smaller ($P < 0.05$), but there was no significant difference in their percentage relative to body weight. BUN, Cre and serum P levels at 20 weeks of age in the CKD group were significantly higher than those in the sham group ($P < 0.05$). Renal tissue sections from the CKD group showed a greater rate of interstitial fibrosis ($P < 0.05$).[Conclusion] CKD model rats induced by adenine diet revealed serologically CKD stage 4. This CKD model rats also presented decreased BMD, bone microstructural deterioration in the cortical bone, and decreased bone strength, although the muscle wet weight as a percentage of body weight did not change.

***Disclosures: Hikaru Saito**, None*

P-748

Pharmacokinetics and Biodistribution of Bone Fracture Targeted Abaloparatide *STEWART LOW[1], Jeffery Nielsen[1], Philip Low[1]. [1]Purdue University, United States

PURPOSE:Previously we have demonstrated the efficacy of a fracture targeted abaloparatide. Following systemic injection, the targeted bone anabolic accumulates selectively on a bone fracture surface and improves the rate of fracture repair as well as the quality of the bone. Here we seek to understand the pharmacokinetics (PK) and elucidate the minimal dosing frequency while maintaining therapeutic concentrations of drugMETHODS:To achieve the above objective, we synthesized a modified abaloparatide. On the C-terminus of the abalo we conjugated a bone mineral-(hydroxyapatite-) targeting acidic oligopeptide forming NOV004.Murine in vivo experiments were conducted on female Swiss Webster mice (3 per group). Femoral fractures stabilized by locking nail. Two weeks post fracture, mice were dosed with 0.03 nmol/kg/dose of radiolabeled NOV004 or non-conjugated (free) radiolabeled abalo. Mice were euthanized at time points 1 h, 2 h, 4 h, 8 h, 16 h, 24 h, 36 h, 48 h, 72 h, 120 h, and 168 h. Blood, heart, lung, liver, spleens, kidney, skin(injection site), healthy femur, and fracture femur samples were collected from each mouse and counted on a gamma counter. SPECT/CT imaging mice were euthanized at 16h and were imaged on a SPEC II CT (MiLabs).RESULTS SECTION:In SPECT/CT imaging studies we observed a marked increase fracture callus accumulation. Small off target accumulation was noted in areas of high cancellous bone. However, accumulation at the fracture site was over 10-fold the accumulation per unit volume of any of the off target skeletal sites.No significant differences between NOV004 and abalo were observed in the blood PK half-life (4.2h and 3.7h respectively). In addition, area under the curve (AUC), a measurement of whole-body exposure were 24.5 and 28.02 for NOV004 and abalo respectively. When comparing the fracture sites 11-fold increase in AUC of NOV004 to abalo and an half-life improvement of 66.6 h and 8.8 h occurred.Conclusions:Previously we observed improved and accelerated fracture repair from NOV004 over abalo or saline during daily dosing over a wide therapeutic range. In this study we observe that less frequent dosing is likely possible due to the long half-life in the fractured bone. Futhermore, we do not observe extra systemic exposures when compared to abalo. Considering this data, it we can reduce dosing frequency to twice a week or fewer without losing efficacy or increasing side effects, making this drug easier for the patient.

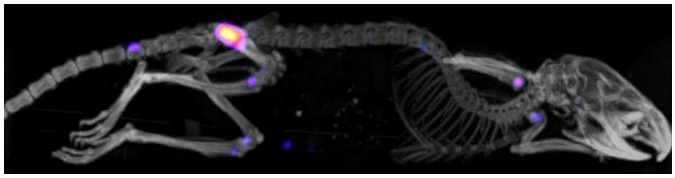

***Disclosures: STEWART LOW**, Novosteo INC., Major Stock Shareholder*

P-749

Intermittent Tryptophan Withdrawal Over a Three-month Period Avoids Severe Weight Loss While Preserving Bone Mass *Kehong Ding[1], Wendy Bollag[2], Meghan McGee-Lawrence[1], Debra L Irsik[1], Xingming Shi[1], William Hill[3], Sadanand Fulzele[1], Mohamed Awad[1], Mark Hamrick[1], Carlos Isales[1]. [1]Augusta University, United States, [2]Augusta University; Charlie Norwood VA Hospital, United States, [3]Medical University of South Carolina/Ralph H. Johnson VAMC, United States

We have previously shown that kynurenine (kyn), a tryptophan (Trp) oxidation product, accumulates with age and contributes to age-induced bone loss. Thus, measures to lower kyn levels could be of benefit in preserving bone mass. One potential approach would be to restrict dietary Trp thus lowering kyn levels. Trp is an essential amino acid used in protein synthesis, serotonin or melatonin synthesis or rapidly broken down to kynurenine through indoleamine 2,3 dioxygenase. Similar to caloric restriction, dietary Trp restriction results in increased lifespan but with detrimental side effects. Dietary Trp restriction results in rapid and sustained weight loss in both human and animal subjects. We have previously shown that in C57BL/6 mice on Trp deficient diet lose about 20% of their body weight within three weeks of initiating this diet, thus limiting its usefulness. We hypothesized that feeding the mice a Trp deficient diet in an intermittent fashion might be better tolerated. In an IACUC-approved protocol using aged (21-month-old) C57BL/6 mice, we fed one group an alternating (one-week interval) 0 or 0.2% (standard) Trp-containing diets (AD) vs the control (Crt) group which was fed a standard (0.2%) Trp containing diet for twelve weeks. There was a small but significant decrease in body weight in the mice fed the 0/0.2% alternating tryptophan diet compared to controls at the end of the twelve week period (Ctr: 32.0.+/-1.5 vs 32.8+/-1.6 vs AD: 31.8+/-2.5 vs 28.8+/-3.0 gm, (Means+SD, Ctr vs AD $p=0.005$, $n=10$/group). Intermittent removal of Trp from the diet did not have a detrimental effect on bone mineral density (BMD). Total BMD: (Ctr: 0.0524+/-0.0009 vs 0.522+/-0.0024 vs AD: 0.0518+/-0.0019 vs 0.0515+/-0.0015, Means+SD, Ctr vs AD at beginning and end of 12-week period). Femoral or Spinal BMD did not change. Thus, intermittent dietary Trp restriction avoided the marked weight loss seen with continuous Trp restriction and preserved BMD.

***Disclosures: Kehong Ding**, None*

P-750

The major components of the widely consumed medium-chain triglyceride ketogenic diet have differential effects on bone *Divya Vohora[1], Shreshta Jain[2]. [1]Jamia Hamdard, India, [2]Jamia Hamdard, New Delhi, India

Purpose: Ketogenic diet consists of high fat, low carbohydrates with a moderate protein intake. The diet has been modified over the years, with modified Atkin's diet and the incorporation of medium-chained triglycerides (MCT). Commonly, the MCT diet is associated with weight loss, fat loss and reduction in body composition referred from clinical and meta-analysis studies performed. They are also endorsed globally as a dietary treatment against neurodegenerative disorders such as refractory epilepsy and Alzheimer's disease, both of which have been associated with bone deficits. To the best of our knowledge, we evaluated for the first time, the role of two major components of MCT ketogenic diet, Caprylic acid and Capric acid to ascertain effects on bone after in vivo administration.Methods: Swiss albino mice were administered oral suspensions of caprylic acid (1100mg/kg, po) and capric acid (1700 mg/kg, po) for 4 weeks. Bone-specific alkaline phosphatase (ALP) and tartrate-resistant acid phosphatase (TRAP5b) along with the microarchitectural parameters, using micro-computed tomography, of the trabecular region of femur and tibia bones, bone mineral density and biomechanical strength were analyzed. Urinary ketone levels were also measured.Results: Remarkable alterations of the trabecular bone microarchitecture, reduced ALP and elevated TRAP5b levels were observed in the caprylic acid treated groups. Interestingly, when used in combination with capric acid, the deteriorating effects on bone were less significant. While the exact mechanisms remain unknown, the role of ketone bodies appears unlikely from our results.Conclusion: We suggest significant negative effects on bone health by caprylic acid. The findings are significant and calls for further validation and dietary modification of the MCT- ketogenic diet composition.Acknowledgement: We thank Dr. Divya Singh and Ms Reena Rai for helping carrying out microarchitecture and biomechanical strength studies at CDRI, Lucknow.

***Disclosures: Divya Vohora**, None*

Posters

P-751

The Role of Pre-existing Infection/Inflammation and Oncology Doses of Zoledronic Acid in the Development of Osteonecrosis of the Jaw after Tooth Extraction in Rice Rats *Evelyn Castillo[1], Abel Abraham[1], Summer Croft[1], Gabriella Gonzalez-Perez[1], Jessica Jiron[1], Samantha Thomas[1], Indraneel Bhattacharyya[1], Donald Kimmel[1], J. Ignacio Aguirre[0]. [1]University of Florida, United States, [0]University of Florida, United States

Osteonecrosis of the jaw (ONJ) is an adverse event affecting osteoporosis and cancer patients taking powerful anti-resorptives (pAR; e.g., zoledronic acid [ZOL]). Local factors (e.g., tooth extraction, periodontitis [PD]) combined with systemic factors (e.g., pARs, etc.) are required for ONJ to occur. ONJ pre-clinical studies using tooth extraction have given inconsistent outcomes and rarely considered the role of infection/inflammation associated with teeth being extracted. We hypothesized that in rice rats receiving an oncologic dose of ZOL, extraction of a periodontally-involved molar causes greater ONJ prevalence than extraction of a periodontally-healthy molar.At age 4-wks, 55 female rats were fed a standard (STD) diet, and administered either saline (VEH) intravenously (IV) or ZOL (80 µg/Kg IV [oncology dose]) q4wks. STD diet induces localized PD at the maxillary molar (M) M2M3 interdental space in ~60% of rice rats by age 16wks. At age 17+/-3 wks, rats were anesthetized, orally-examined for grossly-visible localized PD (LPD) in the M2M3 interdental space and randomized into four groups of 12-15: 1) VEH rats with no LPD; 2) VEH rats with LPD; 3) ZOL rats with no LPD, and 4) ZOL rats with LPD. Rats were anesthetized and one maxillary second molar was extracted from each rat. ZOL treatment continued until the day of necropsy. Rats were euthanized at 56 days post extraction (PE) to determine ONJ prevalence. Maxillae were fixed, decalcified, embedded in paraffin, and serially-sectioned parasagitally at 4µm thickness through the extraction site. Sections were stained with H&E. The whole extraction site and surrounding region was evaluated for necrotic, exposed bone, the hallmark of ONJ.Histopathologic evaluation for ONJ prevalence by group showed: 1) 0% (0/14) in VEH/no LPD rats; 2) 0% (0/12) in VEH/LPD rats; 3) 87% (13/15) in ZOL/no LPD rats; and 4) 79% (11/14) in ZOL/LPD rats. Fisher's Exact Test showed that the ZOL groups differed significantly from both VEH groups (P<.0001), but not from each other. ONJ occurred only in ZOL rats; its prevalence was not influenced by grossly-detectable localized PD at the time/site of tooth extraction. Radiographic examination of grossly-visible localized PD lesions will be considered in future studies to verify the accuracy of localized PD diagnosis. We conclude that tooth extraction in rice rats, as in humans, is an oral risk factor for ONJ in rats treated with a systemically-administered oncology dose of ZOL.

***Disclosures: Evelyn Castillo**, None*

P-752

Magnesium Inhibits Periodontitis Progression via Reducing Expression of Tumor Necrosis Factor-α and Promoting Subperiosteal Bone Formation *Wei He[1], Hai Zhang[2], Jiaxuan Qiu[3], Danfeng Xue[1]. [1]Nanchang University, China, [2]School of Dentistry, University of Washington, United States, [3]The First Affiliated Hospital of Nanchang University, China

Purpose: Periodontitis causes alveolar bone destruction leading to tooth loss. Increased tumor necrosis factor α (TNF-α) in periodontal tissues promotes inflammatory cell recruitment and inhibits bone growth. Magnesium (Mg) was shown to reduce inflammation and promote osteogenesis. The objectives of this study were to determine therapeutic effects of Mg on periodontitis in a rat model, and to elucidate its mechanisms related to TNF-α and bone growth in vivo and in vitro.Methods: Pure Mg rods (Φ1.4mm×5 mm) were implanted in sockets (located under the mandibular first molars) immediately after SD rat incisors were extracted. Titanium rods with same dimensions were used as control (n=6 per group). Periodontitis models were established simultaneously at first molars by ligature. Inflammatory cell infiltration and alveolar bone around first molars were analyzed by histology and micro-CT respectively at 2 and 6 weeks post-operation. In the meantime local Mg content was measured by scanning electron microscopy–energy-dispersive spectroscopy (SEM-EDS). TNF-α concentration in periodontal tissue was semi-quantitatively analyzed by immunohistochemistry. Osteogenic effects of MgCl2 (0.8, 1.8, 5, 10, 20mM) on periosteum-derived cells (PDCs) under TNF-α treatment were evaluated by proliferation (1-3 days) and qRT-PCR of osteogenic genes (2 weeks) assays. Data were statistically analyzed (ANOVA followed by post hoc t-test, α=0.05).Results: H&E staining showed significantly less inflammatory cell infiltration and large amount of new bone formation under periosteum in Mg-implanted rats. Marginal bone loss was significantly lower and alveolar bone volume was significantly higher in Mg group at both time points by micro-CT. SEM-EDS revealed remarkably higher Mg concentration on the surface of alveolar crest in Mg group. TNF-α concentration in gingiva was significantly lower in Mg-implanted group. The proliferation of PDCs was significantly increased at 10 and 20mM MgCl2 groups (p<0.05). The expression of Alp, Col 1 and Opn was significantly higher in PDCs with 5, 10mM MgCl2 and the existence of 5ng/ml TNF-α (p<0.05)Conclusions: Mg implant inhibits progression of experimental periodontitis in rats. This may partially attribute to the suppressive effect of Mg on TNF-α expression and inflammation, as well as stimulation of subperiosteal osteogenesis by Mg. This study provides foundations of a potential therapeutic modality against periodontitis by localized application of Mg.

***Disclosures: Wei He**, None*

P-753

Effects of Infigratinib, a Selective FGFR1-3 Tyrosine Kinase Inhibitor, on Dentoalveolar Development *Sarah Aitken[1], Omar Glover[1], Zachary Michel[2], Emily Chu[1], Francesca Avogadri[3], David Martin[3], Susan Moran[4], Michael Collins[2], Martha Somerman[1]. [1]National Institute of Arthritis and Musculoskeletal and Skin Diseases (NIAMS), National Institutes of Health (NIH), United States, [2]National Institute of Dental and Craniofacial Research (NIDCR), National Institutes of Health (NIH), United States, [3]QED Therapeutics Inc, United States, [4]QED Therapeutics Inc., United States

Fibroblast Growth Factor-Receptor-3 (FGFR3) gain-of-function mutations are linked to achondroplasia in humans. Infigratinib (formerly known as BGJ398) is a tyrosine kinase inhibitor of FGFRs 1-3 and has been shown to improve skeletal growth in an achondroplasia mouse model. However, infigratinib effects on tooth development have not been studied. Existing data demonstrates that multiple FGFs and their receptors have critical roles within the tooth organ. We hypothesized that infigratinib affects dentoalveolar development in a dose-dependent manner. Beginning on postnatal day (PND) 7, male and female Wistar rats received a daily dose of either vehicle, 0.1mg/kg infigratinib (low dose), or 1.0mg/kg infigratinib (high dose). Rats were euthanized at PND21 or 37, and heads were fixed in formalin. Mandibles were dissected and hemisected sagittally. Micro-computed-tomographic (µCT) scans of heads and hemi-mandibles were conducted using a Scanco-µCT-50 Scanner. Qualitative and quantitative 3D µCT analyses were performed using AnalyzePro software. Quantitative data were analyzed using one-way ANOVA with post-hoc Tukey-test for pairwise comparisons, where p<0.05 was considered statistically significant. We report high dose infigratinib (1mg/kg) affects the formation of dentoalveolar tissues and that female rats were more sensitive to infigratinib compared to males. Most notably, in comparison to the other groups, high-dose PND37 female rat molars and surrounding bone exhibited: reduced dentin volume (9-12%); increased dentin densities (2-3%); reduced pulp volume (10-20%) and reduced alveolar bone volume (10-13%). These differences were not detected in PND37 male rats, or in any rats at PND21. Infigratinib did not affect enamel volume or density or alveolar bone density at any timepoint. Mandibular 3rd molars exhibited aberrant crown and root morphology in 100% of high dose female rats and in 80% of high dose male rats at PND37 and PND21. Since the infigratinib doses proposed for achondroplasia treatment are significantly lower than 1.0mg/kg, no effect on dental structures would be anticipated. To better elucidate underlying mechanisms of the effects of infigratinib on dentoalveolar tissues, future studies should include histological analyses, analyses of associated genes/proteins, and dental phenotyping of achondroplasia animal models and patients. These additional studies will inform the best dosing for patients.

***Disclosures: Sarah Aitken**, None*

P-754

Neonatal severe hyperparathyroidism: New analysis causes new guideline. Stephen J. Marx, Ninet Sinaii. Office of the Scientific Director, Section on Genetics and Endocrinology, NICHD/NIH, Bethesda MD 20892 *Stephen Marx[1]. [1]NICHD, United States

Context: Neonatal severe hyperparathyroidism (NSHPT) is a rare and life-threatening emergency. It includes generalized hyperparathyroid bone disease and respiratory distress from combinations among a narrowed thorax, rib fractures, hypotonia, and biochemical disturbances. Neuromotor retardation may persist after otherwise successful therapy. Early intervention seems critical. NSHPT is usually caused by homozygous or heterozygous pathogenic variant(s) of the CASR. Homozygotes and heterozygotes are often not distinguished. In theory, their management should differ. Optimum treatment in homozygotes is early total parathyroidectomy. Optimal management of heterozygotes varies from careful observation without surgery, to bisphosphonates and/or calcimimetics, and/or to subtotal parathyroidectomy. Evidence Acquisition: Each case met strict criteria for "severe" disease. To compare different immunoassays, PTH was analyzed as a ratio (thus without units) of the raw data divided by the upper limit of its normal range. This is a major extension on a recent report (JCEM April 2020). We now include many variables about presentation and therapy. Evidence Synthesis: There were 98 cases with homozygous pathogenic CASR variants and 35 cases with heterozygous pathogenic or likely pathogenic variants. Maximal serum calcium was far higher in homozygotes 5.8 +/- 1.5 versus 3.2 +/- 0.2 (P<.001) (normal 2.2-2.6 mM). Maximal serum PTH as a ratio was also far higher in homozygotes 17 +/- 12 versus 8 +/- 9 (P=.003) (normal ratio 0.3-1.0). We defined extreme hypercalcemia empirically as any calcium value above 4.5 mM. No heterozygote had a maximal calcium above 3.7 mM; however, 30 of 36 (83%) of the homozygotes had maximal calcium above the conservative cutoff of 4.5 mM. A more aggressive cutoff of 4.0 mM would capture 95% of homozygotes and no heterozygotes. The linear regression of the highest levels of extreme hypercalcemia versus day number confirmed frequent clustering of recognition in the first 10 days. Conclusions: Extreme hypercalcemia greater than 4.5 mM was newly identified as a conservative cutoff that was 100% predictive of homozygosity for pathogenic CASR variants. Extreme hypercalcemia in NSHPT is an early, facile, rapid, and inexpensive determinant of homozygosity. It should be sought and used as a guideline to promote early and definitive total parathyroidectomy in homozygotes.

Context: Neonatal severe hyperparathyroidism (NSHPT) is a rare and life-threatening emergency. It includes generalized hyperparathyroid bone disease and respiratory distress from combinations among a narrowed thorax, rib fractures, hypotonia, and biochemical disturbances. Successful therapy is compatible with long life and a healthy prognosis. However, irreversible neuromotor retardation may persist after otherwise successful therapy. The duration and amplitude of hypercalcemia likely correlate with the development of irreversible neuromotor retardation; thus, early intervention seems critical in many cases. NSHPT is usually caused by homozygous or heterozygous pathogenic variant(s) of the *CASR*; a heterozygous variant of this gene is also the usual cause of familial hypocalciuric hypercalcemia (type 1) (FHH or FHH1). Homozygotes and heterozygotes with NSHPT are often not distinguished in the current literature. In theory, their management should differ. Optimum treatment in homozygotes is early total parathyroidectomy. Optimal management of heterozygotes varies from careful observation without surgery, to bisphosphonates and/or calcimimetics, and/or to subtotal parathyroidectomy.

Evidence Acquisition: Each case met strict criteria for "severe"disease and neonatal disease. We analyzed the core biochemical parameters of the maximal serum calcium and maximal PTH. To compare different immunoassays, PTH was analyzed as a ratio (thus without units) of the raw data divided by the upper limit of its normal range. Each case also required information about the allelic dosage of the pathogenic or likely pathogenic *CASR* variant(s).

Evidence Synthesis: There were 36 cases with homozygous pathogenic *CASR* variants and 21 cases with heterozygous pathogenic or likely pathogenic variants. Maximal serum calcium was far higher in homozygotes 5.8 +/- 1.5 versus 3.2 +/- 0.2 (P<.001) (normal 2.2-2.6 mM). Maximal serum PTH as a ratio was also far higher in homozygotes 17 +/- 12 versus 8 +/- 9 (P=.003) (normal ratio 0.3-1.0). We defined extreme hypercalcemia empirically as any calcium value above 4.5 mM. No heterozygote had a maximal calcium above 3.7 mM; however, 30 of 36 (83%) of the homozygotes had maximal calcium above the conservative cutoff of 4.5 mM. A more aggressive cutoff of 4.0 mM would capture 95% of homozygotes and no heterozygotes. Whenever tested early, extreme hypercalcemia was usually recognized in the first week of life.

Conclusions: The main findings were that extreme hypercalcemia greater than 4.5 mM was newly identified as a conservative cutoff that was 100% predictive of homozygosity for pathogenic *CASR* variants. Extreme hypercalcemia in NSHPT is an early, facile, rapid, and inexpensive determinant of homozygosity for pathogenic variants of the *CASR*. It should be sought and used to promote early and definitive total parathyroidectomy, whenever it is identified in NSHPT.

***Disclosures: Stephen Marx**, None*

P-755

Efficacy of burosumab in older adults with X-linked hypophosphataemia (XLH): A subgroup analysis of a randomized, double-blind, placebo-controlled, phase 3 study *Richard Keen[1], Karl Insogna[2], Wei Sun[3], Julian Howell[4], Susan Wood[4]. [1]Royal National Orthopaedic Hospital, United Kingdom, [2]Yale University School of Medicine, United States, [3]Kyowa Kirin Pharmaceutical Development, United States, [4]Kyowa Kirin International, United Kingdom

XLH (X-linked hypophosphataemia) is a rare, chronic and progressive disease. In adults with XLH, acquired bone deformities from childhood, together with ongoing chronic hypophosphataemia and osteomalacia, may lead to substantial musculoskeletal and functional morbidities. Data have shown that treatment with burosumab in adults leads to sustained improvement in biochemical measures, as well as key symptoms and functional impairments. This exploratory post-hoc subgroup analysis of data from CL303 (NVT02526160) assesses how biochemical and clinical outcomes in patients over 50 years of age treated with burosumab compare with younger patients.CL303 is a phase 3 multicentre, randomized, double-blind, placebo-controlled study evaluating the efficacy and safety of burosumab in adults with XLH. Adults were randomly allocated (1:1) to burosumab (1.0mg/kg, SC Q4 Weekly) or placebo (SC Q4 Weekly) for 24 weeks; followed by 24 weeks of open label burosumab. This subgroup analysis examines responses at Week 24 in age-based patient cohorts (>50 years and <50 years) to the primary endpoint of correction of serum phosphate, the key secondary endpoints of pain, stiffness and physical function and exploratory endpoint of (pseudo)-fracture healing.134 subjects were randomized (68 in burosumab and 66 in placebo); 65% female; median age 41 years [18–65 years]; 26 patients were aged >50 years (16 burosumab; 10 placebo); and 108 <50yrs (52 burosumab; 56 placebo). Baseline symptomatology was similar between age and treatment groups.Results at Week 24 are shown in the table. Patients >50yrs treated with burosumab responded at least as well as those <50yrs and better than placebo, for all endpoints.Despite decades of progressive disease, both age cohorts of adult patients with XLH treated with burosumab responded similarly well and better than placebo, improving biochemical markers, symptoms and (pseudo)-fracture healing. In adult patients with symptomatic XLH, advanced age should not be a factor when considering initiation of burosumab treatment.

Outcomes (W24)	>50 years		≤ 50 years	
	Burosumab (B)	Placebo (P)	Burosumab (B)	Placebo (P)
Serum phosphate (%≥LLN)	94%	20%	92%	5%
Changes from baseline				
BPI Worst Pain	-1.26	-0.76	-0.89	-0.36
LS mean difference (SE) B-P	-0.34 (0.730)		-0.44 (0.297)	
WOMAC Stiffness	-19.53	-7.50	-7.84	+0.45
LS mean difference (SE) B-P	-15.66 (8.037)		-6.41(3.605)	
WOMAC Physical Function	-10.56	+0.29	-5.72	-1.20
LS mean difference (SE) B-P	-10.40 (4.370)		-3.32 (2.909)	
% Fracture healing	44%	22%	46%	3%

***Disclosures: Richard Keen**, Kyowa Kirin International, Consultant*

P-756

Real-world evidence of the progressive and cumulative morbidity arising from X-linked hypophosphatemia (XLH) over the adult life course *Kassim Javaid[1], Erik Imel[2], Rafael Pinedo-Villanueva[1], Angela Rylands[3], Angela Williams[3], Karl Insogna[4], Leanne Ward[5]. [1]University of Oxford, United Kingdom, [2]Indiana University of Medicine, United States, [3]Kyowa Kirin International, United Kingdom, [4]Yale School of Medicine, United States, [5]University of Ottawa, Canada

X-linked hypophosphatemia (XLH) is a rare, genetic phosphate-wasting disorder. Musculoskeletal deficits and dental abnormalities begin in childhood, becoming more pronounced and numerous with age. This analysis aimed to explore the disease sequelae of XLH in adulthood according to age groups, using patient-reported data from a multinational online survey.Adults with self-reported XLH were recruited via clinicians and XLH patient advocacy networks to complete the survey. Burosumab-naive adults with XLH were analyzed by age group: 18–29, 30–39, 40–49, 50–59, and >=60 years. Specific manifestations (see Table) were investigated, including musculoskeletal, non-musculoskeletal, and conventional therapy-related sequelae.Data were analyzed from 209 adults (63% United States, 24% Europe, 13% rest of world; mean+/-SD age 45.5+/-13.0 years; 77% women; 38% currently not on therapy). 98% of adults reported >=1 sequelae, with a median of 4 sequelae per person (range 0–11). The proportion experiencing >=5 sequelae increased nearly 9-fold from the youngest to eldest group (8% to 71%, respectively).The proportion experiencing >=1 musculoskeletal sequelae increased from 50% in the 18–29-year group to 77–94% in all older groups. Fracture history prevalence increased across the age groups from 27% in the 18–29-year group, to ~40% in the 30–59-year groups, and 68% in the >=60-year group. The most common fracture site was the femur (19%). Osteoarthritis was reported by 23% of the 18–29-year group, increasing to 71% in the >=60-year group. Other comorbidities increased with age; in the 18–29-year group, osteophytes occurred in 19%, enthesopathy in 4%, and spinal stenosis in 4%, increasing in frequency with age to 52%, 45%, and 39%, respectively, in the >=60-year group.Non-musculoskeletal sequelae were highly prevalent at all ages, increasing from 85% in the 18–29-year group to 94% in the >=60-year group, driven by the presence of dental abscess in most adults (87%). 46% of the 18–29-year-olds reported >=1 conventional therapy-related sequelae, increasing gradually to 65% in the >=60-year group. Of note, hyperparathyroidism was reported by 29% of adults, with prevalence increasing with age from 8% in the 18–29-year group to 61% in the >=60-year group.This analysis of patient-reported data indicates that XLH is a life-long, cumulative, and progressive disease. Important disease manifestations present in early adulthood, and frequency sharply increases after 30 years of age.

Prevalence of musculoskeletal, non-musculoskeletal, and conventional therapy-related manifestations in patients with XLH, according to age group, from a multinational online survey.

Age group, years	*18–29*	*30–39*	*40–49*	*50–59*	*≥60*	*All*
Number of participants	26	45	61	46	31	209
Fracture history prevalence, %	27	40	44	39	68	43.5
Osteoarthritis prevalence, %	23	47	56	70	71	55.0
Osteophyte prevalence, %	19	42	49	50	52	44.5
Enthesopathy prevalence, %	4	16	31	30	45	26.3
Spinal stenosis prevalence, %	4	9	20	22	39	18.9
Adults with ≥1 musculoskeletal-related sequelae, %	50	80	77	87	94	78.9
Dental abscess prevalence, %	69	76	80	85	87	79.9
Hearing loss prevalence, %	15	20	31	41	55	32.5
Tinnitus prevalence, %	38	47	44	50	52	46.4
Adults with ≥1 non-musculoskeletal-related sequelae, %	85	87	85	91	94	88.0
Nephrocalcinosis prevalence, %	42	27	13	13	19	20.6
Kidney problems prevalence, %	4	16	7	17	19	12.4
Hyperparathyroidism prevalence, %	8	20	23	35	61	28.7
Adults with ≥1 conventional therapy-related sequelae, %	46	36	31	46	65	42.1
Median number of disease sequelae (range)	2 (1–6)	4 (0–7)	4 (0–9)	5 (1–9)	6 (1-11)	4 (0-11)
Adults with ≥5 sequelae, %	8	31	33	50	71	38.8

***Disclosures: Kassim Javaid**, Kyowa Kirin International, Grant/Research Support, Kyowa Kirin International, Speakers' Bureau, Kyowa Kirin International, Consultant*

P-757

A Natural History Study In Patients With ENPP1 Deficiency or Severe ABCC6 deficiency *Frank Rutsch[1], Yvonne Nitschke[1], Kristina Kintzinger[1], Mary Hackbarth[2], Ulrike Botschen[1], Sisi Wang[3], Rachel Gafni[4], Kerstin Mueller[3], Gus Khursigara[5], Pedro Huertas[5], William Gahl[2], Carlos Ferreira[2]. [1]Muenster University Children's Hospital, Germany, [2]National Human Genome Research Institute, National Institutes of Health, United States, [3]ICON plc, Canada, [4]National Institute of Dental and Craniofacial Research, National Institutes of Health, United States, [5]Inozyme Pharma, United States

We report on an interim analysis of a retrospective, cross-sectional natural history study (based on chart reviews) in patients diagnosed with generalized arterial calcification of infancy (GACI) or autosomal recessive hypophosphatemic rickets type 2 (ARHR2). The National Institutes of Health (NCT03478839) and Münster University Children's Hospital (NCT03758534) contributed medical data for the study. The study collected full medical data from 127 patients of whom 115 patients were diagnosed with GACI, 36 patients were diagnosed with ARHR2, including 25 patients diagnosed with both GACI and ARHR2. Of 109 probands with genetic confirmation, 88 had mutations in ENPP1 and 21 in ABCC6. Deaths in ENPP1 and ABCC6 subjects were 35 and 4, respectively. Consistent with past observations, arterial calcification (88%, 95%), joint calcification (64%, 33%), hypertension (65%, 67%) and short stature (stature-for-age less than third centile; 42%; 33%) were prevalent in ENPP1 and ABCC6 cohorts, respectively. Organ calcification (78%; 85%) cardiac dysfunction (78%, 85%), renal dysfunction (47%: 40%) and gastrointestinal dysfunction (63%; 58%) were also observed in both ENPP1 and ABCC6 cohorts, respectively. A higher prevalence of neurological complications was observed in the ABCC6 cohort (58% to 40%) while hearing loss (53%; 7%) and rickets (48%; 17%) were higher in the ENPP1 cohort. The data demonstrate similar clinical manifestation between ENPP1 and ABCC6 deficient patients. Significant mortality during infancy, calcification of multiple arteries, organ dysfunction and skeletal abnormalities are reported in both ENPP1 and ABCC6 deficient patients. The overlap of patients diagnosed with both GACI and ARHR2 suggests they may not be distinct conditions. Further analysis will further support and elucidate the progression of the disease. ENPP1 and ABCC6 deficiences are genetic conditions caused by loss-of-function mutations in either the ENPP1 or ABCC6 genes which may manifest in infants as GACI, a life-threatening disorder. Infants present with arterial calcifications, stenoses and cardiac complications. Approximately 50% of GACI infants do not survive the first 6 months of life. Patients with ENPP1 deficiency also manifest hearing loss and ARHR2, characterized by short stature, bone deformities and pain in pediatric and young adults. ABCC6 deficiency also manifests as Pseudoxanthoma elasticum in adults. Disclosure: Grant support and consulting fees from Inozyme Pharma.

***Disclosures: Frank Rutsch**, Inozyme Pharma, Grant/Research Support, Inozyme Pharma, Consultant*

P-758

Inhibition of Activin A with Garetosmab Improved Parameters of Lung Function in Patients with FOP *Cynthia Portal-Celhay[1], Eduardo Forleo-Neto[1], Gregory P. Geba[1], Marcella Ruddy[1], Robert J Pignolo[2], Richard Keen[3], Maja Di Rocco[4], Mona Al Mukaddam[5], Philippe Orcel[6], Christian Roux[7], Jacek Tabarkiewicz[8], Javier Bachiller-Corral[9], Angela M. Cheung[10], Kathryn M. Dahir[11], Thomas Funck-Brentano[6], Sami Kolta[7], Annalisa Madeo[4], Judith S Bubbear[3], Małgorzata Szczepanek[8], Esmée Botman[12], Neena Sarkar[1], Peijie Hou[1], Scott Mellis[1], Andrew J Rankin[1], Aris Economides[1], Dinko Gonzales Trotter[1], Gary Herman[1], David M. Weinreich[1], George D. Yancopolous[1], E. Marelise W. Eekhoff[12], Frederick S. Kaplan[5]. [1]Regeneron Pharmaceuticals, United States, [2]Department of Medicine, Mayo Clinic, United States, [3]Centre for Metabolic Bone Disease Royal National Orthopaedic Hospital NHS Trust, United Kingdom, [4]Department of Pediatrics, Unit of Rare Diseases, IRCCS Istituto Giannina Gaslini, Italy, [5]Departments of Orthopaedics, Medicine and the Center for Research in FOP & Related Disorders, University of Pennsylvania Perelman School of Medicine, United States, [6]Service de Rhumatologie - DMU Locomotion, AP-HP.Nord - Université de Paris, France, [7]Department of Rheumatology, Cochin Hospital, Assistance Publique - Hôpitaux de Paris, France, [8]Rzeszów University, Rzeszów, Poland, [9]Hospital Universitario Ramón y Cajal, Spain, [10]University Health Network, University of Toronto, Canada, [11]Vanderbilt University Medical Center, United States, [12]Department of Internal Medicine section Endocrinology, Amsterdam Bone Center, Amsterdam UMC, Vrije Universiteit, Netherlands

Background: Fibrodysplasia ossificans progressiva (FOP) is characterized by soft tissue inflammation (flare-ups) and cumulative heterotopic ossification (HO) resulting in skeletal deformity, progressive immobility and early mortality. Progressively-diminished chest wall mobility is common and thoracic insufficiency syndrome is the leading cause of death in FOP. LUMINA-1 evaluated safety and efficacy of garetosmab (GAR), a monoclonal antibody (mAb) inhibitor of Activin A, in adults with FOP. Pulmonary function was evaluated as an exploratory outcome.Methods: In LUMINA-1 (NCT03188666), subjects were randomized to IV GAR 10 mg/kg (n=20) or placebo (PBO; n=24) every 4 weeks (Q4w) for 28 weeks and then continued in open-label treatment. Primary efficacy was assessed by 18F-sodium fluoride positron emission tomography (PET) and whole-body low-dose computerized tomography (CT). Spirometry (FVC, FEV1, FEV1/FVC) was performed at baseline and week 28.Results: Pulmonary function of 41 adults (mean age [SD], 27.6 [8.5] years; 43% male overall) in GAR and PBO groups were comparable at study initiation (in L, FEV mean [SD], 1.84 [0.64] and 1.90 [0.80] and FVC, 1.96 [0.69] and 2.12 [0.94], respectively). All exhibited restrictive ventilatory defect at baseline shown by low % predicted FVC and high FEV1/FVC. By week 28, there was a trend toward improved % predicted FVC (mean [SD] baseline: GAR 48.03 [15] vs. PBO 49.81 [18.5]; 28 weeks: GAR 54.67 [20.3] vs, PBO 50.64 [18.2]; change 13.8% GAR vs. 1.6% PBO), or as an improvement in PBO-adjusted absolute change (L) of FVC (GAR, 0.29 [14.7%] vs PBO, 0.05 [2.4%]) of 12.3%, and a statistically significant improvement in % predicted FEV1 (0.32 vs.-1.824; P=0.004) and % change in L FEV1 (7.6% vs 0%; P=-0.003) (Figure).Conclusions: GAR resulted in meaningful increases in lung function parameters with statistically significant improvement in FEV1 and a clinically important increase in FVC. We hypothesize that the chest wall restriction in FOP is mediated in part by soft tissue inflammation and is reversible by inhibiting Activin A with garetosmab. These results may have important implications for the long-term health of individuals living with FOP and should be studied further.Fig:

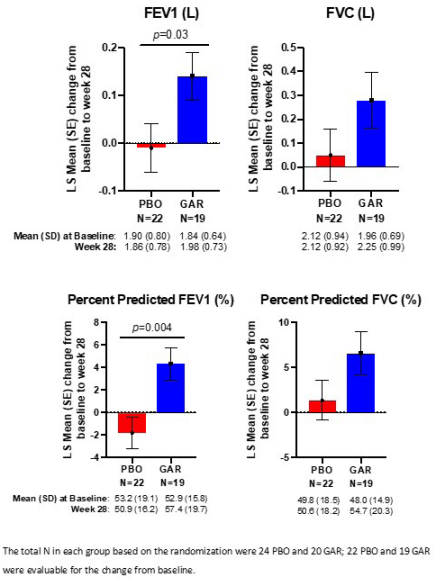

***Disclosures: Cynthia Portal-Celhay**, Regeneron Pharmaceuticals, Major Stock Shareholder*

P-759

A Global Natural History Study of Fibrodysplasia Ossificans Progressiva (FOP): 12-Month Outcomes *Mona Al Mukaddam[1], Robert J Pignolo[2], Geneviève Baujat[3], Matthew A Brown[4], Carmen De Cunto[5], Maja Di Rocco[6], Edward C Hsiao[7], Richard Keen[8], Kim-Hanh Le Quan Sang[3], Andrew Strahs[9], Rose Marino[9], Frederick S Kaplan[10]. [1]Departments of Orthopaedic Surgery & Medicine, The Center for Research in FOP and Related Disorders, Perelman School of Medicine, University of Pennsylvania, United States, [2]Department of Medicine, Mayo Clinic, United States, [3]Département de Génétique, Institut IMAGINE and Hôpital Universitaire Necker-Enfants Malades, France, [4]Guy's & St Thomas' NHS Foundation Trust and King's College London NIHR Biomedical Research Centre, United Kingdom, [5]Pediatric Rheumatology Section, Department of Pediatrics, Hospital Italiano de Buenos Aires, Argentina, [6]Unit of Rare Diseases, Department of Pediatrics, Giannina Gaslini Institute, Italy, [7]Division of Endocrinology and Metabolism, UCSF Metabolic Bone Clinic, Institute of Human Genetics, and UCSF Program in Craniofacial Biology, Department of Medicine, University of California-San Francisco, United States, [8]Centre for Metabolic Bone Disease, Royal National Orthopaedic Hospital, United Kingdom, [9]Ipsen, United States, [10]Departments of Orthopaedic Surgery & Medicine, The Center for Research in FOP and Related Disorders, Perleman School of Medicine, University of Pennsylvania, United States

Background: FOP is an ultra-rare, severely disabling genetic disorder characterized by cumulative heterotopic ossification (HO), often preceded by episodic flare-ups, leading to physical disability and early death. FOP is diagnosed and managed by multiple healthcare professionals, including bone specialists.Objective: A prospective, 36-month, global natural history study (NCT02322255) was designed to investigate the progression of FOP, HO, and impact on physical function. Results are described for the first 12 months.Methods: Individuals with FOP aged <=65 years with documented ACVR1R206H mutation were eligible. HO volume was assessed by low-dose whole-body computed tomography (WBCT; excluding the head) interpreted at a blinded, central laboratory using pre-specified procedures. Physical function was evaluated using the Cumulative Analogue Joint Involvement Scale (CAJIS; total score 0–30 represents degree of ankylosis across 15 joints) and the FOP Physical Function Questionnaire (FOP-PFQ; % total score); higher scores indicate more severe limitations. Changes from Baseline (BL) in HO volume, CAJIS and FOP-PFQ at Month 12 were evaluated.Results: Of 114 participants with BL data, 99 (aged 4–56 years at enrollment, mean 17 years; 56% male) had a Month 12 assessment and 93 had evaluable WBCT HO data at BL and Month 12. Over 12 months, 40% (37/93) developed new HO and 48% (48/99) reported >=1 flare-up. Of participants with new HO, 65% (24/37) reported >=1 flare-up (mean 2.3 flare-ups/year) and 35% (13/37) reported no flare-up. Of participants with no new HO, 43% (24/56) reported >=1 flare-up (mean 1.8 flare-ups/year). Among all participants, mean new HO volume in those who reported flare-ups was 39,718 mm3 (SD: 91,969 mm3; n=48) vs 5,081 mm3 (SD: 14,582 mm3; n=45) in those who did not. Mean changes from BL in CAJIS and FOP-PFQ were minimal (CAJIS: 0.6 [SD: 2.4; median: 1.0; n=99]; FOP-PFQ: 4.4% [SD: 11.2%; median: 3.7%; n=90]) and similar across participants with or without new HO.Conclusions: In participants with FOP, WBCT HO volume increased over 12 months. Among those who experienced new HO, this was not preceded by a flare-up in over one third of cases. Among all participants, mean new HO volume in those who reported flare-ups was ~8 times higher than in those who did not. CAJIS and FOP-PFQ were not sufficiently sensitive to assess FOP disease progression over 12 months. Measuring HO may be a viable way to monitor changes in FOP over short periods of time.

***Disclosures: Mona Al Mukaddam**, Biocryst, Blueprint, Daiichi Sankyo, Keros, Consultant, Research investigator: Clementia/Ipsen, Regeneron; Advisory board (all voluntary): IFOPA Registry Medical Advisory Board, International Clinical Council on FOP, Other Financial or Material Support*

P-760

Long-term trajectory of bone mineral density in pregnancy and lactation-associated osteoporosis with or without bisphosphonate use after teriparatide *Seunghyun Lee[1], Kyoung Jin Kim[1], Namki Hong[1], Yumie Rhee[1]. [1]Department of Internal Medicine, Severance Hospital, Endocrine Research Institute, Yonsei University College of Medicine, Republic of Korea

Pregnancy- and lactation- associated osteoporosis(PLO) is a rare and devastating disorder that leads to limited activity and pain during pregnancy and lactation due to multiple compression fractures. Previous studies showed that teriparatide(TPTD) might be helpful in patients with severe PLO in terms of bone mineral density(BMD) recovery and subsequent fracture risk reduction.[i] However, it is unclear whether TPTD can be discontinued without sequential treatments with anti-resorptives such as bisphosphonates(BP) in premenopausal women with PLO, as recommended in postmenopausal women. In this study, we investigated the changes in BMD in PLO patients treated with TPTD 20 mcg daily injection for one year, with and without sequential BP use. Forty-three premenopausal patients with PLO between 2007 and 2015 in Severance hospital were retrospectively analyzed. Among them, 37 women were treated with TPTD (TPTD with sequential BP treatment, n=17; TPTD without sequential BP treatment, n=20). All subjects maintained regular menstruation cycles after pregnancy and lactation. At baseline, BP users and non-BP users after TPTD were not different in age (31 vs. 32 years), body mass index (20.0 vs. 20.9 kg/m2), duration of TPTD treatment (14.1 vs. 12.6 months), lumbar spine(LS) BMD (0.670 vs. 0.725 g/cm2) and femoral neck(FN) BMD (0.595 vs. 0.550 g/cm2; p > 0.05 for all). Median duration of BP use was 21 months (12 to 26 months) in BP users after TPTD. In overall subjects, average increase in LSBMD was 15.2%, 22.4%, 22.0% after 1,2,3 years from baseline, respectively (P 0.05 for all time points). Similar results were observed for THBMD, with an average increase of up to 4.05%, 7.38%, and 7.37% for 1,2,3 year time points after initiation of TPTD (p<0.05 for each treatment group, at all time points). In conclusion, BMD gain by TPTD use in patients with PLO was well maintained without sequential BP treatment, showing a similar long-term trajectory to that of sequential BP users.[i] Namki Hong, Yumie Rhee et al. Comparison of Efficacy of Pharmacologic Treatments in Pregnancy- and lactation-associated osteoporosis. Clinical Reviews in Bone and Mineral Metabolism (2019) 17:86-93

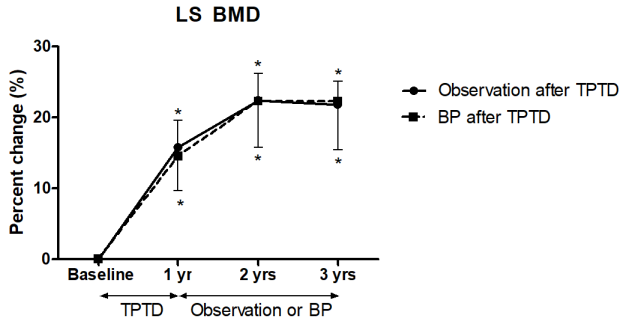

FIGURE 1 Percent change in BMD at the lumbar spine at 1 year, 2 years, 3 years after initiating treatment.

Abbreviations: BMD, bone mineral density; LS, lumbar spine; TPTD, teriparatide; BP, bisphosphonate

*P<0.05 vs baseline; †P<0.05 between TPTD–treated subjects and Sequential bisphosphonate after TPTD –treated subjects.

***Disclosures: Seunghyun Lee**, None*

Posters

P-761

Lesional Sodium Fluoride uptake decreases on PET-CT scan in patients with Fibrous Dysplasia/McCune Albright syndrome treated with Denosumab. *Wouter van der Bruggen[1], Dennis Vriens[1], Maartje E. Meier[1], Frits Smit[1], P. D. Sander Dijkstra[1], Liesbeth E.M. Winter[1], Lioe-Fee de Geus-Oei[1], Natasha M. Appelman-Dijkstra[1]. [1]Leiden University Medical Center (LUMC), Netherlands

Despite the recently described correlation between fibrous dysplasia (FD) disease burden measured with [18F]NaF PET-CT (NaF-PET) and bone turnover markers, the effect of treatment on lesional NaF-uptake in patients with fibrous dysplasia (FD) is unknown. [99mTc]-HDP uptake does not change after bisphosphonate treatment. We retrospectively studied fifteen FD/MAS-patients who underwent NaF-PET scans (37 scans) and received antiresorptive treatment. Baseline and follow-up NaF parameters of healthy bone and FD-lesions and serum markers of bone turnover around treatment with denosumab (n=8) or on bisphosphonates (n=7) were assessed. Individualized patient healthy bone cut-offs on NaF-PET ensured adequate normalization and did not change after denosumab (p=0.237) or bisphosphonates (p=0.575) treatment, reassuring the hypothesis that sites with increased turnover receive the highest dose of treatment. Volumetric parameters of FD-burden on NaF-PET (FTV) showed significant decrease after start of denosumab, median FTV 199 cm3 on baseline scan to 97 cm3 during follow-up, p=0.030. However, FTV did not change in patients receiving bisphosphonates (p=0.249). FTV correlated positively with serum markers Alkaline Phosphatase (ALP) (rSpearman=0.406; p=0.006; n=37) and with P1NP (rSpearman=0.730; p<0.001; n=36). Relative changes in FTV and both serum biomarkers of bone turnover correlated positively (DFTV versus DALP and DP1NP, r Spearman=0.518 and 0.489; p=0.024 and 0.032, respectively). In several patients, either ALP or P1NP (n=5) or both (n=3) showed normal serum levels, still FTV adequately quantified disease and response to antiresoptive treatment, as measured by pain scores, and possibility to reduce pain medication. Changes in serum markers of bone turnover correlate with FD-disease burden measured with FTV on NaF-PET. Therefore NaF-PET could be used as an objective local parameter of treatment response in FD in addition to serum biomarkers of bone turnover, pinpointing location and extension of FD-burden. NaF might be of extra importance in patients with normal(ized) serum markers and clinical complaints.

***Disclosures: Wouter van der Bruggen**, None*

P-762

Infigratinib Therapy in Tumor-Induced Osteomalacia *Iris R. Hartley[1], Kelly L. Roszko[1], Karen Pozo[1], Jamie Streit[1], Jaydira del Rivero[2], Roo Vold[3], Susan Moran[3], Michael T. Collins[4], Rachel I. Gafni[1]. [1]National Institute of Dental and Craniofacial Research, National Institutes of Health, United States, [2]National Cancer Institute, National Institutes of Health, United States, [3]QED Therapeutics, United States, [4]National Institute of Dental and Cranial Facial Research, National Institutes of Health, United States

Tumor-induced osteomalacia (TIO) is a rare disorder caused by fibroblast growth factor 23 (FGF23)-producing phosphaturic mesenchymal tumors (PMTs). Resultant phosphaturia and suppressed 1,25-(OH)2 vitamin D (1,25D) leads to hypophosphatemia, osteomalacia, and fractures. Fibronectin- fibroblast growth factor receptor 1 (FN1-FGFR1) fusions have been identified in up to 40% of PMTs. Infigratinib is a selective FGFR1-3 tyrosine kinase inhibitor with observed anti-tumor activity in phase 2 trials of cancers with FGFR genetic alterations. A previous infigratinib trial, that included 2 TIO patients, normalized FGF23 and phosphate in both, with decreased metastatic PMT burden in one.Four patients (2m, 2f; 26-41y) with TIO due to non-localized or non-resectable PMTs were enrolled in a 24w open-label phase 2 trial of oral infigratinib with the goal of inducing persistent biochemical remission after drug discontinuation. The starting dose was 75 mg/d, which was adjusted to 25-125 mg/d based on biochemical changes and tolerability.Three patients completed 24w of infigratinib; 2 had dose interruptions due to adverse events (AEs). The 4th subject completed 17w of infigratinib, which was then held due to an AE and not restarted because of rising C-terminal FGF23 levels on therapy. Biochemical parameters improved in all patients while on infigratinib including decrease in intact FGF23, and an increase in blood phosphate and 1,25D (Fig). After drug discontinuation, values returned to baseline, indicating a lack of persistent biochemical remission. 68Ga-DOTATATE scans at 24w in the 2 subjects with identified PMTs showed a decrease in PMT activity but not size. After study end, 3 subjects pursued other therapies, and 1 received infigratinib for an additional 42d.All subjects experienced mild to moderate treatment-related, dose-limiting AEs but no serious AEs. The study closed early due to a greater than expected incidence of ocular AEs, possibly due to the continuous daily dosing regimen, and evidence from these first 4 subjects that permanent remission was unlikely on infigratinib.Infigratinib suppression of PMT activity with metabolic remission confirmed the role of FGFR signaling in PMT pathogenesis, consistent with an autocrine feed-forward physiology. Because persistent remission was not achieved with discontinuation, and treatment-related, primarily ocular, AEs were significant, infigratinib should only be considered in those with life-limiting metastatic TIO.

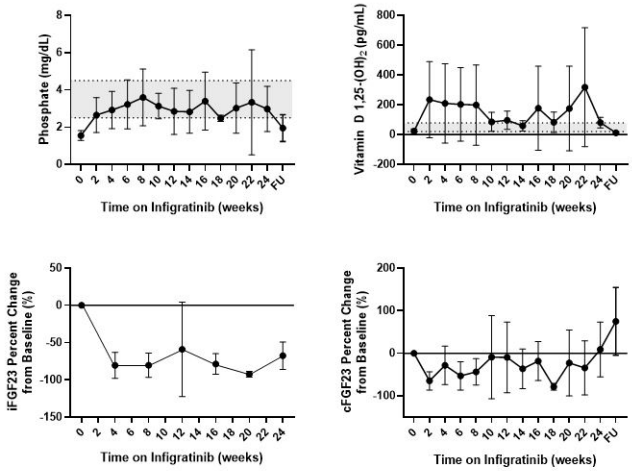

Figure: Biochemical response to infigratinib (mean±SD): Assessments were performed every 2 weeks and at follow up (FU) after at least 7 days off therapy. Phosphate and 1,25D increased to at or above the normal range, while returning to baseline low levels after discontinuation. On infigratinib, intact FGF23 decreased by a mean of 59-92% of the baseline value. C-terminal FGF23 decreased in some patients, but returned to baseline or above after stopping therapy. Shaded area reflects normal range.

***Disclosures: Iris R. Hartley**, QED Therapeutics, Grant/Research Support*

P-763

A Phase 1 PK/PD Study of Once vs Twice Daily Administration of rhPTH(1-84) in Patients With Hypoparathyroidism: Final Analysis *Steven Wai Ing[1], Richard D Finkelman[2], Ping He[3], Aliya A. Khan[4], Michael Mannstadt[5], Lars Rejnmark[6], Ivy Song[3], István Takács[7]. [1]Division of Endocrinology, Diabetes and Metabolism, Ohio State University, United States, [2]Shire Human Genetic Therapies, Inc., a Takeda company, Lexington, MA, USA, United States, [3]Shire Human Genetic Therapies, Inc., a Takeda company, Lexington, MA, USA, United States, [4]McMaster University, Canada, [5]Endocrine Unit, Massachusetts General Hospital and Harvard Medical School, United States, [6]Department of Clinical Medicine, Aarhus University Hospital, Denmark, [7]Department of Medicine, Faculty of Medicine, Semmelweis University, Hungary

Introduction: In the US, recombinant human parathyroid hormone, rhPTH(1-84), is indicated as an adjunct to calcium (Ca) and active vitamin D (vitD) once daily (QD) to control hypocalcemia in patients with hypoparathyroidism (HypoPT). In a phase 1 study, we compared PTH pharmacokinetics (PK) and pharmacodynamic (PD) effects (serum Ca [S-Ca], urinary Ca [U-Ca] excretion) between QD and twice daily (BID) administration over a single day.Methods: Patients with chronic HypoPT (n=34; 30 [88.2%] female; 33 completers) were sequentially enrolled into 1 of 4 rhPTH(1-84) treatment cohorts in a crossover study design. All received single-dose (100 µg QD) plus one of two BID doses (25 µg BID or 50 µg BID) of rhPTH(1-84); without oral Ca (cohorts 1 & 2) or with oral Ca (cohorts 3 & 4). Cohort 1: 25µg BID or 100µg QD, no Ca (n=9). Cohort2: 50µg BID or 100µg QD, no Ca (n=8). Cohort 3: 25µg BID or 100µg QD, with Ca (n=9). Cohort 4: 50µg BID or 100µg QD, with Ca (n=8). Within each cohort, patients were randomized 1:1 to sequence order: QD→ BID vs BID→QD. All received their usual conventional therapy (oral Ca/active vitD) on Day –1, prior to rhPTH(1-84) dose (Day 1). Active vitD was withheld on Day 1. After a washout period, patients crossed over to the opposite rhPTH(1-84) treatment (QD or BID). S-Ca and U-Ca were obtained on Days –1 and 1. Data were summarized using descriptive statistics.Results: S-Ca responses were generally similar among treatments, although S-Ca tended to be numerically higher where treatment included adjunctive oral Ca. Compared with conventional therapy (Day –1), rhPTH(1-84) treatment at 100µg QD, 50µg BID, or 25µg BID markedly reduced 24-h U-Ca excretion in cohorts without oral Ca (1 & 2) by 32.0%, 49.6%, and 47.6%, respectively and in cohorts with oral Ca (3 & 4) by 18.4%, 17.7%, and 31.1%, respectively (Figure). Overall, 18 (52.9%) patients experienced 58 treatment-emergent adverse events (TEAEs), 26 considered treatment-related. All but 2 TEAEs were resolved. No serious TEAEs were reported.Conclusions: S-Ca was not different among the three rhPTH(1-84) regimens. Treatment with rhPTH(1-84) led to a decrease in U-Ca excretion compared with oral Ca/active vitD. With respect to BID administration, U-Ca excretion was reduced incrementally compared with QD but less so when treatment included adjunctive oral Ca. No new safety findings were observed with rhPTH(1-84) whether QD or BID. Data reflect a single day of dosing.

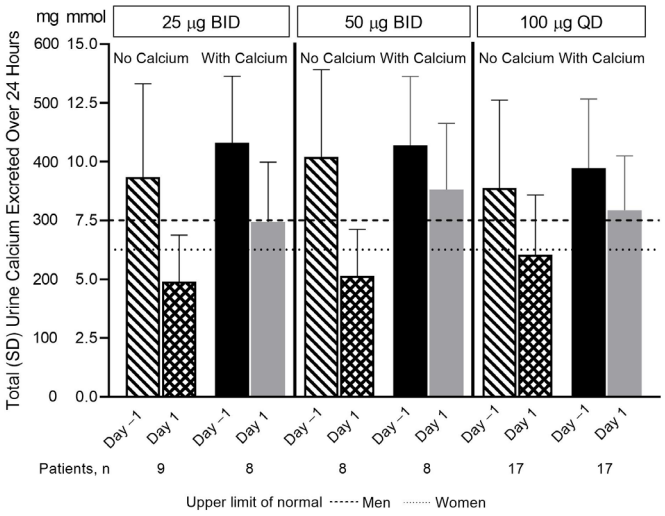

***Disclosures: Steven Wai Ing**, Shire, a Takeda company, Grant/Research Support*

P-764

Calcium and Phosphate Homeostasis in Patients With Chronic Hypoparathyroidism on Conventional Therapy *Olulade Ayodele[1], Lars Rejnmark[2], Allison Briggs[3], Kristina Chen[4], Clara Monleón Bonet[5], Angela Lax[3], Fan Mu[3], Nicole Sherry[6], Elvira Gosmanova[7]. [1]Shire Human Genetic Therapies, Inc., Global Evidence and Outcomes, Data Sciences Institute, United States, [2]Aarhus University and Aarhus University Hospital, Denmark, [3]Analysis Group, Inc., United States, [4]Former, Shire Human Genetic Therapies, Inc., Global Evidence and Outcomes, Data Sciences Institute, Research and Development; Current, Arena Pharmaceuticals, United States, [5]Shire International GmbH, Switzerland, [6]Shire Human Genetic Therapies, Inc., United States, [7]Albany Medical College, United States

Objective: To evaluate longitudinal albumin-corrected serum calcium (Ca), serum phosphate (P), and calcium-phosphate product (Ca × P) levels in patients (pts) with chronic hypoparathyroidism (HypoPT) receiving conventional therapy.Methods: Pts with chronic HypoPT were identified from the Explorys electronic medical record database (Jan 2007–Aug 2019) in the US. Index date was the day after first calcitriol prescription. Ca analysis included pts with >=1 pair of serum albumin and serum Ca values reported on the same date during the 6 mo before index and during 5 years (y) (+/-6 mo) follow up. P and Ca × P analyses were conducted among pts in the Ca analysis sample with >=1 available P value on the same date as their Ca measurement. Pt characteristics before index date were evaluated. Mean proportion of measurements per pt within specified ranges throughout the 5-y period after the index date was assessed using the following ranges for Ca (target range [2.00–2.25 mmol/L], normal range [2.15–2.55 mmol/L], mild hypocalcemia [1.875–2.00 mmol/L], moderate-severe hypocalcemia [2.55 mmol/L]), P (normal range: >=0.81–<=1.45 mmol), and Ca × P (normal range: <=4.4 mmol2/L2).Results: There were 143 pts with available Ca data; mean +/- SD age was 55.3+/-14.9y. Pts had a mean +/- SD (range) of 41.4%+/-24.62% (0–100.00%) of Ca measurements within target range, 28.5%+/-27.06% (0–100.00%) of measurements above target range but within normal range, and 10.4%+/-12.75% (0–50.00%) of measurements within the mild hypocalcemia range (Figure). Also, 15.1%+/-22.34% of Ca measurements were in the moderate-severe hypocalcemia range and 4.7%+/-9.30% were in the hypercalcemia range. The P and Ca × P analysis sample included 31 pts (mean +/- SD age 56.1+15.0y). These pts had a mean +/- SD (range) of 58.8%+/-25.59% (4.55–100.00%) of P measurements and 96.7%+/-6.16% (76.47–100.00%) of Ca × P measurements within normal range.Conclusions: Despite the paramount importance of normal Ca and P homeostasis for health-related outcomes in HypoPT, pts treated with conventional therapy had sub-optimal control of Ca, with wide fluctuations in Ca and P during the 5-y period. Having Ca and/or P measurements outside the target range has been shown to be associated with poor long-term outcomes in pts with HypoPT, including increased risk of renal and cardiovascular complications.

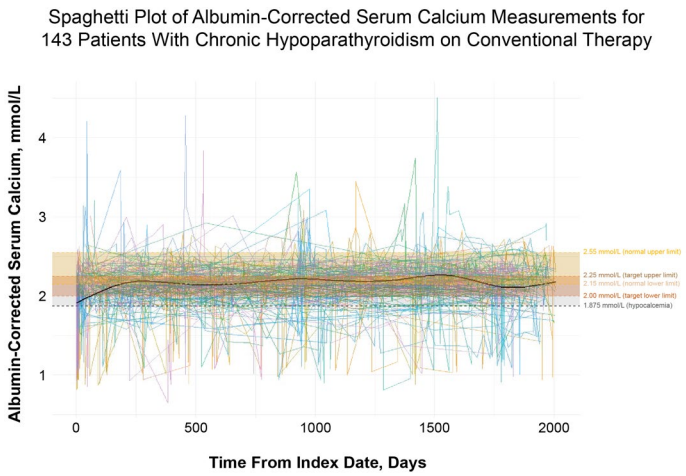

***Disclosures: Olulade Ayodele**, Takeda, Other Financial or Material Support*

P-765

Clinical responses in adult XLH patients not achieving consistent serum phosphate normalization: A subgroup analysis of a randomized, double-blind, placebo-controlled, Phase 3 study (CL303 NCT02526160) *Maria Luisa Brandi[1], Susan Wood[2], Mark Nixon[3], Jennifer Liu[3], Robin Lachmann[4]. [1]Azienda Ospedaliero Universitaria Careggi, Italy, [2]Kyowa Kirin International, United Kingdom, [3]Chilli Consultancy, United Kingdom, [4]Charles Dent Metabolic Unit National Hospital for Neurology and Neurosurgery, United Kingdom

X-linked hypophosphataemia (XLH) is characterised by excess Fibroblast growth factor 23 (FGF23) activity and chronic hypophosphataemia. Burosumab, a fully human anti-FGF23 antibody, restores phosphate homeostasis, thus improving musculoskeletal symptoms and physical function.CL303 is a phase 3 multicentre, randomized, double-blind, placebo-controlled study that evaluated the efficacy and safety of burosumab in adults with XLH. Adults were randomized (1:1) to SC administration of burosumab (1.0mg/kg) or placebo, Q4W for 24 weeks. 92.6% of the burosumab group achieved a mean serum phosphate concentration above the lower limit of normal (LLN) across the midpoints of the dose intervals through W24, compared with only 7.6% of the placebo group ($p < 0.0001$). This exploratory analysis compared clinical outcomes at W24 in subjects with phosphate levels >=LLN for the majority of their visits in the first 24 weeks (>=6/12) (Pi 6+) versus those with fewer (Pi 5-) and was performed in subjects with complete data for both serum phosphate and TmP/GFR measurements.Most subjects treated with burosumab (39/79.6%) had serum phosphate >=LLN for 6 or more visits (Pi6+) versus only 2 (4%) of placebo-treated subjects. Patients treated with burosumab achieved a mean increase in serum phosphate of at least 30% from baseline. All burosumab subjects achieved TmP/GFR measurements >=LLN. Clinical outcomes at Week 24 are shown in the table. Data are not shown for the 2 patients in the placebo Pi 6+ group as small sample size renders results not meaningful.Burosumab consistently improved serum phosphate levels with XLH. Clinical outcomes were improved in subjects treated with burosumab, including those who achieved LLN at less than half of their study visits. A sustained improvement of serum phosphate is a good indicator of clinical effect in these patients even if individual measurements fall short of the LLN.

Clinical outcomes	Pi 6+		Pi 5-	
	Burosumab N=39	Placebo N=2	Burosumab N=10	Placebo N=47
LS Mean (SE)				
BPI Worst Pain				
Baseline	8.1 (0.19)	N/A	8.4 (0.16)	7.9 (0.22)
W24	7.3 (0.31)		7.0 (0.65)	7.5 (0.30)
BPI Average Pain				
Baseline	6.9 (0.19)	N/A	6.9 (0.50)	6.4 (0.21)
W24	5.9 (0.32)		5.9 (0.65)	6.2 (0.32)
WOMAC Stiffness				
Baseline	65.1 (3.29)	N/A	58.8 (8.13)	62.2 (3.35)
W24	56.4 (3.37)		47.5 (5.83)	61.7 (2.97
WOMAC Physical Function				
Baseline	51.0 (3.10)	N/A	44.7 (6.27)	43.3 (2.83)
W24	43.2 (3.23)		47.6 (5.52)	44.0 (3.27)

BPI higher score indicates worst pain; Higher scores on the WOMAC indicated worse stiffness and functional limitations

***Disclosures: Maria Luisa Brandi**, Kyowa Kirin, Consultant*

Posters

P-766

Mild X-linked hypophosphatemia (PHEX c.*231A>G): Normalization of serum phosphorus levels with low-dose burosumab therapy *Gary Gottesman[1], Valerie Wollberg[1], Steven Mumm[2], Michael Whyte[1]. [1]Shriners Hospitals for Children-St. Louis, United States, [2]Washington University School of Medicine, United States

X-linked hypophosphatemia (XLH), from deactivating mutations of PHEX, is the most common heritable disorder featuring renal phosphate (Pi) wasting. Elevated circulating levels of phosphatonin FGF23 cause hypophosphatemia in affected children leading to rickets with skeletal deformity and reduced linear growth. In 2015, we reported uniquely mild XLH in American children and mothers carrying the non-coding PHEX 3'-UTR mutation c.*231A>G. At last year's ASBMR meeting, we reported that a duplication of PHEX exons 13 – 15 was present in 3'-UTR patients. Hence, the 3'-UTR change may represent a molecular marker for this mild XLH phenotype. This year, our retrospective age- and sex-matched 1:1 case-control publication contrasted clinical, biochemical, and DXA findings of 30 people harboring the 3'-UTR mutation versus 30 individuals with classic XLH. We demonstrated the 3'-UTR group had mild XLH, especially the females who were often undiagnosed and untreated. In XLH, burosumab, the fully-human monoclonal antibody targeting FGF23 (approved by the FDA in 2018), improves Pi homeostasis and rickets in children and osteomalacia in adults. Herein, we report our experience treating four children (1 boy, 3 girls) with the 3'-UTR defect who required only low-dose (0.3 mg/kg/dose) burosumab therapy given subcutaneously every two weeks to normalize their serum Pi levels and improve their reported symptoms. For another girl with a family history of XLH, we had started her on a standard burosumab dose of 0.8 mg/kg every 2 weeks (rounded per initial FDA-approved Prescribing Information). She became hyperphosphatemic requiring a reduced dose. Subsequently, PHEX molecular analysis revealed a 3'-UTR mutation. The 3'-UTR PHEX genotype is presently the single known etiology of mild XLH, although our experience with greater than 350 XLH children and their families indicates other PHEX alterations cause mild disease. Identifying XLH patients with this PHEX 3'-UTR variant, or other mild phenotypes, has implications for safe treatment with burosumab or calcitriol and phosphate. Molecular diagnosis of the 3'-UTR PHEX genotype will help guide safe and appropriate therapy.

***Disclosures: Gary Gottesman**, None*

P-767

Characterization of Comorbidity in X-linked Hypophosphatemia: A Prospective Parallel Cohort Study Using the UK CPRD *Samuel Hawley[1], Nick Shaw[2], Antonella Delmestri[1], Daniel Prieto-Alhambra[1], Cyrus Cooper[3], Rafael Pinedo-Villanueva[1], M. Kassim Javaid[1]. [1]University of Oxford, United Kingdom, [2]Birmingham Women's and Children's NHS Foundation Trust, United Kingdom, [3]University of Southampton, United Kingdom

Background and objective: X-linked hypophosphatemia (XLH) is a rare multisystemic disease of mineral homeostasis that has a prominent skeletal phenotype. We have previously demonstrated an unexpected increase in mortality in patient with XLH. We here aimed to describe comorbidity in patients with XLH and compare this to general population controls. Material and methods: The Clinical Practice Research Datalink (CPRD) GOLD was used to identify a cohort of XLH patients (1995-2016), along with a non-XLH cohort matched (1:4) on age, gender and GP practice at date of first XLH diagnosis (index date). Previously published phenotyping algorithms openly available from the online CALIBER portal were used to identify the first primary care diagnosis (and associated age) of 273 defined comorbid conditions during any eligible patient follow-up. For primary analysis, the individual conditions were merged into 15 major disease categories and the proportion of patients having >=1 diagnosis in each category was compared between cohorts using univariable logistic regression. In secondary analysis individual conditions were compared. Only categories/conditions affecting >=10% of either cohort were included in these comparisons given the large number of comorbidities screened relative to a limited sample size. Bonferroni corrected P-values were used to account for multiple testing.Results: There were 64 and 256 patients in the XLH and non-XLH cohort, respectively. Of these, 45% were aged over 16 years at index date and 70.5% were female. Average follow-up per patient was 10.2 years. Recorded comorbidities (categorized) are presented in the table (below). In secondary analyses of individual conditions, eight were recorded in at least 10% of XLH patients which in age ascending order were: acne, dermatitis, asthma, rhinitis, migraine, depression, enthesopathy and hypertension. Four conditions were at least twice as likely to be present in the XLH relative to non-XLH cohort, but only depression met the Bonferroni threshold: odds ratio= 2.95 [95%CI: 1.47 to 5.92]; p=0.0023.Conclusion: Findings suggest XLH patients have elevated levels of comorbidity broadly defined as endocrinological and neurological, in addition to nearly three times the occurrence of depression. These findings should raise awareness of the non-skeletal effects of this rare bone disease.

Table: Counts, age and odds ratios of having at least 1 diagnosis of a comorbid condition within major condition categories

Condition category [1]	XLH cohort (n=64)			non-XLH cohort (n=256)			Odds Ratio			
								95% CI		
	Number with ≥1 condition	%	Mean age at earliest diagnosis	Number with ≥1 condition	%	Mean age at earliest diagnosis	Estimate	Lower	Upper	p-value [2]
Circulatory/CV System	8	12.5	50.8	25	9.8	56	1.32	0.57	3.08	0.5211
Digestive System	10	15.6	45.8	49	19.1	36.5	0.78	0.37	1.64	0.5173
Endocrine System	10	15.6	38.8	13	5.1	49.5	3.46	1.44	8.31	0.0054*
Genitourinary System	15	23.4	43.1	49	19.1	41	1.29	0.67	2.49	0.4429
Mental Health Disorders	17	26.6	36.4	41	16	37.7	1.90	0.99	3.62	0.0527
Musculoskeletal Conditions	13	20.3	47.3	36	14.1	46.3	1.56	0.77	3.15	0.2169
Neurological Conditions	13	20.3	32.6	20	7.8	34.5	3.01	1.41	6.44	0.0046*
Respiratory System	21	32.8	26.7	63	24.6	22.2	1.50	0.83	2.71	0.1839
Skin Conditions	23	35.9	20.8	108	42.2	18.7	0.77	0.44	1.36	0.3639

[1] Only including categories affecting ≥10% of either XLH cases or controls

[2] An astrix (*) indicates p-value was below the Bonferroni corrected threshold, which was p=0.0055556

***Disclosures: Samuel Hawley**, None*

P-768

A qualitative thematic analysis of the burden of illness of x-linked hypophosphatemia across the life course *Juddith Bubbear[1], Angela J Rylands[2], Angela Williams[2], Karen Bailey[3], Jacqui Bernarde[3], Moira Cheung[4]. [1]Royal National Orthopaedic Hospital NHS Trust, United Kingdom, [2]Kyowa Kirin International, United Kingdom, [3]OPEN VIE, United Kingdom, [4]Evelina London Children's Hospital, United Kingdom

X-linked hypophosphatemia (XLH) is a rare, genetic phosphate-wasting disorder. Bone, muscular and dental problems begin early in childhood, widening to include multiple complications and symptoms in adulthood. This qualitative analysis aimed to explore the symptoms or complications from XLH that interfere most with life using a sub-set of data from burosumab-naïve participants completing a large multinational online patient survey. Responses to two open-ended questions from adults (n=209) and children (n=86 via proxy report) with self-reported XLH (59% US, 24% EU, 17% Rest of World) were analysed by age group (1-4, 5-11, 12-17, 18-29, 30-39, 40-49, 50-59, 60+ years) using hybrid deductive and inductive thematic analysis. Two researchers independently coded and analysed the responses, with any differences settled in consensus with a multifaceted research group. Dominant themes, across the life course, were identified according to the most frequently applied codes, and grouped into three categories. The categories were: 1. "clinical signs and symptoms", 2. "impact of signs and symptoms" and 3. "negative treatment experiences". Within category 1, 'pain' was the most dominant theme across the life course, with frequent reports of 'joint pain' in adults and 'bone pain' in children, 'bone and joint pathology' interfered with life most frequently in children. 'Dental problems' were problematic across life, beginning in early years, with 'stiffness' emerging as a symptom in early adulthood. For category 2, interference with 'movement and physical exertion' was a major theme across all age groups. Impact on 'emotional wellbeing' was widely reported, in particular 'depression' and 'worries about the future' in adults and 'frustration' and 'lack of self-esteem' in children. 'Social impacts' was an important theme, largely due to 'feeling different from peers' for teenagers and 'social isolation' for adults. For category 3, 'medication frequency' was most burdensome for children, with adult groups focussing more on lack of 'access to appropriate treatment'. This qualitative analysis highlights that symptoms and complications of XLH can be physical, emotional and social in nature, presenting throughout the lifetime, although the symptoms or complications that interfere most notably vary between children, adolescents and adults. Findings contribute new insights to age-specific impacts of XLH, illustrating the need for age-appropriate multidisciplinary care.

***Disclosures: Juddith Bubbear**, Kyowa Kirin International, Consultant*

P-769

A Clinical Trial to Assess Safety and Efficacy of Burosumab in Cutaneous Skeletal Hypophosphatemia Syndrome (CSHS) *Rachel Gafni[1], Andrea Estrada[2], Alison Boyce[1], Mirini Kim[3], Lindsay Weigley[3], Elmer Rajah[3], Austin Gillies[3], Laura Tosi[3]. [1]Skeletal Disorders and Mineral Homeostasis Section, National Institute of Dental and Craniofacial Research, National Institutes of Health, United States, [2]Division of Endocrinology and Diabetes, Children's National, United States, [3]Bone Health Program, Division of Orthopaedics & Sports Medicine, Children's National, United States

Purpose:CSHS is a rare multi-lineage mosaic disorder due to somatic gain-of-function RAS variants, manifesting with skin lesions, skeletal dysplasia, neoplasms, and FGF23-mediated hypophosphatemia. Conventional therapy includes phosphate and active vitamin D, but the regimen is often poorly tolerated and associated with complications. Burosumab is a fully human monoclonal antibody against FGF23 approved for X-linked hypophosphatemia. As FGF23 levels are elevated in CSHS, we initiated a 52-week investigator-sponsored trial evaluating burosumab in an 18-year-old skeletally-mature woman with debilitating CSHS. Methods: Oral calcitriol and phosphate were stopped 1 week prior to the 1st dose. Burosumab was given q4w (starting at 0.3mg/kg), with biochemistries q2-4w. The dose was titrated to keep trough Pi levels normal. Additional results including skeletal imaging, fitness testing, and patient-reported outcomes are pending completion of 52 weeks.Results:Data reflects 36 weeks of treatment. Screening FGF23 was 224 RU/ml (normal < 180). At baseline, fasting

Pi was 1.6 mg/dL (2.5-4.5), 1,25 (OH)2-Vitamin D 16 pg/mL (1,25D,18-72), TmP/GFR 1.4 mg/dL (2.5-4.2). Two weeks after the 1st dose, all 3 rose into the normal range to 3 mg/dL, 68 pg/mL, and 3.2 mg/dL, respectively, consistent with FGF23 blockade. Burosumab was increased to 0.6 mg/kg with the 3rd injection, when the trough Pi was 2.1 mg/dL; Pi, 1,25D, TmP/GFR, alkaline phosphatase, Ca, and PTH remained in the normal range on this dose (Figure). Of note, the patient had a history of primary hyperparathyroidism with nephrolithiasis; curative resection of a parathyroid adenoma occurred 1 year prior to study enrollment. Renal ultrasound at screening demonstrated small asymptomatic nephroliths without nephrocalcinosis however, after 7w of burosumab, she passed several calcium oxalate kidney stones, without concurrent hypercalciuria. It is unclear if burosumab promoted new stone formation or simply led to mobilization of pre-existing stones. Otherwise, burosumab has been well-tolerated and the patient reports subjective reduction in fatigue and improvement in strength.Conclusion: 36 weeks of burosumab normalized Pi, 1,25D, and TmP/GFR in an adult with FGF23-mediated hypophosphatemia due to CSHS, similar to patients with XLH. While the increased passage of kidney stones was documented, relationship to the drug remains unclear. These early data suggest burosumab may be a safe and effective treatment for CSHS.

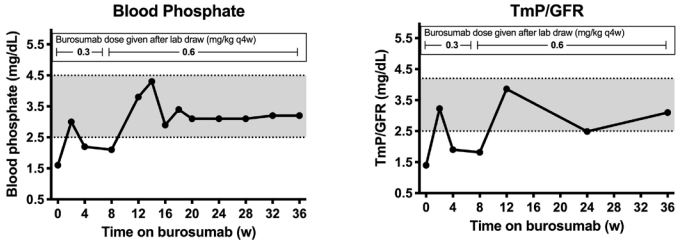

***Disclosures: Rachel Gafni**, Ultragenyx Pharmaceutical, Grant/Research Support*

P-770

Persistent Hypophosphatasemia and its Musculoskeletal Repercussion

*Ariela Kitaigrodsky[1], Luisa Plantalech[1], Sebastian Marciano[1], Maria Diehl[1], Graciela Jimenez[1]. [1]Hospital Italiano de Buenos Aires, Argentina

Introduction: Low alkaline phosphatase (ALP) or hypophosphatasemia due to hypophosphatasia or to secondary causes; although rare and probably underdiagnosed, could have clinical implications. The aim of this report is to estimate the hypophosphatasemia prevalence and describe our clinical findings in adults with persistent hypophosphatasemia. Methods: An electronic medical record search of adult members of our health care system between 2013 and 2017 was made. Those members with two or more ALP <= 30 IU/l, no ALP > 30 IU/l, and no diagnosis of secondary causes were selected. Clinical reports and available complementary studies were analyzed. The categorical variables were expressed as absolute number and percentage, the numerical ones in median and interquartile range 25% -75% (RIC). Results: Persistent hypophosphatasemia was detected in 0.07% (0.06-0.09) of 105.925 members. One patient was excluded because of celiac disease as a secondary cause, 77 cases were included; 61.1% were women, with a median age of 44 (34-56) years old, ALP was 24 (20-27) IU/l and phosphatemia 4.1 (3.8-4.6) mg/dl. Osteoarthritis, vascular calcifications and fractures were detected in 45, 13 and 12 patients respectively; nephrolithiasis, diffuse idiopathic skeletal hyperostosis (DISH), tooth loss and seizures were less frequently reported. At least one of those clinical manifestations was observed in 63.6% of the cases, but in only 5.2% of them hypophosphatasemia had been registered in their clinical record. Densitometric analysis showed osteopenia or osteoporosis in 76.2%. The majority of the 19 fractures observed were of the radius, with no gender predominance. Four patients received bisphosphonates, with low ALP before starting them. No atypical fractures were observed, one patient presented with multiple fractures (pelvis, olecranon and wrist) after antiresorptive treatment. Conclusions: The prevalence of hypophosphatasemia was 0.07%. Findings in medical records were not taken into account in most cases, but far from being asymptomatic, varied clinical manifestations were observed, similar to what had been previously reported in other hypophosphatasemia and adult hypophosphatasia series. In the presence of hypophosphatasemia without a secondary cause, adult hypophosphatasia should be suspected. An adequate diagnosis of hypophosphatasia is relevant due to its clinical and therapeutical implications (antiresorptives should be avoided) as well as for genetic counseling.

***Disclosures: Ariela Kitaigrodsky**, None*

P-771

Whole Exome Sequencing (WES) Reveals Likely Pathogenic Variants in a Small Subset of Premenopausal Women with Idiopathic Osteoporosis

*Adi Cohen[1], Joseph Hostyk[2], Evan H. Baugh[2], Christie M. Buchovecky[2], Vimla S. Aggarwal[2], Robert R. Recker[3], Joan M. Lappe[3], Mafo Kamanda-Kosseh[1], Mariana Bucovsky[1], Julie Stubby[3], David B. Goldstein[2], Elizabeth Shane[1]. [1]Columbia University Irving Medical Center, United States, [2]Columbia University Institute for Genomic Medicine, United States, [3]Creighton University Medical Center, United States

Premenopausal women with idiopathic osteoporosis diagnosed in adulthood (PremenIOP) have profound bone structural deficiencies and commonly report both adult and childhood fractures (Fx) and family history (FH) of osteoporosis. Some have very low bone formation rates suggesting osteoblast dysfunction. These features led us to investigate potential genetic etiologies of bone fragility.In 75 PremenIOP, we performed WES using our variant analysis pipeline to select candidate variants. All had transiliac bone biopsies after tetracycline labeling of bone forming surfaces. The variant analysis pipeline highlights rare (<= 6.29e-5 allele frequency) and novel genotypes likely to affect known disease genes, including known pathogenic variants, compound heterozygous variants, protein-truncating variants in susceptible genes, and other novel variants absent from our in-house variant database and external control reference samples.We ran burden analyses both on all genes individually and on a set of implicated osteoporosis genes. For LRP5 in particular, we also assessed the frequency of all (including common) variants in subjects vs controls (reference cohort, n=18,746 without a diagnosis of osteoporosis).59 women had adult low trauma Fx and 16 had low BMD but no adult Fx. No novel genotype was identified. The cases had no increased burden of common LRP5 variants when compared to controls. Our cohort-wide collapsing results showed that no gene had genome-wide significance between rates of cases and controls with qualifying variants. The variant analysis pipeline did not highlight variants in COL1A1, COL1A2, WNT, or ALPL. The pipeline identified 4 heterozygous variants in LRP5 and PLS3 (encoding Plastin 3) that confidently contribute to osteoporosis. All 4 were either protein-truncating/loss-of-function variants or occurred at sites within the protein that have known pathogenic variants in ClinVar or HGMD. All 4 women had adult Fxs, and 3 had multiple Fxs, childhood Fxs and a FH of osteoporosis. Two presented during pregnancy or lactation. Tissue level bone formation rate was below normal in 3 and just above the lower normal limit in one.In summary, WES revealed likely pathogenic variants in LRP5 and PLS3 in only 4 of 75 women with PreMenIOP. All 3 LRP5 variants were highlighted as rare. In the rest of the group, the LRP5 variant rate was similar to controls. Further functional studies are planned to investigate phenotypic effects of the identified variants.

	All Subjects N=75 Mean±SD	Subject #1	Subject #2	Subject #3	Subject #4
Gene		PLS3	LRP5	LRP5	LRP5
HGVS		ENST00000420625.2:c.367+1G>A	ENST00000294304.7:c.4157delC ENSP00000294304.6:p.Ile1387SerfsTer52	ENST00000294304.7:c.1519G>C ENSP00000294304.6:p.Gly507Arg	ENST00000294304.7:c.3758G>T ENSP00000294304.6:p.Cys1253Phe
Effect		Loss of Function: Splice-donor Variant	Loss of Function: Frame-shift	Missense	Missense
Age (years)	38±7	31	44	44	38
Ht (cm)	163±7	154	162	161	167
Wt (kg)	59±11	56	74	62	64
BMI (kg/m^2)	22.2±3.7	23.6	28.1	23.9	23.0
BMD Z scores LS TH FN DR	 -1.9 ± 1.1 -1.3 ± 0.9 -1.6 ± 0.9 0.1 ± 0.9	 -3.8 -2.4 -2.2 -0.8	 -2.1 -1.0 -1.5 -0.8	 -3.1 -1.6 -2.6 -0.1	 -1.7 -0.8 -0.7 0.4
# of adult Fx	2.3 ± 2.5	7	2	1	2
Fx Types	--	Wrist, rib, multiple vert: T3,T4,T6,T8,T9	Ankle and wrist	Rib	Right hip x 2
History of pregnancy or lactation associated Fx	14/75 = 19%	YES	NO	NO	YES
History of vertebral Fx	18/75 = 24%	YES	NO	NO	NO
History of multiple Fx in adulthood	37/75=49%	YES	YES	NO	YES
History of childhood Fx	28/75 = 37%	YES	NO	YES	YES
Family history of osteoporosis	48/75 = 64%	YES	YES	YES	NO
Bone formation rate (histomorphometry of bone biopsy sample; N=71; mm^2/mm/year)	0.010 ± 0.008	0.000 (undetectable)	0.000 (undetectable)	0.007	0.002
Low bone turnover as previously defined (< 0.006 mm^2/mm/year)	17/71 = 24%	YES	YES	NO	YES

***Disclosures: Adi Cohen**, None*

Posters

P-772

Vitamin B6 Sufficiency In Children With Hypophosphatasia *Michael P. Whyte[1], Fan Zhang[2], Deborah Wenkert[2], Karen E. Mack[2], Karen L. Ericson[3], Vinieth N. Bijanki[2], Stephen P. Coburn[4]. [1]Center for Metabolic Bone Disease and Molecular Research, Shriners Hospitals for Children-St. Louis; and Div. of Bone and Mineral Diseases, Dept. of Internal Medicine, Washington University School of Medicine at Barnes-Jewish Hospital, United States, [2]Center for Metabolic Bone Disease and Molecular Research, Shriners Hospitals for Children-St. Louis, United States, [3]Department of Chemistry, Purdue University-Fort Wayne, United States, [4]Dept. of Chemistry, Purdue University-Fort Wayne, United States

Hypophosphatasia (HPP) is the metabolic bone disease caused by loss-of-function mutation(s) of the ALPL gene that encodes the tissue non-specific isoenzyme of alkaline phosphatase (TNSALP). In HPP, autosomal dominant and autosomal recessive inheritance from among ~ 400 usually missense defects located throughout ALPL largely explains the broad-ranging severity of this inborn-error-of-metabolism. TNSALP is a cell-surface phosphohydrolase expressed especially in the skeleton, liver, and developing teeth. Thus, in HPP its substrates accumulate extracellularly and include pyridoxal 5′-phosphate (PLP), the principal circulating form of vitamin B6 (B6). In neonates and babies with life-threatening HPP, markedly compromised dephosphorylation of PLP by TNSALP can lower circulating pyridoxal (PL), the B6 metabolite capable of cell entry, and thereby cause B6-dependent seizures. For milder HPP, our initial findings from relatively few patients showed circulating PL levels were not low and thereby indicated B6 homeostasis was intact. Then in 2015 our 25-year experience with 173 affected children and adolescents expanded the clinical nosology for pediatric HPP to include, by increasing severity, odonto HPP, mild childhood HPP, severe childhood HPP, infantile HPP, and perinatal HPP. In 2018, having used our cation-exchange high-pressure liquid chromatography method since 1985 to study this cohort, we documented invariably elevated plasma PLP that reflected HPP severity in all 150 patients tested. Herein, from that study, we show both plasma PL and the vitamin B6 degradation product 4-pyridoxic acid (PA) were normal or elevated, but not low: PL mean (SD) 66.7 (59.0) nmol/L [control 39.2 (41.0)] ($p = 0.1293$), and PA 40.2 (25.1) nmol/L [control 39.4 (33.9)] ($p = 0.8152$). Furthermore, L-tryptophan challenge of 5 children with HPP revealed no evidence of B6 deficiency. Thus, in children and adolescents with non-life-threatening HPP, B6 sufficiency is intact, including PL, the form of B6 capable of cell entry.

***Disclosures: Michael P. Whyte**, None*

P-773

High Bone Mass From Mutation Of Low-Density Lipoprotein Receptor-Related Protein 6 (LRP6) *María Lorena Brance[1], Lucas R. Brun[2], Nicolás M. Cóccaro[3], Andrés Aravena [4], Shenghui Duan[5], Steven Mumm[6], Michael P. Whyte[7]. [1]Reumatología y Enfermedades Óseas. Rosario. Argentina; Bone Biology Laboratory. School of Medicine, Rosario National University, Argentina; National Council of Scientific and Technical Research (CONICET), Argentina, Argentina, [2]Bone Biology Laboratory. School of Medicine, Rosario National University, Argentina; National Council of Scientific and Technical Research (CONICET), Argentina, Argentina, [3]Servicio de Diagnóstico por Imágenes, Sanatorio Británico. Rosario. Argentina, Argentina, [4]Bone Biology Laboratory. School of Medicine, Rosario National University, Argentina, Argentina, [5]Division of Bone and Mineral Diseases, Department of Internal Medicine, Washington University School of Medicine at Barnes-Jewish Hospital, United States, [6]Division of Bone and Mineral Diseases, Department of Internal Medicine, Washington University School of Medicine at Barnes-Jewish Hospital; Center for Metabolic Bone Disease and Molecular Research, Shriners Hospitals for Children-St. Louis, United States, [7]Center for Metabolic Bone Disease and Molecular Research, Shriners Hospitals for Children-St. Louis; Division of Bone and Mineral Diseases, Department of Internal Medicine, Washington University School of Medicine at Barnes-Jewish Hospital, United States

Background: Wnt-signaling is important for skeletal development and health. Eleven heterozygous gain-of-function missense mutations within the first β-propeller of LRP5 are known to cause the autosomal dominant disorder called high bone mass (HBM). Recently, the HBM phenotype was identified in two American families harboring different heterozygous LRP6 missense mutations.Case report: A 19-year-old Argentinian man was referred for "osteopetrosis" with nine years of generalized, medium-intensity bone pain and arthralgias of both knees. His jaw and nasal bridge were broad and several teeth were missing (Figure A). Routine biochemical testing, including of mineral homeostasis, was normal. Urinary deoxypyridinoline and serum CTX were slightly increased. Radiographic skeletal survey showed diffusely increased radiodensity (Figure B). DXA revealed substantially elevated BMD Z-scores. Digital orthopantomography confirmed agenesis of maxillary and mandibular lateral incisors and the second left superior premolar. Cranial magnetic resonance imaging showed diffuse thickening of the calvarium and skull base, dilation of the sheath of the optic nerves containing increased fluid and associated with subtle stenosis of the optic canal, and narrow internal auditory canals. Mutation analyses identified a heterozygous missense mutation in exon 4 of LRP6 leading to a 6-nucleotide/2-amino acid deletion (c.678T>Adel679-684, p.His226Gln-del227-228ProPhe) compromising the first β-propeller of LRP6. Notably, LRP6 HBM seemed distinguishable from LRP5 HBM solely by mutation analysis, except in LRP6 HBM there is distinctive absence of adult lateral incisors.

***Disclosures: María Lorena Brance**, None*

P-774

Clinical, Biochemical and Genetic Study in Patients with Odontohypophosphatasia in Japan *Takuo Kubota[1], Yasuhisa Ohata[1], Yasuki Ishihara[2], Makoto Fujiwara[2], Shinji Takeyari[1], Kenichi Yamamoto[1], Yukako Nakano[1], Taichi Kitaoka[1], Hirofumi Nakayama[1], Chieko Yamada[1], Takeshi Ishimi[1], Rena Okawa[3], Kazuhiko Nakano[3], Tomoyuki Akiyama[4], Haruna Kakimoto[5], Shunsuke Araki[6], Shinichiro Sano[7], Tsutomu Ogata[8], Keiichi Ozono[1]. [1]Department of Pediatrics, Osaka University Graduate School of Medicine, Japan, [2]Department of Pediatrics, Osaka University Graduate School of Medicine; The first Department of Oral and Maxillofacial Surgery, Osaka University Graduate School of Dentistry, Japan, [3]Department of Pediatric Dentistry, Osaka University Graduate School of Dentistry, Japan, [4]Department of Child Neurology, Okayama University Graduate School of Medicine, Dentistry and Pharmaceutical Sciences, Japan, [5]Department of Pediatrics, Kagoshima University Hospital, Japan, [6]Department of Pediatrics, University of Occupational and Environmental Health, Japan, [7]Department of Pediatrics, Hamamatsu Medical Center, Japan, [8]Department of Pediatrics, Hamamatsu University School of Medicine, Japan

Hypophosphatasia (HPP) is characterized by defective mineralization of bone and/or teeth in the presence of low serum alkaline phosphatase (ALP) activity and caused by mutations in the ALPL gene encoding tissue-nonspecific ALP. Odontohypophosphatasia (odonto HPP) is characterized by dental complications without abnormalities of the skeleton system. However, the clinical course and biochemical and genetic features of odonto HPP are limited. Thus, we aimed to investigate clinical, biochemical and genetic features in patients with odonto HPP in Japan. We analyzed 16 unrelated Japanese patients with odonto HPP. The median (min.–max.) duration of follow-up was 2.2 (0.1–12.9) years. The first primary tooth loss occurred at the age of 1.8 (0.7–4.0) years. The age of referral to the department of pediatrics was 3.9 (1.7–11.4) years. Height SDS and weight SDS at the first visit was −0.12 (−2.57 to +1.51) and 0.29 (−1.92 to +1.77), respectively. Serum ALP levels were decreased, 259 (66–361) U/L (The normal range at the age of 3 years is 420 to 1200 [male] or 1130 [female] U/L). Urine phosphoethanolamine (PEA) levels were elevated, 644 (166–1853) nmol/mgCr. In 9 patients, serum levels of pyridoxal 5'-phosphate (PLP) and pyridoxal (PL) were measured. PLP levels were high, 322.7 (132.6–706.7) nmol/L. PL levels were 32.4 (10.8–70.1) nmol/L. PLP/PL ratio was high, 10.7 (6.3–32.5). Ages at the first primary tooth loss were not associated with ALP levels and PLP/PL ratio. ALP levels were negatively correlated with PEA levels and PLP/PL ratio. PEA levels were positively correlated with PLP/PL ratio. The ALPL gene analysis showed 12 patients with a heterozygous mutation and 3 with compound heterozygous mutations, including two novel mutations. ALP and PEA levels in patients with compound heterozygous mutations were decreased and increased, respectively, compared to those with a heterozygous mutation. Two patients began to exhibit skeletal symptoms such as bone pain and muscle weakness during elementary school and then were diagnosed with childhood HPP. Our study in Japan showed that odonto HPP, the mildest form of HPP, has the biochemical characteristics of HPP and that serum ALP levels are negatively correlated its substrate levels. Genotype-phenotype analysis indicated that compound heterozygous mutations result in more profound biochemical abnormalities than a heterozygous one. Patients with odonto HPP may develop childhood HPP as they grow.

***Disclosures: Takuo Kubota**, Alexion Pharmaceuticals, Grant/Research Support*

P-775

Hypophosphatasia: ALPL c.1133A>T, p.D378V and c.1250A>G, p.N417S are the most prevalent dominant American mutations *Steven Mumm[1], Gary Gottesman[2], Shenghui Duan[1], Gabriel Haller[1], Karen Mack[2], Valerie Wollberg[2], Sarah Loving[2], Vinieth Bijanki[2], Fan Zhang[2], C. Charles Gu[1], Christina Gurnett[1], Michael P. Whyte[2]. [1]Washington University School of Medicine, United States, [2]Shriners Hospitals for Children-St. Louis, United States

Hypophosphatasia (HPP) is the rare inborn-error-of-metabolism featuring the consequences of impaired skeletal mineralization caused by loss-of-function mutation(s) in the gene ALPL that encodes the tissue non-specific isoenzyme of alkaline phosphatase. HPP manifests with dental disease, sometimes with rickets in infants and children or osteomalacia in adults. Severity ranges from neonatal lethality to asymptomatic carrier status in adult life. HPP is inherited as an autosomal dominant or recessive trait. Generally, recessive HPP disease is more severe. To better understand the molecular basis and inheritance of HPP, we performed mutation analysis of ALPL in >300 HPP probands over the past 32 years, primarily individuals from North America. Typically using leukocyte DNA and advancing methods of mutation analysis, one ALPL missense mutation, c.1133A>T, p.D378V was found in 39 probands without a second ALPL mutation, making this defect the most prevalent dominant ALPL mutation in our cohort. Co-segregation of the mutation with HPP findings in the large kindreds, confirmed dominant inheritance. Genealogy thus far has not disclosed a common ancestor among these families, who all have early American heritage, although limited haplotype analysis suggests p.D378V in our cohort reflects a shared founder. The patients generally have mild disease (ranging from odonto, mild or severe childhood, to adult HPP). HPP can manifest in carriers as they age. There are literature reports of severe or lethal cases when p.D378V is compound heterozygous with a second ALPL mutation. The other prevalent dominant ALPL mutation, c.1250A>G, p.N417S, was identified in 26 families, and causes relatively mild HPP disease (odonto, mild or severe childhood, or adult HPP) with significant clinical variation among patients when inherited singly, but more severe HPP when inherited with a second ALPL defect. Therefore, surprisingly broad clinical expression of HPP occurs in these 65 families with either of these single dominant ALPL mutations. Additional genetic or environmental factors likely contribute to their HPP phenotype. Exome sequencing to identify modifier genes to help explain this variation is underway.

***Disclosures: Steven Mumm**, None*

P-776

Longitudinal rhPTH(1-84) Data From the Observational PARADIGHM Registry of Patients With Chronic Hypoparathyroidism *Bart Clarke[1], Sigridur Björnsdottir[2], Maria Luisa Brandi[3], Pascal Houillier[4], Aliya A. Khan[5], Michael Levine[6], Michael Mannstadt[7], Lars Rejnmark[8], Tamara Vokes[9], Stefanie Hahner[10], Lorenz Hofbauer[11], Dolores Shoback[12], John Germak[13], Claudio Marelli[14], Pinggao Zhang[13], Neil Gittoes[15]. [1]Mayo Clinic Rochester, United States, [2]Karolinska Institutet, Sweden, [3]University Hospital of Careggi, Italy, [4]Centre de Recherche des Cordeliers, INSERM, Sorbonne Université, France, [5]McMaster University, Canada, [6]Children's Hospital of Philadelphia, United States, [7]Massachusetts General Hospital and Harvard Medical School, United States, [8]Aarhus University and Aarhus University Hospital, Denmark, [9]University of Chicago, United States, [10]University Hospital Würzburg, Germany, [11]Technische Universität Dresden, Germany, [12]San Francisco Veterans Affairs Medical Center; University of California, San Francisco, United States, [13]Shire Human Genetic Therapies, Inc., a Takeda company, United States, [14]Shire International GmbH, a Takeda company, Switzerland, [15]University of Birmingham, United Kingdom

This is the first report of longitudinal data from PARADIGHM, an actively recruiting, prospective, observational registry collecting data for >=10 years per patient with chronic hypoparathyroidism (NCT01922440/EUPAS16927). Monitoring key disease-specific parameters will chart the effectiveness of recombinant human parathyroid hormone, rhPTH(1-84), treatment and conventional therapy (CT; oral calcium and active vitamin D) in patients under routine clinical care. We present 2-year longitudinal data of adult patients who had values for each measured parameter at baseline, 12-months, and 24-months as of August 31 2019. Registry inclusion criteria are patients with hypoparathyroidism for >6 months and receiving CT, rhPTH(1-84) plus CT, or rhPTH(1-84). Baseline was defined as the value entered at the time of enrollment; for rhPTH(1-84)-treated patients, baseline was the most recent value before the first dose of rhPTH(1-84). Only patients who had data at baseline per definition were included in this analysis. The variability in patient numbers across parameters is due to data availability. Patients with outlier data were excluded: serum calcium 20 mg/dL; serum phosphate 8 mg/dL; serum creatinine 10 mg/dL; eGFR no lower limit/ except negative values excluded, >200 mL/min/1.73 m2.Median and mean data are shown in the Table. Both patient groups had stable serum calcium. There was an apparent trend for serum phosphate decline in patients treated with rhPTH(1-84) contrasting with no change in patients receiving CT. There was no differential trend apparent in serum creatinine and eGFR consistent with the short period of observation. Limitations are small sample size and short observation time. Additional years of longitudinal data should result in robust future analyses and demonstrate the growing utility of the PARADIGHM registry for assessing the effectiveness and safety of routine clinical care of patients with chronic hypoparathyroidism treated with rhPTH(1-84) and CT.

Serum Calcium, Serum Phosphate, Serum Creatinine, and eGFR Over Time

	rhPTH(1-84)		Conventional Therapy	
Parameter*	Median (range)	Mean (SD)	Median (range)	Mean (SD)
Serum calcium, mg/dL	n=26		n=110	
Baseline	8.3 (6.3, 14.1)	8.6 (1.71)	8.9 (6.8, 12.6)	8.8 (0.80)
12 months	8.9 (6.7, 13.4)	8.9 (1.39)	8.9 (6.4, 11.0)	8.9 (0.75)
24 months	8.6 (6.8, 11.5)	8.8 (1.23)	8.9 (6.6, 10.8)	8.8 (0.66)
Serum phosphate,† mg/dL	n=10		n=49	
Baseline	3.9 (2.4, 5.2)	3.8 (0.76)	3.9 (2.2, 5.8)	4.0 (0.69)
12 months	3.4 (2.1, 4.4)	3.3 (0.70)	3.9 (3.1, 6.0)	4.1 (0.68)
24 months	3.3 (2.4, 4.4)	3.3 (0.71)	4.0 (2.8, 5.7)	4.1 (0.64)
Creatinine, mg/dL	n=21		n=109	
Baseline	0.9 (0.5, 2.7)	1.0 (0.48)	0.9 (0.5, 1.9)	1.0 (0.25)
12 months	0.9 (0.3, 1.5)	0.9 (0.28)	0.9 (0.5, 1.8)	1.0 (0.28)
24 months	0.9 (0.4, 1.4)	1.0 (0.27)	0.9 (0.4, 2.8)	1.0 (0.33)
eGFR, mL/min/1.73 m²	n=21		n=109	
Baseline	85.5 (22.4, 117.3)	79.7 (24.29)	74.8 (32.4, 123.2)	76.9 (21.04)
12 months	83.3 (36.6, 137.8)	84.7 (22.66)	72.2 (25.8, 130.4)	76.2 (22.47)
24 months	87.5 (43.2, 124.4)	80.2 (21.13)	77.0 (22.6, 139.9)	76.6 (23.77)

eGFR=estimated glomerular filtration rate
*n is based on number of patients with longitudinal data available for each specific parameter, †Inorganic phosphate measured

***Disclosures: Bart Clarke**, Shire, Grant/Research Support, Shire, Consultant*

P-777

Clinical Characteristic of Pregnancy and Lactation Associated Osteoporosis (PLO): Results from an Online Survey *Mafo Kamanda-Kosseh[1], John M. Williams[1], Mariana Bucovsky[1], Ivelisse Colon[1], Elizabeth Shane[1], Adi Cohen[1]. [1]Columbia University Irving Medical Center, United States

PLO is a rare form of early-onset osteoporosis in which young women experience spontaneous or low trauma fractures(Fx), most commonly multiple vertebral Fx, during late pregnancy or lactation. Although cohort studies have described this condition, the pathogenesis is poorly understood.Between 5/2018 and 1/2020, we recruited women who self-identified with PLO from our clinical practice and PLO online support groups. Participants completed an anonymized Qualtrics survey with questions on reproductive, nutrition, exercise and family history, and medical conditions/medication exposures that could potentially be related to PLO.Responses were received from 126 women aged (mean+/-SD) 37.5+/-8.2, BMI 22.1+/-4.9 kg/m2; 94% reported white race, 7% Latina ethnicity.Only 5% had a history of osteoporosis before the PLO Fx. 48% reported family history of osteoporosis and 46% reported childhood Fx.Among responders,113(91%) reported vertebral Fx. Of these, age at Fx was 32.9+/-6.5 and 105(93%) reported multiple vertebral Fx (mean,3.5+/-2.5). In 99(88%), the Fx occurred during lactation.Another 8 women(6%) reported hip Fx.Among these, age at Fx was 35.1+/-8.5, 2 had bilateral Fx, and in 7, the Fx occurred during pregnancy.With regard to history of conditions associated with bone fragility, 53 women(43%) reported none, 9(7%) had celiac disease, 5(4%) had anorexia nervosa, 4(3%) had exercise induced amenorrhea, 4(3%) had hyperthyroidism and 9 (7%) had nephrolithiasis. In 28(23%), physical activity had been restricted prepartum. Use of medications associated with bone fragility included 14(11%) with history of glucocorticoid exposure>=3 wks, 14(11%) on thyroid hormone, 36(29%) on progestin-only OCP and 22(18%) with history of heparin or low molecular weight heparin therapy during pregnancy.Use of thyroid hormone and heparins was more frequent than expected based on recent reports of prevalence among pregnant women. Women with these exposures did not differ by age, ht, wt, type or timing of Fx.These survey data indicate that a substantial proportion of women with PLO have a history suggestive of or leading to underlying bone fragility. Particularly common were family history, a Fx that antedated pregnancy, diseases or medications known to be associated with bone loss and Fx. This leads us to hypothesize that genetic or developmental factors may contribute to susceptibility to PLO, and that conditions and medications affecting bone metabolism may also contribute to risk.

***Disclosures: Mafo Kamanda-Kosseh**, None*

P-778

Premature manifestation and accumulation of musculoskeletal-related diseases in adults with X-linked hypophosphatemia (XLH): an analysis of baseline medical history clinical trial data *Kassim Javaid[1], Leanne Ward[2], Rafael Pinedo-Villanueva[1], Angela Rylands[3], Angela Williams[3], Karl Insogna[4], Erik Imel[5]. [1]University of Oxford, United Kingdom, [2]University of Ottawa, Canada, [3]Kyowa Kirin International, United Kingdom, [4]Yale School of Medicine, United States, [5]Indiana University of Medicine, United States

X-linked hypophosphatemia (XLH) is a rare, genetic, phosphate-wasting disease causing chronic hypophosphatemia and characterized in childhood by short stature, lower-limb deformities, and dental defects. These deficits persist into adulthood, compounded by further

complications from XLH and its treatment. This analysis uses baseline XLH medical history data from an international, phase 3, randomized controlled trial of burosumab versus placebo in adults with XLH (NCT02526160) to explore complications across age groups.Adults with XLH and a Brief Pain Inventory "worst pain" score >=4 at screening were grouped by age: 18–29, 30–39, 40–49, and >=50 years. Five prespecified musculoskeletal manifestations (fracture, osteoarthritis [OA], osteophytes, enthesopathy, and spinal stenosis) and associated orthopedic surgeries were investigated (see Table).Data were analyzed for 127 adults (mean+/-SD age 39.8+/-12.3 years [range 18.5–65.5]; 66% women). 90% of adults had received oral phosphate and/or active vitamin D therapy before enrolment, with 70% taking the therapy within 2 years of study baseline. In each age cohort, >65% of adults reported >=1 musculoskeletal manifestation. Those with >=3 manifestations increased from 23% in the 18–29-year group to 58% in the >=50-year group.Overall, 43% of patients reported a history of fractures (37% of the 18–29-year group; 30% of the 30–39-year group and 51–54% of those >=40-years). Fractures were predominantly in the lower limbs (26% femoral). OA was reported by 37% of 18–29-year-olds, increasing to 74–77% in those >=30-years of age. A medical history of osteophytes increased with age from 26% (18–29-year group) to 42% (>=50-year group). A history of enthesopathy was noted in 23% of 18–29-year-olds, which gradually increased with age to 54% in the >=50-year group. Spinal stenosis history was reported in none of the 18–29-year-olds compared with 11% of the 30–39-year-olds, and in a third of adults aged >=40 years. Hip or knee replacements were recorded in 9% of all adults, with none in those <39 years. Hip replacements were reported in 13% in the 40–49-year group and in 8% of the >=50-year group. Knee replacements were reported in 5% in the 40–49-year group and in 19% of the >=50-year group.In this trial population of adults with XLH and moderate to severe baseline pain, musculoskeletal sequelae that are usually associated with ageing in the general population developed in early adulthood, with progressive accrual with age.

Prevalence of musculoskeletal manifestations and their associated surgeries in patients with XLH, according to age group, using baseline XLH medical history data from a phase 3 trial (NCT02526160).

Age group, years	*18–29*	*30–39*	*40–49*	*≥50*	*All*
Patients, n	35	27	39	26	127
Fracture history prevalence, %	37	30	51	54	43.3
Osteoarthritis prevalence, %	37	74	74	77	64.6
Osteophytes prevalence, %	26	37	59	47	41.7
Enthesopathy prevalence, %	23	41	44	63	39.4
Spinal stenosis prevalence, %	0	11	33	35	19.7
Adults who had hip replacements, %	0	0	13	8	5.5
Adults who had knee replacements, %	0	0	5	19	5.5
Median number of musculoskeletal disease sequelae	1	2	3	3	2.0
Adults with ≥1 musculoskeletal-related sequelae, %	66	89	90	89	82.7
Adults with ≥3 musculoskeletal-related sequelae, %	23	33	51	58	40.9

***Disclosures: Kassim Javaid**, Kyowa Kirin International, Grant/Research Support, Kyowa Kirin International, Speakers' Bureau, Kyowa Kirin International, Consultant*

P-779

X-Linked Hypophosphatemia: HR-pQCT and Finite Element Analysis Uniquely Show Benefits from Burosumab Therapy in Fraternal Twins Crossing Puberty *Vinieth N. Bijanki[1], Hiram D. Stahl[2], Valerie Wollberg[3], William H. McAlister[4], Steven Mumm[5], Gary S. Gottesman[6], Michael P. Whyte[7]. [1]Center for Metabolic Bone Disease and Molecular Research, Shriners Hospitals for Children - St. Louis; Clinical Research Department, Shriners Hospitals for Children - St. Louis, United States, [2]Radiology Department, Shriners Hospital for Children - St. Louis, United States, [3]Center for Metabolic Bone Disease and Molecular Research, Shriners Hospitals for Children - St. Louis, United States, [4]Mallinckrodt Institute of Radiology, Washington University School of Medicine at St. Louis Children's Hospital, United States, [5]Division of Bone and Mineral Diseases, Department of Internal Medicine, Washington University School of Medicine at Barnes-Jewish Hospital; Center for Metabolic Bone Disease and Molecular Research, Shriners Hospitals for Children - St. Louis, United States, [6]Center for Metabolic Bone Disease and Molecular Research, Shriners Hospitals for Children - St. Louis, United States, [7]Center for Metabolic Bone Disease and Molecular Research, Shriners Hospitals for Children - St. Louis; Division of Bone and Mineral Diseases, Department of Internal Medicine, Washington University School of Medicine at Barnes-Jewish Hospital, United States

X-linked hypophosphatemia (XLH) features rickets during growth and osteomalacia in adults due to renal phosphate (Pi) wasting caused by mutations in PHEX leading to increased FGF23 expression. For decades, standard of care medical therapy for XLH was oral Pi and active vitamin D. In 2018, burosumab, a fully human anti-FGF23 monoclonal antibody, became available to treat XLH. Clinical trials for burosumab involved validated scales of rickets severity: the radiographic global impression of change (RGI-C) and the Thacher rickets severity score (RSS). Both scales require open growth plates. High resolution peripheral quantitative computed tomography (HR-pQCT) precisely delineates bone quality, typically at the distal radius and distal tibia. The HR-pQCT standard evaluation assesses skeletal density, structure, and geometry in detail, while finite element analysis (FEA) predicts bone quality by calculating strength, strain, and stress. Here, we document benefits from burosumab therapy in 14.7-year-old fraternal twin brothers with XLH following conversion from conventional calcitriol and Pi treatment. Calcitriol and Pi supplementation had improved their rickets radiographically, more so for twin 1 than twin 2. Nine months after the change to burosumab therapy, rickets assessed radiographically improved in both patients. Additionally, the HR-pQCT evaluation analysis and FEA both documented substantial improvement. In the tibia, twin 1 increased total volumetric bone mineral density (Tt.vBMD) from 261.5 to 309.3 mg HA/cm3 and twin 2 from 245.1 to 331.7 mg HA/cm3 (18.3% and 35.3% increases, respectively). For both twins, FEA revealed increased failure load and stiffness in both the radius and the tibia. In the tibia, failure load (absolute value) and stiffness increased in twin 1 by 34.7% (10206.1 N to 13755.9 N) and 37.7% (188605.8 N/mm to 259724.5 N/mm), respectively. Remarkably in the tibia of twin 2, failure load and stiffness increased by 59.4% (7710.8 N to 12290.5 N) and 58.1% (145907.7 N/mm to 230615.0 N/mm), respectively. Assessment of radiographic changes in XLH has primarily involved the physes, which close at the end of puberty. HR-pQCT evaluation with FEA now provides a sensitive and robust tool for evaluating treatment of pediatric XLH including crossing puberty.

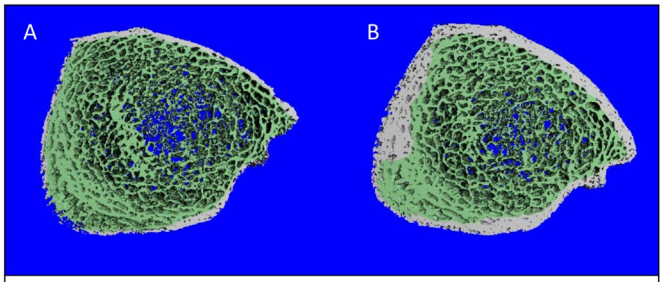

HR-pQCT 3D reconstruction of distal tibia in twin 2 at the end of calcitriol and Pi therapy (A) shows thin cortex and trabeculae. After 9 months of burosumab therapy (B), there is cortical and trabecular thickening

***Disclosures: Vinieth N. Bijanki**, None*

P-780

Incidence of osteophyte, spinal ligament ossification, enthesopathy, nephrocalcinosis, dental disease, and hearing impairment in 25 adult X-linked hypophosphatemic rickets *Minae Koga[1], Hajime Kato[1], Nobuaki Ito[1]. [1]Department of Nephrology and Endocrinology, The University of Tokyo, Japan

?Background?X-linked hypophosphatemia (XLH) is the inherited disorders related to loss of function mutations in the phosphate-regulating endopeptidase (PHEX). Loss of function in PHEX leads to inappropriately increased serum fibroblast growth factor 23 with hypophosphatemia. Clinical manifestations of XLH can vary but most patients present with rickets. Adult XLH develops complications including common treatment related adverse events, which are osteophytes around large joints, ossification in spinal ligament, enthesopathy, nephrocalcinosis, dental disease and hearing impairment. However, these manifestations have not been systemically reviewed and the prevalence and severity remains uncertain. ?Method?The present study includes 25 adult XLH. The clinical records of the participants were retrospectively reviewed. ?Results?The participants consisted of 13 males and 12 females from 21 families, with a median age of 40.3 (18-72) years. 20 patients (80 %) developed ossification of spinal ligament (ossification of the anterior longitudinal ligament/posterior longitudinal ligament/ligamentum flavum (OALL/OPLL/OLF)). The median score of OA/OP/OF/OS index were 3.3 (0-20), 1.6 (0-11), 1.7 (0-12) and 6.7 (0-28), independently. 18 cases (82 %) developed enthesopathy. Osteophytes around hip and knee joints were reported in all cases (100%) and 20 cases (80 %), respectively. The average KL grade was 3 in hip joint and 2 in knee joint. 13 patients (52 %) had O-shaped deformity, and 5 patients (20 %) had X-shaped deformity in the legs. Ultrasound revealed nephrocalcinosis in 18 patients (72%). Median number of residual tooth and intact tooth were 25.4 (15 - 32) and 14.6 (0 - 32), respectively. Hearing impairment developed in seven cases (30 %) and was all in sensorial pattern.?Discussion?Osteophytes around the joint and ossification of spinal ligament were more severe and frequent than in the general population with the reported incidence of hip/knee osteophyte and spinal ligament ossification being 46 – 68 % and 1.5 - 6.0 %, respectively. Because XLH is relatively common inherited disorder (1/20,000) and the isolated cases are not uncommon, there might be not a few undiagnosed cases of XLH included in the patients with OALL/OPLL/OLF and severe hip/knee OA patients. The clarification of un-

derlying cause of ectopic ossification in some inherited FGF23rHR is intriguing unresolved research agenda possibly leading to the development of treatment for these comorbidities.

***Disclosures: Minae Koga**, None*

P-781

Ectonucleotide Pyrophosphatase/Phosphodiesterase 1 (ENPP1) Deficiency Appears to be Associated with an Evolving Skeletal Dysplasia in Addition to Ectopic Calcifications and Rickets *Deborah Wenkert[1], William McAlister[2]. [1]Wenkert & Young, LLC, United States, [2]Department of Pediatric Radiology, Mallinckrodt Institute of Radiology at St. Louis Children's Hospital, Washington University School of Medicine, United States

Introduction: Recessive, loss-of-function mutations in the gene encoding ectonucleotide pyrophosphatase/phosphodiesterase 1, (ENPP1) result in Generalized Arterial Calcification of Infancy (GACI) (OMIM # 208000) and Autosomal Recessive Hypophosphatemic Rickets type 2 (ARHR2) (OMIM # 613312). Dominant inheritance has been reported as associated with osteoporosis in adults. Among the >200 publications describing patients with these disorders, the radiographic descriptions understandably focus on the prominent findings that help a clinician make the diagnosis (e.g., ectopic calcification and/or the signs of rickets). Published radiographs, however, display a number of other ENPP1 deficiency (ENPP1-D) associated skeletal features. We undertook a review of all available published plain x-rays of patients with ENPP1-D disorders as a first step in developing a rating scale to be used in establishing the natural history of the skeletal features of the disorder.Methods: The following terms were searched in PubMed: [ENPP1] or [GACI] or [Generalized arterial calcification of infancy] or [autosomal recessive hypophosphatemic rickets] or [Ectonucleotide pyrophosphatase/phosphodiesterase I] AND [x-ray] or [radiograph]. Additional radiographs were identified searching Google images using the same search strategy.Results: A unique combination of >10 radiographic skeletal abnormalities affected patients who had not been previously treated with bisphosphonates (table). Metaphyseal tongues of radiolucency and craniosynostosis were only seen in patients who had received etidronate.Conclusions: Our review of published skeletal radiographs of patients with ENPP1-D, uncovered >10 abnormalities including some that have not, and others that have only rarely, been mentioned before. Many abnormalities, were apparent only in radiographs of older children implying ENPP1-D is an evolving dysplasia. In addition, although rickets is known to appear in survivors of GACI, we also found rickets in the radiographs of infants with ENPP1-D associated GACI. Thus, rather than being two distinct disorders, GACI and ADHR2 appear to represent stages of the natural evolution of ENPP1-D. Ascertaining the prevalence of all of the skeletal features of ENPP1-D and the natural history of their evolution will be important to understand the response to treatment being developed for ENPP1-D.

location		ENPP1-D characteristics	Extra detail
Global		Ectopic calcification	
		Osteoporosis	Including vertebral compression fracture (one patient)
		Osteosclerosis	Variable
Upper and Lower Extremity	Both Upper and Lower Extremity	Modeling errors	Metaphyseal under-tubulation, expanded metadiaphysis
		Mid-diaphyseal loss of medullary cavity	
		Rickets (beginning in infancy)	Physeal line widenning, metaphyseal flaring or beaking; distal metaphyseal sclerosis, fraying, and cupping
	Upper extremity	Delayed bone age	
		Negative ulnar variance	
		Rounding of the distal radius	
		Abnormal epiphyseal shape	
	Lower extremity	Bowing	
Spine		Small vertebral bodies	
		Neural arch fusion	
		Spinous process fusion	
		Degenerative changes	One middle-aged patient
Ribs and clavicles		Thin	Infants only

***Disclosures: Deborah Wenkert**, Inozyme Pharma, Consultant*

P-782

Addressing a Knowledge Gap: Characterizing the Physical, Functional, and Cognitive Performance in Adults with Hypophosphatasia *Christina Dourrough[1], Kathryn Dahir[2]. [1]Vanderbilt Pi Beta Phi Rehabilitation Institute, Nashville, TN, United States, [2]Vanderbilt University Medical Center, United States

Introduction: Limited data exist regarding physical and cognitive functioning of adults with hypophosphatasia (HPP), and no guidelines for evaluation by physical therapists (PT), occupational therapists (OT), or speech-language pathologists (SLP) exist. We evaluated physical, functional, and cognitive performance among adults with HPP through comprehensive assessments and patient reported outcome tools. Methods: Fifteen subjects with HPP (median age 42 (32.5-50.5) yrs, 73% female, 100% Caucasian, 50% on enzyme replacement therapy) completed standardized assessments of mobility, balance, fine motor, activities of daily living, cognition, and self-reported measures of health-related quality of life, fatigue, depression and anxiety. This study was conducted in accordance with the Declaration of Helsinki and approved by the IRB. Results: Compared with normative data from community dwelling adults, subjects traveled less distance on a Six-Minute Walk Test (1,376 +/- 431** ft vs 1873+/-299) and had slower gait on a 10-Meter Walk Test (1.04+/-0.21 vs 1.39-1.46m/s). Subjects were slower to respond on the Nine Hole Peg Test (20.6+/-2.4s** for right & 21.7+/-2.4s** for left hand vs 16.5s to 18.5s), and 2 had an abnormally slow reaction time via Dynavision (0.9s* [0.85,0.96], functional speed is <1.15s). 20% scored in the low average/borderline range of performance on the Repeatable Battery for the Assessment of Neuropsychological Status (RBANS), suggestive of cognitive impairment. On the Short Form-36 (SF36), 75% reported limitations in their ability to fulfill life roles due to physical problems (25%+/-39%ile**), 75% reported below average energy (30%+/-23ile**), and 100% rated their health as unlikely to improve (32%+/-15%ile**). Fatigue Severity Scale scores were well above the median for a healthy population (47 [34,60.5]* vs 2.3). Median scores for Depression, Anxiety, and Stress (DASS) were within the normal range, but severe depression was reported by 4 subjects. Subjects reported moderate (4), severe (1), or extremely severe (1) anxiety; and 4 reported severe (2) or extremely severe (2) stress. Conclusions: Objective functional assessments indicate mild deficits, but subjects' self-reported significant limitations due to physical dysfunction, indicating that current objective testing is inadequate in the HPP population. Impaired reaction time may indicate potential safety concerns with driving or certain occupations, and screening may be indicated. A subgroup of subjects was significantly affected by depression, stress, and/or anxiety. Guidelines and additional assessment tools should be created to further evaluate physical and cognitive functioning among adults with HPP. The use of PT, OT, and SLP specialists can aid in establishing baseline assessment of impairment and developing treatment plans with objective metrics for assessing efficacy of treatment. *median **mean

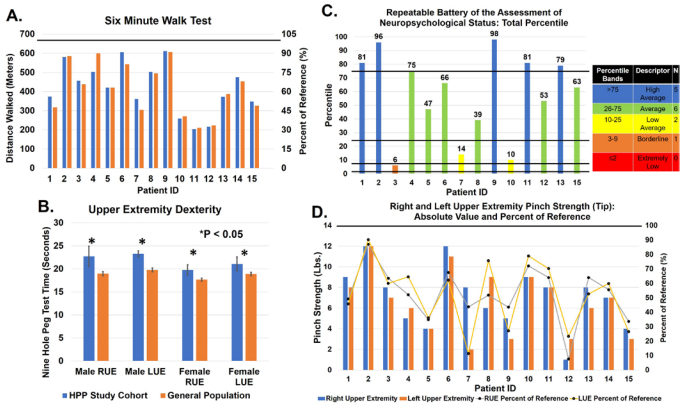

A. HPP Study Cohort Performs Below an Age and Sex-Matched General Population in the Six Minute Walk Test. The six-minute walk test was administered to 15 HPP patients in which all performed below the normal reference distance for their age and sex. Reference: Gibbons et al JCR 2001, 21(2)87-93.

B. HPP Study Cohort Scores Lower in the Upper Extremity Dexterity Compared to a Sex-Matched General Population. Compared to the general population, the HPP study cohort took longer to complete the task whether compared by sex or upper extremity laterality (* = p < 0.05). RUE = Right Upper Extremity. LUE = Left Upper Extremity. Reference: Grice K, Vogel KA, Le V, Mitchell A, Muniz S, Vollmer MA. Adult norms for a commercially available Nine Hole Peg Test for finger dexterity. *Am J Occup Ther*. 2003;57:570–573. 10.5014/ajot.57.5.570

C. Repeatable Battery of the Assessment of Neuropsychological Status (RBANS) Overall Percentile in HPP Study Cohort by Individual Patient. Out of 14 HPP patients, 5 patients scored 'high average' (36%), 6 patients score 'average' (43%), 2 patients score 'low average' (14%), and one patient score 'borderline' (7%). Reference: Randolph, C. (1998). Repeatable battery for the assessment of neuropsychological status (RBANS). San Antonio, TX: Psychological Corporation

D. HPP Study Cohort Performs Below an Age and Sex-Matched General Population in Bilateral Upper Extremity Pinch Strength. Pinch strength was determined in 15 HPP patients. When compared to an age and sex-matched general population, all 15 patients performed worse. Reference: Mathiowetz, V., Kashman, N., Volland, G., Weber, K., Dowe, M., & Rogers, S. (1985). Grip and pinch strength: normative data for adults. *Arch Phys Med Rehabil, 66*(2), 69-74. Retrieved from https://www.ncbi.nlm.nih.gov/pubmed/3970660

***Disclosures: Christina Dourrough**, None*

P-783

Medications Used by Individuals with Fibrodysplasia Ossificans Progressiva (FOP): Data from a Global Natural History Study *Richard Keen[1], Mona Al Mukaddam[2], Geneviève Baujat[3], Carmen De Cunto[4], Edward C Hsiao[5], Robert J Pignolo[6], Kathleen Harnett[7], Rose Marino[7], Frederick S Kaplan[2]. [1]Centre for Metabolic Bone Disease, Royal National Orthopaedic Hospital, United Kingdom, [2]Departments of Orthopaedic Surgery & Medicine, The Center for Research in FOP and Related Disorders, Perelman School of Medicine, University of Pennsylvania, United States, [3]Département de Génétique, Institut IMAGINE and Hôpital Universitaire Necker-Enfants Malades, France, [4]Pediatric Rheumatology Section, Department of Pediatrics, Hospital Italiano de Buenos Aires, Argentina, [5]Division of Endocrinology and Metabolism, UCSF Metabolic Bone Clinic, Institute of Human Genetics, and UCSF Program in Craniofacial Biology, Department of Medicine, University of California-San Francisco, United States, [6]Department of Medicine, Mayo Clinic, United States, [7]Ipsen, United States

Background: FOP is an ultra-rare genetic disorder characterized by episodic progressive heterotopic ossification (HO) and flare-ups, causing cumulative disability and early

Posters

death. There are no established disease-modifying therapies to prevent HO in FOP. However, treatment guidelines for the symptomatic relief of FOP have recently been published by the International Clinical Council on FOP (ICC).1Objective: To report use of medications to manage symptoms of FOP in a natural history study (NHS), as per standard clinical practice. Methods: Individuals with FOP aged <=65 years with a documented ACVR1R206H mutation were eligible to participate in a 36-month, prospective, global NHS (NCT02322255). This analysis reports interim data on medication use during that observational study (data cut 31 August 2019). Use of medications (acute and chronic) was assessed at Baseline (BL), by telephone at Weeks 1–3 and every 3 months thereafter, and at clinic visits (Months 12, 24, and 36). Medication prescribed for symptomatic treatment of reported flare-ups was recorded on flare-up Days 1, 42, and 84. Data were collected using a standardized list and are summarized here by preferred term (PT).Results: 73/114 (64.0%) participants were taking prior medications that were ongoing at BL in the NHS. The most common medications ongoing at BL by PT were prednisone (25.4%), ibuprofen (22.8%), and montelukast (19.3%), all of which are included in the ICC guidelines (Table). Pain relief medications ongoing at BL also included (among others): paracetamol (11.4%), naproxen (8.8%), and celecoxib (7.9%). Most participants (91/114; 79.8%) initiated treatment with new medications during the NHS. The most frequent newly-initiated medications by PT were prednisone (31.6%), ibuprofen (28.1%), and paracetamol (21.9%). Glucocorticoids were commonly administered upon onset of flare-ups (155/217; 71.4%), in accordance with ICC guidelines.Conclusions:- To manage their symptoms during this NHS, individuals with FOP used various medications, which were generally consistent with current ICC guidelines. Although the objective of this study was not to evaluate efficacy or safety of medications used, it highlights the need for disease-modifying therapies to treat or prevent the symptomatic progression of FOP.Reference: 1. Kaplan FS. ICC FOP Treatment Guidelines. Available at: http://www.iccfop.org/dvlp/wp-content/uploads/2020/03/Guidelines_January-2020.pdf [Accessed: 14 May 2020].

	Ongoing prior medications at BL[a] N=114	Newly initiated medications N=114
ICC FOP Class I medications:[b]		
Prednisone	25.4%	31.6%
Non-steroidal anti-inflammatory drugs (NSAIDs)		
Ibuprofen	22.8%	28.1%
Celecoxib	7.9%	3.5%
Indomethacin	3.5%	0.9%
ICC FOP Class II medications:[b]		
Montelukast	19.3%	4.4%
Cromoglicate/ cromoglicic acid	5.3%	1.8%
Zoledronic acid	0.9%	-
Pamidronate	-	4.4%
Imatinib	-	1.8%

[a] Medications taken upon study entry (within 30 days prior to BL study visit); [b] Medications classified into one of three categories based on experimental or anecdotal experience with the drug and knowledge of safety profiles. Class I: Medications widely used to control symptoms of acute flare-ups in FOP or chronic arthropathy, with generally minimal side effects; Class II: Medications with theoretical application to FOP, approved for the treatment of other disorders and with limited and well-described effects. Can be considered with caution, at physicians' discretion. BL: baseline; ICC: International Clinical Council on FOP; FOP: fibrodysplasia ossificans progressiva.

***Disclosures: Richard Keen**, Research investigator: Clementia/Ipsen, Kyowa Kirin, Regeneron; Advisory board: IFOPA FOP Registry Medical Advisory Board, International Clinical Council on FOP, Other Financial or Material Support*

P-784

Use of Assistive Devices and Adaptations by Individuals with Fibrodysplasia Ossificans Progressiva (FOP): Data from a Global Natural History Study

*Edward C Hsiao[1], Mona Al Mukaddam[2], Geneviève Baujat[3], Carmen De Cunto[4], Richard Keen[5], Robert J Pignolo[6], Kathleen Harnett[7], Rose Marino[7], Frederick S Kaplan[8]. [1]Division of Endocrinology and Metabolism, the UCSF Metabolic Bone Clinic, the Institute of Human Genetics, and the UCSF Program in Craniofacial Biology, Department of Medicine, University of California-San Francisco, United States, [2]Departments of Orthopaedic Surgery & Medicine, The Center for Research in FOP and Related Disorders, Perelman School of Medicine, University of Pennsylvania, United States, [3]Département de Génétique, Institut IMAGINE and Hôpital Universitaire Necker-Enfants Malades, France, [4]Pediatric Rheumatology Section, Department of Pediatrics, Hospital Italiano de Buenos Aires, Argentina, [5]Centre for Metabolic Bone Disease, Royal National Orthopaedic Hospital, United Kingdom, [6]Department of Medicine, Mayo Clinic, United States, [7]Ipsen, United States, [8]Deparments of Orthopaedic Surgery & Medicine, The Center for Research in FOP and Related Disorders, Perelman School of Medicine, University of Pennsylvania, United States

Background: FOP is an ultra-rare, severely disabling genetic disorder of progressive heterotopic ossification (HO). HO is episodic, causing cumulative disability. Most individuals with FOP are confined to a wheelchair by the third decade of life.Objective: To characterize the use of assistive devices and adaptations (ADA) in individuals with FOP in a natural history study (NHS).Methods: Individuals with FOP aged <=65 years with a documented ACVR1R206H mutation were eligible to participate in a prospective, 36-month NHS (NCT02322255). This analysis describes the use of ADA at Baseline (BL) and new ADA reported annually. Participants indicated which ADA they were using via a list grouped into 12 categories. The proportion of participants using >=1 ADA in each category was stratified by age group and analyzed using descriptive statistics.Results: Data on ADA usage were available for 111/114 participants, and use of new ADA for 84/99 participants with any assessment at Month 12. The most common ADA categories used overall at BL (N=111) were personal care tools/aids (82.9%), bedroom aids and devices (75.7%), care attendants (73.0%), eating tools (66.7%), and mobility aids (65.8%). The same devices were used at Month 12 (n=97) by 84.5%, 75.3%, 72.2%, 62.9%, and 70.1% of participants, respectively. In younger participants, use of school adaptations was similar (2–7 years: 81.3% [13/16]; 8–14 years: 79.4% [27/34]). A relatively high proportion of participants aged 8–14 years used medical therapies for daily living (79.4% [27/34]) compared with other age groups. Several categories of ADA were used more frequently in older versus younger age groups including mobility aids, personal care tools/aids, bathroom and bedroom aids/devices, and home adaptations. The most common new ADA at Month 12 across age groups were personal care tools/aids, care attendants, bathroom and bedroom aids/devices, and home adaptations; there was a notable rise in the use of new ADA from these categories in participants aged >=25 years (Figure).Conclusions: At least 83% of participants in the NHS used >=1 ADA to manage their disabilities at Baseline and at least 40% used >=1 new ADA at Month 12. Specific types of ADA used varied across age groups and over 12 months; however, longer follow-up to capture the increase in number and complexity of ADA is needed to further demonstrate the physical and financial burden of FOP, and the rate of progression of ADA use.

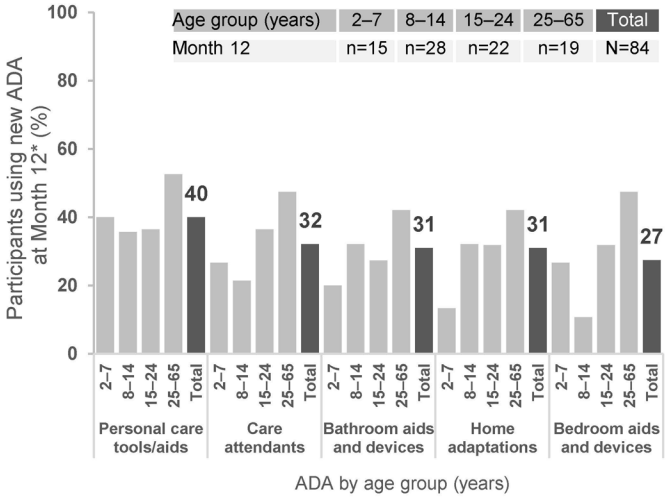

*New ADA reflect those not already used at Baseline. Other categories included: mobility aids, eating tools, work environment, technology, sports/recreation and school adaptations, and medical therapies for daily living. ADA: assistive device or adaptation.

***Disclosures: Edward C Hsiao**, Clementia/Ipsen, Regeneron, Grant/Research Support, : Advisory board (all voluntary): Fibrous Dysplasia Foundation, IFOPA Registry Medical Advisory Board, International Clinical Council on FOP; Research investigator: Clementia/Ipsen, Other Financial or Material Support*

P-785

Impaired Bone Microarchitecture in patients with Tumor Induced Osteomalacia assessed by HR-pQCT *maria belen zanchetta[1], Cesar Bogado[1], Selva Nuñez[1], Yamile Morcalbel [2], Analía Pignatta[2], Natalia Elias[3], Adriana Diaz[2], Carlos Vigovich [4], Carolina Cohen [2], Celeste Balonga[1], Sofia Gonzalez[5], jose ruben zanchetta[1]. [1]IDIM, Universidad del Salvador, Argentina, [2]Hospital de Clínicas, Argentina, [3]Hospital Británico, Argentina, [4]Hospital Gobernador Centeno, Argentina, [5]Hospital Churruca, Argentina

Tumor-induced osteomalacia (TIO) is a rare paraneoplastic syndrome characterized by persistent hypophosphatemia. Hypophosphatemia is caused by increased renal phosphate wasting consequent to elevated levels of circulating fibroblast growth factor 23 (FGF23). Besides causing phosphaturia, FGF23 inhibits renal 1α-hydroxylase, resulting in low levels of 1,25-dihydroxy vitamin D. This pathophysiology leads to deter mineralization of the osteoid matrix causing bone pain, fragility fractures, muscle weakness and severe bone quality impairment. Deterioration of bone microarchitecture parameters in patients presenting osteomalacia has been described by histomorphometric analysis of bone biopsies samples.The aim of this study was to assess the status of bone microarchitecture parameters in patients with TIO using high-resolution pQCT (HR-pQCT), a non-invasive procedure.We studied 8 TIO patients (5 female, 3 male) consulting or referred to our bone clinic. Mean age was 47.4 +/-12.6 (SD) years, range 28.5-64 years. Bone microarchitecture parameters were assessed at the distal radius and tibia by HR-pQCT using Xtreme CT (Scanco Medical AG, Bassersdorf, Switzerland). Results were compared with a group of 16 healthy subjects (10 female, 6 male) obtained from our data base, paired by age and sex in a 2:1 ratio. Mean age of the control group was 47.3 +/-12.2 (SD) years, range 28.8-68 years. Mean percent difference between the patients and control groups was calculated and the results are depicted in Table 1.In the radius, cortical thickness was 24.7% lower in patients than controls (0.61 +/- 0.28 vss 0.81 +/- 0.18 mm) and trabecular density was 31 % lower (128.4 +/- 56.7 vss 186.7 +/- 53.6 mg HA/cm3). In the tibia, cortical thickness was 41% lower in patients than controls (0.72 +/- 0.42 vss 1.22 +/- 0.32 mm) and trabecular density was 52.5 % lower (83.0 +/- 62.4 vss.174.7 +/- 50.5 mg HA/cm3)The results confirm severe bone microarchitecture deterioration in patients with TIO. Deterioration of bone microarchitecture was more evident at the distal tibia, most probably due to impaired mobility as a result of severe muscle weakness. HR-pQCT is a suitable method for the evaluation of bone microarchitecture in patients with TIO and can be a useful tool to evaluate the degree of deterioration and eventually follow the response to treatment.

	Patients (n=8) Mean ±SD	Controls (n=16) Mean ±SD	Difference Mean %
Distal radius			
D100 (mg HA/cm³)	258.9 ± 85.7	338.5 ± 65.6	-23,5
Dcomp (mg HA/cm³)	795.6 ± 136.5	876.5 ± 57.8	-9,2
Ct. Th (mm)	0.61 ± 0.28	0.81 ± 0.18	-24,7
Dtrab (mg HA/cm³)	128.4 ± 56.7	186.7 ± 53.6	-31,2
BV/TV (%)	10.7 ± 4.7	15.6 ± 4.5	-31,4
Tb.N (1/mm)	1.56 ± 0.49	2.02 ± 0.34	-22,8
Tb.Th (mm)	0.067 ± 0.012	0.077 ± 0.015	-13,0
Distal tibia			
D100 (mg HA/cm³)	173.1 ± 97.9	306.0 ± 71.3	-43,4
Dcomp (mg HA/cm³)	780.7 ± 140.8	881.6 ± 54.2	-11,4
Ct. Th (mm)	0.72 ± 0.42	1.22 ± 0.32	-41,0
Dtrab (mg HA/cm³)	83.0 ± 62.4	174.7 ± 50.5	-52,5
BV/TV (%)	7.0 ± 5.2	14.5 ± 4.2	-51,7
Tb.N (1/mm)	0.94 ± 0.56	1.98 ± 0.42	-52,5
Tb.Th (mm)	0.064 ± 0.046	0.074 ± 0.017	-13,5

***Disclosures: maria belen zanchetta**, ultragenyx, Grant/Research Support*

P-786

Multicentric Carpotarsal Osteolysis Syndrome (MCTO) Has a Generalized High Turnover Bone Phenotype, High s RANKL and Responds to Denosumab *Ravit Regev[1], Ronald Laxer[1], Kristi Whitney-Mahoney[2], Yesmino Elia[1], Kornelia Filipowski[2], Damien Noone[1], Amer Shammas[1], Reza Vali[1], Etienne Sochett[1]. [1]The Hospital for Sick Children, University of Toronto, Canada, [2]The Hospital for Sick Children, Canada

Background: MCTO is a rare disorder, caused by mutations in the MABF gene, a negative regulator of RANKL. Manifestations include carpal tarsal osteolysis and renal failure. Pathophysiology is poorly understood, and no effective treatment is available. Clinical case: A 5y old boy presented with R wrist pain and diffuse swelling. MRI showed pan-carpal synovitis with joint effusion. Plain films showed central loss of the proximal row of carpal bones. His mother was followed as an adolescent with presumed juvenile rheumatoid arthritis. Genetic testing confirmed MAFB gene mutation (c.206C>T,p.Ser69Leu) in both. At 7y, skeletal survey showed diffuse osteopenia and mild height loss in T1. DXA (L1-4) Z-score -0.7. Calcium phosphate metabolism indices were within reference ranges. Bone Specific Alk Pi was modestly increased and C-telopeptide markedly increased. He received Denosumab (0.5-0.75 mg/Kg) 4-monthly for two years and had less pain with improved R wrist function. Osteolysis stabilized and none was noted in the L wrist or ankles. BMD Z-score was -0.2. Following each treatment C-telopeptide showed a significant decrease, while bone specific alkaline phosphatase remained stable. (fig. 1) At 13y, radiology showed R knee osteopenia, R wrist almost complete destruction of the carpal bones. Neither ankle nor L wrist showed osteolysis. BMD Z-score was -1.2. Serum calcium, 25(OH)Vitamin D and PTH were normal. Bone specific alkaline phosphatase and C-Telopeptide were elevated. eGFR 150 ml/min/1.73m2, ACR 6.6 ([normal< 3.5] mg/mmol), no hypercalciuria or nephrocalcinosis. High resolution peripheral quantitative computerized tomography (HRpQCT) of the L distal radius and distal tibia compared with 7 age-matched healthy males showed reduced total volumetric BMD (186.4;198.2-306.4), normal trabecular volumetric BMD and markedly reduced cortical volumetric BMD (320.4;636.5-792.5). HRpQCT measurements of the R wrist and tibia were similar. Consecutive sRANKL levels at 6 weeks and 12 weeks after Denosumab were markedly increased in both undiluted (35.4, 26.62 pmol/L) and averaged diluted samples (83.73, 58.98 pmol/L) when compared with healthy age-matched children (0.21-0.41pmol/L).Clinical Lessons: The MAFB, mutation c.206C>T,p.Ser69Leu), has a generalized high turnover osteoporosis, likely driven by very high levels of sRANKL. Denosumab is a targeted treatment for the osteoporosis associated with this form of MCTO.

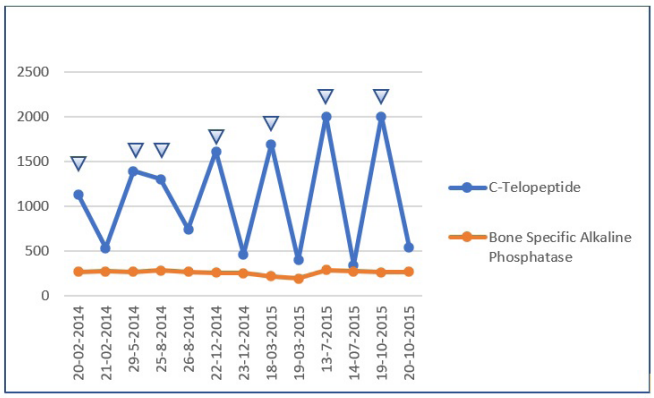

Figure 1: Treatment with Denosumab and bone turnover markers
Arrowheads mark day of treatment with Denosumab

***Disclosures: Ravit Regev**, None*

P-787

Long-term effectiveness of Asfotase Alfa in adults with pediatric-onset Hypophosphatasia in routine clinical practice *Franca Genest[1], Dominik Rak[1], Anna Petryk[2], Lothar Seefried[1]. [1]1Orthopaedic Clinic King-Ludwig-Haus, University of Würzburg, Würzburg, Germany, Germany, [2]2Alexion Pharmaceuticals, Inc., Boston, MA, USA, United States

Introduction: Hypophosphatasia (HPP) is a rare, inherited, metabolic disorder caused by low tissue nonspecific alkaline phosphatase activity. Heterogeneous presentation in adults includes musculoskeletal symptoms, impaired physical function, and reduced health-related quality of life (HRQoL). We evaluated real-world, long-term effectiveness of asfotase alfa, on physical function and HRQoL among adults with pediatric-onset HPP (NCT03418389). Methods: Adults aged >=18 years (y) receiving care at the Orthopedic Institute of the Julius-Maximilians-University of Wu¨rzburg (Germany) were treated with Asfotase Alfa for >=24 months (mo). Physical function evaluation included the 6-Minute Walk Test (6MWT), Timed Up-and-Go (TUG) test, Lower Extremity Functional Scale (LEFS), and Short Physical Performance Battery (SPPB). HRQoL was assessed with the 36-item Short-Form Health Survey, version 2 (SF-36v2); pain was also evaluated. Safety data were collected throughout the study. Results: The study included 14 (11 women, 3 men) patients, with a median (min, max) age of 53 (20, 78) y for women and 46 (19, 57) y for men at treatment initiation. All had compound heterozygous ALPL gene variants, >=1 HPP bone manifestation and history of >=1 fracture. We previously reported score changes from baseline to 12 mo; here, we report changes from 12–24 mo. Improvements were observed over the first 12 mo on treatment and maintained another 12 mo. Median (min, max) 6MWT distance was similar at 12 mo (320 [0, 605] m) and 24 mo (316 [60, 600] m) (n=13; P=0.115). An increase in median time to complete the TUG test from 11.3s–13.75s was not statistically significant (n=7; P=0.382). Specific SPPB component results were stable. Decreases in median 4m usual gait speed from 1.12m/s–1.02m/s (n=9; P=0.61) and median repeated chair rise time from 12.53s–12.48s (n=8; P=0.398) were not statistically significant. Improvements in LEFS (n=10) and SF-36v2 Physical Component Summary (n=9) scores were seen early at 3 and 6 mo and remained stable over 24 mo. Changes in pain level (n=5) were variable between 12 and 24 mo. No new safety signals were identified. Conclusions: These data suggest adults with pediatric-onset HPP treated with asfotase alfa in real-world settings have marked improvements in clinical and functional outcomes, which were observed within the first 12 mo and sustained over 24 mo of treatment.

***Disclosures: Franca Genest**, Alexion, Other Financial or Material Support*

P-788

Safety and Efficacy of Burosumab in Cutaneous Skeletal Hypophosphatemia Syndrome (CSHS) *Thomas Carpenter[1], Laila Tabatabai[2], Diana Luca[3], Mary Scott Roberts[3], Dale Hamilton[2]. [1]Yale University School of Medicine, United States, [2]Houston Methodist Hospital and Research Institute; WCM Affiliate, United States, [3]Ultragenyx Pharmaceutical Inc., United States

CSHS is a rare syndrome caused by somatic RAS mutations often in a mosaic pattern. CSHS is characterized by epidermal and/or melanocytic nevi, skeletal dysplasia, and excess FGF23, resulting in chronic hypophosphatemia, renal phosphate wasting, impaired 1,25(OH)2D synthesis, and rickets/osteomalacia. Current medical management is oral phosphate and/or active vitamin D analogs, but these have limited efficacy. Burosumab is a fully human monoclonal antibody against FGF23 approved to treat X-linked hypophosphatemia (XLH) and is being investigated in tumor-induced osteomalacia (TIO) and CSHS, all characterized by excess FGF23. An ongoing, open-label, phase 2 trial of burosumab safety and efficacy (NCT02304367) enrolled 17 adults with TIO or CSHS. Primary endpoints were changes in serum phosphorus and osteomalacia. Here we focus on the subject with CSHS with data through week 144.The 20-yr-old white male had multiple linear nevi, skeletal dysplasia, and chronic FGF23-mediated hypophosphatemia and suffered from bone pain, distal lower extremity valgus deformities, left femur varus deformity, leg length discrepancy, and multiple fractures. He had been treated with oral phosphate and active vitamin D for 16 yrs prior to study entry.The subject was maintained on the burosumab starting dose (0.3 mg/kg SC Q4W) throughout the study, which resulted in normalization of serum phosphorus through W144. TmP/GFR and 1,25(OH)2D also increased with burosumab (table). The baseline bone biopsy lacked sufficient integrity for accurate measures of osteomalacia. However at W48, osteoid surface/bone surface was 16%, osteoid thickness was 8.7 µm, and mineralization lag time was 12.2 days, indicative of no osteomalacia. The subject had 19 areas of increased uptake on baseline radionucleotide bone scan, indicative of fractures/pseudofractures. All were fully (68.4%) or partially (31.6%) healed by W144. Bone turnover markers decreased over the study (table).Changes in patient-reported pain and fatigue were variable and inconclusive. No changes in sit-to-stand repetitions were seen.The subject had 19 treatment-emergent adverse events; all mild or moderate, none serious, and none considered related to burosumab.In conclusion, burosumab normalized phosphorus homeostasis and improved fracture/pseudofracture healing in this subject with CSHS. Improvements were maintained through W144. Adverse events were tolerable, and efficacy was similar to the broader study population with TIO.

	Baseline	W24	W48	W72	W144
Pharmacodynamic Markers					
Serum phosphorus, mg/dL	1.6	3.5	2.9	3.4	2.6
TmP/GFR, mg/dL	1.8	3.7	NA	2.9	3.0
Serum 1,25(OH)$_2$D, pg/mL	20.9	53.0	67.4	38.7	40.2
Bone Turnover Markers					
Serum BALP, ug/L	33.7	20.2	12.8	12.8	11.5
CTx, ng/mL	NA	1.2	1.1	0.7	0.4
P1NP, ng/mL	172.4	186.2	135.2	95.8	69.0
Osteocalcin, ng/mL	99.6	118.4	73.7	48.6	31.9

TmP/GFP = renal tubular phosphate reabsorption; BALP = bone-specific alkaline phosphatase; CTx = carboxy terminal cross-linked telopeptide of type 1 collagen; P1NP = procollagen type 1 N propeptide; NA = not available.

***Disclosures: Thomas Carpenter**, Ultragenyx, Inozyme, Tegeneron, Kyowa Kirin, Consultant, Ultragenyx Pharmaceutical Inc, Grant/Research Support, Ultragenyx, Inozyme, Other Financial or Material Support*

P-789

Clinical characteristics, therapeutic outcome and follow up of 66 patients of Paget Disease from South India *Krishna Mori[1], Adlyne Reena Asirwatham[1], Shriraam Mahadevan[1], Karthik Balachandran[1], Amulya Yalamanchi[1], Sathish Kumar[1]. [1]Sri Ramchandra Medical College, India

Introduction: Paget disease of bone (PDB) is a disorder of altered bone remodeling mainly characterized by increased osteoclastic activity. While the exact Indian prevalence remains unknown, a clustering of published cases suggests South Indian predominance.Objective: To study the clinico-biochemical profile and therapeutic response of patients with PDB and briefly review the epidemiology of PDB from an Indian perspective.Methods: Retrospective data was collected from the charts of patients who have been seen in Endocrine out-patient clinics in Tamilnadu over a 12 year period. Published literature on PDB from India was reviewed.Results: A total of 66 patients (71% males) predominantly from Tamilnadu were studied. Mean age at presentation was 67+/-8 years. Polyostotic involvement was seen in 89% and familial occurrence of PDB in 5 patients. Symptoms at presentation mainly included bone pain (51%) and skeletal deformities (18%). Scalp vein sign (21%) and sensorineural hearing loss (64%) were also noted. Incidental PDB detection by raised serum alkaline phosphatase (SAP) levels was observed in 17% and by abnormal FDG-PET scan in 6% of cases. Mean SAP at presentation was 606+438 IU/L (Normal, 76-140). Major skeletal site involvement includes pelvis (62.1%) and spine (34.8%). Mean (range) follow up of the cohort was 3.4 years (1-12 years). From the cohort, 64 subjects received zoledronate and two received alendronate and mean (SD) SAP at 1-year was 73+/-42 IU/L. All but two showed remission at the end of 1 year. Two had pathological fractures and two had sarcomas. Review of epidemiology of PDB in Indian literature clearly showed a south Indian predilection for unclear reasons.Conclusion: PDB was considered rare in Asians, especially Indians. Most of the case series and other studies were mainly from Caucasians in UK or the migrant English population in Australia. However, in little over a decade, there were several case studies and two case series from India, suggesting that PDB is not uncommon in India. Hence, in this retrospective study, we intend to present the clinical and therapeutic aspects of 66 patients with PDB from Tamilnadu and provide a focused review of the epidemiology of this disorder

from an Indian perspective. Interestingly, most of the cases reported are exclusively from South India and this needs more exploration.Keywords: Paget disease of bone; South India, Alkaline phosphatase; Zoledronate

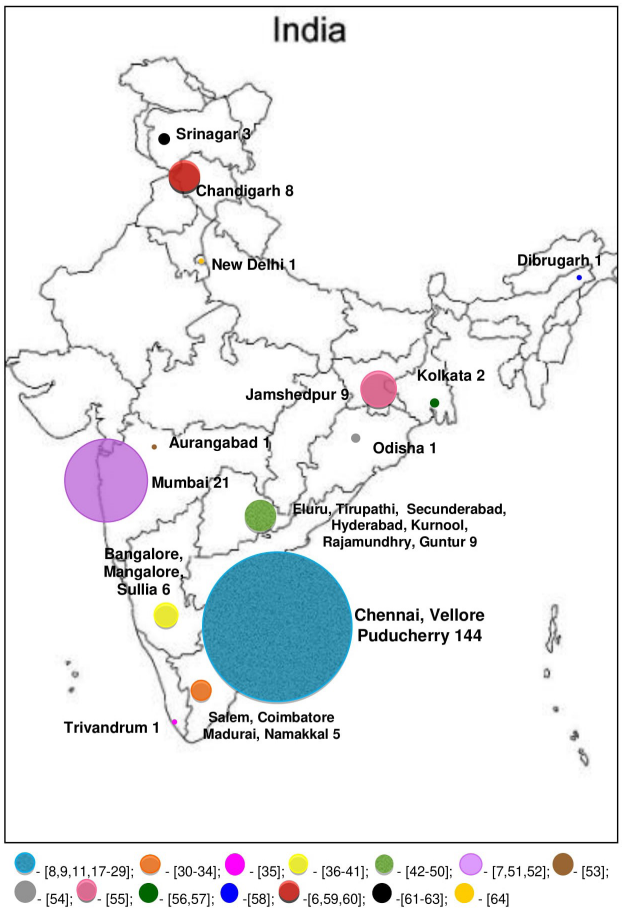

***Disclosures: Krishna Mori**, None*

P-790

X-Linked Hypophosphataemic Rickets: Description of 16 Cases in the Adulthood in Argentina *Tatiana Martinez[1], Laura Maria Schiro[1], Patricia Rodriguez[1], Evangelina Giacoia[1]. [1]Hospital Nacional Prof. A. Posadas, Argentina

Introduction: X-linked hypophosphatemic rickets (XLH) is an inherited disorder that results from an inactivating mutation of the PHEX gene. The familiar form comprises most cases. Its incidence is 4.8 per 100000 persons1. XLH is characterized by bowed or bent legs, short stature, tooth abscesses, hearing loss, joint pain and impaired mobility, which can alter quality of life.Aim: To describe clinical characteristics, laboratory and imaging findings of XLH adult patients attending to our hospital; to evaluate physical function and impact on the quality of life; to estimate adherence to conventional treatment. Methods: A retrospective, observational study from 16 XLH patients' medical records was performed. Age, sex, BMI, age at diagnosis, number of fractures, bone deformities, corrective surgeries, biochemical and genetic profile were evaluated. Physical functionality, pain and stiffness were measured with WOMAC and PROMIS scale; and quality of life (QOL) with SF36. Adherence to treatment was assessed with the CQR questionnaire. Renal ultrasound and brain CT scan were performed.Results: 16 patients were evaluated 14 (88%) female, 2 (12%) male, with a mean (?) age 40.06 years (+/-12.4), Age at diagnosis ?:12.68 years (SD+/-18.37), BMI ?:38.5 kg/m2 (13.07), stature ?:129.9 cm (+/-33.9), fractures 8/16 (50%) and skeletal deformities 16/16 (100%), number of corrective surgeries required 15/16 (94%), pseudofractures 13/16 (81%), kyphoscoliosis 8/16 (50%). Laboratory: calcemia ?:9.5mg/dl (+/-0.37) phosphatemia ?:2.07mg/dl (+/-0.41), PTH ?:88.31 pg/ml (+/- 36.1), 25OHD ?:26.77 ng/ml (+/-11.48), RTP?:76.76% (+/-11.19), FAO ?:37.08 (+/-26.94), CTX ?:1646 (+/-1119), FGF23 ?:58.85pg/ml (+/-27.7). Genetic profile: 1/14 had a definitely pathogenic not previously described in the literature mutation. 14/16 (88%) patients showed NOT to adhere to conventional treatment. Application of WOMAC function scale ?:47.87 (+/-25.23); PROMIS ?:31.5 questionnaire (+/-9.23); SF36 ?:34.95 (+/- 8.5). Renal ultrasound abnormalities 2/16 (13%) nephrocalcinosis and 3/16 (19%) renal lithiasis; no brain calcifications in the CT were described. Conclusion: The high percentage of patients not adherent to conventional treatment leads to marked impaired physical function with important skeletal deformities, fractures and pseudofractures, bone pain and altered QOL. Early diagnosis, adequate treatment and follow-up by a multidisciplinary team will avoid complications and improve the patient's quality of life.

Introduction: X-linked hypophosphatemic rickets (XLH) is an inherited disorder that results from an inactivating mutation of the PHEX gene. The familiar form comprises most cases. Its incidence is 4.8 per 100000 persons1. XLH is characterized by bowed or bent legs, short stature, tooth abscesses, hearing loss, joint pain and impaired mobility, which can alter quality of life.
Aim: To describe clinical characteristics, laboratory and imaging findings of XLH adult patients attending to our hospital; to evaluate physical function and impact on the quality of life; to estimate adherence to conventional treatment.
Methods: A retrospective, observational study from 16 XLH patients' medical records was performed. Age, sex, BMI, age at diagnosis, number of fractures, bone deformities, corrective surgeries, biochemical and genetic profile were evaluated. Physical functionality, pain and stiffness were measured with WOMAC and PROMIS scale; and quality of life (QOL) with SF36. Adherence to treatment was assessed with the CQR questionnaire. Renal ultrasound and brain CT scan were performed.
Results: 16 patients were evaluated 14 (88%) female, 2 (12%) male, with a mean (X̄) age 40.06 years (±12.4), Age at diagnosis X̄:12.68 years (SD±18.37), BMI X̄:38.5 kg/m2 (13.07), stature X̄:129.9 cm (±33.9), fractures 8/16 (50%) and skeletal deformities 16/16 (100%), number of corrective surgeries required 15/16 (94%), pseudofractures 13/16 (81%), kyphoscoliosis 8/16 (50%).Laboratory: calcemia X̄:9.5mg/dl (±0.37) phosphatemia X̄:2.07mg/dl (±0.41), PTH X̄:88.31 pg/ml (± 36.1), 25OHD X̄:26.77 ng/ml (±11.48), RTP
X̄:76.76% (±11.19), FAO X̄:37.08 (±26.94), CTX X̄:1646 (±1119), FGF23 X̄:58.85pg/ml (±27.7). Genetic profile: 1/14 had a definitely pathogenic not previously described in the literature mutation. 14/16 (88%) patients showed NOT to adhere to conventional treatment. Application of WOMAC function scale X̄:47.87 (±25.23); PROMIS X̄:31.5 questionnaire (±9.23); SF36 X̄:34.95 (± 8.5). Renal ultrasound abnormalities 2/16 (13%) nephrocalcinosis and 3/16 (19%) renal lithiasis; no brain calcifications in the CT were described.
Conclusion: The high percentage of patients not adherent to conventional treatment leads to marked impaired physical function with important skeletal deformities, fractures and pseudofractures, bone pain and altered QOL. Early diagnosis, adequate treatment and follow-up by a multidisciplinary team will avoid complications and improve the patient's quality of life.

***Disclosures: Tatiana Martinez**, None*

P-791

Bone Turnover and Mineral Metabolism in Adult Patients With Pediatric-Onset Hypophosphatasia (HPP) Treated With Asfotase Alfa *Lothar Seefried[1], Dominik Rak[1], Anna Petryk[2], Franca Genest[1]. [1]Orthopedic Clinic König-Ludwig-Haus, Julius-Maximilians-Universität Würzburg, Germany, [2]Alexion Pharmaceuticals, Inc., United States

Introduction: Evaluate changes in bone turnover markers in adults with pediatric-onset HPP who were treated with asfotase alfa.Methods:Observational study of adult patients (age >=18 years [y]) with pediatric-onset HPP who were treated with asfotase alfa for 12 months (mo) as part of routine care at 1 center (NCT03418389).Results: Data from 14 patients, ages 19-78y (median 52y), with compound heterozygous ALPL mutations and histories of skeletal (at least 1 fracture) and other HPP manifestations, were analyzed. Levels of Parathyroid Hormone 1-84 (PTH), mostly in the lower normal range before treatment, exhibited a transient increase at 3 mo of treatment, returning back towards baseline levels at 3 and 6 mo. This effect was not accompanied by changes in calcium or phosphate levels. Significant transient increases were observed regarding procollagen type 1 N-propeptide (PINP) at 3 mo and osteocalcin at 3 and 6 mo; both reverted to near baseline by 12 mo (Table). Numeric temporary increases in N-telopeptide of type 1 collagen (NTx) and tartrate-resistant acid phosphatase 5b (TRAP 5b) were not statistically significant. Serum concentrations of pyridoxal 5'-phosphate (PLP) were elevated at baseline with a median of 286ng/mL and decreased significantly (n=12, P=0.005) after12 mo of treatment to 8.5ng/mL (normal: 5-30). Similarly, significant reductions occurred in urine phosphoethanolamine (PEA)/creatinine ratio (n=11, P=0.008), with a decrease from 54.9mmol/mol creatinine at baseline to 22.4mmol/mol creatinine at 12 mo (normal: 2.3-11.3).Conclusions: This is the first systematic evaluation of bone turnover markers during asfotase alfa treatment. Results of this study suggest that beyond significantly reducing PLP and PEA, improvements in bone mineralization may be reflected by specific changes in biochemical markers, indicating facilitated bone remodeling during treatment with asfotase alfa.

***Disclosures: Lothar Seefried**, Alexion Pharmaceuticals, Inc., Consultant*

P-792

Flawed Fractures: Are some fractures pathognomonic for non-accidental injury? *Amy Bobyn[1], Oana Caluseriu[2], Breanne Frohlich[3], Mary Jetha[4], Chelsey Grimbly[5]. [1]University of Alberta, Canada, [2]Department of Medical Genetics, University of Alberta, Canada, [3]Division of General and Community Pediatrics, Department of Pediatrics, University of Albert, Canada, [4]Division of Pediatric Endocrinology, Department of Pediatrics, University of Alberta, Canada, [5]Department of Pediatrics, Division of Endocrinology, University of Alberta, Canada

Introduction: Non-accidental injury (NAI) is a diagnosis of exclusion in children presenting with multiple unexplained fractures. Features highly suggestive of NAI include metaphyseal corner fractures and posterior rib fractures. Osteogenesis Imperfecta (OI) is a rare monogenic class of disorders with vast clinical and genetic heterogeneity characterized by multiple fractures and additional features. OI is often included in the differential diagnosis of NAI. We present a case of siblings with metaphyseal corner fractures and rib fractures due to FKBP10 mutations, a rare cause of OI (MIM 259450; 610960). We performed a lit-

Posters

erature review to address the overlap between OI and NAI fractures. We aim to demonstrate that OI requires careful consideration in cases being investigated for NAI. Cases: A healthy 18-month-old male born to nonconsanguineous parents presented with asymmetric shoulder alignment. Xrays showed multiple fractures of varying healing stages including rib, bilateral ulnar, and metaphyseal corner fractures leading to investigations for NAI. He had isolated gross motor delay and no family history of recurrent fractures. Physical exam showed short stature (Height Z score -2.0), mildly blue sclera, joint hyperlaxity, and kyphosis. There was no dentinogenesis imperfecta (DI) or contractures. Genetic testing showed compound heterozygous likely pathogenic variants in FKBP10, and parents were confirmed carriers. The mother was pregnant at the time, and there was no suspicion of OI through multiple fetal ultrasounds; fetal growth tracked between 25th -50th centile. However, a skeletal survey at birth showed multiple rib fractures, metaphyseal corner fractures and long bone fractures. Genetic testing confirmed the same FKBP10 variants as in the sibling. A literature review identified 191 articles describing fracture patterns in NAI and OI. Thirteen articles reported 79 children investigated for NAI, later found to have OI; 75 children had clinical and radiological signs of OI. Thirty-seven cases proceeded to legal trial and 38 children were removed from family care due to suspicion of NAI. Conclusion: This report highlights that there are no pathognomonic fractures in NAI. OI can present with metaphyseal corner fractures, posterior rib fractures, and fractures at various stages of healing. Our work supports the importance of exploring a diagnosis of OI in cases suspected of NAI with multiple implications for patient and family management.

***Disclosures: Amy Bobyn**, None*

P-793

Quality of Life and Stigma Outcomes in the Surgical Treatment of Craniofacial Fibrous Dysplasia *Andrea Burke[1], Brian Leroux[2], Amanda Konradi[3]. [1]University of Washington School of Dentistry, United States, [2]University of Washington, United States, [3]Loyola University Maryland, United States

Purpose: Craniofacial fibrous dysplasia (CFD), a rare disease of bone marrow stromal cells, may distort facial features, cause functional/esthetic problems or pain. Our work has shown that quality of life (QoL) outcomes in CFD, as measured by the SF-36, were not significantly different in subjects treated operatively vs. non-operatively. Given the variable severity of CFD and important psychosocial implications, the purpose of this study was to measure the association between operative treatment and QoL measures, when taking into account demographic/disease variables and stigma. Methods: This is a retrospective cross-sectional study of subjects enrolled in the Fibrous Dysplasia Foundation Patient Registry, July 2016-December 2018. The primary predictor variable was operative treatment (no surgery, one surgery, more than one surgery); covariates included diagnosis (monostotic FD, polyostotic FD, McCune-Albright Syndrome), lesion location, and demographic data. Outcome variables were QoL and stigma measures obtained from the validated SF-36, HADS anxiety/depression scale, Brief Pain Inventory, and NeuroQoL survey. Multiple linear regression was conducted for the eight SF-36 domains, anxiety, depression, impact of pain, and experienced/internalized stigma to assess associations ($p<0.05$). Since stigma may influence both demographic/disease variables and QoL outcomes, the models were rerun with stigma as a control variable. Results: The sample was composed of 117 CFD adult subjects, with mean age 40 years, 84% female. Forty-nine subjects (41%) had at least one surgical treatment, of which 78% had an operation on facial bones. The number of craniofacial operations was not associated with physical and psychosocial QoL outcomes in any model. Higher disease burden (McCune-Albright Syndrome/polyostotic disease) was associated with worse physical function and pain, before and after adjustment for stigma. Body pain, general health and vitality were worse in females. Subjects who reported greater levels of stigma had significantly worse outcomes for all QoL measures, including pain. Those reporting internalized stigma significantly experienced anxiety and depression. Conclusion: Experienced and internalized stigma may play a role in the relationships between disease severity and QoL measures. Along with surgery, treatment of CFD should address the social effects of the disease.

***Disclosures: Andrea Burke**, None*

P-794

STOPFOP: A Phase II Clinical Trial of Saracatinib (AZD0530) in FOP *Bernard J Smilde[1], Richard Keen[2], Clemens Stockklausner[3], Dong Liu[4], Alex Bullock[5], Annette von Delft[5], Natasja M van Schoor[6], Paul B Yu[7], E Marelise W Eekhoff[1]. [1]Department of Internal Medicine, Amsterdam University Medical Center, Netherlands, [2]Department of Rheumatology, Royal National Orthopaedic Hospital, United Kingdom, [3]Department of Paediatrics, Klinikum Garmisch-Partenkirchen, Germany, [4]BioPharmaceuticals R&D, AstraZeneca, United States, [5]Nuffield Department of Medicine, University of Oxford, United Kingdom, [6]Department of Epidemiology and Biostatistics, Amsterdam University Medical Center, Netherlands, [7]Department of Medicine, Brigham and Women's Hospital, United States

Background: Fibrodysplasia Ossificans Progressiva (FOP) is an autosomal dominant, debilitating disorder marked by severe heterotopic ossifications (HO), progressive loss of mobility and early death. There are currently no approved treatments.Classic FOP is caused by a gain-of-function mutation (Acvr1[R206H]), resulting in a mutated ALK2-Kinase. AZD0530 (saracatinib) was identified by our team as a potent inhibitor of ALK2-kinase and was effective in preventing heterotopic ossification in FOP mouse models. The purpose of this study is to investigate the repositioning of AZD0530, originally designed for ovarian cancer treatment, to treat patients with FOP. This study is funded by the Innovative Medicines Initiative (IMI).Methods: The Saracatinib Trial to Prevent FOP (STOPFOP) is a phase 2a, multicentre, 6-month double blind randomized controlled trial of AZD0530 versus placebo, followed by a 12 month open-label trial comparing extended AZD0530 treatment with historical data. We will include 20 otherwise healthy FOP patients, aged 18-65 years, with the classic FOP mutation. Endpoints are an objective change in heterotopic bone volume measured by low-dose whole-body computer tomography (CT), [18F] NaF PET activity and patient reported outcome measures such as the FOP-IADL assessment.Discussion: Drug repositioning - using existing, previously researched but unapproved drugs for the treatment of a different disease - is especially useful in rare diseases with limited study populations. It represents an ideal solution for limiting risks in early clinical studies. Using existing pre-clinical and clinical knowledge may also allow more effective use of resources. With positive study outcome, AZD0530 may provide a rapidly translatable therapy for FOP due to the availability of extensive safety data from over 600 patients in more than 28 registered clinical trials using AZD0530.Trial registration: NCT04307953 / EudraCT number 2019-003324-20

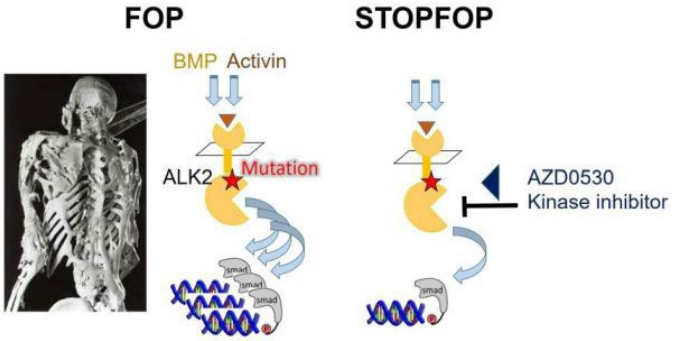

***Disclosures: Bernard J Smilde**, None*

P-795

Reduced Trabecular Bone Score is Associated with Non-Vertebral Fractures and Nephrolithiasis in Transfusion-Dependent Thalassemia *Nisal Punchihewa[1], Anne Trinh[2], Zane kaplan[3], Madhuni Herath[3], Frances Milat[2], Phillip Wong[2]. [1]Monash University, Australia, [2]Hudson Institute, Australia, [3]Monash Health, Australia

Although hypercalciuria, osteoporosis, fractures and nephrolithiasis are well described in thalassemia, there is limited literature to guide clinical surveillance of the renal-bone disease in this group. Bone mineral density as assessed by dual-energy x-ray absorptiometry (DXA) is cannot adequately capture the microarchitectural changes seen in thalassaemia bone disease. The trabecular bone score (TBS), derived from the lumbar spine using DXA provides a surrogate measures of bone microarchitecture. There is limited information available on the utility of TBS for fracture risk assessment in the thalassemia cohort. In this cross-sectional study of 71 subjects with transfusion-dependent thalassemia, the relationship between TBS, BMD, fractures, nephrolithiasis and biochemical parameters were investigated. TBS was significantly associated with non-vertebral fractures (OR 1.99 [95% CI 1.28 - 3.09]) and nephrolithiasis (OR 1.98 [1.33, 2.95]). Nephrolithiasis was highly prevalent (40.6%) and common in men (60%). Conventional DXA parameters were not significantly associated with nephrolithiasis but were associated with all types of fracture. This study demonstrates the potential use of TBS in predicting non-vertebral fractures and nephrolithiasis in transfusion-dependent thalassemia. The association between TBS and nephrolithiasis deserves further study.

***Disclosures: Nisal Punchihewa**, None*

P-796

Skeletal Abnormalities Confirmed by Chest Radiography in Childhood Could Provide a Clue to Diagnose Gorlin Syndrome *Makoto Fujiwara[1], Takuo Kubota[1], Taichi Kitaoka[1], Yasuhisa Ohata[1], Hirofumi Nakayama[1], Shinji Takeyari[1], Yukako Nakano[1], Kenichi Yamamoto[1], Chieko Yamada[1], Takeshi Ishimi[1], Tomonao Aikawa[2], Mikihiko Kogo[2], Akinori Takeshita[3], Narikazu Uzawa[3], Keiichi Ozono[1]. [1]Department of Pediatrics, Osaka University Graduate School of Medicine, Japan, [2]The first Department of Oral and Maxillofacial Surgery, Osaka University Graduate School of Dentistry, Japan, [3]Department of Oral and Maxillofacial Surgery 2, Osaka University Graduate School of Dentistry, Japan

Background: Gorlin syndrome, also called basal cell nevus syndrome, is a disorder characterized by malformations of the skin, nerves, eyes, and bones. Heterozygous mutations of PTCH1, PTCH2, or SUFU which are involved in the SHH-PTCH1 pathway cause the syndrome, and de novo mutations account for 20 to 30% of cases. Because the patients with Gorlin syndrome have a predisposition to various tumors including basal cell carcinoma (BCC) and keratocystic odontogenic tumor (KCOT), early diagnosis is of great importance. Although the major criteria including BCC and KCOT are often not evident until the childhood, the radiological manifestations of various skeletal abnormalities may contribute to make early diagnosis. Especially, rib anomalies such as bifid ribs, whose overall prevalence is estimated lower than 3% in general population, are common with high specificity in Gorlin syndrome.Objectives: The aim of this study was to verify the usefulness of occasional chest X-ray to detect skeletal abnormalities in pediatric patients with Gorlin syndrome.Methods: We retrospectively assessed the chest X-ray films of Gorlin syndrome patients aged under15 year old who have been followed at Osaka University Medical and/or Dental Hospital since 2001.Results: Six patients (2 males and 4 females) were analyzed. Family history was found in 3 patients. All patients showed calcification of the falx cerebri, two patients presented cleft lip and palate, and one patient revealed cardiac fibroma. All patients have developed KCOT and the resection was performed. Genetic analysis was performed in 3 patients, in all of whom heterozygous PTCH1 mutations were detected. All chest X-ray photographs were taken as a preoperative examination at 6.6 – 14.2 years old (average 11.3 years old). Rib abnormalities were found in 3 patients, and vertebral anomalies were identified in 2 patients. Previous chest X-ray could be traced in two patients and all of them showed the same skeletal abnormalities. Two patients were diagnosed with Gorlin syndrome by the rib abnormalities.Conclusion: Patients with Gorlin syndrome exhibit skeletal anomalies in their childhood at high rates, which could be detected by chest X-ray and provide a clue to the diagnosis. Therefore, it is worth considering Gorlin syndrome even when bone abnormalities in chest radiography are observed by chance.

***Disclosures: Makoto Fujiwara**, None*

P-797

Erdheim-Chester disease - Unusual presentation with isolated skeletal lytic lesions *Amulya Yalamanchi[1], Adlyne Reena Asirwatham[1], Karthik Balachandran[1], Shriraam Mahadevan[1], Sathish Kumar[1], Krishna Mori[1]. [1]Sri Ramachandra medical college, India

Background: Erdheim Chester disease (ECD) is a rare, non-langerhans cell histiocytosis characterized by CD68+ and CD1a- foamy histiocytes with multisystem involvement and characteristic sclerotic musculoskeletal lesions. First case was described as “lipogranulomatosis” by Jakob Erdheim and William Chester in 1930. Since then only 650 cases have been reported so far.Case report: A 48-year-old peri-menopausal women, presented with persistent headache and tender swelling of the left shoulder and hip joint for 5 years and with difficulty in walking for 18 years due to multiple long bone fractures. Roentograms showed large mixed expansile lytic sclerotic lesions involving left humerus and acetabulum. Technetium 99m bone scan showed discrete hot spots in the skull, right humerus, left humerus, left femur and iliac crests. MRI brain showed multiple lytic lesions in the skull vault. Biopsy from humeral lesion showed characteristic histologic findings: clusters of foamy histiocytes positive for vimentin, CD68 and negative for S-100 and CD1a, typical of ECD histiocytes. Conclusion: Symmetrical long bone osteosclerosis is the most specific radiological finding for ECD whereas in Langerhans cell histiocytosis (LCH), bone involvement is mostly osteolytic and do not involve long bones. Only 5-8% of the patients with ECD have osteolytic lesions either on the flat bones, or long bones. As our patient has overlapping features of Langerhans cell histiocytosis as well as Erdheim Chester disease, it lead to misdiagnosis for about 20 years. This case represents the unusual presentation of the spectrum of ECD. Keywords: Erdheim Chester disease; Osteosclerosis; non-langerhans cell histiocytosis; Lytic bone lesions;

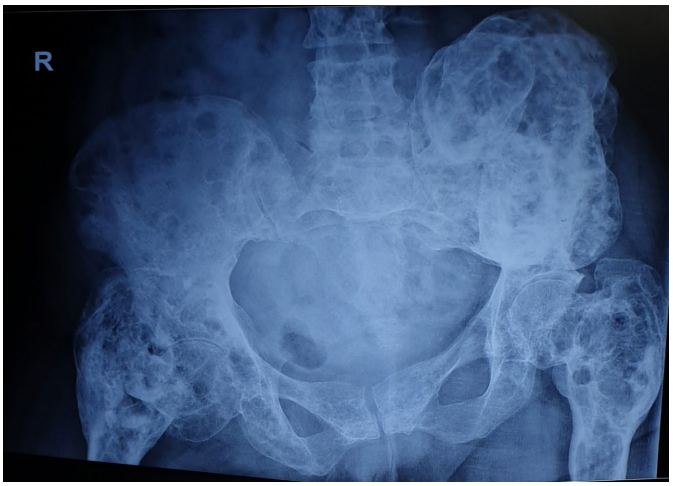

***Disclosures: Amulya Yalamanchi**, None*

P-798

The Role of Lysine Specific Demethylase 1 in Osteoclast Differentiation *Kristina Astleford[1], Kim Mansky[1]. [1]University of Minnesota, United States

Changes in gene expression help bone respond to developmental, repair and remodeling cues in a rapid manner. Healthy skeletal growth and maintenance requires carefully coordinated cycles of bone formation and resorption. Osteoclasts are large, multinucleated cells that are responsible for bone degradation by secreting acids and proteolytic enzymes to dissolve bone mineral and extracellular matrix. Increased activity of osteoclasts has a detrimental effect on the skeleton and therefore, have become a therapeutic target for many skeletal diseases including osteoporosis. Progression from multipotent progenitors into specialized, terminally differentiated cells involves carefully regulated patterns of gene expression to control lineage specification and development of the cellular phenotype. This process requires synchronized action of transcription factors with co-activators and co-repressors to initiate proper activation and inhibition of gene expression. Lysine-specific demethylase 1 (LSD1 or KDM1A) is a member of the histone demethylases which is a group of transcriptional co-repressors/co-activators known for regulating gene expression via removal of mono- and di-methyl groups from histone 3 lysine 4 (H3K4 and histone 3 lysine 9 (H3K9). Demethylation of H3K4 represses transcription while demethylation of H3K9 activates transcription. The mechanism by which LSD1 regulates osteoclast differentiation is currently unknown. As measured by RNA and protein, LSD1 is expressed throughout osteoclast differentiation. Treatment of bone marrow macrophages with the LSD1 chemical inhibitor S2101, enhances osteoclast differentiation and mono-methylation of H3K4. Furthermore, shRNA knockdown of LSD1 exhibits a similar phenotype with an increase in the osteoclast gene markers, Nfatc1, Dcstamp and Cathepsin K. Furthermore, shRNA knockdown of LSD1 results in an increase in multiple osteoclast fusion genes including Adam8 and Oscar, suggesting that osteoclast fusion may be regulated by LSD1. Lastly, knockdown of LSD1 enhances osteoclast resorptive ability. Currently, we are investigating LSD1’s epigenetic role in regulating osteoclast differentiation and activity using mice who are conditionally deleted for LSD1 in osteoclasts by determining their in vivo skeletal and in vitro osteoclast phenotype.

***Disclosures: Kristina Astleford**, None*

P-799

Melorheostosis: Successful Pain Management with Medical Marijuana *Anjali Manavalan[1], Donna Lee[1], Julia Arnsten[2], Vafa Tabatabaie[1]. [1]Division of Endocrinology, Montefiore Medical Center, Albert Einstein College of Medicine, United States, [2]Division of General Internal Medicine and Psychiatry, Montefiore Medical Center, Albert Einstein College of Medicine, United States

Background: Melorheostosis is a rare bone disorder first recognized in 1922. It is characterized by osteosclerosis of cortical bone and adjacent soft tissue. Pain is the most common symptom and correlates with periosteal bone formation. Involvement of the surrounding soft tissue or joint capsule may result in deformities. Localized, asymmetric lesions may help distinguish it from other conditions that are radiologically similar. Sporadic somatic mutations in MAP2K1, SMAD 3 and the RAS pathway have been implicated in isolated melorheostosis (1). Treatment is focused on pain control. The utility of medical marijuana for pain control in patients with melorheostosis has not been described previously.Clinical Case: A 25-year-old man presented to our metabolic bone clinic for the management of worsening melorheostosis that had been diagnosed by bone biopsy at an outside hospital. Genetic testing was unavailable but no family history suggestive of bone disease was reported. Physical exam uncovered tender sites in the left lower extremity without deformity or

joint involvement. Progression of sclerosis was noted on imaging. Vitamin D deficiency and secondary hyperparathyroidism were treated with supplementation. Suboptimal analgesia with opiates led to a referral to the medical cannabis clinic. Pain improved significantly and opiates were weaned. Laboratory Results: Calcium 9.7mg/dl (8.5-10.5), Creatinine 1.1mg/dl (<1.5), Vitamin D 25-OH 30), Intact Parathyroid hormone 73.5pg/ml (15-65), TSH 1.04uU/ml (0.4-4.60), C-Telopeptide 704pg/ml, Osteocalcin 27ng/ml (9-38). Prior Skeletal Survey: Cortical thickening involving the left femoral shaft and iliac bone, consistent with melorheostosis. Current X-Ray Tibia and Fibula: Flowing ossifications in the left distal femur, fibular shaft and calcaneus, compatible with melorheostosis. Conclusion: Treatment of melorheostosis is centered on symptom management. Non-steroidal analgesics may be inadequate and opiates are fraught with the development of tolerance, side effects and potential for addiction and abuse. Bisphosphonates and denosumab may be used but can increase the risk of atypical fractures. Medical marijuana has proven efficacy in the management of pain and anxiety and could represent a safe and effective approach to analgesia in patients with melorheostosis.References:1)P. Wordsworth and M.Chan;Melorheostosis and Osteopoikilosis: A Review of Clinical Features and Pathogenesis;Calcified Tissue International volume 104,530–543(2019)

***Disclosures: Anjali Manavalan**, None*

P-800

The developmental phenotype of the great toe in fibrodysplasia ossificans progressiva *Will Towler[1], Eileen Shore[1], Fred Kaplan[1]. [1]University of Pennsylvania, United States

Fibrodysplasia ossificans progressiva (FOP) is a genetic disorder in which extensive heterotopic ossification begins to form during early childhood and continues to progress throughout life. Although heterotopic bone formation does not occur during embryonic development, children who carry the ACVR1R206H mutation that causes most cases of FOP characteristically exhibit malformation of their great toes at birth, indicating that the mutation also alters skeletal formation. Despite the prevalence of the great toe malformation in the FOP population, it has received relatively little attention due to its apparently clinically benign nature. In this study, we examined radiographs from a cohort of 41 FOP patients ranging from 2 months to 48 years of age to provide a detailed analysis of the developmental features, progression, and variability of the great toe malformation of FOP, which include absent skeletal structures, malformed epiphyses, ectopic ossification centers, malformed first metatarsals and phalangeal fusion.

***Disclosures: Will Towler**, None*

P-801

Tumor-induced Osteomalacia under treatment with burosumab *Daniel Salica[1], Ariel Sanchez[2]. [1]School of Medicine. National University of Cordoba. Argentina, Argentina, [2]Center of Endocrinology, Argentina

Introduction:Tumor-induced Osteomalacia (TIO) is a rare paraneoplastic syndrome, related to excessive production of FGF-23 by tumors of mesenchymal origin. This report is about a patient with TIO whose tumor relapsed after surgery in 2008; she started treatment with burosumab, a fully human monoclonal antibody to FGF23, a year ago.Clinical Case:A 51-year-old woman started in 2004 with muscle weakness, progressive muscle and bone pain, prostration and multiple fractures in vertebrae, both hips, humerus and left shoulder. X-rays studies revealed a tumor in the left ischiopubic bone. The biopsy revealed a mesenchymal tumor. Surgery was performed in 2008, with removal of the affected bone; pathological studies suggested fibrous dysplasia. Symptoms improved and eventually disappeared; the patient remained asymptomatic until 2011, when her clinical picture recurred, causing disability and prostration; she also presented lumbosacral radicular compression syndrome. Treatment with burosumab (started in May 2019), at the current dose of 60 mg per month, increased serum phosphate levels, and decreased pain and fatigue, improving her quality of life,.Laboratory tests before burosumab were: serum calcium 9.1 mg/dl, serum phosphate 1.2 mg/dl, FGF-23 1127.5 pg/dl (NR 0-134); serum alkaline phosphatase 235 IU/l (NR 60-120), serum calcitriol 15.4 pg/ml (NR 19-54); ionic calcium (pH 7,40) 1.21 mmol/l (NR 1.10-1.28); serum PTH 271 pg/ml (NR 10-65); 25-hydroxyvitamin D 38 ng/ml (NR 30-150) urine calcium 200 mg/24 h; tubular reabsorption of phosphate 52% (normal >83).The medical imaging (CT scans, FDG-PET) was negative for tumor, but showed multiple uptake in bone areas attributed to increased remodelling and bone fractures.Laboratory tests during treatment with burosumab were: serum calcium 8.9 mg/dl; ionized calcium 4.76 mg/dl; serum phosphate 2.9 mg/dl; serum alkaline phosphatase 301 IU/l; 25-hydroxyvitamin D 27 ng/ml; serum PTH 269 pg/ml; urine calcium 90 mg/24 h.Conclusion:Burosumab treatment in this case of TIO increased serum phosphate levels, improved mobility, pain and fatigue during 12 months of follow-up, without adverse events.

***Disclosures: Daniel Salica**, None*

P-802

Orbital Fibrous Dysplasia: Visual Loss Due To New Lesion 50 Years After Initial Diagnosis *Abhilasha Singh[1], Vishnu Sundaresh[1], Massiell German[1]. [1]University of Utah, United States

IntroductionFibrous dysplasia (FD) is a rare bone disorder in which normal bone is replaced by fibro-osseous tissue resulting in pathological fractures. It is monostotic in 75-80% of cases, while remaining are polyostotic. Craniofacial involvement is 10-27% in monostotic and 50% in the polyostotic form. Of these, orbital lesions occur in about 20-39%. Majority of craniofacial lesions occur within 3.4 years of diagnosis. We describe a patient presenting with new progressive lesions 5 decades after initial diagnosis.CaseA 56-year-old white female was referred to our clinic by ophthalmology after being evaluated for progressive loss of vision in the left eye over 4 months. Medical history included polyostotic fibrous dysplasia diagnosed at age 14 years when she presented with multiple fractures with onset at age 5 years. History of lobectomy for a benign goiter. Magnetic resonance imaging (MRI) brain reported mass effect on left optic nerve at the orbital apex. Oral and IV prednisone was not helpful. Examination revealed only finger counting in the left eye, with restricted superior and inferior temporal fields. Right eye was normal. No signs of hypercortisolism, acromegaly, and skin lesions. Labs revealed normal calcium, albumin, phosphorus, magnesium levels with PTH: 27 (15-65 pg/ml), Vit D: 57 (30-80 ng/ml), BUN: 13 (8-24 mg/dl), Cr: 0.74 (0.57-1.11 mg/dl), TSH: 0.29 (0.35-4.94 mU/l), FT4: 1.4 (0.8-1.7 ng/dl), TSI: 104 (<122%), PRL: 5.6 (2.8-26 pg/ml), IGF-1: 95 (48-235 ng/ml), Alkaline phoshatase: 156 (38-126 U/L), BSAP: 26.5 (7.0 - 22.4 ug/L), and C-telopeptide: 619 (104-1008 pg/mL). Tc99m Bone scan reported osteoblastic activity in the right calvarium including parietal, temporal, skull base, humeri, pelvis, and femur. Decompressive surgery for the left eye or prophylactic surgery in the right eye was deemed not to be beneficial. Zoledronate was recommended.DiscussionMost cases of FD are identified in early childhood and lead to deformity of the involved bone over time making them prone to fractures. Although, patients develop complications in pre-existing lesions decades after diagnosis, it is extremely rare to present with new lesions. We report the development of new progressive lesions 50 years after initial diagnosis. We suggest to follow these patients lifelong to monitor for new lesions. Timely diagnosis and intervention may reduce fractures, visual and hearing loss, and rarely malignant transformation, with improved quality of life.

***Disclosures: Abhilasha Singh**, None*

P-803

Uncommon disease presenting with common symptom-Tumoral calcinosis presenting as bilateral pedal edema *ASHOK VENKATANARASU[1], RAMAN BODDULA[2], CHIMUTAI CHINTE[2], VIDYA TICKOO[3], PRANITH RAM MAMIDI[3]. [1]SANJEEVANI THYROID, SUGAR AND HORMONES CLINIC, India, [2]Yashoda hospital, India, [3]YASHODA HOSPITAL, India

Introduction:Tumoral calcinosis (TC) is a rare metabolic disorder characterized by ectopic calcification (periarticular or dermal) that results from abnormality in phosphate homeostasis due to an increase in renal phosphate reabsorption, often associates with normal calcitriol. Commonly presents as periarticular soft tissue mass or rarely as calcinosis cutis. Here we are reporting such case that presented with bilateral symmetrical pedal edema, which is uncommon presentation.Clinical caseA 55 years old gentleman who is known case of type 2 diabetes mellitus presented with swelling of feet and legs on both sides since 2 years. It was associated with stiffness, pain and hardness of legs. There was no history of redness of skin over swelling, fever or localized swellings elsewhere in the body. Similar history is present in his mother and younger brother. His parent's and grandparent's marriage was consanguineous marriage. On examination, there was symmetrical bilateral pedal edema that extending upto below knee of the legs and stony hard on palpation. There were no signs of vascular insufficiency and local infection. X- Ray of both legs showed diffuse subcutaneous calcification on both sides(X-ray picture).Laboratory tests revealed, serum calcium-10.0mg/dL, serum phosphorous-6.2mg/dL, serum creatinine -1.1mg/dL, TMP-GFR-6.014, serum parathyroid hormone-24.5pg/mL, 25 (OH)2 Vitamin D3-22ng/mL, 1,25(OH)2 Vitamin D3- 100pmol/L, fibroblast growth factor 23 (FGF-23, C-terminal)- 1038 RU/mL (upto 150) (ELISA) and HbA1C -6.7%. His mother laboratory reports also revealed that serum calcium-10.6, serum phosphorous -6.8, serum albumin 4.1g/dL and serum creatinine-1mg/dL. Genetic work up revealed a homozygous missense variation in exon 6 of the GALNT3 gene, with amino acid substitution of Arginine for Leucine at codon 366 (c.1097 T>G (p.Leu366Arg)). FGF-23 levels are high as it was C- terminal (inactive FGF-23) estimation, expected to be high in this case. Diagnosis of familial tumoral calcinosis made and started on phosphate-restricted diet along with Sevelamer. After 4months, there were improvement noted clinically and also in lab parameters, serum calcium-9.6, serum phosphorous-5.4mg/dL.Conclusion-Familial tumoral calcinosis, which is a rare disease, presented with common general symptom as pedal edema. Sevelamer and phosphate restricted diet showed improvement in presented symptoms and serum phosphorous levels.

***Disclosures: ASHOK VENKATANARASU**, None*

P-804

Delayed Administration of a Selective ALK2 Inhibitor, VU002, Reduces Injury-Induced Endochondral Heterotopic Ossification (HO) by Stopping HO Expansion in Fibrodysplasia Ossificans Progressiva (FOP) Mice *Jessica Pierce[1], Shivangi Dave[2], Paulo Melo[2], Cody Elkins[1], Huili Lyu[1], C. Henrique Serezani[2], Daniel Perrien[1]. [1]Emory University, United States, [2]Vanderbilt University Medical Center, United States

Expression of aberrantly active variants of ACVR1/ALK2 in muscle-resident cells is required for flare initiation and endochondral HO (EHO) in FOP. Daily treatment with clinically-relevant small molecule ALK2 inhibitors started at the time of injury or 2 days post-injury (dpi) can block EHO in FOP mice. However, the role of ALK2 at later stages of flare development and the ability of ALK2 inhibitors to reduce EHO when treatment is further delayed are unclear. Since the trigger for FOP-flares in patients is often unknown, it is important to understand the stages during which ALK2 inhibitor treatments are effective. Muscle injury in tamoxifen-inducible ALK2R206H-FlEx/wt (tamFOP) mice causes hyperinflammation detectable at 2-6 dpi, cartilage formation by 6-8 dpi, and radiographically detectable mineralization by 7-11 dpi. Thus, we hypothesized that oral delivery of a highly potent and selective small-molecule ALK2 inhibitor (VU002) in tamFOP mice would block HO formation when treatment is delayed up to 7 dpi. Following tamoxifen-induced permanent expression of ALK2R206H, 33-35 day old tamFOP mice received bilateral pinch injuries of lower hindlimb muscles. Mice remained untreated (CON) or received 20 mg/kg VU002 b.i.d. by oral gavage starting immediately at the time of injury (D0), or 5-, 7-, or 14-dpi (n=3-6 per group), and treatment continued daily until sacrifice at 35 dpi. As expected, CON mice developed extensive EHO by 14 dpi which continued to expand until 35 dpi, and this was completely prevented in mice that received VU002 starting at the time of injury (d0-35 $p<0.0001$). Mice in the d5-35 and d7-35 groups also developed HO by 14 dpi (64+/-16 $p<0.05$ and 45+/-18 $p<0.01$, respectively), but this was significantly less than in CON mice (103+/-16). Further, the amount of EHO in d5-35 and d7-35 groups did not expand from 14-35 dpi. In contrast, starting treatment at 14 dpi (d14-35 group) did not alter HO area vs. Untreated mice at any timepoint. Surprisingly, immature intramuscular cartilage and mature EHO were present in histological sections of legs from mice treated with VU002 at d5-35 and d7-35, suggesting that ALK2-inhibition may block cartilage maturation and mineralization. Mechanistically, these data suggest that expansion of mineralized HO in FOP mice may be independent of ALK2 signaling. This also indicates the window to initiate oral ALK2 kinase inhibitor treatment may be limited to the inflammatory, prechondrogenic phase of a flare.

***Disclosures: Jessica Pierce**, None*

P-805

New Ifitm5 S42L mouse model for atypical type VI Osteogenesis Imperfecta recapitulates patient phenotype. *Gali Guterman Ram[1], Ghazal Hedjazi[2], Chris Stephan[3], Stéphane Blouin[2], Victoria Schemenz[4], Wolfgang Wagermaier[4], Jochen Zwerina[2], Peter Fratzl[4], Kenneth M Kozloff[3], Nadja Fratzl-Zelman[2], Joan C Marini[5]. [1]Section on Heritable Disorders of Bone and Extracellular Matrix, Eunice Kennedy Shriver National Institute of Child Health and Human Development, National Institutes of Health, United States, [2]Ludwig Boltzmann Institute of Osteology at the Hanusch Hospital of OEGK and AUVA Trauma Centre Meidling, 1st Medical Department, Hanusch Hospital, Austria, [3]Department of Orthopaedic Surgery, University of Michigan, United States, [4]Max Planck Institute of Colloids and Interfaces, Dept. of Biomaterials, Germany, [5]Section on Heritable Disorders of Bone and Extracellular Matrix, Eunice Kennedy Shriver National Institute of Child Health and Human Development, United States

Osteogenesis Imperfecta (OI) is a type I collagen-related bone dysplasia. Type V OI, caused by a recurrent dominant mutation in IFITM5/BRIL, and type VI OI, caused by recessive null mutations in SERPINF1/PEDF, each have distinctive features. IFITM5 S40L, reported in 9 patients, causes severe dominant OI with phenotype, bone histology and decreased cellular PEDF secretion similar to type VI OI, rather than type V. Our aim is to understand the role of the pathways connecting IFITM5 and SERPINF1 in bone development.We generated an Ifitm5 S42L knock-in mouse model with NICHD-ACUC approval. Mice were analyzed by X-Ray, aBMD, qBEI, µCT, bone mechanics, serum chemistry and in-vitro OB differentiation.Newborn Ifitm5 S42L mice, both heterozygous (HET) and homozygous (HMZ), are non-lethal, have flared rib cage, shoulder and knee dislocations; HMZ pups also have rib fractures. On x-Rays, HET mice exhibit »50% humeral fractures at 1,2- and 6-months, while HMZ incur fractures in 96% of humerii, femora and pelvis. Like aVI OI patients, young HET males have increased serum ALP and normal serum PEDF level ($p<0.01$) vs. WT. Mechanical testing of 2-month HET and HMZ show reduced stiffness, yield and ultimate load, with markedly increased brittleness. Biomechanics are not explained by bone size, suggesting material differences. On µCT, HET mice have decreased Ct.Th, but increased BV/TV and Tb.N, as well as increased vascular pore volume/BV. Whole-body DXA-aBMD was significantly decreased in 1,2-and 6-month-old mice with a step effect, suggesting HMZ are more severe than HET($p<0.01$). qBEI of cortical bone revealed hypermineralization in 1-and 2-month HET vs. WT males, with increased CaMean, CaPeak (all, $p<0.01$) and CaHigh ($p=0.0133$, $p=0.0027$ respectively); 2-month HET show increased density and decreased area (both $p<0.001$) of osteocyte lacunar sections. Second harmonic generation florescence microscopy revealed bones from HET mice contain mostly disordered matrix (60% vs 20% WT, $p<0.0001$). Cultured calvarial osteoblasts from HET mice deposit increased mineralization by alizarin red staining ($p<0.05$). HET mice have increased expression of osteoblast differentiation markers, including Ifitm5; OB BRIL level is normal on western blot.We demonstrated our mouse model recapitulates patient phenotype and revealed differences in bone fragility, mineralization, vascularity, matrix organization. Continuing investigation will reveal cellular mechanisms involving Ifitm5 and Serpinf1.

***Disclosures: Gali Guterman Ram**, None*

P-806

Skeletal and Epidermal Contributons of FGF23 Excess in Cutaneous Skeletal Hypophosphatemia Syndrome *Zachary Michel[1], Diana Ovejero[2], Amanda Saikali[1], Christophe Cataisson[3], Stuart Yuspa[3], Michael Collins[1], Luis Fernandez de Castro[1]. [1]Skeletal Disorders and Mineral Homeostasis Section, National Institute of Dental and Craniofacial Research, National Institutes of Health, Bethesda, Maryland, United States, [2]Musculoskeletal Research Unit, Hospital del Mar Institute of Medical Investigation (IMIM), Barcelona, Spain, Spain, [3]Laboratory of Cancer Biology and Genetics, National Cancer Institute, National Institutes of Health, Bethesda, Maryland, United States

Cutaneous skeletal hypophosphatemia syndrome (CSHS) is a rare, mosaic genetic disease caused by gain-of-function RAS mutations during embryogenesis. It prominently affects skin and bone, causing skeletal dysplasia and a variety of skin lesions. It is associated with elevated circulating FGF23, an osteocyte-derived phosphaturic hormone, resulting in hypophosphatemia and often osteomalacia and rickets. Early studies suggested skin lesions are the source of a “phosphaturic factor” causing osteomalacia. Consequently, some patients still undergo painful resections of lesional skin, despite no improvement in hypophosphatemia. Previous studies indicate that skin lesions do not express FGF23 but failed to prove that RAS mutated bone cells are the source of FGF23 excess.We hypothesized that the origin of FGF23 excess in CSHS is RAS-mutated bone, not skin. To test this, we studied two mouse models with mosaic-like expression of human HRAS G12 gain-of-function mutations: one restricted to the appendicular skeleton and cranial areas (by a Prrx1 promoter), and doxycycline-inducible (Bone HRAS G12V); and another with an orthotopic graft of keratinocytes transduced with a mutant HRAS (Epidermal HRAS G12R). Both models result in constitutive HRAS signaling restricted to bone or squamous papilloma, respectively. In both models, we measured blood levels of active FGF23 (intact, iFGF23) and total FGF23 (iFGF23 plus its inactivated c-terminal fragment, cFGF23), as well as vertebral bone volume by micro-CT analysis of the L5 vertebral bone to assess for possible osteomalacia due to FGF23 excess.Bone HRAS G12V mice exhibited dramatically increased total FGF23 and iFGF23

(approximately 17-fold and 30-fold higher than WT, respectively), and decreased vertebral trabecular bone volume. Epidermal HRAS G12R mice showed elevated total FGF23 (3-fold change) but no significant change in iFGF23. Epidermal HRAS G12R did not show bone loss, but L5 vertebrae showed trabecular thinning.In this study, we demonstrated marked excess of active iFGF23 and vertebral bone loss in mice with mosaic-like bone HRAS G12V expression. We are currently investigating the cause of inactive cFGF23 excess and the moderate bone microarchitecture changes observed in epidermal HRAS G12R mice, e.g. systemic inflammation. Further studies will also assess vertebral osteomalacia by histomorphometry, serum phosphate levels, and Fgf23 expression in bone and skin in both models.

***Disclosures: Zachary Michel**, None*

P-807

Skeletal defects in Rps19+/- models of Diamond Blackfan anemia are mediated in part by failure of the meschymal lineage *Jimmy Hom[1], Hiren Patel[1], Mushran Khan[1], Douglas J Adams[2], Lydie M Da Costa[3], Luanne L Peters[4], Cheryl L Ackert-Bicknell[2], Jeffrey M Lipton[1], Lionel Blanc[1]. [1]Feinstein Institute for Medical Research, United States, [2]Departament of Orthopedics, University of Colorado Anschutz Medical Campus, United States, [3]Service d□Hématologie Biologique, Hôpital Robert Debré, France, [4]The Jackson Laboratory, United States

Diamond Blackfan Anemia (DBA) is a bone marrow failure syndrome characterized by red cell aplasia, craniofacial defects, and abnormalities of the forelimbs. Causative mutations for DBA are often found in genes encoding ribosomal proteins, most commonly RPS19. In a 37-week gestation stillborn RPS19+/- DBA patient, we observed decreased trabecular bone and an expanded hypertrophic zone in the ribs. To study this mutation further, 2 mouse models were generated, each with Rsp19 haploinsufficiency: an embryonic stem cell (mESC) line harboring a gene trap in Rps19 and an in vivo model using Prrx1-Cre with a floxed Rps19 allele. Rps19+/- mESCs differentiated into osteoblasts showed decreased ability to form mineralized nodules compared to controls. In these cells at day 23 post differentiation we saw decreased expression of Bmp2 (fold = -4.00, p<0.001) and Runx2 (fold = -6.91, p<0.001), and an increase in the osteoclast stimulating factor Tnfsf11 (RANK Ligand, fold = 8.66, p<0.001). As we reported previously, Prrx1-Cre;Rps19fl/+ mice were born with dysmorphic forelimbs, and shortened hindlimbs. We now show that these growth defects are concurrent with an expanded and disorganized hypertrophic chondrocyte zone in the distal femur. We observed an increase in apoptosis in the pre-hypertrophic zone and a decrease in the hypertrophic zone. The decreased hypertrophic chondrocyte apoptosis may in part be explained by an observed reduction of SOX9 expression. Femur length was reduced at 10 weeks of age in males (p<0.001). We also saw a reduction in trabecular bone volume fraction (BV/TV) in the distal femur and an increase in TRAP+ cells in the metaphysis. Patients with DBA present with increased TRP53 activation in erythroid progenitors. As we reported previously, when TRP53 levels were reduced by crossing Trp53fl/fl with Prrx1-Cre;Rps19fl/+ mice to generate animals with loss of 1 or 2 alleles of Trp53, the forelimbs defects resolved in a dose-dependent manner. We now report that RUNX2 expression at the metaphysis and the femoral growth plate disorganization were both resolved upon Trp53 deletion. Trabecular bone was increased in the Rps19+/-,Trp53-/- 10 week old male mice compared to Rps19+/-,Trp53+/+. These data suggest a fundamental role for Rps19 in skeletal biology that are associated with alterations in TRP53 levels and that skeletal defects seen in DBA patients appear due to RPS19 action in the mesenchymal cells.

***Disclosures: Jimmy Hom**, None*

P-808

Gnas heterozygous inactivation in a mouse model of Albright hereditary osteodystrophy differentially affects cortical bone formation based upon parental inheritance of mutation *Patrick McMullan[1], Peter Maye[2], David Rowe[2], Emily Germain-Lee[3]. [1]Depts of Pediatrics and Center for Regenerative Medicine and Skeletal Development, UConn Health, United States, [2]Center for Regenerative Medicine and Skeletal Development, UConn Health, United States, [3]Depts of Pediatrics and Center for Regenerative Medicine and Skeletal Development, UConn Health and Division of Pediatric Endocrinology, Connecticut Children's, United States

Albright hereditary osteodystrophy (AHO) is caused by heterozygous inactivation of GNAS, which encodes the α-stimulatory subunit (Gαs) of GPCRs. AHO skeletal signs include adult short stature, brachydactyly and subcutaneous ossifications. AHO patients with maternally-derived GNAS mutations develop pseudohypoparathyroidism type 1A and are obese with resistance to hormones requiring Gαs (eg., PTH, TSH and GHRH) due to tissue-specific paternal imprinting of GNAS. Paternally-derived GNAS mutations cause pseudopseudohypoparathyroidism in which patients have AHO skeletal features but do not develop severe obesity or hormonal resistanceThis study aimed to identify if bone formation is affected within Gnas+/- adult (12 wk) mice, and if the parental inheritance of the Gnas mutation differentially affects bone formation. We utilized our AHO mouse model created by targeted disruption of exon 1 of Gnas, resulting in global heterozygous inactivation of Gnas+/- (bred on a pure 129/SvEv background). Previous reports identified adult PPHP (Gnas+/-p) mice had reduced cortical bone quality compared to PHP1A (Gnas+/-m) due to elevated endosteal resorption; no evaluation of bone formation was performed in adults.1We assessed bone formation in vivo by serum P1NP ELISA and dynamic histomorphometry. Statistical analyses include data from male and female mice. Serum P1NP was significantly elevated in Gnas+/-m mice compared to both Gnas+/-p and WT mice. Osteoblast activity (MAR) was also significantly elevated in Gnas+/-m on trabecular and endosteal surfaces compared to Gnas+/-p mice. BMSCs from 6-8 week Gnas+/-m mice treated with osteogenic-inducing media for 14 days demonstrated a significant increase in Bglap1 expression by RT-PCR compared to Gnas+/-p and WT BMSCs. Bglap1 expression was significantly decreased in flushed tibia specimens from Gnas+/-p mice compared to WT. Bglap1 expression in Gnas+/-m specimens was comparable to WT but trended higher than Gnas+/-pThis work identifies distinct phenotypic differences within cortical bone formation between adult Gnas+/-p and Gnas+/-m mice caused by increased osteoblast activity in Gnas+/-m mice. These data provide an additional explanation for the phenotypic differences in cortical bone parameters in adult Gnas+/- mice and suggest imprinting may be involved in bone remodeling1.Ramaswamy,G. et al. Gsα Controls Cortical Bone Quality by Regulating Osteoclast Differentiation via cAMP/PKA and β-Catenin Pathways.Sci. Rep7,1–11(2017)

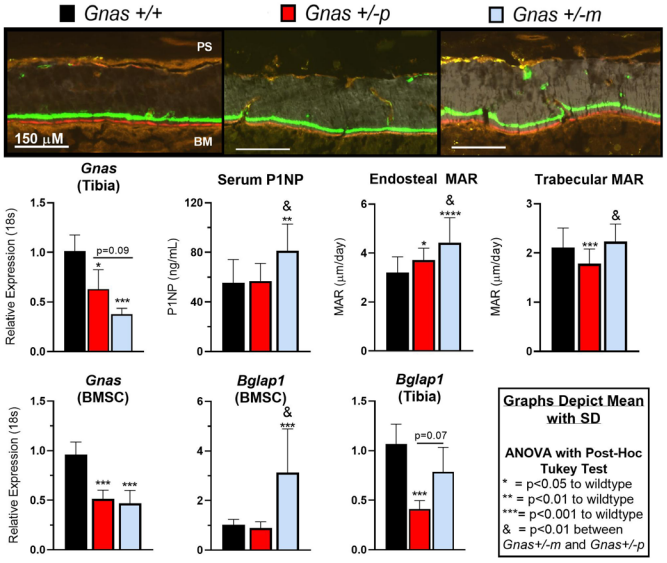

***Disclosures: Patrick McMullan**, None*

P-809

Bone Tissue and Osteoblasts from X-linked type XVIII OI with defects in Regulated Membrane Proteolysis have Distinct Features *Allahdad Zarei[1], Nadja Fratzl-Zelman[2], An Dang Do[3], Megan Glassford[4], Mark Hannibal[4], Paul W Esposito[5], Kristin Lindstrom[6], Jochen Zwerina[2], Marianne Knue[3], Sara Talvacchio[3], Joan C. Marini[1]. [1]Section on Heritable Disorders of Bone and Extracellular Matrix, National Institute of Child Health and Human Development, National Institutes of Health, United States, [2]Ludwig Boltzmann Institute of Osteology at the Hanusch Hospital of OEGK and AUVA Trauma Centre, Austria, [3]Office of Clinical Director, Eunice Kennedy Shriver National Institute of Child Health and Human Development, National Institutes of Health, United States, [4]Division of Genetics, Department of Pediatrics and Communicable Diseases, University of Michigan Medical School, United States, [5]Department of Pediatric Orthopaedic Surgery University of Nebraska Medical Center, United States, [6]Division of genetics and Metabolism, Phoenix Childern's Hospital, United States

Background: Site-2 protease (S2P), encoded by MBTPS2, is a Golgi transmembrane proprotein convertase of membrane-bound transcription factors, well-known for its role in cholesterol metabolism. We previously identified an X-linked recessive form of osteogenesis imperfecta (type XVIII OI) with defects in S2P metal ion coordination site. These mutations cause impaired regulated intramembrane proteolysis (RIP) of SREBP, ATF6 and OASIS, with decreased secretion of type I collagen and increased LP/HP collagen crosslink ratio. Methods: We identified the 3rd and 4th probands with type XVIII OI: a 2yr4m boy with S2P p.N459S, as in prior Thai pedigree, and a 1yr5mos boy with a novel p.L455Q (c.1364T>A) mutation. Bone and primary osteoblasts (OB) with p.N459S were investigated with qBEI, histomorphometry, qPCR and RNAseq.Results: The new S2P mutation is associated with short stature, blue sclerae, limb fractures and deformity, undertubulated long bones with LE rhizomelia, multiple vertebral compression fractures, and L1-L4 DXA z-score= -7.36. Bone turnover markers were elevated: total ALP 1574 (ref range 104-345IU/L), bone specific ALP 420 (25-221mcg/L), osteocalcin 68.9 (7.3-38.5ng/ml). OASIS processing in fibroblasts with p.L455Q mutation showed decreased 50kD S1P/S2P cleavage product, and increased 55kDa S1P cleavage band. A cortical bone sample obtained as surgical discard from the S2P p.N459S had notable marrow fibrosis and was not hypermineralized on qBEI, as found in

classical OI. Histomorphometric analysis of cortical bone revealed increased osteoblast surface per bone surface (Ob.S/BS=14.1%,Tb ref range 8.5+/-4.1), and osteoid surface per bone surface (OS/BS=46.8%, Tb ref range: 34.0+/-6.7). In vitro, the hemizygous S2P p.N459S mutation hampered osteoblastogenesis. Early osteoblast markers, OSX, RUNX2, COL1A1, COL1A2, SPARC were downregulated in proband vs age-matched normal primary OB, whereas, late osteoblast/early osteocyte markers, SPP1, BGLAP, DMP1 and MEPE were upregulated in proband OB. In vitro mineralization was severely delayed in proband primary OB. Transcript profiling revealed that p.N459S alters expression of genes that are constituents of ECM and involved in ECM organization.Conclusions: These MBTPS2 missense mutations further support a critical role of RIP in normal bone development. Analysis of proband bone tissue and OB identifies distinctive features of type XVIII OI, and will reveal insights into the tissue-specific mechanism of RIP.

***Disclosures: Allahdad Zarei**, None*

P-810

Response of the ENPP1-deficient skeletal phenotype to oral phosphate supplementation and/or enzyme replacement therapy: Comparative studies in Humans and Mice. *Demetrios Braddock[1], Carlos Ferreira[2], Ralf Oheim[3], Kristin Zimmerman[1], Dillon Kavanagh[1], Paul Stabach[1], Bjorn Busse[3], Thorsten Schinke[3], Simon van Kroge[3], Michael Levine[4], Thomas Carpenter[5], Mark Horowitz[6]. [1]Yale University, Department of Pathology, United States, [2]Medical Genomics and Metabolic Genetics Branch, National Human Genome Research Institute, National Institutes of Health, United States, [3]Department of Osteology and Biomechanics, University Medical Center Hamburg-Eppendorf, Germany, [4]Department of Pediatrics, University of Pennsylvania Perlman School of Medicine, United States, [5]Department of Pediatrics at Yale University School of Medicine, United States, [6]Department of Orthopædics and Rehabilitation, Yale University School of Medicine, United States

Human ecto-nucleotide pyrophosphatase/phosphodiesterase (ENPP1) deficiency can result in early-onset osteoporosis (EOOP) in heterozygous deficiency and Autosomal Recessive Hypophosphatemic Rickets (ARHR2) in homozygous deficiency. ARHR2 patients are frequently treated with phosphate supplementation to ameliorate the rachitic phenotype, but elevating plasma Pi concentrations in ENPP1 deficiency increases the risk of ectopic calcifications and nephrocalcinosis. To determine the efficacy of ENPP1 enzyme replacement to ameliorate these risks, we treated Enpp1asj/asj mice on a high phosphate diet with recombinant murine Enpp1-Fc and examined the effects on the skeletal and renal phenotype. Similar to Enpp1asj/asj mice on normal chow, 5-week Enpp1asj/asj mice on a diet high in phosphate and low in magnesium (acceleration diet) exhibit markedly lower trabecular bone mass (Tb. BV/TV 70%, Tb.Sp 125%, and TbN 82% of wild type, WT), reduced cortical bone mass (Ct. BV/TV 90%, Ct. Thickness 72% of WT), and higher bone fragility (maximum load and stiffness was 52% and 45% of WT, respectively, and total work-to-fracture was 27% of WT). Treating the Enpp1asj/asj mice with Enpp1-Fc between weeks 2-5 of age normalized trabecular bone mass, normalized or improved bone biomechanical properties (significant improvement in stiffness and total work-to-fracture, and maximum load normalized compared to WT), and prevented the development of nephrocalcinosis and renal failure. Evaluation of a cohort of patients with biallelic ENPP1 deficiency demonstrated low bone mineral density in all adults analyzed and in one adolescent, whose bone mineral density exhibited progressive decline while on conventional treatment with oral phosphate and calcitriol. Medullary nephrocalcinosis occurred in half the patients treated with oral phosphate and calcitriol supplementation, which improved the rickets phenotype but did not prevent progressive reductions in bone mineral density in a closely-followed adolescent. Overall, these data confirm the validity of the Enpp1asj/asj mouse model for the study of skeletal and renal complications of human ENPP1 deficiency and suggest that ENPP1 enzyme replacement therapy may address the aberrant skeletal phenotype present in ENPP1 deficiency.

***Disclosures: Demetrios Braddock**, Inozyme Pharma, Grant/Research Support*

P-811

NFAM1 Regulates SAPK/JNK Signaling to Enhance Osteoclast Differentiation and Bone Resorption in Paget's Disease of Bone *Purushoth Ethiraj[1], Yuvaraj Sambandam[2], Sakamuri Reddy[3]. [1]Darby Childens Research Institute, United States, [2]Northwestern University, United States, [3]Darby Childrens Research Institute, MUSC, United States

Paget's disease of bone (PDB) is marked by focal activity of abnormal osteoclasts (OCLs) with excess bone resorption. We previously detected measles virus nucleocapsid protein (MVNP) transcripts in OCLs from patients with PDB. In addition, MVNP stimulates pagetic OCL formation in vitro and in vivo. MVNP transduced normal human PBMC showed an increased NFAT activating protein with ITAM motif 1 (NFAM1) mRNA expression without RANKL treatment. Further, bone marrow cells from patients with PDB demonstrated elevated levels of NFAM1 mRNA expression. We have also demonstrated NFAM1 signaling enhances OCL formation/bone resorption activity in the PDB, however, the molecular mechanisms underlying the NFAM1 regulation of OCL differentiation and bone resorption are unclear. Here, we showed that the activation of receptor activator of nuclear factor-B ligand (RANKL) enhances NFAM1 expression in preosteoclast cells. Conditioned media obtained from RANKL stimulated RAW264.7 NFAM1 knock-down (NFAM1-KD) stable cells showed a significant inhibition in the levels of IL-6 (2.5-fold), TNF-α (2.2-fold) and CXCL-5 (3-fold) compared to control (WT) cells. Further, RANKL stimulation significantly increased p-STAT6 expression (5.5-fold) in WT cells, but no significant effect was observed in NFAM1-KD cells. However, no changes were detected in STAT3 levels in either of cell groups. Interestingly, NFAM1-KD suppressed the RANKL stimulated c-fos, p-c-Jun expression and c-Jun N-terminal kinase (JNK) activity in preosteoclast cells. We further showed that the suppression of JNK activity is through inhibition of p-SAPK/JNK in these cells. In addition, the expression of NFATc1, a key transcription factor associated with OCL differentiation is significantly inhibited in NFAM1-KD preosteoclast cells. NFAM1 inhibition suppressed the OCL formation/bone resorption activity in mouse bone marrow cell cultures. We also demonstrated inhibition of TRAP expression in RANKL stimulated NFAM1-KD preosteoclast cells. Collectively, our results suggest that MVNP modulation of the NFAM1 regulates SAPK/JNK signaling to enhance OCL formation and bone resorption in Paget's disease.

***Disclosures: Purushoth Ethiraj**, None*

P-812

Measuring Outcomes in Ultra-Rare Bone Diseases: Methodology of the Palovarotene Fibrodysplasia Ossificans Progressiva (FOP) Clinical Development Program *Robert J Pignolo[1], Geneviève Baujat[2], Matthew A Brown[3], Carmen De Cunto[4], Maja Di Rocco[5], Edward C Hsiao[6], Richard Keen[7], Mona Al Mukaddam[8], Andrew Strahs[9], Donna R Grogan[9], Rose Marino[9], Frederick S Kaplan[8]. [1]Department of Medicine, Mayo Clinic, United States, [2]Département de Génétique, Institut IMAGINE and Hôpital Universitaire Necker-Enfants Malades, France, [3]Guy's & St Thomas' NHS Foundation Trust and King's College London NIHR Biomedical Research Centre, United Kingdom, [4]Pediatric Rheumatology Section, Department of Pediatrics, Hospital Italiano de Buenos Aires, Argentina, [5]Unit of Rare Diseases, Department of Pediatrics, Giannina Gaslini Institute, Italy, [6]Division of Endocrinology and Metabolism, UCSF Metabolic Bone Clinic, Institute of Human Genetics, and UCSF Program in Craniofacial Biology, Department of Medicine, University of California-San Francisco, United States, [7]Centre for Metabolic Bone Disease, Royal National Orthopaedic Hospital, United Kingdom, [8]Departments of Orthopaedic Surgery & Medicine, The Center for Research in FOP and Related Disorders, Perelman School of Medicine, University of Pennsylvania, United States, [9]Ipsen, United States

Background: FOP is an ultra-rare genetic disorder characterized by heterotopic ossification (HO) of soft and connective tissues (often preceded by flare-ups), cumulative disability, and early mortality. Palovarotene (PVO) is a selective retinoic acid receptor gamma agonist under investigation for treatment of FOP. Conducting trials in FOP has multiple challenges, including the low number of confirmed cases worldwide, a limited understanding of disease progression, and the need to identify disease-specific biomarkers and optimize assessment of HO progression.Objective: To develop a methodological approach addressing the challenges of conducting clinical trials in underexplored rare bone diseases.Methods: Here, we describe the methodology of: a non-interventional, prospective, protocol-specified, longitudinal natural history study (NHS; NCT02322255); a multicenter, randomized, double-blind, placebo-controlled phase II trial (NCT02190747); an ongoing open-label extension (OLE) to the phase II trial (NCT02279095) (Table). Studies were designed adaptively. PVO doses were administered episodically (high dose for 2 or 4 weeks, followed by low dose for 4 or >=8 weeks, from flare-up onset) or chronically (daily). In the double-blind period of the phase II trial, participants were randomized in two cohorts: 0:3:1 (aged >=15 years) or 3:3:2 (>=6 years) to PVO 5/2.5 mg, PVO 10/5 mg or placebo, episodically for 2 weeks (high dose) then 4 weeks (low dose). HO incidence and volume are assessed annually by standardized low dose whole-body computed tomography and/or at 12 weeks during the course of flare-ups (defined as >=2 [>=1 in OLE Part C] of pain, swelling, stiffness, decreased range of motion, redness, or warmth). Other clinical, functional and patient-reported outcomes are assessed using FOP-specific measures of physical function, including the Cumulative Analogue Joint Involvement Scale (CAJIS) and FOP Physical Function Questionnaire (FOP-PFQ). Studies were approved by independent ethics committees. 151 unique participants were enrolled. Learnings informed the design of the ongoing phase III MOVE trial (NCT03312634; 107 enrolled participants).Conclusions: Novel methodological approaches are needed to expedite availability of disease-modifying treatments for serious, ultra-rare diseases. HO is the main cause of disability in patients with FOP. This program could be used as an example to inform development of new treatments in rare bone diseases.

	NHS N=114	Phase II trial N=40	Phase II OLE			
			Part A N=40 [a]	Part B N=54 [b]		Part C N=48 [c]
Patient age/ skeletal maturity	0–65 years	≥6 years	≥6 years	Skeletally immature [d]	Skeletally mature [e]	≥6 years
PVO dosing regimen	N/A	Episodic (2/4 wks)	Episodic (2/4 wks)	Episodic (≥4/8 wks)	Chronic (daily) + Episodic (≥4/8 wks)	
PVO dose (mg)	None	5/2.5; 10/5; PBO	10/5	20/10	Chronic 5 + Episodic 20/10	

PVO doses were weight-adjusted in skeletally immature children; [a] Including all 40 pts from the phase II trial; [b] Including 36 pts from OLE Part A and 18 new pts; 52 pts received PVO [c] 48 pts from OLE Part B; [d] <90% skeletal maturity on hand/wrist radiography; [e] ≥90% skeletal maturity on hand/wrist radiography. FOP: fibrodysplasia ossificans progressiva; NHS: natural history study; OLE: open-label extension; PBO: placebo; pts: participants; PVO: palovarotene; wks: weeks.

***Disclosures: Robert J Pignolo**, Research investigator: Clementia/Ipsen, Regeneron; Advisory board: President of the International Clinical Council on FOP; Chair of the Publications Committee for the IFOPA Registry Medical Advisory Board, Other Financial or Material Support*

P-813

Sclerostin-antibody Effect on Dental Pathologies in Hyp Mice *Kelsey Carpenter[1], Elizabeth Guirado[2], Yinghua Chen[2], Anne George[2], Ryan Ross[1]. [1]Rush University, United States, [2]University of Illinois at Chicago, United States

X-linked hypophosphatemia (XLH) is the most common form of inherited rickets, affecting approximately 1 in 20,000 people. XLH is caused by an inactivating mutation in the phosphate regulating neutral endopeptidase on the X-chromosome (PHEX). This mutation leads to elevated fibroblast growth factor 23 (FGF23) levels, which subsequently impair phosphate reabsorption in the kidney and inhibit skeletal mineralization. Dental abnormalities are also common in patients with XLH and include tooth fractures, abscesses, and periodontal disorder. Our previous study demonstrated that sclerostin anti-body (Scl-Ab) improves phosphate metabolism and increases endochondral bone mass in Hyp mice (XLH murine model). This study aims to investigate the efficacy of Scl-Ab on the dentin-alveolar bone phenotype in Hyp mice.Male hemizygous and female heterozygous Hyp mice and wild type littermates (37 male; 45 female) were used for this study. Mice were randomly assigned to biweekly subcutaneous injections of 25 mg/kg Scl-Ab or vehicle (saline) treatment starting at 12-weeks of age until sacrifice at 20 weeks of age. Left and right hemi-mandibles were collected at sacrifice. Left hemi-mandibles were analyzed with micro-computed tomography (μCT) for assessing phenotypic changes in alveolar bone, dentin, and periodontal ligament (PDL) space. Right hemi-mandible were decalcified, paraffin embedded, stained with Hemotoxylin-Eosin (H&E), and compared for the presence of osteoid and osteocytic halos.Consistent with our previous data in the femur, Scl-Ab treatment significantly increased bone volume over total volume (BV/TV) in the alveolar bone region (p=0.001 males; p=0.002 females). Gross comparison of H&E stained alveolar bone shows a decrease in osteoid and osteocytic halos. There was no Scl-Ab treatment effect on dentin thickness or the volume of the periodontal ligament space.The current study demonstrates that Scl-Ab treatments improve alveolar bone mass and mineralization in 20-week old Hyp mice. These findings suggest that Scl-Ab treatment may help to improve some of the alveolar bone phenotypes of XLH patients. While no significant dentin or PDL improvements were detected with μCT analyses, future studies are needed to investigate further, such as PDL fiber-orientation and gene expression analysis.

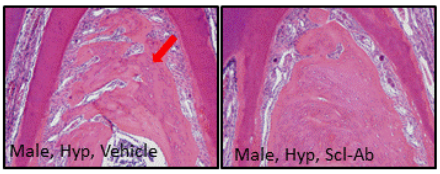

Figure 1. Representative images of H&E stained male Hyp vehicle and Scl-Ab treated mandibles. Region shown is of alveolar bone between the roots of the first molar. Vehicle treated animals have more osteoid (red arrow) present than Scl-Ab treated animals.

***Disclosures: Kelsey Carpenter**, None*

P-814

Osteoblasts and osteoclasts communicate through a chemokine self-amplifying positive feedback loop in sporadic lesions of Paget's Disease of Bone *Britta Petersen[1], Cynthia Alander[1], Hannah Hardy[1], Joseph Lorenzo[2], Marc F. Hansen[1]. [1]Center for Molecular Oncology, UConn School of Medicine, United States, [2]Division of Endocrinology and Metabolism, Department of Medicine, UConn School of Medicine, United States

Paget's Disease of Bone (PDB) is a focal disorder characterized by an exaggerated form of bone remodeling affecting 1.5 million people in the United States. Despite the frequency of PDB, its pathogenesis remains elusive. Sequestosome 1 (SQSTM1) mutations and measles virus nucleocapsid protein (MVNP) are commonly associated with PDB. Our lab has previously found that a subset of osteoblasts (OB) within a somatic PDB lesion possess the SQSTM1 mutation. To elucidate how SQSTM1 mutations impact OB chemokine expression, mRNA analysis was performed on PBD OB isolated by laser capture microdissection. We found substantial fold increases in the expression of chemokines, CCL5 (3.0 +/- 0.2) and CXCL6 (6.5 +/- 0.5) ($p< 0.05$ for both). In vitro experiments comparing a pagetic stromal cell line possessing a heterozygous SQSTM1 mutation (PSV10) to a normal osteogenic cell line (hFOB1.19) treated with 15nM 1α,25-(OH)2D3 and 1mg/mL LPS found increased fold mRNA expression for CCL5 and CXCL6 (5.5 +/-0.25 and 5.7 +/-0.3 respectively, $p <0.05$ for both) and protein expression (30 fold +/-15 and 3 fold +/-1, respectively, $p <0.05$ for both) in the PSV10 cells and in the PSV10 culture media. Transfection of hFOB1.19 with a SQSTM1 mutation increased mRNA expression of the chemokines (7.5 +/-2.0 and 6.0 +/-1.0 fold respectively, $p <0.001$) compared to wildtype hFOB1.19 cells following 1α,25-(OH)2D3 treatment. Analysis of gene expression data found in the Genome Expression Omnibus (GEO) (GEO Data Series GSE29106) of MVNP-transduced, RANKL and M-CSF stimulated human bone marrow derived non-adherent cells (BMM) found that BMMMVNP expressed greater levels of the CCL5 and CXCL6 receptors, CCR5 (6.0 fold) and CXCR1 (5.0 fold), compared to similarly treated SQSTM1P392L-transduced BMMs (GEO data series GSE29107) ($p< 0.001$ for both). Immunostaining of pagetic lesion samples found robust CXCR1 expression in the pagetic osteoclasts (OC). GEO data analysis also revealed that BMMMVNPexpressed greater levels of the chemokine, CXCL5 (70 fold, $p< 0.001$), compared to BMMP392L. CXCL5 is known to facilitate recruitment of OB and OC. Given this information, we propose a model of sporadic PDB wherein a somatic SQSTM1 mutation in an OB upregulates chemokine expression to recruit MVNP-containing OC precursors. Together, they form a self-amplifying positive feedback loop to facilitate recruitment of normal OB and OC to the growing pagetic lesion in a growth-by-recruitment model.

***Disclosures: Britta Petersen**, None*

P-815

Development of a 3D bioprinted human-based bone model using patient-derived cells *Anke de Leeuw[1], Jianhua Zhang[1], Pei Jin Lim[2], Matthias Rüger[3], Marianne Rohrbach[2], Cecilia Giunta[2], Ralph Müller[1], Marina Rubert[1]. [1]Institute for Biomechanics, ETH Zurich, Switzerland, [2]Connective Tissue Unit, Division of Metabolism and Children's Research Center, University Children's Hospital Zurich, Switzerland, [3]Department of Pediatric Orthopaedics and Traumatology, University Children's Hospital Zurich, Switzerland

The current gold standard for understanding bone biology and pathology involves the use of animal models. While extremely valuable, the generation of transgenic animals remains a costly and inefficient process, which is ultimately not representative of human bone pathophysiology. We aim to establish personalized and clinically relevant in vitro bone models to study bone pathophysiology of rare bone disorders such as osteogenesis imperfecta (OI) by developing novel 3D bioprinted bone models using patient-derived cells. Human bone specimens (n = 2) were obtained from pediatric patients undergoing subtractive osteotomies. Cells were isolated based on tissue culture plastic adherence. After expansion, cells were combined with alginate-gelatine (0.8-4.1% w/v) hydrogels and bioprinted to 3D cell-laden scaffolds (n = 3) to mimic the trabecular bone structure (Zhang, 2019). 3D bioprinted scaffolds were cultured in static bioreactors for 6 or 7 weeks under osteogenic conditions. Live/dead assays were performed to determine cell viability after bioprinting. Weekly micro-CT scans were taken non-invasively to assess mineral volume. Osteoblast and osteocyte cell phenotypes of the 3D bioprinted scaffolds were assessed by histology, immunohistochemistry and gene expression analysis after 6 or 7 weeks of culture. Scaffolds were compared to human bone tissues to demonstrate resemblance to in vivo bone architecture and phenotype. Over 90% of patient-derived cells survived the bioprinting process. Alizarin Red S staining showed a high degree of mineralization after 6 weeks of culture and micro-CT data revealed an average mineral volume of 53.6 +/- 4.3 mm3 in our 3D bioprinted scaffolds. Cells resided in cavities in the mineralized bone-like tissue (Figure 1A), resembling the morphology of osteocytes embedded in lacunae (Figure 1B). Osteocalcin expression in 3D bioprinted scaffolds was similar to this of bone explants. Furthermore, the upregulation of PHEX showed that our 3D bioprinted bone models support cell differentiation towards the osteocyte lineage. These results are a proof of concept for 3D bioprinted organotypic bone model using patient-derived cells supporting co-existence and bioactivity of both osteoblastic and osteocytic cells. The established 3D bioprinted bone model will be an especially powerful tool to elucidate pathomechanisms in OI and other rare human bone diseases and facilitate the development and testing of advanced therapies on a patient-specific level.

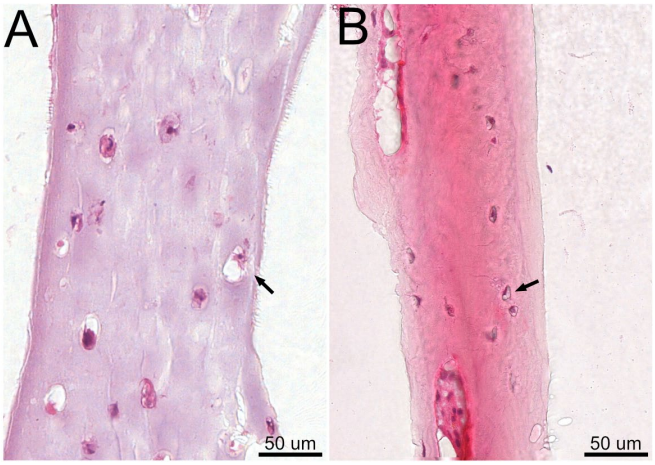

Figure 1: Hematoxylin and eosin (H&E) images of a 3D bioprinted organotypic bone model (A) and a decalcified section of human femur (B). Arrows indicate the comparable cell morphologies of osteocyte-like cells in 3D bioprinted mineralized bone-like tissue and osteocytes embedded in lacunae.

***Disclosures: Anke de Leeuw**, None*

P-816

Mice heterozygous for the Clcn7G213R mutation display osteopetrosis and compromised bone biomechanics *Wenping Song[1], Benjamin Greene[1], Wei Fan[1], Megan Cox[1], Alexander Verbitsky[1], Xiaoyou Ying[1], Robert Fogle[1], Jennifer Johnson[1], Sue Ryan[1], Sheila Cummings[1], Dinesh Bangari[1], Markella Katidou[1], Mostafa Kabiri[1], Yves Sabbagh[1], Stefano Zanotti[1]. [1]Sanofi, United States

Autosomal dominant osteopetrosis type II (ADO2) is a severe rare disease that manifests with generalized bone accumulation and susceptibility to fragility fractures of the appendicular skeleton. ADO2 is characterized by a high number of osteoclasts and elevated tartrate-resistant acid phosphatase (TRAP)5b serum levels, without an increase in collagen type I cross-linked C telopeptide (CTXI). The disorder is caused by dominant mutations in CLCN7, which encodes a homodimeric Cl-/H+ antiporter required for osteoclastic bone resorption. The most common disease-causing CLCN7 mutation leads to a Gly to Arg substitution at position 215. To investigate the mechanisms by which heterozygosity for the CLCN7G215R allele causes bone fragility, we generated the homologous Clcn7G213R mutation in mice by Cas9-directed mutagenesis of 129SvJ single-cell embryos. Initial efforts led to precise editing of both Clcn7 alleles, thereby generating Clcn7G213R homozygotes that did not survive beyond one month of age due to severe osteopetrosis. Optimization of editing conditions allowed creation of Clcn7G213R heterozygotes, which appeared normal and fertile. Analysis of areal bone mineral density and skeletal microarchitecture by dual-energy X-ray absorptiometry and microcomputed tomography, respectively, revealed generalized and marked osteopetrosis in heterozygous mutants. Cancellous bone volume was more than doubled in femurs and lumbar 6 vertebrae from heterozygous Clcn7G213R mice of both sexes due to increased trabecular number, connectivity density, and trabecular thickness. Three-point-bending analysis indicated that femurs from Clcn7G213R heterozygotes had a reduced capacity to absorb energy before failure, secondary to increased brittleness and stiffness. Conversely, compression testing demonstrated that lumbar vertebrae from mutant females required higher maximum force to failure than bones from wild type littermates, although this is consistent with the observation that ADO2 rarely presents with vertebral compression fractures. These findings were complemented by elevated TRAP5b serum levels without a corresponding increase in CTXI, which indicated presence of a high number of osteoclasts with a reduced ability to resorb bone. The phenotype was sustained in 6-month-old mice but did not worsen with aging. In conclusion, heterozygous Clcn7G213R mice recapitulate the clinical features of ADO2 and are an ideal translational model for the human condition.

***Disclosures: Wenping Song**, Snofi, Grant/Research Support*

P-817

A noncanonical focal adhesion pathway initiated by LAMA5 regulates skeletogenesis and produces a distinct bent bone dysplasia *Ivan Duran[1], Maya Barad[2], Deborah Krakow[2], Fabiana Csukasi[2]. [1]University of Malaga/CIBER-BBN, Spain, [2]University of California Los Angeles, United States

In addition to its structural role in skeletogenesis, the extracellular matrix (ECM) facilitates communication with intracellular signaling pathways and cell to cell interactions to control differentiation, proliferation, migration and survival. Alterations in extracellular proteins cause a number of skeletal disorders and one attributed mechanism results from the deleterious effects of mutated proteins on ECM structure. Yet, the consequences of abnormal ECM on cellular communication remains less well understood. Herein, we describe an unclassified distinct form of bent bone dysplasia caused by recessively inherited mutations in gene LAMA5. This finding uncovered a mechanism of disease driven by ECM-cell interactions between alpha5-containing Laminins, and Integrin mediated focal adhesion signaling within the skeleton, particularly in cartilage. Loss of LAMA5 altered b1 Integrin signaling through the non-canonical and tissue specific pathway regulated by PYK2 and the specific-SRC kinase FYN. Loss of LAMA5 negatively impacted WNT signaling, tying focal adhesion complexes to key skeletal signaling molecules. This newly described mechanism underlies the role of a LAMA5-b1 Integrin-PYK2-FYN focal adhesion complex regulating skeletogenesis and when dysregulated produces a distinct bent bone skeletal disorder.

***Disclosures: Ivan Duran**, None*

P-818

Consistent Dental Defects Associated with ALPL Mutations in Humans and Sheep with Hypophosphatasia *Joshua Bertels[1], Michael Chavez[2], Alyssa Falck[1], Shannon Huggins[1], Kaitrin Kramer[2], Charles Long[1], Larry Suva[1], Brian Foster[2], Dana Gaddy[1]. [1]Texas A&M University, United States, [2]Ohio State University, United States

TheALPL gene encodes tissue non-specific alkaline phosphatase (TNAP), an enzyme expressed primarily in bones, teeth, liver, and kidney. Loss-of-function mutations in ALPL are the cause of hypophosphatasia (HPP), an inborn error-of-metabolism that produces skeletal and dental mineralization defects that can affect all dental hard tissues: enamel, dentin, and cementum. However, it is unclear how dental defects correlate to specific genetic mutations. Therefore, a large animal model of HPP was created using sheep to define the structural nature of HPP dental defects. The HPP sheep model was created based on a female child (proband) diagnosed with HPP and compound heterozygous for ALPL mutations (exon 5: c.346G>A, p.A116T; exon 10: c.1077C>G, p.I359M). The corresponding human exon 10 mutation of ALPL was introduced into the Rambouillet sheep genome. Dental effects in the primary dentition of the proband and HPP sheep were analyzed by radiography, high-resolution micro-computed tomography (micro-CT), and histology. We hypothesized that all dental mineralized tissues would exhibit effects of HPP and aimed to establish quantitative measurements of dental tissues in HPP. Both sheep and the proband exfoliated primary teeth prematurely, increased retained root length and mantle dentin mineralization defects. In addition, the proband had lack of functional cementum on some but not all teeth. In the proband, enamel density and thickness were not adversely affected by HPP; however, density variation was greater vs. control teeth. HPP sheep teeth featured decreased crown dentin density, but no difference in root dentin density compared to controls. Histology supported the micro-CT analysis, revealing little to no cementum and altered periodontal ligament fiber organization in HPP teeth. The characterization of mantle dentin defects provides novel insights into the mechanisms of dental pathology in HPP. These data implicate the ALPL mutation in exon 10 (c.1077C>G, p.I359M) as the responsible mutation driving the dental manifestations observed in the proband. Continued examination of the HPP sheep will inform ongoing studies of etiopathologies and therapeutic interventions to improve the musculoskeletal and dental anomalies in HPP.

***Disclosures: Joshua Bertels**, None*

P-819

Introduction to a Multinational, Long-term, Prospective Outcomes Disease Monitoring Program (DMP) in Patients With X-linked Hypophosphatemia *Thomas Carpenter[1], Leanne Ward[2], Marise Lazaretti-Castro[3], Hamilton Cassinelli[4], Alison Skrinar[5], Christine Wang[5], Linda Rees[5], Erik Imel[6]. [1]Yale University School of Medicine, United States, [2]University of Ottawa, Canada, [3]Instituto de Medicina Avancada, Brazil, [4]Hospital de Niños Ricardo Gutiérrez, Argentina, [5]Ultragenyx Pharmaceutical Inc., United States, [6]Indiana University School of Medicine, United States

In X-linked hypophosphatemia (XLH), excess FGF23 causes hypophosphatemia, leading to chronic debilitating musculoskeletal impairments. XLH treatment options include a combination of oral phosphate and active vitamin D, or burosumab, a fully-human monoclonal antibody to FGF23 approved to treat patients with XLH.The XLH Disease Monitoring Program (XLH-DMP) is a prospective, multinational, outcomes study examining the longitudinal progression of clinical, radiographic, and biochemical features of XLH. This 10-year study is collecting real-world safety and effectiveness data of both conventional therapy and

burosumab and includes patients irrespective of age or treatment modality. Enrollment is targeted at >= 500 patients with a confirmed clinical diagnosis of XLH, of whom >= 200 will be children < 18 years.As of 29 February 2020, we have enrolled 566 patients (age range: 1 month to 76 years), including 334 adults and 232 pediatric patients. Of these, 34% (114/334) of adult patients and 36% (83/232) of pediatric patients completed the year 1 visit as of the analysis cutoff date. Overall, 28% of patients (89 adults, 67 children) had previously participated in burosumab clinical trials and were continuing this therapy (Group 1), 37% were non-trial patients (102 adults, 109 children) who initiated burosumab by prescription before or during the XLH-DMP (Group 2), and 35% of patients (143 adults, 56 children) never received burosumab (Group 3). At XLH-DMP enrollment, 53% (176/334) of adults reported a history of enthesopathy/bone spurs/osteophytes, and 22% (74/334) of adults reported spinal stenosis or cord compression. Bowing of the legs was reported in 79% (184/232) of pediatric patients. Burosumab-related adverse events were reported in 13% (25/191) of adult and 10% (17/176) of pediatric patients and were consistent with the known safety profile of burosumab. To date, there have been no burosumab-related serious adverse events. XLH-DMP enrollment is ongoing.The XLH-DMP is establishing a comprehensive real-world dataset in one of the largest populations of this rare disease studied to date. Results from this ongoing 10-year study will improve understanding of the natural history of XLH. These results, and the added potential to link XLH-DMP outcomes with previous clinical trial assessments, will provide further insight into the long-term safety and effectiveness of XLH therapy.

***Disclosures: Thomas Carpenter**, Ultragenyx Pharmaceutical Inc., Consultant, Ultragenyx Pharmaceutical Inc., Grant/Research Support*

P-820

Hypophosphatemia Gene Panel Sponsored Program: A High Yield of Molecular Diagnoses from Clinically Confirmed XLH and Suspected Genetic Hypophosphatemia *Kathryn Dahir[1], Eric Rush[2], Daniel Beltran[3], Scott Eisenbeis[4], Britt Johnson[3], Prameela Ramesan[4], Soodabeh Sarafrazi[4], Rebecca Truty[3], Nicole Miller[4]. [1]Vanderbilt University Medical Center (VUMC), United States, [2]Department of Internal Medicine, University of Kansas Medical Center, United States, [3]Invitae Corporation, United States, [4]Ultragenyx Pharmaceutical Inc., United States

X-linked hypophosphatemia (XLH), a dominant disorder caused by a disease-associated variant in the PHEX gene, affects males and females of all ages. Rickets and osteomalacia may be present along with short stature, lower limb deformity, muscle pain and/or weakness/fatigue, bone pain, joint pain/stiffness, hearing difficulty, enthesopathy, osteoarthritis and dental abscesses. Patients with XLH have below-normal serum phosphate and elevated serum FGF23. XLH is one of multiple etiologies of hypophosphatemia; depending on genetic cause, management may differ. Acquired hypophosphatemia (e.g. tumor induced osteomalacia) is non-genetic in nature. The program provides a no-charge test to confirm a clinical XLH diagnosis or to aid suspected genetic hypophosphatemia diagnosis. Program eligibility: >/= 6 months and either clinical XLH diagnosis or suspicion of genetic hypophosphatemia as evidenced by 2 or more clinical signs/symptoms. The next generation sequencing panel includes 13 genes: ALPL, CLCN5, CYP2R1, CYP27B1, DMP1, ENPP1, FAH, FAM20C, FGF23, FGFR1, PHEX, SLC34A3 and VDR. Copy number variant (CNV) detection was performed. Results704 individuals (671 unrelated probands) have been tested as of 3/24/2020. Of 704 samples received, 510 (72.4%) had a PHEX variant: 47 (9.2%) were variants of uncertain significance (VUS) and 463 (90.8%) were either pathogenic or likely pathogenic (P/LP). Of the 194 cases (27.6%) where no PHEX variant was found, 29 (15%) had molecular diagnoses associated with other genes/disorders: 3 had a variant (P/LP) in FGF23 (autosomal dominant [AD] hypophosphatemic rickets), 2 had two variants (P/LP) in CYP27B1 (autosomal recessive [AR] vitamin D dependent rickets), 1 had P/LP variants in ENPP1 (AR hypophosphatemic rickets Type 2). There were 20 cases with single P or LP variants in ALPL (AD hypophosphatasia, HPP); 3 cases carried two variants (P/LP) in ALPL (AR form). Of 203 unique P/LP PHEX variants detected: 53 were deletions, duplications or insertions; 35 were CNVs; 42 were splicing; 73 were single nucleotide variants. Additional family member testing/clinical information resulted in 38 cases having VUS reclassified to P/LP, highlighting the value of family testing/clinical information to resolve VUS. RNA analyses to resolve VUS/unidentified variants may further improve molecular diagnostic yield. Program results demonstrate a high diagnostic yield for XLH/ genetic hypophosphatemia and new insight into XLH-associated PHEX variants.

***Disclosures: Kathryn Dahir**, Ultragenyx Pharmaceutical Inc, Consultant, Regeneron, Grant/Research Support, Mereo, Grant/Research Support, SoftBones Hypophosphatasia Research Grant, Grant/Research Support, Alexion, Grant/Research Support, Alexion, Consultant, Ultragenyx Pharmaceutical Inc, Grant/Research Support*

P-821

Impaired Mitochondrial Respiration and Altered Fiber Type in Hypophosphatasia Sheep Skeletal Muscle *Joshua Bertels[1], Alyssa Falck[1], Shannon Huggins[1], Sarah White[1], Charles Long[1], Larry Suva[1], Dana Gaddy[1]. [1]Texas A&M University, United States

Hypophosphatasia (HPP) is a rare inherited disorder of mineral metabolism, the result of inactivation of the tissue-nonspecific alkaline phosphatase (TNSALP) gene (ALPL) characterized by decreased mineralization and profound muscle weakness in humans. Since murine genetic models have not demonstrated the muscle phenotype of HPP, a large animal model of HPP using Rambouillet sheep was generated. Based upon a novel compound heterozygous female child diagnosed with HPP, (exon 5: c.346G>A, p.A116T; exon 10: c.1077C>G, p.I359M) the Isoleucine -> Methionine (c.1077 C>G) mutation of ALPL was introduced into the sheep genome. Characterization of founder (F0) HPP sheep skeletal muscle demonstrated aberrant mitochondrial cristae and variable muscle fiber size. To better characterize the muscle defects observed in HPP sheep, gluteus medius (GM) fiber type was determined in 6-mo-old F1 sheep expressing the wild-type (WT; n = 3), heterozygous (Het; n = 1), and homozygous (Hom; n = 2) genotypes for the ALPL mutation by immunofluorescence. The percentage of myosin heavy chain (MyHC) Type 1 and 2a fibers was greater in Hom compared to WT sheep ($P<0.05$) at the expense of MyHC Type 2x fibers. At 1 yr of age, GM samples from the same sheep were analyzed for mitochondrial characteristics. Mitochondrial volume density (citrate synthase activity; CS) was numerically decreased in Het and Hom compared to WT, but low power prevented statistical significance. Mitochondrial function (cytochrome c oxidase activity) was similar between all groups but Hom had approximately 50% lower integrative (relative to tissue wet weight) oxidative phosphorylation (OXPHOS) capacity with complex I+II (PCI+II) compared to WT ($P=0.04$). After normalizing to CS activity, intrinsic PCI+II was similar between groups, indicating the decrement in capacity was likely due to lower CS activity. However, the flux control ratio of PCI+II, an indicator of the coupling efficiency of mitochondrial electron transfer with ATP production was lower in Het and Hom compared to WT (P0.02). Overall, HPP sheep exhibited lower skeletal muscle OXPHOS capacity, likely due to decreased mitochondrial volume density, despite an increase in oxidative fiber type populations. Further, HPP sheep had lower mitochondrial coupling efficiency, which may lead to excess production of damaging intermediates (e.g. reaction oxygen species) during respiration. Collectively, these data provide a mechanistic basis for muscle weakness in HPP.

***Disclosures: Joshua Bertels**, None*

P-822

RNA-based bone histology and histomorphometry *Elena Makareeva[1], Laura Gorrell[1], Shakib Omari[1], Edward Mertz[1], Sergey Leikin[1]. [1]NICHD, NIH, United States

Traditional histological staining identifies many cell types in bone sections, but subjective morphological evaluation of these cells limits the information content and ambiguity of such analysis. To develop a more objective approach to bone histopathology and characterize cell differentiation, functional state, and crucial molecular pathways, we replaced the traditional staining with fluorescent labeling of RNA transcripts. We adapted commercial tape-transfer cryo-sectioning (Section Lab) and fluorescent RNA labeling (RNAScope™) technologies for simultaneous imaging of multiple transcripts in the same cryosection of a fully mineralized mouse bone. We developed automated analysis procedures for counting different bone cells and evaluating relative expression of key RNA transcripts within these cells. For instance, we identify active osteoclasts and osteoblasts as bone surface cells with high Ctsk and Col1a1 expression, respectively. We characterize osteoblast differentiation by visualizing expression of Bglap, Dmp1, Sost, and other transcripts relative to Col1a1. To test this approach, we utilized a G610C mouse model of osteogenesis imperfecta (OI). RNA-based histological analysis combined with RNA-based histomorphometry demonstrated altered differentiation of G610C osteoblasts and resolved multiple inconsistencies between histopathological, micro-CT, and biomechanical measurements in this animal model. We found that reduced mineral apposition rate in G610C mice is likely caused by deficient osteoblast maturation. The animals appear to compensate for this deficiency and normalize their bone formation rate by recruiting additional osteoblasts without an accompanying increase in the number of active osteoclasts, explaining an otherwise puzzling increase in trabecular thickness. We are currently developing approaches to identifying molecular mechanisms of bone cell pathology by combining single cell transcriptomic analysis with visualization of key RNA transcripts in histological sections.

***Disclosures: Elena Makareeva**, None*

P-823

In Vivo Binding of Fluorescence-Labeled Asfotase Alfa to Sites of Physiological Mineralization and Ectopic Calcification *Flavia Amadeu de Oliveira[1], Sonoko Narisawa[1], Massimo Bottini[1], José Luis Millán[1]. [1]Sanford Burnham Prebys Medical Discovery Institute, United States

A mineral-targeted form of recombinant tissue-nonspecific alkaline phosphatase (TNAP), asfotase alfa, was approved multinationally as an enzyme replacement therapy for hypophosphatasia in 2015. Two reports to date have shown evidence of binding of this drug to mineralizing tissues using histochemistry1 and immunohistochemistry2. Here, we sought to expand on those earlier studies by directly visualizing the in vivo binding of asfotase alfa conjugated with AnaTag HiLyte Fluor 750 or Alexa Fluor 647 fluorescent dye to sites of skeletal/dental mineralization and ectopic calcification. We utilized 40-day-old Tagln-Cre; HprtALPL/Y mice3, a model of severe medial vascular calcification; Tie2-Cre; HprtALPL/Y mice4, a model of severe intimal calcification; and sibling WT HprtALPL/Y mice, devoid of soft-tissue calcification. A single dose of 8 mg/kg labeled asfotase alfa was injected via the retro-orbital route. Skeletal tissues and soft organs were imaged ex vivo 2 days after the injection. Strong fluorescence signal was observed in all skeletal tissues (calvaria, vertebra, long bones, jaw, and mandibles) from mutant and WT mice. Fluorescence analysis

of histological sections from bones revealed strong binding of asfotase alfa. Asfotase alfa binding to sites of ectopic calcification in the heart, aorta, and renal artery were found in both the Tagln-Cre; HprtALPL/Y and Tie2-Cre; HprtALPL/Y mice but not in WT mice. In addition, asfotase alfa binding was also found in the kidney stroma and brain of the Tie2-Cre; HprtALPL/Y mice. Our results show that fluorescence-labeled asfotase alfa administered in vivo binds not only to sites of skeletal and dental mineralization but also to sites of ectopic calcification in these animal models5. 1 Millán JL et al. 20082 Yadav MC et al. 20123 Sheen CR et al. 20154 Savinov AY et al. 20155 Amadeu de Oliveira F et al. 2020

***Disclosures: Flavia Amadeu de Oliveira**, None*

P-824

Partial Depletion of Ccr2+ Myeloid Cells Reduces Endochondral Heterotopic Ossification without Inhibiting Muscle Repair in Fibrodyplasia Ossificans Progressiva Mice *Cody M Elkins[1], Nikash Hari[2], Joshua R Johnson[2], Daniel S Perrien[1]. [1]Emory University, United States, [2]Vanderbilt University Medical Center, United States

Fibrodysplasia ossificans progressiva (FOP) is a rare genetic disorder caused by point mutations in Type 1 BMP receptor ACVR1/ALK2 and is characterized by episodes of endochondral heterotopic ossification (EHO) in skeletal muscle known as "flares". Unfortunately, there is no approved therapy for FOP. Inflammation is strongly implicated in FOP flares, and depletion of phagocytic macrophages (MΦs) was previously shown to reduce, but not eliminate, EHO in FOP mice. However, the role of non-phagocytic MΦs has not been described. Thus, we sought to determine the effects of extensive depletion of the entire MΦ lineage on EHO and muscle repair in FOP mice. Ccr2DTR mice, in which administration of diphtheria toxin (DT) selectively depletes Ccr2+ cells, were crossed with tamoxifen-inducible FOP mice to create Ccr2DTR/wt;ALK2FlEx-R206H/wt;R26creERt2/creERt2 (Ccr2DTRFOP) mice. In separate studies, DT was injected at 50ng/g of bodyweight then tapered to 10ng/g every 3 days or given at 10ng/g throughout. FACs analysis revealed the higher dose protocol depleted 90% of F4/80+CD11b+ MΦs (full depletion), while the lower dose depleted 20% (partial depletion), in Ccr2DTR mice. Ccr2DTRFOP and Ccr2wtFOP mice received DT from 3-5 days before muscle injury until sacrifice. Data were analyzed by Mann-Whitney U test. Partial MΦ depletion significantly reduced EHO in Ccr2DTRFOP mice vs Ccr2wtFOP mice as measured in radiographs ($p<0.01$), μCT ($p<0.02$), and histology ($p<0.01$) at d21 post-injury. Areas of necrotic or regenerating myofibers and cartilage weren't significantly affected by partial MΦ depletion. Full MΦ depletion also decreased EHO in Ccr2DTR FOP vs Ccr2wtFOP mice by all three measurements ($p<0.001$ for all) and cartilage area ($p<0.02$). However, full depletion also reduced body weight ($p<0.01$), decreased regenerating myofiber area ($p<0.0001$), and increased necrotic myofiber area ($p<0.03$) vs Ccr2wtFOP mice. Importantly, significant areas of intramembranous dystrophic heterotopic bone ($p=0.0002$ vs Ccr2wt FOP) were found in injured muscles of fully depleted mice. Hence, while 90% depletion of Ccr2+ cells reduced EHO by 94%, it also inhibited muscle repair and induced dystrophic heterotopic bone formation. However, inclusion of non-phagocytic MΦs allowed a relatively mild 20% MΦ depletion to achieve 75% EHO reduction without inhibiting muscle repair, suggesting that targeting non-phagocytic MΦs may be a viable therapeutic strategy.

***Disclosures: Cody M Elkins**, None*

P-825

Bone compartments respond differently to short- and long-term sclerostin antibody treatment in Brtl/+ osteogenesis imperfecta mouse during growth *Christopher Stephan[1], Anne Ryan[1], Camden Felgner[1], Katie Ferguson[1], Ernesto Quiroz[1], Michelle Caird[1], Kurt Hankenson[1], Kenneth Kozloff[1]. [1]University of Michigan Department of Orthopaedic Surgery, United States

Romosozumab, a sclerostin antibody (SclAb), is an FDA-approved anabolic for treatment of osteoporosis in postmenopausal women at high risk of fracture. Potential additional applications include osteogenesis imperfecta (OI), which due to high fracture rates through adolescence, require long-term treatment options. Continuous use of Romosozumab in adults is limited due to waning anabolic effects over time, yet the effects of treatment duration and age on anabolic efficacy have not been fully explored in OI. The purpose of this study was to determine if extended SclAb exposure shows attenuated bone-forming effects during bone growth. Male wildtype (WT) and Brtl/+ OI mice received anti-sclerostin therapy (SclAb VI Amgen and UCB; 25mg/kg) or vehicle 2x/wk over a short 2wk duration at three different ages (3-5, 7-9 or 13-15wks) and were compared to endpoint-matched long-term treatment groups (3-9 or 3-15wks). Sample sizes ranged from 2-10/group. 2wks of SclAb had similar increases in trabecular BV/TV (Fig 1) across all ages driven by both thickness (TbTh) and number (TbN). Gains in TbN vs. age-matched controls were strongest when 2wk SclAb started at young, not older ages, while extending treatment duration further increased gains. In contrast, TbTh gains were strongest when 2wk treatment started at mid- and late, but not young ages, or with extended treatment. In Brtl/+ diaphyses, 2wk SclAb at any age reduced marrow area, but increased treatment duration actually increased marrow area expansion. CFU-F from marrow harvested at sacrifice demonstrate a reduction in progenitors after 6 wks SclAb compared to age-matched mice treated for 2 wks. Conversely, total cortical area increased in a treatment duration-dependent manner with 2wk delayed treatments having no effect, while 6 and 12 wk treatments resulted in profound periosteal expansion. In summary, extended SclAb exposure induces different effects at different sites compared to short term treatments. Early and extended treatments preserve TbN, while TbTh is enhanced with increased drug exposure. Contrasting duration effects in the endosteal and periosteal diaphysis suggest the endosteum is more sensitive to treatment attenuation, possibly due to progenitor cell depletion, but that the periosteum remains responsive. These findings emphasize the need to understand mechanisms responsible for SclAb attenuation in pediatric applications such as OI which require long-term sustained treatment for therapeutic benefit.

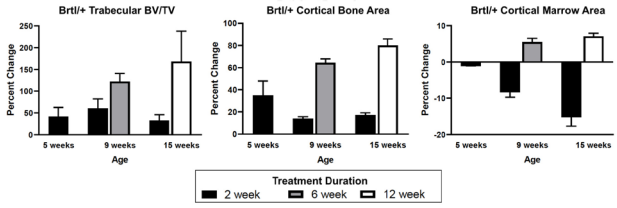

Figure 1: Changes in trabecular and cortical bone and marrow area (mean±SD) relative to age-matched controls. Mice treated with SclAb for short (2 wk) treatment starting at 3, 7, or 9 wks of age (black) compared to extended (6 or 12 wk) endpoint- matched treatment groups.

***Disclosures: Christopher Stephan**, None*

P-826

Semaphorin-3F, a potential biomarker for Lymphatic Anomalies and Bone Cell Function *Ernesto Solorzano[1], Fayez Safadi[1], Michael Kelly[1]. [1]NEOMED, United States

Lymphatic anomalies (LA) are rare conditions characterized by abnormal vascularization of lymphatic vessels (lymphangiogenesis). Gorham-Stout Disease (GSD) is an aggressive type of LA which invades cortical bone and makes it "disappear". There is little evidence elucidating the etiology of GSD and its osteolytic tendencies due to the rarity of the disease. In addition, there are no biomarkers capable of predicting GSD progression or treatment outcome. Normal bone does not have lymphatic vessels. It is believed that in GSD lymphatic endothelial cells (LEC) undergo genetic changes early in development that facilitate their migration and vessel formation in bone. LECs and their secretome are likely both crucial to lymphatic migration into bone and the cortical destruction seen in GSD. In this study, we focused on the LEC secretome with the goal of identifying proteins capable of modifying LEC and bone cell interactions. We initially assessed the effects of normal LEC conditioned media (LEC-CM) on bone cell differentiation and function in vitro and found that LEC-CM stimulates osteoclast differentiation. Next, we subjected LEC-CM to mass spectrometry and over 500 proteins were identified. One of these proteins, Semaphorin-3F (SEMA3F), effectively inhibits lymphangiogenesis in part, by competing with vascular endothelial growth factor-C (VEGF-C), for binding to the neuropilin-2 (Nrp2) receptor. We measured mRNA expression of both SEMA3F and VEGF-C in untreated and Rapamycin treated LECs, a clinically effective therapy for patients with lymphatic anomalies (LA). SEMA3F mRNA expression was upregulated while VEGF-C was downregulated in Rapamycin treated versus untreated LEC cultures. We next assessed the effects of exogenous SEMA3F on LEC viability and on osteoblast differentiation and function. We found that SEMA3F reduced LEC viability in a dose-dependent fashion. In addition, SEMA3F inhibited osteoblast differentiation and function independent of its effects on osteoblast viability or proliferation. Experiments are currently underway to determine the expression/localization of SEMA3F, VEGF-C and Nrp2 in LA tissues obtained from pediatric patients. We expect that SEMA3F expression will be downregulated while VEGF-C will be upregulated in LA compared to normal lymphatics. In summary, our data suggest that SEMA3F might be a possible biomarker for patient with LA conditions or contributes to their pathogenesis.

***Disclosures: Ernesto Solorzano**, None*

P-827

Mutation of PFN1 Gene Causes an Early Onset, Polyostotic Paget's-like Disease Less Responsive to Amino-bisphosphonate Treatment *Daniela Merlotti [1], Maria Materozzi [1], Simone Bianciardi [1], Vito Guarnieri[2], Domenico Rendina[3], Luca Volterrani[1], Cristiana Bellan[4], Christian Mingiano[1], Tommaso Picchioni[1], Alessandro Frosali[1], Ugo Orfanelli [5], Simone Cenci[5], Luigi Gennari[1]. [1]Department of Medicine, Surgery and Neurosciences, University of Siena, Italy, Italy, [2]Medical Genetics Service, IRCCS "Casa Sollievo della Sofferenza" Hospital, San Giovanni Rotondo (FG), Italy, Italy, [3]Department of Clinical and Surgical Medicine, Federico II University Medical School, Naples, Italy, Italy, [4]Department of Medical Biotechnologies, University of Siena, Italy, Italy, [5]Division of Genetics and Cell Biology, San Raffaele Scientific Institute, Milan, Italy;, Italy

Purpose. Paget's disease of bone (PDB) is a focal, metabolic bone disease whose genetic cause remains unknown in up to 50% of familial cases. Our aim was to investigate the underlying genetic defect in a four generations pedigree with a severe, early onset, autosomal dominant form of PDB for which mutations in all known genes involved in PDB or PDB-like diseases had been excluded.Methods. Whole exome sequencing was performed in 5 affected and 5 unaffected family members, across 3 generations. Then mutation screening

was extended to a sample of 41 PDB cases with early-onset, polyostotic PDB without mutations in SQSTM1 or other known PDB-related genes, selected from a large cohort of 893 unrelated PDB patients.Results. We identified a frameshift D107Rfs*3 mutation in PFN1 (encoding for profilin1, a highly conserved regulator of actin-polymerization and cell motility) causing the truncation of the C-terminal part of the protein. The mutation was also detected in a 17-yrs old asymptomatic family member, that upon biochemical and radiological analyses was indeed found to be affected. Sequencing of the entire PFN1 coding region in unrelated PDB cases identified the same mutation in one patient. All mutation carriers had a reduced response to bisphosphonates such as intravenous pamidronate or neridronate, and required multiple zoledronate infusions (up to 5) to control bone pain and achieve biochemical remission over a long term. Moreover, the skeletal distribution of lesions was less focal than generally described in PDB (involving the skull, vertebral bodies and the lower limbs in most cases) and the radionuclide bone scans showed a patched-like pattern of tracer uptake at affected bones rather than the uniform uptake typically described in PDB. These features, together with the very early onset of the lesions (possibly arising in adolescence) suggest that the disease affecting this pedigree is distinct from classical PDB. In vitro osteoclastogenesis in PBMCs from mutation carriers showed a higher number of osteoclasts with PDB-like features. A similar phenotype was observed upon PFN1 silencing in murine bone marrow-derived monocytes, suggesting that the frameshift PFN1 mutation confers a loss of function in profilin 1 activity that induces PDB-like features in the osteoclasts, likely due to enhanced cell motility and actin ring formation.Conclusions. Our findings indicate that PFN1 mutation causes a severe, early onset, polyostotic PDB-like disorder.

Disclosures: Daniela Merlotti, *None*

P-828

Urine Phosphoethanolamine (PEA) Is An Underutilized Biomarker For Hypophosphastasia (HPP) *Nadia Ayala-Lopez[1], Zahra Shajani-Yi[2], Margo Black[1], Kathryn Dahir[2]. [1]Vanderbilt University Medical Center, United States, [2]Vanderbilt University School of Medicine, United States

HPP is a rare disease caused by a loss-of-function mutation in the ALPL gene leading to a deficiency in the tissue-non-specific isoenzyme alkaline phosphatase (ALP) and excess of extracellular inorganic pyrophosphate (PPi) and pyridoxal 5'phosphate (PLP). HPP has a widely variable clinical phenotype, from neonatal seizures and hypomineralization to isolated dental or musculoskeletal disease in adults leading to significant diagnostic challenges, particularly in those with minor disease manifestations. Patients present with ALP activity levels below their age-adjusted reference interval and elevations in PLP. Biomarkers for diagnosing HPP and monitoring patients on enzyme replacement therapy (ERT) are limited. Low ALP activity is not specific for HPP; it can be low in other conditions including untreated hypothyroidism, and other skeletal dysplasias. Accurate PLP assessment is limited in patients on ERT due to hydrolysis of the substrate. PEA is a substrate hydrolyzed by ALP and elevated levels of PEA may be observed in HPP, supporting the diagnosis of HPP, but have been reported to be non-specific. We hypothesized that urine PEA levels could be used to diagnose HPP and as a surrogate marker for ERT compliance. We performed a retrospective analysis on 85 adult patients (64F: 21M) presenting for investigation or follow-up of HPP from 7/1/2014 to 1/7/2020. Urine was sent to the Children's Hospital in Colorado for PEA testing. Patients were diagnosed with HPP if they had of all of the following: ALP levels persistently below the age-adjusted reference interval, an ALPL gene mutation/family history of HPP and had musculoskeletal/dental symptoms pathology. Patients were negative for HPP if ALP was not persistently low, vitamin B6 levels were normal without supplementation, and when tested negative for ALPL variants, and either had absence of musculoskeletal/dental symptoms or explained by an alternative disease state. PEA levels were not considered for diagnosis. The following was collected from the EMR: PEA results, diagnosis, and ERT status. PEA levels were higher in patients with HPP not on ERT (median=126.0, N=51) vs. those negative for HPP (median=20.5, N=16, p<0.0001). The receiver operator curve for PEA in diagnosing HPP had an AUC of 0.95 (SE=0.026, p53.5 ng/ml (sensitivity=82.35%) with an NPV of 66.6% and PPV of 100%. Initial PEA values in patients with HPP and not on ERT were higher (median 126.0, N=51) than patients on ERT (median 65.0, N=16, p=0.004). Patients who began ERT had a decline in PEA levels after treatment (mean decrease 68.1%). PEA is a specific diagnostic marker for HPP in patients undergoing investigation for HPP and may be used as a surrogate marker to monitor ERT compliance. Future studies are necessary to evaluate the association between PEA levels and functional performance.

Disclosures: Nadia Ayala-Lopez, *None*

P-829

Differences in static and dynamic cortical bone histomorphometry between patients with typical osteoporotic and BP-induced atypical femoral fractures *Shijing Qiu[2], George Divine[2], Elizabeth Warner[2], Mahalakshi Honasoge[2], Ruban Dhaliwal[3], Sudhaker Rao[2]. [2]Henry Ford Health System, United States, [2]Henry Ford Health System, Uruguay, [3]SUNY Upstate Medical University, United States

Bisphosphonates (BPs) are commonly used for the prevention and treatment of typical osteoporotic fractures (TOF). However, long-term BP treatment is prone to cause atypical femoral fracture (AFF) in cortical-rich femoral diaphysis. Compromised cortical bone quality would increase the risk of both TOF and AFF. To date, there is little information on the differences in cortical bone structure and turnover between patients with TOF and AFF. Trans-iliac bone biopsies were obtained after double tetracycline labeling from 79 postmenopausal women with TOF (aged 66.3 +/- 6.18) and 73 postmenopausal women with >=2y of alendronate treatment; 57 without AFF (non-AFF, aged 68.2 +/- 7.4y) and 16 with AFF (aged 67.6 +/- 7.7y). The mean duration of BP treatment was 7.3 +/- 4.7y in non-AFF and 11.1 +/- 5.0y in AFF patients. Bone histomorphometry was performed in intracortical and endocortical envelopes and results are combined. The variables included bone volume (BV/TV), cortical thickness (Ct.Th, μm) wall thickness (W.Th, μm), erosion surface (ES/BS, %), osteoclast surface (Oc.S/BS, %), osteoid surface (OS/BS, %), osteoid thickness (O.Th, μm), osteoblast surface (Ob.S/BS, %), mineralizing surface (MS/BS, %), mineral apposition rate (MAR, μm/day), and bone formation rate (BFR/BS, μm3/μm2/year).There was no significant difference in BV/TV among the 3 groups. Ct.Th was significantly thicker in non-AFF and AFF patients compared to TOF patients, but it had no significant difference between the BP treated groups (Table 1). Notably, W.Th decreased progressively from TOF to non-AFF to AFF patients (Table 1). Other bone remodeling-related variables, including OS/BS, ES/BS, MS/BS, MAR and BFR/BS were significantly higher in TOF group than in non-AFF and AFF groups, but did not show significant differences between the BP treated groups (Table 1).Our results indicate that BP treatment substantially increases Ct.Th by inhibiting bone resorption and remodeling, which increases bone mass (and presumably bone strength), and reduces the risk of TOF. The decreases in ES/BS and W.Th in BP-treated patients indicates that both the extent and depth of bone resorption are reduced after long-term BP treatment. Moreover, W.Th is significantly thinner in AFF vs non-AFF patients, suggesting that decreased resorption depth is an independent risk factor for AFF. We propose that decreased resorption depth would increase the volume of aged interstitial bone that is vulnerable to fatigue failure.

Table 1. Comparison of cortical bone histomorphometric variables in patients with and without BP treatment

	No BP	With BP		
	TOF	non-AFF	AFF	p
BV/TV	93.5 (5.17)	94.7 (3.50)	93.9 (3.62)	0.380
Ct.Th	0.859 (0.258)	1.09 (0.312)[a]	0.988 (0.324)	<0.001
W.Th	44.4 (7.66)	40.3 (5.11)[a]	35.3 (4.35)[a b]	<0.001
OS/BS	19.0 (10.8)	5.57 (4.19)[a]	8.21 (5.65)[a]	<0.001
ES/BS	8.80 (5.54)	2.84 (2.19)[a]	4.42 (2.69)[a]	<0.001
MS/BS	11.7 (8.16)	3.29 (3.22)[a]	3.12 (3.01)[a]	<0.001
O.Th	8.26 (2.12)	6.95 (2.66)[a]	7.25 (2.90)	0.008
MAR	0.549 (0.165)	0.351 (0.183)[a]	0.334 (0.143)[a]	<0.001
BFR/BS	25.3 (20.1)	4.95 (6.60)[a]	4.23 (4.54)[a]	<0.001

[a] $p < 0.05$ vs.TOF; [b] $p < 0.05$ vs. non-AFF

Disclosures: Shijing Qiu, *None*

P-830

Effect of Parathyroid Hormone (1-34) on Gross ONJ-like Lesions in Rice Rats Treated with Oncology Doses of Zoledronic Acid *Evelyn Castillo[1], Jessica Jiron[1], Gabriella Gonzalez-Perez[1], Samantha Thomas[1], Summer Croft[1], Indraneel Bhattacharyya[1], Donald Kimmel[1], J. Ignacio Aguirre[1]. [1]University of Florida, United States

Osteonecrosis of the jaw (ONJ) is a severe adverse event occurring in osteoporosis and cancer patients taking powerful anti-resorptives, including nitrogen-containing bisphosphonates, such as zoledronic acid (ZOL). Multiple clinical case series describe successful treatment of ONJ with surgical and non-surgical approaches. Parathyroid hormone (PTH [1-34]) has been used off-label clinically to treat ONJ in uncontrolled trials and pre-clinically in a few small experiments. We hypothesize that administration of PTH in an osteoporosis-like regimen reduces the size and severity of gross ONJ-like lesions. At age 4wks, 64 rice rats (32 M/32 F) were fed a standard (STD) diet and given oncologic doses of ZOL (80μg/kg IV q4wks), to induce maxillary gross ONJ-like lesions. From age 10wks until the end of the experiment, biweekly oral exams of the maxillary molar (M) M2M3 interdental space and surrounding region were used to assign an in vivo gross quadrant grade (GQG, 0-4) that reflected lesion severity. Previous studies in rice rats showed that GQG>=2 lesions are usually histologically-positive for ONJ. Therefore, forty rats (22M, 18F) having one maxilla with GQG>=2 entered study after 30+/-10 (All data=Mean+/-SD) weeks of ZOL. Rats were randomized by GQG and body weight into two groups (N=20 each) of matching gender ratio. As ZOL continued, one group received saline subcutaneously (SC) 3X/wk (ZOL+VEH) and the other received 40μg/kg of PTH (Bachem) SC 3X/wk (ZOL+PTH). After 6 wks, rats were euthanized, high resolution (HR) photographs were taken, and jaws were fixed for histopathologic analyses. Using the HR photograph, a treatment-blinded operator measured gross lesion area (GL.Ar) and total maxilla area (TMx.Ar) with the Axiovision software. GL.Ar/TMx.Ar (expressed as a percentage) in the ZOL+PTH group (8.1+/-4.6%) was significantly smaller compared to the ZOL+VEH group (14.4+/-5.4%) (P=0.003, t-test of means). T-test of pairs showed that during treatment, GQG in the ZOL+PTH group fell from 2.55+/-0.51 at enrollment to 2.35+/-0.49 (P<0.04), while GQG in the ZOL+VEH group rose from 2.35+/-0.49 at enrollment to 2.65+/-0.49 (P<0.01), resulting in a net improvement in GQG of 0.50+/-0.47 with PTH (P<0.002). We conclude that six weeks of PTH improved

established gross ONJ-like lesions, as reflected by reduced severity and smaller lesion size. Histopathologic analyses are currently ongoing to evaluate the amount of necrotic bone in present in oral lesions and wound healing end-points.

***Disclosures: Evelyn Castillo**, None*

P-831

Studies of OI Patient and Murine Osteoblasts to Investigate Phenotypic Variability of Dominant Osteogenesis Imperfecta *Milena Jovanovic[1], Apratim Mitra[2], Ryan K Dale [3], Joan C Marini[1]. [1]Section on Heritable Disorders of Bone and Extracellular Matrix, National Institute of Child Health and Human Development, National Institutes of Health, United States, [2]Bioinformatics and Scientific Programming Core, National Institute of Child Health and Human Development, National Institutes of Health, United States, [3]Bioinformatics and Scientific Programming Core, National Institute of Child Health and Human Development, National Institutes of Health, Bethesda, United States

Introduction: Osteogenesis Imperfecta (OI) is a heterogeneous group of bone disorders characterized by bone fractures, growth deficiency and skeletal defects. An important and unexplained feature of OI and many dominant disorders is phenotypic variability with the same mutation. We present the first comparative study of osteoblast differentiation from normal pediatric controls vs OI patients with phenotypic variability. In addition, phenotypic variability in OI mouse models focused on comparison of COL1A1 G349C mice with new G349S.Methods: Differentiated osteoblasts (OB) cultured from healthy pediatric donor surgical discard and OI patients were subjected to transcriptome profiling by RNA-Seq. Mineralization of OB was evaluated by Alizarin Red. Collagen chain modification, folding and fibrils were studied by 3H steady-state assay, 14C intracellular folding assay, and electron microscopy. Murine X-rays and BMD were examined by Faxitron. Whole mount skeletal staining was done on P1 pups.Results: We focused on COL1A1 mutations Gly352Ser and Gly589Ser, each in two unrelated patients differing in phenotypic severity. Patient OB cell layer and secreted collagen was overmodified, indicating delayed folding; quantitative comparison of Hyl is ongoing. Patient OB deposit significantly less mineral in vitro than controls, while severe patient OB deposit significantly less mineral than mild patients. RNA-Seq transcriptomics showed proteasomal protein degradation, autophagy, and vesicle organization pathways upregulation vs controls, while protein translation was downregulated. OB from both severe patients have upregulation of pathways related to ubiquination vs controls. In parallel, we study the effect of the collagen glycine substituting residue on murine skeletal phenotype, comparing our Brtl(Cys) mouse (COL1A1 Gly349Cys) and a new model with Gly349Ser. Both mice are small but Brtl(Ser) has a more severe phenotype with rib fractures, limb bowing, flared ribcage, kyphosis and skeletal undermineralization by BMD. Brtl(Ser) calvarial osteoblasts have slower collagen folding, lower secreted collagen and lower mineral deposition than wt. Brtl(Ser) dermal collagen fibrils are smaller in diameter than wt or Brtl(Cys).Conclusion: This combined human/mouse approach will lead to novel insights into OI osteoblast differentiation, the roles of OB and matrix in phenotypic variability and the effect of substituting residue and position along the collagen helix.

***Disclosures: Milena Jovanovic**, None*

P-832

The Safety of Withdrawal from Denosumab Therapy in Fibrous Dysplasia and McCune Albright Syndrome *Maartje Meier[1], Stance Clerkx [1], Liesbeth Winter[1], Sander Dijkstra[2], Michiel Van de Sande[1], Natasha Appelman-Dijkstra[1]. [1]Leiden University Medical Center, Netherlands, [2]Leiden University Medical Center, Netherlands

Introduction: In fibrous dysplasia/McCune Albright Syndrome (FD/MAS) Denosumab (Dmab) suppresses the RANKL-mediated increased bone resorption. In a FD mouse model RANKL-inhibition reduced lesional growth, but after withdrawal the lesions reoccurred. In humans Dmab has been used in case of bisphosphonate resistant FD/MAS but data on withdrawal in humans are scarce, with only one pediatric case with a massive rebound phenomenon including hypercalcemia, increased markers of bone turnover (BTMs) and lesional growth. Therefore we aimed to study the safety of Dmab withdrawal in adults with FD/MAS treated in our hospital.Methods: All FD/MAS patients using and taken off Dmab were included. Health records were screened for fractures, lesional growth, pain flares and serum levels of calcium, alkaline phosphatase (ALP), procollagen type 1 N-terminal propeptide (P1NP) and β-crosslaps (CTX). Values during treatment (baseline, BL) were compared with values at 3, 6 and 12 months after the last injection. Data were calculated as median (IQR). Results: 14 patients were included, 2 had only 1 injection and 12 had multiple injections for a median of 1.6 (+/-IQR 1.2) years. Reasons for stopping were: no effect on pain (n=9, 64.3%), side effects (n=4, 28.6%), child wish (n=1, 7.1%) or other (n=3, 14.3%). Median follow up after treatment was 3.4 (+/-2.2) years, wherein no fractures, lesional growth or pain flares occurred. Calcium remained normal in all but 1 patient who had a mild asymptomatic hypercalcemia of 2.73 mmol/L 5 months after therapy withdrawal. In 9/10 patients (90%) at least one BTM exceeded pretreatment values. ALP exceeded the upper limit of normal (ULN) in 20% of the patients (n=2), rose in 50% (n=5) beyond pretreatment values, from 64 (+/-29) to 124 (+/-89) U/L at 6 months, but returned to BL levels at 12 months. P1NP passed the ULN in 6 patients (60%), increased in 4 patients (40%) above pretreatment values, from 24 (+/-22) to 80 (+/-157) ng/ml at 3 months and stabilized thereafter. CTX followed an identical curve. CTX transcended the ULN in in 30% (n=3) and rose in 80% of the patients (n=8) above pretreatment values.Conclusion: These results show that in adults, pretreated with bisphosphonates, withdrawal from Dmab causes a biochemical, asymptomatic rebound phenomenon mainly after treatment with multiple injections. Yet, a longer treatment does not seem to induce a stronger rebound. Further studies on the safety of Dmab and of withdrawal are needed and currently ongoing.

***Disclosures: Maartje Meier**, None*

P-833

Human and Murine Dentin Anomalies in Loeys Dietz Syndrome *Priyam Jani[1], Cyrus Keyvanfar[1], Quynh Nguyen[1], Olivier Duverger[1], Natasha Curry[1], Marian Young[2], Janice Lee[1]. [1]Craniofacial Anomalies and Regeneration Section, National Institute of Craniofacial and Dental Research, National Institutes of Health, United States, [2]Molecular Biology of Bones and Teeth Section, National Institute of Craniofacial and Dental Research, National Institutes of Health, United States

Objectives: Loeys–Dietz syndrome (LDS), a multisystemic autosomal dominant rare connective tissue disorder, is caused by mutations in the TGF-β signaling pathway genes. Major manifestations include vascular tortuosity, aneurysms and craniofacial anomalies. We previously reported and characterized significant enamel defects in a cohort of 40 patients diagnosed with LDS. However, it is not clear if dentin and the surrounding bone, connective tissue derivatives, are also affected in LDS. We, therefore, compared teeth and alveolar bone obtained from a patient and mouse model of LDS-2.Methods: Shed deciduous teeth were obtained from a patient with LDS Type-2 (LDS-2) having a heterozygous mutation in the TGFBR2 gene (TGFBR2 p.M457K). Mandibles and teeth were harvested from Tgfbr2G357W/+ mice recapitulating LDS-2. Human and Murine teeth were characterized using X-ray radiography, micro-CT, histology, scanning electron microscopy, and second harmonic generation. Micro-indentation was performed to assess the hardness of the dentin tissue. Shed deciduous teeth from a healthy donor were used as control for human teeth and age and gender matched littermates were used as controls for murine teeth.Results: X-ray radiography showed increased alveolar bone loss in mandibles of Tgfbr2G357W/+ mice. Micro-CT analysis revealed a decrease in the volume of dentin in Tgfbr2G357W/+ mice compared to controls and confirmed a significant decrease in the alveolar bone volume surrounding the teeth in Tgfbr2G357W/+ mice. Human teeth from a patient with LDS-2 also showed decreased dentin volume. Confocal imaging of FITC stained dentinal tubules showed sparse and irregular dentinal tubules in Tgfbr2G357W/+mice. SEM imaging showed disorganization of collagen fibers surrounding the tubules and excess mineral deposition in both human and murine teeth. Dentin was harder in Tgfbr2G357W/+ mice and LDS-2 human teeth compared to control teeth.Conclusion: Dentin structure is altered in both human and murine teeth with LDS-2. Changes in dentinal tubules and disorganization of collagen were striking in SEM and confocal imaging. Increased hardness of dentin may suggest excess mineral deposition and further biomechanical changes which will need further investigation. These data indicate, for the first-time, that dentin and alveolar bone are affected by the abnormal TGF-b signaling in Loeys-Dietz syndrome.

***Disclosures: Priyam Jani**, None*

P-834

A patient-derived in vitro disease model for Muenke Syndrome reveals defects in neural crest development. *Fahad Kidwai[1], Pamela Robey[1], Janice Lee[1]. [1]NIH, United States

Craniofacial malformation, including macrocephaly, craniosynostosis, midfacial hypoplasia, high arch palate, and temporal bossing is associated with rare craniofacial diseases. One of the most common inherited forms of craniofacial malformation is Muenke syndrome (MS), which is caused by a p.Pro250Arg (c.749C>G) gain-of-function mutation in fibroblast growth factor receptor 3 (FGFR3). Bone deformities in MS patients, in contrast to patients with other FGFR mutations, are mostly limited to the facial neural crest (NC)-derived bones with mild axial and appendicular skeletal abnormalities. NC gives rise to craniofacial bone, whereas mesoderm gives rise to the rest of the skeletal. Bone deformities limited to the craniofacial region in MS leads to the question: By what mechanism does FGFR3 p.Pro250Arg disrupts neural crest-derived craniofacial bone or suture development while sparing axial and appendicular skeletal growth? For this, we aimed to track the effect of FGFR3 p.Pro250Arg gain-of-function mutation on neural crest differentiation by establishing human induced pluripotent stem cells (hiPSCs) derived from MS patients as an in vitro disease model. First, we have successfully created hiPSCs lines from two unrelated MS patients (MUT-MS-hiPSCs) as verified by using standard characterization methods including colony morphology, p.Pro250Arg mutation confirmation, nuclear staining for expression of OCT4 and NANOG, karyotype analysis, Short Tandem Repeat (STR) analysis, and teratoma formation assay. Interestingly, we found higher endogenous FGF1 in MUT-MS-hiPSCs compared with the control cell line (WT-hiPSCs). These data suggest that FGFR3 can initiate its own positive feedback loop, suggesting that FGF1-FGFR3 p.Pro250Arg signaling may cause earlier and higher expression of both ligand and receptor. Second, to study the effect of the mutation causing MS in neural crest differentiation, we integrated a SOX10-GFP reporter into both MS-hiPSCs and WT-hiPSCs to track the neural crest cells. Interestingly, the MUT-MS-hiPSCs-SOX10 population displayed higher SOX10 levels as compared with WT suggesting FGFR3 p.Pro250Arg mutation plays a role in neural crest differentiation.

Ongoing studies aim to further characterize the molecular mechanism causing MS and may also reveal a novel mechanism through which FGFR-linked pathologies arise.

***Disclosures: Fahad Kidwai**, None*

P-835

Angiogenesis Inhibitors (AgIs) and Chemotherapy Drugs Associated with Osteonecrosis of the Jaw Exhibit In Vivo Anti-resorptive Activity *Evelyn Castillo[1], Summer Croft[1], Gabriella Gonzalez-Perez[1], L. Shannon Holliday[1], Lorraine Perciliano de Faria[0], J. Ignacio Aguirre[1], Donald Kimmel[1]. [1]University of Florida, United States, [0]University of Florida, United States

Introduction: Osteonecrosis of the jaw (ONJ) is an adverse event linked to powerful anti-resorptives (pARs) (e.g., zoledronic acid [ZOL] and anti-RANKL antibodies) in osteoporosis and cancer patients. Angiogenesis inhibitors (AgIs) (e.g., anti-vascular endothelial growth factor A ([VEGFA] antibodies, anti-VEGFA) and tyrosine kinase inhibitors (TKIs) (e.g., sunitinib [SU], dasatinib [DA]) are also associated with ONJ in cancer patients in the absence of pARs. Though pARs' mechanism is very specific for blocking osteoclast activity in vivo and AgIs are best known for their ability to inhibit angiogenesis, AgIs have more off-target activities than pARs. For instance, certain AgIs inhibit osteoclast differentiation and/or activity in vitro. Similar effects have been described for chemotherapy drugs (CHEMOs) (e.g., cisplatin [CP], paclitaxel [PTX]) that are co-administered with AgIs to cancer patients. We hypothesized that AgIs and CHEMOs inhibit bone resorption in vivo.Research Design and Methods: We tested the bone resorption effects of the above AgIs and CHEMOs in rapidly growing rats (Schenk Assay). 100 male SD rats aged 6 wks were randomized into 12 groups (N=8-12). Vehicle (VEH) rats received either saline intravenously (IV), IgG IV, or DMSO/PEG by oral gavage (OG) daily. ZOL rats received 80 µg/kg IV ZOL on Day 1. Anti-VEGFA rats received 3 or 10 mg/kg IV B20-4.1.1 (Genentech) on Days 1, 4, and 7. SU rats received 6 or 20 mg/kg daily by OG. DA rats received 3 or 10 mg/kg daily by OG. CP rats received 1.2 or 4mg/kg IV on Days 1 and 8. PTX rats received 1.5 or 5 mg/kg IV on Days 1 and 8. Rats were euthanized and serum TRAcP5b was assessed. Femurs were fixed for histomorphometric analysis of calcified cartilage volume (Ca.V/TV) and other endpoints in the distal femoral metaphysis. Group differences were tested by ANOVA+Tukey's T-test post-hoc test ($P<0.05$).Results: Serum TRAcP5b was lower than VEH with ZOL, anti-VEGFA10, DA10, and SU20. Ca.V/TV was higher than VEH in rats given ZOL, anti-VEGFA3, SU6, SU20, DA10, CP1.2, CP4, and PTX1.5. Trabeculae were thicker than VEH in rats given ZOL, anti-VEGFA10, and SU20. Osteoclast number was lower than VEH in rats given ZOL, anti-VEGFA10, SU20, DA3, and PTX5. The effect of AgIs and CHEMOs was always much less than ZOL.Conclusion: Our data indicate that AgIs and CHEMOs have moderate in vivo anti-resorptive activity that may play a role in their association with ONJ in the absence of pARs.

***Disclosures: Evelyn Castillo**, None*

P-836

Real-World Practices and Perceptions on X-Linked Hypophosphatemia Care Among Interdisciplinary Teams in Four Large US Healthcare Systems *Namrata Dass[1], Rasha Alam[2], Cherilyn Heggen[2], Jeffrey Carter[2], Tamar Sapir[2]. [1]Premier Endocrinology, United States, [2]PRIME Education, LLC, United States

Early identification and treatment of patients with x-linked hypophosphatemia (XLH) is critical to prevent or delay life-long disability, yet system-, team-, and individual-level barriers may challenge optimal care. In a quality improvement initiative, we assessed referral, diagnosis, and care coordination perceptions and practices among 55 interdisciplinary team members providing care to patients with XLH through surveys conducted between 2/2020 and 4/2020 across 4 US academic systems. To address identified barriers, teams participated in audit-feedback sessions to develop action plans. Survey participants comprised 4 metabolic bone specialists, 25 endocrinologists, 10 nephrologists, 4 pediatricians, 1 primary care physician, 2 nurse practitioners, 4 nurses, and 5 other healthcare providers. Over half of respondents (57%) estimated that the average length of time between symptom onset and referral to their center exceeded 2 years for adults; 25% estimated over 2 years for pediatric patients. Top barriers were identified as referring providers' lack of knowledge about XLH (71% of respondents), belief that symptoms are related to other health problems (45%), and uncertainty about where to refer patients (42%). Survey findings also revealed gaps related to genetic risk and testing. Although 75% of respondents believed that XLH family members should be tested for hypophosphatemia, only 60% reported often/always discussing family history and genetics of XLH with patients and only 25% believed that XLH patients understand genetic risks for family members. Only 47% agreed/strongly agreed that patients understand their XLH and available treatment options. On 5-point Likert scales, providers reported being fairly/extremely satisfied on the following XLH care processes: timely referrals of patients with XLH to their center (53%), timely receipt of testing results to confirm diagnosis (42%), counseling patients on the role of family history (55%), appropriate application of pharmacologic therapy (53%), and team-based coordination of care (44%). During audit-feedback sessions, teams identified and formulated action plans for implementation of improved referral processes, care coordination, genetic testing, shared decision making practices, and patient and provider education. These findings can inform additional initiatives to improve timely and appropriate referral, diagnosis, treatment, and care coordination to optimize outcomes for patients with XLH.

***Disclosures: Namrata Dass**, None*

P-837

Development of a New Therapeutic Modality for Bisphosphonate-Related Osteonecrosis of the Jaw *Hiroko Okawa[1], Akishige Hokugo[1], Takeru Kondo[1], Jesus J. Campagna[2], Varghese John[2], Shuting Sun[3], Frank H. Ebetino[3], Charles E. McKenna[4], Ichiro Nishimura[1]. [1]UCLA School of Dentistry, United States, [2]Department of Neurology, David Geffen School of Medicine at UCLA, United States, [3]BioVinc, United States, [4]Department of Chemistry, University of Southern California, United States

Antiresorptive therapy has been reported to be associated with a rare but serious oral morbidity characterized by jawbone necrosis, often with pain and infection. Bisphosphonate-related osteonecrosis of the jaw (BRONJ) represents the largest population of such oral complications, particularly in cancer patients. We previously found that bisphosphonate (BP) adsorption to bone mineral can be reversed by a subsequent application of other BPs. The objective of this research was to develop a trans-oral epithelial formulation of a low potency BP, and to test its efficacy for the prevention and treatment of BRONJ in a mouse model.A fluorescent-BP or MHDP was encapsulated in microfluidics-derived nanoparticles to develop deformable nano-scale vesicles (fBP-DNV and MHDP-DNV). Trans-oral epithelial drug delivery was demonstrated using an in vitro human oral epithelial model (EpiGingival, MatTek Corp) and in mouse maxilla in vivo using fBP-DNV. BRONJ-like symptoms were experimentally induced in C57Bl6/J mice (female, 8-wo) with a bolus IV injection of zoledronate followed by maxillary first molar extraction. In this model, MHDP-DNV was topically applied on the palatal gingiva, prior to or 1 week after the left maxillary first molar extraction. Two weeks after extraction, mouse maxillary tissues were harvested for standardized photography, microCT and decalcified histology.fBP-DNV (170+/-10 nm diameter and +34 +/-4 mV zeta potential) demonstrated greater trans-oral epithelial delivery of BP than without DNV, in vitro, and as detected by the fluorescent signal on the underlining alveolar bone after a topical application in vivo. Mice receiving a ZOL administration followed by tooth extraction, consistently exhibited ONJ-like lesions. Pre-treatment with MHDP-DNV eliminated alveolar bone exposure and reduced gingival swelling. MicroCT images demonstrated significantly better socket healing in the MHDP-DNV topical application group. Separately, after ONJ-like lesions were established at week 1 (ONJ-like lesion prevalence: 100%), MHDP-DNV was topically applied. All MHDP-DNV treated mice exhibited a closed oral wound. By contrast, 83% of untreated control mice exhibited ONJ symptoms with an open oral wound at week 2, which was also still observed in 33% of mice at week 4.This study suggests an efficient treatment of BRONJ by topical application of an MHDP-DNV trans-oral epithelial drug formulation, creating the possibility of a translatable therapy in clinical dentistry.Supported by NIH/NIDCR R01DE022552, R44DE025524, NIH/NCRR C06RR014529

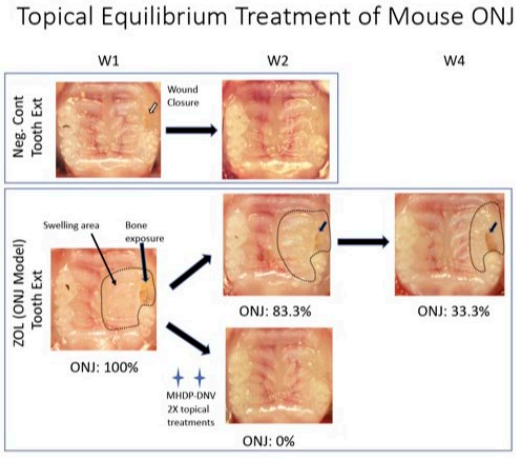

***Disclosures: Hiroko Okawa**, None*

P-838

Establishing a Critical-Sized Segmental Defect in a Mouse Model of Osteogenesis Imperfecta *Kyle Kavaseri[1], David Bertrand[1], Frank Rauch[1], Reggie Hamdy[1], Bettina M. Willie[1]. [1]McGill University, Shriners Hospital for Children Research Centre, Canada

Purpose: Osteogenesis Imperfecta (OI) is a rare bone fragility disorder, typically caused by mutations in COL1A1 or COL1A2. Bisphosphonates are given during growth to prevent fractures. Although fractures appear to heal normally, osteotomies often result in non-union

or delayed healing.1 Osteotomies are performed to correct limb deformities. No studies have investigated osteotomy or defect healing in mouse models of OI. The aim of our study was to establish a critical size femoral segmental defect stabilized under controlled mechanical conditions in the osteogenesis imperfecta murine (oim) model. Methods: Female oim -/-, oim -/+, oim +/+ mice (n=7-8 mice/genotype) were injected with 0.05 mg/kg zoledronic acid from weeks 5-9 of age. At 10 weeks of age, a double osteotomy was performed to create a 2mm segmental defect in the left femoral midshaft using a gigli saw. The osteotomy was stabilized with a unilateral external fixator. The defect was filled with a bovine collagen scaffold, saturated with saline. Healing at the osteotomy defect was assessed using in vivo µCT on days 0, 7, 14, 21 and 28 (8-µm voxel size) and histology on day 28. The effects of scan day, genotype and interactions were assessed by ANOVA and post hoc t-tests (α=0.05). Results: Stabilization of the osteotomy was not possible in oim -/- mice due to fracture at the pin sites, but was successful in the oim -/+ and oim +/+ mice. Osteotomy defects in both oim -/+ and oim +/+ did not achieve bony bridging over 28 days (Fig1A). All µCT-based microstructural parameters of the callus (BV, BV/TV, vTMD, TMC) were not significantly affected by either scan day or genotype (Fig1B). TV was the exception, but demonstrated no significant difference between oim -/+ and oim +/+ on day 28. Histological analysis confirmed these findings.Conclusions: We show that 2mm is a critical sized femoral segmental defect in the oim -/+ and wild-type mice treated with bisphosphonates. Even with bisphosphonate treatment, the bones of oim -/- mice are too fragile to support an external fixator. The established osteotomy defect model stabilized under controlled mechanical conditions will allow for investigation of novel cell-based therapies and/or biomaterial scaffolds to treat non-unions in oim -/+ mice.References: 1- Anam et al. JBMR. 30:1362-1368. 2015. 2- Munns et al. JBMR. 19:1779-1786. 2004.

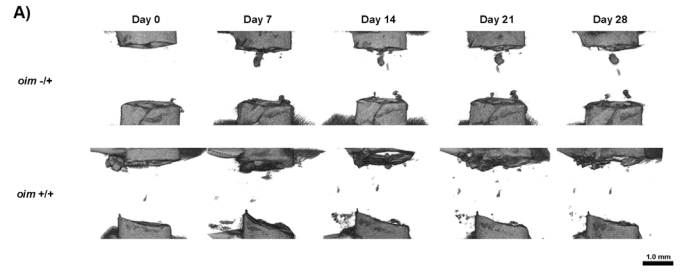

B)

Bone Volume (BV) (mm³)	oim -/+ (n = 8)	oim +/+ (n = 7)
Day 0	1.26 ± 1.07	1.05 ± 0.79
Day 7	1.26 ± 1.07	1.07 ± 0.77
Day 14	1.23 ± 1.15	2.30 ± 1.82
Day 21	2.23 ± 1.32	1.27 ± 1.07
Day 28	1.37 ± 1.53	1.41 ± 1.43

Total Volume (TV) (mm³)	oim -/+ (n = 8)	oim +/+ (n = 7)
Day 0	5.81 ± 1.21	6.09 ± 1.11
Day 7	5.80 ± 1.21	6.60 ± 1.50
Day 14	6.62 ± 1.63	7.92 ± 1.77
Day 21	7.18 ± 2.21	6.43 ± 1.84
Day 28	7.26 ± 1.87	6.79 ± 1.44

Bone Volume Fraction (BV/TV) (mm³/mm³)	oim -/+ (n = 8)	oim +/+ (n = 7)
Day 0	0.21 ± 0.17	0.19 ± 0.14
Day 7	0.21 ± 0.17	0.18 ± 0.15
Day 14	0.19 ± 0.19	0.28 ± 0.21
Day 21	0.32 ± 0.19	0.19 ± 0.14
Day 28	0.17 ± 0.16	0.20 ± 0.18

Volumetric Tissue Mineral Density (vTMD) (mgHA/cm³)	oim -/+ (n = 8)	oim +/+ (n = 7)
Day 0	1020 ± 51	1001 ± 88
Day 7	1003 ± 78	1005 ± 65
Day 14	1034 ± 113	1046 ± 121
Day 21	1124 ± 252	1092 ± 184
Day 28	1041 ± 99	1156 ± 143

Tissue Mineral Content (TMC) (mg)	oim -/+ (n = 8)	oim +/+ (n = 7)
Day 0	1.27 ± 1.06	1.04 ± 0.79
Day 7	1.27 ± 1.06	1.06 ± 0.77
Day 14	1.31 ± 1.25	2.47 ± 2.01
Day 21	2.55 ± 1.40	1.45 ± 1.31
Day 28	1.45 ± 1.61	1.69 ± 1.76

***Disclosures: Kyle Kavaseri**, None*

P-839

Longitudinal and Flare-Up-Specific Biomarkers in Fibrodysplasia Ossificans Progressiva (FOP): Data from a Global Natural History Study

*Robert J Pignolo[1], Mona Al Mukaddam[2], Geneviève Baujat[3], Carmen De Cunto[4], Edward C Hsiao[5], Richard Keen[6], Kathleen Harnett[7], Rose Marino[7], Frederick S Kaplan[2]. [1]Department of Medicine, Mayo Clinic, United States, [2]Departments of Orthopaedic Surgery & Medicine, The Center for Research in FOP and Related Disorders, Perelman School of Medicine, University of Pennsylvania, United States, [3]Département de Génétique, Institut IMAGINE and Hôpital Universitaire Necker-Enfants Malades, France, [4]Pediatric Rheumatology Section, Department of Pediatrics, Hospital Italiano de Buenos Aires, Argentina, [5]Division of Endocrinology and Metabolism, UCSF Metabolic Bone Clinic, Institute of Human Genetics, and UCSF Program in Craniofacial Biology, Department of Medicine, University of California-San Francisco, United States, [6]Centre for Metabolic Bone Disease, Royal National Orthopaedic Hospital, United Kingdom, [7]Ipsen, United States

Background: FOP is an ultra-rare, severely debilitating genetic disorder characterized by episodic heterotopic ossification (HO) and flare-ups. Identification of biomarkers would be useful to predict flare-ups and monitor FOP disease progression, and to identify when interventions are warranted and assess responses to these interventions. Objective: To evaluate putative serum and urine biomarkers at Baseline (BL), annually, and during the course of flare-ups in a longitudinal FOP natural history study (NHS).Methods: Individuals with FOP aged <=65 years with a documented ACVR1R206H mutation were eligible to participate in a prospective, 36-month NHS (NCT02322255) investigating the longitudinal progression of FOP. This analysis evaluated biomarker data at BL and Month 12, and during flare-ups. Blood and urine samples were collected at BL and annual study visits, and at Days 1, 42, and 84 of imaged flare-ups to measure biomarkers of inflammation, angiogenesis, and bone/cartilage turnover. Low-dose whole-body computed tomography (WBCT, excluding the head) was performed to assess HO at Months 12, 24, and 36; flare-up HO volumes were assessed by CT at the flare-up sites. Magnetic resonance imaging (MRI) or ultrasound was used to assess flare-ups for the presence of edema. Data were analyzed using descriptive statistics.Results: BL and Month 12 assessments were completed for 99/114 participants; 93 had evaluable WBCT HO at both timepoints, of whom 37 (39.8%) had new HO at Month 12. Overall, biomarker values did not change substantially from BL to Month 12, and mean values were similar between participants with versus those without new HO at Month 12 (Table). A total of 52 flare-ups were CT-imaged, of which 14 (26.9%) resulted in new HO at Day 84. Out of 42 flare-ups assessed at Day 1 by MRI or ultrasound, 29 (69.0%) had edema; of these, 10 (34.5%) had new HO at Day 84 (versus 19 [65.5%] with no new HO). No serum biomarker was identified that was predictive of flare-ups with BL edema or that resulted in development of new HO.Conclusions: The identification of biomarkers to predict disease progression could greatly benefit the clinical management of FOP. As results from this NHS did not identify a signal for a longitudinal or flare-up-specific biomarker for FOP, potentially due to the limited panel of biomarkers tested, a narrow sampling window, and/or missing data for some participants, further research is required.

Biomarker	Mean change from Baseline (SEM)	
	Without new HO	With new HO
Erythrocyte sedimentation rate (mm/h)	3.3 (1.7); n=32	–3.9 (1.9); n=21
C-reactive protein (mg/L)	–0.4 (1.9); n=45	–1.0 (1.0); n=31
Interleukin-6 (ng/L)	–1.0 (0.4); n=44	–0.3 (0.4); n=26
Interleukin-1 beta (ng/L)	0.0 (0.0); n=44	0.1 (0.1); n=26
Tumor necrosis factor alpha (ng/L)	–0.3 (0.1); n=44	–0.1 (0.1); n=26
Creatine phosphokinase (U/L)	–5.8 (5.9); n=45	3.1 (7.1); n=31
Lactate dehydrogenase (U/L)	–18.7 (4.5); n=45	–20.5 (7.8); n=31
Fibroblast growth factor/urine creatine (µg/kg)	0.8 (0.7); n=32	–1.1 (0.6); n=21
Vesicular endothelial growth factor (ng/L)	–22.6 (12.1); n=44	–16.4 (27.2); n=25
Osteocalcin (µg/L)	–6.9 (3.7); n=44	–12.0 (5.4); n=29
Bone-specific alkaline phosphatase (µg/L)	–4.1 (2.0); n=44	3.9 (4.3); n=29
C-terminal propeptide of type 1 procollagen (µg/L)	–22.0 (13.6); n=44	0.6 (23.3); n=27
N-terminal propeptide of type 1 procollagen (µg/L)	–66.6 (32.4); n=44	–110.6 (46.9); n=28
Collagen-derived retinoic acid protein (ng/L)	–120.0 (56.5); n=45	–87.3 (95.2); n=26
C-terminal telopeptide (µg/L)	–0.1 (0.0); n=42	–0.1 (0.1); n=27

Data not available for all participants at all timepoints. Biomarkers measured in serum, except fibroblast growth factor/urine creatine (urine) and erythrocyte sedimentation rate (blood). BL: Baseline; HO: heterotopic ossification; SEM: standard error of the mean.

***Disclosures: Robert J Pignolo**, Research investigator: Clementia/Ipsen, Regeneron; Advisory board: President of the International Clinical Council on FOP; Chair of the Publications Committee for the IFOPA Registry Medical Advisory Board, Other Financial or Material Support*

P-840

Impact on osteoblasts/osteocytes in vitro of a novel genetic variant of the OFD1 gene linked to X-linked osteoporosis, dental/facial hypoplasia and spontaneous adult-onset multiple long bone insufficiency fractures similar to atypical femur fractures

*Laetitia Michou[1], Marie-Eve Boisvert[1], Emile Couture[1], Rachel Laframboise[2], Frederic Fournier[1], Suzanne N Morin[3], Edith Gagnon[1], Claudia Gagnon[1], Fabrice Mac-Way[1], Mahmoud Rouabhia[4], Louis-Georges Ste-Marie [5], Arnaud Droit[1], Jacques P Brown[1]. [1]CHU de Québec-Université Laval Research Centre, Canada, [2]CHU de Québec-Université Laval, Canada, [3]McGill University, Canada, [4]Faculté de médecine dentaire, Université Laval, Canada, [5]Centre de recherche du CHUM, Universite de Montreal, Canada

Purpose – We identified a novel variant, p.Ala642Asp, of the OFD1 gene in a French-Canadian family in which eleven relatives have X-linked osteoporosis and/or dental and facial hypoplasia and/or adult-onset multiple long bone insufficiency fractures. In bone biopsies from this variant carriers a profound tissular and cellular osteoblastic depression was observed. Mutations of the OFD1 gene are linked to the oral-facial-digital syndrome, belonging to genetic disorders of the primary cilia. We reported another OFD1 variant in a woman with bisphosphonate (BP)-associated atypical femur fracture (AFF). We aimed to investigate the functional effects of the p.Ala642Asp variant, in silico predicted to be pathogenic, on osteoblasts/osteocytes cell lines in vitro.Methods – We reproduced the murine equivalent of this variant using PCR-directed mutagenesis in a lentiviral vector containing the murine ofd1 gene. These vectors, containing the p.Ala642Asp variant or a wild-type vector were transfected into murine cell lines: MC3T3-E1 (pre-osteoblast) and MLO-Y4 (osteocyte-like). Osteoblasts were differentiated over three weeks, before assessing the im-

Posters

pact on osteoblasts proliferation and bone formation abilities using alizarin red. The proliferation of osteocytes and length of primary cilia were quantified in both rare variant and wild-type vectors. To explore the effect of BP on these in vitro experiments, we treated the two cell lines with 10-12 M of alendronate, equivalent of a short-term therapeutic exposure in humans. One-way Anova and Tuckey's post hoc tests were performed.Results – In presence of the p.Ala642Asp variant, there was a significant ($p<0.01$) decrease of osteoblastic proliferation as compared to the wild-type osteoblasts (Fig 1). As expected, the proliferation of wild-type osteoblasts was higher under BP (142 cells versus 217 with BP). Although the mineralization significantly increased in wild-type osteoblasts treated by BP ($p<0.01$), no increase was observed in osteoblast carriers of the variant. The osteocytes proliferation was not modified by the variant (Fig 1). However, the length of primary cilia was significantly ($P<0.0001$) decreased in presence of this variant (4 versus 1.5 µm).Conclusions - Our results are consistent with a pathogenic effect of this OFD1 rare variant on osteoblast proliferation and osteocyte cilia length in vitro, and may be linked to the pathogenesis of long bone insufficiency fractures in oral-facial-digital syndrome.

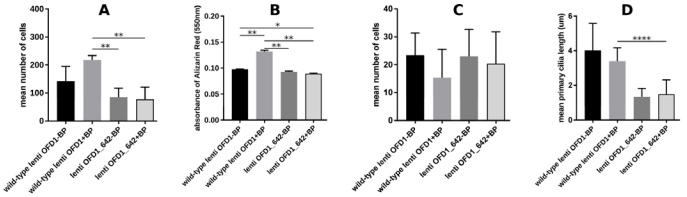

Figure 1: A) *In vitro* differentiated MC3T3-E1 cells into mature osteoblasts transduced by lentiviral vector containing wild-type *OFD1* gene or p.Ala642Asp variant; B) Absorbance of Alizarin Red in cells differentiated in A; C) MLO-Y4 cells in culture transduced by lentiviral vector containing wild-type *OFD1* gene or p.Ala642Asp variant; D) Primary cilia length of MLO-Y4 cells mentioned in C. * $p < 0.05$ ** $p < 0.01$ *** $p < 0.001$ **** $p < 0.0001$

***Disclosures: Laetitia Michou**, None*

P-841

The Diagnostic Journey in Fibrodysplasia Ossificans Progressiva: Insights from the FOP Registry *L. Adam Sherman[1], Kin Cheung[1], Carmen De Cunto[2], Sammi Kile[1], Robert Pignolo[3], Frederick Kaplan[4]. [1]International FOP Association, United States, [2]Department of Pediatrics, Hospital Italiano de Buenos Aires, Argentina, [3]Department of Medicine, Mayo Clinic School of Medicine, Mayo Clinic, United States, [4]Perelman School of Medicine, The University of Pennsylvania, c/o Department of Orthopaedic Surgery, Penn Musculoskeletal Center, United States

Fibrodysplasia Ossificans Progressiva (FOP) is an ultra-rare, disabling genetic disease that causes bone to form in muscle, tendons, ligaments, and other connective tissues. One of the hallmark characteristics of FOP is the malformation of the great toes, which is present in nearly all individuals with FOP. The great toe malformation, along with heterotopic ossification, are early signposts for a definitive clinical diagnosis. However, given its rarity, a diagnosis of FOP is often missed at birth and delayed for years.The International FOP Association (IFOPA), a global patient association, developed the FOP Registry to advance our understanding of FOP. Data from the FOP Registry shows that the mean age of symptom onset is 6.2 years (range, 0 – 45), whereas the mean age at correct diagnosis is 8.3 years (range, 0 – 48). Diagnosis takes longer for patients who have the non-classical versus the classical FOP mutation (18.6 vs. 7.0 years). The diagnostic journey has shortened over the last five years, taking on average 1.5 years to receive a correct diagnosis after first symptom, compared to 2.2 years.Prior to receiving a correct diagnosis, patients see on average 3.3 physician specialties (range, 1 – 10); this average has remained remarkably stable over time. Misdiagnosis occurred in 52.5% of Registry participants, with the most common misdiagnoses noted: cancer (29%), juvenile fibromatosis (13%), myositis ossificans (10%), and Klippel-Feil Syndrome (4%).Orthopedists (25.5%), geneticists (25.1%), and pediatricians (13.7%) are the most common physician specialties providing a definitive diagnosis for FOP. When first symptom onset occurs after the age of 12, rheumatologists (19.0%) play a larger role in making the correct diagnosis. Several physician specialties have high rates of misdiagnosis as a ratio of correct diagnoses given. General physicians are 8.9 times more likely to make an incorrect diagnosis for every correct diagnosis given, followed by pediatricians (5.5), orthopedists (2.5), rheumatologists (1.9) and geneticists (0.9).Patient registries can help medical communities better understand the diagnostic journey taken to make the correct diagnosis, which is critical to ensuring that patients receive the proper clinical care and support services. With a misdiagnosis rate over 50%, greater disease awareness is essential to increase clinicians' index of suspicion for FOP.

***Disclosures: L. Adam Sherman**, None*

P-842

Uncontrolled Serum Calcium and Phosphate Levels and Risk of Cardiovascular Disease in Patients With Chronic Hypoparathyroidism *Lars Rejnmark[1], Kristina Chen[2], Olulade Ayodele[3], Clara Monleón Bonet[4], Nicole Sherry[5], Emma Billmyer[6], Erin Cook[6], Elyse Swallow[6], Elvira Gosmanova[7]. [1]Aarhus University and Aarhus University Hospital, Denmark, [2]Former, Shire Human Genetic Therapies, Inc., Global Evidence and Outcomes, Data Sciences Institute, Research and Development; Current, Arena Pharmaceuticals, United States, [3]Shire Human Genetic Therapies, Inc., Global Evidence and Outcomes, Data Sciences Institute, United States, [4]Shire International GmbH, Switzerland, [5]Shire Human Genetic Therapies, Inc., United States, [6]Analysis Group, Inc., United States, [7]Albany Medical College, United States

Objective: This study evaluated the association of albumin-corrected serum calcium (Ca), serum phosphate (P), and calcium-phosphate product (Ca × P) with risk of developing cardiovascular (CV) events in patients (pts) with chronic hypoparathyroidism (HypoPT). Methods: A nested case-control study using the Explorys electronic medical record database (Jan 2007–Aug 2019) was conducted among US adults with chronic HypoPT (>=2 diagnosis codes for HypoPT occurring >=6 mo apart) on conventional therapy. Index date was the day after first calcitriol prescription. Baseline (BL) period was the 6 mo before the index date and exposure window was the time between the index date and development of a CV event. Pts with a CV event (defined as >=1 diagnosis code for cerebrovascular disease, coronary artery disease, heart failure, or peripheral vascular disease) before the index date, and those receiving parathyroid hormone, were excluded. Controls without a CV event were matched 1:1 to cases with a CV event based on age+/-5y, index date+/-1y, exposure duration, and sex. Associations between levels of Ca, P, and Ca × P and odds of developing CV events were assessed in adjusted logistic regression analyses.Results: Analyses included 264 matched pairs with Ca, and 100 matched pairs with P or Ca × P. Overall, cases and controls had similar BL characteristics, except cases had more comorbidities than controls. Mean age was 59y for the Ca pairs (76% women); mean follow-up 3.0y. Mean age was 57y for cases and 56y for controls for the P and Ca × P pairs (73% women); mean follow-up 2.6y. In the adjusted analyses, compared with pts with <33% of Ca measurements outside the target range, pts with >=67% of measurements outside the target range had 1.94 times higher odds of developing a CV event ($P<0.05$) (Table), but there was no statistically significant association between having 33%–<67% of Ca measurements outside the target range and developing a CV event. Having any P measurements above the target range, or Ca × P outside the target range was associated with higher odds of developing a CV event than pts without any measurements above or outside the target range (OR 3.86, $P<0.01$; OR 4.21, $P<0.05$; Table).Conclusions: In pts with chronic HypoPT treated with conventional therapy, a higher proportion of Ca or Ca × P measurements outside the target range, or any P measurements above the target range was associated with higher odds of developing a CV event.

Association of Biochemical Parameters and Cardiovascular Event

Variable	OR	95% CI	*P* value
Serum calcium outside target range*			
Proportion of serum calcium measurements outside 2.00–2.25 mmol/L*			
≥67%	**1.94**	**1.13–3.33**	**<0.05**
33% – <67%	1.39	0.82–2.37	0.22
<33%	1.00	reference	
Serum phosphate above target			
Any serum phosphate measurements >1.45 mmol/L			
Yes	**3.86**	**1.54–9.68**	**<0.01**
No	1.00	reference	–
Calcium-phosphate product outside target range			
Any calcium-phosphate product measurement >4.40 $mmol^2/L^2$			
Yes	**4.21**	**1.32–13.45**	**<0.05**
No	1.00	reference	–

CI=confidence interval; OR=odds ratio
*Normal range for albumin-corrected serum calcium is 2.00–2.55 mmol/L which is wider than the recommended target range for patients with hypoparathyroidism

***Disclosures: Lars Rejnmark**, Shire, a Takeda company, Consultant, Shire, a Takeda company, Speakers' Bureau, Shire, a Takeda company, Grant/Research Support*

P-843

Characterization of the skeletal phenotype of a new mouse model for Smith-McCort dysplasia *Milena Dimori[1], Irina Pokrovskaya[1], Qiang Fu[1], Vladimir Lupashin[1], Brian Storrie[1], Roy Morello[1]. [1]University of Arkansas for Medical Sciences, United States

Smith-McCort (SMC) and Dyggve-Melchior-Clausen (DMC) dysplasia are rare, autosomal recessive, severe osteochondrodysplasias that share identical radiologic features and cartilage histology. Skeletal defects present after birth, between 12 and 36 months of age and are progressive resulting in significant deformities. The first genetic locus for Smith-McCort dysplasia-1 (SMC1) was identified on chromosome 18q21 and associated with homozygous or compound heterozygous mutations in the DYM gene (encoding for Dymeclin, a novel intracellular protein involved in Golgi organization and intracellular vesicle trafficking). Mutations in the same gene also cause Dyggve-Melchior-Clausen disease, making SMC and DMC allelic disorders. A second locus for Smith-McCort dysplasia-2 (SMC2) was identified on chromosome 4q31 where homozygous or compound heterozygous mutations in the

RAB33B gene were identified. RAB33B encodes a small GTP-binding protein that also plays important roles in Golgi organization, vesicular transport, endocytosis pathway and autophagy. Based on the roles of the Golgi apparatus in protein processing, glycosylation and secretion and the importance of the extracellular matrix (ECM) to bone development, we hypothesize that the underlying disease mechanism is defective Golgi-dependent protein processing/glycosylation leading to defective accumulation of ECM/cell surface protein(s). To study this we generated a new mouse model using CRISPR/Cas9 technology and designed it to mimic a RAB33B 136A>C (p.K46Q) human mutation into the mouse ortholog gene. This mutation was described to change the conserved lysine residue in the guanine nucleotide-binding domain, lead to protein deficiency and cause SMC2. Heterozygous Rab33b+/A136C mice were generated and mated to obtain homozygous mice. Skeletal phenotyping at 6 weeks of age indicated reduced BMD and BMC in male Rab33bA136C / A136C mice (but not females) compared to WT littermate controls. MicroCT scanning of the male Rab33bA136C /A136C mice showed a trend towards reduction in BV/TV at the femur and spine with concurrent reduction of trabecular thickness. Ongoing studies aim to elucidate the potential consequences of this Rab33b mutation on the glycosylation patterns of cell surface and secreted glycoproteins that are important to bone biogenesis.

***Disclosures: Milena Dimori**, None*

P-844

Zoledronate Treatment Improves Trabecular Bone without Affecting Bone Biomechanical Properties in +/G610C Mouse Model of Osteogenesis Imperfecta *Jukka Morko[1], Jaakko Lehtimäki[1], Jukka P Rissanen[1], Jukka Vääräniemi[1]. [1]Pharmatest Services, Finland

Human Osteogenesis Imperfecta (OI) is a group of genetic disorders that results in heterogeneous symptoms ranging from low bone mass and occasional fractures to perinatal lethality. The clinical management of OI aims to maximize bone strength and minimize injuries. Bisphosphonate therapy has been shown to increase bone mass in OI patients. In most cases, human OI is caused by autosomal dominant mutations in type I collagen genes. Accordingly, most animal models of OI are gene-modified mice mimicking these genetic disorders. One animal model is 'Amish variant' mouse with a dominant negative G610C mutation in Col1a2 gene. Previously, we have demonstrated that young adult heterozygous (+/G610C) mice are an excellent animal model of mild-to-moderate OI and that treatment with zoledronate increases the amount of their trabecular bone. In this study, we characterized the bone phenotype of young adult +/G610C male mice in more detailed and investigated the effects of zoledronate treatment on their bone biomechanical properties. At 2 months of age, the tibia of +/G610C and wild-type (+/+) male mice was analyzed by in vivo micro-computed tomography (µCT). Then, +/G610C mice were treated with zoledronate (25 µg/kg, s.c.) or vehicle, and +/+ mice with vehicle once a week for 2 months. At 4 months of age, the mice were terminated, and their femora, tibiae and lumbar vertebrae were harvested for ex vivo µCT, peripheral quantitative computed tomography (pQCT), dual-energy X-ray absorptiometry (DXA), and biomechanical testing. At 2 months of age, +/G610C mice were lighter, and had smaller tibia and less trabecular bone than +/+ mice. At 4 months of age, +/G610C mice were still lighter, and had smaller tibia, femur and lumbar vertebral body, and less trabecular bone. As functional consequences of G610C mutation, femoral neck exhibited smaller maximum load and work-to-fracture in cantilever bending test, and tibial diaphysis demonstrated smaller post-yield displacement and work-to-fracture in three-point bending test. Treatment with zoledronate increased the amount of trabecular bone in femur, tibia and lumbar vertebral body. However, the anti-catabolic zoledronate treatment was not sufficient to improve bone biomechanical properties in young adult +/G610C male mice. This study supports the use of young adult +/G610C mice as the excellent animal model of mild-to-moderate OI and indicates that the improvement of bone strength is a major challenge in the therapy of human OI.

***Disclosures: Jukka Morko**, None*

P-845

The fibrodysplasia ossificans progressiva-causing ACVR1[R206H] and ACVR1[R258G] mutations exhibit distinct skeletal phenotypes in neonatal mice. *John Lees-Shepard[1], Sarah Hatsell[1], Nyanza Rothman[1], Saathyaki Rajamani[1], Ron Deckelbaum[2], Lily Huang[2], Lili Wang[2], Aris Economides[1], Andrew Murphy[2], Kalyan Nannuru[2], Vincent Idone[2], Qian Zhang[1]. [1]Regeneron, United States, [2]regeneron, United States

Gain of function mutations in the intracellular domain of the type I BMP receptor ACVR1 are associated with fibrodysplasia ossificans progressiva (FOP), a rare but catastrophically debilitating disease of ectopic intramuscular bone formation. Although the vast majority of FOP cases are caused by a R206H mutation the GS domain of ACVR1 (ACVR1[R206H]), FOP-causing mutations occur throughout the GS and the kinase domain of ACVR1. Of particular note, all three reported cases of a R258G mutation in the ACVR1 kinase domain exhibited more severe developmental skeletal and non-skeletal defects than are observed for ACVR1[R206H] bearing FOP patients. In an effort to model this phenotypic variance, we engineered a Cre-regulated 'conditional-ON' allele of ACVR1[R258G] in the mouse (Acvr1[R258G]FlEx/+), similar to the previously described Acvr1[R205H]FlEx/+mouse (Hatsell, Idone et al. 2015). As observed in the previously published Acvr1[R206H]FlEx/+;Gt(ROSA26)SorCreERT2/+ mouse, body-wide activation of the FOP allele in adult Acvr1[R258G]FlEx/+;Gt(ROSA26)SorCreERT2/+mice resulted in heterotopic ossification, which was entirely ameliorated by treatment with an Activin A blocking antibody. When recombination was driven by early-embryonic expression of Cre-recombinase, both ACVR1[R206H] and ACVR1[R258G] muteins exhibited skeletal deformities and neonatal lethality. Detailed skeleletal and soft-tissue imaging via iodine-contrast micro-CT confirmed that the skeletal phenotype presented more severely in ACVR1[R258G] mice than ACVR1[R206H] mice, consistent with the increased rarity and severity of ACVR1[R258G] relative to ACVR1[R206H] within the human FOP patient population. Indeed, ACVR1[R258G] mice presented with novel fusions and overgrowths in craniofacial and axial skeletal elements that were not observed in ACVR1[R206H] mice. Further, although ACVR1[R258G] mice are born alive and respond to stimulus, advanced imaging revealed that the lungs of ACVR1[R258G] mice were uninflated, indicating that ACVR1[R258G] likely die due to failure to breathe. Experiments are presently underway to determine whether Activin A neofuction contributes to the embryonic phenotype of either the ACVR1[R258G] or ACVR1[R206H] mice and if the increased severity of the ACVR1[R258G] phenotype is due to enhanced ligand dependent signaling, ligand independent signaling, and/or neoresponsivess to TGF-β or BMP family ligands.

***Disclosures: John Lees-Shepard**, Regeneron, Grant/Research Support*

P-846

BIOCHEMICAL ALGORITHM TO IDENTIFIFY INDIVIDUALS WITH ALPL VARIANTS BETWEEN SUBJECTS WITH PERSISTENT HYPOPHOSPHATASAEMIA *C. Tornero[1], V. Navarro-Compán[1], J. A Tenorio[2], S. García-Carazo[1], A. Buño[3], I. Monjo[1], C. Plasencia-Rodriguez[1], J.M Iturzaeta[3], P. Lapunzina[4], K.E Heath[5], A. Balsa[6], P. Aguado[6]. [1]Department of Rheumatology. La Paz University Hospital., Spain, [2]Institute of Medical and Molecular Genetics (INGEMM). La Paz University Hospital., Spain, [3]Department of Clinical Biochemistry. La Paz University Hospital., Spain, [4]Institute of Medical and Molecular Genetics (INGEMM. La Paz University Hospital., Spain, [5]Institute of Medical and Molecular Genetics (INGEMM). La Paz University Hospital, Spain, [6]Department of Rheumatology. La Paz University Hospital, Spain

BACKGROUND: Studies show a long diagnostic delay in Hypophosphatasia (HPP) and the accessibility for the genetic testing is not always possible. Our previous cross-sectional study (Tornero et al. OJRD (2020) 15:51) revealed alkaline phosphatase (ALP) levels < 25 IU/L seemed to be useful to identify individuals with ALPL variants among subjects with persistent hypophosphatasaemia. These data highlight the importance of establishing a specific biochemical profile and the value of including TNSALP substrates is a matter of interest.OBJECTIVES: First, to confirm our previous results in a one-year follow-up of a longitudinal study. Second, to determine the value of including TNSALP substrates (serum pyridoxal phosphate-PLP-and urinary phosphoetanolamine-PEA) in a specific biochemical profile to detect variants in ALPL in individuals with persistent low ALP levels.METHODS: Biochemical parameters of subjects included in a prospective longitudinal study conducted at La Paz Hospital were employed. Subjects were divided into two groups according to their genetics (+ GT or -GTgroup). Substrates were determined at baseline and at one-year visit and ALP levels also at six-months. To confirm the threshold, diagnostic utility measures were calculated at the 3 visits. ROC curves were employed to determine PLP and PEA best cut-off levels. Hierarchical binary logistic regression analysis was used to determine how well the different models fit (Nagelkerke R2). Finally, diagnostic utility measures for each model were calculated.RESULTS: Using ALP data from the three visits, Specificity (E) ranged between 84-91%; positive predictive value (PPV), 76-87% and +LR 3-6.1%. The ROC curves revealed cut-off PLP levels with the best combination of S and E for PLP were 180 nmol/L (S: 72%, E:86%) and for PEA, 35 (S:58%, E89%) umol/g creat. The regression model showed an OR (95% IC) for ALP180 and PEA>35 of 6.52 (1.07-39.6), 8.06 (2.2-29.9) and 4.4 (1.03-18.9). Compared to the model just including ALP, R2 improved (0.161 to 0.526) when substrates were added (E and PPV:100% and S:22%), especially when PLP was included (Table 1).CONCLUSION: This study confirms that ALP levels <25 IU/L could be useful to identify individuals displaying ALPL variants. Additionally, the combination of this threshold with the proposed cut-off levels of its substrates, especially PLP, have shown a very high specificity to detect the disease and could help vigorously in the diagnostic work-up of HPP.

Table 1. Regression logistic models for the detection of genetic *ALPL* variants including ALP, PLP and PEA cut-off levels.

	Biochemical variables	R^2 Nagelkerke	B	Odds Ratio (95% CI:)	p-value	Diagnostic utility measures
Model 1:	ALP<25	0.161	ALP:1.935 C: -0.325	6.923 (1.81-26.39)	0.005	S: 36.6 E: 92% PPV: 83% NPV: 58%
Model 2:	ALP<25 + PLP>180	0.461	ALP: 1.483 PLP 2.593 C: -1.283	4.407 (0.94-20.5) 13.364 (4.01-44.5)	0.059 0.000 0.001	S: 29% E: 97% PPV: 92% NPV: 56%
Model 3:	ALP<25 + PLP>180 + PEA>35	0.526	ALP: 1.875 PLP: 2.087 PEA: 1.486 C: -1.619	6.521 (1.07-39.6) 8.06 (2.18-29.9) 4.4 (1.03-18.9)	0.042 0.002 0.045 0.000	S: 22% E: 100% PPV: 100% NPV: 55%

***Disclosures: C. Tornero**, None*

P-847

Validity and Reliability of the Fibrodysplasia Ossificans Progressiva Physical Function Questionnaire (FOP-PFQ), a Patient-Reported, Disease-Specific Measure *Robert J Pignolo[1], Miriam Kimel[2], John Whalen[4], Ariane Kawata[2], Dennis Revicki[2], Rose Marino[4], Frederick S Kaplan[5]. [1]Department of Medicine, Mayo Clinic, United States, [2]Evidera, United States, [4]Ipsen, United Kingdom, [4]Ipsen, United States, [5]Departments of Orthopaedic Surgery & Medicine, The Center for Research in FOP and Related Disorders, Perelman School of Medicine, University of Pennsylvania, United States

Background: Fibrodysplasia ossificans progressiva (FOP) is an ultra-rare genetic disorder characterized by heterotopic ossification (HO), leading to progressive disability and functional limitations in joint mobility. To measure the ability of individuals with FOP to conduct activities of daily living, age-specific versions of the FOP physical function questionnaire (FOP-PFQ) were designed based on FDA guidance on patient-reported outcome (PRO) development.Objective: To evaluate the reliability and validity of the FOP-PFQ. Methods: Test-retest reliability was evaluated by comparing scores between Baseline and Week 1–3 visits in an FOP natural history study (NHS; NCT02322255); participants' clinical status was expected to remain stable during this time. Convergent validity was assessed by comparing scores with the Cumulative Analogue Joint Involvement Scale (CAJIS; a whole-body joint function measure), the Patient-Reported Outcomes Measurement Information System Global Health Scale (PROMIS; a quality of life measure), and whole-body HO volume assessed by computed tomography; the validation used pooled FOP-PFQ data from the NHS, an FOP patient registry (NCT02745158), and phase II trials evaluating palovarotene for individuals with FOP (NCT02190747; NCT02279095).Results: Test-retest reliability was high, with correlation coefficients >0.90 for all age-specific versions, well above the 0.70 threshold, indicating that FOP-PFQ scores were stable over the 1–3 week interval between questionnaires. In convergent validity assessments, adult FOP-PFQ scores were highly correlated with CAJIS (Spearman coefficient: 0.71, p<0.0001), indicating that loss of joint function has a significant impact on the ability to conduct activities of daily living as measured by the FOP-PFQ. Lower correlations were observed with the PROMIS physical health subscore (–0.49, p<0.0001) and HO volume (0.33, p<0.05). Findings for the pediatric versions of the FOP-PFQ were generally similar to the adult version, but were limited by small sample sizes, particularly for those aged 2–4 years (n=11).Conclusions: The FOP-PFQ is the first validated PRO developed specifically for FOP, and performed well on test-retest reliability and convergent validity, although some evaluations were inconclusive for pediatric versions, which had small sample sizes. The FOP-PFQ may help individuals with FOP and clinicians better understand the impact of FOP on physical function in trials and clinical practice.

***Disclosures: Robert J Pignolo**, Research investigator: Clementia/Ipsen, Regeneron; Advisory board: President of the International Clinical Council on FOP; Chair of the Publications Committee for the IFOPA Registry Medical Advisory Board, Other Financial or Material Support*

P-848

Bone Health in Children and Youth with Autism Spectrum Disorder: A Systematic Review and Meta-Analysis *Mahdi Rostami Haji Abadi[1], Saija Kontulainen[1]. [1]University of Saskatchewan, Canada

A higher risk of fracture reported in individuals with autism spectrum disorder (ASD) may relate to poor bone health and development in childhood and adolescence. We aimed to systematically review studies comparing imaged bone outcomes between children and youth with ASD and typically developing children and youth, and perform a meta-analysis to compare commonly reported bone outcomes. We searched articles published between January 1991 and December 2018 from PubMed, Cochrane Library, Web of Science, EMBASE and Scopus databases. We included studies comparing areal bone mineral density (aBMD) between children with ASD and typically developing children in the meta-analysis, and evaluated other imaged bone outcomes qualitatively. We assessed the quality of included studies using the modified version of the National Heart, Lung and Blood Institute's Quality Assessment Tool. We used random-effects models with an inverse variance method to pooled effect sizes (ES) of included studies. We estimated publication bias visually by re-displayed funnel plots after Duval and Tweedie's Trim and Fill adjustment for those measures reported in three or more studies. Seven publications were identified for the systematic review, and four studies were included in the meta-analysis. Studies had a fair (n=6) and poor (n=1) quality rating. The meta-analysis indicated that aBMD of the total body (ES=-0.77; 95% CI, -1.26 to -0.28; n=2), lumbar spine (-0.69; -1.00 to -0.39; 4), total hip (-1.00; -1.82 to -0.17; 3) and femoral neck (-1.07; -1.54 to -0.60; 3) were lower in children with ASD compared to typically developing children (Figure 1). There was no evidence of publication bias. Based on our qualitative review, limited evidence suggested 13% lower total body bone mineral content and 10-20% lower cortical and trabecular thickness (distal radius), cortical area and bone strength (distal radius and tibia) in children with ASD. Meta-analysis indicated that children and youth with ASD have lower aBMD at total body, lumbar spine, hip and proximal femur compared to typically developing children. Limited evidence also suggested deficits in bone mineral content, microarchitecture and strength in children and youth with ASD. Future studies are warranted to complement the preliminary findings of bone microarchitecture and strength deficits in children and youth with ASD.

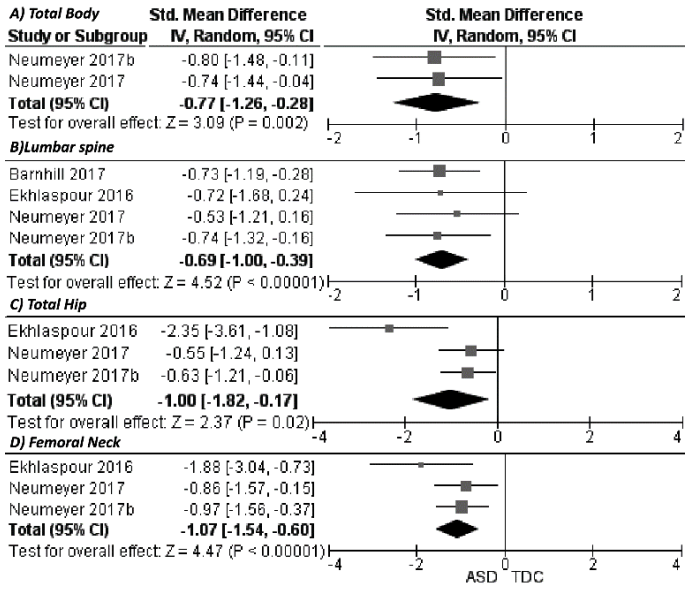

***Disclosures: Mahdi Rostami Haji Abadi**, None*

P-849

Functional characterization of a unique mutant of ALK2, p.K400E, that is associated with a skeletal disorder, diffuse idiopathic skeletal hyperostosis *Sho Tsukamoto[1], Mai Kuratani[2], Takenobu Katagiri[2]. [1]Division of Biomedical Sciences, Research Center for Genomic Medicine, Saitama Medical University, Japan, [2]Division of Biomedical Sciences, Research Center for Genomic Medicine, Saitama Medical Universityity, Japan

Bone morphogenetic protein (BMP) signaling regulates the physiological and pathological development of skeletal tissues. Activin receptor-like kinase 2 (ALK2) is a BMP type I transmembrane serine/threonine kinase receptor. Recently, a p.K400E mutation was found in ALK2 in a patient with diffuse idiopathic skeletal hyperostosis (DISH), which is a disorder characterized by calcification and ossification of spinal ligaments and entheses. We report here the functional characterization of ALK2 p.K400E in vitro. Cells overexpressing ALK2 p.K400E activated BMP signaling in response to osteogenic BMP ligands. However, ALK2 p.K400E was not activated by a nonosteogenic ligand, Activin A. BMP signaling through ALK2 p.K400E was further enhanced by the coexpression of a BMP type II recep-

tor. The type II receptor increased the phosphorylation level of ALK2 p.K400E, suggesting that ALK2 p.K400E is a hypersensitive mutant to the BMP type II receptor kinases. Our findings suggest that pathological calcification and ossification in DISH are caused by over-activated BMP signaling through ALK2 p.K400E enhanced by type II receptors in response to osteogenic BMPs rather than Activin A.

***Disclosures: Sho Tsukamoto**, None*

P-850

Stem Cell Therapy for Osteogenesis Imperfecta: A Systematic Review and Meta-analysis of Preclinical Studies using Mouse Models *Lauren Battle[1], Shoshana Yakar [2], Alessandra Carriero[1]. [1]The City College of New York, United States, [2]New York University College of Dentistry, United States

Osteogenesis imperfecta (OI) is a genetic collagen-related disease characterized by poor bone quality, osteopenia and increased fracture risk1. Bisphosphonates and other existing treatments can only partially correct the bone phenotype, providing symptomatic relief but not addressing the underlying genetic defect. Stem cell therapy is a promising treatment as it holds potential to correct the bone phenotype at the cellular level by utilizing genetically healthy cells early in their development to improve the quality and increase the quantity of OI bone. Here, we conduct a meta-analysis to investigate the efficacy of stem cell therapy on mouse models of OI. A literature review was performed to identify studies treating mouse models of OI with stem cells, including bone marrow, mesenchymal stem cells, and human fetal stem cells. Effect size of fracture incidence, maximum load, stiffness, cortical thickness, BV/TV, and raw engraftment rates were pooled in a random-effects meta-analysis. Moderator analyses were run to estimate the influence of variables including cell type, cell number, injection route, mouse age, irradiation, anatomical bone, and follow-up time. Consistent with clinical case studies2, bone fracture incidence greatly decreased with stem cell therapy, although the small raw engraftment rate. Cell therapy had a beneficial effect on maximum load, with follow-up time and anatomical bone having an influence on it. Stiffness, cortical thickness and BV/TV were not affected by cell therapy in mouse models of OI.This study demonstrates the promising potential of stem cell therapy to reduce fractures in OI despite the low cell engraftment. The mechanism of stem cell engraftment and its participation in bone modeling and remodeling is yet to be understood. Results support the hypothesis that transplanted cells produce beneficial effects by secreting paracrine factors and other soluble molecules3. It was not possible to investigate further parameters due to the lack of standards of investigation between the studies. Being bone fracture the primary symptom of OI, there is a critical need to measure the fracture toughness of OI bone treated with stem cells to assess the actual efficacy of the treatment to rescue OI bone brittleness. Understanding the mechanism of cellular therapy on bone (re)modeling as well as its actual efficacy on enhancing the strength and toughness of OI bone is crucial for the successful implementation of this therapy in the clinic.Van Dijk FS, Sillence DO. Am J Med Genet A. 164A(6), 2014.Horwitz EM, Prockop DJ, Gordon PL, et al. Blood. 97(5), 2001.Prockop DJ. Cytotherapy.19(1), 2017.

Outcome	# of Studies	Effect Size (CI)
Fracture Incidence (RR)	5	0.27 (0.19, 0.38)*
Engraftment (Raw %)	6	6.35 (0.14, 12.55)
Maximum Load (SMD)	6	2.37 (0.43, 4.32)*
Stiffness (SMD)	6	2.09 (-0.45, 4.64)
Cortical Thickness (SMD)	5	0.72 (-0.79, 2.23)
BV/TV (SMD)	3	1.37 (-1.26, 4.00)

Table 1 Meta-analysis conducted on 6 outcomes common to the studies analyzed. The effect size, representing the magnitude of the observation, was considered significant (*) if the relative 95% confidence interval (CI) did not include 0. Risk ratio (RR) of fracture incidence was calculated as the total number of fractured long bones over the total number of long bones. Risk ratios lower than one signify a decrease in risk in the stem cell treated OI bone. Engraftment rate was expressed as the raw percentage of engrafted transplanted cells to total (mouse) cells. Stem cell treated bones showed low and variable rates of engraftment. Standardized mean differences (SMD) were calculated for the other outcomes as the mean difference over the pooled standard deviation. Only Maximum Load was significantly higher in stem cell treated OI bone.

***Disclosures: Lauren Battle**, None*

P-851

The Association Between STX16 and the Imprinting of GNAS in the Pathogenesis of Pseudohypoparathyroidism *Cagri Aksu[1], Monica Reyes[1], Claire Remillard[1], Qing He[1], Murat Bastepe[1]. [1]Massachusetts General Hospital, United States

Autosomal dominant pseudohypoparathyroidism type-Ib is characterized by renal parathyroid hormone resistance, with resultant hypocalcemia and hyperphosphatemia. This disorder is associated with an isolated loss of methylation at GNAS exon A/B and most patients carry maternal microdeletions in the neighboring STX16 gene. The shortest deletion overlap is a 1.2-kb region spanning STX16 exon 4 and thought to harbor a cis-acting element regulating GNAS A/B methylation. However, ablation of the orthologous mouse region does not recapitulate the patient findings and no functional data exists supporting the association between the STX16 gene and GNAS imprinting. The A/B methylation is established in the female germline and maintained throughout the development in somatic cells. We thus investigated the role of the 1.2-kb STX16 region in the maintenance of A/B methylation, employing HCT116 cells, a near-diploid human cell line derived from colorectal carcinoma. To delete this region, we used CRISPR/Cas9 and suitable guide-RNAs targeting upstream and downstream of exon 4. We first generated HCT116 cells stably expressing Cas9 and introduced the guide-RNAs into those cells by lentiviral delivery. After antibiotic enrichment of the transduced cells, the presence of a 2.1-kb deletion spanning STX16 exon 4 and flanking intronic regions was confirmed by PCR, followed by TA-cloning and Sanger sequencing of the products. Multiplex ligation-dependent probe amplification (MLPA) indicated a modest reduction in the STX16 exon 4 copy number, suggesting that the deletion was present only in a subset of cells. Methylation specific-MLPA analysis, which was performed in non-clonal cells, indicated normal methylation status at GNAS exon A/B, and this finding was confirmed by the combined bisulfite restriction analysis. Thus, our initial findings suggest that the putative cis-acting element within STX16 does not regulate the maintenance of exon A/B methylation. To further confirm these results, we are in the process of selecting and analyzing clonal HCT116 cells homozygous or heterozygous for this deletion. In addition, we are introducing the same deletion into human ES cells, so that we can determine its impact on GNAS imprinting during early development.

***Disclosures: Cagri Aksu**, None*

P-852

Histochemical Quantification of FGF23 Expression in the Bone with Phosphor Integrated Dot Nanoparticles *Minae Koga[1], Hajime Kato[1], Nobuaki Ito[1]. [1]The University of Tokyo Hospital, Japan

Background: Tumor-induced osteomalacia (TIO) is a fibroblast growth factor 23 (FGF23)-related hypophosphatemic disorder caused by FGF23 producing tumors. TIO represents bone pain, fracture/pseudofracture, muscle weakness, etc. which could sometimes lead a patient bedridden. TIO is completely cured only by the removal of the tumor, but localization of the tumor is occasionally challenging as the tumor could be very tiny, could develop in any part of the bones or the soft tissue. In our hospital, seven out of 43 cases missed the identified tumor. In TIO patients, FGF23 production in normal bone tissue is expected to be suppressed due to low serum phosphate. Therefore, in those patients with the clinical diagnosis of TIO with an unidentified tumor, it is possible to determine if they actually possess FGF23 producing tumor or suffer from other conditions with overproduction of FGF23 in the bone by confirming the expression level of FGF23 in the bone. However, conventional immunostaining methods are not sensitive enough to confirm the suppression of FGF23 due to relatively low physiological expression levels of FGF23. Also, it is difficult to confirm the local FGF23 production by PCR or Western blotting due to the complexity of extracting mRNA or protein from the tough bone tissue. Phosphor Integrated Dot nanoparticles staining (PID) was developed to detect the target proteins with extremely high sensitivity and quantifiability. Therefore, here we exploit this method to confirm FGF23 suppression in suspected patients with TIO.Methods: The bone samples from 13 patients (STD-bone) and 2 dialysis patients (HD-bone) were collected on the event of hip arthroplasty. Also, the bone samples from 2 patients with FGF23 producing bone tumor were collected during the removal of the tumors (TIO-bone). FGF23 immunostaining using PID was performed for each sample, and the average number of PID particles within 5.5 μm from the cell nucleus for each nucleus was counted with the attribution method.Result: The mean number of PID particles per nucleus was 153.7 in STD-bone, 357.7 in HD-bone, and 19.0 in TIO-bone, with a significant difference between the STD-bone and TIO-bone ($P<0.001$). Discussion: PID method undoubtedly revealed physiological suppression of FGF23 expression in the bone from TIO patients. This method allows us to clearly differentiate the etiology of acquired FGF23 related hypophosphatemic rickets/osteomalacia patients.

***Disclosures: Minae Koga**, None*

P-853

Association of Biochemical Parameters With Chronic Kidney Disease in Chronic Hypoparathyroidism Using Electronic Medical Record Data

*Elvira Gosmanova[1], Kristina Chen[2], Olulade Ayodele[3], Clara Monleón Bonet[4], Nicole Sherry[5], Erin Cook[6], Fan Mu[6], Joshua Young[6], Lars Rejnmark[7]. [1]Albany Medical College, United States, [2]Former, Shire Human Genetic Therapies, Inc., Global Evidence and Outcomes, Data Sciences Institute, Research and Development; Current, Arena Pharmaceuticals, United States, [3]Shire Human Genetic Therapies, Inc., Global Evidence and Outcomes, Data Sciences Institute, United States, [4]Shire International GmbH, Switzerland, [5]Shire Human Genetic Therapies, Inc., United States, [6]Analysis Group, Inc., United States, [7]Aarhus University and Aarhus University Hospital, Denmark

Objective: This study evaluated the association of albumin-corrected serum calcium (Ca), serum phosphate (P), and calcium-phosphate product (Ca × P) with risk of developing chronic kidney disease (CKD; defined as >=1 diagnosis code for CKD stage 3–5 or >=2 outpatient estimated glomerular filtration rate values <60 mL/min/1.73 m2 >3 mo apart) in patients (pts) with chronic hypoparathyroidism (HypoPT).Methods: A nested, case-control study using the Explorys electronic medical record database (Jan 2007–Aug 2019) was conducted among US adults with chronic HypoPT (>=2 diagnosis codes for HypoPT occurring >=6 mo apart) on conventional therapy. Index date was the day after first calcitriol prescription, baseline (BL) period was the 6 mo before the index date, and exposure window was the time between the index date and development of CKD. Pts with CKD before the index date and those receiving parathyroid hormone were excluded. Controls without CKD were matched 1:1 to cases with CKD based on age+/-5 y, index date+/-1 y, exposure duration, and sex. Associations between longitudinal levels of Ca, P, and Ca × P product and odds of developing CKD were assessed in adjusted logistic regression analyses.Results: The analyses included 150 matched pairs with Ca, and 40 matched pairs with P or Ca × P. Overall, cases and controls had similar BL characteristics. Mean age was 58 y for the Ca pairs (83% women); mean follow-up 2.8 y. Mean age was 57 y for cases and 58 y for controls for the P or Ca × P pairs (83% women); mean follow-up 2.5 y. In the adjusted analyses, compared with pts with <33% of Ca measurements outside the target range, pts with >=67% of Ca measurements outside, above, or below the target range had 3.46, 2.85, and 2.68 significantly increased odds, respectively, of developing CKD. Pts with 33%–<67% of Ca measurements above or outside the target range had increased odds of developing CKD, but the associations were not statistically significant (Table). There were no statistically significant associations between developing CKD and any P measurements above the target range, or Ca × P measurements outside the target range (Table).Conclusions: In pts with chronic HypoPT treated with conventional therapy a higher proportion of Ca measurements outside, above, or below the target range was associated with higher odds of developing CKD. Future studies are needed to evaluate the effects of calcium fluctuations and risk of CKD in pts with chronic HypoPT.

Association of Biochemical Parameters and CKD

Variable	OR	95% CI	*P* value
Serum calcium outside target range			
Proportion of serum calcium measurements outside 2.00–2.25 mmol/L*			
≥67%	**3.46**	**1.82–6.56**	**<0.001**
33% to <67%	1.36	0.72–2.56	0.337
<33%	1.00	reference	–
Serum calcium above target range			
Proportion of serum calcium measurements >2.25 mmol/L			
≥67%	**2.85**	**1.30–6.28**	**<0.01**
33% to <67%	1.53	0.87–2.70	0.139
<33%	1.00	reference	–
Serum calcium below target range			
Proportion of serum calcium measurements <2.00 mmol/L			
≥67%	**2.68**	**1.16–6.15**	**<0.05**
33% to <67%	0.71	0.38–1.33	0.286
<33%	1.00	reference	–
Serum phosphate above target range			
Any serum phosphate measurements >1.45 mmol/L			
Yes	0.95	0.32–2.86	0.927
No	1.00	reference	–
Calcium-phosphate product outside target range			
Any calcium-phosphate product measurements >4.40 $mmol^2/L^2$			
Yes	0.79	0.16–4.01	0.776
No	1.00	reference	–

CI=confidence interval; CKD=chronic kidney disease; OR=odds ratio
*Normal range for albumin-corrected serum calcium is 2.00–2.55 mmol/L which is wider than the recommended target range for patients with hypoparathyroidism

***Disclosures: Elvira Gosmanova**, Shire, a Takeda company, Consultant*

P-854

Design of primers for direct sequencing of nine coding exons in the human ACVR1 gene

*Masaru Matsuoka[1], Sho Tsukamoto[2], Yuta Orihara[1], Rieko Kawamura[1], Mai Kuratani[2], Nobuhiko Haga[3], Kenji Ikebuchi[1], Takenobu Katagiri[4]. [1]Department of Clinical Laboratory, Saitama Medical University, Japan, [2]Division of Biomedical Sciences, Research Center for Genomic Medicine, Saitama Medical University, Japan, [3]Department of Rehabilitation Medicine, Graduate School of Medicine, The University of Tokyo, Japan, [4]Division of Biomedical Sciences, Research Center for Genomic Medicine, Saitama Medical University, Japan

The human ACVR1 gene encodes a transmembrane protein consisting of 509 amino acids called activin A receptor, type I (ACVR1) or activin receptor-like kinase 2 (ALK2) and has nine coding exons. The ALK2 protein functions as a signaling receptor for ligands of the transforming growth factor-β family. In the human ACVR1 gene, approximately 20 types of heterozygotic mutations in the coding exons have been associated with congenital disorders and a somatic cancer, such as fibrodysplasia ossificans progressiva (FOP), diffuse intrinsic pontine glioma, diffuse idiopathic skeletal hyperostosis and some congenital heart disorders. In the present study, we designed primers for direct sequencing of the nine coding exons in the human ACVR1 gene. The reliability of the primers was examined by PCR and DNA sequencing using genomic DNA prepared from peripheral blood or swab samples of three patients with FOP who had different mutations in the ACVR1 gene. A single nucleotide heterozygotic mutation was identified in each genomic sample without additional mutations in other regions. Therefore, the primers designed for the nine coding exons of the ACVR1 gene could be useful for the genetic diagnosis of patients who may have disorders associated with mutations in the ACVR1 gene.

***Disclosures: Masaru Matsuoka**, None*

P-855

Sarcopenic obesity according to the EWGSOP II criteria and four different concepts of obesity in regards to physical frailty in Brazilian older adults: data from the SARCOS study.

*Alberto Frisoli Jr[1], Sheila Ingham[1], Jairo Borges[1], Angela Paes[1], Valdir Ambrosio[1]. [1]Universidade Federal Sao Paulo, Brazil

Sarcopenic obesity has been linked to impaired physical capacity, functional loss and incidence of frailty. However, its diagnosis is not yet defined due to the diversity of criteria for obesity (overweight or over regional body fat). Aim: To assess which phenotype of sarcopenic obesity has the greatest association with physical frailty. Method: cross-sectional analysis of the SARCopenia and OSteoporosis in 369 community-dwelling older adults from an outpatient clinic. Appendicular skeletal lean mass and regional fat were assessed by DXA. Frailty was defined by Fried's criteria. The phenotypes were composed by the presence of sarcopenia, that was diagnosed according to recommendations given by EWGSOP II, and obesity, which was diagnosed by four different criteria: BMI >=30 kg/m2 (BMI obesity); appendicular fat percentage ³ 30% (Appendicular obesity); percentage of total body fat ³ 35% women and ³25% men (Total body obesity); and trunk fat percentage ³ 30% (Trunk obesity). The phenotypes were then separated into 4 groups: sarcopenic obesity, sarcopenia, obesity and controls. Then, we evaluated the association of each group with physical frailty. Results: Mean age of 78.45 (+/- 7.2) years old with 53.2% (n=189) women, 67.3% Caucasians. Physical frailty was diagnosed in 38.5%. Sarcopenia EWGSOP II was present in 19.8%, BMI obesity in 23.6%, trunk obesity in 88.4%, total body obesity in 81.9% and appendicular obesity in 66.1%. The prevalence of sarcopenic obesity due to BMI obesity was 1.6% (n = 6), 13.3% (n = 49) due to appendicular obesity, 15.6% (n = 58) due to trunk obesity and 14.2% (n = 53) for total body obesity. Sarcopenia without BMI obesity occurred in 18.2%, 6.5% without appendicular obesity, 5.4% without trunk obesity and 4% by total body obesity. Adjusted regression analyzes are shown in figure 1.Conclusion: Sarcopenic obesity diagnosed by regional obesity was more associated with physical frailty, compared to obesity sarcopenic by BMI obesity, which did not reach a significant association.Sarcopenia of all phenotypes was less associated with physical frailty compared to sarcopenic obesity

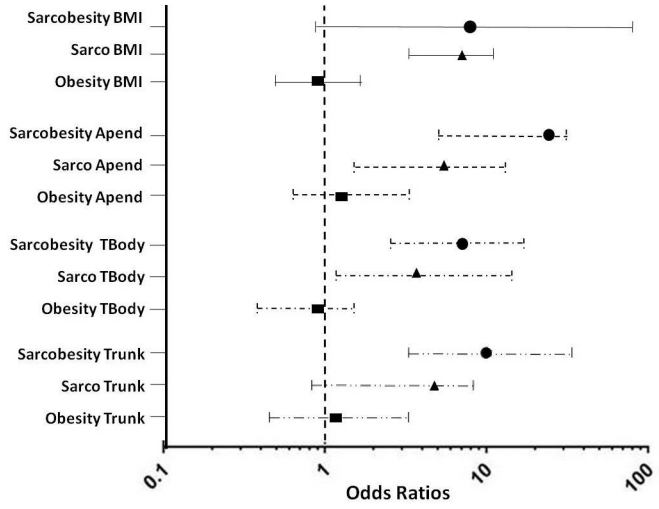

***Disclosures: Alberto Frisoli Jr**, None*

P-856

Skin autofluorescence, a non-invasive biomarker for advanced glycation end-products, is associated with Sarcopenia: The Rotterdam study *Komal Waqas[1], Jinluan Chen[2], Katerina Trajanoska[2], M. Arfan Ikram[2], Fernando Rivadeneira[2], Andre G Uitterlinden[2], M. Carola Zillikens[1]. [1]Department of Internal Medicine, Erasmus Medical Centre, Netherlands, [2]Department of Epidemiology, Erasmus Medical Centre, Netherlands

Accumulation of advanced glycation end-products (AGEs) in skeletal muscle might be related to sarcopenia development and its components namely appendicular skeletal mass index (ASMI), hand grip strength (HGS) and gait speed (GS). No studies have so far investigated skin AGEs in relation to sarcopenia in a general population of European background.In a cross-sectional analysis, 2,744 participants were included from the Rotterdam Study with a mean age of 74.1 years (56% females, 13% diabetics). Skin AGEs were measured using AGE readerTM as Skin autofluorescence (SAF), ASMI with iDXA (GE-Lunar), HGS with a hydraulic hand dynamometer and GS measured on an electronic walkway in a subgroup (n=2,079). We defined probable sarcopenia (low HGS) and sarcopenia (low HGS + low ASMI) based on European working group on Sarcopenia in older people revised criteria (EWGSOP2). Multivariate linear and logistic regression analysis were performed adjusting for age, sex, body fat percentage, height, renal function, diabetes and smoking status. Data was also analyzed in sex-stratified, age-adjusted SAF quartiles for literature comparison. Prevalence of low ASMI was 7.7%, of probable sarcopenia 19%, of low GS 2.9% and of sarcopenia 3.5%. SAF was consistently inversely associated with ASMI (β=-0.064, p=3E-5), HGS (β=-0.054, p=2E-5) and GS (β=-0.077, p=3E-4). SAF was an independent predictor of low ASMI (odds ratio per SAF SD, [OR]= 1.98, 95% confidence interval [CI] 1.47-2.67), probable sarcopenia OR=1.34 (95% CI: 1.07-1.67) and sarcopenia OR=1.98 (95% CI: 1.30-3.03) in fully adjusted models using EWGSOP2 cut-offs. As compared to the bottom three SAF quartiles combined (Q1-3), individuals in the Q4 had higher odds of low ASMI (OR=1.62 (95% CI: 1.18-2.23), probable sarcopenia (OR=1.16 (95% CI: 0.91-1.47) and sarcopenia (OR=1.67 (95% CI: 1.06-2.65).Higher skin AGEs are associated with low muscle mass, strength and performance which is in line with the hypothesis that AGEs play a role in age-related sarcopenia.

***Disclosures: Komal Waqas**, None*

P-857

Pro-inflammatory Diet is Associated with Higher Odds of Frailty in Middle-aged and Older Adults *Courtney Millar[1], Daniel Habtemariam[1], Alyssa Dufour[1], Marian Hannan[1], Nitin Shivappa[2], James Hebert[2], Joanne Murabito[3], Emelia Benjamin[3], Shivani Sahni[1]. [1]Hebrew Senior Life, Harvard Medical School, United States, [2]University of South Carolina, United States, [3]Boston University, School of Medicine; Framingham Heart Study, United States

Systemic inflammation, a key determinant of frailty, is highly modifiable by diet. The dietary inflammatory index (DII) estimates the inflammatory potential of diet (higher scorers indicate a more pro-inflammatory diet). Our objective was to determine whether a pro-inflammatory diet was associated with higher odds of frailty in middle-aged and older adults from the Framingham Heart Study Offspring Cohort. This prospective study included non-frail individuals with baseline diet assessment from a food frequency questionnaire (FFQ) in 1998-2001 and a follow-up frailty measurement in 2011-2014. DII scores were calculated from foods and nutrients (e.g. macronutrient, vitamin, mineral intake) from the FFQ. Frailty was defined as fulfillment of 3 or more Fried frailty phenotype criteria of unintentional weight loss, exhaustion, low physical activity, slowness (of gait speed), and weakness (of grip strength). Participants with missing gait/grip tests due to physical limitation were assumed to be slow (n=14) or weak (n=21), respectively. Logistic regression was used to calculate odds ratios (OR) and 95% confidence intervals (95% CI) for frailty onset adjusting for baseline age, sex, energy intake, current smoking, treatment for diabetes and/or cardiovascular disease, and non-melanoma cancers. Of the 1,805 non-frail individuals at baseline (mean age: 59 (SD=8) years, range: 33 – 81; 44% male), 174 individuals became frail over ~16 years. Mean DII for all participants was -0.10 (SD=1.8; range: -4.5 – 4.8). Mean DII in frail individuals was 0.02 (SD=1.8; range: -3.8 – 3.9), while in non-frail individuals it was -0.11 (SD=1.8; range: -4.5 – 4.8). In the model adjusted for age and sex, a one unit difference in DII was associated with 11% higher odds of developing frailty (p=0.02). The associations became strong after further adjustments for energy intake and current smoking (Table). Additional adjustments for disease indicators did not further change the association. In this cohort of middle-aged and older adults, a pro-inflammatory diet was associated with higher odds of frailty onset over follow-up. Thus, dietary modification may be a useful strategy for frailty prevention.

Title

Pro-inflammatory Diet is Associated with Higher Odds of Frailty in Middle-aged and Older Adults

Authors

Millar, CL. Habtemariam, D. Dufour, AB. Hannan, MT. Shivappa, N. Hebert, JR. Murabito, JM. Benjamin, EJ. Sahni, S.

Table. Associations between the dietary inflammatory index (DII)[a] and odds of frailty in the Framingham Heart Study Offspring Cohort over ~16 years.

Model[b]	All participants (N=1,805)	
	OR (95% CI)	P value
Model 1	1.11 (1.02-1.22)	0.02*
Model 2	1.14 (1.03-1.25)	0.01*
Model 3	1.14 (1.04-1.26)	0.01*

[a] The DII was calculated from 26 foods and nutrients, where higher scores represent a pro-inflammatory diet.
[b] Model 1 is adjusted for baseline age and sex. Model 2 further adjusts for energy intake and current smoking, and Model 3 adjusts for covariates in Model 2 as well as diabetes and/or cardiovascular disease treatment, and non-melanoma cancer.
* P< 0.05 was considered statistically significant.

***Disclosures: Courtney Millar**, None*

P-858

Association of D3Cr muscle mass with short term declines in BMD and bone strength in older men in late life: The MrOS Study *Peggy Cawthon[1], Steven Cummings[1], Andrew Burghardt[2], Lisa Langsetmo[3], Kristine Ensrud[3], Jane Cauley[4], Kristen Beavers[5], Ashley Weaver[5], William Evans[6], Mary Bouxsein[7], Eric Orwoll[8]. [1]California Pacific Medical Center, Research Institute, United States, [2]University of California, San Francisco, United States, [3]University of Minnesota, United States, [4]University of Pittsburgh, United States, [5]Wake Forest University, United States, [6]University of California, Berkeley, United States, [7]Harvard University, United States, [8]Oregon Health and Sciences University, United States

Men with low muscle mass by D3-creatine dilution (D3Cr muscle mass) have a higher risk of fractures and lower volumetric bone mineral density (vBMD) and estimated failure load (FL) at the distal radius and tibia (as assessed by high resolution peripheral quantitative computed tomography, HR-pQCT). Whether D3Cr muscle mass is also associated with decline in BMD is unknown. We tested the hypotheses that low D3Cr muscle mass (or low weight) are associated with greater short term declines in BMD and FL by HR-pQCT, and areal (aBMD) by dual energy x-ray absorptiometry (DXA) in community dwelling men in late life.MrOS men (mean age 77+/-3.8 yrs) had D3Cr muscle mass, HR-pQCT imaging of the distal radius and tibia, and hip DXA assessed at the Year 14 exam. An average of 1.6 years (SD=0.2) later, a subset (N=235) returned for HR-pQCT and DXA. Generalized linear models calculated age- and weight- adjusted mean percent change in BMD and FL, by quartile of D3Cr muscle mass. We also calculated mean percent change by quartiles of weight (adjusted for age and D3Cr muscle mass). Longitudinal changes were measured in common co-registered images for both HR-pQCT and DXA, and included: total vBMD (Tt.BMD), cortical BMD (Ct.BMD) trabecular vBMD (Tb.BMD), and FL at the distal radius and tibia; and aBMD at the femoral neck and total hip.Mean percent change was -1.4%+/-2.4 for distal radius Tt.BMD; -1.1%+/-1.7 for distal tibia Tt.BMD; -1.6%+/-6.0 for distal radius FL, -1.5%+/-4.5 for distal tibia FL, -0.4%+/-3.8 for femoral neck aBMD, and -0.9%+/-2.6 for total hip aBMD. Men with higher levels of D3Cr muscle mass at the Year 14 visit had smaller declines in Tt.BMD and Ct.BMD at the distal radius and distal tibia than men with lower levels of D3Cr muscle mass (p for trend<0.05, Figure). Patterns of change in FL were similar but did not reach statistical significance; D3Cr muscle mass appeared unrelated to change in Tb.BMD. D3Cr muscle mass was not significantly associated with change in total hip or femoral neck aBMD. Weight was not associated with change in BMD or FL at any site.In summary, men with higher D3Cr muscle mass had smaller declines in vBMD at distal sites, particularly in cortical vBMD, than men with lower levels of D3Cr muscle mass. D3Cr muscle mass was not significantly related to change in trabecular vBMD at distal sites, or aBMD at the hip. Weight was unrelated to change in BMD. Low muscle mass may influence vBMD declines at distal sites.

Figure. Age- and weight-adjusted mean percent change in vBMD and FL over 1.6 years at distal radius and tibia, across quartiles of D_3Cr muscle mass

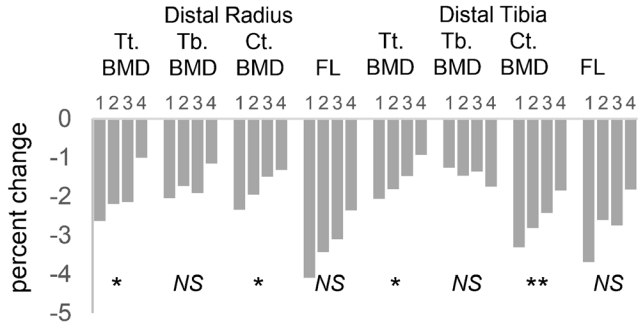

*p<0.05, **p<.001. P value is test for trend across quartiles

***Disclosures: Peggy Cawthon**, None*

P-859

A Longitudinal Study of Sarcopenia in Older Community Dwelling Women *Hampus Ekstubbe[1], Patrik Bartosch[1], Fiona McGuigan[1], Kristina E. Akesson[1]. [1]Lund University, Department of Clinical Sciences Malmö, Sweden

Background: Musculoskeletal ageing is a worldwide public health concern. Loss of muscle mass and strength (sarcopenia) contributes to the decline into frailty and to numerous adverse outcomes, including osteoporosis and fracture.Purpose: To longitudinally investigate prevalence of sarcopenia in a population-based cohort of community-dwelling older women, and its overlap with frailty and body composition. We also investigated the association between sarcopenia, frailty and mortality.Methods: The OPRA cohort were all 75y at inclusion (n=1044); and reassessed at 80y (n=715) and 85y (n=382). Extensive data was collected, including measures of muscle strength (hand grip strength (HGS); knee extension, Biodex), muscle mass (DXA), physical function (gait speed) and body composition; a frailty index (FI) was also available. Based on low muscle strength (HGS <16kg or knee <175 Nms); low mass (<5.5 kg/m2), low gait speed (<=0.8m/s) and total body fat (>40%), individuals were categorized as having Probable Sarcopenia, Sarcopenia and Severe Sarcopenia as outlined by the 2018 European Working Group on Sarcopenia in Older People. Frail was defined as FI>0.25.Results: Sarcopenia prevalence increased from 3.3% at 75 to 5.1% and 10.1% at 80 and 85. Proportionally, sarcopenia with obesity was 0.8%, 1.6%, 5.4% respectively.A substantial increase in frailty was also apparent with increasing severity of sarcopenia; having probable sarcopenia at 75y increased the odds (OR) of being frail at 80y (OR 3.77, CI 2.18-6.49). By age 85 three quarters of all women were both sarcopenic and frail.The odds of death at 5yrs was increased already among those with probable sarcopenia (4.07, CI 2.28-7.28), and higher again when combined with low body fat mass (OR: 6.02, CI 2.48-14.62). It was not increased in those with higher fat mass (OR: 0.54, CI 0.07-4.10). In those with probable sarcopenia in combination with frailty the odds of death were highest (6.33, 3.15-12.75).Conclusion: With the loss of muscle mass, strength and function that typifies musculoskeletal aging, comes an elevated risk of frailty and mortality. Evaluation for sarcopenia may facilitate intervention to maintain musculoskeletal competence; as a way of reducing falls, a major cause of fractures in the elderly.

***Disclosures: Hampus Ekstubbe**, None*

P-860

Adjusting Fracture Probability for Prior Falls: A Registry-Based Cohort Study. *William Leslie[1], Suzanne Morin[2], Lisa Lix[1], Eugene McCloskey[3], Helena Johansson[3], Nicholas Harvey[4], John Kanis[3]. [1]University of Manitoba, Canada, [2]McGill University, Canada, [3]University of Sheffield, United Kingdom, [4]University of Southampton, United Kingdom

BACKGROUND: FRAX® estimates 10-year fracture probability from multiple risk factors but does not currently consider the risk associated with falls. FRAX has been shown to underestimate fracture risk in those with one or more falls in the preceding 12 months, and the magnitude of this underestimation increases the greater the number of number of prior falls.OBJECTIVE: To derive a simple adjustment to FRAX probability based upon the number of falls in the preceding 12 months and assess its impact on risk reclassification. METHODS: Using the population-based Manitoba Bone Mineral Density (BMD) Program registry, we identified women and men age 40 years or older with baseline BMD and FRAX measures. Number of self-reported falls in the prior 12 months was collected from September 1, 2012 onwards. We identified incident major osteoporotic fractures (MOF) and hip fracture (HF) to March 31, 2018 from population-based healthcare data. We compared the effect of applying a simple risk adjustment to FRAX that varied from +10% to +100% per fall in steps of 10%. Cox regression analysis was used to determine the optimal adjustment that minimized the residual effects of falls (model Chi-square). We computed categorical net reclassification improvement (NRI) using 20% MOF and 3% HF intervention thresholds, and integrated discrimination improvement (IDI).RESULTS: The study population consisted of 20,767 individuals (age 65.7 +/- 10.1 years; 85% women). After mean 2.6 years of observation there were incident MOF in 640 and HF in 146. HR for MOF (adjusted for FRAX with BMD) progressively increased with the number of number of prior falls: 1.53 (95% CI 1.25-1.86) for one fall, 1.91 (1.43-2.55) for two falls, 2.57 (1.95-3.38) for 3+ falls (referent no falls). Adjusted HRs were slightly greater for HF (one fall 1.59 [95% CI 1.07-2.38], two falls 1.99 [1.12-3.52], 3+ falls 3.05 [1.80-5.15]). Model Chi-square for falls was minimized for an adjustment to FRAX of +70% per fall for MOF and +50% per fall for HF (FIGURE). Applying the lower FRAX adjustment of +50% per fall reclassified MOF risk in 6.1% and improved MOF prediction (total NRI +0.071; IDI +0.003; both p<0.001); reclassified HF risk in 3.4% and improved HF prediction (total NRI +0.021; IDI +0.003; both p<0.001). CONCLUSIONS: A simple risk adjustment to FRAX based upon the number of falls in the preceding 12 months significantly improves MOF and HF risk prediction, and reclassifies a moderate proportion of individuals.

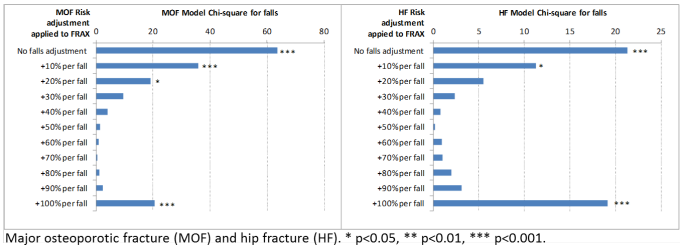

Major osteoporotic fracture (MOF) and hip fracture (HF). * p<0.05, ** p<0.01, *** p<0.001.

***Disclosures: William Leslie**, None*

P-861

Dairy food intake is not associated with frailty in adults *Shivani Sahni[1], Alyssa Dufour[1], Courtney Millar[1], Douglas Kiel[1], Paul Jacques[2], Marian Hannan[1]. [1]Marcus Institute, Hebrew SeniorLife and Harvard Medical School, United States, [2]Jean Mayer USDA HNRCA, Tufts University School of Nutrition, United States

Dietary protein is associated with lower risk of frailty, which occurs in 10-15% of community-living older adults. Yet, little evidence exists for the consumption of dairy foods (a good source of high quality protein) being related to the risk of frailty. It is unclear if high-fat dairy foods have a protective role in frailty given that anorexia and low-calorie intakes are often seen in frail individuals. The aim of this study was to determine the association of dairy food intake [milk, yogurt, cheese, total dairy (milk+yogurt+cheese), low-fat, and high-fat dairy, servings/week] with the odds of frailty in older adults from the Framingham Offspring study.In this cross-sectional study, 2,888 men and women completed food frequency questionnaires (FFQ) and had frailty assessments using Fried's frailty phenotype (1998-2001). Average intake of each dairy food was calculated from FFQs in 1998-2001, 1995-1998, and 1990-1995. Fried's frailty phenotype was defined as presence of >=3 criteria for unintentional weight loss, exhaustion, slowness (gait speed), low physical activity, and weakness (grip strength). Logistic regression was used to calculate odds ratios and 95% confidence intervals adjusting for age, sex, energy intake (residual analysis), current smoking, multivitamin use, self-reported health status (excellent, good, fair/poor), and presence of disease indicators (cognitive impairment, type 2 diabetes treatment, cardiovascular disease, non-skin cancer, and chronic kidney disease).Mean age (+/-SD) was 61y (+/-9, range 33-87y), and 54% were female. Mean dairy food intakes [(+/-SD), servings/week] were 5.7 (+/-5) (total milk), 1.0 (+/-1.6) (yogurt), 2.8 (+/-2.8) (cheese), 9.5 (+/-6.4) (total dairy), 6.1 (+/-5.7) (low-fat dairy), and 4.4 (+/-3.9) (high-fat dairy), Prevalent frailty was 2.3%. In age and sex adjusted models, yogurt was associated with 4% lower odds of frailty and high-fat dairy intake was associated with 3% higher odds of frailty (Table). These association became non-significant after adjustment for other variables. Further adjustment for disease indicators did not change the associations (data not shown).In this study of adults with wide age-range, dairy food intake was not associated with frailty. These analyses were limited by low number of frail individuals (n=67). The observed trend for a deleterious association with high-fat dairy intake should be re-examined in longitudinal studies with frailty assessed over time, particularly in older adults.

Table. Association of dairy food intake (servings/week) with odds of frailty in cross-sectional study of men and women from the Framingham Offspring Study.

Dairy food intake (servings/week)[a]	Model 1[b] (n=2,888)		Model 2[c] (n=2,849)	
	OR (95%CI)[d]	P Value	OR (95%CI)	P Value
Milk	1.00 (0.98-1.02)	0.72	1.00 (0.99-1.02)	0.39
Yogurt[e]	0.96 (0.92-0.99)	0.02*	0.97 (0.93-1.01)	0.18
Cheese	1.02 (0.99-1.06)	0.18	1.02 (0.98-1.05)	0.38
Total dairy	1.00 (0.99-1.02)	0.68	1.00 (0.99-1.02)	0.32
Low-fat dairy	0.99 (0.98-1.01)	0.57	1.00 (0.98-1.02)	0.69
High-fat dairy	1.03 (1.00-1.06)	0.007*	1.02 (0.99-1.05)	0.09

[a] The primary predictor was energy-adjusted residuals of dairy food intake added to a constant, where the constant equals the nutrient intake for the mean energy intake of the study population
[b] Model 1 adjusted for sex and age
[c] Model 2 adjusted for model 1 and energy intake, smoking status, multivitamin supplement use, and self-reported health status
[d] Odds ratios (OR) and 95% Confidence Intervals (95%CI)
[e] Logarithmic transformation was applied to yogurt intake before the residuals were created

***Disclosures: Shivani Sahni**, Ad-hoc reviewers, Egg Nutrition Council, Other Financial or Material Support, Institutional grants from Dairy Management Inc., Grant/Research Support, Unpaid consultant, Protein committee, ILSI North America, Consultant*

P-862

Global Balance of the Spine, an Independent Contributor to Physical Function and Falls in Older Adults: the SAFE Cohort Study *Melany Hars[1], Antonio Faundez[2], Jacques Fechtenbaum[3], Karine Briot[3], Christian Roux[3], Francois Herrmann[4], Serge Ferrari[1], Stephane Genevay[5], Sana Boudabbous[6], Andrea Trombetti[7]. [1]Division of Bone Diseases, Department of Medicine, Geneva University Hospitals and Faculty of Medicine, Switzerland, [2]Hôpital La Tour & Division of Orthopaedics and Trauma Surgery, Department of Surgery, Geneva University Hospitals and Faculty of Medicine, Switzerland, [3]Department of Rheumatology, Cochin Hospital, Assistance Publique-Hôpitaux de Paris, France, [4]Division of Geriatrics, Department of Readaptation and Geriatrics, Geneva University Hospitals and Faculty of Medicine, Switzerland, [5]Division of Rheumatology, Department of Medicine, Geneva University Hospitals and Faculty of Medicine, Switzerland, [6]Division of Radiology, Department Diagnostic, Geneva University Hospitals and Faculty of Medicine, Switzerland, [7]Division of Bone Diseases, Department of Medicine & Division of Geriatrics, Department of Readaptation and Geriatrics, Geneva University Hospitals and Faculty of Medicine, Switzerland

Purpose: Falls are common among older adults and remain the leading cause of fractures. They may result from several intrinsic and extrinsic risk factors. Among them, the role of the global balance of the spine has never been fully established. We conducted a preliminary cross-sectional analysis to determine the association between global balance of the spine, physical function and falls in community-dwelling older adults.Material and Methods: The SAFE study is an ongoing prospective, longitudinal cohort study conducted in Geneva (Switzerland) among community-dwelling adults aged >=65 years without history of instrumented spinal surgery. All subjects underwent a comprehensive assessment battery including: full skeleton 2D/3D radiographs in the standing position by EOS® low-dose biplane X-ray imaging system, DXA imaging, clinical examination, fall history in the past 12 months, and physical function tests. Spino-pelvic parameters collected included, among others, the spino-sacral angle (SSA) and the C7-central sacral line (C7-CSL) distance for sagittal and coronal balance, respectively.Results: 50 subjects (mean age, 74 years; 76% female) were included. Among them, 18 (36%) reported one or more falls in the past 12 months, 19 (38%) reported a history of low-trauma fracture, 15 (30%) were osteoporotic, while 12 (24%) had a Short Physical Performance Battery (SPPB) score <=9. Global sagittal balance was independently associated with physical performances after controlling for potential confounders (adjusted regression coefficient for SPPB score and SSA= 0.09, 95% CI [0.03, 0.16]; p=0.007), as well as some sagittal pelvic and lumbar curve measures. In addition, imbalanced subjects or balanced subjects thanks to compensations had more falls as compared to balanced subjects with no compensation (IRR=1.46, 95% CI [0.13, 2.79; p=0.031]). After controlling for age, sex, comorbidities, vertebral fractures and SPPB score, increased C7-CSL distance was independently associated with increased fall risk (OR=2.28, 95% CI [1.06, 4.92]; AUC=0.79, 95% CI [0.65, 0.92]).Conclusions: The findings of this study suggest that global balance of the spine is an independent contributor to physical impairments and falls in older adults. Further analysis from this longitudinal cohort study will reveal the role of compensating mechanisms in the sagittal plane, and should help to clarify whether global balance of the spine relates to incident falls and fractures in older adults.

***Disclosures: Melany Hars**, None*

P-863

Decreased Lower-extremity Muscle Performance is Associated with Decreased Hip Bone Mineral Density and Increased Fracture Risk in Community-dwelling Postmenopausal Women *Dexing Dai[1], Feng Xu[1], Ruoman Sun[1], Yali Ling[1], Zhongjian Xie[1]. [1]National Clinical Research Center for Metabolic Diseases, Hunan Provincial Key Laboratory for Metabolic Bone Diseases, and Department of Metabolism and Endocrinology, The Second Xiangya Hospital of Central South University, China

Abstract: Postmenopausal women are at high risk for osteoporotic fractures. It has been shown that decreased lower-extremity muscle performance is associated with osteoporotic fractures. The purpose of this study was to investigate the relationship between lower-extremity muscle performance and bone mineral density (BMD) or fracture risk in community-dwelling postmenopausal women. A total of 247 postmenopausal women aged 50-85 years old (age = 65.9; SD = 8.6 years) participated in this study. The short physical performance battery (SPPB) tool including the chair stand test (CST), gait speed test (GST) and balance test (BT) was used to determine lower-extremity functioning and the CST, GST, BT and SPPB total scores were recorded. The BMD of lumbar spine (LSBMD), femoral neck (FNBMD) and total hip (THBMD) were measured by dual-energy X-ray absorptiometry (DXA) and the vertebral fracture was confirmed by lateral spine X-rays radiographs. In addition, patients' 10-years major osteoporotic fracture risk and hip fracture risk were assessed by the Fracture Risk Assessment Tool (FRAX). Linear regression analysis was used to analyze the association between muscle performance and BMD. The results showed that the CST, GST and SPPB total scores were positively associated with LSBMD, THBMD, and FNBMD before adjustment for age, height, and weight. Besides, the SPPB total scores were positively associated with FNBMD and THBMD, but not with LSBMD after adjustment for age, height, and weight. However, the BT score was positively associated with FNBMD and THBMD, but not with LSBMD before and after adjustment for age, height, and weight. Moreover, the CST, GST, BT and SPPB scores were negatively associated with the FRAX score. These data suggest that decreased lower-extremity muscle performance is associated with decreased hip BMD and increased fracture risk in community-dwelling postmenopausal women with BMD.Nothing to ***Disclosures:*** DD, FX, RS, YL, ZX. Sources of Research Support: The National Natural Science Foundation of China (No. 81072219, 81272973, 81471055, and 81672646)

***Disclosures: Dexing Dai**, None*

P-864

Prevalence of Frailty and Associated Factors in a National Observational Cohort of Rheumatic Diseases. *Katherine D. Wysham[1], Joshua F. Baker[2], Kristin Wipfler[3], Patricia P. Katz[4], Kaleb Michaud[5]. [1]VA Puget Sound Health Care System/University of Washington, United States, [2]University of Pennsylvania, United States, [3]The National Databank for Rheumatic Diseases, United States, [4]University of California, San Francisco, United States, [5]University of Nebraska/National Databank for Rheumatic Diseases, United States

Purpose: Frailty is associated with poor outcomes in the general population and recently studies have highlighted its importance in rheumatic musculoskeletal diseases (RMDs). Self-reported measures of frailty are validated in the general population but have not been studied in RMDs. We aimed to describe the prevalence of self-reported frailty across RMDs and associated factors in a large observational cohort. Methods: Data were from participants in FORWARD, The National Databank for Rheumatic Diseases, the largest patient reported RMD research databank in the US, with biannual questionnaires from 1998. The January 2020 questionnaire included a 5-item validated patient-reported frailty scale querying fatigue, ability to walk several blocks, climb ten stairs, weight loss and 11 comorbidities. Those meeting >=3 of the 5 criteria were listed as frail. 1422 responses were collected as of May 21st, 2020 which represents 28% of the total cohort. Multivariable logistic regression analysis was performed to identify factors independently associated with frailty.Results: Top RMDs were rheumatoid arthritis (RA) (N=901, 63%) and osteoarthritis (OA) (N=213, 15%). Those categorized as frail (N=420, 30%) were older, had longer disease duration, a higher pain scale, a higher percentage of obese participants and more historical fractures than those who were not frail (Table 1). Systemic lupus erythematosus (SLE) had the highest proportion of frailty (40%) despite being the youngest group (61+/-12 years). The top three factors contributing to frailty scores were inability to walk several blocks, inability to climb 10 stairs and >=5/11 comorbidities (Table 1). In the multivariable model age, disease duration, pain scale and prior fracture were associated with elevated odds ratios of frailty (ORs 1.04, 1.01, 1.23 and 2.02 respectively, all p<0.05). Within RMDs, using OA as the referent, SLE was associated with 2.74-fold increased odds of frailty (p=0.002). Using normal weight as the referent, overweight and obesity were also associated with increased high odds of frailty (ORs 1.98 and 4.92, p<0.001).Conclusion: Self-reported frailty was prevalent in a third of participants with RMDs with the highest rate in those with SLE. SLE, prior fracture and obesity had the greatest odds of frailty in the multivariable model. Future longitudinal analyses to determine factors associated with incident frailty and fractures are needed in this high-risk population.

Table 1- Cohort characteristics as a whole and by frailty status determined by a five question, patient-reported index. Frailty index range 0-5 and frailty ≥3/5 criteria. Reported as N (%) or mean (SD).

	Overall (N=1422)	Not Frail (N=1002, 70%)	Frail (N=420, 30%)
Female	1230 (86.5%)	857 (85.5%)	373 (88.8%)
Age (years)	65.4 (11.4)	64.5 (11.6)	67.4 (10.4)
White Race	1292 (90.9%)	918 (91.6%)	374 (89.0%)
Disease Duration (years)	23.7 (12.3)	22.8 (12.0)	25.9 (12.8)
Primary Diagnosis			
-RA	901 (63.4%)	643 (64.2%)	258 (61.4%)
-SLE	90 (6.3%)	54 (5.4%)	36 (8.6%)
-Osteoarthritis	213 (15.0%)	147 (14.7%)	66 (15.7%)
-Fibromyalgia	63 (4.4%)	40 (4.0%)	23 (5.5%)
-Other[a]	100 (7.0%)	76 (7.6%)	24 (5.7%)
Pain Scale[b]	3.26 (2.59)	2.78 (2.42)	4.42 (2.62)
Body Mass Index[c]			
-Underweight	22 (1.5%)	18 (1.8%)	4 (1.0%)
-Normal	446 (31.4%)	377 (37.6%)	69 (16.4%)
-Overweight	420 (29.5%)	309 (30.8%)	111 (26.4%)
-Obese	534 (37.6%)	298 (29.7%)	236 (56.2%)
Prior Fracture	426 (30.0%)	246 (24.6%)	180 (42.9%)
Frailty Categories[d]			
-Fatigue	818 (57.5%)	580 (57.9%)	238 (56.7%)
-Stair Climb	464 (32.6%)	131 (13.1%)	333 (79.3%)
-Walking	632 (44.4%)	249 (24.9%)	383 (91.2%)
-Illnesses	533 (37.5%)	243 (24.3%)	290 (69.0%)
-Weight Loss	233 (16.4%)	92 (9.2%)	141 (33.6%)

-RA: rheumatoid arthritis; SLE: systemic lupus erythematosus.
[a]-Other category comprised of >20 primary rheumatic disorders other autoimmune and musculoskeletal syndromes.
[b]-Pain by visual analog scale. Range 0 (no pain at all) to 10 (worst pain imaginable).
[c]-Based on World Health Organization Body Mass Index categories: Underweight (<18.5 kg/m^2), Normal (18.5-24.9 kg/m^2), Overweight (25-29.9 kg/m^2) and Obese (>30 kg/m^2).
[d]-Frailty categories: self-reported fatigue, inability to climb 10 stairs, inability to walk several blocks, ≥5/11 comorbidities, ≥5% weight loss in the last year.
-Missing >5% data: Disease Duration (N=242) and Primary Diagnosis (N=110).

***Disclosures: Katherine D. Wysham**, None*

P-865

Neither Baseline Nor Change in Leg Muscle Strength and Balance Are Associated with the Incidence of Falls in Middle-aged Women: A 5-year Population-based Prospective Study *Mengmeng Wang[1], Feitong Wu[1], Michele Callisaya[2], Graeme Jones[1], Tania Winzenberg[1]. [1]Menzies Institute for Medical Research, University of Tasmania, Australia, [2]Menzies Institute for Medical Research, University of Tasmania; Peninsula Clinical School, Central Clinical School, Monash University, Australia

Objective: Muscle strength and balance are major modifiable factors of falls in older adults, but their associations with falls in middle-aged adults are under investigated. We aimed to examine the association of baseline and change in leg muscle strength (LMS) and balance with the incidence of falls in a cohort of middle-aged women.Material and Methods: This was a five-year follow-up of a population-based sample of 273 women aged 36-57 years at baseline (2011-2012). Data on LMS (by dynamometer) and balance (timed up and go test [TUG], step test [ST], functional reach test [FRT], and lateral reach test [LRT]) were obtained at baseline and five years later (2017-2018). After five years, falls were recorded monthly for one year by questionnaire (2017-2019). Negative binomial/Poisson and log binomial regressions were used as appropriate to assess associations of baseline and change in LMS and balance with any falls, injurious falls and multiple falls.Results: Over one-year, 115 participants (42%) reported at least one fall. Neither baseline nor 5-year change in LMS and balance measures were associated with the risk of any falls, injurious falls, or multiple falls five years later, with or without adjusting for potential confounders at baseline (incidence rate ratio/relative risk ranging from 0.91 to 1.14, 0.94 to 1.16, and 0.88 to 1.23, respectively; P>0.05 for all).Conclusion: Baseline or change in LMS and balance measures are not associated with incident falls among middle-aged women. These findings suggest that risk factor profiles for falls in middle-aged women may be different from those in older adults. Upon further confirmation of these findings different preventive strategies for falls may be needed in this population.

***Disclosures: Mengmeng Wang**, None*

P-866

Grip Strength Reference Values to Identify Sarcopenia in Youth *Fátima Baptista[1], Kathleen F Janz[2], Pedro St Maurice[3], Elena Letuchy[4], Luis Gracia-Marco[5], Enrique G Artero[6], Francisco Ortega[7], Jonatan R Ruiz[8], Luis A Moreno[5], German Vicente-Rodriguez[5], Steven M Levy [9]. [1]CIPER, Faculdade de Motricidade Humana, Universidade de Lisboa, Portugal, [2]Department of Health and Human Physiology, University of Iowa, United States, [3]Metabolic Epidemiology Branch, Division of Cancer Epidemiology and Genetics, National Cancer Institute, NIH, United States, [4]Department of Epidemiology, University of Iowa, United States, [5]University of Zaragoza, Spain, [6]SPORT Research Group (CTS-1024), University of Almería, Spain, [7]School of Sport Sciences, University of Granada, Spain, [8]University of Granada, Spain, [9]Department of Epidemiology; Department of Preventive and Community Dentistry, College of Dentistry, The University of Iowa, United States

Purpose Sarcopenia is a condition characterized by loss of skeletal muscle mass and strength. In adults it is diagnosed via the assessment of grip strength (identification) and the assessment of muscle mass index (confirmation). In adults, the cut-off values for the lower limits of grip strength and muscle mass index are 2.5 standard deviations (SD) and 2.0 SD below the peak of the average of healthy adults, respectively. Sarcopenia is not, however, exclusive to adults; it also manifests itself in children and adolescents due to various clinical conditions and lifestyle. The recognition of sarcopenia in youth is comprised by the lack of reference values. This study aimed to determine and validate handgrip strength reference values of for the identification of sarcopenia in adolescents.Methods The sample consisted of 880 participants divided into 2 sub-samples: a sub-sample for the development of grip strength cut-off values that included 525 healthy youth from Iowa (USA) (14.1 +/-2.3yrs) and a validation sub-sample comprising 355 healthy adolescents from Zaragoza, Spain (14.9 +/-1.2yrs). Handgrip strength was measured with a dynamometer and whole-body lean mass index (LBMI, kg/m2) without bone was determined using dual-energy x-ray absorptiometry. Grip strength performance was used to discriminate decreased LBMI of 2 SD and also of 1 SD (for primary prevention purposes). By gender, statistical analysis included the area under the curve (AUC), sensitivity (Se), specificity (Sp), and predictive odds ratios.Results The AUC varied from 0.72 to 0.81 for grip strength cut points with values for Se and Sp between 53.7 to 82.9% in the development sample. Results were similar in the validation sample. Those not meeting the grip strength cut points were 3 to 13 times more likely to have decreased LBMI, depending on gender, and the cut point being considered (LBMI < -2 SD vs. < -1 SD). Grip strengths of -1.1 SD for males and - 1.2 SD for females were associated with a -2 SD LBMI decrease.Conclusions Grip strength is a valid marker for the identification of sarcopenia in adolescents. We propose the adoption of grip strength of -1.1 SD in males and -1.2 SD in females for the identification of sarcopenia in 10 -18 yrs old.

***Disclosures: Fátima Baptista**, None*

P-867

Recent Fall and High Imminent Risk of Fracture *Kyoungmin Kim[1], Li-Yung Lui[1], Marcia L Stefanick[2], Steven R Cummings[1]. [1]San Francisco Coordinating Center, California Pacific Medical Center Research Institute, United States, [2]Stanford Prevention Research Center, School of Medicine, Stanford University, United States

Purpose: We tested the hypothesis that a recent fall predicts a high risk of fracture in the next year.Methods: We used data from the prospective SOF and MrOS studies. SOF enrolled 9704 women and MrOS, 5994 men age >= 65 years and participants were asked every 4 months about falls or fractures (FXs) in the preceding 4 months. FXs were validated by x-rays reports and follow-up for FXs and falls was > 90% complete over 14.8 years for SOF and 12.6 years for MrOS. 34% in women and men had history of falls within the previous 1 year and about half of those subjects in both sexes had fallen in the preceding 4 months. Non-spine FXs occurred in 4257 (43.9%) women and 1280 (21.4%) men and hip FX in 1444 (14.8%) women and 340 (5.7%) men, respectively. Total hip bone mineral density (BMD) was measured at baseline and every follow-up visit. Multivariate logistic models included history of falls and FXs during preceding 4 or 12 months, age, sex, and total hip BMD to predict over 1, 2 and 3 years.Results: In women and men, falls within 4 months indicated a high risk of non-spine and of hip fractures in the next year that was greater than the risk conferred by fall in the past year (Figure). In women, a recent fall carries an 8.1% risk of a non-spine FX within 1 year, a 2.5-fold greater risk than women without falls, and 2.5% risk of hip FX, a 3-fold increased risk. Those risks of FX diminished in 2nd and 3rd years after the fall (5.0% in 2nd year and 4.4% in 3rd year for non-spine FX and 1.6% in 2nd year and 1.4% in 3rd year for hip FX). In the multivariate models, in both women and men, recent history of fall, in the preceding 4 or 12 months, indicated a greater increase in 1-year risk of FX than did a history of FX during the same intervals: A fall within 4 months indicated a 2.3-fold (95% C.I. = 2.2-2.4) increased risk of non-spine FX while a FX indicated only 1.2-fold (1.1-1.3) increased risk. A fall within 4 months indicated a 2.7-fold [2.5-2.9] increased risk of hip FX while a FX in that period was not significantly associated with an increased risk of hip FX (odds ratio =1.0 [0.8-1.2]).Conclusions: A fall, especially within 4 months, indicates a high risk of fracture in the next 12 months. In multivariate models, a recent fall predicts non-spine and hip FXs more strongly than does a recent FX. Older women and men with recent falls warrant measures to prevent falls and should be considered for drug treatment to reduce their imminent risk of fracture.

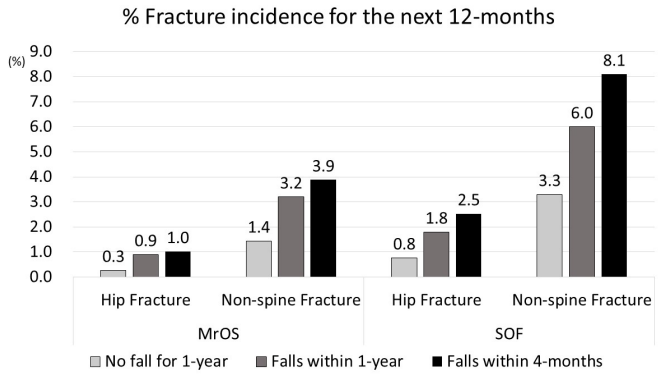

***Disclosures: Kyoungmin Kim**, None*

P-868

Evaluating the Muscle-Bone Unit in Severe Obesity with and without Type 2 Diabetes *Alessandra Amato[1], Jenna C. Gibbs[2], Claudia Gagnon[3], Anne-Frédérique Turcotte[3], Guy Hajj Boutros[4], Fabrice Mac-Way[3], Mylène Aubertin-Leheudre[5], Vanessa Tardio[6], Suzanne N. Morin[7]. [1]Department of Kinesiology and Physical Education, McGill University, Canada, [2]Department of Kinesiology and Physical Education, McGill University; Research Institute of the McGill University Health Centre, Canada, [3]Endocrinology and Nephrology Research Axis, CHU de Quebec Research Centre; Department of Medicine, Université Laval, Canada, [4]Research Institute of the McGill University Health Centre, Montréal, Canada, [5]Department of Exercise Science, Université du Québec à Montréal, Canada, [6]Division of Endocrinology and Metabolism, McGill University Health Centre, Canada, [7]Research Institute of the McGill University Health Centre; Department of Medicine – Division of General Internal Medicine, McGill University Health Centre, Canada

Background: Individuals with severe obesity and type 2 diabetes (T2D) are at a higher risk of fracture despite having higher areal bone mineral density (aBMD). Obesity is an important risk factor for T2D and has negative effects on bone health due to inflammation, higher visceral adipose tissue, functional limitations, and muscle fat infiltration. Muscle-related force production protects against T2D but also increases bone strength by stimulating bone turnover rates. However, data comparing the muscle-bone unit in severe obesity with and without T2D are lacking.Purpose: To describe and compare the associations between measures of muscle quality, bone quality, and physical performance in obese adults with and without T2D.Methods: We aim to recruit obese men and women (age >= 18 y, BMI >35 kg/m2) with (n=20) and without T2D (n=20) for one-time measures in two university research centres. Quantitative computed tomography (QCT) will be used to determine bone quality parameters at the lumbar spine (total and trabecular volumetric BMD (vBMD)), proximal femur, tibia and radius (total, trabecular and cortical vBMD; cortical thickness) using the Mindways QCTPro software. Cross-sectional analysis of the lean and fat soft tissue from these sections will be performed using the Tissue Composition Module of the QCTPro software. Peripheral QCT (pQCT) will also be performed for a subset of participants to compare the bone and muscle data with those of QCT. Handgrip and knee extensor muscle strength will be measured using validated Jamar and Biodex Pro3 dynamometer protocols. Performance-based tests of mobility, balance, and submaximal aerobic capacity, and biochemical analyses of hormones involved in bone metabolism will also be performed (Table 1). Independent t-tests will be used to compare outcomes between groups (T2D versus non-T2D participants). Pearson/Spearman correlation and multivariable linear regression analyses adjusting for potential confounders including, age, sex, and T2D status will be conducted. Expected Results: Greater muscle quality (cross-sectional area, handgrip, and knee extensor strength) will be associated with better bone quality and physical performance. Conclusions: Our research will provide new knowledge on the muscle-bone unit in severe obesity and T2D and inform future multimodal intervention studies to enhance muscle and bone health and prevent falls and fractures in these high-risk populations.

Table 1. Summary of the study measurements.

Variables	Outcome Measures
Bone Quality Variables	QCT Lumbar spine (L2-L3) (total and trabecular vBMD), proximal femur, radius (distal one-third), tibia (distal one-third) (total, trabecular and cortical vBMD; cortical thickness) pQCT Femur (distal), radius (distal, proximal), tibia (distal, proximal) (total, trabecular and cortical vBMD; cortical thickness) DXA Areal BMD at lumbar spine (L1-L4), femoral neck, total hip, radius
Muscle Quality Variables	QCT Lumbar, quadriceps, calf, forearm muscle cross-sectional area pQCT Quadriceps, calf, forearm muscle cross-sectional area and density Strength Hand Grip, Isometric Knee Extensor
Physical Performance Variables	6 Minute Walk Test Timed Up and GO Fullerton Advanced Balance Scale
Biochemical Markers	Glucose, HbA1c, insulin, 25OHD, PTH, calcium, IGF-1, AGEs, FFA, bone turnover markers (P1NP, CTX)

QCT: quantitative computed tomography; vBMD: volumetric bone mineral density; pQCT: peripheral quantitative computed tomography; DXA: dual-energy X-ray absorptiometry; HbA1c: glycated hemoglobin; 25-OHD: 25-hydroxyvitamin D; PTH: parathyroid hormone; IGF-1: Insulin-like growth factor 1; AGEs: advanced glycation end-product; FFA: free fatty acid; P1NP: N-terminal propeptide of type 1 procollagen; CTX: C-terminal telopeptide

***Disclosures: Alessandra Amato**, None*

Posters

Author Index